#ICPEAC2021

VIRTUAL

ICPEAC 2021

32nd International Conference on Photonic, Electronic and Atomic Collisions

July 20 - 23, 2021

www.icpeac2021.ca

www.icpeac2023.ca

OTTAWA • CANADA

icpeac 2023

July 25 - August 1, 2023

CONTENTS

WELCOME

We are excited to welcome you to the **32nd International Conference on Photonic, Electronic and Atomic Collisions** – held from **July 20-23, 2021** – in virtual format (ViCPEAC 2021). Welcome to those of you who have been with us for many years, as well as to those of you who are new to the community. Our deepest thanks go to all of you for staying with us while we transformed (hopefully only as a singular occurrence) the revered in-person event to a virtual one. The conference would not be possible without your scientific contributions and your participation.

“Make sure, it will not just be yet another Zoom-meeting!” We received several comments along these lines when starting out planning ViCPEAC. This clearly indicated after one and a half years of pandemic isolation, the urge within our community for real-life scientific (and social) interaction among colleagues and collaborators. So, we tried to find a corresponding solution by combining two different conference systems. “Pheedloop” is the part of our conference platform to experience special and progress reports and our plenary tutorial and IUPAP prize lectures. If you missed a talk, you can watch its recording on Pheedloop at later times during the conference. In addition, Pheedloop provides messenger-like networking opportunities – simply start a chat with other conference participants or create groups for discussions among several people.

Our poster sessions are organized almost as in a real-life ICPEAC. We set up a conference venue in “GatherTown” where the posters are located in several dedicated rooms. Resembling video games from the 90s, in GatherTown you can walk around using a small avatar, approach a poster, and interact with the presenter just as in real life. Furthermore, this platform (our “ViCPEAC summer resort”) is open 24/7 during the conference for direct social interaction. As soon as you approach another participant, a video chat starts and you can discuss latest science, or simply meet friends and colleagues which you have not been able to meet during the last one and a half years due to pandemic restrictions.

Finally, we would like to express our gratitude to our sponsors for their support which has helped transform this event into a digital reality.

We look forward to meeting you virtually at ViCPEAC 2021

TILL JAHNKE
Chair of the non-Local Organizing Committee of ViCPEAC 2021

ABOUT ICPEAC

ICPEAC has a long history dating back to 1958 when the first meeting was held in New York City. Since then ICPEAC has been held every two years on five continents, and grown to attract as many as 800 participants. The ICPEAC central website can be found **here**.

The conference brings together the world's leading scientists who are working in the field of collisions involving photons, electrons, ions, atoms, molecules, clusters, surfaces, and exotic particles. At this meeting scientists will present their latest research on topics such as ultrafast dynamics at the femto- or attosecond scale, ion-induced radiation damage in particular of biomolecules, atomic spectroscopy and molecular physics of antimatter, free electron lasers, particle acceleration generated by high-power lasers, and ultracold collisions.

Since 2019 ICPEAC is recognized as a separate section within the Atomic, Molecular and Optical Physics Division of the **European Physical Society.** ViCPEAC is recognized as a Europhysics conference.

GUIDE TO USING THIS INTERACTIVE PROGRAM

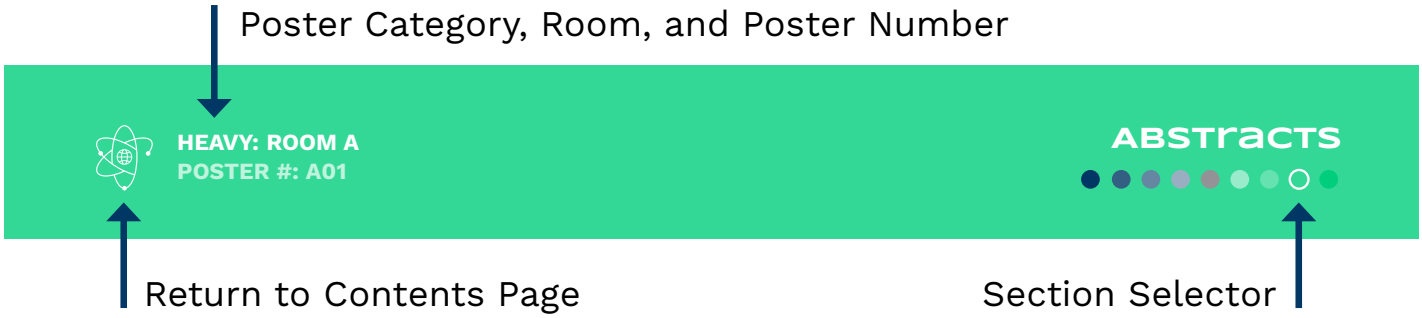

ABOUT VICPEAC

As outlined before, apart from providing a platform for excellent scientific presentations, we focused on enabling as much real-life interaction as possible when implementing ViCPEAC. Let us briefly explain the main features of our conference platform. More detailed information will be available online.

As you log in to the conference, you will be in “Pheedloop”. This is the part of our platform where you can listen to the plenary tutorial lectures and the special and progress reports. Additionally, you can contact any of the ViCPEAC participants here using a messenger-like chat feature.

VIRTUAL PLATFORM - PHEEDLOOP

Below you can see the Pheedloop main window as it appears in your browser.

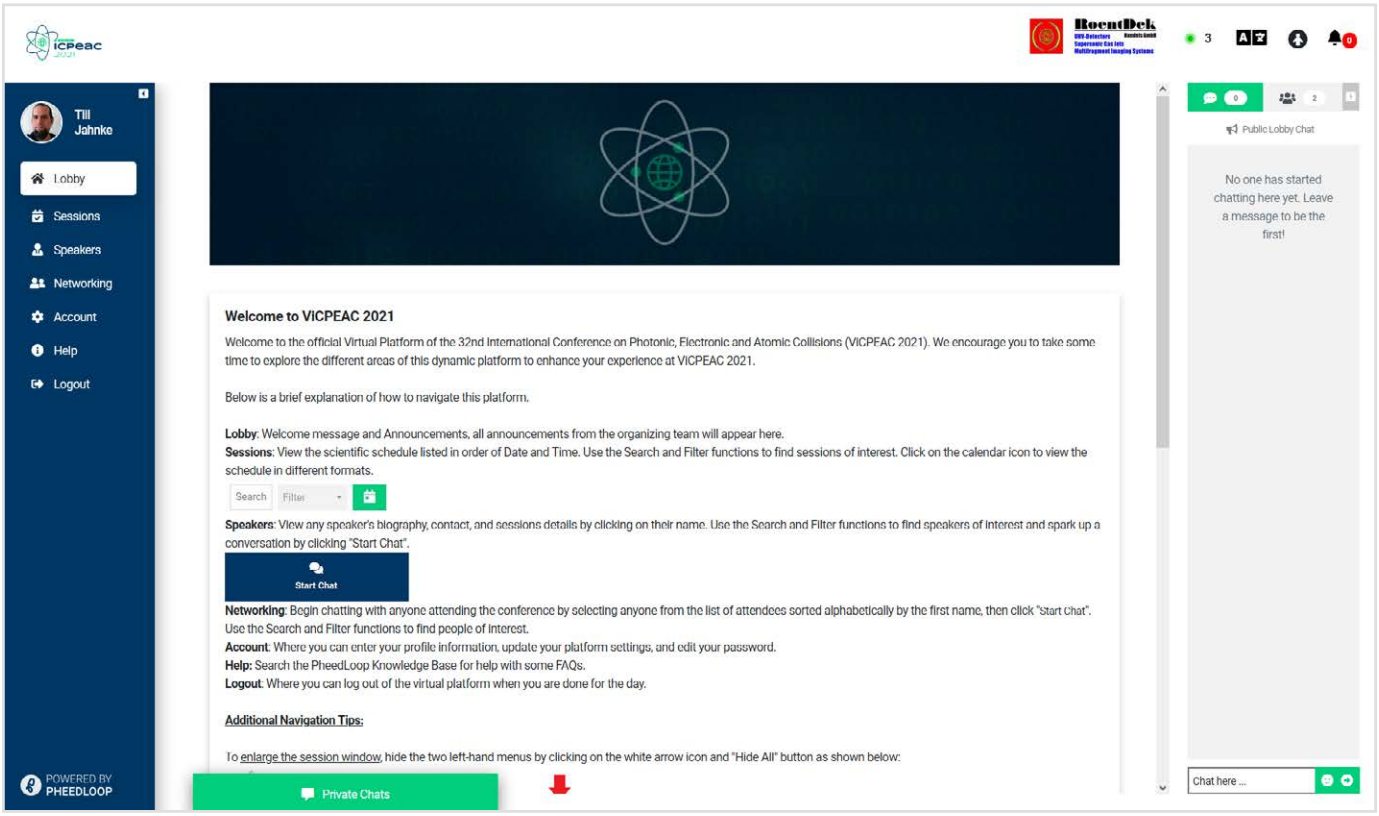

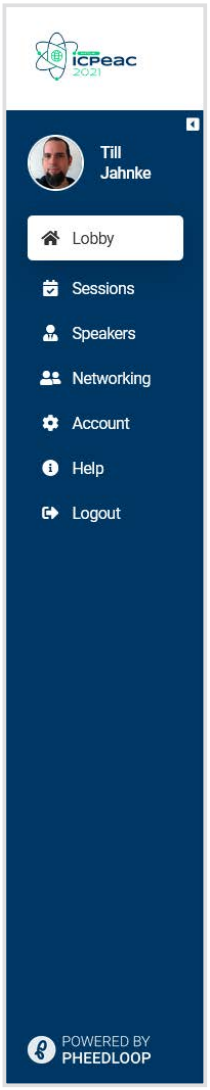

On the left you will find a menu, which consists of the following buttons:

Lobby:

Clicking this Button will display the welcome message and general information and instructions in the main panel in the center. Announcements from the organizing team will appear here, too. The lobby screen displays a public chat on the right.

Sessions:

Here you have access to the scientific schedule and the actual oral presentations. By default, the sessions are listed in order of date and time. You can click on a session item in order to obtain more information (i.e., speaker details and abstracts) or to access the session as it progresses or see its recording if you missed the session.

Speakers:

A list of all speakers providing more information like biography and contact and the speakers' sessions. After selecting a speaker, you can contact them by simply clicking the big "Start Chat" icon. Please note: due to peculiarities of the Pheedloop platform, session chairs are recognized as speakers, as well. You can search and filter the list of speakers using the corresponding fields above the list.

Networking

Provides a list of all participants (similar to the speakers list). Contact a participant by pressing the large "Start Chat" button. You can search for participants or filter the list using the corresponding fields above the list.

Account

Change and review your account settings

Help

Access to the Pheedloop help pages.

Logout

Click here to log out.

POSTER AND NETWORKING PLATFORM - GATHERTOWN

Our poster session and more lifelike socializing takes place in our “ViCPEAC summer resort” on the platform GatherTown. You can access it during poster session times from Pheedloop by selecting the corresponding poster session or enter the site using the link posted in Pheedloop independently from the poster sessions. The GatherTown platform will be open 24/7 during the conference via this link. Below you see a screen shot of how GatherTown looks in your browser.

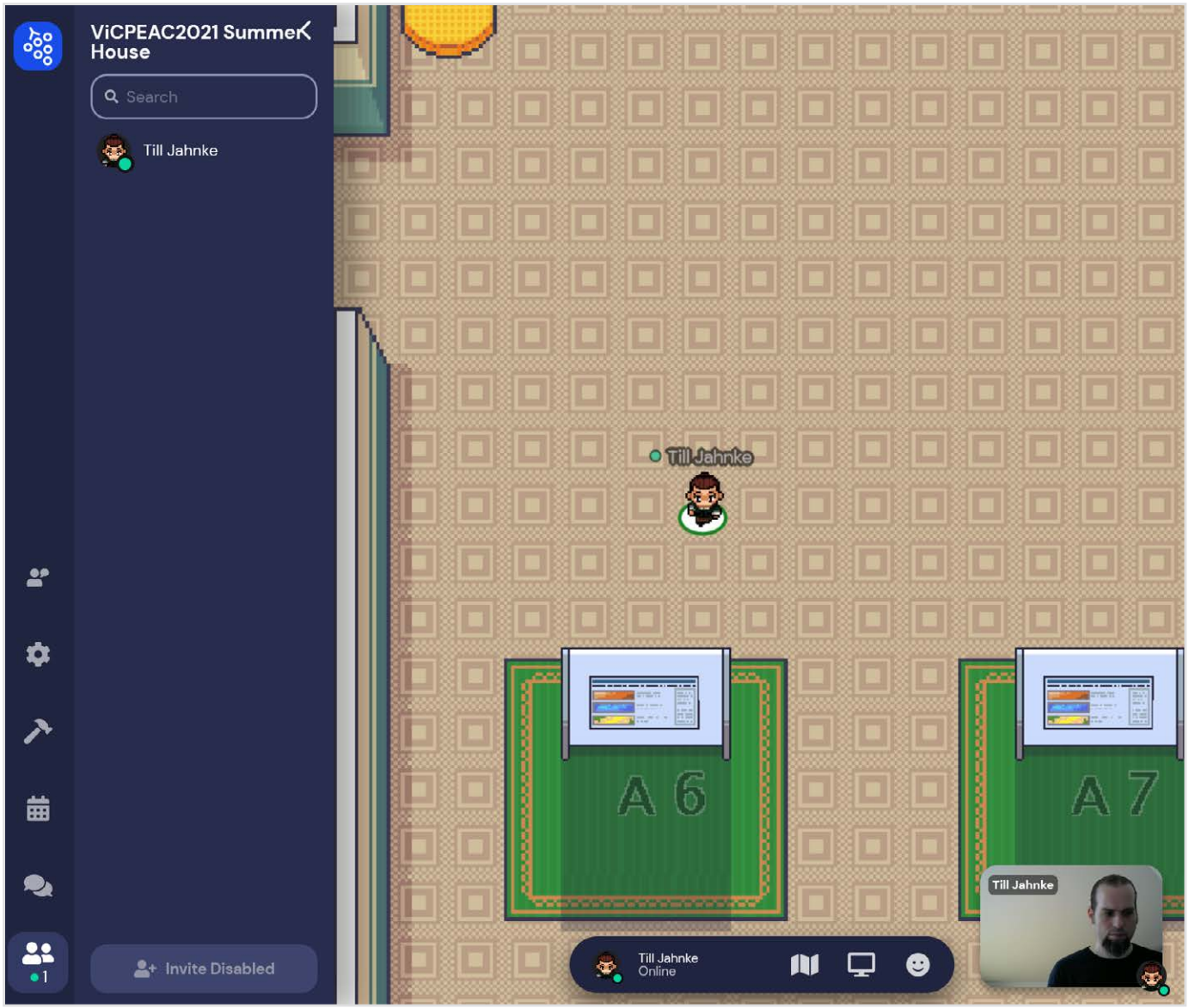

You can use the cursor keys (on your keyboard) to navigate your avatar (the small person with your name on). Above you see an example of one of our poster rooms. By walking up to a poster you may have a detailed look at it after pressing ”x” (as indicated on the screen upon approaching the poster).

As you approach other avatars (by walking up to them) a video chat is opened and you can talk directly to participants in your closer proximity. Please note, on first use, you need to confirm, that your browser is allowed to access your webcam and your microphone. Typically, a prompting message appears, which you need to confirm. As in real life, people can block your way. By holding the letter "g" on your keyboard while moving, you can "ghost" your way through other people. Nevertheless, please avoid standing in front of doorways or narrow walkways blocking the passage for other people.

In a nutshell:

- Move avatar: use cursor keys
- Interact with object (e.g. display poster): press “x”
- Close poster view/map view: press “x”
- Tunnel through other participants: press (and hold) “g”

Apart from the main screen showing your current surrounding, you find a list of all participants, that are currently online on the left. If you want to locate a specific person on the map, you can click their name and either select “locate on map” or “follow”. The former will draw a line leading the way to the person. The latter will automatically navigate your avatar to the location of the selected person.

On the very left there is a narrow menu bar which allows to switch from participants list (icon on the very bottom) to the built-in chat system (speech bubbles). The calendar and build-features are not enabled in the ViCPEAC summer resort. The gear wheel-icon provides access to your account and system settings (i.e. user and video/audio preferences).

At the bottom in the middle you can access your avatar setting by clicking on your name. A map of the room you are in is displayed when clicking the map-icon in the middle. Be careful not to get confused between the map and the actual room after opening the map. The map can be closed by pressing “x” (or clicking on the “x”-icon in the top right corner). The computer screen-icon will share your screen with those people who are currently connected via video chat (i.e. those in your close proximity).

Bottom right you see your current webcam feed (if enabled). By hovering over this area, you can turn on and off your webcam and your microphone.

This was just a brief summary of how to use our platform. Make sure to check out more detailed information (like a full map of the ViCPEAC summer resort and more details on our Q&A sessions) which is provided online (please check out Pheedloop’s lobby section).

committees

EXECUTIVE COMMITTEE

Friedrich Aumayr
Chair
Institute of Applied Physics, Vienna University of Technology, Wiedner Hauptstr. Austria

Emma Sokell
Secretary
University College Dublin, School of Physics Science Centre, Dublin

Stefan Schippers
Treasurer
Institute of Experimental Physics I, Strahlenzentrum, Leihgesterner, Germany

Kiyoshi Ueda
Past Chair
Tokohu University, Sendai, Japan

Dajun Ding
Vice Chair
Jilin University, Changchun, China

Dominique Vernhet
Past LOC Chair
Institut des Nanosciences de Paris, France

Olivier Dulieu
Past LOC Co-Chair
Institute, Laboratoire Aimé Cotton, CNRS-Univ., France

Lamri Adoui
Past LOC Co-Chair
Grand Accélérateur National d'Ions Lourds (GANIL), France

Tom Kirchner
LOC Chair 2023
Department of Physics and Astronomy, York University, Canada

André Staudte
LOC Co-Chair 2023
National Research Council Canada and University of Ottawa, Canada

Michael Meyer
LOC Co-Chair Hamburg
European XFEL research campus Schenefeld Holzkoppel, Germany

Robin Santra
LOC Co-Chair Hamburg
Center for Free-Electron Laser Science, Germany

Toshiyuki Azuma
LOC Chair Sapporo
RIKEN, Japan

Kenichi Ishikawa
LOC Co-Chair Sapporo
School of Engineering, the University of Tokyo, Japan

Masahiko Takahashi
LOC Co-Chair Sapporo
Tohoku University, Japan

Jimena Gorfinkiel
Member
School of Physical Sciences, Robert Hooke building, The Open University, Walton Hall, United Kingdom

Till Jahnke
Member
European XFEL, Germany

Ann Orel
Member
Department of Chemical Engineering and Materials Science, USA

James Sullivan
Member
Australian National University, Australia

NON-LOCAL ORGANIZING COMMITTEE

Till Jahnke
Chair
European XFEL, Germany

Emma Sokell
Co-Chair
University College Dublin, School of Physics Science Centre, Dublin

Tom Kirchner
Co-Chair
Department of Physics and Astronomy, York University, Canada

Jimena Gorfinkiel
Member
School of Physical Sciences, Robert Hooke building, The Open University, Walton Hall, United Kingdom

Markus Schöffler
Member
Institut für Kernphysik, Goethe-Universität, Germany

André Staudte
Member
National Research Council Canada and University of Ottawa, Canada

Dominique Vernhet
Member
Institut des Nanosciences de Paris, France

GENERAL COMMITTEE

Members

Diego Arbó
Argentina

Dariusz Banaś
Poland

Sadia Bari
Germany

Iva Březinová
Austria

Paola Bolognesi
Italy

Michael Bromley
Australia

Romarly Costa
Brazil

Xiangjun Chen
China

Jan Marcus Dahlström
Sweden

Alicja Domaracka
France

Nirit Dudovich
Israel

Ilya Fabrikant
USA

Juraj Fedor
Czech Republic

Gleb Gribakin
Northern Ireland

Rosario González-Férez
Spain

Elena Gryzlova
Russia

Alexandre Gumberidze
Germany

Yasushi Kino
Japan

Holger Kreckel
Germany

Edwin Kukk
Finland

Allen Landers
USA

Heather Lewandowski
USA

Chetan Limbachiya
India

Igor Litvinyuk
Australia

Philippe Martin
France

Takashi Mukaiyama
Japan

Nobuyuki Nakamura
Japan

Antonio Picon
Spain

Francoise Remacle
Belgium

Daniel Rolles
USA

Henning Schmidt
Sweden

Thomas Schlathölter
Netherlands

Lucas Sigaud
Brazil

Olga Smirnova
Germany

Lokesh Tribedi
India

Katalin Varju
Hungary

Oleg Vasyutinskii
Russia

Zong-Chao Yan
Canada

Jianmin Yuan
China

Shaofeng Zhang
China

Award Recipients

Prestigious prizes for young scientists will be awarded at the XXXII virtual ICPEAC:

The IUPAP Young Scientist Prize in Atomic, Molecular, and Optical Physics

The IUPAP Young Scientist Prize (YSP) of the IUPAP C15 Committee is granted to nominees, with not more than 8 years research experience (excluding career interruption) following the PhD, who have made original and outstanding contributions to the field of AMO Physics.

Award Winner 2020:

Philipp Hauke
University of Trento,
Italy

Award Winner 2021:

Carlos Hernández-García
Universidad de Salamanca,
Spain

Both prize winners are presenting their work in the IUPAP Prize Talks session on Wednesday, 21st July.

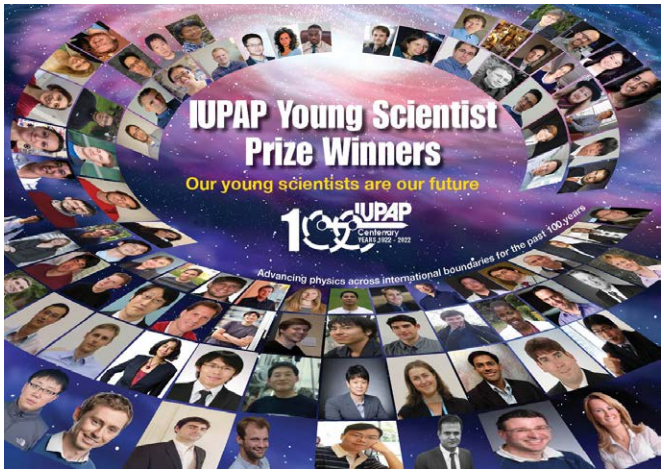

Sheldon Datz Prize for an Outstanding Young Scientist attending ICPEAC.

Sheldon Datz was a pioneer in the field of atomic and molecular collision physics and a staunch supporter of ICPEAC. The Sheldon Datz Prize was established to support an outstanding young researcher (graduate student/post-doc) to attend ICPEAC and this year will recognise such a participant in ViCPEAC. More information can be found at **www.ucd.ie/icpeac/sheldon_prize.html**

The prize will be awarded at the ICPEAC Business Meeting on Wednesday 21st July.

Award Winner:

Madhusree Roy Chowdhury
Tata Institute of Fundamental Research,
Mumbai, India

The prize winner is presenting their work as a Special Report in the Complex Systems session on Tuesday 20th July.

WE ARE VERY GRATEFUL FOR THE SUPPORT OF THE FOLLOWING INSTITUTIONS:

IUPAP

Amplitude

APS physics PHYSICAL REVIEW JOURNALS

EPJ D Recognized by European Physical Society
Atomic, Molecular, Optical and Plasma Physics

FASTLITE

NRC · CNRC
uOttawa
JCEP
Joint Centre for Extreme Photonics
Centre conjoint de la photonique extrême

few-cycle different solutions

RoentDek Handels GmbH
Supersonic Gas Jets
Detection Techniques
Data Acquisition Systems
Multifragment Imaging Systems

UFI UltraFast Innovations

SCIENTIFIC PROGRAM

DAY 1: TUESDAY, JULY 20, 2021

*time zone of CEST

14:50 - 15:00 **Opening Remarks**
Fritz Aumayr & Till Jahnke

15:00 - 16:00 **Attosecond Molecular Science: A Theoretical Point of View**
Fernando Martin
Session Chair: Eva Lindroth
Tutorial Lecture | pg 24

16:00 - 17:00 **Antimatter**
Session Chair: James Danielson

- **16:00 - 16:30** **Accurate Experimental Cross Sections for Electron and Positron Scattering**
  Rina Kadokura
  Progress Report | pg 40
- **16:30 - 16:45** **Many-Body Theory Calculations of Positron Scattering and Annihilation in H_2, N_2, CH_4 and CF_4**
  Charlie Rawlins
  E30 | pg 82
- **16:45 - 17:00** **Production of Antihydrogen Pulses at AEgIS**
  Antoine Camper
  H18 | pg 64

16:00 - 17:00 **Astrophysics**
Session Chair: Ioan Schneider

- **16:00 - 16:30** **Mutual Neutralization of H^- and Metal Ions: Theory, Experiment and Astrophysical Applications**
  Jon Grumer
  Progress Report | pg 36
- **16:30 - 17:00** **Sputtering of Planets and Moons by Ion Impact**
  Paul Szabo
  Progress Report | pg 54

16:00 - 17:00 **Plasma**
Session Chair: Ronnie Hoekstra

- **16:00 - 16:30** **Collisional Radiative Modeling of Plasmas Involving Dielectronic Resonances**
  Dipti Dipti
  Progress Report | pg 33
- **16:30 - 17:00** **Atomic Systems Under Plasma and Cavity Confinements**
  Jayanta Saha
  Progress Report | pg 51

17:00 - 17:10 **BREAK**

DAY 1: TUESDAY, JULY 20, 2021 (CONTINUED)

*time zone of CEST

17:10 - 19:10 **Weak Field Dynamics I**
Session Chair: Stacey Sörensen

17:10 - 17:40	**Experiments with Laser Aligned Molecules at FERMI** **Michele Di Fraia** Progress Report | pg 32
17:40 - 18:10	**Ultrafast Resonant Interatomic Coulombic Decay Induced by Quantum Fluid Dynamics** **Aaron LaForge** Progress Report | pg 43
18:10 - 18:40	**Cage-Opening Dynamics of Adamantane** **Sylvain Maclot** Progress Report | pg 44
18:40 - 18:55	**The Travel Time of Light Across a Molecule** **Sven Grundmann** M08 | pg 71
18:55 - 19:10	**Photo-Induced Molecular Catapult. Imaging Molecular Rotation During Ultrafast Dissociation** **Oksana Travnikova** N29 | pg 88

17:10 - 19:10 **Strong Field Dynamics**
Session Chair: Caterina Vozzi

17:10 - 17:40	**Two-Photon Single Ionization of Helium: From Below-Threshold to Doubly-Excited States** **Diego Boll** Progress Report | pg 30
17:40 - 18:10	**Nonadiabatic Subcycle Linear Momentum Transfer in Tunneling Ionization** **Hongcheng Ni** Progress Report | pg 48
18:10 – 18:40	**Probing Strong-Field QED Using High-Power Lasers Doppler-Boosted by Curved Relativistic Plasma Mirrors** **Henri Vincenti** Progress Report | pg 57
18:40 - 18:55	**Holographic Angular Streaking of Electrons (HASE)** **Sebastian Eckart** I32 | pg 68
18:55 - 19:10	**Strong-Field Photoelectron Emission From Metal Nanoparticles** **Uwe Thumm** O12 | pg 85

DAY 1: TUESDAY, JULY 20, 2021 (CONTINUED)

*time zone of CEST

17:10 - 19:10	**Complex Systems** Session Chair: Marcio Bettega	
	17:10 - 17:40	**Solvent Effects in Low Energy Electron Scattering** **Lucas Cornetta** **Progress Report** | pg 31
	17:40 - 18:10	**Fragmentation Dynamics of Hydrated Tetrahydrofuran Induced by Electron Impact Ionization** **Enliang Wang** **Progress Report** | pg 58
	18:10 - 18:25	**Ultrafast Dynamics of Correlation Bands Following XUV Molecular Photoionization** **Alexie Boyer** **L28** | pg 63
	18:25 - 18:40	**Photoemission and State-Selected Fragmentation in Cyclic Dipeptides Containing an Aromatic Amino Acid** **Laura Carlini** **L31** | pg 65
	18:40 - 18:55	**Intramolecular Charge Migration in Betaine by Impact of Fast Atomic Ions** **Jesús González-Vázquez** **B15** | pg 70
	18:55 - 19:10	**Radiosensitizing Effect of Halouracils in Hadron Therapy** **Madhusree Roy Chowdhury** **B30** | pg 83
19:10 - 20:10	**Posters Viewing in GatherTown**	

DAY 2: WEDNESDAY, JULY 21, 2021

*time zone of CEST

12:30 - 13:00 **Speakers Q&A in GatherTown**

13:00 - 14:00 **Posters Viewing in GatherTown**

14:00 - 16:00 **Fundamental Collisions**
Session Chair: Baoren Wei

14:00 - 14:30 **Quantum-State-Controlled Chemi-Ionization Reactions**
Katrin Dulitz
Progress Report | pg 34

14:30 - 15:00 **Development of an RF-Carpet Gas Cell to Obtain an Ion Beam of Thorium-229**
Atsushi Yamaguchi
Progress Report | pg 59

15:00 - 15:15 **On How Classical Uncertainties Enfeeble Quantum Coherence**
Raul Oscar Barrachina
B08 | pg 52

15:15 - 15:30 **Imaging the Ultrafast Umbrella (Inversion) Motion in Ammonia**
Blanca Belsa
L22 | pg 62

15:30 - 15:45 **Charge Transfer Reactions of Polar Molecules and Rare Gas Ions**
Andriana Tsikritea
C27 | pg 89

15:45 - 16:00 **Polarization Phenomena in Electron Resonant Elastic Scattering on One-Electron Ions**
Daria Vasileva
F29 | pg 90

14:00 - 16:00 **Ultrafast Physics**
Session Chair: Akiyoshi Hishikawa

14:00 - 14:30 **R-Matrix Calculations for Ultrafast Two-Colour Spectroscopy of Noble Gas Atoms**
Kathryn Hamilton
Progress Report | pg 37

14:30 - 15:00 **Ultrafast, All-Optical and Highly Enantio-Sensitive Imaging of Molecular Chirality**
David Ayuso
Progress Report | pg 28

15:00 - 15:30 **Retrieving of an Attosecond Pulse Waveform Based on the High Harmonic Generation**
Tatiana Sarantseva
Progress Report | pg 52

15:30 - 15:45 **Inner-Shell-Ionization-Induced Femtosecond Structural Dynamics of Water Molecules Imaged in Real Time at an X-ray Free-Electron Laser**
Ludger Inhester
M15 | pg 73

15:45 - 16:00 **Coherent Control of Ultrafast XUV Transient Absorption**
Peng Peng
N06 | pg 80

DAY 2: WEDNESDAY, JULY 21, 2021 (CONTINUED)

*time zone of CEST

14:00 - 16:00 **Exotic Systems and Ultracold Collisions**
Session Chair: Masanori Tachikawa

- **14:00 - 14:30** **Ionization of Atoms and Molecules by Twisted Electron Beams**
  Aditi Mandal
  Progress Report | pg 45
- **14:30 - 15:00** **Relativistic Effects on Loosely Bound States of Positronic Alkali-Metal Atom**
  Takuma Yamashita
  Progress Report – E21 | pg 60
- **15:00 - 15:30** **Microwave Control of Ultracold Molecular Collisions**
  Tijs Karman
  Progress Report | pg 41
- **15:30 - 15:45** **Complete Quantum Coherent Control of Ultracold Molecular Collisions**
  Adrien Devolder
  B11 | pg 67
- **15:45 - 16:00** **Ultrafast Electron Cooling in an Expanding Ultracold Plasma**
  Juliette Simonet
  D19 | pg 87

16:00 - 16:10 **BREAK**

16:10 - 17:10 **The Physics of Radio-Frequency Traps in a Collision Physics Perspective**
Caroline Champenois
Session Chair: Xinwen Ma
Tutorial | pg 33

17:10 - 18:30 **IUPAP Prize Talks & ICPEAC Business Meeting**
Session Chair: Roberto Rivarola

- **17:10 - 17:40** **High-Energy Physics at Ultra-Cold Temperatures – Quantum Simulating Lattice Gauge Theories**
  Philipp Hauke
  IUPAP Prize Talk | pg 26
- **17:40 - 18:10** **Light Pulses Structured at the Attosecond Timescale**
  Carlos Hernández-García
  IUPAP Prize Talk | pg 27
- **18:10 - 18:30** **ICPEAC Business Meeting**
  Emma Sokell

18:30 - 19:00 **Speakers Q&A in GatherTown**

DAY 3: THURSDAY, JULY 22, 2021

*time zone of CEST

13:00 - 14:00 **Weak Field Dynamics II**
Session Chair: Danielle Dowek

- **13:00 - 13:30** **Photoinduced Dynamics of Biochromophores Studied in an Ion-Storage Ring**
  Elisabeth Gruber
  Progress Report | pg 35
- **13:30 - 14:00** **Multi-Coincidence Studies of Molecules Using Synchrotrons and XFELs**
  Florian Trinter
  Progress Report | pg 56

13:00 - 14:00 **Ion Molecule**
Session Chair: Károly Tőkési

- **13:00 - 13:30** **Fragmentation Dynamics of Molecular Ions in Cluster Environment**
  Xiao'Qing Hu
  Progress Report | pg 38
- **13:30 - 14:00** **Classical Trajectory Time-Dependent Mean-Field Calculations for Ion-Molecule Collisions**
  Alba Jorge
  Progress Report | pg 39

13:00 - 14:00 **Electron Molecule**
Session Chair: Peter van der Burgt

- **13:00 - 13:30** **Vibrational Autodetachment Following Excitation of Electronic Resonances**
  Miloš Rankovíc
  Progress Report | pg 49
- **13:30 - 13:45** **Low Energy Electron Interactions with 5-Aminoimidazole-4-Carboxamide**
  Mónica Mendes
  G20 | pg 78
- **13:45 - 14:00** **Excitation and ionisation cross-sections of condensed-phase biomaterials by electrons down to very low energy**
  Pablo de Vera
  H09 | pg 66

14:00 - 14:10 **BREAK**

DAY 3: THURSDAY, JULY 22, 2021 (CONTINUED)

*time zone of CEST

14:10 - 16:10 **Multiphoton Dynamics**
Session Chair: Thomas Pfeifer

14:10 - 14:40	**Ultrafast Electronic and Nuclear Dynamics in the Nanoparticle Induced by the Hard-X-ray Laser** **Yoshiaki Kumagai** Progress Report | pg 42
14:40 - 15:10	**Time-resolved imaging of light-induced dynamics in isolated nanoparticles** **Daniela Rupp** Progress Report | pg 50
15:10 - 15:25	**A Molecular Road Movie: Capturing Roaming Molecular Fragments in Real Time** **Heide Ibrahim** M13 | pg 72
15:25 - 15:40	**Time Resolved Atomic Ionization Processes and Tests of the Fundamental Threshold Laws** **Anatoli Kheifets** J02 | pg 75
15:40 - 15:55	**The Imaginary Part of the High-Order Harmonic Cutoff** **Emilio Pisanty** J29 | pg 81
15:55 - 16:10	**Proper Time Delays from Streaking Measurements** **Ulf Saalmann** J40 | pg 84

14:10 - 16:10 **Storage Ring/Traps & Beams**
Session Chair: Marek Pajek

14:10 - 14:40	**Higher-Order Recombination Processes in HCI's** **Weronika Biela-Nowaczyk** Progress Report | pg 29
14:40 - 15:10	**First Dielectronic-Recombination Experiments at CRYRING@ESR** **Esther Menz** Progress Report | pg 46
15:10 - 15:25	**Dissociative Recombination of OH^+ at the Cryogenic Storage Ring** **Ábel Kálosi** F35 | pg 74
15:25 - 15:40	**Laser Spectroscopy of Forbidden Transitions Between Metastable Excited States of I^{7+} in an Electron Beam Ion Trap** **Naoki Kimura** C12 | pg 76
15:40 - 15:55	**Structured Ion Beams Produced by Radiative Recombination of Twisted Electrons** **Anna Maiorova** C15 | pg 77
15:55 - 16:10	**VMI Photoelectron Spectroscopy Probing the Rotational Cooling Dynamics of Hot Trapped OH^- Ions** **Abhishek Shahi** K36 | pg 86

DAY 3: THURSDAY, JULY 22, 2021 (CONTINUED)

*time zone of CEST

14:10 - 16:10 **Electron Scattering**
Session Chair: Sylwia Ptasinska

- **14:10 - 14:40** **Scattering of Attosecond Electron Pulse Trains by Atomic Targets**
  Yuya Morimoto
  Progress Report | pg 47
- **14:40 - 15:10** **Direct Observation of Atomic Motion in Molecules Using Atomic Momentum Spectroscopy**
  Yuichi Tachibana
  Progress Report | pg 55
- **15:10 - 15:40** **Rovibrationally-Resolved Electron Scattering on H_2: Molecular Convergent Close-Coupling Calculations**
  Liam Scarlett
  Progress Report – G34 | pg 53
- **15:40 - 15:55** **Imaging the Structural Dynamics in the Photo-Induced Proton Transfer Reaction of O-Nitrophenol by Ultrafast Electron Diffraction**
  Joao Pedro Figueira-Nunes
  H03 | pg 69
- **15:55 - 16:10** **The Electron-Thiophene Scattering Dynamics Under the Influence of Multichannel Coupling Effects**
  Giseli Moreira
  G21 | pg 79

16:10 - 17:10 **Posters Viewing in GatherTown**

17:10 - 18:10 **Cold Physics and Chemistry: Collisions, Ionization and Reactions Inside Helium Nanodroplets**
Paul Scheier
Session Chair: Friedrich Aumayr
Tutorial Lecture | pg 25

18:10 - 18:40 **Speakers Q&A in GatherTown**

DAY 4: FRIDAY, JULY 23, 2021

*time zone of CEST

13:00 - 20:00 **Conference Hang Out**

17:00 - 18:00 **ICPEAC Diversity Forum**

ABSTRACTS

Instructions: Click on a Abstract Category below to transport to the first abstract in that section. To navigate back to this Abstract Categories Page, click on the second last circle in the top right corner.

Abstracts are displayed in Alpha-numerical order by their Poster Number.

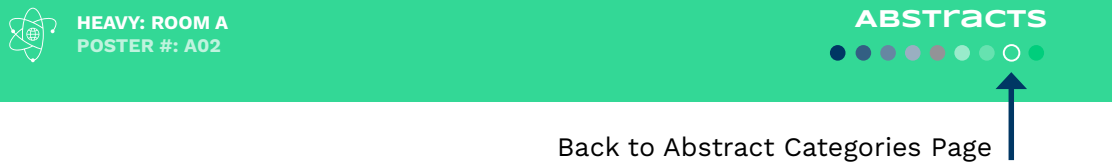

ABSTRACT CATEGORIES

All abstracts were reviewed by at least two members of the ICPEAC Committees prior to inclusion in this Book of Abstract and formal acceptance for presentation at the conference.

The physics of radio-frequency traps in a collision physics perspective

C Champenois[1] *

[1]Aix-Marseille Univ, CNRS, PIIM, Marseille, France

Synopsis This tutorial introduces the physics of radio-frequency traps and how to use basic laser-cooling methods in this context. It justifies the assets of using them to control small charged particle samples and in the same time, identifies its main limitations. Few applications are chosen to illustrate how Coulomb collisions can be studied and turned into a tool to reach capture and detection of charged projectile. These exemples involve different sample sizes and projectile-to-target mass-ratios to highlight different kind of experimental configuration.

The radio-frequency (RF) traps were invented in the mi-50's to confine charged particles, atoms or molecules, over time scales reaching few minutes. With the advent of laser cooling technics, trapping times are not limited anymore and the size and temperature of the trapped sample can be tuned over several orders of magnitude. With all these tight control knobs in hand, RF trap applications now cover optical frequency metrology, quantum information processing, measurement of fundamental constants, as well as cold chemistry.

Depending on the purpose of the experiment, and on the number of trapped particles, Coulomb interactions can be turned as a powerful tool to correlate particle motion or considered as a source of drawback to avoid. More generally, inter-particles interactions or collisions can be considered as binary or collective processes, and if the laser-cooled cloud is larger than few hundreds of ions, its collective behaviour can be understood as if it were a non-neutral plasma [1].

This tutorial will focus on several experimental strategies that take advantage of the interactions between particles. The first one, called sympathetic cooling, works in the very low energy regime and allow to cool to the mK range the motion of atoms or molecules that can not be laser-cooled because of an out of reach transition wavelength or because of the lack of cycling transitions. It relies on their thermalisation with a co-trapped laser-cooled species, through Coulomb interactions. This method is used to cool molecules as large as Alexa Fluor 450 to the mK range [2]. When the to-cool species is produced out of the RF-trap, it implies its capture by the target ion cloud, most of the time after several back-and-forth transit to increase the energy loss of the projectile. This energy loss mechanism is at the core of the capture of $^{40}Ar^{13+}$ highly charged ions by a cloud of $^{9}Be^{+}$ [3]. It is also the scenario for the future GBAR experiment [4] which aims at cooling an anti-hydrogen ion through its Coulomb interaction with co-trapped $^{9}Be^{+}$ ions before it is neutralized to fall under gravity. The energy exchange between a laser-cooled ion cloud and a charged projectile has a signature that can be looked for in the laser induced fluorescence rate of the cloud. To that purpose, RF heating-a side effect of RF trapping- becomes an ally as it can amplify the temperature increase of the cloud and makes it detectable by photon counting methods. This could allow for the detection of single very heavy molecules (larger than 1 MDa) for which few detection device are efficient [5].

References

[1] Champenois C 2009 *J. Phys. B* **42** 154002
[2] Ostendorf A *et al* 2006 *Phys. Rev. Lett.* **97** 243005
[3] Schmöger L *et al* 2015 *Science* **347** 1233
[4] Walz J *et al* 2004 *General Relativity and Gravitation* **36** 561
[5] Poindron A *et al* 2021 *J. Chem. Phys.* **154** 184203

*E-mail: caroline.champenois@univ-amu.fr

Attosecond molecular science: a theoretical point of view

F. Martín [1,2,3]*

[1]Departamento de Química, Módulo 13, Universidad Autónoma de Madrid, 28049 Madrid, Spain
[2]Instituto Madrileño de Estudios Avanzados en Nanociencia (IMDEA-Nanociencia), Cantoblanco, 28049 Madrid, Spain
[3]Condensed Matter Physics Center (IFIMAC), Universidad Autónoma de Madrid, 28049 Madrid, Spain

Synopsis Recent theoretical efforts aimed at providing a realistic description of the observables actually recorded in current attosecond experiments performed in molecules will be reviewed

In most attosecond experiments performed on molecules with high-harmonic generation sources or ultrashort X-ray free-electron lasers, a single broadband pulse or a train of attosecond pulses suddenly ionize the system and create an electronic wave packet that subsequently evolves under the influence of the nuclear motion until it is interrogated by a second pulse at a given time delay. To access the early electron dynamics induced by the first pulse, the experiments usually record photoelectron and/or fragmentation yields as a function of the temporal delay between the two pulses with attosecond resolution. However, in spite of the successful observation of sub- and few-fs dynamics in the recorded yields [1, 2, 3, 4], it is not yet clear how the early electron dynamics leaves its signature in molecular fragments that may be created long after those initial steps (usually after going through a series of non adiabatic processes) or why one should expect a reminiscence of such electron dynamics at all. To answer these questions, theory must describe i) the ionization by the first pulse, ii) the coupled electron and nuclear dynamics that follows, iii) the ionization by the second pulse of a molecular cation in a coherent superposition of states, and iv) the coupled electron and nuclear dynamics that follows the previous step and eventually leads to fragmentation of the molecule. Every step is in itself is a theoretical and computational challenge for molecules containing more than two nuclei. In this talk I will review recent theoretical efforts to account for these four steps and discuss the optimum conditions to visualize electron dynamics in molecules [5].

References

[1] Calegari F *et al* 2014 *Science* **346** 336
[2] Nisoli M, Decleva P, Callegari F, Palacios A, and Martín F 2017 *Chem. Rev.* **117** 10760
[3] Lara-Astiaso M *et al* 2018 *J. Phys. Chem. Lett.* **9** 4570
[4] Delgado J *et al* 2020 *Faraday Discussions* DOI: 10.1039/D0FD00121J
[5] Palacios A and Martín F 2020 *WIREs Comput. Mol. Sci.* e1430

*E-mail: fernando.martin@uam.es

Cold physics and chemistry: collisions, ionization and reactions inside helium nanodroplets

P Scheier[1] *, F Zappa[1], F Laimer[1], L Tiefenthaler[1], E Gruber[1], P Martini[1,2], M Gatchell[1,2], S Albertini[1], A Schiller[1], M Meyer[1], S Bergmeister[1], S Kollotzek[1], L Lundberg[1], O Echt[1,3], DK Böhme[4], S Krasnokutskiy[5]

[1]Institut für Ionenphysik und Angewandte Physik, Universität Innsbruck, Innsbruck, 6020, Austria
[2]Department of Physics, Stockholm University, Stockholm, 106 91, Sweden
[3]Department of Physics, University of New Hampshire, Durham NH 03824, USA
[4]Department of Chemistry, York University, Toronto, Ontario M3J 1P3, Canada,
[5]Laboratory Astrophysics Group of the MPI for Astronomy at the University of Jena, Jena, 07743, Germany

Synopsis Helium nanodroplets provide an inert matrix, free of walls with outstanding properties to grow complexes and clusters at sub-Kelvin temperatures [1]. The conditions inside helium nanodroplets are perfect to simulate cold and dense regions of the interstellar medium and to perform spectroscopy of molecules and ions solvated by helium. Barrierless reactions triggered by radicals or ions have been observed and studied by optical spectroscopy and mass spectrometry [2]. The present contribution summarizes developments of experimental techniques and methods and recent results they enabled.

Almost every existing method of cluster and nanoparticle formation leads to a wide distribution of sizes. Thus, the limiting factor in all cluster studies is creating a sufficiently high concentration of the desired species and separating them from the overall distribution [3]. Recently, we discovered that large helium droplets HNDs can become highly-charged [4]. The charges self-organize as two-dimensional Wigner crystals at the surface of the droplets and act as seeds for the growth of dopant clusters [5].

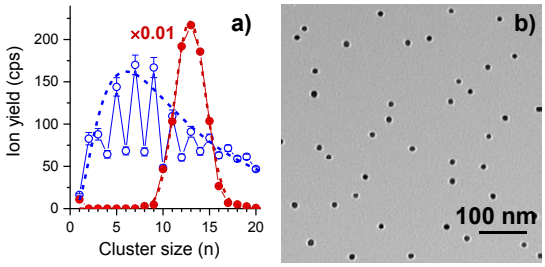

Figure 1 a) gold cluster size distributions obtained via pickup into neutral helium droplets (blue open symbols) and multiply charged helium droplets (red solid symbols). The dashed lines represent a log-normal fit (blue) and Poisson fit (red) to the data. b) TEM image of gold nanoparticles deposited onto amorphous carbon.

Cluster ions of a specific size and composition can be formed by this technique with unprecedented efficiency (Fig. 1a). Soft-landing of metal nanoparticles formed in highly-charged HNDs can be achieved by deposition onto a target surface. Fig. 1b) shows a transmission electron microscope (TEM) image of amorphous carbon surfaces decorated with gold nanoparticles formed upon pickup of gold atoms into multiply charged HNDs. Due to the fact that several hundred nanoparticles are formed simultaneously in one helium droplet, the deposition time was only two minutes. Furthermore, the size distribution is exceptionally narrow. Several applications utilizing pickup into multiply charged HNDs for cluster physics, ion spectroscopy and nanotechnology will be presented.

This work was supported by the Austrian Science Fund FWF (P31149, T1181, I4130 and W1259), the Deutsche Forschungsgemeinschaft DFG (KR 3995/4-1) and the European Union (K-Regio Project No EFRE 2016-4)

References

[1] Mauracher A *et al* 2018 *Phys. Rep.* **751** 1
[2] Albertini S *et al*[3] Tyo EC and Vajda S, 2015, *Nat. Nanotechnol.* **10** 577
[4] Laimer F *et al* 2019 *Phys. Rev. Lett.* **123** 165301
[5] Tiefenthaler L *et al* 2020 *Rev. Sci. Instrum.* **91** 033315

* E-mail: paul.scheier@uibk.ac.at

High-energy physics at ultra-cold temperatures – Quantum simulating lattice gauge theories

P Hauke[1] *

[1]INO-CNR BEC Center & Department of Phyics, University of Trento, Trento 38123, Italy

Synopsis Gauge theories are of fundamental importance for modern physics, yet extremely challenging to tackle with classical computers. In this overview talk, I will review recent progress towards solving gauge theories on quantum simulator devices based on ultracold atoms. I will highlight common challenges, ways to overcome them, and the current state of art of the field.

Gauge theories are at the heart of modern physics. They represent the corner stone of the Standard Model of Particle physics, emerge in exotic phases of matter, and can find application in topological quantum computation. Despite this importance, solving their out-of-equilibrium dynamics on classical computers is extremely challenging. This difficulty is currently stimulating a worldwide effort to implement them in dedicated quantum simulators.

In this talk, I will discuss recent progress towards quantum simulation of gauge theories using ultracold atoms. I will show approaches towards overcoming the main challenge, the realization of a dynamics that respects the local gauge symmetry (corresponding to Gauss' law in the example of quantum electrodynamics). In particular, I will present recent breakthrough experiments, one exploiting angular momentum conservation [1] and one based on engineering of suitable energy penalties [2]. The second of these experiments has realized a many-body gauge theory in a 71-site Hubbard model and has certified the fulfilment of Gauss's law for the first time. I will also illustrate some of the fascinating physics attainable in quantum simulators of gauge theories even for simple target models [3,4].

Finally, I will discuss the state of art and common issues, and thus aim at outlining a roadmap towards mature and practically relevant quantum simulation of gauge theories.

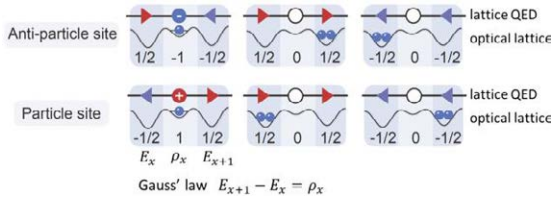

Figure 1. A model of lattice quantum electrodynamics (QED) consisting of electrons and positrons (bullets) and electric field (arrows) can be mapped to an optical superlattice. Only few occupation configurations are allowed by the descrete lattice version of Gauss' law. The challenge for quantum simulation is to realize the dynamics, e.g., of particle-anti-particle generation, while at all times remaining constrained to the subspace of allowed configurations. Figure adapted from [2].

References

[1] Mil, Zache, Hegde, Xia, Bhatt, Oberthaler, Hauke, Berges, Jendrzejewski 2020 *Science* **367** 1128-1130

[2] Yang, Sun, Ott, Wang, Zache, Halimeh, Yuan, Hauke, Pan 2020 *Nature* **587** 392-396

[3] Zache, Mueller, Schneider, Jendrzejewski, Berges, Hauke 2019 *Phys. Rev. Lett.* **122** 050403

[4] Zache, Hebenstreit, Jendrzejewski, Oberthaler, Berges, Hauke 2018 *Quantum Sci. Technol.* **3** 034010

* E-mail: philipp.hauke@unitn.it

Light pulses structured at the attosecond timescale

C Hernández-García[1] *

[1]Grupo de Investigación en Aplicaciones del Láser y Fotónica, Departamento de Física Aplicada, Universidad de Salamanca, Salamanca E-37008, Spain

Synopsis Coherent and structured EUV/soft x-ray sources at the attosecond scale are nowadays realizable through high harmonic generation (HHG). Thanks to the high coherence of HHG, angular momentum properties can be mapped into short wavelength regimes where circularly polarized attosecond pulses, structured in their temporal, spectral and spatial domains can be obtained. The use of such sources in ultrafast magnetism is particularly appealing to achieve a complete understanding of the electronic and spin interactions that govern sub-femtosecond magnetization dynamics.

The development of ultrafast laser sources with new properties is a key ingredient to advance our knowledge about the fundamental dynamics of electronic and spin processes in matter. In particular, coherent extreme-ultraviolet (EUV)/soft x-ray pulses structured in their temporal, spectral and angular momentum (polarization and topological charge) properties is nowadays possible thanks to high harmonic generation (HHG). Such sources are opening new opportunities to explore light-matter interaction at the attosecond and nanometer scales.

In this talk we review our recent work in the generation of structured laser pulses at the attosecond scale. To do so, the angular momentum of light has opened a rich variety of possibilities to tailor EUV/soft x-rays pulses at their generation through HHG. In HHG, an intense, infrared laser pulse is up-converted into EUV/soft x-ray radiation in a high nonlinear, non-perturbative process. Though the mapping of the infrared laser properties into the higher frequency domain is not trivial, we demonstrate how we can control the spectral, temporal and polarization properties of EUV/attosecond pulses through the angular momentum of the driving beam.

Remarkably, the HHG up-conversion mapping takes places at the sub-femtosecond scale, which allows to generate circularly polarized attosecond pulses [1-3], attosecond pulse trains with time-ordered polarization states [4], or low-divergence harmonic combs with controlled frequency line spacing extending into the soft x-rays [5]. Such high coherence of the HHG process has also allowed to provide laser beams with tailored, time-dependent orbital angular momentum, or self-torque [6] (Fig. 1).

* E-mail: carloshergar@usal.es

These achievements are enabling the practical implementation of a novel class of laser-driven coherent EUV/soft x-ray sources. Particularly promising is their application to advance the field of ultrafast magnetism. For example, we have recently predicted that intense, ultrafast magnetic fields, isolated from the electric field, can be obtained from azimuthally structured laser beams [7]. Such structured sources offer an appealing alternative to study sub-femtosecond magnetization dynamics, where a complete understanding of the electronic and spin interactions remains unexplored.

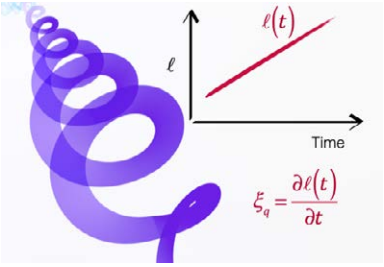

Figure 1. Representation scheme of an ultrafast pulse with self torque (dℓ/dt), carrying a subfemtosecond variation of its topological charge (ℓ) through the high-frequency EUV laser pulse [8].

References

[1] Huang P.-C. et al 2018 Nature Photonics **12**, 349-354
[2] Chang K.-Y. et al 2021 Optica, **8**, 484-492.
[3] Dorney K. et al 2019 Nat. Photon. **13**, 123-130
[4] Rego L et al 2020 Opt. Lett. **45**, 5636-5639
[5] Rego L et al 2019 Science **364**, eaaw9486.
[6] Rego L et al "Necklace-structured high harmonic generation for low-divergence, soft X-ray harmonic combs with tunable line spacing", submitted.
[7] Blanco M et al 2019 ACS Photonics **6**, 38-42.

Ultrafast, all-optical and highly enantio-sensitive imaging of molecular chirality

D Ayuso[1,2*], A Ordonez[2,3], P Decleva[4], M Ivanov[1,2,5] and O Smirnova[1,6]

[1]Department of Physics, Imperial College London, SW7 2BW, United Kingdom
[2]Max-Born-Institut, Berlin, 12489, Germany
[3]Institut de Ciencies Fotoniques, The Barcelona Institute of Science and Technology, Castelldefels, 08860, Spain
[4]Dipartimento di Scienze Chimiche e Farmaceutiche, Università degli Studi di Trieste, 34127, Italy
[5]Institute für Physik, Humboldt-Universität zu Berlin, Berlin, Germany
[6]Technische Universität Berlin, Berlin, Germany

Synopsis. Light allows us to image and even control the electronic clouds of atoms, molecules and solids. However, its applications to molecular chirality are limited by the weakness of magnetic interations, restricting our ability to tell apart opposite versions of a chiral molecule (enantiomers). Here, I will discuss how we can tailor the polarisation of light in *time* and *space* in order to overcome this fundamental limitation. Such optical shaping enables ultrafast and highly enantio-sensitive imaging of molecular chirality, and it opens new opportunitites for efficient control of chiral matter.

Chirality, or handedness, is a ubiquitous geometrical property of light and matter. Chiral molecules appear in pairs of left- and right-handed enantiomers, two non-superimposable "mirror twins". They behave identically, unless they interact with another chiral "object". Distinguishing them is vital, as, for instance, most biomolecules are chiral, and thus the interactions between them are enantio-sensitive.

Traditional chiro-optical methods rely on the electronic response of matter to both the electric and magnetic components of a circularly polarised wave, i.e. on the chiral molecule "feeling" the spatial helix of the light field. However, the pitch of this helix is too large compared to the size of the molecules, leading to weak enantio-sensitivity and making chiral discrimination difficult, especially on ultrafast time scales.

Here, I will present 3 ways of imaging molecular chirality using tailored light, with high enantio-sensitivity and on ultrafast time scales.

First, I will introduce *synthetic* chiral light [1], which is *locally* chiral: unlike circularly polarised light, its chirality does not rely on its spatial structure. Instead, the tip of the electric field vector draws a chiral, 3D Lissajous curve in time, at each point in space. Synthetic chiral light that is also *globally* chiral allows us to quench the nonlinear response of a selected enantiomer while maximising it in its mirror twin.

Second, I will show how to structure light's local handedness in space to realise an enantio-sensitive version of Young's double slit experiment. Such chirality-structured light creates chiral and achiral "slits" upon interaction with isotropic chiral media, which radiate at new optical frequencies from different positions in space. If the distribution of light's handedness breaks left-right symmetry—i.e. the light becomes *chirality polarised*—then the multi-centre interference leads to unidirectional bending of the emitted light, in opposite directions in media of opposite chirality. Shaping the spatial distribution of light's handedness enables control over the enantio-sensitive response, allowing us to bend light to the left, or to the right, depending on the molecular handedness.

Third, I will show how to exploit the transverse spin arising upon spatial confinement of light for efficient chiral recognition. When an intense and ultrashort laser pulse is tightly focused into a medium of randomly oriented chiral molecules, it generates elliptically polarised light, which has opposite polarisation in media of opposite handedness. Sub-cycle optical control of the incident light wave enables full control over the enantio-sensitive response.

The possibility of generating highly enantio-sensitive optical signals using tailored light, either at the level of total intensity of emission [1], or in the direction [2] or polarisation [3] of the emitted harmonic light, creates new opportunities for efficient imaging of molecular chirality and ultrafast chiral dynamics. It also opens new routes for highly enantio-sensitive control of chiral matter.

References

[1] Ayuso et al, *Nat. Photon.* **13**, 866 (2019)
[2] Ayuso et al, *Nat Comm* (accepted, 2021), arXiv:2004.05191
[3] Ayuso et al, arXiv:2011.07873

* E-mail: david.ayuso@imperial.ac.uk

Higher-order recombination processes in HCI's

W. Biela-Nowaczyk[1*], A. Warczak[1], P. Amaro[2], M. Lestinsky[3], D. La Mantia[4], E. Menz[3], S. Schippers[5], J. Tanis[4]

[1]Jagiellonian University, Institute of Physics, Poland
[2]Department of Physics, Universidade NOVA de Lisboa, Portugal
[3]GSI Helmholtzzentrum für Schwerionenforschung, Darmstadt, Germany
[4]Western Michigan University, Kalamazoo, MI 49008 U.S.A.
[5]I. Physikalisches Institut, Justus-Liebig-Universität Gießen, Germany

Synopsis Multielectron recombination processes, like dielectronic (DR) and trielectronic (TR) recombination, form an important topic in atomic physic as well as in astophyscis. This presentation will focus on x-ray results of these higher-order recombination processes in Ar ions collected by using the UJ-EBIT. In the near future it is planned to investigate DR and TR in He-like O ions at the CRYRING@ESR storage ring. This new approach and preliminary results are planned to be presented as well.

The electron-electron interaction is a crucial aspect of atomic reactions involving electron-ion collisions. An effective way to investigate electron-electron interaction is to study the higher-order recombination processes.

The most basic of these recombination processes is DR. DR is the time reversal to the Auger process and is investigated in many different highly-charged systems [1, 2]. The recombination is completed through radiative stabilization of the excited ion.

The research presented here was conducted at the UJ-EBIT (Jagiellonian University EBIT) [3]. Very good resolution of the x-ray detector enabled the K-LL DR resonances to be distinguished for He- up to N-like Ar ions. In the observed x-ray energy region, in addition to the K-LL DR, a trace of the intrashell TR has been seen [2]. These results encouraged the more detailed present studies of TR, specifically of the KK TR. Here, the resonant capture of a free electron to an ion-bound state transfers simultaneously two K-shell electrons to a higher atomic shell. This way, a doubly-excited K-shell state is produced and, in most cases, it decays via emission of two photons. The first transition with two vacancies in the K shell is responsible for emission of the K_α^h hypersatellite photon with an energy slightly higher than energy of the following K_α^s satellite transition. This TR process has been not reported yet to the best of our knowledge. This work presents a maximum-like behavior of the intensity ratio between K_α^h and K_α^s (Figure 1). The position of the observed maximum suggests a successful observation of the KK-LMM TR process in Ar ions.

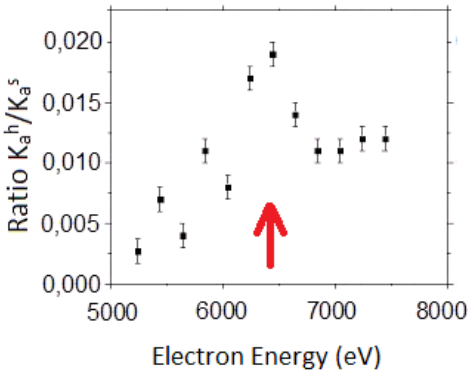

Figure 1. Ratio of Ar K_α^h/K_α^s scanned in the expected KK-LMM TR electron energy range. The arrow shows the calculated TR maximum.

Currently, complementary experiments are planned. It should be possible with application of the collision spectroscopy of highly charged ions merged in a cold electron beam of the CRYRING@ESR cooler [4]. So far, this experimental technique has been used successfully in electron-ion recombination experiments at several storage rings (TSR in Heidelberg, ESR in Darmstadt, CRYRING in Stockholm). Here, it is planned to apply this technique for identification of the TR process in O ions.

References

[1] T.M.Baumann. Z.Harman, J.Stark, *et al.* Phys. Rev. A **90**, 052704 (2014)
[2] C.Beilmann, P.H.Mokler, Z. Harman, *et al.* Phys. Scr. **T144,** 014014 (2011)
[3] G.Zschornack, M.Schmidt and A.Thorn, CERN Yellow Report **007**, 165-201 (2013)
[4] Fogle M, Badnell NR, Glans P *et al.* Astron. & Astrophys. 442, 757 (2005)

* E-mail: weronika.biela@doctoral.uj.edu.pl

Two-photon single ionization of helium: from below-threshold to doubly-excited states

D I R Boll[1,3]*, L Martini[1] O A Fojón[1,2] and A Palacios[3,4]†

[1]Laboratorio de Colisiones Atómicas, Instituto de Física Rosario (CONICET-UNR), Rosario, 2000, Argentina
[2]Escuela de Ciencias Exactas y Naturales, FCEIA, UNR, Rosario, 2000, Argentina
[3]Depto. de Química, Módulo 13, Facultad de Ciencias, UAM, Madrid, 28049, España
[4]Institute of Advance Research in Chemical Science (IAdChem), UAM, Madrid, 28049, España

Synopsis We analyze the two-photon single ionization of helium by ultrashort pulses with photon energies ranging from threshold to 67 eV. We study how the angular correlation and the pulse duration may influence the results obtained on different energy regions. Then, based on some of the previous results, we focus on the two-color polarization control scheme. For that setup of the fields, we show for the first time that a larger degree of control that can be attained when the short wavelength photon energy is below the ionization threshold.

The interest in multiphoton processes has undergone a resurgence in the current century with the advent of femtosecond and subfemtosecond pulses in the UV/EUV and x-ray frequency domains. Nowadays, Free Electron Laser (FEL) facilities are able to provide the necessary intensities for the observation of multiphoton transitions, not only between bound-bound, but also between bound and continuum states. Additionally, the high spectral resolution, together with a fine-tunability in frequency and light polarization state, achieved by FELs enable the possibility of exploring new control schemes combining two-color fields [1, 2, 3].

Based on the current experimental status, we firstly discuss the angularly resolved two-photon single ionization yields of helium resulting after the interaction with an ultrashort EUV pulse. These angular distributions, obtained by numerically solving the full dimension time-dependent Schrödinger equation, reveal the underlying dominant mechanism, which depends on the effective photon energy absorbed and the pulse parameters. Exploring the contributions of radial and angular electron correlation terms, we find that a single-active electron picture is a qualitatively valid approach for the lowest photon energies, even in the above-threshold ionization region. Nonetheless, angular correlation plays a detectable role in the low-energy region and a major role at higher energies when autoionizing states are populated. In particular, when doubly-excited states are populated, we show that a fine tuning of the central EUV frequency offer the means to control the relative contribution of the dipole-allowed photoionization channels, ultimately shaping the angular distributions [4].

A conceptually different approach to steer the relative contributions of photoionization channels with different angular momenta is that of polarization control. In this two-color scheme, the single-photon ionization (pump) of atomic and molecular targets by EUV light pulses gives rise to a photoelectron distribution in the continuum. The additional exchange of photons with the IR light source (probe) generates a sequence of secondary photoelectron peaks called sidebands. Previous experimental results captured a modulation in the sideband signal when the relative polarization angle between the interacting laser fields is modified [5]. We use here a perturbation theory approach to show that it is indeed possible to achieve a larger degree of control over the sideband signal when the photon energy of the pump stage is tuned below the ionization threshold. This largely unexplored energy region offers unique possibilities to achieve polarization control of the reaction [6].

References

[1] Meyer M *et al* 2010 *J. Phys. B* **43** 194006
[2] Prince K C *et al* 2016 *Nat. Photon.* **10** 176
[3] Giannessi L *et al* 2018 *Sci. Rep.* **8** 7774
[4] Boll D I R *et al* 2019 *Phys. Rev. A* **99** 023416
[5] Meyer M *et al* 2008 *Phys. Rev. Lett.* **101** 193002
[6] Boll D I R *et al* 2020 *Phys. Rev. A* **101** 013428

*E-mail: boll@ifir-conicet.gov.ar
†E-mail: alicia.palacios@uam.es

Solvent effects in low energy electron scattering

L M Cornetta[1]* and M T do N Varella[2]†

[1]Instituto de Física Gleb Wtaghin, Universidade Estadual de Campinas, São Paulo, 13083-859, Brazil
[2]Instituto de Física, Universidade de São Paulo, São Paulo, 05508-090, Brazil

Synopsis We present recent advances on the electron attachment characterization in solvated molecules. The studies are based on scattering calculations on clusters, which in turn have been obtained by classical simulations. The discussion focus on thermal distributions of solute-solvent features that can significantly affect vertical attachment energies.

Solvent effects on physical and chemical properties are essential when dealing with molecular processes of biological interests. We introduce a methodology for incorporating the environment influence on the low-energy electron scattering using microsolvation modeling and cluster selection. We have combined classical Monte Carlo simulations and the Schwinger Multichannel method[1] for both approaching the aggregates collection and performing quantum scattering calculations, respectively. Several features of the solute-solvent interaction affect the electron attachment process[2], and we mainly focus on thermal distributions of these contributions.

It will be discussed the cases of native and modified versions of uracil nucleobase[3]. In those cases, the water molecules typically stabilize the anion states, and the lower lying resonances can become bound states in a large fraction of the clusters. We corroborate that the distribution of H-bonds plays a major role in such effect[4], and we also discuss how the strength, the number and the characters of these bonds can affect energies and electronic structures.

The results point out a quasi-continuum range of attachment energies for the clusters, from 0 eV to $\lesssim$ 2.5 eV, although modulated by the probability densities. The broad range of attachment energies essentially arises from the statistics of the rotation-translation configuration space in the liquid, not necessarily from shorter autoionization lifetimes (broader autoionization widths). We did not take vibrational distributions into account, since only the fixed-nuclei resonances, whose peaks define the vertical attachment energies, were calculated. In general terms, the solvent-induced stabilization is accompanied by longer autoionization lifetimes (narrower autoionization widths).

References

[1] da Costa, R F *et al* 2015 *Eur. Phys. J. D* **69** 159
[2] Gorfinkiel, J D *et al* 2017 *J. Phys. B: Atomic, Molecular and Optical Physics* **50** 18
[3] Cornetta, L M *et al* 2020 *J. Chem. Phys.* **8**, 152
[4] de Oliveira, E M *et al* 2014 *J. Chem. Phys.* **141** 051105

*E-mail: lucascor@unicamp.br
†E-mail: mvarella@if.usp.br

Experiments with laser aligned molecules at FERMI

M Di Fraia[1]*,

[1] Elettra - Sincrotrone Trieste S.C.p.A., Trieste, 34149, Italy

Synopsis In this progress report recent experimental results will be presented on aligned molecules probed with FEL radiation at the Low Density Matter beamline of the FERMI Free Electron Laser.

Steering quantum mechanical processes occurring in atomic and molecular targets has been achieved in the 80's [1]. This technique has recently received a strong boost from the advances made in laser technologies and thanks to a parallel development of coherent light sources.
In particular when the angular distribution of electrons (or ions) can be determined, additional information about photoionization and photoemission processes can be gained and controlled thanks to coherent control techniques [2].
Molecular Frame Photoelectron Angular Distributions (MFPADs) measurements allow a better understanding of ultrafast photochemical processes and extraction of detailed structural information.
Laser induced molecular alignment is a well established technique for fixing the molecular axis with respect to the laboratory frame [3]. Such a technique has become a crucial tool in molecular dynamics studies [4, 5, 6, 7].
The Low Density Matter (LDM) endstation [8] of the seeded FEL FERMI is devoted to atomic and molecular dynamics experiments and recent results have been obtained in the field of coherent control of atomic targets by means of PAD measurements [2, 9, 10].
Non-adiabatic alignment of molecules has been investigated at LDM and the very first results on aligned OCS molecules will be presented [11].
The enhancement of the degree of alignment by means of double alignment pulses has also been successfully tested on CO_2 molecules. These two results have demonstrated that laser induced molecular alignment is a consolidated technique at the beamline, and it is now available for LDM users.
A recent experimental user's campaign has been performed on aligned acetylene molecules and preliminary results will be presented.
Moreover, using the unique properties of FERMI, very preliminary results have been obtained on aligned N_2 molecules probed by two-color phase-locked FEL pulses.
Recent innovative operational schemes of FERMI will also be presented [12], which enable to open interesting scenarios and possible experiments on aligned molecular targets with few-fs FEL pulses.

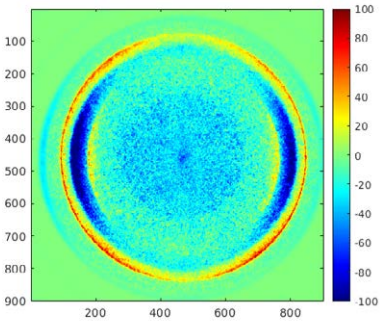

Figure 1. Raw Velocity Map Image. Difference between N_2 aligned and N_2 anti-aligned molecules probed with two-color phase-locked FERMI FEL pulses.

The results that will be presented originate from the joint effort of many international research groups, whose work is gratefully acknowledged.

References

[1] Brumer P *et al* 1986 *Chem. Phys. Lett.* **126** 541
[2] Prince K C *et al* 2016 *Nature Photonics* **10** 176
[3] Stapelfeldt H *et al* 2003 *Rev. Mod. Physics* **76** 543
[4] Bisgaard H *et al* 2009 *Science* **323** 1464
[5] Holmegaard L *et al* 2009 *Nature Physics* **10** 6 4428
[6] Vozzi C *et al* 2011 *Nature Physics* **7** 822
[7] Karamatskos E *et al* 2019 *Nat. Comm.* **10** 3364
[8] LDM beamline at *FERMI* 2021 **Elettra** website
[9] Di Fraia M *et al* 2019 *Phys. Rev. Lett.* **123** 213904
[10] You D *et al* 2020 *Phys. Rev. X* **10** 031070
[11] Di Fraia M *et al* 2017 *Ph. Ch. Ch. Phys.* **19** 19733
[12] Najmeh M S *et al* 2021 *Nature Photonics* **doi**

*E-mail: michele.difraia@elettra.eu

Collisional radiative modeling of plasmas involving dielectronic resonances

Dipti

National Institute of Standards and Technology, Gaithersburg, MD 20899, USA

Synopsis An overview of the collisional-radiative modeling involving dielectronic resonances along with all other important physical processes is presented. Simulations are performed using the non-Maxwellian collisional -radiative code NOMAD utilizing the atomic data produced with a fully relativistic structure code FAC. Comparisons with the benchmark data produced at the electron beam ion trap facility of the National Institute of Standards and Technology are also given.

The importance of dielectronic recombination (DR) for the correct description of ionization balance and other physical parameters such as radiation power loss has been frequently demonstrated in high-Z plasmas such as those in tokamaks, laser-produced plasmas, and astrophysics. Additionally, DR also contributes to the emission of satellite lines which are often used for diagnostics of various plasma parameters, e.g. electron temperature and density. The interpretation of the observed data in highly non-equilibrium conditions is an extremely challenging task which requires comprehensive and verified collisional-radiative (CR) models that account for the important atomic processes that occur in such plasmas.

An electron beam ion trap (EBIT) is a widely used device to produce benchmark data for studying DR and producing atomic data as well as tests of CR models due to the well-controlled and relatively simple plasma environment (e.g. no self-absorption, low densities). Additionally, the emission produced in an EBIT originates from ions excited by a unidirectional electron beam, rather than an isotropic electron distribution. Therefore, the emitted radiation can be anisotropic and linearly polarized, and the measurement with polarization-sensitive spectrometers allows study of the magnetic sublevel population kinetics.

I shall present the recent investigations of inner-shell dielectronic resonances of highly-charged ions measured at the EBIT facility of National Institute of Standards and Technology [1-3]. Theoretical analysis is based upon the large scale CR modeling using the NOMAD code [4], including atomic kinetics at magnetic sublevels which allowed the unambiguous identification of numerous DR associated with excitations of the inner-shell in the measured spectra as well as quantifying the effect of polarization of photons. The details of the theoretical methods and the comparison with the experimental results will be presented and discussed.

* E-mail: fnu.dipti@nist.gov

References

[1] Dipti *et al* 2020 *Phys. Rev. A* **101** 032503

[2] Gall *et al* 2020 *J. Phys. B* **53** 145004

[3] Dipti *et al* 2020 *J. Phys. B* **53** 115701

[4] Ralchenko Yu and Maron Y 2001 *J. Quant. Spec. and Rad. Trans.* **71** 609

Quantum-state-controlled chemi-ionization reactions

T Sixt[1], J Guan[1], J Grzesiak[1], T Muthu-Arachchige[1], A Tsoukala[1], S Hofsäss[1], V Behrendt[1], L Bienkowski[1], M Debatin[1], F Stienkemeier[1] and K Dulitz[1]*

[1]Institute of Physics, University of Freiburg, Hermann-Herder-Str. 3, 79104 Freiburg, Germany

Synopsis In a chemi-ionization reaction, an atom or molecule is ionized by another species in a long-lived, electronically excited (metastable) state. Our work is aimed at understanding the mechanistic details of such collision processes and at actively and passively controlling their outcome.

Besides the conventional means of chemical reaction control, e.g., through the change of temperature and pressure, the exploitation of quantum effects offers many further possibilities for influencing the outcome of chemical events. We develop laser- and magnetic-field-based techniques to precisely control the quantum states of two reaction partners, and thus, the reaction process itself. My group is specialized in the study of so-called chemi-ionization processes in the gas phase [1], in which an atom or molecule is ionized by another species in a long-lived, electronically excited (metastable) state. In order to control such processes, we prepare the atoms and molecules in well-defined quantum states prior to the reaction [2, 3].

Our experimental results for reactive metastable He-Li collisions show that chemi-ionization is efficiently suppressed owing to the conservation of both the total electron spin and Λ, i.e., the projection of the total molecular orbital angular momentum along the internuclear axis, even at room temperature [3]. Recently, we have been able to study reactions, in which both metastable He and Li are prepared in selected magnetic sublevels. Our experimental results imply that the measured reaction rates critically depend on the relative orientation of the reactants' electron spins.

Besides that, we use chemi-ionization as a very sensitive probe of NO molecules in the metastable $a^4\Pi_i$ state [4]. Our approach allows us to probe NO molecule densities as low as ≈ 600 molecules/cm^3 in a supersonic beam [4].

If time permits, I will also present our experimental approach towards the coherent control of chemi-ionization reactions between metastable He atoms in the 2^3S_1 and 2^1S_0 states.

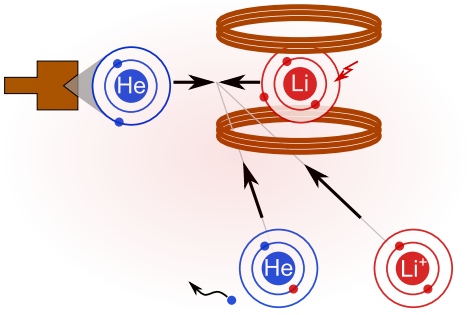

Figure 1. Graphical illustration of a chemi-ionization reaction between a metastable He atom and a Li atom.

References

[1] Grzesiak J *et al* 2019 *J. Chem. Phys.* **150** 034201.
[2] Guan J *et al* 2019 *Phys. Rev. Appl.* **11** 054037.
[3] Dulitz K *et al* 2020 *Phys. Rev. A* **102** 022818.
[4] Guan J *et al* 2020 *J. Phys. B: At. Mol. Opt. Phys.* **53** 245201.

*E-mail: katrin.dulitz@physik.uni-freiburg.de

Photoinduced dynamics of biochromophores studied in an ion-storage ring

E. Gruber[1] * and L. H. Andersen[1†]

[1]Department of Physics and Astronomy, Aarhus University, Aarhus, 8000, Denmark

Synopsis Light-driven processes play a crucial role in nature and in many man-made devices. To study the photophysics of key-molecules of these processes, gas-phase action-spectroscopy has been established as the first-choice method. Several methods have been developed, among them, the electrostatic ion storage ring technique. The combination of this technique with a fs-laser system enables to study ultrafast photo-initiated dynamics of molecular ions. In this contribution, the working principle as well as recent results on photoinduced dynamics of biomolecules by using this method are presented.

Molecular chromophores, the photo active part of photoactive proteins, are of great interest because of their significant role for functioning of living organisms and various applications, but also to study elementary processes, such as light-driven energy transfer, charge separation and photo-initiated isomerization. These processes proceed typically on a timescale of several femto-to-picoseconds. Hence, ultrafast optical techniques are required in combination with detection schemes to register the status of the molecules in real time.

The combination of a fs-laser system with the electrostatic ion-storage ring SAPHIRA [1] has been realized at Aarhus University, enabling fs-pump-probe spectroscopy of stored molecular ions. In short, the setup combines the pump-probe time delay with the action-response time registered in the ring. The setup opens a new approach to study ultrafast photo-initiated dynamics of positive as well as negative molecular ions in the gas phase and is highly advantageous for mapping out the excited-state decay as well as the ground-state recovery time.

By using this setup, the excited-state dynamics of protonated Schiff–base retinal [2] and of the chromophore in green fluorescent protein [3] were studied. The excited-state lifetime has shown a strong dependence on the temperature of the molecules, revealing the role of the energy barriers in the electronically excited states. Recently, we managed to perform pump-probe measurements of charge-tagged and ligand-bounded chlorophyll*a* molecules, which will be presented and discussed.

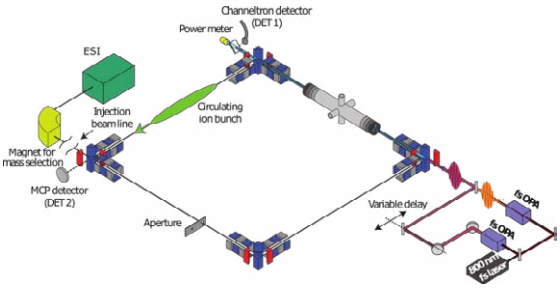

Figure 1. Schematic of the SAPHIRA setup at Aarhus University, which combines an electrostatic ion storage ring with a fs-laser system and enables to study photoinduced dynamics of molecular ions on a femto-to-picosecond timescale.

This work was supported by a research grant (17512) from VILLUM FONDEN.

References

[1] Pedersen H B *et al* 2015 *Rev. Sci. Instrum.* **86** 063107
[2] Kiefer H V *et al* 2019 *Nat. Commun.* **10** 1210
[3] Svendsen A *et al* 2017 *J. Am. Chem. Soc.* **139** 8766

* E-mail: E.Gruber@uibk.ac.at
† E-mail: lha@phys.au.dk

Mutual neutralization of H^- and metal ions: Theory, experiment and astrophysical applications

J Grumer[1]*, G Eklund[2], A M Amarsi[1], P S Barklem[1], S Rosén[2], M C Ji[2], A Simonsson[2], H Cederquist[2], H Zettergren[2], and H T Schmidt[2]

[1]Theoretical Astrophysics, Department of Physics and Astronomy, Uppsala University, Box 516, S 75120, Uppsala, Sweden

[2]Department of Physics, Stockholm University, Stockholm 10691, Sweden

Synopsis Mutual neutralization (MN) between atomic ions are important processes to consider in our understanding of astrophysical objects. The determination of MN processes has seen rapid experimental development over the past decade with the emergence of merged-beams and imaging detector techniques. This has allowed for final-state resolved measurements at meV collision energies also of systems with relatively large mass ratios, thus reaching temperatures and elements of relevance to astrophysical objects such as stellar atmospheres. In this contribution, I will review the current status and future hopes for measurements, calculations, and astrophysical applications of mutual neutralization at low energies.

Collision processes involving atoms and atomic ions play important roles in our understanding of astrophysical objects, their spectra, and thus also in the determination of their physical properties. In particular, accounting for mutual neutralization (MN) processes with hydrogen anions, e.g. $Li^+ + H^- \rightarrow Li + H$, including also possibly excited states, in stellar models can have drastic effects on the measured abundances (see e.g. Refs. [1, 2]). MN processes are also important to our understanding of plasmas such the earth's ionosphere and the atmospheres of other planets and their satellites, as well as in the diagnostics of fusion plasma environments and other high-energy physics experiments involving negative ions.

Even though MN reactions have a generally important role in many astrophysical and laboratory applications, experiments on this type of inelastic heavy collisions processes are few and were until recently limited to total cross-section measurements. However, new developments in merged-beams and imaging detector techniques have allowed for the detection of MN reaction products in coincidence, which has made determinations of kinetic energy releases, and thus final state resolved MN cross-sections in the meV energy range relevant for stellar atmosphere temperatures, possible. Over the past few years measurements of MN using such detection schemes have been carried out for number of systems, including single-pass experiments of O^+/O^- and N^+/O^- [3], Li^+/D^- [4], and with stored ion beams in DESIREE at Stockholm University of Li^+/D^- [5], Na^+/D^-[6], Mg^+/D^- and O^+/D^- (unpublished) reactions.

The present theoretical calculations for charge transfer of e.g. H^- with Li^+, Na^+, Mg^+ and O^+ are expected to be accurate to roughly a factor of two for the strongest rates, but it is important to test the results through experiments - with the new generation of experiments we can for the first time carry out experimental benchmarks at low energies of systems, including those with relatively large mass differences.

In this contribution I will briefly outline the experimental techniques used in low-energy MN measurements, review the obtained results so far, compare the results with old and new theoretical calculations, and discuss the impact in astrophysical spectral modeling and abundance determinations as well as challenges ahead.

References

[1] Barklem (2016) *A&A Rev.* **24**, 9
[2] Barklem, *et al.* (2021) *ApJ* **908**, 245
[3] de Ruette, *et al.* (2018) *PRL* **121**, 083401
[4] Launoy *et al.* (2019) *ApJ* 883, **85**
[5] Eklund *et al.* (2020) *PRA* **102**, 012823
[6] Eklund *et al.* (2021) *PRA* **103**, 032814

*E-mail: jon.grumer@physics.uu.se

R-Matrix calculations for ultrafast two-colour spectroscopy of noble gas atoms

K R Hamilton[1]*

[1]Department of Physics and Astronomy, Drake University, Des Moines, IA 50311, USA

Synopsis The R-Matrix with Time-dependence method (RMT), an *ab initio*, multielectron method, is applied to the study of photoionization delays in noble gas atoms using variants of the RABBITT technique.

R-matrix methods have achieved much success in the areas of time-dependent and time-independent computational atomic physics [1]. Originally developed to describe nuclear resonances, R-matrix theory has been extensively applied to the treatment of atomic and molecular physics problems since the late 1960s. One of the more recently developed R-matrix approaches, and the focus of this progress report, is the R-matrix with time-dependence (RMT) method [2].

RMT solves the time-dependent Schrödinger equation for general, multielectron atoms and ions interacting with laser light. The code has been significantly updated since its first release in 2011, with extensions to describe dynamics in arbitrarily polarized light fields [3], time-dependent processes in molecules [4], and treat semi-relativistic effects [5]. However, where RMT distinguishes itself from competing approaches is its ability to describe the behaviours of truly complex systems, such as irradiated noble gas atoms.

In this Progress Report I will describe recent progress on extracting photoionization delays in neon and argon using variants of the RABBITT (Reconstruction of Attosecond Beating By Interference of Two-photon Transitions) technique. Results from RMT calculations are compared against experimental data from the Harth group at the Max-Planck Institute for Nuclear Physics, Heidelberg, with the goal of extracting continuum-continuum delays in a multi-sideband RABBITT scheme with an argon target [6]. In collaboration with the Sansone group at the University of Freiburg and the Grum-Grzhimailo group at Moscow State University, experimental approaches, RMT, and Perturbation Theory calculations are used to determine attosecond delays near the ionization threshold of neon [7].

*E-mail: kathryn.hamilton@drake.edu

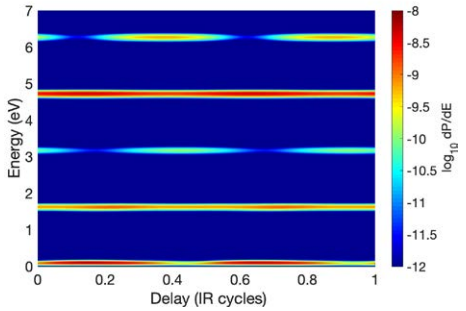

Figure 1. RABBITT spectrum for neon determined by RMT. The IR probe wavelength is 800 nm, and the time-delayed APT contains the 13^{th} to 25^{th} harmonics of the probe. The first sideband exhibits a prominent phase shift from the higher-order sidebands as a result of one pathway involving a bound-bound rather than bound-continuum XUV transition.

This work was supported by the United States National Science Foundation under PHY-1803844, PHY-2012078, OAC-1834740, and XSEDE PHY-090031, and the Frontera Pathways allocation PHY20028. The RMT code is part of the UK-AMOR suite [8], and benefited from computational support by CoSeC, the Computational Science Centre for Research Communities, through CCPQ.

References

[1] Burke P G 2011 *"R-matrix theory of atomic collisions: Application to atomic, molecular and optical processes"*, (Springer, Berlin, Heidelberg)
[2] Brown A C *et al* 2020 *Comp. Phys. Commun.* **250** 107062
[3] Clarke D D A *et al* 2018 *Phys. Rev. A* **98** 053442
[4] Benda J *et al* 2020 *Phys. Rev. A* **102** 052826
[5] Benda J *et al* 2019 *Phys. Rev. Lett.* **123** 163001
[6] Bharti D *et al* 2021 *Phys. Rev. A* **103** 022834
[7] Moioli M *et al* 2021 *52nd Annual Meeting of the APS Division of Atomic, Molecular and Optical Physics*, May 31st–June 4th, Virtual Meeting
[8] https://www.ukamor.com/

Fragmentation dynamics of molecular ions in cluster environment

X Hu[1] *, X Zhu[2,3], S Yan[2], Y Peng[4], D Guo[2], Y Gao[2], S Zhang[2], D Zhao[2], Y Wu[1], X Ma[2] and J Wang[1]

[1]Institute of Applied Physics and Computational Mathematics, Beijing 100088, China.
[2]Institute of Modern Physics, Chinese Academy of Sciences, Lanzhou 730000, China.
[3]University of Chinese Academy of Sciences, Beijing 100049, China.
[4]Nanjing University of Science and Technology, Department of applied physics, Nanjing 210014, China

Synopsis In the past few years, semi-classical and quantum molecular dynamics time-dependent methods are respectively developed based on high-precision potential energy surface (PES) calcaltions to investigate the many-body fragmentation dynamics of weakly bound molecular systems of $ArCO^{3+}$ and N_2Ar^{2+} etc. [1-3] with our experimental collaborators. For the case of $ArCO^{3+}$, it is found that the dissociation of CO^{2+} is greatly delayed due to the obvious difference between the initial vibrational wave packet of CO^{2+} and the interaction region of dipole and radial coupling transitions. Besides, it is found that $ArCO^{3+}$ changes from its initial T shape into the more stable linear shape within a timescale of 100 fs due to the interaction between the metastable CO^{2+} and Ar^{+}, which is hundreds of times faster than the field free case and the widely used Coulomb-explosion imaging technique is found fail to reconstructure the geometry of ArCO. For the breakup of N_2Ar^{2+} induced by 1 MeV Ne^{8+} ions collision, an exotic heavy N^+ ion transfer channel of N_2^{2+}·Ar → N^+ + NAr^+ was found for the first time, for which our PESs calculations show that the neighboring Ar atom significantly decreases the N_2^{2+} barrier height and width, resulting in significant shorter lifetimes of the metastable molecular ion state $N_2^{2+}(X^1\Sigma_g^+)$. Consequently, the breakup of the covalent N^+–N^+ bond, the tunneling out of the N^+ ion from the N_2^{2+} potential well, as well as the formation of an N^+–Ar bound system take place almost simultaneously, resulting in a Coulomb explosion of N^+ and NAr^+ ion pairs.

Figures 1 and 2 show the theoretical results for the three-body breakups of $ArCO^{3+}$ and the heavy N^+ ion transfer channel N_2^{2+}·Ar → N^+ + NAr^+. More details can be found in Refs [1] and [2].

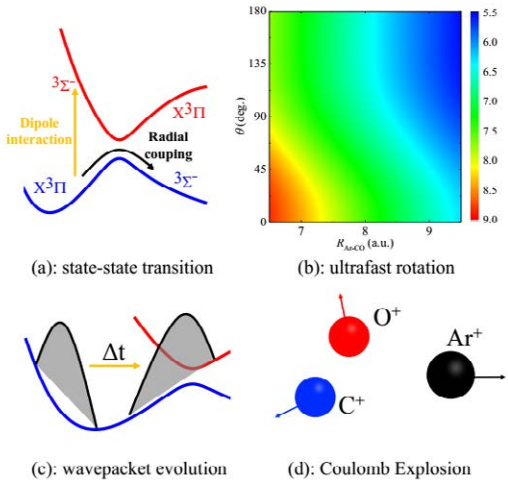

Figure 1. The considered interactions in present simulations for the ultrafast breakups of $ArCO^{3+}$. (a): the dipole transition driven by laser field and the radial coupling transition caused by symmetry breaking; (b): the ultrafast rotation of CO^{2+}; (c): the evolution of vibrational wavepacket for CO^{2+}; (d): the coulomb explosion.

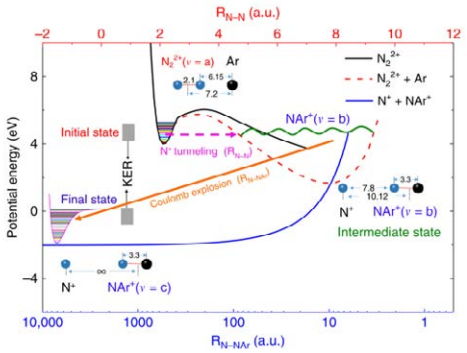

Figure 2. Schematic diagram of heavy ion transfer process through tunneling. The PECs of $N_2^{2+}(X^1\Sigma_g^+)$·Ar with/without the presence of neutral Ar along R_{N-N} (upper horizontal axis) and N^+–NAr^+ along R_{N-NAr} (bottom horizontal axis). The black solid curve for N_2^{2+} without the neutral Ar, the red dashed curve for $N_2^{2+}(X^1\Sigma_g^+)$·Ar at fixed distance R_{N2-Ar} = 7.2 a.u, and the blue solid curve indicates the PEC of N^+–NAr^+ with R_{N-Ar} = 3.3 a.u.

References

[1] X Hu *et al* 2020. *Phys. Rev. A.* **96** 052701
[2] X Zhu *et al* 2020. *Nat. Commun.* **11** 2987
[3] X Ding *et al* 2017. *Phys. Rev. Letts.* **118** 233402

* E-mail: xiaoqing-hu@foxmail.com

Classical trajectory time-dependent mean-field calculations for ion-molecule collisions

A. Jorge*

Departamento de Química, Universidad Autónoma de Madrid, Madrid, 28049, Spain

Synopsis We investigate the dynamics of ion-molecule collisions in the impact energy range from 0.1 to 100 MeV with the Classical Trajectory Monte Carlo method. We focus on the treatment of the multielectronic aspect of the collision through a time-dependent screening model that takes into account the change of the electronic cloud during the dynamics. The effects of these changes on electron capture and ionization processes in collisions involving water molecules are analyzed and results are compared with experimental data where available.

The study on electron emission due to ion collisions on water is of high importance due to its applications in radiobiology. We here study both the final electron emission energy and direction.

This model was presented in [1]. The quantum description of the electron dynamics is approximated by a classical statistical ensemble for each molecular orbital. The statistical distribution interacts with the water cation through a multicenter potential [2]. In order to study the influence of the dynamical response due to the electron loss, we introduce dynamical screening charges in the target potential. During the collision dynamics, the time-evolution is monitored in small time-steps ($\Delta t = 0.05$ a.u.) in the region where the collision happens so that the time-dependent target potentials are updated on a fine time grid.

We present results here for the water molecule. We have checked that for medium charged ions ($Z \sim 6 - 13$) and high impact energies (∼10-100 MeV), there is a notable change in the absolute double differential cross sections (DDCS) and single differential cross sections (SDCS). It must be specially noticed the change in the the forward-backward asymmetry, showing the importance of not considering molecular targets as frozen potentials for this range of energies (See Fig1 (a) and (b)). We have also found that for lower impact energies (250 keV) and a low charged projectile (proton), where the electron loss of the molecule is much lower, the dynamic screening and non-dynamic screening versions show little differences [4].

An in-depth discussion of the model and detailed comparisons with experiments will be presented at the conference.

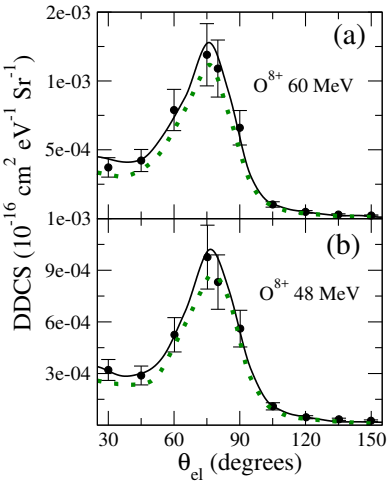

Figure 1. DDCS for ionization in ion-water collisions. •: Measurements [3]. Present CTMC results are shown as solid black and green dotted lines, with static and with time-dependent screening, respectively.

References

[1] Jorge, A. *et al* 2019 *Physical Review A* **99** 062701
[2] Illescas, C. *et al* 2011 *Physical Review A* **83** 052704
[3] Bhattacharjee, S. *et al* 2018 *Eur. Phys. J. D* **72**, 15 (2018)
[4] Bhogale, A. *et al* (in preparation)

*E-mail: albamaria.jorge@gmail.com

Accurate experimental cross sections for electron and positron scattering

R Kadokura[1]*, A Loreti[1], Á Köver[2], A Faure[3] J Tennyson[1] and G Laricchia[1]

[1]UCL Dept. of Physics and Astronomy, University College London, Gower Street, London WC1E 6BT, United Kingdom

[2]Institute for Nuclear Research (Atomki), Bem ter 18/c, H-4026 Debrecen, Hungary

[3]University Grenoble Alpes, 621 avenue Centrale. 38400 Saint-Martin-d'Heres, France

Synopsis Total cross section measurements of positron and electron scattering from H_2O have been investigated using an electrostatically guided beam with a field-free interaction and detection region, enabling a high angular resolution of $\sim$ (0.7° - 1°) against forward elastic scattered projectiles. The precision and accuracy achieved by our present measurements allow us to directly compare experimental values against theoretical determinations, and in the case of electrons, extract the differential elastic cross section.

A fully electrostatic beam [1] characterised by a high angular discrimination ($\sim$ 0.7° - 1°) has been used to measure the total cross section of electron (σ_T^-) and positron (σ_T^+) scattering from water vapour in the energy range (3 - 100) eV and (10 – 300) eV, respectively.

Although measurements for electron systems have been investigated since the early 20th century, discrepancies had remained among experimental and theoretical results at low energies e.g. [2], [3]. The new results for σ_T^- are presented in figure 1, together with previous experimental and theoretical determinations [4]. The effect of forward scattering has also been probed in the angular range 0° – 3.5° and estimates of the average (rotationally and vibrationally summed) differential elastic cross sections for energies $\leq$ 12 eV have been obtained at a scattering angle $\sim$ 1°. These measurements provide the first test of theoretical predictions in an angular region experimentally unexplored until now.

High angular discrimination measurements for σ_T^+ have previously been carried out on the same equipment [5]. When compared with earlier experiments the new results yielded values of σ_T around 50 - 100% higher than previous direct measurements. Agreement among experiments is achieved once allowance is made for forward elastic scattering using the theoretical differential elastic cross section calculated using the (rotationally summed) R-matrix method.

This work was supported by the Engineering and Physical Sciences Research Council (UK) (Grant No. EP/P009395/1) and the Hungarian Scientific Research Fund (Grant No. K128621).

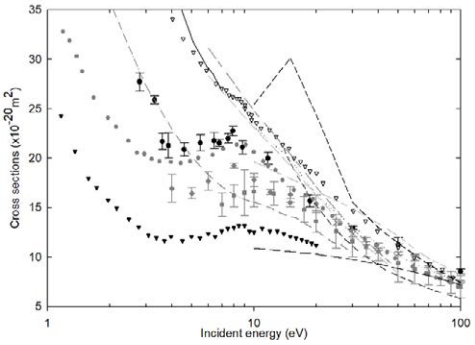

Figure 1. Cross sections for electron scattering from H_2O. Solid symbols denote direct measurements, hollow symbols denote measurements corrected for forward angle elastic scattering and lines denote theories [4].

References

[1] Köver Á *et al* 2014 *Meas. Sci. Technol.* **25** 075013
[2] Itikawa Y 2005 *J. Phys. Chem. Ref. Data* **34** 1
[3] Szmytkowski C and Mozejko P 2006 *Optica Applicata* **36** 543
[4] Kadokura R *et al* 2019 *Phys. Rev. Lett.* **123** 033401
[5] Loreti A *et al* 2016 *Phys. Rev. Lett.* **117** 253401

*E-mail: rina.kadokura.11@ucl.ac.uk

Microwave control of ultracold molecular collisions

Tijs Karman*
Radboud University, Institute for Molecules and Materials, Heyendaalseweg 135, 6525 AJ Nijmegen, the Netherlands

Applications of ultracold molecules – such as quantum simulation – rely on their tunable long-range dipole-dipole interactions. Accessing these interactions requires polarizing molecules using static or microwave electric fields. In this talk I will discuss the interactions induced both ways [1]. For ground state molecules polarized by a static electric field, the dynamics are accurately described by first-order dipolar interactions. For microwave dressing, instead, the collision process is dominated by resonant dipolar collisions, in which molecules reorient along the intermolecular axis and interact with the full strength of the transition dipole. The resonant dipolar interactions can be either attractive or repulsive. Attractive interactions can be observed experimentally as fast collision rates [2], whereas repulsive interactions shield molecules from collisional losses [3].

[1] T. Karman, Z.Z. Yan, and M. Zwierlein arXiv:2106.01610
[2] Z.Z. Yan, J.W. Park, Y. Ni, H. Loh, S. Will, T. Karman, and M. Zwierlein *Phys. Rev. Lett.* **125**, 063401 (2020)
[3] L. Anderegg, S. Burchesky, Y. Bao, S.S. Yu, T. Karman, E. Chae, K.-K. Ni, W. Ketterle, and J.M. Doyle arXiv:2102.04365

*Electronic address: t.karman@science.ru.nl

Ultrafast electronic and nuclear dynamics in the nanoparticle induced by the hard-x-ray laser

Yoshiaki Kumagai[1] *

[1]Institute of Multidisciplinary Research for Advanced Materials, Tohoku University, Sendai, 980-8577, Japan

Synopsis To study ultrafast electronic and nuclear dynamics in the nanoparticle induced by the hard-x-ray laser, we performed electron and ion spectroscopies for atomic clusters irradiated with an x-ray free electron laser pulse. For providing theoretical insight, we employed dedicated molecular-dynamics simulations, which track the real-space dynamics of the atoms and charged particles. Our results elucidate the entire dynamics which happens in the nanoparticle induced by the hard x-ray pulse, and demonstrate a versatile method with weak laser fields as probe for tracking the ultrafast dynamics of the nanoplasma.

The advent of x-ray free-electron lasers (XFELs) has been pioneering the diverse research frontiers. It admits of no doubt that the understanding of the intense x-ray pulse-matter interaction and the subsequent processes promises us to reach the frontiers of science.

To study light-induced dynamics, atomic clusters are ideal objects because their size can be varied in a controlled way. In a cluster composed of heavy atomic species, hard x-ray pulses occur deep inner-shell ionization of heavy atoms followed by a cascade of Auger decays producing many electrons with various kinetic energies, which can excite further electrons through sequential electron impact ionizations. The low-energy electrons are then trapped by the ionized cluster potential, forming a nanoplasma.

We performed electron and ion spectroscopies for the atomic clusters at the XFEL facility, SACLA, to study ultrafast electronic and nuclear dynamics in the nanoparticle induced by the hard x-ray laser. For the theoretical analysis, we employed an extended version of XMDYN, which tracks the real-space dynamics of the atoms, atomic ions, and emitted electrons. To extend the insight, we applied additional near-infrared (NIR) laser pulses to probe the dynamics in time.

The theoretical data obtained for electron and ion kinetic energy spectra as well as for the fragment yields agree with the experimental results of argon clusters with the average size of 1,000 atoms, capturing the essential processes steering the dynamics [1]. The simulations capture the features of the energy absorption from the NIR field by the nanoplasma electrons [2].

As the thermal electron emissions from the ionized krypton clusters with the average size of 50,000 atoms is highly suppressed, the recombination features together with prompt electron emission signal and possible traces of correlated decay phenomena are the only signatures of the transient nanoplasma in the electron spectra [3].

Dramatically improved temporal resolution of the pump–probe scheme allowed to monitor the birth of a nanoplasma by capturing the ultrafast population and depopulation of excited states of atoms during nanoplasma formation in xenon clusters with the average size of 5,000 [4].

Our results elucidate the entire dynamics, from the birth of nanoplasma to the breakup, which happens in the nanoparticle induced by the hard x-ray pulse. The probing with weak laser fields is a versatile method that can be applied to track the ultrafast electron and nuclear dynamics of the nanoplasma.

This work has been carried out in fruitful collaborations with all authors in Refs. [1, 2, 3, 4], especially with W. Xu, H. Fukuzawa and K. Nagaya in the experiments and groups of R. Santra at CFEL and A. Kuleff at Universität Heidelberg for theory, mainly supported by the XFEL Priority Strategy Program of the MEXT with K. Ueda as PI.

References

[1] Kumagai Y, Jurek Z *et al* 2018 *Phys. Rev. Lett.* **120** 223201

[2] Kumagai Y, Jurek Z *et al* 2020 *Phys. Rev.* A **101** 023412

[3] Kumagai Y, Jurek Z *et al* 2021 *J. Phys.* B **54** 044001

[4] Kumagai Y *et al* 2018 *Phys. Rev.* X **8** 031034

*E-mail: kumagai@go.tuat.ac.jp

Ultrafast resonant interatomic Coulombic decay induced by quantum fluid dynamics

A. C. LaForge[1,2]*

[1]Department of Physics, University of Connecticut, Storrs, Connecticut, 06269, USA
[2]Physikalisches Institut, Universität Freiburg, 79104 Freiburg, Germany

Synopsis Bubbles in helium droplets form around excited atoms and greatly accelerate interatomic Coulombic decay, showing how environment enhances this biologically relevant energy-sharing process among atoms and molecules.

When a free atom or molecule is excited by an energetic photon, the only means to release its energy is through internal decay or radiation emission. In contrast, when atoms or molecules are weakly bound to one another, the excitation energy from one site can be transferred to a neighboring one. A particularly interesting energy-sharing process is interatomic Coulombic decay (ICD), in which the release of energy from one atom or molecule leads to ionization of a neighbor. This process plays an important role in the response of biological tissue to radiation. Here, we show that ICD is dramatically enhanced by the response of the medium surrounding the excitations.

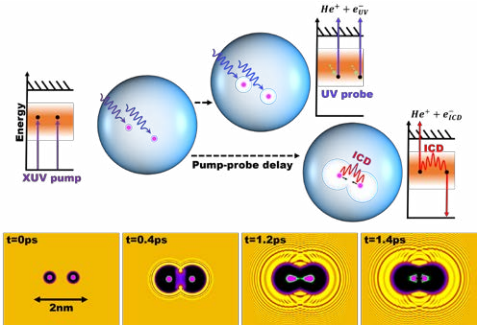

Figure 1. (top) A free-electron laser is used to excite atoms within a helium nanodroplet. Each excited atom is encapsulated inside of a "bubble". Over time, the bubbles can merge leading to interatomic Coulombic decay (ICD). Using a pump-probe technique, the timescale of ICD can be resolved. (bottom) simulation, based on time-dependent density functional theory of the bubble dynamics.

In many condensed systems, such as fluids and small droplets, not only do the interacting atoms and molecules matter, but the local environment can also strongly influence the interatomic decay process. To study this influence, we use ultrashort, extreme-UV laser pulses to directly map ICD of laser-excited superfluid helium nanodroplets over time. State-of-the-art theoretical modeling of the process reveals that a localized bubble, or cavity, forms around each excited atom. Neighboring bubbles then merge into one, thereby pushing the excited atoms together. This causes the atoms to decay by ICD within a few hundred femtoseconds, which is orders of magnitude faster than previously expected.

Similar processes are likely to occur in other fluids such as water, where the formation of nanobubbles plays a role in the solvation of electrons and the unfolding and aggregation of proteins. Our results demonstrate the importance of bubble dynamics in interatomic decay processes and open up a new approach for understanding the basic processes causing radiation damage in biological systems. The results hacve recently been published [1].

References

[1] LaForge A. C. *et al.* 2021 *Phys. Rev. X* **123** 012021

*E-mail: aaron.laforge@uconn.edu

Cage-opening dynamics of adamantane

S Maclot[1,2]*, J Lahl[2], J Peschel[2], H Wikmark[2], F Brunner[2], H Coudert-Alteirac[2], S Indrajith[3], N G Aguirre[4] B A Huber[3], S Díaz-Tendero[5], P Rousseau[3], and P Eng-Johnsson[2]

[1]Department of Physics, University of Gothenburg, Origovägen 6B, 41296, Gothenburg, Sweden
[2]Department of Physics, Lund University, P.O. Box 118, 22100 Lund, Sweden
[3]Normandie Université, ENSICAEN, UNICAEN, CEA, CNRS, CIMAP, 14000 Caen, France
[5]Departamento de Química, Módulo 13, Universidad Autónoma de Madrid, 28049 Madrid, Spain
[4]Theoretical Division, Los Alamos National Laboratory, Los Alamos, New Mexico, 87545, USA

Synopsis Adamantane is the simplest of the diamondoid molecules, which due to their high stability are of great interest both in astrophysics and nanotechnology. This work investigates the molecular photodissociation after ionization by different photon sources. The fragmentation dynamics is inferred by means of ion and electron spectroscopy techniques and quantum chemistry calculations.

Diamondoids are a class of carbon nanomaterials based on carbon cages with well-defined structures formed by $C(sp^3)$-$C(sp^3)$-hybridised bonds and fully terminated by hydrogen atoms. All diamondoids are variants of the adamantane molecule, the most stable among all the isomers with formula $C_{10}H_{16}$. Today, diamondoids are attracting increasing interest for use as an applied nanomaterial [1]. In space, diamondoids have been found to be the most abundant component of presolar grains [2], and due to their high stability, they are expected to be abundant in the interstellar medium [3].

A recent experiment was performed at Lund University using femtosecond XUV pulses produced via high-order harmonic generation to study the photodissociation of adamantane cations [4]. Photoions and photoelectrons were detected by a velocity map imaging spectrometer [5]. The ion mass spectrum and the ion momentum distribution were recorded on a single shot basis, allowing for the use of covariance analysis to disentangle the dissociation dynamics.

As a main result we were able to show that the doubly charged adamantane molecule is metastable and will spontaneously dissociate. But, preceding dissociation, the cage structure will open and hydrogen migration(s) will occur (see Fig. 1). In addition, we were able to assess the energetic picture of the dication processes thanks to the measured ion and electron kinematics combined with theoretical calculations, allowing us to discuss the internal energy distribution of the system.

To delve deeper into adamantane's properties we recently performed a set of complementary studies such as time-resolved photoionisation experiments using pump-probe techniques (XUV-IR at the Lund Attosecond Science Center and XUV-XUV at the Free-electron laser FLASH2), core-ionisation measurements at the synchrotron SOLEIL (FR) and time-dependent photoabsorption spectroscopy at the cryogenic ring DESIREE (SE) from which preliminary results will be presented.

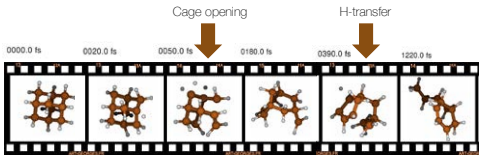

Figure 1. Molecular dynamics simulations showing the opening of the carbon cage.

References

[1] S. Stauss 2017 *Pan Stanford* "Diamondoids: Synthesis, Properties, and Applications"
[2] E. Anders *et al* 1993 *Meteoritics* **28** 490
[3] T. Henning *et al* 1998 *Science* **282** 2204
[4] S. Maclot *et al* 2020 *Sci. Rep.* **10** 2884
[5] L. Rading *et al* 2018 *Appl. Sci.* **8** 998

*E-mail: sylvain.maclot@physics.gu.se

Ionization of atoms and molecules by twisted electron beams

A Mandal[1]*, R Choubisa[1]†, N Dhankhar[1] and D Sébilleau[2]

[1]Department of Physics, Birla Institute of Technology and Science, Pilani, Pilani Campus, Pilani, Rajasthan, 333031, India

[2]Univ Rennes, CNRS, IPR (Institut de Physique de Rennes) - UMR 6251, F-35000 Rennes, France

Synopsis In recent times, ionization of atoms and molecules by twisted electron beams has gathered the centre stage. In optics, vortex beams have been the building blocks of whole fields of research such as communication, quantum computing and many others. Electron vortex beams (EVBs) or twisted electron beam are a quantum state of free electrons that exhibit novel properties such as orbital angular momentum (projected along the propagation axis) and phase vortices. These dynamics of twisted electron beam have been extended as a new probe to single and double ionization of atoms and molecules.

During the last century, electrons have played a significant role in the development of many fields of physics and their wave-like features correctly predict the behaviour of electrons in various physical systems including atoms, molecules and solid-state materials. Twisted electron beam which has been properly described and experimentally demonstrated a decade ago has the ability to carry discrete quantities of Orbital Angular Momentum (OAM) along the propagation direction of electron beam. They are characterized by their opening angle which relates transverse and longitudinal momenta.

Electron vortices have several applications: they can be used to probe multiple sources of perturbation in various physical systems. For instance, they can be used to probe nanoscale magnetic materials and to manipulate nanoparticles. The possible applications of these matter vortex waves are numerous and a fundamental understanding of their interactions with atoms and molecules needs to be developed. The coincident study of ionization of atoms and molecules by the impact of an electron has always been an important topic in atomic and molecular physics for decades to study the basic few-body Coulomb problem, correlation effects, target structure and the spin dependent effects at microscopic level. There is a growing interest to revisit these processes with the twisted electron beam [1, 2]. So, naturally twisted electron beam can act as a new tool for information pertaining to electric, magnetic or crystalline strain properties that can be extracted by examining how electrons are inelastically and elastically scattered by the material. Recently, Harris et al. [3] studied the single ionization of Hydrogen by electron vortex beam within first Born approximation (FBA) which gave some insight on the interaction with atoms. The double ionization of He atoms has also been studied very recently [4]. We are also exploring the relativistic (e, 2e) process by twisted electron beam on atomic targets like Cu and Ag [5] which gave us some very interesting results. Here, we will discuss and share some of these interesting results involving ionization of atoms and molecules with twisted electron beam which has been reported so far.

References

[1] Serbo V *et al* 2015 *Phys. Rev A* **92** 012705
[2] Boxem R V *et al* 2015 *Phys. Rev A* **92** 032703
[3] Harris A L *et al* 2020 *J. Phys.B: At. Mol. Opt. Phys.* **53** 109501
[4] Dhankhar N *et al* 2020 *J. Phys.B: At. Mol. Opt. Phys.* **53** 155203
[5] Mandal A *et al* 2020 *arXiv:2003.06459v1 [physics.atom-ph]* **Under review**

*E-mail: p2016009@pilani.bits-pilani.ac.in
†E-mail: rchoubisa@pilani.bits-pilani.ac.in

First dielectronic-recombination experiments at CRYRING@ESR

EB Menz[1,2]*, M Lestinsky[1] S Fuchs[3,4], W Biela-Nowaczyk[5], A Borovik, Jr.[3], C Brandau[1,3], C Krantz[1], G Vorobyev[1], B Arndt[1], A Gumberidze[1], PM Hillenbrand[1], T Morgenroth[1,2], RS Sidhu[1], S Schippers[3,4], Th Stöhlker[1,2]

[1]GSI Helmholtzzentrum für Schwerionenforschung, Darmstadt, 64291, Germany
[2]Helmholtz Institute Jena, 07743, Germany
[3]I. Physikalisches Institut, Justus Liebig University Giessen, 35390 Germany
[4]Helmholtz Forschungsakademie Hessen für FAIR, Campus Gießen, 35392 Gießen, Germany
[5]Jagiellonian University, Institute of Physics, Poland

Synopsis The first merged-beam DR measurements were performed at the CRYRING@ESR electron cooler since its move from Stockholm. This talk will focus on the newly established particle detection and data acquisition setup and the results of DR measurements of astrophysically relevant neon ions in low charge states.

The analysis of data from astrophysical spectra relies heavily on acurate modelling of the systems involved. For most ions in a thin plasma dielectronic recombination (DR) is the dominant capture process and thus, precise absolute data are vital for determining the charge state balance in plasma modelling. Merged-beam experiments on electron-ion collisions in heavy ion storage rings have so far proven to be the best experimental approach to provide the needed data. During its Stockholm years, CRYRING and its electron cooler facilitated many DR experiments which benefitted from the excellent vacuum conditions and ultra-cold electron beam [1]. At GSI, CRYRING@ESR is now back in operation and with the upstream accelerator complex, intense beams of previously inaccessible ion species are available for experiments.

In merged-beam DR experiments the electron cooler is used both to reduce the momentum spread of the ion beam and as an electron target. An energy range in the ions centre-of-mass system is scanned by detuning the electron energy from the cooling value and the downcharged ions produced at variable relative collision energy are detected with a particle counter installed behind the next downstream dipole magnet. Both the detuning and the data acquisition were achieved by using a single dedicated setup.

Besides injection from the GSI accelerator chain, a local injector can supply a range of ion species from a local source for both testing and experiments. After the installation of a new ECR ion source, Ne^{7+} was chosen for tests of the DR measurement setup prior to scheduled experiments to improve our understanding of the electron beam temperatures of the electron cooler and to commission our experiment controls. The Ne^{7+} test measurement took place in May 2020 and demonstrated an undegraded resolution compared to the previous measurement (see Fig. 1)[2]. It was followed up in May 2021 by a scheduled experiment on astrophysically relevant low-energy DR of Ne^{2+} which this talk will focus on. Ne^{2+} has low-energy DR resonances associated with 2s → 2p core excitations and theory data is available from AUTOSTRUCTURE calulations.

This talk will focus on our new DR measurement setup and detail the results of the test run and the Ne^{2+} measurements which was one of the first scheduled experiments at CRYRING@ESR.

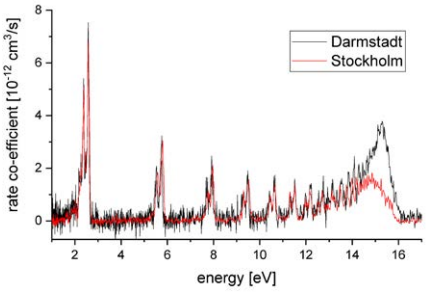

Figure 1. Ne^{7+} DR measurements performed at CRYRING in Stockholm and at GSI.

References

[1] Schuch R, Böhm S 2007 *J. Phys. Conf. Ser.* **305** 61-65

[2] Boehm S *et al* 2005 *Astronomy & Astrophysics* **88** 012002

*E-mail: e.menz@hi-jena.gsi.de

Scatteting of attosecond electron pulse trains by atomic targets

Y Morimoto[1,2*], P Baum[3], L B Madsen[4] and P Hommelhoff[1]

[1]Department of Physics, Friedrich-Alexander-Universität Erlangen-Nürnberg, Erlangen 91058, Germany
[2]RIKEN Center for Advanced Photonics, RIKEN, Saitama 3510198, Japan
[3]University of Konstanz, Konstanz 78457, Germany
[4]Department of Physics and Astronomy, Aarhus University, Aarhus C 8000, Denmark

Synopsis Ultrashort electron pulses provide access to atomic-scale dynamics and new opportunities in collision physics. Here we report the generation and application of attosecond electron pulse trains at sub-relativistic energies. The temporal compression of the electron pulses is achieved by the light-field-driven periodic acceleration at a membrane. A diffraction pattern of a crystalline silicon is recorded with the attosecond pulses. We theoretically demonstrate a quantum interference in the scattering of attosecond electron pulses by an atomic target, which modulates the scattering probability.

Attosecond light pulses produced via high harmonic generation continues to reveal electronic processes with unprecedented temporal resolution. However, it is still challenging to directly visualize atomic-scale attosecond dynamics because of the available wavelength. We here report the temporal compression of sub-relativistic electron beams of picometer wavelength to attosecond duration [1,2]. The broad momentum distribution of attosecond electron pulses can induce a quantum interference when they are scattered by an atomic target [3].

Figure 1(a) shows an experimental setup. Sub-picosecond electron beam at 70 keV is produced by a dc photocathode gun. The electron beam passes through a membrane (50-nm Si_3N_4 for 1-µm laser and 10-nm Al for 7-µm laser) which is excited by a laser beam. The electron is periodically accelerated at the laser cycle and reshapes its temporal shape after the free-space propagation. The temporal structure of the modulated beam is measured by the laser-cycle-driven deflection at the second stage.

Figures 1(b) and (c) show the observed temporal structures modulated by a multi-cycle 1-µm pulse [1] and a single-cycle mid-infrared pulse at 7-µm [2], respectively. The compression by the multi-cycle 1-µm pulse produces a train of nearly identical sub-femtosecond (800 as) pulses separated by the laser cycle (3.4 fs) [1,2]. On the other hand, the single-cycle modulation generates an individual attosecond peak [2].

Figure 1(d) shows a measured electron diffraction pattern of a single-crystalline Si recorded with the attosecond pulses shown in Fig. 1(b). We observe up to 6th-order diffraction spots, demonstrating the atomic spatial resolution.

When the optically-modulated electron beam is spatially focused and scattered by an atomic target, different momentum components of the beam can contribute to the scattering probability of the same final momentum. Accordingly, a quantum interference occurs. Figure 1(e) shows the simulated modulation of the total elastic scattering probability induced by the temporal shaping, as a function of the impact parameter. The interference modulates the scattering probability by more than 20% [3].

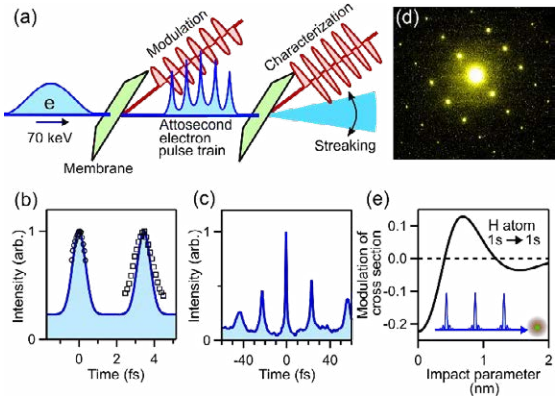

Figure 1. (a) Attosecond electron pulse generation (b),(c) Observed temporal structures. (d) Observed electron diffraction pattern. (e) Modulation of scattering probability.

References

[1]Morimoto Y and Baum P 2018 *Nat. Phys.* 14, 252
[2]Morimoto Y and Baum P 2020 *Phys. Rev. Lett.* 125, 193202
[3]Morimoto Y, Hommelhoff P and Madsen L B 2021 *Phys. Rev. A.*103, 043110

* E-mail: yuya.morimoto@fau.de

Nonadiabatic Subcycle Linear Momentum Transfer in Tunneling Ionization

H Ni[1,2,*], S Brennecke[3], X Gao[2], P-L He[4], S Donsa[2], I Březinová[2], F He[4], J Wu[1], M Lein[3], X-M Tong[5] and J Burgdörfer[2]

[1]State Key Laboratory of Precision Spectroscopy, East China Normal University, Shanghai 200241, China
[2]Institute for Theoretical Physics, Vienna University of Technology, 1040 Vienna, Austria, EU
[3]Institut für Theoretische Physik, Leibniz Universität Hannover, 30167 Hannover, Germany, EU
[4]Key Laboratory for Laser Plasmas (Ministry of Education) and School of Physics and Astronomy, Collaborative Innovation Center for IFSA (CICIFSA), Shanghai Jiao Tong University, Shanghai 200240, China
[5]Center for Computational Sciences, University of Tsukuba, Tsukuba, Ibaraki 305-8573, Japan

Synopsis We study the subcycle phase (or time) resolved linear momentum transfer to an atom accessible by an attoclock protocol. We demonstrate an interplay between nonadiabatic and nondipole effects in strong-field tunneling ionization [1].

Interaction of a strong laser pulse with matter transfers not only energy but also linear momentum of the photons. It is found that the photon momentum transferred in the tunneling step is not given entirely to the ion due to the action of the laser magnetic field during tunneling, resulting in the final linear momentum of the ionized electron in the laser propagation direction [2, 3]

$$\langle p_z \rangle = E/c + I_p/3c, \tag{1}$$

where E is the electron energy and I_p is the ionization potential.

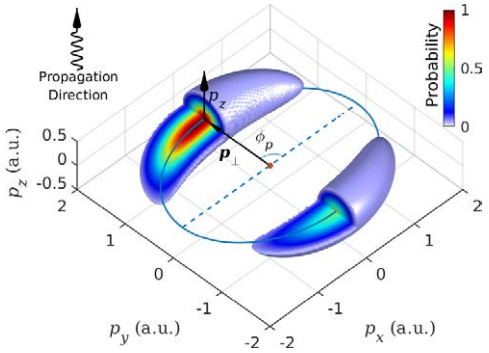

Figure 1. Attoclock protocol for subcycle resolved electron emission with momentum $\boldsymbol{p} = (\boldsymbol{p}_\perp, p_z)$ with the longitudinal component p_z along the propagation direction and the transverse component $\boldsymbol{p}_\perp$ in the polarization plane. The classical cycle-averaged radiation pressure picture suggests $\langle p_z \rangle > 0$.

While most previous studies focused on the momentum transfer by the entire ultrashort pulse, we present here the first ab-initio quantum simulation of the subcycle linear momentum transfer of the electron in strong-field ionization resolved in time [1] accessible by the attoclock protocol [4] (Fig. 1). By employing the backpropagation method [5, 6, 7] and extending the strong-field approximation to the nondipole regime (ndSFA), we decompose the linear momentum transferred during the tunneling process and during the continuum motion of the liberated electron on a subcycle time scale [1]:

$$\langle p_z(t) \rangle = \Delta E/c + \langle v_z(t) \rangle, \tag{2}$$

where ΔE is the energy the electron acquired during the continuum motion after tunneling and

$$\langle v_z(t) \rangle = \frac{\widetilde{I}_p(t)}{3c} \left[1 - \frac{2\alpha_Z F(t)}{(2I_p)^{3/2}} \right] \tag{3}$$

is the linear momentum the electron gained during the tunneling process. One should note the difference of Eq. (2) to Eq. (1). The term in the square bracket accounts for the correction from the ndSFA prefactor. The effective ionization potential $\widetilde{I}_p(t) \equiv I_p + \langle v_\perp^2(t) \rangle/2$ accounts for the energy shift by the initial transverse tunneling momentum, which roots in the nonadiabatic tunneling effects. This subcycle decomposition demonstrates a pronounced interplay between the nonadiabatic and nondipole tunneling effects.

*E-mail: hcni@lps.ecnu.edu.cn

References

[1] Ni H *et al* 2020 *Phys. Rev. Lett.* **125** 073202
[2] Klaiber M *et al* 2013 *Phys. Rev. Lett.* **110** 153004
[3] Chelkowski S *et al* 2014 *Phys. Rev. Lett.* **113** 263005
[4] Willenberg B *et al* 2019 *Nat. Commun.* **10** 5548
[5] Ni H *et al* 2016 *Phys. Rev. Lett.* **117** 023002
[6] Ni H *et al* 2018 *Phys. Rev. A* **97** 013426
[7] Ni H *et al* 2018 *Phys. Rev. A* **98** 013411

Vibrational autodetachment following excitation of electronic resonances

M Ranković[1] *, C S Anstöter[2] , G Mensa-Bonsu[2], P Nag[1], R Kumar T P[1], J R R Verlet[2] and Juraj Fedor[1]

[1]J. Heyrovský Institute of Physical Chemistry, Czech Academy of Sciences, Prague, 18223, Czech Republic
[2]Department of Chemistry, Durham University, Durham, DH1 3LE, United Kingdom

Synopsis We probe the electron detachment from electronic resonances in nitrobenzene by 2D electron energy loss and 2D photoelectron spectroscopy.

Under certain conditions, a collision of electron with neutral molecule may lead to a formation of short-lived transient anion called resonance. Knowing the incident and measuring the outgoing electron energy one may study this resonance by means of electron energy loss (EEL) spectroscopy [1]. Generally, upon formation of such resonance two types of vibrational excitations can be distinguished. The first is when the electron energy loss coincides with the energy required for excitation of vibrational quanta of a specific vibrational mode. Here, exces energy is carried away by a spontaneusely ejected (autodetached) electron. The second type is unspecific, where the electron energy is randomly distributed among nuclear degrees of freedom. In this case, a statistical themal electron emission is observed.

A recent development of two-dimensional (2D) EEL spectroscopy [2] enabled a third type of excitation to be observed in a few molecules, which does not fit into any of the previous types. In this case, electrons are emitted with a very low constant energy over a wide range of incident electron energies, but the spectra have the vibrational structure. So far, there has been no explanation for it.

A similar effect has been observed by means of 2D anion photoelectron (PE) spectroscopy [3] were resonances are created by photoexcitation of the bound anions. It features a constant low energy PE spectrum with vibrational structure associated with nonvalence states [4].

In this talk, we will explore this effect in more details and our suggested mechanism [5] for electron emission involving a nonvalence dipole-bound state of nitrobenzene anion will be presented.

* E-mail: milos.rankovic@jh-inst.cas.cz

References

[1] M. Allan, *J. Electron Spectrosc. Relat. Phenom.* 48, 219 (1989).
[2] K. Regeta and M. Allan, *Phys. Rev. Lett.* **110**, 203201 (2013).
[3] C. S. Anstöter, J. N. Bull, and J. R. R. Verlet, *Int. Rev. Phys. Chem.* **35**, 509 (2016).
[4] J. N. Bull and J. R. R. Verlet, *Sci. Adv.* **3**, e1603106 (2017).
[5] C. S. Anstöter, *Phys. Rev. Lett.* **124**, 203401 (2020).

Time-resolved imaging of light-induced dynamics in isolated nanoparticles

D Rupp[1,2,*]

[1]LFKP, ETH Zürich, 8093 Zürich, Switzerland
[2]Max-Born-Institute Berlin for Nonlinear Optics and Ultrafast Spectroscopy, 12489 Berlin, Germany

Synopsis Ultrafast nanoscale dynamics, such as laser-induced melting in a single metal cluster in free-flight, can be made visible and followed in time by employing intense short wavelength pulses from free-electron lasers or high-harmonic sources for coherent diffraction imaging.

With the high-intensity short-wavelength pulses available at free-electron lasers (FELs) and high harmonic sources (HHG), novel experiments with both, extreme spatial and temporal resolution, have become possible. One key example is coherent diffraction imaging of individual, isolated nanoparticles. Here, the elastically scattered photons form an interference pattern, which encodes structural information in a 'snapshot'. The method enables the in-situ study of fragile and short-lived specimen such as superfluid helium nanodroplets which cannot be deposited and analyzed e.g. with other microscopy methods.

In time-resolved configurations using the intense short-wavelength pulses as a probe of the dynamics, fundamental questions of light-matter interaction can be tackled in a near-background-free manner and on their required length and time scales. If one measures in the vicinity of electronic resonances, even changes in the electronic structure, e.g. due to ionization, can alter the scattering response quite dramatically and can thus in principle be followed with diffraction imaging. However, because electron dynamics occur on a timescale shorter than the typical tens of femtosecond pulse durations of FELs, we expect an exciting development in this context from the current progress at X-ray FELs and HHG sources towards high-intensity attosecond pulses.

In my talk I will discuss recent results using extreme ultraviolet (XUV) pulses for diffraction imaging. The comparably long wavelengths allow for the measurement of wide-angle diffraction patterns that contain three-dimensional information even in a single-shot pattern, thus enabling the 3D structural characterization of superfluid spinning droplets and silver nanopolyhedra. Using optical pump pulses with moderate intensities to excite the isolated nanoparticles, we find indications of ultrafast melting and instable phase explosions in superheated silver clusters and observe interesting switching dynamics in the ultrafast electronic response of helium nanodroplets. These recent results demonstrate the capabilities of diffraction imaging to visualize ultrafast nanoscale dynamics in highly excited matter.

* E-mail: ruppda@phys.ethz.ch

Atomic systems under plasma and cavity confinements

A Sadhukhan[1], S Mondal[1], P Amaro[2], J P Santos[2], K D Sen[3], J K Saha[1]*

[1]Department of Physics, Aliah University, Kolkata, 700160, India
[2]Laboratory for Instrumentation, Biomedical Engineering and Radiation Physics (LIBPhys-UNL), Department of Physics, NOVA School of Science and Technology, FCT, NOVA University Lisbon, Portugal
[3]School of Chemistry, University of Hyderabad, Hyderabad 500046, India

Synopsis Recent studies on the modifications of structural properties of atom placed under plasma and cavity confinements are discussed. The idea of atom under impenetrable box has been used to study resonance structure of highly charged helium like ions.

Manipulation of quantum systems with increasingly precise control may be considered as one of the key research activity in atomic, molecular, and optical science and technology in the coming decade. Such manipulation can be realized when the system is placed under various confining situations *e.g.* atoms embedded plasma environments, atoms encaged in zeolite sieves or in endohedral fullerenes, semiconductor quantum dots, ion storage etc. Moreover, the conceptual understanding of confined systems has also been used for biological modelling purposes. Over the years, technical advancements have opened up the horizons of various experimental observations and simultaneously, theoretical research has become crucial to formulate appropriate models for understanding the behavioural changes of such confined quantum systems.

Comprehensive studies on the modification of structural and spectral properties of plasma as well as cavity embedded one and two-electron atoms both in bound and resonance states are studied to explore various novel properties *e.g.* evolution of quasi bound states, incidental degeneracy and subsequent level crossing, ionization potential depression etc. Explicitly correlated Hylleraas type basis set consistent with appropriate boundary condition has been used under the Ritz variational framework. In recent times, we have made some methodological advancements in studying confined three-electron systems both by extending Hylleraas type basis set [1] as well by using model potential based composite variational framework [2].

In a closely related subject concerning, the critical nuclear charge *i.e.* the the nuclear charge that can hold two electrons in a bound state of a confined model two-electron system (Zee) have been derived. We have noted quantum phase transition around the critical nuclear charge which can further be tuned by the range of inter-particle interaction [3]. In case of impenetrable cavity confinement, an analysis of the confined Zee wave function points toward its smooth transition from a hydrogen like to the particle-in-a-box like nature as the system transits through zero energy state from the sufficiently negative to the positive energy regions [4].

The stabilization method has been used under the relativistic configuration-interaction (CI) framework to study the autoionization resonance structure of heliumlike ions [5]. In this method, the idea is to confine the ion within an impenetrable spherical cavity, the size of which has been varied to obtain the resonance parameters. This method has been applied for the determination of the resonance structure of heliumlike uranium ion, where a relativistic framework is essential. In the strong-confinement region, the present method can be useful to simulate the properties of an atom or ion under extreme pressure or to study ions embedded in dense plasma environment.

*E-mail: jksaha.phys@aliah.ac.in

References

[1] Dutta S, Saha J K, Chandra R and Mukherjee T K 2016 *Phys. Plas.* **23** 042107
[2] Saha J K, Bhattacharyya S, Ahmed Sk F 2020 *Int. J. Quant. Chem.* **121** e26570
[3] Sadhukhan A, Nayek S K and Saha J K 2020 *Eur. Phys. J. D* **74** 210
[4] Sadhukhan A, Sen K D and Saha J K 2021 *Chem. Phys. Lett.* **768** 138383
[5] Amaro P, Santos J P, Bhattacharyya S, Mukherjee T K, Saha J K 2021 *Phys. Rev. A* **103** 012811

Retrieving of an attosecond pulse waveform based on the high harmonic generation

T S Sarantseva[1,2]*, A A Romanov[2,3], A A Silaev[2,3], N V Vvedenskii[2,3] and M V Frolov[1,2]

[1]Department of Physics, Voronezh State University, Voronezh 394018, Russia
[2]Department of Radiophysics, University of Nizhny Novgorod, Nizhny Novgorod 603950, Russia
[3]Institute of Applied Physics, Russian Academy of Sciences, Nizhny Novgorod 603950, Russia

Synopsis All-optical non-iterative method for retrieving the temporal profile of an extreme ultraviolet (XUV) attosecond pulse is proposed based on the high harmonic generation process in an intense infrared field and attosecond XUV pulse. Within this method, two retrieving procedures are suggested, which utilize harmonic generation from two predominantly different spectral ranges. The capability of these procedures is discussed.

We propose a new method for retrieving an attosecond pulse waveform based on the analysis of high harmonic generation (HHG) in an intense infrared (IR) field and a weak (perturbative) time-delayed extreme ultraviolet (XUV) attosecond pulse. The theoretical background of the proposed method is based on the recently developed approach [1], which treats electron-laser interaction with an intense IR field quasiclassically (i.e., in terms of closed classical trajectories), while interaction with attosecond XUV pulse is considered within perturbation theory. Generally, the XUV field may induce several alternative channels for HHG, however only one contributes for harmonics beyond the cutoff of IR-induced plateau. In this channel, electron tunnels through the barrier and accelerated by an intense IR field along a closed classical trajectory. At the returning moment $t = t_j$, the liberated electron recombines to the initial state with simultaneous absorbtion XUV photon with frequency Ω and emission harmonic of frequency Ω_h forming additional plateau in the HHG spectrum [2]. Our theoretical analysis shows that contribution of this channel causes a specific dependence of HHG yield on the time delay between IR and XUV pulses, which can be utilized for retrieving attosecond pulse wave form:

$$\begin{aligned}\mathcal{Y}(\Omega_h) &\approx \mathcal{Y}_0(\Omega_h)\\ &+F_{\mathrm{XUV}}\sum_j a_j f(t_j-\tau)\cos(\Omega(t_j-\tau)+\phi_j)\\ &+F_{XUV}^2\sum_j y_j f^2(t_j-\tau),\end{aligned}\qquad(1)$$

where $\mathcal{Y}_0(\Omega_h)$ is the HHG yield in an intense IR field, F_{XUV} and $f(t)$ are field strength and envelope of the attopulse, τ is the time delay between IR and XUV pulses, a_j, y_j and ϕ_j are functions of IR field parameters. The first and second terms contribute on the slope of the IR-induced plateau, while the last term in Eq. (1) dominates on the XUV-induced plateau [2]. According to the explicit expression for the HHG yield we suggest two procedures for the attopulse waveform retrieving: (i) using harmonics just below the cutoff of IR-induced plateau; (ii) using harmonic far beyond IR-induced plateau. These methods consist in measurement of the HHG yield as a function of the time delay. In the first case, the τ-dependence of $\mathcal{Y}(\Omega_h)$ provides full temporal characterization of the attosecond pulse waveform, while in the second case measurements of HHG yield mimic the square of attosecond pulse envelope. Practical realization of the proposed method requires that the difference between two recombination times should be larger than duration of the attosecond pulse.

In order to test our method we perform numerical simulation of HHG in the presence of attosecond pulse within our recently developed time-dependent Khon-Shem code [3]. Our numerical calculations for Ne atom demonstrate the stability and high accuracy of suggested retrieval method of the waveform of the attosecond pulse.

References

[1] Sarantseva T S *et al* 2021 *Opt. Expr.* **29** 1428
[2] Sarantseva T S *et al* 2020 *Phys. Rev. A* **101** 013402
[3] Romanov A A *et al* 2020 *Phys. Rev. A* **101** 013435

*E-mail: sarantseva_ts@phys.vsu.ru

Rovibrationally-resolved electron scattering on H_2: Molecular convergent close-coupling calculations

L H Scarlett[1]*, D V Fursa[1], M C Zammit[2], J S Savage[1], and I Bray[1]

[1]Department of Physics and Astronomy, Curtin University, Perth, Western Australia 6102, Australia
[2]Theoretical Division, Los Alamos National Laboratory, Los Alamos, New Mexico, USA

Synopsis We review the progress made in recent years on the calculation of electron-H_2 cross sections with the *ab initio* molecular convergent close-coupling method: from fixed-nuclei calculations to rovibrationally-resolved adiabatic-nuclei calculations, and finally to electronic-vibrational close-coupling calculations capable of resolving resonances in the scattering cross sections.

Molecular hydrogen is the simplest neutral molecule, and yet there are still substantial gaps in the literature of accurate cross sections for electron-H_2 collisions. Collisional-radiative models of fusion or astrophysical plasmas containing H_2 require cross sections resolved in electronic, vibrational, and rotational levels, leading to data sets containing in excess of 100,000 transitions. Although a number of theoretical methods for modeling electron-molecule collisions have been available for decades, none are capable of performing the large-scale convergence studies required to ensure the accuracy of the calculated cross sections at all incident energies, and in many cases they make use of approximations which limit the processes which can be studied or the energy regions where the methods are valid.

The molecular convergent close-coupling (MCCC) method has been developed with the aim of producing accurate rovibrationally-resolved elastic, excitation, ionization, and total cross sections for electrons and positrons scattering on diatomic molecules. The use of prolate spheroidal coordinates allows the target structure to be accurately described over the range of internuclear separations required to account for the nuclear motion.

In this presentation we describe the MCCC method and the convergence studies which have been performed for scattering on the ground state and electronically-excited states of H_2, and we will present vibrationally-resolved cross sections for transitions between the first 19 electronic states of H_2 and its five isotopologues. We will discuss the application of MCCC cross sections in a collisional-radiative model for the triplet system of H_2 (see Figure 1), calculations of dissociation cross sections, and studies of the Fulcher-α band polarization. Finally, we will present new low-energy cross sections obtained using an electronic-vibrational close-coupling method which does not rely on the adiabatic-nuclei approximation.

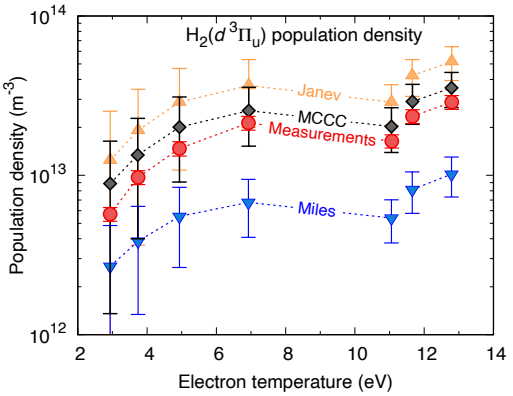

Figure 1. Comparison of measured population densities of the H_2 $d\ ^3\Pi_u$ state with predictions from the Yacora CR model [4] using cross sections from the previously recommended data sets of Janev *et al.* [1] and Miles *et al.* [2], as well as the MCCC cross sections [3]. Figure reproduced from Ref. [4].

References

[1] Janev R K *et al.* 2003 *Collision processes in Low-Temperature Hydrogen Plasmas* (Forschungszentrum Jülich, Zentralbibliothek)
[2] Miles *et al.* 1972 *J. Appl. Phys.* **43** 678
[3] Scarlett *et al.* 2021 *Atom. Data Nucl. Data Tables* **137** 101361
[4] Wünderlich *et al.* 2021 *J. Phys. D: Appl. Phys.* **54** 115201

*E-mail: liam.scarlett@postgrad.curtin.edu.au

Sputtering of Planets and Moons by Ion Impact

P S Szabo[1]*, H Biber[1], N Jäggi[2], D Weichselbaum[1], A Niggas[1], J Brötzner[1], R Stadlmayr[1], D Primetzhofer[3], A Nenning[4], A Mutzke[5], M Sauer[6], J Fleig[4], A Foelske-Schmitz[6], K Mezger[7], H Lammer[8], A Galli[2], P Wurz[2], and F Aumayr[1]†

[1]Institute of Applied Physics, TU Wien, Vienna, 1040, Austria
[2]Physics Institute, University of Bern, Bern, 3012, Switzerland
[3]Department of Physics and Astronomy, Uppsala University, Uppsala, 752 37, Sweden
[4]Institute of Chemical Technologies and Analytics, TU Wien, Vienna, 1060, Austria
[5]Max-Planck Institut für Plasmaphysik, Greifswald, 17491, Germany
[6]Analytical Instrumentation Center, TU Wien, Vienna, 1060, Austria
[7]Institute of Geological Sciences, University of Bern, Bern, 3012, Switzerland
[8]Space Research Institute, Austrian Academy of Sciences, Graz, 8042, Austria

Synopsis The surfaces of planets and moons are significantly eroded due to sputtering by the bombardment of solar wind ions and atmospheric ions, but many aspects of this process are still poorly understood. Using analog minerals for the surfaces of the Moon, Mercury and the Martian moon Phobos, the important contributions to the erosion by multiply charged solar wind ions and by planetary oxygen ions are shown.

The bombardment of planetary surfaces by ions represents an important contribution to the space weathering of airless planets and moons [1]. The major source for ion precipitation is the solar wind (see Figure 1), a steady stream of mostly H^+ and He^{2+} ions at 1 keV/amu [2]. The Martian moon Phobos is additionally also altered by oxygen ions at energies of several keV, which originate in the Martian atmosphere [3].

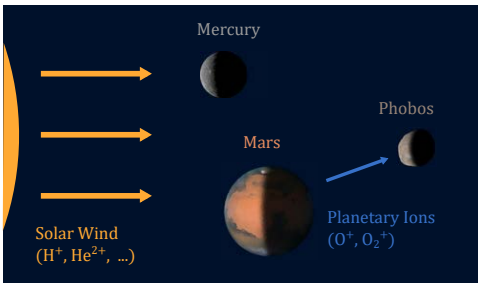

Figure 1. Airless bodies in the solar system are primarily sputtered by the solar wind. Phobos is also exposed to a flux of oxygen ions from the Martian atmosphere. (Image credit: NASA/JPL/USGS/David Crisp and the WFPC2 Science Team/University of Arizona)

In order to get a better understanding of effects that govern ion-solid interaction on planetary surfaces, laboratory experiments with a Quartz Crystal Microbalance (QCM) setup were performed, allowing real-time in-situ mass change measurements [4]. Thin films of different silicate minerals were used as analogs for the surfaces of the Moon, Mercury and Phobos [5, 6]. He^{2+} potential sputtering was found to increase the total sputtering of planetary surfaces by around 40% due to additional desorption of O atoms in accordance with the defect-mediated model of potential sputtering [5, 7]. Sputtering by oxygen ions was found to significantly contribute to the alteration of the surface of Phobos and oxygen implantation was also observed [6]. These results provide new insights into space weathering and will help in understanding the history of the airless bodies in the solar system.

References

[1] Pieters C M and Noble S K 2016 *J. Geophys. Res.: Planets* **121.10** 1865
[2] Russell C T *et al* 2016 *Space Physics: An Introduction (Cambridge: Cambridge Univ. Press)*
[3] Nénon Q *et al* 2019 *J. Geophys. Res.: Planets* **124** 3385
[4] Hayderer G *et al* 1999 *Rev. Sci. Instrum.* **70** 3696
[5] Szabo P S *et al* 2020 *Astrophys. J.* **891** 100
[6] Szabo P S *et al* 2020 *J. Geophys. Res.: Planets* **125** e2020JE006583
[7] Sporn M *et al* 1997 *Phys. Rev. Lett.* **79** 945

*E-mail: szabo@iap.tuwien.ac.at
†E-mail: aumayr@iap.tuwien.ac.at

Direct observation of atomic motion in molecules using atomic momentum spectroscopy

Y Tachibana[1 *], Y Onistuka[1], H Kono[2], and M Takahashi[1 †]

[1]Institute of Multidisciplinary Research for Advanced Materials, Tohoku University, Sendai 980-8577, Japan
[2]Department of Chemistry, Graduate school of Science, Tohoku University, Sendai 980-8578, Japan

Synopsis We demonstrate that atomic motion in a molecule can directly be observed by means of electron-atom Compton scattering experiments or atomic momentum spectroscopy. The key enabler behind this is development of a protocol to extract contribution of intramolecular atomic motion from raw experimental data. It is shown that the measured momentum distribution of the H-atom in the H_2 molecule is in satisfactory agreement with an associated one that has been calculated by using quantum chemistry theory.

Atomic motion in molecules has long been attracting great attention in a broad range of science and technology areas, as it is related to various physical and chemical phenomena. It was suggested recently by M. Vos and others that such intramolecular atomic motion could directly be observed by performing electron-atom Compton scattering experiments [1]. The remarkable feature of this experiment, called atomic momentum spectroscopy (AMS), is that it can measure momentum distributions of each atom, with different mass numbers, in a molecule. However, the unique ability of AMS is scarcely utilized for molecular science because of having no protocol to extract momentum distribution due to intramolecular atomic motion from raw experimental data. It is the purpose of the present work to propose such a protocol and to test its validity by making a comparison between experiment and theory for the H-atom motion in the H_2 molecule.

Basically, AMS measures the energy loss of an incident electron backscattered from a target molecule. The scattering process can be considered as a binary collision of the incident electron and a single atom in the molecule, so that the electron energy loss E can be described as $E = K^2/2M + \boldsymbol{P}\cdot\boldsymbol{K}/M$. Here M, $\boldsymbol{P}$, and $\boldsymbol{K}$ are the target atom mass, initial momentum of the scattering atom, and the electron momentum transfer, respectively. The AMS experiment on H_2 was conducted at a scattering angle of 135° and at incident electron energy of 2 keV by using a multichannel AMS apparatus [2]. The experimental data have been analyzed by using our proposed protocol that employs the convolution theorem to exclude the contribution of the instrumental response function in addition to the method [3, 4] to exclude the contribution of the molecular translational motion.

A preliminary result is presented in Figure 1, which shows the momentum distribution due to the H-atom motion in H_2. Also included in the figure is a theoretical distribution which has been calculated by using a rovibrational wave function of H_2 predicted by quantum chemistry theory. A good agreement between experiment and theory is obtained, indicating not only the validity of our proposed protocol but also feasibility of use of AMS as a completely new molecular spectroscopy technique. In the talk, future prospect of AMS is also disccused.

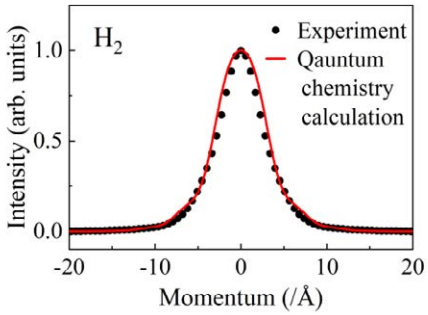

Figure 1. Comparison of momentum dsitribtuion of H in H_2 between experiment and quantum chemistry calculations.

References

[1] Vos M 2001 *Phys. Rev. A* 65 012703
[2] Yamazaki M *et al* 2017 *Rev. Sci. Instrum.* 88 063103
[3] Yamazaki M *et al* 2019 *J. Phys. B* 52 065205
[4] Tachibana Y *et al* 2019 *Phys. Rev. A* 100 032506

* E-mail: yuuichi.tachibana.s7@dc.tohoku.ac.jp
† E-mail: masahiko.takahashi.c4@tohoku.ac.jp

Multi-coincidence Studies of Molecules using Synchrotrons and XFELs

F Trinter[1,2] *

[1]Institut für Kernphysik, Goethe-Universität, Max-von-Laue-Str. 1, 60438 Frankfurt am Main, Germany
[2]Molecular Physics, Fritz-Haber-Institut der Max-Planck-Gesellschaft, Faradayweg 4-6, 14195 Berlin, Germany

Synopsis The talk will cover different multi-coincidence studies of atoms and molecules using synchrotrons and XFELs employing COLTRIMS reaction microscopes.

At the synchrotron light sources ESRF in Grenoble and PETRA III in Hamburg, we observed photoion backward emission in photoionizaton of He and N_2 [1]. We experimentally investigated the effects of the linear photon momentum on the momentum distributions of photoions and photoelectrons generated in one-photon ionization in an energy range of 300 eV < Eγ < 40 keV. Our results show that for each ionization event the photon momentum is imparted onto the photoion, which is essentially the system's center of mass. Nevertheless, the mean value of the ion momentum distribution along the light propagation direction is backward-directed by -3/5 times the photon momentum. These results experimentally confirm a 90-year-old prediction (see Fig. 1).

At the European XFEL in Schenefeld, we studied photoelectron diffraction imaging of a molecular breakup as well as double core-hole generation in O_2 molecules and the corresponding molecular-frame photoelectron angular distributions, both making use of an x-ray free-electron laser.

We show that x-ray photoelectron diffraction can be used to image the increase of the internuclear distance during the x-ray-induced fragmentation of an O_2 molecule [2]. By measuring the molecular-frame photoelectron emission patterns for a two-photon sequential K-shell ionization in coincidence with the fragment ions, and by sorting the data as a function of the measured kinetic energy release, we can resolve the elongation of the molecular bond by approximately 1.2 a.u. within the duration of the x-ray pulse.

In a second study, we report that by measuring two ions and two electrons in coincidence, we investigate double core-hole generation in O_2 molecules [3]. Single-site and two-site double core holes have been identified and their molecular-frame electron angular distributions have been obtained for a breakup of the oxygen molecule into two doubly charged ions. The measured distributions are compared to results of calculations performed within the frozen- and relaxed-core Hartree-Fock approximation.

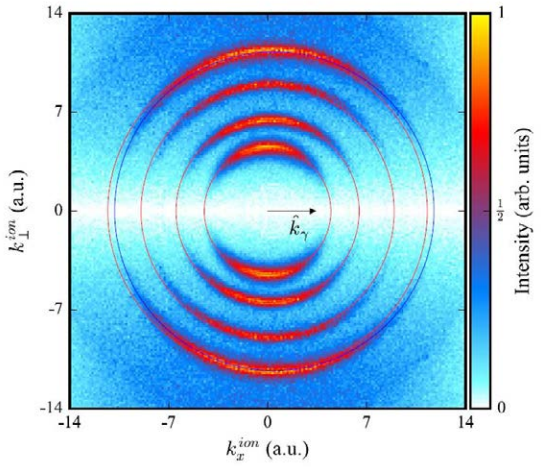

Figure 1. Momentum distribution of He^+ ions from single ionization by circularly polarized photons with Eγ = 300, 600, 1125, and 1775 eV.The blue outer circle is forward shifted by the corresponding photon momentum.

References

[1] Grundmann S *et al* 2020 *Phys. Rev. Lett.* **124** 233201
[2] Kastirke G *et al* 2020 *Phys. Rev. X* **10** 021052
[3] Kastirke G *et al* 2020 *Phys. Rev. Lett.* **125** 163201

* E-mail: trinter@atom.uni-frankfurt.de

Probing strong-field QED using high-power lasers Doppler-boosted by curved relativistic plasma mirrors

H. Vincenti[1] *, L. Fedeli[1], N. Zaim[1], A. Sainte-Marie[1], J-L Vay[2], A. Myers[2], M. Thévenet[3]

[1]LIDYL, CEA-Université Paris-Saclay, CEA Saclay, 91 191 Gif-sur-Yvette, France
[2]Lawrence Berkeley National Laboratory, Berkeley, CA 94720, USA
[3]Deutsches Elektronen Synchrotron (DESY), Hamburg, Hamburg 22607, Germany

Synopsis We propose a scheme to explore regimes of strong-field Quantum Electrodynamics (SF-QED) otherwise unattainable with the currently available laser technology. The scheme relies on relativistic plasma mirrors curved by radiation pressure to boost the intensity of PetaWatt-class laser pulses by Doppler effect and focus them to extreme field intensities. We show that very clear SF-QED signatures could be observed by placing a secondary target where the boosted beam is focused.

Achieving a light source delivering intensities up to the Schwinger limit of 10^{29} W/cm2 would allow exploring novel regimes of strong-field Quantum ElectroDynamics (QED) where the quantum vacuum is ripped apart. A promising candidate to build such a light source is the Curved Relativistic Mirror (CRM) concept that consists in: (i) inducing a Doppler upshift and temporal compression of a counter-propagating incident laser (ii) focusing the upshifted radiation down to a focal spot size much smaller than the one possible with the incident laser. Since its emergence in 2003 [1], many implementations of the CRM concept have been proposed. However, none has led to a detailed and feasible experimental proposal, mainly because they make use of idealized experimental conditions that are either not realistic or beyond present experimental know-how.

In this context, we recently proposed a novel and realistic all-optical scheme [2] to implement the CRM concept using so-called relativistic 'Plasma Mirrors' (PM) formed when an ultra-intense laser with high-contrast is focused on an initially-flat solid target. In this scheme, the PM surface is optically curved, either by radiation pressure or using secondary pre-pulse beams. As we demonstrate, this enables a considerably higher control of the PM shape than the one obtained with all other schemes proposed so far relying on the use of pre-shaped solid targets, which are beyond present State-Of-The-Art of manufacturing techniques.

In my talk, I first present the new scheme and its validation using cutting-edge 3D PIC simulations at an unprecedented scsale using the pseudo-spectral 3D PIC code WarpX. These simulations show that Doppler boosted intensities between 1025W/cm2 and up to 1028W/cm2 can be achieved with a multi-PW laser.

I then present the latest simulation results obtained by my team on the interactions of a Doppler boosted multi-PW laser beam with a secondary solid target placed at PM focus [3]. Our simulations show that very clear SF-QED signatures could be obtained in experiments (gamma-rays, GeV relativistic positron beams) with already available PW lasers. At constant laser power, these signatures are more than 3 orders of magnitude higher to what would be obtained with a non-boosted multi-PW laser beam and should enable the probing of SF-QED dominated regimes in light-matter interactions in the near future.

References

[1] S. V. Bulanov et al, Physical Review Letters, 91, 085001 (2003)
[2] H. Vincenti, Physical Review Letters, 123, 105001 (2019)
[3] L. Fedeli *et al*, Physical Review Letters (in press), ArXiv:2012.07696 (2021)

* E-mail: henri.vincenti@cea.fr

Fragmentation dynamics of hydrated tetrahydrofuran induced by electron impact ionization

Enliang Wang[1,2]*, Xueguang Ren[1,3]†, WoonYong Baek[4], Hans Rabus[4], Thomas Pfeifer[1], and Alexander Dorn[1]‡

[1]Max-Planck-Institut für Kernphysik, Saupfercheckweg 1, 69117 Heidelberg, Germany
[2]J. R. Macdonald Laboratory, Physics Department, Kansas State University, Manhattan, KS 66506, USA
[3]School of Physics, Xi'an Jiaotong University, Xi'an 710049, China
[4]Physikalisch-Technische Bundesanstalt, 38116 Braunschweig, Germany

Synopsis The ionization and fragmentation of tetrahydrofuran (THF) and hydrated THF induced by low-energy (65 eV) electron-collision were studied. The ionic fragments are identified from the measured ion time-of-flight spectra. The corresponding binding energy spectra (BES) are determined by an (e, 2e+ion) triple-coincidence detection by the reaction microscope. The influence of the water environment on the THF is investigated with the ion fragment correlated BES and *ab-initio* calculations. We find that hydration reduces the energy barrier for THF dissociation.

Electron-impact ionization of atoms and molecules is a fundamental process that is relevant to understand and interpret a wide range of scientific phenomenon and technological applications, including radiation damage in biological tissue [1]. In this respect, hydrated biomolecule clusters are interesting targets that allow studying the behavior of biomolecules in an aqueous environment.

In the present work, we report a study on the electron-impact induced ionization and fragmentation processes in clusters consisting of water and bio-relevant molecules, i.e. THF, by the multi-particle coincidence technique (reaction microscope) [2, 3] in which the momentum vectors and, consequently, the kinetic energies of all final state particles (electrons and ions) are measured in coincidence. A molecular ring-break mechanism is observed, which is absent for the THF monomer [4]. As shown in figure 1, the BES of the ring-break channel of hydrated THF (b) and THF dimer (a) corresponds to the highest occupied molecular orbital (HOMO) which is lower about 2.5 eV than the same ring-break channel of the THF monomer (c). By performing theoretical calculations, we find that ionization of the outermost THF orbital initiates significant rearrangement of the dimer structure increasing the internal energy and leading to THF ring-break. These results demonstrate that the local environment in form of hydrogen-bonded molecules can considerably affect the stability of molecular covalent bonds.

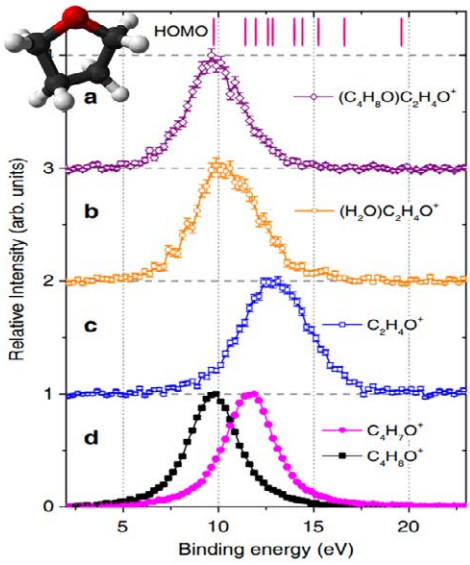

Figure 1. Measured binding energy spectra for various fragment species.

References

[1] Alizadeh E *et al* 2015 *Annu. Rev. Phys. Chem.* **66**, 379
[2] Ren X *et al* 2018 *Nat. Phys.* **14**, 1062
[3] Ren X *et al* 2016 *Nat. Commun.* **7**, 11093
[4] Wang E *et al* 2010 *Nat. Commun.* **11**, 2496

*E-mail: enliang@phys.ksu.edu
†E-mail: renxueguang@xjtu.edu.cn
‡E-mail: alexander.dorn@mpi-hd.mpg.de

Development of an RF-carpet gas cell to obtain an ion beam of thorium-229

A. Yamaguchi[1, 2 *], Y. Shigekawa[3], H. Haba[3], M. Wada[4] and H. Katori[1, 5]

[1]Quantum Metrology Laboratory, RIKEN, Wako, Saitama, 351-0198, Japan
[2]PRESTO, Japan Science and Technology Agency, Kawaguchi, Saitama, 332-0012, Japan
[3]Nishina Center for Accelerator-Based Science, RIKEN, Wako, Saitama, 351-0198, Japan
[4]Wako Nuclear Science Center, Institute of Particle and Nuclear Studies, High Energy Accelerator Research Organization, Wako, Saitama, 351-0198, Japan
[5]Department of Applied Physics, Graduate School of Engineering, The University of Tokyo, Tokyo 113-8656, Japan

Synopsis The first-excited isomeric state of Th-229 (Th-229^m) has an extremely low energy, offering a unique opportunity of laser spectroscopy of an atomic nucleus. An RF-carpet gas cell is developed to obtain an ion beam of Th-229 for trapping and laser spectroscopy of Th-229 ions. The Th-229 ions are obtained as recoil ions from an U-233 source. The nuclear state of 2% of recoil Th-229 ions from U-233 are Th-229^m. The apparatus developed in this study will thus also enable laser cooling and spectroscopy of trapped Th-229^m ions.

The first-excited isomeric state of Th-229 (Th-229^m) attracts attention for its extremely low energy. Existence of Th-229^m was confirmed via the observation of electrons emitted by internal conversion (IC) decays [1]. The excitation energy of the Th-229^m was measured to be approximately 8 eV by IC electron spectroscopy [2] and γ-ray spectroscopy [3-5]. The nuclear transition between the ground and isomeric states of Th-229 thus offers unique opportunities for laser spectroscopy of an atomic nucleus. One of the promising applications is an optical nuclear clock: an atomic clock based on this nuclear transition [6, 7]. The ion trap is an ideal platform for the nuclear clock because the quantum states of isolated Th-229 ions in a trap can be precisely manipulated by lasers.

In this study, we are developing an RF-carpet gas cell which generates an ion beam of Th-229 for the ion trap experiment. Figure 1 shows the schematic of the apparatus. The Th-229 recoil ions emitted from U-233 source are cooled by collisions with He buffer gas and extracted as an ion beam by an RF-carpet [8] with a push filed ($+V_0$) and a quadrupole ion guide.

In the previous ion trap and laser cooling experiments of Th-229 [9, 10], ions were prepared by laser ablation where the nucleus of the Th-229 ion was in the ground state. On the other hand, our apparatus can extract Th-229^m ions because 2% of the recoil Th-229 ions from U-233 are Th-229^m. Thus, by attaching the ion trap apparatus to the gas cell developed in this study, laser cooling and spectroscopy of trapped Th-229^m could also be performed, which should provide more detailed knowledge of this unique nuclear state.

* E-mail: atsushi.yamaguchi.fv@riken.jp

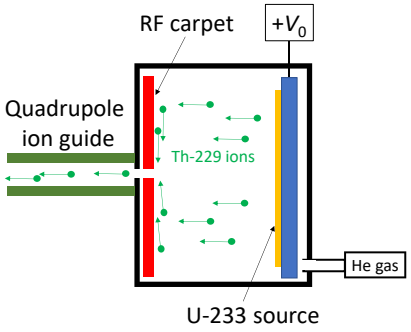

Figure 1. Schematic view of the developed RF-carpet gas cell. Recoil Th-229 ions emitted from an U-233 source are cooled with He buffer gas, extracted by an RF-carpet with a push filed ($+V_0$) and transported by a quadrupole ion guide.

References

[1] L. Von der Wense *et al.* 2016 *Nature* **533** 47
[2] B. Seiferle *et al.* 2019 *Nature* **573** 243
[3] B. R. Beck *et al.* 2007 *Phys. Rev. Lett.* **98** 142501; B. R. Beck *et al.* 2009 Report No. LLNL-PROC-415170
[4] A. Yamaguchi *et al.* 2019 *Phys. Rev. Lett.* **123** 222501
[5] T. Sikorsky *et al.* 2020 *Phys. Rev. Lett.* **125** 142503
[6] E. Peik and C. Tamm 2003 *Europhys. Lett.* **61** 181
[7] C. J. Campbell *et al.* 2012 *Phys. Rev. Lett.* **108** 120802
[8] M. Wada *et al.* 2003 *Nucl. Instrum. Methods Phys. Res. B* **204** 570
[9] C. J. Campbell *et al.* 2009 *Phys. Rev. Lett.* **102** 233004
[10] C. J. Campbell *et al.* 2011 *Phys. Rev. Lett.* **106** 223001

Relativistic effects on loosely bound states of positronic alkali-metal atom

T Yamashita[1,2]*; **Y Kino**[2]

[1]Institute for Excellence in Higher Education, Tohoku University, Sendai, 980-8576, Japan
[2]Department of Chemistry, Tohoku University, Sendai, 980-8578, Japan

Synopsis In contrast to ordinary atoms/ions where the relativistic effects become remarkable in heavy elements, our variational three-body calculation reveals that the positronic alkali-metal atoms show high ratio of relativistic corrections to the binding energy, even for the light elements such as Li and Na. In particular, the positronic sodium atom is found to be as high ratio as Cs^{54+}, which demonstrates a new aspect of relativistic binding mechanism of positronic compounds.

In heavy elements, relativistic corrections $\delta\varepsilon_{\rm rel}$ generally account for binding energy $\varepsilon = \varepsilon_{\rm nr} + \delta\varepsilon_{\rm rel}$ where $\varepsilon_{\rm nr}$ is non-relativistic binding energy. As the ratio of $\delta\varepsilon_{\rm rel}/\varepsilon$ increases, the properties of atoms deviate from the periodic law, which are known as relativistic effect. The effects play an indispensable role in heavy element chemistry.

Positronic alkali-metal atoms, APs^+ (A=Li, Na, ...), have been investigated in lots of theoretical works and are known to have a structure where a positronium ($Ps=e^+e^-$) cloud forms around the alkali-metal ion A^+. It has been known that only Li and Na atoms can form a bound state with positron, and their binding energies are $\varepsilon_{\rm nr} = 0.06$ eV [1] for $LiPs^+$ and 0.01 eV [2] for $NaPs^+$. Owing to such small binding energy coming from the neutralization of e^--e^+ pair, the Ps cloud around A^+ is diffuse like halo [3]. Since the APs^+ exists only in the light elements and the binding energy is small, the relativistic effects have been rarely discussed. However, the electron can access the nucleus even in the loosely bound state, which could account for the non-negligible relativistic contribution to the binding energy.

We calculated the relativistic corrections $\delta\varepsilon_{\rm rel}$ to the non-relativistic binding energies $\varepsilon_{\rm nr}$ of APs^+ using a three-body model (A^+, e^- and e^+). Model potentials between e^-/e^+ and A^+ are constructed so that the calculation including relativistic corrections reproduces the actual energy levels as well as the fine structure of alkali-metal atom A. Using a non-relativistic wavefunction $\Psi_{\rm nr}$ obtained by a Gaussian expansion method [4], $\delta\varepsilon_{\rm rel}$ is calculated by the perturbative Hamiltonian for the relativistic corrections, $H'_{\rm rel}$, including the Breit-Pauli interactions.

Figure 1 displays $\delta\varepsilon_{\rm rel}$ against ε for $LiPs^+$, $NaPs^+$, hydrogen-like alkali-metal ions, neutral atoms and negative ions Li^- and Na^-. The APs^+ systems are found to be positioned at the smallest ε region while the $\delta\varepsilon_{\rm rel}$ is relatively high in compared with the other ordinary atomic systems. In other words, the binding energy $\varepsilon_{\rm nr}$ of the positronic alkali-metal atoms are reduced by binding a positron, but the relativistic corrections $\delta\varepsilon_{\rm rel}$ are hardly reduced. As a result, the ratio $\delta\varepsilon_{\rm rel}/\varepsilon$ is remarkably amplified, e.g., the ratio of $NaPs^+$ is almost comparable to that of Cs^{54+} and neutral Cs [5].

As seen in Fig. 1, the positronic alkali-metal atoms situate a unique position in various atomic systems. Since ε is rather small, the high ratio of $\delta\varepsilon_{\rm rel}/\varepsilon$ can drastically affect the characteristics and reactivity of positronium halo. In summary, they would be suitable for the study of relativistic interactions among the weakly interacting quantum particles.

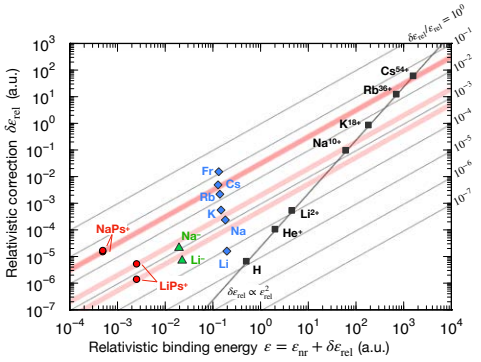

Figure 1. Relativistic correction against binding energy for APs^+ and various alkali-metal atoms, their hydrogen-like ions, negative ions.

References

[1] Ryzhikh G G and Mitroy J 1997 *Phys. Rev. Lett.* **79** 4124
[2] Yuan J 1998 *Phys. Rev. A* **58** R4(R)
[3] Mitroy J 2005 *Phys. Rev. Lett.* **94** 033402
[4] Hiyama E *et al.* 2003 *Prog. Part. Nucl. Phys.* **51** 223
[5] Yamashita T and Kino Y 2019 *Phys. Rev. A* **100** 062511

*E-mail: tyamashita@tohoku.ac.jp

On how classical uncertainties enfeeble quantum coherence

T A Guarda[1], R O Barrachina[1,2,3] *, F Navarrete[4] and M F Ciappina[5,6,7,8]

[1]Centro Atómico Bariloche, Comisión Nacional de Energía Atómica (CNEA), 8400 Bariloche, Argentina
[2]Instituto Balseiro, CNEA and Universidad Nacional de Cuyo, 8400 Bariloche, Argentina
[3]Consejo Nacional de Investigaciones Científicas y Técnicas (CONICET), Argentina
[4]Institute of Physics, University of Rostock, 18051 Rostock, Germany
[5]ICFO–Institut de Ciencies Fotoniques, The Barcelona Institute of Science and Technology, 08860 Castelldefels, Spain
[6]Institute of Physics of the ASCR, ELI Beamlines Project, 18221 Prague, Czech Republic
[7]Physics Program, Guangdong Technion - Israel Institute of Technology, Shantou, Guangdong 515063, China
[8]Technion - Israel Institute of Technology, Haifa 32000, Israel

Synopsis The departure of quantum mechanics from the classical world is the so-called quantum coherence. It is usually defined as the characteristic of systems which are in a superposition of states yielding interference patterns in certain kinds of experiments. In this work we study how classical uncertainties in a mixture of similar states reduce quantum coherence in quantum scattering theory. To this end, we deal with different examples, all of them with roots in the widely studied Feynman's two-slit thought experiment. We finally propose an operational and intuitive definition of the concept of coherence length.

Quantum coherence is the signature that distinguishes the quantum from the classical world. It has demonstrated to be decisive in different areas of physics and has proven to play a decisive role in the theoretical analysis of collision experiments [1,2]. This concept is challenging to both learn and teach [3] and is not usually included in courses and quantum mechanics textbooks. Except for a few exceptions, where this subject is treated briefly and superficially, it is difficult to find any reference to coherence in the index of the most well-known textbooks.

We formally analyzed how to incorporate concepts of quantum coherence in scattering processes employing the coherence length. Its definition allowed us to both describe qualitatively and also quantify the influence of the classical experimental context in the observation of quantum mechanical effects, through a detailed analysis of the two-slit thought experiment. We explored the problem in steps of increasing complexity. We demonstrate how, for a mixed state, the classical uncertainties in the impact parameter of its pure state constituents lead to a decrease of the coherence and the appearance of an effect similar to the van Cittert–Zernike effect, but for the quantum scattering of massive particles. It is worth to notice that, while it was predictable that classical uncertainties would wash out quantum effects of a system in a mixed state, the appearance of this effect in such simple and understandable fashion is a clear advantage of the present theoretical development [4].

* E-mail: barra@cab.cnea.gov.ar

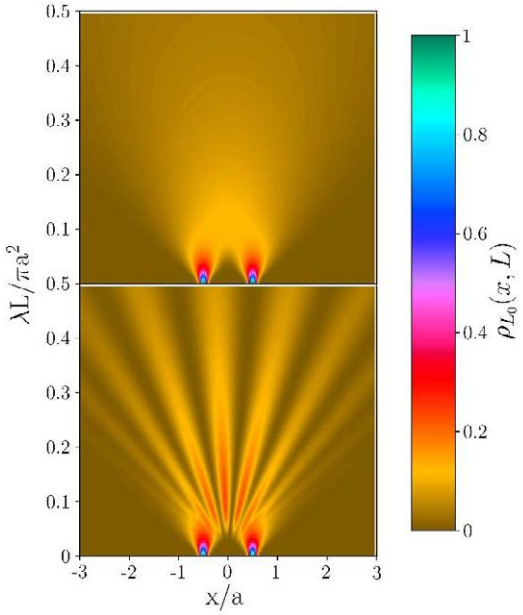

Figure 1. Probability distribution for a mixture of free waves of wavelength λ, initial width d and collimation D which, after travelling a distance L_o, traverse two slits of width δ separated by a distance a = 10 δ, for D = 10 a and d = a/10. The upper and lower panels correspond to $\lambda L_o/\pi a^2 = 0$ and 10, respectively.

References

[1] Navarrete F *et al* 2017 *Nucl. Instr. Meth., B* **408**, 165.
[2] Barrachina R O *et al* 2021 *Atoms* **9**, 5.
[3] Barrachina R O *et al* 2020 *Phys. Rev. Research* **2**, 043353.
[4] Fabre I *et al* 2018, *Eur. J. Phys*. **39** 015401.

Imaging the ultrafast umbrella (inversion) motion in ammonia

B Belsa[1], K Amini[1,2], X Liu[1], A Sanchez[1], T Steinle[1], J Steinmetzer[3], A T Le[4], R Moshammer[5], T Pfeifer[5], J Ullrich[5,6], R Moszynski[2], C D Lin[7], S Gräfe[3] and J Biegert[1,8] *

[1]ICFO - Institut de Ciencies Fotoniques, The Barcelona Institute of Science and Technology, Castelldefels (Barcelona), 08860, Spain
[2]Department of Chemistry, University of Warsaw, Warsaw, 02-093, Poland.
[3]Institute of Physical Chemistry and Abbe Center of Photonics, Friedrich-Schiller-Universität Jena, Helmholtzweg 4, Jena, 07743, Germany
[4]Department of Physics, Missouri University of Science and Technology, Rolla, MO 65409, USA
[5]Max-Planck-Institut für Kernphysik, Saupfercheckweg 1, Heidelberg, 69117, Germany
[6]Physikalisch-Technische Bundesanstalt, Bundesallee 100, Braunschweig, 38116, Germany
[7]Department of Physics, J. R. Macdonald Laboratory, Kansas State University, Manhattan, 66506-2604 KS, USA
[8]ICREA, Pg. Lluís Companys 23, Barcelona, 08010, Spain

Synopsis Exploiting the picometer and femtosecond spatio-temporal resolution achieved with laser-induced electron diffraction (LIED), we image the ultrafast umbrella motion of an isolated ammonia molecule, NH_3. We identified a symmetrically bent, near-planar ammonia cation, NH_3^+, in good agreement with our calculated equilibrium field dressed structure.

Numerous significant processes in nature involve the motion of hydrogen atoms, such as the influence of proton dynamics on the biological function of proteins [1]. The motion of the hydrogen atom denotes the fastest nuclear motion in molecules, occurring only on a few-femtosecond timescale. Thus, to image such rapid molecular motions, we need a method both fast and sensitive enough. In this work, we prove the capabilities of laser-induced electron diffraction (LIED) by capturing the fast motion of hydrogen atoms in the umbrella (inversion) mode of NH_3 [2, 3].

Upon ionization, the NH_3 molecule experiences a major geometrical transformation. Neutral NH_3 at its equilibrium configuration has a pyramidal shape (H-N-H bond angle, Φ_{HNH} = 107°), whereas the ammonia cation, NH_3^+, has a planar equilibrium geometry (Φ_{HNH} = 120°). Kraus and Wörner [4] theoretically investigated this pyramidal-to-planar transition dynamics, and they calculated it to occur on a ~8-fs timescale. Here, we employ LIED to directly retrieve structural information of the NH_3^+ ion. We strong-field ionize a neutral NH_3 molecule with a 3.2 μm driving laser (see black dot), emitting an electron wave packet (blue shaded) which may recollide back onto the target NH_3^+ ion 7-9 fs after ionization (see green dot). We identify a symmetrically, near-planar, NH_3^+ cation (Φ_{HNH} = 117 ± 5°) that agree well with our quantum-chemical calculations (Φ_{HNH} = 114°).

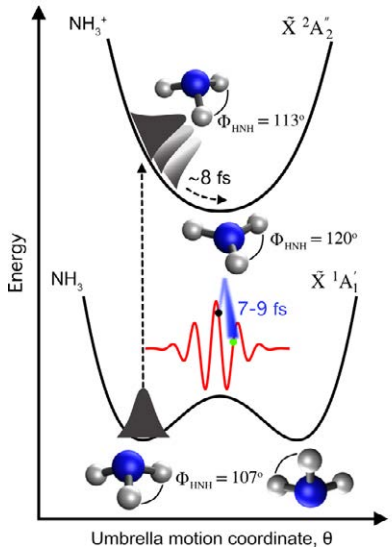

Figure 1. Schematic of the ultrafast umbrella motion in NH_3. The ground-state potential energy curves for the neutral NH_3 (bottom) and the cation NH_3^+ (top) are shown together with the corresponding equilibrium structures. Also, the LIED process is sketched.

References

[1] Parks S *et al* 2013 *Nat. Rev. Cancer* **13**, 611
[2] Pullen M *et al* 2016 *Nat. Commun.* **7**, 11922
[3] Belsa B *et al* 2021 *Struct. Dyn.* **8** 014301
[4] Kraus P M *et al* 2013 *ChemPhysChem* **14** 1445-145

* E-mail: jens.biegert@icfo.eu

Ultrafast dynamics of correlation bands following XUV molecular photoionization

A Boyer[1]*, M Hervé[1], V Despré[2], P Castellanos Nash[3], V Loriot[1], A Marciniak[1], A Scognamiglio[1], G Karras[1], R Brédy[1], E Constant[1], A G G M Tielens[3], A I Kuleff[2] and F Lépine[1]†

[1]Univ Lyon, Univ Claude Bernard Lyon 1, CNRS, Institut Lumière Matière, F-69622, Villeurbanne, France
[2]Theoretische Chemie, PCI, Universität Heidelberg, Heidelberg, Germany
[3]Leiden Observatory, Leiden University, P.O. Box 9513, 2300-RA Leiden, The Netherlands

Synopsis We observe ultrafast dynamics following molecular photoionization by an ultrashort XUV pulse. One corresponds to the dynamics of correlation bands, features created by electron correlation. The second one corresponds to a progressive loss of vibrational selectivity that will eventually lead to a complete intramolecular vibrational energy redistribution. Corresponding timescales, of few tens of femtoseconds, are measured experimentally in several Polycyclic Aromatic Hydrocarbons.

Attosecond technology has brought new perspectives in the real-time observation of ultrafast processes such as nuclear or electron dynamics. It also provides tools to investigate dynamics of highly excited species, commonly encountered in natural environments. While several experiments have investigated ultrafast XUV induced processes in atoms and small molecules, it is only recently that these studies were extended to larger systems [1, 2].

In this work, we study the relaxation of highly excited Polycyclic Aromatic Hydrocarbons (PAHs) using XUV-IR time resolved mass spectroscopy. In the experiment, the neutral molecules are ionized by an ulrashort XUV pulse (15 to 30eV). The resulting cations are left in highly excited electronic states. Due to electron correlation, some of these states are preferentially populated thus creating the so-called correlation bands (CBs). An IR pulse is used to probe the subsequent dynamics. The electronic relaxation of the CBs is observed by measuring the two-color dication yield [3]. On the other hand, the time resolved fragmentation yield of the excited cation allows to observe a second dynamics, associated to a loss of vibrational selectivity of the molecule [4].

These two dynamics were studied for several PAHs, from Anthracene to Hexabenzocoronene. The electronic relaxation of the CBs non-linearly increases with the size of the PAH (purple curve in Fig 1.). This trend is explained by a simple model based on an analogy with solid-state physics. In this model, the electronic relaxation is associated to an electron-phonon scattering process. Interestingly, the timescale of the vibrational dynamics shows an opposite trend and decreases with the size of the PAH (green curve in Fig 1.), providing an onset for coherence loss.

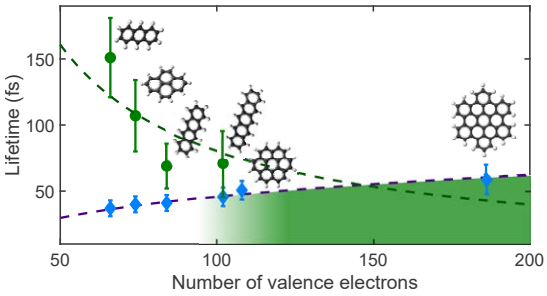

Figure 1. Extracted timescales for the relaxation dynamics in the CB (blue diamonds) and the follow-up vibrational dynamics (green dots).

References

[1] Calegari F *et al.*, Science **346**, 336-339 (2014).
[2] Marciniak A *et al.*, Nat. Commun. **10**, 337 (2019).
[3] Hervé M *et al.*, Nat. Phys. **17**, 327–331 (2021).
[4] Boyer A *et al.*, *submitted*.

*E-mail: alexie.boyer@univ-lyon1.fr
†E-mail: franck.lepine@univ-lyon1.fr

Production of antihydrogen pulses at AEgIS

A Camper[1,2] on behalf of the AEgIS collaboration

[1]Physics Department, CERN, 1211 Geneva, Switzerland. [2]Department of Physics, Univ. of Oslo, Sem Sælandsvei 24, 0371 Oslo, Norway.

Synopsis We report on the first production of antihydrogen pulses by charge exchange between a cold plasma of antiprotons and pulses of positronium atoms excited to Rydberg levels. 90% of the antihydrogen atoms are produced within a window of 250 ns. This achievement brings the AEgIS collaboration one step closer to the first measurement of neutral antimatter atoms free fall in the Earth's gravitational field. The principle of the time of flight measurement through a moiré interferometer will also be presented.

The antiproton decelerator (AD) at CERN was built some 20 years ago to investigate the origin of the baryonic assymetry, which is the reason for our Universe to be made mostly of matter and contain so little antimatter. The AD (soon to be completed by the Extremely Low ENergy Antiproton decelerator) provides different experiments with cold antiprotons that can be used to produce cold antihydrogen, with the idea to search for a violation of the Charge, Parity and Time reversal symmetry in the spectroscopic properties of antihydrogen compared to those of hydrogen and to probe the foundations of General Relativity by measuring the free fall of antihydrogen in the Earth's gravitational field.

Two techniques have been developed to produce antihydrogen $\bar{\mathrm{H}}$: charge mixing [1] (the three-body collision of two positrons and one antiproton $\bar{\mathrm{p}}$) and charge exchange [2] (the collision between one antiproton and a positronium atom). The AEgIS (Antihydrogen Experiment: gravity, Interferometry, Spectroscopy) collaboration developed a new implementation of the charge exchange reaction making use of short pulses of positronium laser excited to Rydberg states (Ps^* in equation 1).

$$Ps^* + \bar{\mathrm{p}} \rightarrow e^- + \bar{\mathrm{H}}^* \qquad (1)$$

Thanks to the controlled timing of the production of positronium pulses, AEgIS improved the accuracy on the antihydrogen production timing by three orders of magnitude compared to previous experiments. The formation process happens within a window of 250 ns (full-width at half-maximum).

This achievement is a milestone that opens the road to the first test of the Weak Equivalence Principle (the fact that everything massive falls at the same rate in a given gravitational field) on neutral antimatter atoms. Controlling the $\bar{\mathrm{H}}$ production time is indeed a requirement to measure the time of flight through the moiré deflectometer thought for the measurement of the free fall of $\bar{\mathrm{H}}$ [5].

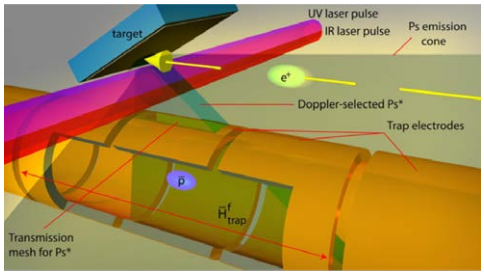

Figure 1. Blow-up of the antihydrogen production region in the AEgIS apparatus. The antiproton trap is located 1.3 cm below the target acting as a positron to positronium converter. The traps' electrodes located below the Ps converter are semi-transparent on top of the antiproton plasma to allow the passage of Ps^*. Two nanosecond laser pulses are used to excite Ps atoms into the Rydberg state [3]. Figure reproduced from [4].

We will present the pulsed production of $\bar{\mathrm{H}}$ at AEgIS and review the following steps towards the first gravity measurement on neutral antimatter.

References

[1] Amoretti M *et al* 2002 *Nature* **419** 456-459
[2] Storry C H *et al* 2004 *Phys. Rev. Lett.* **93** 263401
[3] Antonello M *et al* 2020 *Phys. Rev. A* **102** 013101
[4] Amsler C *et al* 2021 *Comm. Phys.* **4** 1
[5] Aghion S *et al* 2014 *Nat. Comm.* **5** 4538

Photoemission and state-selected fragmentation in cyclic dipeptides containing an aromatic amino acid

L Carlini[1] *, E Molteni[1], P Bolognesi[1], D Sangalli[1], G Mattioli[1], P Alippi[1], A Casavola[1], M Singh[2], C Altucci[2], M Valadan[2], M Nisoli[3,4], Y Wu[3], F Vismarra[3,4], R Borrego Varillas[4], R Richter[5], J Chiarinelli[1], M C Castrovilli[1] and L Avaldi[1]

[1]CNR - Istituto di Struttura Della Materia (CNR - ISM), Area della Ricerca di Roma 1, Monterotondo Scalo, Italy
[2]Università degli Studi di Napoli Federico II, Dipartimento di Fisica, Napoli, Italy
[3]Politecnico di Milano, Dipartimento di Fisica, Milano, Italy
[4]CNR - Istituto di Fotonica e Nanotecnologie (CNR - IFN), Milano, Italy
[5]Elettra, Sincrotrone Trieste S.C.p.A., Trieste, Italy

Synopsis A combined experimental and theoretical study of the electronic structure and the state-selected fragmentation of cyclic dipeptide cations (*c*-GlyPhe, *c*-TrpTrp and *c*-TrpTyr) containing an aromatic amino acid has been performed. The systematic ab-initio study allowed to explore geometry, energy levels, electronic wave-functions and optical properties of these dipeptides.

Among the cyclic(*c*)-dipeptides, the ones containing an aromatic amino acid are of interest for the study of the dynamics involving the transfer of charge and excitation energy [1], which are relevant processes in bio-systems.

We have undertaken a combined experimental and theoretical study of the electronic and optical properties of the *c*-GlyPhe, *c*-TrpTrp and *c*-TrpTyr dipeptides. In this work we report valence photoemission (PES), mass spectrometry (MS) and photoelectron-photoion, PEPICO, measurements done at 60 eV photon energy [2]. From the PEPICO measurements, the partial ion yield of the main fragments as a function of the binding energy (BE) has been extracted. The experiments have been performed at the CIPO beamline [3] of the Elettra synchrotron radiation facility.

In Figure 1 an example of the results for the case of *c*-TrpTyr is shown. The mass spectrum shows a very small amount of parent ion (m/z=349), a dominant contribution at m/z=130 attributed to the aromatic terminal (C_9H_8N) of the Trp aminoacid and a small feature at m/z=107. The fragmentation channel leading to $C_9H_8N^+$ opens at very low BE and is very stable up to the BE=26 eV. This suggests that, independently of the ionized orbital, the charge migrates to the Trp aromatic terminal, which is then lost as a charge fragment during dissociation.

DFT calculations of the electronic levels and density of states (DOS) of the three molecules have been performed with different choices of the exchange-correlation functional and the calculated DOS have been compared with the experimental PES spectra.

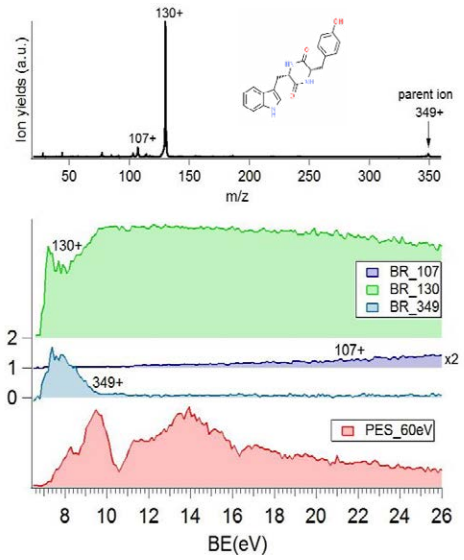

Figure 1. The mass spectrum (top panel), the partial ion yield of the main fragments (central panel) and the PES spectrum (bottom panel) of *c*-TrpTyr molecule obtained at 60 eV incident radiation.

Acknowledgment: PRIN 20173B72NB "Predicting and controlling the fate of biomolecule driven by extreme-ultraviolet radiation".

References

[1] R. Weinkauf et al,J.Phys.Chem.,1996,100,18567-18585.
[2] J. Chiarinelli et al,Phys.Chem.Chem.Phys.,2018,20, 22841-22848.
[3] A. Derossi et al, Rev.Sci.Instrum.,1995,66,1718-1720.

* E-mail: laura.carlini@ism.cnr.it

Excitation and ionisation cross-sections of condensed-phase biomaterials by electrons down to very low energy

R Garcia-Molina[1]*, I Abril[3], and P de Vera[2]†

[1]Departamento de Física – Centro de Investigación en Óptica y Nanofísica, Universidad de Murcia, Murcia, 30100, Spain
[2]Departament de Física Aplicada, Universitat d'Alacant, Alacant, 03080, Spain
[3]European Centre for Theoretical Studies in Nuclear Physics and Related Areas (ECT*-FBK) and Trento Institute for Fundamental Physics and Applications (TIFPA- INFN), Trento, 38123, Italy

Synopsis We present a model for the calculation of excitation and ionisation cross-sections of electrons in biomaterials, which takes into account in a suitable manner the condensed-phase nature of the targets. This theoretical procedure provides both differential and total cross sections, down to very low electron energies, in very good agreement with the available experimental data for water and the DNA/RNA molecular components.

Electronic excitations and ionisations produced by electron impact are key processes in the radiation-induced damage mechanisms in materials of biological relevance, underlying important medical [1] and technological applications [2]. Due to the arduous task of experimentally measuring all the necessary electronic interaction cross-sections for every relevant material, we have developed a predictive model [3], sufficiently accurate and easily implementable, based on the dielectric formalism, to provide reliable ionisation and excitation cross-sections for electron-impact on complex biomolecular media, taking into account their condensed-phase nature.

Our model accounts for the indistinguishability and exchange between the primary beam and excited electrons, for the molecular electronic structure effects in the electron binding, as well as for low-energy corrections to the first Born approximation. The resulting approach yields total ionisation and electronic excitation cross-sections for condensed-phase biomaterials (see Fig. 1), as well as energy distributions of secondary electrons, once the electronic excitation spectrum is known from experiments or a predictive model.

The comparison with the available experimental data of the results obtained for water and DNA/RNA molecular building blocks by this procedure shows a very good agreement and a great predictive power in a wide range of electron incident energies, from the large values characteristic of electron beams down to excitation threshold.

The proposed model constitutes a very useful procedure for computing the electronic interaction cross-sections, which are fundamental ingredients in Monte Carlo simulations, for arbitrary biological materials in a wide range of incident electron energies.

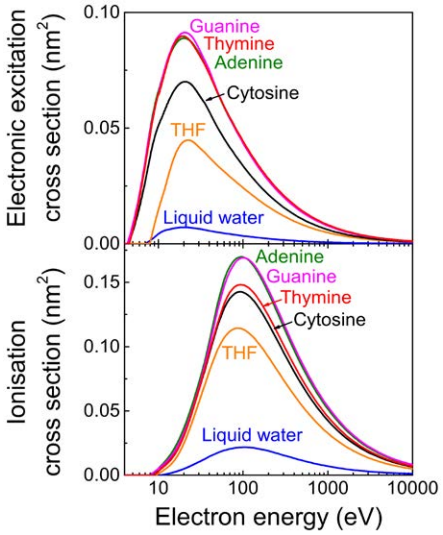

Figure 1. Calculated electronic cross sections of several biomaterials in condensed-phase.

References

[1] Solov'yov A V (ed.) 2017 *Nanoscale Insights into Ion-Beam Cancer Therapy*, Springer International Publishing AG, Cham, Switzerland
[2] de Vera P *et al* 2020 *Sci. Rep.* **10** 20827
[3] de Vera P, Abril I, and Garcia-Molina R 2021 *Phys. Chem. Chem. Phys.* **23** 5079-5095

*E-mail: rgm@um.es
†E-mail: pdeveragomis@ectstar.eu

Complete quantum coherent control of ultracold molecular collisions

A. Devolder[1] *, P. Brumer[1] and T. V. Tscherbul[2]

[1]Chemical Physics Theory Group, Department of Chemistry, and Center for Quantum Information and Quantum Control, University of Toronto, Toronto, Ontario, M5S 3H6, Canada
[2]Department of Physics, University of Nevada, Reno, NV, 89557, USA

Synopsis We show that coherent control is a promising method for tuning the quantum dynamics of ultracold bimolecular collisions. Complete control is demonstrated over ultracold thermoneutral (elastic) scattering and spin-exchange transitions in O_2-O_2 collisions.

Coherent control of scattering events relies on tuning the values of scattering properties (such as collision cross sections) via quantum interferences, induced by prior preparation of coherent superpositions of molecular states [1]. This method has the advantage of being a field-free control method for ultracold collisions rather than being reliant, as other methods are, on the use of external electromagnetic fields.

Two factors limit the extent of coherent control of state-to-state integral cross-sections: the partial wave expansion and the contributions of satellite terms. The former is a problem for coherent control because partial waves are independent and thus do not interfere with one another. The latter are uncontrollable contributions due to the absence of interferences owing to symmetry requirements (i.e. energy conservation, angular momentum projection conservation, etc).

We demonstrate that these two issues can be solved for ultracold thermoneutral (elastic) collisions [2], leading to dramatic control. In this case, only the s-wave is involved before and after the scattering. Furthermore, the satellite contributions are negligible due to the Wigner threshold laws. Then, complete control is achieved with the possibility of complete destructive interference. We develop an analytical model for the control parameters and illustrate the complete control of spin-exchange transitions in O_2-O_2 scattering. An extended range of control over 9 orders of magnitudes is observed for the integral cross-sections, and over 17 orders of magnitude for branching ratios (see figure).

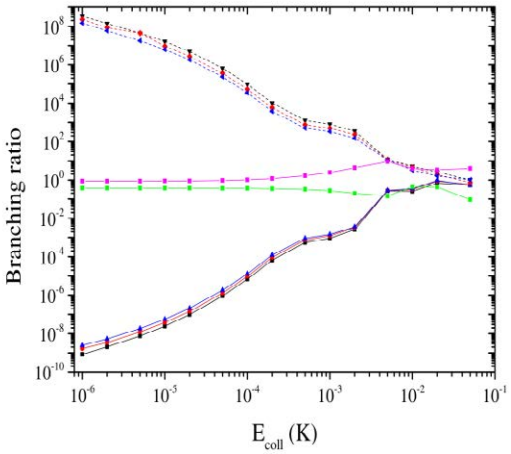

Figure 1. Minimum and maximim branching ratios for several initial superpositions of O_2 spin states, which differ by the satellite terms.The branching ratios in the absence of control are also shown in magenta and green.

References

[1] M. Shapiro and P. Brumer, Quantum control of Molecular Processes (Wiley-VCH, 2012)
[2] A. Devolder, P. Brumer and T. V. Tscherbul, Complete Quantum Coherent Control of Ultracold Molecular Collisions, *Phys. Rev. Lett.* (in press), arXiv: https://arxiv.org/abs/2012.10269

* E-mail: adrien.devolder@utoronto.ca

Holographic Angular Streaking of Electrons (HASE)

S Eckart[1]*, D Trabert[1], K Fehre[1], A Geyer[1], J Rist[1], K Lin[1,2], F Trinter[1,3], L Ph H Schmidt[1], M Schöffler[1], T Jahnke[1], M Kunitski[1], and R Dörner[1]

[1]Institut für Kernphysik, Goethe Universität, Frankfurt am Main, 60438, Germany
[2]State Key Laboratory of Precision Spectroscopy, East China Normal University, Shanghai, 200241, China
[3]Molecular Physics, Fritz-Haber-Institut der Max-Planck-Gesellschaft, Berlin, 14195, Germany

Synopsis Holographic Angular Streaking of Electrons (HASE) is a new, trajectory-based, semi-classical approach towards sub-cycle interference upon strong field ionization by circularly polarized two-color fields. HASE can be used to model the modulation of energy peaks in above-threshold ionization reaching excellent agreement with experimental results. HASE enables the retrieval of attosecond-time delays in strong field ionization just as RABBITT (reconstruction of attosecond harmonic beating by interference of two-photon transitions) can be applied to single-photon ionization.

The strong field ionization [1] of argon atoms is studied experimentally for the regime of co-rotating circular two-color (CoRTC) and counter-rotating circular two-color (CRTC) laser fields that are dominated by the second harmonic [2, 3] (central wavelengths of 780 nm and 390 nm). The three-dimensional electron momenta upon strong field ionization of argon have been measured using cold-target recoil-ion momentum spectroscopy (COLTRIMS) [4]. It is found that sidebands are almost completely suppressed for the CRTC field but are clearly visible for the CoRTC field (see Fig. 1).

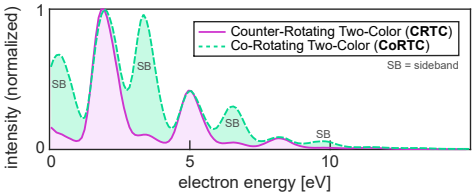

Figure 1. The measured electron energy spectra depend on the relative helicity of circularly polarized two-color fields (with peak intensities on the order of 10^{14} W/cm^2). The measured electron energy spectra upon single ionization of argon are shown for a CRTC and a CoRTC field. The sidebands are very intense for the CoRTC field and are hardly visible for the CRTC field. Sideband peaks are labeled with "SB". Figure and caption taken from [3].

The experimental findings are compared to theoretical results using holographic angular streaking of electrons (HASE) [5]. HASE is a semi-classical, trajectory-based model similar to the approaches in Refs. [6, 7]. The results from HASE are in excellent agreement with our experimental findings. The influence of Coulomb interaction after tunneling is investigated quantitatively employing a modified version of the well-established semi-classical two-step model [6].

Finally, it is shown how HASE allows to access one component of the phase-gradient of the wave function (in momentum space represenation) at the tunnel exit. The link of the phase gradient of the wave function in momentum space at the tunnel exit and the Wigner time delay [8] is explained [5, 9]. Differences with respect to the attoclock-technique [10] are discussed.

References

[1] Keldysh L W 1965 *Sov. Phys. JETP* **20** 1307
[2] Han M *et al* 2018 *Phys. Rev. Lett.* **120** 073202
[3] Eckart S *et al* 2020 *Phys. Rev. A* **102** 043115
[4] Jagutzki O *et al* 2002 *IEEE Transactions on Nuclear Science* **49** 2477
[5] Eckart S 2020 *Phys. Rev. Research* **2** 033248
[6] Shvetsov-Shilovski N I *et al* 2016 *Phys. Rev. A* **94** 013415
[7] Feng Y *et al* 2019 *Phys. Rev. A* **100** 063411
[8] Wigner E P 1955 *Phys. Rev.* **98** 145
[9] Trabert D *et al* 2021 *Nat. Commun.* **12** 1697
[10] Eckle P *et al* 2008 *Nat. Phys.* **4** 565

*E-mail: eckart@atom.uni-frankfurt.de

Imaging the structural dynamics in the photo-induced proton transfer reaction of o-nitrophenol by Ultrafast Electron Diffraction

J P F Nunes[1 *], J Yang[2], T J A Wolf[3], M Williams[2,3,4], R Parrish[2,3,4], B Moore[1], K Wilkin[1], X Shen[2], M Lin[2,3], K Hegazy[3], R Li[2], S Weathersby[2], M Gühr[5], T Martinez[2,3,4], X Wang[2], M Centurion[1]

[1]Department of Physics and Astronomy, University of Nebraska-Lincoln, 855 N 16th Street, Lincoln, USA
[2]SLAC National Accelerator Laboratory, 2575 Sand Hill Road, Menlo Park, USA
[3]Stanford PULSE Institute, SLAC, 2575 Sand Hill Rd, Menlo Park, CA, 94025, USA
[4]Department of Chemistry, Stanford University, 333 Campus Dr., Menlo Park, CA, 94305, USA
[5]Institut für Physik und Astronomie, Universität Potsdam, Potsdam, Germany

Synopsis The relaxation dynamics of o-nitrophenol following excitation to its S_1 and S_4 states were investigated using ultrafast gas-phase electron diffraction. Structural rearrangements leading to the formation of a nitrous acid motif through excited state intramolecular proton transfer, and subsequent motions enabling nitrophenol to access a conical intersection back to ground state were captured with subångström resolution.

O-nitrophenol is prototypical push-pull molecule, where, upon photoexcitation, the proximity between electron donating and withdrawing groups facilitates intramolecular charge transfer transitions and potentiates excited state intramolecular proton transfer (ESIPT); a mechanism crucial to many biological and chemical reactions. Previous spectroscopic studies [1,2] have reported the formation of nitrous acid (HONO) following ESIPT between the OH and NO_2 groups along the first excited state, S_1. This ESIPT is believed to be coupled to an out-of-plane rotation of the HONO group, which allows the system to relax back to ground state through a conical intersection [3].

Here we use megaelectronvolt ultrafast electron diffraction to spatially resolve with subångström resolution the relaxation dynamics of o-nitrophenol photoexcited to its first (S_1) and forth (S_4) excited states, using 330 and 266 nm light, respectively. Motions leading to and ensuing from ESIPT were retrieved directly from the experimental difference-diffraction signal (Figure 1) using a genetical algorithm mediated structure retrieval. Our results revealed that shortly after excitation to the S_1, the OH group moves towards the NO_2 group, causing in a transient compression of $O(H)\cdots O_2N$ separation, leading to ESIPT. Following a 250 fs delay the HONO group rotates out of the plan of the phenol ring, granting access to the S_1/S_0 conical intersection and relaxation back to the ground state. These stepwise dynamics contrast those retrived following excitation to the S_4, where the excess internal energy favours a concerted ESIPT and C-N rotation to access the conical intersection back to the ground state. These differences highlight the impact of potential energy surface topology on the motions mediating relaxation. Our assignment of nuclear motions is complemented by a computational investigation of potential energy landscapes using ab-initio multiple spawning simulations at the FOMO-CASCI(2,2)/6-31G** level of theory.

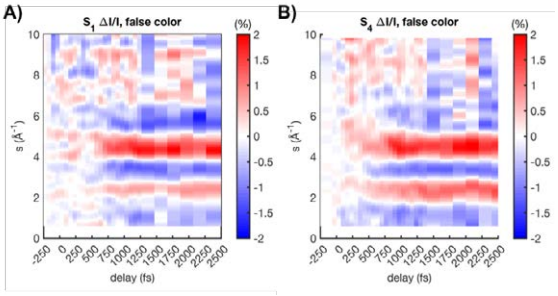

Figure 1. Time-resolved difference-diffraction as a function of momentum transfer vector, s, following excitation to the A) S_1 and B) S_4 states of o-nitrophenol. $\Delta I/I(s,t) = I(s,t>0) - I(s,t<0) / I(s,t<0)$, where $I(s,t<0)$ and $I(s,t>0)$ are the total scattering signals before and after time-zero, respectively.

References

[1] Wang Y Q *et al* 2006 *J. Chem. Phys.* **125** 214506
[2] Nitta Y Q *et al* 2021 *J. Chem. Phys. Lett.* **12** 674−679
[3] Ernst H A *et al* 2015 *J. Phys. Chem. A* **119**, 9225−9235

* E-mail: joao-pedro.figueira-nunes@unl.edu

Intramolecular charge migration in betaine by impact of fast atomic ions

J González-Vázquez[1,2]*, P Rousseau[3], D G Piekarski[1], J Kopyra[4], A Domaracka[3], M Alcamí[1,2,5], L Adoui[3], B A Huber[3], S Díaz-Tendero[1,2,6], and F Martín[1,5,6]

[1]Departamento de Química, Módulo 13, Universidad Autónoma de Madrid, 28049 Madrid, Spain
[2]Institute for Advanced Research in Chemical Sciences (IAdChem), Universidad Autónoma de Madrid, 28049 Madrid, Spain
[3]Normandie Univ, ENSICAEN, UNICAEN, CEA, CNRS, CIMAP, 14000 Caen, France
[4]Faculty of Exact and Natural Sciences, Siedlce University of Natural Sciences and Humanities, 3 Maja 54, 08-110 Siedlce, Poland
[5]Instituto Madrileño de Estudios Avanzados en Nanociencias (IMDEA Nano), 28049 Madrid, Spain
[6]Condensed Matter Physics Center (IFIMAC), Universidad Autónoma de Madrid, 28049 Madrid, Spain

Synopsis Intramolecular charge migration has been observed in the dissociation of the betaine dication following collision with low-energy ions. A rather long timescale of about 40 fs has been found in agreement with quantum chemistry calculations and is attributed to nuclear dynamics occurring in the ground state of the dication.

Electron dynamics governs the fragmentation dynamics occurring at long timescales. Experimentally, it is possible to observe this can be observed using different experimental schemes: On the one hand, it is possible to obtain the time-resolved dynamics by using pump-probe schemes, for example with high harmonic generation or free electron lasers [1]. Alternatively it is possible to clock the electronic dynamics using Coulomb explosion or electron emission after photoionization. On the other hand, electronic dynamics can also be induced with low-energy ion collisions that are characterized by a sub-fs interaction time where one can expect a "sudden" ionization. In this regime, resonant electron captures dominate and are associated with large cross sections, thus low target excitation are expected. The main disadvantage is that currently it is not possible to perform pump-probe experiments at the fs timescale with ion beams and ion collisions are not selective.

Betaine is a zwitterion molecule, i.e. with one end positively charged ($N(CD_3)_3$ group) and the other one negatively charged (CO_2 group) while the whole molecular system remains neutral. During the collision with 3 keV/amu O^{6+}, two electrons are removed from the CO_2 side leading to the formation of a dication with two holes localited at both sides. We observe two main dissociation channels as depicted in Fig.1. Beside the expected direct Coulomb explosion giving the pair $CO_2^+/(CD_2)N(CD_3)_2^+$, we observe a competitive channel following intramolecular charge migration (ICM) and giving the pair $CD_3^+/(CD_2)N(CD_3)_2^+$. These two channels are rationalized by simulating the dynamics with surface hopping semiclassical methodology where the electronic states are represented via perturbation theory based in multireference wavefunctions.

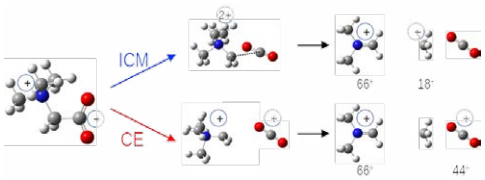

Figure 1. Ion pair coincidences in the dissociation of betaine dication following collisions with 48 keV O^{6+} ions and associated fragmentation schemes.

References

[1] Nisoli M *et al* 2017 *Chem. Rev.* **117** 10760

*E-mail: jesus.gonzalezv@uam.es

The travel time of light across a molecule

S Grundmann[1]*, D Trabert[1], K Fehre[1], N Strenger[1], A Pier[1], L Kaiser[1], M Kircher[1], M Weller[1], S Eckart[1], L Ph H Schmidt[1], F Trinter[1,2,3], T Jahnke[1], M S Schöffler[1] and R Dörner[1]†,

[1]Institut für Kernphysik, Goethe-Universität, 60438 Frankfurt, Germany
[2]Photon Science, Deutsches Elektronen-Synchrotron (DESY), 22607 Hamburg, Germany
[3]Molecular Physics, Fritz-Haber-Institut der Max-Planck-Gesellschaft, 14195 Berlin, Germany

Synopsis Photoelectron emission from the H_2 molecule mimics the double-slit experiment. For one-photon double ionization of H_2 at 800 eV photon energy, we have measured asymmetries in the electron interference pattern that can be interpreted as a result of the finite travel time of light across the molecule.

In a recent experimental work [1], we adressed the question whether a spatially extended molecular orbital reacts simultaneously upon photoionization. We used the P04 beamline at PETRA III (DESY) and applied a reaction microscope to investigate one-photon double ionization of H_2 at 800 eV photon energy. We obtained the double-slit-like photoelectron interference pattern in the molecular frame of reference by measuring the three-dimensional momentum vectors of all reaction fragments [2].

Depending on the angle between the light direction and the molecular axis (β), we found asymmetries in the interference pattern of fast electrons (Fig. 1b, electron energy 735 ± 15 eV). For a quantitative analysis, we determined α_0—the angle to which the zeroth-order interference maximum is shifted—by means of a Gaussian fit (e.g. Fig. 1a for parallel alignment of light and molecule). The mean of the fitted Gauss is presented in Fig. 1c as function of β. The observed asymmetries suggest a phase difference at birth time between the two superimposing waves, which can be the result of the finite travel time of light across the molecule. The birth time delay τ—between electron emission from one of the two protons—and α_0 are related through

$$\tau = \cos a_0 \frac{R}{v_{ph}} , \qquad (1)$$

where R is the internuclear distance and v_{ph} is the phase speed of the photoelectron wave. The time delays as obtained from Eq. (1) are shown in Fig. 1c (right axis). For comparison, the blue line resembles $\tau = (\cos\beta \cdot R)/c$, where c is the speed of light.

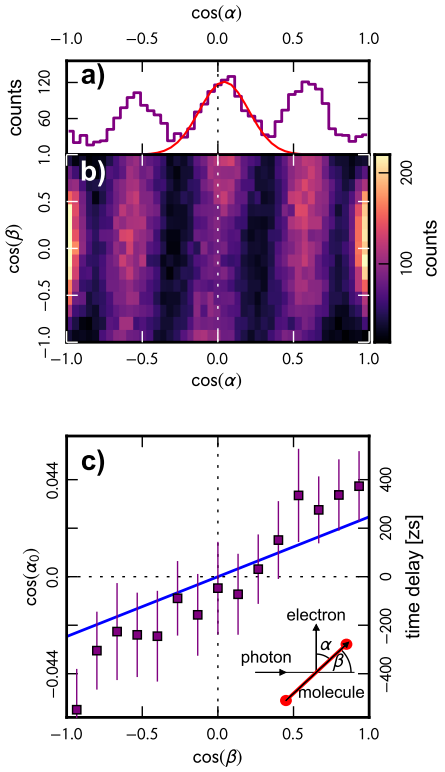

Figure 1. Results of birth time delay measurement. See text for details.

References

[1] Grundmann S *et al* 2020 *Science* **370** 339-341
[2] Akoury D *et al* 2007 *Science* **318** 949-952

*E-mail: grundmann@atom.uni-frankfurt.de
†E-mail: doerner@atom.uni-frankfurt.de

A molecular road movie: capturing roaming molecular fragments in real time

T. Endo[1,2], S. P. Neville[3], V. Wanie[1], S. Beaulieu[1], C. Qu[4], J. Deschamps[1], P. Lassonde[1], B. E. Schmidt[5], H. Fujise[6], M. Fushitani[6], A. Hishikawa[6], P. L. Houston[7,8], J. M. Bowman[4,9], M. S. Schuurman[3,10], F. Légaré[1*], and H. Ibrahim[1†]

[1]Institut National de la Recherche Scientifique, Centre ÉMT, Varennes, QC J3X 1S2 Canada
[2]Kansai Photon Science Institute (KPSI), QST, Kyoto 619-0215, Japan
[3]National Research Council of Canada, 100 Sussex Drive, Ottawa, ON K1A 0R6, Canada
[4]Department of Chemistry & Biochemistry, University of Maryland, Maryland 20742, USA
[5]few-cycle Inc., Montreal, QC H1L 5W5 Canada
[6]Department of Chemistry, Research Center for Materials Science, Nagoya University, Nagoya, 464-8602, Japan
[7]Department of Chemistry and Chemical Biology, Cornell University, Ithaca, NY 14852, USA
[8]School of Chemistry and Biochemistry, Georgia Institute of Technology, Atlanta, Georgia 30332, United States
[9]Dept. of Chemistry and Cherry L. Emerson Center, Emory University, Atlanta, Georgia 30322, USA
[10]Department of Chemistry and Biomolecular Sciences, University of Ottawa, Ottawa, ON K1N 6N5, Canada

Synopsis Roaming molecular fragments are directly observed in the prototypical roaming reaction in the formaldehyde molecule. Despite their statistical nature, roaming is well discriminated from the radical- and molecular dissociation channels, using Coulomb explosion imaging and theoretical modeling for every critical experimental step.

Since the discovery of roaming as an alternative molecular dissociation pathway in formaldehyde (H_2CO) in 2004 [1], it has been indirectly observed in numerous molecules. The phenomenon describes a frustrated dissociation with fragments roaming at relatively large interatomic distances rather than following conventional transition-state dissociation; incipient radicals from the parent molecule self-react to form molecular products. Roaming has been in general identified using high-resolution spectroscopy through static product channel – resolved measurements, but not in real-time observations of the roaming fragment itself. Using time-resolved Coulomb explosion imaging (CEI), a technique sensitive to single molecule, we directly imaged individual "roamers" on ultrafast time scales in the prototypical formaldehyde dissociation reaction [2]. Using high-level first-principles simulations of all critical experimental steps, distinctive roaming signatures were identified. These were rendered observable by extracting rare stochastic events out of an overwhelming background using the highly sensitive CEI method. Also, the identification of transient features allowed to generalize the definition of roaming.

Here presented technique is applicable to the observation of stoachastic events in general.

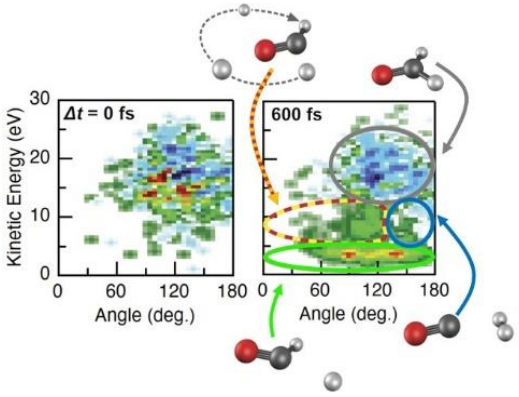

Figure 1. Experimental data of total kinetic energy release vs. angle between both deuteron momentum vectors for time zero (left) and a pump probe time delay of 600 fs (right). Areas corresponding to different dissociation pathways are indicated as: equilibrium (grey), roaming (yellow-orange dashed), molecular dissociation (blue) and radical dissociation (green).

References

[1] D. Townsend et al., *Science* **306**, 1158 (2004)
[2] T. Endo, et al., *Science*, **370**, 1072 (2020)

* E-mail: francois.legare@inrs.ca
† E-mail: heide.ibrahim@inrs.ca

Inner-shell-ionization-induced femtosecond structural dynamics of water molecules imaged in real time at an x-ray free-electron laser

L Inhester[1]*, T Jahnke[2], R Guillemin[3], S-K Son[1], G Kastirke[4], M Illchen[2,5], J Rist[4], D Trabert[4], N Melzer[4], N Anders[4], T Mazza[2], R Boll[2], A De Fanis[2], V Music[2,5], T Weber[6], M Weller[4], S Eckart[4], K Fehre[4], S Grundmann[4], A Hartung[4], M Hofmann[4], C Janke[4], M Kircher[4], G Nalin[4], A Pier[4], J Siebert[4], N Strenger[4], I Vela-Perez[4], T M. Baumann[2], P Grychtol[2], J Montano[2], Y Ovcharenko[2], N Rennhack[2], D E Rivas[2], R Wagner[2], P Ziolkowski[2], P Schmidt[2,5], T Marchenko[3], O Travnikova[3], L Journel[3], I Ismail[3], E Kukk[7], J Niskanen[7], F Trinter[8,9], C Vozzi[10], M Devetta[10], S Stagira[11], M Gisselbrecht[12], A L Jäger[13], X Li[14], Y Malakar[14], M Martins[15], R Feifel[16], L Ph H Schmidt[4], A Czasch[4], G Sansone[13], D Rolles[14], A Rudenko[14], R Moshammer[17], R Dörner[4], M Meyer[2], T Pfeifer[17], M S Schöffler[4], R Santra[1,18], M Simon[3], M N Piancastelli[3,19]

[1]Center for Free-Electron Laser Science, DESY, Hamburg, D-22607, Germany [2]European XFEL GmbH, Schenefeld, D-22869, Germany [3]Sorbonne Université, CNRS, LCPMR, Paris, F-75005, France [4]Institut für Kernphysik, Goethe-Universität, Frankfurt am Main, D-60438, Germany [5]Institut für Physik und CINSaT, Universität Kassel, Kassel, D-34132, Germany [6]Lawrence Berkeley National Laboratory, Chemical Sciences, Berkeley, California 94720, USA [7]Department of Physics and Astronomy, University of Turku, Turku, FI-20014, Finland [8]FS-PETRA-S, DESY, Hamburg, D-22607, Germany [9]Fritz-Haber-Institut der Max-Planck-Gesellschaft, Berlin, D-14195, Germany [10]IFN - Instituto di Fotonica e Nanotecnologie, CNR, Milan, I-20133, Italy [11]Politecnico di Milano, Milan, Italy [12]Department of Physics, Lund University, Lund, SE-22100, Sweden [13]Physikalisches Institut, Universität Freiburg, Freiburg, D-79104, Germany [14]Department of Physics, Kansas State University, Manhattan, Kansas 66506, USA [15]Institut für Experimentalphysik, Universität Hamburg, Hamburg, D-22761, Germany [16]Department of Physics, University of Gothenburg, Gothenburg, SE-412 96, Sweden [17]Max-Planck-Institut für Kernphysik, Heidelberg, D-69117, Germany [18]Department of Physics, Universität Hamburg, Hamburg, D-20355, Germany [19]Department of Physics and Astronomy, Uppsala University, Uppsala, SE-751 20, Sweden

Synopsis We have exposed isolated water molecules to short x-ray pulses from a free-electron laser and detected momenta of all produced ions in coincidence. By combining experimental results and theoretical modeling, we can image the dissociation dynamics of water in unprecedented detail and uncover fundamental dynamical patterns relevant for the radiation damage in aqueous environments.

The response of molecules to ionizing radiation is of utmost relevance to many research areas. Multi-coincidence signals from experiments at x-ray free-electrons lasers provide us new opportunities to study the dynamics of molecules upon inner-shell ionization.

We have exposed water vapor to intense x-ray pulses and recorded coincidently all the resulting ion fragments. With the help of ab-initio simulation employing the XMOLECULE toolkit [1, 2], we have followed the dynamics theoretically involving several photoionizations and Auger decay steps. The resulting ion momenta are in excellent agreement with the coincidence measurements. Through rigorous analysis, we have identified distinct signatures in the final momentum data of highly charged ions that allow us to reveal unique details on the dynamics of water molecules following inner-shell ionization and Auger decay. This way, we show unambiguously that a considerable amount of water molecules exhibit rapid angle opening dynamics and asymmetric dissociation, each of which leaves a characteristic feature in the final momentum data. From their kinetic-energy dependence and their depletion for higher charged ions, we can image how the dynamics evolve on a timescale of a few fs. The identified dynamical patterns provide new insight into the inner-shell-ionization induced dynamics of water that is relevant for our general understanding of radiation chemistry in aqueous environments [3].

*E-mail: ludger.inhester@desy.de

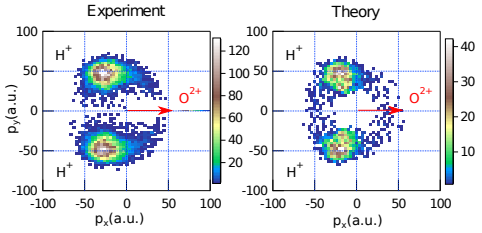

Figure 1. Newton diagram for H_2O^{4+}.

References

[1] Hao Y *et al.* 2015 *Struct. Dyn.* **2** 041707
[2] Inhester L *et al.* 2017 *Phys. Rev. A* **94** 023422
[3] Jahnke T, Guillemin R, Inhester L, *et al. in review*

Dissociative recombination of OH^+ at the Cryogenic Storage Ring

Á Kálosi[1,2]*, K Blaum[2], L Gamer[2], M Grieser[2], R von Hahn[2], L W Isberner[3,2], J I Jäger[2], H Kreckel[2], D Paul[2], D W Savin[1], V C Schmidt[2], A Wolf[2] and O Novotný[2]

[1]Columbia Astrophysics Laboratory, Columbia University, New York, 10027 New York, USA
[2]Max-Planck-Institut für Kernphysik, 69117 Heidelberg, Germany
[3]I. Physikalisches Institut, Justus-Liebig-Universität Gießen, 35392 Gießen, Germany

Synopsis
We have carried out experimental studies of the dissociative recombination (DR) of rotationally cold OH^+ molecules with free electrons at the Cryogenic Storage Ring (CSR) in Heidelberg, Germany. The low-temperature DR rate coefficient of OH^+ in its vibrational and rotational ground state is important for astrochemical models, as it is frequently used to infer the cosmic-ray ionization rate of atomic H and other fundamental parameters of diffuse interstellar clouds from astronomical observations.

The cosmic-ray ionization rate of atomic H is an influential parameter of diffuse interstellar cloud models. OH^+ formation is closely linked to the cosmic-ray ionization rate of atomic H, where charge transfer of the resulting protons with atomic O initiates a reaction chain that may lead to the gas-phase formation of interstellar water. The resulting O^+ can undergo hydrogen abstraction with H_2 to form OH^+. However, reactions with H_2 (forming H_2O^+) can also rapidly destroy the OH^+ ions. A steady-state analysis of this system, including the competing destruction pathway of DR with free electrons, allows to estimate the cosmic-ray ionization rates from the observed OH^+ abundances. But such models require reliable rate coefficients that account for the internal excitation of the reactants.

We have stored fast OH^+ ion beams in the cryogenic environment of CSR. Previous studies showed that infra-red active diatomic hydrides will relax to their lowest rotational states within minutes of storage inside CSR [1]. Here, we present merged beams experiments for OH^+ interacting with free electrons produced in a low-energy electron cooler, which enables electron-ion collision studies at translational temperatures as low as $\sim$ 10 K. At these energies, the electrons can not only neutralize OH^+ via DR but can also rotationally excite and de-excite the molecules. We took special care in the present experiments to prepare the stored ion beam with a well-characterized rotational population while recording DR spectra as a function of center-of-mass collision energy.

Despite the fundamental importance of OH^+, previous high-resolution storage ring experiments are scarce. In Figure 1 we compare our preliminary results with literature values [2] in the collision energy range from 60 meV to 360 meV, to highlight the difference in resolution. Here, we will present our preliminary results for the full DR spectrum.

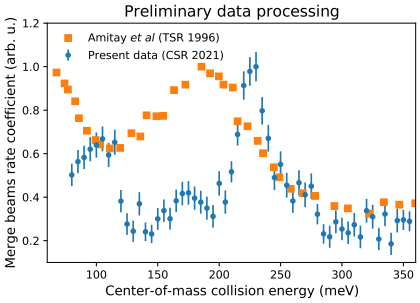

Figure 1. Merged beams rate coefficients plotted as a function of center-of-mass collision energy. The preliminary dataset (CSR) is compared to a previous experiment performed at the Test Storage Ring (TSR) [2], to highlight the gain in experimental resolution. Both datasets are arbitrarily normalized such that the maximum values in the shown energy range are equal to one.

This project is supported, in part, by the NASA Astrophysics Research and Analysis program under grant 80NSSC19K0969 and by the Max Planck Society.

References

[1] O'Connor A P *et al* 2016 *Phys. Rev. Lett.* **116** 113002
[2] Amitay Z *et al* 1996 *Phys. Rev. A* **53** R644

*E-mail: abel.kalosi@hotmail.com

Time resolved atomic ionization processes and tests of the fundamental threshold laws

A S Kheifets[1]*, A W Bray[1] and I Bray[2]

[1]Research School of Physics, The Australian National University, Canberra ACT 2600, Australia
[2]Curtin Institute for Computation and Department of Physics, Curtin University, Perth, WA 6845, Australia

Synopsis Time-resolved atomic photoionization and photodetachment processes are taken towards the reaction thresholds to probe the fundmental physics of one- and two-electron escapes at low energy. This opens up the route towards direct tests of the Wigner and Wannier threshold laws in the time domain.

Discrete and continuous parts of absorption spectra merge continuously across the ionization threshold [1]. A process of reconstruction of attosecond beating by interference of two-photon transitions (RABBITT) reveals a similar phenomenon [2]. In RABBITT, primary XUV driven ionization is aided by secondary IR photon absorption or emission. The latter processes involve transitions between continuous states. We demonstrate that when RABBITT crosses the ionization threshold and proceeds via a discrete bound state, its phase makes a sudden jump, as illustrated in Figure 1, which can be related to the phase of the continuous transitions above the threshold. Up to now, this phase remained undetermined experimentally and could only be estimated theoretically. The under-threshold RABBITT provides alternative means of assessing this quantity. Above the threshold, the RABBITT phase remains a smooth function of the photoelectron energy and can be extrapolated to the limit $E \to 0$.

The photoelectron group delay, also known as the Wigner time delay (WTD), is examined under conditions when it is strongly enhanced by many-electron correlations [3]. To illustrate these cases, we select the lowest excitation and the double detachment thresholds in the H^- and Li^- ions. Near the $n = 2$ excitation threshold in H^-, the WTD remains finite while showing a sharp angular dependence. In contrast, the WTD in Li^- is divergent at the $2p$ threshold due to the Wigner cusp while its angular dependence is mild. Both ions display a divergent WTD above the double photodetachment threshold which is characteristic for the Wannier two-electron escape. Experimental verification of these theoretical predictions can shed new light on the Wigner and Wannier threshold laws studied in the time domain. Up to now, these tests have only been conducted in the energy domain.

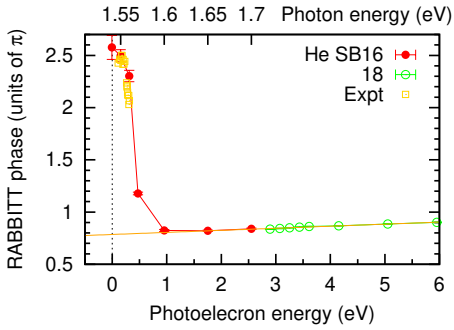

Figure 1. The RABBITT phases of sidebands 16 and 18 in He are plotted as functions of the corresponding photoelectron energy $E_{2q} = 2q\omega - I_p$. The data points are obtained by sweeping the central IR frequency ω across the range $1.53 - 1.70$ eV. The solid line extrapolates the RABBITT phase towards the threshold. Experimental data from [4] are exhibited with orange open circles.

References

[1] Fano U, Cooper JW 1968 *Rev. Mod. Phys.* **40** 441
[2] Kheifets AS, Bray AW 2021 *Phys. Rev. A* **103** L011101 Letter
[3] Kheifets AS, Bray I 2021 *Phys. Rev. Lett.* under review
[4] Swoboda M *et al.* 2010 *Phys. Rev. Lett.* **104** 103003

*E-mail: A.Kheifets@anu.edu.au

Laser spectroscopy of forbidden transitions between metastable excited states of I^{7+} in an electron beam ion trap

N Kimura[1]*, Priti[2], Y Kono[2], P Pipatpakorn[2], K Soutome[2], R Kodama[2], N Numadate[3], S Kuma[1], T Azuma[1] and N Nakamura[2]

[1]Atomic, Molecular and Optical Physics laboratory, RIKEN, Saitama, 351-0198, Japan
[2]Institute for Laser Science, The University of Electro-Communications, Tokyo, 182-8585, Japan
[3]Komaba Institute for Science, The University of Tokyo, Tokyo, 153-8902, Japan

Synopsis We demonstrate time-resolved laser spectroscopy of electric-dipole-forbidden transitions between metastable states in highly charged ions employing palladium-like I^{7+} ions stored in an electron beam ion trap. This novel spectroscopic method enables the observation of transitions with hyperfine-structure, that are not directly accessible by passive spectroscopy.

Optical transitions of highly charged ions (HCIs) are promising approach in exploring fundamental physics. Prospects for a new type of atomic clocks using forbidden transitions in HCIs have spurred further developments in HCI laser spectroscopy [1]. Resonant fluorescence laser spectroscopy and quantum logic spectroscopy of trapped HCIs have already been demonstrated by employing a simple hyperfine- or fine-structure splitting in the ground term [2, 3, 4]. Recent proposals suggest specific transitions in the complicated level structures with a $5s$-$4f$ level crossing as a candidate for an HCI clock transition [1]. Extension of HCI laser spectroscopy to such complex systems involving three or more levels possesses new experimental challenges to be overcome.

Recently, we succeed in observing laser induced fluorescence (LIF) spectra of I^{7+} in an electron beam ion trap (EBIT), as shown in Figure 1. The electric-quadrupole (E2) emission $((4d_{3/2}^{-1}5s)_{J=2} \rightarrow (4d^{10})_{J=0})$ induced by pulsed laser excitation via the magnetic-dipole (M1) transition $((4d_{5/2}^{-1}5s)_{J=3} \rightarrow (4d_{3/2}^{-1}5s)_{J=2})$ was observed by a time-resolved extreme ultraviolet spectrometer with wavelength dispersion directly coupled to the EBIT. The collisional and radiative processes in the EBIT plasma prepare a high population in the long-lived metastable state $(4d^{-1}5s)_{J=3}$ [5] and make it possible to repeatably induce the E2 emission without depletion of the population. The narrow natural width of the transition between the metastable states without electric-dipole (E1) decay paths enables us to perform high-precision wavelength measurements revealing their hyperfine-structure. This method can also be applied to state-selective lifetime measurements that eliminate the contribution of the cascade processes from the higher levels.

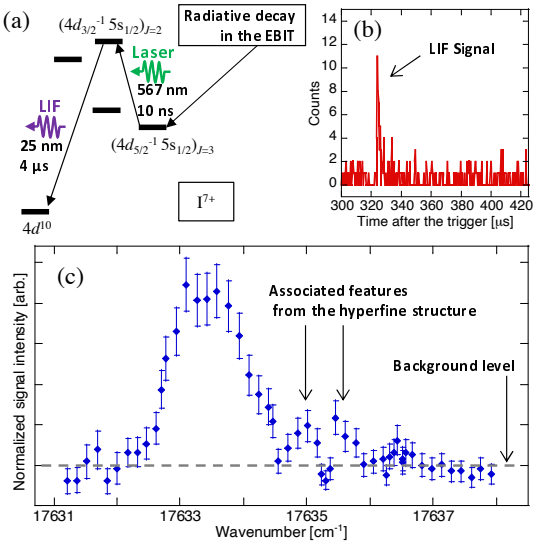

Figure 1. (a) Schematic energy level diagram of I^{7+}. (b) Typical LIF signal from I^{7+} ions trapped in the EBIT. (c) LIF spectrum of the I^{7+} $(4d_{3/2}^{-1}5s)_{J=2}$ - $(4d_{5/2}^{-1}5s)_{J=3}$ transition with hyperfine-structure.

References

[1] Kozlov M *et al* 2018 *Rev. Mod. Phys.* **90** 045005
[2] Klaft I *et al* 1994 *Phys. Rev. Lett.* **73** 2425
[3] Mäckel V *et al* 2011 *Phys. Rev. Lett.* **107** 143002
[4] Micke P *et al* 2020 *Nature(London)* **578** 60
[5] Kimura N *et al* 2020 *Phys. Rev. A* **102** 032807

*E-mail: naoki.kimura@riken.jp

Structured ion beams produced by radiative recombination of twisted electrons

A V Maiorova[1] *, A A Peshkov[2,3] and A Surzhykov[2,3,4]

[1]Center for Advanced Studies, Peter the Great St. Petersburg Polytechnic University, 195251 St. Petersburg, Russia
[2]Physikalisch-Technische Bundesanstalt, D-38116 Braunschweig, Germany
[3]Institut für Mathematische Physik, Technische Universität Braunschweig, D-38106 Braunschweig, Germany
[4]Laboratory for Emerging Nanometrology Braunschweig, D-38106 Braunschweig, Germany

Synopsis We present theoretical study of the radiative recombination of twisted electrons into bound states of initially bare ions. Special emphasis is placed on the magnetic sublevel population of the residual H-like ions. We show that this sublevel population strongly depends on the position of an ion within the incident electron wavefront. This dependence implies that the structured beams of H-like ions can be produced in collisions with Bessel electrons at ion storage rings. Such structured beams have complex intensity and spin patterns and can become a valuable tool for future ion collision studies.

The twisted electron beams are a new tool for atomic collisions studies, which has become available in the last few years [1–3]. These beams have a helical wavefront and can carry a large projection of the orbital angular momentum (and hence a large magnetic moment) onto their propagation direction. Therefore, twisted electron beams provide an effective tool for re-investigations of fundamental atomic processes.

We present theoretical investigation of the radiative recombination of twisted Bessel electrons with initially bare ions [4]. In our analyzis a special attention is focused on the magnetic sublevels population of produced H-like ions, while the properties of recombination radiation remains unobserved. We have employed the density matrix approach and relativistic Dirac's theory to derive the general expressions for statistical tensors, which most naturally describe this population. Based on the obtained expressions, we have shown that the probability to produce an ion in a particular fine-structure state as well as relative population of its magnetic substates depends on the position b of an ion within the incident electron wavefront. This b-dependence indicates that ion beams with a complex internal structure can be produced by the radiative recombination of Bessel electrons.

We considered the capture of Bessel electrons into the ground $1s_{1/2}$ and excited $2p_{3/2}$ hydrogenic states. For the first case, the sublevels population can be visualized in terms of the polarization vector $\mathbf{P}^{(tw)}$. Detailed calculations performed for e-U^{92+} collisions have shown that $\mathbf{P}^{(tw)}$ varies significantly over the ionic positions, producing azimuthally symmetric spin patterns. Moreover, the particle density of the beam possesses azimuthal symmetry and appears as concentric high- and low-intensity rings (see Fig. 1). We also have shown the correlation between polarization and intensity patterns.

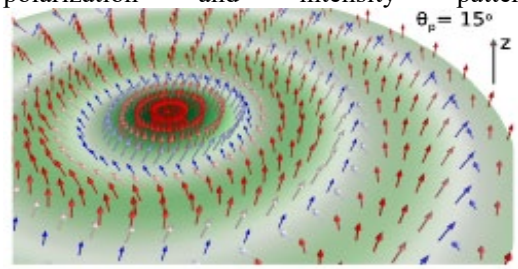

Figure 1. The intensity profile and the polarization pattern of the H-like uranium ions produced in their $1s_{1/2}$ state by the capture of twisted Bessel electrons..

Apart from the K-shell recombination, detailed analysis has been performed for the production of H-like uranium ions in the $2p_{3/2}$ state. We demonstrated that information about the structure of these (excited-ion) beams can be obtained from the analysis of the subsequent Ly-a_1 radiative decay.

References

[1] Bliokh K Y *et al* 2007 *Phys. Rev. Lett.* **99** 190404
[2] Bliokh K Y *et al* 2017 *Phys. Rep.* **690** 1
[3] Lloyd S M *et al* 2017 *Rev. Mod. Phys.* **89** 035004
[4] Maiorova A V *et al* 2020 *Phys. Rev. A* **101** 062704

* E-mail: majorova_av@spbstu.ru

Low energy electron interactions with 5-aminoimidazole-4-carboxamide

M Mendes[1*], J Pereira-da-Silva[1], R Rodrigues[1], J Ameixa[1], L M Cornetta[2], F Ferreira da Silva[1,†]

[1] CEFITEC, Departamento de Física, Faculdade de Ciências e Tecnologia, Universidade NOVA de Lisboa, Campus de Caparica, 2829–516 Caparica, Portugal
[2] Instituto de Física Gleb Wataghin da Universidade Estadual de Campinas, Brazil

Synopsis In the present communication is presented a comprehensive investigation of low energy electron interactions with 5-aminoimidazole-4-carboxamide (AIC). Parent anion formation is formed as the most intense ion apart from a wide assortment of anionic fragments. Ionization yield curves for the most abundant cations were also obtained, up to 150 eV, in order to determine the appearance energies. The obtained experimental results are supported by *ab initio* quantum chemical calculations.

DNA alkylating agents play a central role in several chemotherapy treatments for cancer diseases. Temozolomide (TMZ) is a methylating anticancer drug, and the first choice used in treatments for glioblastomas. After its oral administration, TMZ is spontaneously hydrolyzed at physiological pH in a reaction chain until it is metabolized to 5-aminoimidazole-4-carboxamide (AIC) and methyldiazonium ion. These species produces methyl adducts with DNA bases [1].

The efficiency of TMZ as anti-tumour agent is enhanced when administered concurrently with radiotherapy. The efficacy of the radiation in cancer treatments may be associated to the effect of low energy electrons (LEE) when interacting with the main components of cells, especially DNA molecule [2]. LEEs interactions with modified pyrimidines, cisplatin and nitro-aromatic compounds have shown that radiosensitizer effect is driven by those electron induced reactions [3]. Such studies have shown that the formation negative ions and radical species triggered by electron interactions are a key mechanism in physical-chemical radiosensitization.

In the present study, we describe electron ionization and dissociative electron attachment (DEA) reactions with the AIC molecule ($C_4H_6N_4O$, m/z 126), by using a trochoidal electron monochromator coupled with an orthogonal reflectron time-of-flight mass spectrometer. From the electron ionization study, ionization energy of neutral AIC is found at (9.93 ± 0.70) eV. Several cationic fragments resulted from the dissociation of AIC were also observed, notably $C_4H_4N_3O^+$ (m/z 110) and $C_4H_5N_4^+$ (m/z 109) (Figure 1). The appearance energies for the observed ions have been determined experimentally. We have also observed that electron attachment to AIC leads to the formation of the parent anion as the most abudant negative ion , with two resonances at ~0eV and 0.7 eV. In both electron ionization and electron attachment processes with AIC, the intact molecular ion is most abundant product detected.

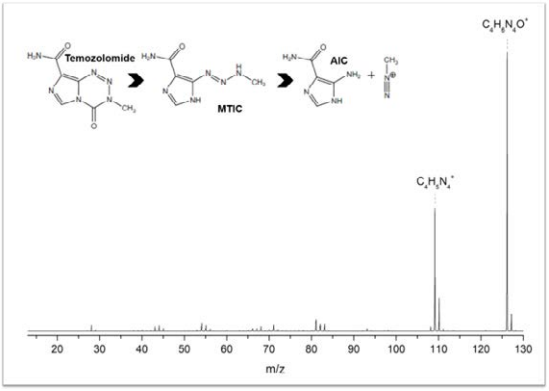

Figure 1. AIC electron ionization mass spectrum recorded at 70 eV incident electron energy.

References

[1] Denny B J *et al* 1994 *Biochemistry* 33 9045-9051
[2] Alizadeh E and Sanche L 2012 *Chem. Rev.* 112 5578
[3] Arthur-Baidoo *et al* 2020 *Angew. Chem. Int. Ed.* 59 17177–17181

* E-mail: mf.mendes@fct.unl.pt
† E-mail: f.ferreiradasilva@fct.unl.pt

The electron-thiophene scattering dynamics under the influence of multichannel coupling effects

G M Moreira[1]*, M H F Bettega[1] and R F da Costa[2]

[1]Departamento de Física, Universidade Federal do Paraná, Caixa Postal 19044, 81531-990 Curitiba, Paraná, Brazil

[2]Centro de Ciências Naturais e Humanas, Universidade Federal do ABC, 09210-580 Santo André, São Paulo, Brazil

Synopsis Integral and differential cross sections for elastic and electronically inelastic scattering of electrons by the thiophene molecule were determined by means of the Schwinger multichannel method within the static-exchange plus polarization (SEP) approximation in the energy range from 3.41 to 50 eV. We investigated the influence of multichannel coupling effects by calculating the cross sections according to an up to 61ch-SEP level of approximation, namely, a scheme where the channel coupling ranged from 1 to 61 open channels along with inclusion of polarization effects. Present results show that the inclusion of more channels in the scattering calculations leads to a significant decrease in the magnitude of the cross sections.

Thiophene is the simplest sulfur-containing heterocyclic compound. It is considered as a prototype system of biological interest and also has important technological applications such as for the development of semiconductors, solar cells, diodes, transistors, and others [1, 2]. In many of these applications, the knowledge of a complete set of cross sections for scattering processes induced by electron impact is determinant.

In the present work the excitation of thiophene by electron impact involving the electronic transitions from ground state to the $^3B_2$, $^3A_1$ and $^1B_2$ excited states was investigated by means of the Schwinger multichannel method [3]. The scattering calculations were carried out according to the MOB-SCI strategy [4] and within an up to 61ch-SEP channel coupling scheme. We report on integral and differential cross sections in the energy range from 3.41 to 50 eV with emphasis on analysing the influence of multichannel coupling on the description of the electronic excitation of thiophene by electron impact. By comparing the results obtained at the 2ch-SEP, 3ch-SEP, 4ch-SEP, 16ch-SEP, 30ch-SEP, 41ch-SEP, 48ch-SEP, 59ch-SEP and 61ch-SEP levels of approximation we found that the magnitude of the cross sections decreases as more channels are included in the calculations. In addition, flux loss due to the competition between the energetically accessible channels becomes more evident as the incident electron energy increases. Present results corresponding to our best level of channel coupling at a given energyy, both for elastic and electronically inelastic electron scattering by thiophene, displays an overall good agreement with the experimental data available in the literature for furan, as can be seen in Figure 1.

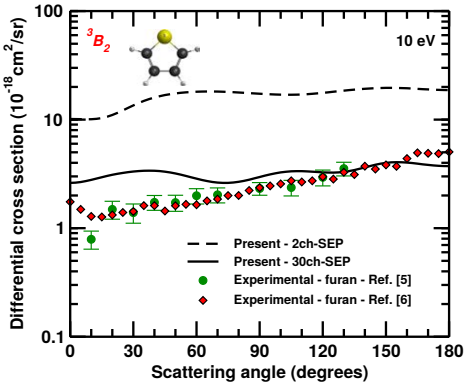

Figure 1. Differential cross section for the electronic transition from ground state to the first excited ($^3B_2$) state of thiophene compared to the experimental data for furan from Refs. [5, 6].

References

[1] Tsivgoulis G *et al* 1997 *Adv. Mater* **9** 39
[2] Staykov A *et al* 2011 *ACS Nano* **5** 1165
[3] da Costa R *et al* 2015 *Eur. Phys. J. D* **69** 159
[4] da Costa R *et al* 2005 *J. Phys. B* **38** 4363
[5] da Costa R F *et al* 2012 *Phys. Rev. A* **85** 062706
[6] Regeta K and Allan M 2015 *Phys. Rev. A* **91** 012707

*E-mail: gmm08@fisica.ufpr.br

Coherent control of ultrafast XUV transient absorption

P Peng[1,2*], Y Mi[1], M Lytova[2], M Britton[2], X Ding[1,2], A Y Naumov[1], P B Corkum[1,2], D M Villeneuve[1,2†]

[1]Joint Attosecond Science Laboratory, National Research Council and University of Ottawa, 100 Sussex Drive, Ottawa ON K1A 0R6 Canada
[2]Department of Physics, University of Ottawa, 25 Templeton St., Ottawa, ON K1N 6N5 Canada

Synopsis We demonstrated coherent control of molecular absorption line shape and optical gain in XUV. The control is achieved by creating a quantum coherence in the ground electronic state of hydrogen molecules. These observations provide new insights into control of spectral line shapes and open the way for achieving lasing-without-inversion in the XUV spectral range.

Ultrafast extreme ultraviolet (XUV) transient absorption is the process by which atoms and molecules absorb light on a timescale faster than the lifetime of the states involved [1]. Coherent control uses quantum coherences to manipulate quantum pathways in light-matter interactions. Here we combine the two. We use an early-arrived near infrared (NIR) laser to create a quantum coherence in the ground state of hydrogen or deuterium molecules, which can last much longer than the NIR pulse duration [2]. This superposition is probed with a broadband XUV pulse.

We show that this field-free coherence is well suited to controlling ultrafast XUV transient absorption. We can control the absorption spectral line shape, changing it from Lorentzian to Fano to inverted Lorentzian and back again. We show that the absorption can become negative at 12 eV, i.e. optical gain.

Fig. 1a shows the transient absorption spectra of rotational excited D_2. The modulation originates from the coherence-induced absorption line shape change. Fig. 1b shows the lineouts of OD at three different delays. The black spots in Fig. 1a and the red line in Fig. 1b show negative OD. This is the signature of optical gain.

There is no population inversion in our experiment for several reasons. First, in the pump step, the upper electronic state is unpopulated as the NIR pulse frequency is far away from resonance. Second, in the probe step, the XUV pulse based on high harmonic generation is very weak, and very little population is transferred to the upper state. Third, the NIR pulse arrives much earlier (~ 6 ps) than the XUV pulse, which removes the influence of multi-photon processes. The optical gain at 12.4 eV is a demonstration of lasing-without-inversion in the XUV. Although the gain is weak, our results greatly extend the lasing-without-inversion idea from the visible to the XUV spectral regime.

Our study provides a benchmark for the coherence-induced line shape change and lasing-without-inversion. This mechanism may widely exist in molecular systems, from rotational and vibrational wave-packets to electron excitations.

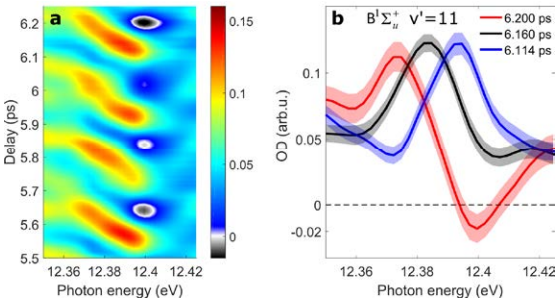

Figure 1. A Transient absorption of D_2. **a**, Transient absorption spectra OD, the black regions demonstrate negative OD. **b**, Lineouts of OD at three different pump-probe delays.

References

[1] C. Ott *et al* 2013 *Science* 340, 716-720.
[2] H. Stapelfeldt *et al* 2003 *Rev. Mod. Phys.* 75, 543.

* E-mail: pengpengnrc@gmail.com
† E-mail: David.Villeneuve@uottawa.ca

The imaginary part of the high-order harmonic cutoff

E Pisanty[1,2]*, M F Ciappina[1] and M Lewenstein[1,3]

[1]ICFO – Institut de Ciencies Fotoniques, 08860 Castelldefels (Barcelona), Spain
[2]Max Born Institute for Nonlinear Optics and Short Pulse Spectroscopy, 12489 Berlin, Germany
[3]ICREA, Passeig de Lluís Companys, 23, 08010 Barcelona, Spain

Synopsis We present a rigorous definition of the high-harmonic cutoff which is applicable to arbitrary driver waveforms. Our definition provides a natural meaning for the imaginary part of the cutoff energy, which controls the strength of quantum-path interference in the plateau. This construction radically simplifies quantum-orbit calculations. Using this definition, we build the Harmonic-Cutoff Approximation to calculate the exact location and brightness of the cutoff at a fraction of the cost of the state of the art – giving access to a much wider class of optimization tasks.

The harmonic cutoff is one of the key concepts in high-harmonic generation, but it is also an elusive object which has escaped a precise definition since its introduction in the early 1990s. In this work we provide the first natural definition for the harmonic cutoff, we show how to find it in a simple and computationally effective way, and we show how it can be used.

We build our construction on a new type of quantum orbit, which recollides at the harmonic-cutoff times t_{hc} defined by a second-order saddle-point equation for the usual action S,

$$\frac{\mathrm{d}^2 S}{\mathrm{d}t^2}(t_{\mathsf{hc}}) = 0. \tag{1}$$

The harmonic-cutoff photon energy is then given by the real part of $\Omega_{\mathsf{hc}} = \frac{\mathrm{d}S}{\mathrm{d}t}(t_{\mathsf{hc}})$. This provides a value for $\mathrm{Im}(\Omega_{\mathsf{hc}})$, which controls the strength of quantum-path interference in the plateau. The quantum orbits emerge as different branches of a unified Riemann surface, and the harmonic-cutoff times t_{hc} are the branch points that unite them.

More practically, the times t_{hc} can be used to classify the solutions of saddle-point equations into individual quantum orbits in a simple and efficient way, making saddle-point calculations much more flexible and effective.

Finally, and more importantly, the information at the times t_{hc} is enough to fully characterize the harmonic spectrum at the cutoff. This allows us to build a new approach – the Harmonic-Cutoff Approximation – which gives a quantitatively accurate estimate of the location and brightness of the cutoff, and a qualitative estimate of the spectrum in the upper plateau. This requires solving a single saddle-point equation – as opposed to dozens or hundreds of equations, as in previous approaches.

*E-mail: emilio.pisanty@mbi-berlin.de

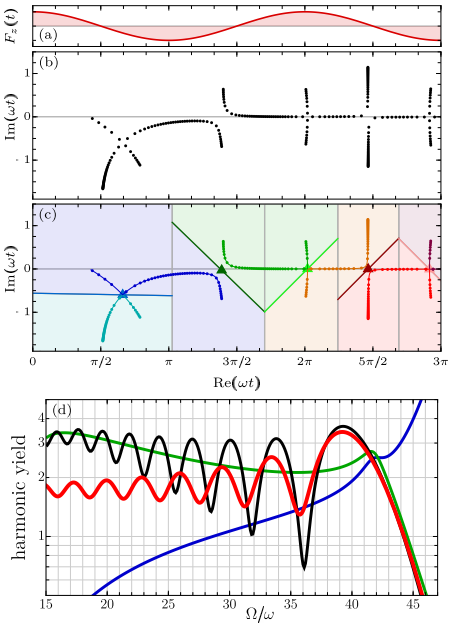

Figure 1. Solving the saddle-point equations for HHG produces an unstructured cloud of solutions, shown in (b), which need to be classified into individual quantum orbits. The harmonic-cutoff times t_{hc} (triangles, in (c)) make this classification simple. (d) The Harmonic-Cutoff Approximation (red line) matches the saddle-point approximation (black line, combining the short (blue) and long (green) trajectories) at the cutoff.

References

[1] Pisanty E *et al* 2020 *J. Phys.: Photon.* **2** 034013

Many-body theory calculations of positron scattering and annihilation in H_2, N_2, CH_4 and CF_4

C M Rawlins[1]*, J Hofierka[1], B J Cunningham[1], C H Patterson[2] and D G Green[1]†

[1]School of Mathematics and Physics, Queen's University Belfast, Belfast BT7 1NN, United Kingdom
[2]School of Physics, Trinity College Dublin, Dublin 2, Ireland

Synopsis *Ab initio* many-body theory calculations of low-energy positron scattering and annihilation on H_2, N_2, CH_4 and CF_4 are performed. The effects of positron-electron and positron-molecule correlations are delineated, and comparison with other theory and experiment is made, where possible.

Understanding the fundamental interactions of positrons with matter is important to e.g., develop positron traps, beams and positron emission tomography, and to properly interpret positron-based materials science techniques and understand positron interactions in the Galaxy.

Progress has been made describing positron-atom interactions, e.g., many-body theory calculations have given positron scattering cross sections, annihilation rates [1] and γ spectra [2], and thermalisation rates [3] all in excellent agreement with experiment. For molecules, calculations of positron binding energies have been performed via numerous approaches including quantum Monte Carlo, configuration interaction, NEO (Nuclear Electronic Orbital framework) and APMO (Any-Particle Molecular Orbital theory), finding agreement with experiment to 25% at best for small polar molecules, and failing to predict binding in non-polar molecules (see e.g., [4]). Calculations of positron scattering or annihilation in molecules are more scarce. Calculations for small molecules have been performed using sophisticated techniques including stochastic variational, *R*-matrix, Kohn-variational, diffusion Monte Carlo and Schwinger-multichannel methods, but only for positron annihilation on the smallest molecule (H_2) does theory agree adequately with experiment (see e.g., [5]).

We have developed a many-body theory description of positron interactions with polyatomic molecules [6]. Here, we use it to calculate *s*-wave positron scattering phase shifts and $Z_{\rm eff}$ *ab initio* for H_2, N_2, CH_4 and CF_4 (which do not bind the positron), delineating the effects of the positron-molecule correlations, and comparing with theory and experiment, where possible, e.g., see Figure 1, which shows the many-body theory calculated $Z_{\rm eff}$ for H_2. We solve the Dyson equation in a Gaussian basis with positron-molecule self energy calculated at the *GW*@(RPA/TDHF/BSE) levels including the virtual-positronium formation (vPs) and positron-hole (p-h) contributions. The Dyson wavefunction normalisation is determined from the energies of discretized positron positive energy pseudostates [7]. The effects of short-range positron-electron correlations on $Z_{\rm eff}$ are included via vertex enhancement factors [2].

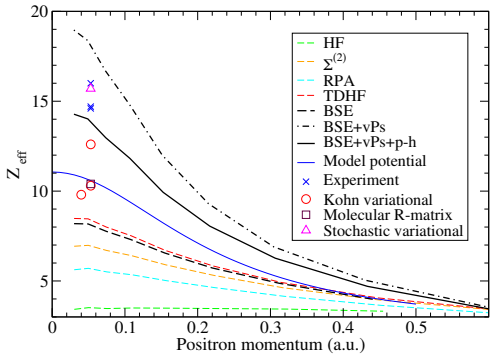

Figure 1. *s*-wave $Z_{\rm eff}$ for positrons on H_2. Many-body theory calculations in different approximations (see legend), model potential calculation [7] (blue line) and room-temperature values (see Table 2 in [5]: experiments are blue symbols, the rest from other methods).

References

[1] Green D G *et al* 2014 *Phys. Rev. A* **90** 032712
[2] Green D G *et al* 2015 *Phys. Rev. Lett.* **114** 093201
[3] Green D G 2017 *Phys. Rev. Lett.* **119** 203403
[4] Gribakin G F *et al* 2010 *Rev. Mod. Phys.* **82** 2557
[5] Green, D G *et al* 2012 *New J. Phys.* **14** 035021
[6] Cunningham B J *et al, In preparation*
[7] Swann, A. R. and Gribakin, G. F. 2020 *Phys. Rev. A.* **101** 022702

This work is funded by European Research Council grant 804383 "ANTI-ATOM".

*E-mail: c.rawlins@qub.ac.uk
†E-mail: d.green@qub.ac.uk

Radiosensitizing effect of halouracils in hadron therapy

M Roy Chowdhury[1], A Mandal[1], D Misra[1] , J M Monti[2], R D Rivarola[2], P F Weck[3] and L C Tribedi[1,*]

[1]Tata Institute of Fundamental Research, Mumbai 400005, India
[2]Instituto de Fisica Rosario, CONICET, Universidad Nacional de Rosario, 2000 Rosario, Argentina
[3]Sandia National Laboratories, Albuquerque, NM 87185, United States of America

Synopsis We present a detailed study of double differential cross section measurements for keV energy proton impact ionization of uracil and bromouracil. A large enhancement, by a factor of about 2.0, in the low energy electron production from bromouracil over uracil has been observed. This study was also extended for MeV energy highly charged ions and a similar enhancement has been obtained from bromouracil as well as iodouracil. For either projectiles, the comparison with CDW-EIS model shows a qualitative agreement.

The study of interaction of protons and highly charged ions with biological matter has gained immense importance since last decade due to it's application in cancer treatment. The favourable depth dose profile of ions make them suitable candidates for the treatment of deep seated tumours. The low energy electrons which are produced during interaction with the ion beam are responsible for creating damage to the DNA/RNA of the malignant cells[1]. Hadron therapy when combined with nanoparticles is proposed to be more effective method for cancer treatment. Due to the presence of nanoparticle of high Z (atomic number) atoms, there is an amplification in the low energy electron production when the biological matter is interacted with the high energy ion beam[2,3]. This leads to more efficient destroying of the DNA/RNA strands and eventually leads to killing of the malignant cells. Apart from different high Z elements which have shown radiosensitive properties, halouracils (5-XU, X = F, Cl, Br, I) are also expected to act as radiosensitizers.

In the present work we have measured the absolute double differential cross section (DDCS) of the electrons emitted from bromouracil and uracil in collisions with 200 keV protons. The 14.5 GHz ECR ion accelerator at TIFR, Mumbai was used to generate the 200 keV protons. The vapour jet of uracil and bromouracil were prepared by heating the powders in a metallic oven. The electron spectroscopy technique with the hemispherical electrostatic energy analyzer was used to measure the e-DDCS and the data were collected for both the targets successively under the same experimental conditions. Further similar measurements were carried out with 5.5 MeV/u C^{6+} ions obtained from the 14 MV Pelletron accelerator at TIFR. The ratio of the e-DDCS for bromouracil to uracil showed an enhancement by a factor of about 2 times for both the projectiles [4]. This enhancement could not be predicted by the CDW-EIS (continuum distorted wave-eikonal initial state) model which shows a qualitative agreement with the DDCS measurements for every angle individually. The enhancement in electron production may be explained by Auger cascade effect and collective excitation phenomena due to the presence of Br atom. However, collective excitation in Br atom is not well known. In case of 5.5 MeV/u bare C ions, the measurements were extended for iodouracil and the e-enhancement was found to be about 2.4 times [5] and this could be related to the well known atomic giant resonance in the I-atom. The present systematic study of uracil and halouracils along with the quantitative estimate of enhancement in electron production exhibiting radiosensitizing properties are expected to serve as important input for modelling of doses for proton and hadron therapy.

References

[1] Boudaiffa B *et al* 2000 *Science* **287** 1658
[2] Porcel E *et al* 2010 *Nanotech.* **21** 085103
[3] Verkhovtsev A V *et al* 2015 *Phys. Rev. Lett* **114** 063401
[4] Roy Chowdhury M, Tribedi L C *et al* (submitted)
[5] Mandal A, Roy Chowdhury M *et al* 2020 *Phys. Rev. A* **102** 062811

* E-mail: lokesh@tifr.res.in

Proper time delays from streaking measurements

U Saalmann

Max Planck Institute for the Physics of Complex Systems
Nöthnitzer Str. 38 · 01187 Dresden · Germany | https://www.pks.mpg.de/us

Synopsis By means of classical mechanics it is rigorously shown under which condition the shift from a streaking spectrogram provides the Wigner-Smith time delay.

In attosecond science it is assumed that Wigner-Smith (WS) time delays, known from scattering theory, are determined by measuring streaking shifts. Despite their wide use from atoms to solids this has never been proven. Analyzing the underlying process, energy absorption from the streaking light (see the figure, which shows the position-resolved energy absorption for different scenarios), we derive this relation [1]. It reveals that — under specific conditions only — streaking shifts measure WS time delays. For the most relevant case, interactions containing long-range Coulomb tails, we show that finite streaking shifts, including relative shifts from two different orbitals, are misleading.

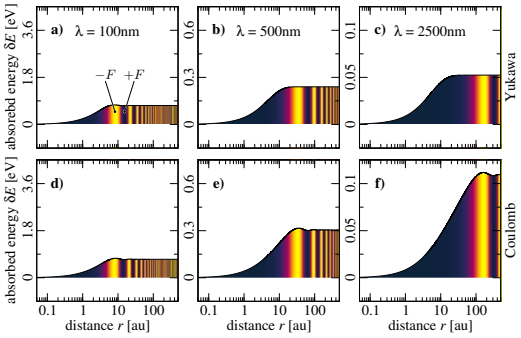

Figure 1. Absorbed energy $\delta E(r) = E(r) - E$ as a function of distance r for the Yukawa and the Coulomb potential for three different laser wavelengths λ, specified in the panels. The color coding represents the instantaneous laser field strength for the time when the electron is at a particular r.

Our analysis shows that streaking time delays become independent of the properties of the streaking laser and approach the WS time delay of short-range potentials for sufficiently weak streaking fields *and* in the limit of small frequencies or long wavelengths [1]. That streaking experiments for atoms measure finite times (despite infinite WS time delays for Coulombic systems) is a consequence of finite laser frequencies used. Those finite streaking delays, however, depend on the laser parameters and the excess energy of the electron. Therefore, both absolute streaking delays and relative ones for different excess energies are not suitable to characterize properties of a Coulombic system. Photo-ionization streaking delays should be measured relative to those of a pure hydrogenic Coulomb potential at the same excess energy of the photo-electron.

The interpretation of streaking measurements requires careful analysis. Even a relative measurement of a time delay between two orbitals of different binding energy in the same atom and with the same streaking laser depends, against any reasonable expectation, on the properties of the streaking light, namely its frequency. However, with the results presented here, it should be possible in the future to design experiments which measure time delays free from properties of the streaking laser.

References

[1] U Saalmann & J M Rost
Phys. Rev. Lett. 125 (2020) 113202

Strong-field photoelectron emission from metal nanoparticles

E. Saydanzad[1], J. A. Powell[1,2], A. Rudenko[1], and U. Thumm[1]

[1]Department of Physics, Kansas State University, Manhattan, Kansas 66506, USA
[2] INRS, Énergie, Matériaux et Télécommunications,1650 Bld. Lionel Boulet, Varennes, Québec, J3X1S2, Canada

Synopsis We modeled strong-field ionization from metal nanoparticles. Our model accounts for plasmon, electron-electron and electron-residual charge interactions, and for electron rescattering and recombination at the nanoparticle surface. Based on simulated photoelectron-momentum distributions for 5 to 70 nm diameter gold nanospheres and two different intensities, and in comparison with measured velocity-map-image (VMI) photoelectron spectra, we scrutinized the effects of electronic correlation, induced plasmonic fields, and electron-residual-charge interactions.

For spherical nanoparticles exposed to intense IR laser pulses, we numerically modeled photoelectron momentum distributions (PEMDs) within a semi-classical two-step approach [1, 2]. We first calculated the number of emitted photoelectrons, using Fowler-Nordheim tunneling rates, as a function of time and location on the particle's surface. In a second step, we solved Newton's equations for the motion of emitted photoelectrons outside the nanoparticle in the presence of the incident laser pulse, transient induced nanoplasmonic fields, and electron-electron and electron-residual charge interactions within a classical trajectory Monte-Carlo-sampling scheme [3, 4].

We investigated effects of the total electric field ($\vec{E}_{tot}$) and of the fields associated with accumulated residual charges ($\vec{F}_{res}$) and electronic repulsion ($\vec{F}_{e-e}$) on PEMDs. Figure 1 shows representative numerical results for gold nanospheres in comparison with our experimental data. The first, second, and third row, show simulated VMI spectra assuming no rescattering, specular, and diffuse photoelectron rescattering. In the calculation excluding rescattering, all photoelectrons that are driven back to the surface are assumed to recombine with the nanoparticle. For specular and diffuse photoelectron rescattering, variable fractions of emitted electrons are modeled to rescatter from the surface.

The dipole character of the PEMDs in the left and second column of Fig. 1 mimics the dipole character of the plasmonic field and is lost due to dominant electron-electron interactions and diffuse rescattering (columns 3 and 4), in agreement with our measured VMI spectrum (column 5). While the residual-charge interaction decreases the electron yield and cutoff energy, the nanoplasmonic field enhancement and electronic interaction increase them. Detected photoelectrons without rescattering occupy the lower part and rescattered photoelectrons the more energetic part of the VMI spectra.

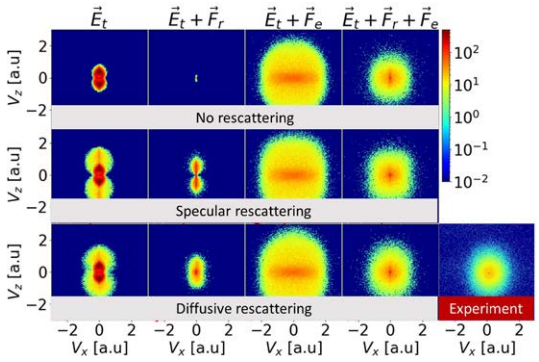

Figure 1. PEMDs for gold nanospheres with a diameter of 30 nm. V_x and V_z are photoelectron-velocity components along the laser propagation and polarization directions. See text.

Supported by the US NSF and DOD.

References

[1] E Saydanzad *et al* 2021 *In progress*
[2] J A Powell *et al* 2019 *Optics Express* **27** 27124
[3] E Saydanzad, J Li, and U Thumm 2017 *Phys. Rev. A* **95** 053406
[4] E Saydanzad, J Li, and U Thumm 2018 *Phys. Rev. A* **98** 063422

VMI photoelectron spectroscopy probing the rotational cooling dynamics of hot trapped OH^- ions

A Shahi[1] *, S. Mishra[1], D. Gupta[1], I. Rahinov[2], O. Heber[1] † and D Zajfman[1]

[1]Department of Particle Physics and Astrophysics, Weizmann Institute of Science, Rehovot, 76100, Israel
[2]Department of Natural Sciences, The Open University of Israel, Ra'anana 4353701, Israel

Synopsis The VMI photoelectron spectrometer installed inside of an electrostatic ion beam trap is used to find the cooling dynamics of many rotational states of hot OH^- ions. Rotational cooling dynamics recorded during 3 s storage time clearly shows the conversion of population (relaxation) from higher to lower rotational states as the time progresses. We estimated the relaxation rate constants of about 30 rotational states as well as the rotational temperature of ions as a function of trapping time. This is the first time the relaxation rate constants of high rotational states of OH^- are reported.

VMI photoelectron spectroscopy inside an electrostatic ion beam trap (EIBT)[1,2] is used to probe the time dependent dynamics of rotational states relaxation. Such relaxation process mainly occurs via spontaneous emission (radiative cooling) and its rate can be measured from time dependent intensity of rotational transitions which is experimentally challenging [3]. Previous works were able to detect either spectroscopy at a single temperature, or dynamics at cryogenic temperature - mostly for the lower rotational states (J<3) [3-7]. The higher rotational states relax faster than the lower rotational states and therefore it is an ideal system to be studied in VMI-EIBT. In this study, we attempt to measure the rotational relaxation dynamics of higher and lower rotational states of "hot" OH^- ion, which are produced in a cesium sputter ion source.

The photodetachment of OH^- ion results neutral OH in its $\Pi_{3/2}$ and $\Pi_{1/2}$ states [8]; the corresponding VMI photoelectron raw data spectra of unresolved P-branch transitions are shown in Figure 1 for different storage times in the EIBT. As the storage time increases, the peak radius of P-transition decreases, indicating the rotational population shift from high to low rotational levels. The calculated rotational temperature resulting from the fitted rotational line intensities ranges from 4100 to 900K for 0.1-2.8 sec trapping time. Further, we have explored relative population change in individual rotational states population as a function of storage time to extract relaxation rate coefficients for a broad range of rotational states of OH^-.

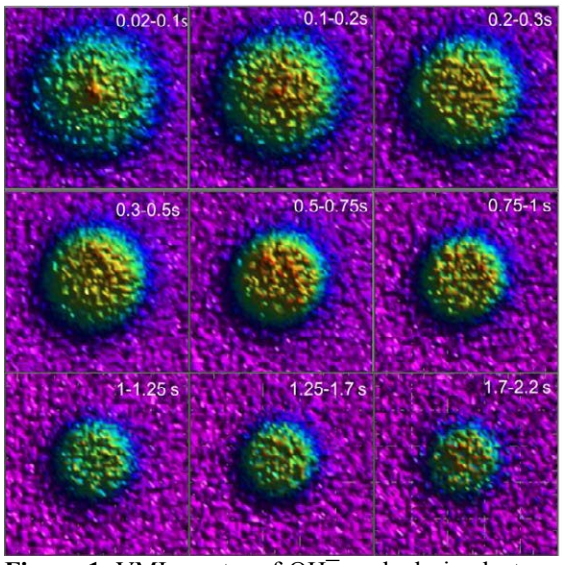

Figure 1. VMI spectra of OH^- probed via electron detachment by a CW laser (682 nm) as a function of trapping time.

References

[1] Zajfman D *et al* 1997 *Phys. Rev. A* **55** R1577
[2] Saha K *et al* 2017 *Rev. Sci. Instrm.* **88** 053101
[3] Meyer C *et al* 2017 *Phys. Rev. Lett.* **119** 023202
[4] Schmidt H T *et al* 2017 *Phys. Rev. Lett.* **119** 073001
[5] Otto R *et al* 2013 *Phys. Chem. Chem. Phys.* **15** 612
[6] Tripple S *et al.* 2006 *Phys. Rev. Lett.* **97** 193003
[7] Hauser D *et al* 2015 *Nat. Phys.* **11** 467
[8] Schulz P A *et al* 1983 *Phys. Rev. A* **27** 2229

* E-mail: abhishek.shahi@weizmann.ac.il
† E-mail: oded.heber@weizmann.ac.il

Ultrafast electron cooling in an expanding ultracold plasma

T. Kroker[1], M. Großmann[1], K. Sengstock[1], M. Drescher[1], P. Wessels-Staarmann[1*] and J. Simonet[1*]

[1]The Hamburg Centre for Ultrafast Imaging (CUI), University of Hamburg, Hamburg, Germany

Synopsis Plasma dynamics critically depends on density and temperature, thus well-controlled experimental realizations are essential benchmarks for theoretical models. The formation of an ultracold plasma can be triggered by a single femtosecond laser pulse that ionizes a controlled number of atoms in a micrometersized volume of a Bose-Einstein condensate. Our experimental setup grants direct access to the plasma dynamics in a so far unexplored regime by combining state-of-the-art techniques of ultrashort laser pulses and ultracold atomic gases.

Ultrashort laser pulses provide new pathways for manipulating atomic quantum gases on femtosecond timescales. In particular the strong light-field of a femtosecond laser pulse is able to instantaneously ionize a tunable number of atoms in a ^{87}Rb Bose–Einstein condensate [1].

Above a critical number of charged particles, the attractive ionic Coulomb potential is deep enough to trap a fraction of the photoelectrons, thus forming an ultracold plasma in a so far unexplored regime. The large atomic densities (above 10^{20} m^{-3}) combined with low ion temperatures (below 40 mK) give rise to a strongly coupled plasma where the Coulomb energies initially exceed the thermal energies by three orders of magnitude [2].

The investigated plasma dynamics reveals striking effects that cannot be captured by a hydrodynamic description. We observe an ultrafast electron cooling in the expanding plasma from initially 5250 K to below 10 K in less than 500 ns. With our experimental setup the electronic kinetic energy distribution can be measured with meV resolution.

The limited number of particles involved in our microplasma (from a few hundred to 4000) is a key feature that allows for an accurate comparison between experimental results and numerical simulations of the plasma dynamics. These computations reveal two cooling mechanisms occurring on distinct timescales: an ultrafast cooling during the plasma formation (picosecond timescale) and a subsequent process driven by the Coulomb expansion of the ionic component (nanosecond timescale).

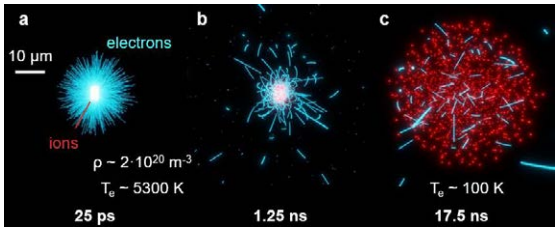

Figure 1. Ultrafast dynamics of an ultracold microplasma. Snapshots from numerical simulations tracing the electrons (blue) and ions (red) after photoionization. Due to their high initial temperature ($T_e \approx 5250$ K), initially half of the photoelectrons leave the ionization volume, while the ions can be regarded as static (a). This charge separation gives rise to a space charge potential leading to the formation of an ultracold plasma (b). During the Coulomb expansion of the ionic component, the electrons are further cooled to temperatures below 10 K (c).

Such a laboratory experiment that grants access to microscopic observables, allows testing the validity of macroscopic models, thus leading to a better understanding of similar systems in nature. Strongly coupled plasmas are of particular interest as the charge carriers should develop spatial correlations and self-assembled ordered structures. Photoionization of ultracold quantum gases paves the way toward plasmas supporting strong ion as well as electron coupling. Indeed, by tuning the ionization process to lower excess energy, the initial temperature of the electrons shall be reduced by orders of magnitude.

This work is funded by the Cluster of Excellence "CUI: Advanced Imaging of Matter" of the Deutsche Forschungsgemeinschaft (DFG) - EXC 2056 - project ID 390715994.

References

[1] Wessels P *et al.* 2018 *Commun. Phys.* **1** 32
[2] Kroker T *et al.* 2021 *Nat. Commun.* **12** 596

* E-mail: jsimonet@physnet.uni-hamburg.de

Photo-induced molecular catapult. Imaging molecular rotation during ultrafast dissociation.

O. Travnikova[1]*, B. Cunha de Miranda[1], S. Carniato[1], V. Kimberg[3], F. Trinter[2], T. Jahnke[2], M. S. Schöffler[2], R. Dörner[2] and M. Simon[1]

[1]LCPMR, CNRS, Sorbonne Université, UMR7614, 75005 Paris, France
[2]Institut für Kernphysik Goethe-Universität Frankfurt, 60438 Frankfurt, Germany.
[3]Department of Theoretical Chemistry and Biology, KTH, 10691, Stockholm, Sweden

Synopsis Ion momenta correlation analysis was performed for Br 3*d* core-excited states of bromochloromethane. This allowed capturing ultrafast photo-induced dissociation mechanisms, which resembles a medieval mangonel-type catapult. A strong tension in the C–Br bond is created by promotion of a Br 3*d* electron to a strongly dissociative molecular orbital, which causes a light CH_2-moiety to be slung from a heavy Br-atom in a matter of a few femtoseconds.

Resonant excitation of a core electron to an anti-bonding molecular orbital may lead to ultrafast nuclear dynamics and even dissociation on a few-fs time scale. Ultrafast dissociation (UFD) is a phenomenon, when the breakage of molecular bonds occurs on the same time scale and, therefore, competes with electronic relaxation, which results in radiative or Auger decay emission from already dissociated fragments. A simple pseudo-diatomic description of UFD, modeling the departing fragments as point-masses and the dissociation along only one coordinate, guided all in-depth studies of the UFD phenomenon to relatively light molecules, where their reduced masses allowed the complete breakage of the chemical bond during the very short core-hole lifetime. [1, 2, 3]

Another mechanism of UFD, recently elaborated [4] based on simple theoretical modelling, implies that bond breakages may be also mediated by the internal motion of light linkages situated between heavy parts of the molecules. For example the rotation of the $(CH_2)_2$-moiety may enable the dissociation of the C–Br bond in the Br 3*d* core-excited state of 1-bromo-2-chloroethane, whose lifetime counts only about 7 fs. In the very early stages of the photodissociation, the carbon atoms experience a significant displacement while the halogen atoms remain nearly still. This mechanism was predicted to be rather general for large polyatomic molecules.

In order to 'capture' the internal rotation of carbon atoms and verify its dominance in the UFD process, we performed coincidence imaging measurements using COLTRIMS coincidence setup at BESSY II synchrotron radiation facility.

Multiple ions were measured in coincidence with electrons following Br 3*d* core excitation and ionisation in bromochloromethane (CH_2BrCl, BCM). Ion momenta correlation analysis allowed disentangling different photo-induced dissociation mechanisms.

The observed nuclear dynamics, occurring in the dominant dissociative channel of BCM, resembles a medieval mangonel-type catapult having CH_2 as a projectile, where CH_2–Cl bond acts as a lever arm (see Fig. 1). Absorption of a photon creates a tension in opposing directions of the strongly dissociative Br*–CH_2 bond and the arm releases up in a radial arc causing the projectile to fling away.

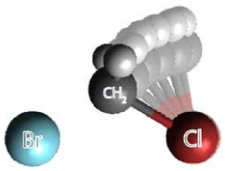

Figure 1. Schematics of nuclear motion in bromochloromethane leading to ultrafast dissociation in Br 3*d* core-excited state within the lifetime of $\tau \sim 7$ fs.

References

[1] Björneholm *et al* 1997 *Phys. Rev. Lett.* **79** 3150
[2] Hjelte *et al* 2003 *Chem. Phys. Lett.* **370** 781
[3] Sann *et al* 2016 *Phys. Rev. Lett.* **117** 243002
[4] Travnikova *et al* 2013 *J. Phys. Chem. Lett.* **4** 2361

*E-mail: oksana.travnikova@sorbonne-universite.fr

Charge transfer reactions of polar molecules and rare gas ions

A Tsikritea[1,2] * and B R Heazlewood[2]

[1]Department of Chemistry, University of Oxford, Physical and Theoretical Chemistry, South Parks Road, Oxford, OX1 3QZ, United Kingdom
[2]Department of Physics, University of Liverpool, Liverpool, L69 7ZE, United Kingdom

Synopsis In the absence of experimental data, astrochemical models typically adopt variants of capture theory to estimate rate coefficients for ion-molecule reactions that take place in interstellar environments. We examine astrochemically-relevant charge transfer reactions between isotopologues of ammonia or water and rare gas ions. Capture theory predictions are evaluated, alongside observed kinetic isotope effects.

Astrochemical models often adopt capture theories to predict low-temperature reaction rate coefficients of experimentally unmeasured reactions. A lack of experimental data is evident, in particular, when considering deuterated reactants –species that play an important role in interstellar chemistry.

The cold and controlled environment of Ca^+ Coulomb crystals, confined in a linear Paul trap, is utilised to undertake the reaction studies. Rare gas ions are sympathetically cooled via their efficient elastic collisions with the laser-cooled Ca^+ ions. Thermal neutral reactants are introduced effusively via a high-precision leak valve. Laser-induced fluorescence images coupled with time-of-flight mass spectrometry allow us to monitor the reactions' progress. Comparison with molecular dynamics simulations yields bimolecular rate constants.

Rate coefficients for the NH_3 or ND_3 reactions with ground-state Xe^+, Kr^+ and Ar^+ ions are experimentally calculated at collision energies lower than 300 K and are compared with capture theory models. The models' predictions overestimate the rate coefficients of all six reaction systems studied. Additionally, an inverse kinetic isotope effect (KIE) is observed; ND_3 reacts faster than NH_3. As illustrated in Figure 1, the magnitude of the KIE shows a dependence on the mass of the rare gas ion. Capture theories cannot account for the presence of the observed KIEs.

Detailed *ab initio* calculations show no energetically-accessible crossing between the reactant and product potential energy curves; the mechanism responsible for electron transfer is not straightforward. We speculate that the properties of the reaction complex, such as its density of vibrational states and lifetime, play a role in the probability of product formation [1, 2].

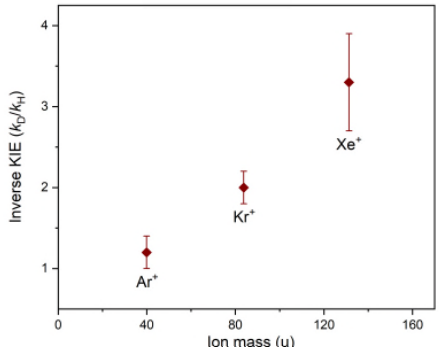

Figure 1. Inverse KIEs observed for the ammonia charge exchange reactions.

Conversely, charge transfer reactions between water isotopologues (H_2O or D_2O) and Kr^+ ions, studied under similar conditions, do appear to be well-described by capture theory. Furthermore, no significant KIE is observed.

Accurately accounting for the reactivity of species such as small rare gas ions and polar molecules such as ammonia and water –all species known to be present in the interstellar medium–is important. Without accurate reaction rate coefficients, models of interstellar chemistry are of limited use. Our work suggests that capture theories do not consistenly describe the reactivity of ion-molecule systems. Further work is needed to establish when capture theories can be confidently utilised.

References

[1] Petralia L S *et al* 2020 *Nat. Comm.* **11** 173
[2] Tsikritea A *et al* 2021 (submitted)

* E-mail: andriana.tsikritea@chem.ox.ac.uk

Polarization phenomena in electron resonant elastic scattering on one-electron ions

D M Vasileva[1]*, K N Lyashchenko[2], O Yu Andreev[1,3] and A B Voitkiv[4]

[1]Department of Physics, St. Petersburg State University, St. Petersburg, 199034, Russia
[2]Institute of Modern Physics, Chinese Academy of Sciences, Lanzhou, 730000, China
[3]Petersburg Nuclear Physics Institute, Gatchina, 188300, Russia
[4]Institute for Theoretical Physics I, Heinrich-Heine-University of Düsseldorf, Düsseldorf, 40225, Germany

Synopsis The polarization properties of the elastic electron scattering on one-electron ions are investigated within the framework of the relativistic QED theory. In this process both the spin-orbit interaction and the spin exchange between the incident and bound electrons play a significant role. The polarization properties can be fully described in terms of five parameters. The behaviour of these parameters is studied for the region of impact energies where the scattering can proceed via the formation and subsequent Auger decay of intermediate LL autoionizing states.

The electron elastically scattered on an ion, atom or molecule changes its polarization due to the combination of the spin-orbit interaction and the exchange interaction between the incident and bound electrons. This polarization change has been extensively studied in terms of three polarization parameters S, T and U for the elastic electron scattering on atoms [1]. In such process the spin-orbit interaction often dominates. Thus, in the calculations of the polarization parameters the exchange interaction is either neglected or approximated by a local potential.

The two most notable features of the elastic electron scattering are:

1. The initially unpolarized electron becomes partially polarized and its polarization is directed perpendicular to the plane of scattering.

2. If the incident electron has nonzero polarization perpendicular to its momentum, the resulting differential cross section becomes dependent on the angle between the incident electron polarization and the scattered electron momentum.

Both features can be described by the Sherman asymmetry function [2] and can be used to produce or detect polarized electrons.

We investigate the elastic electron scattering on one-electron ions for impact energies where the scattering of an electron can proceed via the formation of a doubly excited (autoionizing) state and its subsequent Auger decay. In this case, both the spin-orbit interaction and the exchange interaction are important [3]. In order to account for both of these interactions, the relativistic QED theory developed in [4] was employed.

The spin exchange between the incident and bound electrons leads to the asymmetry in respect to the rotation of the plane of scattering, which necessitates the introduction of two additional parameters for the description of the polarization properties.

We study the behaviour of five polarization parameters for nonresonant scattering as well as in the presence of LL resonances. We consider collisions with a wide range of ions (from B^{4+} to Xe^{53+}).

The formation of intermediate autoionizing states in the resonant electron scattering leads to the abrupt change of the polarization parameters at impact energies close to the resonances. The resulting polarization phenomena are highly dependent on the nature of the intermediate states formed in the process.

*E-mail: summerdacha64@rambler.ru

References

[1] Dapor M 2018 *Sci Rep.* **8** 5370
[2] Sherman N 1956 *Phys. Rev.* **103** 1601
[3] Burke P G and Mitchell J F B 1974 *J. Phys. B: Atom. Mol. Phys.* **7** 214
[4] Lyashchenko K N *et al* 2020 *Phys. Rev. Research* **2** 013087

Treatment of ion collisions with multielectron atomic targets without using independent-event model

I. B. Abdurakhmanov*, C. T. Plowman, A. S. Kadyrov and I. Bray

Curtin Institute for Computation and Department of Physics and Astronomy, Curtin University, GPO Box U1987, Perth, WA 6845, Australia

Synopsis An effective single-electron approach to ion collisions with multielectron atomic targets has been developed. The approach treats all the target electrons on an equal footing and do not employ the commonly used independent-event model. It allows calculating single-ionization and single-electron capture cross sections by including excitation of any one of the inner- or outer-shell target electrons.

Ion-atom collisions involving one- or two-electron targets can be dealt with in an *ab initio* manner without significant approximations. However, as the number of target electrons increases it becomes unavoidable to introduce approximations. Usually, processes involving the outer-shell and inner-shell electrons are treated using an independent-event model. However, the independent-event model becomes impractical when the number of shells is more than two. We develop an effective single-electron approach to ion collisions with multielectron atomic targets that overcomes this difficulty by treating all the atomic electrons on an equal footing [1]. The ground state wave function for the target atom obtained in the Hartree-Fock approximation is used to calculate the probability density for the whole atom. The latter is then averaged over the spatial coordinates and spin variables of all of the target electrons except for the position of one electron from the nucleus. The obtained single-electron probability density is then used to derive a pseudopotential describing the interaction of one electron with an effective field produced by the target nucleus and the other electrons. The procedure reduces the many-body Schrödinger equation effectively into a three-body one.

In Fig. 1 we show the energy dependence of the total cross section for single-electron capture and single ionisation in p-K collisions. For single electron capture the results are in excellent agreement with all the available measurements. The observed hump above 30 keV is mainly due to the projectile capturing one of the inner-shell electrons of the target. For single ionization our results are in good agreement with the experimental measurements at high energies [2] but disagree below 100 keV [3].

*E-mail: ilkhom.abdurakhmanov@curtin.edu.au

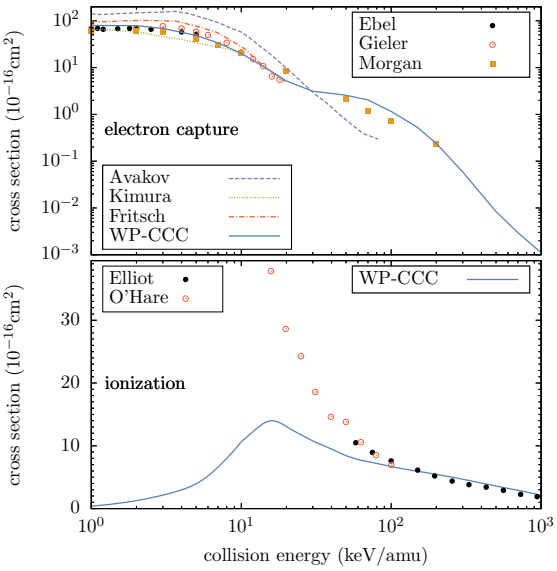

Figure 1. Total cross section for single-electron capture and single ionization in p-K collisions as a function of the impact energy. The results of the present WP-CCC approach are compared with the experimental measurements [2, 3, 4, 5, 6], and theoretical calculations [7, 8, 9].

References

[1] Abdurakhmanov I B *et al* 2021, submitted
[2] Elliot D S *et al* 1986 *J. Phys. B* **19** 3277
[3] O'Hare B G *et al* 1975 *J. Phys. B* **8** 2968
[4] Ebel F *et al* 1987 *J. Phys. B* **20** 4531
[5] Gieler M *et al* 1991 *J. Phys. B* **24** 647
[6] Morgan T J *et al* 1985 *J. Phys. Chem. Ref. Data* **14** 971
[7] Avakov G V *et al* 1992 *J. Phys. B* **25** 213
[8] Kimura R E *et al* 1992 *Phys. Rev. A* **26** 1138
[9] Fritsch W 1984 *Phys. Rev. A* **30** 1135

Formation of united atomic systems during heavy-ion–heavy-atom collisions

R Gupta[1,2], C V Ahmad[1,2], K Chakraborty[1,2], A. Rani[2], S. Mandal[2], D Swami[3], T. Nandi[3], G Sharma[4], D. Mitra[5] and P Verma[1*]

[1]Department of Physics, Kalindi College, University of Delhi, New Delhi 110008, India
[2]Department of Physics and Astrophysics, University of Delhi , New Delhi 110007, India
[3]Inter-University Accelerator Centre, Aruna Asaf Ali Marg, New Delhi 110067, India
[4]Department of Physics, Government Engineering College, Ajmer, Rajasthan 305001, India
[5]Department of Physics, University of Kalyani, Kalyani, Nadia, West Bengal 741235, India

Synopsis Formation of superheavy quasimolecules, with united atomic numbers between 111 and 130, have been studied via collision-induced X-rays.

Superheavy systems, with atomic numbers greater than 100, are particularly interesting owing to several exotic features such as significantly increased binding energies, enhanced spin–orbit splitting for the *p* orbitals, considerably shrinked shell radius and multiple ionization. Such superheavy systems can be formed transiently during a quasiadiabatic heavy-ion–heavy-atom collision. As the collision partners approach each other slowly, their inner-shell electrons adjust adiabatically to the combined nuclear potential of the partners. Consequently, a transient collision molecule or quasimolecule having a united atomic charge $Z_{UA}=Z_1+Z_2$ (Z_1 and Z_2 represent projectile and target atomic numbers, respectively) is formed for the inner-shell electrons. Thus, by taking Z_1 and Z_2 such that $Z_{UA} \geq 100$, superheavy systems can be explored, even in very low energy collisions **[1,2]**, via X-rays.

Investigation of inner-shell ionization cross-sections of $64 \leq Z_2 \leq 83$ targets bombarded by 70–180 MeV Ag^{q+} ($5 \leq q \leq 12$) obtained from the 15UD Pelletron at Inter University Accelerator Centre (IUAC), New Delhi, India were performed. The collision-induced X-rays from both collision partners showed multiple ionization **[3]** as well as enhanced X-ray production cross-sections and target to projectile intensity ratios when observed as functions of Z_2. Furthermore, although Ag^{q+} with completely closed inner shells were bombarded on the targets, Doppler-shifted Ag K X-rays were also observed, as shown in **Figure 1**.

These observations can be understood qualitatively within the framework of the quasimolecular phenomenon **[1,2]** for the inner-shell electrons of united systems $111 \leq Z_{UA} \leq 130$. It is considered that the inner shells of the collision partners become coupled to each other through correlations with the energy levels of the corresponding Z_{UA}, leading to dynamic vacancy transfers between the target and projectile inner shells, thereby giving rise to the observed Ag K X-rays even at such low energy collisions.

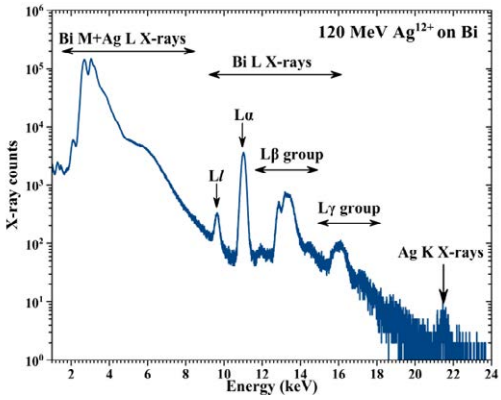

Figure 1. Collision-induced X-ray spectrum for 120 MeV Ag^{12+} bombarded on Bi.

Further investigations are being conducted to examine and verify the origin of these observations using diabatic correlation diagrams **[4]** for Ag–Z_2 ($64 \leq Z_2 \leq 83$) combinations.

References

[1] Greenberg J S *et al* 1985 High-Energy Atomic Physics—Experimental. In: Bromley D.A. (eds) Treatise on Heavy-Ion Science. Springer, Boston, MA.
[2] Verma P *et al* 2006 *NIM B* **245**, **56–60**; 2006 *Rad. Phys. and Chem.* **75**, **2014–2018**; 2011 *Phys. Scripta* **T144**, **014032**.
[3] Verma P *et al* 2000 *Phys. Scripta* **61**, **335–338**; 2017 *J. Phys. : Conf. Ser.* **875**, **092029**.
[4] Verma P *et al* 2015 *J. Phys. : Conf. Ser.* **635**, **022074**.

* E-mail: punitaverma@kalindi.du.ac.in

Molecular orbital formation by low energy Xe-ion impact on Pt and Au

C V Ahmad[1, 2], R Gupta[1, 2], K Chakraborty[1, 2], D Swami[1] and P Verma[2*]

[1]Department of Physics and Astrophysics, University of Delhi, New Delhi, 110007, India
[2]Department of Physics, Kalindi College, University of Delhi, New Delhi, 110008, India
[3]Inter University Accelerator Centre, Aruna Asaf Ali Marg, New Delhi-110067, India

Synopsis M molecular orbital X-ray bands corresponding to the united atomic systems Z_{UA} = 132 and 133 have been observed in the collision-induced X-ray spectra of 2–5 MeV Xe-ions bombarded on Pt and Au thin foils.

The experimental observation of quasimolecular X-rays with low energy projectiles has opened up a remarkable window to investigate the terrain of superheavy elements using collision-induced atomic processes. Under adiabatic condition ($Z_P/Z_T \approx 1$ and $v_P/v_{Ts} \ll 1$, where, P is projectile, T is target and s = K, L, M…shell) i.e., for very symmetric and low energy collisions, molecular orbitals (MO) are formed, and at very small inter atomic distance between the collisional partners there is a probability of formation of transient quasimolecules having atomic number equal to the sum of the atomic numbers of the collisional partners **[1,2]**. This can be well explained by the electron promotion model **[3]**, according to which a change in the internuclear distance changes the ordering of the occupied quasimolecular energy levels that interact with the unoccupied states. This interaction of the occupied state with the unoccupied state creates a vacancy in the inner shells which result in the formation of the X-ray bands.

The low energy ion beam accelerator using an ECR-ion source at Inter-University Accelerator Centre (IUAC), New Delhi, India has been used to accelerate Xe ions to 2–5 MeV. X-rays emitted from both the collision partners have been recorded with silicon drift detectors (SDD) having a resolution of ~129 eV at 5.9 keV. **Figure 1** shows the X-ray spectrum of 4 MeV Xe^{12+}-ions incident on Pt. The observed continuum peak at the higher energy end of the spectrum indicate the formation of MOs during the collision. Furthermore, slight shifts in the target X-ray energies and altered target to projectile intensity ratios have been observed indicating multiple ionization and the presence of spectator vacancies. Additionally, cross-section enhancements have also been observed.

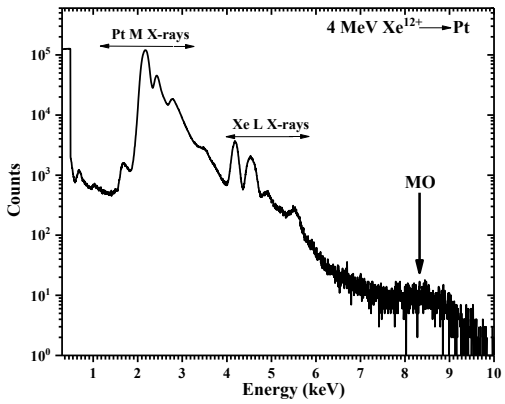

Figure 1. X-ray spectrum of 4 MeV Xe^{12+} incident on Pt showing *M* MO X-ray band at the higher energy end.

In the preliminary analysis, the peak centroid of the observed broad X-ray band has been found to be approximately in the range 7.4–9.8 keV. This X-ray energy range corresponds to the $4f \rightarrow 3d$ transition in the united atomic systems Z_{UA} = 132 and 133 **[4,5]**. Further detailed analysis is being carried out to evaluate the experimental observations for understanding the vacancy transfer mechanisms in such low energy collisions.

References

[1] Anholt R 1985 *Rev. Mod. Phys.* **57**, **995**.
[2] Verma P *et al* 2006 *NIM B* **245**, **56**; 2006 *Rad. Phys. Chem.* **75**, **2014**; 2011 *Phys. Scr.*, **T144**, **014032**; 2017 *J. Phys. : Conf. Ser.* **875**, **092029**.
[3] Barat M *et al* 1972 *Phys. Rev. A* **6**, **211**; Lichten W 1980 *J. Phys. Chem.* **84**, **2102**.
[4] Mokler P H *et al* 1972 *Phys. Rev. Lett.* **29**, **827**.
[5] Lutz H O *et al* 1976 *J. Phys. B* **9**, **L157**.

* E-mail: punitaverma@kalindi.du.ac.in

Collisions between two-Hydrogen atoms

S J Al Atawneh[1, 2] and K Tőkési[1,*]

[1]Institute for Nuclear Research (ATOMKI), Debrecen, 4026, Hungary
[2] Doctoral School of Physics, University of Debrecen, Debrecen, 4032, Hungary

Synopsis: The interaction between two hydrogen atoms is studied employing both the standard 4-body classical trajectory Monte Carlo (CTMC) and the quasi-classical trajectory Monte Carlo method of Kirschbaum and Wilets (QTMC-KW). We present total cross sections for the excitation and ionization of the projectile, and the target. Calculations were performed in the projectile energy range between 3.0 keV and 100 keV, relevant to the interest of the fusion research. Our results are compared with previous theoretical and experimental results. We found that the classical treatment describes reasonably well the cross sections for various final channels. Moreover, we show that the calculations by the QTMC-KW model significantly improve the obtained cross sections.

Classical calculations for determining atomic collision cross sections have received a great deal of interest in the past 20 years. There was a great revival of the CTMC calculations applied in atomic collisions involving four or more particles [1]. The CTMC method is a non-perturbative method, where classical equations of motions are solved numerically [2]. For a better description of the classical atomic collisions, the quasi-classical trajectory Monte Carlo model of the Kirschbaum and Wilets (QTMC-KW) is improving the results of the standard CTMC model [3]. In particular, it is desirable to have a method that consistently treats electron transfer and ionization as well as multiplicities and combinations of these processes with high accuracy. Along this line, in this work, the interaction between two ground state hydrogen atoms is studied using both the standard 4-body CTMC and the QTMC-KW method in the projectile energy range between 3.0 keV and 100 keV. According to our knowledge, this is the first time to present cross section data using the QTMC-KW method for H(1s) + H(1s) system.

In the present work, the four particles (target nucleus, target electron, projectile electron, and projectile nucleus) are presented by their masses and charges. We used Coulomb potential for describing all interactions. Figure 1. shows the projectile ionization cross sections in a collision between two ground state hydrogen atoms as a function of impact energy. Our results were compared with the experimental data. According to the expectation, the QTMC-KW method improved the cross section data compared with the results of the standard CTMC method. We found reasonable good agreement between the experimental data and our results obtaind by QTMC-KW method.

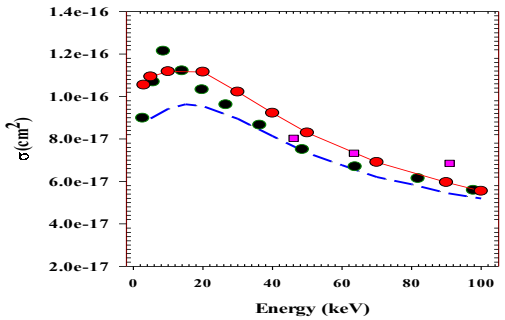

Figure 1. Projectile ionization cross sections in a collision between two ground state hydrogen atoms as a function of impact energy. Red solid-circles line: present 4-body QTMC-KW results, blue solid-dashed line: present standard 4-body CTMC results. Black solid circle: Experimental data by McClure [4]. Pink square: Experimental data by Wittkower *et al* [5].

This work has been carried out within the framework of the EUROfusion Consortium and has received funding from the Euratom research and training programme 2014-2018 and 2019-2020 under grant agreement No 633053. The views and opinions expressed herein do not necessarily reflect those of the European Commission.

References

[1] Saed J. Al Atawneh and K. Tőkési, Journal of Physics B, accepted for publication.
[2] Olson R.E. and Salop A. 1977 *Phys. Rev.* A 16 531-541
[3] Kirschbaum C.L. and Wilets L. 1980 *Phys. Rev.* A 21 834-841
[4] McClure G.W. 1968 *Phys. Rev* 166 22-29
[5] Wittkower A.B., Levy G. and Gilbody H.B. 1967 *Proc. Phys. Soc* 91 306-309

* E-mail: tokesi@atomki.hu

State-resolved KLL cross sections of single electron capture in collisions of swift $C^{4+}(1s2s\ ^3S)$ ions with gas targets

I Madesis[1,2], A Laoutaris[1,2], S Nanos[2,3], T J M Zouros[1], A Dubois[4†] and E P Benis[3,*]

[1]Department of Physics, University of Crete, GR-70013 Heraklion,
[2]Tandem Accelerator Laboratory, INPP, NCSR "Demokritos", GR-15310 Ag. Paraskevi, Greece
[3]Department of Physics, University of Ioannina, GR-45110 Ioannina, Greece
[4]Sorbonne Université, CNRS, Laboratoire de Chimie Physique-Matiére et Rayonnement, F-75005 Paris, France

Synopsis We report on the absolute cross sections determination for the production of the 1s2s2p ^4P and ^2P states via single electron capture in collisions of swift $C^{4+}(1s2s\ ^3S)$ ions with gas targets (H_2, He, Ne and Ar). The absolute cross sections were determined experimentally for all targets using high resolution Auger projectile spectroscopy, as well as theoretically for H_2 and He targets using ab initio calculations based on a three-electron close-coupling semiclassical approach.

In a recent publication [1] we reported on the formation of doubly excited triply open-shell $C^{3+}(1s2s2p\ ^{2,4}P)$ states via single electron capture (SEC) in collisions of swift $C^{4+}(1s2s\ ^3S)$ pre-excited ions with H_2 and He gas targets. Using high resolution Auger projectile spectroscopy and *ab initio* calculations based on a three-electron close-coupling (3eAOCC) semiclassical approach, we resolved a long-standing controversy on the value of the cross sections ratio $R=\sigma(^4P)/\sigma(^2P)$, used as a measure of spin statistics. Our findings invalidate the generally adopted frozen core approximation for the SEC process in multi-electron, multi-open-shell quantum systems and a new screening effect due to the Pauli exclusion principle (Pauli shielding) was proposed.

Here, we report on the determination of the absolute cross sections for the production of the ^4P and ^2P states via SEC in collisions of swift $C^{4+}(1s2s\ ^3S)$ ions with H_2 and He gas targets, as well as with Ne and Ar. The determination of the ratio R requires only relative electron yields and thus the corresponding absolute cross sections were not considered in [1].

The absolute cross sections were obtained experimentally after separating the contributions for the metastable 1s2s ^3S part of the $C^{4+}(1s^2\ ^1S, 1s2s\ ^{1,3}S)$ mixed-state ion beam, delivered by the tandem Van der Graaff accelerator. For this, we have developed a two-measurement technique [2] that exploits two independent spectrum measurements performed with ions having quite different 1s2s ^3S metastable fractions. In addition, the technique provides the value of the 1s2s ^3S metastable fraction that is necessary for the absolute cross section determination of the ^4P state.

The absolute cross sections were also determined within the 3eAOCC calculations [3] for the cases of H_2 and He. In the case of the long-lived ^4P state, selective cascade feeding from higher lying quartet states populated by SEC had to be considered [4].

A good agreement is evident both for H_2 and He targets. Moreover, the cross sections for Ne and Ar targets are shown to roughly scale with the number of electrons that can participate in the SEC process.

References

[1] Madesis I *et al* 2020 *Phys. Rev. Lett.* **124** 113401
[2] Benis E P *et al* 2016 *J. Phys. B* **49** 235202
[3] Gao J W *et al* 2017 *Phys. Rev. A* **96** 052703
[4] Zouros T J M *et al* 2020 *Atoms* **8** 61

We acknowledge support of this work by the project "Cluster of Accelerator Laboratories for Ion-Beam Research and Applications - CALIBRA" (MIS 5002799) implemented under the Action "Reinforcement of the Research and Innovation Infrastructure", funded by the Operational Programme "Competitiveness, Entrepreneurship and Innovation" (NSRF 2014-2020) and co-financed by Greece and the European Union (European Regional Development Fund).

† E-mail: alain.dubois@sorbonne-universite.fr
* E-mail: mbenis@uoi.gr

Pauli Shielding and Breakdown of Spin Statistics in Multielectron, Multi-Open-Shell Dynamical Atomic Systems

I Madesis[1,2], A Laoutaris[1,2], E P Benis[3], T J M Zouros[1†], J W Gao[4] and A Dubois[5*]

[1]Department of Physics, University of Crete, GR-70013 Heraklion, Greece
[2]Tandem Accelerator Laboratory, INPP, NCSR "Demokritos", GR-15310 Ag. Paraskevi, Greece
[3]Department of Physics, University of Ioannina, GR-45110 Ioannina, Greece
[4]Sichuan University, 610064 Chengdu, China
[5]Sorbonne Université, CNRS, Laboratoire de Chimie Physique-Matière et Rayonnement, F-75005 Paris, France

Synopsis State-resolved cross sections of electron capture in collisions of swift $C^{4+}(1s2s\ ^3S)$ ions with He and H_2 are determined to investigate the formation of doubly excited $C^{3+}(1s2s2p)\ ^4P$ and $^2P_\pm$ states and the ratio R of their cross sections as a measure of spin statistics. Using ZAPS measurements and semiclassical close-coupling calculations, a long-standing puzzle and controversy on the value of R and the effect of cascades is resolved invalidating the frozen core approximation generally used in the past when considering electron capture in multielectron, multi-open-shell quantum systems.

We provide experimental results for the 1s2s2p $^4P/^2P_\pm$ line ratio R for single electron capture in fast collisions of $C^{4+}(1s2s\ ^3S)$ with helium and hydrogen targets [1]. Our measured R values shown in Fig. 1 are seen to be close to 2, in contrast to previous findings. In parallel, the ratio R calculated using a sophisticated multielectron close-coupling approach (3eAOCC) [2] is found to be in agreement, for the first time, with experiment, when postcollisional radiative cascades [3] are also taken into account. These results draw attention to the limited predictive power of the frozen core approximation regarding spin statistics in highly correlated dynamical atomic systems. To better understand our findings, we propose an elegant Pauli shielding mechanism related to strong exchange effects which selectively (and counter-intuitively) obstructs specific reaction channels. Systematic isoelectronic studies should further validate these conclusions in a more general context.

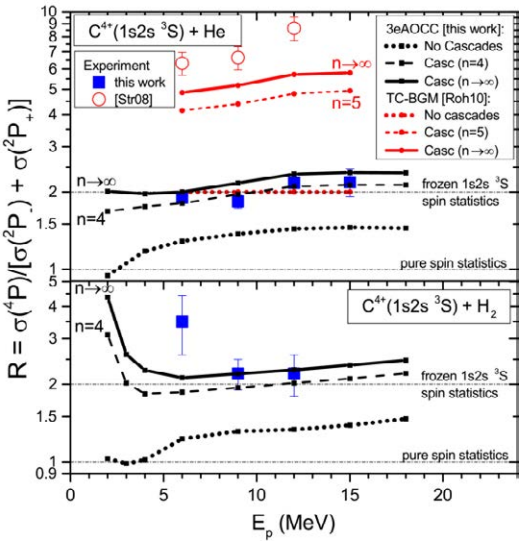

Figure 1. Ratio R for $C^{4+}(1s2s\ ^3S)$ collisions with He (top) and H_2 (bottom) as a function of projectile energy [1]. Experiment (ZAPS): Squares (this work), circles [4]. Theory: Black lines (3eAOCC), red lines [5]. Results without (dotted) and with radiative cascades from 1s2snl ^4L states up to the indicated n (dashed) and extrapolated to $n \to \infty$ (solid) are shown. The frozen 1s2s ^3S core spin statistics and pure spin statistics values are indicated.

* E-mail: alain.dubois@sorbonne-universite.fr
† E-mail: tzouros@physics.uoc.gr

References

[1] Madesis I *et al* 2020 *Phys. Rev. Lett.* **124** 113401
[2] Gao J W *et al* 2017 *Phys. Rev. A* **96** 052703
[3] Zouros T J M *et al* 2020 *Atoms* **8** 61
[4] Strohschein D *et al* 2008 Phys. Rev. A **77** 022706
[5] Röhrbein D *et al* 2010 Phys. Rev. A **81** 042701

We acknowledge support of this work by the project "Cluster of Accelerator Laboratories for Ion-Beam Research and Applications - CALIBRA" (MIS 5002799) implemented under the Action "Reinforcement of the Research and Innovation Infrastructure", funded by the Operational Programme "Competitiveness, Entrepreneurship and Innovation" (NSRF 2014-2020) and co-financed by Greece and the European Union (European Regional Development Fund).

Time-Dependent Close-Coupling Calculations of nl-resolved cross sections for collisions of bare Ne and Mg on atomic hydrogen and helium between 1 - 5 keV/amu

S. Bromley[1]*, **M. Pindzola**[1], **M. Fogle**[1]

[1]Department of Physics, Auburn University, Auburn, 36832, USA

Synopsis Charge exchange between highly charged ions and neutrals introduces a problematic background for every x-ray observation [1]. For H-like ions produced by charge exchange the l states within each n shell are degenerate. While several analytical l-distributions are known and available (see e.g. [2]), the exact distribution of l capture states is unknown. To date, few laboratory measurements are available for benchmarking at the required solar wind velocities (300 - 1000 km/s). We report here explicit calculations of nl-resolved CX cross sections using the time dependent close coupling method for bare Ne and Mg incident on atomic H and He at solar wind velocities. The effect of l distribution on diagnostic line ratios and comparisons to common l-distribution choices are presented.

Charge exchange (CX) is the process by which an ion captures an electron from a neutral, typically into an excited state of the ion, after which the excited state decays to produce an x-ray cascade, γ. The (net) process may be written as

$$A^q + B \rightarrow A^{(q-j)+} + B^{j+} + \gamma \qquad (1)$$

where γ depends on the initial nl state populated by CX and the transition rates of ion $A^{(q-j)+}$. For atomic hydrogen targets (B), only single-electron capture (SEC), $j = 1$, is possible, whereas multi-electron targets open up the possibility of multi-electron capture ($j > 1$). The resulting multiply-excited ion stabilizes via radiative decay or autoionization. To-date, the relative contribution of multi-electron processes to observed x-ray spectra is not well understood.

Following SEC onto a bare ion, the l states within each n shell are degenerate. However, the radiative cascades depend on both n and l. For a given n-resolved cross section, two l distributions are commonly assumed: (1) the low energy distribution favored for energies < 0.1 keV/amu, and (2) the statistical l distribution, favored for energies above $\sim$10 keV/amu [2]. Historically, lab studies of CX focused on high collision velocities relevant to e.g. fusion apparatus' (c.f. [3]), resulting in little to no laboratory data for benchmarking CX cross section calculations at solar wind velocities of $\sim$300 - 1000 km/s (0.5 - 5 keV/amu). Planned experiments at the Clemson University Electron Beam Ion Trap facility are expected to shed light on the exact l distribution following electron capture from hydrogen and helium targets.

We present nl-resolved calculations of CX cross sections for bare Ne and Mg. CX cross section calculations were carried out using the time-dependent close coupling method (TDCC, described in [4]). Level energies and transition rates were generated using the Flexible Atomic Code [5], which were combined with our CX cross sections in an x-ray cascade model. Our cross sections and x-ray spectra are compared to the Multi-Channel Laundau-Zener cross sections and spectra described in [6]. For $n < 5$, we find poor agreement between analytical l distributions and TDCC values at all energies considered here. For $n \geq 6$, the l distribution tends toward the statistical distribution for collision energies between 1 - 5 keV/amu. The effect of our nl distributions on the x-ray spectra and line ratio diagnostics are presented.

References

[1] K. Kuntz 2018 *The Astronomy and Astrophysics Review* **27** 1
[2] P. Mullen *et al.* 2016 *The Astrophysical Journal Supplement Series* **224** 31
[3] L. Wu *et al.* 2007 *Fusion Science and Technology* **52** 4
[4] M. Fogle and M. Pindzola 2020 *Journal of Physics B: Atomic, Molecular and Optical Physics* **53** 9
[5] M. F. Gu 2008 *Canadian Journal of Physics* **86** 5
[6] D. Lyons *et al.* 2017 *The Astrophysical Journal Supplement Series* **232** 2

*E-mail: sjb0068@auburn.edu

Dissociation dynamics of C_nN^- (n = 1-3, 5-7) anions and formation of smaller anions in the interstellar and circumstellar mediums

R Chacko[1]*, S Barik[1] and G Aravind[1]†

[1]Indian Institute of Technology Madras, Chennai - 600036, India

Synopsis The formation and depletion of the nitrogen terminated carbon chain anions in the interstellar and circumstellar regions are studied using collision-induced dissociation experiments of C_nN^- (n=1-3, 5-7) anions. The results reveal rich dissociation dynamics, and we identified three new physico-chemical processes anions can take part in UV-dominant astrophysical environments. A new pathway for the formation of smaller anions in the series of C_nN^- and C_n^- is proposed. The results indicate the possible presence of two new anions, C_2^- and C_2N^- in the circumstellar envelope of the carbon-rich star IRC +10216.

C_nN^-(n=1,3,5) ions are the three out of the six detected anions in the interstellar and circumstellar regions in space. The formation mechanism and stability of these anions, as well as the other probable anions that can be present, have been debated by the frontier researchers in astrochemistry, and this work tries to address these questions. Radiative electron attachment (REA) had been initially proposed as a formation mechanism for these anions but was recently reported as an inefficient process. Instead the reaction $HC_nN + H^- \rightarrow C_nN^- + H_2$ was proposed [1, 2]. We propose a new pathway - the formation of C_nN^-/C_n^- anions from larger C_nN^- anions in interstellar and circumstellar environments upon photoexcitation via anion resonances. The proposed mechanism also throws light on the stability of C_nN^- anions in the UV abundant regions in the astrophysical environments. Our work identifies three new physico-chemical processes that anions can take part in the interstellar and circumstellar regions, viz (i) anion dissociation via resonance states without electron detachment, (ii) non-dissociative double electron detachment and (iii) dissociative double electron detachment.

Collision-induced dissociation (CID) experiment was employed to excite the anions to their resonance states and to study their decay. The results present the first study on the dissociation dynamics of C_nN^- (n=1-3,5-7) anions. The results call for a search of two new anions, C_2^- and C_2N^- in the outer envelope of the carbon-rich star IRC+10216. The kinetic energy release analysis revealed concerted dissociation, leading to rich dissociation dynamics. The significance of the results in the astrophysical context is discussed in the recent publication [3].

*E-mail: robychako@gmail.com
†E-mail: garavind@iitm.ac.in

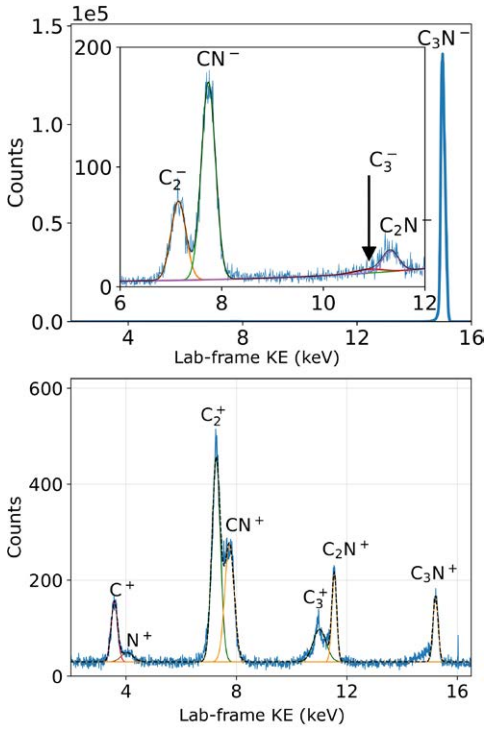

Figure 1. Negative *(top)* and positive *(bottom)* daughter ions formed upon collisional destruction of the ISM anion C_3N^-.

References

[1] Khamesian, M. *et al* 2016 *PRL* **117** 123001
[2] Gianturco, F. A. *et al* 2017 *ApJ* **850** 42
[3] Chacko, R *et al* 2020 *ApJ* **905** 90

Dynamic charge-changing processes in Ne^{7+} ions collision with Ar atoms near the Bohr velocity

Z Wang, R Cheng*, Y H Chen, Y Lei, Y Y Wang, Z X Zhou, J Yang, M G Su and C Z Dong†

Key Laboratory of Atomic and Molecular Physics & Functional Material of Gansu Province, College of Physics and Electronic Engineering, Northwest Normal University, Lanzhou 730070, China

Synopsis Charge state of 1.75 MeV Ne^{7+} ions penetrating through the different areal densities of gaseous argon target are measured. The comparison between experiment and theoretical explanation gives the evidence of multi-electron charge-changing effects on the dynamic evolution of charge state with target areal density.

The roles of charge-changing and related energy loss for highly charged ions penetrating through the matter are important for the investigation of fusion energy research [1,2]. Here, we address the recent progress on the charge state measurement in the case of several tens of keV/u Ne^{7+} ions passing through a gaseous argon target.

The experiments were carried out at the HV-ECR (High Voltage Electronic Cyclotron Resonance ion source) platform at IMP, where ion beams with energy up to 320*q keV (q is charge state of ions) can be provided. After penetrating through the gaseous target, the ion beams were measured by a position sensitive detector coupled the electrostatic plates [3].

Figure 1 shows the experimental result of the average charge state for 1.75 MeV Ne^{7+} ions penetrating the gaseous Ar target with the areal density varying from 0 to 130 μg/cm^2. The average charges predicted by different model are also shown. In this figure, SEL+SEC denotes prediction considering only single-electron loss and capture cross sections; DEL+SEC (a/b), additionally, the double-electron loss cross sections are taken into account properly.

As can be seen in the figure, the experimental result shows a clear dynamic evolution of average charge from non-equilibrium stage to equilibrium stage. The predictions considering the effect of double-electron loss processes provides a better agreement with the experiment than the prediction of SEL+SEC only.

It was also found that the average charge state goes down again at the areal density greater than 30 μg/cm^2 and our present theoretical predictions cannot explain it well. The reason for this phenomenon can be attributed to significant energy loss of projectile [3]. In the future, we plan to propose an analysis model to explain it.

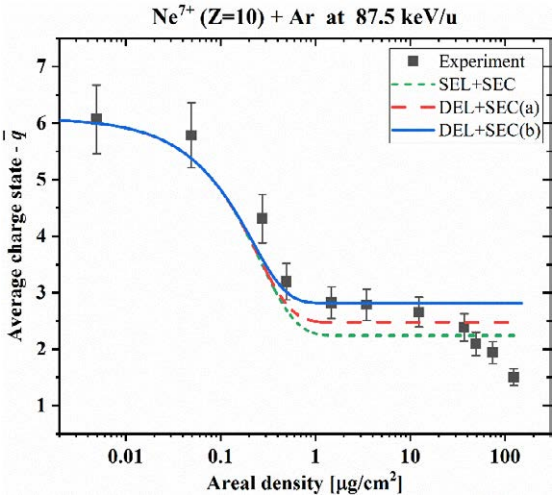

Figure 1. Average charge states of exit ions as a function of the target areal density for Ne^{7+} ions penetrating through gaseous Ar targets.

This work was supported by the State Key Development Program for Basic Research of China (Grant No. 2017YFA0402300) and the National Natural Science Foundation of China (Grant Nos. U1532263, 11505248, 11375034, 11775042).

References

[1] Hurricane O A *et al* 2016 *Nat. Phys.* **12** 800-806.
[2] Kawata S *et al* 2016 *Matter Radiat. at Extremes* **1** 89-113.
[3] Wang Z *et al* 2020 *Phys. Scr.* **95** 105404.

* E-mail: chengrui@impcas.ac.cn
† E-mail: dongcz@nwnu.edu.cn

Inversion of coherent backscattering with interacting Bose–Einstein condensates in two–dimensional disorder : a Truncated Wigner approach

R. Chrétien * **and P. Schlagheck** †

CESAM Research Unit, University of Liege, 4000 Liège, Belgium

We theoretically study the propagation of an interacting Bose–Einstein condensate in a two-dimensional disorder potential, following the principle of an atom laser. The constructive interference between time–reversed scattering paths gives rise to coherent backscattering, which may be observed under the form of a sharp cone in the disorder-averaged angular backscattered current.

As is found by the numerical integration of the Gross–Pitaevskii equation, this coherent backscattering cone is inversed when a non-vanishing interaction strength is present, indicating a crossover from constructive to destructive interferences.

Numerical simulations based on the Truncated Wigner method allow one to go beyond the mean-field approach and show that dephasing renders this signature of antilocalisation hidden behind a structureless and dominant incoherent contribution as the interaction strength is increased and the injected density decreased, in a regime of parameters far away from the mean–field limit.

However, despite a partial dephasing, we observe that this weak antilocalisation scenario prevails for finite interaction strengths, opening the way for an experimental observation with ^{87}Rb atoms [1].

References

[1] R. Chrétien and P. Schlagheck, Phys. Rev. A **103**, 033319 (2021).

*E-mail: rchretien@uliege.be
†E-mail: peter.schlagheck@uliege.be

Distorted wave models for electron emission by impact of dressed proyectiles.

N Esponda[1]*, M A Quinto[1], R D Rivarola[1,2] and J M Monti[1,2]

[1]Grupo de Colisiones Atómicas IFIR-CONICET, Rosario CP2000, Argentina
[2]Laboratorio de Colisiones Atómicas FCEIA-UNR, Rosario CP2000, Argentina

Synopsis
In collisions involving dressed projectiles, partial or total screening of their nuclear charge should be considered. Accordingly, a dynamic effective charge is included in the state-of-the-art CDW and CDW-EIS models. This correction in the exit channel retrieves a two center description from collisions with neutral projectiles. However, some discrepancies are found when the dynamic charge is applied to the initial channel under the CDW-EIS prior version. This may be due to the asymptotic character of the Eikonal approximation. Therefore, further exploration with CDW models will be performed.

Up to date, the continuum distorted wave model (CDW) [1, 2] and its initial Eikonal state approximation (CDW-EIS) [3] can both predict, within a general good agreement, the double differential cross sections for single ionization by impact of swift partially dressed ions over atomic targets. However, some of the approximations made in the seek of maintaining analytical distorted wavefunctions can still be improved to obtain a better physical description of the collision.

In the present work we study the effective charge assigned to the projectile electric field. Due to the electronic structure of the projectile, its nuclear charge may result screened to some extent; for small impact parameters the active electron might be perturbed by a nuclear-like projectile potential whereas an asymptotic net charge is felt by the active electron for a large impact parameter. To take this dynamic screening into account, the effective dressed projectile charge is selected regarding the collision impact parameter. Following the work done in [4], a dynamic effective charge is defined in terms of the projectile form factor.

Using this dynamic effective charge in the final channel, a better agreement with experimental data is achieved for partially dressed ions and atoms as projectiles. Moreover, in the case of neutral ones a two center description is retrieved, not as in the case of using a static net charge (equal to zero) that makes the projectile distortions disappear. Nonetheless, some discrepancies are found when the dynamic charge is applied to the initial channel under the CDW-EIS prior version. This might be expected because of the asymptotic nature of the Eikonal approximation. To test this assumption, a comparison with CDW results will be presented.

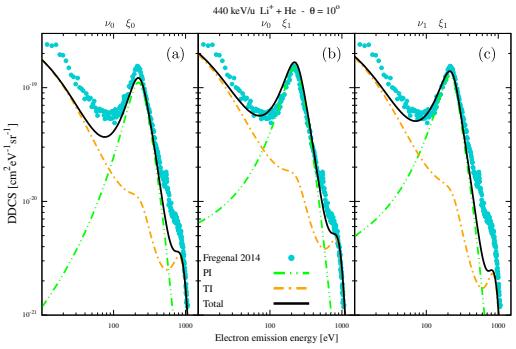

Figure 1. CDW-EIS prior DDCS using (a) an asymptotic net charge in both channels, (b) a dynamic charge correction only in the exit channel and (c) a dynamic charge in both channels. "PI" stands for projectile ionization and "TI" for target ionization. Experimental results are from [2].

References

[1] Monti J. M. *et al* 2010 *J. Phys. B At. Mol. Phys.* **43** 205203
[2] Fregenal D. *et al* 2014 *J. Phys. B At. Mol. Phys.* **47** 155204
[3] Monti J. M. *et al* 2021 *Atoms* **9** 3
[4] R. D. DuBois and S. T. Manson 1990 *Phys. Rev. A* **42** 1222

*E-mail: nesponda@fbioyf.unr.edu.ar

Ejected electron distribution in the particle atom collision

G Zorigt[1] *, L Khenmedekh[1] † and Ch Aldarmaa[1]

[1]Department of Physics, School of Applied Sciences, Mongolian University of Science and Technology, Ulaanbaatar city, 14191, Mongolia

Synopsis For the heavy particle collision with the atom, information's from the fully differential cross sections. We here show that the information's can be obtained directly from the ejected electron probability distribution.

In the particle atom collision process, most information's obtained from the scattering cross sections. But in this paper we will show that the information's may be obtained directly from the electron wave function i.e. from the solution of the time-dependent Schrodinger equation (TDSE) and visualized. For the heavy particle collisions with the atom, the particle treated classically, as moving along the straight line trajectory and the atomic electrons are treated quantum mechanically by solving the TDSE [2, 3]. On the other hand, experimentators are measured the fully differential cross sections (FDCS) for a given scattering angle (or transferred momentum) of the projectile. To compare with the experimental results, one must go from the classical impact parameter (straight line) trajectories to the transferred momentum representation for the projectile scattering amplitude. Instead of to do this, we transform the electron wavefunction from the impact parameter representation to the the transferred momentum representation, which allows us directly visualize the electron distribution probability in space and time. The transformation is the two dimensional Fourier transform:

$$\Psi_{\vec{\eta}}(t,\vec{r}) = \frac{1}{2\pi}\int d\vec{b} e^{i\vec{\eta}\vec{b}} e^{i\delta(b)} \Psi_{\vec{b}}(t,\vec{r}) \qquad (1)$$

where b is the projectile impact parameter, η is the transverse momentum transfer to the projectile, $\delta(b) = \frac{2Z_a Z_p}{v} \cdot \ln(v \cdot b)$. In the Figures 1 and 2 shown the square of the wave function modulus $\left(\left|r\,\Psi_{\vec{\eta}}(t,\vec{r})\right|^2\right)$ at the scattering plane in case of projectile energy of 200 keV, the scattering angle 0.2 mrad (η = 0.519a.u.) .

From the Figure 1. we observe that the ejected electron probability distribution has two lobes corresponding to the binary and recoil peaks of the FDCS for the antiproton scattering from the Hydrogen atom. In the Figure 2. shown the proton collision wth Hydrogen atom, the electron probability distribution has a large peak of ionized electron distribution and small peak around the position of the projectile (z=270a.u.) which corresponds to the captured to the projectile electron.

We conclude that the informations of the heavy charged particle-atom scattering can be obtained directly from the electron probability distribution in the transferred momentum representation of projectile.

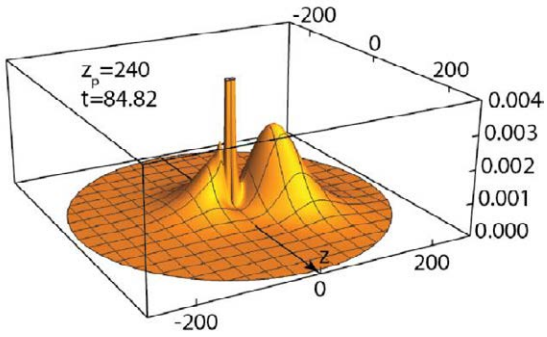

Figure 1. Ejected electron probability density in the scattering plane. Projectile (antiproton) energy 200 keV, scattering angle 0.2 mrad, antiproton z-coordinate equal to 240 a.u..

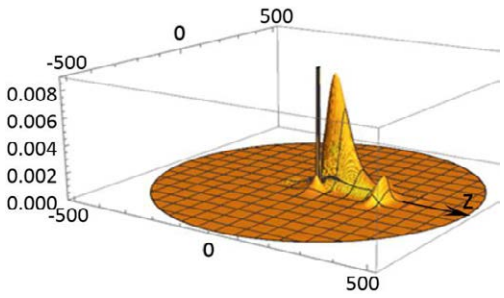

Figure 2. Ejected electron probability density in the scattering plane. Projectile (proton) energy 200 keV, scattering angle 0.2 mrad, proton z-coordinate equal to 270 a.u

REFERENCES

[1] G. Zorigt, L. Khenmedekh, Ch. Aldarmaa, IJMA-10(5), (2019) 19-23.
[2] J. Azuma, N. Toshima, K. Hino, and A. Igarashi, Phys. Rev. A 64, 062704 (2001).
[3] Emil Y Sidky and C D Lin. J. Phys. B: At. Mol. Opt. Phys. 31 (1998) 2949–2960

* E-mail: zorigt@must.edu.mn
† E-mail: khenmed@must.edu.mn

Angular distribution of characteristic radiation following the proton- and electron-impact excitation of He-like uranium

A Gumberidze[1]*, D B Thorn[2], A Surzhykov [3,4,5], C J Fontes[6], D Banaś[7], H F Beyer[8], W Chen[9], R E Grisenti[8,10], S Hagmann[8,10], Regina Hess[8], P-M Hillenbrand[8,10], P Indelicato[11], C Kozhuharov[8], M Lestinsky[8], R Märtin[8,12], N Petridis[8], R V Popov[13], R Schuch[14], U Spillmann[8], S Tashenov[15], S Trotsenko[8,12], A Warczak[16], G Weber[8,12], W Wen[17], D F A Winters[8], N Winters[8], Z Yin[18], and T Stöhlker[8,12,19]

[1] EMMI, GSI Helmholtzzentrum für Schwerionenforschung, 64291 Darmstadt, Germany
[2] Lawrence Livermore National Laboratory, Livermore, California 94550-9234, USA
[3] Physikalisch-Technische Bundesanstalt, D-38116 Braunschweig, Germany
[4] Technische Universität Braunschweig, D-38106 Braunschweig, Germany
[5] Laboratory for Emerging Nanometrology Braunschweig, D38106 Braunschweig, Germany
[6] Computational Physics Division, Los Alamos National Laboratory, Los Alamos NM 87545, USA
[7] Institute of Physics, Jan Kochanowski University, PL-25-406 Kielce, Poland
[8] GSI Helmholtzzentrum für Schwerionenforschung, 64291 Darmstadt, Germany
[9] Chinese Academy of Sciences, Institute of High Energy Physics, Dongguan 523803, China
[10] Institut für Kernphysik, Goethe-Universität Frankfurt, 60486 Frankfurt am Main, Germany
[11] LKB, Sorbonne Université, CNRS, ENS-PSL Research University, Collège de France, F-75005 Paris, France
[12] Helmholtz-Institut Jena, D-07743 Jena, Germany
[13] Department of Physics, St. Petersburg State University, St. Petersburg 198504, Russia
[14] Physics Department, Stockholm University, S-106 91 Stockholm, Sweden
[15] Physikalisches Institut, Ruprecht-Karls-Universität Heidelberg, 69120 Heidelberg, Germany
[16] Institute of Physics, Jagiellonian University, 30-348 Krakow, Poland
[17] Institute of Modern Physics, Chinese Academy of Sciences, 730000, Lanzhou, China
[18] Laboratory for Physical Chemistry, ETH Zrich, 8093 Zürich, Switzerland
[19] IOQ, Friedrich-Schiller-Universität Jena, 07743 Jena, Germany

Synopsis In this work, we studied an angular distribution of characteristic radiation following excitation of He-like uranium in collisions with hydrogen and argon gas targets. The experimental data show a good agreement with fully relativistic calculations which include the projectile excitation due to the interaction with the target nucleus as well as the target electrons. In particular, we clearly identify an important role of the electron-impact excitation on the angular distributions.

In this contribution, we present an experimental and theoretical study of K→L excitation for He-like uranium occurring in collisions with hydrogen and argon targets at 218 and 300 MeV/u energies. The experiment was performed at the Experimental Storage Ring (ESR) at GSI Darmstadt. The excitation process has been studied via observing Kα x-rays of He-like uranium following the decay of the excited L-shell states. In this study, we concentrate in particular on angular distributions of the characteristic Kα radiation. Therefore, we pay special attention to the magnetic sub-level population of the excited $1s2l_j$ states which is directly related to the angular distribution. The experimental data can be well described by fully relativistic calculations taking into account the proton- (or nucleus-) and electron-impact excitation processes. We show that the two processes populate magnetic sublevels of the $1s2l_j$ states differently. Moreover, we demonstrate for the first time an important influence of the electron-impact excitation process on the angular distribution of the Kα_2 radiation produced by excitation of He-like uranium in collisions with the H_2 target [1].

References

[1] Gumberidze A *et al* 2021 *Atoms* **9** 20

*E-mail: a.gumberidze@gsi.de

Multi-electron processes in near-adiabatic collisions of $Xe^{52+....54+}$ +Xe at the ESR Storage ring

S. Hagmann[1*], P.-M. Hillenbrand[1, 2], J. Glorius[1], U. Spillmann[1], Yu. A. Litvinov[1], Y. S. Kozhedub[10], I. I. Tupitsyn[10], M. Lestinsky[1], A. Gumberidze[1, 3], S. Trotsenko[1,4], M. Steck[1], R. Grisenti[1,2], N. Petridis[1,2], Sh. Sanjari[1], C. Brandau[1], E. Menz[1], T. Morgenroth[1], D. Schneider[5], O.Forstner[1,4], R. Chen[1], R. Sidhu[1],L. Varga[1],P.Pfäfflein[9], H. Rothard[6], E. DeFilippo[7], E. P. Benis[8], S. Nanos[8],Th. Stöhlker[1,4,9]

[1]GSI Helmholtz-Zentrum für Schwerionenforschung, 64291 Darmstadt, Germany, [2]Inst. f. Kernphysik, Goethe Universität, 60438 Frankfurt, Germany, [3]Extreme Matter Institute EMMI, 64291 Darmstadt, Germany [4]Helmholtz Institut Jena, 07743 Jena, Germany, [5]Lawrence Livermore National Laboratory, 94550 Livermore, USA, [6]CIMAP-CIRIL-Ganil, F-14070 Caen, France, [7]INFN-LNS Istituto Nazionale de Fisica Nucleare - Laboratori Nazionali del Sud Catania, 95123 Catania, Italy, [8]Dep of Physics, Univ. of Ioannina, 45110 Ioannina,Greece, [9]Institut für Optik u. Quantenelektronik, Universität Jena, 07743 Jena, Germany, [10]Dep of Physics, St Petersburg State Univ., 199034 St Petersburg, Russia

Synopsis We present preliminary results for target and projectile K x ray spectra emitted in 15AMeV and 30AMeV $Xe^{52+,53+,54+}$ + Xe collisions

We are studying multi-electron transfer and –ionization processes in near adiabatic collisions ($v_{proj}/v_K<0.6$) of bare, H-like and He-like $Xe^{54+...52+}$ ions with Xe atoms. We measure emitted target- and projectile K- and L- x rays at 35^9, 90^0 and 145^0 with respect to the beam direction in coincidence with projectiles which have captured 3 to 6 electrons, and with time of flight of recoiling Xe target ions. The target K satellite and hyper-satellite x rays which we observe in these collisions overwhelmingly originate from 2pπ-2pσ rotational coupling (for Xe^{52+} projectiles) and single (for $Xe^{53+,54+}$) and double (only for Xe^{54+}) charge transfer from the target K shell into the projectile K shell. The satellite and hypersatellite K x ray spectra emitted by the projectile, on the other hand, are created following single and multiple outer shell electron transfer from the target into the projectile. The energy resolution of the Ge(i) detectors permits to resolve for K x rays emitted by the projectile satellite from hypersatellite transitions from L-, M-, N-, O-, and P-shells into the K shell with clear evidence that even higher shells beyond the projectile P shell are significantly populated; the K x rays from those high n shells indicate that outer shell transfer dominantly ends in (n,l) states with a low l≈1, i.e $2p_{1/2}$ and $2p_{3/2}$ decaying directly to the K shell. Capture dominantly going into circular states (n,l=n-1) of the projectile would feed mostly the $KL_{2,3}$ transitions via Yrast cascades, which is in conflict with present evidence. Projectile K x ray spectra coincident with multiple (i) capture with i≥3 into the projectile show only capture occurring into states up to n=6, with clear absence of the Rydberg state population, which only appears for single and double capture. We also find that single capture favors capture into the $2p_{3/2}$ over the $2p_{1/2}$ state, whereas for multiple capture n≥3 the $2p_{1/2}$ is more strongly populated than the $2p_{3/2}$ state. For the target satellite and hypersatellite K x ray spectra, we observe that the ratio K- satellite/K-hypersatellite yields is significantly enhanced over the predictions by a relativistic theory, which exhibits a near binomial distribution for single and double K to K charge transfer for bare Xe^{54+} projectiles[1]. This finding is at variance with homologue ratios at low Z collision systems. This enhancement is particularly strong for 3fold capture into the projectile simultaneous with the K-K charge transfer, but decreases with increasing capture multiplicity. Analysis of further details of the emission characteristic is currently in progress. We, the SPARC collaboration E132, acknowledge support by ERC-ASTRUm-ENSAR2(682841,654002) and ERUM FSP APPA (BMBF 05P15R6FAA, 05P19SJFAA).

References

[1] Y. Kozhedub et al. 2022 to be published

* E-mail: s.hagmann@gsi.de

K-shell vacancy production in slow Xe^{54+}-Xe collisions

P-M Hillenbrand[1,2]*, S Hagmann[2], Y S Kozhedub[3], E P Benis[4], C Brandau[2,5], R J Chen[2], D Dmytriiev[2], O Forstner[2,6] J Glorius[2], R E Grisenti[1,2], A Gumberidze[2], M Lestinsky[2], Yu A Litvinov[2], E B Menz[2], T Morgenroth[2], S Nanos[4], N Petridis[2], P Pfäfflein[7], H Rothard[8], M S Sanjari[2], R S Sidhu[2], U Spillmann[2], S Trotsenko[2], I I Tupitsyn[3], L Varga[2], Th Stöhlker[2,6,7]

[1]Institut für Kernphysik, Goethe-Universität, 60438 Frankfurt, Germany
[2]GSI Helmholtzzentrum für Schwerionenforschung, 64291 Darmstadt, Germany
[3]Department of Physics, St. Petersburg State University, 199034 St. Petersburg, Russia
[4]Department of Physics, University of Ioannina, 45110 Ioannina, Greece
[5]I. Physikalisches Institut, Justus-Liebig-Universität Giessen, 35392 Giessen, Germany
[6]Institut für Optik und Quantenelektronik, Friedrich-Schiller-Universität Jena, 07743 Jena, Germany
[7]Helmholtz-Institut Jena, 07743 Jena, Germany
[8]CIMAP-CIRIL-Ganil, 14070 Caen, France

Synopsis We present preliminary experimental and theoretical results for single and double K-shell vacancy production in slow Xe^{54+}-Xe collisions.

Slow symmetric collisions of heavy ions are of fundamental interest due to their relativistic non-perturbative character. In the limiting case of small collision velocities with respect to the orbital velocity of the active electrons, these processes can be considered as quasi-molecular or adiabatic collisions. When the collision occurs between a heavy projectile ion and a similarly heavy target atom, a fully relativistic description is required. A corresponding time-dependent two-center approach was developed in Refs. [1, 2], but comparison to experimental results has been scars [3].

In the presented experiment we studied the collision system Xe^{54+}+Xe at 30 MeV/u and 15 MeV/u. For comparison we also performed measurements for Xe^{53+}+Xe at 15 MeV/u. We used x-ray detectors at three observation angles, a particle detector for recombined projectile ions, a target-ion recoil detector, and an electron spectrometer. In particular, the x-ray spectra of the Ge(i) detector mounted at 35° with respect to the projectile beam proved to be highly sensitive to the occurring electron-transfer mechanisms. At this observation angle, target and projectile radiation of the symmetric collision systems can be distinguished solely by the Doppler shift of the projectile radiation, and the Kα radiation of both collision partners can unambiguously be identified.

*E-mail: p.m.hillenbrand@gsi.de

As a first step we analyzed the target satellite $K\alpha^{s}_{1,2}$ and hypersatellite $K\alpha^{hs}_{1,2}$ radiation. Their intensity ratio is directly related to the cross section ratio of target single-to-double K-shell vacancy production. In slow symmetric collisions of bare projectile ions with neutral target atoms, target K-shell vacancy production occurs dominantly through resonant charge transfer of one or two electrons from the target's K-shell to the projectile's K-shell. This can be seen in our data by the absence of target $K\alpha^{hs}_{1,2}$ radiation for incoming Xe^{53+} projectiles. We will present a preliminary analysis of the measured x-ray spectra, and compare our results to theoretical predictions applying the approach of Refs. [1, 2].

This research has been conducted in the framework of the SPARC collaboration, experiment E132 of FAIR Phase-0 supported by GSI. It is further supported by the European Research Council (ERC) under the European Union's Horizon 2020 research and innovation programme, grant No. 682841 ("ASTRUm") and the grant agreement No. 654002 (ENSAR2). We acknowledge substantial support by ErUM-FSP APPA (BMBF No. 05P15RGFAA and No. 05P19SJFAA).

References

[1] Tupitsyn I I *et al* 2010 *Phys. Rev. A* **82** 042701
[2] Tupitsyn I I *et al* 2012 *Phys. Rev. A* **85** 032712
[3] Kozhedub Y S *et al* 2014 *Phys. Rev. A* **90** 042709

Theoretical study on the hyperpolarizability of Li atoms

T Wang, J Jiang*, Z W Wu, L Y Xie, D H Zhang and C Z Dong

Key Laboratory of Atomic and Molecular Physics and Functional Materials of Gansu Province,College of Physics and Electronic Engineering, Northwest Normal University, Lanzhou, 730070, P. R. China

Synopsis The hyperpolarizability of the ground state of Li atoms is calculated by using the relativistic configuration interaction plus core polarization (RCICP) method. The contributions of different intermediate states to the hyperpolarizability have been analyzed to explain the reason for the difference between the theoretical results of different methods.

With the rapid development of laser trapping and cooling technologies, the accuracies of atomic clocks have reached the level of 10^{-19} [1]. The hyperpolarizability of atoms needs to be determined accurately. In addition, the uncertainty of atomic hyperpolarizability results in uncertainty of 10^{-17} to 10^{-18} level in clock experiments [2, 3, 4]. Therefore, high-precision hyperpolarizability is a very key atomic parameter to obtain high-precision atomic clocks.

For the ground state of Li atoms, the difference of hyperpolarizability calculated by different theoretical methods is more than 10 times. For example, the hyperpolarizability calculated by Kassimi *et al.* with the coupled cluster method is 1100 a.u. [5]. This result is 3 times smaller than the result 3060 a.u. [6] calculated by Tang *et al.* with the Hylleraas basis expansion method, and an order of magnitude smaller than the result 65000 a.u. [7] calculated by Fuentealba *et al.* with the semiempirical pseudopotentials method.

In the present work, the hyperpolarizability of the ground state of Li atoms is calculated by using the relativistic configuration interaction plus core polarization (RCICP) method. In order to explain the reason for these differences, the contributions of different intermediate states to the hyperpolarizability are analyzed in detail. It is found that the summation of the contributions of the $2s \rightarrow np_j (n \geq 3)$ and $np_j \rightarrow nd_j (n \geq 3)$ transitions to hyperpolarizability is approximately equal to that term of $\alpha_0^1\beta_0$, as shown in Table I. The subtraction between the summation of contributions of the different intermediate states and $\alpha_0^1\beta_0$ is relatively small. Consequently, the uncertainty of the hyperpolarizability of the ground state is very large.

Table 1. Contributions to the hyperpolarizability (a.u.) of the ground state of Li atoms. The values in parentheses indicate the uncertainties. γ_0 is the hyperpolarizability of the ground state.

Contr.	RCICP
$\frac{1}{18}T(s,p_{1/2},s,p_{1/2})$	8312(2)
$-\frac{1}{18}T(s,p_{1/2},s,p_{3/2})$	16624(5)
$-\frac{1}{18}T(s,p_{3/2},s,p_{1/2})$	16624(5)
$\frac{1}{18}T(s,p_{3/2},s,p_{3/2})$	33248(11)
$T(s,p_{j'},s,p_{j''})$	74809(13)
$\frac{1}{18}T(s,p_{1/2},d_{3/2},p_{1/2})$	33799(13)
$\frac{1}{18\sqrt{10}}T(s,p_{1/2},d_{3/2},p_{3/2})$	6759(3)
$\frac{1}{18\sqrt{10}}T(s,p_{3/2},d_{3/2},p_{1/2})$	6759(3)
$\frac{1}{180}T(s,p_{3/2},d_{3/2},p_{3/2})$	1352(0)
$\frac{1}{30}T(s,p_{3/2},d_{5/2},p_{3/2})$	72993(40)
$T(s,p_{j'},d_j,p_{j''})$	121661(42)
$Total$	196470(55)
$\alpha_0^1\beta_0$	196128(268)
$\gamma_0(2s)$	4109(3264)

This work has been supported by National Key Research and Development Program of China (2017YFA0402300) and National Natural Science Foundation of China (Grant Nos. 11774292, 11864036, 11804280).

References

[1] Brewer S M *et al* 2019 *Phys. Rev. lett.* **123** 033201
[2] Derevianko A *et al* 2003 *Rev. Mod. Phys.* **83** 331
[3] Katori H *et al* 2003 *Phys. Rev. lett.* **91** 173005
[4] Porsev S G *et al* 2018 *Phys. Rev. lett.* **120** 063204
[5] Kassimi E B *et al* 1994 *Phys. Rev. A* **50** 2948
[6] Tang L Y *et al* 2009 *Phys. Rev. A* **79** 062712
[7] Fuentealba P *et al* 1993 *J. Phys. B: At. Mol. Opt. Phys.* **26** 2245

*E-mail: phyjiang@yeah.net

Transfer of angular momentum at the interaction between spin polarized metastable helium atoms

V.A. Kartoshkin*

Ioffe Institute, Russian Academy of sciences, St. Petersburg, 194021, Russia

Synopsis The cross sections, which characterize the decay and transfer of orientation and alignment of colliding particles as a result of chemiionization and spin exchange are calculated.

In the collision of spin-polarized atoms, the transfer of electron polarization between colliding particles is possible. A similar situation occurs in a collision, for example, between alkali atoms in the ground state. If one of the colliding particles is in an excited state and its energy is sufficient for ionization of the collision partner, then together with the elastic process (spin exchange), an inelastic process (ionization) is also possible, as a result of these processes polarization can also be transferred to the partner. Simultaneously occurring elastic and inelastic processes at the collision between two helium atoms are possible if these atoms are in the metastable (2^3S_1) state [1].The helium metastable atom ($He^*(2^3S_1)$), having a large store of internal energy (19.8 eV), is capable to ionize the molecules or atoms even at the thermal energies of relative motion. In a collision between two excited (metastable) helium atoms both elastic (spin exchange) and inelastic process (chemiionization) are possible. The paper discusses the interaction between spin-polarized metastable helium isotopes under conditions of optical pumping of atoms. The optical orientation of atoms is a method to obtain spin polarized atomic particles during an experiment. It is possible to introduce the cross section σ^{abs} and σ^{tr} which, according to kinetic equations, characterize the decay and transfer of orientation and alignment of colliding particles as a result of chemiionization and spin exchange. Complex interaction potentials of the atoms under study were constructed and on their basis the spin exchange (σ^{abs}) and chemoionization (σ^{tr}) cross sections were calculated.

Using these cross sections, expressions for the transfer of orientation and alignment from one atom to another were obtained. It is known that, in a collision of two triplet metastable helium atoms a quasi-molecule, He_2^* is formed [2]. This quasi-molecule can decay in two channels with the formation of atomic and molecular helium ions.

$$He^*(2^3S_1)+He^*(2^3S_1)\rightarrow He_2^*\rightarrow\begin{cases} He_2^+ + e^- \\ He(1^1S_0)+He^+ + e^-, \end{cases} \quad (1)$$

The quasi-molecule formed in the collision can be described by three states with the total spin $S = 0$, 1, and 2, which corresponds to three molecular terms $^1\Sigma^+$, $^3\Sigma^+$, $^5\Sigma^+$ (singlet, triplet and, quintet). In accordance with the law of conservation of total spin ($m_1+m_2=m_1'+m_2'$) ionization is only possible from the states of low multiplicity, i.e. from the singlet and triplet states, since in this case, the total spin is the same at the exit and entrance of the reaction.

As noted above, simultaneously with the inelastic process an elastic process is also possible:

$$He^*(2^3S_1,m_1)+He^*(2^3S_1,m_2)\rightarrow He_2^* \rightarrow He^*(2^3S_1,m_1')+He^*(2^3S_1,m_2'), \quad (2)$$

where m_1 and m_2 are the projections of the angular moments of the atomic particles.

If in a collision participate atoms polarized in spin, then in processes (1) and (2) the transfer of angular momentum from one atom to another is also possible. It should be borne in mind that the simultaneous occurrence of elastic and inelastic processes leads to their mutual influence. In particular, the cross section of the elastic process changes significantly, and this is the case for both the cross-section of the spin exchange and the magnetic resonance frequency shift cross-section.

References

[1] Kartoshkin V.A. 2008 *Opt.Spectrosc.* **105** 657
[2] Muller M.W. et al 1991 *Z. Phys. D* **21** 89

* E-mail: victor.kart@mail.ioffe.ru

RDEC for F^{9+} and F^{8+} Ions on Graphene: First Observation†

D S La Mantia[1]*, P M Niraula[2], K Bhatt[2], A Kayani[2], and J A Tanis[2]

[1]Department of Physics & Astronomy, Clemson University, Clemson, SC 29634 USA
[2]Department of Physics, Western Michigan University, Kalamazoo, MI 49008 USA

Synopsis First evidence for radiative double-electron capture has been observed for fast ions colliding with single-layer graphene. Preliminary results for 2.11 MeV/u (40 MeV) F^{9+} and F^{8+} compared with those for previous RDEC studies for thin-foil carbon targets ($\sim 10^2$ thicker) show similarities despite the closeness in thickness (∼factor of two) to the N_2 and Ne gas targets. The similarities and differences will be discussed.

Radiative double electron capture (RDEC) is a fundamental atomic collision process wherein two electrons are captured from the target to bound states in the projectile simultaneous with emission of a single photon [1]. RDEC can be considered the inverse of double photoionization for ion-atom collision systems. Preliminary RDEC results for 2.11 MeV/u $F^{9,8+}$ (40 MeV) ions on single-layer graphene are presented.

This work was performed using the tandem Van de Graaff facility at Western Michigan University. The incident beam was directed toward a ∼0.35 nm thick graphene sample mounted on a 200 nm thick silicon nitride grid with ∼6400 holes of 2 μm diameter on a 200 μm thick silicon substrate (commercially purchased). Details of the graphene target can be found in an abstract adjacent to this one. A Si(Li) x-ray detector at 90° to the beamline collected photons. Following magnetic separation, individual silicon surface-barrier detectors collected charge-changed projectiles. Event mode data collection was used to assign coincidences between x rays and charge-changed particle events.

Fig. 1 shows preliminary x-ray gated particle spectra obtained for F^{9+} ions on the graphene target (left side) compared with the same spectra for thin-foil carbon. Similarities and differences are seen, with the data for the graphene showing up in all three outgoing charge states. Previous studies for 40 MeV F^{9+} on C [2] showed similar results due to multi-collision effects with the q-2 and q-1 channels being dominant, whereas the present results attributed to single-collisions because of the thinness of the graphene occur primarily in the q-1 channel. For F^{8+} the graphene counts were dominant in the q channel by about a factor of four, in contrast to thin-foil carbon [2] where the counts were split about equally between channels q-1 and q. On the other hand, previous work for gas targets of N_2 and Ne [3] showed all events to occur as expected in the q-2 channel.

†Supported in part by NSF Grant 1707467.

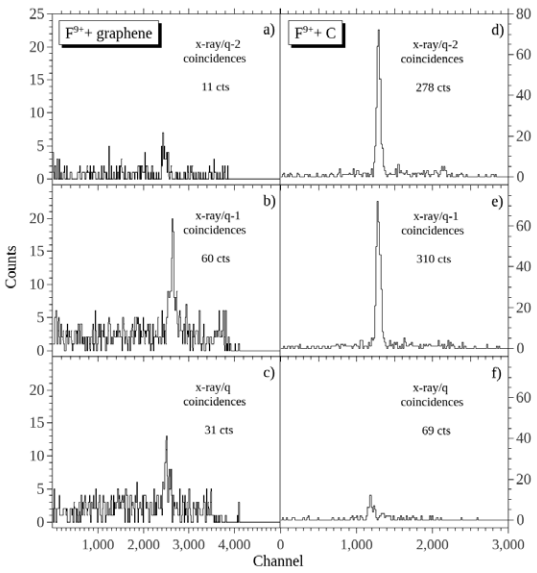

Figure 1. Doubly- (q-2), singly- (q), and no (q) charge changed particle spectra associated with RDEC x-ray events for 2.11 MeV/u F^{9+} (40 MeV) + graphene (left panel, preliminary) and thin-foil C (right panel). The numbers on the graphs are the spectra totals after background subtraction.

References

[1] Miraglia J and Gravielle M. S. 1987 *ICPEAC XV: Book of Abstracts* p. 517 Brighton, U.K.
[2] La Mantia D S *et al* 2020 *Phys. Rev. A.* **102** 060801(R)
[3] La Mantia D S *et al* 2020 *Phys. Rev. Lett.* **124** 133401

*E-mail: dlamant@clemson.edu

Updated compilation, universal empirical and theoretical fits for K x-ray production cross sections by protons

Gregory Lapicki, Department of Physics, East Carolina University, Greenville NC 27858, USA

The relevance of x-ray production cross sections (XRPCS) and the related ionization cross sections (ISC) in many research areas has been described at length and analyzed in detail [1]. X-ray emission cross sections by ion impact are a relevant input in many areas such as e.g., studies of track structure in DNA [2], water [3], and biological matter [4]. Particle Induced X-ray Emission (PIXE) strongly requires trustworthy databases for XRPCS and/or reliable predictions of inner-shell ionization theories as periodically evaluated in Monte Carlo Geant4 simulations [5,6].

To check if theories are accurate across the periodic table of elements and a large range of projectile energies, equally comprehensive databases are essential and a universal fit for them is desired. That fit should be in terms of a variable by which XRPCS are scaled with a minimum of adjustable parameters.

For each target element, the **compiled XRPCS** [1] follow a single curve when plotted versus the ratio of the proton velocity v_1 to the orbital velocity of $v_{2L}=Z_{2L}/n$ of the inner-shell electron. Furthermore, for all elements XRPCS peak at $\sigma_{LX}^{max}(Z_{2L})$ when $v_1 = v_{2L}$. Hence, with $v \equiv v_1/v_{2L}$, a **universal fit** to all compiled data

$$\sigma_{LX}=\sigma_{LX}^{max}(Z_{2L})\cdot\exp[-(1+a_1Z_{2L})v^2+a_2v^7] \quad (1)$$

is made with just two adjustable parameters a_1=0.00484 and a_2=0.005. The predictions of the ECUSAR theory [7] can be also fitted in a similar fashion as done recently based on recently updated data and the revised universal empirical fit [8].

1) **Over three decades old tables of K-shell XRPCS [9,10] will be updated with a new compilation**,

2) **universal empirical and theoretical fits to the updated database will be reviewed as it was done the L shell [8]**,

3) **similar to the L shell, universal empirical and theoretical fits to these updated data will be presented for the K shell**.

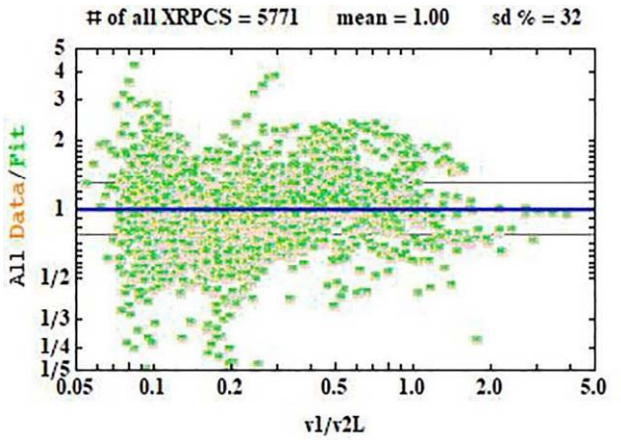

Figure 1. With a standard deviation of 32%, the mean ratio of 5771 measurements to the universal experimental fit for L-shell XRPCS is 1.00. 97% of these ratios are within a factor of 2 from that mean. The compiled data includes target elemnts from $_{24}$Cr to $_{95}$Am and proton energies from 0.035 to 1.000 MeV [8].

References

[1] J. Miranda and G. Lapicki 2014 *At. Data Nucl. Data Tables* **100** 651.
[2] H. Lekadir *et al.* 2009 *Nucl. Instrum. Meth. B* **267** 1001.
[3] G. Bäckström *et al.* 2013 *Med. Phys.* **40** 064101.
[4]M.A. Quinto *et al.* 2020 *Rad.Phys.Chem.* **167** 108337.
[5] M.G. Pia. *et al.* 2010 *J. Phys. Conf. Ser.* **219** 032018.
[6] S. Incerati *et al.* 2015 *Nucl. Instrum. Meth. B* **358** 210.
[7] G. Lapicki 2001 *Nucl. Instrum. Meth. B* **189** 6.
[8] G. Lapicki 2020 *Nucl. Instrum. Meth. B* **467** 123.
[9] G. Lapicki 1989 *J. Phys.Chem. Ref. Data* **18** 111.
[10] H Paul and J. Sacher 1989 *At. Data Nucl. Data Tables* **42** 105.

E-mail : lapickig@ecu.edu

High resolution measurement of the $2p_{3/2} \rightarrow 2s_{1/2}$ intra-shell transition in He-like uranium

R Loetzsch[1 *], U Spillmann[2], D Banas[3], H Beyer[2],P Dergham[4], L Duval[5], J Glorius[2], R Grisenti[2], A Gumberidze[2], P-M Hillenbrand[2], P Indelicato[5], Y Litvinov[2], P Jagodzinski[3], E Lamour[4], N Paul[5], G Paulus[1,6], N Petridis[2], M Scheidel[2], R S Sidhu[2], S Steydli[4], K Szary[3], S Trotsenko[2], I Uschmann[1,6], G Weber[6], T Stoehlker[1,2,7] and M Trassinelli[5 †]

[1]Institut für Optik und Quantenelektronik, Friedrich-Schiller-Universität Jena, 07743 Jena, Germany
[2]GSI Helmholtzzentrum für Schwerionenforschung, 64291 Darmstadt, Germany
[3]Institute of Physics, Jan Kochanowski University, Kielce, Poland
[4]Institut des NanoSciences de Paris, CNRS, Sorbonne Universités, Paris, France
[5]Laboratoire Kastler Brossel, Sorbonne Université, CNRS, ENS-PSL Research Univ., Collége de France, Paris, France
[6]Helmholtz-Institut Jena, Jena,Germany

Synopsis We measured the $2p_{3/2} \rightarrow 2s_{1/2}$ transition in He-like uranium at the ESR, employing a bent crystal Bragg spectrometer. This allows for an energy resolution of ~2.7 eV and an statistical accuracy of ~0.06 eV. By comparing the line to the corresponding transition in Li-like uranium, we aim for an accuracy of ~0.2 eV on the absolute energy of the He-like and ~0.06 eV for the relative measurement of the two lines. This allows for an unmatched test of electron correlation effects and two-loop corrections of Quantum Electrodynamics in few electron systems in strong electric fields.

He-like ions, the simplest multi-body atomic systems, offer the possibility to probe QED correlation and electron interaction effects. The theoretical description of these effects in extrem high electric fields, as for high-Z ions, is still challenging and different approaches leaves to different results. Thus tests by experiments are needed. By measuring the difference in transition energies between He- and Li-like ions, it is additionally possible to effectively isolate the electron correlations effects. Precision spectroscopy of He-like heaviest ions is also experimentally very challenging and the $2p_{3/2} \rightarrow 2s_{1/2}$ transition in uranium was only measured in an pilot experiment [1] at the ESR with limited accuracy.

The experiment was conducted at the internal gas jet target of the ESR at GSI. We employed a twin arm spectrometer with two bent Ge(220) crystals, both under 90° observation angle to the ion beam. The velocity of the ions was tuned to detect the innershell transitions at ~4320 eV. We reached an FWHM resolution of the lines of ~2.7 eV, determined by the crystal reflection curve and a Doppler broadening due to finite size of the gas jet. The collected more than 1000 photons per spectrometer and line allow us to determine the line positions with an statistical accuracy of about 0.06 eV. To control the systematics in the experiment, we also measured reference lines from a stationary Zn fluorescence target as well as the innershell transition from Be-like uranium ions. Preliminary results of the experiment will be given.

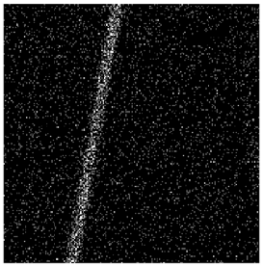

Figure 1. Detector image of the $2p_{3/2} \rightarrow 2s_{1/2}$ transition in He-like uranium. Dispersion is in the horizontal direction. The slant of the line is due to the Doppler shift.

This research has been conducted in the framework of the SPARC collaboration, experiment E125 of FAIR Phase-0 supported by GSI. It is further supported by the Extreme Matter Institute EMMI and by the European Research Council (ERC) under the European Union's Horizon 2020 research as well as by the innovation programme (Grant No 682841 "ASTRUm") and the grant agreement n° 6544002, ENSAR2. We acknowledge substantial support by ErUM-FSP APPA (BMBF n° 05P19SJFAA) too.

References

[1] Trassinelli M *et al* 2009 *EPL.* **87** 63001

* E-mail: robert.loetzsch@uni-jena.de † E-mail: martino.trassinelli@insp.jussieu.fr

Lanthanides, the importance of 4f electrons in the energy loss

A M P Mendez[1 *], C C Montanari[1†], D M Mitnik[1] and J E Miraglia[1]

[1]Instituto de Astronomía y Física del Espacio, CONICET and Universidad de Buenos Aires, Ciudad Autónoma de Buenos Aires, 1428, Argentina

Synopsis In this work we studied lanthanides by using a full-relativistic description of the electronic structure of all shells. We tested the so obtained wave functions in binding energies in stopping power calculations, considering separately the contributions of the valence and bound electrons. Present results for protons in Gd and Er state doubts on the present knowledge of the stopping values in lanthanides, and shows that an appropiate characterization of the 4f-electrons plays a decisive rol.

Knowledge of electronic stopping is important in many fields, from basic physics to technology or medicine [1]. In this case we focused on lanthanides due to its electronic complexity (open 4f-subshell, need of relativistic description [2]); and to low energy experimental data with values much larger than expected [3].

Based on fully relativistic atomic structure results, and to the very close binding energies of the outer shells of Gd and Er, Mendez et al [2] propose that the FEG of these solids should be characterized by 10 (14) electrons and a Wigner-Seitz radio r_S= 1.75 (1.52) for Gd (Er), respectively. These values are in agreement with experimental findings of larger stopping cross sections of rare earths in [3].

Drawing upon our experience in total stopping power calculations in a large energy range [4], we analyzed these values in the two cases mentioned above. The results for H projectile in Gd and Er are displayed in Figure 1. As can be noted, despite the inclusion of the 4f-electrons in the FEG of Gd describes the low energy experimental data, the stopping at intermediate and high energy is highly overestimated. Similar behavior is found for H in Er. In this case, no data is available for impact energies below 100 keV [5]. However, the overestimation of the existing experimental values is clear. In both cases our curves are different from the so accepted SRIM semi empirical values [6].

We conclude that the proposal of the 4f open subshell as part of the FEG should be revised and new experimental data for these and other lanthanides are required.

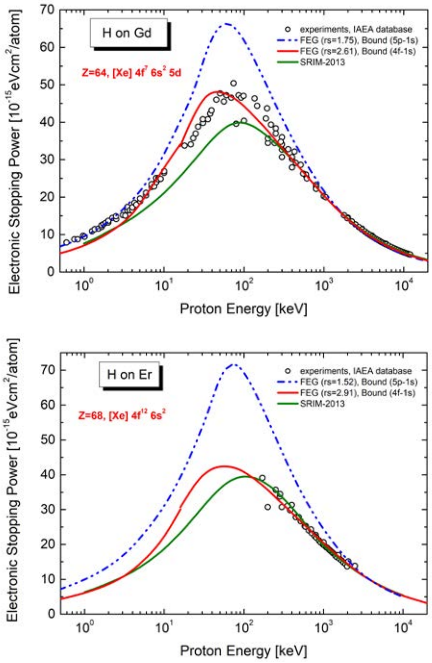

Figure 1. Sopping cross sections for H in Gd and Er. Curves, present results with and without the 4f electrons in the FEG, and SRIM semi empirical values [6]. Symbols, experimental data in [5].

References

[1] H. Paul, A. Schinner, At. Data Nucl. Data Tables 85 (2003) 377
[2] A M O Mendez *et al*, Nuclear Inst. and Meth in Phys. Res. B 460 (2019) 114–118
[3] D Roth *et al*, Phys. Rev. Lett. 118 (2017) 103401
[4] C C Montanari et al, Phys. Rev. A 96 (2017) 012707
[5] *Electronic Stopping Power of Matter for ions*, IAEA database, https://www-nds.iaea.org/stopping/
[6] J.F. Ziegler http://www.srim.org/

* E-mail: alemendez@iafe.uba.ar
† E-mail: mclaudia@iafe.uba.ar

Target used to study radiative-double electron capture in single-layer graphene†

P M Niraula[1*], R Jayathissa[1], D S La Mantia[2], K Bhatt[1], J A Tanis[1] and A N Kayani[1]

[1]Department of Physics, Western Michigan University, Kalamazoo, Michigan, 49008 USA
[2]Department of Physics, Clemson University, Clemson, South Carolina, 29634 USA

Synopsis A special single-layer graphene target is described for measuring radiative double-electron capture by ions passing through. RDEC is a fundamental process occurring when the ion captures two electrons simultaneously with the emission of a single photon. Due to the thinness of the graphene (< 1 nm), it is more difficult to investigate than usual thin-foil or gas targets.

Radiative double-electron capture (RDEC) is a fundamental atomic process that occurs when moving ions pass through a target with the ion capturing two electrons while simultaneously emitting a single photon. The process has been successfully studied for gas [1] and thin-foil [2] targets. However, RDEC has not been investigated to our knowledge for single- or few-layer graphene targets. In an abstract associated with this work, the results of the first attempt for F^{9+} and F^{8+} ions are described. The purpose of this abstract is to describe the special target requirements for a graphene target.

The work was done at the Western Michigan University accelerator laboratory. Beams of F^{9+} and F^{8+} ions obtained from the accelerator were directed onto the target. For the usual gas and thin-foil targets, the beam impacts entirely on the target. For graphene, because of the thinness of the substance, the target must be much smaller and mounted on a grid.

To use a graphene target with single-layer thicknesses as small as ~0.35 nm, a commercially purchased graphene sample on a 200 nm thick silicon nitride supporting grid with ~6400 holes of 2 µm diameter was mounted. This entire assembly was mounted on a 200 µm thick 3.0 mm hexagonal silicon substrate with a 0.5 x 0.5 mm aperture. Figure 1 is a schematic showing the three parts of the assembly. It is noted that all of the incident beam does not strike the graphene in the sample. However, this does not affect the beam used to calculate the estimated cross sections as long as the two charge-changed (q-2 and q-1) and the uncharged-change (q) states of the incident beam are measured. Such is the case in the present experiment done with this target sample. This assembly was used successfully in the RDEC measurements described in the adjoining abstract.

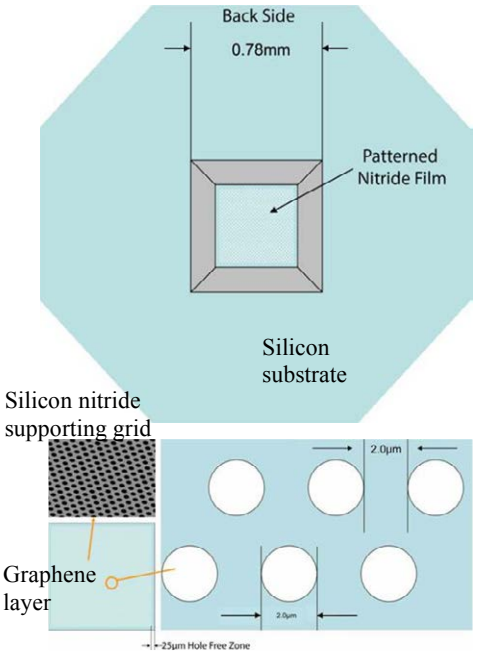

Figure 1. Schematic of the graphene assembly [3] used as the target in the RDEC measurements done.

†Supported in part by NSF Grant No. 1707467.

Reference

[1] D. S. La Mantia *et al*. 2020 *Phys. Rev. Lett.* **124**, 133401).
[2] D. S. La Mantia *et al*. 2020 *Phys. Rev. A* **102**, 060801(R).
[3] ACS Material, 959 E Walnut Street, Pasadena, CA 91106 https://www.acsmaterial.com/graphene-on-silicon-nitride-tem-grids.html

* E-mail: prashantamani.niraula@wmich.edu

;

Measurements of Charge Transfer Cross Sections for Hydrogen Ion Impact on Lithium at Low Energies

P Oxley[1] *

[1]The College of the Holy Cross, Department of Physics, Worcester, 01610, USA

Synopsis We report measurements of the total charge transfer cross section for collisions of protons, deuterium ions, and molecular hydrogen ions with lithium atoms in the energy range 65 – 3000 eV/u. Our proton cross sections are significantly larger than those previously measured, but are in good agreement with the theoretical predictions. Measured deuterium cross sections are equal to the proton cross sections, when scaled to equal ion velocities, while molecular hydrogen ion cross sections are up to a factor of two larger than past measurements.

Charge transfer between ions and atoms is a process of fundamental interest. The transient molecular complex that arises during such a collision is challenging to model accurately, especially at low collision energy, and accurate experimental data are therefore important for testing the validity of different theoretical approaches. In addition, charge transfer plays an important role in a variety of different plasma environments. In tokamak plasmas, charge transfer collisions involving lithium atoms are particularly relevant since lithium is used as a first wall coating in some devices, while neutral lithium beams are injected into the plasma for diagnostic purposes.

We report experimental measurements of total charge transfer cross sections for collisions between lithium atoms and protons in the energy range 130 – 880 eV/u, between lithium atoms and deuterium ions in the energy range 65 – 415 eV/u, and between lithium atoms and H_2^+ ions in the energy range 65 – 3000 eV/u. Our experiments use crossed beams of lithium atoms and ions, unlike most prior experiments that pass the ion beam through a neutral gas cell. Our technique allows efficient detection of the lithium ion produced in a charge transfer collision and can detect impurities present in the lithium beam. In addition, the beam technique enables accurate measurement of the lithium target density by laser absorption spectroscopy.

Figure 1 shows our results for the proton-lithium collision cross sections, along with a prior experiment [1] and several theoretical models [2-5]. At energies below about 700 eV the available theoretical predictions converge towards a single curve that is in close agreement with our data, but not with the prior experimental work. Our cross section data for D^+ collisions with lithium closely match those for proton collisions at the same ion velocity, while our preliminary measurements of H_2^+- lithium collision cross sections are up to a factor of two larger than prior experiments [6]. We hope that our work will stimulate a theoretical study of this collision system, since currently no theoretical predictions for H_2^+- lithium cross sections exist in our energy range.

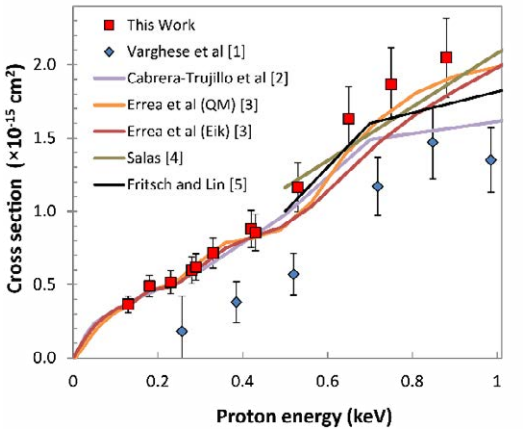

Figure 1. Cross sections for proton-lithium charge transfer collisions. Symbols show experimental data and lines show the results of theoretical calculations.

References

[1] Varghese S L *et al* 1984 *Phys. Rev. A* **29** 2453
[2] Cabrera-Trujillo R 2008 *Phys. Rev. A* **78** 012707
[3] Errea L F *et al* 2008 *Phys. Rev. A* **77** 012706
[4] Fritsch *et al* 1983 *J .Phys. B* **16** 1595
[5] Salas J P, 2000 *J .Phys. B* **33** 3201
[6] Aumayr and Winter 1985 *Phys. Rev. A* **31** 67

* E-mail: poxley@holycross.edu

Charge exchange and excitation cross sections in Li^{2+}-H collisions in the intermediate impact energy domain

S Passalidis*, N Sisourat and A Dubois

Laboratoire de Chimie Physique-Matière et Rayonnement, Sorbonne Université - CNRS, 75005 Paris France

Synopsis Cross sections for shell- and sub-shell selective charge exchange and excitation are presented for collisions between doubly-charged lithium ions and hydrogen atoms for impact energies ranging from 0.1 to 250 keV/u. They are calculated using a semiclassical close-coupling treatment taking into account the two electrons in the dynamics.

Semiclassical close-coupling approaches within the molecular and asymptotic representations have been widely used with great success for one- or quasi-one-active electron ion-atom collisions [1]. For multielectronic systems and for the intermediate energy domain the situation is more complex and a majority of investigations have been performed using the independent electron or independent event approximations [2]. Much less non perturbative calculations taking into account the dynamics of several electrons have been done in the past due to the important computer resources they require. They often presented a limited control of convergence with respect to the number of states included in the basis sets employed. Comparisons with numerous series of experimental data were therefore fundamental to test the accuracy and the adequacy of the theoretical results.

Unlike many ion-atom systems for which wealth of experimental data are available, capture processes in Li^{2+}-H collisions have been more rarely studied, certainly due to the only two existing experimental investigations carried out in the late seventies: both considered the various ionic states of lithium as projectiles, impacting hydrogen at energies ranging from about 10 to 210 keV/u in Shah et al [3] and in the narrow domain 2-4 keV/u in Seim et al [4]. No experimental data therefore exist at low energies.

To study the capture and excitation processes in Li^{2+}-H we applied the semiclassical close-coupling approach based on the asymptotic (atomic) description of the collision partners [5]. The electronic dynamics is then treated quantum mechanically solving the two-electron time-dependent Schrödinger equation within a full configuration interaction (CI) approach.

* E-mail: stylianos.passalidis@sorbonne-universite.fr

In Figure 1, we present the cross sections of total capture for impact energies ranging from 0.1 to 250 keV/u, together with the two existing series of experimental data. In the conference shell and sub-shell selective cross sections will be presented for capture and excitation processes, to validate/invalidate the existing theoretical results and to extend the predictions towards the low energy region.

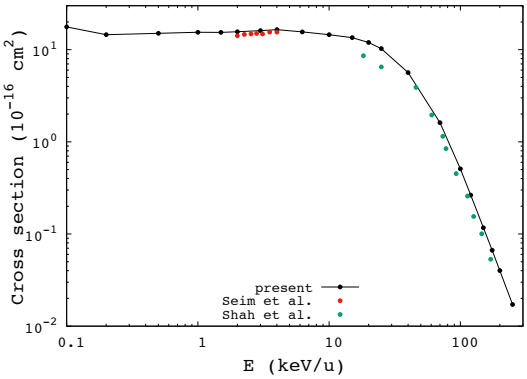

Figure 1. Cross sections of total capture as function of impact energy for Li^{2+}-H collisions. Solid line: present results. Experimental results: green circles from [3] and red circles from [4].

References

[1] Bransden B H and McDowell M R C 1992 Charge Exchange and the Theory of Ion-Atom Collisions (Clarendon Press)
[2] Reading J F et al 1997 *J. Phys. B: At. Mol. Opt. Phys.* **30** L189
[3] Shah M B et al 1978 *J. Phys. B: At. Mol. Phys.* **11** L233
[4] Seim W et al 1981 *J. Phys. B: At. Mol. Phys.* **14** 3475
[5] Gao J W et al 2018 *Phys. Rev. A* **96** 052709

Neutron Impact Ionization of the Fluorine Atom

MS Pindzola[1] * **JP Colgan**[2]

[1]Auburn University, Auburn, AL 36849, USA [2]Los Alamos National Laboratory, Los Alamos, NM, 87545, USA

Synopsis Calculations for neutron-impact ionization of the Fluorine atom.

Neutron-impact single and double ionization cross sections of the Fluorine atom are calculated in support of possible dark matter observations. One of the leading candidates for dark matter are weakly interacting massive particles (WIMPs) The WIMP-impact ionization of atoms would behave in a similar manner to those produced by neutron-impact ionization of atoms. Cross sections for the single and double differential ionization of the 1s, 2s and 2p subshells are found for neutron incident energies from 1.0 MeV to 4.0 MeV.

*E-mail: pindzms@auburn.edu

Differential studies of proton-hydrogen collisions

C T Plowman*, K H Spicer, I B Abdurakhmanov, A S Kadyrov and I Bray

Curtin Institute for Computation and Department of Physics and Astronomy,
Curtin University, GPO Box U1987, Perth, WA 6845, Australia

Synopsis The first unified study of all singly differential cross sections in proton collisions with atomic hydrogen has been conducted using the wave-packet convergent close-coupling method. Using this two-centre approach we calculated scattering amplitudes for all final channels simultaneously, conserving unitarity. Resulting singly differential cross sections for direct scattering, electron capture, and ionisation lead to improved agreement between experiment and theory.

Proton scattering on atomic hydrogen is a fundamental three-body Coulomb problem where all interactions between the particles and the two-body bound-state wave functions in the reaction channels are analytically known, making it an ideal testing ground for theoretical models. Many theoretical approaches to ion-atom collisions have been developed, but most have only been applied to calculate integrated cross sections. We used the wave-packet convergent close-coupling (WP-CCC) approach [1] to calculate singly differential cross sections for all binary and breakup reaction channels in the p+H collision system, including coupling between the channels.

Angular and energy differential cross sections for ionisation are shown in Fig. 1 in comparison with experiment and other calculations, for an incident energy of 20 keV. The WP-CCC results display excellent agreement with experiment. The CTMC and CDW-EIS calculations by Kerby *et al.* [2] fail to consistently replicate the experiment in both ejection angle (a) and ejection energy (b). The FHBS calculations by Reading *et al.* [3] overestimate experiment in angle (a) and become inaccurate with increasing energy (b).

Our approach provides good agreement with experiment for direct scattering, electron capture, and ionisation processes simultaneously, offering improvement over previous theoretical studies. For other processes and incident energies see Ref. [1].

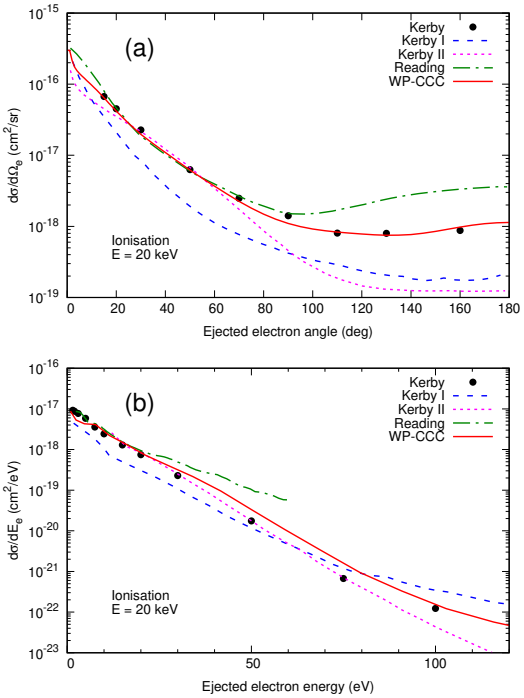

Figure 1. Angular (a) and energy (b) differential cross sections for ionisation in p+H collisions at an incident energy of 20 keV. Experiment data, CTMC (I) and CDW-EIS (II) calculations by Kerby *et al.* [2]; FHBS calculations by Reading *et al.* [3].

References

[1] Plowman C T *et al* 2020 *Phys. Rev. A* **102**, 052810
[2] Kerby G W *et al* 1995 *Phys. Rev. A* **51**, 2256
[3] Reading J F *et al* 2004 *Phys. Rev. A* **70**, 032718

*E-mail: corey.plowman@postgrad.curtin.edu.au

Single-electron capture by He^+ from helium at intermediate energies

K. Purkait, D. Jana and M. Purkait*

Department of Physics, Ramakrishna Mission Residential College, Narendrapur, Kolkata-700103, India

Synopsis A theoretical investigation of single-electron transfer from He in ground state by the impact of He^+ has been presented in the energy range 30 - 4000 keV. Calculations are performed within the framework of four-body one channel distorted-wave model. The angular-differential cross sections (DCS) for ground-state transfer exhibit an oscillatory structure at intermediate energies.

The theoretical description of single-electron capture from helium in interaction with He^+ is rather complicated because of three electrons involved. This collision problem is solved by Gao et al [1] using semiclassical atomic-orbital close-coupling (SCAOCC) method at incident energies between 1 and 225 keV/amu. We observe a prominent maxima and minima (upto second minima) in the DCS for ground state transfer at 30 keV and 100 keV. Under the circumstances, we are motivated to make a parallel investigation to that of our previous work [2] for the above-mentioned processes. The transition amplitudes in the prior and post forms within the framework of four-body one channel distorted-wave (DW-4B) model can be written as

$$T_{if}^{\mp} = N_i \int\int\int d\vec{s}_1 d\vec{s}_2 d\vec{R} \exp(i\vec{q}.\vec{R}) \phi_P(\vec{s}_1)\phi_T(\vec{s}_2)$$
$$\phi_f(\vec{s}_1,\vec{s}_2) V_{i,f_1} F_1\{i\alpha_1;1;i(vs_2+\vec{v}.\vec{s}_2)\}$$
$$_1F_1\{-i\alpha_2;1;i(k_iR-\vec{k}_i.\vec{R})\},$$

where

$$V_i \approx Z_T(\tfrac{1}{R}-\tfrac{1}{x_1})+(\tfrac{1}{r_{12}}-\tfrac{1}{s_2})+V_s(R),$$

and

$$V_f = Z_T(\tfrac{Z_P}{R}-\tfrac{1}{x_1}-\tfrac{1}{x_2})+V_s(R).$$

Here $V_s(R)$ is the interaction potential between the projectile (He^+) and the passive electron in the target. The differential cross section (DCS) is given by

$$\sigma_{if}(\theta_P,E) = (\tfrac{d\sigma}{d\Omega_P}) = \tfrac{\mu_i\mu_f}{(2\pi)^2}\tfrac{k_f}{k_i}|T_{if}^{(\mp)}|^2,$$

where $\vec{k}_i(\vec{k}_f)$ is the initial (final) momenta and θ_P is the projectile scattering angle.

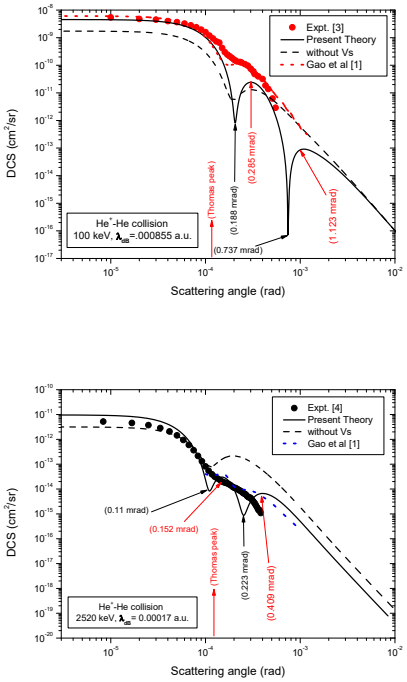

Figure . Differential cross sections as a function of projectile scattering angle θ_P (radian) in the laboratory frame of reference for single electron transfer to the ground state in $He^+ - He$ collisions at 100 and 2520 keV.

This work was supported by the Science and Engineering Research Board (SERB), New Delhi, India, under Grant No. CRG/2018/001344.

References

[1] Gao J W *et al* 2018 *Phys. Rev. A* **97** 052709

[2] Samaddar S *et al* 2020 *J. Phys. B: At. Mol. Opt. Phys.* **53** 245202

[3] Guo D L *et al* 2017 *Phys. Rev. A* **95** 011707

[4] Schöffler M S *et al* 2009 *Phys. Rev. A* **79** 064701

*$E-mail$: $mpurkait\_2007@rediffmail.com$

Electron loss of neutral hydrogen atom impacting on water molecule

M A Quinto[1] *, J M Monti[1] and R D Rivarola[1]

[1] Instituto de Física Rosario, CONICET and Universidad Nacional de Rosario, Rosario, S2000EKF

Synopsis This study focuses on the electron emission from neutral hydrogen impacting on a water molecule. The ionization of the projectile will be investigated using a quantum mechanical description within the first Born approximation with corrected boundary condition (FBA) approximation.

The study of electrons removal in collision of neutral hydrogen with water molecule plays an important role in radiobiology. In particular, in radiotherapy during the continuous slowing-down of the proton beam, a fraction of them will change of state when its energy approaches the Bragg's peak region [1]. In a recent work (Quinto *et al* [2]), the ionization of water molecule induced by neutral hydrogen has been investigated. However, the projectile electron loss process for the same collision system has been scarcely studied. In the literature, three different sets of experimental data [3-5] and two semi-empirical analytical models [6-7] exist, which have studied this reaction for neutral hydrogen – water molecule collisions.

In this work, we present a theoretical approach to describe the electron loss process in the neutral hydrogen – water collision. The total cross section, calculated within a quantum mechanical first Born approximation, are presented in figure 1. The TCS computed within the FBA approximation overestimates the measurements below a few hundreds of keV. To improve this, a Barkas's charge was introduced [8]. This correction is normally used in the calculation of stopping power of charged particles in the matter. As a result, FBA calculations with Barkas's charge correction show a better agreement with experimental data and semi-empirical predictions.

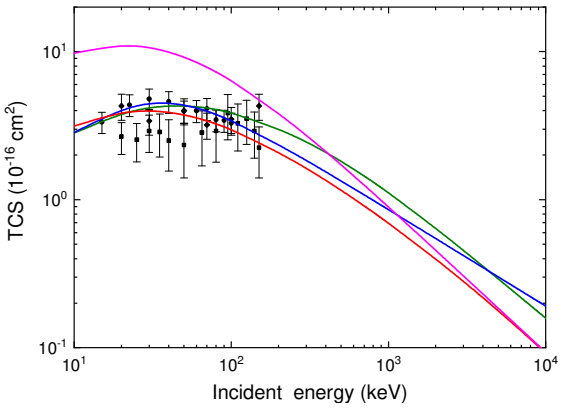

Figure 1. Total cross sections for electron loss of neutral hydrogen impacted on water. Theoretical calculations solid lines: FBA with Barkas's charge, red; FBA without Barkas's charge, magenta; Miller's semi-empirical model, blue [6]; Dingefelder's semi-empirical model, green [7]. Experimental data is taken from diamonds [3], squares [4] and circles [5].

References

[1] Alcocer-Ávila M E *et al* 2019 *Sci. Rep* **9** 14030
[2] Quinto M A *et al* 2019 *Phys. Rev.* A **100** 042704
[3] Bolorizadeh M A and Rudd M E 1986 *Phys. Rev.* A **33 2**
[4] Gobet F *et al* 2006 *Chem. Phys. Lett.* **421** 68
[5] Luna H *et al* 2007 *Phys. Rev.* A **76** 042711
[6] Miller J H and Green A E S 1973 *Radiat. Res.* **54** 343
[7] Dingfelder M *et al* 2000 *Radiat. Phys Chem.* **59** 255
[8] Barkas W H and Berger M J 1964 *Nat. Acad. Sci., Ed. S.i.p.o.c.p.i. Matter* **1133** 103

* E-mail: quinto@ifir-conicet.gov.ar

Electron removal in neutral hydrogen – atom collisions

M A Quinto[1] *, J M Monti[1] and R D Rivarola[1]

[1] Instituto de Física Rosario, CONICET and Universidad Nacional de Rosario, Rosario, S2000EKF

Synopsis This study focuses on the electron emission in neutral hydrogen – atom collisions. Both target and projectile ionization are investigated using a quantum mechanical description within the continuum distorted wave-eikonal initial state (CDW-EIS) approximation.

The study of electrons production in hydrogen – atom collisions is important in many areas (radiation physics, atmospheric physics, astrophysics, plasma physics). Several studies have been carried out for these collisional systems. Among them, the work of Green and McNeal [2] proposing an analytical formula based on the experimental data to describe the ionization process in term of total cross section. Later on, Heil and co-workers have investigated the electron removal in hydrogen – helium and helium – helium collisions. In particular, they focused on the double differential cross sections of the target, the projectile and the simultaneous ionization. These processes were described within the plane wave Born approximation (PWBA) [3].

In this work, we study the electron removal (target ionization and electron loss) by using the continuum distorted wave-eikonal initial state (CDW-EIS) approximation. The results in term of total cross section (TCS) are shown in figure 1. To improve the CDW-EIS approximation in the case of collisions between neutral atoms, we consider the Barkas's charge in the initial channel and the dynamic effective charge in the exit one. The Barkas's charge is a correction used to compute the energy loss of charged particle in the matter [4]. On the other side, the dynamic effective charge was introducing by McGuire *et al* [5] to screen the nuclear projectile charge as a function of the momentum transfer.

When both corrections are introduced into the CDW-EIS approximation, the obtained TCS are in better agreement with the experimental data.

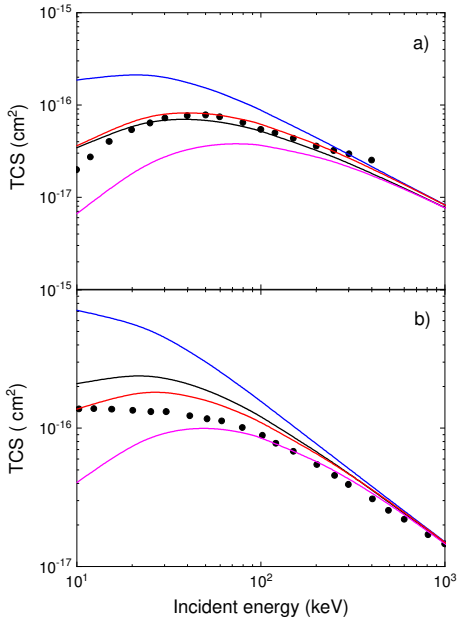

Figure 1. Total cross sections for electron removal in H with He collision. Theoretical calculations: pink line, CDW-EIS; black line, CDW-EIS with dynamic effective charge; blue line: CDW-EIS with Barkas's charge, magenta: CDW-EIS with both dynamic effective charge and Barkas's charge. Experimental data are token [2]. Target ionization (a) and electron loss (b).

References

[1] Monti J M *et al* 2011 *J. Phys. B: At. Mol. Opt. Phys.* **44** 195206
[2] Green A E S and McNeal R J 1971 *J. GeoPhys Res.* **76** 1
[3] Heil O *et al* 1991 NIM B **56** 284
[4] Barkas W H and Berger M J 1964 *Nat. Acad. Sci., Ed. S.i.p.o.c.p.i. Matter* **1133** 103
[5] McGuire J H *et al* 1981 *Phys. Rev.* B **22** 1

* E-mail: quinto@ifir-conicet.gov.ar

On the quest for projectile coherence in C^{6+}/He collisions

L Ph H Schmidt[1], J Rist[1], M Kircher[1], A Mery[2], J Rangama[2], S Grundmann[1], I Vela-Perez[1], D Tsitsonis[1], D Trabert[1], S Eckart[1], G Kastirke[1], K Fehre[1], T Jahnke[1], R Dörner[1], R Moshammer[3], J Ullrich[4], D Fischer[5], M Schulz[5], A Cassimi[2], M S Schöffler[*1]

[1] Institut für Kernphysik, Goethe-Universität, Frankfurt Max-von-Laue-Straße 1, 60438 Frankfurt am Main, Germany
[2] CIMAP Caen, GANIL, Bd Henri Becquerel, BP 55027 14076 Caen Cedex 05, France
3 Max-Planck-Institut für Kernphysik, Saupfercheckweg 1, 69117 Heidelberg, Germany
4 Physikalisch-Technische Bundesanstalt, Bundesallee 100, 38116 Braunschweig, Germany
5 Physics Department and LAMOR, Missouri University of Science and Technology, Rolla, Missouri, USA

Synopsis We have measured fully differential cross sections for single ionization of Helium, induced by 95 MeV/u C^{6+} ions.

20 years ago, single ionization of Helium induced by 100 MeV/u C^{6+} projectiles was investigated in a kinematically complete experiment [1]. The experimentally obtained results, which were in strong contrast to state of the art theories at this time and even most recent calculations. While the electron momentum distribution should exhibit two well separates lobes, the so-called binary- and recoil-lobe, the node between them was mostly filled. This launched an avalanche of controversial discussions, which are still ongoing today. The most heavily debates explanations are a) experimental issues/limited resolution and b) transversal coherence of the projectile, a concept introduced in 2011 by Schulz and coworkers [2].

In order to solve the "C^{6+}-mystery", we used a state-of-the-art COLTRIMS (COLd Target Recoil Ion Momentum Spectroscopy) Reaction-Microscope and redid the initial experiment in Cave D4 of GANIL. As insufficient momentum resolution might have been an issue in the original experiment, ion arm of the spectrometer was build in a time- and space-focussing geometry in order to reduce the diminishing influence of the extended target size. The electron arm was build in a time-focussing Wiley-McLaren-Geometry. On both ends of the spectrometer, hexagonal delay-line-detectors were used, which have an overall non-linearty <100 µm.

Also the gas jet was precooled to 80 K and for both, electrons and ions, separate calibrations, using an additional 25 keV ion source were used. With this, the ion momenta were calibrated, focusing on discrete structures in momentum space as a result of single electron capture ($He^{2+} + He \rightarrow He^{+} + He^{+}$ and $He^{+} + He \rightarrow He^{0} + He^{+}$). An He^{+} momentum resolution of $\Delta p<0.1$ au was achieved. The electron arm of the spectrometer was calibrated via autoionizing states of a Neon target ($He^{2+} + Ne \rightarrow He^{+} + Ne^{2+} + e^{-}$), which create a dozen (below 15 eV) of energetically sharp isotropically emitted electrons.

The experiment was performed in march 2021. Therefore the data are currently analyzed and the results will be presented.

References

[1] M. Schulz, et al., Nature, 422, 48-50, (2003)
[2] K. N. Egodapitiya, et al., Phys. Rev. Lett., 106, 153202, (2011)

[*] E-mail: schoeffler@atom.uni-frankfurt.de

Interference effects in fully differential cusp electron production cross sections for p + He collisions

S Bastola[1], M Dhital[1], R Lomsadze[2], J Davis[1] and M Schulz[1*]

[1]Missouri University of Science & Technology, Rolla, MO 65401, USA
[2]Tbilisi State University, Tbilisi 0179, Georgia

Synopsis A double peak structure observed in the fully differential angular distribution of electrons ejected in p + He collisions is interpreted as interference between a higher-order ionization amplitude, known to lead to cusp electrons, and a first-order amplitude.

We have measured fully momentum analyzed He^+ recoil ions and scattered projectiles in coincidence with each other for 75 keV p + He collisions. From the data, we obtained fully differential ionization cross sections (FDCS) for electrons with an energy of 43.9 eV ejected into the scattering plane. This energy corresponds to an electron speed close to the projectile speed (velocity matching). The measurements were performed for a small collimator slit - target distance corresponding to a relatively small transverse projectile coherence length of about 1.0 a.u. [1].

Previously, we reported FDCS for several ejected electron energies in the velocity matching regime, which were measured for a relatively large transverse projectile coherence length [2]. At large projectile scattering angles, apart from the well-established "binary peak", a signature of the first-order amplitude, another well-separated peak structure in the forward direction was observed.

An enhanced FDCS in the forward direction can be explained by a higher-order amplitude, known as PCI. However, in [2] we pointed out that while the binary peak can to a large extent be explained by a first-order mechanism, the same PCI-amplitude is known to lead to a slight shift towards the forward direction relative to the direction of the momentum transfer q, where the binary peak is expected within a pure first-order description [3,4]. Within a classical picture PCI should lead to a small-angle wing, giving the binary peak an asymmetric shape favoring the forward direction, but it should not lead to a separate forward peak. Qunatum-mechanically, on the other hand, the observed double peak structure can be interpreted as destructive interference between the first-order and PCI-amplitudes leading to a minimum between the direction of q and the forward direction. If this interpretation is correct, the double peak structure should become less pronounced or disappear altogether in the FDCS measured for the smaller coherence length.

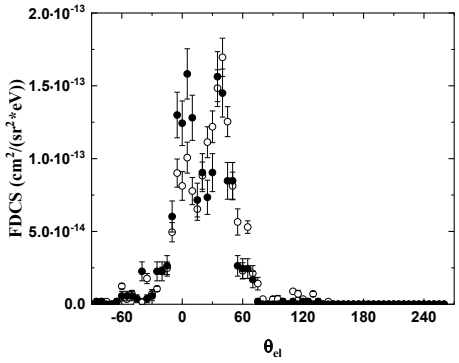

Figure 1. FDCS measured for a large (closed symbols) and small (open symbols) coherence length.

In Fig. 1 the FDCS are shown for a projectile angle of 0.5 mrad and a coherence length of 3.3 a.u. (1.0 a.u.) as closed (open) symbols. Indeed, for the less coherent case the forward peak is reduced relative to the binary peak. At other scattering angles clear differences between the data for the two coherence lengths were observed as well. However, a conclusive interpretation has to await theoretical calculations, which are currently in progress.

This work was supported by the National Science Foundation under grant no. PHY-2011307.

References

[1] Egodapitiya K *et al* 2011 *Phys. Rev. Lett.* **106** 153202
[2] Dhital M *et al* 2020 *Phys. Rev. A* **102** 032818
[3] Schulz M *et al* 2002 *J. Phys. B* **35** L161
[4] Schulz M *et al.* 2013 *Phys. Rev. A* **88** 022704

* E-mail: schulz@mst.edu

Quantum-state-controlled Penning collisions of ultracold lithium atoms with metastable atoms and molecules

T Sixt[1]*, J Guan[1], J Grzesiak[1], M Debatin[1], F Stienkemeier[1] and K Dulitz[1]

[1]Institute of Physics, University of Freiburg, Hermann-Herder-Str. 3, 79104 Freiburg im Breisgau, Germany

Synopsis Our work is aimed at understanding the mechanistic details of reactive collisions and at controlling the outcome of chemical reactions. For this, we study quantum-state-controlled Penning collisions between laser-cooled lithium (Li) atoms and different kinds of metastable atoms and molecules to investigate new ways of controlling the outcome of Penning-ionizing collisions.

The efficient suppression of Penning-ionizing collisions is a stringent requirement to achieve quantum degeneracy in metastable rare gases. In our experiment, we have combined a supersonic beam source for metastable helium (He*) atoms with a magneto-optical trap (MOT) for Li atoms. In order to get full quantum-state control of the reaction partners, the Li atoms are optically pumped into selected electronic hyperfine and magnetic substates. Additionally, we can distinguish the relative contributions from reactive collisions with the metastable $He(2^3S_1)$ and $He(2^1S_0)$ states by optical depletion of the $He(2^1S_0)$ state using a novel excitation scheme [1]. In the first part of this contribution, we report on the efficient suppression of He*-Li Penning ionization by laser excitation of the Li atoms. The results illustrate that not only the electron spin, but also Λ - the projection of the total molecular orbital angular momentum along the internuclear axis - is conserved during the ionization process [2]. Our findings suggest that Λ conservation can be used as a more general means of reaction control, for example, to improve schemes for the simultaneous laser cooling and trapping of He* and alkali atoms.

Furthermore, we report on the sensitive detection of metastable nitric oxide molecules (NO*), produced in a supersonic beam source, by reactive collisions with electronically excited Li atoms in the $2^2P_{3/2}$ state. Since the internal energy of $NO(a^4\Pi_i,\ v \leq 4)$ is lower than the ionization potential of Li in the $2^2S_{1/2}$ electronic ground state, we observe that the product ion yield arising from autoionizing $NO(a^4\Pi_i)$ + $Li(2^2S_{1/2})$ collisions is a factor of 21 lower than the ion yield from $NO(a^4\Pi_i)$ + $Li(2^2P_{3/2})$ collisions. Using this detection method, we infer densities of $\approx$ 600 $NO(a^4\Pi_i)$ molecules/cm^3 in the interaction region. Our results also allow for an estimate of the fractional population of $NO(a^4\Pi_i,\ v \geq 5)$ prior to the collision process [3].

References

[1] Guan J *et al* 2019 *Phys. Rev. Appl.* **11** 054037.
[2] Dulitz K *et al* 2020 *Phys. Rev. A* **102** 022818.
[3] Guan J *et al* 2020 *J. Phys. B: At. Mol. Opt. Phys.* **53** 245201.

*E-mail: tobias.sixt@physik.uni-freiburg.de

Differential direct scattering and electron capture in proton-helium collisions at intermediate energies

K. H. Spicer[1]*, C. T. Plowman[1], Sh. U. Alladustov[2], I. B. Abdurakhmanov[1], A. S. Kadyrov[1], and I. Bray[1]

[1]Curtin Institute for Computation and Department of Physics and Astronomy,Curtin University, GPO Box U1987, Perth, WA 6845, Australia
[2]Uzbek-Israel Joint Faculty, National University of Uzbekistan, Tashkent, 100174, Uzbekistan

Synopsis We investigate the four-body proton-helium differential scattering problem using the two-center wave-packet convergent close-coupling approach in the intermediate energy region. For comparison, a recently developed method that reduces the target to an effective single-electron system is also used. The results of the two methods exhibit a very good level of agreement with experiment. It is concluded that both versions provide a realistic picture of they processes taking place in proton-helium collisions.

We present an investigation of the four-body proton-helium differential scattering problem using the two-center wave-packet convergent close-coupling (WP-CCC) approach. The approach uses fully-correlated two-electron wave functions for the helium target. Here, we focus on the angular differential cross sections for direct-scattering and electron-capture processes in the intermediate energy (75–300 keV) region where coupling between various channels is important.

A brief overview of the theoretical approaches to the differential proton-helium scattering problem indicates that different approaches have only been applied to isolated reaction channels. Some found agreement in their chosen process, however, could not provide information on other concurrent channels. There has been no attempt to calculate all the interconnected processes on equal footing at the same time and in a systematic fashion. The aim is to test if the WP-CCC approach is capable of providing a complete differential picture of all the simultaneous interrelated processes occurring during the collision and, thereby, filling this gap.

For comparison, we also use a recently developed approach [1] that allows one to reduce the two-electron helium atom to an effectively single-electron system convenient for scattering calculations.

We report results for angular differential cross sections for elastic scattering, excitation into the $n = 2$ states (where n is the principal quantum number of the atom in the final state), and state-selective electron capture obtained using both methods. Results for the angular differential cross sections of excitation and electron capture agree well with experiment. For elastic scattering, significant disagreement between the experiment at 100 keV and theory still remains, though agreement in shape between the experiment and the two-electron WP-CCC results is excellent. We suggest that there could be a normalisation error in the experiment. New experiments and independent calculations would shed more light on the situation. We also present results using a recently developed effective single-electron description of the target. Results from this alternative, computationally more efficient, treatment of the target structure exhibit generally good agreement with the correlated two-electron WP-CCC calculations.

It is concluded that both the fully-correlated two-electron and less expensive effective single-electron WP-CCC approaches are capable of providing a complete and reasonably accurate differential picture of the binary processes taking place in proton-helium collisions. We will next turn our attention to proton-helium differential ionisation where there is an abundance of experimental data to compare with.

References

[1] Abdurakhmanov I. B. *et al* 2021 submitted.

*E-mail: kate.bain@student.curtin.edu.au

p-wave elastic collisional properties of Fermi gases confined in quasi-2D

N Takahashi[1] *, K Nagase[1], Y Chen[1], Z Xu[1] and T Mukaiyama[1,2] †

[1]Graduate School of Engineering Science, Osaka University, 1-3 Machikaneyama, Toyonaka, Osaka 560-8531, Japan
[2]Quantum Information and Quantum Biology Division, Institute for Open and Transdisciplinary Research Institute, Osaka University, Osaka 560-8351, Japan

Synopsis We study elastic collisions of ^{6}Li atoms near a *p*-wave Feshbach resonance via cross-dimensional thermalization. The experimental results imply that thermalization is suppressed in quasi-2D due to decrease of the density of the final momentum states after collisions. This study will make an important step toward full understanding of relation between *p*-wave interactions and confinement dimensions.

Ultracold atomic gases are useful playgrounds for research in condensed matter physics, because of its controllability of the interatomic interactions using Feshbach resonances. In fact, various many-body properties have been clarified in the system of ultracold fermionic atoms so far, such as the observation of BCS-BEC crossover, creation of Efimov three-body bound states, determination of thermodynamics of a unitary Fermi gas, and so on.

In contrast to the case of fermions with *s*-wave interactions, *p*-wave superfluid has eluded a realization in ultracold atomic gases. This is mainly because atoms near a *p*-wave Feshbach resonance suffer from strong inelastic collisional losses. To overcome this issue, it is proposed to lower the dimension of the system. Ref. [1] predicts that the quasi-2D BCS *p*-wave condensates are more stable than their 3D counterparts. It is important to experimentally confirm this assertion by measuring elastic and inelastic collisional properties of Fermi gases both in 3D and quasi-2D.

In this experiment, we prepare spin-polarized Fermi gases of ^{6}Li atoms confined in 3D and quasi-2D. Two lasers incident onto the atoms in counter-propagating directions form a quasi-2D Fermi gas. In order to determine the *p*-wave elastic collisional properties of the atom, we used the scheme called cross-dimensional thermalization [2]. We intentionally excite the motion of the atoms along with one of the loosely confined directions by the resonant modulation of the optical trap laser intensity. This makes the momentum distribution of the atoms anisotropic. After holding the atoms near a *p*-wave Feshbach resonance, the anisotropy of the momentum distribution gets relaxed and finally reaches thermal equilibrium. Figure 1 shows thermalization rate in 3D and quasi-2D as a function of magnetic-field detuning. Our experimental results suggest that *p*-wave elastic collision is relatively suppressed for the gas in quasi-2D confinement compared with that in 3D confinement, reflecting the lower density of states in quasi-2D confinement. This study, together with the clarification of inelastic collisional properties, will confirm whether trapping atoms in quasi-2D would help realize *p*-wave superfluids in ultracold atomic gases.

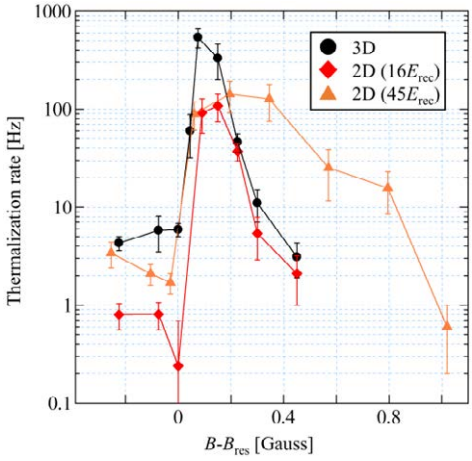

Figure 1. Thermalization rate versus magnetic-field detuning in 3D and quasi-2D. Lattice depth are shown in parentheses.

References

[1] J. Levinsen *et al*. 2008 *Phys. Rev. A* **78** 063616
[2] T. Nakasuji *et al*. 2013 *Phys. Rev. A* **88** 012710

* E-mail: u597606f@ecs.osaka-u.ac.jp
† E-mail: muka@ee.es.osaka-u.ac.jp

Radiative double-electron capture for $F^{9,8+}$ ions in gas and thin-foil targets*

J A Tanis[1], D S La Mantia[1] and P N S Kumara[1]

[1]Department of Physics, Western Michigan University, Kalamazoo, Michigan 49008, USA

Synopsis Radiative double-electron capture has been investigated for 2.11 MeV/u $F^{9,8+}$ ions incident on N_2, Ne and thin-foil carbon targets. Comparison of the outgoing charge states for the gas and foil target results shows very different results. However, total cross sections found for the two cases give values not too different.

Radiative double-electron capture (RDEC) has been investigated for bare and one-electron ions incident on gas and thin-foil targets. RDEC is a process in which a moving projectile captures two electrons from a target to bound states simultaneous with the emission of a single photon [1]. As such, RDEC is considered the inverse of double photoioization for ion-atom collisions. Results for 2.11 MeV/u $F^{9,8+}$ ions on gas N_2 and Ne and thin-foil C targets are combined [2], and are based on earlier work for the gas [3] and the carbon [4] targets.

Experimentally the work was done at Western Michigan University using the tandem accelerator facility. The beam was collimated and directed onto either the gas (inside a differentially pumped cell) or the thin-foil carbon. A Si(Li) detector mounted at 90° to the incident beam recorded emitted photons. Following interaction with the target, the beam was magnetically separated and the charge-changed components were collected with individual silicon surface-barrier detectors. Event mode data acquisition was used to record coincidences between x rays and charge-changed particles.

Figure 1 shows the results obtained for $F^{9,8+}$ ions incident on gaseous N_2 (results for Ne were similar) and thin-foil C targets. The findings are seen to be quite different. For N_2 (panels (a) and (b)) x-rays that signify RDEC events occur only for coincidences with the double-capture charge state q-2 as expected, while for the C foil (panels (c) – (h)) the x-ray coincidences due to RDEC are seen in the three charge states q-2, q-1, and q. This latter effect is attributed to multiple collisions that occur only for the C foil, as opposed to the single collisions conditions for the N_2 target. To compare the total cross sections for the gas and thin-foil targets the events seen in all the charge states must be added, giving values close to one another.

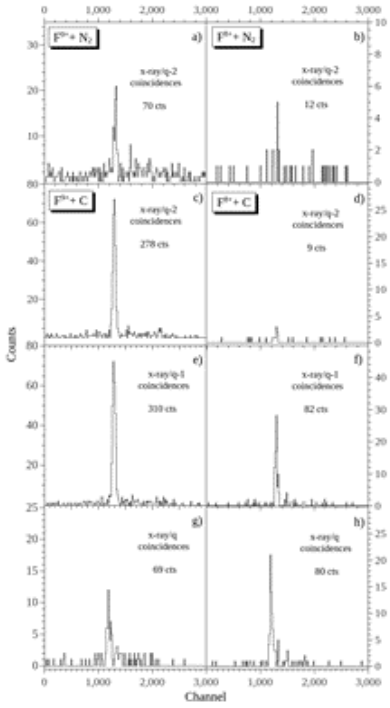

Figure 1. Spectra obtained for 2.11 MeV/u F^{9+} and F^{8+}+ N_2 (panels (a) and (b)) and C (panels (c) – (h), respectively): The panels show x-ray-gated particle spectra associated with charge changed projectiles q-2, q-1, and q. The numbers shown on each graph are the totals for each spectral peak after background subtraction.

*Supported in part by NSF Grant 1707467

References

[1] Miraglia J and Gravielle M. S. 1987 ICPEAC XV: Book of Abstracts p. 517 Brighton, U.K.
[2] Tanis J, La Mantia D S, Kumara P N S 2021 *Phys. Rev. A* (submitted)
[3] La Mantia D S *et al* 2020 *Phys. Rev. Lett*. 124 133401
[4] La Mantia D S *et al* 2020 *Phys. Rev. A*. 102 060801(R)

* E-mail: john.tanis@wmich.edu

Transfer ionization cross sections in collisions between bare light ions and Helium atom

A Taoutioui[1] *, B He[2] and K Tőkési[1] †

[1]Institute for Nuclear Research, Debrecen, 4026, Hungary
[2]Institute of Applied Physics and Computational Mathematics, Beijing, China

Synopsis We present a nonperturbative study of the total and differential cross-sections of the transfer ionization (TI) process in collisions between Helium atom and bare ions A^{q+} (q = 1 - 3) from intermediate to high impact energies (10 keV-1 MeV). We used the 4-body Classical Trajectory Monte Carlo method (CTMC). Our classical cross sections are compared with available experimental data. We found reasonable agreement between the recent calculations and the experimental data.

Inelastic electron processes involving many electron targets in ion-atom collisions play a crucial role in several fields, such as nuclear fusion reactors. Recently, with the advent of supercomputers and parallel facilities, the double electron processes are investigated nonperturbatively [1]. However, the double or multiple electron processes are still not well understood and need more in-depth investigations.

In this work, we present a theoretical investigation of the transfer ionization using the CTMC method. This process was already investigated both theoretically and experimentally by several authors [2–5]. We present the total and differential cross-sections of the transfer ionization in collisions between A^{q+} (q = 1 - 3) ions and ground state Helium. Fig. 1 shows the TI total cross sections obtained by the standard CTMC method for collisions between the bare ions H^+, He^{2+} and Li^{3+} and the ground state Helium atom. According to Fig. 1, the total cross sections of TI in case of H^+ projectile show a remarkable discrepancy between the classical and experimental data where this discrepancy is less pronounced for He^{2+} and Li^{3+} ions. Improving the classical treatment the Kirschbaum and Wilets potential [6] was included in the Hamiltonian of the collisional system. Applying the potential mimicking the quantum feature of the collision the cross sections are closer to the experimental data. Moreover, the differential cross sections are investigated to get a deeper insight on the collision dynamics.

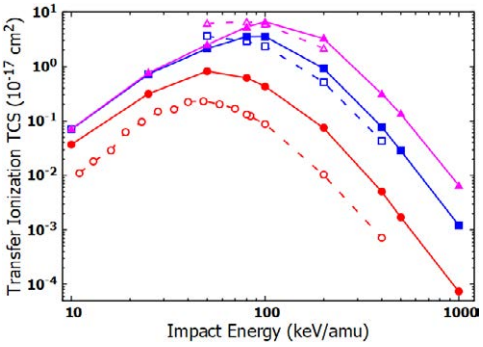

Figure 1. Total cross sections for transfer ionization as a function of projectile impact energy using the 4-body CTMC. Experimental data of Shah et al. [4,5] H^+: open-circles, He^{2+}: open-squares and Li^{3+}: open-triangles. Present 4-body CTMC H^+: filled-circles, He^{2+}: filled-squares and Li^{3+}: filled-triangles.

This work has been carried out within the framework of the EUROfusion Consortium and has received funding from the Euratom research and training programme 2014-2018 and 2019-2020 under grant agreement No 633053. The views and opinions expressed herein do not necessarily reflect those of the European Commission.

References

[1] Gao J W*et al* 2019 *Phys. Rev. Lett.* **122** 093402
[2] Bachi N*et al* 2018*Eur. Phys. J. D* **72** 127
[3] Cohen J S *et al* 1996 *Phys. Rev. A* **54** 573
[4] Sah M B*et al* 1985 *J. Phys. B: At. Mol. Opt. Phys.* **18** 899
[5] Sah M B*et al* 1989 *J. Phys. B: At. Mol. Opt. Phys.* **22** 3037
[6] Kirschbaum C L*et al* 1980 *Phys. Rev. A* **21** 834

*E-mail: Abdelmalek.taoutioui@atomki.hu
†E-mail: tokesi.karoly@atomki.hu

NOON states with ultracold bosonic atoms via resonance- and chaos-assisted tunneling

G Vanhaele[1] * **and P Schlagheck**[1]

[1]CESAM Reasearch Unit of University of Liege, Liège, 4000, Belgium

Synopsis We show that an external perturbation applied to a two-mode ultracold gas could drastically reduce the time required to produce a NOON state. The semiclassical theory resonance- and chaos-assisted tunneling turns out to be suitable to indicate which range of parameters can be chosen.

We theoretically investigate the generation of microscopic atomic NOON states, corresponding to the coherent $|N,0\rangle + |0,N\rangle$ superposition with $N \sim 5$ particles, via collective tunneling of interacting ultracold bosonic atoms within a symmetric double-well potential in the self-trapping regime. We show that a periodic driving of the double well with suitably tuned amplitude and frequency parameters allows one to substantially boost this tunneling process without altering its collective character. The time scale to generate the NOON superposition, which corresponds to half the tunneling time and would be prohibitively large in the undriven double well for the considered atomic populations, can thereby be drastically reduced, which renders the realization of NOON states through this protocol experimentally feasible. Resonance- and chaos-assisted tunneling are identified as key mechanisms in this context. A quantitative semiclassical evaluation of their impact onto the collective tunneling process allows one to determine the optimal choice for the driving parameters in order to generate those NOON states as fast as possible.

*E-mail: guillaume.vanhaele@uliege.be

Accurate binding energy of Yb dimer (Yb_2) from *ab initio* calculations and ultracold photoassociation spectroscopy

G. Visentin, A. A. Buchachenko

CEST, Skolkovo Institute of Science and Technology, Skolkovo Innovation Center, Moscow 121205, Russia

Synopsis The ground-state Born-Oppenheimer potential energy curve for the Yb dimer (Yb_2) is modelled by use of a semi-analytical function, consisting of a short- and a long-range contribution. The former is evaluated with all-electron exact-2-component scalar relativistic CCSD(T) calculations, with the diffuse component of the basis set saturated with atom- or bond-centered primitives, extrapolated to the complete basis set limit through the n = D, T, Q sequence of the correlation-consistent polarized n-zeta basis set. The long-range part is represented by accurate *ab initio* or empirical long-range coefficients for the dipole-dipole and dipole-quadrupole dispersion interaction. Upon scaling the model potential function with a semiclassical constraint of the number of vibrational levels of ^{174}Yb, the dissociation energy of the dimer is bounded within a very narrow range. Our new improved potential may be of interest as references for non-Born-Oppenheimer models.

Recent proposals to use Yb dimer (Yb_2) as a frequency standard and as a sensor for non-Newtonian gravity (see, for instance, Refs. [1,2] imply the accurate knowledge of its interaction potential. However, previous *ab initio* calculations are not fully consistent with each other [3- 5]. Here, the ground-state Born-Oppenheimer Yb_2 potential energy curve is modelled by a semi-analytical function [4], consisting of a short- and a long-range contribution. For the former, systematic *ab initio* all-electron exact 2-component scalar-relativistic CCSD(T) calculations are carried out, where the diffuse component of the basis set is saturated with the atom- or bond-centered primitives, while the complete basis set limit is reached through n = D, T, Q sequence of the correlation-consistent polarized n-zeta basis sets [6]. For the long-range part, similar approaches are used to compute the dipole and quadrupole dispersion terms, by the implementation of the CCSD(3) polarization propagator method[7] for dynamic polarizabilities. Alternatively, empirical dispersion coefficients fitted to photoassociation spectroscopy data [4] are used. A semiclassical constraint on the number of the bound vibrational levels known for the ^{174}Yb isotope is used to scale the model potential function. Upon the scaling, based on the most accurate *ab initio* results, the dissociation energy of the interacting Yb partners is bounded within the very narrow 734 $\pm$ 4 cm^{-1} range. Our results explain the mismatches in previous ab initio potentials and are in reasonable agreement with the previous estimations, attained after accurate *ab initio* calculations. The potentials thus achieved can be used as references for more sophisticated models going beyond the Born-Oppenheimer approximation and bound their uncertainty bars.

We thank P.S. Żukowski, P. Tecmer, M. Borkowski and D. Kędziera for fruitful discussions and Russian Science Foundation for support under the project # 17-13-01466.

References

[1] Borkowski M. (2018), Phys. Rev. Lett. **120**, 083202
[2] Borkowski M. *et al.* (2019), Sci. Rep. **9**, 14807
[3] Mosyagin N.S. *et al.* (2010), Int. J. Quant. Chem. **111**, 3793
[4] Borkowski M. *et al.* (2017), Phys. Rev. A **96**, 063405
[5] Tecmer P. *et al.* (2019), J. Quant. Chem. **119**, e25983
[6] Lu Q. *et al.* (2016), J. Chem. Phys. **145**, 054111
[7] Korona T. *et al.* (2006), Mol. Phys. **104**, 2303

Theoretical study on the tune-out wavelengths of the ground state of Ba atom

X Wang, J Jiang*, Z W Wu, L Y Xie, D H Zhang and C Z Dong†

Key Laboratory of Atomic and Molecular Physics and Functional Materials of Gansu Province,College of Physics and Electronic Engineering, Northwest Normal University, Lanzhou, 730070, P. R. China

Synopsis The energy levels and transition matrix elements of some low-lying states of Ba atom have been calculated systematically using the relativistic configuration interaction with core polarization method. The static polarizabilities and tune-out wavelengths of the ground state are further determined.

The alkali-earth metal atoms trapped in the optical lattice have been widely applied to high-precise optical clocks, quantum information, and Bose-Einstein condensates [1]. When atom is exposed to an electromagnetic field, the energy shift of this atom is proportional to the dipole dynamic polarizability with the change of laser frequency. If the dynamic polarizability is equal to zero, the corresponding laser wavelength is called as tune-out wavelength. The tune-out wavelength can be used in the determination of high-precise atomic parameters and the sympathetic cooling. The optical clocks based on trapped cold Mg, Ca and Sr atoms have achieved great successes in the past few years. The laser cooling and trapping of Ba atom has been reported about 5.7(8) mK in the magneto-optical trap [2]. Therefore, the further research on the polarizabilities and tune-out wavelengths is very essential.

The relativistic configuration interaction with core polarization (RCICP) method using S-spinors and L-spinors basis has been developed by us to deal with the divalent electron systems. By tuning the polarization potential cut-off parameters for individual symmetries, the relative difference of energies between the present RCICP and experimental NIST results is less than 0.5%. Using these energies and wavefunctions, the reduced matrix elements of the electric-dipole transitions are computed. Then the static and dynamic dipole polarizabilities are further determined by the sum-over states approach. The dipole static polarizability of the ground state, 275.47 a.u., agrees well with the recommended value 273.5(2.0) a.u. [3]. It can be seen that there are three tune-out wavelengths in Figure 1. The longest tune-out wavelength is longer about 1 nm than the nonrelativistic value 788.875 nm [4].

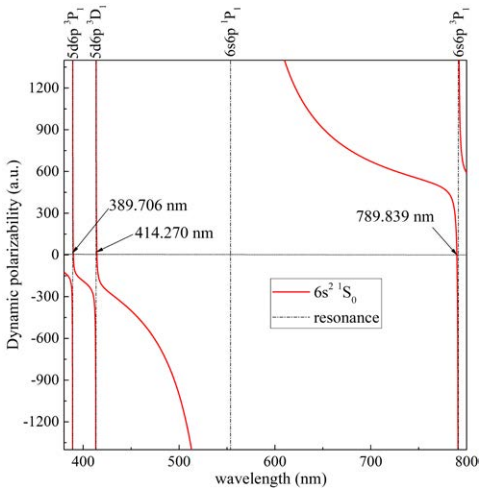

Figure 1. Dynamic polarizability (red lines) of the ground state of Ba atom in the region of visible light. Tune-out wavelengths are indicated by arrows.

This work has been supported by National Key Research and Development Program of China (Grant No. 2017YFA0402300) and National Natural Science Foundation of China (Grant Nos. 11774292, 11864036, 11804280).

References

[1] Safronova M S *et al* 2018 *Rev. Mod. Phys.* **90** 025008
[2] De S *et al* 2009 *Phys. Rev. A* **79** 041402
[3] Porsev S G and Derevianko A 2006 *J. Exp. Theor. Phys.* **102** 195
[4] Cheng Y J *et al* 2013 *Phys. Rev. A* **88** 022511

*E-mail: phyjiang@yeah.net
†E-mail: dongcz@nwnu.edu.cn

Single ionization of helium by high energy proton impact using the parabolic Sturmians representation

S A Zaytsev[1]*, A S Zaytsev[1]†, D S Zaytseva[1], L U Ancarani[2] and K A Kouzakov[3]

[1]Pacific National University, Khabarovsk 680035, Russia
[2]Université de Lorraine, CNRS, LPCT, 57000 Metz, France
[3] Faculty of Physics, Lomonosov Moscow State University, Moscow 119991, Russia

Synopsis We study theoretically the helium ionization by impact of high energy protons. The ionization problem is recast as an inhomogeneous Schrödinger equation for the three-body Coulomb system (e^-, He^+, p). Using a L^2 parabolic Sturmians representation, from the asymptotic behavior of the scattering function we extract analytically the ionization amplitude. The calculated fully differential cross sections are in good agreement with recent experimental data and WP-CCC results.

Ionization of helium by a proton constitutes a very challenging quantum mechanical four-body problem. For fast incident protons, one may reduce the difficulty by employing a frozen-core model for the target, and thus deal with a more tractable Coulomb three-body problem. In this way, the ionization amplitude is cast in the form

$$T_{\mathbf{K},\mathbf{k}_e} = \left\langle \Psi^{(-)}_{\mathbf{K},\mathbf{k}_e}, \psi^{He^+}_{1s} \middle| \hat{V} \middle| \mathbf{K}_0, \Phi^{(0)} \right\rangle, \qquad (1)$$

where $\hat{V}(\mathbf{R},\mathbf{r}) = \frac{1}{R} - \frac{1}{|\mathbf{R}-\mathbf{r}|}$ is the interaction operator. The initial state is represented by the product of a helium ground state $\Phi^{(0)}(\mathbf{r},\mathbf{r}')$ and a plane wave $\mathbf{K}_0$ describing the fast incident proton (position $\mathbf{R}$); $\psi^{He^+}_{1s}(\mathbf{r}')$ is the frozen electron wave function; $\Psi^{(-)}_{\mathbf{K},\mathbf{k}_e}$ is the three-body system (e^-, He^+, p) final state. The amplitude can be formally extracted from the asymptotic behavior of the function generated by the action of the three-body Green's function operator $\hat{G}^{(+)}$ on the driven term of a three-body inhomogeneous Schrödinger equation. We assume that for a high enough incident energy, we can approximate $\hat{G}^{(+)}$ by the Born series

$$\hat{G}^{(+)} = \hat{G}^{(+)}_0 + \hat{G}^{(+)}_0 \hat{U} \hat{G}^{(+)}_0 + \ldots, \qquad (2)$$

where $\hat{G}^{(+)}_0 \equiv [E - \hat{H}_0]^{-1}$ is the Green operator corresponding to

$$\hat{H}_0 = -\frac{1}{2m_p}\nabla^2_{\mathbf{R}} - \frac{1}{2}\nabla^2_{\mathbf{r}} + \frac{1}{R} - \frac{1}{r}, \qquad (3)$$

i.e., the Hamiltonian without the proton-electron interaction $\hat{U}$ which is treated as a perturbation.

In our proposal, we make use of a L^2 parabolic Sturmians representation, which allows us to calculate the amplitude analytically in terms of the expansion coefficients.

We have made FDCS calculations at 1 MeV incident energy, and for several geometrical and kinematical configurations. An example is given in figure 1. Taking the zeroth order, *i.e.* $\hat{G}^{(+)} = \hat{G}^{(+)}_0$, our calculated FDCS (labelled 2C-like) essentially reproduces the 2C model result [1]. Going to the next order, *i.e.* $\hat{G}^{(+)} = \hat{G}^{(+)}_0 + \hat{G}^{(+)}_0 \hat{U} \hat{G}^{(+)}_0$, our FDCS (label PS) reasonably agrees with the experiment [1] and recent WP-CCC results [2].

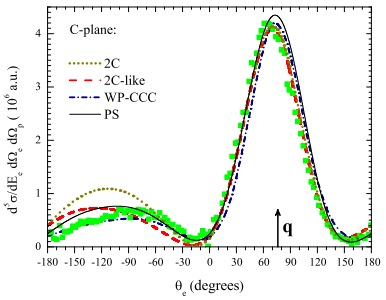

Figure 1. FDCS for single ionization of helium by 1-MeV protons in the collision plane. The ejected-electron energy is $E_e = 6.5$ eV, and the momentum transfer is $q = 0.75$ a.u.

References

[1] Chuluunbaatar O *et al* 2017 *Phys. Rev. A* **96** 042716
[2] Abdurakhmanov I B *et al* 2017 *Phys. Rev. A* **96** 022702; 2019 *Phys. Rev. A* **100** 062708

*E-mail: zaytsevsa@pnu.edu.ru
†E-mail: alzaytsev@pnu.edu.ru

Ion and electron induced molecular growth inside of linear hydrocarbons clusters

S Indrajith[1]*, J Kočišek[2]†, A Domaracka[3], C Nicolafrancesco[3], P Rousseau[3], J Fedor[2], M Farnik[2] and B A Huber[3]

[1]Department of Physics, Stockholm University, Stockholm, 114 21, Sweden
[2]J. Heyrovský Institute of Physical Chemistry v.v.i., The Czech Academy of Sciences, Prague, 18223, Czech Republic
[3]Normandie Univ., ENSICAEN, UNICAEN, CEA, CNRS, CIMAP, Caen, 14000 France

Synopsis Here we report on experimental studies of ion and electron collisions between butadiene and butane clusters. New molecular species are produced by growth mechanism inside of clusters.

Collisions of low energy ions with loosely bound clusters of molecules are studied in the gas phase with the aim to analyze either fragmentation processes, which occur due to the transfer of energy and charge, or, more surprisingly, the growth processes leading to molecular growth and the formation of new larger covalently bound molecules. This second type of processes is based on the transfer of energy into the heavy particle system (molecular nuclei), either by the initial electronic excitation which ends on longer time scales via the electron-phonon coupling in the degrees of vibrational motion, or by the direct fast knockout of an atom from the molecule in an elastic nucleus-nucleus collision. In the case of ion/solid collisions these mechanisms are termed as electronic and nuclear stopping power.

By the knockout of an atom highly reactive radicals and molecular species are formed which on very short time scales (<∼ps) react with their neighbor molecules in the cluster. It has been shown that this triggers reactivity, as observed in C_{60} clusters [1] or PAH (Polycyclic Aromatic Hydrocarbons) ones [2]. When several atoms are kicked out along the ion trajectory in the cluster, large covalently bound systems can be formed.

We present results on cluster systems containing linear chain molecules like butane and butadiene. We will discuss the possible formation of ring structures and the path to aromatic molecules. The irradiation of hydrocarbons clusters using different radiation sources (electrons and ions) allows to determine the balance between ionization induced reactivity and collision induced one. The latter is the typical collision occurring in Titan's atmosphere involving slow and heavy ions (∼ 5 keV O^+ ions) [3].

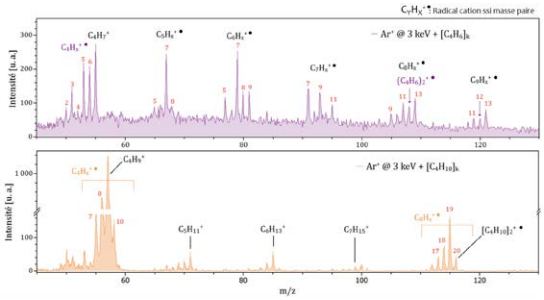

Figure 1. Mass spectra comparison of butadiene (C_4H_6) (top panel) and butane (C_4H_{10}) (bottom panel) clusters in collision with Ar^+ ions at an energy of 3 keV.

References

[1] Delaunay R *et al* 2018 *Carbon* **129** 766-774
[2] Delaunay R *et al* 2015 *J. Phys. Chem. Lett.* **6(9)** 1536-1542
[3] Brown R H *et al* 2009 *Springer*

*E-mail: suvasthika.indrajith@fysik.su.se
†E-mail: jaroslav.kocisek@jh-inst.cas.cz

Splashing of cold doped helium nanodroplets

P Martini[1,2] *, S Albertini[1], F Laimer[1] ,M Meyer[1], M Gatchell[1,2], F Zappa[1], O Echt[3] and P Scheier[1]

[1] Institute for ion and applied physics, University of Innsbruck, Innsbruck, 6020, Austria
[2] Department of Physics, Stockholm University, Stockholm, 10691, Sweden
[3] Department of Physics, University of New Hampshire, Durham, NH 038824, USA

Synopsis Large, doped, charged and neutral helium nanodroplets show a splashing like behavior, like other liquids, upon collision with a stainless steel surface.

New masspectrometric and transmission electron microscopy measurements (TEM) give insight about a splashing like behavior of large helium nanodroplets (HND). Thus, indicate a backscattering mechanism of both, neutral and charged clusters formed in the cold environment of the HNDs. Previoulsly, Laimer et al. could show that the superfluid HNDs, formed via supersonic expansion of precooled and pressurized helium, can efficiently hold many positive or negative charges [1]. Moreover, measurements suggest that the charges embedded in the HNDs can be used as nucleation centers for cluster growth. However, the extraction mechanism of the clusters formed within the environment of the HNDs is not well known. Tiefenthaler et al. showed that small ionic clusters could be extracted form the large HND via multiple collisions with an additional He gas at room temperature in a RF ion guide [2].

Here we explore a new experimental approach optimizing the liberation meachanism of the dopand clusters from the HNDs. An electron impact ion source (EI) is used to ionize the HNDs in a differentially pumped chamber directly after the formation of the droplets. Dopand clusters are then formed by multiple pickups of atoms or molecules into charged HNDs by collision in a pickup chamber. Depending on the charge state of the droplets the dopands get distributed over the charges within the HNDs leading to different dopand cluster size distributions. To exract the ions these doped HNDs collide with a stainless steel surface placed in the flight path of the HNDs beam. Weak electrostatic fields guide the small ionic clusters, which are backscattered towards a time-of-flight mass spectrometer.

* E-mail: paul.martini@fysik.su.se

Measurements comparing positively and negatively charged HNDs show that the charges can be used as nucleation centers for the dopant cluster growth. Furthermore, the high He decoration of the low mass ions for both positively and negatively charged ions indicate a rather soft liberation mechanism.

In addition, TEM images show that there is no upper mass limit for the backscattered clusters for both charged and neutral.

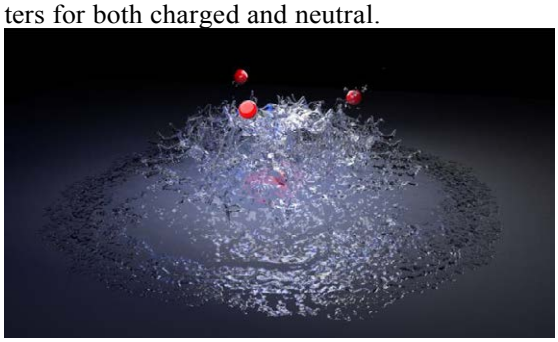

Figure 1. Graphical representation of a helium nanodroplet colliding with a surface and backscattering of small ions (in red).

The high ion yield for the low mass ions and the high amount of He atoms attached to the dopands make action spectroscopy measurement feasible for many different dopand species, especially anioic cases. Furthermore, the backscattering of high mass clusters has an important implementation for the deposition of nano particles and thus allow the deposition on complex surfaces.

References

[1] Laimer F *et al* 2019 Highly Charged Droplets of Superfluid Helium *Phys. Rev. Lett.* **123** 165301

[2] Tiefenthaler L *et al* 2020 An intense source for cold cluster ions of a specific composition *Rev. Sci. Instrum.* **91** 033315

Irradiation of Au-nano-islands with highly charged ions and characterization with AFM and SEM

H Muckenhuber[1] *, G L Szabo[1] †, J Arkadiusz[2], B R Jany[2], M Lehner[1], A Niggas[1], U Kentsch[3], F Krok[2], and R A Wilhelm[1]

[1]Institute of Applied Physics, TU Wien, 1040 Vienna, Austria
[2]Institute of Physics, Jagiellonian University, 30-348 Krakow, Poland
[3]Institute of Ion Beam Physics and Materials Research, Helmholtz-Zentrum Dresden-Rossendorf, 01328 Dresden, Germany

Synopsis Structural changes of metallic Au-nano-islands were observed after irradiation with slow highly charged ions, which was so far not observed for metallic materials. The changes were characterized with AFM and SEM measurements with respect to the change of height and size. We link the alteration of the metallic nano-islands to the potential energy deposition of the projectiles.

Impacts of slow highly charged ions (HCIs) onto a target surface can lead to a change of the materials structure triggered by a phase transition or complex dynamics of trapped electronic excitations [1]. Responsible for this structural transformation is the excitation/ionization of electrons from the target material due to the neutralization of the ion in the area of the impact. Subsequent lattice heating mediated by the electron-phonon-coupling finally leads to the material modification.

So far, such effects were only observed when irradiating semi-conducting or insulating target materials. Metal films are inert to the potential energy deposition

We now present measurements of irradiated Au-nano-islands with lateral sizes of 5-90 nm and an average height of about 7 nm. Irradiations were performed with Xe^{1+} and Xe^{40+} (both with 180 keV kinetic energy). Using SEM before and after irradiation, figure 1 shows the difference of the intensity resulting from Xe^{1+} and Xe^{40+} charge impacts. The nano-islands appear less bright for the irradiation with Xe^{40+}, which is a strong indication for structural changes of the nano-island. The threshold at 14 nm specifies the minimal lateral size where no changes are observed, because above this threshold the nano-island melting enthalpy exceeds the ion's potential energy.

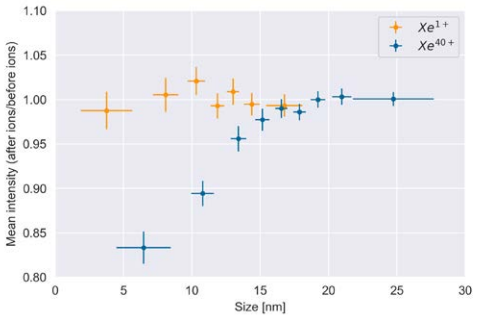

Figure 1. Brightness analysis of the nano-islands in dependence of their lateral size indicates a certain size threshold for potential energy effects.

Further investigations are ongoing to show a charge-state dependence of this threshold, promising to improve our understanding of nano-structuring of metallic quantum dots as a consequence of electronic excitation confinement.

References

[1] Aumayr F *et al* 2008 *J. Phys.: Cond. Matt.* **23** 393001
[2] Pomeroy J M *et al* 2007 *Phys. Rev. B* **75** 241409
[3] Stabrawa I *et al* 2017 *Nucl. Instr. and Meth. B* **408** 235-240

*E-mail: helmut.muckenhuber@tuwien.ac.at
†E-mail: gszabo@iap.tuwien.ac.at

Observing the submersion of rubidium clusters in helium nanodroplets

A Schiller[1] *, P Martini[1,2] and P Scheier[1]

[1] Institut für Ionenphysik und Angewandte Physik, Universität Innsbruck, A-6020 Innsbruck, Austria
[2] Department of Physics, Stockholm University, Stockholm, 106 91, Sweden

Synopsis While small alkali clusters attach to the surface of helium droplets, larger clusters of Li through Rb were predicted to become submerged in the droplet beyond an element-specific critical size, which was soon after confirmed experimentally for Na and K. This contribution presents a study that observed the submersion transition and determined the critical cluster size for the submersion of rubidium clusters for the first time.

Helium nanodroplets (HNDs) are a fascinating tool which can be used for a number of different applications. Their ability to pick up virtually any dopant atoms and molecules and allow these dopants to coagulate at a temperature of 0.4 K is widely exploited to synthesize clusters and nanoparticles. Whereas most dopant atoms and molecules locate in the HND interior, alkali atoms and small alkali clusters occupy dimple sites at the surface of the HND. It was predicted, however, that for alkali clusters (Li_n through Rb_n) exceeding a certain critical size n_c, an interior location becomes energetically favorable, resulting in the submersion of the alkali cluster into the HND [1]. This was later confirmed experimentally for sodium [2] and potassium [3]. Here, a study observing the submersion of large rubidium clusters by means of time-of-flight mass spectrometry (ToF-MS) is presented [4].

In the experiment, HNDs were doped with rubidium atoms, subjected to an incident electron beam followed by analysis of ionic fragments via ToF-MS. Mass spectra extending to about 200 Rb atoms were recorded at different incident electron energies between 8 and 160 eV.

By monitoring the ion yield of cationic rubidium clusters Rb_n^+ as a function of the incident electron energy and cluster size n, we were able to observe a gradual submersion transition and determine the critical size for the full submersion of rubidium clusters as n_c ~100.

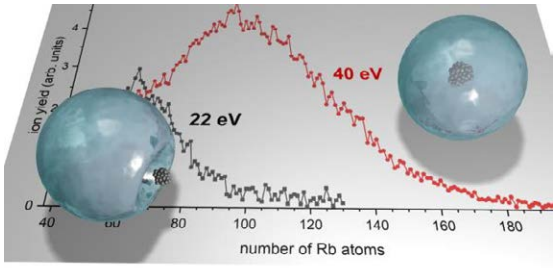

Figure 1. Artist impression of two Rb clusters attached to HNDs. While with the smaller Rb cluster resides in a surface dimple, the larger one is submerged in the droplet. In the background, two cluster size distributions recorded at different incident electron energies are shown.

This work was supported by the Austrian Science Fund FWF, project number P31149.

References

[1] Stark C and Kresin VV 2010, *Phys. Rev. B* **81**, 085401
[2] An der Lan L *et al.* 2011, *J. Chem. Phys.* **135**, 044309
[3] An der Lan L *et al.* 2012, *Phys. Rev. B* **85**, 115414
[4] Schiller A *et al.* 2021, *Eur. Phys. J. D* **75**, 124

* E-mail: arne.schiller@uibk.ac.at

Development of α-particle track structure simulations for targeted radiation therapy in oncology

M E Alcocer-Ávila[1]*, M A Quinto[2], J M Monti[2], R D Rivarola[2] and C Champion[1]†

[1]Centre Lasers Intenses et Applications, Université de Bordeaux, Talence, 33405, France
[2]Instituto de Física Rosario, CONICET - Universidad Nacional de Rosario, Rosario, 2000, Argentina

Synopsis In this study, we report the extension of the homemade numerical platform *TILDA-V* for simulating the slowing-down of α-particles in water, and its first application for evaluating the performance of promising α-particle emitters for targeted therapy of tumors. Results for several α-particle emitters are presented in terms of S-values (Gy·Bq^{-1}·s^{-1}), considering the cell nucleus as the critical target for radiation-induced cellular death.

The long search for a "magic bullet" against cancer has awaken in recent years a great interest in coupling radionuclides to tumor specific carrier molecules to deliver cytotoxic radiation doses to tumor cells, a technique known as targeted radionuclide therapy. Particular attention has been given to Auger electron and α-particle emitters, because they would provide a localized irradiation ideal for eradicating single tumor cells and micrometastases. However, appropriate simulation tools are needed to carry out preclinical studies and thus determine the true potential of these radionuclides.

We recently extended the Monte Carlo track structure code *TILDA-V*, initially developed for protons [1, 2], to include the physical processes required to describe the transport of α-particles of 10 keV/u – 100 MeV/u in water. The code was validated by computing the stopping power and range of α-particles, and comparing our results with data found in the literature.

TILDA-V was then used to simulate the α-particles emitted by ^{211}At, ^{212}Pb/^{212}Bi, ^{213}Bi, ^{223}Ra, ^{225}Ac and ^{227}Th. We computed the S-values for these radionuclides distributed in a single spherical cell of 14 μm diameter with a centered nucleus of 10 μm diameter. We considered four different distributions of the radionuclide: on the cell surface (CS), intracytoplasmic (Cy), intranuclear (N), and a uniform whole cell distribution (C). In all cases the nucleus was taken as the target region. We compared the effect on S-values of considering only the radiations emitted directly by the radionuclide alone, and including the contribution of its decay series. Our results were in excellent agreement with calculations obtained with other codes [3, 4].

Figure 1 depicts the decay series of ^{211}At, while the results for this radionuclide are reported in Table 1.

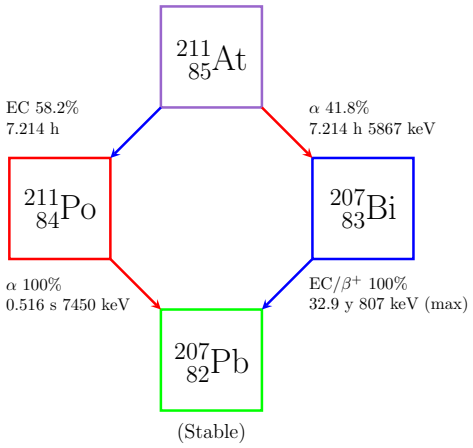

Figure 1. Simplified decay scheme of ^{211}At.

Table 1. S-values for ^{211}At (Gy·Bq^{-1}·s^{-1}).

	S(N ← CS)	S(N ← Cy)
Alone	1.07×10^{-2}	1.57×10^{-2}
Series	2.19×10^{-2}	3.22×10^{-2}
	S(N ← N)	S(N ← C)
Alone	3.99×10^{-2}	2.43×10^{-2}
Series	8.43×10^{-2}	5.09×10^{-2}

References

[1] Quinto M A *et al* 2017 *Eur. Phys. J. D* **71**
[2] Alcocer-Ávila M E *et al* 2019 *Sci. Rep.* **9** 14030
[3] Vaziri B *et al* 2014 *J. Nucl. Med.* **55** 1557
[4] Lee D *et al* 2018 *Radiat. Res.* **190** 236

*E-mail: maen.alav@gmail.com
†E-mail: christophe.champion@u-bordeaux.fr

Ionization and fragmentation of PAH molecules by swift projectile ions

C Bagdia[1] *, A Mandal[1], D Misra[1] and L C Tribedi[1] †

[1]Department of Nuclear and Atomic Physics, Tata Institute of Fundamental Research, Mumbai, 400005, India

Synopsis We present the ionization and fragmentation study of the fluorene ($C_{13}H_{10}$), and acenaphthene ($C_{12}H_{10}$) molecule in collision with swift C, O and F ions. The TOF spectrum of these molecules is measured to identify various fragmentation products. The ratio of double- to single-ionization is studied as a function of projectile charge state (q_p) and velocity (v_p).

The polycylic aromatic hydrocarbons are established to be present in the interstellar medium [1,2]. The PAHs interact with the radiations present in the ISM that leads to the various processes, such as, excitation, ionization, fragmentation etc. The fragmentation of the molecules leads to the production of smaller molecules, which is also know as the top-down channel of molecule formation in the ISM [3]. The PAHs are in general planar molecules having delocalized π-electron cloud that can oscillate collectively upon external perturbation [4-5]. The collective excitation are also known as giant plasmon resonance (GDPR), which results from strong e^--e^- correlations.

Hence, in this work, the experimets are performed with the fluorene ($C_{13}H_{10}$) and acenaphthene ($C_{12}H_{10}$) molecules to study the effect of the structure of the molecule. We measured the ionization and fragmentation of these molecules in collisions with C, O and F-ions using the double field time-of-flight (TOF) spectrometer. The ion beams are obtained from the 14 MV Pelletron accelerator at TIFR, Mumbai. The effusive jet of the target molecules are obtained by heating the molecules.

The ionization and fragmentation yields are measured as a function of projectile charge state (q_p) and velocity (v_p). The figure 1 shows the typical TOF spectrum of the acenaphthene upon 60 MeV O^{6+} ion impact. The various fragmentation channels and products for both the PAHs have been identified from the TOF spectrum. The q_p and v_p dependence of the single- (SI) and double-ionization (DI) has been studied. We have compared the ratio of DI to SI with that for He from literature and O_2 molecules from the same experiment. The ratio is higher for PAHs as compared to gaseouse targets, particularly C-based molecules. The apparently large ratios in case of PAHs indicates the effect of strong e^--e^- correlation among the collectively excited plasmon in such PAH molecules.

The detailed results will be presented.

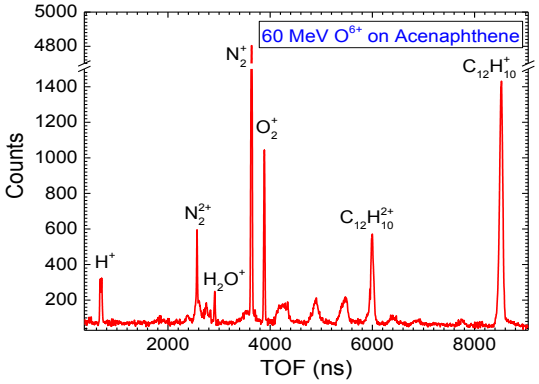

Figure 1. Time of flight spectrum of the acenaphthene upon 60 MeV O^{6+} ion impact.

References

[1] Tielens A G G M 2008 *Annu. Rev. Astron. Astrophys.* **46** 289
[2] Lopez-Puertas M *et al* 2013 *Astrophys. J.* **770** 132
[3] Tielens A G G M 2013 *Rev. Mod. Phys.* **85** 1021
[4] Gutfreund H *et al* 1969 *J. Chem. Phys.* **50** 4478
[5] Biswas S *et al* 2015 *Phys. Rev. A* **92** 060701

* E-mail: chandanbagdia@gmail.com
† E-mail: ltribedi@gmail.com

On how a target atom might hide in plain sight due to a loss of coherence of the projectiles beam

R O Barrachina[1,2,3 *], F Navarrete[4] and M Ciappina[5,6,7,8]

[1]Centro Atómico Bariloche, Comisión Nacional de Energía Atómica (CNEA), 8400 Bariloche, Argentina
[2]Instituto Balseiro, CNEA and Universidad Nacional de Cuyo, 8400 Bariloche, Argentina
[3]Consejo Nacional de Investigaciones Científicas y Técnicas (CONICET), Argentina
[4]Institute of Physics, University of Rostock, 18051 Rostock, Germany
[5]ICFO–Institut de Ciencies Fotoniques, The Barcelona Institute of Science and Technology, 08860 Castelldefels, Spain
[6]Institute of Physics of the ASCR, ELI Beamlines Project, 18221 Prague, Czech Republic
[7]Physics Program, Guangdong Technion - Israel Institute of Technology, Shantou, Guangdong 515063, China
[8]Technion - Israel Institute of Technology, Haifa 32000, Israel

Synopsis We demonstrate how, due to an atomic masking effect, the cross section of a collision can strongly decrease in magnitude when the coherence length of the incident beam is much smaller than the characteristic dimensions of the target.

One of the most basic assumptions in almost every collision experiment and any corresponding theoretical development is that the projectiles' beam is coherent in lengths greater than that of the target atoms or molecules, a. However, it has been recently shown that it is possible to experimentally manipulate the coherence length l and to go from a coherent situation for $l>a$ to an incoherent one in the opposite case [1]. An unequivocal manifestation of this transition is the disappearance of interference effects when the previous condition is not attained [2,3].

However, this effect is not always easy to observe experimentally. On the contrary, in this communication we discuss a much clearer subproduct of the loss of coherence, namely a strong decrease in the magnitude of the cross section [4].

Surprisingly enough, this effect was already there in the first experimental and theoretical results regarding the manipulation of the coherence length (see, eg. [1] and [5]) but, as far as we can tell, it went mostly unnoticed.

As a working example, let us consider the case of a molecular target. The characteristic length a is representative of the internuclear distances in the molecule. When l is larger than a, the incoming projectiles' beam coherently illuminates each individual molecule in the target. This means that all the atoms in the molecule coherently participate in the collision event and interference effects might appear [6].

On the other hand, in the incoherent situation, each atom in the molecule is illuminated separately from the others. In other words, if a projectile "hits" one atom, it does not hit any other atom in the molecule. This means that any interference effect should disappear. But it also means that the cross section, being it total or differential, would be greatly reduced. In particular, for the case of an hydrogen molecule, the cross section will be two times smaller than in the coherent case [4], an effect that is confirmed by experimental results [1].

Unfortunately, despite the efforts done by different authors (see references in [4]), there is no generalization of the standard scattering theory that might deal with the transition between a coherent and an incoherent collision.

However, in this communication we will discuss the basic framework of this generalized theory and present comprehensive results that can explain both limiting cases.

References

[1] Egodapitiya K N *et al* 2011 *Phys. Rev. Lett.* **106** 153202
[2] Schulz M 2017 *Adv. Atoms. Mol. Opt. Phys.* **66** 507
[3] Barrachina R O *et al* 2019 *Coherence and contextuality in scattering experiments*. In "Ion-Atom Collisions" Ed. Schulz M, (De Gruyter: Berlin) p. 61
[4] Barrachina R O 2021 *Atoms* **9** 5
[5] Sarkadi L *et al* 2016 *Phys. Rev. A* **93** 032702
[6] Barrachina R O *et al* 2019 *Eur. J. Phys.* **40** 065402

* E-mail: barra@cab.cnea.gov.ar

Ionization of water under the impact of 250 keV proton beam

A Bhogale[1]*, M Roy Chowdhury[1] J M Monti[2] A Jorge[4] M Horbatsch[3] T Kirchner[3] R D Rivarola[2] and L C Tribedi[1]†

[1]Tata Institute of Fundamental Research, Homi Bhabha Road, Colaba, Mumbai 400005, India
[2]Instituto de Fisica Rosario (CONICET-UNR), Universidad Nacional de Rosario, 2000 Rosario, Argentina
[3]Department of Physics and Astronomy, York University, Toronto, Ontario, M3J 1P3 Canada
[4]Departamento de Qumica, Universidad Autnoma de Madrid, Madrid, 28049, Spain

Synopsis The double differential cross sections (DDCS) for emitted electrons from water target under the impact of 250keV proton beam are measured. The measured data are compared with the theoretical calculations based on two models i.e. CDW-EIS and CTMC. The single differential cross section (SDCS) and total ionization cross section (TCS) were also obtained. While CDW-EIS gives a reasonable agreement with the data the CTMC model turns out to provide an excellent explanation.

The study of the DDCS for emitted electrons from water vapour by energetic proton impact gains importance in radiobiology. To explore the science behind the radiobiology related to the hadron therapy of cancer, and in general for radiation damage by high energy particles, it is importannt to understand the characteristics of the ionization process and the energy loss etc. in water molecules due to its high abundance in living organisms [1]. The ions interact with the water molecules to give rise to processes like ionization, electron capture or dissociation etc. The prominent process is the emission of electrons with different energies in all directions which may cause further damage [2, 3] Emitted electrons are detected using hemispherical electrostatic analyzer for emission angles within 30 to 160 degree. The highly collimated proton beam of energy 250 keV was available from the 14.5 GHz ECR based ion-accelerator in the DNAP, TIFR. The absolute DDCS, $d^2\sigma/d\epsilon_e d\Omega_e$, as function of the emission energy (ϵ_e) and emission angle (Ω_e), have been obtained and compared with the CDW-EIS and CTMC [4] calculations. The CTMC calculations show excellent agreement with the experimental DDCS data particularly in the backward angles. In case of forward angles both the CDW-EIS and the CTMC provide reasonable agreement (Fig.1). The TCS values as obtained from the experiment, the CDW-EIS and the CTMC model are 1.62x10^{-16}, 2.99x10^{-16} and 2.14x10^{-16} cm^2, respectively. The experimental data falls much closer to the CTMC prediction.

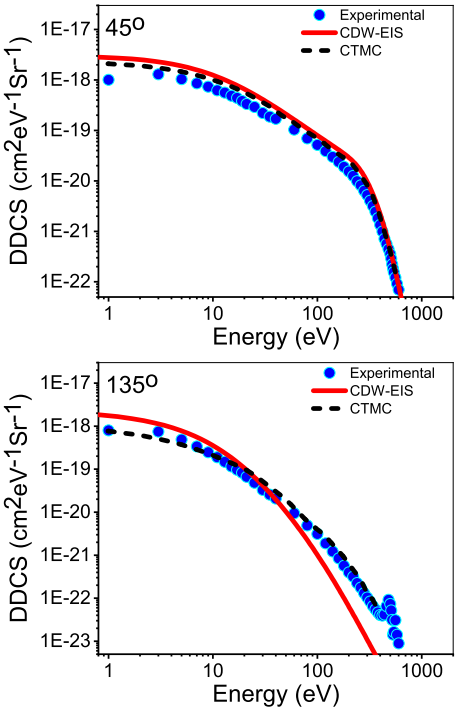

Figure 1. DDCS for (a) 45° and (b) 135° with CDW-EIS (solid-red line) and CTMC (dashed black line) predictions.

References

[1] Gobet F *et al* 2004 *Phy. Rev. A* **70** 062716
[2] Bernal MA *et al* 2007 *Nucl. Instrum. Methods Phys. Res., B* **262** 1-6
[3] Bhattacharjee S *et al* 2017 *Phy. Rev. A* **96** 052707
[4] Jorge A *et al* 2019 *Phy. Rev. A* **99** 062701

*E-mail: abhibhogale@gmail.com
†E-mail: lokesh@tifr.res.in

Energy transfer from keV and lower energy Sn ions to H_2 molecules

K I Bijlsma[1,2] *, S Rai[1,2], M Salverda[1], O O Versolato[2,3], R Hoekstra[1,2]

[1] Zernike Institute for Advanced Materials, University of Groningen, Groningen, 9747 AG, The Netherlands
[2] Advanced Research Center for Nanolithography, Amsterdam, 1098 XG, The Netherlands
[3] Department of Physics and Astronomy, and LaserLaB, Vrije Universiteit, Amsterdam, 1081 HV, The Netherlands

Synopsis The transfer of energy from keV and lower energy Sn ions to H_2 molecules is and will be studied both experimentally and by using simulations and calculations.

Nanolithography machines of the latest generation work with light in the extreme ultraviolet (EUV) regime. This light is generated by a laser-produced plasma (LPP) of Sn. Apart from the EUV photons, the plasma also emits energetic, highly-charged Sn ions. These ions, with up to several tens of keV of energy, may damage plasma-facing surfaces including the EUV multilayer collector mirror. Therefore, one can use a buffer gas to slow these ions. The only gas that barely absorbs the EUV light is H_2 [1].

The most widely used software package to simulate energy loss, scattering, and penetration depths of particles in solids and gases is SRIM (Stopping and Range of Ions in Matter) [2]. However, heavy and low-energy Sn ions colliding with a light target as H_2 is a system not in the well-tested, core region of validity of SRIM. Aspects that are not explicitly considered are for example the charge state of the ions, the molecular nature of H_2, the polarizability of the target, and the validity of the generic ZBL potential for Sn^{q+} - H_2 interactions.

To address these aspects we have designed and are commissioning a crossed-beam type of experiment to perform energy loss and scattering measurements. The experimental aim is to perform high-resolution Time-of-Flight (ToF) spectroscopy on the scattered projectiles and target fragments. The setup is connected to our ZERNIKELEIF facility in Groningen, at which a beam of Sn^{q+} ions of a specific isotope, charge-state, and energy can be generated using a 14 GHz Electron Cyclotron Resonance Ion Source (ECRIS) of supernanogan type. In the build-up and test phase of the experimental setup, experiments on electron capture in Sn^{3+} - H_2 collisions have already been performed [3].

Here we focus on the energy transfer from a Sn ion to a target H_2 molecule. The shapes of the H_2^+ and H^+ peaks in the target ToF spectra show broadening beyond the Gaussian shape expected from standard contributions (beam pulse length, trajectories through the ToF spectrometer, and electronics), which relates to the energy transfer from projectile to target. In this contribution, we discuss the interpretation of the broadening and its link to the energy transfer. In addition, beam broadening results (integral scattering) are presented as a function of target density. The integral H_2 density along the beam path has been accurately determined by conducting experiments on charge exchange interactions between protons and H_2, a system for which the cross-sections are well-established.

The experimental results will be compared to predictions from SRIM as well as to calculations of projectile-target interactions for various adjusted interatomic potentials.

* E-mail: k.i.j.bijlsma@rug.nl

References

[1] Versolato O O 2019 *Plasma Sources Sci. Technol.* **28** 083001
[2] Ziegler J F *et al* 2010 *Nucl. Instrum. Methods Phys. Res. B* **268** 1818
[3] Rai S *et al* ViCPEAC 2021

Ionization and fragmentation dynamics of collisionally excited small hydrocarbon derivatives, a theoretical study

L López-Pacios[1] and S Díaz-Tendero[1,2,3] *

[1]Departamento de Química, Universidad Autónoma de Madrid, 28049 Madrid, Spain
[2]Condensed Matter Physics Center (IFIMAC), Universidad Autónoma de Madrid, 28049 Madrid, Spain
[3]Institute for Advanced Research in Chemical Science (IAdChem), Univ. Autónoma de Madrid, 28049 Madrid, Spain

Synopsis We use density functional theory (DFT) and ab initio molecular dynamics to study the ionization potentials, dissociation energies, and fragmentation dynamics of small hydrocarbon derivatives. We thus provide a theoretical insight into the main factors that govern the behaviour of these molecules after ionization and excitation in a collision with energetic particles: electrons, atomic ions, or photons. We focus our discussion mainly on fragmentation channels that involve (atomic and/or molecular) hydrogen loss, and hydrogen migration.

In the interstellar medium and circumstellar envelopes, several polyatomic chemical compounds have been identified [1], in particular hydrocarbon molecules and its derivatives. In such media, they are exposed to harsh environments, where the interaction with energetic particles, coming from e.g. solar winds, can trigger various reactions. Typically, excitation and/or ionization produced in the collision is followed by the fragmentation of the molecule.

In this communication we present a theoretical study on several ionized and excited small hydrocarbons and hydrocarbon derivatives, considering different functional groups. We have studied ionization potentials, dissociation energies, and fragmentation dynamics using density functional theory and ab initio molecular dynamics simulations. The combination of these two methodologies has been successfully used in the past to study fragmentation of positively charged molecules and clusters after ionization and excitation with atomic ions and energetic photons (see e.g. [2-4]).

An important research activity during the last years focuses on understanding the way the charge and the excess of energy is distributed among the molecular degrees of freedom in the collision process [5]. In this communication we have considered the fragmentation of neutral, singly and doubly-ionized species with excitation energy in the range of 7-15 eV. The comparison of the results obtained in each case allows us to understand the key aspects of the fragmentation.

As an example, we present in Fig.1 the degree of fragmentation of methane in the three ionization states considered in this work (CH_4, CH_4^+ and CH_4^{2+}) as a function of the excitation energy. It has been computed from the molecular dynamics simulations as follows: First, we run several trajectories distributing randomly the excitation energy in nuclear degrees of freedom. For each charge and energy value, we run statistics over the channels that have been populated after 200 fs. Finally, the fragmentation degree is obtained by weighining those channels with the same number of fragments by a given factor.

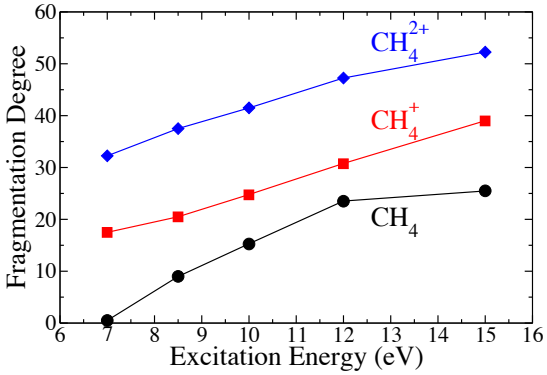

Figure 1. Degre of fragmentation of neutral, singly- and doubly-ionized methane as a function of the excitation energy.

References

[1] Tielens AGGM 2013 *Rev. Mod. Phys.* **85** 1021
[2] Maclot S et al 2013 *J. Phys. Chem. Lett.* **4** 3903.
[3] Maclot S et al 2016 *Phys. Rev. Lett.* **117** 073201.
[4] Rousseau P et al 2020 *Nat. Comm.* **11** 3818.
[5] Aguirre NF et al 2021 *Theor. Chem. Acc.* **140** 22.

* E-mail: sergio.diaztendero@uam.es

Cooling of C_2^- in ion traps with H_2 as a partner gas

J Franz[1,2]*, B P Mant[3], R Wester[4], F A Gianturco[4]

[1]Faculty of Applied Physics and Mathematics, Gdańsk University of Technology, Gdańsk, 80-233, Poland
[2]Advanced Materials Center, Gdańsk University of Technology, Gdańsk, 80-233, Poland
[3]Department of Chemistry, University College London, London, WC1H 0AJ, UK
[4]Institut für Ionenphysik und Angewandte Physik, Universität Innsbruck, Innsbruck, A-6020, Austria

Synopsis Computed scattering cross sections and corresponding rate coefficients for rotationally inelastic collisions of C_2^- with $H_2$are presented. The cross sections are computed with quantum scattering theory using a new ab initio potential energy surface.

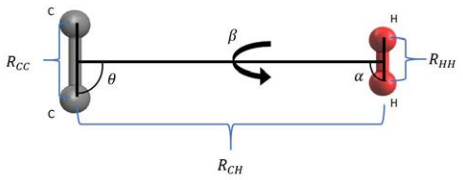

Figure 1. Definition of the body-fixed coordinates system.

Laser-cooled negative ions have been suggested for sympathetic cooling of antiprotons [1]. A very efficient cooling gas for this process could be the molecular anion C_2^-, because of its many inner degrees of freedom (rotational, vibrational and electronic) [2, 3, 4]. This requires, that first C_2^- can be cooled down to subkelvin temperatures. In a series of studies Mant *et al.* have simulated rates for rotational cooling of C_2^- with the noble gases He, Ne and Ar [5, 6, 7]. A more efficient gas for cooling molecular anions is molecular hydrogen [8]. Here we will present results for rotational cooling of C_2^- with molecular hydrogen [9]. For this purpose we have computed a new ab initio potential energy surface and calculated rotational inelastic cross sections [9]. Currently we are working on cooling rates involving vibrational inelastic collisions. The cross section data is used for simulating the thermalization rates. These rates are compared with those obtained for the noble gases.

References

[1] Kellerbauer A and Walz J, 2006 *New J. Phys.* **8** 45
[2] Yzombard P *et al.*, 2015 *Phys. Rev. Lett.* **114** 213001
[3] Fesel J *et al.*, 2017 *Phys. Rev. A* **96** 031401(R)
[4] Gerber S *et al.*, 2018 *New J. Phys.* **20** 023024
[5] Mant B P *et al.*, 2020 *J. Phys.B: At. Mol. Opt. Phys.* **53** 025201
[6] Mant B P *et al.*, 2020 *J. Int. Mass Spectrom.* **457** 116426
[7] Mant B P *et al.*, 2020 *Phys. Rev. A* **102** 062810
[8] González-Sánchez L *et al.*, 2020 *ApJ* **897** 75
[9] Mant B P *et al.*, 2021 *Mol. Phys.* submitted

*E-mail: janfranz@pg.edu.pl

Quantum calculations of O_2-N_2 scattering: *Ab initio* investigation of the N_2-perturbed fine structure lines in $O_2(X^3\Sigma_g^-)$

M. Gancewski[1]*, H. Jóźwiak[1], E. Quintas-Sánchez[2], R. Dawes[2], F. Thibault[3], P. Wcisło[1]†

[1]Institute of Physics, Faculty of Physics, Astronomy and Informatics,
Nicolaus Copernicus University, Toruń, Poland
[2] Department of Chemistry, Missouri University of Science and Technology, Rolla, MO, USA
[3]Institute of Physics of Rennes, Univ. Rennes, Rennes, France

Synopsis Collisional perturbations of fine structure lines in $O_2(X^3\Sigma_g^-)$ diluted in N_2 bath are analyzed for the first time in terms of fully quantum calculations involving a new *ab initio* potential energy surface.

The O_2-N_2 interactions play a role in the modelling and understanding of collisional perturbations of the Earth's atmosphere spectral lines. However, in order to faithfully represent the collision dynamics in such system, the non-zero electronic spin of the ground electronic $^3\Sigma_g^-$ state of O_2 needs to be taken into account in the description of quantum scattering. We present our methodology as well as the results of fully quantum calculations of the O_2-N_2 scattering and the pressure broadening parameters for $O_2(X^3\Sigma_g^-)$ immersed in molecular nitrogen bath. It is the first theoretical *ab initio* investigation of this collisional system in the context of the shapes of molecular lines. The PES for this study was constructed automatically using the AUTOSURF code [1]. The data provided through this investigation is important for the terrestrial atmospheric measurements and can be used for populating the spectroscopic databases such as HITRAN or GEISA.

References

[1] Quintas-Sánchez, Ernesto, and Richard Dawes. "AUTOSURF: A freely available program to construct potential energy surfaces." *Journal of chemical information and modeling* **59**, no. 1 (2018): 262-271

*E-mail: 291447@stud.umk.pl
†E-mail: piotr.wcislo@umk.pl

Collisional effects in the self- and H_2-perturbed spectra of D_2

H Jóźwiak[1]*, N Stolarczyk[1], M Zaborowski[1], A Cygan[1], S Wójtewicz[1], M Gancewski[1], K Stankiewicz[1], P Jankowski[2], K Patkowski [3], K Szalewicz[4], F Thibault[5], R Ciuryło[1], D Lisak[1] and P Wcisło[1]

[1]Institute of Physics, Faculty of Physics, Astronomy and Informatics, Nicolaus Copernicus University in Toruń, 87-100 Toruń, Poland
[2]Faculty of Chemistry, Nicolaus Copernicus University in Toruń, 87-100 Toruń, Poland
[3]Department of Chemistry and Biochemistry, Auburn University, Auburn, Alabama 36849, United States
[4]Department of Physics and Astronomy, University of Delaware, Newark, Delaware 19716, United States
[5]Univ. Rennes, CNRS, IPR (Institut de Physique de Rennes)-UMR 6251, Rennes F-35000, France

Synopsis We perform an experimental and theoretical study of the self- and H_2-perturbed 2-0 S(2) transition in D_2. Accurate experimental spectra allow us to test subtle collisional effects, such as the centrifugal distortion of the potential energy surface or the phenomenon of quantum indistinguishability.

Accurate measurements of rovibrational transitions in the ground electronic state of molecular hydrogen allow for stringent tests of quantum electrodynamics for molecules [1] and can be used in searches for physics beyond the Standard Model [2]. Recently, we reported the most accurate measurement of the position of the weak quadrupole 2-0 S(2) transition in D_2 [3], using frequency-stabilized cavity ringdown spectrometer operating in the frequency-agile, rapid scanning spectroscopy mode. Despite working in the Doppler-limited regime, we reached the accuracy of 170 kHz.

Molecular collisions perturb the shape of optical resonances and affect the accuracy of determined transition frequencies. This is particularly important in the spectra of molecular hydrogen, where, for instance, the speed-dependence of collisional shift results in an asymmetric line profile [4]. Systematic errors in the experimental analysis can be reduced if one uses realistic line-shape models, such as the speed-dependent billiard-ball profile (SDBBP) [5], the parameters of which are derived from quantum scattering calculations. Such a theoretical approach has recently led to an unprecedented agreement with the cavity-enhanced He-perturbed H_2 spectra [6]. On the other hand, employing the very same technique for the self-perturbed 2-0 S(2) line in D_2 resulted in a 27% discrepancy in the collisional shift [7]. This disagreement could be caused by the centrifgual distortion of the potential energy surface (PES) or the quantum indistinguishability phenomenon, which were disregarded in the original calculations.

Here, we investigate the self- and H_2-perturbed 2-0 S(2) line in D_2 – two distinct collisional systems which involve indistinguishable and distinguishable colliding partners. Quantum scattering calculations are performed using a new, full-dimensional PES that was fitted to energies at the highest practical level of electronic structure theory and that is valid for a much broader range of intramonomer distances than any published PES for this system. Scattering S-matrix elements are used to obtain line-shape parameters of the SDBBP. Spectral line-shape measurements in pure D_2 and 2% D_2-H_2 mixture are performed using optical-frequency-comb-locked cavity ring down spectrometer. Each of the samples is measured in temperatures between 296 and 333 K and pressures ranging from 0.5 to 2.2 atm. This study provides a unique opportunity to quantify the interference term in the scattering cross sections [8] and constitutes a first test of quantum indistinguishability in the spectral line-shape theory.

*E-mail: hubert.jozwiak@doktorant.umk.pl

References

[1] Komasa J *et al.* 2019 *Phys. Rev. A* **100** 032519
[2] Ubachs W *et al.* 2016 *J. Mol. Spectrosc.* **320** 1
[3] Zaborowski M *et al.* 2020 *Opt. Lett.* **45** 1603
[4] Farrow R L *et al.* 1989 *Phys. Rev. Lett.* **63** 746
[5] Ciuryło R *et al.* 2002 *Phys. Rev. A* **65** 012502
[6] Słowiński M *et al.* 2020 *Phys. Rev. A* **101** 052705
[7] Wcisło P *et al.* 2018 *J. Quant. Spectrosc. Radiat. Transf.* **213** 41
[8] Huo W M *et al.* 1996 *J. Chem. Phys.* **104** 7572

Ab initio investigation of the CO–N_2 quantum scattering: The collisional perturbation of the pure rotational R(0) line in CO

H Jóźwiak[1]*, F Thibault[2], H Cybulski[3] and P Wcisło[1]

[1]Institute of Physics, Faculty of Physics, Astronomy and Informatics, Nicolaus Copernicus University in Toruń, 87-100 Toruń, Poland
[2]Univ. Rennes, CNRS, IPR (Institut de Physique de Rennes)-UMR 6251, Rennes F-35000, France
[3]Institute of Physics, Kazimierz Wielki University, ul. Powstańców Wielkopolskich 2, 85-090 Bydgoszcz, Poland

Synopsis We report the first fully quantum investigation of the shape of the N_2-perturbed molecular resonance of CO. The results agree well with the available experimental data. This work is the first step towards populating the spectroscopic databases with *ab initio* collisional line-shape parameters for atmosphere-relevant systems.

Collisions with the nitrogen molecule perturb the absorption lines of less abundant molecules in the Earth's atmosphere, leading to the pressure broadening of the spectra which constitutes the primary broadening mechanism in the troposphere [1]. Accurate values of pressure broadening and shift coefficients are essential for reducing atmospheric-spectra fit residuals, which might affect the values of the quantities retrieved from the fit, such as the volume mixing ratio (VMR) of the absorbing compound [2]. This is especially important in terms of remote sensing of gaseous pollutants, such as the CO molecule. Accurate pressure broadening coefficients of the N_2-perturbed CO lines are also needed in the analysis of the nitrogen-dominated atmospheres of Titan [3], Triton [4] or Pluto [5].

We report fully quantum calculations of the collisional perturbation of the N_2-perturbed pure rotational R(0) line in CO [6]. The results agree well with the available experimental data [7, 8, 9, 10]. This work constitutes a significant step toward populating the spectroscopic databases with *ab initio* collisional line-shape parameters for atmosphere-relevant systems. The calculations were performed using three different recently reported potential energy surfaces (PESs) [11, 12, 13]. We conclude that all three PESs lead to practically the same values of the pressure broadening coefficients.

References

[1] Hartmann D L *Atmospheric radiative transfer and climate*, in *Global Physical Climatology*, 2nd ed., edited by Hartmann D L, Elsevier, Boston, 2016
[2] Hartmann J M *et al.* 2018 *J. Quant. Spectrosc. Radiat. Transf.* **213** 178
[3] Muhleman D O *et al.* 1984 *Science* **223** 393
[4] Lellouch E *et al.* 2010 *Astron. Astrophys.* **512** L8
[5] Stern S A *et al.* 2015 *Science* **350** aad1815
[6] Jóźwiak H *et al.* 2021 *J. Chem. Phys.* **154** 054314
[7] Colmont J M *et al.* 1986 *J. Quant. Spectrosc. Radiat. Tranf.* **35** 81
[8] Connor B J *et al.* 1986 *J. Mol. Spectrosc.* **119** 229
[9] Nissen N *et al.* 1999 *Z. Nat. A* **54** 218
[10] Puzzarini C *et al.* 2002 *J. Mol. Spectrosc.* **246** 428
[11] Surin L A *et al.* 2018 *J. Chem. Phys.* **148** 044313
[12] Liu J-M *et al.* 2018 *Phys. Chem. Chem. Phys.* **20** 2036
[13] Cybulski H *et al.* 2018 *Phys. Chem. Chem. Phys.* **20** 12624

*E-mail: hubert.jozwiak@doktorant.umk.pl

Rotational excitation followed by collision-induced molecular dissociation in 10-keV $O^+ + H_2$ and $O^+ + D_2$ collisions

Z Juhász[1*], V Vizcaïno[2], J-Y Chesnel[2], S T S Kovács[1], P Herczku[1], S Demes[1], R Rácz[1], S Biri[1], N Sens[2], D V Mifsud[3,1], L Ábrók and B Sulik[1]

[1] Institute for Nuclear Research, Hungarian Academy of Sciences (Atomki), Debrecen, H-4026, Hungary
[2] Normandie Univ, ENSICAEN, UNICAEN, CEA, CNRS, CIMAP, Caen, 14000, France
[3] Centre for Astrophysics and Planetary Science, School of Physical Sciences, University of Kent, Canterbury CT2 7NH, United Kingdom

Synopsis We studied fragmentation of H_2 and D_2 by 10-keV O^+ impact. A time-of-flight setup was developed to detect fragment ions with low emission energies. The velocity components of the H^+ or D^+ fragments were recorded. A significant fraction of the fragments stems from the kick-out of a target atom following a binary encounter with the projectile. In the velocity distribution the binary ridge due these fragments is split into two parts, which is a signature for a kick-out process from rotating molecules. The asymmetry of the two parts provides evidence for rotational excitation of the target.

The interaction between ions and molecules is an essential process in various areas of physics and chemistry. Emission of low-energy fragment ions is a significant output channel following excitation and moderate ionization of the target molecules [1]. Its experimental investigation is difficult since slow ions are sensitive to disturbing electric fields. A time-of-flight setup was thus developed at Atomki for reliable measurement of absolute cross sections for emission of fragment ions with kinetic energies down to 0.1 eV. The emitted ions fly through a well-shielded field-free region before their detection on a 2D position sensitive detector which can be rotated around the center of the chamber.

We measured the velocity distribution of the H^+ (or D^+) fragments ejected from H_2 (or D_2) molecules bombarded with 10-keV O^+ ions. Figure 1 depicts the velocity distribution of the D^+ fragments whose kinetic energy is lower than 2 eV. In this range, the velocity distribution shows a maximum at velocities close to 0.001 a.u., *i.e.* at energies on the order of 0.1 eV. In accordance with a recent thermodynamic model for molecular collisions [2], the slowest fragments are most likely due to dissociation of H_2^+ (or D_2^+) ions created by single electron capture from the target.

The velocity distribution shows a ridge due to enhanced fragment emission in the transverse direction after binary knock out by the projectile. Compared to its expected position for a target at rest, this binary ridge is split and shifted towards two opposite directions. These shifts are due to the speed of the atoms in the rotating target molecule. As expected from their mass ratio, the shift is found to be twice as large for H_2 as for D_2. The shift towards a negative longitudinal velocity component is found to be more likely than that towards a positive component, showing that the active target atom is attracted by the incoming projectile. This result provides evidence for rotational excitation of the target molecule before dissociation.

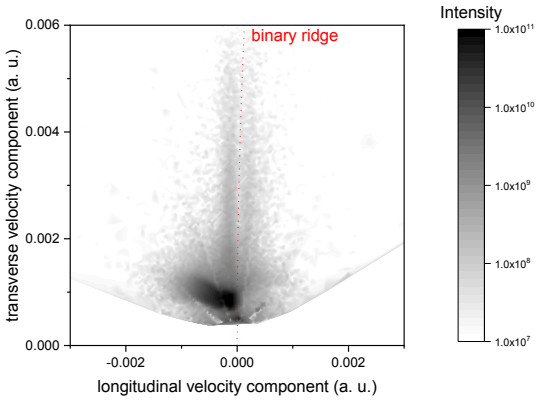

Fig. 1. Velocity distribution of D^+ fragments stemming from 10-keV $O^+ + D_2$ collisions. The longitudinal velocity component is the component along the beam axis.

This work was supported by Hungarian NRDIO-OTKA Grants No. K109440 and K128621, the CNRS International Emerging Action (IEA-PICS-CNRS No. 7739 / NKM-115/2017), and by the Hungarian NIIF Institution.

References

[1] Juhász Z *et al* 2019 *Phys. Rev. A* **100** 032713
[2] Juhász Z 2016 *Phys. Rev. A* **94** 022707

* E-mail: zjuhasz@atomki.hu

Proton collisions with fluorine-containing biomolecules: an exploratory study based on an independent atom model including geometric overlap

H J Lüdde[1]*, M Horbatsch[2]†, and T Kirchner[2]‡

[1]Center for Scientific Computing, Goethe-Universität, D-60438 Frankfurt, Germany
[2]Department of Physics and Astronomy, York University, Toronto, Ontario, M3J 1P3, Canada

Synopsis We present independent-atom-model pixel-counting-method calculations for net ionization and net capture in proton collisions with fluorine-containing compounds of radiobiological relevance.

Compounds containing fluorine-18 are widely used in medical applications such as positron emission tomography. A prominent example is fluorodeoxyglucose (FDG), which is used for imaging tumors. Motivated by the question if there are added benefits to proton therapy if the tumor has taken up FDG or other ^{18}F containing compounds before irradiation, we study ionization and capture processes in proton collisions with these molecules.

Our study is based on the independent-atom-model pixel counting method (IAM-PCM) introduced recently [1, 2]. The IAM-PCM represents a refined version of the additivity rule (IAM-AR) for calculating a net ionization or a net capture cross section for an ion-molecule collision system in that it takes into account the overlapping nature of the effective cross-sectional areas of the atomic contributions. The overlap effect can lead to strong reductions of the net cross sections and, as demonstrated in a number of calculations for biologically relevant molecules [3, 4], improved agreement with experimental data compared to the IAM-AR.

As in our previous works, the atomic cross sections are calculated using the two-center basis generator method and the relevant geometrical information for the molecules studied are taken from the available literature.

In Fig. 1 we compare total cross section results for proton collisions with FDG and H_2O. Not surprisingly, the former are significantly larger than the latter. For the case of net ionization (shown by the blue curves) we observe an almost constant enhancement by about a factor of ten over the entire impact energy range from 10 keV to 10 MeV, which is in line with the scaling behavior discussed in [5].

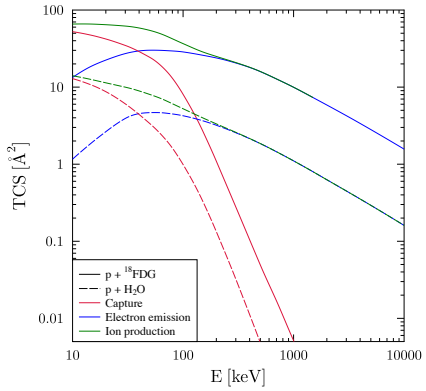

Figure 1. Net capture, electron emission (i.e., net ionization), and recoil ion production cross sections for proton collisions with FDG ($C_6H_{11}FO_5$) and water (H_2O) as functions of impact energy: present calculations.

At the conference we will present results for collisions with a number of fluorine-containing compounds and discuss their implications for radiotherapy.

References

[1] Lüdde H J *et al* 2016 *Eur. Phys. J. D* **70** 82
[2] Lüdde H J *et al* 2018 *Eur. Phys. J. B* **91** 99
[3] Lüdde H J *et al* 2019 *Eur. Phys. J. D* **73** 249
[4] Lüdde H J *et al* 2020 *Phys. Rev. A* **101** 062709
[5] Lüdde H J *et al* 2019 *J. Phys B* **52** 195203

*E-mail: luedde@itp.uni-frankfurt.de
†E-mail: marko@yorku.ca
‡E-mail: tomk@yorku.ca

Methanol fragmentation probed in electron transfer experiments

A I Lozano[1 *], B Kerkeni[2], S Kumar[1], G García[3] and P Limão-Vieira[1 †]

[1]Atomic and Molecular Collisions Laboratory, CEFITEC, Department of Physics, Universidade NOVA de Lisboa, Caparica, 2829-516, Portugal
[2]Department of Physics, University of Oxford, Oxford OX1 3RH, UK
[3]Instituto de Física Fundamental, CSIC, Serrano 113-bis, Madrid, 28006, Spain

Synopsis We present a comprehensive investigation on the negative ion formation from methanol (CH_3OH) triggered by electron transfer processes in collisions with neutral potassium atoms up to 250 eV collision energies. The fragment anions formed have been assigned to $M\text{-}H^-$, OH^-, O^-, and H^-, where the most intense yield corresponds to the dehydrogenated parent anion $(M\text{-}H)^-$, in the whole collision energy range investigated. Relevant information about the main electronic states accessible has been obtained through potassium cation energy loss spectra in the forward scattering direction.

Molecules in the interstellar medium (ISM) are exposed to high-energy radiation, as well as to different secondary species such as ions and low-energy electrons. Nowadays, it is known that these secondary species are responsible to trigger the synthesis of prebiotic molecules in the ISM [1,2], where one of the prevalent interaction mechanisms yields molecular dissociation. However, most of the advances in the spectroscopy of ISM molecules are related to photo- induced dissociation processes.

Methanol (CH_3OH), the simplest primary alcohol, is known to play an important role in astrochemistry. First, it is widely observed in the ISM [3]. Also, it may serve as an initial step to further understand the processes that give rise to the formation of prebiotic molecules in the ISM [1].

Here, we have obtained by means of time-of-flight mass spectrometry the anion yields of methanol in electron transfer from collisions with potassium atoms. The anions' branching ratios (BR) (see Fig. 1) show a strong energy dependence in the range investigated. The dehydrogenated parent ion $(M\text{-}H)^-$ is found to be the sole fragment at the lowest collision energy probed.

The complex behaviour observed from the BRs is likely related to the opening of different dissociation channels as the collision energy increases. In order to explore the role of main electronic states involved, we have also performed potassium cation energy loss spectra measurements (post-collision) in the forward scattering direction. Additionally, the experimental findings are supported by *ab initio* quantum chemical calculations for the lowest-lying unoccupied molecular orbitals of methanol in the presence of the potassium atom.

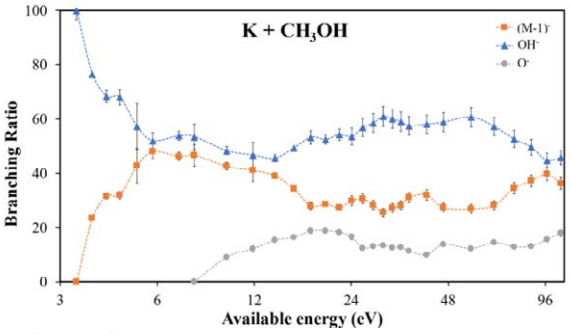

Figure 1. Methanol branching ratios of $(M\text{-}H)^-$, OH^-, and O^- as a function of the available energy.

References

[1] Arumainayagam C R *et al* 2019 *Chem. Soc. Rev.* **48** 2293-314
[2] Sandford S A *et al* 2020 *Chem. Rev.* **120** 4616-59
[3] Wirström E S *et al* 2011 *Astron. Astrophys.* **35** 297-308

* E-mail: ai.lozano@fct.unl.pt
† E-mail: plimaovieira@fct.unl.pt

Initial state-selected molecular reactive scattering with non-equilibrium ring polymer molecular dynamics

A Marjollet[1]*, **L Inhester**[1]† **R Welsch**[1]

[1] Center for Free-Electron Laser Science, DESY, Notkestrasse 85, 22607 Hamburg, Germany

Synopsis Integral cross sections (ICS) of the reactions Mu/H/D+H_2 and H+CH_4 for the vibrational ground and first excited states of H_2, CH_4, and its isotopic variants (excited C-H stretch) are computed employing an extension of the ring polymer molecular dynamics approach (RPMD). In our method, aspects of the quasiclassical trajectory approach (QCT) are implemented in RPMD by employing non-equilibrium initial conditions. The good accuracy of our results firmly hints that our method is a promising, viable and, computationally efficient approach for describing nuclear quantum effects (NQE) in reactive molecular collisions.

The state-resolved knowledge of reaction dynamics in chemisorption processes or gas-phase reactions is paramount for the understanding and control of reactions important to catalysis and atmospheric chemistry.

To gain this knowledge we need simulations including nuclear quantum effects. However, employing rigorous quantum dynamics approaches is prohibitively expensive. As exact calculations can take up months of computer time [3], most studies rely on the quasiclassical trajectory (QCT) approach. In the QCT approach, the nuclei are treated classically and, therefore, the approach is subject to shortcomings such as the absence of both zero-point energy and tunneling effects. The RPMD approach has emerged as a viable and efficient method to mimic quantum effects in classical-like simulations of thermal equilibrium processes [4]. However, so far no state-resolved information could be obtained from these simulations.

We propose an approach combining the advantages of RPMD with procedures from the QCT method to compute initial state-resolved cross sections [5,6]. The approach is systematic to implement, numerically efficient and scalable, so that it can be applied to other scenarios such as surface reactions. We applied our method for the Mu/H/D+H_2 and H+CH_4 reactions. We compare the obtained ICS with its QCT and exact quantum counterparts and find substantial improvement over QCT. Specifically, we find that our method correctly describes zero-point energy as well as tunneling effects. From the simulation data, we discuss the role of these NQEs in the two reactions.

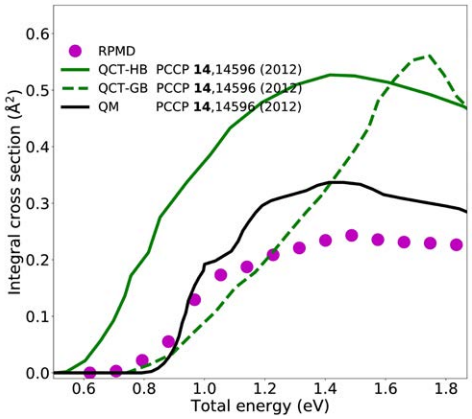

Figure 1. ICS for the reaction Mu+H_2 → MuH+H as a function of energy. Black line: Exact quantum results; Green line: QCT and QCT with histogram/gaussian binning of the products; Purple dots: our extension of RPMD.

References

[1] R Welsch and U Manthe. J. Chem. Phys. (2015) **142** 064309
[2] T. F. Miller III *et al* Annual Review of Physical Chemistry (2013) **64**:387-413
[3] A Marjollet and R Welsch. J. Chem. Phys. 152, 194113 (2020) **152** 194113
[4] A Marjollet and R Welsch. Int J Quantum Chem. (2020) **121**:e26447

*E-mail: adrien.marjollet@desy.de
†E-mail: ludger.inhester@desy.de

Universal scaling rule for the ionization of molecules by impact of ions

A M P Mendez[1]*, C C Montanari[1] and J E Miraglia[1]

[1]Instituto de Astronomía y Física del Espacio, CONICET–UBA, Ciudad Autónoma de Buenos Aires, 1428, Argentina

Synopsis Theoretical and experimental data sets for the single ionization of complex molecules of biological interest are submitted to a two-fold scaling rule. The rule depends on the projectile charge and the number of active electrons of the molecular target. Consequently, the cross sections become independent of the collisional system, and a large number of data sets lay into a single curve.

In a recent work [1], we combined continue distorted–wave calculations (CDW) for atoms and the simple stoichiometric model (SSM) to compute the ionization cross sections of complex molecular targets by charged ions. The CDW–SSM approximation showed reasonable results for over a hundred ion–molecule systems.

In the high energy range, the ionization cross sections present the Z^2 dependence given by the first Born approximation. However, at intermediate energies, the dependence with Z is more complex, and non–perturbative models are mandatory. Following the scaling rule proposed by Montenegro and co–workers [2, 3] $\sigma/Z^\alpha = f(E/Z^{2-\alpha})$, which keeps the Z^2/E relationship, we found that the parameter that best converges the CDW–SSM cross sections of the 96 collisional systems considered over the broadest energy range is $\alpha = 1.2$.

Following Toburen's rule [4, 5], we noticed that CDW ionization cross section σ_A scale with the number of active electrons as $\sigma_e = \sigma_A \nu_A$, where ν_A is 1 for H, and 4 for C, N, and O. Then, employing the SSM, we defined the number of active electrons per *molecule* as $n_M = \sum_A n_A \nu_A$, where n_A is the number of atoms of the element A in the molecule.

Combining the projectile charge reduction of the ionization cross section and the scaling with the number of active electrons of the molecule, we obtained an independent cross section $\widetilde{\sigma}$, which is expressed as a function of $E/Z^{2-\alpha}$ and given by

$$\widetilde{\sigma} = \frac{\sigma_e}{Z^\alpha} = \frac{\sigma_M/n_M}{Z^\alpha}\,, \qquad (1)$$

where σ_M is the ionization cross section for the molecular target. In the figure below, the CDW–SSM theoretical values for 96 collisional systems were submitted to the two-folded scaling rule (solid lines). As noted, the scaling works well, and the cross sections $\widetilde{\sigma}$ lay in a narrow band valid for any ion in any molecule with a dispersion of 25% respect to a fitted mean value (dashed line). Furthermore, the experimental data sets shown are within 35% (see references in [6]).

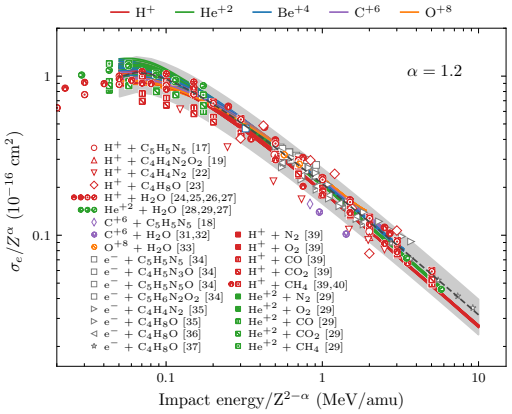

References

[1] A. M. P. Mendez *et al.* 2020 *J. Phys. B: At. Mol. Opt. Phys.* **53**, 055201
[2] R. D. DuBois *et al.* 2013 *AIP Conference Proceeding* **1525**, 679
[3] E. C. Montenegro *et al. Phys. Rev. A* **87** 012706
[4] W. E. Wilson *et al.* 1975 *Phys. Rev. A* **11**, 1303
[5] D. J. Lynch *et al.* 1976 *J. Chem. Phys.* **64**, 2616
[6] A. M. P. Mendez *et al.* 2020 *J. Phys. B: At. Mol. Opt. Phys.* **53**, 175202

*E-mail: alemendez@iafe.uba.ar

Theoretical study of collisions of multicharged ions with water molecules

C Illescas, A. Jorge, L Méndez*, I Rabadán and J Suárez

Laboratorio Asociado al CIEMAT de Física Atómica y Molecular en Plasmas de Fusión. Departamento de Química, módulo 13, Universidad Autónoma de Madrid, 28049-Madrid, Spain.

Synopsis We present calculations of ionization and electron capture in collisions of He^{2+}, Li^{3+} and C^{3+} with water molecules at energies between 20 and 500 keV/u. Three different classical and semiclassical methods are compared.

Ion collisions with water are relevant in cancer ion therapy. Also, electron capture in ion-water collisions leads to X-ray emission from cometary and planetary atmospheres. In this work we have carried out a computational study of collisions of He^{2+}, Li^{3+} and C^{3+} with water molecules at energies above 20 keV/u. We have performed the calculations within the framework of the independent electron approximation and we have used both classical (CTMC) and semiclassical methods [1]. In the semiclassical calculations we have applied a direct numerical solution of the time-dependent Schrödinger equation, by employing the GridTDSE code [2], and the so-called asymptotic frozen molecular orbitals (AFMO) method, where the collision wavefunction is expanded in a set of molecular orbitals (MOs), obtained at large ion-molecule separations.

As found in our previous calculations [3], we have checked that orientation-averaged cross sections can be well approximated by a single trajectory calculation, which is particularly useful to avoid lengthy calculations in numerical methods. We have also found that all methods lead to similar opacity functions for the electron removal from the valence MOs of the water molecule. We find good agreement between the electron-loss and electron-production total cross sections calculated with the three methods. We have shown the importance of many-electron removal in order to qualitatively reproduce the experiment of Ref. [4] for C^{3+} + H_2O collisions.

The GridTDSE method allows to follow the collision mechanism by inspecting the electron density along the collision. This is illustrated in Figure 1, where we plot a cut of the electron density captured by the ion in a Li^{3+} + H_2O collision with the electron initially in the $1b_1$ MO. In the illustration the Li^{3+} nucleus is fixed on the origin and the H_2O molecule follows a rectilinear trajectory with velocity v = 1.8 a.u. (81 keV/u), $\boldsymbol{v} \parallel \hat{Y}$, and impact parameter b = 2.0 bohr, $\boldsymbol{b} \parallel \hat{X}$. One can note that the wave packet formed in the collision rotates anticlockwise as a consequence of the transfer of angular momentum in the electron capture. The rotation of the wave packet is due to the interferences between the exit wave functions of different energy levels, and, therefore, it disappears at low velocities as only one level is significantly populated.

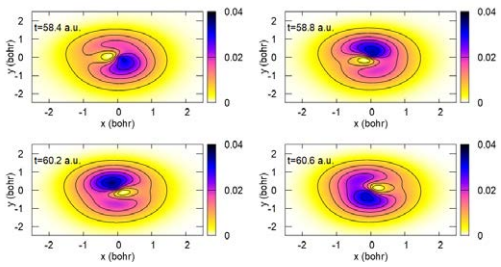

Figure 1. Contour plots of $|\Psi|^2$ on the collision plane at four time values t = 58.4, 58.8, 60.2 and 60.6 a.u., for electron capture in Li^{3+} + H_2O collisions (see text for details).

References

[1] Illescas C *et al* 2020 *Phys. Chem. Chem. Phys.* **22** 19573
[2] Suarez J *et al* 2009 *Comput. Phys. Commun.* **180** 2025
[3] Illescas C *et al* 2011 *Phys. Rev. A* **83** 052704
[4] Luna H and Montenegro E C 2005 *Phys. Rev. Lett* **94** 043201

*E-mail: l.mendez@uam.es

High-Fluence S^+ Implantation in Simple Oxide Astrophysical Ice Analogues

D V Mifsud[1,2 *], Z Kaňuchová[3,4], P Herczku[2], Z Juhász[2], S T S Kovács[2], B Sulik[2], P A Hailey[1], A Traspas Muiña[5], S Ioppolo[5], R W McCullough[6], and N J Mason[1]

[1]Centre for Astrophysics & Planetary Science, University of Kent, Canterbury, CT2 7NH, UK
[2]Institute for Nuclear Research (Atomki), Debrecen, H-4026, Hungary
[3]Astronomical Institute, Slovak Academy of Sciences, Tatranska Lomnicá, SK-059 60, Slovakia
[4]INAF Osservatorio Astornomico di Roma, Monte Porzio Catone, RM-00078, Italy
[5]School of Electronic Engineering & Computer Science, Queen Mary University of London, London, E1 4NS, UK
[6]School of Mathematics & Physics, Queen's University Belfast, Belfast BT7 1NN, UK

Synopsis The implantation of reactive charged species within low-temperature solids is relevant to astrochemistry and may lead to physico-chemical changes within the solid, such as the formation of new molecules which incorporate the projectile. We have performed the high-fluence (>10^{16} ions cm^{-2}) implantation of S^+ into CO, CO_2 and H_2O ices at 20 and 70 K. Our results show that implantation into CO and CO_2 results in the formation of SO_2 at 20 K, although no evidence of SO_2 was observed at 70 K. Implantation into H_2O yields H_2SO_4 hydrates. These results are applicable to the Galilean moons of Jupiter.

Implantation of magnetospheric sulphur ions (S^+) into the icy surfaces of the Galilean moons of Jupiter is known to be a source of sulphur-containing molecules. Laboratory studies have confirmed that H_2SO_4 hydrates are efficiently formed via implantation into H_2O ice [1]. However, there has been some debate as to whether S^+ implantation into surface CO or CO_2 frosts may form SO_2.

Studies conducted at high-fluence using ices at 20 K have shown that SO_2 is a radiolysis product, and have suggested that S^+ implantation may yield the observed quantity of surface SO_2 in ~10^4 years [2]. This temperature is too low to be directly relevant to the surface of the Galilean moons, however, and the failure to detect SO_2 in studies using lower fluences has led to some uncertainty as to the provenance of the SO_2 observed at the surfaces of these moons [3].

To address this issue, we have systematically implanted energetic (290-400 keV) S^+ ions into pure CO, CO_2 and H_2O ices at 20 K, and into the latter two at 70 K. Ices were prepared and processed using the Ice Chamber for Astrophysics-Astrochemistry facility [4]. In order to maximise the formation of sulphur-bearing product molecules, we have made use of high projectile ion fluences throughout (>10^{16} ions cm^{-2}).

Our results have shown that, although SO_2 is among the radiolysis products arising as a result of S^+ implantation into CO and CO_2 ice at 20 K (Figure 1), no evidence for its formation could be detected after implantation into CO_2 at 70 K. These results imply that S^+ implantation into CO and CO_2 ices is likely not a dominant formation pathway for SO_2 at the surfaces of the Galilean moons, and that its formation depends on an endogenic sulphur source. S^+ implantation into H_2O ice at 20 and 70 K yielded H_2SO_4 hydrates, in line with previous investigations [1].

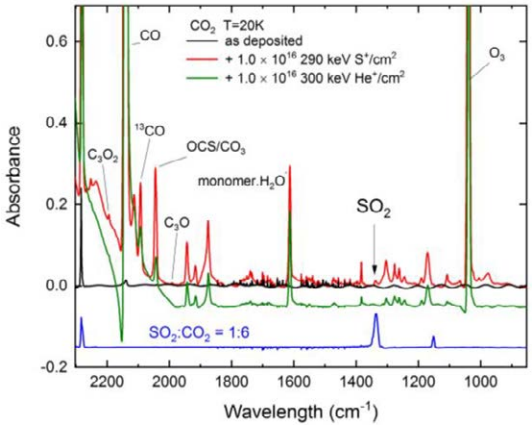

Figure 1. Mid-IR spectra for S^+ implantation into CO_2 ice at 20 K. He^+ implantation was performed as a control experiment. No SO_2 was detected when the experiment was repeated at 70 K.

References

[1] Ding J J *et al.* 2013 *Icarus* 226 860
[2] Lv X Y *et al.* 2014 *MNRAS* 438 922
[3] Boduch P *et al.* 2016 *Icarus* 277 424
[4] Herczku P *et al.* 2021 *Rev. Sci. Instrum.* submitted

* E-mail: duncanvmifsud@gmail.com

New Lifetime Limit of the Ground State Vinylidene Anion H_2CC^-

F Nuesslein[1]*, K Blaum[1], S George[2], J Göck[1], M Grieser[1], R von Hahn[1], Á Kálosi[3,1], H Kreckel[1], D Müll[1], O Novotný[1], H B Pedersen[4], V C Schmidt[1] and A Wolf[1]

[1]Max-Planck-Institut für Kernphysik, Heidelberg, 69117, Germany
[2]Institut für Physik, Universität Greifswald, Greifswald, 17487, Germany
[3]Columbia Astrophysics Laboratory, Columbia University, New York, 10027, USA
[4]Department of Physics and Astronomy, Aarhus University, Aarhus, 8000, Denmark

Synopsis From photodetachment measurements at the electrostatic Cryogenic Storage Ring (CSR) we report a ground-state vinylidene anion (H_2CC^-) lifetime on the order of several 10^3 s.

The C_2H_2 molecule with its two isomers acetylene (HCCH) and vinylidene (H_2CC) is one of the simplest systems for studying isomeric reactions involving hydrogen. In the past decades, their neutral, cationic and anionic species have been subject to theoretical and experimental investigations.

For the anion, the state with lowest total energy has the vinylidene structure, H_2CC^-, and a vertical electron affinity of about 0.5 eV. This state lies 1.5 eV above the lowest neutral level of the acetylene structure, opening up the principal possibility that isomerization linked with electron emission could intrinsically limit the lifetime of the vinylidene anion.

Indeed, an experiment at a room-temperature storage ring reported indications of a finite intrinsic lifetime of about 110 s [1]. This experiment compared the ion beam decays of H_2CC^- and a lighter reference ion for which an isomerization decay path cannot exist. Both beam lifetimes ($1/k \sim 10$ s) were limited by residual-gas collisions and the small difference of the decay rates was ascribed to the intrinsic H_2CC^- lifetime.

To re-address this issue, we employed the electrostatic Cryogenic Storage Ring (CSR) at the Max-Planck-Institut für Kernphysik in Heidelberg [2] for measuring the ground-state H_2CC^- lifetime.

CSR provides a cryogenic environment with strongly suppressed blackbody radiation and extremely low residual gas density, allowing to store and observe fast ion beams over time scales on the order of an hour. The measured rest-gas induced neutralization rates indicated that even these long lifetimes are not limited by residual gas collisions. Hence, the storage-ring induced loss rates should be largely independent of the ion beam composition in our experiment.

We used photodetachment to monitor the decays of simultaneously stored H_2CC^- and CN^- ion beams. Here, CN^- served as a stable reference ion with nearly identical mass-to-charge ratio. Comparing the two decays at storage times up to 3000 s allowed us to cancel a large part of the storage-ring induced losses. Also, by using the novel isochronous mass spectrometry method [3], we were able to prove that no other contaminant ions could affect the observed lifetimes.

We present preliminary results which suggest that the intrinsic lifetime of the ground-state of H_2CC^- is at least 3500 s, i.e., more than an order of magnitude longer than assumed previously.

References

[1] Jensen M *et al* 2000 *Phys. Rev. Lett.* **84** 1128
[2] von Hahn R *et al* 2016 *Rev. Sci. Instrum.* **87** 063115
[3] Grieser M *et al* (in preparation)

*E-mail: felix.nuesslein@mpi-hd.mpg.de

Engineering intermolecular interactions with light to prevent destructive ultracold collisions

A Orbán[1], T Xie[2], M Lepers[3], R Vexiau[2], O Dulieu[2] and N Bouloufa-Maafa[2]

[1]Institute for Nuclear Research (ATOMKI), Debrecen, Pf. 51, 4001, Hungary
[2]Laboratoire Aimè Cotton, Universitè Paris-Saclay, CNRS, Orsay, 91405 , France
[3]Laboratoire Interdisciplinaire Carnot de Bourgogne, CNRS, Universitè de Bourgogne Franche-Comtè, Dijon, 21078 , France

Synopsis An optical shielding mechanism is proposed to suppress destructive chemical reactions between ultracold ground-state NaRb molecules. The proposed shielding scheme leads to dramatic suppression of inelastic collisions which opens the possibility for strong increase of trapping time and efficient evaporative cooling.

Ultracold polar quantum gases are promising systems with possible applications in quantum simulation or quantum computation. Due to their large permanent electric dipole moment polar molecules in electric field exhibit strong long-range anisotropic dipole-dipole interactions (DDIs). The creation and trapping of ultracold dipolar diatomic molecules of various species are feasible in many experimental groups nowadays. However long time trapping is still a challenge even in the case of the so called nonreactive molecules [1]. Various hypothesis have been invoked to explain the possible mechanisms for the loss, however the check of their pertinence is not trivial since the final products can not be easily detected [2]. To overcome the loss, we propose to suppress inelastic collisions using optical shielding (OS). OS relies on the modification of long-range interactions between ground-state and excited molecules by laser light. The first experimental proof of the OS process was demonstrated in case of the collision between identical ultracold alkali-metal atoms [3].

One of the polar bialkali molecule for which unexpected losses were reported experimentally is the bosonic ^{23}Na^{87}Rb molecule [2], [4]. We will present our theoretical results on the OS of ultracold collision between two bosonic ^{23}Na^{87}Rb molecule in their lowest rovibrational level of the ground electronic state.

By applying a laser with a frequency blue-detuned from the transition between the lowest rovibrational level of the electronic ground state $X^1\Sigma^+(v_X = 0, j_X = 0)$, and the long-lived excited level $b^3\Pi_0(v_b = 0, j_b = 1)$, the long-range DDI between the colliding molecules can be engineered. We have used a quantum close coupling method in the dressed-state framework to describe the two-body collision between ground-state ^{23}Na^{87}Rb molecules in the presence of the OS field . The long range potential energy curves (PEC) between the two ground state molecule and between one ground state molecule and one excited molecule have been determined using a long-large multipolar expression [5]. Among a bunch of PECs, those with long-range repulsive behaviour were identified as they are the best candidates for an efficient OS.

We have carefully analysed the ratio between the elastic and destructive (reactive and photoinduced inelastic) collisional rate ratio as a function of Rabi frequency and detuning to map the conditions for maximizing this ratio, which leads to efficient OS. Our calculations show that the proposed OS leads to a dramatic suppression of reactive and photoinduced inelastic collisions, for both linear and circular laser polarizations. We demonstrate that the spontaneous emission from $b^3\Pi_0(v_b = 0, j_b = 1)$ does not deteriorate the shielding process. This opens the possibility for a strong increase of the lifetime of ultracoldcold molecule traps and for an efficient evaporative cooling. We also predict that OS is can also be an effective mechanism for other heteronuclear alkali-metal diatoms with sufficiently large permanent dipole moment [6].

References

[1] Żuchowski P S *et al* 2010 *Phys. Rev. A* **81** 060703(R)
[2] Guo M *et al* 2016 *Phys. Rev. Lett.* **116** 205303
[3] Weiner J *et al* 1999 *Rev. Mod. Phys.* **71** 1
[4] Ye X *et al* 2018 *Sci. Adv.* **4** eaaq0083
[5] Vexiau R *et al* 2015 *J. Chem. Phys.* **142** 214303
[6] Xie T *et al* 2020 *Phys. Rev. Lett.* **125** 153202

Neutralization of fullerene- and PAH-cations in collisions with atomic anions

R Paul[1*], M Gatchell[1], M C Ji[1], S. Rosén[1], Å Larson[1], H Cederquist[1], H T Schmidt[1] and H Zettergren[1]

[1]Department of Physics, Stockholm University, SE-114 21, Stockholm, Sweden

Synopsis We have performed pilot studies of charge transfer processes in sub 100 meV collisions - involving large molecular cations and atomic anions at the cryogenic double electrostatic storage ring facility DESIREE. Here we report the measured excitation energy distributions of C_{60} and pyrene ($C_{16}H_{10}$) and compare the results with Landau-Zener model calculations of the branching ratios for the electronic states populated in such collisions.

C_{60}^+ has been identified as carrier of a handful of diffuse interstellar bands [1,2] and Polycyclic Aromatic Hydrocarbons (PAHs) are believed to be omnipresent in space in ionic as well as neutral forms [3]. The neutralization of fullerene and PAH-cations in low energy collisions with atomic or molecular anions may thus be important for the charge balance in e.g. the interstellar medium. The DESIREE facility [4] is designed for studying such reactions.

We have recently studied sub 100 meV $C_{60}^+ + Au^- \rightarrow C_{60}^* + Au$ and $C_{16}H_{10}^+ + Si^- \rightarrow Si + C_{16}H_{10}^*$ collisions in DESIREE. In these pilot studies the electron donors are chosen for experimental reasons to match the velocities of the two stored ion beams [4]. By analyzing the kinetic energy of the neutral products formed in the reactions, we determine the excitation energy (E_{exc}) distributions for the neutral fullerenes (C_{60}^*) and pyrene ($C_{16}H_{10}^*$) formed in the collision.

The results from the fullerene measurements are shown in Fig. 1 together with the Landau-Zener [5] calculations of the branching fractions for the electronic states being populated in the collisions. In these calculations, we use interaction potential from Ref 6, the coupling elements from Ref. 7, and the singlet state excitation energies from Ref. 8. In Fig. 1., the state with the largest calculated branching fraction (at 3.67 eV) was normalized with respect to the maximum value of the measured distribution and the calculated branching fractions for the other states were adjusted by the same factor. The Landau-Zener results agree reasonably well with the experiments as they fall within the measured distribution. We aim to perform electronic structure calculations of triplet states to investigate if they may also contribute to the measured distribution.

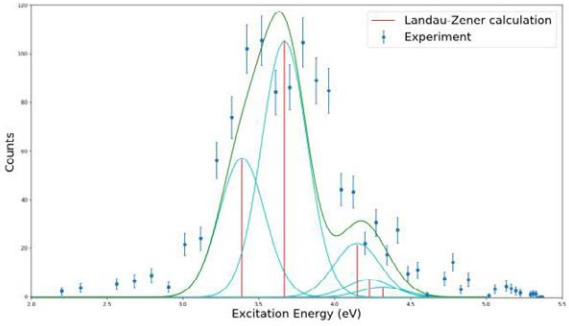

Figure 1. Excitation energy distribution for C_{60}^* in $C_{60}^+ + Au^- \rightarrow C_{60}^* + Au$ collisions. The vertical red lines are the results from Landau-Zener calculations (see text).

References

[1] E K Campbell, M Holz, D Gerlich and J P Maier, *Nature* 523, 322 (2015)
[2] M A Cordiner et al, *The Astrophysical Journal Letters* 875, L28 (2019)
[3] A G G M Tielens, *Rev Mod Phys*, 85, 1021 (2013)
[4] R D Thomas et al 2011 *J. Phys.: Conf. Ser.* 300 012011
[5] C Zener, Proc. *R. Soc. London Ser. A* 137 696 (1932)
[6] H Zettergren, *Phys. Chem. Chem. Phys.*, 14, 16360–16364 (2012)
[7] R E Olson, *J. Chem. Phys*. 56, 2979 (1972)
[8] R Fukuda and M Ehara, J. Chem. Phys. 137, 134304 (2012)

* E-mail: raka.paul@fysik.su.se

Single charge capture in collisions of protons with poliatomic molecules

I Rabadán*, **Clara Illescas, L Méndez**

Laboratorio Asociado al CIEMAT de Física Atómica y Molecular en Plasmas de Fusión. Departamento de Química, módulo 13, Universidad Autónoma de Madrid, 28049-Madrid, Spain.

Synopsis We present calculations of electron capture cross sections in collisions of H^+ with CO_2 and 2-aminooxazole for impact energies between 0.1 and 50 keV/u. Wave functions and non-adiabatic couplings are obtained using multi-reference configuration interaction methods.

Single electron capture (SEC) cross sections are valuable data to model the interaction of ions and molecules in a variety of areas, from the interaction of solar winds with planetary magnetospheres and ionospheres to the biological media in cancer hadron therapy. For collision energies below 10 keV/u, non-perturbative methods are necessary to describe the electronic degrees of freedom and, if there are more than two active/valence electrons in the system, one could take advantage of established quantum chemistry methods to obtain the necessary wave functions and non-adiabatic couplings. In this work, we test CASSCF and multi-reference configuration interaction methods to adress the study of SEC in collisions of protons with CO_2 and 2-aminooxazole molecules, which are of interest in planetary atmospheres and prebiotic environments. The anisotropy of the target molecules could be an issue in the non-perturbative regime and it is taken into account following the ion-trajectory integration of the time-dependent Schrödinger equation, as detailed in [1]. the Franck-Condon approximation is employed to freeze the internal nuclear degrees of freedom of the target during its interaction with the ion, and the use of multielectronic wave functions makes unnecessary to rely on independent electron approximations.

As an illustration, we show in Fig. 1 the SEC cross sections in collisions of H^+ with CO_2 compared with experimental data [2, 3, 4, 5]. The lines are obtained considering projectile trajectories parallel the CO_2 molecular axis. The calculation separates the contribution of the ground and first excited states of CO_2^+ to the total SEC cross section. Also included is the SEC cross section in collision of H^+ with 2-aminooxazole parallel to the molecular plane. For both systems, a π electron is captured by the proton, which results in very similar cross sections.

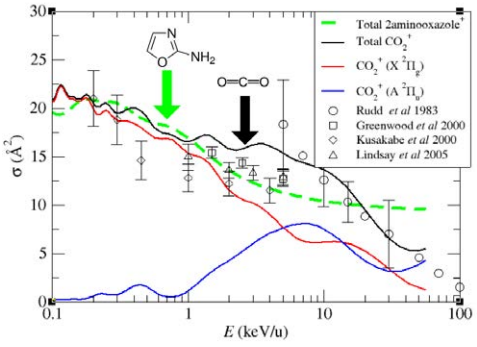

Figure 1. State-selected single electron capture cross sections in H^++CO_2 collisions. Lines, present calculations, symbols correspond to experimental measurements. Also included is the SEC cross section for H^++2-aminooxazole.

This work is partially supported by the project FIS2017-84684-R (Spanish Ministerio de Ciencia e innovación (Spain).

References

[1] Rabadán I and Méndez, L. 2017. *J. of Phys: Conf. Ser.*, **875** 012009
[2] Rudd M E *et al* 1983 *Phys Rev A* **28** 3244
[3] Greenwood J B *et al* 2000 *The Astrophysical Journal* **529** 605
[4] Kusakabe T *et al* 2000 *Phys Rev A* **62** 062714
[5] Lindsay B G *et al* 2005 *Phys Rev A* **71** 032705

*E-mail: ismanuel.rabadan@uam.es

Charge exchange interactions of 9 – 51 keV Sn^{3+} with H_2 molecules

S Rai [*1,2], K I Bijlsma[1,2], P A J Wolff[1], M Salverda[1], O O Versolato[2,3], R Hoekstra[1,2]

[1] Zernike Institute for Advanced Materials, University of Groningen, Groningen, 9747 AG, The Netherlands
[2]Advanced Research Center for Nanolithography, Amsterdam, 1098 XG, The Netherlands
[3]Department of Physics and Astronomy, and LaserLaB, Vrije Universiteit, Amsterdam, 1081 HV, The Netherlands

Synopsis Charge exchange interactions of 9 – 51 keV Sn^{3+} ions with H_2 molecules have been investigated experimentally and the total single electron capture cross-sections have been determined. The results are then compared with predictions of various standard theoretical models.

In modern state-of-the-art extreme ultraviolet (EUV) nanolithography tools, laser-produced tin plasma (LPP) is used to generate EUV light. Energetic highly-charged Sn ions, coming from the LPP with energies up to several tens of keV, may damage the EUV collector mirrors, if not mitigated. Therefore one uses H_2 buffer gas, to stop and mitigate these ions [1].

At the ZERNIKELEIF facility in Groningen, isotope, charge-state, and energy selected Sn^{q+} ions are generated using a 14 GHz Electron Cyclotron Resonance Ion Source (ECRIS) of supernanogan type. The ions are then transported to dedicated setups where their interactions with various types of targets are investigated. The experiments reported here have been carried out at the CHEOPS (CHarge Exchange Observed by Particle Spectroscopy) setup and the ion under study is Sn^{3+}.

In the experiments, a monoenergetic Sn^{3+} ion beam (9 - 51 keV) crosses a jet of neutral H_2 gas. A collision between the energetic Sn^{3+} ion and a H_2 molecule can result in the capture of one or two electrons from the H_2, thus leading to single or double electron capture respectively. Consequently, the charge state of the ion reduces, leading to a drop in ion beam current which is recorded using a Faraday cup (FC). At the same time, fragments of hydrogen (protons and H_2^+) are created that are then extracted and analysed using a Time-of-Flight (ToF) spectrometer.

From the FC data, "apparent" total single electron capture cross-sections for Sn^{3+} are determined. The "apparent" cross-sections are corrected for a small bound double capture contribution by measuring the relative strength of the bound double capture channel with respect to the single capture channel from the ToF spectrum (see figure 1). Double collision corrections at higher target densities are also taken into account.

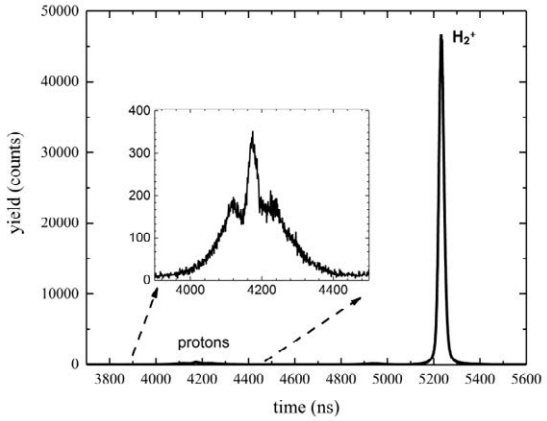

Figure 1. ToF spectrum of H_2 fragments created after collisions of 48 keV Sn^{3+} ions with H_2 molecules.

The corrected final cross-sections are compared with available theoretical predictions. There is good agreement with our Landau-Zener type calculations. Towards lower energies, the data show a clear increase in cross-section, a trend in line with the well-known v^{-1} Langevin behavior, with impact velocity v.

References

[1] Versolato O O 2019 *Plasma Sources Sci. Technol.* **28** 083001

* E-mail: s.rai@rug.nl

Ultra-fast dynamics in quantum systems revealed by particle motion as clock

M. S. Schöffler[1], L. Ph. H. Schmidt[1], S. Eckart[1], R. Dörner[1], A. Czasch[1,2], O. Jagutzki[1,2], T. Jahnke[3], J. Ullrich[4], R. Moshammer[5], R. Schuch[6] and H. Schmidt-Böcking[1,2] *

[1] Institut für Kernphysik, Universität Frankfurt, Max-von-Laue-Str. 1, 60438 Frankfurt, Germany
[2] Roentdek GmbH, 65779 Kelkheim, Germany
[3] European XFEL, Holzkoppel 4, 22869 Schenefeld, Germany
[4] PTB, Braunschweig, Germany
[5] MPI für Kernphysik, Heidelberg, Germany
[6] Physics Department, Stockholm University, Alba Nova, 107 67 Stockholm, Sweden

Synopsis We report on the possibilities of using ion-atom collision experiments to explore dynamics on ultrafast time scales.

To explore ultra-fast dynamics in quantum systems one needs detection schemes which allow time measurements in the attosecond regime. During the recent decades, the pump/probe two-pulse laser technique has provided milestone results on ultra-fast dynamics with femto- and attosecond time resolution. Today this technique is applied in many laboratories around the globe, since complete pump/probe systems are commercially available. It is, however, less known or even forgotten that ultra-fast dynamics has been investigated several decades earlier even with zeptosecond resolution in ion-atom collision processes. A few of such historic experiments, are presented here, where the particle motion (due to its very fast velocity) was used as chronometer to determine ultra-short time delays in quantum reaction processes.

In order to reveal the "entangled" electron dynamics inside the same molecule, it is typically not sufficient to perform single parameter measurements on the same molecular object at two shortly successive instants in time. To reveal entangled dynamics, the simultaneous detection of the momenta of all fragments emitted from the same single molecule is required. Thus, a multi-fragment coincidence measurement imaging the complete momentum space with high resolution is necessary. Such high-resolution multi-coincidence detection systems are available since about two decades: The COLTRIMS-reaction microscope (C-REMI) possesses all necessary properties to perform such high-resolution multi-coincidence investigations.

Finally, an outlook is given when in near future relativistic heavy ion beams are available which allow a novel kind of "pump/probe" experiments on molecular systems with a few zeptosecond resolution. However, such experiments are only feasible if the complete many-particle fragmentation process can be imaged with high momentum resolution by state-of-the-art multi-particle coincidence technique.

*E-mail: schmidtb@atom.uni-frankfurt.de

Fragmentation dynamics of CO_2^{4+} : Contributions of different electronic states

S Srivastav[1*], A Sen[1], D Sharma[1] and B Bapat[1]

[1]Indian Institute of Science Education and Research Pune, Homi Bhabha Road, Pune 411008, India

Synopsis Fragmentation dynamics of CO_2^{4+} , created by the impact of slow, highly charged ions (96 keV Ar^{q+}; $8 \le q \le 14$) on CO_2 , has been studied by recoil ion momentum spectrometry. Kinetic energy release distributions of both three-body dissociation channels of CO_2^{4+} were derived. *Ab initio* quantum chemical calculations were carried out to obtain the potential energy curves of CO_2^{4+}. The relative probability of accessing different electronic states of CO_2^{4+} was estimated. These probabilities were found to depend on the projectile charge q.

In ion-molecule collision, the charge of the projectile ion is an important parameter that decides the strength of the perturbation, and hence experiments on the creation and fragmentation of molecular ions under a range of projectile charges open up the possibility of preferentially populating different excited states. In the slow collisions with highly charged ion (HCI), various electronic states of target molecule may get populated by different ionization mechanisms such as direct ionization or, more probably, by electron capture from the target molecule. These different ionization mechanisms causing excitation into various electronic states may result the differences in the fragmentation dynamics.

We have investigated both dissociation channels $O^+ + C^{2+} + O^+$ (121) and $O^{2+} + C^+ + O^+$ (211) of CO_2^{4+} created by impact of slow HCIs (Ar^{q+}; $8 \le q \le 14$) at 96 keV on CO_2 [1]. Ar-ion beam is obtained from electron beam ion source (EBIS) installed at IISER Pune, India [2]. We observe total KER distributions of both fragmentation channels. *Ab initio* quantum chemical calculations at the multi-configuration self-consistent-field configuration-interaction level of theory are carried out to obtain the potential energy curves of CO_2^{4+} from which the expected KER values are derived. With the help of computed potential energy curves and fitting of experimental KER distributions to sum of multiple Gaussian distributions, relative probabilities of accessing different electronic states of CO_2^{4+} has been estimated. These relative probabilities are found to depend on the projectile charge q and in which Ar^{10+} and Ar^{12+} are showing more stark differences in both dissociation channels. Ar^{10+} is populating higher lying electronic states and Ar^{12+} is populating rather low lying states of CO_2^{4+}. With the help of Dalitz plot analysis, it is also found that for (211) channel, the contribution of sequential process to total events is higher around 6% for Ar^{12+} and lesser around 3% for Ar^{10+} ion.

These results reveal that low energy HCIs are suitable candidates to influence the fragmentation dynamics of polyatomic molecular ions and preponderance of certain ionization mechanisms for certain projectile could be the primary reason which alter the probabilities of accessing different electronic states and thereby affect the fragmentation dynamics.

Presently, we are installing the 'post collision charge state analyzer' to separate involved ionization mechanisms and get more insight into the fragmentation dynamics. We expect to present some more detail results at the conference.

References

[1] Srivastav S *et al* 2021 *Phys. Rev. A* 103, 032821
[2] Bapat B *et al* 2020 *J. Phys.: Conf. Ser.* 1412 152070

* E-mail: sumit.srivastav@students.iiserpune.ac.in

Accurate theoretical studies from first principles of HD-He collisional system in molecular spectra

K. Stankiewicz[1]* **H. Jóźwiak**[1] **M. Gancewski**[1] **N. Stolarczyk**[1] **F. Thibault**[2] **P. Wcisło**[1]

[1]Institute of Physics, Faculty of Physics, Astronomy and Informatics, Nicolaus Copernicus University, Grudziadzka 5, Toruń, 87-100, Poland

[2]Univ Rennes, CNRS, IPR (Institut de Physique de Rennes)-UMR 6251, F-35000 Rennes, France

Synopsis We report results of quantum scattering *ab initio* calculations of the impact of collisional effects on HD molecule spectrum in HD-He collisional system. The present study contains a great number of transitions and will contribute to creating a highly accurate collisional line-shape parameters database for all hydrogen isotopologues relevant from the perspective of hydrogen-helium interactions in planetary atmospheres.

The abundance of molecular hydrogen and atomic helium in the universe makes them an important system to study in various fields. A mixture of molecular hydrogen and helium is the main component of the atmospheres of gas giants in the Solar System and is predicted to be a dominant constituent of the atmospheres of some types of exoplanets [1]. The hydrogen molecule is also the simplest molecule, the structure of which can be calculated from first principles, which makes it well suited for accurate tests of *ab initio* calculations. In particular HD molecule, despite its lower abundance than H_2 isotopologue is noticeable in spectroscopic studies due to the presence of its dipole moment even in the electronic ground state. Studies show [2] that in some cases the uncertainty of astronomical observations of hydrogen molecule spectra is dominated by the uncertainties of collisional parameters, including pressure broadening and pressure shift coefficients. An accurate list of the line–shape parameters is necessary for a correct interpretation of molecular spectra from the atmospheres of gas giants [2] and exoplanets [3]. Moreover, studies of the H_2–rich atmospheres are well suited for measuring the D/H ratio, which is crucial for understanding the evolution of the Universe and planets' atmospheres [4, 5].

We present the methodology and results of *ab initio* calculations of collisional effects for 12 purely rotational and 60 rovibrational electric dipole transitions in R and P branches: from R(0) to R(5) and from P(1) to P(6) in the 0–0 to 5–0 vibrational bands. We used state-of-the-art potential energy surface [6] - an improved version of the one reported by Bakr, Smith, and Patkowski [7]. We also carefully examined the validity of the usually assumed approximation for rovibrational transitions - centrifugal distortion neglection - in the case of the HD-He system. Available experimental studies [8][9] are in good agreement with our calculations for most transitions, however, some of the results are beyond the estimated uncertainty. The experimental values for rovibrational lines only consist of $R_1(0)$ and $R_1(1)$ transitions at 77 K. This, together with the fact that the measurements were using less accurate line-shape models, and current experimental techniques are more accurate, show that there is a strong need for new accurate experimental studies of collisional line-shape parameters.

References

[1] Miller-Ricci E *et al* 2009 *J. Phys.: ApJ* **690 1056**
[2] Feuchtgruber *et al* 2013 *Astron. Astrophys* **551 A126**
[3] Fortney J *et al* 2019 *arXiv* **1905.07064**
[4] Smith W *et al* 1989 *ICARUS* **81 429**
[5] Fortney J *et al* 1995 *ICARUS* **114 328**
[6] Thibault F *et al* 2017 *J Quant Spectrosc Radiat Transf* **202 308**
[7] Bakr B *et al* 2013 *J Chem Phys* **139 144305**
[8] Lu Z, *et al* 1993 *Phys. Rev. A* **47, 1159**
[9] McKellar A, *et al* 1984 *Can J Phys* **62, 211**

*E-mail: 305679@stud.umk.pl

The first comprehensive data set of beyond-Voigt line-shape parameters for the H_2-He system for the HITRAN database

P Wcisło[1], F Thibault[2], N Stolarczyk[1]*, H Jóźwiak[1], M Słowiński[1], M Gancewski[1], K Stankiewicz[1], M Konefał[1], S Kassi[3], A Campargue[3], Y Tan[4], J Wang[4], K Patkowski[5], R Ciuryło[1], D Lisak[1], R Kochanov[6], L S Rothman[6] and I E Gordon[6]

[1]Institute of Physics, Faculty of Physics, Astronomy and Informatics, Nicolaus Copernicus University in Toruń, Grudziadzka 5, 87-100 Toruń, Poland
[2]Univ. Rennes, CNRS, IPR (Institut de Physique de Rennes)-UMR 6251, Rennes F-35000, France
[3]University of Grenoble Alpes, CNRS, LIPhy F-38000 Grenoble, France
[4]Hefei National Laboratory for Physical Sciences at Microscale, iChEM, University of Science and Technology of China, 230026 Hefei, China
[5]Department of Chemistry and Biochemistry, Auburn University, Auburn, Alabama 36849, USA
[6]Harvard-Smithsonian Center for Astrophysics, Atomic and Molecular Physcis Division, Cambridge, Massachusetts, USA

Synopsis We present the methodology of populating spectroscopic line-by-line databases with fully *ab initio* line-shape parameters. We are able to provide beyond-Voigt collisional parameters for numerous bands, branches and temperature ranges. We also present the first such data set of the 3480 transitions of H_2 perturbed by He.

Molecular collisions are manifested as a perturbation of the shapes of molecular optical resonances. Therefore, on the one hand, the line-shape analysis of accurate molecular spectra constitutes an important tool for studying quantum scattering and testing *ab initio* molecular interaction [1]. On the other hand, the collisional effects can deteriorate the accuracy of atmospheric measurements of the Earth and other planets, modify the opacity of the exoplanetary atmospheres as well as influence the accuracy in optical metrology based on molecular spectroscopy [2, 3]. Development of molecular-spectroscopy-based tools requires an accurate and accessible reference such as data sets of accurate beyond-Voigt spectral line-shape parameters.

We demonstrate a new method for populating line-by-line spectroscopic databases with beyond-Voigt line-shape parameters based on *ab initio* quantum scattering calculations [4]. We report a comprehensive data set for the benchmark system of He-perturbed H_2 (we cover all the rovibrational bands that are present in the HITRAN spectroscopic database [5]). We generate the entire data set of the line-shape parameters i.e., broadening and shift, their speed dependence, and the complex Dicke parameter. The results are projected on a simple structure of the quadratic speed-dependent hard-collision profile [6, 7]. We report a simple and compact formula that allows the speed-dependence parameters to be calculated directly from the generalized spectroscopic cross sections. For each line and each line-shape parameter, we provide a full temperature dependence within the double-power-law (DPL) representation, which makes the data set compatible with the HITRAN database [8]. The temperature dependences cover the range from 20 to 1000 K, which includes the low temperatures relevant for the studies of the atmospheres of giant planets. The final outcome from our data set is validated on highly-accurate cavity ring-down experimental spectra . The methodology can be applied to many other molecular species important for atmospheric and planetary studies.

*E-mail: nikodemstolarczyk319@gmail.com

References

[1] Wcisło P *et al* 2015 *Phys. Rev. A* **91** 052505
[2] Moretti L *et al* 2013 *Phys. Rev. Lett.* **111** 060803
[3] Wcisło P *et al* 2016 *Phys. Rev. A* **93** 022501
[4] Demeio D *et al* 1995 *J. Chem. Phys.* **102** 9160
[5] Gordon I E *et al* 2017 *J. Quant Spectrosc. Radiat. Transfer* **203** 3
[6] Pine A S N *et al* 1999 *J. Quant Spectrosc. Radiat. Transfer* **64** 397
[7] Ngo N *et al* 2013 *J. Quant Spectrosc. Radiat. Transfer* **129** 89
[8] Stolarczyk N *et al* 2020 *J. Quant Spectrosc. Radiat. Transfer* **240** 106676

CO-Ar collisions: sub-percent agreement between *ab initio* model and experimental spectra at pressures varying within four order of magnitude

E A Serov,[1] N Stolarczyk,[2]* D S Makarov,[1] I N Vilkov,[1] G Yu Golubiatnikov,[1] A A Balashov,[1] M A Koshelev,[1] P Wcisło,[2] F Thibault,[3] and M Yu Tretyakov[1]

[1]Institute of Applied Physics, Russian Academy of Sciences, 46 Ulyanov str., Nizhny Novgorod, 603950, Russia
[2]Institute of Physics, Faculty of Physics, Astronomy and Informatics, Nicolaus Copernicus University in Toruń, Grudziadzka 5, 87-100 Toruń, Poland
[3]Univ. Rennes, CNRS, IPR (Institut de Physique de Rennes)-UMR 6251, Rennes F-35000, France

Synopsis We report a broad-pressure-range spectroscopic study of the CO-Ar collisional system. We present the results of our *ab initio* quantum scattering calculations and experimental data collected with three independent techniques. We achieve sub-percent agreement between theory and experimental data, which confirms the validity of our *ab initio* calculations at pressures spanning four orders of magnitude.

CO-Ar molecular system is a prototype of atmospherically relevant cases. It is, on the one hand, affordable for calculation of the line shape parameters by modern *ab initio* methods [1, 2], and, on the other hand, is very convenient for experimental studies because of its regular, well spaced rotational spectrum having a moderate intensity [3]. The shapes of molecular optical resonances are strongly dependent on pressure. To test that our quantum-scattering calculations are valid in a broad pressure range, we performed our spectroscopic study of the CO-Ar collisional system at pressures spanning four orders of magnitude.

Three independent spectroscopic techniques [5, 6, 7] were used to record the spectral line shape of the first rotational overtone of the CO molecule preturbed by Ar. Simultaneously we performed fully *ab initio* quantum scattering calculations on two recent potential energy surfaces [3, 4]. We employed the sophisticated spectral line-shape model to simulate the shapes of the molecular optical resonance.

We show that the simulated collision-perturbed spectra, which are based on our fully *ab initio* calculations, agree with the experimental line profiles at sub-percent level over a wide range (more than four orders of magnitude) of pressures.We demonstrate that the agreement between theory and experiment can be further improved if the model accounts for the collisional transfer of an optical coherence between different rotational transitions (the line-mixing effect). We show that the two surfaces tested in this work lead to a very similar agreement with the experiment. Capability of calculating line shape parameters in a broad range of temperatures is therefore demonstrated.

Experiment was supported in parts by the Russian State project (0030-2021-0016) and Russian Science Foundation (17-19-01602). P.W. was supported by National Science Centre, Poland, Project No. 2018/31/B/ST2/00720. N.S. was supported by National Science Centre, Poland, Project No. 2019/35/B/ST2/01118. The project was cofinanced by the Polish National Agency for Academic Exchange under the PHC Polonium program (dec. PPN/X/PS/318/2018).

References

[1] Kowzan G *et al* 2020 *J. Quant Spectrosc. Radiat. Transfer* **243** 106803
[2] Stolarczyk N *et al* 2020 *J. Quant Spectrosc. Radiat. Transfer* **240** 106676
[3] Kowzan G *et al* 2020 *Phys. Rev. A* **102** 012821
[4] Sumiyoshi Y *et al* 2015 *J. Chem. Phys.* **142** 024314
[5] Golubiatnikov G *et al* 2014 *Radiophys. Quantum El.* **56** 599
[6] Tretyakov M Yu *et al* 2008 *Instrum. Exp. Tech.* **51** 78
[7] Koshelev M A *et al* 2018 *IEEE Trans. Terahertz Sci. Technol.* **8** 773

*E-mail: nikodemstolarczyk319@gmail.com

Fragmentation of tyrosine under low-energy electron impact

J Tamuliene[1] *, L Romanova[2], V Vukstich[2], and A Snegursky[2†]

[1]Vilnius University, Institute of Theoretical Physics and Astronomy, 3 Sauletekio av., 10257 Vilnius, Lithuania
[2]Institute of Electron Physics, Ukr. Nat. Acad. Sci., 21 Universitetska str., 88017 Uzhgorod, Ukraine

Synopsis Here we present the study of tyrosine fragmentation under low electron impact. Results obtained allow us to explain some specific features of the mass spectrum of this amino acid that is quite different from that of other amino acids.

Tyrosine is one of the 20 standard amino acids used by cells to synthesize proteins. Proteins containing tyrosine can be converted into various degradation products via several distinct mechanisms including low-energy electron impact [1]. Degradation products can change the physical-chemical properties of proteins [2, 3] and, as consequence, cause several diseases. Regulation of cellular functions in many diseases, including cancer, could be disturbed due to the degradation of tyrosine. The potential role of this amino acid damage as a causative factor in human disease remains largely unknown. Currently, experimental studies exhibited a role of low-energy electrons in radiation-induced damage to biologically relevant molecules [4]. Hence, the data on the cleavage of tyrosine is urgent to determine protein and peptide chemical composition and their sequence. We have performed the study of tyrosine fragmentation aiming to shed some light on the behavior of this amino acid under low-energy electron impact. The chemical composition of the cations formed and the way of their formation are suggested. The specificity of the measured mass spectrum of this amino acid is explained, too. The experimental research is accompanied by a theoretical study.

We obtained the ionization energy of the parent molecule and compared it with the appearance energies of the fragments produced under low electron impact. The results indicate that the appearance energies of the vast majority of cations are much higher than the ionization energy of tyrosine. The exception are the m/z = 164, 107, 92, 28 fragments, for which the appearance energies are less than ~2 eV higher than the ionization potential. The m/z = 164 and 28 fragments are complementary ones, i.e. they could be formed via the same channels. As consequence, the intensities of both above peaks are low. Formation of the m/z = 92 fragment is rather complicated because it requires decomposition of both C-C and OH bonds. On the other hand, the appearance energy of this fragment is similar to the ionization potential of the tyrosine molecule. This indicates that decomposition of this amino acid could start during ionization. However, theoretical investigation did not prove decomposition of the ionized tyrosine. It means that the appearance energy for the m/z = 92 fragment could indeed be lower than the ionization potential (activation energy), thus, it could not be observed experimentally. Hence, the most probable tyrosine fragmentation pathway suggested is as follows:

$$C_9H_{11}NO_3 + e \rightarrow C_7H_7O^+ + C_2H_4NO_2^- + e$$

The statement is based on one of the lowest appearance energies for this fragment and the absence of competing fragmentation pathways.

Present study was supported in part by the Ukrainian National Research Fund (Grant No. 2020.01/0009 "Influence of ionizing radiation on the structure of amino acid molecules").

References

[1] Huan Kang H *et al*. 2019 *Mol. Pharmaceutics* 16, 258−272
[2] Hermeling S *et al.* 2006 *J. Pharm. Sci*. 95 (5),1084−96
[3] Cockrell G Met al 2015 *Mol. Pharmaceutics* 12 (6),1784−97
[4] Boudaïffa B P. *et al* 2000 *Science* 287 (2000), 1658-1660

* E-mail: Jelena.Tamuliene@tfai.vu.lt
† E-mail: snegursky.alex@gmail.com

Marks of charge transfer and complexes formation processes revealed in cation-induced fragmentation spectra of pyridine

T. J. Wasowicz[1*]

[1]Division of Complex Systems Spectroscopy, Gdansk University of Technology, 80-233 Gdańsk, Poland

Synopsis Charge transfer and formation of the collisional complexes have been investigated experimentally in M^+ + pyridine (M = H, H_2, He) collisions. The fragmentation spectra of pyridine (C_5H_5N) have been measured using collision-induced emission spectroscopy (CIES). Production of helium atoms in the excited 1s4p $^3P^0$, 1s4d $^1D_2$, $^3D_{1,2,3}$ states directly shows charge transfer from pyridine to He^+ cations. The relative cross-sections of dissociation products have prominent resonance-like maxima suggesting the formation of the $[M{-}C_5H_5N]^+$ transient complexes before fragmentation.

Molecular fragmentation can be initiated by electromagnetic waves or a beam of particles. In contrast to the fragmentation induced by collisions with photons and electrons, the charged particles' impact leads to the electrostatic interactions between reacting species preceding decomposition. Therefore, two processes may occur, namely the charge transfer and the transient complexes formation. These reactions take part in various chemical and biological phenomena, for example, oxygenic photosynthesis or cellular respiration.

The present work focuses on deciphering these collisional processes leading to the fragmentation of pyridine molecules under the H^+/H_2^+/He^+ cations impact in the velocity range ~20–450 km/s. Pyridine is a heteroaromatic building block of vitamins, pharmaceuticals, and agrochemicals. The experiments were performed at the University of Gdansk using a spectrometer for the CIES [1], [2].

These mechanisms were identified by analyzing the optical fragmentation spectra (see examples in Figures 1a and b). Among the recognized emitters, the luminescence of helium atoms excited to the higher-lying states was recorded (Fig. 1b). The helium atom is not built into the pyridine structure. Therefore, observation of its emission lines confirms a collisional reaction where the electronic charge is transferred between interacting objects. The marks of this reaction are also seen in collisions with hydrogen ions, where increased production of excited hydrogen atoms over other fragments occurs (Fig. 1a). The recorded spectra show considerable variations of intensities with the velocity change. In particular, at the lowest velocities, the relative cross-sections reveal prominent resonance-like maxima (see Fig. 1c), which result from the formation of the $[M{-}C_5H_5N]^+$ transient complexes before fragmentation [3].

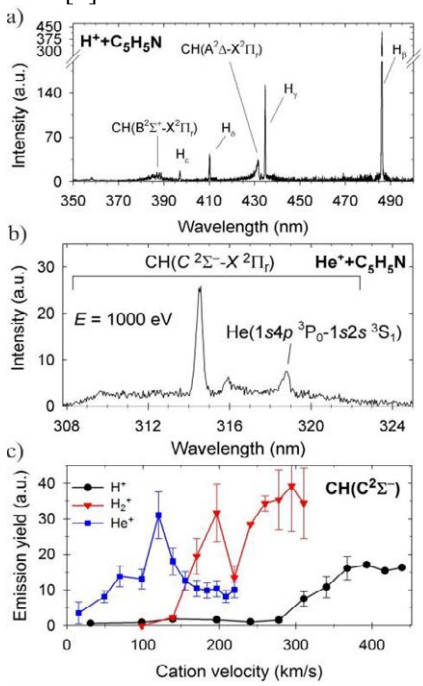

Figure 1. Luminescence spectra measured for collisions of pyridine with (a) H^+ (b) He^+ c) Emission yields of the excited $CH(C^2\Sigma^-)$ fragments.

References

[1] Wasowicz TJ *et al* 2015 *J. Phys. Chem. A* 119 581
[2] Wasowicz TJ 2020 *Res. Phys.* **18** 103244
[3] Wasowicz TJ *et al* 2019 *Int. J. Mol. Sci.* **20** 6022

* E-mail: tomasz.wasowicz1@pg.edu.pl

Delayed fragmentation of propyne and allene in collisions with highly charged ions

H. Yuan[1,2], S. Xu[1,3]*, D. B. Qian[1,3], T. T. Li[2], Y. Liu[2], D. L. Guo[1,3], X. L. Zhu[1,3], and X. Ma[1,3]†,

[1]Institute of Modern Physics, Chinese Academy of Sciences, Lanzhou 730070, China
[2]School of Physics, Xi'an Jiaotong University, Xi'an 710049, China
[3]School of Nuclear Science and Technology, University of Chinese Academy of Sciences, Beijing 100049, China

Synopsis Delayed deprotonation dissociation of dications of two C_3H_4 isomers, propyne and allene, induced by 50 keV/u Ne^{8+} ions is investigated employing the reaction microscope technique. The survival time of the precursor ${C_3H_4}^{2+}$ is retrieved according to the time-of-flight difference between the two ionic fragments. It was found that the initial structure of the isomer does not play a key role in the delayed fragmentation process and the delayed fragmentation of both isomers can be well described by the power-law decay.

Delayed deprotonation dissociation of C_3H_4 isomers, propyne and allene, induced by 50 keV/u Ne^{8+} are investigated employing the reaction microscope at the 320-kV platform [1]. As shown in Fig. 1, the long tail structure in the time-of-flight (TOF) coincidence spectrum is a typical feature of the delayed dissociation with different survival times of the metastable di-cations. The survival times of ${C_3H_4}^{2+}$ are retrieved by utilizing the TOF difference between the two ionic fragments, as shown in Fig. 1(b).

The exponential fitting and power-law fitting of the survival time distributions are presented in Figs. 1c-f accompanying with the experimental data. Obvious discrepancy is observed between the exponential fitting and experiment results for both CH_3CCH and CH_2CCH_2. Such discrepancy is mainly attributed to the fact that the exponential fitting is suitable for the contribution of only one state with a definite lifetime in the delayed dissociation process, while in the present molecular system a series of vibrational states with different modes can be populated on different electronic states. Thus, the power-law fitting reaches much better agreement with the experiment.

The two isomers exhibit the very similar survival time distributions and almost the same fitting parameters, indicating that the initial structure of the isomer does not play an important role in the delayed deprotonation dissociation process. The present work indicates that the power-law fitting is not only applicable to larger ensembles, but is probably a general behavior of the delayed deprotonation dissociation of dications of hydrocarbon molecules with the size bigger than C_3H_4 [1] and C_2H_4 [2] .

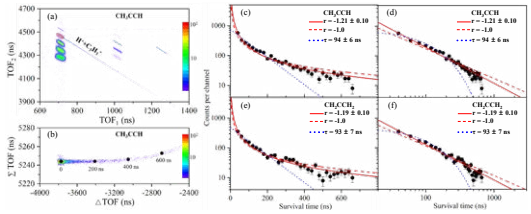

Figure 1. (a) TOF coincidence spectrum for CH_3CCH. (b) Correlation plot as a function of ΔTOF and ΣTOF for CH_3CCH. Black dots display selected samples of the time delay between ionization and fragmentation retrieved from ΔTOF. (c)-(f) ${C_3H_4}^{2+}$ survival time distributions against the deprotonation dissociation channel. The blue dot curves present the fits by exponential function. The red solid curves present the fits by function of power-law decay, whereas the red dashed curves present 1/t distributions.

References

[1] H. Yuan *et al* 2020 *Physical Review A*. **102** 062808
[2] S. Larimian *et al* 2016 *Physical Review A*. **93** 053405

*E-mail: s.xu@impcas.ac.cn
†E-mail: x.ma@impcas.ac.cn

Using Coulomb collisions in a radio-frequency trap to detect a single heavy molecule

A Poindron[1], J Pedregosa-Gutierrez[1], A Janulyte[1], C Jouvet[1], M Knoop[1], and C Champenois[1]*

[1]Aix Marseille Univ, CNRS, PIIM, Marseille, France

Synopsis We show by means of molecular dynamics simulations how a laser-cooled ion cloud, confined in a linear radio-frequency trap, can reach the ultimate sensitivity providing the detection of individual charged heavy molecular ions. The detection signal is the laser induced fluorescence drop due to a significant temperature variation of the cloud, triggered by the Coulombian repulsion. We identify the optimum initial energy for the molecular ion to be detected and analyse the impact of the cloud confinement parameters.

Today, mass spectrometry covers a broad range of species from light atoms up to giant molecules. In these devices, a mass filter is coupled to a charged particle detectors like microchannel plate (MCP). The need to expand the sensitivity range of charged particle detectors towards very large mass has appeared already in the 90's [1] with the achievement of heavy molecules ionising sources like MALDI and ESI. In this context, the low detection efficiency of MCPs for the mass range beyond 10^4 a.m.u is an issue as the produced mass spectrum does not accurately reflect the mass abundance of the incoming ions. Our novel approach consists in detecting the molecular ion, based on the perturbation that it induces in crossing a laser-cooled cloud of trapped ions. This method has the potential to non-destructively detect single molecules without limitation in the mass range.

The key element of the detector is a cloud of Ca^+ laser-cooled atomic ions stored in a linear RF quadrupole trap, chosen due to the commercial availability of the lasers required for photoionisation, and laser-cooling, as well as for the observation efficiency. The injected charged molecule is heavy enough not to be deviated by the trap potential neither by the ion cloud and a small part of its kinetic energy is deposed in the ion cloud, which perturbs its equilibrium state. In a second step, the heating process is amplified by radio-frequency heating. The temperature of the cloud is not accessible to measurements and its indirect observation is based on the laser induced fluorescence whose long-lasting drop is a signature of the projectile crossing.

Laser-cooled ion clouds are a practical realisation of finite-size one-component plasma and this device could be made sensitive enough to quantify the energy exchange between the injected molecule and trapped ion cloud, which remains an open question in the context of the stopping power of strongly correlated one-component plasma [2]. This communication will present the results of the molecular dynamics simulation built to assess the optimum conditions for an efficient detection, regarding the projectile initial energy and the cloud size and shape [3]. The status of the experiment built to demonstrate this detection process will also be presented.

References

[1] Frank M *et al* 1999 *Mass Spectrometry Reviews* **18** 155
[2] Bernstein D *et al* 2019 *Physics of Plasmas* **26** 082705
[3] Poindron A *et al* 2021, submitted

*E-mail: caroline.champenois@univ-amu.fr

Ultraviolet photon detection system for precision laser spectroscopy of Lithium-like $^{16}O^{5+}$ ions at CSRe

D Y Chen[1,2], H B Wang[2] †, Z K Huang[2], D M Zhao[2], J L Liu[2], C C Li[2], D C Zhang[1] *, W Q Wen[2], X Ma[2] and Laser Cooling Collaboration

[1]School of Physics and Optoelectronic Engineering, Xidian University, Xi'an, 710071, PR China
[2]Institute of Modern Physics, Chinese Academy of Sciences, Lanzhou, 730000, PR China

Synopsis Laser cooling of relativistic lithium-like $^{16}O^{5+}$ ion beams has been realized at the experimental Cooler Sorage Ring (CSRe). In order to perform precision laser spectroscopy experiment of $^{16}O^{5+}$ ions at the CSRe, a new non-destructive photon detection system has been developed for efficient detection of the forward-emitted ultraviolet photons. The collection efficiency for the forward-emitted photons is improved by more than 50 times as compared to the previously used optical detector. The new detection system will be used in the upcoming experiments at the CSRe.

In order to efficiently detect the forward-emitted ultraviolet fluorescence photons during laser cooling and precision laser spectroscopy experiments of relativistic lithium-like $^{16}O^{5+}$ ion beams at the storage ring CSRe[1], we developed a new non-destructive photon detection system, the structure of the detection system is shown in Figure 1. Based on the experiences of optical detection at the ESR[2] and the CSRe[3], this new detection system includes a moveable parabolic reflector with a central slit and a MCP coated with CsI which will efficiently collect the fluorescence photons emitted under very small angles with respect to the ion beam direction. The reflector will focus those collected photons into the MCP without affecting the operation of the ion beams in the storage ring. By converting incident photons into photoelectrons with a 300 nm thick CsI coating on the MCP surface, the detection efficiency of the MCP can be improved and the response wavelength range of the MCP can be extended from 150 nm to 200 nm. Since the detectable forward-emitted photons wavelength will be around 50 ~ 100 nm in $^{16}O^{5+}$ experiment, the material of SiC has been chosen as the reflector because its reflectivity is higher than any other material in this wavelength range. In addition, the SiC also has high radiation resistance, high thermal conductivity, and extremely low outgassing rates, which all meet the requirements for storage ring experiments. The reflector and MCP are movable by a stepper motor.

Compared to the previous used fluorescence detector installed inside the CSRe, the collection efficiency for the forward-emitted photons of this new photon detection system is improved by more than 50 times. This new detection system has been already installed in the CSRe, and will be firstly employed for the upcoming precision laser spectroscopy experiments of lithium-like $^{16}O^{5+}$ ions at the CSRe.

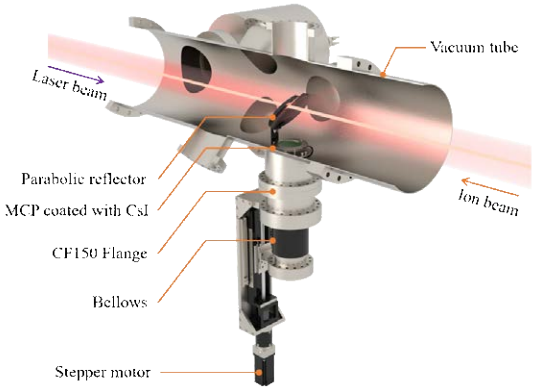

Figure 1. Schematic view of the new photon detection system at the CSRe.

References

[1]W Q Wen *et al.*, *Hyperfine Interact.* 240:45, 2019.
[2]V Hannen *et al.*, *Jinst.* 8:14, 2013.
[3]H B Wang *et al.*, *Nucl. Instrum. Methods B* 480: 180-284, 2017.

†E-mail: wanghanbing@impcas.ac.cn
*E-mail: dch.zhang@xidian.edu.cn

Detailed simulation of carbon ions track-structure in liquid water: from ab initio excitation spectrum to biodamage on the nanoscale

P de Vera[1]*, S Taioli[1], P E Trevisanutto[1], S Simonucci[2], I Abril[3], M Dapor[1], and R Garcia-Molina[4]†

[1]European Centre for Theoretical Studies in Nuclear Physics and Related Areas (ECT*-FBK) and Trento Institute for Fundamental Physics and Applications (TIFPA- INFN), Trento, 38123, Italy
[2]School of Science and Technology, University of Camerino, Camerino, 62032, Italy; INFN, Sezione di Perugia, Perugia, 06123, Italy
[3]Departament de Física Aplicada, Universitat d'Alacant, Alacant, 03080, Spain
[4]Departamento de Física, CIOyN, Universidad de Murcia, Murcia, 30100, Spain

Synopsis Carbon ion beams are used in cancer radiotherapy and are present in cosmic radiation, affecting space exploration. Lethal biodamage is related to the clustering of inelastic events within nanometric DNA targets, which are here approximated by liquid water. Its electronic excitation spectrum has been calculated by TDDFT and used to obtain reliable electronic cross sections for carbon ions and secondary electrons. Monte Carlo simulations are used to estimate the relative role of different physical mechanisms on direct complex biodamage, finding that ionizations contribute around 70% to it.

Carbon ions are promising projectiles for radiotherapy [1] and can be found in cosmic radiation, affecting human integrity during space exploration [2]. Their high relative biological effectiveness is related to the large clusters of inelastic events that they and their secondary electrons produce within a few turns of the sensitive DNA molecules, inhibiting their repair mechanisms.

Probability distributions of electronic excitations in liquid water, the main constituent of human tissues, can be reliably obtained if its electronic excitation spectrum is accurately known. The latter has been obtained from time-dependent density functional theory (TDDFT) [3] in excellent agreement with the available experimental data [4]. From it, differential and total cross sections for electronic excitation and ionization have been obtained and used in detailed Monte Carlo simulations of the carbon ions track structure, in order to assess the clustering of damaging events in nanocylinders of volume equivalent to two DNA convolutions [3].

The simulations reproduced fairly well the nanodosimetric measurements of ionization cluster size distributions. At the same time, they allowed to assess how other physical mechanisms, namely electronic excitations leading to molecular dissociation and dissociative electron attachment (DEA), contribute to the direct complex biodamage during carbon irradiation. The results, depicted in Fig. 1, show how ionizations, the only event directly measurable, contribute ∼70% to the average damage cluster size, independently of the ion energy and impact parameter, while DEA only plays a minor role.

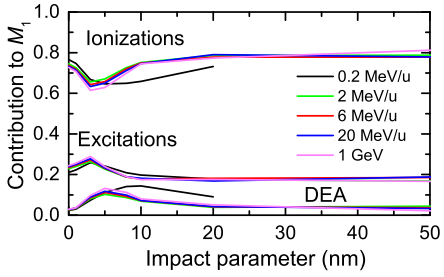

Figure 1. Relative contributions of ionizations, electronic excitations leading to molecular dissociation and DEA to the average damage cluster size M_1 in liquid water, as a function of carbon ion energy and distance to the DNA-like target [3].

References

[1] Ebner D K, Kamada T 2016 *Front. Oncol.* **6** 140
[2] Durante M, Cucinotta F A 2011 *Rev. Mod. Phys.* **83** 1245–1281
[3] Taioli S, Trevisanutto P E, de Vera P, Simonucci S, Abril I, Garcia-Molina R, Dapor M 2021 *J. Phys. Chem. Lett.* **12** 487–493
[4] Hayashi H et al. 2000 *PNAS* **97** 6264–6266

*E-mail: pdeveragomis@ectstar.eu
†E-mail: rgm@um.es

Rotational excitation of H_3O^+ by H_2: enhanced collisional data to explore water chemistry in interstellar clouds

S Demes[1]* **and F Lique**[1]

[1]Univ Rennes, CNRS, IPR (Institut de Physique de Rennes) - UMR 6251, Rennes, F-35000, France

Synopsis Rotational excitation of hydronium cations by molecular hydrogen was studied for the first time from a close-coupling method using a new highly correlated 5D potential energy surface to describe the collisional system. State-to-state inelastic cross sections were computed and the corresponding thermal rate coefficients were obtained for kinetic temperatures up to 300 K. Both the *ortho*- and *para*- nuclear spin isomers of the H_3O^+ were considered. The calculated rates can be used to estimate the abundance of hydronium both in the diffuse and dense regions of the interstellar medium, which leads to a better understanding of interstellar water chemistry.

The hydronium cation (H_3O^+) has been detected in both dense and diffuse molecular clouds of the interstellar medium (ISM) [1]. It plays a crucial role in oxygen and water chemistry [2] in these regions. Finding the abundance of H_3O^+ cations thus could be used as an indirect path to determine the abundance of interstellar water.

While the spectroscopy of the H_3O^+ was intensively studied over the past [3], there are only limited works devoted to its collisional excitation by the dominant interstellar colliders (He and H_2). The interaction of hydronium with He atoms was studied only very recently [4]. For collisions involving H_2 (i.e. the most abundant colliding partner in the ISM) the situation is even worth since only scaled scattering data derived from the isoelectronic NH_3 ones are available. As one can see, accurate rate coefficients for the H_3O^+ – H_2 collision are obviously needed.

We have studied the rotational excitation of hydronium by molecular hydrogen. First we proposed a new, accurate 5D potential energy surface (PES) for the collisional system [6]. Then state-to-state rotational de-excitation cross sections were calculated along with the corresponding thermal rate coefficients in a wide collision energy (up to $E_{col} = 1500\,cm^{-1}$) and kinetic temperature (up to $T_{kin} = 300$ K) range. The cross sections were computed from a close-coupling method, using the `HIBRIDON` scattering code.

In astrophysical media the collisional and radiative excitation of molecules are two competing processes, which are necessary to study in order to properly analyse the physical conditions. Our new collisional rates allows one to interpret the astrophysical observations of H_3O^+ both in the dense and diffuse interstellar clouds by using appropriate radiative transfer models.

*E-mail: sandor.demes@univ-rennes1.fr

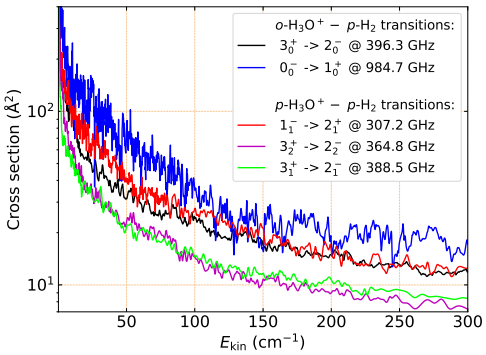

Figure 1. Rotational de-excitation cross sections for collision of *ortho*- and *para*-H_3O^+ with *para*-H_2 as a function of collision energy.

The cross sections for some selected transitions in rotational de-excitation of *ortho*- and *para*-H_3O^+ by *para*-H_2 are shown in Fig. 1. The initial and final rotational states for the symmetric top H_3O^+ are denoted by j^{ϵ}_k, where j is the total angular momentum of H_3O^+, k is its projection on the C_3 rotational axis, and $\epsilon = \pm$ is the symmetry index. Further results will be be presented during the conference.

References

[1] van der Tak F F S *et al* 2008 *A&A* **477** L5
[2] Sternberg A *et al* 1987 *Ap. J.* **320** 676
[3] Melnikov V V *et al* 2016 *PCCP* **18** 26268
[4] El Hanini H *et al* 2019 *PCCP* **21** 11705
[5] Offer A R *et al* 1992 *Chem. Phys.* **163** 83
[6] Demes S *et al* 2020 *J. Chem. Phys.* **153** 094301

Differential Cross Sections for $Na^+ + O^-$ mutual neutralization

A Dochain[1] * **and X Urbain**[1] †

[1]Université catholique de Louvain, Louvain-la-Neuve, Belgium

Synopsis We have measured the first partial differential cross section for a mutual neutralization reaction and developed a simple model to account for its main features.

Partial cross section measurements for the Na^++O^- mutual neutralization (MN) performed at UCLouvain have shown that the main products are $Na(3p)$+$O(^3P)$. These measurements are part of a series of branching ratio measurements done in parallel at UCLouvain [1] and at the DESIREE facility in Stockholm [2] that allow us to assess the validity of the models [3] in use. On the other hand, no experimental result was available on the differential cross section, besides the theoretical work dealing with Li^++F^-, H^++H^- and He^++H^- [4].

To fill this gap, we selected Na^++O^- as a test case (see Figure 1), since it is dominated by a single exit channel, $Na(3p)$+$O(^3P)$. This conclusion could be reached independently by comparing the partial cross section measurement of Weiner *et al.* [5] with the total cross section measurement of Moseley *et al.* [6] The angular differential cross section was measured for collision energies E between 5 meV and 500 meV using the experimental setup described in [1]). An update of the data analysis method allowed us to obtain both the channel-specific kinetic energy release (KER) and the scattering angle with respect to the beam propagation axis.

Two classical trajectory models were used: the analytical Interrupted Rutherford (IR) model, and the impact parameter method (IPM) combined with the multichannel Landau-Zener model. The first one could be described as follows: The initial trajectory of the ions follows the Rutherford hyperbole up to the point where the ions neutralize, the deflection being interrupted at the first or second passage through the avoided crossing between the ionic and the covalent channel. The Landau-Zener transition probability is obtained from a modified version of the anion-centred asymptotic model [7].

Despite its simplicity, the IR model reproduces the overall shape of the angular differential cross section, except for the rainbow scattering caused by the strongly avoided crossing between the ionic channel and the $Na(3s)$+$O(^3P)$ channel, which is well reproduced by the IPM.

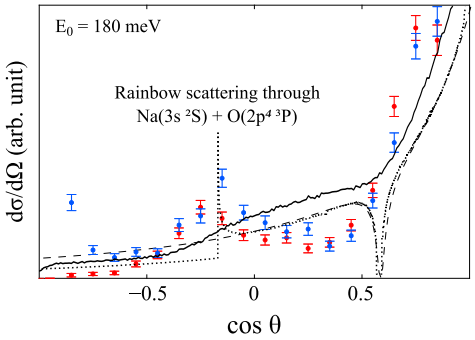

Figure 1. Na^++O^- MN differential cross section. Blue/red symbols: experiment; dashed line: IR model; dotted line: IPM; full line: IPM convoluted with the collision velocity distribution.

References

[1] de Ruette N *et al* 2018 *Phys. Rev. Lett.* **121** 083401; Launoy T *et al* 2019 *ApJ* **883** 85
[2] Eklund G *et al* 2020 *Phys. Rev. A* **102** 012823; 2021 *Phys. Rev. A* **103** 032814
[3] Barklem P S *et al* 2021 *ApJ* **908** 245
[4] Nkambule S M *et al* 2015 *Chem. Phys.* **462** 23; 2016 *Phys. Rev. A* **93** 032701; Larson Å *et al* 2016 *Phys. Rev. A* **94** 022709
[5] Weiner J *et al* 1970 *Phys. Rev. Lett.* **25** 79; 1971 *Phys. Rev. A* **4** 1824
[6] Moseley, J *et al* 1972 *J. Geophys. Res.* **77(1)** 255
[7] Janev R K 1976 *J. Chem. Phys.* **64** 1891

*E-mail: arnaud.dochain@uclouvain.be
†E-mail: xavier.urbain@uclouvain.be

Dirac R-matrix calculations for singly ionised Nickel.

N. L. Dunleavy[1]*, J. C. Gouldie[1], C. P. Ballance[1] and C. A. Ramsbottom[1]

[1]Centre for Theoretical Atomic, Molecular and Optical Physics, Queen's University Belfast, University Road, Belfast, BT7 1NN, United Kingdom

Synopsis Theoretical atomic structure and scattering calculations are necessary to underpin the interpretation of a variety of astrophysical spectra. Iron-peak elements in particular are observed in a variety of different astrophysical environments. However, beyond models involving only a restricted number of target configurations there is a modelling need for a more comprehensive dataset for the second most abundant iron peak element, Ni II. We shall address these issues through use of the GRASP0 atomic structure code and the relativistic atomic scattering code DARC.

Emission lines of Ni II have been observed in a variety of astrophysical spectra. These astrophysical sources include filaments of the luminous blue variable (LBV) star, η Carinae [1], stars evolved to red giants [2], stars which became white dwarfs [3], Seyfert galaxies [4], and also γ-ray bursts [5].

From early theoretical calculations [6] employing only the lowest two configurations to a 5 configuration calculation [8]. the focus was upon low temperature nebular spectra and calculations were constrained by computational limitations.

We shall present a more sophisticated 11 configuration structure containing higher excited state configurations involving 4d, 5s, and 5p orbitals. Previous studies did not include these higher excited states that reveal a wealth of spectral lines, not previously available to modellers.

Specifically, we employ target atomic structures derived from the Multi-Configuration Dirac-Hartree-Fock method as implemented within the General Purpose Relativistic Atomic Structure Package (GRASP0) [10]. The R-matrix DARC scattering calculations are implemented through the parallel relativistic Dirac Atomic R-matrix Codes (DARC) [11]. Our data set is formatted for future integration within more powerful modelling programs, such as CLOUDY [13] and ADAS [14].

References

[1] Davidson, K. et al 2001, AJ, **121** 1569
[2] Richardson, N. D. et al. 2011, The Astronomical Journal, **142** 201
[3] Klein, B. et al. 2011, ApJ, **741** 64
[4] Véron-Cetty, M. P. et al. 2006, AA, **451** 851
[5] Cucchiara, A. et al. 2011, ApJ, **743** 154
[6] Bautista, M. A. Pradhan, A. K. 1996, AAS, **115** 551
[7] Bautista, M. A. 2004, AA, **420** 763
[8] Cassidy, C. M. et al. 2010, AA, **513** A55
[9] Cassidy, C. M. et al 2016, AA, **587** A107
[10] Dyall, K. et al. 1996, Comp. Phys. Comm., 94, 249
[11] Ballance, C. P. 2019, DARC
[12] Bates, David Robert, et al. 1962, **267**
[13] Ferland, G. J. et al. 2017, Rev. Mexicana Astron. Astrofis., **53** 385
[14] University of Strathclyde ADAS

*E-mail: ndunleavy01@qub.ac.uk

Dirac R-matrix calculations for near-neutral ion stages of tungsten in support of magnetically-confined fusion experiments.

N. L. Dunleavy[1]*, C. P. Ballance[1], C. A. Ramsbottom[1], R. T. Smyth[1], C. A. Johnson[2], S. D. Loch[2] and D. A. Ennis[2]

[1]Centre for Theoretical Atomic, Molecular and Optical Physics, Queen's University Belfast, University Road, Belfast, BT7 1NN, United Kingdom
[2]Department of Physics, Auburn University, Auburn, Alabama 36849, USA

Synopsis Tungsten has been chosen for use as a plasma facing component in the divertor for the ITER experiment, is currently being used on existing tokamaks such as JET, and has been the subject of a number of tokamak experiments such as those on DIII-D. The successful use of W as a plasma facing component depend upon reliable erosion diagnostics which in turn are underpinned by reliable atomic scattering calculations that enable the characterisation of tungsten impurity influx into the core plasma. We present illustrative results from electron impact excitation calculations using the DARC R-matrix codes for the near neutral tungsten species: W I and W II. Comparison with the Compact Toroidal Hybrid (CTH) experiment (Auburn University) allow us to explore tungsten diagnostic capabilities for future experiments.

Due to the high temperatures attainable in tokamaks, tungsten may be used for plasma facing components (PFCs) in the divertor region. Significant wall erosion of the tungsten may quench the plasma if impurity influx reach sufficient concentrations in the core. Regardless, as the impurity influx from PFCs is unavoidable it must be characterized by accurate tungsten models critical to erosion determination on large scale experiments such as ITER [1]. The erosion of tungsten (W), determines the lifetime of the PFCs, and is extensively discussed in the work of Brezinsek et al 2019 [2]. Spectroscopic methods along with theoretical atomic physics coefficients, known as SXB ratios, provide a less invasive diagnostic capability if results can be generalized to a wide variety of experiments involving tungsten.

Highly-charged tungsten species have been studied in recent years [3, 5, 6, 7], but there has been less focus on the more challenging near neutral stages of tungsten. Extensive calculations for neutral tungsten [4] and singly ionized tungsten shall be presented. The atomic structures are created using the Multi-Configuration Dirac Hartree Fock method, implemented by the General Purpose Relativistic Atomic Structure Package (GRASP0) [8]. The electron-impact excitation is investigated using the parallel relativistic Dirac Atomic R-matrix Codes (DARC) [9]. Electron-impact ionisation from both the ground and especially excited states is also required if accurate erosion diagnostics are to be determined, though this is theoretically demanding. Collisional radiative modelling incorporating these atomic structure and scattering datasets with ADAS [10] and ColRadPy [11], helps identify strong tungsten lines and ultimately whether they have diagnostic capabilities within certain wavelength windows.

*E-mail: ndunleavy01@qub.ac.uk

References

[1] Rebut, P.-H. 1995, Fusion Engineering and Design, **27** 3
[2] Brezinsek, S. 2019, Nuclear Fusion, **59** 9 096035
[3] Turkington, M. D. et al. 2016, Phys. Rev. A **94** 022508
[4] Smyth, R. et al. 2018, Phys. Rev. A, **97** 052705
[5] Hussein, A. A. A. et al. 2019, Journal of Electron Spectroscopy and Related Phenomena, 234, 86
[6] El-Maaref, A. A. et al. 2019, Journal of Qunatitative Spectroscopy and Radiative Transfer, 224, 147
[7] Aggarwal, K. M. 2019, Journal of Qunatitative Spectroscopy and Radiative Transfer, 231, 136
[8] Dyall, K. et al. 1996, Comp. Phys. Comm., 94, 249
[9] Ballance, C. P. 2021, DARC, R-Matrix Codes http://connorb.freeshell.org
[10] Summers, H. P. 2004, The ADAS User Manual, version 2.6
[11] Johnson, C. et al. 2019 Nuclear Materials and Energy **20** 100579

Time dependent dynamics of ions in an electrostatic ion beam trap

D Gupta[1] *, R Singh[2], R Ringle[3,4], C Nicoloff[3,4], I Rahinov[5], S Mishra[1], A Shahi[1], O Heber[1] † and D Zajfman[1]

[1]Department of Particle Physics and Astrophysics, Weizmann Institute of Science, Rehovot 7610001, Israel
[2]CIMAP, Ganil, Caen 14000, France
[3]Facility for Rare Isotope Beams, East Lansing, MI, USA
[4]Department of Physics and Astronomy, Michigan State University, East Lansing, MI, USA
[5]Department of Natural Sciences, The Open University of Israel, Raanana 43107, Israel

Synopsis The time dependent dynamics of trapped ions have been investigated in the dispersive and self-bunching mode of the trap both experimentally and numerically to study the effect of ion-ion collision and its dynamics in the trap.

Electrostatic Ion Beam Traps (EIBT) [1] are used to study time-dependent dynamics of trapped molecular ions. One important aspect is the influence of the ion-ion collision, which leads to interesting collective behavior of the molecular ions in such devices. So far, no good common tool was available specifically for EIBTs to study the effect of ion-ion interaction numerically. Here we present a study of the dynamics of ions trapped in an EIBT, both experimental and numerical, using a new tool developed at MSU and employed at WIS. The study examines the ion-ion dynamics both in dispersive (faster ions less oscillation time) and self-bunching (faster ions longer oscillation time) [2] mode of the trap. SF_5^+ ion bunches with certain initial width and velocity distribution were trapped in the experimental device, and the evolution of the bunch width vs. time was studied. The ion bunch dynamics of diffusion and synchronization was investigated previously using a one dimensional model [3]. One-dimensional models are clearly a crude approximation to the real experimental conditions, and hence, there is a need for a better simulation technique, which can more accurately capture the initial conditions and physics involved, to understand the role of ion-ion collision using a longer simulation time in the dispersive, as well as in the self-bunching, mode.

Here, we have developed a new simulation technique which more closely reproduces the experimental conditions using the two-dimensional particle-in-a-cell code in cylindrical coordinates (2DCylPIC) that enabled us to study the effect of space charge (ion-ion) interactions inside the EIBT. We have performed the simulation both with and without ion-ion collisions and the effect of ion-ion collisions is clearly reflected by getting the enhanced diffusion of bunches in the dispersive mode from 8~10 ms without collisions to about 1.5 ms with collisions (depends on the ion density). Similarly the bunch width preserved for more than 100 ms (the length of the simulation) in the self-bunching mode of the trap. Figure 1 shows the comparison of full width half maxima (FWHM) in the self-bunching mode of the trap showing a good agreement with the experiment for 20 ms.

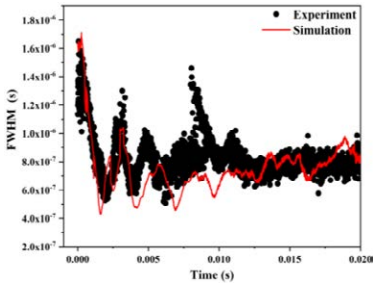

Figure 1. comparison of evolution of FWHM with time in the self-bunching mode of the trap.

Additional external time dependent forces applied to the trap electrodes were also studied exhibiting inner bunch collective oscillations.

References

[1] Zafjman D *et al*., 1997 *Phys. Rev. A* 55 R1577
[2] Pedersen H B *et al*., 2001 *Phys. Rev. Letts.* 119 103202
[2] Pedersen H B *et al*., 2002 *Phys. Rev. A* 65 042704

* E-mail: dhanojsanjay@gmail.com
† E-mail: oded.heber@weizmann.ac.il

Excitation, electron capture and ionization in Be^{4+}+H($n = 1, 2$) collisions: a comparative study

Clara Illescas*, **A. Jorge, L. Méndez, I Rabadán**

Laboratorio Asociado al CIEMAT de Física Atómica y Molecular en Plasmas de Fusión.
Departamento de Química, módulo 13, Universidad Autónoma de Madrid, 28049-Madrid, Spain.

Synopsis We present calculations of ionization, total and state-selective excitation and electron capture cross sections in collisions of Be^{4+} with hydrogen in its ground state ($1s$) and in the excited $n = 2$ states. We have employed two theoretical methods, the classical trajectory Monte-Carlo method and a direct numerical solution of the time-dependent Schrödinger equation.

The study of inelastic processes between fully stripped ions and hydrogen atoms is a main subject of interest in various domains, from fusion research to astrophysics research. In particular, collisions involving Be^{q+} ions are relevant because Be will be used as the armor material of the first wall of ITER. The diagnostics of impurity density and temperature in the plasma core are obtained through charge exchange recombination spectroscopy (CXRS), following the injection of a neutral beam of H or D, which requires fundamental atomic data such as nl-state selective cross sections.

We have performed calculations for Be^{4+}+H(n=1,2) collisions employing two non-perturbative treatments, a semiclassical method, in which we solve numerically the time-dependent Schrödinger equation, by using the GridTDSE package [1] and, the classical trajectory Monte-Carlo method (CTMC) [2]. The present semiclassical calculations for H($2s$) collisions were carried out with a broad box of $L_{max} = 80$ a_0. We have obtained the hybrid orbitals due to the Be^{4+} charge. The calculated initial wavefunction is located in the center of the grid (0, 0, 0) while the moving Be^{4+} charge is located at (b, 0, z_{ini}) where $z_{ini} = -80$ a.u. has been obtained with convergence tests. The initial wave function is therefore calculated for each v and b. The details of the calculations with H($1s$) targets can be found in [3]. In the case of the classical description of the excited hydrogen atom, the electron dynamics have been described by means of a microcanonical phase space distribution discretized in terms of $N = 2 \times 10^6$ non-interacting trajectories and the Hamilton equations have been integrated from $t_{ini} = -200$ a.u. up to $t_{fin} = \frac{1000}{v}$ a.u.

As an illustration, we show in Fig. 1 preliminary cross sections for state-selective excitation to the most populated levels in Be^{4+} + H($2s$) collisions,

$$Be^{4+} + H(2s) \rightarrow Be^{4+} + H(nl)$$

The comparison of both calculations shows a good agreement at the two energies of 20 keV/u and 100 keV/u.

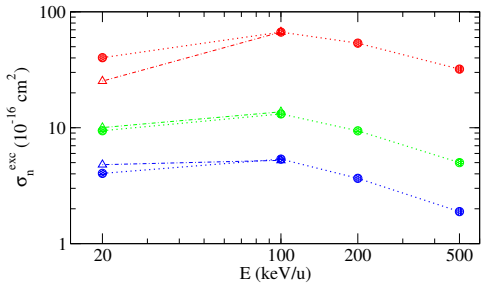

Figure 1. State-selective excitation cross sections in Be^{4+}+H($2s$) collisions for $n = 3$ in red, $n = 4$ in green and $n = 5$ in blue. Present calculations: classical (circles) and semiclassical (triangles).

This work is partially supported by the project FIS2017-84684-R (Spanish Ministerio de Ciencia e innovación).

References

[1] Suarez J *et al* 2009 *Comput. Phys. Commun.* **180** 2025
[2] Abrines and Percival 1966 *Proc. Phys. Soc.* **88**, 861
[3] Jorge A *et al* 2016 *Phys. Rev. A* **94**, 032707

*E-mail: clara.illescas@uam.es

Laser-Microwave Double-Resonance Spectroscopy: Toward Measurement of Magnetic Moments in Heavy, Highly Charged Ions

Kanika[1,2*], J Klimes[1,2,3†], P Baus[4], G Birkl[4], Z Guo[1,2,3], W Quint [1,2] and M Vogel[1]

[1] GSI Helmholtz Center for Heavy Ion Research, Planckstraße 1, Darmstadt, Germany [2] Physics Institute, Heidelberg University, Im Neuenheimer Feld 226, Heidelberg, Germany [3] Max Planck Institute for Nuclear Physics, Saupfercheckweg 1, Heidelberg, Germany [4] Institute for Applied Physics, TU Darmstadt, Schlossgartenstraße 7, Darmstadt, Germany

Synopsis In the ARTEMIS experiment, large ensembles of highly charged ions (HCIs) are stored and cooled in a Penning trap for subsequent g-factor measurements. A Laser-Microwave double-resonance technique will be used to probe the transitions and thus measure the Larmor frequency of the electron bound to these HCIs.

In ARTEMIS [1, 2] laser-microwave double-resonance spectroscopy [3] will be used to measure the intrinsic magnetic moments of both electrons and nuclei in heavy, highly charged ions (HCIs). This provides a probe of strong-field quantum electrodynamics. Figure 1 shows the level scheme for boron-like argon(Ar^{13+}) and the transitions used for the measurement. Ion densities up to 10^6 cm^{-3} can be stored for several days or even weeks [4]. This is possible due to the vacuum pressure $< 10^{-15}$ mbar in the trap center, which is in turn made possible by a cryogenic environment at nearly 4 K.

The ARTEMIS Penning trap has two sections: the spectroscopy trap (ST) and creation trap (CT). The ST uses a half-open design for optical and ion access. On the closed side spectroscopic access is provided by a transparent endcap electrode with a conductive indium-tin-oxide coating. This provides ≈ 2 sr conical access to the trap center for irradiation and detection of fluorescence light but maintains a well-defined trap potential. On the open side HCIs can be injected from the adjacent CT, where they can be created in situ via electron impact ionization or captured from an external source. Currently, ARTEMIS is working toward a measurement of the 2p electron in a test ion, Ar^{13+}, which has a well known and accessible fine-structure transition. Also the experiment is preparing for capture of heavy HCIs such as Pb^{81+} and Bi^{82+} from the HITRAP facility at GSI.

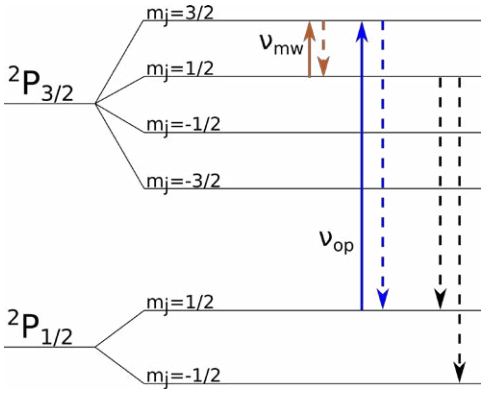

Figure 1. Level scheme of Ar^{13+} with relevant spectroscopic transitions. ν_{op} denotes a closed-cycle optical transition, and dotted lines are spontaneous or stimulated decay channels. The Zeeman transition of interest, ν_{mw}, is in the microwave regime for the given charge state and magnetic field strength.

References

[1] Quint W *et al* 2008 Physical Review A **78** 03251
[2] Sturm S *et al* 2017 Atoms **5** 4
[3] Lindenfels D V *et al* 2013 Physical Review A **87** 023412
[4] Ebrahimi M S *et al* 2018 Physical Review A **98** 023423

This research has been conducted in the framework of the SPARC collaboration, experiment E130 of FAIR Phase-0 supported by GSI. We acknowledge substantial support by BMBF to TU-Darmstadt and support by IMPRS for Quantum Dynamics in Heidelberg.

*E-mail: k.kanika@gsi.de
†E-mail: j.klimes@gsi.de

Spontaneous decay of highly excited C_2^-: electron emission versus fragmentation

N. Kono*, R. Paul, E. K. Anderson, M. Gatchell, H. Zettergren† and H. T. Schmidt

Department of Physics, Stockholm University, Roslagstullsbacken 21, Stockholm, 114 21, Sweden

Synopsis We report a study of the competition between electron emission and fragmentation for C_2^- on milliseconds timescales. Internally hot C_2^- ions were stored in the cryogenic ion-beam storage ring, DESIREE, for 200 ms. The preliminary result shows that the electron emission is the most prominent decay pathway in the beginning of the storage and then fragmentation dominates after about 25 ms. This is surprising given the fact that the energy threshold for the electron emission is so much smaller than the threshold for fragmentation.

Homonuclear diatomic molecules have no permanent dipole moment and may therefore remain trapped in the rovibrational states in which they are produced unless they are hot enough to decay by fragmentation or electron emission. Delayed fragmentation is possible for highly excited rovibrational states where tunneling through the so-called centrifugal barrier determines the lifetime for such metastable states. The total fragmentation rate for an ensemble of anions having a broad distribution of rovibrational states then displays a power law dependence as a function of time, as suggested in pioneering studies of the spontaneous decay of Ag_2^- in ELISA [1]. Recently, we have confirmed this scenario and in addition shown that electron emission becomes the most dominant decay pathway for storage timescales exceeding 100 ms [2]. The latter observation was highly surprising as there are no avoided crossings between the adiabatic potential energy curves of the anion and the neutral dimers, and electron emission must in such cases lead to a significant decrease in vibrational excitation.

Here, we studied the competition between electron emission and fragmentation for C_2^- as a function of storage time. The experiment was carried out using one of DESIREE rings [3], where both detectors for neutral particles (ND) and charged fragment ions (FD) were used in parallel (see fig. 1 (a)).

Figure 1 (b) and (c) show preliminary results of the decay curves and the branching ratios, respectively. These show that electron emission is the most prominent decay pathway up to about 25 ms, while fragmentation dominates on longer timescales. This is surprising given the fact that the electron affinity (3.3 eV) of C_2 is so much smaller than the dissociation energy (8.3 eV) of C_2^-. A possible explanation is that there is a population of highly rotationally excited ions that preferentially decay through fragmentation, but which cool more slowly that the rest of the stored population.

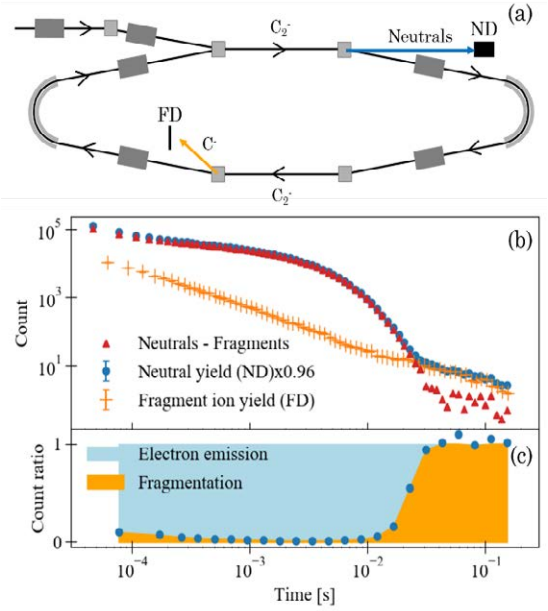

Figure 1. Schematic of experimental setup (a), spontaneous decay curves (b) and ratio between neutrals and fragments (c). Results are preliminary.

References

[1] J. Fedor *et al* 2005 *Phys. Rev. Lett.* **94** 113201
[2] E. K. Anderson *et al* 2020 *Phys. Rev. Lett.* **124** 173001
[3] H. T. Schmidt *et al* 2013 *Rev. Sci. Instrum.* **84** 055115

* E-mail: naoko.kono@fysik.su.se
† E-mail: henning@fysik.su.se

Atomic physics research at HIAF and future perspectives

X Ma[1,2 *], S F Zhang[1,2], W Q Wen[1,2], J Yang[1,2], Z K Huang[1,2], H B Wang[1,2], D L Guo[1,2], X L Zhu[1,2], Y Gao[1,2], S Yan[1,2], D B Qian[1,2], S Xu[1,2], D Yu[1,2], R Cheng[1,2], R T Zhang[1,2], D M Zhao[1], L J Mao[1,2], J C Yang[1,2], H S Xu[1,2], X H Zhou[1,2], Y J Yuan[1,2], J W Xia[1,2], H W Zhao[1,2], and W L Zhan[1,2]

[1]Institute of Modern Physics, Chinese Academy of Sciences, Lanzhou, 730000, China
[2]University of Chinese Academy of Sciences, Beijing, 100049, China

Synopsis The physics programs at the new large-scale scientific facility HIAF is briefly introduced and a detection system is proposed for the study of vacuum decay in super-critical field at the upgrading HIAF complex.

The High Intensity heavy ion Accelerator Facility (HIAF) is a new large-scale scientific project under construction in Huizhou city, Guangdong Province of South China. The HIAF consists of an ion-Linac (iLinac) with a length of 100 m, a super-conducting Booster Ring (BRing), a radioactive beam line of fragmentation type, a spectrometer ring (SRing), and various experimental setups for external and in-ring experiments as shown in Fig. 1 [1].

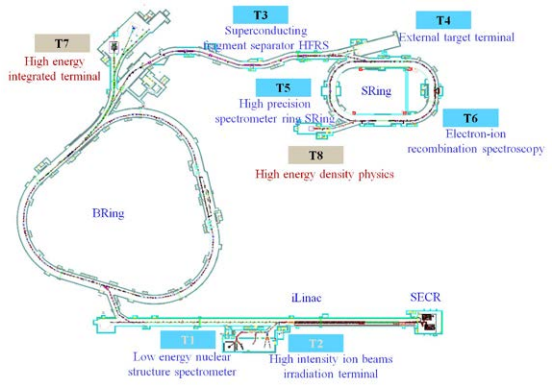

Figure 1. A schematic view of the HIAF complex.

The atomic physics experiments will be mainly peformed at the SRing and the high energy density physics will be performed at terminal T8. Stable and unstable heavy ions with high energies, high intensities and high quality will be stored at the SRing [2]. The atomic physics research covers the test of quantum electrodynamics (QED) effects in strong fields, parity nonconservation in highly charged ions, few-body dynamics in relativistic collisions, and nonlocality/decoherence/environmental effects of massive particles in collision dynamics. Unstable ions far from stability will be employed for precision atomic spectroscopy as well. Furthermore, the upgrade HIAF will provide unprecedented opportunities for QED tests in super-critical electromagnetic fields beyond the Schwinger limit [3], where QED vacuum decay will be manifested [4] by identification of spontaneous e+e- pair creation in heavy ion-ion collisions at CM energies below Coulomb barrier in the merge rings. The proposed detector system is shown in Figure 2.

In parallel, the international project – FAIR is being built in Germany, which will offer unique experimental opportunities for atomic physics [5]. The two projects have collaborations and are supporting each other. HIAF is funded by National Development and Reform Commission of China.

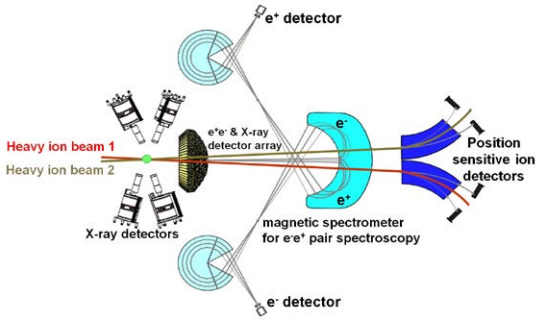

Figure 2. A schematic view of the experimental setup for study of vacuum decay in super-critical field [6].

References

[1] J. C. Yang, et al. 2013 *NIM* B **317**, 263;
[2] X. Ma, et al. 2017 *NIM* B **408**, 169;
[3] X. Ma, et al. 2020 *SCIENTIA SINICA Physica, Mechanica & Astronomica*, **50**, 112008;
[4] I. A. Maltsev, et al. 2019 *PRL*, **123**, 113401
[5] T. Stöhlker et al, 2015 *Phys. Scr.* T**166**, 014025
[6] http://apex.impcas.ac.cn/

* E-mail: x.ma@impcas.ac.cn

How to observe the vacuum decay in supercritical heavy-ion collisions

I A Maltsev[1]*, R V Popov[1], V M Shabaev[1]†, D A Telnov[1], I I Tupitsyn[1], Y S Kozhedub[1], A I Bondarev[2], N V Kozin[1], X Ma[3], G Plunien[4], T Stöhlker[5,6,7], D A Tumakov[1], and V A Zaytsev[1]

[1]St. Petersburg State University, St. Petersburg, 199034, Russia
[2]Peter the Great St. Petersburg Polytechnic University, St. Petersburg, 195251, Russia
[3]Institute of Modern Physics, Lanzhou, 730000, China
[4]Institut für Theoretische Physik, TU Dresden, Dresden, D-01062, Germany
[5]GSI Helmholtzzentrum für Schwerionenforschung GmbH, Darmstadt, D-64291, Germany
[6]Helmholtz-Institut Jena, Jena, D-07743, Germany
[7] Institut für Optik und Quantenelektronik, Friedrich-Schiller-Universität Jena, D-07743 Jena, Germany

Synopsis We propose a method to detect the spontaneous vacuum decay in heavy-ion collisions.

Quantum electrodynamics (QED) is known as the most established example of the quantum field theory. The QED predictions have been tested with high precision in numerous experiments. However, all the tests were performed for relatively weak electromagnetic fields, in which there exists a stable vacuum state. In extremely strong (supercritical) fields, the QED vacuum becomes unstable and can decay spontaneously via production of electron-positron pairs. This fundamental phenomenon was predicted many years ago but has never been observed experimentally.

The field of required strength can achieved in collision of two heavy ions if their total charge exceeds the critical value $Z_C \approx 173$. The detection of the emitted particles would be the direct evidence of the spontaneous vacuum decay. However, in heavy-ion collisions, the electron-positron pairs can be also produced dynamically by the time-dependent potential of the moving nuclei. Therefore, in order to detect the signal from the vacuum decay, one has to distinguish the spontaneous pair production mechanism from the dynamical one.

For decades it was widely accepted that spontaneous contribution cannot be separated from the dynamical background and, therefore, it is impossible to find the evidence of the vacuum decay. Nevertheless, in the present work, we show that the vacuum decay can be detected. The approach is based on the different behavior of the pair-production probability as a function of ion velocities in the subcritical and supercritical cases. One can observe the desired difference in experiment using the impact-sensitive measurements of the pair-production probabilities. Possibility of such observation is shown utilizing the numerical calculations of pair production.

It is also demonstrated the positron energy spectra can provide even a stronger evidence of the transition to the supercritical regime. For instance, it becomes very pronounced in collisions of bare uranium nuclei. We also consider the possibility of extending this study to collisions of bare nuclei with neutral atoms. It is shown that the relatively large probability of a vacancy in the the ground state of a quasimolecule formed in such collisions make them suitable for detection of the vacuum decay.

The details of the present research can be found in Refs. [1, 2].

This work was supported by RFBR-Rosatom (Grant No. 20-21-00098), by the President of the Russian Federation (Grant No. MK-1626.2020.2), and by the "BASIS" foundation.

References

[1] Maltsev I M, Shabaev V M, Popov R V, Kozhedub Y S, Plunien G, Ma X, Stöhlker Th, and Tumakov D A 2019 *Phys. Rev. Lett.* **123** 113401

[2] Popov R V, Shabaev V. M., Telnov D A, Tupitsyn I I, Maltsev I A, Kozhedub Y. S., Bondarev A I, and Zaytsev V A, 2020 *Phys. Rev. D* **102** 076005

*E-mail: i.maltsev@spbu.ru
†E-mail: v.shabaev@spbu.ru

Interatomic Coulombic decay driving the de-excitation of highly charged ions inside of atomically thin materials

A Niggas[1]*, S Creutzburg[2], J Schwestka[1], B Wöckinger[1], T Gupta[3], P L Grande[4], D Eder[3], J P Marques[5], B C Bayer[3,6], F Aumayr[1], R Bennett[7]† and R A Wilhelm[1]

[1] Institute of Applied Physics, TU Wien, 1040 Vienna, Austria
[2] Institute of Ion Beam Physics and Materials Research, Helmholtz-Zentrum Dresden-Rossendorf, 01328 Dresden, Germany
[3] Institute of Materials Chemistry, TU Wien, 1060 Vienna, Austria
[4] Insituto de Fisica, Universidade Federal do Rio Grande do Sul, 91500 Porto Alegre, Brazil
[5] Laboratório de Instrumentação e Física Experimental de Partículas (LIP) and Faculdade de Ciências, Universidade de Lisboa, Portugal
[6] Faculty of Physics, University of Vienna, 1090 Vienna, Austria
[7] Department of Physics and Astronomy, University of Glasgow, Glasgow, G12 8QQ UK

Synopsis Our investigation reveals the charge state evolution of ions inside a solid, a quantity otherwise hidden from experiments. We further describe theoretically what drives the dynamics by means of a new self-consistent ab-initio model based on the virtual photon model. Our description of the inter-particle energy transfer in form of the interatomic Coulombic decay is applicable even for small interatomic separations. Our results are largely universal und apply to all ion beams methods, whereas we use highly charged ions as probes.

The charge state of an ion is one of its most important properties, because it can change depending on its environment and leads consequently to energy transfer. This sets ion beams apart from any other particle and photon-based method and may allow for controlled damage production and determination of the distance travelled in a material. In our joint experimental and theoretical contribution, we focus on the evolution of the ion charge state *inside* materials.

As a model system we use single- and multilayer graphene samples, which enable us to adjust the thickness of our targets with monolayer precision. We probe our samples via transmission of highly charged Xe ions analysed in regard to their final charge state. Experimentally, we find that the ion neutralisation depends solely on the time the ion spends in close proximity to material layers, i.e., we observe the same charge exchange for ions transmitted through one graphene layer as for ions with twice the velocity transmitted through two layers of graphene.

Recently, it was shown that direct Auger de-excitation, which we will refer to as the interatomic Coulombic decay (ICD) [1], is the dominant process in the neutralisation of highly charged ions [2]. By means of a new ab-initio model based on the virtual photon model [3], we are able to provide a self-consistent description for our system - even for small interatomic separations R. Figure 1 shows the extracted ICD rates $\Gamma(R)$ for various incident Xe charge states, which confirms our experimental findings that the neutralisation is limited to a small area around each material layer. This allows us to quantify the charge state evolution in a material for the very first time.

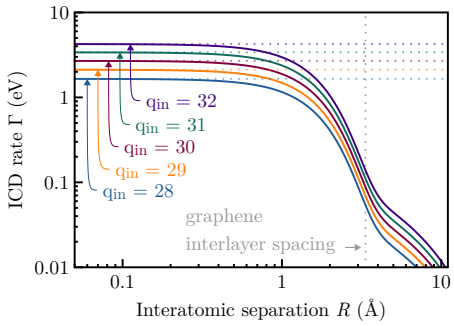

Figure 1. ICD rate Γ in dependence of the interatomic separation for five incident Xe charge states.

References

[1] Jahnke T *et al.* 2020 *Chem. Rev.* **120** 11295
[2] Wilhelm R A *et al.* 2017 *Phys. Rev. Lett.* **119** 103401
[3] Averbukh V *et al.* 2004 *Phys. Rev. Lett.* **93** 263002

*E-mail: niggas@iap.tuwien.ac.at
†E-mail: robert.bennett@glasgow.ac.uk

Rotational cooling effect on the reaction rate constant of translationally cold $Ca^+ + CH_3F \rightarrow CaF^+ + CH_3$ reaction

K Okada[1]*, T Nakamura[1], and K Sakimoto[1]

[1]Department of Materials and Life Sciences, Sophia University, Tokyo 102-8554, Japan

Synopsis We have investigated the rotational cooling effect on the reaction rate constants between laser-cooled Ca^+ and velocity-selected CH_3F generated by the wavy Stark velocity filter combining with a cold buffer gas molecular source. The increases in the rate constants at low buffer-gas temperatures (∼30 K) show a strong rotational temperature dependence at low translational reaction temperatures. The theoretical capture rate constants calculated by the Perturbed Rotational State (PRS) theory supports the present experimental results.

Recent astronomical observations provide us with further details of chemical compositions of molecular clouds and urge astrochemists to update the existing astrochemical models. In order to reproduce the observation results [1], fuller information about gas-phase chemical processes, such as temperature dependences, is needed. In this context, we have been working on the experimental study of ion-polar molecule reactions at low temperatures using the technique of Stark velocity filters combined with laser cooling [2]. In this paper, we report the rotational cooling effect on the reaction rate constant of $Ca^+ + CH_3F \rightarrow CaF^+ + CH_3$ by introducing a cold buffer gas cell for the rotational cooling of velocity-selected CH_3F molecules. We used a helium gas as the buffer gas to cool CH_3F molecules to the cold wall temperature (∼30 K). The elastic collision times of He + CH_3F were estimated to be about 80. The CH_3F molecules extracted from the gas cell are guided by a wavy Stark velocity filter [3]. The translational temperatures of the velocity-selected molecules can be set in the range of approximately 10 to 40 K by changing applied guide voltages. The rotational state distributions of the velocity-selected CH_3F molecules were determined by numerical simulations of the velocity filtering and were used to calculate the rotationally-averaged capture rate constants. The rotational-state selected data were obtained by the Perturbed Rotational State (PRS) theory [2]. In the reaction rate measurements, we first generated a Ca^+ Coulomb crystal and observed the decrease in a laser induced fluorescence (LIF) image occupied by Ca^+ ions with increasing reaction time. Figure 1 shows the LIF images of Ca^+ Coulomb crystals before and after $Ca^+ + CH_3F$ reactions. The translational reaction temperature was evaluated to be about 15 K [2, 4]. As shown in Fig.1(b), a part of product ions (CaF^+) are sympathetically cooled by crystallized Ca^+ ions. Comparing to the results obtained under the condition of room temperature gas cell, we observed the notable increase in the reaction rate constant at low buffer-gas temperatures (∼30 K). This clearly shows a strong rotational state dependence at low translational reaction temperatures. The theoretical capture rate constants calculated by the PRS theory supports the present experimental findings [2].

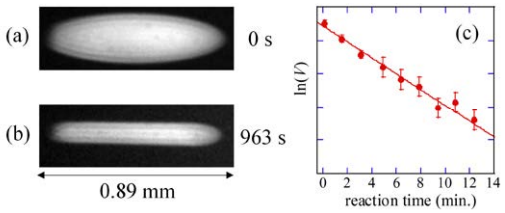

Figure 1. Fluorescence images of Ca^+ Coulomb crystals before (a) and after (b) $Ca^+ + CH_3F$ reactions. (c) A decay curve of the relative number of Ca^+ ions during the reactions between Ca^+ and translationally cold CH_3F extracted from the helium buffer gas cell at about 30 K.

References

[1] Sakai N *et al.* 2014 *Nature* **507**, 78
[2] Okada K *et al.* 2020 *J. Chem. Phys.* **153** 124305
[3] Okada K *et al* 2017 *Rev. Sci. Instrum.* **88** 083106
[4] Okada K *et al.* 2015 *Phys. Rev. Appl.* **4**, 054009

*E-mail: okada-k@sophia.ac.jp

Study of charge transfer reactions between oxygen ions in a unique cryogenic double storage ring apparatus.

M Poline[1]*, A Dochain[2], S Rosén[1], M Ji[1], G Eklund[1], X Urbain[2], M Larsson[1], N S Shuman[3], S G Ard[3], A A Viggiano[3], H Cederquist[1], H T Schmidt[1], H Zettergren[1], P S Barklem[4], and R D Thomas[1]

[1]Department of Physics, Stockholm University, Stockholm, Sweden.
[2] Department of Physics, University of Louvain, Louvain, Belgium.
[3]AFRL/RVBXT, Albuquerque, New Mexico, United States, 87116.
[4]Department of Physics, Uppsala University, Uppsala, Sweden.

Synopsis The mutual neutralisation of O^+ and O_2^+ with O^- has been studied in a unique cryogenic double storage ring apparatus using combined imaging and timing techniques.

In the upper part of our atmosphere, oxygen species are constantly exposed to UV radiation from the sun. This produces O_2^+ and O^+ which, during the night, neutralize by recombining with free electrons or by interacting with O^-. These exothermic processes result in highly excited and kinetic neutrals, which then emit photons characteristics of the airglow in the atmosphere[1].

While free electron-cation recombination processes have been studied extensively in the past, electron transfer from an anion to a cation, also known as mutual neutralisation, has not been considered with any great attention due to technical limitations. The double electrostatic storage ion ring experiment (DESIREE), has been constructed for this purpose, and allows oppositely charged ions to be stored in two separate rings, with a common straight section in which charge transfer can occur[2].

We present here the first stored merged beams study of O^+ with O^-. Using imaging and timing techniques, we have measured the three dimensional distance between the products r, a direct measure of the kinetic energy released in the reaction. Aided by theoretical calculations, we have identified the corresponding products, and were able to determine the branching ratio into the different final product electronic states of the reaction. Contributions from the metastable $O^+(^2D^o)$ state were identified and compared with previous data from single pass (non stored) merged beam results[3].

We also present here preliminary results on the mutual neutralisation of O_2^+ with O^-. Based on the total displacement (TD) of the three fragments from the beam center, the neutral products could be identified. This represents the first mutual neutralisation study involving a molecular ion in which the products were identified.

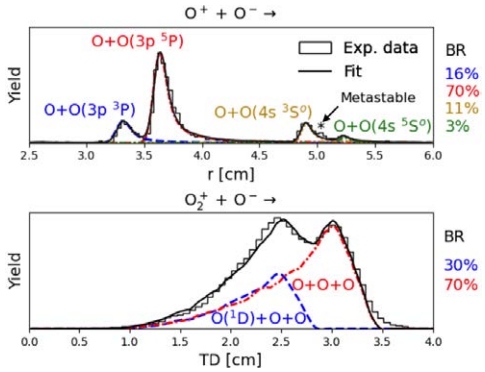

Figure 1. Recorded spectra for the mutual neutralisation of O^+/O_2^+ with O^-. From the measured quantities, branching ratio (BR) into the different set of electronically excited states, were determined

References

[1] J. Qin *et al* 2015, *J. Geophys. Res. Space Phys.* **20**, 10116
[2] R. D. Thomas *et al* 2011, *Rev. Sci. Instrum.* **82**, 065112
[3] N. de Ruette *et al* 2018, *Phys. Rev. Lett.* **121**, 083401

*E-mail: mathias.poline@fysik.su.se

Collisional-radiative modeling of the EUV spectrum of W^{6+}–W^{13+} ions observed in an electron beam ion trap

Priti[1]*, M Mita[1] D Kato[2,3] I Murakami[2,4]H A Sakaue[2] N Nakamura[1]

[1]Institute of Laser Science, The University of Electro-communications, Tokyo, 182-8585 Japan
[2]National Institute for Fusion Science, Toki, Gifu 509-5292, Japan
[3]Interdisciplinary graduate school of engineering sciences, Kyushu University, Fukuoka 816-8580, Japan
[4]Department of Fusion Science, The Graduate University for Advanced Studies, SOKENDAI, Toki, Gifu 509-5292, Japan

Synopsis We present the investigation of EUV transitions for W^{6+} and W^{13+} ions from the spectra observed using an electron beam ion trap. The analysis is based on relativistic configuration interaction structure calculation and collisional-radiative (CR) modeling.

Atomic data of few times ionized tungsten have great importance due to its prospective application in diagnostics of divertor plasma of the ITER [1]. Moreover, spectral studies of these ions are challenging as these ions have very complex atomic structures with the open $4f$ subshell, and competition of orbital energies between $4f, 5s$, and $5p$ electrons. In fact, for the few ions even ground state is still uncertain. Therefore, such studies are very important not only from the application but also from the atomic physics point of view. However, in literature, only very few studies are available [2] and there is still no data available for W IX to W XIII in the Atomic Spectra Database of the NIST [3].

We present spectroscopic measurements and detailed theoretical analysis of charged tungsten W^{6+}-W^{13+} ions in EUV range. The EUV emission from W^{6+} through W^{13+} was recorded at the compact electron beam ion trap (CoBIT) facility [4] at the University of Electro-Communications with with a grazing-incidence flat-field spectrometer for electron-beam energies between 90-280 eV [5]. The analysis of the observed spectra is based on the detailed collisional-radiative (CR) modeling with fine structure sublevels atomic kinetics. The present model includes basic kinetic processes such as electron impact excitation (de-excitation), ionization and radiative decay. All the atomic data for energy levels, transition probabilities, and cross-sections are calculated using the wavefunction obtained within the relativistic configurational interaction (RCI) method using FAC 1.1.5. The present CR model is used to identify the charged states and corresponding lines observed from CoBIT. Most of the lines are belong to 5p-5d, 4f-5d and 5s-5p transitions.

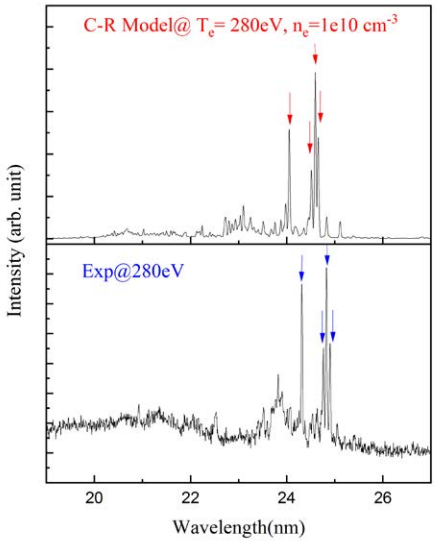

Figure 1. Experimental and simulated spectra (5s-5p transitions) of W^{13+} ion in the EUV range.

References

[1] Clementson J, *et al* 2010 *J. Phys. B: At. Mol. Opt. Phys.* **43** 063104
[2] Ralchenko Y, *et al* 2013 *JPlasma Fusion Res.* **8** 2503024
[3] Kramida A, *et al* 2020 *NIST Atomic Spectra Database (version 5.7.1).*
[4] Nakamura N, *et al* 2008 *Rev. Sci. Instrum.* **79** 144009
[5] Mita M, *et al* 2017 *J. Phys.: Conf. Ser.* **675** 012019

*E-mail: priti@ils.uec.ac.jp

Experimental branching fractions of the mutual neutralization of Li^+ and H^- at DESIREE

A F Schmidt-May[1]*, G Eklund[1], S Indrajith[1], M Poline[1], S Rosén[1], M C Ji[1], R D Thomas[1], J Grumer[2], P S Barklem[2], H Cederquist[1], H Zettergren[1], and H T Schmidt[1]†

[1] Stockholm University, Stockholm, 114 19, Sweden
[2] Uppsala University, Uppsala, 752 36, Sweden

Synopsis We studied the mutual neutralization of Li^+ and H^- at effective collision temperatures of around 2000 K, which corresponds to few hundred meV, and obtained branching fractions for the three observed product states of neutral lithium, 3s, 3p and 3d. These are compared to theoretical investigations of Ref. [1] and [2] and previous measurements of Ref. [3] and [4], which focused on the heavier isotope deuterium. Preliminary analysis finds best agreement with the full quantum calculations and the presence of an isotope effect.

The mutual neutralization (MN) between Li^+ and H^- has been identified as a significant process in non-local thermodynamical equilibrium (non-LTE) modelling of stellar atmospheres [5, 6]. The non-LTE model links the observable lithium lines to the lithium abundance which in turn gives information e.g. about processes occurring during stellar evolution. Its accuracy depends on the used cross sections. Different theoretical methods have been used to calculate the cross section of MN between Li^+ and H^- resulting in different branching fractions [1, 2]. So far, experimental attention, including ours, has focused on Li^+ and D^- for technical reasons. Branching fractions for Li^+ and H^- in the relevant energy range have only been reported at one collision energy in Ref. [3]. Here, we present recent results on our MN study of Li^+ and H^- at few hundred meV collision energies. We compare the extracted branching fractions for the three observed product states of neutral lithium, 3s, 3p and 3d, to the results of different theoretical models, namely full quantum (FQ) [2] and Landau-Zener based calculations using coupling strengths calculated via linear combination of atomic orbitals (LCAO) [7] or from semi-empirical considerations (SE) [8]. Our preliminarily branching fractions agree well and best with the FQ results. No significant deviation is found to the published branching fractions at 3 meV of Ref. [3] but, contrary to their MN studies, our results on H^- vs D^- speak for the presence of an isotope effect.

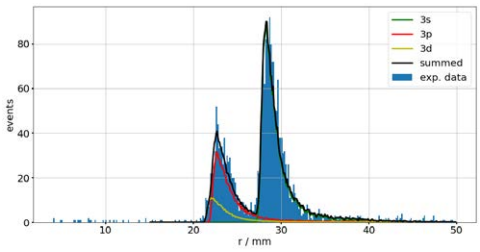

Figure 1. Histogram of measured separations of neutral products in blue together with scaled-to-fit simulations for the kinetic energy releases of MN into the 3s, 3p and 3d state of lithium.

References

[1] Barklem P S *et al* 2021 *Astrophys. J.* **908** 245
[2] Croft H *et al* 1999 *MNRAS* **304** 327
[3] Launoy T *et al* 2019 *Astrophys. J.* **883** 85
[4] Eklund G *et al* 2020, *Phys. Rev. A* **102** 012823
[5] Barklem P S *et al* 2003 *A&A* **409** L1
[6] Lind K *et al* 2009, *A&A* **503** 541
[7] Barklem P 2016 *Phys. Rev. A* **93** 042705
[8] Olson R *et al* 1971 *ApOpt* **10** 1848

*E-mail: alice.schmidt-may@fysik.su.se
†E-mail: schmidt@fysik.su.se

Planned Laboratory Studies of N_2 reacting with H_3^+ Isotopologues

D Schury[1]*, C Bu[1], P-M Hillenbrand[2], X Urbain[3], and D W Savin[1]†

[1]Columbia Astrophysics Laboratory, Columbia University, New York, NY 10027, USA
[2]GSI Helmholtzzentrum, Darmstadt, 64291, Germany
[3]Université catholique de Louvain, Louvain-la-Neuve, 1348, Belgium

Synopsis Astronomical observations of N_2D^+ and N_2H^+ abundances are used to trace the properties of cosmic objects, such as prestellar cores and protoplanetary disks. These studies require an accurate understanding of the molecular physics forming these ions. Here we describe how we plan to measure some of the key reactions leading to the formation of these ions.

Deuterated molecules are used to infer the temperature, chemistry, and thermal history of cosmic objects such as prestellar cores and protoplanetary disks [1]. In the very dense cold regions found in prestellar cores and the outer midplane of protoplanetary disks, most molecules beside hydrogen freeze onto dust grains, leaving HD as the primary deuterium reservoir in the gas phase. The HD can react with H_3^+ to form deuterated isotopologues of the ion. Subsequent ion-neutral reactions pass on the deuteration to other gas-phase species. Of particular importance is the abundance ratio for N_2D^+ and N_2H^+. Their formation occurs near the N_2 snow line of prestellar cores and protoplanetary disks and they are commonly used to trace the properties of these objects. However, to reliably interpret observations of these ions, an accurate understanding of their formation process is needed. We will use our dual-source, ion-neutral, merged-fast-beams apparatus [2, 3] to measure the integral cross sections of the reaction of N_2 with H_3^+ and its isotopologues, to an accuracy of about 15%. From these results, we will derive the thermal rate coefficients used in astrochemical models. In addition, our results will help the astrophysics community to determine the validity of the commonly assumed scaling of available kinetics data for H-bearing reactions to deuterated isotopologues and also of the assumed statistical branching ratios used for the relative fractions of H-bearing and D-bearing daughter products.

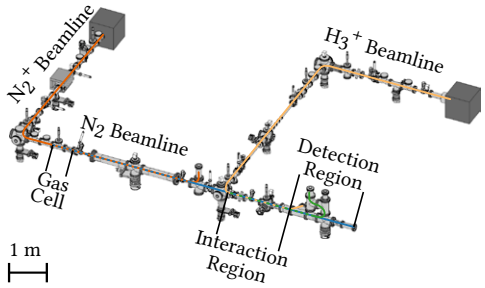

Figure 1. Schematic of the experimental setup with particle beam trajectories indicated. The initial N_2^+ beam (dark orange) neutralizes in the gas cell and forms N_2 (blue). In the interaction region, it reacts with the superimposed H_3^+ beam (light orange) and N_2H^+ is created (green). All initial and product beams are collected in Faraday cups and particle detectors.

References

[1] Albertson T *et al* 2013 *Astrophys. J. Suppl. Ser.* **207** 27
[2] O'Connor A P *et al* 2015 *Astrophys. J. Suppl. Ser.* **219** 6
[3] Bowen K P *et al* 2021 *J. Chem. Phys.* **154** 084307

*E-mail: daniel.schury@physik.uni-giessen.de
†E-mail: savin@astro.columbia.edu

Measurement of ion-induced desorption yields for accelerator vacuum application

S Steydli[1*], R Levallois[2], V Baglin[5], M Bender[3], S Bilgen[4], L Kirsch[3], E Lamour[1], A Lévy[1], B Mercier[4], G Sattonnay[4], D Schury[1], C Stodel[2] and V Velthaus[3]

[1] Institut des Nanosciences de Paris, Sorbonne Université, CNRS UMR 7588, Paris, 75005, France
[2] GANIL, Grand Accélérateur d'Ions Lourd, Caen, 14076, France
[3]GSI Helmholtzzentrum für Schwerionenforschung, Darmstadt, 64291, Germany
[4]IJCLab, Université Paris Sud, CNRS, Orsay, 91405, France
[5] CERN, Geneva, Switzerland

Synopsis: Ion induced desorption is a severe intensity limitation in modern high luminosity accelerators. The surface treatment/preparation may have a strong impact in the reduction of the desorption yield. Desorption yields have been measured on various samples of copper, stainless steel and tungsten (materials often used in accelerator construction).

The outgassing due to ion induced desorption is a severe intensity limitation in modern accelerators. It is produced when the ion beam impact on a target and remove the gas molecules trapped over and inside a material. In accelerators, the targets are mainly the wall of vacuum vessels but also beam dumps, slits, mostly made of stainless steel, copper and tungsten. The number of particles removed by incident beam ion (desorption yield) can vary between one and several thousand depending on the beam energy and irradiated material. That is why the pressure rise due to ion-induced desorption can be easily 1 or 2 order of magnitude over the base pressure which affects strongly the transmission of a beam [1, 2, 3].

During the past decade, ion induced desorption has been investigated to be decreased. The surface quality of the material irradiated is the key parameter to reach this goal. So, for their future facilities, GSI/FAIR, CERN but also GANIL/SPIRAL2 for the future Super Spectrometer Separator (S3) try to find the best treatment to minimize the desorption yield.

Samples of copper, stainless steel and tungsten with various treatments (chemical attacks, annealing, beam conditioning) have been bombarded with 4.8 MeV/u Ca^{19+} ions at the UNILAC accelerator of GSI. The goal was to determine the best treatment that minimizes the ion-induced desorption yield. The "scrubbing" effect that is the cleaning of the surface by the beam itself was investigated over a long time of irradiation.

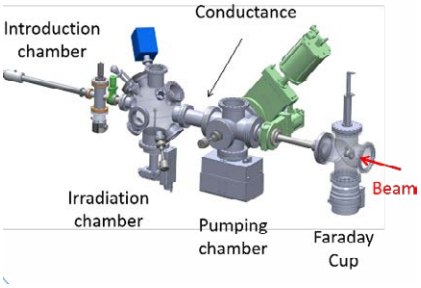

Figure 1. The setup at the M-Branch of GSI

Desorption yields are evaluated by determining the pressure increase in the chamber when the ion bombardment is on (the base line pressure before irradiation was around 10^{-10} mbar). After a description of the experimental setup (Figure 1), the different results will be presented and compared.

References

[1] E Mahner 2009 *PRST* **11** 104801
[2] Z Q Dong *et al* 2017 *NIMA* **870** 73–78
[3] E Hedlund *et al* 2009 *NIMA* **599** 1–8

* E-mail : sebastien.steydli@insp.jussieu.fr

Generation of picosecond ion pulses using a fast pulse electron beam ion source

G L Szabo[1]*, J Fries[1], A Niggas[1], and R A Wilhelm[1]†,

[1]Institute of Applied Physics, TU Wien, 1040 Vienna, Austria

Synopsis An experiment is presented which aims to generate and measure ultra-fast ion pulses with pulse widths in the ps range. Thereby we will be able to perform time-resolved measurements of ion-solid-interactions.

Ion beams in the range from few keV up to MeV are known to induce nano-structures on different materials. While the processes leading to structural transformations are generally well understood, little is known from experiments about the timescale at which, for example, collisional cascades take place. Therefore, a pump-probe experiment using a fs-laser to create ultra-fast ion pulses on the one hand and to probe the excited system on the other hand is required. To realize such an experiment, the pulse width of the probing ion beam has to be in the range of the life time of a collisional cascade, which is estimated to be in the order of a few ps. We present simulations to create ion pulses in the ps regime, using a modified concept of an electron beam ion source (EBIS), such that a pulsed electron beam generates ions by electron impact ionisation. We also present a new approach to measure ion pulses in the ps range, using an energy-filtered streak-camera.

For first simulations of the fast-pulse EBIS, we used a similar geometry as it can be found in a Dreebit EBIS-A [1], where we optimized the extraction parameters, such as field gradient for acceleration of the ions and temperature of the gas atoms (Hydrogen). The ionization process is induced by electron impact ionization, where pulsed electrons are generated using a fs-laser focused on the cathode of the EBIS. While the pulse width of the electrons is in the range of the pulse width of the laser (12 fs), the one of the ions is a few magnitudes higher, resulting from the atoms initial momentum distribution. To minimize the initial momentum distribution (especially parallel to the electron beam), a temperature of 10 mK was assumed for the gas atoms, which can be realized by expanding a gas-jet into the drift tube (similarly to the technique of Golombek *et al.* [2]).

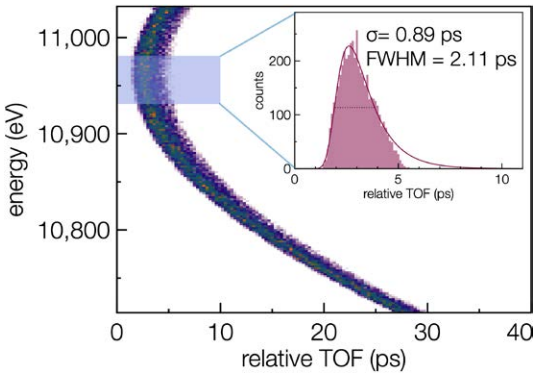

Figure 1. Kinetic energy of ions in dependence of their time of flight.

This leads to a pulse width of approximatley 2.11 ps, as it can be seen in the insert in figure 1. For this pulse width calculation, a kinetic energy window ΔE (blue rectangle) is taken into account in figure 1. To analyse such pulse widths, an adapted streak-camera will be used and its concept will be presented as well.

References

[1] Zschornack G *et al* 2008 *Rev. Sci. Instrum.* **79** 02A703

[2] Golombek A *et al* 2021 *New J. Phys.* in press https://doi.org/10.1088/1367-2630/abe443

*E-mail: gszabo@iap.tuwien.ac.at
†E-mail: wilhelm@iap.tuwien.ac.at

Comparison of classical trajectory and quantum calculations of reactions of O^- with H_2 at low temperatures

J Táborský*, M Čížek† and K Houfek

Charles University, Faculty of Mathematics and Physics, Institute of Theoretical Physics, Prague, 180 00, Czech Republic

Synopsis The associative detachment reaction $O^- + H_2 \longrightarrow H_2O + e^-$ is calculated using the classical trajectory Monte-Carlo method and the quantum Multi Configuration Time Dependent Hartree (MCTDH) package. Both approaches are then compared with experimental results.

Formation of water molecules in interstellar clouds in gas phase can proceed through the associative detachment reaction $O^- + H_2 \longrightarrow H_2O + e^-$. It takes place as an exothermic reaction with large cross section at very low energies exceeding the Langevin cross section, as it was shown in a recent experiment [1]. The production of OH^- by hydrogen transfer, which is the second possible channel in this interaction, is also exoenergetic but much less probable at low energies.

The full description of all three potential energy surfaces connected to ground state $O^- + H_2$ asymptote has been studied in detail using the MRCI method in previous works [1, 2] as well as the electron resonances in the autodetachment region using the R-matrix method.

The presented work focuses on detailed classical trajectory Monte-Carlo calculations of reaction cross sections $O^- + H_2$, which are in good agreement with recent experiments [3]. The classical trajectory calculations are then compared with full quantum simulations using the Multi Configuration Time Dependent Hartree (MCTDH) package [4] on the same potential energy surface. Possible different approaches to the simulation of the electron autodetachment region are then further discussed from both physical and numerical point of view while using the POTFIT program included in the MCTDH package.

Acknowledgement: This work has been supported by the Charles University under contract GAUK 552419.

References

[1] Jusko P *et al.* 2015 *J. Chem. Phys.* **142** 014304
[2] Houfek K and Čížek M 2016 *Eur. Phys. J. D* **70** 107
[3] Plašil R *et al.* 2017 *Phys. Rev. A* **96** 062703
[4] Worth G A *et al.* 2007 The MCTDH Package, Version 8.4

*E-mail: jiri1.taborsky@email.cz
†E-mail: martin.cizek@mff.cuni.cz

Simulation of bunched Schottky spectrum for laser-cooled O^{5+} ions at CSRe

H B Wang[1,2], D Y Chen[1,2], W Q Wen[1,2], Y J Yuan[1,2 *], X Ma[1,2 †] and Laser Cooling Collaboration

[1] Institute of Modern Physics, Chinese Academy of Sciences, Lanzhou, 730000, China
[2] University of Chinese Academy of Sciences, Beijing, 100049, China

Synopsis Laser cooling of bunched lithium-like O^{5+} ion beams with an energy of 275.7 MeV/u was successfully achieved at the heavy-ion storage ring CSRe, and the cooling dynamics were measured by the Schottky pick-up system. We have simulated the bunched Schottky spectrum of laser-cooled O^{5+} ions by the multi-particle tracking method for the first time. With the simulation of the Schottky spectrum, we achieve a better understanding of dynamics for the laser cooling of bunched ion beams.

Laser cooling of lithium-like O^{5+} ion beams with an energy of 275.7 MeV/u was successfully achieved at the storage ring CSRe in Lanzhou, China [1]. In order to explain the experimental results, by employing the multi-particle tracking method we made simulations of the bunched Schottky spectrum of O^{5+} ions with and without laser cooling. In the simulation, both of the transverse oscillation and the photon-ion resonant interaction process are considered while intrabeam scattering is ignored. Without laser cooling, the phase space distribution of the bunched ion beams and the corresponding experimental and simulated Schottky spectra are shown in Figure 1(a)-(c). The bucket is filled by the ions, and the Schottky power is nearly a Gaussian distribution. For laser-cooled bunched ion beams, the phase space distribution is shown in Figure 1(d), and Figure 1(e) and (f) show the experimentally observed and simulated Schottky spectra. With more ions laser-cooled to the center of the bucket, the distribution of the Schottky spectrum becomes narrower than that of the un-cooled ion beams in Figure 1(b). However, the simulated bunched Schottky spectrum for laser-cooled ion beams in Figure 1(f) shows strong sidebands at the position where laser resonant interacts with ions. The reason is that the beta-oscilation in the laser cooling straight section is simplified by using a mean betatron-function value. The further simulation is in progress. With this simulation, the dynamics for the laser cooling of bunched ion beams are fully understood for the first time. We will present the detailed simulation results at this ViCPEAC conference.

References

[1] Wen W *et al* 2019 *Hyperfine Interact.* **240** 45

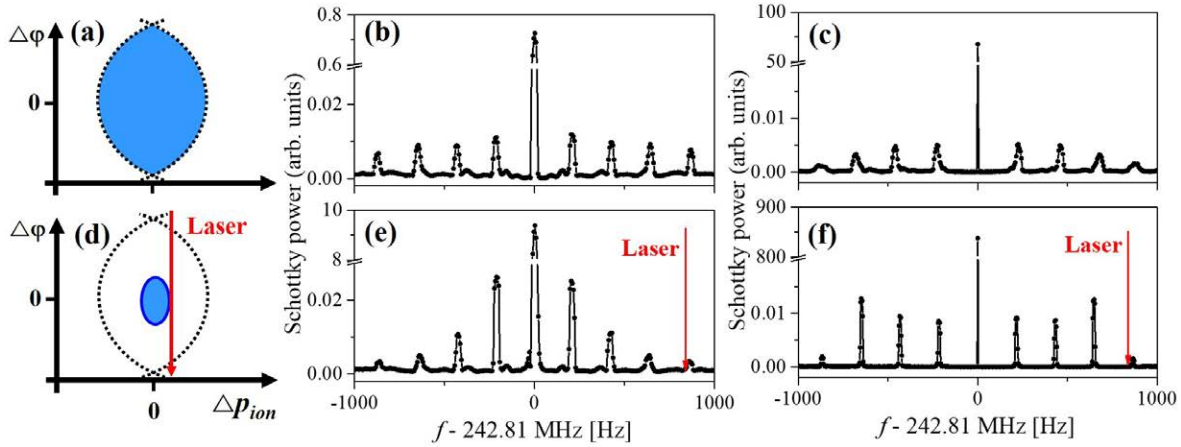

Figure 1. Experimental and simulated bunched Schottky spectra of uncooled and laser-cooled O^{5+} ions at the CSRe. Figure (a) and (d) are the phase space distribution of the ions inside of the bucket with and without laser interaction, the color represent the phase space density of the ions inside of the bucket. Figure (b) (c) and (e) (f) are the corresponding experimental and simulated Schottky spectra of figure (a) and (d).

* E-mail: yuanyj@impcas.ac.cn † E-mail: x.ma@impcas.ac.cn

Non-radiative charge exchange in an ultracold Li-Ba$^+$ hybrid trap

X Xing[1] * P Weckesser[2] F Thielemann[2] R Vexiau[1] T Xie[1] E Luc-Koenig[1] N Bouloufa-Maafa[1] T Schaetz[2] † and O Dulieu[1] ‡

[1]Laboratoire Aimé Cotton, Université Paris-Saclay/CNRS, Orsay, 91400, France
[2]Physikalisches Institut, Albert-Ludwigs-Universität Freiburg, Freiburg, 79104, Germany

Synopsis We have developed several theoretical models of increasing complexity to determine the governing interactions when a single ion Ba$^+$ is immersed in an ultracold Li gas. The fine structure quenching, parity-dependent non-radiative charge exchange and non-radiative quenching processes are identified. The agreement with the experimental results demonstrates the crucial importance of the rotational coupling.

The precise control at the single quantum level of ultracold collisions is one of the most challenging goal of researches on ultracold gases. Collisions between cold trapped atoms and ions have the practical advantage to provide the possibility to observe the reactants and products with long trapping lifetimes. Over the past few years various achievements [1, 2, 3, 4, 5, 6] have been obtained in investigating a single ion immersed within an ultracold neutral atomic bath, to explore various reactions, such as radiative/non-radiative charge/excitation exchange, spin flip, non-radiative quenching, radiative molecular formation.

In Freiburg we set up a hybrid ion-atom trap experiment involving ultracold polarized ^{6}Li($2s$) atoms colliding with a long-lived ultracold ^{138}Ba$^+$ ion in an excited metastable state ($5d^2D_{5/2,3/2}$). Non-radiative charge exchange (NRCE), fine structure quenching (FSQ) and non-radiative quenching (NRQ) are probed simultaneously.

In Orsay we designed a series of theoretical models of increasing complexity to identify the main interactions at play during such collisions: Landau-Zener (LZ) model, and full quantum scattering (QS) model involving various number of channels, spin-orbit couplings (SOCs), and rotational couplings. As expected, the LZ model is suitable to identify the main channels but only provides a qualitative picture of the collision. The full QS approach demonstrates the competing contributions of the SOCs and the rotational couplings induced by the initial high angular momentum of the ion.

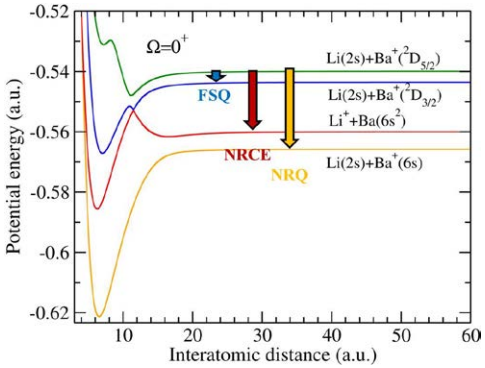

Figure 1. Computed potential energy curves of LiBa$^+$ relevant for the present experiment, with the various processes indicated.

Our results for branching ratios between the various processes from the QS model are found in good agreement with experimental observations around 0.2 mK collisional temperature. Although the parity of the total wave function of the colliding complex cannot be distinguished in experimental measurements, our model proves a particular parity-dependent quantum effect for non-radiative collisions.

References

[1] Sikorsky T *et al* 2018 *Nat. commun.* **9** 920.
[2] Feldker T *et al* 2020 *Nat. Phys.* **16** 413-416.
[3] Ben-shlomi R *et al* 2020 *Phys. Rev. A* **102** 031301(R).
[4] Joger J *et al* 2017 *Phys. Rev. A* **96**, 030703(R).
[5] Saito R *et al* 2017 *Phys. Rev. A* **95** 032709.
[6] Mohammadi A *et al* 2021 *Phys. Rev. Research* **3** 013196.

*E-mail: xiaodong.xing@universite-paris-saclay.fr
†E-mail: tobias.schaetz@physik.uni-freiburg.de
‡E-mail: olivier.dulieu@universite-paris-saclay.fr

Spin-state dependence of the Charge-Exchange collision in a hybrid system of ultracold ^{6}Li atoms and $^{40}Ca^{+}$ ions

Y. Naito[1*] , R. Saito[1] , S. Haze[2] , T. Oyama [1] , T. Osawa [1] , O. Dulieu[3] , T. Mukaiyama[1 †]

[1]Graduate School of Engineering Science, Osaka University, Machikaneyamamachi1-3, Toyonaka, Osaka 560-8531, Japan
[2]Institut für Quantenmaterie and Center for Integrated Quantum Science and Technology (IQST), Universität Ulm, 89069 Ulm, German
[3]Laboratoire Aimé Cotten, CNRS, Univerité Paris-sud, ENS Cachan, Université Paris-Saclay, 91405 Orsay Cedex, France

Synopsis We experimentally investigate magnetic-sublevel dependence of the charge-exchange collision between ultracold neutral ^{6}Li atoms and laser-cooled $^{40}Ca^{+}$ ions. We precisely control the spin states of the atoms and ions to independently observe the chemical reactions in the triple potentials. This study contributes to detail understanding of ultracold the chemical reactions.

At extremely low temperatures, wave nature of a particle start to appear and the quantum statistics of particles emerges in physical and chemical properties. Investigation of the chemical reactions in the ultralow temperature regime provide us detailed understanding of the quantum aspect of the chemical reactions.

A hybrid system of ultracold atoms and ions has several ideal features for the study of ultracold chemical reactions. First, a micro Kelvin temperature regime can be realized with laser cooling techniques. Second, quantum states of the atoms and ions undergoing chemical reactions can be precisely controlled by optical means. Third, the reaction product may sometimes be kept trapped in an isolated condition, which makes it possible to sensitively detect the chemical reactions at a single atom level.

In this experiment, we prepare $^{40}Ca^{+}$ ions and neutral ^{6}Li atoms separately and mix them using optical tweezers technique to observe the chemical reaction. It has already been revealed by mass spectrometry that this chemical reaction is a charge exchange process [1]. The important contribution of the spin-orbit interaction to the chemical reaction has already been shown by the discovery that ions in the $D_{5/2}$ and $D_{3/2}$ states exhibit different charge exchange collision coefficients[2]. In the present experiment, we introduce a highly-stabilized 729-nm laser to drive a $S_{1/2}$-$D_{5/2}$ transition of a $^{40}Ca^{+}$ ions with a natural linewidh on the order of 1 Hz. The narrow transition can be used to select arbitrarily magnetic-sublevels of the $D_{5/2}$ state, and therefore, the ion-state dependence of the chemical reactions can be probed in the system. Figure 1 shows the spectrum of the transition between $|S_{1/2}, m_F = 1/2\rangle$ and $|D_{5/2}, m_F = 5/2\rangle$. The square, triangle, and circle markers show a 1st red sideband, a 1st blue sideband, and a carrier transition, respectively. The peaks are separated with one another by the trapping frequency which is much larger than the linewidth of the transition. By exciting any of these transiton, we can selectively prepare the ion in the $m_F = 5/2$ state. Furthermore, the red sideband transition can be used for sideband cooling of the ions to reach ultralow temperature regime on the order of tens of microkelvin. In the presentation, we report our experimental investigation of the state-dependent charge exchange collisions toward full understanding of an ultracold atom-ion reactions.

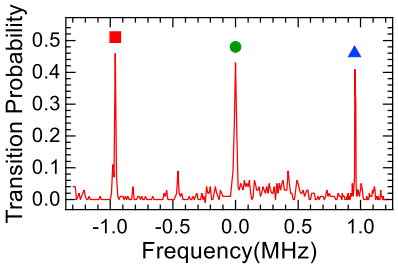

Figure 1. A typical spectrum of $S_{1/2}$-$D_{5/2}$ transition of a $^{40}Ca^{+}$ ion. The square, triangle, and circle markers show a 1st red, a 1st blue and a carrier transition, respectively.

References

[1] S.Haze *et al.* 2015 *Phys.Rev.A* **91** 032709
[2] R.Saito *et al.* 2017 *Phys.Rev.A* **95** 032709

* E-mail: u808975b@ecs.osaka-u.ac.jp
† E-mail: muka@ee.es.osaka-u.ac.jp

Observation of X-ray spectroscopy from H-like Lead at CRYRING@ESR

B Zhu[1,2*], G Weber[1,3], T Over[2], Z Andelkovic[3], R Chen[3], D Dmytriiev[3], O Forstner[1,2,3], A Gumberidze[3], C Hahn[1,2,3], M O Herdrich[1,2,3], P M Hillenbrand[3], A Kalinin[1], Th Köhler[2], F M Kröger[1,2,3], M Lestinsky[3], Y A Litvinov[3], E Menz[1,2,3], T Morgenroth[3], N Petridis[3], F Herfurth[3], Ph Pfäfflein[1,2,3], M S Sanjari[3], R S Sidhu[3], U Spillmann[3], S Trotsenko[1,3], L Varga[3], G Vorobyev[3] and Th Stöhlker[1,2,3]

[1] Helmholtz-Institute Jena, Jena, 07743, Germany
[2] Friedrich-Schiller-Universität Jena, Institut für Optik und Quantenelektronik, Jena, 07743, Germany
[3] GSI Helmholtzzentrum für Schwerionenforschung GmbH, Darmstadt, 64291, Germany

Synopsis One of the frontiers of quantum electrodynamics (QED) is the study of electrons in extreme electromagnetic fields. Especially, the 1s Lamb shift in the heaviest stable hydrogen-like ions available in the laboratory, may serve as the ultimate testbed for rigorous experiments at high field strength. The coupling of the CRYRING and ESR storage rings, for the first time, enable state-of-the-art test of X-ray spectra registration from H-like Lead (Pb^{81+}) at electron cooler of CRYCRING, providing proof of the favorable conditions for planned spectroscopy precision study.

The aim of the current investigation is to measure the 1s Lamb shift in hydrogen-like uranium (U^{91+}) with an accuracy of better than 1 eV to test the non-perturbative bound-state QED on the level of 2nd order corrections. Recently, some significant parts of the experiment setup had been prepared and installed at the CRYRING electron cooler. In addition, several critical aspects regarding to accelerator settings were also successfully demonstrated in the commissioning beam time in May 2020.

The bare lead ions (Pb^{82+}) were injected from ESR into CRYRING decelerated down to 10 MeV/u, which is allowed for a commissioning run for E138 experiment, as the beam lifetimes, ion trajectories and x-ray energies are expected to be quite similar as for U^{92+}. At the electron cooler, equipped with dedicated chambers for housing of the view ports for x-ray detection under 0° and 180° with respect to the ion beam axis, standard high-purity germanium x-ray detectors were mounted. In order to suppress the strong background of photons (mainly bremsstrahlung) emitted from the electron beam, an ion detector (channel electron multiplier) was successfully operated downstream to the cooler, enabling to record x-rays in coincidence with recombined ions (Pb^{81+}) in the electron cooler section.Even though in this very first beam time with bare Pb^{82+} ions in CRYRING only a low intensity of max. 2×10^5 ions per injection was achieved, a few days of continuous operation were sufficient to accumulate meaningful spectral information when combining the signals in both x-ray detectors with the particle detector. The x-ray spectrum associated with radiative recombination, observed at the 0-deg and 180-deg view port at the electron cooler were observed, the eliminated tails of Ly-α transition lines together with intense state selective Balmer spectrum due to beryllium view-ports, are compared with that at ESR with U^{91+} beam energy of 43 MeV/u [1],

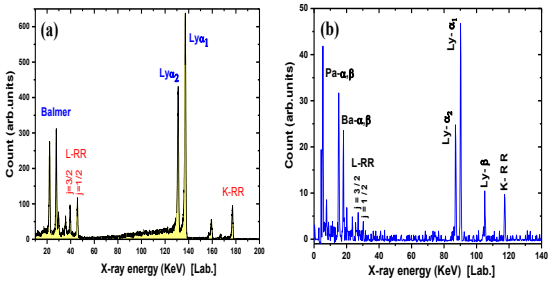

Figure 1. X-ray spectrum observed (a) at close to 0 deg for $U^{92+}\rightarrow e^-$ collisions at 43 MeV/u at ESR, and (b) at exactly 0 deg for $Pb^{82+}\rightarrow e^-$ collisions at 10 MeV/u.

This research has been conducted in the framework of the SPARC collaboration, experiment E125 of FAIR Phase-0 supported by GSI. It is further supported by the Extreme Matter Institute EMMI and by the European Research Council (ERC) under the European Union's Horizon 2020 research as well as by the innovation programme (Grant No 682841 "ASTRUm") and the grant agreement n° 6544002, ENSAR2. We acknowledge substantial support by ErUM-FSP APPA (BMBF n° 05P19SJFAA) too.

[1] A Gumberidze *et al*. 2005 *Phys.Rev.Lett*. **94** 223001

* E-mail: binghui.zhu@uni-jena.de

Collisional-radiative model of the visible spectrum of W^{13+} ion

Y. L. Liu[1], X. B. Ding[1]*, F. L. Zhang[2], Y. Yang[3], K. Yao[3], L. Zhang[2], F. Koike[4], I. Murakami[5], D. Kato[5], H. A Sakaue[5], and C Z Dong[1]

[1]Key Laboratory of Atomic and Molecular Physics and Functional Materials of Gansu Province,College of Physics and Electronic Engineering, Northwest Normal University, Lanzhou, 730070, P. R. China
[2]Institute of Plasma Physics, Chinese Academy of Sciences, Hefei 230000, China
[3]Key Laboratory of Applied Ion Beam Ministry of Education, Institute of Modern Physics, Fudan University, Shanghai 200433, China
[4]Department of Physics, Sophia University, Tokyo 102-8554, Japan
[5]National Institute for Fusion Science, National Institutes of Natural Sciences, Toki, Gifu 509-5292, Japan

Synopsis The visible spectrum of W^{13+} ion was investigated by collisional-radiative model (CRM) with the implementation of relativistic configuration interaction (RCI) method. The M1 transition wavelength of the ground doublet was assigned to 549.5 nm according to the present theoretical calculation.

The knowledge of the atomic structure, properties, kinetic process, and emission spectrum of moderate ionization tungsten ions are very important for the diagnosis of the edge and divertor plasma in the next generation fusion reactor, such as ITER. The W^{13+} ion and adjacent ions were predicted to be observed in these region. Thus, their atomic data and properties are necessary for the future application. Z. Zhao et al. measured the visible spectrum of W^{13+} ion on Shanghai EBIT and assigned the peak around 549.5±0.06 nm as the M1 transition between the ground configuration ($4f^{13}5s^2$) fine structure levels[1]. Later, Y. Kobayashi et al. made a further observation on the visible spectra of W^{12+} - W^{14+} ions on Tokyo EBIT[2]. They assigned another line at 560.25 nm to be the M1 transition of the fine-structure levels of the ground configuration of W^{13+} ion.

However, the ground configuration of W^{13+} ion has only a doublet level structure. The M1 transition wavelength of the ground doublet is the difference between the two energy levels. To clarify the confusion, the spectrum of the M1 transition of W^{13+} ion was investigated in the work.

The CRM includes important atomic processes, such as spontaneous radiative transitions, collision excitation, and deexcitation[3]. The configurations included in the CRM of W^{13+} ion are $4f^{13}5s5l(l = 0\text{-}4)$, $4f^{13}5p5l(l = 1\text{-}3)$, $4f^{12}5s^25l(l = 1,2)$, $4f^{12}5s5p^2$and $4f^{14}5l(l = 0\text{-}2)$. In order to take the configuration interaction effect into account, the configurations, such as, $4f^{13}5d5l(l = 2\text{-}4)$, $4f^{13}5f5l(l = 3,4)$, $4f^{13}5g^2$, $4f^{13}5d5g$, $4f^{13}5g^2$, and $4f^{13}5p5g$ are considered as interaction configuration to improve the accuracy of atomic data. The theoretical visible spectrum of the W^{13+} ion at T_e=280 eV and different electron densities is shown in Fig. 1. With the variation of the electron density, the peak around 549.5 nm becomes weaker while 560.25 nm peak become strong. According to the dependence of the intensity on the electron density, the M1 transition wavelength of the ground doublet of the W^{13+} ion should be 549.5 nm, rather than 560.25 nm.

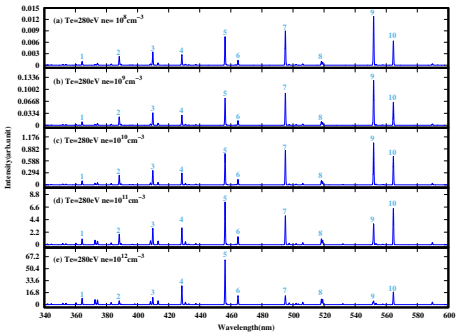

Figure 1. The M1 transition spectra of W^{13+} ion with different electron densities.

References

[1] Z Z Zhao *et al* 2015 *J. Phys. B* **48** 115004
[2] Y Kobayashi *et al* 2015 *Phys. Rev. A* **92** 022510
[3] X B Ding *et al* 2020 *Phys. Rev. A* **101** 042509

*E-mail: dingxb@nwnu.edu.cn

A new experimental apparatus for ion and electron impact studies on astrophysical ice analogues

P Herczku[1], D V Mifsud[1,2 *], Z Juhász[1], S T S Kovács[1], B Sulik[1], P A Hailey[2], Z Kaňuchová[3,4], A Traspas Muiña[5], S Ioppolo[5], R W McCullough[6], B Paripás[7] and N J Mason[2]

[1]Institute for Nuclear Research (Atomki), Debrecen, H-4026, Hungary
[2]Centre for Astrophysics & Planetary Science, University of Kent, Canterbury, CT2 7NH, UK
[3]Astronomical Institute, Slovak Academy of Sciences, Tatranska Lomnicá, SK-059 60, Slovakia
[4]INAF Osservatorio Astornomico di Roma, Monte Porzio Catone, RM-00078, Italy
[5]School of Electronic Engineering & Computer Science, Queen Mary University of London, London, E1 4NS, UK
[6]School of Mathematics & Physics, Queen's University Belfast, Belfast BT7 1NN, UK
[7]Department of Physics, University of Miskolc, Miskolc, H-3515, Hungary

Synopsis A new end-station, the Ice Chamber for Astrophysics-Astrochemistry (ICA), was commisioned recently at a Tandetron beamline of the Institute for Nuclear Research (Atomki) in Debrecen, Hungary. The apparatus has been dedicated for studying the chemical evolution and changes in physico-chemical properties of astrophysical ice analogues during ionising radiation and thermal processing.

Since the discovery of the first molecular species in the 1930s (see [1] and refs. therein), much interest has been devoted to the formation and fates of interstellar molecules. To study the formation processes and reactivity of of molecules, we have to simulate the interstellar environment. Astrophysical ice analogues have been processed with Lyman-α, vacuum- or extreme-UV photons, electrons and ions [2] for a long time. Experiments have revealed much information on the chemical reactivity. However, systematicity, repeatability, and reproducibility have sometimes been difficult to achieve [3,4].

Here we report a new end-station for ion irradiation studies relevant to experimental astrochemistry located at the Institute for Nuclear Research (Atomki) in Debrecen, Hungary.

The Chamber for Astrophysics- Astrochemistry (ICA) is designed to perform systematic studies wherein a selected number of parameters (e.g. ice thickness, morphology, temperature, projectile ion nature and energy, etc.) may be controlled and varied. The main advantage of the ICA set-up lies in its provision of four deposition substrates, for creating ice replicates under identical conditions. Thermal, ion and electron, processings are available, allowing for various combinations of them. Heavy ion beams in the mid-energy (0.2-18 MeV) range may be delivered to ices deposited on cold (20-300 K) ZnSe substrates. Those are vertically mounted on a copper holder connected to a closed cycle cryostat, a 360° rotation stage and a z-linear manipulator. The ions may cross the ice layer with small relative energy loss, or may get implanted to the ice. Irradiation induced physico-chemical changes are monitored by FTIR spectroscory. A temperature controller allows us to perform thermal-programmed desorption (TPD) studies on both non-irradiated and irradiated ices. Sublimating volatiles, particles sputtered during irradiation and desorbed molecules in TPD experiments are monitored by a quadrupole mass spectrometer (QMS). The ice layers are created through background deposition. The gas-mixtures are prepared in a dosing-line and introduced in the main chamber by means of an all leak metal valve. The set-up is equipped with an electron gun, it provides electron beams of a few μA in the 5 eV – 2 keV energy range.

At the conference, we will present preliminary results of e^-, H^+ and S^{2+} impact on ice mixtures deposited at 20 K.

* E-mail: herczku.peter@atomki.hu

References

[1] PA Feldman, Can. J. Phys. 79, 89 (2001)
[2] G Strazzulla, et al, Nucl. Phys. News 27, 23 (2017)
[3] PA Gerakines, RL Hudson, Astrophys. J. Lett. 808, L40 (2015)
[4] GA Baratta, ME Palumbo, Astron. Astrophys. 608, 81 (2017)

Status of the FISIC platform for future ion-ion collisions

E Lamour[1]*, A Méry[2], L Adoui[2], A Bräuning-Demian[3], J-Y Chesnel[2], A Gumberidze[3], C Hahn[4], A Lévy[1], M Lestinsky[3] S Macé[1], C Prigent[1], JM Ramillon[2], J Rangama[2], P Rousseau[2], D Schury[1], U Spillmann[3], S Steydli[1], Th Stöhlker[3,4,5], M Trassinelli[1] and D Vernhet[1]

[1]Institut des Nanosciences de Paris, Sorbonne Université, CNRS UMR 7588, Paris, 75005, France
[2]CIMAP, CEA/CNRS/ENSICAEN/Université de Caen Normandie, Caen, 14050, France
[3]GSI Helmholtzzentrum für Schwerionenforschung, Darmstadt, 64291, Germany
[4]Friedrich-Schiller-Universität Jena, Jena, 07743, Germany
[5]Helmholtz-Institut Jena, Jena, 07743, Germany

Synopsis In ion-ion collisions for Atomic Physics, the control of both ion charge states before and after the interaction is crucial to investigate the many-body electronic dynamics in an energy regime where cross sections of elementary electronic processes are rather unknown, both experimentally and theoretically. We present the status of a mobile platform that will deliver keV/u energy ion beams and that will be easy to install at another ion facility that provide MeV/u ion beams.

Ion-ion collisions provide a unique scenario for testing our knowledge of fundamental electronic processes such as capture, ionization and excitation [1]. By scanning the initial charge state of each ion partner, we even have the opportunity to investigate the quantum dynamics of N-body systems. Indeed, besides the possibility to reach the pure three-body problem (a bare ion on a hydrogen-like one) as a benchmark, the role of additional bound electrons -added one by one to one or to both partners- should permit to quantify various effects such as the role of electron-electron interactions or/and of multi-electron processes for instance. For such studies, crossed-beam experiments must be performed at different collision energies since the probabilities of electronic processes strongly depend on the collision energy. So far only results have been obtained in the low-energy domain where electron capture is the dominant process [2].
To go further and investigate the unexplored regime where the ion stopping power (energy transfer) is maximum, we develop a low-energy (keV/u) ion mobile platform divided into two parts. The first one, upstream the collision zone, is equipped with an ECR ion source connected to a beam transport line well-adapted to shape the beam and clean it from non-desired charge states thanks to a purification system [3]. The second part of the platform includes the collision chamber and an ion spectrometer to analyse the different charge states of the low-energy ion products that will be tested at the ARIBE facility (GANIL in Caen) and at the SIMPA installation (INSP/Sorbonne Université in Paris). Proposed experiments at CRYRING@ESR [4] to perform fast (MeV/u) ion - slow (keV/u) ion collisions and the status of the integration of our platform (Figure 1) into the ring will be presented.

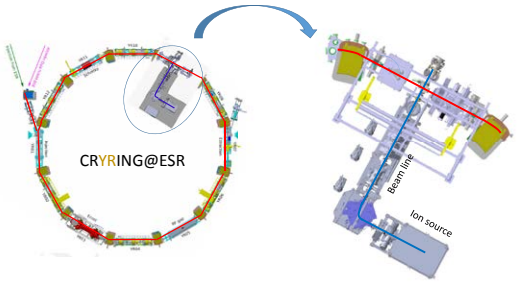

Figure 1. Ion-ion experiments at CRYRING@ESR (FAIR/GSI). The low-energy ion platform is connected at 90 degrees with respect to the ion beam direction in the CRYRING@ESR.

References

[1] Aumayr F *et al* 2019 *J. Phys. B* **52** 171003
[2] Bräuning H *et al* 2005 *J. Phys. B* **38** 2311
[3] Schury D *et al* 2019 *Rev. Sci. Instrum.* **90** 083306
[4] Lestinsky M *et al* 2016 *Eur. Phys. J* **225,** 797-882

*E-mail: emily.lamour@sorbonne-universite.fr

APEX: A collaboration on Atomic Processes at EXtremes

X Ma[1,2 *], S F Zhang[1,2], W Q Wen[1,2], J Yang[1,2], X L Zhu[1,2], S C Yan[1,2], R T Zhang[1,2], S Y Xu[1,2], D B Qian[1,2], R Cheng[1,2], and APEX Collaboration

[1]Institute of Modern Physics, Chinese Academy of Sciences, Lanzhou, 730000, China
[2]University of Chinese Academy of Sciences, Beijing, 100049, China

Synopsis The collaboration on Atomic Processes at Extremes (APEX) is introduced and calls for participation.

APEX is an international collaboration for scientific research on **A**tomic **P**rocesses at **EX**treme conditions based on the large scale modern accelerator complex HIRFL and HIAF. HIRFL is the Heavy Ion Research Facility in Lanzhou which is in operation currently. HIAF is the High Intensity heavy ion Accelerator Facility in Huizhou, in the coast area of South China, which is under construction and will be ready for day-one experiment in 2025[1]. The logo for APEX collaboration is shown in Fig. 1.

The collaboration research topics include experimental and theoretical investigations of quantum electrodynamic (QED) effects in strong Coulomb fields, even the decay of QED vacuum at super critical electromagnetic fields beyond Schwinger limit, the ultrafast dynamics in collisions of highly charged ions /XUV photons /electrons with atoms, molecules and clusters, precision measurements on electron-ion reaction rates which are important to astrophysics plasmas and fusion plasmas, the ion beam-plasma interactions to understand high energy density matter produced by intense heavy ion beams and their properties, and nuclear properties of radioactive ions using precision atomic spectroscopy, etc. The research topics and the structure of APEX are presented in Fig. 2.

The APEX research program aims at a better understanding of the universe since, as it is already known, more than 95% of visible matter in the universe is in plasma state, where high temperature, strong couplings, extremely strong fields, and highly charged ions prevail. Similar extreme conditions could also be found in artificial plasmas, like fusion plasma driven by strong lasers or intense ion beams, etc. More information can be found at the websites below: http://apex.impcas.ac.cn/, http://amdimp.impcas.ac.cn/

Figure 1. The logo for APEX collaboration.

References

[1] J. C. Yang, *et al*. 2013 *NIM B* **317**, 263
[2] X. Ma, *et al*. 2017 *NIM B* **408**, 169
[3] X. Ma, *et al*. 2020 *SCIENTIA SINICA Physica, Mechanica & Astronomica*, **50**, 112008

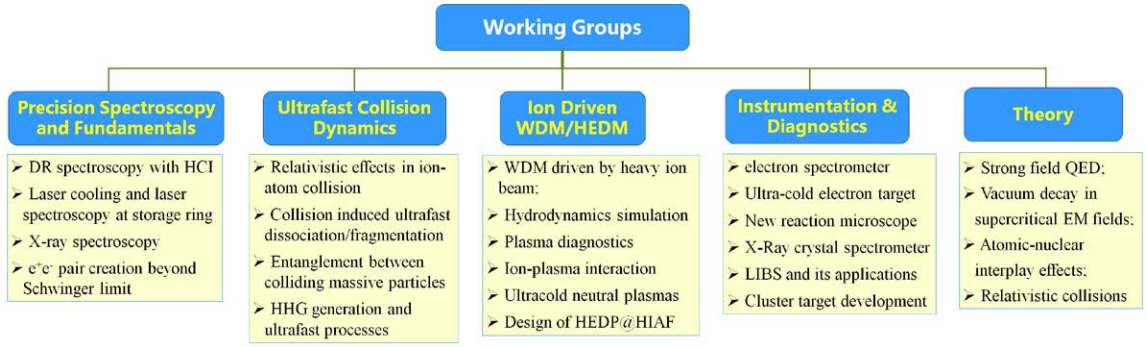

Figure 2. The proposed research directions for APEX collaboration.

* E-mail: x.ma@impcas.ac.cn

Neutral Particle Imaging for Beam Analysis at CRYRING@ESR

E B Menz[1,2,3]*, M Lestinsky[1], W Biela-Nowaczyk[4], S Buaruk[5], B Walasek-Höhne[1], A Reiter[1], C Krantz[1], Th Stöhlker[1,2,3]

[1]GSI Helmholtzzentrum für Schwerionenforschung, Darmstadt, 64291, Germany
[2]Helmholtz Institute Jena, Jena, 07743, Germany
[3]Friedrich Schiller University Jena, Jena, 07743, Germany
[4]Jagiellonian University, Institute of Physics, Poland
[5]Prince of Songkla University, Hat Yai District, Songkhla 90110, Thailand

Synopsis An imaging setup for neutral particles has been taken into operation at the CRYRING@ESR heavy-ion storage ring. The setup consists of a multi-channel plate (MCP), a phosophor screen and a camera and is used to determine the size of stored ion beams and the effect of electron cooling. This provides a much needed diagnostic tool for experiments using singly charged ions.

An important factor for successful experiments at storage rings is the ability to observe and optimise the electron cooling of a stored ion beam. CRYRING@ESR is equipped with an ionization profile monitor (IPM), to assess the quality of electron-ion overlap in the electron cooler by minimizing the widths of the transverse profiles of the circulating ion beam. However, inherent electric fields inside the IPM produce a distortion of the closed orbit. For several proposed experiments at CRYRING@ESR, beam injection is achievable only from source potential of the local injector beamline. For these very soft beams, the IPM would destroy the closed orbit and thus has to be turned off. This leaves only a very faint and ambiguous Schottky signal as an aid for beam tuning. This "blind spot" of the existing beam diagnotics setup meant that the establishment and optimisation of electron cooling of such beams was both difficult and time consuming. To close this gap in beam diagnostics a new imaging system has been implemented.

One loss channel for stored ions is charge exchange (CX) with residual gas [1]. A characteristic of CX is the negligible momentum transfer, which means that down-charged product particles retain their initial trajectory making them easy to distinguish from other important loss channels such as electron stripping or Rutherford scattering. Observing beam fragments after neutralization gives access to the beam profile and the position of the stored ion beam.

The imaging setup consists of a double stack of multi-channel plates in a chevron configuration that are installed at a free zero degree port in the dipole chamber of one of the main ring magnets. Neutral atoms striking the front-end of the MCP produce an electron cascade along the channels. The electrons exiting the back-end are further accelerated onto a P43 phosphor screen were they produce visible light. Signal readout is done using a camera system and delivers instant visual feedback to the operators.

The setup was successfully taken into operation using a Mg^+ beam and showed its usefulness in establishing electron cooling.

Acknowledgement: Results presented here are based on a SPARC R&D project in the context of FAIR Phase-0 at GSI, Darmstadt (Germany).

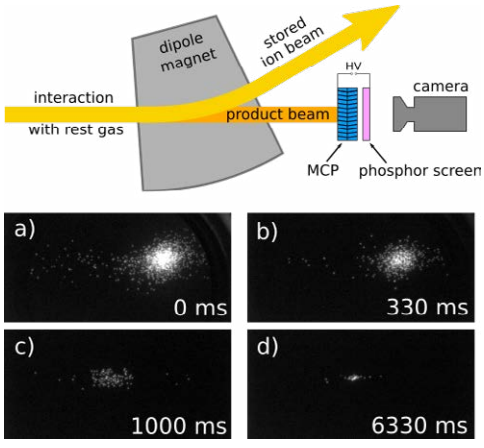

Figure 1. Measurement principle and images recorded during electron cooling of a Mg^+ beam.

References

[1] Schlachter A S *et al* 1983 *Phys. Rev. A* **123** 012021

*E-mail: e.menz@hi-jena.gsi.de

The confined Helium atom with a moving nucleus

M F Morcillo Arencibia[1]*, J M. Alcaraz-Pelegrina, J M Randazzo[2]†, A J Sarsa Rubio[1]

[1]Departamento de Física, Universidad de Córdoba, España.
[2]Consejo Nacional de Investigaciones Científicas y Técnicas, Argentina.

Synopsis We explore convergence of Configuration Interaction expansions for one and two-electron atomic systems under off-center spherical confinement, for two different choices of the spherical coordinate systems, i. e. the one associated to the atom and the one associated to the spherical cavity, where a partial wave decomposition is used both for the off-center potential and the electronic repulsion.

Endohedrally confinement of atomic systems has been a subject of active research during the recent rears [1, 2]. Besides a few exceptions [3, 4], the system is studied under spherical confinement, i. e. where the atom is located at the center of the spherical potential.

In this work we address the problem of one and two electron atoms under off-centered spherical confinement using two different spherical coordinate systems: a) the one associated to the Coulomb charge of the atom and b) the one associated to the spherical cage. Off-centered treatment imply that the potential which is not centered (the confinement in case a) and the Coulomb charge in case b)) need to be treated through a partial wave expansion approach, which gives rise to different levels of approximations for the wave-functions.

The purpose of this study is the characterization of the convergence behaviour of the wave functions and energies as a function of the displacement in each one of the aforementioned approximations for a Helium atom confined by a combination of two Woods-Saxon potentials in order to model a C_{60} fullerene cage [5].

Our results show a better performance of the first scheme. In Figure 1 we plot the energy of the ground state of the He atom as a function of the position of the nucleus inside the fullerene cage for different number of partial waves in the expansion. A good accuracy on the energy is obtanied in the full range of positions of the nuclei with wave functions including up to $L = 4$ in the partial wave expansion. The minimum value of the energy coincides with the position of the structure of the confining cavity close to the nucleus, therefore this indicates that the atom tend to be in that place.

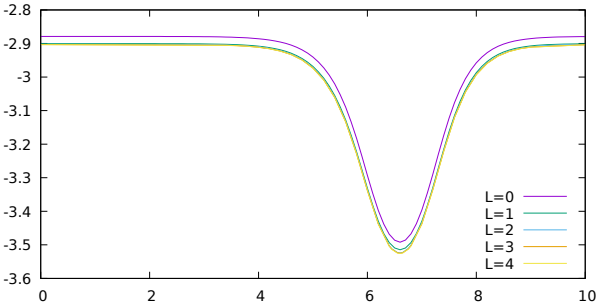

Figure 1. Convergence of the ground state energy of the confined Helium atom with a moving nucleus as a function of the displacement and for different partial waves.

References

[1] Amusia M Y, Liverts E Z and Mandelzweig V B 2006 *Phys. Rev. A* **74** 042712.
[2] Frapiccini, A L and Mitnik D M 2021 *Eur. Phys. J. D* **75** 41.
[3] Neek-Amal M, Tayebirad G and Asgari R 2007 *J. Phys. B* **40** 1509.
[4] Randazzo J M and Rios C A 2016 *J. Phys. B* **49** 235003.
[5] Martínez-Flores C and Cabrera-Trujillo R 2018 *J. Phys. B* **51** 055203.

*E-mail: f22moarm@uco.es
†E-mail: randazzo@cab.cnea.gov.ar

Studies of DD reactions in Deuterated Crystals at HELIS in astrophysical energy region

O D Dalkarov[1], M A Negodaev[1], A S Rusetskii[1]
T.A.Tukhfatullin[2*]

[1]Lebedev Physical Institute RAS, 119991, Moscow, Russia
[2]Tomsk Polytechnic University, 634050, Tomsk, Russia

Synopsis The results of the computer simulation and comparison with experiments of the orientation effect in the D+D reaction yield in dense targets.

The cross sections for nuclear fusion reactions at low energies are of considerable interest, both for the creation of new generation power plants and for understanding the processes inside stars, see [1-3] and references therein. The significant effect of the fusion reaction yield enhancing in dense targets at energies in the Gamow peak is attributed to the screening effect of ions by target electrons. It makes easier to overcome the Coulomb barrier in the synthesis of nuclei and increases the yield of the reaction. Recent experiments at HELIS facility [1-3] with 10 - 25 keV deuteron (D) beam on D-enriched polycrystalline Ti, Pd and CVD-diamond targets revealed the new feature – orientation effect on the yield of the reaction D+D → n (2.45 MeV)+ ^{3}He(0.8 MeV).

The computer simulations based on the computer code BCM-2.0 [4] qualitatively describe the flux-peaking effect on reaction yield (Fig.1). Here, we present comparative analysis of experimental data on channeling effect to DD reactions yield from CVD-diamond and Pd and improved computer code to consider anisotropy of the DD reaction products yield. The new schemes of the experiments with one and double CVD diamond targets are suggested.

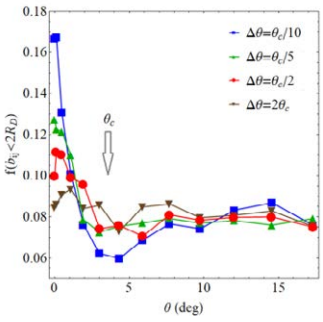

Figure 1. Simulations of D (200) channeling in Pd: fraction of trajectories $f(b_{ij}<2R_D)$ versus incident angle θ for different angular spread $\Delta\theta$ of incident beam. Here, b_{ij} – is impact parameter of D moving in jth trajectory with nearest ith D located in (200) Pd channel, and R_D the D radius. The arrow indicates the critical channeling angle θ_c=3.58°.

References

[1] Bagulya A V *et al* 2015 *Nucl. Instrum. Methods Phys. Res.* **B 355** 340
[2] Bagulya A V *et al* 2017 *Nucl. Instr. and Meth.in Phys. Res.* **B 402** 243
[3] Dalkarov O D *et al* 2019 *Phys. Rev. Accel. and Beams* **22** 034201
[4] Abdrashitov S V *et al* 2017 *Nucl. Instrum. Methods Phys. Res.* **B 402** 10 6

* E-mail: tta@tpu.ru

Half-Wavelength-Crystal channeling of relativistic heavy ions and its possible application

O V Bogdanov[1], T A Tukhfatullin[1*], H Geissel[2], N Kuzminchuk-Feuerstein[2], S Purushothaman[2] and C Scheidenberger[2]

[1]Tomsk Polytechnic University, Tomsk, 634050, Russia
[2]GSI, Darmstadt, 64278, Germany

Synopsis The results of computer simulations of half-wavelength crystal channeling of high-Z Relativistic Heavy Ions and its possible application for beam deflection and focusing.

In a half-wavelength crystal (HWC) a channeling particle experiences "mirroring" (HWC channeling) due to only one collision with a crystallographic plane. The HWC channeling was observed for 400 GeV protons at CERN-SPS [1] and for 255-MeV electrons at the SAGA-LS Facility [2, 3]. Compared to protons and electrons, in the case of Relativistic Heavy Ions (RHI), there appear two additional parameters: ion charge Ze and mass number A. The channeling critical angle becomes sensitive to $(Z/A)^{1/2}$. The computer simulations of HWC channeling of low-Z isotopes [4] revealed the remarkable isotopic effect. Here, we present the results of computer simulations of HWC channeling of high-Z RHI (^{129}Xe, ^{208}Pb, ^{238}U) with almost the same values of $(Z/A)^{1/2}$ in Si, Ge and W crystals, using the computer code BCM-2.0 [5]. The assembly of N sequentially placed and rotated by the critical channeling angle HWC increases almost N times the deflection angle. Fig. 1 shows simulated 2D beam intensity diagram of ^{238}U RHI passed through the two (200) tungsten HWC as a function of the crystal rotation angle θ_l and of the beam deflection angle $\theta_{def.}$

The applications of HWC channeling for RHI beam deflection and focusing on the downstream target are discussed, in view of atomic physics experiments with RHIbeams planned for Super-FRS Experiment Collaboration [6].

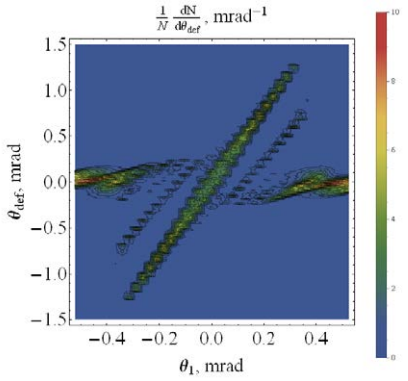

Figure 1. Beam intensity diagram of 300 MeV/u ^{238}U RHI passed through the two (200) tungsten HWC as a function of the crystal rotation angle θ_l and of the beam deflection angle θ_{def} for incident beam with angular spread $\Delta\theta = \theta_c/10 = 0.034$ mrad

References

[1] Scandale W *et al* 2014 *Phys. Lett.* **B 734, 1**
[2] Takabayashi Y *et al* 2015 *Phys. Lett.* **B 751, 453**
[3] Takabayashi Y *et al* 2015 *Nucl.Instr. and Meth.* **B 355, 188**
[4] Bogdanov O V *et al* 2020 *Phys. Lett.* **B 802 135265**
[5] Abdrashitov SV *et al* 2017 *Nucl. Instr. and Meth.* **B 402, 106**
[6] Geissel H *et al* 2017 *GSI Scientific Report* 179

* E-mail: tta@tpu.ru

HWC Channeling of Relativistic Isotopes

O V Bogdanov[1], T A Tukhfatullin[1*], H Geissel[2], N Kuzminchuk-Feuerstein[2], S Purushothaman[2] and C Scheidenberger[2]

[1]Tomsk Polytechnic University, Tomsk, 634050, Russia
[2]GSI, Darmstadt, 64278, Germany

Synopsis Result of computer simulations of isotopic effect in half-wavelength crystal channeling in different crystals and for isotopes energies.

A half-wavelength crystal (HWC) is a thin crystal where a channeling particle experiences only one collision with a crystallographic plane ("mirroring") during passing through a crystal. The HWC channeling was observed for 400 GeV protons at CERN-SPS [1] and for 255-MeV electrons at the SAGA-LS Facility [2]. Recent computer simulations [3] of HWC channeling in (100) Si crystal of low-Z H (p, d, t) and Li (^{6}Li, ^{9}Li, ^{11}Li) isotopes with kinetic energy E_k =300 MeV/u revealed that the angular distributions of transmitted through HWC isotopes are sensitive to a mass number A, i.e. there appears an isotopic effect, Fig.1.

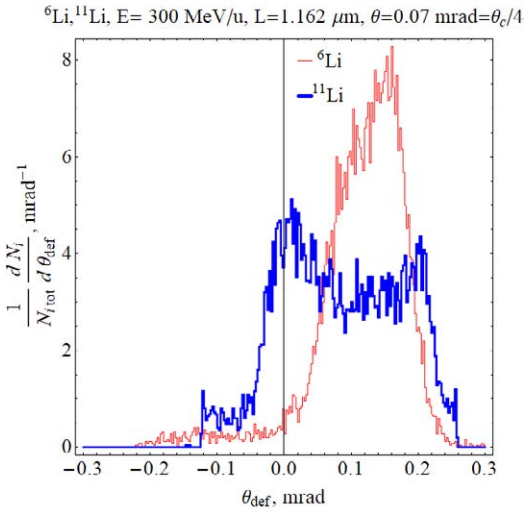

Figure 1. The distributions in deflection angle θ_{def} of 300 MeV/u ^{6}Li (red thin line) and ^{11}Li (blue bold line) passed through a (220) Ge HWC.The angle of incidence is a quarter of critical channeling angle:$\theta=\theta_c/4$=0.07 mrad.

In Fig.1, the crystal thickness L=1.162 μm just fits the requirement to HWC thickness for E=300 MeV/u ^{6}Li isotopes and their mirroring is clearly seen. Changing E of mixed isotopic beam at fixed L or changing L at fixed E allows spatial separation of isotopes. At greater E, the L of HWC becomes greater which is important for operation with very thin crystals. Here, we present extended computer simulations of isotopic effect in HWC-channeling in different crystals and for isotopes energies up to 25 GeV/u, planned at Super-FRS GSI/FAIR [4].

References

[1] Scandale W *et al* 2014 *Phys. Lett.* **B 734 1**
[2] Takabayashi Y *et al* 2018 *Phys. Lett.* **B 785 347**
[3] Bogdanov O V *et al* 2020 *Phys. Lett.* **B 802 135265**
[4] Conceptual Design Report for the Scientific Program of the Super-FRS Experiment Collaboration. *GSI Report* 2016-3.

* E-mail: tta@tpu.ru

Very grazing incidence effects on fast He diffraction from KCl(001)

G A Bocan[1]*, H Breiss[2], S Szilasi[2], A Momeni[2,3], E M Staicu Casagrande[2], M S Gravielle[4], E A Sánchez[1], and H Khemliche[2]

[1]Instituto de Nanociencia y Nanotecnología - Nodo Bariloche (CONICET-CNEA) and Instituto Balseiro (U. N. Cuyo), Centro Atómico Bariloche, S.C. de Bariloche, 8400, Argentina
[2]Université Paris-Saclay, CNRS, Institut des Sciences Moléculaires d'Orsay, Orsay, 91405, France
[3]CY Cergy Paris Université, Cergy, F-95000, France
[4]Instituto de Astronomía y Física del Espacio (CONICET-UBA), Buenos Aires, C1428EGA, Argentina

Synopsis We present theoretical and experimental evidence of an anomalous behavior of the KCl(001) surface corrugation obtained from diffraction patterns of very grazing He atoms. Experiments show an impressive $\gtrsim$85% increase for incidence along ⟨110⟩; an intriguing feature not due to van der Waals (vdW) interactions but to the combination of dynamical effects and the evolution of He-cation and He-anion interactions with the normal He-surface distance Z. This feature, not previously analyzed on alkali-halide surfaces, may favor the alignment properties of weakly interacting overlayers.

In this contribution we probe the corrugation of the KCl(001) surface using grazing incidence fast atom diffraction (GIFAD) [1, 2]. For incidence of ^{4}He projectiles along ⟨110⟩ (Fig. 1a) the corrugations ΔZ independently obtained from the experimental and simulated (surface initial value representation, SIVR [3]) GIFAD patterns intriguingly increase with decreasing normal energy. The intrinsic corrugation ΔZ^{PES}, obtained from the DFT-based He-KCl(001) potential energy surface (PES), also shows an increasing behavior. We explain this increase in terms of two factors: a) The different evolution of the He-K^+ and He-Cl^- interactions, which result in the increase of ΔZ^{PES} and b) Dynamical effects due to the softness of the He-surface interaction. This latter contribution corresponds to the difference between the SIVR corrugation (ΔZ^{SIVR}) and ΔZ^{PES}. In contrast, for incidence along ⟨100⟩ ΔZ^{PES} monotonously decreases with decreasing $E_\perp$ while the experimental and SIVR corrugations show a slight increase for $E_\perp < 30$ meV.

Despite the stronger dynamical effects for ⟨110⟩ (already visible at $E_\perp = 200$ meV), GIFAD provides satisfactory structural information for both channels in the $E_\perp > 30$ meV range. For lower normal energies dynamical effects take hold, resulting in both the sharp increase for ⟨110⟩ [4] and the change in the slope sign for ⟨100⟩. These features can ultimately be traced to the presence of shallow attractive regions in the PES.

*E-mail: gisela.bocan@cab.cnea.gov.ar

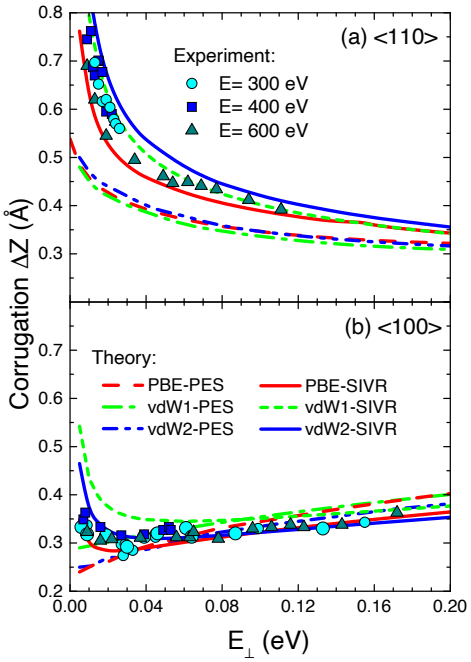

Figure 1. Experimental and theoretical corrugation (see text for details). "PBE" curves do not include vdW interactions. "vdW1" and "vdW2" do, with two different approaches.

References

[1] Schüller A *et al* 2007 *Phys. Rev. Lett,* **98** 016103
[2] Rousseau P *et al* 2007 *Phys. Rev. Lett,* **98** 016104
[3] Gravielle M S *et al* 2014 *Phys. Rev. A* **90** 052718
[4] Bocan G A *et al* 2020 *Phys. Rev. Lett.* **125** 096101

Probing surface magnetism with highly charged ions by X-ray spectroscopy

P Dergham[1*], M Werl[2], D Vernhet[1], E Lamour[1], C Prigent[1], F Aumayr[2], R A. Wilhelm[2], S Steydli[1], S Macé[1], M Trassinelli[1]

[1]Sorbonne Université, Institut des NanoSciences de Paris (INSP), Paris, 75005, France
[2]TU Wien, Institute of Applied Physics, Vienna, 1040, Austria

Synopsis: We report on a new set-up to investigate magnetic surface states via X-ray spectroscopy of highly charged ions that collide at grazing incidence. An atomic cascade code taking into account spin transfer during the ion radiative relaxation will be presented.

Study of magnetic domains on the surface of materials with the use of highly charged ions (HCI) represents an alternative to conventional methods such as the Kerr effect, X-ray dichronism and neutron scattering more sensitive to the bulk magnetization properties. Grazing collisions of HCI on surfaces are known to be sensitive to the first atomic layers offering the possibility to characterize the surface magnetic state. When a HCI comes close enough to the surface, electrons are transferred from the surface to the ion excited states while conserving their spin polarization [1]. The study of the ion relaxation via radiative and Auger processes that follows gives then information on the magnetization properties.

Previous experiments have detected magnetic domains by studying the Auger emission [2]. Only qualitative results can be obtained in this context due to the complexity of Auger spectra and the influence of the material work function. X-ray spectroscopy is expected to provide more quantitative information. The goal of our project is to probe the surface magnetization state by investigating the X-ray emission of HCIs for a quantitative and deep characterization of unknown magnetic properties.

In that respect, we have built a new set-up (Figure 1) that is connected to our SIMPA facility (acronym for multi-charged ion source in Paris) that delivers keV/u ion beams. A first experiment will be performed with hydrogen-like argon ions colliding on a monocrystalline nickel sample for a proof of principle. In a second step, coincidence measurements of the X-ray emission with the final ion charge state will permit, in particular, to exclude Interatomic Coulombic decay, recently highlighted by Aumayr et al. [3], which do not conserve the spin state. The study will be then extended to other more complex samples like FeRh that has an antiferrognatic phase at ambiant temperature.

One critical aspect is the possible loss of information of the captured electron spin orientation due to the atomic cascade in the ion relaxation processes. A cascade code based on Kirchner's past work [4] is under development. With appropriate approximations, spin transfer and depolarization are taken into account and first predictions from this code will be presented for different ion types and populated states.

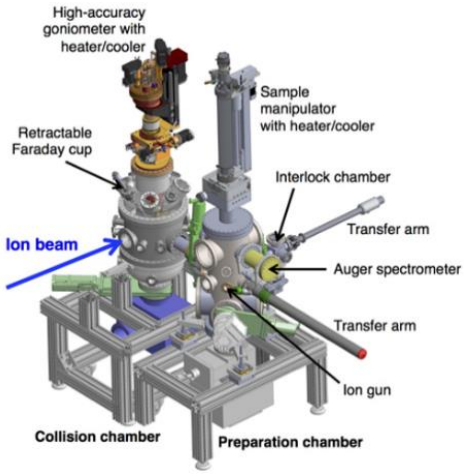

Figure 1. The new setup with the ion collision chamber and the sample preparation one.

* E-mail: perla.dergham@insp.jussieu.fr

References

[1] H. Winter 2002 *Phys. Rep. 367, 387*
[2] M. Unipan *et al.* 2006 *Phys. Rev. Lett. 96, 177601*
[3] R.A. Wilhelm *et al. 2017 Phys. Rev. Lett. 119, 103401*
[4] A Salehzadeh and T Kirchner 2013 *J. Phys. B: At. Opt. Phys.*46 025201

Sodium isocyanide: helium potential energy surface and astrophysical applications

C. Gharbi[1,2]* , Y. Ajili[3] , D. Ben Abdallah[1], M. Hochlaf[2]

[1]Laboratoire de Spectroscopie et Dynamique Molculaire,Universit de Tunis, Ecole Nationale Suprieure d'Ingnieurs de Tunis, 5 Av Taha Hussein, 1008 Tunis,Tunisia
[2]Universit Gustave Eifel, COSYS/LISIS, 5 Bd Descartes,77454 Champs-sur-Marne, France
[3]Laboratoire de Spectroscopie Atomique, Molculaire et Applications LSAMA, Universit de Tunis El Manar,Tunis, Tunisia

Synopsis : We presente a new 2D potential energy surface for l-NaNC-He($X^1\Sigma^+$) along the intermonomer Jacobi coordinates. This PES is incorporated later into dynamical computations in order to deduce the rotational excitation cross-sections and coefficient rates of NaNC colliding with He. The scattering calculations were performed, via close coupling (CC) and coupled state (CS) approach.

Abstract

In this work, we generated the two-dimensional potential energy surface (2D-PES) of the l-NaNC–He van der Waals interact-ing system. The electronic computations are done at the CCSD(T)-F12 [1, 2]/aug-cc-pVTZ [3, 4] level. This 2D-PES exhibits a unique shallow minimum for helium approaching l-NaNC from the Na atom side. Afterward, we derived an analytical form for this ab initio 2D-PES, which is incorporated into quantum scattering code to compute the rotational (de-)excitation cross sections (rate coeicients) of l-NaNC by collision with He atom for total energies up to 2000 cm^{-1} (from 5 to 300 K). The propensity rules that favor $\triangle$j=–1 transitions are less pronounced than in the case of t-NaCN isomer. Our data may be used for the determination of the abundances, in astrophysical media, of the candidate isomer l-NaNC with respect to those of the already detected t-NaCN isomer. We also performed comparison with the astrophysical relevant Al- and Mg-bearing (iso) cyanide systems interacting with He.

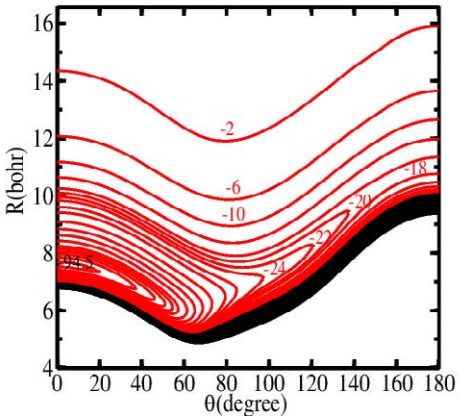

Figure 1. Two-dimensional contour plots of the potential energy surface of l-NaNCHe as a function of R and θ. The energies are in cm^{-1}.

References

[1] Adler TB *et al* 2007 *J. Chem. Phys.* **127** 221106
[2] Knizia G *et al* 2009 *J. Chem. Phys.* **130** 054104
[3] Dunning TH 1989 *J. Chem. Phys.* **90** 1007
[4] Kendall RA *et al* 1992 *J. Chem. Phys.* **96** 6796

*E-mail: chaimagharbi27@hotmail.com

The influence of the crystal temperature on grazing-incidence fast atom diffraction from LiF(001)

L Frisco[1*] **and M S Gravielle**[1†]

[1] Instituto de Astronomía y Física del Espacio (UBA-CONICET), Buenos Aires, C1428EGA, Argentina

Synopsis Grazing-incidence fast atom diffraction (GIFAD) is a sensitive method for surface analysis, which can be used even at high crystal temperatures. In this work we study the influence of temperature on GIFAD patterns from insulator surfaces by applying the phonon-surface initial value representation (P0-SIVR) approximation to the He-LiF(001) system. The P0-SIVR approach is a semiquantum method that includes the phonon contribution to the elastic scattering, allowing us to investigate the main features introduced by thermal lattice vibrations on GIFAD distributions.

We study thermal effects on angular distributions of fast He atoms grazingly scattered from LiF(001). This system has been extensively investigated with GIFAD at room temperature, becoming a prototype of the GIFAD phenomenon. However, most of the theoretical descriptions have been based on static crystal models, with the crystal atoms at rest at their equilibrium positions, while thermal vibration effects have been studied to a much lesser extent [1,2]

To investigate the influence of temperature on GIFAD we make use of the recently developed P0-SIVR approach [3]. The P0-SIVR method is based on the previous SIVR approximation for grazing scattering from a rigid surface, incorporating lattice vibrations (i.e., phonon contributions) through a quantum description of the surface given by the harmonic crystal model.

P0-SIVR projectile distributions for He-LiF(001) scattering under a fixed incidence condition are analyzed considering temperatures T in the 250–1000 K range. With the goal of determining the contribution of thermal lattice vibrations, P0-SIVR differential probabilities, as a function of the final azimuthal φ_f and polar θ_f angles, are contrasted with the angular distribution for a rigid crystal, derived within the SIVR approximation. Also, azimuthal and polar spectra of scattered helium atoms are separately analyzed as a function of T, finding different behaviors along both directions [4]. Present P0-SIVR results at room temperature are validated through the comparison with available experimental data.

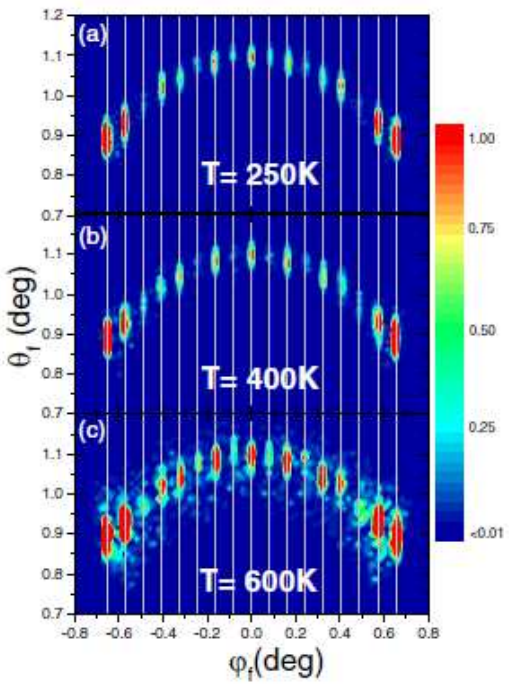

Figure 1. P0-SIVR distributions for 1.25 keV ^{4}He → <110> LiF(001) at the grazing angle θi = 1.1 deg, considering different temperatures T of the sample.

References

[1] Manson J R *et al* 2008 *Phys. Rev. B* 78 155408
[2] Roncin P *et al* 2017 *Phys. Rev. B* 96 035415
[3] Frisco L *et al* 2019 *Phys. Rev. A.* 100 062703
[4] Frisco L *et al* 2020 *Phys. Rev. A* 102 062821

* E-mail: lfrisco@iafe.uba.ar
† E-mail: msilvia@iafe.uba.ar

The role of internal dielectronic excitation in relaxation of Rydberg hollow atoms

Ł Jabłoński[1]*, D Banaś[1] P Jagodziński[1] A Kubala-Kukuś[1] D Sobota[1] I Stabrawa[1] K Szary[1] and M Pajek[1]†

[1]Institute of Physics, Jan Kochanowski University, Kielce, 25-406, Poland

Synopsis The M-X-rays emitted from Rydberg hollow atoms created in collisions of Xe^{q+} ions (q=23-36) with Be surface were measured and interpreted as the electric dipole nf-3d X-ray transitions. A contribution of the internal dielectronic excitation (IDE) process was extracted from the measured X-ray yields using the developed q-dependent X-ray emission model of relaxation. In particular, the contributions of IDE processes involving 3d and 3p electrons were determinded. The measured intensities of M-X-rays for a wide range of charge states are in good agreement with proposed model of relaxation process.

The beams of highly charged ions (HCI) produced in the electron beam ion source (EBIS) were used to study the X-ray emission from slow ($\sim$ 8 keV/q) Xe^{q+} (q=23-36) ions colliding with Be target. In such collisions the Rydberg hollow atoms (RHA) with ($n_c \sim 30$) are created in the ion neutralization process at the metal surface, which subsequently deexcite by various radiationless processes, including two-electron interatomic Coulombic decay (ICD) [1], internal dielectronic excitation (IDE) [2] and Auger transitions, and alternatively the radiative (R) transitions. In the present study the emitted X-rays were observed by a silicon drift detector (SDD) having energy resolution of about 60-100 eV for the observed X-rays of energy 0.5-3 keV. The measured M-X-rays were interpreted in terms of the electric-dipole allowed nf-3d transitions (Paschen series), including their hypersatellites. The measured X-ray spectra were interpreted in terms of the MCDF calculations implemented in the GRASP2K code [3]. We found that the observation of X-ray Paschen series having a sharp cut-off at $n \leq 10 - 20$) supports the scenario that in the first stage deexcitation of RHA proceeds via the ICD process [1]. For lower n-states both the radiative and Auger processes take place, while for about $n = 10$ the rapid IDE process is energetically possible, giving important contribution to M-X-ray emission, in particular, by creating additional vacancies in the M-shell. Performed MCDF calculations demonstrate that strong 4f-3d($5p^5$) hypersatellite observed for Xe^{35+} indicates formation of 3p vacancies in the M-shell by IDE(3p-4s), while the observed M-X-ray emission for Xe^{26+} ions, having no initial vacancies in the M-shell, is fully explained by their creation in the 3d state by IDE(3d-4p). The X-ray yields measured for Xe^{q+} ions of different charge states are well reproduced by the developed q-dependent X-ray emission model (q-XEM) allowing separation of contributions of IDE(3p-4s) and IDE(3d-4p) processes.

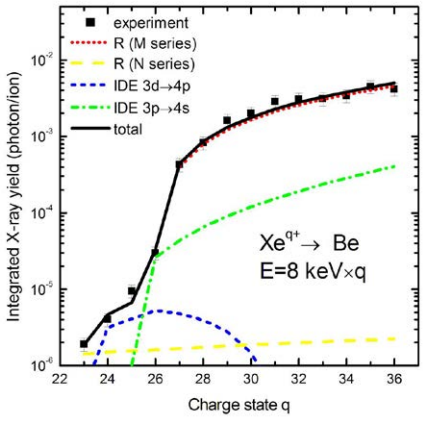

Figure 1. Measured charge state dependence of M-X-ray yield for Xe^{q+} ions showing contributions of direct radiative (R) and IDE processes.

References

[1] Wilhelm R *et al* 2017 *Phys. Rev. Lett.* **119** 103401
[2] Schuch R *et al* 1993 *Phys. Rev. Lett.* **70** 1073
[3] Jönsson P *et al* 2013 *Comp. Phys. Comm.* **184** 2197

*E-mail: l.jablonski@ujk.edu.pl
†E-mail: m.pajek@ujk.edu.pl

Coincidence measurements between secondary ions and scattered projectiles in collisions of MeV-energy heavy ion with submicron droplets

T Majima[1 *], S Mizutani[1], Y Mizunami[1], K Kitajima[1], H Tsuchida[1,2] and M Saito[1,2]

[1]Department of Nuclear Engineering, Kyoto University, Kyoto 615-8540, Japan
[2]Quantum Science and Engineering Center, Kyoto University, Uji 611-0011, Japan

Synopsis Positive and negative secondary ions emitted from ethanol microdroplet surfaces by 4-MeV C^{3+} were investigated using a new coincidence technique between secondary ions and forward-scattered projectiles. Notably, this technique enabled positive fragment ions to be observed by suppressing the strong background originating from gas-phase molecules more than 10^4-fold. Furthermore, the energy loss by scattered ions was used to evaluate the target thickness at a submicron level. The results highlight the unknown mechanism of "submicron effects" observed in secondary ion emission processes.

Fast heavy ions cause violent physicochemical reactions in materials along their trajectory. The molecular-level mechanism of complicated reactions has been studies for decades to gain a correct understanding of the phenomena and to further improve their application. Secondary ion emission from surfaces is a powerful probe of reactions in heavy-ion tracks. However, as mass spectrometry requires a high-vacuum environment, special experimental techniques are needed to be applied to volatile liquid surfaces.

Recently, we have developed an experimental system using microdroplets as an approach to performing mass spectrometry on liquid surfaces [1,2]. We have reported the generation of various types of product ions emitted from ethanol droplets[2]. However, only positive fragment ions could not be identified due to the large background from gas-phase molecules. Another goal of using droplet targets is to observe the reaction process at the nanoscale. However, droplets applicable in the current experiments have a broad size distribution, ranging from nanometers to micrometers in diameter.

In this study, we have developed a new coincidence technique between secondary ions and forward-scattered projectiles to solve the above problems[3]. With the removal of gas-phase background signals, secondary ion emission probabilities, including positive fragment ions, are obtained. Furthermore, the coincidence measurement provides selective information depending on the penetration length.

A schematic diagram of the experimental setup is shown in Fig.1. Correlations between the time-of-flight (TOF) of positive or negative secondary ions and the energy of forward-scattered ions are recorded.

The production of H^+, H_3O^+, $C_2H_5^+$, and EtO^+ ions was identified as major fragment ions. These ions except for H^+ are produced from protonated ethanol $EtOH_2^+$ through intermolecular proton transfer. The present results prove the competition between rapid hydrogen ion emission and intermolecular proton transfer accompanied by further fragmentation.

Furthermore, variations in secondary ion yield, mass distribution, and kinetic energies depending on the penetration length were observed below 1 μm. These results highlight the unknown mechanism of "submicron effects" observed in secondary ion emission processes as a new phenomenon.

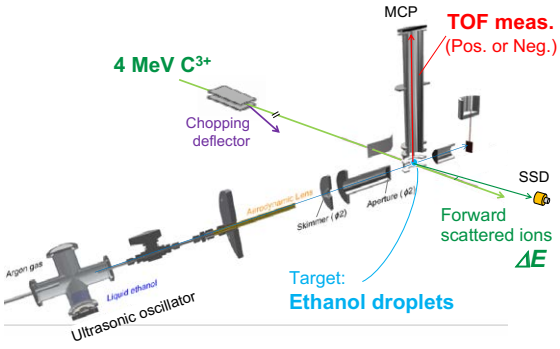

Figure 1. .Schematics of the experimental setup [3].

References

[1] Majima T *et al* 2015 *J. Phys. : Conf. Ser.* **635** 012021
[2] Kitajima K *et al* 2018 *Nucl. Instrum. Methods. Phys. Res., Sect. B* **424** 10
[3] Majima T *et al* 2020 *J. Chem. Phys.* **153** 224201

* E-mail: majima@nucleng.kyoto-u.ac.jp

Computer simulations of the spatial and temporal distribution of 1 MeV proton microbeam guided through a poly(tetrafluoroethylene) macrocapillary

G U L Nagy[1,2] *, Z T Gaál[1,2], I Rajta[1] and K Tőkési[1] †

[1]Institute for Nuclear Research (ATOMKI), Debrecen, 4026, Hungary
[2]University of Debrecen, Debrecen, 4026, Hungary

Synopsis We present computer simulations about the spatial and temporal evolution of the guided transmission of 1 MeV proton microbeam through an insulating macrocapillary. We found that at different phases of the transmission, different atomic processes result in the evolution of the beam distribution, including a scattering phase, a mixed phase and the stabilized, guided transmission, where the beam is concentrated into a small spot, and the transmitted protons keep their initial kinetic energy.

Ion beams are able to pass through insulating capillaries keeping their initial kinetic energy and charge state, even if the capillary target is tilted with respect to the incident beam and thus preventing geometrical transmission. The phenomenon is called ion guiding and caused by the self-organized charge-up of the insulating material. At the beginning the incident beam hits the inner capillary wall and deposits its charge on, which will repulse the ions arriving later due to the Coulomb interaction. Once a dynamical equillibrium is established between the charges being put on the surface and the leakage currents flowing away, a stable transmission is realized.

In the present work we performed computer simulations in order to investigate the dynamic features of the beam transmitted through an insulating macrocapillary. The incident beam was 1 MeV proton beam with 10 – 1000 pA intensity, focused down to a few µm. The length of the poly(tetrafluoroethylene) capillary target was 45 mm, the inner diameter was 800 µm, and the axis of the capillary was tilted to 1° relative to the axis of the incident beam, which ensured geometrical non-transparency.

The simulation is based on the combination of stochastic (Monte-Carlo) and deterministic methods. It involves 1) random sampling of the initial conditions, according to distributions generated by the widely used and freely available computer software packages, namely SRIM and WinTRAX, 2) the numerical solution of the governing equations for following the classical trajectory of the projectiles, and 3) the description of the field-driven charge migration on the surface and in the bulk of the insulator material.

We found that our simulation describes reasonably all of our previous experimental observations, indicating the functionality and reliability of the applied model. In addition, we found that at different phases of the beam transmission, different atomic processes result in the evolution of the beam distribution. First, in a scattering phase, the multiple small angle atomic scattering dominates in the beam transmission, resulting an outgoing beam into a wide angular range and in a wide energy window. Later, in a mixed phase, scattering and guiding happens simultaneously, with a continuously increasing contribution of the guiding. Finally, in the phase of the stabilized, guided transmission, a quadrupole-like focusing effect is observed, i.e. the transmitted beam is concentrated into a small spot, and the transmitted protons keep their initial kinetic energy.

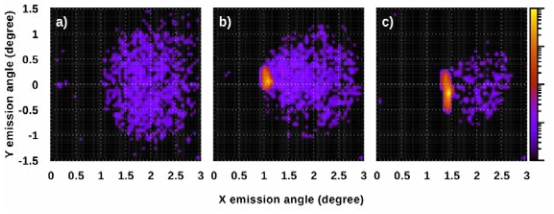

Figure 1. Simulated angular distributions of the transmitted beam, using 100 pA incident intensity. a) At the beginning of transmission; b) during the formation of the charge patch; c) at stabilized transmission.

References

[1] Nagy G U L, Gaál Z T, Rajta I and Tőkési K 2021 *Phys. Rev. A* **103** 042801

* E-mail: nagy.gyula@atomki.hu
† E-mail: tokesi.karoly@atomki.hu

Measuring charge exchange and energy loss of highly charged ions colliding with surfaces under grazing incidence

M. Werl[1]*, A. Niggas[1], F. Aumayr[1], and R. A. Wilhelm[1]

[1] TU Wien, Institute of Applied Physics, 1040 Vienna, Austria

Synopsis When a slow highly charged ion approaches a surface, it resonantly absorbs electrons into highly excited states. At small interatomic separations from the surface, the ion subsequently de-excites via intra-atomic decay; while at larger distances, the atom decays predominantly radiatively or via Auger processes. Previous experiments within our lab studied the charge exchange and energy loss of ions in transmission experiments. As a first step to study the radiative and Auger decay, small-angle-scattering experiments are performed with the same experimental setup.

When a highly charged ion (HCI) approaches a surface, electrons are resonantly absorbed by the ion into highly excited states, forming a *hollow atom*. At close distances from the surface, the hollow atom quickly decays (in the order of $\approx 10^{-15}$ s) via an intra-atomic Auger process known as interatomic Coulomb decay (ICD). [1] Due to this ultra-fast decay, the potential energy of the incident ion is deposited in the very first atomic layers of a surface. The rate Γ at which ICD occurs strongly decreases with the interatomic distance R between the projectile and the target ($\Gamma \propto \frac{1}{R^6}$). At larger distances from the surface, the atom will favor decay via radiative or Auger pathways.

In our lab at the TU Wien, a setup to irradiate samples with HCIs and measure the charge exchange as well as energy loss of the projectiles due to the interaction with the sample is present. [2] In this setup, the HCIs are first created in and then extracted from an electron beam ion source (EBIS). Kinetic energies are tunable in a range of 1-400 keV and charge states can be selected by means of a Wien filter. The ion beam is then focused onto a sample. A deflection plate and a Roentdek delay line detector (DLD) behind the sample measures the charge state and scattering angle distribution of the scattered ions. Their energy after the collisions (and therefore the energy loss) is determined using a time-of-flight (TOF) measurement from the sample to the DLD.

Up to this point, the spectrometer was used for transmission experiments with 2D materials, such as graphene. For future HCI-based analysis techniques, the x-ray and Auger-spectra of the projectiles are of interest. To ensure the projectile does not undergo ICD, scattering experiments under small angles of incidence are performed where small angle scattering trajectories are selected with the DLD. Preliminary results, showing the charge exchange and energy loss in small-angle-scattering experiments, will be shown in this presentation.

References

[1] Richard Wilhelm *et al* 2017 *Phys. Rev. Lett.* **119** 103401

[2] Janine Schwestka *et al* 2018 *Rev. Sci. Instrum.* **89** 085101

*E-mail: werl@iap.tuwien.at

Ionization potentials of the superheavy element Rg(Z=111) and its homolog element Au

T. C. Zhang, X. B. Ding*, C. Z. Dong

Key Laboratory of Atomic and Molecular Physics and Functional Materials of Gansu Province, College of Physics and Electronic Engineering, Northwest Normal University, Lanzhou 730070, P. R. China

Synopsis Ionization potential is one of the fundamental properties of the superheavy elements. In the present work, the ionization potentials (IP_1-IP_4) of the superheavy element $Rg^{q+}(q = 0, 1, 2, 3, 4)$ and it's homolog element Au are calculated by using the MCDF method. The relativistic effects, electron correlation, Breit interaction, and QED effects were included.

Elements with the atomic number greater than 103 are superheavy elements. The study on the superheavy elements has been a hot topic in both atomic physics and nuclear physics. Due to the superheavy elements have short half-life and low productivity, the experimental study on their atomic structure, physical, and chemical properties are very difficult. Meanwhile, the strong relativistic effects and electron correlation effects of the superheavy elements played important role on the difference of the physical and chemical properties. Therefore, precisely theoretical calculations may help us to understand these "unknown" elements. Especially, the accurate ionziation potential will be helpful for the laser resonance ionization technology.

The total energy of the ground states and ionization potentials of Rg^{q+} and $Au^{q+}(q = 0, 1, 2, 3, 4)$ are calculated by using GRASP2K code[1] based on the multi-configuration Dirac-Fock(MCDF) method. Firstly, a small configuration space was used to search for the the ground states of the Rg and Au atoms and ions. The valence electrons in {(n-1)d;ns} are excited into active space {(n-1)d;nsp;(n+1)spd} by single and double excitation to take the VV correlation into account. The Breit interaction and QED effect are also included perturbatively in this work. The calculated ground states of Au^{0+-4+} are consistent with the avaiable experiments. The calculated ground states of Rg^{0+-4+} ions are $[Rn]4f^{14}6d^97s^2\ {}^2D_{5/2}$, $[Rn]4f^{14}6d^87s^2\ {}^3F_4$, $[Rn]4f^{14}6d^77s^2\ {}^4F_{9/2}$, $[Rn]4f^{14}6d^77s^1\ {}^5F_5$, and $[Rn]4f^{14}6d^7\ {}^4F_{9/2}$, respectively, which agrees with the recent CIPT results[2].

Once the ground states of Rg ions have been determined, the ionization potentials are calculated by the large-scale calculations, in which the valence electrons in {(n-1)d;ns} are excited into active space {(n-1)d;nspf;(n+1)spdf; (n+2)spdf; (n+3)spdf; (n+4)spdf} by single and double excitation to consider the correlation effect between valence electrons. The calculated ionization potentials of Rg and Au (IP_1-IP_4) are given in Table 1. The diffence between the calculated IP and the available experimental results of Au ions are no more than 1 eV, and agrees well with CIPT results. There are still minor difference between CIPT and present resutls, which might caused by the lack of the core-core and core-valence correlation effects.

Table 1. Ionization potentials calculations using MCDF method for Rg and the homolog elements Au are presented in eV. △=|MCDF-Expt|.

	IP_s			
Ion	MCDF	Expt	△	CIPT[2]
$Au \rightarrow Au^{1+}$	8.72	9.23	0.51	9.40
$Rg \rightarrow Rg^{1+}$	10.21			11.17
$Au^{1+} \rightarrow Au^{2+}$	19.83	20.00	0.37	20.47
$Rg^{1+} \rightarrow Rg^{3+}$	20.63			21.32
$Au^{2+} \rightarrow Au^{3+}$	31.77			32.26
$Rg^{2+} \rightarrow Rg^{3+}$	30.40			
$Au^{3+} \rightarrow Au^{4+}$	45.54			45.74
$Rg^{3+} \rightarrow Rg^{4+}$	41.83			42.00

References

[1] P. Jnsson*et al* 2013 *Comput. Phys. Commun.* **184** 2197

[2] V.A.DzuBa *et al* 2020 *Phys. Rev. A.* **177.7** 597-622

*E-mail: dingxb@nwnu.edu.cn

Theoretical study of TEOP transition probabilities in He-like ions

K N Lyashchenko[1]*, O Yu Andreev[2,3]† and D Yu[1]‡

[1]Institute of Modern Physics, Chinese Academy of Sciences, Lanzhou 730000, China
[2]Department of Physics, St. Petersburg State University, 7/9 Universitetskaya nab., St. Petersburg, 199034, Russia
[3]Petersburg Nuclear Physics Institute named by B.P. Konstantinov of National Research Centre Kurchatov Institute, Gatchina, Leningrad District 188300, Russia

Synopsis We study the process of two-electron one-photon (TEOP) transitions to the ground state with the emission of a single photon in He-like ions. The corresponding transition probabilities and transition energies are calculated within the QED theory. The branching ratios between the TEOP transitions and the other major transitions are presented. The calculations are performed for ions with nuclear charge number $5 \leq Z \leq 92$.

We study two-electron one-photon (TEOP) transitions, which are single photon transitions where two electrons change their quantum numbers. Such transitions occur only due to the interelectron interaction and represent a process that is very sensitive to the description of the interelectron correlation.

We consider TEOP transitions from autoionizing LL states to the ground state of He-like ions. The main attention is paid to the TEOP transition probabilities for $(2s2p_{1/2})_1{}^3P_1$ and $(2s2p_{3/2})_1{}^1P_1$ states to the ground states $(1s)^2\ {}^1S_0$ of the He-like sequence of atomic ions $5 \leq Z \leq 92$. The calculation was performed within the QED theory. The line-profile approach (LPA) was used [1, 2].

To compare the intensities of TEOP transitions with those for other transitions, we present the branching ratios Γ_{TEOP}/Γ and $\Gamma_{TEOP}/\Gamma_{OEOP}$, where Γ_{TEOP} is related to the TEOP transition probability (W) as $\Gamma_{TEOP} = \hbar W$ and Γ_{OEOP} denotes the radiative widths corresponding to all the possible one-electron one-photon (OEOP) transitions, Γ are the total widths.

We compare our results with available results obtained by other authors. For the spin-allowed $(2s2p_{3/2})_1{}^1P_1 \rightarrow (1s)^2\ {}^1S_0$ transition, we compare our results with the work of U. Safronova [3], in which the perturbation theory for the electron-electron interaction was used, and with the results of R. Kadrekar and L. Natarajan [4, 5], where the GRASP2K code was used. A reasonable agreement with the results of U. Safronova was found. The reason for the discrepancy is that our work takes into account the second order (and partly higher orders) in the interelectron interaction and the radiative corrections. However, there is significant disagreement with the works [4, 5]: the difference in the results significantly exceeds the accuracy of our calculation, which is estimated as the difference between the results in velocity and length gauges. In the case of the spin-forbidden $(2s2p_{1/2})_1{}^3P_1 \rightarrow (1s)^2{}^1S_0$ transitions (which are not considered in work [3]) our results for the TEOP transition probabilities are roughly in two times larger than results obtained in [4, 5].

References

[1] O. Yu. Andreev, L. N. Labzowsky, G. Plunien, and D. A. Solovyev 2008 *Phys. Rep.* **455**, 135.
[2] O. Yu. Andreev, L. N. Labzowsky, and A. V. Prigorovsky 2009 *Phys. Rev. A* **79**, 032515
[3] U. I. Safronova and V. S. Senashenko 1977 *J. Phys. B* **10**, L271
[4] R. Kadrekar and L. Natarajan 2011 *Phys. Rev. A* **84**, 062506
[5] L. Natarajan and R. Kadrekar 2013 *Phys. Rev. A* **88**, 012501

*E-mail: k.n.lyashenko@impcas.ac.cn
†E-mail: o.y.andreev@spbu.ru
‡E-mail: d.yu@impcas.ac.cn

Classical description of the electron-impact ionization of Carbon

N. Bachi[1] *, S Otranto[1] † and K Tőkési[2] ‡

[1] Instituto de Física del Sur (IFISUR), Departamento de Física, Universidad Nacional del Sur (UNS), CONICET, Av. L. N. Alem 1253, B8000CPB - Bahía Blanca, Argentina
[2] Institute for Nuclear Research, 4026 Debrecen Bem tér 18/c, Hungary

Synopsis The electron-impact ionization of C is studied using the classical trajectory Monte Carlo method. Total cross sections are benchmarked against the reported experimental data and the predictions of numerically intensive theoretical methods.

The ITER project aims to demonstrate the feasibility of fusion as a large-scale energy source. It is currently under construction in Cadarache, France, and relies on the efforts of 35 countries to build the world's largest tokamak. Since the reactor has carbon components in their divertors, accurate data on collisions of electrons with carbon atoms are needed for plasma diagnostics, such as impurity influx studies.

Despite the potential interest in this topic, the number of experimental reports is quite limited [1]. From a theoretical point of view, during the last decade efforts have been devoted to calculate the total ionization cross sections for the present collision system, either from the ground state or from excited states, by means of highly numerically intensive methods, such us the time dependent close coupling and time independent distorted wave methods [2] or the B-spline R-matrix-with-pseudostates [3]. These studies have considered impact energies up to 60 eV and 100 eV respectively, range which encompasses the peak region.

In the present work, we show the performance of the 3-body classical trajectory Monte Carlo method for the calculation of ionization cross sections for collisions of electrons with carbon atoms. Ionization cross sections obtained by different effective potentials, such as effective charges and potential models derived from Hartree-Fock calculations, are presented and analyzed. Moreover, predictions based on the simple addition rule $2\sigma_{2p} + 2\sigma_{2s}$ are compared to those obtained by means of the independent electron (IEL) and the independent event (IEV) models.

In Figure 1, we show the total ionization cross sections (TCS) in collision between electron and Carbon atom up to an impact energy of 1 keV. We observe that in the low energy range our results tend to overestimate the experimental data. Furthermore, the maxima of the different models exhibit a clear shift towards lower impact energies compared to the experimental data. In contrast, our calculations tend to agree with each other and with the experimental trends at the larger impact energies considered.

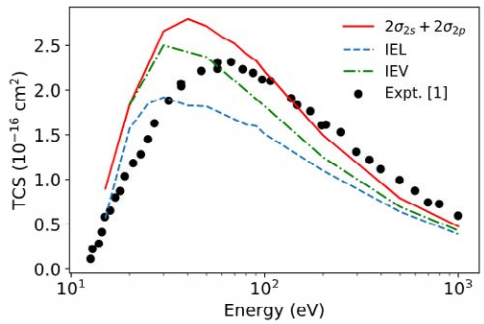

Figure 1. Total ionization cross section as a function of the impact energy for collisions of electrons with carbon atoms. For details please see the text.

This work has been carried out within the framework of the EUROfusion Consortium and has received funding from the Euratom research and training programme 2014-2018 and 2019-2020 under grant agreement No 633053. The views and opinions expressed herein do not necessarily reflect those of the European Commission.

References

[1] E Brook *et al* 1978 *J. Phys. B: Atom. Mol. Phys.* **11** 3115
[2] Sh. A. Abdel-Naby *et al* 2013 *Phys. Rev. A* **87** 022708
[3] Y Wang *et al* 2013 *Phys. Rev. A* **87** 012704

* E-mail: nicolas.bachi@uns.edu.ar
† E-mail: sotranto@uns.edu.ar
‡ E-mail: tokesi@atomki.hu

Autoionization and direct ionization of Cs atoms by electron impact

O Borovik*

Institute of Electron Physics, Uzhgorod, 88017, Ukraine

Synopsis On the basis of experimental data on the total cross sections for single ionization and $5p^6$ autoionization, an analysis of the theoretical description of single ionization of Cs atoms by electron impact is carried out.

Experimental studies of electron-impact ionization of heavy alkali atoms (K, Rb, and Cs) reveal a rapid increase in cross section immediately after the excitation threshold of the p^6 subvalent shell [1-3]. None of *ab initio* calculations of the ionization cross section for these atoms, which included the subvalent shell in the analysis, could correctly describe the form of the autoionization contribution or evaluate its absolute value [4, 5]. The availability of experimental data on the autoionization cross section and the total single ionization cross section would make it possible to determine the quantitative relationship between these processes and find a criteria to evaluate the accuracy of theoretical calculations. In this work, we present such an analysis for Cs atoms.

Figure 1 shows the experimental data on the total single ionization cross section of cesium σ^+_{tot} [1] normalized to the absolute data [2] at 500 eV and the $5p^6$ autoionization cross section σ_{aut} [6]. The calculated ionization data are presented by the total ionization cross section σ^+_{tot} [4] and the sum $\sigma^+(6s+5p^6)$ of the ionization cross sections for 6s and $5p^6$ shells [7].

Comparing the total ionization cross section [1] and the sum $\sigma_{aut}+\sigma^+(6s+5p^6)$ one can see their almost complete agreement (both in shape and magnitude) in the impact energy range from the excitation threshold of the $5p^6$ subshell to 40 eV. However, at higher impact energies, the sum $\sigma_{aut}+\sigma^+(6s+5p^6)$ noticeably exceeds the data [1]. This behavior indicates weakness in the calculations [7], in particular, their overestimated character at energies above 100 eV. Meanwhile, the actual behavior of the ionization cross section in the energy region above 30 eV is determined by the difference between the cross sections σ^+_{tot} [1] and σ_{aut} [6] (see cross section $\sigma^+_{tot}[1]-\sigma_{aut}$). Taking into account experimental errors [1, 6], this cross section can serve as a reference point for further calculations in Cs atoms.

The calculated total ionization cross section σ^+_{tot} [4] describes the general behavior of the cross section $\sigma_{aut}+\sigma^+(6s+5p^6)$ in the near-threshold impact energy region well. This confirms the correctness of the assumption made in [4] about the predominantly resonant excitation of the $5p^5n_1l_1n_2l_2$ atomic autoionizing states in Cs atoms.

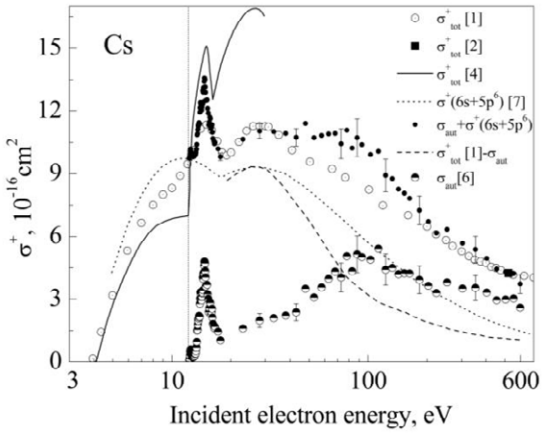

Figure 1. Total single ionization cross section of Cs by electron impact. Vertical dashed line marks the $5p^6$ excitation threshold at 12.307 eV [8].

This study was funded by the National Academy of Sciences of Ukraine under the project #0117U000651.

References

[1] Tate J *et al* 1934 *Phys. Rev.* **46** 773
[2] McFarland R *et al* 1965 *Phys. Rev.* **137** A1058
[3] Nygaard K 1975 *Phys. Rev. A* **11** 1475
[4] Roy B *et al* 1973 *Phys. Rev. A* **8** 849
[5] Lukomski M *et al* 2006 *Phys. Rev. A* **74** 032708
[6] Borovik A *et al* 2013 *J. Phys. B* **46** 215201
[7] Kupliauskiene A 2011 *Phys. Scr. A* **8** 849
[8] Pejcev V *et al* 1977 *J. Phys. B* **10** 2935

* E-mail:baa1948@gmail.com

Generalized oscillator strengths of the valence-shell excitations of neon studied by fast electron impact

X J Du[1], S X Wang[1] and L F Zhu[1]*

[1] Hefei National Laboratory for Physical Sciences at Microscale and Department of Modern Physics, University of Science and Technology of China, Hefei, Anhui 230026, People's Republic of China

Synopsis The different electric multipolar transitions and corresponding generalized oscillator strengths of the valence-shell excitations of neon were measured with an fast-electron energy-loss spectrometer at an incident electron energy of 1500 eV and an energy resolution of about 80 meV. The accuracy of the generalized oscillator strengths is improved by the adopted relative flow technique.

The studies of the generalized oscillator strengths (GOSs) for the valence-shell excitations of neon atom have the significance from both the fundamental and applied points of view. Since the GOS is determined by the wavefunctions of both initial and final states of an atom or a molecule, accurate experimental GOSs can be used to evaluate the theoretical models and calculational code rigorously[1]. Therefore, the GOSs of the valence-shell excitations of neon have been studied extensively both experimentally and theoretically. Furthermore, the present experimental results can be used to estimate the validity condition of the first Born approximation (FBA).

The present experiment was performed at a high-resolution fast-electron energy loss spectrometer at an incident electron energy of 1500 eV and an energy resolution of about 80 meV. In our experiment, the standard relative flow technique was used to simplify the normalization processes and improve the accuracy of the experimental results. The GOSs of the electric dipole excitation of $2p^5 3s'[1/2]_1$ of neon is shown in Fig.1 along with the previous high-energy and intermediate-energy scattering results[2, 3], IXS ones[4] and some theoretical calculations based on the RPAE and the RDW[5]. As shown in Fig.1, the same momentum transfer dependence behaviors are presented between the present and previous GOSs for the $2p^5 3s'[1/2]_1$ transition and a minimum at about 2.7 a.u. is observed. Since the IXS results[4] are free from the high-order Born terms, the well agreement among the present results with IXS ones in $K^2 < 1.5 a.u.$ indicates that FBA is satisfied at 1500 eV in this region. As for the region of $K^2 > 1.5 a.u.$, may be nonnegligible the contribution of the high-order Born terms.

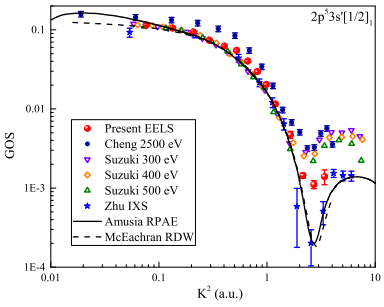

Figure 1. The present GOSs for the electric dipole excitations to $2p^5 3s'[1/2]_1$ of neon comparing with the experimental results and theoretical calculations.

In summary, the GOSs of the valence-shell excitations of neon have been determined by fast electron impact. The validity of the FBA of the electric dipole transition to $2p^5 3s'[1/2]_1$ of neon have been discussed by comparing the present results with the previous experimental and theoretical results.

References

[1] Molaro P *et al* 2001 *Astrophys. J.* **549** 90
[2] Suzuki T Y *et al* 1994 *Phys. Rev. A* **49** 4578
[3] Cheng H D *et al* 2005 *Phys. Rev. A* **72** 012715
[4] Zhu L F *et al* 2012 *Phys. Rev. A* **85** 030501(R)
[5] Amusia M Ya *et al* 2007 *Phys. Rev. A* **75** 062703

*E-mail: lfzhu@ustc.edu.cn

An investigation into low temperature dielectronic recombination rate coefficients

J Isaac Garcia[1]*, M Fogle[1] and S D Loch[1]†

[1]Auburn University, Auburn, AL 36849, USA

Synopsis In this project we aim to improve the accuracy of theoretical calculations of dielectronic recombination rate coefficients in the low temperature regime. We expand on existing computational methods for modeling atomic structure and transition rates, for applications in low temperature photoionized plasmas.

In both astrophysical and laboratory plasmas, understanding the charge state balance of an element is key in interpreting the spectral emission. One of the dominant recombination mechanisms in both types of plasmas is dielectronic recombination (DR), requiring both accurate atomic structures and transition rates. For astrophysical photoionized plasmas, low electron temperature DR rate coefficients are critically important in the ionization balance and are known to have large uncertainties in their calculated values [3, 4]. In this work, we seek to address this problem of accurate low temperature DR.

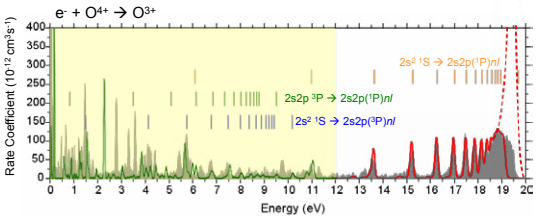

Figure 1. Dielectronic recombination measurements and theoretical calculations for O^{4+}.

Although effective in the high temperature case, current theoretical methods (e.g., [1, 2]) are known to have large uncertainties in the low temperature regime due to uncertainties in calculating low-n doubly excited states. This can be seen from differences with storage ring measurements [3]. Large configuration-interaction atomic structure calculations and the R-matrix approaches are both candidates for producing a more accurate atomic structure [5]. We explore the use of large CI AUTOSTRUCTURE calculations to improve the low temperature DR rate coefficients, comparing with existing storage ring measurements. This work is in collaboration with new measurements being performed at the heavy ion storage ring CRYRING@ESR at the FAIR facility in Darmstadt, Germany.

We also consider the commonly used method for calculating dielectronic capture rates: the detailed balance relation with the Auger rates resulting from the time dependent perturbation of a passing Coulomb potential. Although Fermi's golden rule has been the standard approach, it can be shown that the integral used in Fermi's golden rule is equivalent to the first order term of the Dyson series [6], a more complete picture of quantum transitions. We outline a method to quantify the uncertainty of Fermi's golden rule for Auger rates by determining the rate of convergence of the Dyson series.

In summary, we explore methods to more accurately calculate both resonance positions and heights for low temperature dielectronic recombination rate coefficients.

References

[1] Badnell N. R., 2016, http://ascl.net/1612.014
[2] Gu M. F., 2018, http://ascl.net/1802.001
[3] Fogle M., Badnell N. R., Glans P., Loch S. D., Madzunkov S., Abdel-Naby S. A., Pindzola M. S., et al., 2005, A&A, **442**, 757
[4] Bryans P., Badnell N. R., Gorczyca T. W., Laming J. M., Mitthumsiri W., Savin D. W., 2006, ApJS, **167**, 343
[5] Sochi T., Storey P. J., 2013, ADNDT, **99, 633**
[6] Dyson F. J., 1949, **75, 486**

*E-mail: jig0005@auburn.edu
†E-mail: loch@physics.auburn.edu

Benchmark Calculations for Electron Collisions with Ytterbium

K R Hamilton and K Bartschat *

Department of Physics and Astronomy, Drake University, Des Moines, IA 50311, USA

Synopsis We have applied the relativistic Dirac B-Spline R-matrix method to obtain cross sections for electron scattering from ytterbium atoms. The results are compared with those obtained from a semi-relativistic (Breit-Pauli) model-potential approach and a few available experimental data.

Accurate cross sections for electron collisions with ytterbium atoms are needed in the modelling of the enrichment process for the creation of Lu-177, which carries great promise in the treatment of a variety of cancers [1]. While a few experimental data and theoretical predictions are available in the literature [2, 3, 4], the comprehensive dataset needed to perform the relevant modeling requires calculations for a large number of discrete transitions as well as ionization over an extended energy range.

We used the relativistic Dirac B-Spline R-matrix (DBSR) method described in [5] to perform such calculations. The method is based upon the all-electron Dirac-Coulomb Hamiltonian, and thus may be employed for any complex atom or ion, without the use of phenomenological core potentials.

Our first results were obtained in a reduced 20-state model (DBSR-20), in which we coupled the $(4f^{14}5p^6 6s^2)^1S_0$ ground state with all states of dominant configurations $4f^{14}5p^6 6s6p$, $4f^{14}5p^6 5d6s$, $4f^{14}5p^6 6s6d$, $4f^{14}5p^6 6s7s$, and $4f^{14}5p^6 6s7p$, as well as the important $(4f^{13}5p^6 5d6s^2)^1P_1$ state, which provides an optically allowed 4f → 5d single-electron excitation pathway from the ground state.

Figure 1 shows examples of our initial results. Comparing the DBSR predictions for elastic scattering with those obtained from a standard semi-relativistic 28-state Breit-Pauli model (BBRM-28) and the experimental data of Predojević *et al* [2, 3] shows good agreement for incident energies above ≈ 0.1 eV. Below that energy, the results become extremely sensitive to the details of the model. DBSR calculations using much larger numbers of physical and pseudo-states (to describe ionization) are currently in progress.

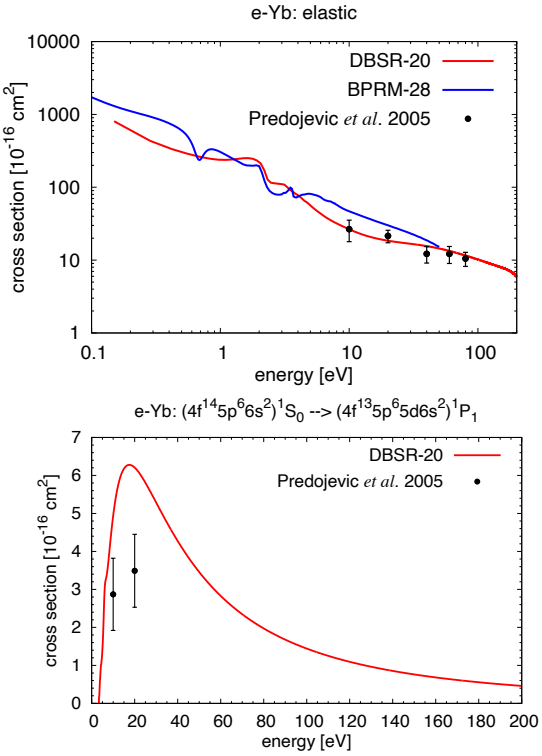

Figure 1. Top: Cross section for elastic e-Yb scattering obtained in the DBSR-20 and BPRM-28 models. The experimental data are taken from [2]. Bottom: Cross section for electron impact excitation of the $(4f^{14}5p^6 6s^2)^1S_0 \rightarrow (4f^{13}5p^6 5d6s^2)^1P_1$ transition in Yb. The DBSR-20 results are compared with the experimental data of [3].

This work was initiated by our late colleague Dr. Oleg Zatsarinny. It is supported, in part, by the NSF and Oak Ridge National Laboratory.

References

[1] ORNL News 2020
[2] Predojević B *et al* 2005 *J. Phys. B* **38** 1329
[3] Predojević B *et al* 2005 *J. Phys. B* **38** 3489
[4] Bostock C J *et al* 2012 *Phys. Rev. A* **83** 052710
[5] Zatsarinny O and Bartschat K 2008 *Phys. Rev. A* **77** 062701

*E-mail: klaus.bartschat@drake.edu

Azimuthal plane ionization using electron vortex projectiles

A L Harris *

Department of Physics, Illinois State University, Normal, IL 61790, USA

Synopsis We present triple differential cross sections for ionization of helium by electron vortex projectiles into the azimuthal plane. We show that at low energy, the ionization mechanism is similar for vortex and non-vortex projectiles. At high energy, vortex ionization can proceed through both single and double collisions, resulting in an enhancement of electron emission in a perpendicular geometry.

Triple differential cross sections (TDCS) have long been used to study the mechanisms that lead to ionization. In particular, if both final state electrons are ejected into the plane perpendicular to the incident beam (azimuthal plane), it is possible to distinguish double and single scattering mechanisms [1,2]. For a single binary collision between the projectile and the target electron, the outgoing electrons are most likely to be emitted in a back-to-back geometry in the azimuthal plane due to momentum conservation. This results in a single peak structure in the TDCS at low projectile energies. However, at larger projectile energies, double scattering mechanisms lead to perpendicular emission of the electrons and a double peak structure in the TDCS [1,2].

In the last decade, a new type of twisted electron wave packet has been experimentally realized that has non-zero transverse linear momentum and orbital angular momentum [3]. Known as electron vortex beams (EVBs), little is known about how they interact with individual atoms. In order to realize the many proposed applications for EVBs, it is crucial to understand how EVB interactactions with atoms on a fundamental level. Unfortunately, there are no experimental results for collisions between EVBs and atomic targets, making theoretical results the only insight into these interactions.

Our previous studies have shown that the TDCS for EVB ionization are qualitatively and quantitatively different from those of non-vortex projectiles [4,5]. Here, we examine whether the mechanisms leading to ionization by vortex projectiles are different than those of their non-vortex counterparts. Figure 1 shows TDCS for ionization of helium into the azimuthal plane using vortex and non-vortex pro jectiles calculated in a distorted wave Born approximation. The vortex projectile is characterized by its opening angle α, which is defined by the ratio of transverse to longitudinal projectile momenta, $\tan \alpha = k_{i\perp}/k_{iz}$. At low energy, our results predict that ionization by vortex projectile proceeds primarily through single collisions, as evidenced by the back-to-back emission peak at $\varphi_e = 180°$. The magnitude of the binary peak at large vortex opening angles is increased due to double scattering mechanisms. At higher energy, our results predict that ionization in a perpendicular emission geometry is enhanced by the vortex transverse momentum.

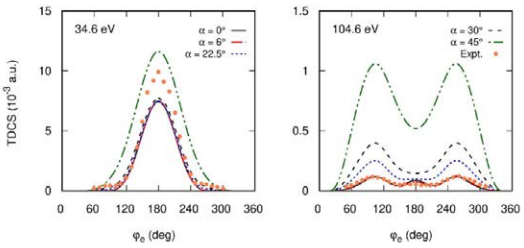

Figure 1. TDCS for ionization of helium by vortex ($\alpha \neq 0$) and non-vortex ($\alpha = 0$) projectiles into the azimuthal plane as a function of relative angle between the outgoing electrons φ_e. The final state electrons have equal energy and the incident projectile energy is listed in the figure. Experimental data are from [2] for non-vortex projectiles and normalized to the $\alpha = 0$ curve at 104.6 eV.

References

[1] Zhang X, Whelan C T and Walters H R J 1990 *J. Phys. B: At. Mol. Opt. Phys.* **23** L173–8
[2] Murray A J, Woolf M B J and Read F H 1992 *J. Phys. B: At. Mol. Opt. Phys.* **25** 3021–36
[3] Verbeeck J, Tian H and Schattschneider P 2010 *Nature* **467** 301–4
[4] Harris A L, Plumadore A and Smozhanyk Z 2019 *J. Phys. B: At. Mol. Opt. Phys.* **52** 094001
[5] Plumadore A and Harris A L 2020 *J. Phys. B: At. Mol. Opt. Phys.* **53** 205205

* E-mail: alharri@ilstu.edu

Many-body theory calculations of positron-atom binding energies using a Gaussian-orbital basis

J Hofierka[1]*, B J Cunningham[1], C M Rawlins[1], C H Patterson[2] and D G Green[1]†

[1]School of Mathematics and Physics, Queen's University Belfast, Belfast BT7 1NN, United Kingdom
[2]School of Physics, Trinity College Dublin, Dublin 2, Ireland

Synopsis Positron-atom binding energies are calculated using many-body theory via self-consistent solution of the Dyson equation including the positron-molecule self energy calculated at GW@RPA/TDHF/BSE+virtual-Positronium levels, and compared against existing theoretical results.

The positron-atom system is characterised by strong many-body correlations, including polarisation of the electron cloud by the positron, screening of the electron-positron Coulomb interaction, and the non-perturbative process of virtual-positronium formation [1, 2]. These correlations can modify scattering, enhance annihilation rates, and even cause positron binding to atoms. Whilst positrons have been measured to bind to ~ 75 molecules [3], no measurements of positron binding to atoms have yet been performed. Yet, the ability of positrons to bind to atoms is now firmly established, after first being predicted by many-body calculations [4] and subsequently proved in variational calculations of the e^+Li [5, 6]. There is now a wealth of theoretical predictions, see e.g., [7] for a comprehensive study of the periodic table using coupled-cluster theory, and where recommended values are given. However, the error $\sim$100 meV is still significant, and thus further study is warranted.

We have developed an *ab initio* Gaussian-orbital based implementation of positron-atom diagrammatic many-body theory that enables full account of positron-atom correlations, including polarisation of the electron cloud by the positron, screening of the electron-positron Coulomb interaction, and the non-perturbative process of virtual-Positronium formation. These interactions are treated at increasing level of approximation by solving the Dyson equation with a positron-atom self energy including the so-called *GW* contribution (at various levels: RPA, TDHF, and BSE), which describes the polarisation, screening and electron-hole interactions, and the infinite ladder series of electron-positron interactions describing virtual-Positronium formation, via the solution of the Bethe-Salpeter equations for the respective two-particle propagators [8]. We will present calculations of the positron binding energies and electron-positron contact densities (annihilation rates in the bound state) for neutral atoms including Be, Mg, Zn atoms and several halide ions, discussing basis-set sensitivity and convergence, and making comparison to other theory where possible [9].

Figure 1. The calculated positron density for Mg in a plane including the atom (filled circle) from 1/3 of maximum (white) to maximum (darkest red).

References

[1] Gribakin G F, Ludlow J 2004 *Phys Rev A* **70** 032720
[2] Green D G, Ludlow J, Gribakin G F, 2014 *Phys Rev A* **90**, 032712
[3] Gribakin G F *et al* 2010 *Rev. Mod. Phys.* **82** 2557
[4] Dzuba V A *et al* 1995 *Phys. Rev. A* **52**, 4541
[5] Ryzhikh G G, Mitroy J, 1997 *Phys. Rev. Lett.* **79**, 4124
[6] Strasburger K, Chojnacki H, 1998 *J. Chem. Phys.* **108**, 3218
[7] Harabati C, Dzuba V A, Flambaum V V 2014 *Phys Rev A* **89** 022517
[8] Cunningham B J, Hofierka J, Rawlins C M, Patterson C H and Green D G *In preparation*
[9] Hofierka J, Cunningham B J, Rawlins C M, Patterson C H and Green D G *In preparation*

This work is funded by DGG's European Research Council grant 804383 "ANTI-ATOM".

*E-mail: jhofierka01@qub.ac.uk
†E-mail: d.green@qub.ac.uk

Search for metastable muonic atoms toward observation of atomic parity violation

S Kanda[1] *

[1]Institute of Materials Structure Science, KEK 1-1 Oho, Tsukuba, Ibaraki, 305-0801, Japan

Synopsis Atomic parity violation in muonic atoms provides a unique opportunity to search for physics beyond the standard model at the low energy scale. We have proposed a new experiment to perform X-ray spectroscopy of muonic atoms in the 2S metastable state. As a feasibility test for the experiment, a search for 2S metastable muonic carbon atoms was performed using a low-density methane gas target.

When a negative muon is captured by a nucleus, it forms a bound-state called a muonic atom. The muon is 200 times heavier than the electron, so the Bohr radius of a muonic atom is about 1/200 of that of ordinary atoms. Therefore, the muon acts as a probe with high sensitivity to interactions with nuclei. Immediately after formation, the muonic atom is in excited states with a principle quantum number n of approximately $n \sim \sqrt{m_\mu/m_e} = 14$. Muonic atom is de-excited by radiative or Auger transitions leading to the ground-state within a short time. A few percent of muonic atoms remain in the long-lived metastable 2S state in low-pressure gases with small atomic number Z. During the de-excitation processes, electrons in the orbitals are ejected one after another, and for atoms with small Z, all electrons except the K-shell are often lost. We can investigate the parity violation due to neutral weak current by observing the parity-odd transitions in the de-excitation processes of muonic atoms. The interaction between the nucleus and the muon results in the parity non-conserving mixing of the 2S and 2P states. This atomic parity violation (APV) effect leads to a one-photon M1 transition from 2S to 1S associating a monochromatic light with angular asymmetry. From the asymmetry of this one-photon transition, the Weinberg angle can be determined via the weak charge of the nucleus. The Weinberg angle is an energy-dependent parameter that describes the mixing of the electromagnetic and weak interactions. Measurements of the Weinberg angle at various energy scales are essentially important as a precision test of the standard model and search for physics beyond the standard model. In the 1990s, several experiments aiming at observation of APV in muonic atom were performed at Paul Scherrer Institute (PSI) [1]. However, no parity-odd transition was observed because of difficulties in the experiment. To revisit this topic, we proposed a new experiment using a high-intensity pulsed muon beam at J-PARC and a fast calorimeter consisting of Ce:LYSO crystals and silicon photomultipliers (SiPMs). Figure 1 illustrates an experimental setup. In April 2021 we conducted our first experiment with a low-density methane gas target. In this contribution, we present an overview of the experiment and preliminary results.

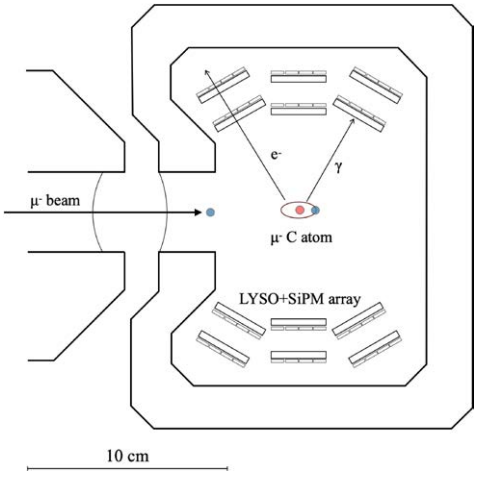

Figure 1. Schematic of the experimental setup.

References

[1] Kirch K *et al* 1997 *Phys. Rev. Lett.* **78** 4363

*E-mail: kanda@post.kek.jp

Distorted Wave Born Approximation and Optical Potential Methods in Calculation of Cross Sections for Electron-Potassium Elastic Scattering

P K Kariuki[1] *, J Okumu[1] and C S Singh[1] †

[1]Kenyatta University, Nairobi, - 00100, Kenya

Synopsis The first-order distorted wave Born approximation (DWBA) and the optical potential (OP) methods are systematically compared in the elastic scattering of electrons by potassium atom at the intermediate energies 7 – 200 eV using the same distorting potential including a non-local polarization potential. Both methods are found to yield results that compare well with measured results at all electron-impact energies considered.

Although potassium atom has a relatively simple atomic structure and is adequately described using the Hartree-Fock approximation, theoretical calculation of scattering cross sections (Madison *et al*., [1],) has yielded results that are not in complete agreement with absolute measurements (Vuskovic and Srivastava [2] and Buckman *et al*. [3]). It is therefore desirable to carry out more calculations to investigate how the atom interacts with energetic electrons especially at intermediate energies.

We have compared the OP and the DWBA methods in the problem of elastic scattering of intermediate-energy electrons by the potassium atom using a distorting potential of the form

$$V_{opt} = V_{st}(r) + V_{ex}(r) + V_{pol}(r) + iV_{abs}(r) \qquad (1)$$

where V_{st} is the static potential , V_{ex} is the Furness-McCarthy exchange potential [4], V_{pol} is a non-local polarization potential [5], and V_{abs} is the absorption potential [6]. Since the polarization potential for potassium is dominated by excitation to the 4^2P state, only a few low-lying states are included namely, 4^2P, 5^2P, 3^2D, and 5^2S, to obtain the polarization potential. The present OP and DWBA calculations are then carried out using the static (S), static-exchange (SE), static-exchange-polarization (SEP), and static-exchange-polarization-absorption (SEPA) potentials. The DCS results at $100eV$ are shown in Figure 1. The results at other electron impact energies will be presented at the Conference.

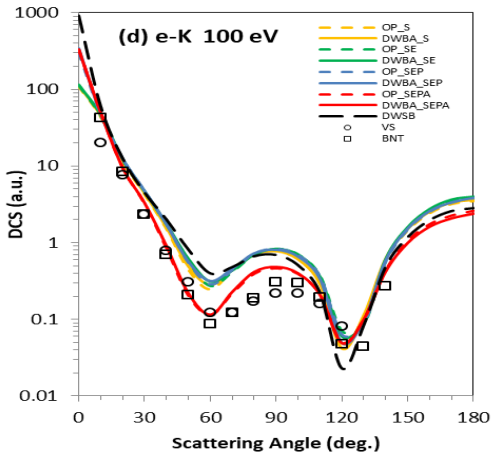

Figure 1. Differential cross sections for electron-potassium elastic scattering at 100 eV. Theory: OP, present optical potential calculation; DWBA, present first-order distorted wave Born approximation; DWSB, second-order distorted wave Born approximation calculation of Madison *et al* [1]. Experiment: VS, Vuskovic and Srivastava [2] and Buckman *et al* [3].

References

[1] Madison D H *et al* 1995 *J. Phys. B: At. Mol. Opt. Phys*. **28** 105
[2] Vuskovic L and Srivastava S K 1980 *J. Phys. B: At. Mol. Phys*. **13** 4849
[3] Buckman S J *et al* 1979 *J. Phys. B: At. Mol. Phys*. **12** 3077
[4] Furness J B and McCarthy I E 1973 *J. Phys. B: At. Mol. Phys*. **6** 2280
[5] Kariuki P K *et al* 2015 *The African Review of Physics* **10** 0018 131
[6] Staszewska G *et al* 1984 *Phys. Rev. A*. **29** 3078

* E-mail: pekika2017@gmail.com
† E-mail: singh_cs@hotmail.com

Double ionization of argon by impact of fast electrons

I Kada[1], A Herbadji[1], C Dal Cappello[2], and A Mansouri[1*]

[1]LPQSD, Department of physics, Faculty of Science, University Sétif-1, 19000, Setif, Algeria
[2]SRSMC, UMR CNRS 7565, University of Lorraine, BP 70239, 54506 Vandoeuvre-les-Nancy, France

Synopsis : The differential fivefold cross section is calculated using a model where the fast electrons (incident and scattered) are described by plane waves and the two ejected electrons by distorted waves [1]. In this work, the incident electron-target interaction is described by a potential taking into account all the electrons of the target. The results of our model are compared with the experimental results of El Marji et al [2].

The study of collisions allows us to understand the properties of atoms and molecules. Thus, the double ionization gives us very accurate information on the electronic correlation in an atom or a molecule. The (e, 3e) experiments refer to electron impact double ionization experiments in which the scattered projectile and the two target ejected electrons are detected in coincidence where the scattered electron is fast (5500 eV) while the two ejected electrons are slow (10 eV-10eV). Measurements of the fivefold cross section (FDCS) yields fundamental information on electronic correlation. This particular situation allows us to apply the first Born approximation. Very few theoretical studies have been carried out because the experiment cannot separate the contributions of the three states of the Ar++ ion, namely 3P, 1D and 1S.
Dal Cappello[2] had applied a model (2CWG) in which the two ejected electrons were described by a Coulomb wave and where the Gamow factor had been taken into account. Then Herbadji et al [1] had described the two ejected electrons by distorted waves(2DWG) instead of Coulomb waves. In this study, we use the equation (7) of [3] obtained by integrating on the 16 electrons of the target. This model, denoted 2DWSRG,is then applied to the double ionization of argon for which the scattering angle is fixed at 0.45 deg. Figure 1 shows an example of the application of our model (2DWSRG), compared to the other two models (2CWG and 2DWG) and to the experimental results [2]. In this example, we present the FDCS for the case($\theta_2 =$ 127°) of the experiment[2] we compare our theoretical results : blue dotted line model with fixed charge (2CWG), red dashed line (2DWG) and black solid line (2DWSR)
The (2DWG) model with the variable charge makes important corrections to 2CWG cross sections, but the FDCS calculated by 2DWSRG are much better than the 2DW model.

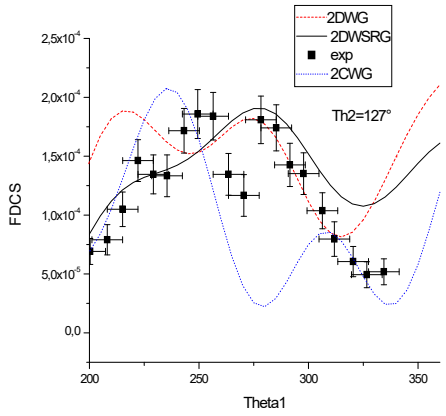

Figure1: FDCS for argon atoms, the incident electron energy is E_i = 5500 eV and the ejected electrons energies are (E_1,E_2) = (10eV,10eV).
The scattering angle is θ_s = 0.45°and θ_2 = 127°.

References

[1] Herbadji A et al, 2019 (XXX ICPEAC), Deauville, France, July 23-30
[2] El Marji *et al* 1997 *J. Phys. B: At. Mol. Opt. Phys.* **30** 3677
[3] Kada I, Dal Cappello C and Mansouri A, 2017 Eur. Phys. J. D. 71,41

* E-mail: mansouria@univ-setif.dz

Relativistic Distorted Wave Approach to Electron Impact Excitation of Argon Gas Using a Complex Potential

Alex M. Marucha[1*], Peter K. Kariuki[1], John Okumu[1], Chandra S. Singh[1]

[1]*Department of Physics, Kenyatta University, Nairobi, Kenya*

We apply relativistic effects to the problem of excitation of the lowest lying resonance states of argon gas with inclusion of absorption, polarization and exchange effects to the electrostatic distortion potential to form an overall complex distortion potential. The atomic wave functions are constructed using the GRASP code [6] while differential cross sections (DCS) and integral cross sections (ICS) have been obtained using our new code RDWA1. Results from this study predict that use of a complex distortion potential generally lowers ICS and DCS as impact energies of the incident electron increases, more specifically beyond 50 eV, and that it is the energy dependent polarization potential adopted in this work that plays a major role in improving shapes of cross-sections at near threshold impact energies up to around 20 eV, where available distorted wave methods fail to give satisfactory results when compared to experiments.

Previous non-relativistic [1, 3] studies on electron impact excitation of rare gases have not applied energy dependent polarization nor absorption potentials in their calculations while relativistic distorted wave (RDWBA) studies [5], despite having energy independent polarization lacks the effect of absorption and uses a non-local exchange potential to distort the free incident electron.

We consider an atom target excited by an incident free electron causing the atom electron to transit from an initial state 'a' to a final state 'b' represented by an electron transition matrix $T_{a\to b}^{RDW} = \langle \chi_b^- \mid \mathrm{V} - U \mid A\chi_a^+ \rangle$ in which calculation of the electrons wave-functions $\chi^{\pm}$ is achieved by employing a complex distorting potential U together with the interaction potential V. We present results in which we have applied static (S), local electron exchange (SE) and an energy dependent polarization (SEP) potential [2] to the real part and an absorption of incident electrons potential [4] (SEPA) to the complex part.

From the figure 1, it is clear that S and SE results alone cannot give accurate atomic collisions results and the overlapping SEP and SEPA results greatly improve cross section shapes with polarization playing a major role. Furthermore, the overlap shows that the absorption potential has negligible effect on results at low energies close to excitation threshold.

E-mail: * magembe.marucha@gmail.com

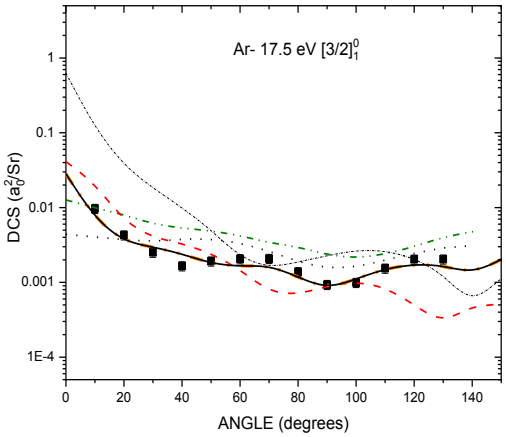

Figure1. DCS for electron excitation of the lowest resonance states of argon. _ . _ . _ . _ . _ . _ ,S RDWBA present; _ _ _ _ _ _ , SE RDWBA present ; _ _ . _ . _ _ . _ . _ _ ,SEP RDWBA present ; ———— , SEPA RDWBA present; Khakoo *et al.* [7]: ■ , experimental; — · · — , DWBA; ····· , RM.

References

[1] Bartschat K and Madison D H 1987 *J. Phys.* B **20** 5839
[2] Jhanwar B L and Khare S P 1976 *J. Phys. B* **9** 17
[3] Madison D H, Maloney C M and Wang J B 1998 *J. Phys. B* **31** 873
[4] K. Sharma, Acta Phys. Pol. A 126, 3 (2014)
[5] Zuo T, McEachran R and Stauffer A D 1992 *J. Phys. B* **25** 3393
[6] Dyall K G *et al* 1989 *Comput. Phys. Commun.* **55**, 425
[7] Khakoo M et al 2004 *J. Phys. B* **37** 247.

Theoretical and experimental determination of Au I-III lines within Collisional-Radiative and LTE plasma regimes.

M. McCann[1]*, S. J. Bromley[2], C. P. Ballance[1], S. D. Loch[2]

[1]CTAMOP, Queen's University of Belfast, Belfast, Northern Ireland, BT7 1NN
[2]Dept. of Physics, Auburn University, Auburn , AL, USA, AL 368349

Synopsis Neutron binary star mergers have long been proposed as sufficiently neutron rich environments that could support the synthesis of rapid neutron capture elements (r-process), elements such as gold. However, NIST reveals that beyond neutral and singly ionised systems, there is a lack of accurate wavelengths for the majority of levels. We shall take several independent theoretical and experimental approaches to ensure self-consistency in the identification of Au I-III energy levels and therefore accurately determine spectral lines from these ions.

With the advent of detecting gravitational waves from a binary neutron star merger (NSM) in 2017 by the LIGO collaboration [1] and its electromagnetic counterpart [2] interest in heavy r-process elements has increased dramatically. Immediately following a NSM, physical conditions are expected to produce significant abundances of r-process elements, including the lanthanides, actinides, and platinum-group elements [3].

From [4] we see that the ejecta from NSM include heavy r-process elements these elements cause difficulty for opacity calculations due to them being open f shell. This shows a necessity for accurate calculations of the atomic structure of r-process elements to accurately model the NSM environment.

Our calculations are informed by two ongoing efforts, spanning both the astrophysical and magnetically-confined plasma regimes. Experimental measurements of Au I and Au II spectra in [5] many emission lines for heavy elements such as gold may be heavily influenced by excitation from long-lived metastable levels. Theoretically, accurate modeling of the emission spectra at these conditions requires both accurate atomic structure and electron-impact excitation calculations if the resulting synthetic spectra is to be matched to observation.

For our atomic structure models we use a modified version of the General-purpose Relativistic Atomic Structure Package (GRASP^0) [6] for Dirac-Coulomb Hamiltonian's determined from a Multi-Configuration Dirac-Fock approach. These GRASP^0 calculations shall be presented alongside an independent Flexible Atomic Code (FAC) [7] model to compare the accuracy of our target level designations and their respective energies. Additionally we have compared our calculated data to experimental measurements from the gold literature, where available.

Using the structure data from these calculations we hope initially to find simple line ratios within a low temperature, low density astrophysical plasma regime before considering the metastable resolved picture of magnetically-confined plasmas.

References

[1] Abbott B P *et al* 2017 *PhRvL.* **119** 161101
[2] Coulter D A *et al* 2017 *Sci.* **358** 1556
[3] Kajino T *et al* 2019 *Prog. Part. Nucl. Phys.* **107** 109
[4] Fontes C J *et al* 2020 MNRAS **493** 4143
[5] Bromley S J *et al* 2020 *ApJS* **250** 19
[6] Parpia F A *et al* 1996 *Comp. Phys. Comm.* **94** 249
[7] Gu M F *et al* 2008 *Can. J. Phys.* **86** 675

*E-mail: mmccann80@qub.ac.uk

Electron-Impact single ionization of lithium: Benchmark data

D M Mootheril[1]*, J Zhou[1,2], X Ren[1,2], A Dorn[1]

[1]Max-Planck-Institute of Nuclear Physics, Heidelberg, 69115, Germany
[2]School of Physics, Xi'an Jiaotong University, Xi'an 710049, China

Synopsis We present the fully differential cross section of lithium after single ionization by 110 eV electron impact. Considerable emission in perpendicular plane shows the higher order effects in the projectile-target interactions. Furthermore, we motivate and show preliminary results for double ionization studies producing one K- and one L-shell vacancy.

Kinematically complete experiments like (e,2e) and (e,3e) allow to measure the final state momentum vectors of all the outgoing particles and thereby the determination of fully differential cross sections (FDCS). This enables the stringent test of theoretical models which describes the dynamics of quantum few-body systems. There have been many successful efforts of such experiments on helium from high to threshold energy regime thereby measuring FDCS for nearly all scattering geometries [1, 2, 3, 4]. Non-perturbative models like time-dependent close-coupling (TDCC) and convergent close-coupling (CCC) showed excellent agreement with the experimental data [4]. Lithium is an atom of particular interest since it is of next higher degree of complexity than helium and due to the fact that the single ionization process takes place predominantly from the 2s shell. Double ionization studies at threshold are stimulated from the theoretical predictions of a 'T' shape three electron emission pattern owing to the different initial states of the emitted electrons [5, 6].

Our experiment employs an efficient multi-electron recoil ion momentum spectrometer, 'Reaction microscope' (ReMi) [7] to detect all the outgoing fragments for single and double ionization of lithium. The vapour target beam is produced by an effusive oven heated to a temperature of 750^0C. Momenta of all the outgoing electrons are reconstructed with excellent resolution whereas that of the recoil ion must be calculated from the momentum conservation due to its poorly resolved momentum as a consequence of the high target temperature.

Here, we present the first preliminary results of ongoing (e,2e) measurements after single ionization of lithium with 110 eV electron impact. One salient feature present in the FDCS is the considerable emission in the perpendicular plane due to the higher order projectile-target interactions. A second feature is a shoulder in the binary lobe in the scattering plane. This was also observed in the FDCS after the ionization of an ultra-cold lithium target with O^{+8} ions of 24 MeV energy [8].

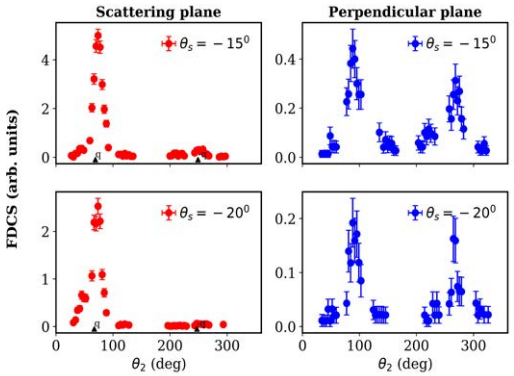

Figure 1. FDCS in the scattering plane and perpendicular plane as a function of angle of the emitted electron of energy E= 12 eV with projectile scattering angles $\theta = 15^0, 20^0$. Arrows shows momentum transfer direction.

References

[1] A. Dorn *et al* 1999 *Phys. Rev. Lett.* **82** 2496-2499
[2] X. Ren *et al* 2008 *Phys. Rev. Lett.* **101** 093201
[3] M. Dürr *et al* 2008 *Phys. Rev. A* **77** 032717
[4] X. Ren *et al* 2011 *Phys. Rev. A* **85** 052711
[5] J. Colgan *et al* 2013 *Phys. Rev. Lett.* **110** 063001
[6] A. Emmanouilidou *et al* 2008 *Phys. Rev. Lett.* **100** 063002
[7] R. Moshammer *et al* 1994 *Phys. Rev. Lett* **73** 3371
[8] R. Hubele *et al* 2013 *Phys. Rev. Lett* **110** 133201

*E-mail: deepthy.mootheril@mpi-hd.mpg.de

Electron Impact Ionization of the Neon Atom

JP Colgan[1] **MS Pindzola**[2]*

[1]Los Alamos National Laboratory, Los Alamos, NM, 87545, USA [2]Auburn University, Auburn, AL 36849, USA

Synopsis Time-dependent close coupling coupling calculations for the single ionization of the Neon atom.

Time-dependent close-coupling methods are used to calculate the single ionization of the Neon atom. The inner subshells are treated using pseudopotentials, while interaction with the remaining core electrons of the outer subshell is handled in a configuration-average approximation. A 2D radial lattice is used to calculate single and triple differential cross sections. The calculations are in support of the modeling of runaway electrons in plasma ionization studies.

*E-mail: pindzms@auburn.edu

Critical minima in the differential cross sections of electron elastic scattering by the atoms of 2nd and 3rd periods

V Kelemen[1], Sh Demes[2], E Remeta[1*] and V Roman[1†]

[1]Institute of electron physics of National Academy of Sciences of Ukraine, Uzhhorod, 88017, Ukraine
[2]Institute for Nuclear Research (ATOMKI), Debrecen, 4026, Hungary

Synopsis The characteristics of critical minima in the differential elastic cross sections of electron scattering by the atoms of sequences Li-Ne and Mg-Ar are calculated in the relativistic optical potential approach.

Minima in differential elastic cross sections (DCSs) of electron scattering by the atoms are investigated a fairly long time (see [1-4] and ref. there). Among the minima in DCSs, the deepest, so-called, critical minima (CM) are distinguished. In vicinity of these minima for the direct f(E,θ) and spin-flip g(E,θ) amplitudes the unequality is fulfilled $|f(E,\theta)|^2 < |g(E,\theta)|^2$ and as a result the polarization of the scattering electrons reaches large and maximum (±100%) values. The positions of CM are determines by the critical energy E_c and angle θ_c, in small vicinity of which the scattering amplitudes Ref(E,θ) and Imf(E,θ) simultaneously pass through the zero value.

We have determined the energies and angles of CM in DCSs for the sequences of Li-Ne and Mg-Ar atoms. The calculations were performed in our relativistic RSEP and RSEPA approximations (see, for example, [4]).

On fig.1 $E_c(Z)$ dependences for high-angle minima in DCSs of the atoms sequences Li-Ne and Mg-Ar calculated in the RSEP approximation are presented. Based on the smooth behaviour of this dependence for the atoms of p-elements, here for the Si atom are predicted following values E_c=22 eV and θ_c=141°. The angles θ_c for high-angle CM are vary from 96.33° (Li) to 99.89°-(Ne) and from 146.89° (Mg) to 140.31° (Ar).

DCSs values in the CM are (in 10^{-20} m^2/sr): 0.0233 (Li) and vary from $0.120\cdot10^{-6}$ (Be) to $0.561\cdot10^{-6}$ (Ne); vary from $0.150\cdot10^{-5}$ (Mg) to $0.272\cdot10^{-5}$ (Ar).

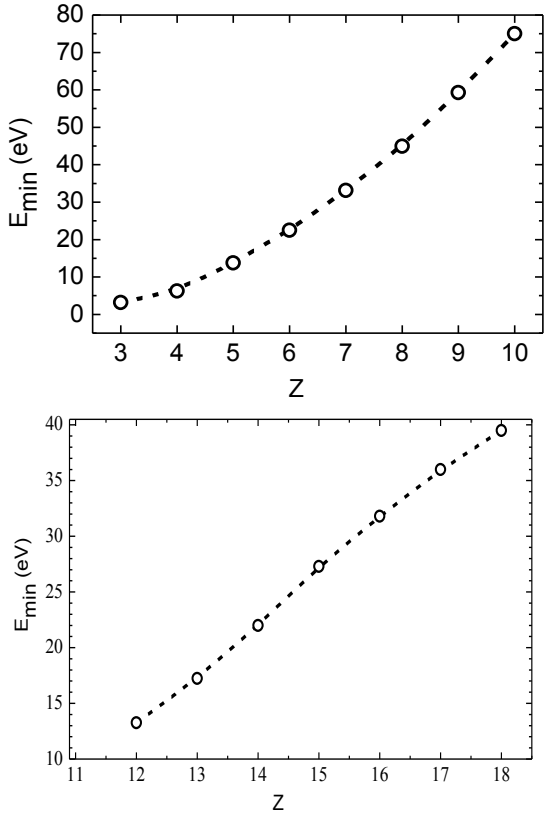

Figure 1. $E_c(Z)$ dependences for the Li-Ne and Mg-Ar atomic sequences.

*E-mail: remetoveyu@gmail.com
†E-mail: viktoriyaroman11@gmail.com

References

[1] Buhring W 1968 *Z. Phys.* **208** 286
[2] Khare S, Raj D 1980 *J. Phys. B: At. Mol. Phys.* **13** 4627
[3] Milosavljević A *et al* 2004 *Eur. Phys. J. D* **29** 329
[4] Kelemen V, Remeta E 2012 *J. Phys. B: At. Mol. Opt. Phys.* **45** 185202

Ionization and recombination coefficients of the dense nonideal hydrogen plasma: effects of screening and quantum diffraction

E O Shalenov[1,2]*, M M Seisembaeva[1], M N Jumagulov[1] and K N Dzhumagulova[1,2]

[1]Institute of Experimental and Theoretical Physics, al-Farabi Kazakh National University, Almaty, 050040, Kazakhstan
[2]Department of Physics, Nazarbayev University, Nur-Sultan, 010000, Kazakhstan

Synopsis Problems connected with the investigation of the excitation cross section of electron levels of atoms and atom ionization by electron impact were solved by finding phase shifts based on the solution of the Calogero equation. The results of the investigation of these elementary processes (their cross sections) were used to calculate the kinetic coefficients of ionization and recombination. Based on the effective interaction potential of particles of a nonideal semiclassical plasma, elementary processes are studied: electron capture, ion excitation and ionization.

To solve the actual problem of realizing thermonuclear controlled fusion (TCF) with inertial confinement, as well as to study the processes taking place in astrophysical objects (white dwarfs, the Sun, the bowels of giant planets, etc.), reliable data on the physical characteristics of a nonideal semiclassical plasma arising on Earth and in the Cosmos in many processes associated with the heating and compression of matter are needed. A nonideal dense plasma is observed, for example, when the target substance is compressed by a high-power laser radiation in nuclear fusion, in nuclear explosions, at supersonic motion of bodies in dense layers of planetary atmospheres, at impact of high-intensity energy fluxes on the surface of various materials.

The Saha equation allows us to determine the number of particles of different types per unit volume for the case when the plasma is in a state of thermodynamic equilibrium. In the general case, the composition of the plasma is determined on the basis of the so-called ionization kinetics equations. These equations describe the rate of change in the number of particles (growth or decrease) in a certain state (free, bound, etc.), due to various reactions.

In the work, we used the original potential for interaction between an electron and an atom that we developed earlier in [1–5]. This effective potential takes into account the quantum mechanical effect of diffraction at small distances, because of which it has a finite value at distances close to zero.

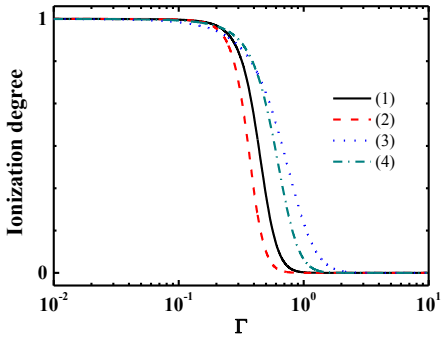

Figure 1. Dependence of the degree of ionization of a hydrogen plasma on the coupling parameter for various values of the density parameter. Solution of the kinetic equation of ionization 1) $r_s = 10$; 2) $r_s = 5$; solution of the Saha equation 3) $r_s = 10$; 4) $r_s = 5$.

The calculated dependences of the ionization degree on the coupling parameter for different values of the density parameter are shown in figure 1.

References

[1] Shalenov E O *et al* 2018 *Phys. Plasmas.* **25** 082706
[2] Shalenov E O *et al* 2019 *Contrib. Plasma Physics.* **59** e201900024
[3] Shalenov E O *et al* 2019 *J. Phys.: Conf. Ser.* **1400** 077035
[4] Shalenov E O *et al* 2019 *J. Phys.: Conf. Ser.* **1385** 012031
[5] Jumagulov M N *et al* 2020 *High Energy Density Physics.* **36** 100832

* E-mail: shalenov.erik@physics.kz

Electron impact excitation of autoionizing states of lithium and potassium using distorted wave method with absorption potential

C. S. Singh*

Department of Physics, Kenyatta University, P.O. Box 43844-00100, Nairobi, Kenya

Synopsis Calculations for electron impact excitation of the lowest autoionizing states of lithium ($1s2s^2$) and potassium ($3p^54s^2$) have been made using distorted wave method with Staszewska's absorption potential. It is found that when using Staszewska's absorption potential, the choice of the value of the threshold parameter Δ is very crucial. The value of Δ when taken to be small, gives results which are close to the experimental results of Borovik *et al* at low impact energy.

We have made calculations for electron impact excitation of the lowest autoionizing states $(1s2s^2)^2S$ of lithium and $(3p^54s^2)^2P$ of potassium using distorted wave method with absorption potential of Staszewska *et al* [1] and exchange potential of Furness and McCarthy [2]. In the initial channel we have used the initial state static potential and in the final channel a linear combination of static potentials of initial and final states with equal weight.

In our calculation, we have used the multi-zeta wavefunctions of Clementi and Roetti [3]. We have modified the computer program DWBA1 written by Madison and Bartschat [4] so that it can be used for complex potential.

We have used the following formula to determine the energy dependent threshold parameter,

$$\Delta(E) = K + \frac{E - I}{2} \qquad (1)$$

where K is the value of the threshold parameter Δ chosen at some specific energy I where it gives cross section result close to the experimental result (it was chosen as 0.225eV for Li at 56.55eV electron impact energy and 0.8eV for K at 20.40 electron impact energy), E is the electron impact energy. Values of Δ for all other impact energies were determined using the above formula.

It is seen that in using the Staszewska's absorption potential, the choice of the threshold parameter Δ is very crucial. In our electron-lithium scattering for the excitation of the autoionizing state ($1s^22s \rightarrow 1s2s^2$) and in electron-potassium excitation ($3p^64s \rightarrow 3p^54s^2$), close to threshold, if we take the value of Δ very small as given by equation (1), the results come close to the experimental results of Borovik and Krasilinek [5] and Borovik *et al*. [6]. This choice of very small value of threshold parameter can be justified on the ground that the channel of elastic scattering which opens at very low impact energy (any value > 0) is absorption channel when we consider inelastic processes like those being considered in this study. As we go towards higher impact energy, the effect of absorption becomes less and less, and the threshold parameter values become high.

Integral cross section results for electron-lithium scattering are shown in the figure.

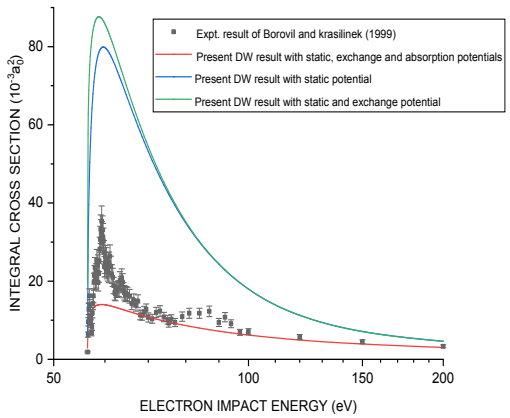

Figure 1. Integral cross section for electron impact excitation of ($1s^22s \rightarrow 1s2s^2$) state in lithium

References

[1] Staszewska G *et al* 1984 *Phys. Rev. A* **29** 3078
[2] Furness J B and McCarthy I E 1973 *J. Phys. B* **6** 2280
[3] Clementi E and Roetti C 1974 *Atomic Data and Nuclear Data Tables* **14** 177
[4] Madison D H and Bartschat K 1996 *Computational Atomic Physics* ed. K. Bartschat, Springer-Berlin, p. 65
[5] Borovik A A and Krasilinek V N 1999 *J. Phys. B* 32 1941
[6] Borovik A A *et al* 2005 *J. Phys. B: At. Mol. Opt. Phys.* **38** 1081

*E-mail : singh.chadra@ku.ac.ke

Positron collisions with alkali atoms

R Utamuratov *, N A Mori, D V Fursa, A S Kadyrov and I Bray

Department of Physics, Curtin University, Perth, Australia

Synopsis Convergent close-coupling method has been applied to positron scattering by the alkali atoms Li, Na, K, Rb and Cs. Obtained results form the most complete and comprehensive positron-alkali collision dataset with cross sections of total and elastic scattering, direct ionization, target excitations and Ps formation.

Positron-alkali atom collision problem still remains of interest due to lack of either experimental or theoretical comprehensive studies. The most up to date cross section estimates for these collision systems have uncertainties above 20% [1]. The experimental studies are very limited due to technical challenges associated with positron beams as well as alkali atoms. On the other hand, theoretical studies are also restricted in scope of considered collision processes due to challenges arising from two-centric nature of the positron collision processes.

In this work we apply convergent close-coupling (CCC) approach to positron collisions with atomic targets of Li, Na, K, Rb and Cs. The CCC method allows to use both single- and two-centre approaches to the positron scattering problem [2], thus letting convergence checks independently using different expansion types. This allows a convenient test of the calculations, which is particularly important in the absence of other benchmark experimental or theoretical results. In this work we present integrated cross sections for elastic scattering, target excitation, ionization and Ps formation in the ground and excited states.

As an example, figure 1 presents our preliminary results for total Ps-formation cross sections obtained using large two-centre expansions.

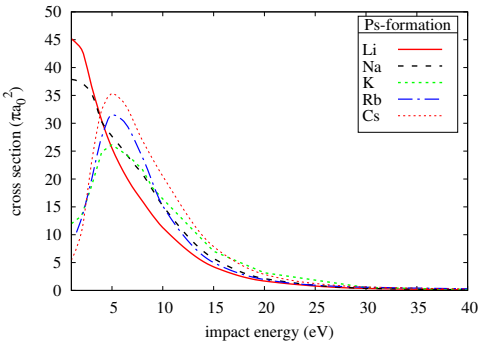

Figure 1. CCC results for total Ps formation cross sections in positron collisions with alkali atoms.

References

[1] Ratnavelu K, Brunger M J and Buckman S J 2019 *J. Phys. Chem. Ref. Data* **48** 023102
[2] Bray I *et al.* 2016 *Eur. Phys. J.* D**70** 6

*E-mail: r.utamuratov@curtin.edu.au

Positron impact excitation of lowest autoionizing state of potassium atom using distorted wave method with absorption and polarization potentials

N N William[1]*, E O Jobunga[2] and C S Singh[1]

[1]Department of Physics, Kenyatta University, Nairobi, Kenya
[2]Department of Mathematics and Physics, Technical University of Mombasa, Mombasa, Kenya

Synopsis Integral cross-sections of the lowest autoionizing state of potassium $\left(3p^5 4s^2\right)\ ^2\mathrm{P}$ were calculated using a non-relativistic distorted wave method to investigate the effect of absorption and polarization potentials. The inclusion of polarization potential has shown the near-threshold resonance structure revealed in electron impact excitation experimental results. The absorption potential has a small effect at low impact energies near the excitation threshold.

In the recent decades, positron scattering from alkali atoms has triggered considerable involvement of both experimentalists and theoreticians due to their intriguing features such as low ionization potential and high polarizability [1, 2]. The alkali atoms have a comparatively simple electronic structure with the outermost shells consisting of a single electron.

In this study, the full distortion potential comprised static, polarization [3], and absorption [4] potentials. In the initial channel, the static potential was the static potential of the target atom in its initial state while in the final channel it was is a simple average of target atom static potentials in its initial and final states[5]. We used Roothan- Hartree-Fock (RHF) multizeta atomic wave functions given in Clementi and Roetti tables [6]. The single configuration Hartree-Fock model used is not highly accurate for the lowest states. Also, the Contribution of the transitions from other excited states to the lowest autoionizing level was neglected. The study was based on the understanding that the interaction potential can be chosen arbitrarily to reproduce reliable results.

Integral cross-section results using static potential only have the same trend as the only available theoretical results of [7]. The disparity at low and intermediate energies is attributed to the choice of distorting potential. That is, choice of static potential in the final channel. The effect of absorption was noted at low impact energies near the excitation threshold. This is because inelastic processes such as positronium formation as well as excitation and ionization of the target have a contribution to the integral cross sections at low impact energies

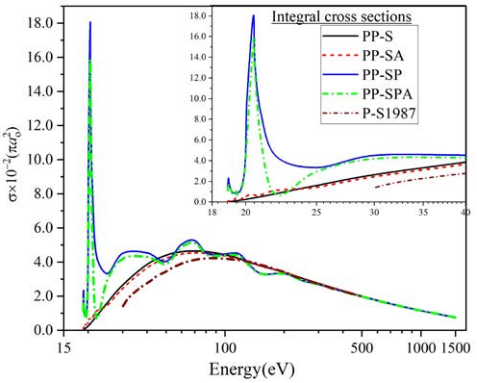

Figure 1. Integral cross section results for e^+ impact excitation of lowest autoionizing state of potassium. PP-S - static only; PP-SA - static + absorption; PP-SP - static + polarization ; PP-SPA - static + polarization + absorption; P-S1987 - e^+ impact results of [7]

Inclusion of polarization potential produced results that have sharp resonance structure near the excitation threshold. An implication that the behaviour of the target as the projectile approaches (polarization) has a high contribution to the integral cross sections in this energy region.

References

[1] Salah Y 2007 *Mod. Phys. Lett. B* **51**:625–637
[2] Nidhi S *et al* 2018 *J. Phys. B* **51**:015204
[3] Nahar S and Wadehra J 1986 *Phys. Rev. A* **35**:5
[4] Staszewska G *et al* 1984 *Phys. Rev. A* **29**:3078
[5] Singh S 2004 *EAJS* **5**:85–98
[6] Clementi E and Roetti C 1974 *At. Data Nucl. Data Tables* **14**:177 – 478
[7] Pangantiwar A and Srivastava R 1987 *J Phys B-At Mol Opt* **20**:5881 – 5902

*E-mail: noahnzeki@gmail.com

Antihydrogen positive ion formation in antihydrogen-positronium collision

T Yamashita[1,2]*, Y Kino[2], E Hiyama[3,4], S Jonsell[5], P Froelich[6]

[1]Institute for Excellence in Higher Education, Tohoku University, Sendai, 980-8576, Japan
[2]Department of Chemistry, Tohoku University, Sendai, 980-8578, Japan
[3]Department of Physics, Tohoku University, Sendai, 980-8578, Japan
[4]Nishina Center, RIKEN, Wako, Saitama 351-0198, Japan
[5]Department of Physics, Stockholm University, Stockholm, SE-10691, Sweden
[6]Department of Chemistry, Uppsala University, Uppsala, Box 518 751-20, Sweden

Synopsis We present a 4-body calculation of the antihydrogen-positronium scattering with particular focus on the antihydrogen positive ions ($\bar{H}^+$) formation that enters the chain of reactions designed to produce ultra-cold antihydrogen atoms for matter-antimatter gravity tests. From the numerically obtained scattering wavefunctions, we determine the S-matrix and state-to-state cross sections in the vicinity of the threshold energy for $\bar{H}^+$ formation. The near-threshold behaviour of these cross sections shows an agreement with the Wigner's law.

The antihydrogen positive ion ($\bar{H}^+$) consisting of an antiproton ($\bar{p}$) and two positrons (e^+) can be a gateway for antimatter chemistry. $\bar{H}^+$ may be manipulated by electric fields and be used in studies of particle physics and atomic physics. $\bar{H}^+$-ion formation from the reaction between an antihydrogen atom ($\bar{H} = \bar{p}e^+$) and positronium ($Ps = e^+e^-$) enters a production chain of ultra-cold antihydrogen atoms for studies of gravity between matter and antimatter [1, 2]. The cold $\bar{H}$ atoms are meant to prepared by sympathetic cooling of $\bar{H}^+$ with Be^+ ions and the subsequent photodetatchment. The $\bar{H}^+$ formation reaction,

$$\bar{H}(1s) + Ps(nl) \rightarrow \bar{H}^+ + e^-, \qquad (1)$$

is endothermic for $n \leq 3$ and exothermic for $n \geq 4$. This rearrangement reaction (1) competes with several inelastic reactions of Ps (de-)excitation and requires rigorous theoretical treatment.

In order to calculate the cross section for the reaction (1), we perform a four-body coupled-rearrangement channel scattering calculation [3, 4]. The total scattering wavefunction Ψ is written as $\Psi = \sum_\upsilon a_\upsilon \Phi_\upsilon + \sum_c \psi_c$, where Φ_υ are square integrable four-body functions that, together with the expansion coefficients a_υ, describe the "intermediate state" of the collision, and ψ_α are open channel functions that describe the asymptotically non-vanishing component. Construction of the set $\{\Phi_\upsilon\}$ plays a primary role in the accurate determination of the cross sections. Each Φ_υ is described in terms of finite range Gaussian functions and satisfies $\langle \Phi_{\upsilon'}|H|\Phi_\upsilon\rangle = E_\upsilon \delta_{\upsilon'\upsilon}$ where H is the total 4-body Hamiltonian. The Schrödinger equation, $H\Psi = E\Psi$, is converted to a set of coupled integro-differential equations under proper boundary conditions of the asymptotic behaviour of scattering wavefunction, and is solved using a finite difference method. State-to-state cross sections are obtained from the S-matrix elements.

As shown in figure 1, we determine the cross sections σ_{rearr} of the reaction (1) and of all competing inelastic processes for $n \leq 3$. Partial waves s–h are included. σ_{rearr} of $Ps(n = 3) + \bar{H}(1s)$ collision shows drastic change against the collision energy while that of $Ps(n \leq 2) + \bar{H}(1s)$ collisions show steady behaviour. We will show that this behaviour is consistent with the Wigner's threshold law [5].

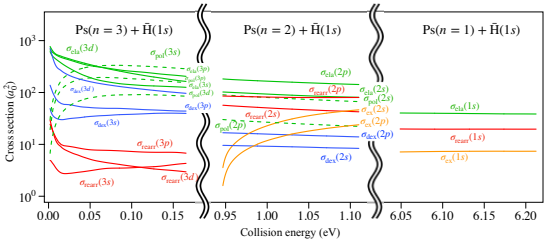

Figure 1. Elastic/inelastic cross sections against the collision energy in center-of-mass reference frame [4]. Red: $\bar{H}^+$ formation, blue: deexcitation, orange: excitation, green solid: elastic, green dashed: polarization.

References

[1] Perez P and Sacquin Y 2012 *Class. Quantum Grav.* **29** 184008
[2] Sacquin Y 2014 *Eur. Phys. J. D* **68** 31
[3] Yamashita T *et al* 2020 *J. Phys. Conf. Ser.* **1412** 052012
[4] Yamashita T *et al* 2021 *New J. Phys.* **23** 012001
[5] Wigner E P 1948 *Phys. Rev.* **73** 1002

*E-mail: tyamashita@tohoku.ac.jp

Laser-assisted elastic electron scattering by Xe in the quasi-Sturmian-Floquet approach

S A Zaytsev[1]*, A S Zaytsev[1], D S Zaytseva[1], L U Ancarani[2] and K A Kouzakov[3]†

[1]Pacific National University, Khabarovsk 680035, Russia
[2]Université de Lorraine, CNRS, LPCT, 57000 Metz, France
[3]Department of Nuclear Physics and Quantum Theory of Collisions, Faculty of Physics, Lomonosov Moscow State University, Moscow 119991, Russia

Synopsis We consider scattering of 1 keV electrons on Xe in an intense laser field of 1.55 eV photons, corresponding to the experimental conditions of [1]. To take into account the light-dressing effect we use Zon's polarization potential in the framework of the quasi-Sturmian-Floquet method [2]. In comparison with the Born approximation (the Zon's model), we show that a better agreement with experiment is found, in particular regarding the peak that the cross section exhibits at small scattering angles.

We consider the laser-assisted electron collision on atomic Xe:

$$e^- + \mathrm{Xe} + \ell\omega \to \mathrm{Xe} + e^-, \qquad (1)$$

where a net number ℓ of photons of frequency ω can be exchanged between the projectile-target system and the external field. We take into account the laser-dressing by taking Zon's potential in the lab frame, namely

$$V(\mathbf{r}) = V_A(r) + \frac{\omega^2\alpha(\omega)}{r^3}(\mathbf{a}(t)\cdot\mathbf{r}), \qquad (2)$$

where V_A is a static atomic potential, $\alpha(\omega)$ is the atomic polarizability, and $\mathbf{a}(t)$ is the free-electron displacement in a laser field. In the Kramers–Henneberger frame the problem is reduced to scattering on the space-translated potential $V[\mathbf{r}+\mathbf{a}(t)]$. We solve this scattering problem within the Hermitian Floquet theory

$$\psi(\mathbf{r},t) = e^{-iEt}\sum_{\ell=-\mathcal{N}}^{\mathcal{N}} e^{-i\ell\omega t}F_\ell(E,\mathbf{r}). \qquad (3)$$

The Fourier-Floquet components F_ℓ are expanded in terms of the parabolic quasi-Sturmian functions [2], and from the solution we calculate the angular cross section.

The result for electrons elastically scattered from Xe with absorption of a single photon is shown in figure 1; the number $\mathcal{N}$ of Fourier-Floquet component in (3) is varied from 1 to 7.

It is found that the minimum position and the subsequent slope are in better agreement with experimental observations [1] than the prediction of Zon's scattering model, which treats the electron scattering in the potential (2) within the Born approximation.

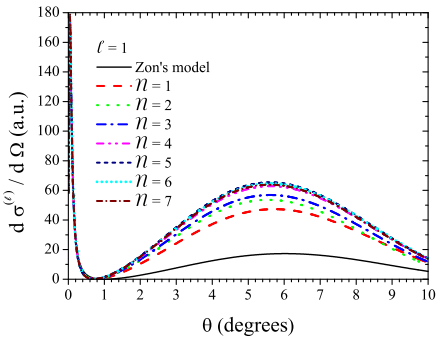

Figure 1. Convergence behavior of the one-photon exchange cross section as the number of photons $\mathcal{N}$ in the expansion (3) is varied from 1 to 7.

References

[1] Morimoto Y *et al* 2015 *Phys. Rev. Lett.* **115** 123201
[2] Zaytsev A S *et al* 2018 *Phys. Rev. A* **97** 043417

*E-mail: zaytsevsa@pnu.edu.ru
†E-mail: kouzakov@srd.sinp.msu.ru

Positron binding and annihilation with nitrogen- and oxygen-containing molecules

J P Cassidy[1]*, A R Swann[1]† and G F Gribakin[1]

[1]School of Mathematics & Physics, Queen's University Belfast, Belfast BT7 1NN, United Kingdom

Synopsis Calculations of positron binding energies and annihilation rates for nitrogen- and oxygen-containing molecules are presented. Where possible, comparisons with experiment are made.

It is now well established that positrons are capable of binding to a variety of polyatomic molecules. By observing vibrational Feshbach resonances (VFRs) in the dependence of the annihilation rate on the positron energy, binding energies have been measured for about 90 molecules using trap-based positron beams [1, 2, 3, 4]. However, due to strong electron-positron correlations, performing accurate calculations of positron binding energies remains a difficult problem.

Here, we extend the method which employs a model correlation potential proposed by Gribakin and Swann [5] to calculate positron bound states and annihilation rates for several nitrogen- and oxygen-containing organic molecules. These molecules are acetonitrile (C_2H_3N), propionitrile (C_3H_5N), 2-methylpropionitrile (C_4H_7N), acrylonitrile (C_3H_3N), cyanoacetylene (C_3HN), formaldehyde (CH_2O), acetaldehyde (C_2H_4O), propanal (C_3H_6O), and propanone (C_3H_6O). The positron is considered to be subject to the potential due to the field of the static molecule plus a model-correlation potential, viz., $V_{\rm cor}(\mathbf{r}) = -\frac{1}{2}\sum_A \alpha_A|\mathbf{r}-\mathbf{r}_A|^{-4}[1-\exp(-|\mathbf{r}-\mathbf{r}_A|^6/\rho_A^6)]$, where $\mathbf{r}$ is the position of the positron, $\mathbf{r}_A$ is the position of the A-th constituent atom, α_A is the hybrid polarizability of atom A [6] and ρ_A is a cutoff radius used to parameterize short-range correlations. We take $\rho_{\rm C} = \rho_{\rm H} = 2.051$ a.u.[7], $\rho_{\rm N} = 1.829$ a.u. and $\rho_{\rm O} = 1.765$ a.u. The latter two are chosen to reproduce the measured positron binding energies of acetonitrile and acetaldehyde, respectively [4]. Figure 1 presents a comparison of some of the calculated binding energies with the corresponding experimental values [4]. We find our binding-energy calculations to be in excellent agreement with experiment, with all errors less than 7%. Where experimental data aren't available, our calculations serve as predictions of the positron binding energy for that molecule. The positron wave function is also used to calculate the annihilation rates.

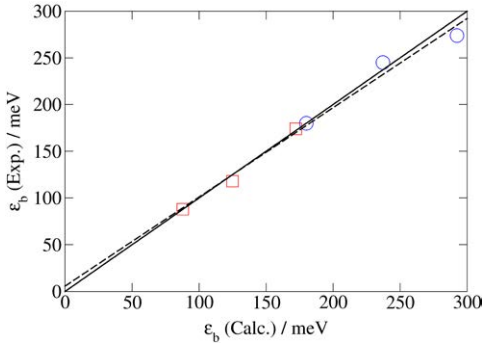

Figure 1. Comparison of the measured and calculated positron binding energies for molecules containing nitrogen (blue cirlces)mand oxygen (red squares). Solid line: identity line; dashed line: regression line $\varepsilon_b^{\rm exp} = 5.6453 + 0.9551\varepsilon_b^{\rm calc}$.

References

[1] Danielson J R, Young J A and Surko C M 2009 *J. Phys. B* **45** 235203
[2] Gribakin G F, Young J A and Surko C M 2010 *Rev. Mod. Phys.* **82** 2557
[3] Danielson J R, Gosselin J J and Surko C M 2010 *Phys. Rev. Lett.* **104** 233201
[4] Danielson J R *et al* 2012 *Phys. Rev. A* **85** 022709
[5] Swann A R and Gribakin G F 2018 *J. Chem. Phys.* **149** 244305
[6] Miller K J 1990 *J. Am. Chem. Soc.* **112** 8533
[7] Swann A R and Gribakin G F 2020 *Phys. Rev. A* **101** 022702

*E-mail: jcassidy18@qub.ac.uk
†E-mail: a.swann@qub.ac.uk

Many-body theory of positron binding in polyatomic molecules

B J Cunningham[1], J Hofierka[1], C M Rawlins[1], C H Patterson[2] and D G Green[1]*

[1]School of Mathematics and Physics, Queen's University Belfast, Belfast BT7 1NN, United Kingdom
[2]School of Physics, Trinity College Dublin, Dublin 2, Ireland

Synopsis Many-body theory of positron binding in polyatomic molecules is developed and used to calculate binding energies for a range of polar and non-polar molecules. We find the best agreement with experiment to date (to within a few percent in some cases). Delineating the effects of the correlations, we show, in particular, that virtual-positronium formation significantly enhances binding in organic polar molecules, and moreover, that it is essential to support binding in non-polar molecules including CS_2, CSe_2 and benzene.

Positrons bind to molecules leading to vibrational excitation and spectacularly enhanced annihilation (see [1] for a review). Whilst positron binding energies have been measured via resonant annihilation spectra for around 75 molecules in the past two decades [1], an accurate *ab initio* theoretical description has remained elusive. Of the molecules studied experimentally, calculations exist for only 6, and for these, standard quantum chemistry approaches have proved severely deficient, agreeing with experiment to at best 25% accuracy for polar molecules, and failing to predict binding in non-polar molecules. The theoretical difficulty lies in the need to accurately account for strong positron-molecule correlations including polarisation of the electron cloud, screening of the positron-molecule Coulomb interaction by molecular electrons, and the unique process of virtual-positronium formation (where a molecular electron temporarily tunnels to the positron). Their roles in positron-molecule binding have yet to be elucidated.

We have developed a diagrammatic many-body description of positron-molecule binding in polyatomic molecules that takes *ab initio* account of the correlations [2]. We solve the Dyson equation for the positron quasiparticle wavefunction in a Gaussian basis, constructing the positron-molecule self-energy including the *GW* contribution that describes polarisation, screening and electron-hole interaction interactions (at RPA/TDHF/BSE levels), the ladder series of positron-electron interactions that describes virtual positronium formation, and the ladder series of positron-hole interactions.

We have used it to calculate binding energies for a range of polar and non-polar molecules, focussing chiefly on the molecules for which both theory and experiment exist [2]. Delineating the effects of the correlations, we show, in particular, that virtual-positronium formation significantly enhances binding in organic polar molecules, and moreover, that it is essential to support binding in non-polar molecules including CS_2, CSe_2 and benzene. Overall, we find the best agreement with experiment to date (to within a few percent in some cases). The method also enables the calculation of the positron bound wavefunction (see Fig. 1), and of the positron-electron contact density (annihilation rate in the bound state).

Our approach can be extended to enable predictive *ab initio* calculations of positron scattering and annihilation γ spectra in molecules, providing insight that should support the development of fundamental experiments and the myriad of antimatter-based technologies and applications. Moreover, the positron-molecule problem provides a testbed for the development of methods to tackle the quantum many-body problem, for which our results can serve as benchmarks.

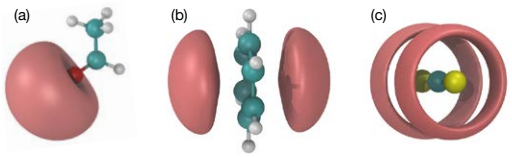

Figure 1. Present many-body theory calculated bound-state positron density for (a) acetaldehyde (polar, isovalue at 0.62 of maximum density), (b) benzene (non-polar, isovalue at 0.83 of maximum density), and (c) CS_2 (non-polar, isovalue at 0.99 of maximum density).

References

[1] Gribakin G F *et al* 2010 *Rev. Mod. Phys.* **82** 2557
[2] Cunningham B J, Hofierka J, Rawlins C M, Patterson C H and Green D G *In preparation*

This work is funded by DGG's European Research Council grant 804383 "ANTI-ATOM".

*E-mail: d.green@qub.ac.uk

Bound positron molecule annihilation resonances beyond fundamental modes

S Ghosh*, J R Danielson†, and C M Surko

Physics Department, University of California San Diego, La Jolla, CA 92093, USA

Synopsis Evidence is presented that in positron-molecule interactions, vibrational Feshbach resonances can occur by excitation of vibrational modes other than the fundamentals.

Positrons bind to most molecules through Feshbach resonant excitation of dipole- and quadrupole-active fundamental vibrational modes, and this leads to greatly enhanced annihilation rates [1]. These resonances ride on a broad background of annihilation which is also above the level expected from a simple collision process [2, 3]. Although it has been proposed that this background could be due to annihilation on combination and overtone vibrations, no direct evidence is yet available. Here, measurements are presented that resolve new resonances, likely due to combination and overtone modes [4].

Positrons from a ^{22}Na radioactive source are moderated to $\sim$ eV energies using a layer of solid Ne at 8 K then magnetically guided into a Penning-Malmberg-style buffer gas trap (BGT) at 293 K. They thermalize to the ambient via inelastic collisions with N_2 and CF_4 molecules. The room temperature positrons are then guided into a second trap and cooled to 50 K through collisions with CO, to form a cold (CT) beam (FWHM $\sim$ 20 meV) [5].

Figure 1 shows the energy resolved annihilation spectrum in the region of the fundamental C-H stretch vibrational modes (cf. blue bars) for cyclopentane (C_5H_{10}). The expected resonance from these modes is indicated by the red curve. A distinct peak in the annihilation spectrum at $\sim$ 0.27 eV is evidence of a new resonance which must be due to modes other than fundamentals. Lower resolution data for other ring and chain hydrocarbons using the BGT beam will be presented that exhibit similar features.

The relation of these new resonances to IR spectra (e.g., blue curve, Fig. 1) and correlation with the combination and overtones of the fundamental vibrational modes will be discussed. This study provides evidence that positron interactions with modes other than the fundamental vibrations in molecules can result in annihilation resonances and greatly enhanced annihilation rates.

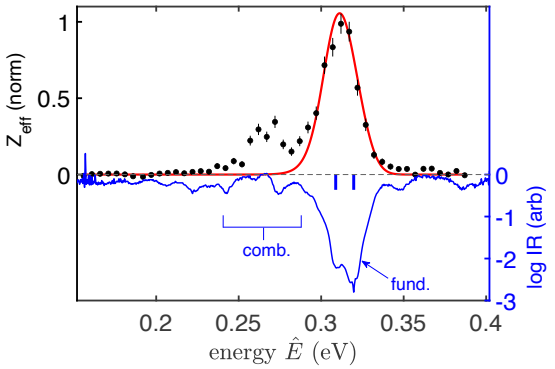

Figure 1. (Color online) Normalized, background-subtracted annihilation rate Z_{eff} for cyclopentane as a function of peak total energy $\hat{E}$ using the CT beam (black circles). Red curve represents the resonance due to fundamental modes (blue bars). These modes and the IR spectrum (blue curve) have been downshifted by the 48 meV binding energy.

Work supported by the U. S. NSF, grant PHY-2010699.

References

[1] G. F. Gribakin, J. A. Young, and C. M. Surko, Rev. Mod. Phys. **82**, 2557 (2010).
[2] A. C. L. Jones, J. R. Danielson, M. R. Natisin, C. M. Surko, and G. F. Gribakin, Phys. Rev. Lett. **108**, 093201 (2012).
[3] G. F. Gribakin, J. F. Stanton, J. R. Danielson, M. R. Natisin, and C. M. Surko, Phys. Rev. A **96**, 062709 (2017).
[4] S. Ghosh, J. R. Danielson and C. M. Surko, Phys. Rev. Lett., **125**,173401 (2020).
[5] M. R. Natisin, J. R. Danielson, and C. M. Surko, Appl. Phys. Lett. **108**, 024102 (2016).

*E-mail: soumen@physics.ucsd.edu
†E-mail: jrdanielson@ucsd.edu

Theoretical and experimental study of positron-pyrazine collisions

V Graves[1]*, D Edwards[2], D Stevens[2], Z Cheong[2], F Blanco[3], J D Gorfinkiel[1], G García[4], M J Brunger[5], R D White[6], and J P Sullivan[2]

[1]School of Physical Sciences, The Open University, Walton Hall, Milton Keynes, UK
[2]Laser Physics Centre, Research School of Physics, Australian National University, Acton ACT, Australia
[3] Dept. de Estructura de la Materia, Física Térmica y Electrónica, Universidad Complutense de Madrid, Spain
[4]Instituto de Física Fundamental, Consejo Superior de Investigaciones Científicas, Madrid, Spain
[5]College of Science and Engineering, Flinders University, Adelaide, SA, Australia
[6]College of Science and Engineering, James Cook University, Townsville, Qld., Australia

Synopsis We present and compare recent experimental and theoretical cross sections for positron scattering from non-polar pyrazine. At low energy, agreement between the measured and calculated elastic cross sections is not as good as for similar polar targets.

Understanding positron interactions with biomolecules, e.g. DNA nucleobases, is important for modelling their medical uses, particularly in Positron Emission Tomography. Nucleobases have low symmetry and are hard to bring into gas the phase, so more volatile model systems with higher symmetry are often investigated instead. Diazines have been studied to gain insight into electron and positron scattering from pyrimidinic nucleobases. Of these, pyrazine has the highest symmetry and is non-polar.

Experimental data was measured using the Surko trap and beam system at ANU, described in detail in [1], and using well established measurement techniques [2]. Measurements were made of grand total, total elastic (rovibrationally averaged), total positronium, ionisation and electronic excitation cross sections. Elastic differential cross sections (DCS) were also measured, at energies from 1 to 10 eV.

Low energy cross sections were calculated at the Static-plus-Polarization level using the R-matrix method [3] and electron-diazine models as a starting point. Calculations indicate that a more accurate description of the polarization effects is required for positron scattering versus electron scattering. At higher energies, the well known IAM-SCAR method was employed [4].

Figure 1 shows the DCS at 5 eV. Here, the shape of the experimental data agrees better with the IAM-SCAR calculation at low scattering angles, being strongly forward peaked. This is likely due to the influence of the large dipole polarizability of the molecule. At intermediate scattering angles, the R-matrix and Schwinger multichannel (SMC) data of Moreira and Bettega [5] have better agreement. This is expected as these two theoretical approaches model the molecular structure effects much more accurately. No theory is able to reproduce well the experimental data for all angles hinting at limitations in our ability to accurately describe low energy positron scattering from high-polarizability molecules.

*E-mail: vhg7@open.ac.uk

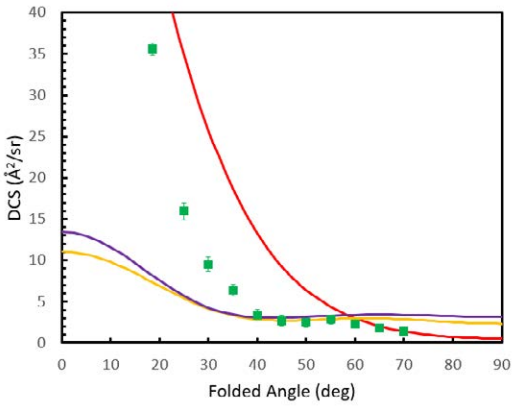

Figure 1. DCS for positron scattering from pyrazine at 5 eV. Experiment: circles. Calculations: red line, IAM-SCAR, yellow line, R-matrix, purple line, SMC [5].

References

[1] Sullivan J P *et al* 2008 *Rev. Sci. Instr.* **79** 113105
[2] Sullivan J P *et al* 2002 *Phys. Rev.* A **66** 042708
[3] Mašín Z *et al* 2020 *Computer Phys. Comm.* **249** 107092
[4] Barbosa, A S *et al* 2019 *Phys. Rev.* A **100** 042705
[5] Moreira G M and Bettega M H F 2019 *J. Phys. Chem.* A **42** 9132

Positron binding to chlorinated hydrocarbons

A R Swann[1]*, G F Gribakin[1]†, J R Danielson[2], S Ghosh[2], M R Natisin[2] and C M Surko[2]

[1]School of Mathematics & Physics, Queen's University Belfast, Belfast BT7 1NN, United Kingdom
[2]Department of Physics, University of California San Diego, La Jolla, California 92093, USA

Synopsis Measurements and calculations of positron affinities are presented for a selection of chlorinated hydrocarbons.

Calculations of positron-molecule binding are challenging, due to the strong electron-positron correlations that determine the binding energies and, for nonpolar species, ensure the very existence of binding. However, binding energies have been found experimentally for around 90 species using a trap-based positron beam, by observing vibrational Feshbach resonances in the positron-energy dependence of the annihilation rate.

Here we present measurements of binding energies for a selection of chlorinated hydrocarbons with up to 6 carbon atoms and one or two Cl atoms. These data were taken over many years, using positron beams with different parameters and different analysis procedures [1, 2, 3, 4]. The new and previous data sets are corrected for the differences in beam parameters, and the binding energies are obtained from a consistent analysis of the annihilation rates for these molecules. We also present calculations of these binding energies using the model-potential method [5], where the positron-molecule interaction potential is taken to be the sum of the electrostatic potential and a model potential that accounts for the positron-molecule correlations, viz., $V_{\rm cor}(\mathbf{r}) = -\frac{1}{2}\sum_A \alpha_A |\mathbf{r} - \mathbf{r}_A|^{-4}[1 - \exp(-|\mathbf{r} - \mathbf{r}_A|^6/\rho_A^6)]$, where $\mathbf{r}$ is the position of the positron; the sum is over the molecule's constituent atoms; and α_A, $\mathbf{r}_A$, and ρ_A are the hybrid polarizability [6], position, and cutoff radius (a parameter) of constituent atom A. Using past experience of calculations for alkanes and other small molecules, we take $\rho_{\rm C} = \rho_{\rm H} = 2.15$ a.u., except for n-hexyl chloride, for which we take $\rho_{\rm C} = \rho_{\rm H} = 2.25$ a.u. [7, 8]. To understand the sensitivity of the results to the choice of $\rho_{\rm Cl}$, we carried out the calculations using two different values, viz., $\rho_{\rm Cl} = 2.20$ and 2.24 a.u. Figure 1 compares the measured and calculated binding energies for 19 molecules.

*E-mail: a.swann@qub.ac.uk
†E-mail: g.gribakin@qub.ac.uk

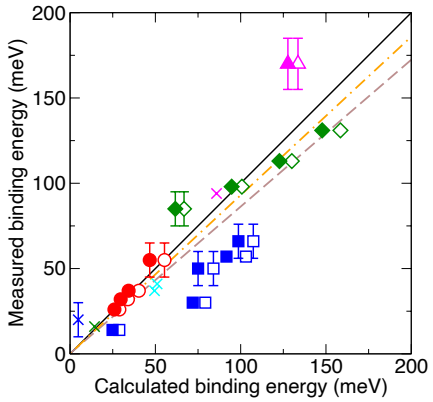

Figure 1. Open (filled) symbols, $\rho_{\rm Cl} = 2.20$ (2.24) a.u: circles, methanes; squares, ethylenes; diamonds, propanes; triangles, n-hexyl chloride. Crosses: hydrocarbons. Lines: solid, identity; dashed (dot-dashed), fit for $\rho_{\rm Cl} = 2.20$ (2.24) a.u.

Overall, there is strong positive correlation between the measured and calculated positron binding energies. The strongest outliers, viz., the chlorinated ethylenes, are planar molecules. This suggests that the anisotropy of the molecular polarizability (unaccounted for by the present model potential) plays an important role in determining the binding energy.

References

[1] Gilbert S J *et al* 2002 *Phys. Rev. Lett.* **88** 043201
[2] Gribakin G F, Young J A and Surko C M 2010 *Rev. Mod. Phys.* **82** 2557
[3] Danielson J R, Gosselin J J and Surko C M 2010 *Phys. Rev. Lett.* **104** 233201
[4] Danielson J R *et al* 2012 *Phys. Rev. A* **85** 022709
[5] Swann A R and Gribakin G F 2018 *J. Chem. Phys.* **149** 244305
[6] Miller K J 1990 *J. Am. Chem. Soc.* **112** 8533
[7] Swann A R and Gribakin G F 2019 *Phys. Rev. Lett.* **123** 113402
[8] Swann A R and Gribakin G F 2020 *Phys. Rev. A* **101** 022702

Calculated cross sections for elastic scattering of slow positrons by polar molecules

G M Moreira[1]*, A S Barbosa[1], S D Sanchez[1], R F da Costa[2] and M H F Bettega[1]†

[1]Departamento de Física, Universidade Federal do Paraná, Caixa Postal 19044, 81531-980 Curitiba, Paraná, Brazil
[3]Centro de Ciências Naturais e Humanas, Universidade Federal do ABC, 09210-580 Santo André, São Paulo, Brazil

Synopsis We present calculated cross sections for elastic positron impact by polar molecules using the Schwinger multichannel method. The calculations were performed at the static plus polarization level of approximation, for impact energies up to 10 eV. In order to improve the description of the long-range dipole potential, the Born-closure procedure was employed.

In recent years, there has been an effort by theoreticians and experimentalists to improve the description of the collision process of positron with atoms and molecules. Particularly, from the theoretical point of view, the description of the positron-molecule collision process is still a very difficult task.

The importance of obtaining reliable cross sections for the scattering of positrons by molecules comes from the fact that these data are of great relevance in many areas of science and technology. For instance, in the simulation of positron tracking in biologically relevant media, the cross section data for positron-molecule interactions are crucial input parameters in Monte Carlo codes [1].

This study focuses on positron scattering by polar molecules with different applications. Ammonia (NH_3) and phosphine (PH_3) have great significance in the astrophysical environments; the alcohols methanol (CH_4O) and ethanol (C_2H_6O) have high application in organic chemistry; and uracil ($C_4H_4N_2O_2$) is a system of biological relevance for its one of the constituents of the RNA nucleobases.

We employed the Schwinger multichannel (SMC) method [2] to obtain the scattering amplitude and thus calculate the integral and differential cross sections. To account for the long-range dipole interaction, we used the Born-closure scheme [3] to improve the description of scattering amplitudes. In order to obtain a trusty set of results, we have performed extensive studies to improve the description of the polarization potential, as well as, a careful choice of the basis set to describe in an accurate way the molecular target.

The results obtained in this study were compared with previous theoretical and/or experimental data available in the literature. Additionally, for ethanol, methanol and uracil molecules we used our calculated differential cross section in order to provide a correction to the experimental total cross section to account for the lack of angular resolution in the experimental apparatus used by the authors in Refs. [4, 5].

References

[1] Sanz A G *et al* 2012 *Int. J. Radiat. Biol.* **88** **71**
[2] Germano J S E and Lima M A P 1993 *Phys. Rev. A* **47** 3976
[3] da Costa R F *et al* 2015 *Eur. Phys. J. D* **69** 159
[4] Zecca A *et al* 2008 *Phys. Rev. A* **78** 022703
[5] Anderson E K *et al* 2014 *J. Chem. Phys.* **141** 034306

*E-mail: gmm08@fisica.ufpr.br
†E-mail: bettega@fisica.ufpr.br

An atomic momentum spectroscopy study for elucidating the range of the validity of the plane wave impulse approximation

Y Onitsuka[1] *, Y Tachibana[1], and M Takahashi[1] †

[1]Institute of Multidisciplinary Research for Advanced Materials, Tohoku University, Sendai 980–8577, Japan

Synopsis We have investigated the range of the validity of the plane wave impulse approximation (PWIA) in atomic momentum spectroscopy by measuring energy loss spectra for H_2 at incident electron energies (E_0) ranging from 0.5 to 2.0 keV. Furthermore, subtracted spectra have been generated by subtracting contribution of molecular translational motion and the instrumental response function from each energy loss spectrum. It is found that with the increase in E_0 the spectral shape of the subtracted spectrum becomes more symmetric and that it can be recognized as momentum distribution due to the intramolecular atomic motion at E_0 = 2.0 keV.

Within the plane wave impulse approximation (PWIA), atomic momentum spectroscopy (AMS) [1] can provide direct information about atomic motion in matter as a Compton profile. Elucidation of the range of the validity of PWIA is therefore essential for applying AMS as a molecular spectroscopy technique. Once the experiment reaches the PWIA high-energy limit, the AMS spectrum should be symmetric against the atomic momentum (P) and unaltered against the increase in the incident electron energy (E_0). Thus the validity of PWIA is experimentally verifiable. Indeed, such a study was made for H_2 by Vos [2]. He observed that failure of the PWIA description appears as asymmetry of the AMS spectral shape, and this observation is consistent with the theoretical prediction [3] that the dominant correction term is odd with respect to P. However, the reported AMS spectra [2] involve contribution of the instrumental response function that is dependent on E_0. Clearly, further studies are required for elucidating more completely the validity of PWIA.

In this study, we have carried out AMS experiments on H_2 at several E_0 values ranging from 0.5 to 2.0 keV by using our multichannel AMS apparatus [4-6]. Briefly, electron backscattering (θ = 135°) occurred where an incident electron beam of E_0 collided with a H_2-gas beam. The energy loss of the scattered electron was measured, while the instrumental response function at different E_0 values being set identical to each other by adjusting the decereration ratio in electron energy analysis. Here the instrumental response functions were assumed to be the same as the AMS spectra for Xe.

An example of the results is depicted in Figure 1, which shows the AMS spectra of H_2 measured at E_0 = 1.0 and 2.0 keV, together with their right-and-left reversed ones. Difference spectra between the two are also included as a measure of spectral symmetry. Asymmetry of the AMS spectrum of H_2 at E_0 = 1.0 keV is noticeably large, while that at 2.0 keV is minimal. In this way, the validity or failure of PWIA can be evaluated qualitatively. In the talk, we present results of quantitative data analysis, which employs the convolution theorem to exclude the contribution of the instrumental response function. E_0-dependence of an AMS spectrum due only to intramolecular atomic motion becomes, for the fist time, directly visible.

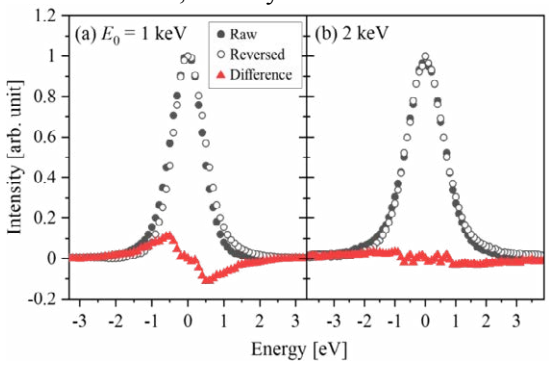

Figure 1. AMS spectra of H_2 at E_0 = 1 and 2 keV.

References

[1] Vos M 2001 *Phys. Rev. A* **65** 012703
[2] Vos M 2016 *J. Phys. B* **49** 145202
[3] Sears V F 1984 *Phys. Rev. B* **30** 44
[4] Yamazaki M *et al* 2017 *Rev. Sci. Instrum.* **88** 063103
[5] Yamazaki M *et al* 2019 *J. Phys. B* **52** 065205
[6] Tachibana Y *et al* 2019 *Phys. Rev. A* **100** 032506

* E-mail: yuuki.onitsuka.e8@tohoku.ac.jp
† E-mail: masahiko@tohoku.ac.jp

Elastic positron collision with acetone molecule: a study in the low-energy region

R O Lima*, G M Moreira, M H F Bettega and S D Sanchez†

Departamento de Física, Universidade Federal do Paraná, Caixa Postal 19044, 81531-980 Curitiba, Paraná, Brazil

Synopsis We report integral (ICS) and differential (DCS) cross sections for positron elastic low-energy collisions with acetone. For this purpose, we employed Schwinger multichannel method in the static plus polarization approximation. The effects of permanent electric dipole moment were taken into account through the Born-closure scheme. We compared our results with experimental data available in the literature and our results agree qualitatively well with the most recent experimental data available in all energy regions.

Acetone is one of the simplest carbonyl with important investigations of absorption spectra [1]. It also plays an important role in industrial applications as a solvent [2] and a agent in the manufacture of cordite [3], and it is of relevance as a biomarker for people with diabetes [4]. For many of these applications, it is essential to obtain data that can be used to model interactions and applications of this system.

There are previous experimental works on the total cross section (TCS) available in the literature. However, the most recent data from Ref. [5] do not agree at very low energy region with the other two data reported in Refs. [5, 6]. Therefore, the theoretical study of positrons collisions with this system is of interest in order to compare with the experimental results. In this work, we employed the Schwinger multichannel method [7] in the static plus polarization level of approximation(SP), which takes into account the distortion of electronic cloud due to the incoming charged particle, to study the interactions of low-energy positron with the acetone molecule. To describe the long-range interactions due to the permanent electric dipole moment, we used the Born-closure scheme [8]. Additionally, we employed our differential cross sections to properly correct the total cross sections reported in Ref. [5] in order to account for the lack of angular resolution in the apparatus used by these authors.

Our present integral cross sections are shown in figure 1, which are in good qualitative agreement with most recent experimental results from Ref. [5]. The correction of experimental measurements due the angular resolution of apparatus shows a better accordance with our calculations. With respect to the differential cross sections calculations, they exhibited dominant patterns associated with p- d- and f- partial waves depending on the incident energy.

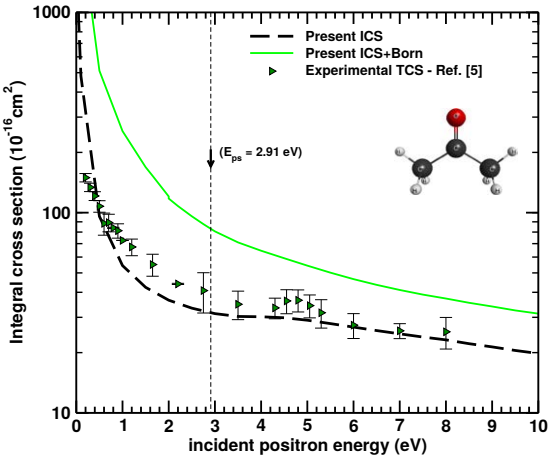

Figure 1. Present ICS with and without Born corrections, and experimental TCS data from Ref. [5]. E_{ps} represents the positronium threshold energy.

References

[1] Nobre M *et al* 2008 *Phys.Chem.Chem.Phys.* **10** 550
[2] Mohadesi M *et al* 2020 *Fuel* **273** 117736
[3] Anbarasan P *et al* 2012 *Nature* **491** 235
[4] Manolis A *et al* 1983 *Clin.Chem.* **29** 5
[5] Zecca A *et al* 2010 *PMC Phys. B* **3** 4
[6] Kimura M *et al* 2000 *Adv. Chem. Phys.* **111** 537
[7] Germano J *et al* 1993 *Phys. Rev. A* **47** 3976
[8] da Costa R J *et al* 2015 *Eur. Phys. J. D* **69** 159

*E-mail: rafael@fisica.ufpr.br
†E-mail: ssanchez@fisica.ufpr.br

Electron and Positron scattering by lactic acid molecule

R V B Morás*, C A Amaral, G M Moreira, A S Barbosa† and S D Sanchez

Departamento de Física, Universidade Federal do Paraná, Caixa Postal 19044, 81531-990 Curitiba, Paraná, Brasil

Synopsis In this work we study low energy electron and positron interactions with lactic acid molecule. The Schwinger Multichannel Method were employed in the calculations of integral and differential cross sections, in the static-exchange plus polarization and static plus polarization approximations, for electron and positron scattering, respectively. The calculations were performed for the two most stable conformers of the lactic acid.

The interest in low energy electron scattering by molecules of biological interest was greatly increased by the work of Boudaïffa *et al* [2], in which it was shown that secondary electrons, coming from ionizing radiation, may cause molecular breaks through the Dissociative Electron Attachment process. Whereas, understanding interaction of positron with organic molecules is desirable to help understand positron track in human tissue, since Positron Emission Tomography[4] is an important tool for tumor localization.

Lactic acid is a biologically relevant molecule, since it is a simple organic acid commonly present in the human body. Seven conformers of this molecule were experimentally reported[1]. Despite the relevance of this target, to the best of our knowledge, there is only one work reporting electron interactions with latic acid [3]. In particular, the authors reported theoretical results for DEA, with the use of *ab initio* molecular dynamics simulation, for the second most stable conformer of lactic acid [3].

The present work proposes to study the low energy electron and positron scattering by the two most stable conformers of latic acid, shown in Figure 1. Both electron and positron scattering calculations were performed with the Schwinger Multicanal Method [5, 6]. The former was performed in the static exchange and static exchange plus polarization approximation, while the latter in the static plus polarization approximation. The targets were described in the Born-Oppenheimer approximation at the Hartree-Fock level. The electron calculations employed Bachelet, Hamann and Schluter pseudopotentials[7] and were carried out including both singlets and triplets and only singlets.

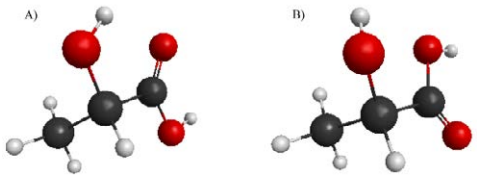

Figure 1. Structural formula of A) first and B) second most stable conformers of lactic acid (generated with McMolPlt[8])

The results of the Elastic Cross Section for electron and positron scattering were compared. For the former, we characterized the position of a π^* resonance, related to the double bound in the carboxylic group, in the different approximations carried out. Once there is no experimental data in the literature for electron scattering by lactic acid, we compared our results with a semi empirical scale rule, accordingly to Aflatooni[9]. Finally, an analysis of the Differential Cross Section for both particle's scattering were performed.

References

[1] Jarmelo S *et al* 2012 *J. Phys. Chem.B* **116(1)** 9-21
[2] Boudaïffa B *et al* 2000 *Science* **287** 1658
[3] Zhang Y *et al* 2019 *Sci Rep* **9(1)** 19532
[4] Bailey D L *et al* 2007 **Springer: London**
[5] Germano J S E and Lima M A P 1993 *Phys. Rev.A* **47** 3976
[6] Lima M A P *et al* 1990 *Phys. Rev.A* **41** 327
[7] Bettega M H F *et al* 1993 *Phys. Rev.A* **47** 1111
[8] Bode B M and Gordon M S 1998 *J. Molec. Graph. Model.* **16** 133-138
[9] Aflatooni K *et al* 2001 *J. Chem. Phys.* **115** 6489

*E-mail: rvmoras@fisica.ufpr.br
†E-mail: alessandra@fisica.ufpr.br

Positron cooling in N_2 and CF_4 gases

A R Swann[1]* **and D G Green**[1]†

[1]School of Mathematics and Physics, Queen's University Belfast, Belfast BT7 1NN, United Kingdom

Synopsis We perform Monte Carlo simulations of positron cooling in N_2 and CF_4 via rotational and vibrational excitations, examining the effects of positron-positron interactions.

Developments in positron trapping have enabled the study of low-energy antimatter interactions with atoms and molecules [2, 3], and antihydrogen formation [4]. In a typical setup, ∼500 keV positrons from a ^{22}Na source are slowed to eV energies by a solid-neon moderator and guided into a Surko trap [5], where thermalization to room temperature is achieved via collisions with N_2 and/or CF_4 gases. Regarding theory, recently, a Monte Carlo approach [6] using accurate many-body-theory cross sections [7] gave a complete description of thermalization in noble gases, obtaining excellent agreement with experiment [8, 9]. But cooling in molecular gases is not well understood theoretically, even for N_2 and CF_4, despite their important use. Recent experiments for CF_4 indicated that the positron momentum distribution remains Maxwellian throughout the cooling, suggesting a mechanism beyond simple excitation of the dominant ν_3 and ν_4 vibrational modes (which alone would be expected to lead to 'pile-ups' of the distribution below the vibrational thresholds; see Fig. 1).

Here, we calculate the evolution of the momentum distribution $f(k)$ and positron temperature T during cooling in N_2 (via rotational excitation) and CF_4 (via vibrational excitation) using a Monte Carlo approach, simulating the experiments of Natisin *et al* [10]. We use the Born-dipole and Born-quadrupole cross sections, respectively. Figures 1 and 2 show the evolution of $f(k)$ and T, respectively, for CF_4, calculated with the inclusion of the dominant ν_3 and ν_4 modes, and the ν_1 mode. The predicted evolution of T is in excellent agreement with experiment, and although we observe 'pile-ups' at the vibrational thresholds, the inclusion of ν_1 enables combination cooling below the lowest threshold (ν_4). We are now investigating the effect of positron-positron collisions, determining whether the experimental positron-to-gas-density ratio is sufficient to effect rapid Maxwellianization.

*E-mail: a.swann@qub.ac.uk
†E-mail: d.green@qub.ac.uk

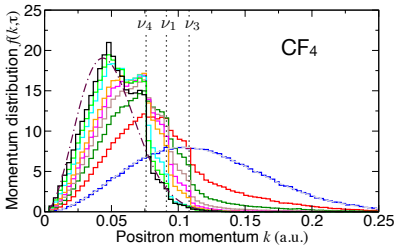

Figure 1. $f(k)$ for cooling in CF4. Values of time density (in ns amg): 0 (blue), 0.002 (red), 0.004 (dark green), 0.006 (brown), 0.008 (magenta), 0.01 (orange), 0.02 (cyan), 0.03 (light green), 0.06 (black). Dashed line: initial MB for T = 1700 K. Dot-dashed line: MB for 300 K. Dotted lines: vibrational thresholds.

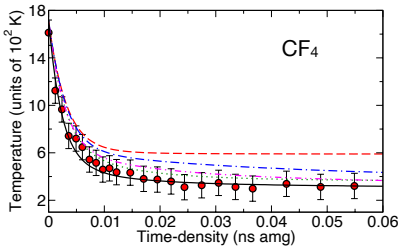

Figure 2. T for cooling in CF4. ν_3 only (red), $\nu_3 + \nu_4$ (blue), $\nu_3 + \nu_4$ with scaling (green), $\nu_3 + \nu_4 + \nu_1$ (magenta), $\nu_3 + \nu_4 + \nu_1$ with scaling (black), experiment [10] (red circles).

References

[1] Danielson J R *et al* 2015 *Rev. Mod. Phys.* **87** 247
[2] Surko C M *at al* 2005 *J. Phys. B* **38** R57
[3] Gribakin G F *et al* 2010 *Rev. Mod. Phys.* **82** 2557
[4] ALPHA Collaboration 2011 *Nat. Phys.* **7** 558
[5] Surko C M *et al* 1989 *Phys. Rev. Lett.* **62** 901
[6] Green D G 2018 *Comp. Phys. Comm.* **224** 362
[7] Green D G *et al* 2014 *Phys. Rev. A* **90** 032712
[8] Green D G 2017 *Phys. Rev. Lett.* **119** 203403
[9] Green D G 2017 *Phys. Rev. Lett.* **119** 203404
[10] Natisin M R *et al* 2014 *J. Phys. B* **47** 225209

This work is funded by European Research Council grant 804383 "ANTI-ATOM".

Positronium Scattering by O_2 and CO_2

R S Wilde[1] *, H B Ambalampitiya[2] and I I Fabrikant[2] †

[1]Oregon Institute of Technology, Dept. of Natural Sciences, Klamath Falls OR, 97601-8801, USA
[2]University of Nebraska-Lincoln, Dept. of Physics and Astronomy, Lincoln NE, 68588-0299, USA

Synopsis We calculate elastic and positronium (Ps) break-up cross sections for collision of Ps with O_2 and CO_2 in the fixed-nuclei approximation. The results exhibit similarity between electron and Ps scattering cross sections when plotted as a function of the projectile velocity confirming experimental observations. Below the Ps break-up threshold we observe resonance structures similar to those obtained earlier for Ps-N_2 scattering.

The similarity between electron and positronium (Ps) scattering discovered ten years ago [1] continues to attract attention of experimentalists and theorists. In particular a recent observation of resonant Ps-N_2 scattering [2] similar to resonant e–N_2 scattering was confirmed by theory [3].

Although a low-energy Π_g resonance is observed in both e–N_2 and e–O_2 scattering, the latter resonance is extremely narrow and can be observed only in experiments with a very high energy resolution. In the case of CO_2 a sharp Π_u resonance exists in electron scattering from this molecule and there is evidence of a resonance in Ps scattering as well [4].

In the present work we have performed calculations of elastic Ps-O_2 and Ps-CO_2 scattering using exchange and correlation potentials derived from the free-electron-gas (FEG) approximation developed earlier for the Ps-atom and Ps-molecule interaction [5].

Apart from elastic scattering the most important inelastic process is Ps break-up or ionization. We calculate Ps ionization for the present targets using the binary-encounter approximation [3].

In Figure 1 we show our results for the total Ps-O_2 and Ps-CO_2 cross sections compared with experiment and the recommended total electron scattering cross sections as a function of projectile velocity.

For both targets we see scattering resonances below the Ps ionization threshold which is at a velocity of 0.5 a.u. Above the threshold our total cross sections exhibit good agreement with the experimental results and become similar to the total electron scattering cross section.

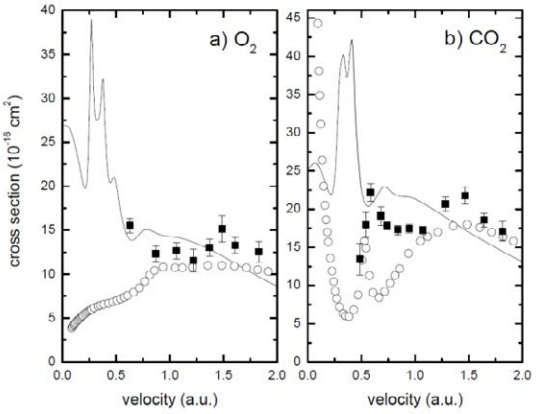

Figure 1. Total scattering cross sections for Ps and e^- scattering by a) O_2 and b) CO_2. Solid lines: present results; Squares: Ps experiment, O_2 [1] and CO_2 [4]; Circles: recommended e^- total scattering cross sections for O_2 [6] and CO_2 [7].

References

[1] Brawley S J *et al* 2010 *Science* **330** 789
[2] Shipman M *et al* 2017 *Phys. Rev. A* **95** 032704
[3] Wilde R S and Fabrikant I I 2018 *Phys. Rev. A* **97** 052708
[4] Brawley S J *et al* 2010 *Phys. Rev. Lett.* **105** 263401
[5] Fabrikant I I and Wilde R S 2018 *Phys. Rev. A* **97** 052707
[6] Itikawa Y. 2009 *J. Phys. Chem. Ref. Data* **38** 1
[7] Itikawa Y. 2002 *J. Phys. Chem. Ref. Data* **31** 749

Acknowledgments

Supported by the US National Science Foundation.

* E-mail: robyn.wilde@oit.edu
† E-mail: ifabrikant@unl.edu

Low-energy electron impact dissociative recombination and vibrational transitions of N_2^+

A Abdoulanziz[1], V Laporta[2], K Chakrabarti[3], A Bultel[4], J Tennyson[5], I. F. Schneider[1,6*] and J Zs Mezei[1,7†]

[1]LOMC UMR CNRS 6294, Université du Havre, Le Havre, 76058, France
[2]Istituto per la Scienza e Tecnologia dei Plasmi, CNR, 70126 Bari, Italy
[3]Dept. Of Mathematics, Scotish Church College 1&3 Urquhart Sq., Kolkata 700 006, India
[4]CORIA, UMR CNRS 6614, Université de Rouen, Saint Etienne du Rouvray, 76801, France
[5]Dept. of Physics and Astronomy, University College London, London WC1E 6BT, UK
[6]Laboratoire Aimé-Cotton CNRS-UPR-3321, Université Paris-Sud, 91405 Orsay, France
[7]Institute for Nuclear Research, Hungarian Academy of Sciences, Debrecen, H-4001, Hungary

Synopsis Cross sections and thermal rate coefficients are computed for electron-impact dissociative recombination and vibrational excitation/de-excitation of the N_2^+ molecular ion on its lowest six vibrational levels, for collision energies/temperatures up to 2.3 eV/5000 K.

The nitrogen molecule is very stable at low temperature and is one of the most widely studied species so far in plasma physics. It is very abundant in the Earth atmosphere and is notably present in other planetary atmospheres such as Titan, Triton, Pluton, Venus, and Mars. The N_2^+ cation is also of huge interest, its production on excited vibrational states playing a significant role in the characteristics of the Earth's thermosphere due to the solar irradiation. During the atmospheric entry of a spacecraft in Earth's and Titan's atmospheres, the hypersonic compression of the gases leads to the formation of a plasma departing from local thermodynamic equilibrium[1].

Using the Multichannel Quantum Defect Theory (MQDT) [2-5], we computed the cross sections and the rate coefficients for the dissociative recombination (DR) (1.1) and the related competitive processes - vibrational excitation or de-excitation (VE or VdE) (1.2) ($v_f^+ > v_i^+$ or $v_f^+ < v_i^+$ respectively):

$$N_2^+(v_i^+) + e^- \longrightarrow N + N \quad (1.1)$$

$$\longrightarrow N_2^+(v_f^+) + e^- \quad (1.2)$$

Here v_i^+ and v_f^+ stand for the initial and final vibrational quantum number of the target ion.

Based on molecucular datas used on ref. [5], the cross section and rate coefficients are calculated for the ground electronic state and the lowest six vibrational levels of the molecule for an incident electron energy up to 2.3 eV.

In fig.1 we display the rate coefficients recently computed [6].

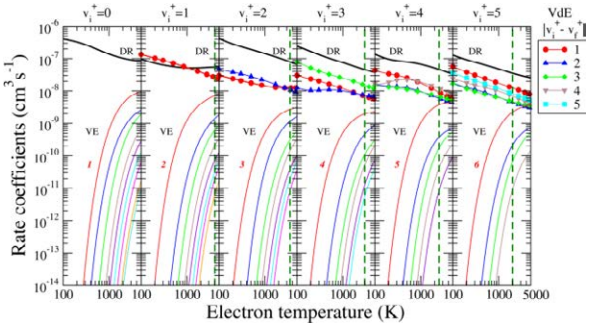

Figure 1. Maxwell rate coefficients for all the relevant electron-induced processes on N_2^+ initially on v_i^+=*0-5* vibrational levels: Dissociative recombination (black line), vibrational excitation (thin colored lines), and vibrational de-excitation (symbols and thick colored lines). For the vibrational excitations, all the transitions are shown up to (v_f^+=*9*) with the lowest final level being labeled in each figure.. The green dashed line gives the precision limit of our calculation.

References

[1] Annaloro J and Bultel A 2020 *Phys. Plasmas* **21**, **123512**
[2] Giusti A 1980 *J. Phys. B* **13 3867**
[3] Guberman S L *et al* 1991 *The Journal of Chemical Physics* **95 2602**
[4] Chakrabarti K *et al* 2013 *Phys. Rev. A*, **87 022702**
[5] Little D A *et al* 2014, *J. Phys. B* **47 105204**
[6] Abdoulanziz A *et al* 2021 *J. Appl. Phys.* **129, 053303**

* E-mail: ioan.schneider@univ-lehavre.fr
† E-mail: mezei.zsolt@atomki.hu

Electron Impact Dissociation and Ionization of ND_3^+

M O A El Ghazaly[1,2 *,†], J J Jureta[1,3], O Al-Hagan[2] , N Al-Aziz[2] and and P. Defrance[1]

[1]IMCN, Catholic University of Louvain, Chemin du Cyclotron, 2, 1348 Louvain-la-Neuve, Belgium
[2]Department of Physics, King Khalid University, Guraiger 62529, Saudi Arabia
[3]Institute of Physics, University of Belgrade, Belgrade 11081, Serbia

Synopsis Absolute cross sections for electron impact ionization and dissociation of ND_3^+ ions have been measured in a single-pass crossed electron-ion beams experiment. The dissociative excitation or ionization into D_2^+, N^+, N_2^+, and ND^+ along with the ionization were investigated in details.

Molecular ions play a significant role in interstellar space, in atmospheres of planets and in planetary ionospheres, as well. Likewise, they are an important player in laboratory plasmas such as of combustion engines or in the divertor and edge regions of ITER-like fusion devices [1]. In either type of plasma, molecular ions undergo various excitation and ionization reactions, which, in turn, mostly lead to dissociation. In particular, nitrogenated ions are of significance in planetary aeronomy and in ion-chemistry of interstellar clouds. Electron-induced dissociative excitation (DE) or ionization (DI) of interstellar NH_3^+ ammonia cation is a significant process in nitrogen-rich regions of space, likely on Pluto, on Titan's upper atmosphere [2], in interstellar ices, molecular clouds and interstellar grains. These reactions likely occur in interstellar space, within the interaction of solar-wind with interstellar nitrogen-rich molecular clouds.

Electron-impact ionization and dissociation processes have been widely studied in the single-pass electron-ion experiment at the Catholic University of Louvain, Belgium, and the present investigation is a part of a series dedicated to nitrogenated molecular ions [3-5]. ND_3^+ ions are extracted from an ECR, being accelerated to 8 keV and mass purified, the ion beam crosses the electron beam at right angle. The electron energy is tunable from a few eV up to 2.5 keV. Figure 1 shows the absolute cross section for electron impact ionization of ND_3^+. Cross-sections for various DE and DI channels were measured, as well. Detailed results for D_2^+, N^+, N_2^+, ND^+ and ND_3^{2+} will be presented and discussed at the Conference.

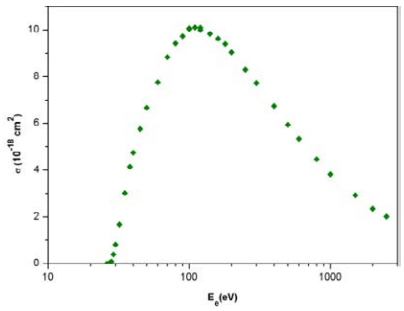

Figure 1. Absolute electron-impact ionization cross-section of ND3+..

References

[2] J Braams and H.-K. Chung 2015 Chung, *J. Phys. : Conf. Ser.* **576** 011001
[2] H. B., Niemann, *et al* 2010 *JGR* **115** E12006
[3] El Ghazaly M O A *et al* 2014 *J. Phys. Chem. A* **118** 10020−10027
[4] El Ghazaly M O A *et al* 2004 *J. Phys. B: At. Mol. Opt. Phys.* **37** 2467–2483
[5] Bahati E M *et al* 2001 *J. Phys. B: At. Mol. Opt. Phys.* **34** 2963

* E-mail: melghazaly@kku.edu.sa
† E-mail: pierre.defrance@uclouvain.be

Electron Impact Dissociation of N_3^+ Trinitrogen Ion

M O A El Ghazaly[1,2 *,†], J J Jureta[1,3], O Al-Hagan[2], A Algarni[2] and and P. Defrance[1]

[1]IMCN, Catholic University of Louvain, Chemin du Cyclotron, 2, 1348 Louvain-la-Neuve, Belgium
[2]Department of Physics, King Khalid University, Guraiger 62529, Saudi Arabia
[3]Institute of Physics, University of Belgrade, Belgrade 11081, Serbia

Synopsis Cross sections for electron impact dissociation of N_3^+ ions have been measured in a crossed-beams apparatus. In this experiment, the two singly-charged dissociation products, N^+ and N_2^+ were collected separately. Excitation and ionization mechanisms are analyzed.

Dissociative excitation or ionization of molecular ions are predominant processes in many types of either naturally-occurring or manmade plasmas [1]. In interstellar molecular clouds, the interactions with thermalized or low-energy low energy ionization-based electrons or with solar wind's electrons give arise to the different reactions of recombination, ionization, dissociative excitation or ionization, or charge-exchange [2]. These reactions occurring in their respective energy balance, compete against each-other in e.g. a ionization process and its counterbalancing electron-ion recombination, in a typical equilibrium that determines the charge state balance in the plasma of the cloud [3]. Likewise, in the plasma of divertor and edge regions of fusion reactors, electron-ion collisions, similarly lead to the same reactions, which occur with a significant prodominace, as well. Nitrogenated ions and clusters are a key player in many planetary atmospheres and ionospheres including Earth and interstellar nitrogen-rich molecular clouds [4]. In essence, the homonuclear N3+ trinitrogen ion is likely of a great abundance in e.g. Titan's atmosphere [5].

Electron-induced dissociative excitation or ionization have long been investigated using the single-pass electron-ion experiment at the Catholic University of Louvain, Belgium [6], and the present investigation is a part of a series dedicated to nitrogenated molecular ions [3,6]. N_3^+ ions were produced in an ECR source, then extracted and accelerated to 8 keV. The ion beam is subsequently mass-selected using a magnet sector and the ion beam steered to cross the electron beam at right angle. The electron energy is tunable from a few eV up to 2.5 keV. Figure 1 shows the apparent inclusive cross section for electron impact dissociative excitation and ionization of N_3^+. In this experiment, single ionization and dissociative excitation or ionization cross-sections for channels were measured, as well. Detailed results for N_2^+ channel will be presented and discussed at the Conference.

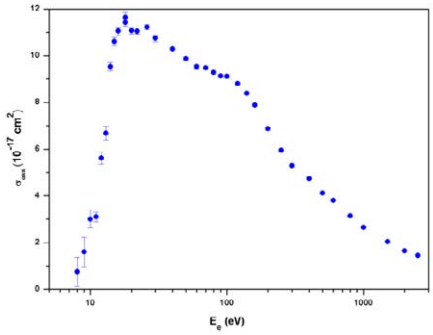

Figure 1. Absolute electron-impact Dissociative excitation or ionization cross-section of N_3^+ into N_2^+.

References

[1] J Braams and H.-K. Chung 2015 Chung, *J. Phys.: Conf. Ser.* **576** 011001
[2] Moradmand A. *et al.* 2018 *Astrophys J Suppl* Ser, **234**.1 14.
[3] Schmidt H T *et al.* 2008 *Int. J of Astrobiology* **7** (3 & 4): 205–208
[4] El Ghazaly M O A *et al* 2014 *J. Phys. Chem. A* **118** 10020−10027
[5] Niemann H B *et al* 2010 *JGR* **115** E12006
[6] El Ghazaly M O A *et al* 2004 *J. Phys. B: At. Mol. Opt. Phys.* **37** 2467–2483
[7] Bahati E M *et al* 2001 *J. Phys. B: At. Mol. Opt. Phys.* **34** 2963

* E-mail: melghazaly@kku.edu.sa
† E-mail: pierre.defrance@uclouvain.be

PolarX-EBIT: A versatile tool for high-resolution resonant photoexcitation spectroscopy with highly charged ions

S Bernitt[1,2,5]*, S Kühn[2], R Steinbrügge[3], M Togawa[2], P Micke[4], Th Stöhlker[1,5], J R Crespo López-Urrutia[2]

[1]Helmholtz-Institut Jena, 07743 Jena, Germany
[2]Max-Planck-Institut für Kernphysik, 69117 Heidelberg, Germany
[3]Deutsches Elektronen-Synchrotron DESY, 22607 Hamburg, Germany
[4]Physikalisch-Technische Bundesanstalt, 38116 Braunschweig, Germany
[5]Friedrich-Schiller-Universität, 07743 Jena, Germany

Synopsis Experiments with the compact electron beam ion trap PolarX-EBIT, employed at ultrabrilliant x-ray light sources, are presented. By resonantly exciting electronic transitions in trapped highly charged ions and recording subsequent fluorescence, spectroscopic data was provided for astrophysical applications as well as for benchmarking atomic structure theory.

The PolarX-EBIT is an electron beam ion trap, providing targets of trapped highly charged ions for photon beams from ultrabrilliant UV and x-ray light sources. Its compact design replaces the commonly used cryogenic superconducting magnets with room-temperature permanent magnets [1]. A novel off-axis electron gun allows the photon beam to leave the interaction region and be made available for downstream setups. This enables high-precision spectroscopy experiments with applications in atomic physics and astrophysics, and furthermore makes PolarX-EBIT a promising diagnostics tool for a wide range of current and future UV and x-ray photon beamlines.

In experiments with the high-resolution monochromator of beamline P04 at the synchrotron PETRA III, we were able to measure spectra of Ne-like Fe^{16+} with unprecedented accuracy, addressing disagreements of astrophysical and laboratory observations with the best available calculations, that have persisted for more than four decades [2].

Measurements of the K-shell Rydberg spectrum of molecular oxygen were conducted at beamline U49-PGM2 of BESSY II, while simultaneously observing resonantly excited transitions in few-electron ions in PolarX-EBIT. This allowed us to uncover a previously unknown systematic energy shift in widely used literature values for the molecular spectrum, which impacts many past and future spectroscopy experiments [3]. This has also demonstrated how well-known electronic transitions in few-electron ions can serve as precise and reproducible x-ray wavelength references.

In another experiment, we found strong two-electron-one-photon (TEOP) relaxation following the resonant excitation of K-series transitions in Li-like O^{5+} ions, which can dominate over normal radiative decay and become comparable in strength with Auger decay, due to correlation effects [4].

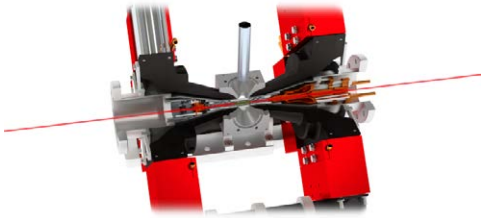

Figure 1. A sectional view of the PolarX-EBIT. The photon beam is overlapped with the prolate ion cloud in the center.

These different experiments highlight the potential of PolarX-EBIT as a tool for different applications, including astrophysics, metrology, and fundamental studies of the structure of electronic systems.

References

[1] Micke P *et al* 2018 *Rev. Sci. Instrum.* **89** 063109
[2] Kühn S *et al* 2020 *Phys. Rev. Lett.* **124** 225001
[3] Leutenegger M A *et al* 2020 *Phys. Rev. Lett.* **125** 243001
[4] Togawa M *et al* 2020 *Phys. Rev. A* **102** 052831

*E-mail: bernitt@mpi-hd.mpg.de

Status of the Transverse Free-Electron Target for the Heavy-Ion Storage Ring CRYRING@ESR

A Borovik Jr.[1]*, C Brandau[1]†, B M Döhring[1], A Müller[2] and S Schippers[1]

[1]I. Physikalisches Institut, Justus-Liebig-Universität Gießen, Giessen, D-35392, Germany
[2]Institut für Atom- und Molekülphysik, Justus-Liebig-Universität Gießen, Giessen, D-35392, Germany

Synopsis We report on the status of the transversal free-electron target for CRYRING@ESR which is currently being assembled at our university in Giessen. After the envisaged setup in the section YR09 of the heavy-ion storage ring CRYRING@ESR at FAIR in Darmstadt in several months, it will allow for novel electron-ion-collision experiments involving free electrons and stored heavy ions.

In order to facilitate new electron-ion collision experiments with free electrons, a specially tailored free-electron target for the heavy-ion storage ring CRYRING@ESR has been developed and built at the University of Giessen. The project builds on the decades-long experience of operating free-electron targets [1, 2] in single-pass electron-ion-collision experiments. The new device allows for the production of a ribbon-shaped, high-intensity electron beam with energies up to 12.5 keV (in the laboratory coordinate system) and electron densities in the interaction region reaching as high as 10^9 cm^{-3} (at 1keV). In addition to an optimal adaptation to the storage ring environment, the target permits an open view into the interaction region thus providing a large solid angle for photon spectroscopy. Delayed photons from long-lived states can be observed in a spectroscopy chamber down-beam of the electron target or by using an x-ray detector array located around the chamber of the gas-jet target that is installed in the same experimental section of the CRYRING [3]. The target bridges the gap between low-collision-energy experiments in electron coolers and those employing quasi-free electrons of gas-jet targets. Compared to the latter, the absence of a target nucleus enables unambiguous studies of processes, which are otherwise are masked by competing reactions with the target nucleus.

We report on the completion of the assembly and start of the offline commissioning in our laboratory in Giessen, during which the operation and performance of the target will be evaluated before its transfer to FAIR later this year and on-site commissioning with heavy ion-beams at CRYRING in 2022.

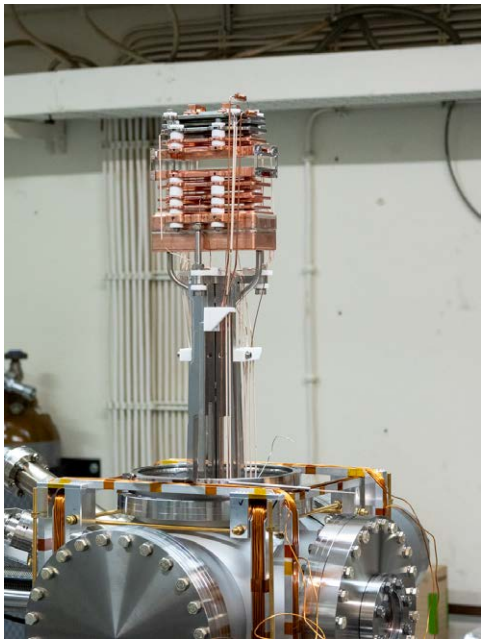

Figure 1. The electron target during assembly in the "offline" setup at JLU Gießen.

This research was supported by the ErUM-FSP APPA (BMBF grant no. 05P19RGFA1, https://fsp-appa.fair-center.eu).

References

[1] R. Becker *et al* 1985 *Nucl. Instrum. Methods B* **9** 385
[2] B. Ebinger *et al* 2017 *Nucl. Instrum. Methods B* **408** 3017
[3] M. Lestinsky *et al* 2016 *Eur. Phys. J Spec. Top.* **225** 797

*E-mail: Alexander.Borovik@physik.uni-giessen.de
†E-mail: C.Brandau@gsi.de

Commissioning of a new energy-scan-system for electron-ion crossed-beams experiments with a high-power electron gun

B M Döhring[1,2]*, A Borovik Jr[1], K Huber[1], A Müller[3] and S Schippers[1]†

[1]I. Physikalisches Institut, Justus-Liebig-Universität Gießen, 35392 Giessen, Germany
[2]GSI Helmholtzzentrum für Schwerionenforschung GmbH, 64291 Darmstadt, Germany
[3]Institut für Atom- und Molekülphysik, Justus-Liebig-Universität Gießen, 35392 Giessen, Germany

Synopsis We report on the commissioning of a new measurement and control system of our high-power electron-gun with an available collision-energy range of up to 3500 eV. The new control system allows us to set the voltages remotely with significantly better accuracy. In addition, an energy-scan-mode with fine energy steps in the meV range is established which allows us to resolve small resonance and step features in the measured cross-sections for electron-impact ionization of ions.

During recent years we have developed and commissioned a new high-power electron-gun for the Giessen electron-ion crossed beams experiment which extends our previous available energy range of 1000 eV up to 3500 eV [1]. A fast energy-scan-system to investigate fine details in the cross-section curves similar to the system presented in [2] for our old gun up to 1000 eV was not available up to now. This new scan system needed to be newly developed since the new gun has more electrodes, the voltages of which need to be controlled independently from each other for highest flexibility. From the technical side, this is very challenging because more than 300 parameters (e.g. electrode voltages, loss currents) are needed for controlling the gun as well as for keeping the voltage ripple on the electrodes as low as possible. For scans, we set the electron gun in a fixed position of maximum overlap between the electron beam and the ion beam. The electron energy is varied with simultaneous registration of signal plus background, ion current and electron current. These scan measurements yield relative cross sections which have to be adjusted to absolute cross-sections. Scans are repeated hundreds of times to average out possible fluctuations in beam overlap, beam currents and counting rates.

First scans were performed for the prominent $1s2s3s3d\ ^3D^e$ resonance of O^{5+} at about 591 eV (Fig. 1). These first results show that the energy resolution of the new gun is comparable to the previous one [3]. The measured resonance appears to have an experimental width of 1.7 eV. In the near future, we will use the new gun for measuring detailed cross sections for single and multiple electron-impact ionization of heavy low-charged ions of interest for the understanding of kilonovae [4]. The new electron gun serves also as a prototype of a high-intensity electron target, which is currently under construction and which shall be employed at the low-energy heavy-ion storage ring CRYRING of the international FAIR accelerator facility in Darmstadt, Germany [5].

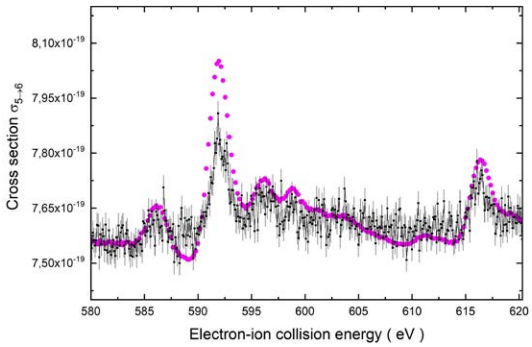

Figure 1. New scan (black squares); old scan [3] (magenta points); single ionization O^{5+}

References

[1] Ebinger B *et al* 2017 *Nucl. Instrum. Meth. B* **408** 317
[2] Müller A *et al* 1988 *Phys. Rev. Lett.* **61** 70
[3] Müller A *et al* 2000 *Phys. Rev. A* **62** 062720
[4] Watson D *et al* 2019 *Nature* **574** 497-500
[5] Lestinsky M *et al* 2016 *Eur. Phys. J. ST* **225** 797

*E-mail: michel.doehring@physik.uni-giessen.de
†E-mail: stefan.schippers@physik.uni-giessen.de

Semiclassical theory of laser-assisted dissociative recombination

I I Fabrikant[1]*, H B Ambalampitiya[1] and I F. Schneider[2,3]

[1]University of Nebraska-Lincoln, Lincoln, 68588, USA
[2]Université Le Havre Normandie, 76058 Le Havre, France
[3]Université Paris-Saclay, 91405 Orsay, France

Synopsis A semiclassical theory is developed for the process of laser-assisted dissociative recombination. Results are presented for the case of H_2^+. Compared to the field-free case, laser-assisted cross sections are significantly higher due to the Coulomb focusing effect.

The application of classical mechanics to a microscopic system of charged particles interacting via Coulomb potential can be justified for the *low*-energy regime [1]. In the case of laser-assisted processes, like laser-assisted bremsstrahlung [2] and radiative recombination [3], the classical electron dynamics leads to interesting effects such as the occurrence of fractals and Coulomb focusing. The latter effect typically enhances cross sections due to a broader range of impact parameters contributing to the process.

In the present work, we study the process of laser-assisted dissociative recombination (DR):

$$e^- + AB^+ \to A + B,$$

and present the results for the case of H_2^+. In our calculations, we first divide the configuration space using a reaction sphere whose radius r_0 is of a few atomic units. Outside this sphere the electron motion is treated classically. The electron-laser interaction is described in the electric-dipole approximation, so that the force on electron is

$$F(t) = F_0 \cos(\omega t + \phi_0),$$

where F_0 is the force amplitude, ω is the angular frequency, and ϕ_0 is the initial constant phase. For each impact parameter the electron trajectory is checked for reaching the reaction sphere. Inside the sphere the laser field is neglected, and the DR probability for a given energy E and angular momentum l within the sphere is calculated from quantum-mechanical field-free cross sections. For DR to H_2^+ we assume that only trajectories whose classical angular momenta are in the vicinity of $l = 2$ are contributing. The laser-assisted DR cross section is then obtained by integrating the DR probabilities over a range of impact parameters.

In Fig. 1 we show the phase-averaged DR cross sections for H_2^+ for the field intensity I =2.09 GW/cm^2 and the wavelength λ =22.8 μm. In the energy region above 1 meV the cross section is significantly enhanced, as compared to the field-free case, due to the Coulomb focusing effect. The quantum calculations for the field-free case show Rydberg resonances which are washed out by the field effects.

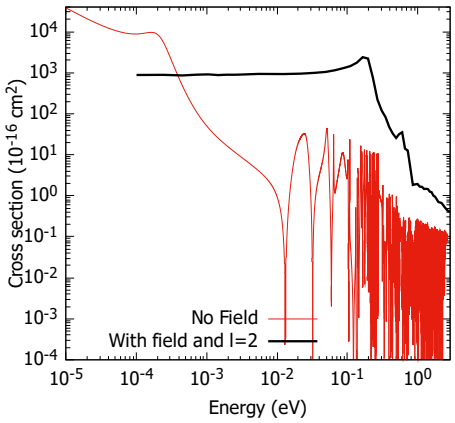

Figure 1. Laser-assisted DR cross section for H_2^+ (thick dark line) is compared with the field-free quantum DR cross section (thin red line).

This work is supported by the US National Science Foundation.

References

[1] Landau L D and Lifshitz E M 1977 *Quantum Mechanics: Nonrelativistic Theory* ((Pergamon, Oxford)
[2] Ambalampitiya H B and Fabrikant I I 2019 *Phys. Rev. A* **99** 063404
[3] Fabrikant I I and Ambalampitiya H B 2020 *Phys. Rev. A* **101** 053401

*E-mail: ifabrikant@unl.edu

Collisions of excited Ps with antiprotons: Ps break-up and antihydrogen formation

H B Ambalampitiya[1], I I Fabrikant[1]*, M Charlton[2], D V Fursa[3], A S Kadyrov[3] and I Bray[3]

[1]University of Nebraska-Lincoln, Lincoln, 68588-0299, USA
[2]Swansea University, SA2 8PP, United Kingdom
[3]Curtin University, Perth, WA 6845, Australia

Synopsis Benchmark quantum and classical scattering calculations are reported for collisions of excited Ps with antiprotons. For highly excited Ps, classical calculations become more efficient and reliable.

In low-energy antimatter experiments involving antihydrogen ($\bar{\mathrm{H}}$), the major requirement is to first obtain cold $\bar{\mathrm{H}}$ atoms in abundance. The following charge-transfer collision between positronium (Ps, the bound state of e^+ and e^-) and $\bar{p}$, has shown to be a promising pathway to maximize the $\bar{\mathrm{H}}$ yields [1].

$$\mathrm{Ps}(n_{\mathrm{Ps}}, l_{\mathrm{Ps}}) + \bar{p} \rightarrow \bar{\mathrm{H}}(n_{\mathrm{H}}, l_{\mathrm{H}}) + e^-, \qquad (1)$$

where $n_{\mathrm{Ps}}, l_{\mathrm{Ps}}$ and $n_{\mathrm{H}}, l_{\mathrm{H}}$ are the principal and angular momentum quantum numbers of Ps and $\bar{\mathrm{H}}$, respectively.

To guide and benchmark future $\bar{\mathrm{H}}$ experiments exploiting Ps collisions, accurate scattering cross sections for the reaction (1) are of a great importance. However, the current available data for reaction (1) are limited to a few lower Ps states [2]. In this report, we provide exact quantum and classical results for a broad range Ps states. In addition to reaction (1), we discuss the Ps break-up and Ps state-changing channels which are also important for experiments.

The quantum calculations are carried out using the convergent close coupling (CCC) calculations [3]. In CCC, the total wavefunction of the scattering system is expanded by the final atomic, and projectile Ps pseudostates. Next, to determine the transition matrix, a set of momentum-space coupled Lippman-Schwinger equations are solved using the partial-wave expansion in total orbital angular momentum.

The classical results are obtained by using the classical trajectory Monte Calro (CTMC) approach [4]. In CTMC, an initial microcanonical ensemble of Ps states are propagated towards the target for each impact parameter. The final energies, and angular momenta of the paired particles are then checked for probabilities. The final cross sections are obtained by integrating the probabilities over a range of impact parameters.

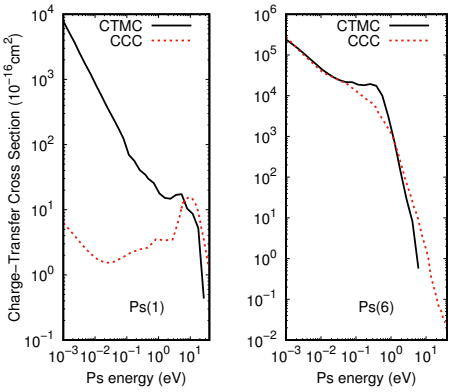

Figure 1. Summed $\bar{\mathrm{H}}$ formation cross sections for Ps(n_{Ps}) initial states, averaged over initial Ps angular momentum states.

As shown in Fig. 1, for low Ps states, CCC and CTMC disagree because of the importance of quantum effects. But as n_{Ps} grows, CTMC method becomes reliable and more efficient.

This work is supported by the US National Science Foundation, and Australian Research Council.

References

[1] Charlton M 1990 *Phys. Lett. A* **143** 143
[2] Ambalampitiya H B *et al* 2020 *J. Phys. B: At. Mol. Opt. Phys.* **53** 155201
[3] Kadyrov A S *et al* 2015 *Phys. Rev. A* **114** 183201
[4] Abrines R and Percival I C 1966 *Proc. Phys. Soc.* **88** 861

*E-mail: ifabrikant@unl.edu

High-Resolution Electron-Ion Collision Spectroscopy with Slow Cooled Pb^{78+} Ions in the CRYRING@ESR Storage Ring

S Fuchs[1,2]*, C Brandau[1,3], E B Menz[3,4], M Lestinsky[3], A Borovik Jr[1], Y Zhang[5], Z Andelkovic[3], F Herfurth[3], C Kozhuharov[3], C Krantz[3], U Spillmann[3], M Steck[3], G Vorobyev[3], D Banaś[6], M Fogle[7], S Fritzsche[4,8], E Lindroth[9], X Ma[10], A Müller[1], R Schuch[9], A Surzhykov[10,11], M Trassinelli[12], Th Stöhlker[3,4,7], Z Harman[13], and S Schippers[1,2] for the SPARC Collaboration

[1]JLU Gießen, [2]HFHF Campus Gießen, [3]GSI, [4]HI Jena, [5]Xi'an Jiaotong University, [6]JKU Kielce, [7]Auburn University, [8]FSU Jena, [9]Stockholm University, [10]TU Braunschweig, [11]PTB, [12]UMPC Paris, [13]MPIK

Synopsis We report on very recent results from the first DR experiment with highly charged ions in the heavy-ion storage ring CRYRING@ESR of the international FAIR facility in Darmstadt, Germany.

The experimental technique of dielectronic recombination (DR) collision spectroscopy is a very successful approach for studying the properties of highly charged ions [1, 2]. Due to its versatility and the high experimental precision DR spectroscopy plays an important role in the physics program of the SPARC collaboration as is outlined, e.g., in the CRYRING@ESR Physics Book [3]. The range of topics that is covered using DR as a spectroscopic tool comprises among others, tests of QED in strong-fields, investigations of nuclear properties via isotope shift or hyperfine splitting, lifetime studies, and measurements of input data for plasma modelling and astrophysics. CRYRING@ESR is particularly attractive for DR studies, since it is equipped with an electron cooler that provides an ultracold electron beam promising highest experimental resolving power and precision.

Here, we report on the results from the first DR experiment with highly charged ions in the heavy ion storage ring CRYRING@ESR of the international FAIR facility in Darmstadt, Germany. The experiment was carried out in March 2021. The Pb^{78+} ion beam was prepared by using the full GSI accelerator chain to first accelerate the ions to obtain the desired charge state from a foil-stripper that was located in the transfer beamline from the SIS heavy-ion synchrotron to the ESR storage ring. There, the Pb^{78+} ions were stored and cooled, and decelerated to an energy of 11 MeV/u. Finally, up to 5×10^6 ions per cycle were injected into the CRYRING where the beam lifetime was about 30 s, mainly limited by collisions with residual gas particles despite the ultra-high vacuum conditions in the storage ring (background pressure of a few times 10^{-11} mbar).

DR spectra were measured in the 0–40 eV collision-energy range where $2s2p(^3P_1)\,19\ell$ and $2s2p(^3P_1)\,20\ell$ resonances occur that are associated with $2s^2\ ^1S_0 \rightarrow 2s2p\ ^3P_1$ excitations of the Be-like ion core. The measured relative peak positions and peak strengths agree well with theoretical calculations that employed the methodology described, e.g., in Ref. [4]. From the comparison between experiment and theory we infer the longitudinal and transversal electron beam temperatures $k_B T_{||} \approx 0.08$ meV and $k_B T_{\perp} \approx 3$ meV, which are in accord with the expectations. This preliminary result of our experiment already clearly demonstrates that CRYRING@ESR is indeed excellently suited for high-resolution electron-ion collision spectroscopy of very highly charged ions, which makes it a world-unique facility for the investigations of the above mentioned physics cases. More detailed results will become available as the ongoing data analysis proceeds.

This research was supported by the ErUM-FSP T05 "APPA" (BMBF grant 05P19RGFA1, https://fsp-appa.fair-center.eu). The results are based on an experiment in the context of FAIR Phase-0 at GSI, Darmstadt (Germany).

References

[1] Schippers S 2015 *Nucl. Instrum. Methods Phys. Res. B* **350** 61
[2] Brandau C *et al* 2015 *Phys. Scr.* **T166** 014022
[3] Lestinsky M *et al* 2016 *Eur. Phys. J. ST* **225** 797
[4] Harman Z *et al.* 2019 *Phys. Rev. A* **99** 012506

*E-mail: sebastian.fuchs@physik.uni-giessen.de

Quantum control of entangled photon pair emission in electron-ion collisions by laser-synthesized photoelectron wave packets

R E Goetz* **and K Bartschat**

Department of Physics and Astronomy, Drake University, Des Moines, IA 50311, USA

Synopsis We theoretically investigate the coherent control of correlated two-electron dynamics and quantum light emission resulting from the collision of a laser-synthesized photoelectron wave packet with a He^+ ion. The coherence of the tailored wave packet is exploited to control the rearrangement channel, the de-excitation dynamics, and the subsequent photoemission. We demonstrate coherent control over the angular distribution of entangled photon pairs emitted in inelastic scattering and dielectronic recombination by modulating the spectral coherence of the incident electron beam based on interferometric multi-photon ionization of its parent atom.

The correlated electron dynamics initiated by the incident electron in electron-ion collisions manifests itself in a variety of competing rearrangement channels, such as inelastic scattering or dielectronic recombination. The latter involves capture of the incident electron via transient doubly-excited compound resonance states that may, in turn, decay via two competing processes: autoionization or radiative stabilization. The rearrangement channel ultimately dictates the photoemission via spontaneous decay.

Motivated by recent advances to engineer free-electron wave packets with tailored momentum distributions based on resonantly-enhanced multiphoton ionization [1, 2], we propose an extension of coherent control using coherent, Fourier-synthesized photoelectron matter waves, rather than classical light, to coherently control the correlated electron dynamics in electron-ion collisions and the ensuing photocascade emission.

We show that the temporal coherence of the incident projectile can be engineered to control competing rearrangement channels as well as the correlated electron dynamics and underlying processes within each channel. This enables us to control the angular distribution of emitted entangled photon pairs by influencing the de-excitation dynamics in inelastic scattering [3] and correlated de-excitation dynamics in dielectronic recombination. The coherence of the incident electron wave packet is engineered by pulse-shaping the ionizing laser field to promote interfering multi-photon ionization pathways in the parent atom.

Our theoretical treatment is based on numerically solving the time-dependent Schrödinger equation for the fully-correlated two-electron wave packet coupled to the photon field and a time-dependent two-Hilbert-space formulation of multichannel scattering theory of rearrangement collisions to interpret the relevant interfering processes that contribute to the desired control. Control is achieved by manipulating interferences between quantum pathways contributing to the same final state and photon modes.

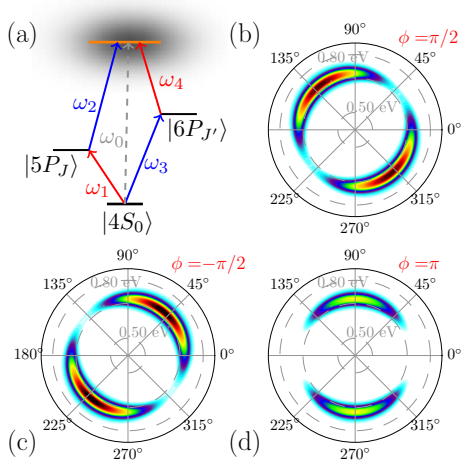

Figure 1. (a) Ionization scheme for the incident wave packet. (b-d) Angular distribution of photon (1) emitted after collision for different relative CEP phases of the fields ω_j shown in (a). The detection direction of the correlated peer (2) is fixed.

This work was supported by the NSF grant No. PHY-1803844.

References

[1] Wollenhaupt *et al* 2013 *ChemPhysChem* **14** 1297
[2] Kerbstadt S *et al* 2019 *Adv. Phys.: X* **4** 1672583
[3] Goetz E and Bartschat K 2021 arXiv:2011.09649

*E-mail: esteban.goetz@drake.edu

Reactive Electron Collision Dynamics And Rate Coefficients With Isotopologues of Beryllium Monohydride

F.Iacob[1], N. Pop[2], J. Zs Mezei[3], S. Niyonzima[4], V. Laporta[5], A. Abdoulanziz[6], E. Djuissi[6], J. Bofelli[6], F. Gauchet[6], J. Tennyson[7], D. Reiter[8], K. Chakrabarti[9] , A. Bultel[10] , I. F. Schneider[6,11]

[1]Physics Faculty, West University of Timişoara, Timişoara, 300223, Romania
[2]Dept. Politehnica University, of Fundamental Physics for Engineers, Timisoara, 300006, Romania
[3]Inst. of Nuclear Research of the Hungarian Academy of Sciences, Debrecen, H-4001, Hungary
[4]Département de Physique, Université du Burundi, Bujumbara, 1550, Burundi
[5]Istituto per la Scienza e Tecnologia dei Plasmi, CNR, Bari, Italy
[6]Laboratoire Ondes et Milieux Complexes, CNRS, Univ. du Havre, Le Havre, 76058, France
[7]Department of Physics and Astronomy, University College London, London WC1E 6BT, United Kingdom
[8]Institute for Laser and Plasma Physics, Heinrich-Heine-University, D-40225 D□usseldorf, Germany
[9]Department of Mathematics, Scottish Church College, Calcutta 700 006, India
[10]CORIA CNRS—Université de Rouen—Université Normandie, F-76801 Saint-Etienne du Rouvray, France
[11]Laboratoire Aimé Cotton, CNRS, ENS Cachan and Univ. Paris-Sud, Orsay, 91405, France

Synopsis Cross sections and Maxwell rate coefficients calculated using MQDT for elementary processes in ionized cold gases will be presented.

Reactive electron collision dynamics will refer to elementary processes in cold ionized gases: dissociative recombination (DR), elastic collisions (EC), vibrational excitation (VE) (inelastic collisions), vibrational de-excitation (VdE) (super-elastic collisions). Using a step-wise method based on Multichannel Quantum Defect Theory (MQDT) [1], cross sections and Maxwell rate coefficients have been obtained. The key challenge in the use of beryllium as main chamber material for experimental and commercial fusion devices is to understand, predict and control the characteristics of the thermonuclear burning plasma. Due to its toxicity no much experimental data can be found. In order to model and diagnose the low-temperature edge plasmas, a complete database for electron-impact collision processes is required for molecular species containing beryllium and hydrogen. We have expanded our studies on **BeH**$^+$ [4] to **BeD**$^+$ [5] and **BeT**$^+$ [6] cations. A complete set of vibrationally resolved rate coefficients for BeT$^+$ cation reactive collisions with electrons below the ion dissociation threshold is provided.

The resulting data are useful in magnetic confinement fusion edge plasma modelling and spectroscopy, in devices with beryllium based main chamber materials, such as ITER and JET, and operating with the deuterium-tritium fuel mix. One of the important results is the studies upon the isotopic effects presented in Figure 1.

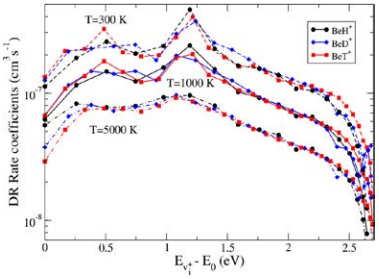

Figure 1. Dissociative recombination Maxwell rate coefficients of H_2^+ and $HD^+(N_i^+=0\text{-}2,\ v_i^+=0)$, via all symmetries of H_2.

References

[1]Jungen Ch 2011 *Handbook of High Resolution Spectroscopy*, Wiley & Sons, New York, 471
[2] Motapon O *et al* 2014 *Phys. Rev. A* **90** 012706
[3] Epée Epée MD *et al* 2015 *MNRAS* **455** 276–281
[4] Niyonzima S *et al* 2017 *Atomic Data and Nuclear Data Tables* **115-116** 287
[5] Niyonzima S *et al* 2018 *Plasma Sources Sci. Technol.* **27** 025015
[6] Iacob F *et al* 2019 *AIP* 2071(1) 020007
[6] N. Pop, et al, Atomic Data and Nuclear Data Table, 139, 101414 (2021).

† E-mail: felix.iacob@e-uvt.ro

Electron-induced excitation and recombination of BeH^+ ions and isotopologues: reactional dynamics and rate coefficients

F. Iacob[1], N. Pop[2], J. Zs Mezei[3], S. Niyonzima[4], V. Laporta[5], A. Abdoulanziz[6], E. Djuissi[6], J. Bofelli[6], F. Gauchet[6], J. Tennyson[7], D. Reiter[8], K. Chakrabarti[9], A. Bultel[10], I. F. Schneider[6,11]

[1]Physics Faculty, West University of Timişoara, Timişoara, 300223, Romania
[2]Dept. of Fundamental Physics for Engineers, Politehnica University, Timisoara, 300006, Romania
[3]Inst. of Nuclear Research of the Hungarian Academy of Sciences, Debrecen, H-4001, Hungary
[4]Département de Physique, Université du Burundi, Bujumbara, 1550, Burundi
[5]Istituto per la Scienza e Tecnologia dei Plasmi, CNR, Bari, Italy
[6]Laboratoire Ondes et Milieux Complexes, CNRS, Univ. Le Havre Normandie, Le Havre, 76058, France
[7]Department of Physics and Astronomy, University College London, London WC1E 6BT, United Kingdom
[8]Institute for Laser and Plasma Physics, Heinrich-Heine-University, D-40225 Düsseldorf, Germany
[9]Department of Mathematics, Scottish Church College, Calcutta 700 006, India
[10]CORIA CNRS, Université de Rouen Normandie, F-76801 Saint-Etienne du Rouvray, France
[11]Laboratoire Aimé Cotton, CNRS, ENS Cachan and Univ. Paris-Sud, Orsay, 91405, France

Synopsis Cross sections and Maxwell rate coefficients for reactive collisons between electrons and Beryllium monohydride cations and isotopologues have been computed using the Multichannel Quantum Defect Theory.

The key challenge in the use of beryllium as main chamber material for experimental and commercial fusion devices is to understand, predict and controle the characteristics of the thermonuclear burning plasma. Due to its toxicity, few experimental data are currently available. In order to model and diagnose the low-temperature edge plasmas, a complete database for electron-impact collision processes is required for molecular species containing beryllium and hydrogen.

Using a step-wise method based on the Multichannel Quantum Defect Theory (MQDT) [1-3], cross sections and Maxwell rate coefficients for dissociative recombination (DR), vibrational excitation (VE, inelastic collisions) and vibrational de-excitation (VdE, super-elastic collisions) have been obtained. We have expanded our studies on **BeH^+** [4] to **BeD^+** [5] and **BeT^+** [6] cations.

One of the important outcomes of our studies is displayed in Figure 1, where the isotopic effects are shown. This figure demonstrates the quasi-independence of the rate coefficients on the isotopologue, if they are represented with respect to the vibrational energy of the target, at a given electron temperature.

New computations on extended energy/temperature range, up to 12 eV/30000 K, are ongoing.

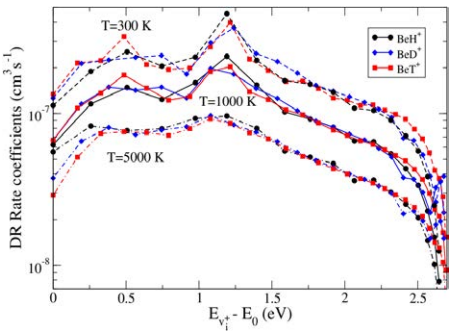

Figure 1. Dissociative recombination Maxwell rate coefficients for BeH^+, BeD^+ and BeT^+.

References

[1] Jungen Ch 2011, in *Handbook of High Resolution Spectroscopy*, Wiley & Sons, New York, 471
[2] Motapon O *et al* 2014, *Phys. Rev. A* **90,** 012706
[3] Epée Epée M D *et al* 2015, *MNRAS* **455,** 276
[4] Niyonzima S *et al* 2017, *Atomic Data and Nuclear Data Tables* **115-116,** 287
[5] Niyonzima S *et al* 2018, *Plasma Sources Sci. Technol.* **27**, 025015
[6] Iacob F *et al* 2019, *AIP* **2071**,,020007
[7] N. Pop, *et al* 2021, Atomic Data and Nuclear Data Tables **139**, 101414 (2021)

† E-mail: felix.iacob@e-uvt.ro

Electron-impact double ionization of B^+

J Koncevičiūtė[1]*, **V Jonauskas**[1]†

[1]Institute of Theoretical Physics and Astronomy, Vilnius University, Saulėtekio av. 3, LT-10257 Vilnius, Lithuania

Synopsis Electron-impact double ionization of the B^+ ion is investigated. Scaled distorted wave cross sections are used to study the collisional ionization and excitation processes. Additional ionization-excitation-autoionization and excitation-ionization-autoionization processes are introduced to the total double ionization.

Boron is important in fusion devices where boronization is used as a powerful wall conditioning method to achieve very pure fusion plasmas. Comprehensive data for electron collisions with the neutral and ionized boron are needed in order to understand erosion processes of these ions in fusion experiments.

The aim of this work is to study electron-impact double ionization (DI) process of the B^+ ion. Contribution of direct and indirect processes is considered. A few-step approach [1] is applied to study direct double ionization (DDI) process. This method threats DDI as a sequence of two- (ionization-ionization (II)) and three-step (excitation-ionization-ionization (EII), and ionization-excitation-ionization (IEI)) processes. Additionally in this work another two few-step processes were applied to study DI of B^+ ion. Those processes include ionization-excitation-autoionization (IE-AI) and excitation-ionization-autoionization (EI-AI).

The Flexible Atomic Code [2], which implements the Dirac-Fock-Slater approach was used to obtain atomic data, needed for the calculation of DI cross sections. Two cases of DDI are investigated, DDI^1: collisional ionization (CI) cross sections obtained in the potentials of the ionizing ions; DDI^2: $B^+ \rightarrow B^{2+}$ CI cross sections obtained in the potential of the ionizing ion but $B^{2+} \rightarrow B^{3+}$ CI cross sections obtained in the potential of the ionized ion.

Electron-impact double ionization cross sections are studied for the ground level of the B^+ ion. The study includes correlation effects for the ground configuration of the B^+ ion and scaled [3] DW cross sections for the electron-impact excitation and ionization processes. It is shown, that contribution of the additional EI-AI and IE-AI processes leads to a good agreement with experimental cross sections at higher energies of incident electron. The II path of the DDI process dominates over the IEI and EII paths. The II contributes ~70% to the total DDI cross sections.

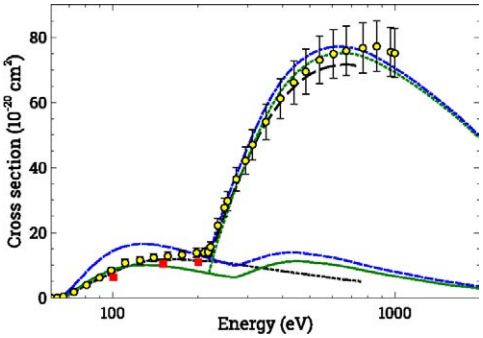

Figure 1. Electron-impact double ionization of B^+ ion. Continuous line (green): DDI^1 cross sections; dashed line (blue): DDI^2 cross sections; dashed-dotted line (green): total DI cross sections with DDI^1; dashed-double-dotted line (blue): total DI cross sections with DDI^2; solid circles (yellow): experimental total DI cross sections [4]; solid squares (red): TDCC calculations [5]; dashed line (black): CADW calculations for the single ionization of the 1*s* subshell of the ground configuration added to a background of TDCC fit (black dashed-double-dotted line) [5]

References

[1] Jonauskas V *et al* 2014 *Phys. Rev. A* **89** 052714
[2] Gu M F 2008 *Can. J. Phys.* **86** 675
[3] Kim Y -K 2001 *Phys. Rev. A* **86** 032713
[4] Shevelko P *et al* 2005 *J. Phys. B: At. Mol. Opt. Phys.* **38** 525
[5] Pindzola M S *et al* 2011 *J. Phys. B: At. Mol. Opt. Phys.* **44** 105202

*E-mail: jurgita.konceviciute@tfai.vu.lt
†E-mail: valdas.jonauskas@tfai.vu.lt

Developing Compact Neomagnet Electron Beam Ion Trap and Penning Trap Beyond 0.7 T at NIST

D. S. La Mantia[1,3]*, A. S. Naing[2,3], and J. N. Tan[3]

[1]Department of Physics & Astronomy, Clemson University, Clemson, SC 29634 USA
[2]Department of Physics & Astronomy, University of Delaware, Newark, DE 19716 USA
[3]National Institute of Standards & Technology, Gaithersburg, MD 20899 USA

Synopsis A permanent-magnet Penning trap and an electron beam ion trap are in development at NIST for generating and isolating a broad range of highly-charged ions, including charge states with low ionization thresholds of interest in atomic clock research, detector innovation, and other applications. This effort builds upon prior prototypes to design a new device that serves as a light source for spectroscopy, as well as a source of highly-charged ions that can be extracted and subsequently isolated for measurements. The development and current state of these devices will be discussed.

The study of highly-ionized atoms has been greatly facilitated by the electron beam ion trap (EBIT), a device developed in the late 1980's [1] for the effective production and trapping of highly-charged ions. The original EBIT used superconducting magnets to intensify the electron beam, a costly setup to build and operate.

In recent years the use of rare-earth permanent magnets –*e.g.*, neodymium iron boron (NdFeB) in so-called neomagnets– has made it possible to attain high magnetic fields at room temperatures, enabling construction of compact ("mini") EBITs and Penning traps. Potential applications include creating certain low ionization threshold highly-charged ions, such as Pr^{9+} and Nd^{10+}, proposed as interesting candidates for the development of next-generation atomic clocks, quantum information processing, or the search for fine-structure constant variation [2].

As proof of principle, a prototype mini-EBIT [3] at NIST employs a pair of axially-magnetized NdFeB rings yoked by electrical iron to produce a peak field of ∼0.32 T at the trap center; subsequent refinements yielded consistent production of Ne^{q+} ($q \leq 8$), $Ar^{\tilde{q}+}$ ($\tilde{q} \leq 15$), $Kr^{\tilde{q}+}$ ($\tilde{q} \leq 20$), and $Xe^{q'+}$ ($q' \leq 25$) [4]. The next-generation unitary Penning trap [5] and mini-EBIT under development will include features to improve performance, including the integration of three pairs of radially-magnetized annular neomagnets into the drift tubes. As illustrated in Fig. 1, results of simulation indicate that appropriate yoking of these neomagnets can increase the peak axial magnetic field beyond 0.7 T.

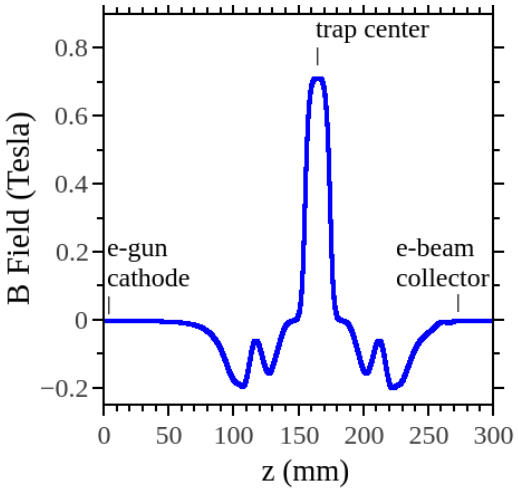

Figure 1. Magnetic field profile (Tesla) produced by three pairs of radially magnetized NdFeB annular magnets with yoking by the soft iron components of the mini-EBIT drift tubes.

References

[1] M. A. Levine, *et al*, Physica Scripta Volume T **22**, 157-163 (1988)
[2] M. Safronova, *et al*, Physical Review Letters **113**, 030801 (2014)
[3] S. F. Hoogerheide, *et al*, Atoms **3**, 367-391 (2015)
[4] A. S. Naing *et al*, 19th International Conference on Physics of Highly Charged Ions Proceedings, Lisbon, Portugal (2018)
[5] A. S. Naing, *et al*, (in preparation)

*E-mail: dlamant@clemson.edu

Precision Measurements of $^2P_{1/2}$-$^2P_{3/2}$ M1 Transitions in Boron-like S^{11+} and Cl^{12+} at EBIT

X Liu[1, 2], X P Zhou[1], Z K Huang[1], Q F Lu[3], C L Yan[3], A V Volotka[4], J Xiao[3*], W Q Wen[1†] and X Ma[1]

[1]Institute of Modern Physics, Chinese Academy of Sciences, 730000, Lanzhou, China
[2]Institute of Quantum Matter, South China Normal University, Guangzhou 510006, China
[3]Shanghai EBIT Laboratory, Institute of Modern Physics, Fudan University, Shanghai 200433, China
[4]GSI Helmholtzzentrum für Schwerionenforschung, D-64291 Darmstadt, Germany

Synopsis Precision measurements of the electric dipole-forbidden transition between the $^2P_{3/2}$ and $^2P_{1/2}$ fine structure levels of boron-like ions S^{11+} and Cl^{12+} have been performed at Shanghai High-Temperature Superconducting electron beam ion trap (SH-HtscEBIT). The M1 transition wavelengths were determined to be 760.976(29) nm and 574.151(31) nm for S^{11+} and Cl^{12+}, respectively. As compared to the previously observed results, the accuracy of current experimental results is improved by 2 times and 21.5 times for S^{11+} and Cl^{12+}, respectively.

Precision measurements of the fine structure transition energy of boron-like ions are considered important not only to investigate the fundamental physics [1], including QED effects, electron correlation effects, relativistic effects and atomic nuclear effects, but also to provide key atomic data for astrophysics [2]. Additionally, the M1 transition of the boron-like ions are considered for highly charged ion optical clocks [3].

We present the experimental results as well as the theoretical calculation of the electric dipole-forbidden transition $^2P_{3/2}$ - $^2P_{1/2}$ in boron-like S^{11+} and Cl^{12+} ions. The experiments were performed by using a high-resolution Czerny-Turner spectrometer at the SH-HtscEBIT [4]. Emission lines from S^{11+} and Cl^{12+} ions are shown in Figure 1 (a) and (b). The observed peaks belong to the $^2P_{3/2}$ - $^2P_{1/2}$ transition of B-like S^{11+} and Cl^{12+} ions are indicated. All random uncertainties including line position errors and standard deviation of wavelength calibration function have been calculated as a "root sum of squares," whereas systematic calibration errors and uncertainties from calibration lines have been added linearly. The final transition wavelengths of S^{11+} and Cl^{12+} are determined as 760.976(29) nm and 574.151(31) nm, respectively. Precision calculations, including QED contribution, are accomplished for S^{11+} and Cl^{12+} and the calculated results are 761.24(18) nm for S^{11+} and 574.36(10) nm for Cl^{12+}, respectively. The present experimental results in agreement with theoretical calculations. Our results will provide a possibility to test QED effect and also for using in astrophysical plasma diagnosis. We will present all of the details on the conference.

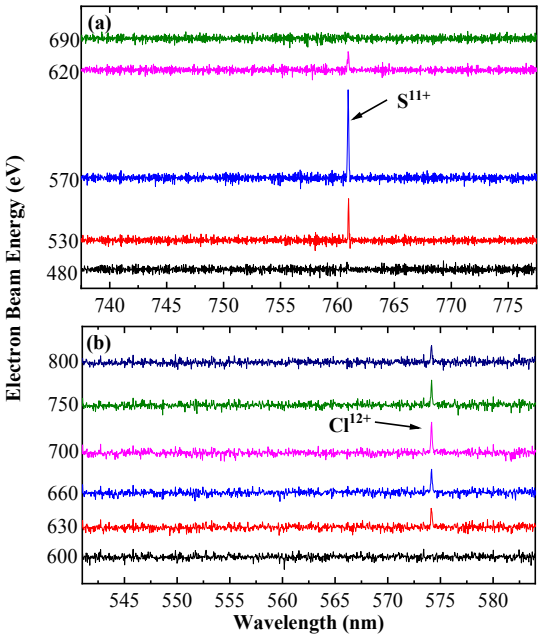

Figure 1 Emission spectra of B-like ions. (a) for S^{11+} in the range of 737–777 nm and (b) for Cl^{12+} in the range of 541–584 nm. The nominal electron beam energies are labeled in the vertical axis respectively for each ions with different colors.

References

[1] I. Draganić *et al*. 2003 *Phys. Rev. Lett*. **91** 183001
[2] G. Y. Liang *et al*. 2012 *A&A*. **547** A87
[3] V. Yudin *et al*. 2014 *Phys. Rev. Lett*. **113** 233003
[4] Q. Lu *et al*. 2020 *Phys. Rev. A*. **102** 042817

* E-mail: xiao_jun@fudan.edu.cn
† E-mail: wenweiqiang@impcas.ac.cn

Visible lines from W^{8+} and W^{10+} in electron beam ion trap

Q Lu[1], C L Yan[1], J Meng[2], N Fu[1], G Q Xu[1], Y Yang[1], C Y Chen[1], J Xiao[1 *], J G Li[2], K Wang[3], J G Wang[2], and Y Zou[1]

[1]Shanghai EBIT Laboratory, Key Laboratory of Nuclear Physics and Ion-Beam Application (MOE), Institute of Modern Physics, Fudan University, Shanghai 200433, China
[2]Institute of Applied Physics and Computational Mathematics, Beijing 100088, China
[3]Hebei Key Lab of Optic-electronic Information and Materials, The College of Physics Science and Technology, Hebei University, Baoding 071002, China

Synopsis To provide spectroscopic data for lowly charged tungsten ions relevant to fusion research, we present measurements and identifications of visible radiation from W^{8+} and W^{10+}. The ions are produced and confined in an electron-beam ion trap (EBIT) at Shanghai EBIT Laboratory, and the spectra are recorded with a Czerny-Turner spectrometer in the wavelength range 300-700 nm. The observed spectral lines (six lines from W^{8+} and five lines from W^{10+}) are identified using detailed collisional-radiative (CR) modeling of the EBIT spectra. In addition, we perform large-scale theoretical calculations for the low-lying energy levels of W^{8+} and W^{10+} using FAC and GRASP codes. Reasonably good agreement is found between our two independent atomic-structure calculations, with ~1.4% and ~0.5% differences on average for W^{8+} and W^{10+} respectively. Finally, the resulting values are adopted to check our line identifications.

Spectroscopic data of lowly charged tungsten related to tokamak divertor region are of great importance to the balance and diagnostics of the forthcoming fusion devices, e.g., the International Thermonuclear Experimental Reactor (ITER) [1]. However, due to the complicated spectra as well as the large uncertainties of theoretical calculations, there is still a shortage of spectroscopic data for lowly charged tungsten ions [2].

Visible spectra of W^{8+} and W^{10+} are measured with Shanghai high temperature superconducting electron-beam ion trap (SH-HtscEBIT) [3], which is specially designed to generate and trap lowly charged ions for fusion-edge plasma research. By tuning the potential difference between cathode and central of the drift tube, tungsten ions with targeted charge states can be produced. The fluorescence emitted from the trapped ions is observed by a Czerny-Turner spectrometer and then detected by an electron multiplying CCD (EMCCD) camera operated at −65 °C. Lines are classified into several charge states according to their intensity variation as a function of electron-beam energy.

The analysis of the observed W^{8+} and W^{10+} spectra is performed by CR modeling of the EBIT plasma using FAC 1.1.5 [4]. Three dynamical physical processes including electron-impact excitation, electron-impact deexcitation, and radiative dacay are considered to construct rate equations to obtain the population of each energy level. The luminosity of each transition, obtained from the multiplication of gA value times the population, is finally calculated and compared with the experimental results.

Large-scale FAC and GRASP [5] calculations for the excitation energies of low-lying energy levels of W^{8+} and W^{10+} are conducted to verify our line identifications. The electron correlation effects, which are typically difficult to handle with for these ions, are studied carefully in our work. To conclude, three lines of W^{8+} are identified to stem from M1 transtions in the $4f^{13}5s^25p^5$ configuration, and three lines from M1 transtions in the $4f^{12}5s^25p^6$ configuration [6]. For W^{10+}, three lines come from M1 transtions in the $4f^{13}5s^25p^3$ configuration, and the other two lines come from M1 transtions in the $4f^{12}5s^25p^4$ configuration [7].

References

[1] Ralchenko Y 2013 Plasma Fusion Res. **8** 2503024
[2] Kramida A E and Shirai T 2009 At. Data Nucl. Data Tables **95** 305
[3] Lu Q *et al* 2019 Phys. Rev. A **99** 042510
[4] Gu M F 2008 Can. J. Phys. **86** 675
[5] Jönsson P *et al* 2013 Comput. Phys. Commun. **184** 2197
[6] Lu Q *et al* 2021 Phys. Rev. A **103** 022808
[7] Lu Q *et al* 2021 J. Quant. Spectrosc. Radiat. Trans. **262** 107533

* E-mail: xiao_jun@fudan.edu.cn

A transverse electron target for electron-impact ionization of highly charged ions at the 320 kV platform

W L Ma[1], S X Wang[1], W Q Wen[2], Z K Huang[2], X Ma[2] and L F Zhu[1]*

[1]Hefei National Laboratory for Physical Sciences at Microscale and Department of Modern Physics, University of Science and Technology of China, Hefei, 230026, China
[2]Institute of Modern Physics, Chinese Academy of Sciences, Lanzhou, 730000, China

Synopsis A transverse electron target for electron impact ionization experiments of highly charged ions is under construction. Its prototype will be installed at the 320 kV platform at the Institute of Modern Physics in Lanzhou, China. The high-intensity electron target will improve the efficiency of crossed-beams electron-ion collision experiments prominently.

Electron impact ionization (EII) is one of the fundamental atomic collision processes in astrophysical and man-made plasmas [1]. Absolute EII cross sections are of great importance to interpret the observed spectra and to diagnose the electron temperature or density of a plasma. Most of the available EII data are produced by theoretical calculations. However, reliable experimental data can not only be regarded as input parameters for plasma models but also as a benchmark for theoretical calculations. Earlier crossed-beams electron-ion collision experiments are limited by the available electron density and energy range of the electron target. The concept of the transverse electron target were proposed to overcome the weakness [1]. Here we present the simulation result of a transverse electron target based on previous designs [2, 3, 4], which will be installed at the 320 kV platform for EII experiments.

Table 1. Parameters of the electron target.

Parameters	Values
Gun perveance (μAV$^{-3/2}$)	5.7
Electron current (mA)	6-1300
Electron energy (eV)	100-3000
Interaction length (mm)	60

A ribbon-shaped electron beam with a perveance of 5.7×10^{-6}AV$^{-3/2}$, e.g., a current of 0.18 A at 1 keV electron energy (Figure 1), was obtained in the simulation. The beam is optimized as parallel as possible in the interaction region, where the beam has a height of 1.2 mm. The energy distribution of the beam in the interaction region centers at 987 eV with an energy spread of about 0.7 eV. The divergence angle of the electron beam along z-direction is $\Delta\theta = \pm0.2°$, comprising more than 90% electrons. In addition, further mechanical design are still in progress to meet the feasibility. After the first attempt on the 320 kV platform, the electron target will be installed at the heavy-ion storage ring CSRe for extended crossed-beams collision experiments including ionization, recombination and excitation.

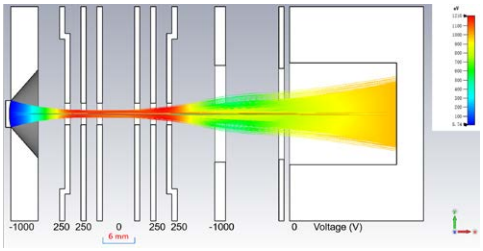

Figure 1. The structure and beam trajectory of the electron gun in the simulation. The electrodes potentials are presented on the bottom.

This work is supported by the National Natural Science Foundation of China (Grant No. U1932207). The authors would like to thank Prof. S. Shippers, Dr. A. Borovik, Jr. and B. M. Döhring for useful discussions.

References

[1] A Müller 2008 *Adv. at. mol. phys.* **55** 293-417
[2] C Brandau *et al* 2017 *J. Phys.: Conf. Ser.* **875** 052040
[3] B Ebinger *et al* 2017 *Nucl. Instrum. Methods B* **408** 317-322
[4] B M Döhring *et al* 2020 *J. Phys.: Conf. Ser.* **1412** 152009

*E-mail: lfzhu@ustc.edu.cn

Polarization of radiative recombination X-rays in highly charged Bi ions

N Numadate[1,2]*, S Oishi[1], H Odaka[3,4], Priti[1], M Sakurai[5], T Takahashi[4,3], Y Tsuzuki[3,4], Y Uchida[6], H Watanabe[7], S Watanabe[8,4], H Yoneda[9] and N Nakamura[1]

[1]Institute for Laser Science, The University of Electro-Communications, Tokyo 182-8585, Japan
[2]Komaba Institute for Science, The University of Tokyo, Tokyo 153-8902, Japan
[3]Department of Physics, The University of Tokyo, Tokyo 113-0033, Japan
[4]Kavli Institute for the Physics and Mathematics of the Universe (WPI), The University of Tokyo, Chiba 277-8583, Japan
[5]Department of Physics, Kobe University, Kobe 657-8501, Japan
[6]Department of Physics, Hiroshima University, Hiroshima 739-8526, Japan
[7]Department of Physics, Chubu University, Aichi 487-8501, Japan
[8]Institute of Space and Astronautical Science, Japan Aerospace Exploration Agency, Kanagawa 252-5210, Japan
[9]RIKEN Nishina Center, Saitama 351-0198, Japan

Synopsis We present polarization measurement for L-shell radiative recombination (RR) X-rays in highly charged Bi ions with a state-of-the-art Si/CdTe semiconductor Compton camera installed on an electron beam ion trap. The experimental azimuthal angular distribution of the Compton scattered X-rays is compared with the distribution obtained with a Monte Carlo simulation based on the theoretical polarization calculated with the Flexible Atomic Code.

Radiative recombination (RR) is one of the important recombination processes between highly charged ions and free electrons. It is well known that this process generally accompanies strongly polarized photon emissions. The polarization feature of RR X-rays for highly charged heavy ions is useful for experimental verification of relativistic effects, quantum electrodynamics and so on [1]. However, polarization measurements in the hard X-ray range have been strictly limited because of the lack of highly sensitive polarimeters. Recently, we developed a new Compton polarimeter for the precise polarization measurements of hard X-rays from highly charged ions [2]. In this poster, we present polarization measurement for L-shell RR X-rays in He- to F-like Bi ions with the new polarimeter installed on the Tokyo electron beam ion trap (Tokyo-EBIT) [3].

Figure 1 shows the measured azimuthal angular distribution of the Compton scattered X-rays detected with the polarimeter. The RR X-rays were also measured with an ordinary pure Ge detector at the same time in order to obtain the charge state distribution from the RR spectral feature. Using the obtained charge state distribution and the theoretical polarization calculated with the Flexible Atomic Code, we made a Monte Carlo simulation for the azimuthal angular distribution, which is compared with the experimental result in Fig. 1.

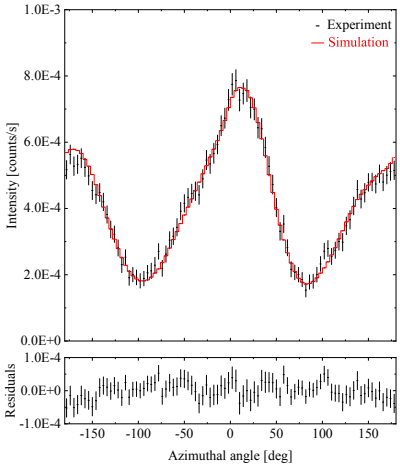

Figure 1. Measured (black points) and simulated (red histogram) azimuthal angular distributions for the Compton scattered RR X-rays.

References

[1] Nakamura N *et al* 2016 *J. Phys. B: At. Mol. Opt. Phys.* **49** 212001
[2] Tsuzuki Y *et al Submitted to Rev. Sci. Instrum.*
[3] Nakamura N *et al* 1997 *Phys. Scr.* **T73** 362

*E-mail: numadate-naoki@g.ecc.u-tokyo.ac.jp

The low-energy scattering of electrons on H_2^+ and HD^+: Dissociative recombination and ro-vibrational transitions

N Pop[1 *], E. Djuissi[2], J. Zs Mezei[3], F Iacob[4], M D Epée Epée[5], O Motapon[5, 6], V. Laporta[7] and I F Schneider[2, 8]

[1]Dept. of Physical Foundation of Engineering, Politehnica University Timişoara, Timişoara, RO30223, Romania
[2]Laboratoire Ondes et Milieux Complexes, CNRS, Université Le Havre Normandie, 76058, Le Havre, France
[3]Institute for Nuclear Research, ATOMKI, Debrecen, 4026, Hungary
[4]Dept. of Physics, West University of Timişoara, Timişoara, RO30223, Romania
[5]LPF, UFD Mathématiques, Informatique Appliquée et Physique Fondamentale, University of Douala, 24157 Douala, Cameroon
[6]Faculty of Science, University of Maroua, Maroua, 814, Cameroon
[7]Istituto per la Scienza e Tecnologia dei Plasmi, CNR, Bari, 70126, Italy
[8]LAC CNRS-FRE2038, Université Paris-Saclay, ENS Cachan, , 91405, Orsay, France

Synopsis The Multichannel Quantum Defect Theory (MQDT) has been employed in computing cross sections and Maxwell rate coefficients for electron-driven reactions involving H_2^+ and D_2^+ molecular cations.

The Dissociative Recombination (DR), the inelastic and the superelastic scattering of low-energy electrons by H_2^+ and HD^+, relevant for the astrochemistry of the early Universe are described using Multichannel Quantum Defect Theory (MQDT) [1].

The results of the present work are an extension of our previous studies [2-4] to a wider range of incident collision energy and to mixed rotational and vibrational transitions.

We report cross sections and Maxwellian rate coefficients, and outline several important features, like isotopic, rotational and resonant effects. The provided collisional data will be integrated in the kinetics models of the early Universe.

The thermal rate coefficients for electron temperatures between 10 and 3000 K are given in Figure 1 for targets in their ground ro-vibrational state $(N_i^+ ; v_i^+) = (0; 0)$. The DR predominates at very low temperatures, being surpassed by the rotational excitation onto the lowest rotational levels above 50 K.

The excitations into higher ro-vibrational levels become notable above 2000 K only.

* E-mail: nicolina.pop@upt.ro

Figure 1 also illustrates the isotopic effects: it is important for $\Delta N^+ = 2$ and 4 rotational excitations and for DR below 100K electron temperature.

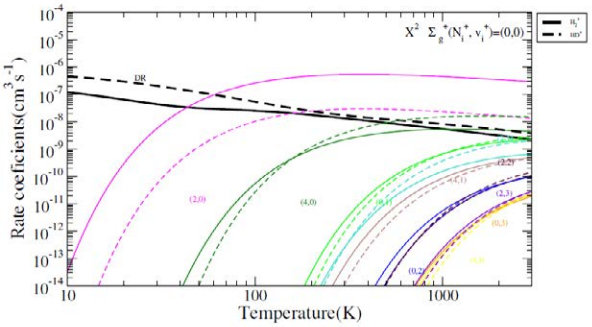

Figure 1. Electron-impact dissociative recombination and ro-vibrational transitions of HD^+ and H_2^+ in their ground state: Maxwell rate coefficients.

References

[1] Jungen Ch 2011 in *Handbook of High Resolution Spectroscopy* 471.
[2]Motapon O *et al* 2014 *Phys. Rev. A*, **90** 012706
[3] Epée Epée M D *et al* 2015 *MNRAS* **455** 276
[4] Djuissi E *et al* 2020 *Romanian Astronomical Journal* **30(2)** 101.

Electron-impact excitation cross section of the 190.8 nm ($6s6p\ ^3P^o_1 \rightarrow 6s^2\ ^1S_0$) intercombination line of the Tl^+ ion

A N Gomonai, A I Gomonai, V Roman* and L Bandurina

Institute of electron physics of National Academy of Sciences of Ukraine, Uzhgorod, 88017, Ukraine

Synopsis The results of investigation of the electron-impact excitation cross section of the λ190.8 nm ($6s6p\ ^3P_1 \rightarrow 6s^2\ ^1S_0$) intercombination line of the Tl^+ ion from the excitation threshold up to 300 eV is presented. The absolute value of the excitation cross section was found to be $0.14\pm0.07\times10^{-16}$ cm^2 at 300 eV.

Here we report on investigation of the electron-impact excitation cross section of the λ190.8 nm ($6s6p\ ^3P_1 \rightarrow 6s^2\ ^1S_0$) intercombination line of the Tl^+ ion from the excitation threshold up to 300 eV:

$$e + Tl^+(6s^2)^1S_0 \rightarrow e + Tl^{+*}(6s6p)^3P^o_1$$
$$\downarrow$$
$$Tl^+(6s^2)^1S_0 + h\nu$$

The experiment was performed by a photon spectroscopy method using the crossed electron and ion beams technique [1].

The measured excitation cross-section for the Tl^+ ion λ190.8 nm intercombination line is shown in Fig. 1 as a function of the incident electron energy. The absolute value of the electron-impact excitation cross section at 300 eV was found to be $0.14\pm0.07\times10^{-16}$ cm^2. The total error of the absolute value determination was estimated to be 50%.

Fig. 1 also contains the electron-impact excitation cross sections of the $6s6p\ ^3P^o_1$ level of the Tl^+ ion calculated using a two-state close coupling method without taking into account (curve 1) and with account of the $6\ ^1P^o_1$ and $6\ ^3P^o_1$ levels configuration mixing (95% $^3P^o_1$ + 5% $^1P^o_1$) (curve 2). As it is seen, account of the configuration mixing results in change of the $6s6p\ ^3P^o_1$ level excitation cross-section value as well as the energy dependence behaviour.

We also calculated the electron-impact excitation cross section of the $6s6p\ ^3P^o_1$ level of the Tl^+ ion in the distorted wave approximation (curve 3) using a complete software package Flexible Atomic Code (FAC) [2]. The radial orbitals for the construction of the basis state wave functions were derived from a modified Dirac-Fock-Slater iteration. The data obtained by this method better describe the electron excitation cross section of the λ190.8 nm line at the excitation threshold.

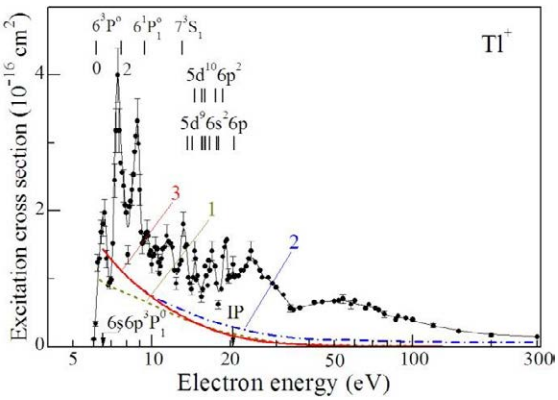

Figure 1. Electron-impact excitation cross section of the Tl^+ ion λ190.8 nm intercombination line.

However, comparison of theoretical and experimental excitation cross sections reveals strong data discrepancies. In particular, the experimental excitation function shows strong resonance contribution of the Tl atom autoionizing states the subsequent electronic decay of which leads to the significant population of the Tl^+ ion $6\ ^3P^o_1$ resonance level.

In order to improve theoretical calculations, one should take into account all possible cascade transitions from high-energy levels as well as correlation effects. Note that no theoretical calculations or other experimental measurements were found in the literature to compare with the present results.

References

[1] Ovcharenko E *et al* 2010 *J. Phys. B: Atom. Mol. Opt. Phys.* **43** 175206
[2] Gu M 2008 *Can. J. Phys.* **86** 675

* E-mail: viktoriyaroman11@gmail.com

Absolute cross-section of electron-impact excitation of the In^+ ion λ158.6 nm resonance line

A N Gomonai, A I Gomonai, V Roman*, Yu Hutych, and V Zvenihorodsky

Institute of Electron Physics of National Academy of Sciences of Ukraine, Uzhgorod, 88017, Ukraine

Synopsis The results of joint experimental and theoretical investigation of the electron-impact excitation cross-section of the λ158.6 nm ($5s5p\ ^1P_1 \rightarrow 5s^2\ ^1S_0$) resonance line of the In^+ ion is presented. The absolute value of the cross-section at 200 eV was found to be $3.0\pm0.9\times10^{-16}$ cm^2.

Electron-impact excitation is the subject of intense study, both experimentally and theoretically, since it is the dominant mechanism of the emission lines formation in many laboratory and astrophysical plasmas. The indium ion spectral lines are of an interest in the plasma spectroscopy and in astrophysical research.

Here we report on study of the electron-impact excitation cross section of the λ158.6 nm ($5s5p\ ^1P_1 \rightarrow 5s^2\ ^1S_0$) resonance line of the In^+ ion from the excitation threshold up to 300 eV. The experiment was performed by photon spectroscopy method using the crossed electron and ion beams technique which allows to carry out the detail investigation with the energy resolution $\Delta E_{1/2} \sim 0.4$ eV and to observe the structure features on the energy dependence. The details of the experimental setup and the experimental procedure can be found in [1].

The obtained experimental result is presented in Fig. 1. The error bars in figure represent one standard deviation statistical uncertainty. The absolute value of the electron-impact excitation cross-section of the In^+ ion resonance line was determined by normalizing the relative value at the electron beam energy of 200 eV to the theoretical data of the cross section for electron impact excitation of the ground $5s^2\ ^1S_0$ state to the excited $5s5p\ ^1P^\circ_1$ state (curve 1) obtained by the relativistic distorted wave method (RDW) [2]. The determination uncertainty of the absolute effective excitation cross-section was about ± 30%.

In Fig. 1 we have compared our experimental result with other theoretical calculations. For comparison, we have performed calculations for the electron-impact cross section of the $5s5p\ ^1P^\circ_1$ state excitation of the In^+ ion by using the semiempirical distorted wave (DW) method of the Los Alamos code [3] (curve 2) as well as the Van-Regemorter formula (curve 3). The results of both quantum-mechanical calculations (curve 1 and curve 2) are seen to be in good agreement with the experimental data at the electron energy $E > 7E_{thr}$ ($E_{thr} \approx 7.8$ eV is the threshold energy).

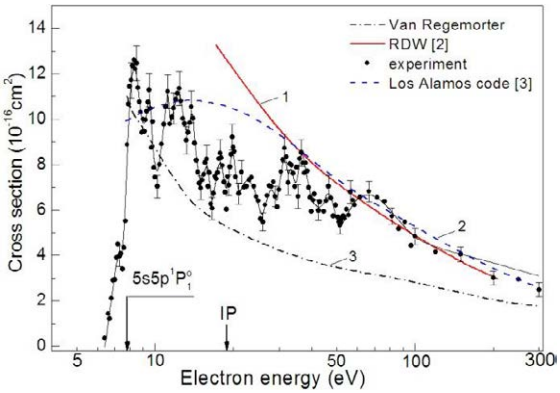

Figure 1. Effective excitation cross section of the λ158.6 nm resonance line of the In^+ ion.

Unfortunately, to date there are no theoretical calculations that could describe the experimentally observed structure in the cross-section energy dependence which results from the cascade effects from higher lying state and collective resonance contribution of close-lying autoionizing states of $4d^{10}5snln_1l_1$, $4d^{10}5p^2nl$ and $4d^9 5s^2nln_1l_1$ configuration.

References

[1] Ovcharenko E *et al* 2010 *J. Phys. B: Atom. Mol. Opt. Phys.* **43** 175206
[2] Bharti S *et al* 2020 *JAMCNP* **7** 83
[3] https://www-amdis.iaea.org/LANL/

* E-mail: viktoriyaroman11@gmail.com

Emission cross-sections of the λ182.2 and λ143.4 nm Pb^+ ion spectral lines

V Roman[1] *, V Jonauskas[2] †, S Kučas[2], A N Gomonai[1], A I Gomonai[1], and Y Hutych[1]

[1] Institute of electron physics of National Academy of Sciences of Ukraine, Uzhgorod, 88017, Ukraine
[2] Institute of Theoretical Physics and Astronomy, Vilnius University, Vilnius, LT-01108, Lithuania

Synopsis Results of experimental and theoretical investigation for electron-impact excitation of the $6s^26d\ ^2D \rightarrow 6s^26p\ ^2P^\circ$ spectral transitions in the Pb^+ ion are presented. The absolute emission cross-section values for the $6s^26d\ ^2D_{5/2} \rightarrow 6s^26p\ ^2P^\circ_{3/2}$ (λ182.2 nm) and $6s^26d\ ^2D_{3/2} \rightarrow 6s^26p\ ^2P^\circ_{1/2}$ (λ143.4 nm) transitions at 100 eV are found to be $(0.31\pm0.15)\times10^{-16}$ cm^2 and $(0.54\pm0.25)\times10^{-16}$ cm^2, respectively.

We report the study of the electron-impact excitation cross-sections for the dipole-allowed $6s^26p\ ^2P^o_{1/2,3/2} \rightarrow 6s^26d\ ^2D_{3/2,5/2}$ transitions of the Pb^+ ion in the 5–110 eV energy range. The experimental excitation functions are measured by a VUV-spectroscopy method using the crossed electron and ion beams technique which allows one to resolve the observed resonance structure for both transitions with sufficient energy resolution, typically of 0.6 eV. The theoretical calculations were performed in the DW approximation using Flexible Atomic Code [1] which implements the Dirac-Fock-Slater approximation. The configuration interaction (CI) method is used to investigate influence of the correlation effects for the considered transitions. Note that the results for electron excitation cross-section of the 143.4 nm Pb^+ ion line were presented in [2]. However, there was no theoretical analysis for these data given.

The experimental cross sections for electron-impact excitation of the $6s^26d\ ^2D_{5/2} \rightarrow 6s^26p\ ^2P^o_{3/2}$ (λ182.2 nm) and $6s^26d\ ^2D_{3/2} \rightarrow 6s^26p\ ^2P^o_{1/2}$ (λ143.4 nm) transitions are shown in Fig. 1. The error bars represent one standard deviation statistical uncertainty. The distinct structure due to autoionizing states contribution is observed in the cross-sections of the lines under investigation. The absolute values of the cross-sections at the energy 100 eV are obtained by normalizing the experimental data on that calculated using Van Regemorter formula. They are found to be $(0.31\pm0.15)\times10^{-16}$ cm^2 and $(0.54\pm0.25)\times10^{-16}$ cm^2, respectively.

The absolute cross-sections calculated using Flexible Atomic Code (DW-CI) are represented as dotted lines in Fig. 1. As it is seen there is a discrepancy with experimental values obtained by normalizing on Van Regemorter formula taking into account the experimental oscillator strengths 0.179 ($^2D_{5/2} \rightarrow {}^2P^o_{3/2}$) and 0.321 ($^2D_{3/2} \rightarrow {}^2P^o_{1/2}$) [3]. In contrast to the experimental data, the calculated cross-section for the $^2D_{5/2} \rightarrow {}^2P^o_{3/2}$ transition appears to be greater than that for the $^2D_{3/2} \rightarrow {}^2P^o_{1/2}$ transition. Note that the same situation is also observed in the case of the cross-sections calculated using the relativistic distorted wave (DW) approximation [4] (see solid lines in Fig. 1). This, in our opinion, is due to the complexity of the Pb^+ ion which is a three-valence-electron system characterized by core-valence correlation, relativistic effects including the Breit interaction, and strong configuration mixing.

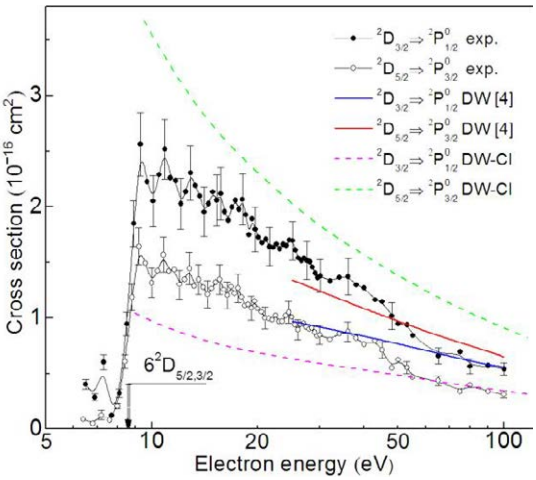

Figure 1. Absolute emission cross-sections of the λ182.2 nm ($6s^26d\ ^2D_{5/2} \rightarrow 6s^26p\ ^2P^\circ_{3/2}$) and λ143.4 nm ($6s^26d\ ^2D_{3/2} \rightarrow 6s^26p\ ^2P^\circ_{1/2}$) spectral lines.

*E-mail: viktoriyaroman11@gmail.com
†E-mail: valdas.jonauskas@tfai.vu.lt

References
[1] Gu M 2008 *Can. J. Phys.* **86** 675
[2] Gomonai A N *et al* 2017 *Eur. Phys. J. D* **71** 31
[3] Heidarian N *et al* 2015 *Astrophys. J.* **808**:112
[4] Bharti S *et al* 2019 *Springer Proceedings in Physics* **230** 250

Theoretical study of resonant electron recombination process of Si^{11+} ions

J L Rui[1], J M Zhang, L Y Xie[1*] and C Z Dong[1†]

[1] Key Laboratory of Atomic and Molecular Physics and Functional Materials of Gansu Province, College of Physics and Electronic Engineering, Northwest Normal University, Lanzhou 730070, People's Republic of China;

Synopsis The Δn=1, 2, and 3 resonant electron-ion recombination process associated with K-shell electron excitations of Si^{11+} ions are systematically studied using the flexible atomic code based on the relativistic configuration interaction method. The theoretical cross sections and rate coefficients are presented, and compared with the experimental measurements at heavy-ion storage ring (TSR), a good agreement is obtained.

Silicon is the eight most abundant element in the solar chemical composition, accurate atomic data of silicon ions are required in order to identify spectral lines, derive ion abundances of solar plasma. Several studies have been performed to investigate the electron-ion recombination process and X-ray spectra of Li-like Si^{11+} ions. Kenntner et al [1] have measured the absolute cross sections of Si^{11+} for K-shell dielectronic recombination (DR) and electron-impact ionization at the Heidelberg heavy ion storage ring TSR. Bartsch et al [2] have measured the enhancement of DR by applied electric fields for L-shell Δn=0 transition using heavy ion storage ring CRYRING at Stockholm University. Recently, Lindroth et al [3] reported experimental measurements of K-shell electron-impact recombination and excitation rates of Si^{11+} ions at the Stockholm electron beam ion trap.

In this work, we systematically investigate the K-shell Δn=1, 2, and 3 resonant electron recombination process of Si^{11+} ion in the ground state ($1s^22s\ ^2S_{1/2}$) by using the flexible atomic code (FAC) [4], the main processes can be described as following

$$Si^{11+}(1s^2 2s) + e^- \rightarrow \begin{cases} Si^{10+}(1s2s2ln'l' + 1s2p^2n'l')^{**} & (\Delta n = 1) \\ Si^{10+}(1s2s3ln''l'' + 1s2p3ln''l'')^{**} & (\Delta n = 2) \\ Si^{10+}(1s2s4ln'''l''' + 1s2p4ln'''l''')^{**} & (\Delta n = 3) \end{cases} \rightarrow Si^{11+*} + h\upsilon$$

where the dominant DR and trielectronic recombinations (TR) channels are included. State-by-state calculations are performed for all resonances up to n', n'', n'''=30, and higher-n contributions can be negligible. We obtained the detailed resonant energies, strengths, recombination cross sections, and rate coefficients for K-shell Si^{11+} ions. As shown in Fig 1, the theoretical cross sections are convoluted using a full width at half maximum of 7 eV experimental resolution to model the experimental recombination spectra [1], a good agreement can be found.

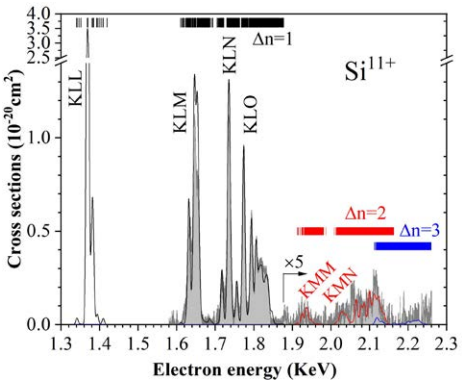

Figure 1. The DR cross section of Si^{11+} ions in the ground state ($1s^22s\ ^2S_{1/2}$) resulting from the K-shell Δn=1, 2, and 3 excitations compared to the experiment [1] (gray area). The vertical bars show the resonant positions for individual resonances.

The work was supported by the National Key Research and Development Program of China under Grant No.2017YFA0402300, the Natural Science Foundation of China (Grant Nos. 12064041, U1530142, 11564036, 11774292, 11464042, 11874051), the Funds for innovative Fundamental Research Group Project of Gansu Province (20JR5RA541) and the Fund of NWNU (NWNU-LKQN-15-3).

References

[1] Kenntner J *et al* 1995 *Nuclear Instruments and Methods in Physics Research B.* **98** 142
[2] Batsch T *et al* 1997 *Phys. Rev. L.* **79** 12
[3] Lindroth E *et al* 2020 *Phys. Rev. A.* **101** 062706
[4] Gu M F 2008 *Can. J. Phys.* **86** 675

* E-mail: xiely@nwnu.edu.cn
† E-mail: dongcz@nwnu.edu.cn

Investigation of electron runaway process on the basis of effective potential taking into account dynamic screening

M M Seisembaeva[1], E O Shalenov[1,2 *], M N Jumagulov[1] and K N Dzhumagulova[1,2]

[1]Institute of Experimental and Theoretical Physics, al-Farabi Kazakh National University, Almaty, 050040, Kazakhstan
[2]Department of Physics, Nazarbayev University, Nur-Sultan, 010000, Kazakhstan

Synopsis In this work, the phenomenon of electron runaway in dense semiclassical plasma was investigated on the basis of the effective interaction potential, which takes into account dynamic screening and the quantum mechanical effect of diffraction. Using the method of phase functions, the transport cross sections for scattering of electrons by ions and other electrons were calculated; on their basis, the mean free path of electrons was determined for various values of the density and coupling parameters.

The electron runaway phenomenon has attracted great attention in many areas of plasma physics. In astrophysics, the role of high-energy electrons in a gamma-ray burst during a supernova is well known. Also energetic electrons can appear as a result of the acceleration of electrons during a solar flare. Under atmospheric conditions, runaway electrons are observed in electrical discharges associated with thunderstorms, where they can cause electrical breakdown. It was also found that electrons with energy $\geq MeV$ can cause serious problems in power plants, for example, the presence of runaway electrons in the plasma of fusion reactors, namely in a tokamak, under certain circumstances is one of the main obstacles to the implementation of the production of fusion energy. It should be noted that these fast electrons underlie many studies in modern laser physics. This is due to the fact that in the interaction of laser radiation of relativistic intensity with a plasma, most of the energy is spent on accelerating electrons.

In the work, we used the original potential for interaction between an electron and an atom that we developed earlier in [1–5]. This effective potential takes into account the quantum mechanical effect of diffraction at small distances, because of which it has a finite value at distances close to zero.

Figure 1 show the reduced Dreiser's critical electric field as a function of the coupling parameter at a fixed value of rs = 4. The dependences show that with decreasing temperature, higher values of the Dreiser's critical field are required for electron runaway.

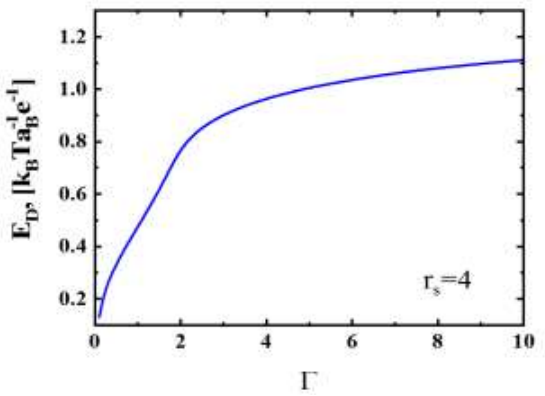

Figure 1. Electric field as a function of the communication parameter.

References

[1] Shalenov E O *et al* 2018 *Phys. Plasmas.* **25** 082706
[2] Shalenov E O *et al* 2019 *Contrib. Plasma Physics.* **59** e201900024
[3] Shalenov E O *et al* 2019 *J. Phys.: Conf. Ser.* **1400** 077035
[4] Shalenov E O *et al* 2019 *J. Phys.: Conf. Ser.* **1385** 012031
[5] Jumagulov M N *et al* 2020 *High Energy Density Physics.* **36** 100832

* E-mail: shalenov.erik@physics.kz

Transitions between multiply-excited states and their contribution to opacity in laser-driven tin plasmas for EUV lithography

J Sheil[1]*, F. Torretti[1,2], R. Schupp[1], M M Basko[3], M Bayraktar[4], R A Meijer[1,2], S. Witte[1,2], W Ubachs[1,2], R Hoekstra[1,5], O O Versolato[1,2], A J Neukirch[6], J Colgan[6]†

[1]Advanced Research Center for Nanolithography, Science Park 106, 1098 XG Amsterdam, The Netherlands
[2]Department of Physics and Astronomy, and LaserLaB, Vrije Universiteit, De Boelelaan 1081, 1081 HV Amsterdam, The Netherlands
[3]Keldysh Institute of Applied Mathematics, Miusskaya Square 4, 125047 Moscow, Russia
[4]Industrial Focus Group XUV Optics, MESA+ Institute for Nanotechnology, University of Twente, Drienerlolaan 5, 7522 NB Enschede, The Netherlands
[5]Zernike Institute for Advanced Materials, University of Groningen, Nijenborgh 4, 9747 AG Groningen, The Netherlands
[6]Los Alamos National Laboratory, Los Alamos, NM 87545, USA

Synopsis We will present recent work investigating the radiative properties of tin plasmas in the context of their role as a light source for EUV lithography. Our calculations reveal that transitions between complex, multiply-excited states are the dominant contributors to EUV emission in laser-driven tin plasmas.

Laser-produced plasmas formed on tin microdroplets act as the light source in new-generation extreme ultraviolet (EUV) lithography machines [1]. This choice is based on their ability to provide sufficiently high doses of EUV radiation in the narrow 2% reflective bandwidth (centered at 13.5 nm) of molybdenum/silicon multilayer mirrors.

Under appropriate experimental conditions, the EUV spectrum of a laser-driven tin plasma exhibits an intense, narrowband emission feature centered near 13.5 nm. For many years, this feature was attributed to overlapping $\Delta n = 0$ transition arrays of the form $4p^6 4d^m - (4p^5 4d^{m+1} + 4p^6 4d^{m-1} 4f)$ in $Sn^{11+} - Sn^{14+}$ ions ($m = 3-0$). However, recent calculations of tin-plasma opacities indicate that these transitions only make a minor contribution to EUV emission from these plasmas [2, 3]. Rather, it is transitions between complex, multiply-excited states (doubly-, trebly- and quadruply-excited states) that dominate the EUV spectrum.

We will present an overview of our recent work on tin plasma opacities for Nd:YAG (laser wavelength $\lambda = 1.064$ μm) and CO_2 ($\lambda = 10.6$ μm) laser-driven plasma conditions [2, 3]. We have employed the Los Alamos ATOMIC code under the assumption of local thermodynamic equilibrium (LTE) conditions. Coupling our opacity calculations with a model for radiation transport in the plasma has enabled comparisons with experimental EUV spectra recorded from Nd:YAG laser-driven tin plasmas (see Figure 1). To model the radiative properties of lower-density, industrially-relevant CO_2 laser-driven plasmas we have employed Busquet's method [3] to effectively "mimic" non-LTE opacities using LTE computations. We have found that transitions between multiply-excited states also make a substantial contribution to EUV emission in lower-density, CO_2 laser-driven tin plasmas.

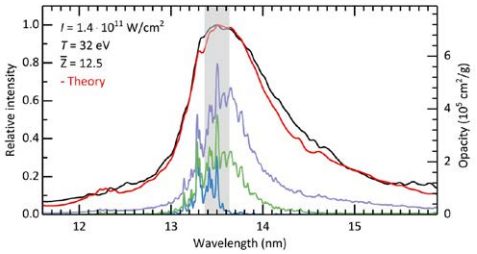

Figure 1. Experimental EUV spectrum (black) and a radiation-transported spectrum (red). Various contributions to the opacity are shown in blue, green and purple, respectively [3].

References

[1] Versolato O O *et al* 2019 *Plasma Sources Sci. Technol.* **28** 083001
[2] Torretti F *et al* 2020 *Nat. Commun.* **11** 2334
[3] Sheil J *et al* 2021 *J. Phys B: At. Mol. Opt. Phys.* **54** 035002

*E-mail: j.sheil@arcnl.nl
†E-mail: jcolgan@lanl.gov

Electron-impact excitation of Sc II

S. S. Tayal[*] [1] and O. Zatsarinny[†] [2]

[*] Department of Physics, Clark Atlanta University, Atlanta, GA 30314, USA
[†] Department of Physics and Astronomy, Drake University, Des Moines, Iowa 50311, USA

Synopsis New large-scale calculations for electron impact excitation collision strengths and radiative parameters for Sc II spectral lines between the 145 fine-structure levels belonging to the $3p^63d^2$, $3p^63d4l$ (l=0-3), $3p^63d5l$ (l=0-3), $3p^63d6s$, $3p^64s^2$, $3p^64s4l$ (l=0-3), $3p^64s5l$ (l=0-1), and $3p^64p^2$ configurations have been performed. The likely uncertainties in our results have been estimated by means of comparison with other calculations and experimental radiative parameters.

Sc II is the first member of the iron-group elements whose several optical and infrared lines have been observed in stellar and nebular spectra. The combination of infrared and optical lines offers good spectral diagnostics. The collision rates and radiative parameters such as transition probabilities are of primary importance for the analysis and interpretation of astrophysical spectra.

Accurate description of the target wave functions and adequate account of the various interactions between target levels have been determined by a combination of the multiconfiguration Hartree-Fock (MCHF) and the B-spline box-based close-coupling methods together with the nonorthogonal orbitals technique. The valence electron wave functions are described by multichannel expansions in a B-spline basis and are subjected to a boundary condition to become negligible at the boundary. This approach generates whole Rydberg series as well as considers the interaction between different series. The short-range correlation and relaxation effects are included using the MCHF method for individual optimization of different ion states and the so-called "perturbers" in the Rydberg series. The calculations of collision strengths have been performed using the close-coupling approximation based on the B-spline Breit-Pauli R-matrix method [1]. The relativistic effects in the scattering calculations have been incorporated in the Breit-Pauli Hamiltonian using the one-body Darwin, mass correction, and spin-orbit operators.

Lawler et al. [2] measured branching fractions for 259 lines of Sc I and Sc II using the Fourier transform spectra. We have shown comparison of the present radiative rates with experimental values of Lawler et al. [2] in Fig. 1. Also indicated in the panel is the average deviation from the present results. There is an overall good agreement between the theory and experiment.

The collision strengths for the fine-structure forbidden transitions from the ground state triplet $3d4s\ ^3D_{1,2,3}$ levels to the excited $3d^2\ ^3F_2$ level exhibit rich resonance structures. The collision strengths for the allowed $3d4s\ ^3D_2$ - $3d4p\ ^3D_2$ transition from the present 145-level model show stronger increase at higher temperatures than the 89-level model [3]. It may be related to the slower convergence of the dipole partial wave expansions. The collision strengths show characteristic energy behavior of log(E) for the allowed transitions. The magnitude of collision strengths at higher electron energies is directly related to the dipole oscillator strengths for the allowed transitions. The 30-state R-matrix calculation [4] shows significant discrepancies with the present 145-level model and the previous 89-level model [3].

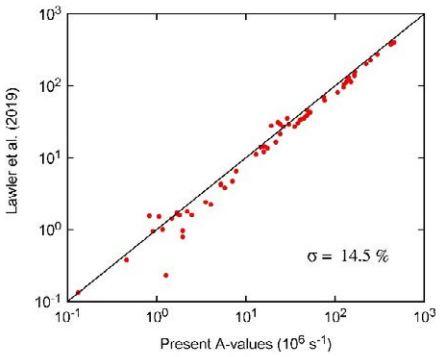

Figure 1. Comparison of the present radiative rates with experimental values [2].

This work was supported by the NSF grants No. AST-1714159 (ST) and No. PHY-0555226 (OZ).

References

[1] O. Zatsarinny 2006 Comp. Phys. Commun. **174** 273
[2] J. E. Lawler et al. 2019 ApJS **241** 21
[3] M. F. R. Grieve and C. A. Ramsbottom 2012 MNRAS **424** 2461
[4] M. A. Bautista et al. 2009 MNRAS **393** 1503

[1] E-mail: stayal@cau.edu
[2] E-mail: oleg.zatsarinny@drake.edu

Precise determination of the transition energy with fluorine-like nickel utilizing a low-lying dielectronic resonance

S X Wang[1], Z K Huang[2], W Q Wen[2], H B Wang[2], W L Ma[1], C Y Chen[3], Z W Wu[4], A V Volotka[5], X Ma[2]*, L F Zhu[1]† and DR collaboration @ CSR

[1] Department of Modern Physics, University of Science and Technology of China, Hefei, 230026, China
[2]Institute of Modern Physics, Chinese Academy of Sciences, 730000, Lanzhou, China
[3]Shanghai EBIT Laboratory, Institute of Modern Physics, Fudan University, Shanghai 200433, China
[4]College of Physics and Electronic Engineering, Northwest Normal University, Lanzhou 730070, China
[5]Helmholtz–Institut Jena, Fröbelstieg 3, D–07743 Jena, Germany

Synopsis Precision dielectronic recombination spectroscopy of fluorine-like nickel was measured by employing the electron-ion merged-beam technique at the heavy-ion storage ring CSRm at the Institute of Modern Physics in Lanzhou, China. By comparing with the recent relativistic configuration interaction calculation, the measured dielectronic resonances are state-resolved. The first resonance at about 82 meV allows precise determination of the $2s^22p^5[^2P_{3/2}] \rightarrow 2s2p^6[^2S_{1/2}]$ transition energy when the Rydberg binding energy of $(2s2p^6[^2S_{1/2}]6s)_{J=1}$ state can be calculated with a high accuracy and high precision. The uncertainty of the associated transition energy could then be improved prominently when compared to the NIST recommended value of 149.05±0.12 eV.

Atomic energy levels of highly charged ions constitutes ideal systems for testing the quantum electrodynamics (QED) and relativistic effects. Dielectronic recombination (DR) spectroscopy is proven to be an effective tool to approach the ionic energy levels [1, 2]. DR resonances, in particular for the ones near threshold, are sensitive to the core transition energies [3, 4]. By employing the electron-ion merged-beam technique at the heavy-ion storage ring, the low-lying DR resonances can be determined accurately and precisely. The core transition energy of highly charged ions with DR resonances near threshold can thus be determined with incredible precision by analyzing the lowest DR resonances [1, 2, 5]. Nevertheless, the binding energy of the Rydberg electron should be calculated with a prominent accuracy and high precision.

By comparing with the relativistic configuration calculation utilizing the FAC code, the first DR resonance of fluorine-like nickel associated with the $(2s2p^6[^2S_{1/2}]6s)_{J=1}$ intermediate state was recognized [6]. The experimental data for the low-lying DR resonances are presented in Figure 1 along with the fitted curves. The energy position for the first DR resonance is determined as 82 meV with an experimental uncertainty of 2 meV, including the errors due to the beam energies, the space-charge effect and the collision angle. The transition energy of $2s^22p^5[^2P_{3/2}] \rightarrow 2s2p^6[^2S_{1/2}]$ could then be determined with an accuracy of several meV as long as the Rydberg binding energy of the $(2s2p^6[^2S_{1/2}]6s)_{J=1}$ state can be calculated with an absolute accuracy comparable to the experimental uncertainty. Further data analysis in collaboration with theoretical calculations are still in progress. We would like to present a full result during the conference.

*E-mail: x.ma@impcas.ac.cn
†E-mail: lfzhu@ustc.edu.cn

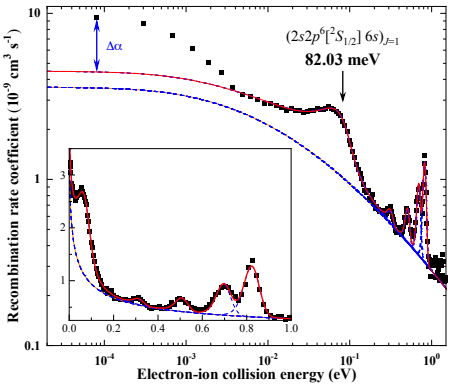

Figure 1. The low-lying DR resonances of fluorine-like nickel ions are presented. The square dots are the measured data and the red line is the fitted curve [6]. The blue lines are the fitted curve for individual resonances superimposed on the RR background (indicated by the orange line).

References

[1] Kieslich S *et al* 2004 *PRA* **70** 042714
[2] Lestinsky M *et al* 2008 *PRL* **100** 033001
[3] Lindroth E *et al* 2001 *PRL* **86** 5027
[4] Schuch R *et al* 2005 *PRL* **95** 183003
[5] Krantz C *et al* 2009 *JPCS* **163** 012059
[6] Wang S X *et al* 2019 *A&A* **627** A171

Rate Coefficients for Dielectronic Recombination of C-Like $^{40}Ca^{14+}$

W Q Wen[1*], Z K Huang[1], S X Wang[2], N Khan[1], H B Wang[1], C Y Chen[3], C Y Zhang[3], S Preval[4], N R Badnell[5], W L Ma[2], D Y Chen[1], X Liu[1], D M Zhao[1], L J Mao[1], J Li[1], X M Ma[1], M T Tang[1], D Y Yin[1], Y J Yuan[1], J C Yang[1], L F Zhu[2], and X Ma[1*]

[1] Institute of Modern Physics, Chinese Academy of Sciences, 730000, Lanzhou, PR China
[2] Department of Modern Physics, University of Science and Technology of China, Hefei, Anhui 230026, PR China
[3]Shanghai EBIT Laboratory, Institute of Modern Physics, Fudan University, Shanghai 200433, China
[4]Department of Physics and Astronomy, University of Leicester, University Road, Leicester, LE1 7RH, UK
[5]Department of Physics, University of Strathclyde, Glasgow G4 0NG, United Kingdom

Synopsis Dielectronic recombination (DR) rate coefficients for carbon-like $^{40}Ca^{14+}$ forming nitrogen-like $^{40}Ca^{13+}$ have been measured using the electron-ion merged-beam technique at the heavy ion storage ring CSRm at the Institute of Modern Physics in Lanzhou, China. The measured DR rate coefficients in the energy range from 0 to 92 eV cover most of the DR resonances associated with $2s^22p^2 \rightarrow 2s^22p^2$ and $2s^22p^2 \rightarrow 2s2p^3$ core transitions ($\Delta N = 0$). Theoretical calculations of the DR cross sections were carried out by using two different state-of-the-art atomic theoretical techniques, multi-configuration Breit-Pauli (MCBP) code AUTOSTRUCTURE and relativistic configuration interaction code FAC, to have comparison with the experimental rate coefficients.

DR rate coefficients for carbon-like and oxygen-like ions have been identified as the most urgent needs for astrophysical applications, and therefore, precision measurements of the DR rate coefficients of these ions which are abundant in astrophysical plasmas to benchmark the theories are required. We have measured DR rate coefficients of C-like Ca^{14+} forming N-like Ca^{13+} and compared the results with theoretical calculations [1]. As shown in Figure 1, the experimental DR resonances associated with ΔN=0 ($2s^22p^2 \rightarrow 2s^22p^2$ and $2s^22p^2 \rightarrow 2s2p^3$) within the energy range of 0 - 92 eV were studied and identified using the Rydberg formula. The AUTOSTRUCTURE code and the FAC code are employed for calculations. A good agreement was found for DR resonance positions and strengths at collision energies higher than 8 eV. However a significant discrepancy was found at low collision energy range, similar to the previous results from storage ring DR experiments of multi-electron highly charged ions.

The plasma recombination rate coefficients were deduced from the experimental DR rate coefficients in the temperature range from 0.1 to 1000 eV and compared with existing literature data. At the temperature range of photoionized plasmas, the most recent results of (Gu 2003) and (Zatsarinny, et al. 2004) are ~30% smaller than the experimental ones. For temperatures range within ~220-630 eV of the collisionally-ionized plasmas, these two calculated data agree well within 20% with the experimental ones. However, the calculated data from (Mazzotta, et al. 1998) and (Jacobs, et al. 1980) significantly underestimate the rate coefficients as compared with the present experimental results in the photoionized temperature range. Our experimental DR data of Ca^{14+} ions thus provide a benchmark for use in astrophysical and laboratory plasma modelling.

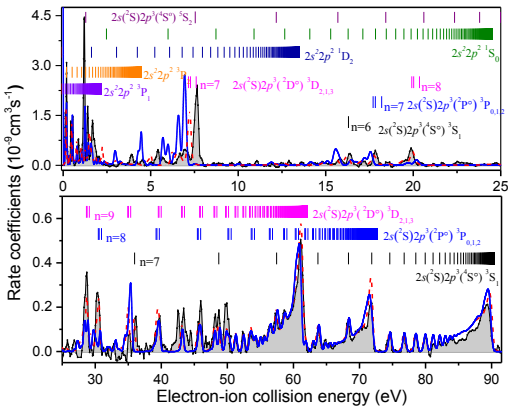

Figure 1. Experimental DR rate coefficients of C-like Ca^{14+} as a function of relative energy (gray area). DR series associated with $2s^22p^2 \rightarrow 2s^22p^2$ and $2s^22p^2 \rightarrow 2s2p^3$ core excitations (ΔN = 0) are observed, and the positions are indicated by short bars of different colors. Theoretical DR rate coefficients from the AUTOSTRUCTURE and FAC codes are shown by the short-dash-dotted red line and the blue solid lines, respectively. Both theoretical curves contain the recombination into Rydberg states with the principal quantum number up to n=1000 and n=300, respectively, which is called the field-ionization-free recombination rate coefficient.

References

[1] W.Q. Wen, Z.K. Huang, S.X. Wang, et al., ***APJ*** 2020 905, 36.

E-mail: wenweiqiang@impcas.ac.cn
E-mail: x.ma@impcas.ac.cn

Electron-impact ionization and excitation of Si^+ for applications in laboratory and astrophysical plasmas.

A P White[1]*, D A Ennis[1], C P Ballance[2], and S D Loch[1]†

[1]Auburn University, Auburn, AL 36849, USA
[2]Queen's University of Belfast, Belfast, UK

Synopsis Silicon is an important element in astrophysics and laboratory plasmas. We report on new R-matrix with pseudostate calculations for the electron-impact excitation and ionization of Si^+.

Silicon is both the seventh-most-abundant element in the universe and a material of interest for applications in plasma facing components of nuclear fusion plasma systems [1, 2]. In many astrophysical and laboratory plasmas, free-electron collisions are the dominant mechanism for ionizing species and exciting bound electrons to excited states. Accurate electron-impact data for Si ions is essential for determining Si abundances in astrophysics and erosion characteristics for laboratory plasma facing components.

One non-perturbative method used for electron-impact excitation/ionization is the R-matrix with pseudo-states (RMPS) method which has been used with much success for other light atomic systems [3, 4, 5]. Therefore, we shall present both the ground state and excited state ionization cross sections for Si^+ compared to the experimental measurements of Djurić et al. [6] and recent perturbative theoretical data [7, 8, 9]. For magnetically-confined plasmas, it has be shown that the ionization from excited states can be the dominant contributor to the effective ionization rates [10]. Thus, it is necessary to calculate Si^+ excited state ionization to determine its role in the net ionization of Si^+. Determining the effective ionization rate requires electron-impact excitation data, which motivates an associated electron-impact excitation calculation using the R-matrix method. This calculation is compared to an earlier R-matrix calculation of Tayal et al. [11]. We note that this excitation calculation also allows for the generation of atomic coefficients known as 'ionizations per photon' (also called S/XBs), which are used in erosion diagnostics for plasma facing components [12]. The S/XBs are being generated in support of work at the DIII-D tokamak in California.

References

[1] Abrams T., et al., 2020, APS DPP Meeting, PO06.005
[2] Wright G. M., et al., 2015, J. Nucl. Mat., **458**, 272
[3] Ballance C. P., et al., 2009, J. Phys. B: At. Mol. Opt. Phys., **42**, 175202
[4] Mitnik D. M., et al., 2003, J. Phys. B: At. Mol. Opt. Phys., **36**, 717
[5] Gorczyca T. W., Badnell, N. R., 1997, J. Phys. B: At. Mol. Opt. Phys., **30**, 3897
[6] Djurić N., et al., 1993, PhRvA, **47**, 4786
[7] Jonauskas V., 2020, A&A, **642**, A185
[8] Colgan J., Zhang H. L., Fontes C. J., 2008, PhRvA, **77**, 062704
[9] Dere K. P., 2007, A&A, **466**, 771
[10] Allain J. P., et al., 2004, Nucl. Fusion, **44**, 655
[11] Tayal S. S., 2008, ApJS, **179**, 534
[12] Behringer K., et al., 1989, PPCF, **31**, 2059

*E-mail: apw0037@auburn.edu
†E-mail: loch@physics.auburn.edu

Electron collision with CH: negative ion states and cross sections

K Chakrabarti[1] *, R Ghosh[2] and B S Choudhury[3]

[1]Department of Mathematics, Scottish Church College, Kolkata 700 006, India
[2] Department of Mathematics, Sukumar Sengupta Mahavidyalaya, Keshpur 721150, India
[3] Department of Mathematics, Indian Institute of Engineering Science and Technology, Shibpur 711103, India

Synopsis The molecular *R*-matrix method is used to study electron collision with the CH radical at low energies. Apart form different cross sections, namely those for electronic excitation to some of the low lying states, approximate calculations for electron impact dissociation and dissociative electron attachment, we have obtained several previously unreported negative ion states which are routes for the dissociative electron attachment.

The methylidyne radical CH and its positive ion CH^+ are of considerable importance in astrophysics, in technology and in flames [1] and is thus a prime candidate for electron collision studies.

In this work, we have used the *R*-matrix method to study electron collision with the CH radical with an emphasis on determining the anionic states which are not well studied. Yet these anionic states are of considerable interest because these are the routes to dissociative electron attachment (DEA), a process that is responsible for the dissociation of CH.

A good quality target calculation is first made to obtain the ground and several excited states of the CH target. Scattering calculations are then performed to obtain cross sections for elastic scattering and electronic excitation to some of the low lying states [1].

We have also performed calculations for the bound states of CH^- and resonances in the e + CH system. The $X\ ^3\Sigma^-$ ground state of CH^- is found to be bound, while the first $^1\Delta$ was found to be weakly bond.

Several Feschbach resonances of singlet, triplet and quintet symmetries have been obtained, of which only two of $^5\Sigma^-$ and $^3\Pi$ symmetry were reported previously [2] but their widths were never reported. Along with the resonances, we have also found the resonance widths which were previously unknown. Detailed calculations were done for Feshbach resonances and their widths as a function of the internuclear distance. Moreover, we have also traced the continuation of the resonances as bound states below the CH $X\ ^2\Pi$ ground state. This allowed us to completely construct the valence CH^- states that may be relevant for DEA studies.

* E-mail: kkch.atmol@gmail.com

As a preliminary calculation, we tried to estimate the DEA cross section using the $^5\Sigma^-$ and its width computed at the CH equilibrium geometry [1] using an approximate method proposed by Munro *et. al.* [3] that uses the survival probability of the resonance.

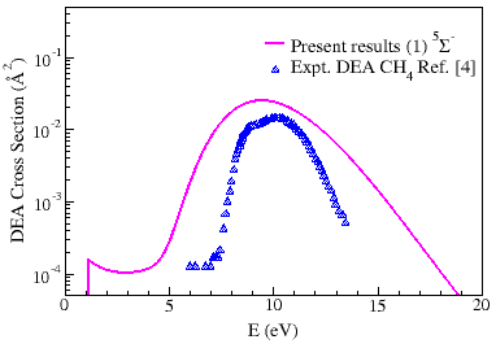

Figure 1. Approximate DEA calculation using the CH^- resonance of $^5\Sigma^-$ symmetry calculated at CH equilibrium R_e = 2.116 a_0. Experimental DEA cross section for CH_4 form Ref. [4] is used for comparison since no other data is available.

We are in the process of undertaking a full DEA calculation using the CH^- resonant states and their widths that we have obtained.

References

[1] Ghosh R *et al* 2020 *Plasma Souces Sci. Technol.* 29 095016
[2] Sun H and Freed K F 1982 *J. Chem. Phys.* **76** 5051
[3] Munro J *et al* 2012 *J. Phys.: Conf. Ser.* **388** 012013
[4] Vane C R *et al* 2007 *Phys. Rev.* A **75** 052715

A detailed investigation of temporary states of H_2^-

P Bingham[1], T Meltzer[2], Z Mašín[2] and J D Gorfinkiel[1]

[1]School of Physical Sciences, Faculty of STEM, The Open University, Milton Keynes, UK
[2]Institute of Theoretical Physics, Faculty of Mathematics and Physics, Charles University, Prague, Czechia

Synopsis We present a detailed analysis of the resonances in electron collisions with H_2 converging to the H(2l) + $H^-(1s^2)$ dissociation limit. Little information is available in the literature on these resonances despite their relevance in dissociative electron attachment.

Experiments on electron scattering from H_2 have revealed a complex spectra of resonances, many of which are known to be linked to dissociative electron attachment (DEA) of the molecule. The simple nature of H_2 makes the study of DEA particularly insightful. Recent DEA experiments [1] looking at higher electron scattering energies have reported a loss of symmetry in the angular distributions of the hydrogen anions from what would be expected when the dissociation is via a single resonant state. Although there have been significant efforts made in understanding and modelling H_2 resonances, only those at the lower electron scattering energies have been well characterised so far.

The lower energy resonances have been the subject of several theoretical works, with a comprehensive study [2] characterising them up to energies of approximately 13 eV above the ground state (at equilibrium geometry). The interpretation of the recent velocity slice imaging (VSI) DEA experiments at higher energies requires knowledge of resonances that have mostly either not been characterised or only partially so.

We have thus performed calculations to identify and describe resonances in electron scattering from H_2 between energies of approximately 12.5 eV and 15 eV and for bondlengths between 1 and 4 a_0. This energy interval encompasses several target state excitation thresholds, which makes identifying and following the resonances as a function of bondlength difficult.

The calculations were performed using the *ab initio* R-matrix method [3] as implemented in the UKRmol+ suite [4]. We used the aug-cc-pVTZ basis set, 29 target states (in D_{2h} symmetry), full configuration interaction and a continuum modelled using B-splines. An inner region radius of 40 a_0 was used with propagation to 600 a_0 sufficient for most bondlengths. It was essential, in order to obtain converged results for all bondlengths, to include partial waves up to l=6. This model, although necessarily less sophisticated (and therefore computationally cheaper) than that recently employed to determine highly accurate cross sections for electron scattering from H_2 [5], provides a good description of the system.

The results of our calculations show a large number of resonances of various symmetries over the range of bondlengths studied. Some of these can be clearly identified for the whole of this range, while others seem to be present for only some of the bondlengths. No obvious candidates that match the two resonances hypothesized by Krishnakumar *et al.* to explain their VSI results were identified. This fact, together with the large number of resonances identified and their characteristics, points at a more complex mechanism responsible for the asymmetric anion distribution than that proposed in [1].

References

[1] Krishnakumar E 2017, *et al Nature Physics* **14** 149.
[2] Darian T Stibbe and Jonathan Tennyson 1998, Journal of Physics B **31** 815
[3] P. G. Burke 2011, *R-Matrix Theory of Atomic Collisions: Application to Atomic, Molecular and Optical Processes*. Springer.
[4] Mašín Z *et al* 2020 *Computer Phys. Comm.* **249** 107092
[5] T Meltzer *et al* 2020 *J. Phys. B: At. Mol. Opt. Phys.* **53** 145204

Resonant dissociative excitation of rare gas molecular ions by electron impact

K S Kislov[1]*, A A Narits[1]† and V S Lebedev[1]

[1]P.N. Lebedev Physical Institute, Leninskiy prospect 53, Moscow 119991, Russian Federation

Synopsis The role of different physical mechanisms of destruction of heteronuclear and homonuclear inert gas ions is studied theoretically. Particular attention is paid to the role of the resonant non-adiabatic mechanism of dissociative excitation of molecular ions by electron impact. It is shown that the resonant process of dissociative excitation dominates over the process of dissociative recombination of molecular ions in a wide range of electron temperatures of rare gas plasma.

We report the results of comparative theoretical studies of different physical mechanisms of destruction of rare gas molecular ions. The studied processes include the dissociative excitation by electron impact and dissociative recombination of molecular ions resulting in population of highly excited and lower states of inert gas atoms. All the studied processes are due to the non-adiabatic energy exchange between the outer and inner electrons of a collision system $BA^+ + e$. For their description an original theoretical approach was developed based on the use of a quantum-mechanical version of the theory of non-adiabatic transitions between the electronic terms of the system. The key feature of this approach is that it allows one to take into account the integral contribution of the entire quasicontinuum of the rovibrational states of the molecular ions BA^+ to the dynamics of the studied decay processes. This feature allows us to calculate the Boltzmann-averaged rates of the dissociative recombination and dissociative excitation of weakly bound heteronuclear rare gas ions and carry out theoretical modelling of the low-temperature plasmas in the wide range of parameters typical for the afterglows of pulse discharges in noble gas mixtures.

The main goal of the work was to carry out theoretical study of dissociative excitation of molecular ions of inert gases by electron impact, and to compare the contribution of this process to that of the widely known mechanism of dissociative recombination. Specific calculations were performed for a wide range of heteronuclear ($HeXe^+$, $NeXe^+$, $ArXe^+$ and $KrXe^+$) and homonuclear (Ar_2^+, Xe_2^+) inert gas ions in conditions typical for experimental studies. It has been shown that in the case of molecular ions with low dissociation energies $D_0 \lesssim 0.1$ eV, dissociative excitation is predominant in the entire temperature range of $T_e \gtrsim 300$ K and $T \gtrsim 300$ K. In case of moderately bound and strongly bound ions with $D_0 \gtrsim 0.1 - 1$ eV, the efficiency of dissociative excitation turns out to be low in the temperature range $T_e \lesssim 2000$ K, but rapidly increases with increasing electron temperature. According to calculations, it begins to make a decisive contribution to the destruction of strongly bound ions at $T_e \gtrsim 10000$ K (see Fig. 1).

This work was supported by the Russian Science Foundation (grant 19-79-30086).

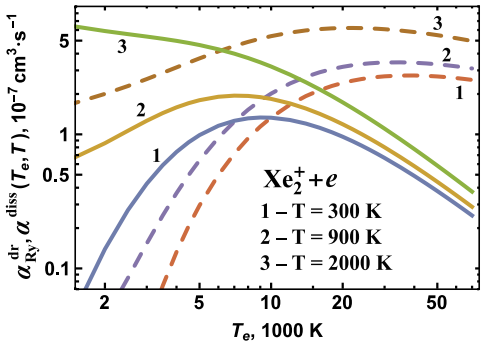

Figure 1. Solid curves, rate constants of electron-impact dissociative excitation of Xe_2^+ at gas temperatures $T = 300$ K (line 1), 900 K (line 2) and 2000 K (line 3). Dashed curves, integral contribution of dissociative recombination populating Rydberg atomic states.

*E-mail: kislov93@mail.ru
†E-mail: narits@sci.lebedev.ru

New insights in the low energy electron-driven reactivity of molecular cations

János Zsolt Mezei[1,2]*, Jeoffrey Boffelli[2], Frédéric Gauchet[2], Andrea Orbán[1], Kalyan Chakrabarti[3], Dahbia Talbi[4] and Ioan F Schneider[2,5]†

[1] Institute for Nuclear Research (ATOMKI), Debrecen, H-4001, Hungary
[2] LOMC, University Le Havre Normandy, Le Havre, 76600, France
[3] Scottish Church College, University of Calcutta, Calcutta, 700006, India
[4] LUPM, Montpellier University, Montpellier, 34095, France
[5]LAC, University Paris-Saclay, Orsay, 91405, France

Synopsis The major mechanisms governing the fragmentation dynamics induced by the reactive collisions of electrons with molecular cations will be illustrated in the case of the positive molecular hydrogen ions and several diatomic and triatomic hydrides.

Electron-impact dissociative recombination, ro-vibrational (de)excitation and dissociative excitation of hydride cations

$$AB^+ + e^- \rightarrow AB^{*,**} \rightarrow \begin{cases} A + B \\ AB'^+ + e^- \\ A + B^+ + e^- \end{cases} , \quad (1)$$

are in the heart of molecular reactivity in the cold ionized media [1], being major charged particles destruction reactions and producing often atomic species in metastable states, inaccessible through optical excitations. They involve super-excited molecular states undergoing predissociation and autoionization, having thus strong resonant character. Consequently, they are subject to beyond-Born-Oppenheimer theoretical approximations, and often require rather quasi-diabatic than adiabatic representations of the molecular states. In addition, they involve particularly sophisticated methods for modelling the collisional dynamics, able to manage the superposition of many continua and infinite series of Rydberg states.

We use the Multichannel Quantum Defect Theory [2], capable to account the strong mixing between ionization and dissociative channels, open - direct mechanism - and closed - indirect mechanism, via capture into prominent Rydberg resonances [3, 4] correlating to the ground and excited ionic states, and the rotational effects. These features will be illustrated for several cations of high astrophysical and cold plasma physical relevance such as SH^+ [5] and CH^+ [4, 6, 7], comparisons with other existing theoretical and experimental results being performed.

Advancement in the theoretical treatment - as the effect of the energy-dependence of the quantum defect on vibronic interactions for the benchmark cation H_2^+, the spin-orbit coupling for HCl^+, the isotopic effects for polyatomic systems like N_2H^+, etc. - will be presented.

Research supported by the Normandy region, CNRS-PCMI, ANR Labex EMC^3 and NKFIH-OTKA.

References

[1] I. F. Schneider, O. Dulieu, and J. Robert (editors) 2015 *Eur. Phys. J. Web of Conf.* **84**
[2] Ch. Jungen (editor), 1996 *Molecular Applications of Quantum Defect Theory*, (IoP Publish. Bristol)
[3] I. F. Schneider *et al* 1991 *J. Phys. B* **24**, L289
[4] Mezei J Zs et al 2019 ACS Earth and Space Chen,3 2376
[5] D. O. Kashinski *et al* 2017 *J. Chem. Phys.* **146**, 204109
[6] A. Faure *et al* 2017 *MNRAS* **469**, 612
[7] K. Chakrabarti *et al* 2018 *J. Phys. B* **51**, 104002

*E-mail: mezei.zsolt@atomki.hu
†E-mail: ioan.schneider@univ-lehavre.fr

Nonlocal multidimensional vibrational dynamics of anions: Testing of various Krylov subspace methods on model examples

M Šarmanová*, J Dvořák and M Čížek

Charles University, Faculty of Mathematics and Physics, Prague, Czech Republic.

Synopsis We test performance of various Krylov subspace iterative methods for solution of class of nonlocal models for vibrational excitation of molecules by electron impact. Up to three vibrational modes and two discrete anion states are included.

Nonlocal model was very successful in description of electron-molecule collisions involving resonance or virtual states (see for example [1]). In the last 30 years it has been applied to number of diatomic molecules. The treatment of the resulting equations for larger molecules is very difficult.

In this contribution we suggest to use Krylov subspace methods to solve the nonlocal dynamics for the discrete state component of the wave function with two or three active vibrational degrees of freedom. The model is inspired by [2], where two dimensional dynamics was treated for model of conical intersection in continuum. In this model the dynamics was treated by chain fraction method because of the block diagonal structure of the matrix of the problem. We realized that such model can be extended in a very flexible way leaving the matrix of the problem more complicated but still sparse, so that it is ideally suited for Krylov subspace methods.

In this contribution we will start by explaining the set up of used model. We then show the working equations of the nonlocal model and their representation as the "black box" for a general Krylov subspace method. Finally several methods, both specially designed for complex-symmetric and general matrices, are described. We mainly study the folowing methods: Conjugate orthogonal conjugate gradient method (COCG), Conjugate Aorthogonal conjugate residual method (COCR), Iterative method for complex symmetric matrices (CSYM), Generalized minimal residual method (GMRES) and Bi-conjugate gradient method (BiCG). The performance of iterative solution of the working equations is compared among the different methods for all test models.

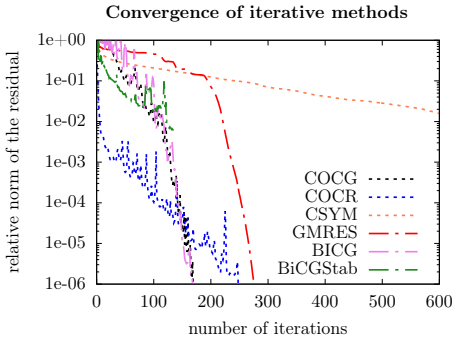

Figure 1. Convergence of iterative methods applied on complex-symmetric matrix arising from a model, which describes a vibrational dynamics of anion. The order of used matrix is $N = 1800$.

Acknowledgements: The work was supported by Charles University by grant GAUK 552120.

References

[1] Čársky P, Čurík R (Editors), *Low-Energy Electron Scattering from Molecules, Biomolecules and Surfaces,* CRC Press 2012.
[2] Estrada H *et al* 1986 *J. Chem. Phys.* **84** 152

*E-mail: martina.sarmanova@email.cz

The role of the environment in quenching the production of H_3^+ from the dicationic clusters of methanol

Enliang Wang[1,2]*, **Xueguang Ren**[1,3]† and **Alexander Dorn**[1]‡

[1]Max-Planck-Institut für Kernphysik, Saupfercheckweg 1, 69117 Heidelberg, Germany
[2]J. R. Macdonald Laboratory, Physics Department, Kansas State University, Manhattan, KS 66506, USA
[3]School of Physics, Xi'an Jiaotong University, Xi'an 710049, China

Synopsis H_3^+ is the most prevalent molecular ion in interstellar space and plays an important role in astrochemistry due to its high activity to initiate various chemical reactions. The ionization and subsequent isomerization of organic molecules is suggested to be an important source of H_3^+. We studied electron impact ionization of a cold methanol supersonic jet target containing small clusters in order to simulate cold molecular clouds in outer space. It was found that the H_3^+ production which is identified in double ionization of monomers is quenched in clusters, i.e., by the chemical environment.

The trihydrogen H_3^+ cation is regarded as the "engine" of interstellar chemistry due to its high activity in donating a proton through the proton hopping reaction [1], $H_3^+ + X \rightarrow HX^+ + H_2$. The protonated unit becomes far more reactive than the neutral one and, thereby, chains of reactions are launched that produce larger and more diverse molecules. Molecular dynamical studies suggest a mechanism concerning double ionization of alcohols that can produce H_3^+ via isomerization processes of the dication. In the first step, an ultrafast (less than 15 fs) double hydrogen migration takes place forming an intermediate neutral H_2. Secondly, the neutral H_2 roams around the dication and ends in formation of H_3^+ by attracting a proton from the dication [2, 3].

In this work, we study the influence of chemical environment on the formation of H_3^+ from methanol [4] using a reaction microscope. The molecular target was generated in a supersonic expansion through a 30 μm nozzle using helium as carrier gas. The temperature of the target was about 20 K which is in line with the conditions in the cold molecular clouds in interstellar space. The target was doubly ionized by the low-energy electron (90 eV) which initiated the isomerization and dissociation process of the dication. While a pronounced two-body coincidence between H_3^+ and COH^+ from the methanol monomer dicatoin was observed, the H_3^+ production was quenched from the methanol clusters.

The molecular dynamics simulation, potential energy surface, and classical-over-the-barrier model analysis reveal a fast charge transfer mechanism. The decisive aspect is that if a dication in its electronic ground state is placed within a dimer or cluster the whole system is in an electronically excited state. As a result, new reaction channels are open where charges, i.e. electrons or protons but also neutrals are transferred between the constituents of the cluster. As the roaming mechanism takes about 100 fs for formation of H_3^+, such ultrafast charge transfer greatly outperforms the production of H_3^+.

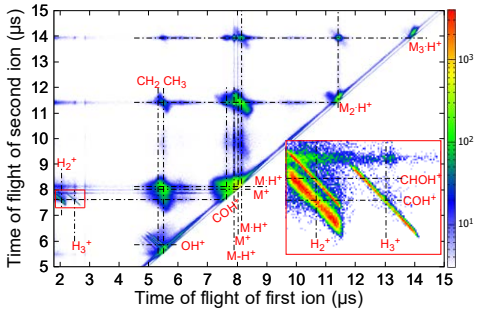

Figure 1. Time correlation map of two ions from methanol.

References

[1] T. Oka, 2006 *Proc. Natl. Acad. Sci. U.S.A.***103**, 12235
[2] N. Ekanayake, *et al*, 2018 *Nat. Commun.* **9**, 5186
[3] E. Wang, *et al*, 2020 *J. Phys. Chem. A* **124**, 2785
[4] E. Wang, *et al*, 2021 *Phys. Rev. Lett.* **126**, 103402

*E-mail: enliang@phys.ksu.edu
†E-mail: ren@mpi-hd.mpg.de
‡E-mail: alexander.dorn@mpi-hd.mpg.de

Hydrogen migration in the dissociation of hydrocarbon dications

Y Zhang [1], B Ren [2], C-L Yang [3], L Wei [2], B Wang [2], J Han [2], W Yu [2], Y Qi [1], Y Zou [2], L Chen [2], E Wang [4] and B Wei [2 *]

[1]School of Mathematics, Physics and Information Engineering, Jiaxing University, Jiaxing, 314001, China
[2]Key Laboratory of Nuclear Physics and Ion-beam Application (MOE), Institute of Modern Physics, Fudan University, Shanghai, 200433, China
[3]School of Physics and Optoelectronics Engineering, Ludong University, Yantai, 264025, China
[4]J. R. Macdonald Laboratory, Physics Department, Kansas State University, Manhattan, KS 66506, USA

Synopsis H_3^+ has great astronomical significance, but its formation mechanisms are not fully understood. Here a combined experimental and theoretical study of H_3^+ formation dynamics from ethane dications shows that roaming occurs at a much longer timescale than the transition state, and is accompanied by nuclear motion of larger amplitudes. In addition to the H_3^+ channels, other hydrogen-migration-induced dissociation channels are investigated.

Hydrogen migration plays an important role in the chemistry of hydrocarbons which considerably influences their chemical functions. The migration of one or more hydrogen atoms occurring in hydrocarbon cations has an opportunity to produce the simplest polyatomic molecule, i.e. H_3^+ and isomerization channels. Here we present a combined experimental and theoretical study of hydrogen migration in those channels from small hydrocarbon dications [1, 2]. The experiments are performed by 300-eV electron and 3-keV/u Ar^{8+} collisions with hydrocarbons using the cold target recoil ion momentum spectroscopy (COLTRIMS). The kinetic energy releases (KERs) and relative yields of corresponding hydrogen migration channels are determined. On the theoretical side, quantum chemistry calculations including reaction path calculation and *ab initio* molecular dynamics simulation are carried out. Also, theoretical KERs are extracted and compared with experimental ones.

Taking the dissociation of ethane dication for example, the calculations show that the H_3^+ formation channel can be opened on the ground-state potential energy surface of ethane dication via transition state and roaming mechanisms (see Figure 1). The *ab initio* molecular dynamics simulation shows that the H_3^+ can be generated in a wide time range from 70 to 500 fs. Qualitatively, the trajectories of the fast dissociation follow the intrinsic reaction coordinate predicted by the conventional transition state theory. The roaming mechanism, compared to the transition state, occurs within a much longer timescale accompanied by nuclear motion of larger amplitude. In addition, the hydrogen-migration-induced isomerization is found responsible for both the symmetric and asymmetric C-C bond breakup channels.

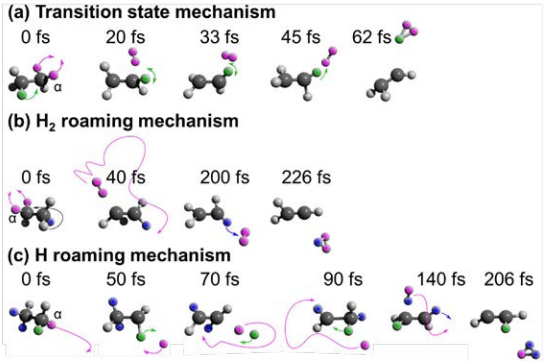

Figure 1. Structural evolution of ethane dication along three typical trajectories leading to $H_3^+ + C_2H_3^+$.

References

[1] Zhang Y *et al* 2019 *Phys. Rev. A* **100** 052706
[2] Zhang Y *et al* 2020 *Commun. Chem.* **3** 160

* E-mail: brwei@fudan.edu.cn

Formation of negative ions from gas-phase and clusters of precursor molecules for FEBID and EBISA by low-energy electron impact

P Papp[1] *, D Mészáros[1], R A Cartaya López[2], P Swiderek[2†] and Š Matejčík[1]

[1] Department of Experimental Physics, Faculty of Mathematics, Physics and Informatics, Comenius University in Bratislava, Mlynska dolina F2, 842 48 Braltislava, Slovakia
[2] Institute for Applied and Physical Chemistry, University of Bremen, Fachbereich 2 (Chemie/Biologie), Leobner Strasse/NW 2, Postfach 330440, 28334 Bremen, Germany

Synopsis Low-energy electron attachment and dissociative attachment to gas-phase $Co(CO)_3NO$ and $Fe(CO)_5$ precursors will be compared to pure clusters and their mixtures with acetic acid. Dissociative electron attachment cross-sections for ionic products of molecules and clusters will be compared. The activation of surface in deposition techniques will be described via electron attachment studies of mixed precursor and acetic acid cluster.

High-energy electron beam techniques based on focused electron beam induced deposition (FEBID) [1] or electron beam induced surface activation (EBISA) [2] are tools for preparing 3D nanustructures of ~nm sizes. Low-energy electrons <50 eV originating from surface ionization with the primary beam or back-scattering of primary electrons play important role in the deposition. Unfortunately, codeposition of impurities via electron induced dissociations and broadening of the deposited structers out of the primary beam focus is often seen. Crossed-beams techniques were used to study the electron attachment (EA) and dissociative electron attachment (DEA) to gas phase $Co(CO)_3NO$ precursor [3] and clusters of $Fe(CO)_5$ precursors [4]. The present work reports new results of DEA to $Co(CO)_3NO$ clusters in Ar (Figure 1) comapared with He nanodroplet results [5].

The HKUST-1 surface activation with EBISA has been studied for $Co(CO)_3NO$ and $Fe(CO)_5$ [2], with differences for the efficiency of autocatalytic growth. The activation of carboxylic groups of the linkers of surface-anchored metal-organic frameworks was proposed [2]. Due to that DEA studies to precursor/acetic acid mixed clusters were performed and compared to pure clusters and gas-phase.

This research was supported by Slovak Research and Development Agency project nr. APVV-19-0386 and Grant Agency VEGA project nr. 1/0489/21. This project has received funding from the European Union's Horizon 2020 research and innovation programme under the Marie Skłodowska-Curie grant agreement No 722149.

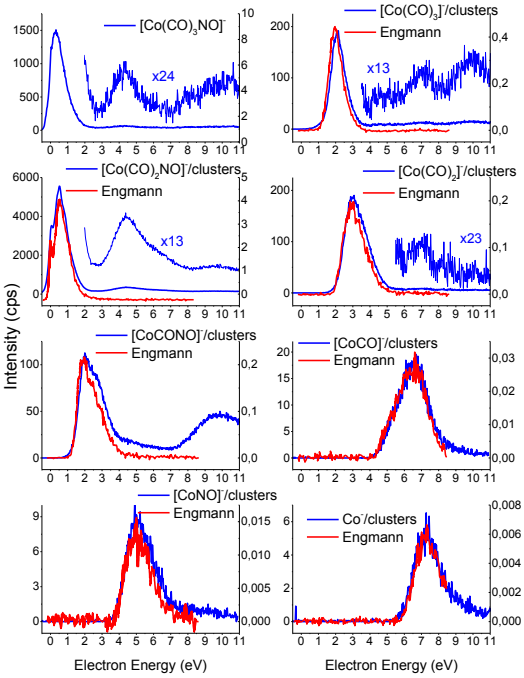

Figure 1. DEA molecular fragments of $Co(CO)_3NO$: red are gas-phase [3], blue are clusters (recent work).

References

[1] Utke I *et al* 2008 *J. Vac. Sci. Technol. B* **26** 1197
[2] Ahlenhoff K *et al* 2018 *J. Phys. Chem. C* **122** 26658
[3] Engmann S *et al* 2013 *J. Chem. Phys.* **138** 044305
[4] Lengyel J *et al* 2017 *Beilstein J. Nanotechnol.* **8** 2200
[5] Postler J *et al* 2015 *J. Phys. Chem.* **119** 20917

* E-mail: peter.papp@uniba.sk
† E-mail: swiderek@uni-bremen.de

Multicenter description of the electron-impact ionization of aligned H_2 molecules

E Acebal[1]* and S Otranto[1]

[1]Instituto de Física del Sur (IFISUR), Departamento de Física, Universidad Nacional del Sur (UNS), CONICET, Av. L. N. Alem 1253, B8000CPB - Bahía Blanca, Argentina

Synopsis Fully differential cross sections (FDCS) for the single ionization of oriented H_2 molecules by electron-impact are calculated by means of a multicenter CDW-EIS model, where the multicenter nature of the molecular ion is explicitly taken into account. Present results are contrasted with recent experimental data and reported theoretical calculations obtained with the time-dependent close-coupling method (TDCC). These exhibit a good overall description of the angles at which the FDCS peaks and the width of these structures.

The electron-impact ionization of atoms and molecules has represented a challenging field for decades. Regarding fully differential studies, since the mid 1990s the introduction of reaction microscopes has allowed for an unprecedented experimental level of detail. Concerning simple targets, and from a theoretical point of view, the experimental structures were accurately reproduced by numerical intensive treatments and perturbative methods, but the extension to complex molecular targets is far from being understood.

In this sense, we have recently introduced a multicenter CDW-EIS model, which, unlike the usual CDW-EIS model, explicitly considers the multicenter nature of the recoiling molecular ion in the final-state wave function [1]. Within this formalism, we have performed calculations of fully differential cross sections for the single ionization of aligned H_2 molecules at an impact energy of 54 eV, and benchmarked our results to the recent experimental data from Ren *et al.* [2] and other theoretical methods used to describe these data, such as the TDCC method.

In this work, we present the calculations regarding this collision system by means of three different models within the CDW-EIS formalism. The first one considers the residual ion as a single center of charge $Z = +1$ (1C), the second one incorporates the multicenter nature of the target by neglecting the remaining-electron repulsive potential terms (2C), and the third one accounts for the complete anysotropic nature of the molecular ion (MC).

In Figure 1, we contrast our results with the experimental data and the numerical intensive TDCC method as a function of the emission angle of one electron into the perpendicular xy plane and for equal energy sharing and a particular orientation of the target. It can be seen that the MC model correctly reproduces the peaks positions along the direction of the atoms' positions (light gray dashed vertical lines in Figure 1), in contrast to other theories.

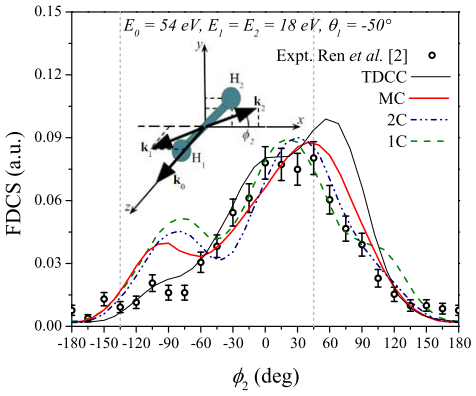

Figure 1. FDCS for electron-impact ionization of aligned H_2 molecules, for the perpendicular plane xy. Experimental and theoretical data from Ref. [2] scaled to the present theoretical results.

We also present calculations for six more geometries rotating the molecular target and, in addition, we analyse the FDCS as a function of the angle between the continuum electron momenta $\mathbf{k}_1$ and $\mathbf{k}_2$, a representation to which not much attention has been paid so far for these data.

References

[1] Acebal E and Otranto S 2020 *Phys. Rev. A* **102** 042808
[2] Ren X *et al* 2012 *Phys. Rev. Lett.* **109** 123202

*E-mail: emiliano.acebal@uns.edu.ar

Electron-molecule scattering calculations with Quantemol-EC

H B Ambalampitiya[1]*, B Cooper[1,2], M Tudorovskaya[1], S Mohr[1], M Hanicinec[1], M A P Turner[1], A Dzarasova[1] and J Tennyson[1,2]

[1]Quantemol Ltd, London, United Kingdom
[2]Department of Physics and Astronomy, University College London, London, United Kingdom

Synopsis Quantemol Electron Collisions (QEC) is a state-of-the-art software to generate accurate and reliable electron-molecule scattering cross sections. The latest QEC features include the non-resonant vibrational excitation and the implementation of effective-core potentials for ionization cross sections.

Low-energy electron-molecule scattering is informed by a rich amount of physics and it plays a fundamental role in a multitude of atmospheric, biological, and plasma processes. Quantitative studies of these processes can help design and advance important practical applications associated with plasma etching, fusion plasma, radiation therapy, and more. However, *ab initio* electron scattering calculations can become notoriously difficult and time-consuming for complex molecules.

To facilitate efficient electron-molecule scattering calculations, Quantemol introduces its newest and updated software: QEC [1]. Equipped with a Graphical User Interface (GUI), QEC presents an optimized user-friendly environment to run Molpro [2] and the UKRMOL+ [3] codes together. The latter conducts the advanced R-matrix calculations on the molecule whose quantum chemistry is provided by Molpro. With this combination, QEC generates accurate and reliable cross sections for total elastic and differential scattering, momentum-transfer, electronic excitation, electron-impact ionization and dissociation, dissociative electron attachment, and high-energy electron scattering. The updated QEC is also capable of calculating non-resonant vibrational-excitation (VE) cross sections [4] and implementing effective-core potentials (ECP) for calculating binary-encounter-Bethe (BEB) ionization cross sections of heavier atoms [5].

Figure 1 shows QEC calculations for a five-atom dipolar molecule: CH_3F (fluoromethane). Results compare the total elastic-scattering cross section with the experimental data [6]. The higher calculated cross section at low-energy is due to forward-scattered electrons which are hard to be detected in experiments. The present work will demonstrate and explain the steps involved in a sample QEC calculation as shown in Fig. 1. In addition, this poster will highlight the newest QEC features including VE and BEB ionization cross sections with ECP.

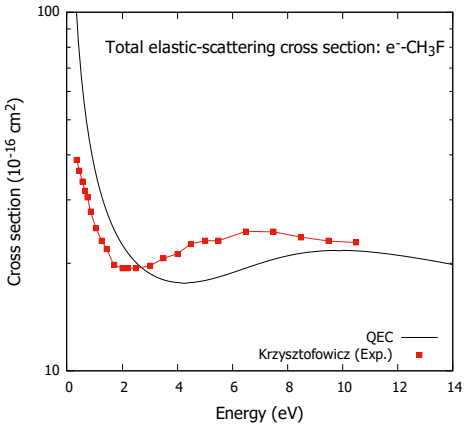

Figure 1. Total elastic scattering cross section for fluoromethane: CH_3F. Experimental data [6] are compared with the QEC results.

References

[1] Cooper B *et al* 2019 *Atoms* **7** 97
[2] Werner H J *et al* 2012 *WIREs Comput. Mol. Sci.* **2** 242
[3] Masin Z *et al* 2020 *Comput. Phys. Comms* **249** 107092
[4] Douguet N *et al* 2012 *Phys. Rev. Lett.* **108** 023202
[5] Graves V *et al* 2021 *J. Chem. Phys.* **154** 114104
[6] Krzysztofowicz A M *et al* 1995 *J. Phys. B* **28** 1593

*E-mail: harin@quantemol.com

Electron attachment induced dehydrogenation of benzaldehyde

J. Ameixa[1,2*], E. Arthur-Baidoo[1], J. Pereira-da-Silva[2], M. Ryszka[3], I. Carmichael[3], L.M. Cornetta[4], M. T. do N. Varella[4], F. Ferreira da Silva[2], S. Ptasińska[3,5] and S. Denifl[1†]

[1]Institut für Ionenphysik und Angewandte Physik, Leopold-Franzens Universität Innsbruck, Technikerstraße 25/3, 6020 Innsbruck, Austria
[2]Centro de Física e Investigação Tecnológica (CEFITEC), Department of Physics, NOVA University of Lisbon, 2829-516 Caparica, Portugal
[3]Radiation Laboratory, University of Notre Dame, Notre Dame, Indiana 46556, USA
[4]Instituto de Física, Universidade de São Paulo, Rua do Matão 1731, 05508-090 São Paulo, Brazil
[5]Department of Physics, University of Notre Dame, Notre Dame, Indiana 46556, USA

Synopsis Dissociative electron attachment to benzaldehyde (C_6H_5CHO) leads to the formation of the dehydrogenated parent anion. Here, we show that the dehydrogenation position, either at the formyl moiety (CHO), or at the phenyl moiety (C_6H_5), depends on the incident electron energy.

Dissociative electron attachment (DEA) plays a key role in the fragmentation of biomolecules including DNA. Low-energy electrons (<15 eV) can be attached by a molecule to produce a temporary negative ion (TNI), which decays either by spontaneous electron emission (autodetachment) or by dissociation into an anionic fragment and neutrals (DEA). [1] Here, we show that the dehydrogenation of benzaldehyde upon DEA is site selective. The study was carried out by means of a crossed molecular-electron beam experiment, quantum chemical calculations and elastic electron scattering calculations using the Schwinger multichannel method implemented with pseudopotentials (SMCPP). [2]

Figure 1 shows that the formation of the dehydrogenated benzaldehyde anion occurs through two core-excited resonances at 7.6 and 9.2 eV as well as through the π_4* shape resonance at 4.6 eV, according to the SMCPP calculations. Since the experimentally determined onset at 3.6 eV lies above the calculated thermodynamic thresholds for H-loss from the different hydrogen positions, we have investigated the dehydrogenation reaction for partially deuterated benzaldehyde-α-d_1 (C_6H_5CDO, d-benzaldehyde). As shown in Figure 1, the two core-excited resonances are common for both compounds, whereas the π_4* shape resonance is quenched in d-benzaldehyde. This occurs because, after the electron is attached, the slower dissociation dynamics promotes autodetachment. In summary, the dehydrogenation from the formyl moiety is thus triggered by electrons having an energy of 4.6 eV, while the higher-lying resonances lead to dehydrogenation from the phenyl moiety.

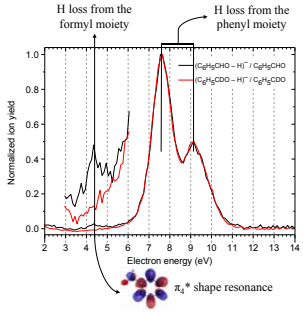

Figure 1. Ion yield for the dehydrogenated parent anion from benzaldehyde (black line) or from d-benzaldehyde (red line) showing that the π_4* shape resonance is suppressed in d-benzaldehyde. The ion yield intensity was normalized with respect to the maxima of the signal at 7.6 eV.

This work was partially supported by the FWF (P30332) and by the Radiation Biology and Biophysics Doctoral Training Programme (RaBBiT, PD/00193/2012); UID/Multi/ 04378/2019 (UCIBIO); UID/FIS/00068/2019 (CEFITEC).

References

[1] J. D. Gorfinkiel and S. Ptasińska, J. Phys. B At. Mol. Opt. Phys. **50**, 182001 (2017).
[2] J. Ameixa *et al.*, Phys. Chem. Chem. Phys. **22**, 8171 (2020).

* E-mail: j.ameixa@campus.fct.unl.pt
† E-mail: Stephan.Denifl@uibk.ac.at

Selective fragmentation in the tirapazamine molecule by low-energy electrons

E Arthur-Baidoo[1*], J Ameixa[1,2], P Ziegler[1], F Ferreira da Silva[2], M Ončák[1] and S Denifl[1†]

[1]Institute for Ion Physics and Applied Physics, University of Innsbruck, Technikerstrasse 25/3, 6020 Innsbruck, Austria.
[2]Atomic and Molecular Collisions Laboratory, Department of Physics, CEFITEC, Universidade NOVA de Lisboa 2829–516 Caparica, Portugal;

Synopsis Tirapazamine (TPZ) was proposed as a radiosensitizer drug for hypoxic tumor cells. Under hypoxia, the bioactive role of the drug is suggested to follow two pathways, the release of hydroxyl radical or the benzotrianzyl radical. Here, we present a detailed study on low-energy (<10 eV) electron attachment to TPZ in the gas phase. We found that TPZ is efficiently decomposed upon the interaction with a low-energy electron, with loss of OH as the most preferred pathway. Based on quantum chemical calculations, we suggest that other pathways are accompanied by roaming of OH.

Radiosensitizers, including tirapazamine (TPZ), are chemical agents administered as part of the cancer treatment to increase the lethal effect of ionizing radiation. Their sensitization capacity may depend on their affinity for electrons and the formation of radicals [1]. Low-energy electrons are known to induce bond cleavages in molecules due to dissociative electron attachment (DEA), which leads to the formation of a fragment anion and neutral(s) [2]. In this contribution we present our recent findings on DEA studies with TPZ [3,4]. Experiments were carried out using a crossed electron-molecular beams setup and were supported by quantum chemical calculations.

As the principal result in this study, we detected the formation of the $(TPZ - OH)^-$ anion, which appeared as the most abundant fragment anion [3], see Figure 1. This finding indicates that the suggested channel of DNA damage in the biological medium via the release of $OH^\bullet$ is highly favored in the gas phase. Although, we were also able to observe the intact parent anion within the detection limit of the apparatus.

The dynamics of the molecular fragmentation is such that the loss of OH destabilizes the initial planar conformation of the molecule. In addition, the quantum chemical calculations showed that the $OH^\bullet$ upon dissociation may stay in the vicinity of the molecule that could lead to further minor channels via a so-called roaming-mechanism [3]. This also lead to the formation of C-N-centered anions via rearrangement and multiple bond cleavages [4]. Interestingly, the fragment anions are associated with the substantial rupture of the triazine ring.

In contrast, the benzene moiety of the molecule is not distorted, and it forms the basic unit for most of the fragment anions with heavier mass. Other minor fragments formed are associated with further bond cleavages and are not directly related to the OH loss [4].

We also investigated theoretically the effect of micro-hydration on the observed pathways. Hypothetically, we suggest that under such conditions, the roaming is restricted and thus the pathways to the minor channels are blocked [3].

The work was supported by the FWF (P30332).

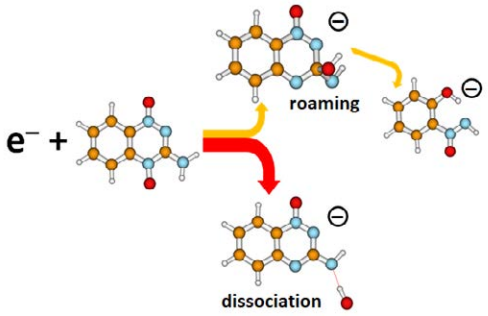

Figure 1. Suggested electron-induced pathways of TPZ upon DEA showing some possible fragments.

References

[1] Wang H *et al* 2018 *Trends. Pharm. Sci.* **39** 24-48
[2] Panajotovic R *et al* 2006 *Phys. Rev. Lett.* **165** 452-459
[3] Arthur-Baidoo E *et al* 2020 *Angew. Chemie Int. Ed.*. **59** 17177-17181
[4] Arthur-Baidoo E *et al* 2021 *Int. J. Mol. Sci.* **22** 3159

* E-mail: eugene.arthur-baidoo@student.uibk.ac.at
† E-mail: Stephan.Denifl@uibk.ac.at

Neutral dissociation of methane by electron impact and a complete and consistent cross section set

D. Bouwman[1]*, A. Martinez[1,2] B. Braams[1] U. Ebert[1,2]

[1]Multiscale Dynamics Group, Centrum Wiskunde & Informatica (CWI), Amsterdam, The Netherlands
[2]Department of Applied Physics, Eindhoven University of Technology, Eindhoven, The Netherlands

Synopsis We present cross sections for neutral dissociation of methane by electron impact. Combined with existing cross sections this gives a complete and consistent set without the need for any data fitting.

We present cross sections for the neutral dissociation of methane, in a large part obtained through analytical approximations. With these cross sections the work of Song *et al.* [1] can be extended which results in a complete and consistent set of cross sections for the collision of electrons with up to 100 eV energy with methane molecules. Notably, the resulting cross section set does not require any data fitting to produce bulk swarm parameters that match with experiments. Therefore consistency can be considered an inherent trait of the set, since swarm calculations (with a Monte-Carlo code) are used exclusively for validation of the cross sections. Neutral dissociation of methane is essential to include (1) because it is a crucial electron energy sink in methane plasma, and (2) because it largely contributes to the production of hydrogen radicals that can be vital for plasma-chemical processes. Finally, we compare the production rates of hydrogen species for a swarm-fitted data set with ours. The two consistent cross section sets predict different production rates, with differences of 45% (at 100 Td) and 125% (at 50 Td) for production of H_2 and a similar trend for production of H. With this comparison we underline that the swarm-fitting procedure, used to ensure consistency of the electron swarm parameters, can possibly deteriorate the accuracy with which chemical production rates are estimated. This is of particular importance for applications with an emphasis on plasma-chemical activation of the gas.

References

[1] M. Song *et al.* J. Phys. Chem. Ref. Data, **44**, 023101, (2015)

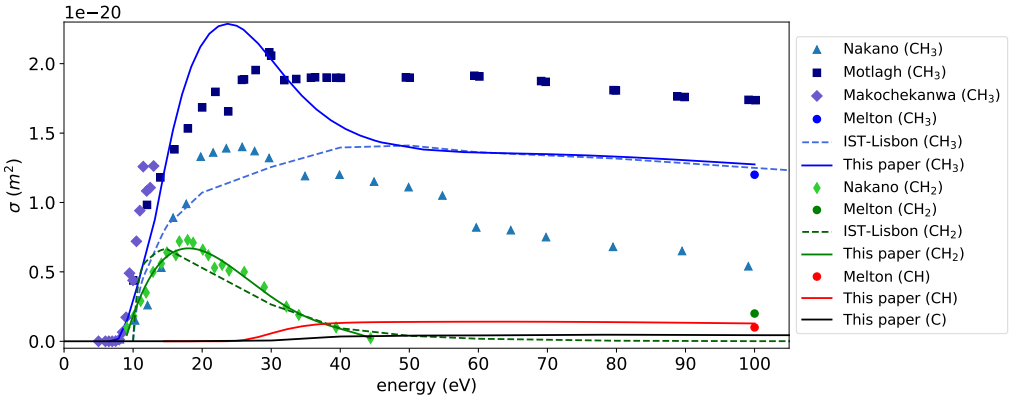

Figure 1: Cross sections for neutral dissociation of methane by electron impact.

*E-mail: Dennis.Bouwman@cwi.nl

Electron-impact dissociation of H_2 and its isotopologues into neutral fragments

D K Boyle[1]*, L H Scarlett[1]†, D V Fursa[1], M C Zammit[2], and I Bray[1]

[1]Curtin Institute for Computation and Department of Physics and Astronomy, Curtin University, Perth, Western Australia 6102, Australia

[2]Theoretical Division, Los Alamos National Laboratory, Los Alamos, New Mexico 87545, USA

Synopsis We present dissociation cross sections for electrons scattering on vibrationally-excited molecular hydrogen and its isotopologues (H_2, HD, HT, D_2, DT, and T_2) considering the contributions from dissociative excitation, excitation-radiative-decay dissociation, and predissociation. The calculations were performed using the molecular convergent close-coupling (MCCC) method considering excitations from all bound vibrational levels of the ground electronic state to singlet and triplet states up to $n = 3$, where n is the atomic limit principle quantum number.

Dissociation of H_2 and its isotopologues due to electron impact is an important process in modelling astrophysical and fusion plasmas. The isotopologues can behave differently due to differences in the reduced mass and therefore the vibrational spectrum of each molecule. Cross sections for the deuterated and triterated isotopologues are required as these species will be present in the fusion reactor ITER. Previous calculations for electron-impact dissociation of the heavier isotopologues of H_2 considered only two species, H_2 and D_2, and considered dissociation via the excitation of the $B\ ^1\Sigma_u^+$ and $C\ ^1\Pi_u$ states as well as the $b\ ^3\Sigma_u^+$ state [1]. There have also been no measurements of the dissociation cross sections for the heavier isotoplogues of H_2, hence the need for accurate theoretical data.

The MCCC method has been used to calculate vibrationally-resolved excitation cross sections from the ground state of H_2 and its isotopologues [2]. Contributions from dissociative excitation (DE), excitation-radiative-decay dissociation (ERDD), and predissociation (PD) are calculated to obtain cross sections for dissociation of each isotopologue into neutral atomic fragments. The total dissociation cross sections for electrons scattering on H_2 starting in the vibrational levels of the electronic ground state $X\ ^1\Sigma_g$ are shown in Figure 1. We present results that extend previous work covering electron impact dissociation of H_2 [3] to include all the isotopologues of H_2. Previously recommended cross sections for low-energy dissociation predicted large isotope effects [4]. These have recently been shown to be unphysical [5]. Here we investigate the dissociation of the isotopologues from 4.5 to 500 eV. We find that dissociation via singlet states is dominated by ERDD processes. The singlet state contribution to the total dissociation cross section becomes larger then the triplet state contribution above 40 eV [3].

*E-mail: daniel.k.boyle@student.curtin.edu.au
†E-mail: liam.scarlett@postgrad.curtin.edu.au

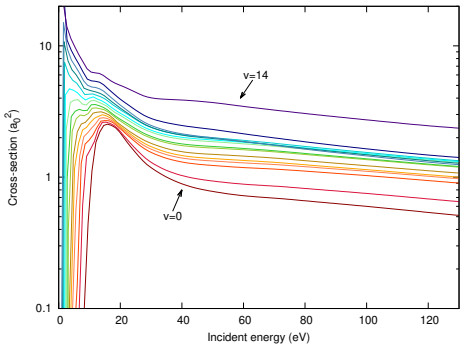

Figure 1. Vibrationally resolved total dissociation cross sections for electron impacting on H_2 in the vibrational level v. Cross sections increase monotonically starting with $v = 0$.

References

[1] Celiberto *et al.* 2002 *Phys. Scr.* **2002** 32
[2] Scarlett *et al.* 2021 *Atom. Data Nucl. Data Tables* **137** 101361
[3] Scarlett *et al.* 2018 *Eur. Phys. J. D.* **72** 34
[4] Trevisan and Tennyson 2002 *Plasma Phys. Control* **44** 1263
[5] Scarlett *et al.* 2021 *Phys. Rev. A* **103** L020801

Processes of excitation of glutamine molecules by electron impact

A I Bulhakova*, N M Erdevdi, O B Shpenik, A N Zavilopulo

Institute of Electron Physics, Nat. Acad. Sci. of Ukraine, 88017, Uzhhorod, Ukraine

Synopsis It is known that amino acids play a very important role in the human body. Therefore, it is extremely relevant to study the effect of various external factors on amino acids, especially such as interaction with slow electrons. During the interaction of electrons with amino acid molecules, a number of competing elementary processes occur, among which the most significant are ionization and excitation, which lead to changes in the structure and energy state of molecules. We have studied the processes of excitation of glutamine, one of the important amino acids.

In the process of ionization, charged particles arise [1], and upon excitation, the spectral bands of molecules and their fragments are emitted. Studyies of fluorescence and excitation of electronic states of molecules enable the efficiency of conversion of internal energy into optical radiation to be determined.

The experiment was performed on an experimental setup, a detailed description of which is given in [2]. The measurements were carried out optically using a vapor-filled cell, in which a required concentration of glutamine vapor was created. The residual gas pressure in the vacuum chamber was $1.3 \cdot 10^{-4}$ Pa. An electron beam of 2 mm in diameter was formed by a 4-electrode gun, with the electron current of ~20 μA, the monoenergeticity of electrons in the beam was not worse than 0,5 eV. The radiation emitted by the diffraction monochromator was detected by a photoelectron multiplier FEU-106, its single-photoelectron pulses were amplified, formed, and fed to the pulse counter.

Figure 1 shows the emission spectra at various energies of the exciting electrons, with a step of 0.814 nm, with $\Delta\lambda$ = 2 nm. Our thorough analysis of the obtained spectra allows us to conclude that at the collision of electrons with glutamine molecules various decay channels are possible. The most probable of them are the detachment of hydrogen atoms or an OH fragment in an excited state with subsequent emission, i. e. the emissions in the range of 280-330 nm belong to the H^* and OH^* atom according to such schemes:

$$C_5H_{10}N_2O_3+e^- \rightarrow C_5H_9N_2O_3+H^*+e^-,$$

$$C_5H_{10}N_2O_3+e^- \rightarrow (C_5H_{10}N_2O_3)^{**}+e^- \rightarrow C_5H_9N_2O_3+OH^*+e^-$$

To elucidate the mechanisms of the glutamine molecule decay at collisions with electrons, we studied the energy dependences of excitation of individual bands and determined their excitation thresholds. Figure 1**a** shows the excitation functions of the hydroxyl group OH the (λ = 316 nm band) and the spectral line (the λ = 292 nm). The excitation thresholds of these emissions are close to each other, but the nature of their excitation differs significantly in the studied energy range: the excitation of the λ = 316 nm band has a pronounced threshold, an increase in intensity followed by a plateau at an energy of 18-20 eV. The excitation of the λ = 292 nm band has a not so pronounced threshold, a small plateau at an energy of 15-22 eV, and an intense growth with increasing electron energy.

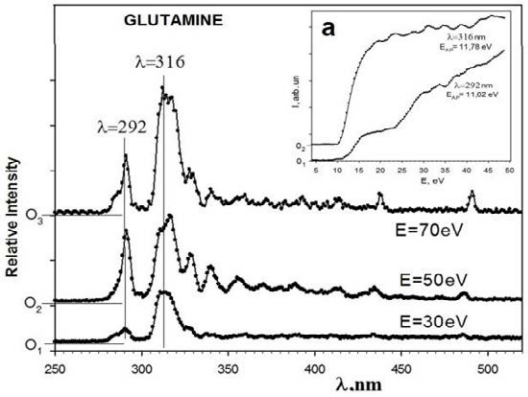

Figure 1. The emission spectra of glutamine at 30, 50 and 70 eV. Insert: excitation functions.

References

[1] Zavilopulo A N *et al* 2019 *Int. J. Mass Spectr.* **441** 1-7

[2] Erdevdi N M *et al* 2013 *Optics and Spectroscopy* **114** 1-6

* E-mail: alla.bulgakova.uzh@gmail.com

Ionization and fragmentation of glutamic acid and glutamine molecules in the gas phase by electron impact

A I Bulhakova[1] *, S Demes[2], A N Zavilopulo[1], E Yu Remeta[1]

[1] Institute of Electron Physics, Nat. Acad. Sci. of Ukraine, Uzhhorod, 88017, Ukraine
[2]Normandie University Le Havre, Le Havre Cedex, 76058, France

Synopsis In this work, we studied the processes of electron ionization of Glu-Acid and Gln molecules in the gas phase by the mass spectrometric method at various temperatures. *Ab initio* calculations of ionization potentials of these molecules and the binding energies of their HOMO orbitals were performed.

In the experiment, a setup with a monopole mass spectrometer was used [1]. The experiment was carried out in two stages: at the first stage mass spectra and temperature dependences were studied (Fig. 1), at the second stage total cross sections for single positive ions of Glu-Acid and Gln yield were studied.

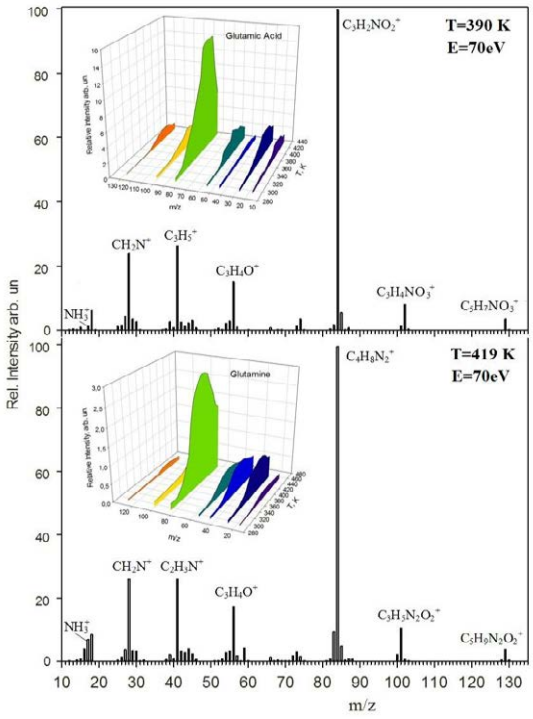

Figure 1. Mass spectra of Glu-Acid, Gln and temperature dependences (inserts).

The temperature dependences for different fragments are similar (Fig. 1): initially the signal intensity increases, followed by saturation at T = 370-410 K and then a rather sharp decline related to the onset of decomposition of the substance under study. The ionization energy was determined from the initial part of the energy dependence of the total cross section for the formation of positive ions.

Table 1 shows the calculation results and the experimental data of ionization energies E_{IE}. Theoretically the ionization potentials I(M) of molecules were calculated in two *ab initio* approximations [2]: adiabatic I(M) = $E_t[M^+]$ - $E_t[M]$ where $E_t[M]$ and $E_t[M^+]$ are the total energies of the parent neutral molecule and its ion, respectively, and in molecular orbital approximation from the binding energy E_b^{HOMO} of the HOMO (highest occupied molecular orbital) of the molecule. It was found that the values calculated in the adiabatic approximation for the Gln molecule are by ~0.08-0.09 eV, and for Glu-Acid by ~0.06 eV are smaller than the experimental data.

Table 1. Energy characteristics

Gln $C_5H_{10}N_2O_3$		**Glu-Acid $C_5H_9NO_4$**	
Energy	D-Gln	Energy	D-Glu-Acid
Adiabatic approximation			
$E_t[M]$, a.o.	-531.848802	$E_t[M]$, a.o.	551.723672
$E_t[M^+]$, a.o.	-531.534418	$E_t[M^+]$, a.o.	551.397838
I(M), eV	**8.555**	I(M), eV	**8.866**
Molecular orbital approximation			
E_b^{HOMO}, a.e.	-0.257323	E_b^{HOMO}, a.e.	-0.269497
I(M), a.e.	0.257323	I(M), a.e.	0.269497
I(M), eV	7.002	I(M), eV	7.333
Experiment			
E_{IE}, eV	**8.64 ±0.25**	E_{IE}, eV	**8.86 ±0.25**

References

[1] Zavilopulo A M *et al* 2019 *Technical Physics Letters* **45** 1252-1257
[2] Demesh Sh Sh *et al* 2015 *Eur. Phys. J. D.* **69** 168-176

* E-mail: alla.bulgakova.uzh@gmail.com

Single ionization of valine amino acid molecule

Sh Demes[1], A Zavilopulo[2], A Bulhakova[2], A Vasiliev[2] * and E Remeta[2]

[1]Institute for Nuclear Research (ATOMKI), 4026, Debrecen, Hungary
[2]Institute of electron physics NAS of Ukraine, Uzhhorod, 88017, Ukraine

Synopsis Calculations of ionization potentials and cross sections of D-, DL-, L-isomers of valine amino acid molecule by electron impact are given. The relative values of the experimental total ionization cross sections are normalized to the theoretical value in the near-threshold region.

The calculations of the cross sections were perfomed with analytical expressions used in known approximations – Binary-Encounter-Bethe (BEB), Gryzinski (Gryz) [1-4].

The energy characteristics of molecular orbitals (MO), binding energies and average kinetic energies of electrons, D-, DL-, and L-forms of the valine molecule $C_5H_{11}NO_2$ (Val, m/z=117) and its Val^+ ion were calculated in the density functional theory (DFT) according GAUSSIAN code [5]. In the adiabatic approximation the ionization potentials were calculated (in eV): D-Val 9.367, DL-Val 9.367, L-Val 9.359. Exprimental value is 8.66±0.22 eV. According to the binding energy of HOMO-orbital the ionization potentials of the D-, DL-, L-forms valine molecule are equal (in eV): 6.887, 6.888, 6.893.

Using the energy characteristics of 32 MO D- and DL-forms of the molecule the summerized single ionization cross section (SICS) by electron impact, from the thresholds to 200 eV, were calculated. The SICS of both forms of valine are similar on shape and size. Experimental total ionization cross section values, in 5.2-60 eV energy region, are normalized to BEB D-SICS and to DL-SICS at energy 8.8 eV, near the threshold. According to the appropriate formulas (BED, BEB and Gryzinski) it is possible to approximate these absolute values.

The fitting parameters can be used to calculate total ionization cross sections at intermediate and high energies and to calculate the ionization rates of these molecules by electrons.

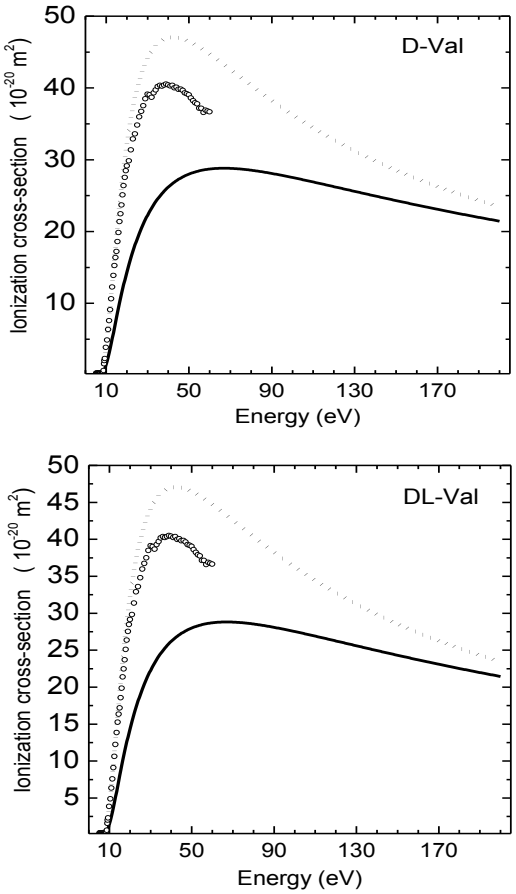

Figure 1. Summerized single ionization cross sections of D- and DL-forms of valine molecules: Experimental values (ooo); BEB-DFT (——); Gryz-DFT (**.....**).

One of the authors (E.R.) is grateful for partial financial support from the NRFU (grant N 2020.01 / 0009 "Effect of ionizing radiation on the amino acid molecules structure'')

References

[1] Yong-Ki K, Rudd M 1994 *Phys. Rev.* A. **50** 3954
[2] Yong-Ki K *et al* 2000 *J. Res. NIST* **105** 285
[3] Tanaka H *et al* 2016 *Rev. Mod. Phys.* **88** 1
[4] Gryziwski M 1965 *Phys. Rev.* **138** A336
[5] Frisch M J *et al* Gaussian 09, Revision E.01. (Gaussian Inc., Wallingford CT. 2009).

* E-mail: nucleargoga@gmail.com

On implementation of PO formalism into R-matrix calculations.

M Čížek*, Z Mašín and J Benda

Charles University, Faculty of Mathematics and Physics, Prague, Czech Republic.

Synopsis We will present the implementation of the projection operator formalism into R-matrix calculations. The basic formulation including the definition of the background scattering R-matrix is explained on examples of shape resonance in potential scattering. Then we show the results of test calculations for diatomic molecules using UK-Rmatrix codes.

Projection-operator formalism of Feshbach has been successfully used as diabatization procedure to remove resonances from the scattering continuum and parametrize the fixed-nuclei electron-molecule scattering for subsequent calculation of vibrational excitation and dissociative attachment processes [1]. The formalism has been implemented explicitly only for H_2 molecule in [2] and since then it is used only as a concept for fitting resonance and virtual state parameters from scattering data.

Here I will discuss the simple formula to recover energy-dependent resonance width and level-shift from R-matrix calculations. I then introduce the formula for the background scattering R-matrix and for explicit construction of the discrete-state continuum coupling. The formulation is then demonstrated on potential scattering example featuring shape resonance (Fig. 1).

Finally we show the implementation of the approach into UK R-matrix codes [3] for diatomic molecules studied previously by other methods.

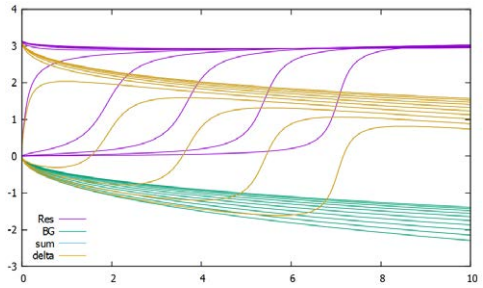

Figure 1. Resonance-background separation of scattering phase-shifts for a shape resonance.

Acknowledgements: The work was supported by grant agency of Czech republic GACR19-20524S.

References

[1] Domcke W 1991 *Phys. Rep.* **208** 97
[2] Berman M *et al* 1985 *Phys. Rev. A* **31** 641
[3] Mašín Z *et al* 2020 *Comput. Phys. Comm.* **249** 107092

*E-mail: Martin.Cizek@mff.cuni.cz

Low-energy electron collisions with cubane

T C Freitas[1]*, G M Moreira[1], A S Barbosa[1] and M H F Bettega[1]

[1]Universidade Federal do Paraná, Curitiba, PO Box 19044, 81531-980, Brazil

Synopsis Calculations of low-energy electron collisions with cubane were performed using the Schwinger multichannel method with pseudopotentials in order to obtain elastic cross sections.

The cubane molecule (C_8H_8) is a high symmetry hydrocarbon with a cubic structure with some remarkable properties associated with its filled and empty electronic levels. The first vertical ionization energy is lower than related alkanes, the molecule is also prone to interact with external charges, among other characteristics related to the electron-donor properties.

Besides, the cubic cage structure enhances some electron-acceptor behaviour. The described properties make the C_8H_8 molecule a very interesting system to be a target in an electron-molecule interactions studies.

Electron transmission spectrum experiment showed three resonances at 2.93, 6.44 and 10.4 eV [1]. Calculated cross sections using the model potential [2] displayed two strong resonances at 8 and 14 eV together with high energy structures, and the evidence of a Ramsauer-Townsend minimum. In this conference, we will present our results for elastic electron collisions with cubane molecules.

We have employed the Schwinger multichannel method [3] with pseudopotentials [4] to compute the integral, differential and momentum transfer cross sections. In particular, we want to investigate the very low-energy features of the cross section, like the Ramsauer-Townsend minimum and an eventual virtual state.

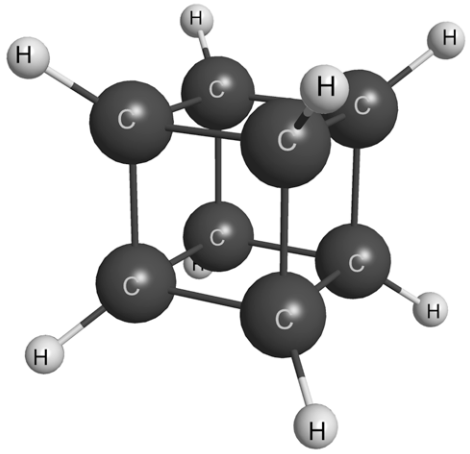

Figure 1. Geometrical structure of cubane.

References

[1] Modelli A and Martin H-D 2004 *J. Electron Spectrosc. Relat. Phenom.* **134**, 191
[2] Gianturco F A *et al* 2004 *J. Chem. Phys.* **120**, 4172
[3] Takatsuka K and McKoy V 1984 *Phys. Rev. A* **30**, 1734
[4] Bettega M H F *et al* (1993) *Phys. Rev. A* **47**, 1111

*E-mail: tcf@ufpr.br

Elastic scattering of low-energy electrons by borazine

E B da Silva[1]*, L V S Dalagnol[1] and M H F Bettega[1]†

[1]Departamento de Física, Universidade Federal do Paraná, Curitiba, 81531-980, Brazil

Synopsis We used the Schwinger multichannel method with pseudopotencials to study elastic scattering of low-energy electrons by borazine in the static-exchange and static-exchange plus polarization approximations.

In this work we present the study of the elastic scattering of low-energy electrons by borazine ($B_3H_6N_3$). This molecule is a heterocyclic inorganic compound, called "inorganic benzene", due to its similarity with benzene. Furthermore, borazine is of technological relevance, being used as a processing plasma. It is well known that electron-molecule collision cross sections are important in the description and understanding of chemical processes that occur in cold plasmas [1].

Our goal in the present study is to obtain the shape resonance spectra of borazine through electron-molecule collisions calculations. For the elastic scattering calculations we employed the Schwinger multichannel method [2, 3] implemented with norm-conserving pseudopotentials of Bachelet, Hamann and Schlüter [4, 5]. The calculations were carried out in the static-exchange (SE) and static-exchange plus polarization (SEP) approximations. We present integral, differential and momentum transfer cross sections for energies up to 30 eV. Along with the integral cross section, we present its symmetry decomposition according to the C_{2v} group, in order to characterize the structures that appear in the integral cross section below 10 eV.

In Figure 1 we present the elastic integral cross section for electron scattering by borazine in the SE approximation for energies up to 30 eV. Although the SE approximation overestimated the position of the shape resonances, it is useful to predict these resonances. There are two pronounced structures in the cross section at around 5 and 13 eV.

Besides the scattering calculations, electronic structure calculations were also performed using GAMESS (The General Atomic and Molecular Electronic Structure System) [6] in order to estimate the position of the resonances using an empirical scaling relation [7].

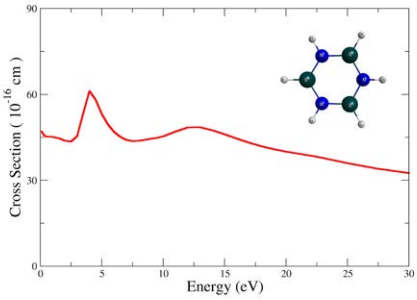

Figure 1. Elastic integral cross section for borazine.

References

[1] McKoy V *et al* 1998 *J. Vac. Sci. Technol. A* **16** 324
[2] Takatsuka K and McKoy V 1981 *Phys. Rev. A* **24** 2473
[3] Takatsuka K and McKoy V 1984 *Phys. Rev. A* **30** 1734
[4] Bachelet G *et al* 1982 *Phys. Rev. B* **26** 4199
[5] Bettega M H F *et al* 1993 *Phys. Rev. A* **47** 111
[6] Schmidt M W *et al* 1993 *J. Comput. Chem.* **14** 1347
[7] Staley S W and Strnad J T 1994 *J. Phys. Chem.* **98** 116

*E-mail: bandeira@fisica.ufpr.br
†E-mail: bettega@fisica.ufpr.br

Shape-Resonance Spectra of 1,4–$C_6H_4X_2$ (X = F, Cl, Br, I)

L V S Dalagnol*, G M Moreira and M H F Bettega†

Departamento de Física, Universidade Federal do Paraná, Curitiba, 81531-980, Brazil

Synopsis We used the Schwinger multichannel method implemented with norm-conserving pseudopotentials to obtain elastic cross sections for scattering of low-energy electrons by 1,4–$C_6H_4X_2$ (X = F, Cl, Br, I). Our main focus is on the shape resonance spectra of the para-dihalobenzenes.

In this work we present the study of the shape resonance spectra of the para-dihalobenzenes 1,4–dfluorobenzene (1,4–$C_6H_4F_2$), 1,4–dichlorobenzene (1,4–$C_6H_4Cl_2$), 1,4–dibromobenzene (1,4–$C_6H_4Br_2$) and 1,4–diiodobenzene (1,4–$C_6H_4I_2$). These are molecules are interesting since they are a dopant worn to ionize the soluble organic species present in mineral coal, and is also used in Nuclear Magnetic Resonance (NMR); a carcinogenic pesticide; an intermediate dyestuff used for organic synthesizing; and a precursor used in the preparation of martinellic acid and 1,4-bis(p-R-phenylethynyl)benzenes, and in the surface-mediated synthesis of epitaxially aligned and separated polyphenylene lines on Cu(110) via Ullmann dehalogenation reaction, respectively. These dihalobenzenes are obtained by the effect of double halogenation of the benzene (C_6H_6) molecule when the positions of the hydrogen one and four are replaced by halogen atoms. The aim of this work is to obtain, through electron-molecule scattering calculations, the shape resonances (temporary attachment of the incident electron, forming a temporary negative ion) for these molecules. The cross section calculations were performed with the Schwinger multichannel method (SMC) [1, 2] implemented with norm-conserving pseudopotentials [3, 4]. We also carried out auxiliary electronic structure calculations using the GAMESS (The General Atomic and Molecular Electronic Structure System) [5] package in order to estimate the position of the resonances using an empirical scaling relation [6, 7]. For this electronic structure calculations, the basis set 6-31G(1d) was employed with Møller–Plesset second-order perturbation theory to optimize the ground state geometries and the total energy calculations were performed at the Hartree-Fock level. Unfortunately, the basis set 6-31G(1d) is not available for iodine atoms, and therefore the basis set 3-21G(1d) was employed for 1,4–diiodobenzene. For all molecules, the orbitals responsible for the resonances are presented. Our calculated cross sections are compared with experimental data available in Ref. [8].

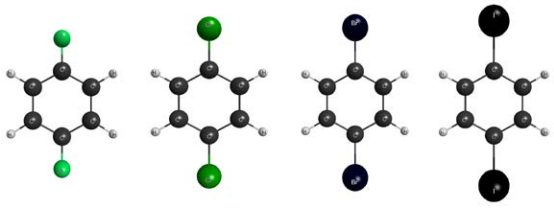

Figure 1. Geometrical structures of 1,4–dihalobenzene molecules (obtained using the MacMolPlt [9]).

Figure (1) shows a representation of the geometric structure of the target molecules investigated in this work.

References

[1] Takatsuka K and McKoy V 1981 *Phys. Rev. A* **24** 2473
[2] Takatsuka K and McKoy V 1984 *Phys. Rev. A* **30** 1734
[3] Bachelet G *et al* 1982 *Phys. Rev. B* **26** 4199
[4] Bettega M H F *et al* 1993 *Phys. Rev. A* **47** 111
[5] Schmidt M W *et al* 1993 *J. Comput. Chem.* **14** 1347
[6] Staley S W and Strnad J T 1994 *J. Phys. Chem.* **98(1)** 116
[7] Aflatooni K *et al* 2000 *J. Phys. Chem. A* **104** 7359
[8] Olthoff J K *et al* 1985 *J. Chem. Phys.* **83** 5627
[9] Bode B M *et al* 1998 *J. Mol. Graph. Model.* **16(3)** 133

*E-mail: lvsd15@fisica.ufpr.br
†E-mail: bettega@fisica.ufpr.br

Multidimensional vibrational dynamics of $e^- + CO_2$ collisions within the nonlocal approach

J Dvořák*, **K Houfek and M Čížek**

Charles University, Faculty of Mathematics and Physics, Institute of Theoretical Physics, V Holešovičkách 2, Prague, 180 00, Czech Republic

Synopsis We present our calculation of vibrational dynamics of $e^- + CO_2$ collisions within the nonlocal model that includes all vibrational modes, three electronic states of CO_2^- and coupling to electron s and p partial waves. We discuss our preliminary results, specifically the two-dimensional electron energy-loss spectrum.

The $e^- + CO_2$ system has been attracting scientific attention for a long time, but there are still questions that need to be answered. We present the first nonlocal calculation of the full vibrational dynamics of $e^- + CO_2$ collisions. We generalized the vibronic coupling model of Estrada *et al* [1] to include the $^2\Pi_u$ shape resonance and the $^2\Sigma_g^+$ virtual state of CO_2^- in combination with all vibrational modes - symmetric stretching, asymmetric stretching and bending.

The degeneracy of the $^2\Pi_u$ resonance is lifted upon bending due to the Renner-Teller effect and one of the components interacts with the $^2\Sigma_g^+$ state [2, 3]. The $^2\Pi_u$ and $^2\Sigma_g^+$ states are represented by diabatic potential energy surfaces that interact directly with each other and also with s and p partial-wave components of electronic continuum. As a result, final vibrational states of CO_2 with Σ_g^+, Σ_u^+, Π_g, Π_u, and Δ_g symmetries can be excited.

Utilizing the molecular symmetry, we expanded elements of the effective Hamiltonian around the equilibrium linear geometry into low-order polynomials in normal vibrational coordinates. The symmetry considerations were essential for obtaining values of the model parameters from ab-initio fixed-nuclei R-matrix calculations. In order for the numerical solution of the dynamics to be feasible, we considered only harmonic vibrations of the neutral molecule. However, the representation of the molecular anion goes beyond the harmonic approximation. Iterative matrix methods based on Krylov subspaces were used to solve the Schrödinger equation.

We will discuss our preliminary results, particularly the two-dimensional electron energy-loss spectrum, see Figure 1. Because of the harmonic approximation and some other simplifications, we primarily aim to describe qualitative features of the multidimensional dynamics. We will also compare our predictions with experimental results that have been originally measured by Currell and Comer [4] and recently with a good resolution by Fedor *et al* (to be published).

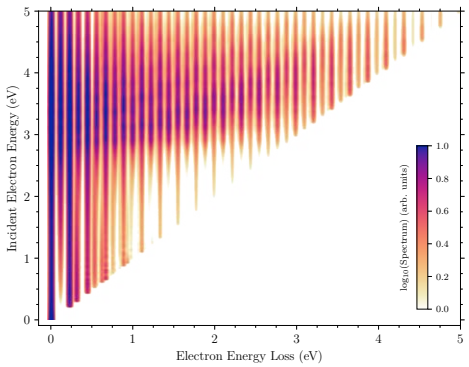

Figure 1. The 2D electron energy-loss spectrum of CO_2 calculated as integral cross sections.

Our model does not include the Fermi resonance but we can appropriately mix the harmonic T-matrices to partially incorporate this effect (not shown in Figure 1). Thus, we can predict excitations of individual members of Fermi polyads.

References

[1] Estrada H *et al* 1986 *J. Chem. Phys.* **84** 152
[2] Sommerfeld T *et al* 2004 *Phys. Chem. Chem. Phys.* **6** 42
[3] Köppel H *et al* 1981 *J. Chem. Phys.* **74** 2945
[4] Currell F and Comer J 1995 *Phys. Rev. Lett.* **74** 1319

*E-mail: jan.dvorak@utf.mff.cuni.cz

Electron energy deposition in molecular hydrogen : a monte-carlo simulation using convergent close coupling cross sections

R K Horton*, D V Fursa†, L H Scarlett, I Bray

Curtin Institute for Computation and Department of Physics and Astronomy, Curtin University, Perth, Western Australia 6102, Australia

Synopsis A Monte-Carlo simulation of electron energy deposition in a gas of molecular hydrogen at STP was conducted with the aim of reproducing standard energy deposition parameters such as the mean energy per ion pair (w). Molecular convergent close coupling (MCCC) cross sections were used as input. The simulation produced agreement with previous calculations and excellent agreement with experiment.

The calculation of parameters characterising the energy deposition of charged particles incident on matter has long been the focus of several different fields, including radiation dosimetry and astrophysics. The damage caused by the incident particle is usually analysed in two different regions of incident energy. A 'high energy' region above the ionisation potential of the target, and a low energy region below it.

Quantities characterising the damage caused in the high energy region include the mean energy per ion pair (w) and mean penetration distance. Energy apportionment techniques [1] and Monte-Carlo simulations have long been used in calculations of these quantities.

The low energy region is the so called 'nanodosimetry' range, which is instead characterised by the number of induced processes such as molecular dissociation. Monte-Carlo simulations are currently the primary method of analysing this region [2].

It is often stressed that the accuracy of scattering cross sections for various processes greatly affects the results of calculations of these quantities. Nevertheless, even for simple systems such as e-H_2 scattering accurate sets of cross sections are often unavailable.

Due to the recent development of the molecular convergent close-coupling method (MCCC), such a data set has become available for e-H_2 scattering [3]. This data set has been used in a Monte-Carlo simulation of electron energy deposition in a gas of H_2.

Excellent agreement with experiment was found. A high energy value of $w = 36.3$ eV was found, in agreement with the accepted value of 36.5 ± 0.3 eV [6]. The code was also benchmarked using the well-know data set compiled by Miles, Thompson and Green [4] by comparing to a previous simulation that made use of their data [1].

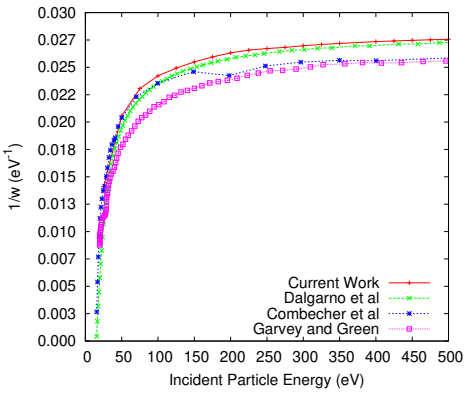

Figure 1. Calculated values of $\frac{1}{w}$. The current work is compared to the simulation of Dalgarno [6], experimental results of Combecher [5] and the simulation of Garvey [1].

References

[1] Garvey R *et al* 1976 *Phys Rev A* 10.1103/PhysRevA.14.946
[2] Solov'yov A 2017 Springer 10.1007/978-3-319-43030-0
[3] Scarlett L *et al* 2020 *Eur. Phys. J. D* 10.1140/epjd/e2020-100549-0
[4] Miles W *et al* 1972 *Journal of Applied Physics* 10.1063/1.1661176
[5] Combecher D 1980 *Radiation Research* 10.2307/3575293
[6] Dalgarno A 1999 *ApJS* 10.1086/313267

*E-mail: reese.horton@student.curtin.edu.au
†E-mail: D.Fursa@curtin.edu.au

Applications and developments of the Schwinger multichannel method to electron-molecule collisions

A G Falkowski[1], M B Kiataki[2], L S Maioli[3], M T N Varella[2], M H F Bettega[3], M A P Lima[1] and F Kossoski[4]*

[1] Instituto de Física "Gleb Wataghin", Universidade Estadual de Campinas, Campinas, 13083-859 ,Brazil
[2] Instituto de Física, Universidade de São Paulo, Rua do Matão 1731, São Paulo, 05508-090 , Brazil
[3] Departamento de Física, Universidade Federal do Paraná, Caixa Postal 19044, Curitiba, 81531-990, Brazil
[4] Laboratoire de Chimie et Physique Quantiques (UMR 5626), Université de Toulouse, CNRS, UPS, France

Synopsis We report on theoretical results for low-energy electron collisions with cyanamide, carbodiimide, CF_3Br, CF_3I, and ethanol. Several open questions are addressed, including the assignments of the shape resonances and the magnitudes of cross sections. We support that the rare tautomer carbodiimide leaves a distinct signature on the previously measured dehydrogenation signal, and we explain why vibrational Feshbach resonances had not been observed. Up to 431 open target states have been considered in the case of ethanol, which allowed us to discuss key aspects of our underlying approximations.

Recent applications of the Schwinger multichannel (SMC) method [1] to low-energy electron-molecule scattering are reported.

The first target molecule is cyanamide, a well-known prebiotic found in the interstellar medium (ISM). Understanding its interaction with free electrons is required for building accurate models for the chemical evolution of the ISM. Available dissociative electron attachment (DEA) measurements [2] showed that dehydrogenation takes place at impact energies of 1.5 eV and around 2.5 eV. Our calculations [3] support that a π^* shape resonance of cyanamide accounts for the latter, while the former arises from the analogous state of the rare tautomer carbodiimide. Despite its smaller population, a more efficient π^*/σ^*_{NH} coupling plays in favor of DEA in the case of carbodiimide. Interestingly, cyanamide does not undergo dehydrogenation via vibrational Feshbach resonances (VFRs), even though it is able to support a dipole-bound state (DBS). We show that the coupling of the DBS with the dissociative σ^*_{NH} resonance does not provide a potential barrier for hydrogen tunnelling, effectively quenching the VFR dissociation mechanism.

Electron-induced reactions also play a central role in plasma-based technologies, and CF_3I has been considered a promising substitute to CF_3Br. Modelling such environments requires accurate electron collision cross sections, yet available results for these two molecules have been contradictory. In addition, different assignments of their shape resonances have been put forward. We have recently contributed to these questions as well [4]. In particular, our assignments of the shape resonances support one out of the two previously proposed interpretations. We also discuss the impact of different sets of orbitals on the computed cross sections and on the convergence of polarization effects.

Above the electronic excitation threshold, accounting for multichannel coupling effects represent a major challenge for theoretical models. Recent calculations for molecules larger than diatomics have considered between 10 and 100 electronic states [5]. Even more recently, we have performed SMC calculations with a record of 431 open target states [6], for electron scattering from both conformers of ethanol (gauche and trans). While the importance of increasing the number of open channels has been established in previous publications, the present results demonstrate other factors that must also be addressed in the future.

*E-mail: fkossoski@irsamc.ups-tlse.fr

References

[1] da Costa R F *et al* 2015 *Eur. J. Phys. D* **69** 159
[2] Tanzer K *et al* 2015 *J. Chem. Phys.* **142** 034301
[3] Maioli L S *et al* 2020 *Phys. Chem. Chem. Phys.* **22** 7894
[4] Kiataki M B *et al* 2020 *J. Phys. Chem. A* **124** 8660
[5] da Costa R F *et al* 2018 *J. Chem. Phys.* **149** 174308
[6] Falkowski A *et al* 2020 *J. Chem. Phys.* **152** 244302

Effect of slicing in velocity map imaging for the study of dissociation dynamics in electron collision with isolated molecules

N Kundu*, D Biswas, A Paul and D Nandi†

Indian Institute of Science Education and Research Kolkata, Mohanpur, 741246, India

Synopsis Here, we report the implementation of solid angle weighted slicing that helps us to overcome the drawback that arises in the conventionally used parallel slicing method mainly due to the inclusion of total Newton spheres having a diameter ≤ time window of the parallel slices. Unlike parallel slicing, the solid angle weighted slicing technique reveals the best representation of the dissociation dynamics, particularly for the ions with low kinetic energy (KE).

A high-resolution image is nothing but well optimization of its positional parameters. Thus, the estimation of phenomenally closest images (degree of accuracy) depends on the techniques one go through. Our previous reports on dissociative electron attachment [1] and dipolar dissociation [2] to carbon monoxide were based on the analysis of data using time-gated unweighted parallel slicing. In the case of fragments that have a reasonable contribution to generate low energetic (≈ 0 eV) ions, this technique seriously exaggerates those contributions than its higher energy counterparts. To compensate for this drawback, we need to make sure that the contribution of ions with the entire momentum range will contribute equally to the extracted KE distributions. To overcome this difficulty, solid angle weighted slicing has been implemented. A linear scale factor is used for extracting the z values from the time of flight data to reconstruct the entire Newton sphere. For parallel slicing, the time window is 50 ns and in the case of solid angle weighted slicing, the solid angle is set up considering 10° azimuth angle in both sides from the initial meridian plane which roughly corresponds to 50 ns time-slicing at its maximum. Nevertheless, the weak contribution from the forward lobe is also preserved in solid angle weighted velocity slice image (VSI). The KE distributions (b_2) resolves the exaggerated nature in the lower KE range, the two most probable peak positions for O^-/CO at 11.5 eV beam energy are distinguishable but not well resolute for 10.5 and 11 eV beam energy due to the insufficient resolution of the electron beam. The KE distributions (b_2) at 10.5, 11 & 11.5 eV incident electron energy also reveal that the intensity of the low energetic peak is comparably small concerning the high energetic one which may inconclusive for parallel slicing. However, we have determined the angular distribution (AD) of O^-/CO for various KE bands of fragmented ions using solid angle weighted slicing which is almost identical as extracted using parallel slicing because the magnitude of anisotropy in AD is independent of linear momentum or KE of the fragments.

*E-mail: nk18rs002@iiserkol.ac.in
†E-mail: dhananjay@iiserkol.ac.in

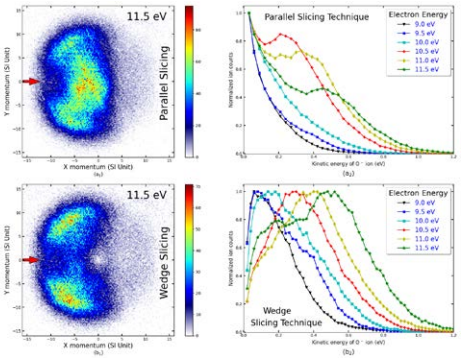

Figure 1. (a_1,b_1) velocity slice images of O^-/CO at 11.5 eV incident electron energy, extracted using parallel slicing and solid angle weighted slicing techniques, respectively, and (a_2,b_2) KE distributions of O^-/CO at various incident electron energies, analysed using parallel slicing and solid angle weighted slicing techniques, respectively.

References

[1] Nag P *et al.* 2015 *Phys. Chem. Chem. Phys.* **17** 7130
[2] Chakraborty D *et al.* 2016 *Phys. Chem. Chem. Phys.* **18** 32973

Dissociative σ^* states in electron-molecule collisions and their interpretation

Zdeněk Mašín[1]*, J. Benda[1], J. D. Gorfinkiel[2] and K. Houfek[1]

[1]Institute of Theoretical Physics, Faculty of Mathematics and Physics, Charles University, V Holešovičkách 2, 180 00 Prague 8, Czech Republic

[2]School of Physical Sciences, The Open University, Walton Hall, MK7 6AA, Milton Keynes, UK

Synopsis Dissociative electron attachment to molecules often involves electronic anion states with σ^* symmetry. In particular the role and existence of wide σ^* resonances has been the topic of active debate in the field for many years. We present an R-matrix approach to localization of all Siegert states in molecules and demonstrate that while in some molecules the σ^* state dissociative pathway includes a feature resembling a wide resonance it does not in fact correspond to a physical resonant state. Instead, depending on the molecule, it originates in a dipole-bound or virtual state.

Ab initio scattering calculations generate elastic and inelastic cross sections of complicated shapes which typically include peaks and dips which may not be straightforward to interpret. Those features are often caused by Siegert states (poles of the S-matrix): resonant, virtual and near-threshold bound states. Knowledge of the positions and properties of the Siegert states provides a clear physical interpretation of the computed results.

In this contribution we describe an R-matrix approach enabling localization of all Siegert states for a multi-electron target molecule. Siegert states are exponentially increasing in the lower-half complex momentum plane which makes them difficult to handle using standard numerical methods. This problem is avoided in the R-matrix approach [1] which uses a division of space and treats the asymptotic part of the wavefunction as a one-electron problem for which analytical methods can be used [2].

We have applied our method to analysis of calculations of low-energy electron collisions with molecules of increasing complexity: N_2, HNCO, HCOOH and the ring molecule pyrrole. All S-matrix poles are traced as a function of molecular geometry. We show how the permanent dipole moment influences the trajectories of S-matrix poles in different molecules [3]. For the first time we are able to correlate the presence of Siegert states with features in scattering cross sections computed on the real energy axis, see Figure 1. We show that the broad feature in the elastic cross section for pyrrole (around 8 eV) is surprisingly caused by the formation of two broad resonances.

Finally, we show that neither pyrrole nor HCOOH possess a broad σ^* resonance which has been assumed in some previous works to form in strongly dipolar systems and used to explain the dissociative electron attachment process. Instead, we show how the resonant-like effect ascribed to it arises as a consequence of formation of a virtual or dipole-bound state, depending on the strength of the permanent dipole moment.

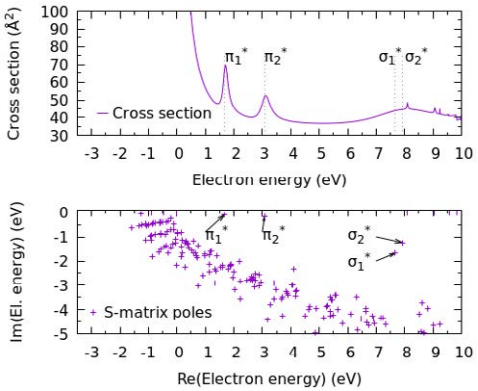

Figure 1. Electron scattering cross section and S-matrix poles for pyrrole for a bent geometry.

References

[1] Z. Mašín et al., Comp. Phys. Comm. **249**, (2020), 107092

[2] Morgan, L. A. and Burke, P. G., J. Phys. B. **21**, (1988), 2091–2105

[3] Estrada, H. and Domcke, W., J. Phys. B. **17**, (1984), 279–297

*E-mail: zdenek.masin@utf.mff.cuni.cz

Calculation of the single differential cross section for electron-impact ionization of atoms and molecules

N A Mori[1]*, R Utamuratov[1], D V Fursa[1], M C Zammit[2] and I Bray[1]

[1]Curtin Institute for Computation, Curtin University, Perth, Western Australia 6102, Australia
[2]Los Alamos National Laboratory, Los Alamos, New Mexico 87545, USA

Synopsis A technique has been developed which calculates the electron-impact ionization single differential cross section from the integrated cross sections of positive-energy pseudostates found via the close-coupling method. This method was tested against existing theoretical and experimental benchmarks for atomic hydrogen and helium. This technique was then applied to molecular hydrogen.

The ionization of atoms and molecules by electron-impact is of both fundamental and practical interest within scientific research. The final energy distribution of the electrons, as measured by the single differential cross section (SDCS), is one important aspect of this reaction. In particular the SDCS is essential for astronomical, plasma and radiation research.

In this report we present a numerical method of calculating the SDCS that is applicable to pseudostate close-coupling techniques, and is far less computationally expensive than previous techniques (based on close-coupling approaches). The ability to obtain true target continuum functions is typically a requirement of close-coupling based approaches, such as the collisional close-coupling (CCC) method, to calculate differential ionization. However, with this newly developed technique we shall show that the SDCS may be accurately obtained without the knowledge of true target continuum functions. As a result this technique can be applied to all targets for which a close-coupling approach has been implemented for electron-impact excitation to positive-energy pseudostates.

There exists benchmark data for testing any new approach to calculating the SDCS. Substantial experimental and theoretical research has been undertaken into the ionization of atomic hydrogen and helium by electron impact. Due to the computational costs and complexities involved in the modelling of molecular ionization collisions molecular targets have been studied mostly experimentally.

We have utilized the CCC method to demonstrate that this approach is as valid for molecular targets such as H_2, as it is for H and He targets. As an example, figure 1 shows a SDCS result calculated with this method for an incident electron with energy of 100 eV on H_2, with comparisons to existing theory and experiment.

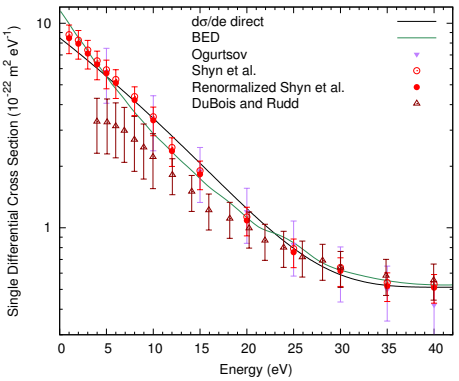

Figure 1. CCC-calculated SDCS for 100 eV electrons incident upon H2 presented alongside the BED model of Kim and Rudd [1] and the experimental results of Shyn et al [2], Ogurtsov [3] and DuBois and Rudd [4].

References

[1] Kim Y-K and Rudd M E 1994 *Phys Rev. A.* **50** 3954
[2] Shyn T W *et al* 1981 *Phys Rev. A.* **24** 79
[3] Ogurtsov G N 1998 *J. Phys. B: At. Mol. Opt. Phys.* **31** 1805
[4] DuBois R D and Rudd M E 1978 *Phys Rev. A.* **17** 843

*E-mail: nicolas.mori@postgrad.curtin.edu.au

Cross sections measurements and calculations for low energy electron scattering from titanium tetrachloride

N Tańska[1 *], S Stefanowska-Tur[1], Cz Szmytkowski[1], E Ptasińska-Denga[1] and P Możejko[1†]

[1]Institute of Physics and Applied Computer Science, Gdańsk University of Technology, Gdańsk, 80-233, Poland

Synopsis Total cross section for electron scattering from $TiCl_4$ molecules have been measured for collisional energies from 0.5 to 300 eV. Integral eleastic cross section have been also calculated using R-matrix method.

Accurate experimental data concerning electron interactions with molecules in the gas phase are very important for understanding and modelling many technological processes including focused electron beam deposition (FEBID) method. In our latest experiments we have measured absolute total cross sections for low- and intermediate-energy electron scattering from basic precursors of tin, silicon and germanium nanostructures i.e. $SnCl_4$ [1], $Si(CH_3)_4$ [2], and $Ge(CH_3)_4$ [2]. Titanium tetrachloride ($TiCl_4$) is one of the simplest molecular compound which can be used as a precursor of titanium nanostructures produced in FEBID. For this reason we have measured absolute *grand*-total cross section (TCS) for electron scattering from titanium tetrachloride at electron-impact energies extending from 0.5 to 300 eV.

Measurements have been carried out with the electrostatic 127° electron spectrometer [3] working in the linear transmission mode. The TCS $\sigma(E)$ at given electron impact energy E has been obtained according to the attenuation formula:

$$I_n(E)=I_0(E)\exp[-nL\sigma(E)].$$

Here, $I_n(E)$ and $I_0(E)$ are the measured intensities of the electron beam passing the distance L through the reaction volume in the presence and absence of the target vapour, respectively; n is the number density of the target molecule in scattering cell. Preliminary TCS for electron scattering from $TiCl_4$ molecule for electron energies ranging between 0.5 and 7 eV is shown in figure 1.

Integral elastic cross section (ECS) of low-energy electron scattering from $TiCl_4$ was calculated with the R-matrix method implemented in the UKRmol+ suite [4]. The results of calculations within the static-exchange (SE) and static-exchange-polarization (SEP) approximation in 6-31G* basis, with 49 virtual orbitals and R-matrix radius a=18a_0 are depicted in figure 1. A quadruple precision was applied. With the parameters used, no resonance structures below 7 eV were detected. It is evident from figure 1 that ECS obtained within SEP approximation (not like SE) quite well reflects energy dependence of the measured TCS.

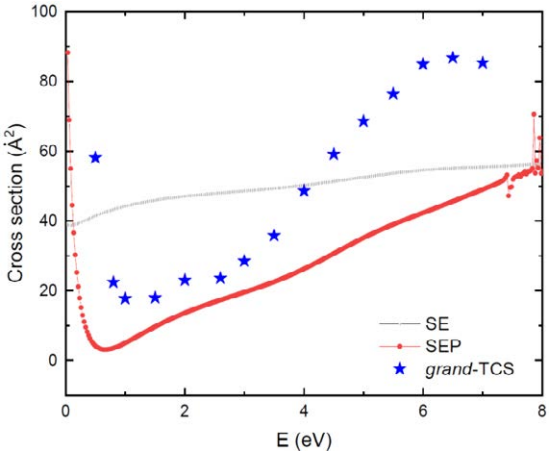

Figure 1. Comparision of experimental *grand*-TCS with computed ECS for electron scattering from $TiCl_4$.

Calculations were carried out at the Centre of Informatics Tricity Academic Supercomputer & Network (TASK).

References

[1] Możejko P *et al* 2019 *J. Phys.Chem.* **151** 064305
[2] Stefanowska-Tur S *et al* 2019 *J. Phys.Chem.* **150** 094303
[3] Szmytkowski Cz *et al* 2001 *Vacuum* **63** 549
[4] Mašín Z *et al* 2020 *Comput. Phys. Comm.* **249** 107092

* E-mail: natalia.tanska@pg.edu.pl
† E-mail: paw@pg.edu.pl

Total cross section calculations for electron-impact ionization of germanium tetrafluoride, GeF_4, and germanium tetrachloride, $GeCl_4$, molecules

P Możejko[1*]

[1]Institute of Physics and Applied Computer Science, Gdańsk University of Technology, Gdańsk, 80-233, Poland

Synopsis Total cross sections for single electron-impact ionization of GeF4 and GeCl4 molecules have been calculated for energies from the ionization threshold up to 1 keV.

New accurate experimental data on electron interactions with matter, including collisional cross sections are still crucial and desired for understanding a wide variety of natural and technological processes occurring and carried on in complex environments [1]. In this contribution cross sections calculations for electron-impact ionization (ICS) of two tetrahedral molecular targets i.e. germanium tetrafluoride, GeF_4, and germanium tetrachloride, $GeCl_4$, in a wide collisional energy range spanned between the ionization threshold and 1 keV, are reported.

Calculations have been performed using the binary-encounter-Bethe method (BEB) [2]. Within this formalism the electron-impact ionization cross section of a given molecular orbital can be calculated due to the following formula:

$$\sigma^{BEB} = \frac{S}{t+u+1}\left[\frac{\ln t}{2}\left(1-\frac{1}{t^2}\right)+1-\frac{1}{t}-\frac{\ln t}{t+1}\right],$$

where $u=U/B$, $t=T/B$, $S=4\,\pi a_0^2 N R^2/B^2$, $a_0=0.5292$ Å, $R=13.61$ eV, and T is the energy of the impinging electron. The total cross section for electron-impact ionization can be obtained as a sum of ionization cross sections calculated for all molecular orbitals:

$$\sigma^{ION} = \sum_i^{n_{MO}} \sigma_i^{BEB},$$

where n_{MO} is the number of the given molecular orbital. The electron binding energy, B, kinetic energy of the given orbital, U, and orbital occupation number, N, have been calculated for the ground state of the geometrically optimized molecules with the Hartree-Fock method using quantum chemistry computer code GAUSSIAN. To include the effect of electron correlations within molecule, we have performed also outer valence Green function (OVGF) calculations of ionization potentials using the GAUSSIAN code [3].

Figure 1 shows calculated electron-impact ionization cross sections for GeF_4 and $GeCl_4$ molecules for energies ranging from the ionization threshold up to 1 keV.

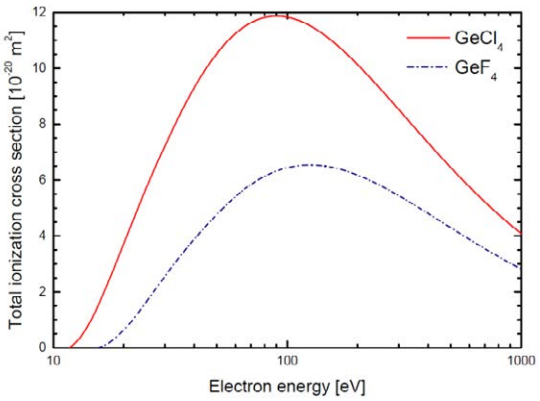

Figure 1. Comparison of calculated total ionization cross sections for GeF_4 and $GeCl_4$ molecules.

It is worth to notice that the BEB method usually provides ionization cross sections which are in quite good agreement (within ±15%) with experimental data see e.g. [4].

Calculations were carried out at the Centre of Informatics Tricity Academic Supercomputer & Network (TASK).

References

[1] Szmytkowski Cz *et al* 2020 *Eur. J. Phys. D* **74** 90
[2] Kim Y-K *et al* 1994 *Phys. Rev. A.* **50** 3954
[3] Zakrzewski VG *et al* 1993 *J. Comp. Chem.* **14** 13
[4] Karwasz GP *et al* 2014 *Int. J. Mass Spectrom.* **365-366** 232

* E-mail: paw@pg.edu.pl

Oxygen excitation induced by electron impact

J Országh[1] *, D Bodewits[2] †, S. J. Bromley[2], B Stachová[1] and Š Matejčík[1]

[1]Comenius University in Bratislava, Mlynská dolina F2, Bratislava, 84248, Slovakia.
[2]Auburn University, Physics Department, Leach Science Center, Auburn, AL, 36832, USA.

Synopsis The optical emission spectrum following electron impact on O_2 was studied in a crossed-beam experiment. The spectrum was measured at 50 eV electron energy within the spectral range of 200-650 nm. Emissions of O_2^+ were detected along with the spectral lines of neutral O I and ionized O II atoms. Energy-dependent emission cross sections of selected transitions were measured within a range of 10-100 eV electron energy.

Electron induced processes are abundant in various environments from space and planetary atmospheres to the laboratory. They can act as remote probe of physical properties of astrophysical environments since every molecule or atom has a unique spectrum which is further affected by ambient conditions.

Analysis of the Rosetta mission data has shown that the emission from the 67P/Churyumov-Gerasimenko comet coma is induced mostly by electron impact if outside the 2 AU pre-perihelion [1]. To assess such its implications and potential diagnostics, it is necessary to understand the electron impact fluorescence of molecules forming coma including the cross sections of the processes. Unfortunately currently available laboratory data are incomplete or insufficient.

Our experiment is based on a crossed-beams method using trochoidal electron monochromator as an electron source and effusive capilary to generate molecular beam at abmient laboratory temperature. The experimental setup was described previously [2].

The emission spectrum (see fig.) was determined at 50 eV electron energy within the spectral range of 200-650 nm and corrected for the apparatus wavelength-dependen(t/d?) sensitivity. The second negative system $O_2^+(A^2\Pi_u - X^2\Pi_g)$, several bands of the first negative system O_2^+ ($b^4\Sigma_g^- - a^4\Pi_u$) and atomic O I and O II lines were identified according to [3]. For selected transitions, the emission cross sections were determined within 10-100 eV electron energy.

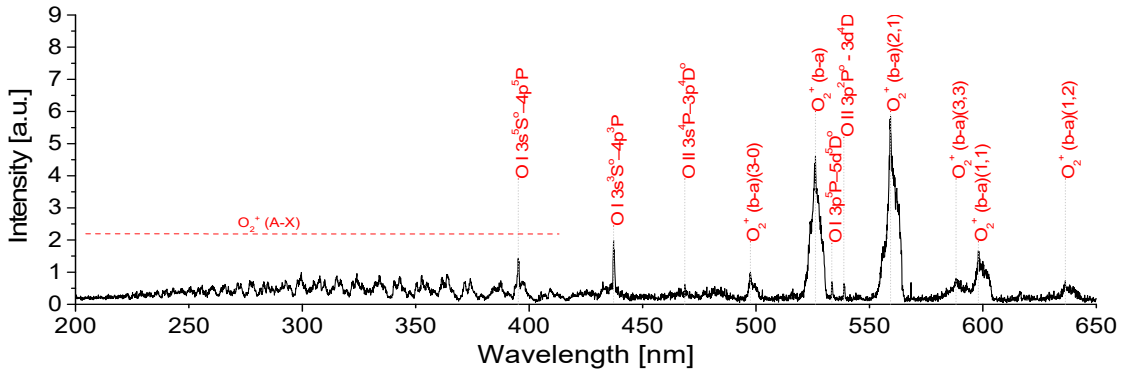

This research was supported by the Slovak Research and Development Agency APVV-19-0386, Grant Agency VEGA project nr. 1/0489/21. Europlanet 2024 RI has received funding from the European Union's Horizon 2020 research and innovation programme under grant agreement No 871149. DB and DJB acknowledge support from the NASA RPAP program.

References

[1] Bodewits D *et al* 2016 *ApJ* **152**, 130.
[2] Bodewits D *et al* 2019 *ApJ* **885**, 167.
[3] Terrel C A *et al* 2004 *J. Phys. B* **37**, 1931.

* E-mail: juraj.orszagh@uniba.sk
† E-mail: dennis@auburn.edu

Investigating resonant low-energy electron attachment to formamide

G Panelli[1]*, A Moradmand[2], B Griffin[1], K Swanson[1], T Weber[3], T N Rescigno [3], C W McCurdy[3,4], D S Slaughter[3], and J B Williams[1]

[1] Department of Physics, University of Nevada, Reno, Nevada 89557, USA
[2] Department of Sciences and Mathematics, California Maritime Academy, Vallejo, California 94590, USA
[3] Chemical Sciences Division, Lawrence Berkeley National Laboratory, Berkeley, California 94720, USA
[4] Department of Chemistry, University of California, Davis, California 95616, USA

Synopsis New experimental results are presented on dissociative electron attachment to gaseous formamide with a momentum imaging technique. Emphasis is given to NH_2^-, O^-, and H^- fragmentation channels. Results for NH_2^- dissociation are accompanied by theoretical predictions.

Formamide ($HCONH_2$) is widely considered an archetypal model molecule for the investigation of protein and peptide chemistry due to its simple yet rich structure which includes an amide bond. Formamide is comprised of many of the progenitors of complex biological molecules such as proteins and nucleic acids and is considered an important link in the evolution of simple biomolecules into complex structures. This feature makes formamide a prototypical molecule for the study of electron-capture-induced peptide bond breaking. Investigation of low-energy electron disruption of peptide bonds is necessary for a more complete understanding of protein stability.

Until recently, experimental investigations of dissociative electron attachment (DEA) to formamide have focused solely on the enrgy dependence of fragment yields. We report experimental results on three-dimensional momentum imaging measurements of anions generated via DEA to gaseous formamide for incident electron energies between 5eV and 12eV [1]. From the momentum images, we analyze the kinetic energy and angular distributions for NH_2^-, O^-, and H^- fragments and discuss the possible electron attachment and dissociation mechanisms for multiple resonances for two ranges of incident electron energies, from 5.3 eV to 6.8 eV, and from 10.0 eV to 11.5 eV. *Ab initio* theoretical results for the angular distributions of the NH_2^- anion for ∼6 eV incident electrons are also provided and, when compared with the experimental results, suggest that the two resonances producing this fragment.

*E-mail: gpanelli@nevada.unr.edu

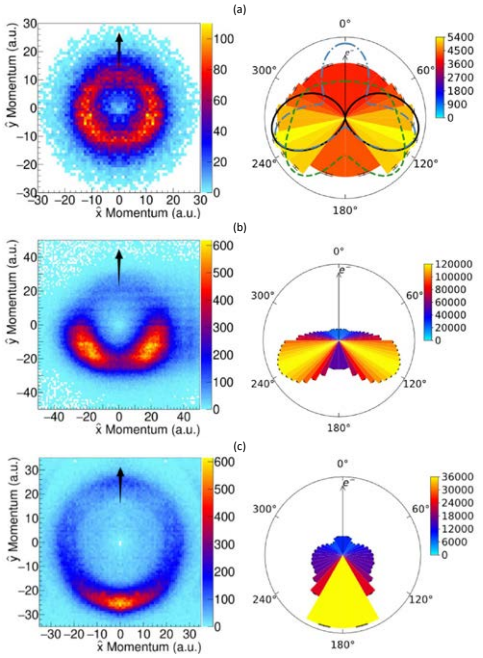

Figure 1. (Left) Momentum image of fragmented anion from DEA process - black arrow represents incident electron direction. (Right) Polar plot of fragment dissociation angle measured from incident electron direction. (a) NH_2^- at incident electron energy 6.3 eV. Includes theoretical angular distributions for Feshbach resonances ^{2}A" (black, solid), ^{2}A' (blue, dot-dashed), and ^{2}A' with 30 deg. rotation (green, dashed) (b) O^- at incident electron energy 10.5 eV. (c) H^- at incident electron energy 10.5 eV.

References

[1] Panelli G *et al* 2021 *Phys. Rev. Research* **3** 013082
[2] Hamann T *et al* 2011 *Phys. Chem. Chem. Phys* **13** 12305

Electron impact ion-pair dissociation dynamics of nitrous oxide

Anirban Paul*, **Narayan Kundu and Dhananjay Nandi**†

[1] Indian Institute of Science Education and Research Kolkata, Mohanpur, 741246, India

Synopsis Molecular ion-pair states have higher energy compared to the neutral ground electronic state, they can be accessed by the impact of electrons of low to intermediate energy. The complete dynamics of electron impact ion-pair dissociation of nitrous oxide have been studied. Using the velocity map imaging (VMI) spectrometer and wedge slicing technique the kinetic energy and the angular distribution of the negative ion fragments produced by the electron impact ion pair dissociation have been measured.

Molecular ion-pair states are unusual compared to normal neutral electronic states of the molecule, they have higher energy compared to the neutral ground electronic state but can be quite strongly bound and dissociation from these states leads to pairs of positive and negative ions. For example, the ion-pair states of O_2 have larger equilibrium internuclear separation than its ground electronic state.The $^3\Sigma_u(O^+, O^-)$ ion-pair state of O_2 is more strongly bound than its ground electronic state, and more strikingly, over a much larger range of internuclear distances [1].

Electron impact ion-pair dissociation is a non-resonant inelastic process [2] in which the incident electron partially transfers its kinetic energy to the molecule to excite the molecule to an ion pair state or to a higher-lying Rydberg state of the molecule and subsequently decays into a positive and a negatively charged fragment. Nitrous oxide N_2O is a linear triatomic molecule, it dissociates into O^- and N_2^+ fragments.

$e^-(\epsilon) + N_2O \rightarrow e^-(\epsilon - E) + N_2O^*$

$N_2O^* \rightarrow O^- + N_2^+$

We obtained the ion yield curve of O^- ions and found that the threshold for this process is 17.2 eV. We have taken the velocity map imaging (VMI) data of only O^- ions at five different incident electron energies 19.4, 23.4, 27.4, 31.4, and 35.4 eV. The VMI data contains all information of the newton sphere of the O^- ions and by using the wedge slicing method the kinetic energy and the angular distribution have been measured. The kinetic energy distribution of the O^- ions showing a broad peak with a long tail at around 0.5 eV and the peak position almost remains the same with the increase in the incident electron energy. Since N_2O is a triatomic molecule, and it dissociates into O^- and N_2^+ fragments, the N_2^+ fragments may be formed in the higher vibrationally excited state and thus the kinetic energy distribution curve has that kind of shape.

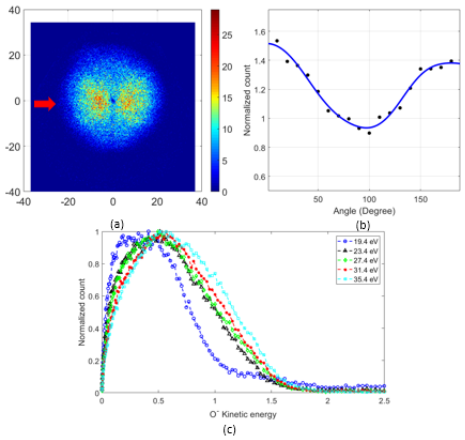

Figure 1. (a) Wedge sliced image of ions, (b) Angular distribution of the ions and (c) Kinetic energy distribution of the fragment ions at different incident electron energies.

We have fitted the angular distribution with the formula given by Van Brunt [3] and found that the best fit is for $\Sigma \rightarrow \Sigma + \Pi$ transition, and thus concluded that the ion-pair states of symmetry Σ and Π are involved for the dissociation process.

References

[1] D H Parker *et al* 2009 *J. Chem.Phys.* **129** 214306
[2] E Szymańska *et al* 2014 *Int. J. Mass.Spectrom.* **365-366** 356
[3] R. J. Van Brunt 1974 J. Chem. Phys. **60** 3064

*E-mail: ap18rs006@iiserkol.ac.in
†E-mail: dhananjay@iiserkol.ac.in

Frustrated ionization in strongly driven triatomic molecules.

M B Peters[1]*, G P Katsoulis[1] V P Majety[2] R Sarkar[1] and A Emmanouilidou[1]†

[1]Department of Physics and Astronomy, University College London, Gower Street, London WC1E 6BT, United Kingdom

[2]2Department of Physics and Center for Atomic, Molecular and Optical Sciences and Technology, Indian Institute of Technology Tirupati, Tirupati 517506, India

Synopsis A Monte-Carlo simulation is performed for strongly driven triatomic molecules using a three-dimensional semi-classical model. Statistical results are obtained for frustrated ionization in both a 2 electron and 3 electron setting.

Frustrated" double ionization accounts for roughly 10% of all ionization events in the breakup of strongly-driven molecules and therefore is of fundamental interest to strong field physics.

We employ a three-dimensional semi-classical model, to demonstrate a significant enhancement of "frustrated" double ionization in the two-electron triatomic molecule D_3^+, driven by counter-rotating two-colour circular laser fields. The enhancement of the probability is due to a pathway, which does not appear in strongly driven molecules with linear fields. In this pathway, the first ionization step is "frustrated" and electronic correlation is negligible. We also employ a simple model that predicts many of the main features of the probabilities of the "frustrated" double ionization.

We adjust our previous model to treat three-electron escape dynamics in a strongly-driven linear triatomic molecule, HeH_2^+. To avoid autoionization, we employ criteria to switch on and off the Coulomb forces between electrons at appropriate times. We investigate triple and "frustrated" triple ionization and see that two pathways prevail as seen before in "frustrated" double ionization. Our results indicate that in triple and "frustrated" triple ionization, electronic correlation is weak. Moreover, we find that the fragmenting molecule can deviate from its initial linear configuration.

References

[1] G. P. Katsoulis, R. Sarkar, and A. Emmanouilidou 2020 *Phys. Rev. A* **101** 033403

[2] M. B. Peters, V.P. Majety, A. Emmanouilidou 2020 *arXiv* 2010:16216

*E-mail: ucapete@ucl.ac.uk
†E-mail: ucapaem@ucl.ac.uk

Rotational excitation of H_2 by electron impact with the molecular convergent close-coupling method

U S Rehill[1], L H Scarlett[1]*, M C Zammit[2], D V Fursa[1], I Bray[1]

[1]Department of Physics and Astronomy, Curtin University, Perth, Western Australia 6102, Australia
[2]Theoretical Division, Los Alamos National Laboratory, Los Alamos, New Mexico 87545, USA

Synopsis We calculated rotationally-resolved cross sections using the adiabatic-nuclei molecular convergent close-coupling method. Rovibrational cross sections are presented for scattering within the $X\ ^1\Sigma_g^+$ state and excitation of the $d\ ^3\Pi_u$ state. Linear polarisation fractions obtained from the $d\ ^3\Pi_u$ cross sections are also presented.

Cross sections for electron-H_2 scattering are of fundamental importance for fusion research as molecular hydrogen is found in the edge and divertor regions of fusion devices. To accurately model plasmas containing H_2, cross sections are required for a large number of electronic, vibrational and rotational transitions.

Previous studies of rotationally-resolved collisions have found reasonable agreement between theory and experiment for low-lying rotational excitations within the ground electronic state. However, there is little data available for simultaneous electronic, vibrational and rotational excitation.

The adiabatic-nuclei molecular convergent close-coupling (MCCC) method has been applied to the electron-H_2 scattering system with the goal of obtaining a complete set of scattering cross sections. Electronic and vibrationally resolved cross sections have been obtained previously, and now we extend the data set to include rotationally-resolved cross sections.

We present cross sections for pure rotational and rovibrational excitation of the $X\ ^1\Sigma_g^+$ state (see Figure 1), as well as simultaneous electronic and rovibrational excitation of the $d\ ^3\Pi_u$ state. The $d\ ^3\Pi_u$ state is the upper state of the Fulcher-α band, which is frequently used in plasma spectroscopy due to it's particularly strong emission intensity. The degree of polarisation of light emitted in the decay of the $d\ ^3\Pi_u$ state can be measured and used to determine plasma properties. We present linear polarisation fractions calculated using the MCCC $d\ ^3\Pi_u$ cross sections resolved in rotational sublevels.

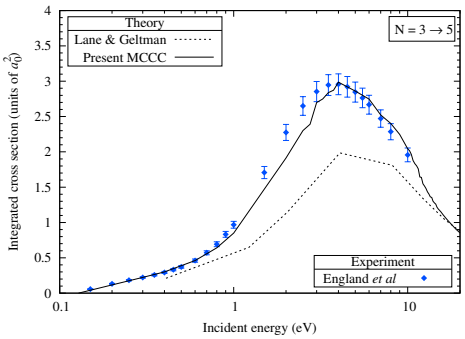

Figure 1. Integrated cross section for the $X\ ^1\Sigma_g^+(v=0, N=3) \rightarrow X\ ^1\Sigma_g^+(v=0, N=5)$ transition. The MCCC results are compared with the theoretical calculations of Lane & Geltman [1] and the experimental results of England *et al* [2].

References

[1] N Lane & S Geltman 1967 *Phys. Rev.* **160** 53
[2] England *et al* 1988 *Aust. J. Phys.* **41** 573

*E-mail: liam.scarlett@postgrad.curtin.edu.au

Elastic electron scattering by the amino acid threonine molecule

Sh Demes[1], A Vasiliev[2] *, E Remeta[2] and V Roman[2] †

[1]Institute for Nuclear Research (ATOMKI), 4026, Debrecen, Hungary
[2]Institute of electron physics of National Academy of Sciences of Ukraine, Uzhhorod, 88017, Ukraine

Synopsis Integral and differential cross sections of the potential electron scattering by amino acid D-threonine molecule are calculated in the independent atom model. An analysis of the energy and angle dependences of cross sections were carried out.

The differential cross sections (DCSs) of elastic electron scattering by the amino acid D-threonine molecule (Thr, $C_4H_9NO_3$) were calculated in 2 approximations, IAM and Ad, of independent atom model (see descriprion and ref. in [1]). Amplitudes and CSs of elastic electron scattering by atoms C, H, N, O, that consist this biomolecule were found in the optical potential method, SEPA approximation (taking into account absorption effects) according to ELSEPA code [2] (also see [1]).

The DCSs in the IAM approximation takes into account the so-called interference terms that arise due to the spatial arrangement of atoms of threonine molecule. In the Ad approximation the DCSs are equal th the simple sum of the DCSs electron scattering by 17 atoms of the threonine molecule.

On figure 1 presented a comparison of DCSs of these 2 approximations for collision energies 20 and 150 eV. Integral elastic and momentum transfer Ad-CSs at 20 and 150 eV are (in 10^{-20} m^2): 91.721, 47.364, 20.158, 5.004.

At the collision energies of 20, 40 and 60 eV IAM-DCSs differ the most from Ad-DCSs in the region of small scattering angles. Thus, at 20 eV such difference is up to 70°, for 40 eV up to 40°, for 60 eV up to ~25. However, with increasing energy IAM-DCSs gradually differ from AD-DCSs in the whole range of angles.

The largest difference between the DCSs of these approximations is for an energy of 150 eV. The excess of IAM-DCSs over Ad-DCSs is only in a narrow range of forward scattering angles – ~15°. In the range of angles up to 130° IAM-DCSs have certaine angular structure. This is a important role of the interference terms from the scattering amolitydes from different atoms of the threonine molecule.

*E-mail: nucleargoga@gmail.com
†E-mail: viktoriyaroman11@gmail.com

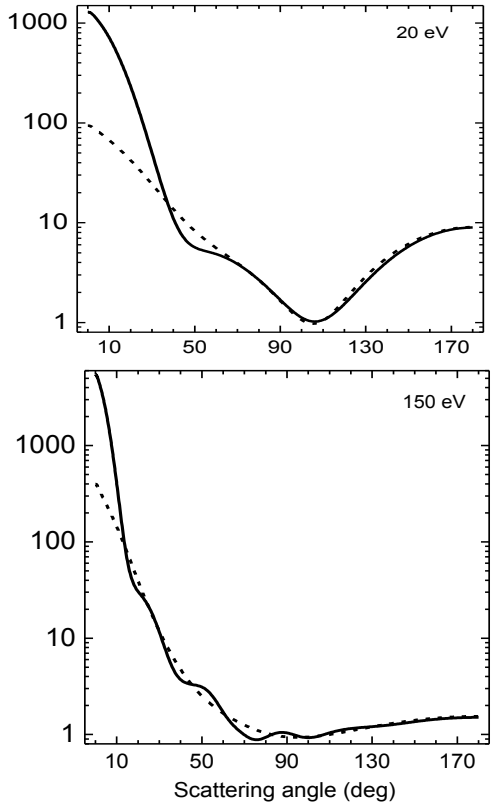

Figure 1. Angle dependences of elastic DCSs (in 10^{-20} m^2/sr) for e+D-Thr scattering at 20 and 150 eV. IAM- (–—) and Ad- (-----) approximations of IAM.

The study was perfomed with partial financial support from the NRFU (grant N 2020.01 / 0009 "Effect of ionizing radiation on the amino acid molecules structure'')

References

[1] Demes Sh *et al* 2020 *Scientific Herald of Uzhhorod University. Series Physics* **48** 102
[2] Salvat F *et al* 2005 *Comp. Phys. Commun.* **165** 157

Resonances in the low-energy electron interaction with the D-ribose molecule

I Chernyshova, E Kontros and V Roman*

Institute of electron physics of National Academy of Sciences of Ukraine, Uzhhorod, 88017, Ukraine

Synopsis Using a hypocycloidal electron spectrometer, total dissociative electron attachment and total elastic cross sections for electron scattering by D-ribose molecule are studied at incident electron energies E<20 eV. A clear structure near 0 eV and in the 5.5–9.5 eV range has been observed in the dissociative electron attachment cross section. These features appear due to the formation of negative molecular ion fragments. In the total cross-section of electron scattering by molecules, resonance structure is observed in the range 6–9.5 eV where negative ions are formed related to the molecule heterocycle destruction.

D-ribose ($C_5H_{10}O_5$) belongs to mono-saccharides, the most abundant group of biomolecules, with five C atoms. This molecule is a part of the building blocks that form DNA and RNA molecules. D-ribose is also contained in ATP and NADH, which are critical for the metabolism. Here we report on the results of our studies on the total cross sections for the production of negative ions of the D-ribose molecule and total elastic cross sections for electron scattering by D-ribose by slow (<20 eV) electrons.

In our experiments, a hypocycloidal electron monochromator [1] was used to produce an electron beam with at least 0.2 eV energy resolution. The ribose powder (Sigma-Aldrich, 99% purity) placed into a quartz ampoule was heated up to ~80ºC in a stainless-steel reservoir, filling thus the gas cell (at $P \approx 10^{-3}$ Torr). Ions produced were extracted to the collector mounted perpendicularly to the electron beam direction. A low positive potential was applied to the collector for detecting the negative ions. Scattered electron current was detected directly at the collision chamber walls.

Figure 1 shows the total dissociative electron attachment cross section for the D-ribose molecule measured at 80ºC in the 0–16.0 eV electron energy region. An intense peak near zero energy and two lower-intensity maxima in the region of 6.0–9.5 eV can be observed. Based on the results of Ref. [2, 3] we assume that the observed features appear due to the formation of the $C_5H_8O_4$–, $C_5H_6O_3$–, $C_4H_5O_3$–, $C_3H_4O_2$–, $C_3H_3O_2$–, $C_2H_3O_2$– and OH– ion fragments.

The energy dependence of the total electron-ribose molecule scattering cross section has been measured within the incident electron energy range from 0 to 9.0 eV. A drastic decrease below 1.0 eV is a specific feature of the above cross section.

In the 5.0 – 9.0 eV energy region, the distinct features are observed. They are due to the influence of resonances formed at a temporary (10^{-15} s) electron capture by molecule. Such resonance structure is shown in Fig. 1 (curve 2). The energy positions of the maxima are 5.8 eV, 6.6 eV, 7.4 eV, 8.2 eV and ~8.4 eV. Note that our results agree well with calculations [4].

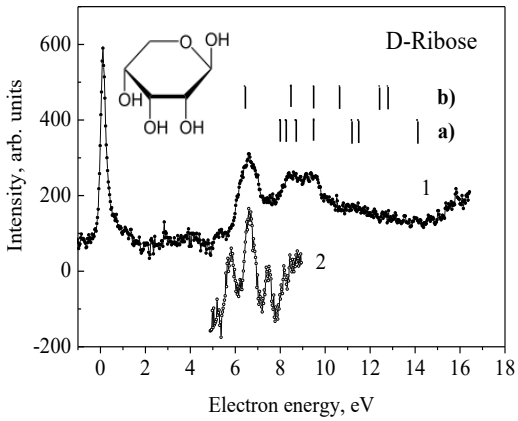

Figure 1. The total dissociative electron attachment cross section for the D-ribose molecule (curve **1**). The resonance structure found in the total scattering cross section (curve **2**). The letters **a)** and **b)** denote the calculated resonance positions [4].

Comparing the resonance structure (curve 2 in Fig. 1) with the total dissociative attachment cross section (curve 1 in Fig. 1) has confirmed the resonant nature of negative ion production in the 5.5 – 9.5 eV incident electron energy region.

References

[1] Kontros J *et al* 2002 *J. Phys. B* **35** 2195
[2] Bald I *et al* 2006 *Angew. Chem. Int. Ed.* **45** 4851
[3] Baccarelli I *et al* 2007 *J. Am. Chem. Soc.* **129** 6269
[4] Baccarelli I 2008 *J. Phys. Conf. Ser.* **115** 012009

* E-mail: viktoriyaroman11@gmail.com

METHYLATION EFFECT ON ELECTRON SCATTERING: GLYCOLIC ACID AND LACTIC ACID

C A Amaral*, R V B Morás, A S Barbosa and S D Sanchez†

Departamento de Física, Universidade Federal do Paraná, Caixa Postal 19044, 81531-980 Curitiba, Paraná, Brazil

Synopsis In this work we investigated the effect of methylation in the electron scattering process by glycolic acid and lactic acid, since both molecules differ by a methyl group. Our focus is to analyze how it affect resonance position in electron scattering due to the fact that resonance can cause single and double DNA strand breaks, and methylation on a nitrogenous basis is not an unusual process. We employed the Schwinger's Multichannel method with pseudopotentials to obtain the integral cross section. Our preliminar results show that the resonance in lactic acid is higher than in the glicolic acid molecule.

Understanding low energy electrons scattering by molecules is of fundamental importance for different areas of knowledge. Particularly, in the human body, through the resonant process known as dissociative electron attachment, low-energy electrons can cause single and double DNA strand breaks [1]. Also, it is common to observe methylated nitrogenous basis in DNA [2, 3] and hence, it is of great importance to understand how a methyl group can affect resonance position .

In the human body, lactic acid, in the form of lactate, plays an important role in anaerobic and aerobic exercises. Glycolic acid is a compound widely used in cosmetics and found in some sugar plants. Also, its simplicity makes them ideal to understand methylation in electron scattering processes.

In this way, we present the results for integral and the differential cross section for electron scattering for glycolic acid and lactic acid, in which the first one differs from lactic acid by the substitution of a hydrogen atom by methyl group (figure 1). Due to the methyl radical present in the lactic acid, the integral and differential cross sections are expected to have greater amplitude than in the case of glycolic acid. In addition, we investigated the π^* shape resonance for both molecules, due to the fact that this type of resonance is responsible for the single and double DNA strand breaks.

Such a study is being performed using Schwinger's Multichannel method with pseudopotentials in the static exchange and static exchange plus polarization levels of approximations [4]. Preliminary results thus far show the desastibilization of the resonance due to the presence of the methyl group as was previously observed at [5]. Also, electronic structure calculations using the Hartree-Fock method, to assist in the characterization of the resonance.

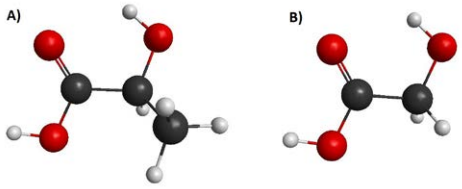

Figure 1. Representation of A) lactic acid and B) glycolic acid.

References

[1] B Boudaïiffa *et al* 2000 *American Association for the Advancement of Science* **287** 5458
[2] O T Avery *et al* 1944 *J Exp Med* **79** 137
[3] M McCarty *et al* 1946 *J Exp Med* **83** 89
[4] R F Costa *et al* 2015 *Eur Phys* **69** 159
[5] F B Nunes, M H F Bettega and S D Sanchez 2016 *J. Chem. Phys.* **145** 214313

*E-mail: cesar_amaral@ufpr.br
†E-mail: ssanchez@fisica.ufpr.br

Neutral H_2 production from ethylene electron and photon ionization

L Sigaud[1] * and E C Montenegro[2] †

[1] Instituto de Física, Universidade Federal Fluminense (UFF), Niterói, 24210-346, Brazil
[2] Instituto de Física, Universidade Federal do Rio de Janeiro (UFRJ), Rio de Janeiro, 21941-972, Brazil

Synopsis The production of molecular hydrogen in the interstellar medium and in planetary atmospheres is intrinsically dependent on other molecules. Direct measurement data of neutral species following molecular ionization and fragmentation, on the other hand, is scarce. Here we present a methodology for obtaining H_2 production following ethylene (C_2H_4) ionization, for which this particular molecule can contribute significantly to neutral hydrogen formation in any environment where it is present.

In a myriad of astrophysical media the ionization of light hydrocarbons produces fragments which serve as building blocks of heavier molecules and lead to the formation of interstellar dust. These granular structures are currently considered the main mechanism in assisting molecular hydrogen formation, since the binding of two free hydrogen atoms is ineffective, due to the excess energy that cannot be disposed of by electric dipole radiation.

Ethylene (C_2H_4) ionization has many different produced fragments that can possibly lead to molecular hydrogen. In order to identify and quantify these possible pathways, a second-order magnifying lens was used: a combination of the Delayed-Extraction Time-Of-Flight (DETOF) technique, which provides absolute cross sections for the different kinetic energy distributions of each produced fragment, and the fragmentation matrix, which is able to link the experimental cross sections with the theoretical cross sections for electron removal from each molecular orbital (MO) [1].

Experimental DETOF data for electron impact, analyzed using calculated MO ionization cross sections, are shown in Figure 1. The production of H_2 after ethylene ionization is not only relevant, but is one order of magnitude higher than that of methane fragmentation, which was widely regarded as the main pathway for H_2 production prior to the formation of interstellar dust [1].

For electron impact energies where TS2 processes are negligible in comparison to single ionization, the fragmentation and subsequent H_2 production depend only on the molecular orbital from which the ionized electron was removed, regardless of the projectile type. This allows the use of the fragmentation matrix also for photon irradiation. To this end, photoionization experimental data from Grimm *et al*. [2] and MOs photoionization cross sections from Toffoli and Decleva [3] were employed.

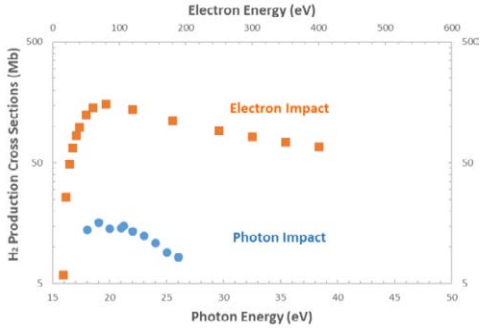

Figure 1. Cross sections for the production of H_2 from ethylene ionization by electrons (orange squares, upper *x* axis) and photons (blue circles, lower *x* axis).

This procedure allows one to determine the cross sections for production of H_2 for the ethylene photoionization (see Figure 1). This shows molecular hydrogen must be present in ethylene-containing systems bombarded by photons in this energy range. This is the case, for instance, of Titan's atmosphere and the He I emission line (~21.2eV, for which there is a maximum on the cross sections) from the Sun.

References

[1] Sigaud L and Montenegro E C 2020 *Phys. Rev. A* **102** 052809
[2] Grimm F A *et al* 1991 *Chem. Phys.* **154** 303
[3] Toffoli D and Decleva P 2016 *J. Chem. Theory Comput.* **26** 4996

* E-mail: lsigaud@id.uff.br
† E-mail: montenegro@if.ufrj.br

Elastic and electronically inelastic scattering of low-energy electrons by the 2H-pyran molecule

M O Silva[1], R F da Costa[2] and M H F Bettega[1]*

[1]Departamento de Física, Universidade Federal do Paraná, Caixa Postal 19044, 81531-990 Curitiba, Paraná, Brazil

[2]Centro de Ciências Naturais e Humanas, Universidade Federal do ABC, 09210-580 Santo André, São Paulo, Brazil

Synopsis We report on integral and differential cross sections for elastic and electronically inelastic electron scattering by the 2H-pyran molecule obtained by means of the Schwinger multichannel method with pseudopotentials. The aim of this work is to investigate the formation of resonances in the elastic channel as well as to analyze the influence of multichannel coupling effects on the magnitude of elastic and electronically inelastic cross sections.

The 2H-pyran molecule is a six-membered heterocyclic compound consisting of five carbon atoms and one oxygen atom and containing two double bonds in the ring structure. It can be considered as the simplest representative of an important class of biologically active natural and synthetic products and, due to this fact, has been the subject of recent investigations [1, 2].

In the present work we employed the Schwinger multichannel method implemented with pseudopotentials [3] to study low-energy electron collisions with the 2H-pyran molecule. As a first step of our investigation we carried out elastic scattering calculations at the static-exchange (SE) and the static-exchange plus polarization (SEP) levels of approximation. Partial cross section for the resonant symmetry A'', shown in the top panel in Figure 1, indicates the presence of two resonances. As can be seen in Table 1, the values of the resonance positions obtained according to the SEP level of approximation are in good agreement with the vertical attachment energies (VAEs) estimated by means of an empirical scaling relation.

Table 1. Values for the resonance positions (in eV) obtained according to the SE and SEP approximations together with the estimated VAE.

	SE	SEP	VAE
π_1^*	2.80	1.02	0.93
π_2^*	6.80	4.02	3.33

With the aim to evaluate the effect of multichannel coupling effects we are also performing a calculation within the spirit of the MOB-SCI strategy [4] which includes the coupling and competition of up to 33-coupled channels. Preliminary differential cross section results are presented in the bottom panel in Figure 1.

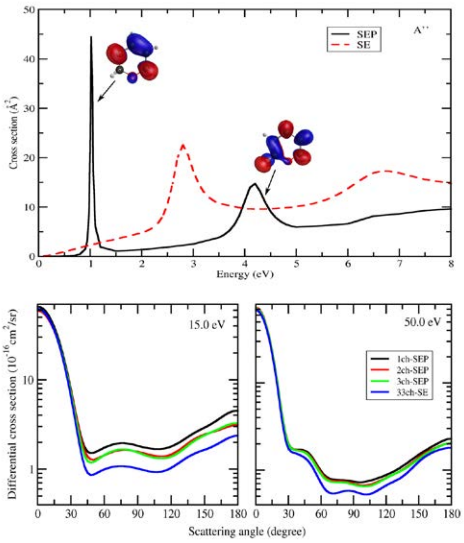

Figure 1. (Top panel) A'' partial integral cross section for elastic electron scattering by 2H-pyran obtained at the SE and SEP levels of approximation. Calculated inelastic differential cross sections (Bottom panel) considering up to 33 open channels.

References

[1] Goel A *et al* 2009 *Tetrahedron* **65** 7865
[2] Kumar K A *et al* 2015 *J. Chem. Pharm. Res.* 693
[3] da Costa R *et al* 2015 Eur. Phys. J. D **69** 159
[4] da Costa R *et al.* 2005 J. Phys. B **38** 4363

*E-mail: bettega@fisica.ufpr.br

Carboxylation effects in low-energy electron scattering by molecules

A S Barbosa*

Departamento de Física, Universidade Federal do Paraná, Caixa Postal 19044, 81531-990 Curitiba, Paraná, Brasil

Synopsis This work presents a theoretical study on low-energy electron interactions with furan- and pyrrol-2-carboxylic acids. The scattering cross sections have been calculated employing the Schwinger Multichannel Method, whereas electronic structure calculations have been carried out in order to support the characterization of the resonances as well to provide some preliminar discussion on the dissociation pathways for these systems.

It is well-known that substitution of a hydrogen atom by other atoms or groups in molecules affects the electron-molecule dynamics, in particular, at lower energies where this substitution exerts some influence on the tempo-rary anions formation. For example, halogenation of unsaturated molecules not only gives rise to a σ^* resonance, but also affects the π^* resonance energy [1]; methylation affects the low-energy electron-molecule interaction so much that it can stabilize or destabilize resonances and also suppress some dissociation channels [2].

Recently it was shown that carboxylation strongly affects the elastic electron-pyrrolidine scattering at impact energies up to 4.0 eV. In particular, the cross sections for low-energy electron scattering by proline, which can be seen as a carboxylated pyrrolidine, is dominated by the shape resonance associated to the carboxylic group [3]. More recently, the dissociative electron attachment in 2-furoic acid, which can be seen as a carboxylic group attached to a furan ring, has been measured revealing that the carboxylation enhances the fragmentation upon electron attachment [4].

In this work, we present a theoretical study on low-energy electron interactions with cyclic acids. Some of the target molecules are furan- and pyrrol 2-carboxylic acids. The Schwinger multichannel method implemented with pseudopotentials [5] has been employed to obtain the elastic integral and differential cross sections, in the static-exchange plus polarization approximations, for impact energies up to 15 eV. Some additional electronic structure calculations have also been carried out to support the characterization of the resonance spectrum and provide some preliminary discussion on the dissociation pathways for these molecules. We also compare the present results with previous data available from the literature for the parent molecule furan and pyrrol.

References

[1] Barbosa A S *et al* 2016 *J. Chem. Phys.* **145** 084311
[2] Kossoski F and Varella M T do N 2017 *J. Chem. Phys.* **147** 164310
[3] Barbosa A S, Freitas T C, Bettega M H F 2018 *J Chem. Phys.* **148** 074304
[4] Zawadzki M *et al.* 2020 *J. Phys. Chem. A* **124** 9427
[5] Costa R F *et al.* 2015 *Eur. Phys. J. D* **69** 159

*E-mail: alessandra@fisica.ufpr.br

Theoretical study of the collision dynamics in electron-impact ionization of atomic and molecular targets

T Khatir[1] *, S Houamer[1] and C Dal Cappello[2]

[1] LPQSD, Department of Physics, Faculty of Sciences, University Sétif1, Setif 19000, Algeria
[2] LPCT, UMR CNRS 7019, University of Lorraine, BP 70239, 54506 Vandoeuvre-les-Nancy, France

Synopsis A new theoretical approach is used to calculate the triple differential ionization cross-sections for atomic and molecular targets by electron impact. The distortion effects and the short-range potential are simultaneously taken into account. The method is applied for specific atoms and molecules, the results are compared to available experiments and other theories performed in coplanar asymmetric geometries.

The electron impact ionization of matter is a basic process in collision physics, which plays a significant role in number of fundamental areas. The triply differential cross section (TDCS) obtained in (e, 2e) experiments represent the most detailed description of the ionization process. A new theoretical approach is used to calculate (TDCS) of (e,2e) reactions, which is the most sensitive test for theoretical models.

Here, we present an improved description regarding the reaction dynamics in the case of simple ionization of atomic and molecular targets. We use here three models to calculate the TDCS, where the post collisionnal interaction (PCI) between the outgoing electrons is taken into account. The First model, called BDW, where the ejected electron is represented by a distorted wave and the scattered electron is described by a Coulomb wave. The second model called BSR where the final state is described by three Coulomb waves representing the interaction of the scattered and the ejected electrons with the residual ion as well as the PCI between these two electrons. Then we tried to improve the treatment via the BDWSR model where the distortion effects and the short-range potential are taken into account at the same time. The main idea was to use a variable charge Z(r) representing these approximated distortion effects, enabling an interesting analytical mathematical scheme and consequently important time calculation economy. The method is applied to specific atomic and molecular targets, and the results are compared to available experiments and other sophisticated models.

In figure 1 the TDCS of $1t_2$ orbital of CH_4 is displayed and compared to the relative measurements performed at 500 eV scattered energy.

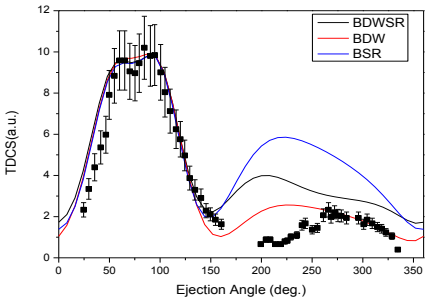

Figure 1. TDCS vs ejection angle for the ionization of the $1t_2$ orbital of CH_4 . Kinematical parameters are: θ_s =6º ,E_s = 500 eV , Eb =12 eV [2].

As it can be seen in figure1, that the experiments exhibit a considerable recoil peak, indicating an important participation of the residual ion in the collision dynamics. The data are overall explained by BDW and BDWSR, which both practically predict a significant recoil structure. The BSR model substantially over-estimates the data in the recoil region, this indicates the role of the distortion effects which are not accounted by this model. The advantage of our models manifest themselves in the case of molecules, where a result is obtained in a few hours with the more complicated BDWSR model [1] instead of a few days [3].

References

[1] Khatir T, Houamer S, Dal Cappello C 2019 *J. Phys. B: At. Mol. Opt. Phys*. 52 245201
[2] Lahmam-Bennani A, Naja A, Staicu Casagrande E M, Okumus N, Dal Cappello C, Charpentier I and Houamer S 2009 *J. Phys. B: At. Mol. Opt. Phys*. 42 165201
[3] Madison D H and Al-Hagan O 2010 *J. At. Mol. Opt. Phys*. 2010 367180

* E-mail: tarek.khathir@univ-setif.dz

Electron-attachment energies predicted using TD-DFT methods

G Thiam[1]*, F Rabilloud[1]†, P M Dinh[2] and H Abdoul-Carime[3]

[1]Université of Lyon, Université Claude Bernard Lyon 1, CNRS, Institut Lumière Matière, UMR5306, F-69622, Villeurbanne, France

[2]Laboratoire de Physique Théorique, Université Paul Sabatier, F-31062 Toulouse, France [3]Université of Lyon, University Lyon 1, Institut de Physique des 2 Infinis, CNRS/IN2P3, UMR5822, F-69003 Lyon, France

Synopsis Presenting a new method for calculating, using TD-DFT method, electron-attachment energies.

Understanding the attachment of low energy electrons to molecules constitutes a key subject from a fundamental perspective but also for innovative applications in various fields of science: radiation chemistry and biology, beam- and photon-induced surface chemistry,astrophysics, etc.

Computational methods for temporary anions uses either very computationally demanding tasks, or, on the contrary, very simple empirical approches.

Here, we present a new TDDFT-based method for predicting the electron attachment energies. The method has been performed using separated range corrected functional ωB97x and compares well with more computationnally expensive methods such as Coupled-Cluster ones. It can be used for small or large molecules, and it does not use any empirical parameters.

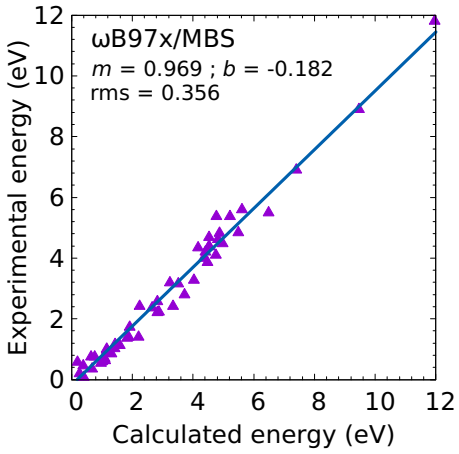

Figure 1. Experimental energies vs Calculated energies using TD-DFT methods and different basis-set to evaluate separetely the vertical electron affinity and the excitation energies

*E-mail: guillaume.thiam@univ-lyon1.fr
†E-mail: franck.rabilloud@univ-lyon1.fr

Theoretical study of electron-impact vibrational excitation of isocyanic acid HNCO using two dimensional nonlocal model

J Trnka*, K Houfek, M Čížek†

Institute of Theoretical Physics, Faculty of Mathematics and Physics, Charles University, V Holešovičkách 2, 180 00, Praha 2

Synopsis We present our theoretical description of vibrational excitation of HNCO induced by collision with electron using a two-dimensional nonlocal resonance model including HN stretch and HNC bending modes.

The collisions of slow electrons with atoms and molecules have been successfully studied using the nonlocal resonance model [1] in numerous molecular systems [2]. However, the use of the nonlocal model has been mostly limited to one-dimensional models. We present our ongoing efforts to extend the use of the nonlocal resonance model to multidimensional systems and the application of the theory to vibrational excitation of HNCO.

The vibrational excitation, as well as dissociative electron attachment in HNCO, has been investigated in combined experimental and theoretical studies [3, 4]. For the purpose of those studies, only radial coordinate along HN bond was considered in the construction and the dynamics of the model and the rest of the molecule was kept at its equilibrium geometry. We have expanded this model to include HNC bending by adding azimuthal angular coordinate of the hydrogen atom.

An important step in the construction of the model is the parametrization of the electron-molecule scattering data using the discrete-state-in-continuum model. For this purpose, we performed the fixed-nuclei R-matrix calculations using the UK molecular R-matrix suite of codes [5] for a large number of HN-bond lengths and HNC bond angles. We parametrize these results using the generalized Breit-Wigner formula to obtain an appropriate form of coupling for the nonlocal model.

The dynamics of the collision is described in the time-independent picture. To treat the angular coordinate we employ expansion in spherical harmonics. This leads to a set of coupled integral equations which is solved using the Schwinger-Lanczos algorithm. In this way we obtain scattering cross sections of elastic scattering, HN stretch excitations, and previously unavailable HNC bending mode excitations. We compare the results with the results of the 1D model and with available experimental data.

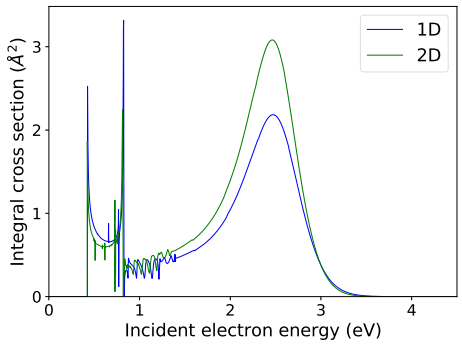

Figure 1. Excitation curves for the HN stretch vibration (0→1). Green line is calculated using 2D model, blue using the same model restricted to equilibrium geometry and treated as 1D problem

References

[1] Domcke W 1991 Phys. Rep. **208** 97
[2] Čárský and Čurík R 2012 Low-energy electron scattering from molecules, biomolecules and surfaces (CRC Press, Boca Raton)
[3] Ragesh Kumar T P *et al* 2020 Phys. Rev. A **102** 062822
[4] Zawadski M *et al* 2018 Phys. Rev. Lett. **121** 143402
[5] Carr J M *et al* 2012 Eur. Phys. J. D **66** 58

*E-mail: trnkajirka@seznam.cz
†E-mail: Martin.Cizek@mff.cuni.cz

Fragmentation of anthracene molecules following double ionization by 70 eV electron impact

P J M van der Burgt[1] * and M L Gradziel[1]

[1]Department of Experimental Physics, National University of Ireland Maynooth, Maynooth, Co. Kildare, Ireland

Synopsis We have performed coincidence mass spectrometry of fragmentation of anthracene molecules by 70 eV electron impact. Double ionization results in a number of prominent fragmentations producing two singly-ionized fragments. A field programmable gate array was used for the timing and the recording of mass spectra on an event-by-event basis. Bespoke software was developed both for the computer control of the field programmable gate array and for the acquisition of the coincident events. A detailed model of the coincidence data acquisition was developed, fully accounting for the effect of instrumental imperfections such as detector dead time and for random coincidences, increasing the fidelity of the final coincidence maps.

In our earlier studies of electron impact on anthracene and phenanthrene [1, 2] we measured mass spectra for positive ions using a reflectron time-of-fight mass spectrometer. Mass spectra were recorded using a multichannel scaler and the electron impact energy was varied from 0 to 100 eV in steps of 0.5 eV. Ion yield curves and appearance energies of most of the fragment ions of anthracene and phenanthrene were determined. In these mass spectra clear evidence was observed for double ionization by electron impact at energies above 21 eV.

In order to study double ionization, we have implemented a new data acquisition system in which a field programmable gate array (FPGA, National Instruments cRIO9075) is used for the timing of the pulsing of the electron gun and the ion extraction voltage, and for the recording of mass spectra on an event-by-event basis. We have developed LabVIEW code for both the communication between the FPGA and a PC, running on the FPGA chassis, and the control of the experiment and the acquisition of the event-by-event data, running on the PC.

Python software has been developed to analyse the file with event data, and to assemble a coincidence matrix for all electron pulses for which two or more ions were detected. A detailed model of the coincidence data acquisition was developed, fully accounting for instrumental imperfections such as detector dead time and for random coincidences. This model was implemented in Python and enables us to reliably obtain the map of true coincidences.

* E-mail: peter.vanderburgt@mu.ie

Double ionization processes can be written as:

$e^- + C_{14}H_{10} \rightarrow C_{14}H_{10}^{++}$

$\rightarrow C_aH_m^+ + C_bH_n^+ +$ neutral fragments

Our measurements show that fragmentations for which the total number $a + b$ of carbon atoms in both fragments is even are generally significantly stronger than fragmentations for which the total is odd.

The strongest fragmentations are the groups $(a, b) = (4, 6)$, $(3, 5)$ and $(3, 7)$. In these three groups the strongest fragmentations are $C_4H_2^+ + C_6H_2^+$, $C_3H_3^+ + C_5H_3^+$, and $C_3H_3^+ + C_7H_3^+$. The diagonal groups (4, 4) and (5, 5) also contain a few strong fragmentations, but because of detector dead time our experiment does not fully resolve fragmentations producing fragments of exactly equal mass.

In most of the groups, the fragmentations in which each of the fragments has 2 or 3 hydrogen atoms are the strongest. The exceptions are for the groups $(a, b) = (4, 10)$, $(3, 11)$ and $(2, 12)$. In these groups the strongest fragmentations are $C_4H_2^+ + C_{10}H_6^+$, $C_3H_3^+ + C_{11}H_7^+$, and $C_2H_3^+ + C_{12}H_6^+$.

Essentially no fragmentations are observed for groups with $a + b = 13$. The only weak fragmentations producing one fragment with only one carbon atom are $CH_3^+ + C_5H_3^+$, $CH_3^+ + C_9H_3+$ and $CH_3^+ + C_{13}H_{6\text{-}7}^+$. All these fragmentations involve the rearrangement of hydrogen atoms.

References

[1] van der Burgt P J M, Dunne M, and Gradziel M L 2018 *Eur. Phys. J. D* **72**, 31

[2] van der Burgt P J M, Dunne M, and Gradziel M L 2019 *J. Phys. Conf. Ser.* **1289**, 012008

The study of the low-lying valence-shell excitations of carbon tetrachloride by fast electron impact

Li-Han Wang[1,2], Xiao-Jiao Du[1,2], Yuan-Chen Xu[1,2], and Lin-Fan Zhu[1,2]*

[1]Hefei National Laboratory for Physical Sciences at Microscale and Department of Modern Physics, University of Science and Technology of China, Hefei, Anhui 230026, Peoples Republic of China

Synopsis Generalized oscillator strengths of the valence-shell excitations of carbon tetrachloride have been determined by means of EELS at an incident electron energy of 1.5 keV and an energy resolution of about 70 meV. By analysing the variations of intensity and shape of the feature in the range of 5.0-7.7 eV, the excitation energies of the states in this region are determined.

Carbon tetrachloride (CCL_4) can be decomposed by ultraviolet radiations in the stratosphere, which would produce significant amounts of chlorine atoms and leads to the destruction of atmospheric ozone [1]. Thus, the valence-shell excitations of carbon tetrachloride have been studied extensively by optical methods and electron collision methods. Because of the limitations of experimental resolutions and the restriction of the optical selection rules, some puzzles still exist in the previous studies about the assignments of some states. Due to the relaxation of the selection rules at nonzero scattering angles in the fast electron collision experiment, these states are reassigned in this work.

Using the fast electron energy loss spectroscopy, the generalized oscillator strengths (GOSs) of the valence-shell excitations of CCL_4 have been measured in this work at an incident electron energy of 1.5 keV and an energy resolution of 70 meV. The present GOS for the 1^1T_1 state of CCL_4 is illustrated in Fig.1, and the excitation energy of 6.10 eV of this state has been determined. As shown in Fig.1, the 1^1T_1 state, which should have optical forbidden characteristics, retains certain excitation probability when $K^2 \to 0$, which might be caused by the vibronic effect [2]. However, since the optical oscillator strength of this state is less than 0.01, it has been hidden in the previous experiments.

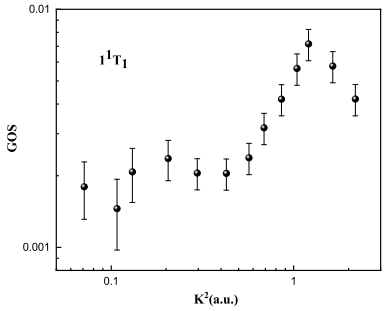

Figure 1. The GOSs of the 1^1T_1 state. The black dots are the present GOSs.

In summary, the GOSs of the valence-shell excitations of CCL_4 have been determined by a fast electron impact method, which provide some new information about the valence-shell excitations and can serve as basic data to modeling planetary atmospheric phenomena and evolution of the atmosphere of the earth.

References

[1] F Sherwood Rowland and Mario J Molina. *Reviews of Geophysics*, 13(1):1–35, 1975.

[2] Noboru Watanabe, Daisuke Suzuki, and Masahiko Takahashi. *The Journal of chemical physics*, 134(23):234309, 2011.

*E-mail: lfzhu@ustc.edu.cn

Measurement of the forward-backward asymmetry in electron impact ionization of CO

N Watanabe[1] * and M Takahashi[1]

[1]Institute of Multidisciplinary Research for Advanced Materials, Tohoku University, Sendai 980-8577, Japan

Synopsis We investigate the molecular-orientation dependence of high-energy electron-impact ionization of CO. The $3^2\Pi$ ionization cross section measured at low momentum transfer is found to be considerably larger when the momentum transfer vector points toward the C atom along the molecular axis than when it is in the opposite direction, which is a nontrivial molecular orientation effect in charged-particle-induced ionization.

The molecular-orientation dependence of electron-impact ionization is shown to provide valuable information on the shape of excited molecular orbitals [1]. To apply it to heteronuclear molecules, such as CO, it is necessary to distinguish the difference between the C and O sides. The ionization rate of CO may, in principle, be different depending upon whether the momentum transfer vector points towards the C or O atom. Despite its fundamental nature of electron induced processes, however, such asymmetry has not yet been observed. We therefore investigate the molecular-orientation dependence of the inner valence ionization of CO to elucidate how the inversion asymmetry appears in the ionization process [2].

(e, e+ion) experiments on CO were carried out using an electron-ion coincidence apparatus developed in our laboratory [3]. It consists of an electron gun, an energy-dispersive electron spectrometer, and an ion momentum imaging spectrometer. The coincidence data were obtained using incident electron energy of ~1.4 keV. The direction of the molecular-axis with respect to the momentum transfer vector $\boldsymbol{K}$ was deduced from the angular correlation between the fragment ion and the scattered electron.

Figure 1 shows the angular distributions of C^+ ions having kinetic energy of 1.8-2.3 eV, which are presented as a function of angle between the momentum transfer vector and the recoil direction of C^+, ϕ_K. They were constructed using the coincidence data measured for electron energy loss of E = 28-30 eV, at which the C^+ ions detected are formed by dissociation of the $3^2\Pi$ state into the C^+ (^2P) + O(^1D) limit.

It can be seen from the figure that the ionization cross section exhibits anisotropic molecular-orientation dependence. For K^2 = 0.16 a.u., the distribution has a maximum around ϕ_K = 0° and its intensity is appreciably higher than that at 180°, in contrast to the symmetric angular distribution of photoions [4]. A higher intensity for the C side is observed also for K^2 = 0.56 a.u. This molecular orientation effect observed in non-dipole regime offers a challenge to scattering theory as the influences of anisotropic molecular potential and the outgoing-wave boundary condition have to be correctly taken into account for describing the asymmetry [2].

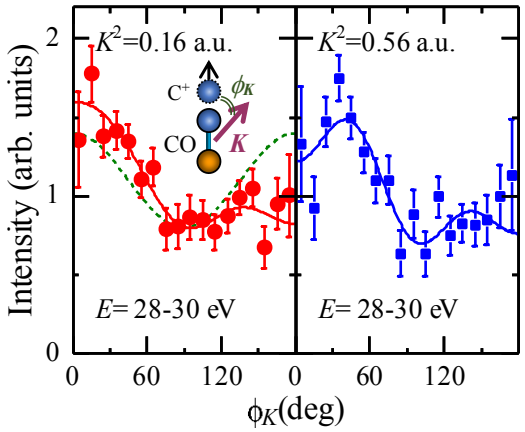

Figure 1. Molecular orientation dependence of the $3^2\Pi$ ionization. Dashed line is the associated photoion angular distribution with respect to the polarization vector [4].

References

[1] Watanabe N *et al* 2019 *Phys. Rev. A* **99** 022704
[2] Watanabe N and Takahashi M 2020 *J. Chem. Phys.* **152** 164301
[3] Watanabe N *et al* 2018 *Rev. Sci. Instrum.* **89** 043105
[4] Lebech M *et al* 2009 *J. Chem. Phys.* **130** 194307

* E-mail: noboru.watanabe.e2@tohoku.ac.jp

Electron scattering by molecules relevant to plasma processing

P A S Randi*, G M Moreira and M H F Bettega†

Departamento de Física, Universidade Federal do Paraná, Curitiba, 81531-980, Brazil

Synopsis We present the elastic momentum-transfer cross section for the scattering of low energy electrons by $Si(CH_3)_4$, $Ge(CH_3)_4$, $SnCl_4$ and $Ga(CH_3)_3$. The scattering amplitudes were calculated with the Schwinger multichannel method implemented with norm-conserving pseudopotentials. Some features of the calculated cross sections, such as shape resonances and Ramsauer-Townsend minimum, are discussed.

Plasma environments are rich in low-energy electrons and are used in many modern manufacturing techniques. For instance, in plasma-enhanced chemical vapor deposition (PECVD) a plasma is used to dissociate precursor molecules and deposit its constituents onto a substrate [1]. $Si(CH_3)_4$, $Ge(CH_3)_4$, $SnCl_4$ and $Ga(CH_3)_3$ are used as such precursor molecules. Therefore, the interaction between low-energy electrons and these molecules play a key role in these techniques.

In this work, we present the elastic integral, differential and momentum transfer cross sections for the scattering of low-energy electrons by $Si(CH_3)_4$, $Ge(CH_3)_4$ [2], $SnCl_4$ [3] and $Ga(CH_3)_3$. The scattering amplitudes were calculated with the Schwinger multichannel method implemented with norm-conserving pseudopotentials [4] in the static exchange approximation for $Ga(CH_3)_3$ (where we omit all polarization effects of the molecular target) and in the static exchange plus polarization approximation for $Si(CH_3)_4$, $Ge(CH_3)_4$ and $SnCl_4$.

The momentum transfer cross sections (MTCSs) for $Si(CH_3)_4$, $Ge(CH_3)_4$, $Ga(CH_3)_3$ and $SnCl_4$ are presented in Figure 1. Each system shows resonant structures in the calculated MTCS. The low energy behavior of the s-wave cross sections and eigenphases supports the presence of a Ramsauer–Townsend (RT) minimum for $Si(CH_3)_4$, $Ge(CH_3)_4$ and $SnCl_4$. The position of the resonances and the RT minimum are summarized in Table 1. We also compare our results for $Si(CH_3)_4$, $Ge(CH_3)_4$ and $SnCl_4$ with the total cross sections (TCS) measurements of Stefanowska-Tur *et al.* [5] and Możejko *et al.* [6], finding a good agreement.

*E-mail: pasr@fisica.ufpr.br
†E-mail: bettega@fisica.ufpr.br

Table 1. Position of the resonances and the RT minimum found in the calculated MTCS, s-wave cross sections and eigenphases (in eV).

Molecules	Resonances	RT
$Si(CH_3)_4$	6.0	0.32
$Ge(CH_3)_4$	6.0	0.40
$SnCl_4$	1.2, 5.6	0.10
$Ga(CH_3)_3$	2.2, 9.0	–

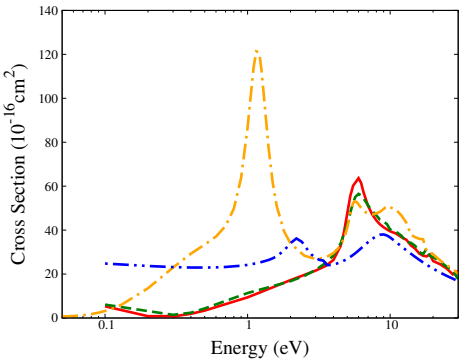

Figure 1. MTCS for $Si(CH_3)_4$, solid red line; $Ge(CH_3)_4$, dotted olive line; $SnCl_4$, dot-dashed orange line and $Ga(CH_3)_3$, blue dot-dot-dashed line.

References

[1] Lieberman M A and Lichtenberg A J 2005 *Principles of Plasma Discharges and Materials Processing* (John Wiley & Sons)
[2] Randi P A S *et al* 2020 *Phys. Rev. A.* **102** 022812
[3] Randi P A S and Bettega M H F 2020 *J. Appl. Phys.* **127** 233301
[4] da Costa R F *et al* 2015 *Eur. Phys. J. D.* **69** 012069
[5] Stefanowska-Tur S *et al* 2019 *J. Chem. Phys.* **150** 094303
[6] Możejko P *et al* 2019 *J. Chem. Phys.* **151** 064305

Bulk water effect upon π_1^* orbital of the 1-methyl-4-nitroimidazole

M B Kiataki[1], K Coutinho[1]* and M T do N Varella[1] †

[1]Instituto de Física da Universidade de São Paulo, Rua do Matão 1731, 05508-090, São Paulo, SP, Brazil

Synopsis We have investigated the effect of bulk water upon π_1^* virtual orbital of the 1-methyl-4-nitroimidazole (1M4N). Monte Carlo simulations were performed to generate liquid configurations comprised of one 1M4N surrounded by 1000 molecules of water. Quantum mechanics/molecular mechanics (QM/MM) calculations were carried out for different QM region sizes. Overall, the polarization of the QM region due to the presence of external MM solvent proved to be important.

Radiosensitizers, such as nitroimidazolic compounds [1], are chemical compounds used to improve the efficiency of radiotherapy in cancer treatment. Low-energy electrons, abundant species generated by the incident radiation in the biological medium, can attach into radiosensitizing drugs forming transient anion states (resonances), which in turn, can induce bond cleavages, producing chemically reactive species precursors to DNA damage. A resonance is typically formed when the incident electron is temporarily trapped by the target molecule into some virtual orbital. The electron attachment process can also form a non-decomposed parent anion which may play an important role in the radiosensitising effect of nitroimidazolic compounds [2].

Water solvent effects upon electron attachment and dissociation processes are under investigation in the last years and significant differences between isolated and solvated systems have been observed [2, 3]. A complete understanding of the aqueous environment's effects upon the physical and chemical properties of molecules is still necessary. QM/MM methods have been employed in several studies to investigate bulk solvent effects upon the physical and chemical properties of molecules.

In the present study, we have investigated the bulk water effect upon the virtual orbital π_1^* of the 1M4N. Metropolis Monte Carlo simulations were carried out in normal conditions of temperature and pressure, to generate liquid configurations comprised of one 1M4N surrounded by 1000 water molecules. We obtained from these liquid simulations different statistically uncorrelated configurations where hydrogen bonds between 1M4N and water molecules were present.

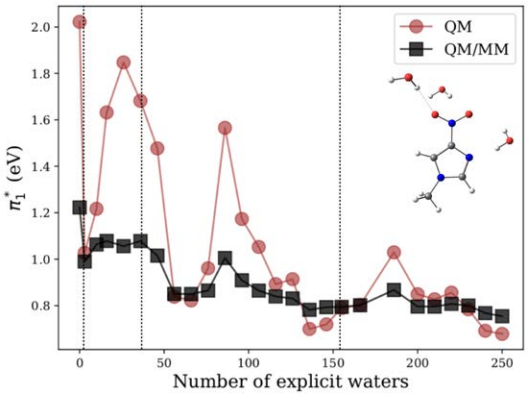

Figure 1. π_1^* orbital energy of the 1M4N according to QM region. Brown circles: only QM calculation. Black squares: QM/MM calculation. Vertical dotted lines indicate the solvation shells.

Figure 1 shows the results of the QM and QM/MM (electrostatic embedding) calculations for different QM regions of the representative configuration. The bulk water effect taken into account with the QM/MM approach proved to be important.

References

[1] P. Wardman 2007 *Clin. Oncol.* **19** 397
[2] R. Meiner *et al* 2019 *Nat. Commun.* **10** 2388
[3] J. Kohanoff *et al* 2017 *J. Phys.: Condens. Matter* **29** 383001

*E-mail: kaline@if.usp.br
†E-mail: mvarella@if.usp.br

Design of a charged particle transport method using electrostatic field

K Okutsu[1*], T Yamashita[1], Y Kino[1], R Nakashima[1], K Miyashita[1], K Yasuda[1], S Okada[2], M Sato[2], T Oka[3], N Kawamura[4], S Kanda[4], K Shimomura[4], P Strasser[4], S Takeshita[4], M Tampo[4], S Doiuchi[4], Y Nagatani[4], H Natori[4], S Nishimura[4], A D Pant[4], Y Miyake[4], K Ishida[5]

[1]Tohoku University, Sendai, 980-8578, Japan
[2]Chubu University, Kasugai, 487-8501, Japan
[3]Japan Atomic Energy Agency (JAEA), Tokai, 319-1184, Japan
[4]High Energy Accelerator Research Organization (KEK), Tsukuba, 305-0801, Japan
[5]RIKEN, Wako, 351-0198, Japan

Synopsis A charged particle transport method gathering and transporting the charged particle emitted from the surface was developed. The method is especially effective for particles emitted isotopically from the surface, which was difficult to focus or gather for increase in the yield rate with usual methods. Utilizing the merit of the method, we applied it to transportation of the "recycling muon" released from the solid deuterium thin layer after the muon catalyzed fusion.

A negatively charged muon (μ) is one of the elementary particles with a mass 207 times larger than an electron and the same charge as the electron. It acts like a heavy electron in materials. The μ can form a muonic molecule with two hydrogen isotope nuclei. The molecule consisting of two deuterons (d) and μ, ddμ, is regarded as an analogous system of D_2^+ molecule, where the electron is replaced by μ; however, ddμ shows unique characteristics different from D_2^+. Due to the small spatial size of the ddμ molecule, a nuclear fusion (ddμ → ^{3}He + n + μ or p + t + μ) occurs inside the muonic molecule. This reaction is called muon-catalyzed fusion (μCF) [1] because the μ does not participate directly in the nuclear reaction but promotes the fusion reaction.

The "recycling muon" that is the muon released after the fusion plays a critical role in triggering the next fusion reaction. It is expected to have a continuous kinetic energy distribution of approximately 10 keV on average. This energy reflects the wavefunction of the ddμ at the moment of the fusion reaction because the muon in the muonic molecule is "liberated" almost as it is when the molecule immediately dissociates into fragments after the fusion. The observation of the recycling muon can directly provide rich information on few-body quantum mechanics.

The recycling muon could be extracted to the vacuum by using the solid deuterium thin layer [2]. However, it is difficult to distinguish the recycling muon with the scattered muon initially from the accelerator. Also, the solid deuterium could vaporize easily when the hot parts such as coils with high current applied is near by. In order to protect the cryogenic target and transport the recycling muon far away from the solid deuterium, we have developed a charged particle transport method consisting of a grounded tube and a center wire with high voltage applied (See figure 1) [3,4].

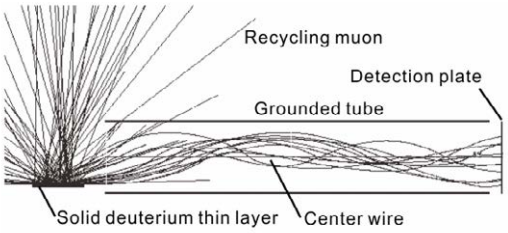

Figure 1. Simulated trajectories of recycling muon relased from the deuterium thin layer in which the muons from the accelerator stop and cause the muon cataliezed fusion.

References

[1] Froelich P 1992 *Adv. Phys.* **41** 405
[2] Strasser P *et al* 2000 *Nucl. Instr. Meth. Phys. Rev. A* **460** 451
[3] Nagatani Y *et al* Japanese patent application No. 2020-178286
[4] Okutsu K *et al Fusion Engineering and Design* submitted

A Science Gateway for Atomic and Molecular Physics: Democratizing Atomic and Molecular Physics Research and Education

B I Schneider[1]*, S Pamidighantam[2], A Scrinzi[3], K R Hamilton[4], K Bartschat[4], O Zatsarinny[4], I Bray[5], L D Carr[6], J D Gorfinkiel[7], F Martin[8], J G Vasquez[8], R R Lucchese[9], A C Brown[10], C F Fischer[11], N Douguet[12], and S F dos Santos[13]

[1]National Institute of Standards and Technology, [2]Indiana University, [3]Ludwig-Maximilians-University, [4]Drake University, [5]Curtin University, [6]Colorado School of Mines, [7]Open University, [8]University of Madrid, [9]Lawrence Berkeley Laboratory, [10]Queens University, [11]University of British Columbia, [12]Kennesaw State University, [13]Rollins College

Synopsis The objective of this project is to create a comprehensive and long-lasting cyberinfrastructure (CI) for the atomic and molecular physics (AMP) community, where practitioners can access a synergistic, full-scope platform for computational AMP through the AMPGateway.

The creation of a comprehensive cyberinfrastructure (CI) for atomic and molecular physics (AMP), where the AMP community can simply access and directly use a broad range of computational tools for research and education, has the potential of transforming the way AMP is conducted [1]. These state-of-the-art resources become available to a much larger set of practitioners and students, which has the effect of democratizing research and education in AMP. The AMPGateway is currently hosting nine state-of-the-art AMP software suites. It is powered by an advanced CI enabling a flexible and easy-to-use platform for the broad AMP community. The gateway-hosted AMP applications are contributed by an internationally recognized group of AMP theorists who have developed best-of-breed approaches for computing atomic/ionic structure, electron collision/photoionization cross sections, and control of atomic and molecular systems by laser-atom/molecule interactions.

The AMP scientific group is complemented by experts in CI and computational science capable of delivering advanced CI and high-performance computing integration expertise to the broader AMP community, an end-user base of over 3,000 in the American Physical Society's Division of Atomic, Molecular, and Optical Physics (DAMOP) alone. The combined efforts of the group will enable a significantly larger fraction of the AMP community to perform AMP science at a level currently only available to a few isolated groups. Without such a coordinated and combined effort, it is unlikely for this ambitious project to succeed. The group is dedicated to making the AMPGateway the premier CI for researchers, students, and educators interested in AMP.

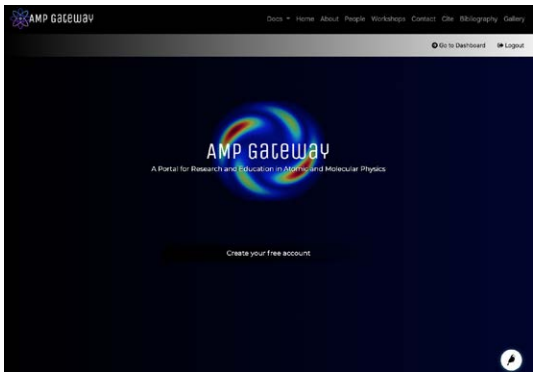

Figure 1. The website for the AMPGateway [2].

References

[1] Schneider B I, Bartschat K, Zatsarinny O, Hamilton K R, Bray I, Scrinzi A, Martın F, Vasquez J G, Tennyson J, Gorfinkiel J D, Lucchese R R and Pamidighantam S 2020 *Proc. PEARC20* Atomic and Molecular Scattering Applications in an Apache Airavata Science Gateway

[2] Atomic and Molecular Physics Science Gateway

*E-mail: bis@nist.gov

On the stability of the aromatic molecules benzonitrile and toluene under electron impact in Titan´s atmosphere

Wania Wolff[1],* Lucia H Coutinho[1], Fabio de A. Ribeiro[2], Diana P. Andrade[3], Gerhard Hilgers[4], and Volker Dangendorf[4]

[1]Physics Institute, Federal University of Rio de Janeiro, Rio de Janeiro, 21941-972, Brazil
[2]Federal Institute of Rio de Janeiro, Rio de Janeiro, 26530-060, Brazil
[3]Observatorio do Valongo, Federal University of Rio de Janeiro, Rio de Janeiro, 20080-090, Brazil
[4]Physikalisch-Technische Bundesanstalt (PTB), Bundesallee 100 Braunschweig D-38116 Germany

Synopsis We present experimental rate of formation constant of fragment ionic species and the half-life of the aromatic molecules benzonitrile and toluene, proxy for benzene the most well-known aromatic hydrocarbon identified in Titan's upper atmosphere. Data from the Cassini and Voyager flyby of Titan show that the magnetosphere electron flux is the major source of the ionization of neutrals in the moon's nightside ionosphere. We estimate half-lifes that suggest that benzonitrile as well as toluene exist at relative abundances.

We report an experimental study motivated by the detection of the aromatic molecule benzonitrile (BN) within the interstellar Taurus Molecular Cloud using radio astronomy [1] and the prediction of relative abundances of toluene (MeB) in Titan, Saturn's largest moon [2]. Titan spends about 95 percent of the time within Saturn's magnetosphere and super-thermal electron populations can precipitate along the magnetic field lines into its dense atmosphere.

Multiple Titan encounters by the Voyager and Cassini missions have shown that the ionization of neutrals by precipitation of these magnetospheric electrons into the upper atmosphere of Titan [3] is the major source of the nightside ionosphere, at least for altitudes above 1000 km.

Large abundances of ions just below and above 100 amu were measured by the plasma spectrometer's ion beam sensor during Cassini spacecraft encounters with Titan's upper atmosphere [4]. Chemical models incorporating neutral and/or ion chemistry have been created to explain the observed ion densities. Therefore, experiments are called for to improve the chemistry of molecules including aromatics at Titan.

In order to assess the stability of benzonitrile and toluene under electron impact in Titan's atmosphere, time of flight mass spectrometry experiments have been performed, using a pulsed electron gun to produce electrons at energies from 20 eV up to 2000 eV. Within this electron energy range spectral electron fluxes were measured by Cassini Plasma Spectrometer-Electron Spectrometer at altitudes ranging from 1000 to 2700 km [3]. To our knowledge, ionization and fragmentation data of BN in this wide electron energy range are not available in the literature.

Using the derived results, we were able to quantify the abundance of benzonitrile and toluene ionic fragments, and estimate the formation rate constant of these fragments and the half-life of the molecules in dependence of the electron impact energy and the altitude in Titan´s ionosphere. The results confirm previous results which suggest that BN and MeB can be considered as a proxy for benzene, the most well-known aromatic hydrocarbon identified in Titan's upper atmosphere [4] as well in the cold interstellar medium (ISM) [1]. Similar approach will be extended to other aromatic molecules and other moons of the solar planets.

References

[1] McGuire B A *et al* 2018 *Science* **359** 202–205
[2] Loison J C *et al* 2019 *Icarus* **259** 55-71
[3] Richard M S *et al* 2015 *Journal of Geophysics Research and Space Physics* **120** 1-18
[4] Crary F J *et al* 2009 *Planetary and Space Science* **57** 1847–1856

*E-mail: wania@if.ufrj.br

Free wave packet model vs semi-classical model for the energy loss distribution of light particles in plasmas

Claudio Archubi* [1], **Diego Arbó*** [2], **and Nestor R. Arista**†

* Instituto de Astronomía y Física del Espacio, Universidad de Buenos Aires, Ciudad Universitaria, 1428 Buenos Aires, Argentina
† División Colisiones Atómicas, Centro Atómico Bariloche, 8400 S. C. Bariloche, Argentina,

Synopsis We present a free wave packet model approach to describe the interaction of positrons and electrons with an electron gas that applies to arbitrary values of densities and temperatures, covering the whole nonrelativistic range of projectile energies. We compare the results with those raising from an extension of the Peter-Meyer [1] classical stopping model for plasmas. We analyze cases of interest for fusion and astrophysical studies.

In this work, we propose a free wave packet model (FWPM) to evaluate the three moments of the energy loss distribution of positrons and electrons traversing a hot and dense electron gas, including energy losses, mean free paths, straggling and thermalization ranges. To formulate this method, we introduce modifications to our wave-packet method for light targets [2-3], which allows us to describe changes in target density and temperature.

We compare the results of this method with semi-classical (SM) results obtained from modificating the Peter-Mayer classical stopping model. We perform these modifications extending the classical scheme to calculate the different moments of the energy-loss distribution and introducing quantum restrictions to the behaviour of light projectiles traversing a hot electron gas. In the case of electrons these restrictions arise from the Pauli's principle, the electronic correlations between the projectile and the target electrons, the statistics of identical particles and quantum aspects of the interactions and energy loss of charged particles in cold solids [4] and hot plasmas [2]. The purpose is to evaluate the contributions of free electrons to the energy loss distribution of light particles traversing an electron gas on an extensive range of parameters that include low, intermediate, and high energies, with densities and temperatures going from normal laboratory conditions to very high values, such as those of interest for inertial fusion and astrophysical studies.

Figure 1 shows a comparison between SM and FWPM results for the stopping of positrons when increasing the temperature, showing both models an increase of the stopping with temperature for high velocities.

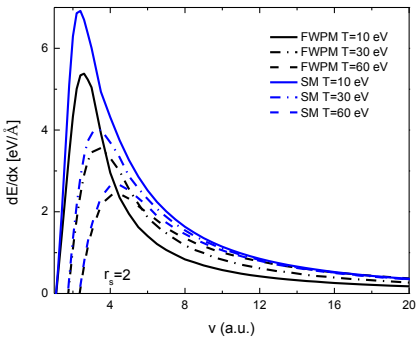

Figure 1. Stopping power for positrons traversing a hot electron gas with r_s=2 for different temperatures as a function of the projectile velocity.

References

[1] T. Peter and J. Meyer-ter-Vehn 1991 *Phys Rev A* 43 1998
[2] C. D. Archubi and N. R. Arista 2020 *Phys Rev A* 102 052811
[3] C. D. Archubi and N. R. Arista, *Rufus Ritchie, A gentleman and a Scholar*, *Advances in Quantum Chemistry*, edited by J. Sabin and J. Oddershede (Academic Press, New York, 2019), Vol 80, Chap. 10, pp. 247-269.
[4] C. D. Archubi and N. R. Arista 2017 *Eur. Phys. J.B.* 90: 18

[1] E-mail: archubi@iafe.uba.ar
[2] E-mail: diego@iafe.uba.ar

Generation of twisted photons by charged particles in cholesteric liquid crystals with large pitch

O V Bogdanov[1,2]*, P O Kazinski[1], P S Korolev[1] and G Yu Lazarenko[1]

[1]Physics Faculty, Tomsk State University, Tomsk, 634050, Russia
[2]Tomsk Polytechnic University, Tomsk, 634050, Russia

Synopsis We study the radiation from charged particles crossing a cholesteric plate in the shortwave approximation where the wavelength of photons is much smaller than the pitch of the cholesteric helix. It is shown that in the paraxial shortwave regime the main part of radiated photons is linearly polarized with the projection of the orbital angular momentum $l = \pm 1$. As the examples, we consider the production of 6.3 eV twisted photons from uranium nuclei and the production of X-ray twisted photons from 120 MeV electrons

The vortex waves are called the electromagnetic waves with a helical phase front characterized by the phase dependence of the form $e^{il\varphi}$, where l is the projection of the orbital angular momentum (OAM) and φ is the azimuthal angle. Evolving in time, this wave front twists around the average direction of propagation of the electromagnetic wave and so these waves are also referred to as twisted ones [1]. The notion of twisted waves is generalized to the nonparaxial regime where the photons constituting such a wave possess the projection of the total angular momentum m and the helicity s. Because of their peculiar properties, the twisted photons found many applications in physics, biology, and telecommunication technologies [2]. To take advantage of the properties of twisted photons in various fields of fundamental science and technology, there is a pressing need in the development of new pure bright sources of twisted photons in various spectral ranges.

It was shown in [3] that the use of helical media allows one to produce the twisted photons with large values of OAM in transition radiation. In the present paper, we apply the shortwave approximation [4] to describe the radiation of photons produced by charged particles moving rectilinearly in the cholesteric liquid crystal (CLC) plate of a finite width.

The CLCs are a particular case of a helical medium with the permittivity tensor of the form

$$\varepsilon_{ij}(k_0, z) = \varepsilon_\perp(k_0)\delta_{ij} + (\varepsilon_\parallel(k_0) - \varepsilon_\perp(k_0))\tau_i(z)\tau_j(z), \quad (1)$$

where $\boldsymbol{\tau}(z) = (\cos(qz), \sin(qz), 0)$ is the director, $\varepsilon_\parallel$ is the permittivity along $\boldsymbol{\tau}(z)$, and $\varepsilon_\perp$ is the permittivity in the direction perpendicular to it. The period of variations of the director, $2\pi/q$, is the helix pitch of the CLC. For the different CLCs, it varies from dozens of angstroms to several micrometers [5].

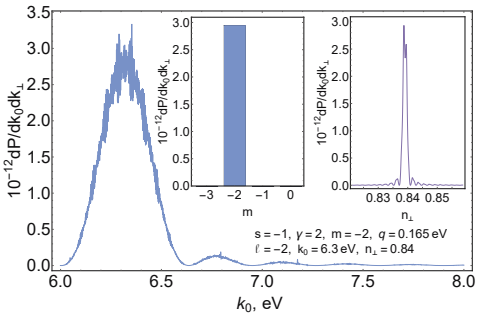

Figure 1. Transition radiation of twisted photons from the ions $^{238}U^{92+}$ traversing normally the CLC plate.

As is seen from Fig. 1, transition radiation from a charged particle traversing normally the CLC plate is a pure source of twisted photons with the projection of the total angular momentum $m = -2$. In the paraxial regime, $n_\perp = \sin\theta \ll 1$, we have $l = m - s$.

This work was supported by the Russian Science Foundation (Project No. 17-72-20013).

References

[1] Molina-Terriza G *et al* 2007 *Nature Phys.* **3** 305
[2] Rubinsztein-Dunlop H *et al* 2017 *J. Opt.* **19** 013001
[3] Bogdanov O V *et al* 2019 *Phys. Rev. A* **100** 043836
[4] Aksenova E V *et al* 2001 *Opt. Spectrosc.* **91** 969
[5] Belyakov V 2019 *Diffraction Optics of Complex-Structured Periodic Media* (Springer: Cham, Switzerland)

*E-mail: bov@tpu.ru

Four-body calculation of muonic molecular resonances in the electron cloud

K Yasuda[1]*, T Yamashita[1,2], K Okutsu[1] and Y Kino[1]

[1]Department of Chemistry, Tohoku University, Sendai, 980-8578, Japan
[2]Institute for Excellence in Higher Education, Tohoku University, Sendai, 980-8576, Japan

Synopsis We investigate muon molecular resonance states (dtμ^*e) is embedded in an electron cloud with a four-body (d, t, μ and e) calculation. This system would take part in the muon-catalyzed fusion cycle because dtμ^* can be formed through the same process as the bound state dtμ. Our precise four-body variational calculation reveals that the resonant states shrink by the electron cloud. We also discuss the radiative dissociation of dtμ^* as well.

A negative muon (μ) binds more tightly nuclei than an electron because the muon mass is 207 times heavier than electron mass. The sizes of muonic atoms/molecules are about 200 times smaller than electron ones. When a μ binds a deuteron d and a triton t and forms muonic molecule dtμ, tails of the two nucleus wavefunctions overlap so that the nuclear fusion reaction occurs. This phenomenon is called muon-catalyzed fusion (μCF) [1], where μ is not directly involved in the nuclear reaction but acts as a catalyst.

The dtμ is considered to be formed in the D_2 molecule by the collision between t$\mu(1s)$ and D_2 (tμ + D_2 $\rightarrow$ [dtμ]e-de), which is called the Vesman mechanism [3]. A similar process for the excited tμ would be allowed, t$\mu(n = 2)$ + D_2 $\rightarrow$ [dtμ^*]e-de, where dtμ^* is a resonance state of dtμ. The latter process appears in the μCF side-path model [2] and would be indispensable in the comprehensive understanding of the μCF. While a number of calculations of dtμ and dtμ^* have been reported so far, few studies have considered the effect that the molecule exists in the electron cloud. However, even in the case of dtμ in the electron cloud, the binding energy of surrounding electron slightly changes due to the finite size of the dtμ [4]. Since the size of the dtμ^* is much larger than dtμ, and the binding would change more.

Recently we reported a four-body variational calculation of d, t, μ and e system to study the energy shift for dtμ in the electron cloud [5]. In the present work, we adopt the similar approach to dtμ^* in the electron cloud (denoting the system as dtμ^*e). The wavefunction is described using the Gaussian expansion method [6]. We introduce two types of configurations. One consists of dtμ^* subsystem and e (Type I), and other consists of subsystem of tμ and de (Type II). The Gaussian basis functions are described with the Jacobian coordinates based on the configurations.

*E-mail: kazuhiro.yasuda.p7@dc.tohoku.ac.jp

Table 1 shows the resonance energies of dtμ^*e (v = 7–9) calculated with the different sets of basis functions and energy shifts due to addition of Type II basis sets to Type I. Since the main component of the dtμ^* is dtμ^* + e, the dtμ^* which can be formed by the Vesman mechanism, the contribution from the Type II basis sets is not negligible because their energy levels are close to the brake-up threshold energy of t$\mu(1s)$ + de(nl). The energy shifts are 0.2–0.7 eV which are critical value in the Vesman mechanism. Thus, the improvement of the energy levels can contribute to analysis of the μCF cycle rate with the side-path model. Utilizing the complex coordinate rotation method [7, 8], we will also report the stability of dtμ^*e against the radiative dissociation process, dtμ^*e $\rightarrow$ t$\mu(1s)$ + de(nl) + γ.

Table 1. Resonance energies (eV) of dtμ^*e (J = 0) calculated by Type I basis sets and Type I + II ones. v denotes vibrational quantum number. The energy in parentheses denotes the energy above the threshold energy of t$\mu(n = 2)$+de$(1s)$, −691.416.

v	Type I	Type I + II	Shift
7	−693.923	−694.206	0.283
8	−692.070	−692.535	0.465
9	(−690.919)	−691.686	0.767

References

[1] Froelich P 1992 *Adv. Phys.* **41** 405
[2] Froelich P *et al* 1995 *Phys. Rev. Lett.* **75** 2108
[3] Vesman E A 1967 *Pis'ma Zh. Eksp. Teor. Fiz.* **5** 113 [1967 *JETP Lett.* **5** 91]
[4] Harston M R *et al* 1997 . *Phys. Rev. A* **56** 2685
[5] Niiyama M *et al* 2020 *J. Phys.: Conf. Ser.* **1412** 222013
[6] Hiyama E *et al* 2003 *Prog. Part. Nucl. Phys.* **51** 223
[7] Ho Y K 1983 *Phys. Rep.* **99** 1
[8] Buchleitner A *et al* 1994 *J. Phys. B: At. Mol. Opt. Phys.***27** 2663

Absolute Rate Coefficients for Dielectronic Recombination of Na-like Kr^{25+}

Z. K. Huang[1], W. Q. Wen[1*], S. X. Wang[2], N. Khan[1], H. B. Wang[1], C. Y. Chen[3], C. Y. Zhang[3], S. P. Preval[4], N. R. Badnell[5], W. L, Ma[2], X. Liu[1], D. Y. Chen[1], D. M. Zhao[1], L. J. Mao[1], X. M. Ma[1], J. Li[1], M. T. Tang[1], R. S. Mao[1], D. Y. Yin[1], W. Q. Yang[1], J. C. Yang[1], Y. J. Yuan[1], L. F. Zhu[2] and X. Ma[1†]

[1] *Institute of Modern Physics, Chinese Academy of Sciences, 730000, Lanzhou, China*
[2] *Hefei National Laboratory for Physical Sciences at Microscale, Department of Modern Physics, University of Science and Technology of China, 230026, Hefei, China*
[3] *Shanghai EBIT Laboratory, Institute of Modern Physics, Fudan University, and the Key Laboratory of Applied Ion Beam Physics, Chinese Ministry of Education, Shanghai 200433, China*
[4] *Department of Physics and Astronomy, University of Leicester, Leicester, LE1 7RH, UK*
[5] *Department of Physics, University of Strathclyde, Glasgow, G4 0NG, UK*

Synopsis Absolute dielectronic recombination (DR) rate coefficients for sodium-like Kr^{25+} have been measured at the storage ring CSRm at the Institute of Modern Physics, Lanzhou. The measured DR spectrum covers the energy of 0-70 eV and the Δn=1 DR resonances were found surprisingly strong contributed therein. All the DR resonances are carefully identified and compared with the theoretical calculations and good agreement can be achieved only by carefully considering the strong mixing among the low-energy Δn=0 and Δn=1 DR resonances.

The precision DR rate coefficients for sodium-like Kr^{25+} ions are of great importance in interpreting the observed emission-lines from the ionized krypton ions in fusion plasmas and testing the reliability of atomic structure calculations. As shown in figure 1, we have measured the precision DR spectrum of Na-like Kr^{25+} and compared with the theoretical calculations by using FAC and AUTOSTRUCTURE codes. In addition to the DR resonances due to $3s \rightarrow 3p$ and $3s \rightarrow 3d$ ($\Delta n=0$), the DR resonances associated with the $3s \rightarrow 4l$ ($\Delta n=1$) core excitations were found surprisingly strong contributed in the measured DR rate coefficients. By considering the strong mixing effects among the low-energy DR resonances associated with $\Delta n=0$ and $\Delta n=1$ core excitation in both calculations, a good agreement has been achieved between the experimental results and the theoretical calculations. The temperature dependent plasma recombination rate coefficients have been obtained by convolved the experimentally-derived DR spectrum with a Maxwellian-Boltzmann distribution and then compared with previously available results from the literature. The present experimental result yields a precise plasma rate coefficients at the low temperature range up to ~ 1×10^6 K thus provide a benchmark for use in astrophysical and laboratory plasma modelling. For the high temperature above 2×10^6 K, which is out of the scope of present measurements, the calculated data by Altun et al. (2006) can still provide the reliable plasma rate coefficients.

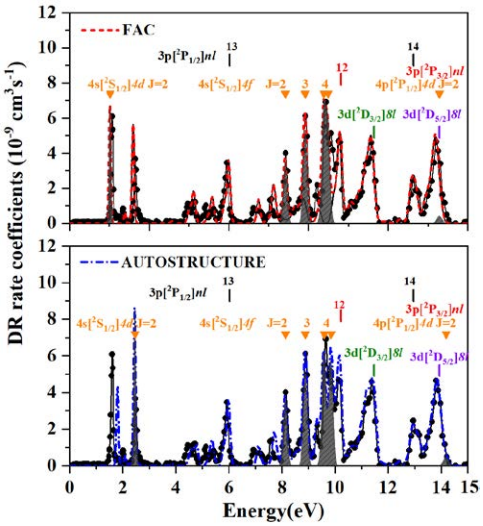

Figure 1. Detailed comparison between the FAC code (upper panel) and AUTOSTRUCTURE (lower panel) calculated and measured DR rate coefficients of Na-like Kr^{25+} within the energy rage of 0-15 eV. The connected black circles are the measured DR spectrum with background subtracted. The dashed red and dash-dotted blue curves are the FAC and AUTOSTRUCTURE calculated DR rate coefficient. The gray areas give the DR rate coefficient associated with $3l \rightarrow 4l$ ($\Delta n=1$) core excitation.

References

[1] Z.K. Huang, W.Q. Wen, S.X. Wang, et al., *Phys. Rev. A*, **102**, 062823 (2020).

* E-mail: wenweiqiang@impcas.ac.cn
† E-mail: x.ma@impcas.ac.cn

Electronic excitation spectra of cerium oxides: an ab initio–informed study supported by Monte Carlo transport simulations

P de Vera[1]*, A Pedrielli[1], N Pugno[2], P E Trevisanutto[1], R Garcia-Molina[4], I Abril[3], M Dapor[1], and S Taioli[1]

[1]European Centre for Theoretical Studies in Nuclear Physics and Related Areas (ECT*-FBK) and Trento Institute for Fundamental Physics and Applications (TIFPA- INFN), Trento, 38123, Italy
[2]Laboratory of Bio-inspired, Bionic, Nano, Meta Materials & Mechanics, Department of Civil, Environmental and Mechanical Engineering, University of Trento, Trento, 38122, Italy
[3]Departament de Física Aplicada, Universitat d'Alacant, Alacant, 03080, Spain
[4]Departamento de Física, Centro de Investigación en Óptica y Nanofísica, Universidad de Murcia, Murcia, 30100, Spain

Synopsis Cerium oxides present promising applications ranging from fuel cells to catalysis or nanoparticle radiosensitization in cancer treatment. Their implementation requires a precise description of electron transport. Here, TDDFT calculations of the electronic properties of the two stable oxides CeO_2 and Ce_2O_3 are reported, which are used to obtain inelastic cross sections for electrons, whose transport is described by Monte Carlo simulations. The good agreement with available REELS experiments validates the TDDFT calculated spectra.

Cerium oxides are materials relevant in many applications ranging from fuel cells to catalysis [1], to nanoparticle radiosensitization for cancer radiotherapy [2]. A precise knowledge of their electronic properties is essential for these applications and, in particular, to understand the electron production and propagation through them.

In this work, we report linear-response time-dependent density functional theory (TDDFT) calculations of the complex dielectric function of the two stable oxides CeO_2 and Ce_2O_3 over a wide range of energy and momentum transfers. For CeO_2, the agreement with experimental optical data is remarkable, while experimental information for Ce_2O_3 is scarcer. The TDDFT results can be combined with the dielectric formalism to produce reliable differential and total electronic cross sections in condensed matter, which then can feed detailed Monte Carlo simulations [3].

This strategy has been followed to test the calculated electronic spectra by comparison with experimental reflection electron energy loss spectroscopy (REELS) measurements in these materials [4]. The results, depicted in Fig. 1, show that the main features of the REELS can be interpreted in terms of the CeO_2 and Ce_2O_3 spectra. The position of the most intense energy loss peaks correspond mainly to Ce_2O_3, while lower energy loss structures point out to the coexistence of CeO_2 and Ce_2O_3 phases in the measured samples, which is a situation typically encountered in sputtered-cleaned metal oxides. The fair agreement of the simulated and experimental REELS supports the TDDFT calculated electronic properties of cerium oxides.

*E-mail: pdeveragomis@ectstar.eu

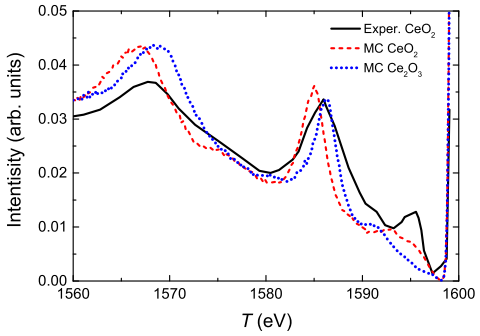

Figure 1. Experimental REELS spectrum for 1.6 keV electrons in cerium oxide [4], together with present simulations in CeO_2 and Ce_2O_3.

References

[1] Gunasekar G H, Shin J, Jung K-D, Park K and Yoon S 2018 *ACS Catalysis* **8** 4346–4353
[2] McKinnon S, Guatelli S, Incerti S, Ivanchenko V, Konstantinov K, Corde S, Lerch M, Tehei M and Rosenfeld A 2016 *Physica Medica* **32** 1584–1593
[3] Taioli S, Trevisanutto P E, de Vera P, Simonucci S, Abril I, Garcia-Molina R and Dapor M 2021 *J. Phys. Chem. Lett.* **12** 487–493
[4] Pauly N, Yubero F, Espinós J P and Tougaard S 2017 *Applied Optics* **56** 6611–6621

Monte-Carlo simulations of electron emission from liquid water

K Wiciak-Pawłowska[1]*, J Franz[1,2]†, M Franz[1], P de Vera[3,5], S Taioli[3], M Dapor[3], I Abril[4], R Garcia-Molina[5]

[1]Faculty of Applied Physics and Mathematics, Gdańsk University of Technology, Gdańsk, 80-233, Poland
[2]Advanced Materials Center, Gdańsk University of Technology, Gdańsk, 80-233, Poland
[3]European Centre for Theoretical Studies in Nuclear Physics and Related Areas (ECT*), Trento, 38123, Italy
[4]Departament de Física Aplicada, Universitat d'Alacant, Alacant, 03080, Spain
[5]Departamento de Física - Centro de Investigación en Óptica y Nanofísica, Universidad de Murcia, Murcia, 30100, Spain

Synopsis We will present results from studies of the influence of different scattering models on the simulations of the secondary electron yield from liquid water after irradiation by a beam of energetic electrons.

For many applications in medical physics and radiation biology it is important to be able to model the transport and effects of electrons in liquid water. Physical quantities of interest include the range, the stopping power, the interaction volume and the secondary electron yield. Frequently Monte-Carlo simulation techniques are used to compute these quantities.

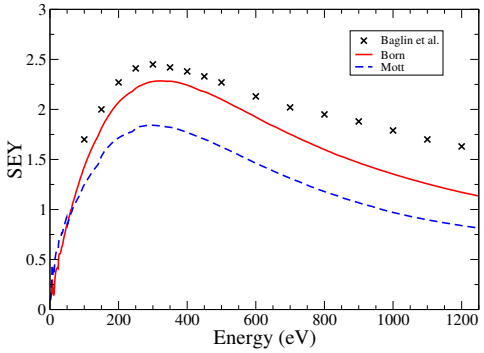

Figure 1. Secondary electron yields as functions of incident electron energy for different elastic scattering models and experiments by Baglin *et al.*[4].

In computer program packages for Monte-Carlo simulation (see e.g. Geant4-DNA [1]) the particles are tracked down until their kinetic energy is below a certain cutoff value. Recently Mehnaz et al. [2] have demonstrated that the choice of this cutoff threshold has a large influence on the computed secondary electron yield from liquid water. Therefore it is important to describe as accurately as possible the different interactions of electrons with water, particularly at low energies.

In this work we investigate the influence of different scattering models for elastic and inelastic collisions at low energies on the computed secondary electron yield (SEY). The simulations are performed with the Monte-Carlo simulation code SEED [3]. Preliminary results are shown in Figure 1 for the Born dipole model and the relativistic Mott model with interference terms together with the experimental results from Baglin *et al.*[4].

References

[1] Incerti S *et al.*, 2018 *Medical Physics* **45** 722
[2] Mehnaz *et al.*, 2020 *Medical Physics* **47** 759
[3] Dapor M, 2020 *Transport of Energetic Electrons in Solids, 3rd edition*, Springer-Nature, Cham/Switzerland
[4] Baglin V *et al.*, 2000 The secondary electron yield of technical materials and its variation with surface treatments, Proc. EPAC, Vienna, Austria.

*E-mail: wkpol@outlook.com
†E-mail: janfranz@pg.edu.pl

High resolution measurement of electronic K x rays from muonic atoms in metal

T Okumura[1]*, T Azuma[1], D A Bennet[2], P Caradonna[3], I Chiu[4], W B Doriese[2], M S Durkin[2], J W Fowler[2], J D Gard[2], T Hashimoto[5], R Hayakawa[6], G C Hilton[2], Y Ichinohe[7], P Indelicato[8], T Isobe[1], S Kanda[9], D Kato[10], M Katsuragawa[3], N Kawamura[9], Y Kino[11], K M Kubo[12], K Mine[3], Y Miyake[9], K M Morgan[2], K Ninomiya[4], H Noda[4], G C O'Neil[2], S Okada[13], K Okutsu[11], T Osawa[5], N Paul[8], C D Reintsema[2], D R Schmidt[2], K Shimomura[9], P Strasser[9], H Suda[6], D S Swetz[2], T Takahashi[3], S Takeda[3], S Takeshita[9], M Tampo[9], H Tatsuno[6], X M Tong[14], Y Ueno[1], J N Ullom[2], S Watanabe[15], and S. Yamada[7]

[1]RIKEN, Wako 3510198, Japan, [2]National Institute of Standards and Technology, Boulder, CO 80305, USA, [3]Kavli IPMU (WPI), Kashiwa 2778583, Japan, [4]Osaka University, Toyonaka 5600043, Japan, [5]Japan Atomic Energy Agency (JAEA), Tokai 3191184, Japan, [6]Tokyo Metropolitan University, Tokyo 1920397, Japan, [7]Rikkyo University, Tokyo 1718501, Japan, [8]Laboratoire Kastler Brossel, Sorbonne Université, CNRS, ENS-PSL Research University, Collège de France, Case 74, 4, place Jussieu, 75005 Paris, France, [9]High Energy Accelerator Research Organization (KEK), Tsukuba 3050801, Japan, [10]National Institute for Fusion Science (NIFS), Toki 5095292, Japan, [11]Tohoku University, Sendai 9808578, Japan, [12]International Christian University, Tokyo 1818585, Japan, [13]Chubu University, Kasugai 487-8501, Japan, [14]University of Tsukuba, Tsukuba 305-8573, Japan, [15]Japan Aerospace Exploration Agency (JAXA), Sagamihara 252-5210, Japan

Synopsis We observed asymmetric and broad peaks of electronic K x rays from muonic Fe by using state-of-the-art transition-edge sensor microcalorimeters. By comparing with simulation, we reveal that the observed peak profiles reflect the femtosecond dynamics of electrons in the muonic atom during the muon cascade.

A muonic atom consists of a negative muon and an atomic nucleus, sometimes accompanied by bound electrons. When a negative muon encounters an atom, the muon is captured in a highly excited state of the atom and then de-excites to lower energy levels step-by-step with emission of Auger electrons and muonic x rays. Electron holes formed during this cascade process are immediately filled by the upper-level electrons, e.g., via characteristic x-ray emission. In metals, electron filling from the surrounding atoms also occurs, while similar phenomena have been studied through the de-excitation dynamics of highly-charged ions in metal [1]. In this study, we measured electronic K x rays from muonic Fe (μFe) using Transition-Edge Sensor (TES) microcalorimeters at J-PARC [2]. The TES microcalorimeters are state-of-the-art x-ray detectors with a high-energy resolution of 5.2 eV FWHM for 6 keV x rays. As shown in Figure 1, we observed an asymmetric and broad peak of electronic $K\alpha$ x rays from μFe. This broad feature reflects the dynamics of the cascade process because the energies of the μFe K x rays are sensitive to the muon states and electron configurations at the moment of x-ray emission. We simulated the time evolution of the muon cascade considering all processes involved, particularly electron filling from the valence band of Fe. The result of the simulation, represented by the red curve in Fig. 1, shows good agreement with the experimental result.

*E-mail: takuma.okumura@riken.jp

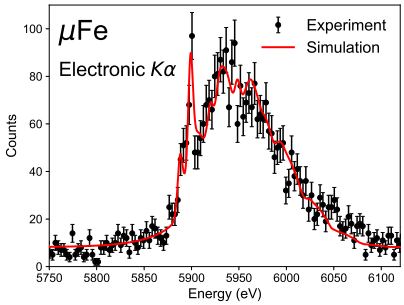

Figure 1. Electronic $K\alpha$ x rays from μFe.

References

[1] Arnau A *et al. Surf. Sci. Rep.* **27** 113.
[2] Okumura T *et al. Phys. Rev. Lett.* submitted.

Oscillator model: A new approach to study the interaction of external charged particle with 2D materials. Application to graphene.

S Segui[1,2]*, J L Gervasoni[1,2,3]†, Z L Mišković[4] and N R Arista[1,3]

[1] Centro Atómico Bariloche (CNEA), 8400 S. C. de Bariloche, Argentina.
[2] Consejo Nacional de Investigaciones Científicas y Técnicas (CONICET), Argentina.
[3] Instituto Balseiro (CNEA - UNCuyo), 8400 S. C. de Bariloche, Argentina.
[4] University of Waterloo, Waterloo, Ontario, Canada N2L 3G1.

Synopsis In this work we adapt the oscillators model approximation to calculate the energy loss of relativistic charged particles interacting with a 2D-material monolayer. We model the material as a monoatomic layer of electronic oscillators, and consider a wide range of incident energies for both parallel and perpendicular trajectories of the external particle. In particular, we apply the model to describe the case of electrons interacting with graphene.

In a recent work [1] we developed a comprehensive framework to calculate the energy loss of external charged particles interacting with a 2D material. We represent it as a planar array of harmonic oscillators, with isotropic or anisotropic electronic vibration modes of characteristic frequencies ω_i. The incident particle travels along a rectilinear trajectory either parallel or perpendicular to the layer, and transfers energy to the oscillators through its electromagnetic field. Using this simple model, we obtain several useful analytical expressions for the energy loss as a function of the relevant parameters of the process, such as the particle's velocity and the material's electronic density.

In this presentation, we apply this model to the case of graphene, using the anisotropic approach since its electrons (oscillators) are constrained to move within the monolayer plane. We consider two regimes of oscillators frequencies: the optical range, where the interband electron transitions give rise to the characteristic frequencies of the π and σ oscillators around 4 and 14 eV; and the THz range of frequencies, relevant for the case of doped graphene where intraband π-electrons excitations give raise to a strongly dispersing sheet plasmon-polariton mode [2]. In both regimes, we obtain the stopping power and total energy loss for parallel and perpendicular trajectories respectively.

In Figure 1, we plot the stopping power $\bar{S}$ for a particle traveling on a parallel trajectory at different values of impact parameter b_0 in terms of the reduced velocity $\beta = v/c$. We compare it with the DPP graphene model from reference [3], using an adequate normalization factor. We observe that the oscillators model is in very good agreement with the dielectric method on a wide range of velocities and impact parameters.

We remark that this versatile model gives a promising alternative to the description of the incident particle's energy loss process to study 2D materials with their respective distinctive properties.

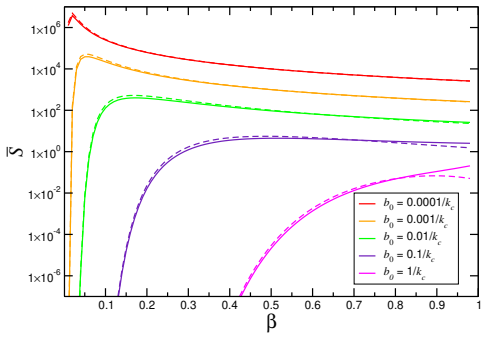

Figure 1. Stopping power (continuous lines) as a function of β in the THz regime. Calculations from ref. [3] (dashed lines) are included.

References

[1] Segui S *et al* 2021 *Nucl. Inst. Meth. B* **490** 18
[2] Mišković Z *et al* 2016 *Phys. Rev. B* **94** 125414
[3] Mišković Z *et al* 2018 *Nucl. Inst. Meth. B* **422** 18

*E-mail: segui@cab.cnea.gov.ar
†E-mail: gervason@cab.cnea.gov.ar

Interecations of electrons and positrons with two-dimensional proton lattice

M Al-Ajaleen[1,2] and K Tőkési [1, *]

[1]Institute for Nuclear Research (ATOMKI), Debrecen, 4026, Hungary
[2] Doctoral School of Physics, University of Debrecen, Debrecen, 4032, Hungary

Synopsis We present theoretical studies of electron and positron interaction with a two-dimensional proton lattice. The periodic proton lattice is generated artificially where the individual protons are fixed in the certain position. The electron and positron trajectories passing through these periodic multiple scattering object are calculated using a Classical Trajectory Monte Carlo method. We found characteristic periodic peak structure after the proton lattice. We analyze and discuss this behavior as a function of the distance between the protons in the lattice.

Two-dimensional (2D) materials are ideally composed of one atomic layer. Atoms in the layer may have a different function than internal atoms, and so the increase in the number of surface atoms leads to a change in the behavior of 2D materials. These materials are unique due to unprecedented properties that are unparalleled when compared to their bulky counterparts.
In this work we are working on the hypothetical ideal 2D lattice. The objects in the lattice are protons where the individual protons are fixed in the certain position. In this case we generate a special periodic multiple scattering object. Based on our model target the electron and positron scattering probabilities are studies. The obtained results may open new way later for the investigation of more realistic targets like graphene.
In this work we treat the collision problem in the framework of a classical trajectory Monte Carlo (CTMC) model. The CTMC method is a nonperturbativ method, where the classical equations of motion are solved numerically. In the present work the CTMC simulations were made in the many-body approximation, where all protons are interact with the projectile. The detail of the calculation procedure can be found in ref [1]. We followed $5x10^6$ primary trajectories for each collision systems. The lattice is uniform and has a constant separation between the protons. During our investigations the separations were 1, 2, 3 and 5 a.u. The projectile kinetic energies were 500 and 1000 eV.
We found characteristic periodic peak structure after the proton lattice (see figure 1.)

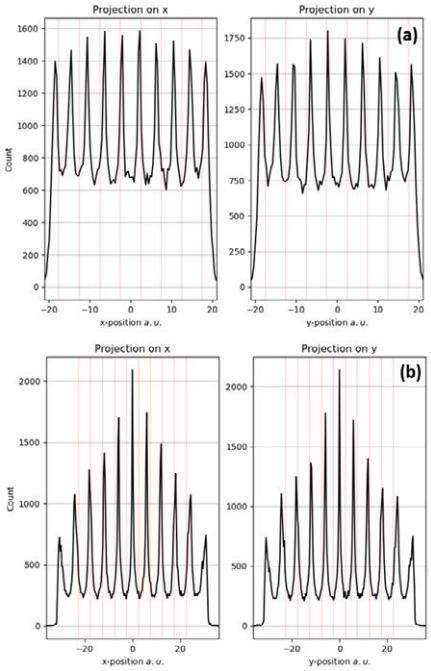

Figure 1. Electron (a), and positron (b) intensities at 50 au. from the lattice after after they passed the proton lattice with separation of 5 au. at 500 eV primary energy. Red lines show the positions of the protons.

This work has been carried out within the framework of the EUROfusion Consortium and has received funding from the Euratom research and training programme 2014-2018 and 2019-2020 under grant agreement No 633053. The views and opinions expressed herein do not necessarily reflect those of the European Commission.

References

[1] K Tőkési and G. Hock 1996 *J. Phys. B* **19** L119–L125.

* E-mail: tokesi@atomki.hu

Observation of quantum fluctuations via position to polarization converter

H Abbas[1,2]*, **T Frenholz**[2]†

[1] University Of Nottingham, Nottingham, NG7 2RD, UK
[2]Jazan University, Jazan, 45142, Saudi Arabia

Synopsis Hybrid quantum system is used to observe the quantum effects like quantum fluctuations. It consists of an optomechanical system where a micromechanical membrane is strongly coupled to a high finesse cavity using position to polarization converter and couple it into Rb atoms.

Hybrid quantum systems are a hot topic, especially transducers that allow us to interface the quantum noise properties of an object of one type to quantum noise properties of an object of another type. A micromechanical membrane coupled to an electromagnetic optical cavity is considered as a new frontier in quantum optics. This coupling gives an opportunity for connecting different quantum resources, manipulating the quantum state of light[1], studying quantum measurement back-action in the optical detection of macroscopic objects[2], and ultra sensitive force detectors [3]. The optomechanical system that is used is composed of a high-stress silicon nitride membrane that placed in the middle of a high finesse cavity. The membrane will have an effect on the behaviour of the cavity which is the focus of our measurements. One way to achieve this would be to measure the phase of the reflected beam from the optical cavity as function of the membrane position by interfering it with a reference beam which has a constant phase relation with the cavity beam. Thus, we can map the position onto polarization and couple the reflected beam to rubidium 87 atoms.

This hybrid quantum system can be used to generate entanglement between atoms and mechanical systems. Such a set-up could be used to facilitate long distance quantum communication, as well as inertial sensing schemes and many other possibilities.

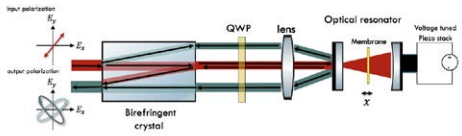

Figure 1. A design of position to polarization converter.

References

[1] Thompson, JD and Zwickl *et al* 2008 *Nature.* **452** 7183
[2] Møller, C.B., Thomas*et al* 2017 *Nature.* **547** 7662
[3] Yu, P.L. 2016 *University of Colorado.*

*E-mail: Hayat.Abbas@nottingham.ac.uk
†E-mail: Thomas.Frenholz@nottingham.ac.uk

Nondipole and channel-interference effects in the case of Kr 4*p* direct photoionization and 3*p*/3*d* Auger decay

L Ábrók[1,2]*, T Buhr[3], S. Schippers[3], Á Kövér[1], A Müller[4], A Orbán[1], †S Ricz[1]

[1]Institute for Nuclear Research, Hungarian Academy of Sciences (MTA Atomki), Debrecen, H-4001, Hungary
[2]Doctoral School of Physics, University of Debrecen, Egyetem sqr. 1, Debrecen, H-4032, Hungary
[3]I. Physikalisches Institut, Justus-Liebig-Universität Gießen, Giessen, 35392, Germany
[4]Institut für Atom-und Molekülphysik, Justus-Liebig-Universität Gießen, Giessen, 35392, Germany

Synopsis We have investigated the photoelectron angular distributions of Kr 4*p* direct ionization in the vicinity of the $3p \longrightarrow ns/md$ and the $3d \longrightarrow np$ resonant excitations. The channel interaction effect observed between the direct photoionization and the participator Auger decay process affects the anisotropy parameters of the angular distributions. We have developed a theoretical model considering higher-order terms beyond the dipole approximation to describe the main features observed in the experiments. In the present model we included the relevant Auger processes as well.

The description of the photoionization process at low photon energies is mostly limited to the dipole approximation, higher-order terms are usually neglected. However, both theoretical and experimental studies confirmed that first and second-order nondipole terms can affect the angular distributions even at photon energies of a few tens of eV [1]. These effects become important for example in the case of Cooper-minima and autoionization. In the latter case the relaxation process of the excited states, realized through inner electron processes, and the direct photoionization interfere. Thus the different anisotropy parameters can vary strongly within a small photon energy range resulting in notable angular distribution changes.

The angular distributions of Kr 4*p* photoelectrons were measured in the vicinity of the resonantly excited states of the inner shells 3*p* and 3*d* at the synchrotron light source DORIS III in Hamburg, Germany applying linearly polarized light. The ESA-22D electron spectrometer was used to detect the electrons in the polar angular range of 0°-360° [2]. The Kr 3d and 3p shells were excited at around 90 eV [3] and 220 eV [4] photon energy, respectively. The interference of the direct ionization and the participator Auger process was investigated at different photon energies. We have calculated angular differential cross section for the ejected electrons considering higher-order terms (electric dipole, quadrupole and octupole) in the interaction Hamiltonian. In our model we also included the Auger decay based on a simplified two step process. The anisotropy parameters were extracted from the experiments by fitting the theoretical expression including higher-order terms.

Strong photon energy dependence was observed with a forward-backward asymmetry that can only be explained by the presence of the multipole terms (Fig. 1).

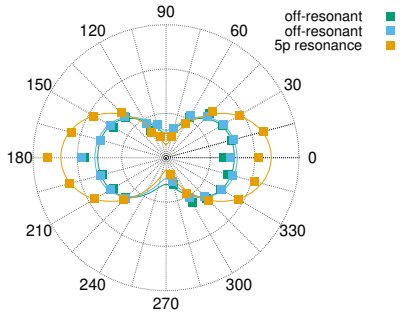

Figure 1. Angular distributions of the Kr 4*p* photoelectrons relative to the photon polarization vector measured at different photon energies : at the 3*d* resonance (91.21 eV) and in its vicinity (90.93 eV, 91.03 eV).

References

[1] Pradhan B G *et al* 2011 *J. Phys. B: At. Mol. Opt. Phys.* **44** 201001
[2] Ricz S *et al* 2002 *Phys. Rev. A* **65** 042707
[3] Ricz S *et al* 2010 *Phys. Rev. A* **81** 043416
[4] Ábrók L *et al*, in preparation

*E-mail: abrok.levente@atomki.hu

Magnetic Dichroism in Few-Photon Ionization of Lithium Atoms

B.P. Acharya[1]*, M. Dodson[2], K. Romans[1], S. Dubey[1], A.H.N.C. DeSilva[1], K. Foster[1], O. Russ[1], K. Bartschat[3], N. Douguet[2], and D. Fischer[1]†,

[1] Physics Department and LAMOR, Missouri University of Science & Technology, Rolla, Missouri 65409, USA
[2] Department of Physics and Astronomy, Drake University, Des Moines, Iowa 50311, USA
[3] Department of Physics, Kennesaw State University, Kennesaw, Georgia 30144, USA

Synopsis We observe a strong magnetic dichroism in the few-photon ionization of a polarized atomic target, i.e., a dependence of the differential cross section on the target's initial magnetic state. While the observed asymmetries can be explained by lowest-order perturbation theory, future experiments in the tunnel ionization regime might lead to a better understanding of the time delays observed in "attoclock" experiments.

The investigation of symmetry breaks in photoelectron angular distributions (PADs) is often a key to a better understanding of atomic dynamics in external electromagnetic fields. Such asymmetries occur, e.g., in the adiabatic tunnel ionization of atoms in "attoclock" experiments, where a shift of the PAD with respect to the direction of the strongest electric field is observed and interpreted in terms of a finite tunneling time [1]. Similar asymmetries have also been found in multiphoton ionization by elliptically polarized light [2]. They can often be explained within lowest-order perturbation theory (LOPT) by the interference of phase-shifted partial waves with different (dipole-allowed) angular-momentum quantum numbers ℓ and m.

In the present contribution, we demonstrate that angular shifts can also occur in atomic few-photon ionization with linearly polarized light, provided the target atom is initially polarized. We use a lithium target in an all-optical laser atom trap (AOT) [3], which is excited to the polarized Li $(2p, m = +1)$ state [4]. The atoms are ionized by the absorption of a few photons in the linearly polarized field of a femtosecond laser whose wavelength is varied between 665 nm and 800 nm. Electron and recoil ion momentum vectors are measured using the COLTRIMS (cold target recoil ion momentum spectroscopy) technique. The experimental results are compared to a model based on the numerical solution of the time-dependent Schrödinger equation (TDSE).

Measured spectra are shown in Figure 1 for a laser wavelength of 770 nm with peak intensity $1.8{\cdot}10^{11}$ W/cm^2. The laser is vertically polarized (i.e., in the y-direction), and the electronic atomic angular momentum points in the z-direction, corresponding to an electron current density rotating in the xy-plane. Both, the momentum distribution and the angular distribution are cuts in the xy-plane, which is perpendicular to the laser propagation direction (z). A significant shift of the main electron emission direction with respect to the laser polarization axis is observed and well reproduced by our model.

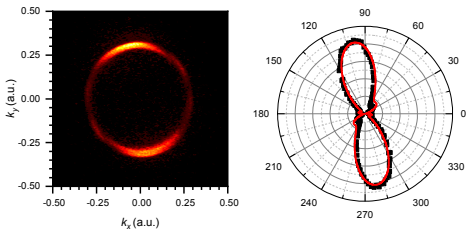

Figure 1. Electron momentum (left) and angular (right) distributions in the xy-plane (see text). The red solid line is the result of our TDSE calculation.

Our observed asymmetries can be qualitatively explained by LOPT, similar to the discussion given in [2]. Possible future experiments in the tunnel ionization regime will be discussed.

This work was supported by the NSF under PHY-1554776, PHY-1803844, PHY-2012078, and XSEDE-PHY-090031.

References

[1] Eckle P *et al* 2008 *Science* **322** 1525
[2] Hofbrucker J *et al* 2018 *Phys. Rev. Lett.* **121** 053401
[3] Sharma S *et al* 2018 *Phys. Rev. A* **97** 043427
[4] Silva A D *et al* 2021 *Phys. Rev. Lett.* **126** 023201

*E-mail: bpa3n3@mst.edu
†E-mail: fischerda@mst.edu

Theoretical treatment of quantum beats in autoinizing nf' states in Argon.

M A Alarcón[1]*, C H Greene[1]†, A Plunkett[2], J Wood[2] and A Sandhu[2]

[1]Department of Physics and Astronomy, Purdue University, West Lafayette, Indiana, 47907, USA.
[2]Department of Physics, University of Arizona, Tucson, Arizona, 85721, USA

Synopsis An accompanying experimental study observed quantum beats in the yield of autoionizing nf electrons in Argon as a function of the time delay between their excitation by an ultrafast laser and a short pulse that can photoionize them. We implement Multichannel Quantum Defect Theory and time-dependent perturbation theory to model this phenomenon. We find that as a consequence of the interference between quantum pathways formed by photoionization, the total and partial electronic yield oscillates with frequencies equal to the separation between the nf quasibound states.

Argon atoms are excited to the nf' states by an extreme ultraviolet (XUV) laser that takes them to the autoionizing region. The experiment studied the total yield of autoionized electrons after a time-delayed 1200 nm pulse hits the excited atoms. They found that the yield oscillated in the time delay; and that the involved frequencies are the difference between the energies of the quasi-bound states. These oscillations manifest in the excess or depletion in the yield without the second laser. See the upper panel of the figure.

To describe this theoretically, we utilized the multichannel quantum defect theory parameters for the relevant symmetry [1] to argue that bound states with a fixed ionic core approximate the electronic wave function. We treated the time-delayed laser semiclassically as a gaussian packet in the length gauge. With the perturbative expansion of the transition matrix [2], we obtained the probability to photoionize and of remaining in the discrete.

We found that the finite bandwidth of the laser is what permits the interference. For photoionization, different resonances can be excited to the same continuum energy and they contribute incoherently to the total probability. For autoionization, there is population redistribution in the discrete using the continuum states as intermediaries. The continuum states transition into a range of bound states. The accumulated phase of the continuum states will interfere with the phase of the bound electrons. The difference between the second-order probability and the initial population approximately describes the experimental data, as is seen in the figure.

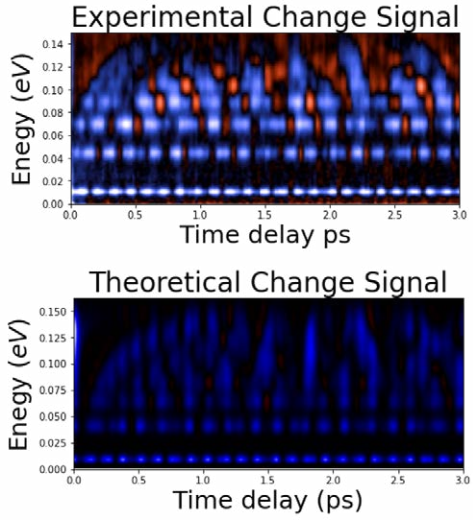

Figure 1. Comparison between experimental and theoretical change for a 1TW/cm^2 80 fs laser. The energy axis is the kinetic energy of the autoionized electrons.

This research is based upon work supported by the U.S. Department of Energy, Office os Science, Basic Energy Sciences, under Award No. DE-SC0010545.

References

[1] Pellarin M *et al* 1998 *J. Phys. B: At. Mol. Opt. Phys.*, 21 **3833**
[2] Faisal, Farhad H. Theory of Multiphoton Processes. Springer Science+Business Media, 1987.

*E-mail: malarco@purdue.edu
†E-mail: chgreene@purdue.edu

The probe of the double photoionization process in He-like and Be-like ions with extreme UV and soft-X-ray laser pulses

M A Albert[1,*], S Laulan[1] and S Barmaki[1]

[1]Laboratoire de Physique Computationnelle et Photonique, Université de Moncton, Shippagan, N-B, E8S 1P6, Canada

Synopsis We investigate the double photoionization process along the He and Be isoelectronic sequences by solving the time-dependent Schrödinger equation with a *B*-spline based spectral method of configuration interaction type. The probe of the electron dynamics in the different systems shows that the way the outer electrons will leave their parent *X* system is systematically dictated by the amount of excess photon energy available to them relative to the ionization potential of the corresponding X^+ ion.

We investigate the removal of the two outer electrons in the X = He, Li^+, C^{4+}, Be, B^+ and Ne^{6+} ions by the absorption of a single photon of energy in the extreme UV and soft X-ray spectral region.

The Be and Be-like ions B^+, Ne^{6+} are in this work treated as two-active electron systems with two outer electrons in a field of a frozen core including the nucleus and the $1s^2$ inner shell electrons [1]. The electrostatic interaction potential $1/r_{12}$ is treated without any approximation by using the multipole expansion of the Coulomb repulsion between the two outer electrons [2].

We have probed the electron dynamics from low to high photon energies in each X system. For a better comparison between the results generated in all the systems, the single P(γ,e) and double P(γ,2e) probabilities are, as shown in Figure 1, presented as function of the reduced excess energy

$$\Delta E = \frac{E_{ex}}{I_{X^+}} = \frac{\hbar\omega - I_2}{I_2 - I_1},$$

with E_{ex} the available excess photon energy shared by the two ejected electrons, I_1 (I_2) the single (double) ionization threshold [3]. The obtained results indicate similar behavior of the dynamic of the double photoionization in all the X systems. The P(γ,2e) probability begins to decrease at about the reduced excess energy ΔE = 0.3. Further probe of the mechanisms of the electron ejection has been made by analyzing the probability density distribution of the ejected electrons at different values of ΔE. The results have shown that in each system, the share of the energy between the two electrons begins to be asymmetric at the specific value of ΔE = 0.3. The observed asymmetry gets more accentuated as the photon energy is increased [3].

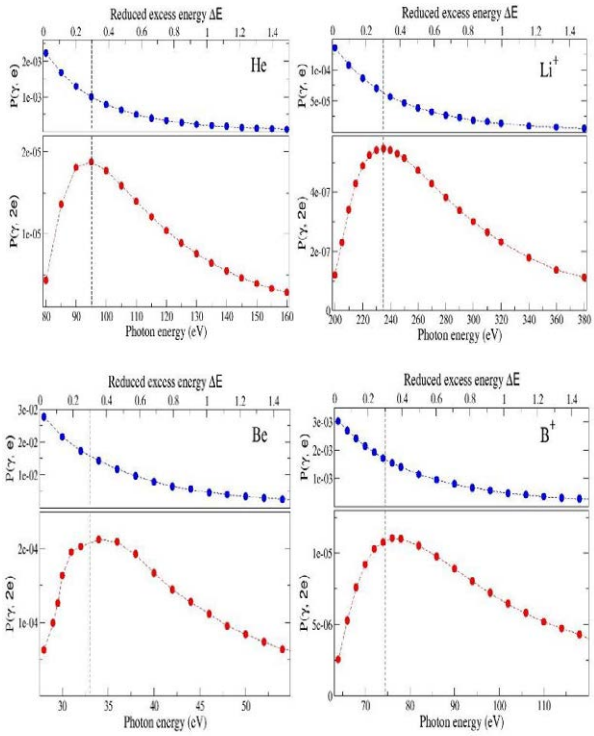

Figure 1. Single P(γ, e) and double P(γ, 2e) photoionization probabilities in He, He-like Li^+, Be and Be-like B^+ [3].

References

[1] Barmaki S *et al* 2018, *J. Phys. B : At. Mol. Opt. Phys.* **51** 105002
[2] Barmaki S *et al* 2014, *Phys. Rev. A* **89** 063406
[3] Barmaki S *et al* 2019 *Chem. Phys.* **517** 24

* E-mail: ema3813@umoncton.ca

Inclination of sidbands in laser assisted photoionization emission

R Della Picca[1] *, S D López[2] and D G Arbó[2,3] †

[1]Centro Atómico Bariloche, Av. Exequiel Bustillo 9500, 8400 Bariloche, Argentina
[2]Institute for Astronomy and Space Physics IAFE (UBA-Conicet), Buenos Aires, 1428, Argentina
[3]Universidad de Buenos Aires, Facultad de Ciencias Exactas y Naturales and Ciclo Básico Común, 1428, Argentina

Synopsis We theoretically investigate on the laser assisted XUV ionization. In this work, we focus on the position of the sidebands in the energy-angle distribution and observe a slight inclination of them as a function of the emission angle. We explore the physical origin of such inclination and its dependence on the time delay between both NIR and XUV pulses.

Laser-assisted photoinization emission (LAPE) involves two-color multiphoton ionization where one of the two radiation fields has low intensity and relatively high frequency while the other is intense with a low frequency. If the XUV pulse is longer than the NIR laser period $T_L = 2\pi/\omega_L$ (where ω_L is the laser frequency), the photoelectron energy spectrum shows a main line associated with the absorption of one XUV photon accompanied by sideband lines, located more or less symmetrically on its sides. The equally spaced sidebands with separation equal to the NIR frequency ω_L are associated with an additional exchange of laser photons through absorption and stimulated emission processes [1]. The analysis of the resulting two-color photoelectron spectra can provide information about the high-frequency pulse duration, laser intensity, and the time delay between the two pulses in experiments [2].

In this work, we carefully analyze the position of the sidebands in the doubly differential energy-angle distribution (see Fig. 1). We observe that there is a slight dependence of the position of the sidebands near threshold as a function of the emission angle θ, which was recently reported by Tong [3]. For example, the sideband shown at energy $E \simeq 1.3\ \omega_L$ is tilted towards higher energies as θ increases (and $cos\theta$ decreases). In order to investigate the origin of such subtle effect we use different envelopes for both XUV and NIR pulses and we vary the time delay between them [4].

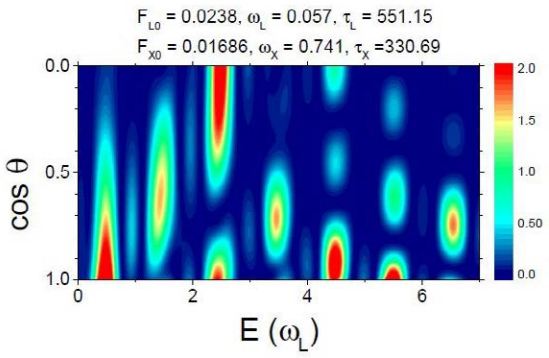

Figure 1. TDSE results for sidebands in the doubly differential E-cosθ distribution for LAPE. Energy is shown in multiples of the NIR photon energy. The laser parameters are indicated in the figure and both pulses have a trapezoidal envelope with the XUV field centered with respect to the NIR one. tL and tX are the duration of the respective NIR and XUV pulse

We make use of the time dependent Schrödinger equation (TDSE) and compare its results with the strong field approximation and the Coulomb-Volkov approximation to study the role of the Coulomb potential in the formation of the intracycle interference pattern [1,2] and its influence on the inclination of the sidebands.

References

[1] A. A. Gramajo *et al* 2018 *Jour. Phys. B* 51, 055603
[2] J Jummert *et al* 2020 *Jour. Phys B* 53 154003
[3] X-M Tong 2019 *Phys. Rev. A* 99, 043422
[4] R Della Picca et al 2020 Phys. Rev. A 102 043106

* E-mail: renata@cab.cnea.gov.ar
† E-mail: diego@iafe.uba.ar

Ionization phases in ω – 2ω above-threshold ionization

S D López[1], S Donsa[2], D G Arbó[1,3] †, and J Burgdörfer[2]

[1]Institute for Astronomy and Space Physics IAFE (CONICET-UBA), C1428ZAA, Buenos Aires, Argentina
[2]Institute for Theoretical Physics, Vienna University of Technology, A-1040 Vienna, Austria, EU
[3]Universidad de Buenos Aires, Facultad de Ciencias Exactas y Naturales and Ciclo Básico Común, 1428, Argentina

Synopsis In this work we theoretically explore the extraction of information on the ionization phases in a ω – 2ω setting. We find significant differences in ionization phases between the strong field approximation and the ab initio results of the time dependent Schrödinger equation even at energies well above the ionization threshold.

Two-color ω-2ω laser fields with well-controlled relative phases have been studied experimentally and theoretically since the last decade of the last century. One key feature is that the broken inversion symmetry of the ω-2ω field allows for interference between odd and even partial waves of the outgoing photoelectron, which leads to a forward-backward asymmetry of the emission signal. Recently, Zipp *et al* [1] extended the measurement of ionization phases and attosecond time delays to the strong-field multiphoton regime, providing new perspectives on time-resolved strong-field ionization. In this novel ω-2ω interference protocol the role of electron wavepackets emitted by absorption of subsequent harmonics in the RABBIT protocol is replaced by adjacent ATI peaks generated by a strong driving field of frequency 2ω. The concomitant weaker field opens up interfering pathways to side bands in between neighboring ATI peaks by absorbing or emitting one ω photon. This approach of measuring the ionization asymmetry as a function of the relative phase - between the ω and the 2 ω fields somewhat resembling the original RABBIT protocol promises to offer insight into the ionization phase and, possibly, timing information of multiphoton processes [2].

We present a theoretical study of the ionization phase in the multi-photon regime accessible by such a ω-2ω interference protocol for two collinearly polarized laser fields. We find strong deviations from the predictions of the strong field approximation clearly indicating that the atomic potential has a crucial influence on the ionization phase of ATI peaks even at energies well above the ionization threshold. Unlike RABBIT, the present ω-2ω protocol opens up a multitude of competing quantum paths, turning the extraction and interpretation of interference phases more complex. In Fig. 1 we show the time delays as a function of the probe intensity.

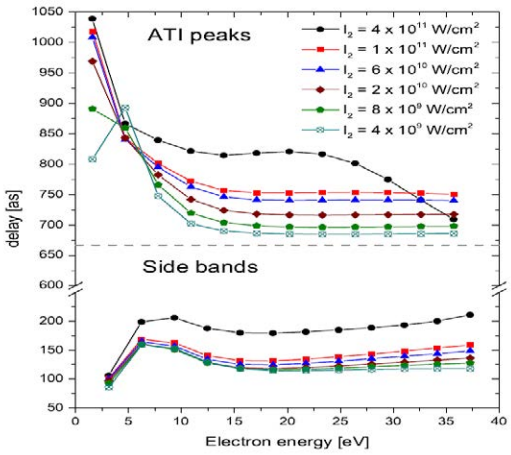

Figure 1. Time delays as a function of the emission energy calculated from asymmetries integrated over half spheres for decreasing probe intensities. The intensity of thee pump is $I_{2\omega} = 8\times10^{13}$ W/cm^2 with ω = 0.057 a.u. and pulse duration of τ = 881.85 a.u.

In order to disentangle short- from long- ranged effects of the atomic potential we perform simulations for atomic model potentials featuring either a Coulombic long-range tail or a Yukawa-type short-range potential.

References

[1] L J Zipp *et al* 2014 *Optica* **1** 361-364
[2] J Fuchs *et al* 2020 *Optica* **2** 154 (2020)
[3] S Donsa *et al* 2019 *Phys. Rev. Lett.* **123** 133203

† E-mail: diego@iafe.uba.ar

Enhancing spin polarization using attosecond angular streaking

G. S. J. Armstrong[1]*, D. D. A. Clarke[2], J. Benda[3], J. Wragg[1], A. C. Brown[1], and H. W. van der Hart[1]

[1]School of Mathematics and Physics, Queen's University Belfast, Belfast BT7 1NN, United Kingdom
[2]School of Physics and CRANN Institute, Trinity College Dublin, Dublin 2, Ireland
[3]Institute of Theoretical Physics, Faculty of Mathematics and Physics, Charles University, V Holešovičkách 2, 180 00 Prague 8, Czech Republic

Synopsis We use the R-matrix with time-dependence method to investigate spin polarization in atomic krypton using an angular streaking scheme. We find that such schemes can produce strong spin polarization, and that they may be applied in domains beyond those in which they are typically used to investigate electron tunneling.

Photoelectron spin alignment represents an exploitable degree of freedom for probing both the structure and dynamics of matter. In this contribution, we demonstrate numerically that the contemporary technique of attosecond angular streaking (or the "attoclock"), traditionally used to investigate electron tunneling [1], can be repurposed to produce strongly spin-polarized electrons. The attoclock employs a few-cycle, near-circularly-polarized laser pulse of infrared wavelength to modify the binding potential of the target to form a rotating barrier, through which an electron may tunnel. The brevity of the pulse serves to localize the ejected-electron wavepacket within an angular interval, allowing a dominant emission direction to be defined. The angle between the dominant emission direction and the major axis of laser polarization is often associated with a 'tunneling time', though considerable controversy exists regarding this interpretation[2].

Regardless of the attoclock's ability to provide a tunneling time, calculations have shown that in an attoclock scheme, $p_{\pm1}$ electrons ejected from noble gases may be spatially separated to some extent. Given their preference for opposite spin orientations, their separation should induce a strong spin polarization. To investigate this process, we apply the R-matrix with time-dependence method [3, 4] to angular streaking of krypton. Through solution of the multielectron, semi-relativistic, time-dependent Schrödinger equation, we show that angular streaking produces strongly spin-polarized electrons. We find that the degree of spin polarization attainable using the angular streaking scheme exceeds that achieved using longer circularly polarized pulses. We also find that the degree of spin polarization increases with the Keldysh parameter, so that angular streaking may be used beyond its traditional tunneling domain to generate spin-polarized electron bunches. Finally, we also explore modifications of the angular streaking scheme that also enhance spin polarization [5].

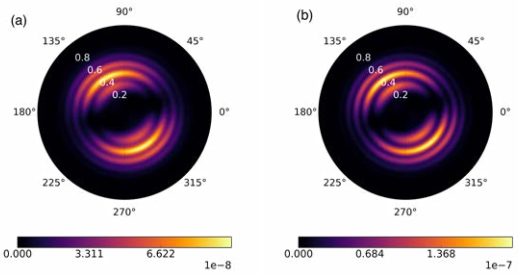

Figure 1. Momentum distribution for (a) spin up and (b) spin down electrons ionized from Kr by an 8-cycle, 780-nm, 2×10^{13} W/cm^2 pulse of ellipticity $\epsilon = 0.87$.

References

[1] P. Eckle *et al.*, *Nature Physics* **4**, 565 (2008).
[2] A. Kheifets *et al.*, *J. Phys. B: At. Mol. Opt. Phys* **53** 072001 (2020)
[3] D. D. A. Clarke *et al.*, *Phys.Rev.A.* **98** 053442 (2018).
[4] A. C. Brown *et al.*, *Comput. Phys. Commun.* **250** 107062 (2020).
[5] G. S. J. Armstrong *et al.*, *to be published* (2021).

*E-mail: gregory.armstrong@qub.ac.uk

EUV spectral measurements and theoretical investigation of Mo^{4+}-Mo^{17+} ions in laser-produced plasmas

M Bakhiet, M G Su*, S Q Cao, W Yanhong, M Li, J Liu and C Z Dong†

Key Laboratory of Atomic and Molecular Physics & Functional Material of Gansu Province, College of Physics and Electronic Engineering, Northwest Normal University, Lanzhou 730070, China.

Synopsis Spectra of laser-produced molybdenum (Mo) plasmas have been measured in the 6.7-14.3 nm wavelength range at different time delays. The Hartree-Fock (HF) method with relativistic corrections (HFR) using Cowan's codes and the Flexible Atomic Code (FAC) show that spectral features are consistent with theoretical spectra of the 4s-*n*p, 4p-*m*s, and 4p-*n*d resonance transitions in Mo^{4+}-Mo^{12+} ions. Double excitations in Mo^{12+}, Mo^{13+}, and Mo^{14+} were also worthy of inclusion because of their important contributions. To obtain the plasma parameters, the steady-state collisional-radiative model has been used. The evolution of the rate coefficients with electron temperatures, fractional populations for each ion, and various physical aspects relating to plasma expansion into a vacuum were provided. Simulated spectra were made for different effective temperatures, which may be reflect different phases of the plasma evolution. The synthetics theoretical spectra agree reasonably well with the experimental results, which indicates the possibility of use for plasma diagnostics. The results should be beneficial for spectroscopic diagnostics of hot plasmas in tokamak and fusion research.

The research on the emission spectra of highly-charged Mo ions of a laser-produced plasma is currently a topic of considerable interest because of their use for plasma diagnostics in tokamak fusion reactors [1]. To understand the processes involved in plasma expansion such as ion emission, ion distributions, the resulting velocities, and kinetic energy distribution, different experimental and theoretical approaches have been undertaken.

In this work, we take the advantage of high-power density (2.04×10^{11} W/cm^2) of the available short-pulse Nd:YAG laser to irradiating a pure Mo and measure the spectrum for different transitions. Several unknown lines appear on the observed spectrum. The Cowan suites of Hartree-Fock (HF) method with relativistic corrections (HFR) [2] and the Flexible Atomic Code (FAC) [3] were used to explain the measured spectral structures.

We aim to provide more comprehensive theoretical investigations concerning highly-charged Mo ions. For this purpose, detailed analysis of the 4s- and 4p-excitations are systematically analyzed and discussed based on a steady-state collisional radiative (CR) model.

The spatial scans of the plasma emission show variations in the ionization stage with the position in the plasma. Figure 1 shows the synthetic spectra produced from the sum of the 4s-*n*p and 4p-*m*s in Mo^{4+}-Mo^{12+} ions at T_e=31 eV and T_e=14.3 eV.

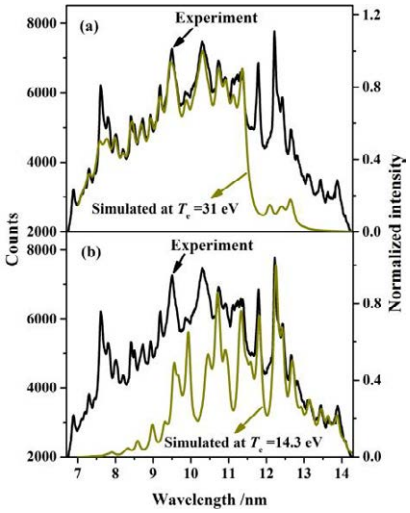

Figure 1. Comparisons between the experimental and simulated spectra. (a) For T_e=14.3 eV and n_e=3.6×10^{20} cm^{-3}. (b) For T_e=31 eV and n_e=7×10^{20} cm^{-3}.

This work is supported by the National Key Research and Development Program of China (Grant no. 2017YFA0402300).

References

[1] Finkenthal M *et al*. 1982 *Phys. Lett. A.* **91** 284-286.
[2] Cowan R D 1981 *The theory of Atomic Structure and Spectra* (University of California Press, Berkeley).
[3] MF Gu 2008 *Can. J. Phys.* **86**, 675.

* E-mail: sumg@nwnu.edu.cn
† E-mail: dongcz@nwnu.edu.cn

Multiphoton interaction phase shifts in attosecond science

M Bertolino[1]*, D Busto[1], F Zapata[1] and J M Dahlström[1]†

[1] Department of Physics, Lund University, Box 118, SE-221 00 Lund, Sweden

Synopsis We use *ab initio* simulations of several interferometric experiments in attosecond and free-electron laser sciences to find that there is a dependence on multiphoton phase shifts in above-threshold ionization. A simple rule of thumb is devised that is able to explain general phase and amplitude effects on an *absolute* scale, relative to known reference experiments. For instance, we show why interferometric ATI experiments are shifted by $\pi/4$ relative to RABBIT-like experiments, and why there is no 2ω-phase modulation (RABBIT-modulation) in laser-assisted photoionization with odd and even harmonics.

Novel types of spectroscopies use probing laser beams to interfere different energy components of the studied system by changing the dynamics in the interferometric arms. This makes it possible to study nonlinear processes like high-order harmonic generation (HHG), but it also makes it hard to disentangle the unperturbed dynamics in e.g. the photoionization process.

In Ref. [1] we use *ab initio* simulations based on the time-dependent configuration interaction singles (TDCIS) method [2] to study recent attosecond experiments, e.g. from Ref. [3, 4, 5], and interpret the dependence on the carrier–envelope phase (CEP), φ, difference between pump and probe field within a unified framework. We derive the following rule of thumb, valid in the limit of a small ponderomotive energy,

$$c_{\mathbf{k}}^{(n)} \approx (-i)^{|n|} J_{|n|} \exp(in\varphi) f_{\mathbf{k}}^{(\mathrm{pump})},$$

which expresses the nth laser-assisted photoionization amplitude as its elementary photoionization amplitude, $f_{\mathbf{k}}^{(\mathrm{pump})}$, the CEP difference between pump and probe fields, a Bessel function and an *interaction phase* $(-i)^{|n|}$ which accumulates for each included interaction.

Using the rule of thumb, we provide a simple explanation why interferometric ATI experiments are shifted relative to RABBIT, and why laser-assisted photoionization with odd and even harmonics has no RABBIT-modulation, due to interference with the direct ionization path and the paths with absorption or emission with two IR-photons, see Fig. 1.

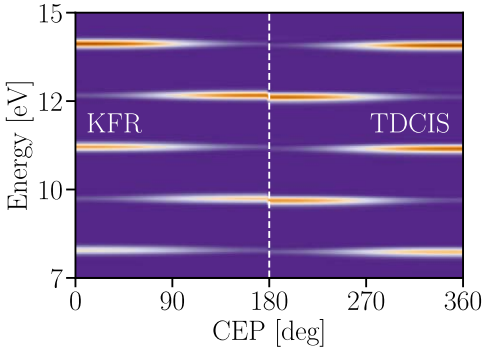

Figure 1. Photoelectron peaks in Ne2p from odd and even high-order harmonics 20–24 using (left) Keldysh–Faisal–Reiss theory and (right) TDCIS as in Ref [3].

References

[1] Bertolino M and Dahlström J M 2021 *Phys. Rev. Research* **3(1)** 013270
[2] Greenman L *et al* 2010 *Phys. Rev. A* **82(2)** 023406
[3] Laurent G *et al* 2012 *Phys. Rev. Lett.* **109(8)** 083001
[4] Maroju P K *et al* 2020 *Nature* **578(7795)** 386–391
[5] Zipp J L *et al* 2014 *Optica* **1(6)**

*E-mail: mattias.bertolino@matfys.lth.se
†E-mail: marcus.dahlstrom@matfys.lth.se

Multi-Sideband RABBITT in Atomic Hydrogen and Argon: Theory and Experiment

D Bharti[1]*, D Atri-Schuller[2], H Srinivas[1], F Shobeiry[1], G Menning[2], K R Hamilton[2], R Moshammer[1], T Pfeifer[1], N Douguet[3], K Bartschat[2], and A Harth[1]†

[1]Max-Planck-Institute for Nuclear Physics, Heidelberg, D-69117, Germany
[2]Department of Physics and Astronomy, Drake University, Des Moines, IA 50311, USA
[3]Department of Physics, Kennesaw State University, Marietta, GA 30060, USA

Synopsis Using the 3-sideband RABBITT technique, we explore the applicability of a universal continuum-continuum coupling phase, derived from the asymptotic approximation, in cases where more than one transition occurs in the continuum.

The reconstruction of attosecond beating by interference of two-photon transitions (RABBITT) is a widely employed technique to measure attosecond time delays in photoionization processes [1]. It is an interferometric technique in which an extreme ultraviolet (XUV) attosecond pulse train (APT) ionizes a target by single-photon absorption, thereby creating main peaks in the photoelectron kinetic energy spectrum. The presence of a temporally and spatially overlapped near-infrared (NIR) field creates a sideband (SB) signal in between these main peaks, which oscillates sinusoidally as the delay between the XUV and the NIR beams is varied. Using the so-called "asymptotic approximation", the atomic part $\Delta\phi_a$ of the measured RABBITT phase difference can be separated into a single-photon ionization contribution $\Delta\phi_W$ and a continuum-continuum (cc) term $\Delta\phi_{cc}$ [1].

Recently, we extended the applicability of this approximation to multi-sideband RABBITT schemes where the atomic part $\Delta\phi_a$, corresponding to N photon interactions, can be written as a sum of the Wigner and multiple cc-contributions:

$$\Delta\phi_a = \Delta\phi_W + \Delta\phi_{cc}^1 + \Delta\phi_{cc}^2 + ... + \Delta\phi_{cc}^{N-1}.$$

This approach was analyzed in detail for atomic hydrogen [2].

In addition to further theoretical results for atomic hydrogen, we present our first realization of a 3-SB RABBITT experiment using argon as the target gas (cf. Fig. 1). Argon is easier to handle experimentally but more challenging for theory, due to its multi-electron nature and the non-vanishing orbital angular momentum of the active 3p electron. Consequently, we use the multielectron R-matrix with time dependence method (RMT) [3] to generate theoretical predictions that will be compared with our experimental data.

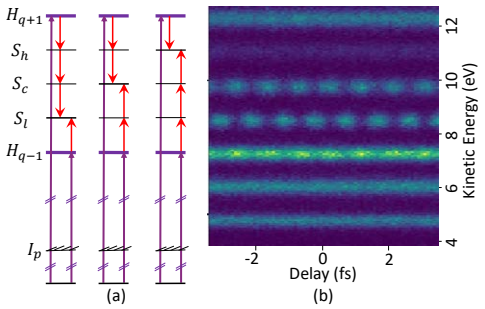

Figure 1. (a) Energy level schemes explaining the formation of three sidebands in between two adjacent main peaks; (b) experimental 3-SB RABBITT trace recorded in argon.

Multi-sideband RABBITT opens a new way to study cc-couplings [4]. By comparing the measurements from 1-SB and 3-SB RABBITT setups, we aim to separate cc transitions from the ionization process and extract $\Delta\phi_{cc}$ individually.

References

[1] Dahlström J M *et al* 2012 *J Phys. B* **45** 183001
[2] Bharti D *et al* 2021 *Phys. Rev. A* **103** 022834
[3] Brown A C *et al* 2020 *Comp. Phys. Commun.* **250** 107062
[4] Harth A *et al* 2019 *Phys. Rev. A* **99** 023410

This work was supported, in part, by the United States National Science Foundation, the DFG-QUTIF program, and IMPRS-QD.

*E-mail: bharti@mpi-hd.mpg.de
†E-mail: harth@mpi-hd.mpg.de

Numerical methods for few body problems in atomic physics

L Biedma[1]*, F D Colavecchia[2] and J Randazzo[2]

[1]FAMAF, Universidad Nacional de Cordoba, Cordoba, X5000, Argentina.
[2]Instituto Balseiro and CONICET, Bariloche, S4140, Argentina.

Synopsis We present a numerical method to solve few body problems, based on the use of spectral decomposition of the wave function, and the application of *latent matrices* to solve the resulting linear algebra system. The method is tailed to multi-core computers and automatically increases the size of the basis set to achieve cross section convergence. Fast and accurate results are presented for Helium-like double photoionization systems.

The formulation of partial differential equations (PDEs) leads in atomic physics simulations, results in the formidable task of solving huge linear algebra system. A more accurate description of a given phenomenon always needs more variables to obtain a satisfactory solution. Because of this, developing fast numerical linear algebra methods is a top priority in computational physics.

In this work, we solve the Schrodinger equation for continuum states in a three-body system, that can be obtained from the solution of the time-independent problem:

$$(H - E)\Psi = W\Psi_0, \tag{1}$$

where Ψ_0 is the initial state of the process and E is the total energy of the system. The operator W is responsible for the transitions from state Ψ_0 to the collisional unknown state Ψ.

A widely used tool to obtain this solution is the spectral method, where we represent Ψ and Ψ_0 as an infinite sum of base functions:

$$\Psi(r_1, r_2) = \sum_{n,m}^{NM} x_{nm}\Omega^L_{nm}(r_1, r_2) \tag{2}$$

The proposed model for the solution of these problems is based on a previous publication, where we describe a task-parallelization approach to the solution of a linear system with an unknown final dimension, using *latent matrices* [1, 2]. For this work, we adapted the method to compute cross-sections of the double photoionization of helium, using Generalized Sturmian Functions to describe the function space.

It is also important to note that the current framework computes solutions for all the intermediate dimensions in the problem, something that is impossible using spectral methods such as the conjugate gradient.

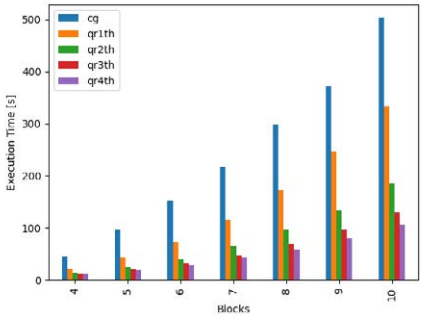

Figure 1. Comparison for execution times for different algorithms: Conjugate Gradient (not parallelized) and the Exact Solution computed with our current algorithm, using 1-4 threads.

The performance studies and the associated plot show that the combination of this change in paradigm and the utilization of state-of-the-art numerical linear algebra libraries, allows us to solve these problems with great speed and provides the capability to tackle even bigger and more complex problems in the future.

References

[1] Biedma L, Colavecchia F and Quintana-Orti E, 2017 *Procedia Computer Science 108* **1743**
[2] Biedma L., PhD Thesis, Universidad Nacional de Córdoba, 2021
[3] McCurdy C W et. al, 2004 *Phys. Rev. A 69* **032707**

*E-mail: lbiedma@famaf.unc.edu.ar

Direct absorption measurements of the two-photon excitation cross-section of the 6p'[3/2]$_2$ and 6p'[1/2]$_0$ levels of Xe I with a new analytical formula

C Blondel[1] * and C Drag[1] †

[1]Laboratoire de Physique des plasmas, Centre national de la recherche scientifique, École polytechnique, Sorbonne Université, Université Paris-Saclay, Observatoire de Paris, Institut polytechnique de Paris, route de Saclay, F-91128 Palaiseau cedex, France

Synopsis The two-photon excitation cross-section of xenon, which is often used for calibration of two-photon absorption laser induced fluorescence (TALIF) measurements but had never been measured directly, has been experimentally quantified by absorption measurements. Absorption measurements have the advantage of not relying on assumed de-excitation branching ratios nor light collection efficiencies, which are weak points of fluorescence-based measurements. A new analytical formula is proposed to describe the medium-absorption regime.

The two-photon excitation cross-section is an essential parameter of the two-photon absorption laser induced fuorescence (TALIF) method, which is commonly used to measure atomic densities in gases, especially for plasma diagnostics. The method consists in recording the fluorescence signal that follows the absorption of two photons of UV light. Calibration usually consists in comparing the signal recorded in the studied sample with the fluorescence produced, at a similar wavelength, in a noble gas vapor, the density of which can be easily known. Obviously the ratio of the involved cross-sections is a key parameter of such measurements. Yet the two-photon excitation cross-section of xenon, which is the usual calibration gas for oxygen density measurements, was never measured directly. The present study has found it to be $1.36^{+0.46}_{-0.34}$ and $1.88^{+0.75}_{-0.54}\times10^{-43}$ m^4 for the 6p'[3/2]$_2$ and 6p'[1/2]$_0$ levels, respectively.

In contradistinction with fluorescence, the absorption measurement that we carry out is not on a zero background. The absorbed power has thus to be a substantial fraction of the incident one, to optimize the signal-to-noise ratio. Lowest-order attenuation, in that regime, is not a sufficient model. Assuming our laser pulse has Gaussian profiles both in space and time (which provides generally valid orders of magnitude), the transmission factor K can be modeled, at all orders, as

$$K = \mathrm{Li}_{3/2}(-a)/(-a)$$

with $\mathrm{Li}_{3/2}$ the polylogarithmic function of order 3/2 and $a = 2\, n\, \sigma^{(2)}(\omega)\, \varphi\, z$, with n the atomic density, $\sigma^{(2)}(\omega)$ the frequency-dependent cross-section, ϕ the peak laser flux and z the cell length. Absorption profiles and obtained integrated cross-sections are presented on figure 1.

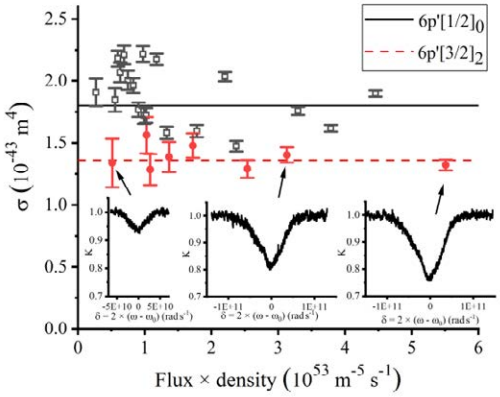

Figure 1. Absorption profiles and integrated cross-sections, for different values of the product $n\ \Phi$ that appears in absorption variable a.

For the commonly used 6p'[3/2]$_2$ level, the value found is more than twice smaller than previously admitted, which suggests that O densities already measured by Xe-calibrated TALIF have to be revised to substantially lower values. Although it has been less often used, the 6p'[1/2]$_0$ level appears as a good alternative, both because of its simplicity due to the absence of a hyperfine structure and to a counter-intuitively larger cross-section.

* E-mail: christophe.blondel@lpp.polytechnique.fr
† E-mail: cyril.drag@lpp.polytechnique.fr

Two-photon decay rates in heliumlike atoms: Finite-nuclear-mass effects

A T Bondy[1]*, D C Morton[2] and G W F Drake[1]

[1] Department of Physics, University of Windsor, Windsor, ON, N9B 3P4, Canada
[2]Herzberg Astronomy and Astrophysics, National Research Council, Victoria, BC, V9E 2E7, Canada

Synopsis Two-photon decay rates are calculated for the helium isoelectronic sequence and for muonic, pionic, and antiprotonic helium. Effects due to the finite mass of the nucleus are included and are studied as a function of the ratio of the reduced mass to the nuclear mass.

Two-photon processes have played an important role in many branches of physics ever since their first theoretical discussion by Maria Goeppert-Mayer [1] as a second-order interaction between atoms and the electromagnetic field. In emission, two-photon decay determines the radiative lifetimes of metastable states such as $2\ ^2S_{1/2}$ of hydrogen and $2\ ^1S_0$ of helium, important in determining their population balance in astrophysical sources such as planetary nebulae [2]. They also largely determine the rate of radiation loss in the early universe to form the cosmological microwave background (CMB) since there is no resonant reabsorption of radiation [3, 4]. In absorption, two-photon transitions can be driven by strong laser fields, giving rise to a wide variety of phenomena and a vast range of technological applications.

In this work, spontaneous two-photon decay rates for the $1s2s\ ^1S_0 - 1s^2\ ^1S_0$ transition in helium and its isoelectronic sequence up to $Z = 10$ are calculated, including the effects of finite nuclear mass. Muonic, pionic, and antiprotonic "heavy" helium species are also studied as extreme cases of the finite mass effect. Correlated variational wave functions in Hylleraas coordinates and discrete pseudostate summations for intermediate states are used to calculate the decay rates. The accuracy of previous work is improved by several orders of magnitude. Length and velocity gauge calculations agree to eight or more figures, demonstrating that the theoretical formulation correctly takes into account the three effects of (1) radiation due to motion of the nucleus in the center-of-mass frame, (2) mass scaling and (3) mass polarization[5]. The first two can be accounted for by simple scaling, and the mass polarization effect can be expressed as a correction factor that can be written as a gauge-dependent power series in powers of μ/M, the ratio of the reduced mass to the nuclear mass. Algebraic relationships relating the length and velocity are derived and tested, yielding a simple formula relating the actual two-photon decay rates to the infinite nuclear mass case that can be used for other helium isotopes or adjusted values of μ/M.

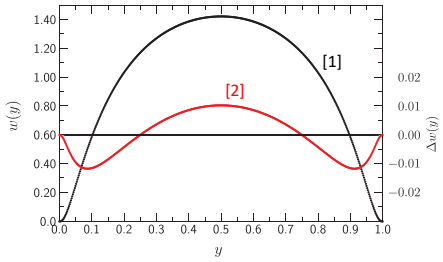

Figure 1. Plots of the [1] two-photon emission rate $w^{(2\gamma)}(^4\mathrm{He})$ and [2] the difference $\Delta w^{(2\gamma)} = w^{(2\gamma)}(\mu^2\text{-}^4\mathrm{He}) - w^{(2\gamma)}(^4\mathrm{He})$ (red) as fractions $y = \omega_1/\Delta$, with $\Delta = (E_i - E_f)/\hbar$, of the unit energy range normalized to unity.

References

[1] M. Goeppert-Mayer 1931 *Ann Phys. (Leipzig)* **401** 273
[2] G. R. Blumenthal, G. W. F. Drake and W. P. Tucker 1972 *Astrophys. J.* **172**, 205
[3] Y. B. Zel'dovich, V. G. Kurt, R. A. Sunyaev 1968 *Sov. Phys. JETP Lett.* **28**, 146
[4] P. J. E. Peebles 1968 *Astrophys. J.* **153**, 1
[5] A. T. Bondy, D. C. Morton , G. W. F. Drake 2020 *Phys. Rev. A* **102**, 052807

*E-mail: bondy11u@uwindsor.ca

Photoionization microscopy in the time domain: classical atomic chronoscopy

P Kalaitzis[1], S Danakas[1], K Ferentinou[1], S Cohen[1] and C Bordas[2] *

[1] Atomic and Molecular Physics Laboratory, Physics Department, University of Ioannina, 45110 Ioannina, Greece
[2] Université de Lyon, CNRS, UMR5306, Institut Lumière Matière, 69622 Villeurbanne, France

Synopsis Detailed analysis of the dynamical aspects of classical electron trajectories in atomic Rydberg states in the presence of an external electric field allows us to extract time-dependent information from the glory oscillations observed in the near-threshold Stark spectrum.

The electron motion in bound atomic Rydberg states constitutes an internal clock of arbitrarily adjustable frequency, not directly accessible other than via a pump-probe ionization scheme. By contrast, Stark resonances in the continuum provide a measurable atomic clock, with an additional degree of external control. Direct measurement of time characteristics of the electronic motion is hardly achievable, however specific spectral characteristics directly related to this internal clock are more easily accessible from the instrumental point of view. For example, glory oscillations in the ionization continuum of an atom in the presence of a static electric field F exhibit striking signatures of the electron motion clock. Glory scattering has been precisely described [1] in the case of photoionization microscopy [2] where it manifests itself by the appearance of an intense peak at the center of the photoelectron momentum distribution. Glory signal exhibits strong oscillations and beating effects over the entire spectral range [1]. In this work we present a comprehensive analysis of the dynamical aspects of classical electron motion in the combination of a Coulomb and a static electric field. As an example, Fig. 1 shows the time-of-flight between ionization and arrival of the electron on a plane perpendicular to the field at a finite distance for the different ejection angles contributing to the glory effect. We show that the experimental glory spectrum carries a signature of the time-of-flight differences ∂t between the different glory angles. The insert in figure 1 shows the short time Fourier transform (STFT) of the glory spectrum (Mg atoms), exhibiting different branches corresponding precisely to the ∂t quantities. Note that the residual difference between these quantities ∂t in a non-hydrogenic atom, observable in principle experimentally, and these same quantities in the pure coulombic case calculated classically here, are the strict analog of the photoemission delays measured in the attosecond regime.

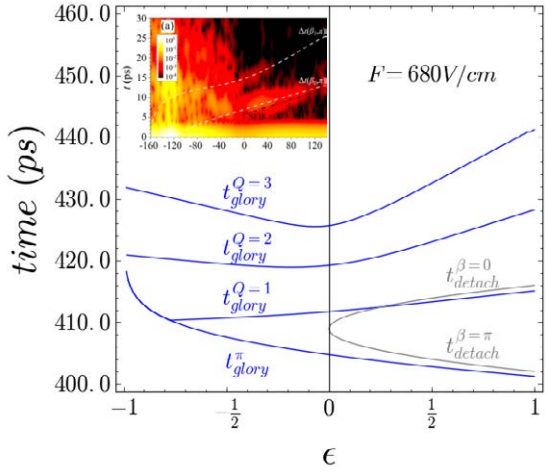

Figure 1. Classical photoionization (blue lines) electron time-of-flight at glory angles (labeled as π and Q=1, 2 and 3) as a function of reduced energy $\epsilon = E/2\sqrt{F}$ (a.u.) as compared to photodetachment (grey lines) at a distance L=1 mm. Insert: short time Fourier transform applied to the Mg glory signal. Computed ∂t are drawn in white dashed lines (F=680 V/cm).

Our present analysis is limited to the glory signal and the deviation between our measurements and the pure coulombic model appears negligible. By exploiting the full experimental data we plan to recover the full information, extract the non-hydrogenic part of the photoemission time and compare it with a complete quantum modeling of the Stark effect taking into account the non-zero quantum defects. This will provide access to the measurement of the photoemission time-delays at femto- or even pico-second time scales, i.e. in slow motion as compared to analogous experiments in the attosecond domain.

References

[1] Kalaitzis P *et al* 2020 *Phys. Rev. A* **102** 033101
[2] Nicole C *et al* 2002 *Phys. Rev. Lett.* **88** 133001-1

* E-mail: christian.bordas@univ-lyon1.fr

Strong-field ionization of FEL-prepared doubly excited states in helium

G D Borisova[1*], S Meister[1], H Lindenblatt[1], F Trost[1], P Schoch[1], V Stooß[1], M Braune[2], R Treusch[2], H Redlin[2], N Schirmel[2], P Birk[1], M Hartmann[1], C Ott[1], R Moshammer[1] and T Pfeifer[1†]

[1]Max-Planck-Institute for Nuclear Physics, 69117 Heidelberg, Germany
[2]Deutsches Elektronen-Synchrotron, 22607 Hamburg, Germany

Synopsis In a two-color extreme ultraviolet (XUV)-infrared (IR) experiment using a reaction microscope (ReMi) we study IR strong-field ionization out of selectively prepared doubly excited states (DESs) in helium in the XUV energy region between 59 eV and 80 eV. Both single- and double-ionization have been observed and the impact of different ionization mechanisms will be discussed, also in comparison with model calculations.

To gain new insights into the role of the initial state for the ionization process, we selectively prepared doubly excited states in He with XUV light provided by the free-electron laser in Hamburg (FLASH), and studied their ionization in the presence of an additional IR field. The XUV photon energy was scanned over the broad region of DESs between 59 eV and 80 eV, reaching as high as the double ionization continuum I_∞. The intensity of the synchronized 800 nm IR pulses is too low to ionize He in its ground state, but strong enough to ionize it from the doubly excited states.

We observed both single and double ionization in a fully differential ReMi measurement. In Fig. 1 we show the data for He^++e^- and He^{2+}+e^- coincidences, both in the cases XUV only and XUV + IR. The diagonal lines in the plots of electron kinetic energy $E_{kin,e}$ vs. XUV photon energy originate from direct XUV ionization above the ionization thresholds I_2, I_3 etc. In the presence of the IR field, we additionally detect electrons with low $E_{kin,e}$ at the energy positions of resonant DESs, indicated in the upper part of the figure. For the lines below I_2, above threshold ionization (ATI) peaks are visible in the distribution of the photoelectron kinetic energy, which is a clear signature of multi-photon strong-field ionization of FEL-prepared DESs. Above 70 eV, for IR-induced double ionization, photoelectrons with $E_{kin,e} \approx 0$ eV and their first ATI peak emerge. In this densely populated region of states the two electrons seem to become free simultaneously, with one of them often having almost no kinetic energy, i.e. just barely escaping the atom. We discuss this and other ionization mechanisms leading to the observed single and double ionization, and compare our findings to 1D model calculations based on the time-dependent Schrödinger equation for two active electrons, accounting also for the electron-electron interaction [1].

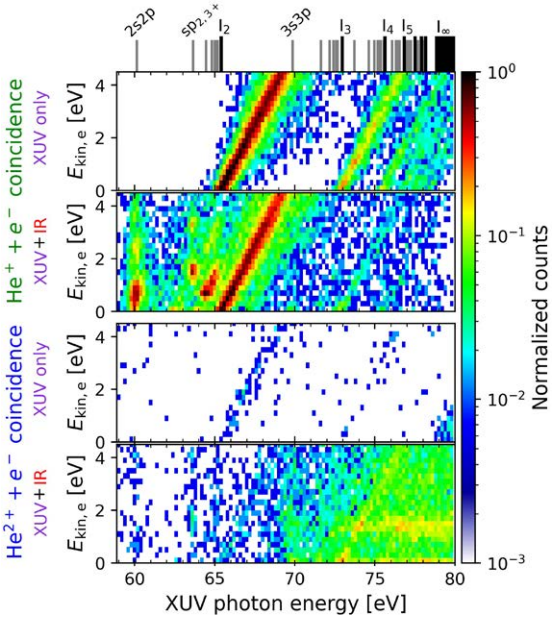

Figure 1. Energy-resolved ionization yield of He^+ and He^{2+} ions, detected in coincidence with one photoelectron. The ionization yield in all cases is normalized to the maximal coincident counts for He^++e^- in the presence of XUV and IR.

References

[1] Borisova G D *et al* 2020 *J. Phys. Commun.* **4** 055012

* E-mail: borisova@mpi-hd.mpg.de
† E-mail: thomas.pfeifer@mpi-hd.mpg.de

Beyond Born-Type Methods in Investigating the Core Dynamics of Excited Helium

A C Bray[1]*, A S Maxwell [2] M Ciappina [3] and C Figueira De Morisson Faria [1] †
Y Kissin [4] M Ruberti [4] and V Averbukh [4]

[1]UCL Department of Physics & Astronomy,University College, Gower St, London WC1E 6BT, UK
[2]Institut de Ciencies Fotoniques, The Barcelona Institute of Science and Technology, 08860 Castelldefels (Barcelona), Spain
[3] Physics Program, Guangdong Technion - Israel Institute of Technology, Shantou, China
[4] Imperial College London - Department of Physics, Prince Consort Rd, SW7 2BW, UK

Synopsis We use the Coulomb Quantum Orbit Strong-Field Approximation (CQSFA) to probe excited states of Helium, revealing rescattering is no longer confined to the polarisation axis and we identify the orbits responsible for a non-vanishing photoelectron signal. Further to this, we use ab initio methods to investigate multi and single electron effects in the given system and how they provide a picture of the core dynamics.

Similarly, to light holography, ultrafast photoelectron holography makes use of a probe and a reference wave to reconstruct a target using phase differences. This makes use of the fact that different pathways for an electron in a strong laser field may be associated with specific interference patterns. Typically, the reference is a direct pathway and the probe is associated to a laser-induced rescattering process. If traditional orbit-based approaches are employed, such as the strong-field approximation, for linearly polarised fields rescattering will occur near and on the polarisation axis. This will make it detrimental for probing targets whose geometry is oriented perpendicular to the field. In the present contribution, we employ a novel approach which goes beyond that and takes into account the residual binding potential and the external laser field on equal footing: The Coulomb Quantum Orbit Strong-Field Approximation (CQSFA) [1,2].

By studying a variety of atomic species prepared in excited states of different geometries, we show that, due to the presence of the Coulomb potential, rescattering will no longer be confined to this axis, which makes it possible to probe orbitals whose polarisation is perpendicular to that of the field. We also identify the main types of orbits responsible for a non-vanishing photoelectron signal within the CQSFA and initial momentum distributions of the instances of tunnelling and re-scattering. We further probe the interplay between the driving field and the binding potential by modifying parameters such as the field intensity and the binding energy. By comparing with ab initio models (such a Qprop and ADC BSplines [3,4]), we are able to asses core dynamics through the description of resonances from multi-electron effects, as well as provide a description of hybrid orbits through single electron effects from CQSFA.

References

[1] A. S. Maxwell, A. Al-Jawahiry, T. Das, and C. Figueira de Morisson Faria " Coulomb-corrected quantum interference in above-threshold ionization: Working towards multitrajectory electron holography", Phys. Rev. A **96**, 023420 (2017).
[2] C. Figueira de Morisson Faria and A. S. Maxwell "It is all about phases: ultrafast holographic photoelectron imaging", Rep. Prog. Phys. **83**, 034401 (2020).
[3] V. Tulsky, D. Bauer "Qprop with faster calculation of photoelectron spectra", Computer Physics Communications, **251**, 107098 (2020).
[4] M. Ruberti and V. Averbukh, ?Chemistry and Molecular Physics on the Attosecond Timescale: Theoretical Approaches?, RSC Theoretical and Computational Chemistry series (2018)

*E-mail: a.bray@ucl.ac.uk
†E-mail: c.faria@ucl.ac.uk

The R-matrix with time (RMT) project

A. C. Brown[1]*, G. S. J. Armstrong[1] J. Benda[2], D. D. A. Clarke[3], J. Wragg[1], K. R. Hamilton[4], Z. Mašín[2], J. D. Gorfinkiel[5], H. W. van der Hart[1].

[1]Queen's University Belfast, Belfast BT7 1NN, United Kingdom
[2]Charles University, V Holešovičkách 2, 180 00 Prague 8, Czech Republic
[3]Trinity College Dublin, Dublin 2, Ireland
[4]Drake University, Des Moines, Iowa 50311, USA
[5]The Open University, Walton Hall, MK7 6AA Milton Keynes, UK

Synopsis The R-matrix with time-dependence (RMT) code is designed to solve the time-dependent Schrödinger equation for atomic and molecular systems driven by strong, ultrashort and arbitrarily polarised laser fields. It offers a detailed and accurate description of electron correlation effects, and has been used to probe attosecond phenomena, including high-harmonic generation, the 'attoclock' and strong-field ionisation of molecules.

In the last several years experimental techniques have become sufficiently advanced to probe the strong-field-driven dynamics of correlated electrons in atomic and molecular systems. Theoretical approaches to describe these processes can fall short when the quantum effects under inspection defy the classical, three-step paradigm, and this presents a uniquely challenging prospect for computational modelling.

It has long been held that a solution of the Time-Dependent Schrödinger Equation (TDSE) is impossible for all but the simplest target systems. Thus simplified approaches– invoking e.g. a single-active electron model– have dominated.

However by making use of the R-matrix approach, and building capability hierarchically on more than half-a-century-worth of atomic, molecular and optical physics software, we have developed the R-matrix with time-dependence (RMT) code explicitly for the solution of the TDSE for general multielectron atomic and molecular systems driven by strong fields [1].

This contribution will report on the capabilities of RMT, and the new scientific insights that it can provide. To demonstrate new capability to describe arbitrarily polarised laser pulses, we will show results of research into electron vortices and the attoclock scheme [2]. Furthermore, by expanding the methodology to account explicitly for spin[3], we can show new schemes to address spin-polarised electrons and polarisation in high-harmonic generation. Finally, RMT can now desribe electronic dynamics in molecular systems. The contribution will show some initial applications of RMT to molecular photoionisation, outline the boundaries of our current capability and our vision for future developments.

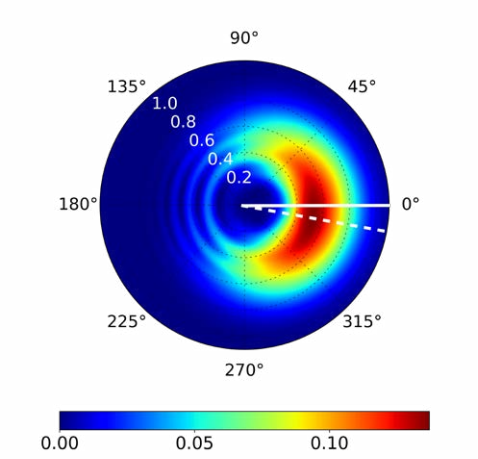

Figure 1. Photoelectron momentum distribution, in the laser polarization plane, arising from F^- in a two-cycle, 800-nm, 5×10^{13} W/cm^2, circularly polarized laser pulse. The small, negative offset angle– between the maximum of the distribution (dashed line) and the x axis (solid line)– can be attributed to contraction of the residual electron cloud following photodetachment of the electron [2].

References

[1] A. C. Brown *et al*, Comp. Phys. Commun. **250**, (2020) 107062
[2] G. S. J. Armstrong *et al*, Phys. Rev. A **101**, (2020) 041401
[3] J. Wragg *et al*, Phys. Rev. Lett. **123**, (2019) 163001

*E-mail: andrew.brown@qub.ac.uk

Optical Measurement of Photorecombination Time Delays

G G Brown[1]*, C Zhang[1], D H Ko[1], and P B Corkum[1,2]

[1]Department of Physics, University of Ottawa, Ottawa, Canada K1N 6N5
[2]National Research Council of Canada, Ottawa, Canada K1A 0R6

Synopsis Measuring the photoionization time delay between electrons from different orbitals is one of the most important accomplishments of attosecond science [1]. These measurements are typically done using attosecond pulses generated through electron recollision to photoionize a target inside a photoelectron spectrometer [2]. In such experiments, the measured delay corresponds to the superposition of all possible paths to ionization and can be difficult to deconvolve. Here, we show that, by characterizing recollision dynamics entirely optically [3], photorecombination time delays due to electron dynamics and structure can be unambiguously measured without obfuscation from ionic structural and propagation effects. This work paves the way for the entirely optical measurement of ultrafast electron dynamics and photorecombination delays due to electronic structure, multielectron interaction, and strong-field driven dynamics in complex molecular systems and correlated solid-state systems.

The process of recollision leading to attosecond pulse emission consists of three steps [4]: (1) in the presence of a strong field, an electron tunnels into the continuum, (2) the electron is accelerated by the strong field, and (3) the electron recombines with its parent ion and emits a high energy photon. In sinusoidal fields, these three-steps repeat every half optical-cycle. The phase of attosecond pulses generated in simple systems is predominantly shaped by the electron's propagation in the continuum and is well understood. In more complex system, the recombination step exhibits time delays which dramatically reshape the attosecond pulse phase similarly to photoionization time delays.

Measuring attosecond pulses is accomplished in one of two ways: (*i*) by ionizing a secondary target with an attosecond pulse, or (*ii*) by perturbing the recollision electron with a co-phased perturbing field [3]. Since the second-class of measurement takes place during attosecond pulse generation is typically referred to as being done *in situ*. *In situ* measurement is advantageous because it is performed entirely optically and it is invariant with respect to attosecond pulse propagation. The domain of attosecond *in situ* techniques, however, is unclear and they are thought to be insensitive to recombination time delay [7].

Here, we demonstrate that *in situ* methods are sensitive to recombination effects pertaining to strong-field driven electron dynamics and electronic structure, but invariant with respect to ionic structure. We first demonstrate this through experimental and theoretical studies of *in situ* characterization of attosecond pulses generated in argon, which exhibits a photorecombination delay around the Cooper minimum [5]. We then present experimental and theoretical studies of recollision-induced plasmonic excitation in xenon and how multielectron interaction can be studied using these techniques [6].

The optical study of photorecombination time delay measurements is advantageous in many ways: these techniques observe strong-field electron dynamics and structure without obfuscation from ionic structure, they are robust with respect to propagation effects, and can be performed entirely optically. Any laboratory capable of generating high harmonics can perform these studies. Finally, combining attosecond *in situ* measurement with photoionization-based measurements will permit the unambiguous isolation of time delays associated with ionic structural effects.

References

[1] Goulielmakis, E *et al* 2010 *Nature* **466** 739-743
[2] Cattaneo, L *et al* 2016 *Opt. Express* **24** 29060-29076
[3] Kim, K T *et al* 2014 *Nature Photon.* **8** 187-194
[4] Corkum, P 1993 *Phys. Rev. Lett.* **71** 1994–1997
[5] Higuet, J *et al* 2011 *Phys. Rev. A* **83** 053401
[6] Shiner, A D *et al* 2011 *Nature Phys.* **7** 464-467
[7] Spanner, M *et al* 2016 *Phys. Rev. A* **94** 023825

*E-mail: graham.brown@uottawa.ca

Comprehensive investigation of nondipole effects in photoionization of the He 1*s* and Ne 2*s* shells

T Buhr[1] *, L Ábrók[2], A Müller[3], S Schippers[1], Á Kövér[2] and S Ricz[2] †

[1]I. Physikalisches Institut, Justus-Liebig-Universität Gießen, Giessen, 35392, Germany
[2]Institute for Nuclear Research (ATOMKI), Debrecen, 4001, Hungary
[3]Institut für Atom- und Molekülphysik, Justus-Liebig-Universität Gießen, Giessen, 35392, Germany

Synopsis Angular distributions of He 1*s* and Ne 2*s* photoelectrons were measured over wide ranges of the polar and azimuthal angles covering a solid angle of about 2π at 100 eV and 200 eV photon energies using linearly polarized synchrotron radiation. The photoelectrons were detected in in-plane as well as in out-of-plane geometry as determined by the photon momentum and polarization vectors. The observed difference between the experimental and theoretical angular distributions might be explained by the neglected terms in the calculation [1].

Nondipole effects strongly modify the polar and azimuthal-angle dependence of the double differential cross section of the photoelectron emission [1]. In order to study these effects in detail, angular distributions of He 1*s* and Ne 2*s* photoelectrons were measured at 100 eV and 200 eV photon energies in the polar angular range (ψ) of ±15° to ±165° relative to the photon momentum vector (**k**) and in the azimuthal angular range (χ) of 0° to 90° as well as of 180° to 270° applying linearly polarized photons. The experiments were carried out at the beamline PTB-XRS of the synchrotron light source BESSY II in Berlin, Germany. The photoelectrons were detected with an ESA-22-type electrostatic electron spectrometer [2, 3] in in-plane and in out-of-plane geometry as determined by the photon momentum (**k**) and polarization vectors (**P**). The experimental data were fitted by the theoretical expression of the angular distribution of photoelectrons for linearly polarized light. The electric dipole and the first-order nondipole (electric quadrupole and magnetic dipole) interactions were taken into account.

Figure 1 shows the ratios of the fitted and the measured intensities for He 1*s* photoelectrons at 100 eV photon energy for the entire angular range. Different colors and symbols denote different polar angles. The deviation of the ratios from unity indicates that the shape of the experimental angular distribution differs from the predicted one. The difference between the experimental and theoretical values might be explained by the neglected terms in the interaction potential and by the neglected higher-order multipoles in the theoretical description.

We would like to thank B. Pollakowski-Herrmann, J. Weser and B. Beckhoff for assistance in using beamline PTB-XRS. We also wish to thank D. Varga for fruitful discussions.

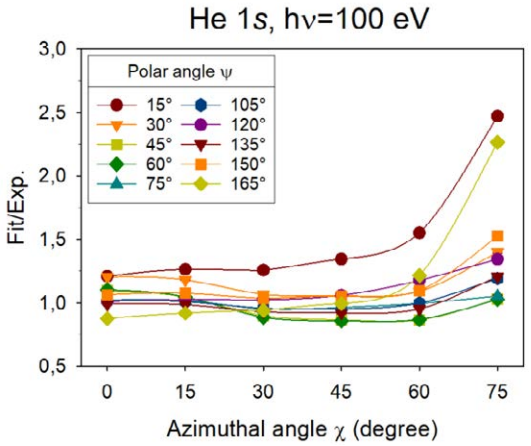

Figure 1. Fitted [1] and experimental intensity ratios for He 1*s* photoelectrons at 100 eV photon energy as a function of the azimuthal angles. Different colors and symbols represent different polar angles.

References

† Deceased
[1] Derevianko A *et al* 1999 *At. Data Nucl. Data Tables* **73** 153
[2] Ricz S *et al* 2002 *Phys. Rev. A* **65** 042704
[3] Ábrók L *et al* 2016 *Nucl. Instrum. Methods B* **369** 24

* E-mail: ticia.buhr@physik.uni-giessen.de

Probing electronic coherence in the vicinity of Fano resonances using high resolution photoelectron interferometry

D Busto[1,2]*, H Laurell[1], C Alexandridi[3], D Finkelstein Shapiro[4], A Escoubas[1], M Isinger[1], S Nandi[1], D Platzer[3], R J Squibb[5], M Turconi[3], S Zhong[1], C L Arnold [1], R Feifel[5], M Gisselbrecht[1], T Pullerits[4], P Salières[3], A L'Huillier[1]

[1]Department of Physics, Lund University, P.O. Box 118, SE-22 100 Lund, Sweden
[2]Physikalisches Institut, Albert-Ludwigs-Universität, Stefan Meier Strasse 19, 79104 Freiburg, Germany
[3]LIDYL, CEA, CNRS, Université Paris-Saclay, CEA Saclay, 91191 Gif-Sur-Yvette, France
[4]Department of Chemical Physics and NanoLund, Lund University, Box 124, SE-221 00 Lund, Sweden
[5]Department of Physics, University of Gothenburg, Origovägen 6B, SE-41296 Gothenburg, Sweden

Synopsis
The photoionization of atoms or molecules by attosecond pulses leads to the emission of photoelectron wave packets. Quantifying the coherence properties of these wave packets is of great interest but very challenging. We use high-spectral-resolution attosecond photoelectron interferometry to measure the spectral amplitude and phase of photoelectron wave packets emitted in the vicinity of the 2s2p Fano resonance in He. We compare the measured amplitude and phase to different models and discuss the effect of decoherence in our measurements.

Photoelectron spectroscopy is a powerful technique that provides detailed information on the electronic structure of matter. The advent of attosecond science has opened the possibility to combine photoelectron spectroscopy with attosecond temporal resolution in order to investigate electronic dynamics in real time.

Attosecond photoelectron interferometry, which relies on the interference of two-photon transitions induced by absorption of an attosecond pulse train followed by absorption or emission of an infrared photon from a phase-locked laser pulse, is a technique that allows measuring the spectral amplitude and phase of photoelectron wavepackets (EWPs) [1]. So far, it has been assumed that the EWPs are coherent so that the measured amplitude and phase reflect that of the photoelectron wavefunction [4, 3]. However, measurements do not always probe all degrees of freedom of the system, resulting in a loss of coherence of the measured wave packet.

In this work, we present high spectral resolution angle-integrated RABBIT measurements in the vicinity of the 2s2p Fano resonance in helium. Fano resonances, which arise from the interference between direct ionization and autoionization, are particularly well suited to investigate decoherence since a loss of coherence will affect the contrast of the interference pattern [2]. The high spectral resolution of our measurements allows us to retrieve the amplitude and phase of the wave packets with unprecedented accuracy and to show that the infrared pulse couples the 2s2p resonance with the $2p^2$ state, whose lifetime is longer than the duration of the measurement, resulting in a loss of coherence of EWPs as shown in Fig. 1. These results pave the way towards the investigation of partially coherent electronic dynamics in more complex systems.

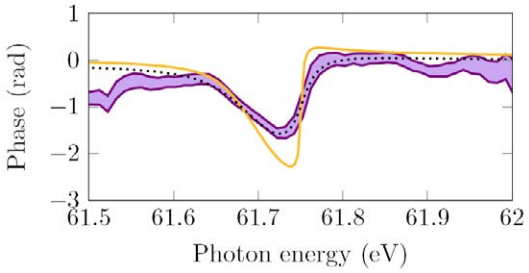

Figure 1. Phase of the PEWP measured in the vicinity of the 2s2p resonance (purple) and comparison with a fully coherent (yellow) and partially coherent (dotted black) model.

References

[1] Paul P M *et al* 2001 *Science* **292** 1689
[2] Bärnthaler A *et al* 2010 *Phys Rev Lett* **105** 056801
[3] Busto D *et al* 2018 *J. Phys. B.* **51** 044002
[4] Gruson V *et al* 2016 *Science* **354** 6313

*E-mail: david.busto@fysik.lth.se

Two-photon ionization using superradiant light from a Free-Electron Laser

J Feist[1], A Palacios[1,*], G Sansone[2], D Garratt[3], J P Marangos[3], T Mazza[4], M Meyer[4], R J Squibb[5], R Feifel[5], M Bonanomi[6,7,8], C Callegari[6,†], M Coreno[9], A Demidovich[6], M Di Fraia[6], L Giannessi[6,10], O Plekan[6], K C Prince[6], R Richter[6], F Sottocorona[6,11], S Spampinati[6]

[1]Universidad Autónoma de Madrid, 28049 Madrid, Spain
[2]Albert-Ludwigs-Universität Freiburg, 79104 Freiburg, Germany
[3]Imperial College London, South Kensington Campus, London SW7 2AZ, United Kingdom
[4]European XFEL, 22869 Schenefeld, Germany
[5]Department of Physics, University of Gothenburg, 412 96 Gothenburg, Sweden
[6]Elettra Sincrotrone Trieste, 34149 Trieste, Italy
[7]Dipartimento di Fisica, Politecnico di Milano, 20133 Milano, Italy
[8]Istituto di Fotonica e Nanotecnologie, Consiglio Nazionale delle Ricerche, 20133 Milano, Italy
[9]ISM-CNR, Istituto di Struttura della Materia, LD2 Unit, 34149 Trieste, Italy
[10]Istituto Nazionale di Fisica Nucleare, Laboratori Nazionali di Frascati, 00044 Frascati, Italy
[11]University of Trieste, 34127 Trieste, Italy

Synopsis The new superradiance mode of the FERMI Free-Electron Laser (FEL) produces 5 fs pulses of high power and was used to investigate two-photon resonant ionization of He through the ^{1}P(2s2p) doubly excited state. The pulse duration was less than a third of the 17 fs lifetime of the resonance, and we measure a photoelectron spectrum that is in agreement with theoretical calculations.

Recently a new mode of operation, superradiance, has been demonstrated at FERMI [1], and it produced tunable, close to transform limited pulses with a duration much shorter than previously generated by a seeded FEL. Here we describe a first application of this radiation to resonant, two-photon atomic ionization.

Doubly excited states of He are a prototypical system for the investigation of correlation effects and many new phenomena [2,3]. Using 60.1 eV pulses of ~5 fs duration, we resonantly excited He to the doubly excited ^{1}P(2s2p) state, which has a lifetime of ~17 fs. The measured two-photon electron spectrum is dominated by n=2 final states, He^+(2s/2p), rather than n=1 He^+(1s) which dominate non-resonant excitation. Other satellite peaks are also present.

In a first theoretical approximation, the process appears to be sequential excitation of both electrons by one photon, followed by ejection of one of these two electrons by a second photon. However, detailed calculations indicate that this picture is incomplete and the role of correlation must be taken into account, being responsible for the intensity of satellite lines.

This work demonstrates that superradiance opens new opportunities for resonant, non-linear ultrafast spectroscopy. We used light of precise, tunable wavelength with a duration less than the lifetime of the excited state. As well as the advantage of using pulses faster than the correlation dynamics we also overcome problems of sample depletion before maximum intensity is reached. We have also characterized the light in terms of harmonic content: the presence of second and third harmonic radiation can be problematic for two- and three-photon processes respectively, and we have quantified these effects.

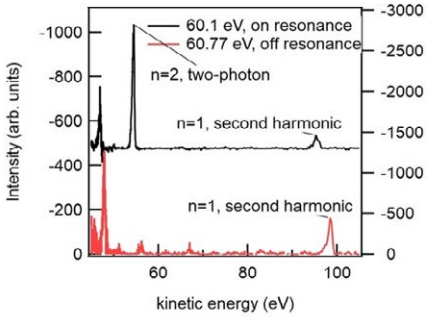

Figure 1. Photoelectron spectra taken on and off resonance. The contributions of the spurious second harmonic are shown and overlap the two-photon ionization to the ground state ion.

References

[1] Mirian N S *et al,* 2021 *Nat. Phot., in press*
[2] Kaldun A *et al,* 2016 *Science* **354** 738
[3] Ott Ch *et al,* 2019 *Phys Rev. Lett.* **123** 163201

*E-mail: alicia.palacios@uam.es †E-mail: carlo.callegari@elettra.eu

A high-harmonic generation source for ultrafast X-ray imaging and spectroscopic applications driven by a high-power mid-infrared optical parametric chirped-pulse amplifier

F Campi[1] *, J H Buss[2], M V Petev[2], T Golz[2], S Starosielec[2], M Schulz[2], R Riedel[2], and P M Kraus[1,3]

[1]Advanced Research Center for Nanolithography, Science Park 106, 1098 XG Amsterdam, The Netherlands
[2]Class 5 Photonics GmbH, Notkestrasse 85, 22607 Hamburg, Germany
[3]Department of Physics and Astronomy, and LaserLaB, Vrije Universiteit, De Boelelaan 1105, 1081 HV Amsterdam, The Netherlands

Synopsis The combination of short pulse durations and short wavelengths resulting from high-harmonic generation in the water window may allow for simultaneous time-dependent spatially-resolved spectroscopic measurements. To that end, the development of a mid-infrared source exceeding 50 W enables the generation of high-flux X-ray pulses, which can be utilized for element-specific metrology of nano-scale structures.

High-harmonic generation (HHG) has enabled the investigation of electronic processes on their intrinsic timescales, owing to the attosecond temporal structure of the generated pulses. At the same time, HHG provides very broad spectra, thus allowing element sensitivity, as well as short wavelengths, which can be employed for imaging nanostructures, down to the resolution limit.

In the past decade, a few groups demonstrated continua spanning the water-window up to and beyond the oxygen K-edge (540 eV) [1], but the widespread application as spectroscopic source has been hindered by the low available fluxes. At the same time, tremendous efforts have been devoted to overcoming the low numerical aperture of X-ray optics, with techniques such as lensless imaging in the extreme-ultraviolet [2].

A mid-infrared high-power laser system (>50W at 50 kHz), delivering femtosecond pulses with energy exceeding 1 mJ, at a wavelength of 2 µm (Figure 1a), was recently installed in our laboratories. The unprecedented power-level achieved, together with outstanding long-term stability of its output (Figure 1b), render this laser an ideal driver for photon-hungry applications in the X-ray spectral range, such as diffractive imaging.

This system will drive an HHG source. Consequently, we expect to generate X-ray pulses up to 600 eV. Such a source should enable wavelength-resolved element-specific broadband lensless imaging on sub-10-nm structures.

In this poster, we present the layout and performance of the laser chain, along with the design of the X-ray HHG beamline, as well as the first experimental X-ray spectra obtained.

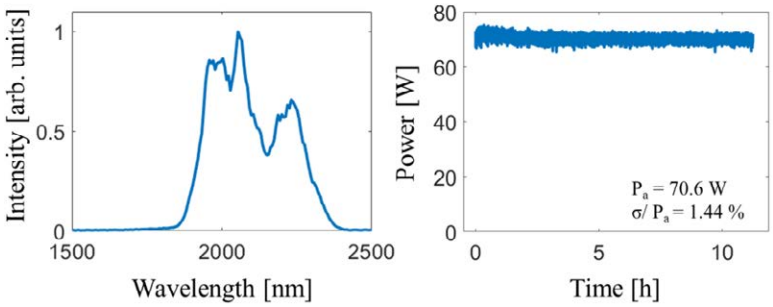

Figure 1. a) Spectrum of the output of the optical parametric chirp-pulse amplifier. b) Long-term power stability.

References

[1] T Popmintchev *et at* 2012 *Science* **336**, 1287-1291
[2] S Witte *et al* 2013 *Light: Science & Applications* **3** (3)

* E-mail: f.campi@arcnl.nl

Stabilization of an autoionizing polariton in attosecond transient absorption

C Cariker[1] *, N Harkema[2], E Lindroth[3], A Sandhu[2], and L Argenti[1] †

[1]University of Central Florida, Orlando, FL, 32814, USA; [2]University of Arizona, Tuscon, AZ, USA; [3]Stockholm University, Stockholm, Sweden, EU

Synopsis We compute *ab initio* the attosecond transient absorption spectrum of argon, where the light-induced coupling between resonances in the continuum causes the autoionizing $3s^{-1}4p$ to split into a pair of polaritonic branches. The computed and measured ATAS are in excellent agreement, both evidencing stabilization of one of the polaritons against ionization. This stabilization is ascribed to the interference between radiative and Auger decay channels, corroborated by an extension of the Jaynes-Cummings model to overlapping autoionizing states.

Intense laser pulses can couple resonances in the continuum, giving rise to a split pair of autoionizing polaritons (AIPs) whose lifetime can be extended as a result of interference between radiative and Auger decay channels [1]. We study this phenomenon both analytically and computationally by simulating *ab initio* [2] attosecond transient absorption spectra (ATAS) in argon. The spectra exhibit multiple avoided crossings between the $3s^{-1}4p$ autoionizing resonance and light-induced states originating from nearby even parity resonances in the continuum. These avoided crossings, which are characteristic of the formation of a polaritonic multiplet, show that some AIPs are stabilized against autoionization. Using an extension of the Jaynes-Cummings model to autoionizing states [3], we confirm that this stabilization is due to the destructive interference between radiative and Auger decay channels. These theoretical predictions are in excellent agreement with recent experiments conducted in parallel [4]. This study indicates a new way to control the electronic structure in the continuum of poly-electronic systems.

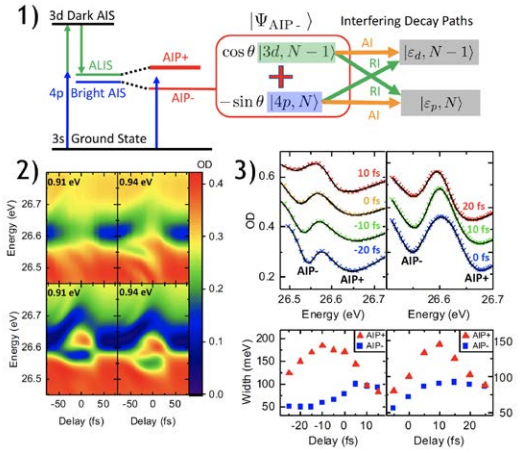

Figure 1. 1) Diagram depicting the excitation and decay of a pair of AIPs in argon. 2) Experimental (top) and theoretical (bottom) ATAS of argon at 2 different IR frequencies, where a pair of AIPS are visible near zero time delay and have markedly different spectral widths. 3) Experimental (left) and theoretical (right) ATAS of argon at an IR energy of 0.94 eV, along with fits of the spectral width, at a sampling of time delays.

References

[1] Y S Kim and P Lambropolous 1982 *Phys Rev Lett* **49** 1698
[2] T Carette L Argenti *et al* 2013 *Phys Rev A* **87** no 2, p 023420
[3] E T Jaynes and F W Cummings 1963 *Proceedings of the IEEE* **51** 89
[4] N Harkema, C Cariker *et al* 2021 arXiv:2103.17077 [physics.atom-ph]

*E-mail: ccariker@knights.ucf.edu
†E-mail: Luca.Argenti@ucf.edu

Core hole motion revealed through interference in above-threshold ionization

S Carlström[1,2]*, JM Dahlström[2], M Yu Ivanov[1], and S Patchkovskii[1]

[1]Max-Born-Institut, Max-Born-Straße 2A, 12489 Berlin, Germany
[2]Department of Physics, Lund University, Box 118, SE-221 00 Lund, Sweden

Synopsis We study the role of spin–orbit hole dynamics and inelastic scattering in the interference between the various pathways the photoelectron may take in above-threshold ionization; 1) direct electrons reaching a maximal kinetic energy of twice the ponderomotive energy ($2U_p$), 2) rescattered electrons reaching up to $10U_p$ kinetic energy, where the scattering may be 2a) elastic or 2b) inelastic, the latter leading to a transition between the spin–orbit states of the ion.

When a spin–orbit split ion is prepared through photoionization, a core hole wavepacket consisting of spin-up and spin-down vacancies is formed, which will oscillate in time. This core hole motion can be observed using *recollisional imaging*, ie exchange of a core electron with the initial photoelectron.

In *above-threshold ionization* (ATI), there are at least two pathways to the same final state of the overall system, ie photoelectron and ion; in the low-energy region $< 2U_p$, direct and (in)elastically rescattered photoelectrons may interfere; between $2U_p$ and $10U_p$, the interference takes place between elastically and inelastically rescattered photoelectrons (see Fig. 1a). The interference patterns depend on the difference in scattering phase between the pathways; this forms the basis for the recollisional imaging.

To investigate these effects, we compute photoelectron spectra from xenon, which has a spin–orbit splitting of approximately 1.3 eV, when ionized by an intense laser field of varying driving frequency ω and pulse duration τ. The spectra are resolved on photoelectron momenta and final ion state; by tracing out the photoelectron we form the *degree of coherence* between the ion cores:

$$\tilde{\rho}_{3/2;1/2} \equiv \frac{\rho_{3/2;1/2}}{\sqrt{\rho_{3/2;3/2}\rho_{1/2;1/2}}},$$

where $\rho_{a;b}$ is the coherence between ion cores a and b, and $\rho_{a;a}$ the population in the ion core a. This is plotted in Fig. 1b). The spectra are calculated using an implementation of time-dependent configuration interaction singles (TD-CIS, see eg [1]), including spin–orbit coupling using a relativistic pseudopotential [2].

*E-mail: stefanos@mbi-berlin.de

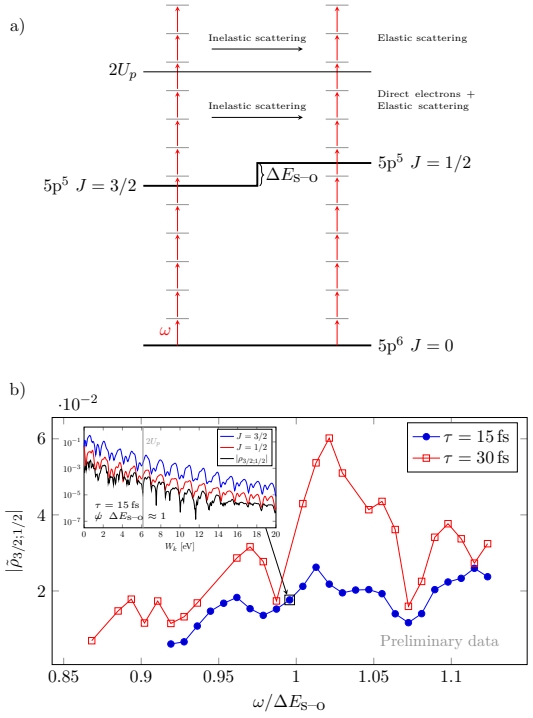

Figure 1. a) Sketch of ATI from xenon. $J = 3/2$ is dominant, so inelastic scattering mainly occurs $3/2 \to 1/2$. b) Computed degree of coherence between the $J = 3/2$ and $J = 1/2$ ion cores of xenon as a function of the relative frequency between the driving IR field and the spin–orbit splitting. Inset: Typical ATI spectrum resolved on J of the ion, along with the coherence between the ion states.

References

[1] Greenman L *et al* 2010 *Phys. Rev. A* **82**(2), 023406
[2] Peterson KA *et al* 2003 *J. Chem. Phys.* **119**(21), 11113–11123

Role of carrier-envelope phase on below-threshold high-order harmonic generation of Ar atom

Y-Y Chen[1], Z-H Jiao[1]*, X-R Hong[1], and P-C Li[1,2,3]†

[1]College of Physics and Electronic Engineering, Northwest Normal University, Lanzhou 730070, China
[2]Research Center for Advanced Optics and Photoelectronics, Department of Physics, College of Science, Shantou University, Shantou, Guangdong 515063, China
[3]Key Laboratory of Intelligent Manufacturing Technology of MOE, Shantou University, Shantou, Guangdong 515063, China

Synopsis We theoretically study the carrier-envelope phase (CEP) dependence of the below-threshold harmonics generation (BTHG) of argon atom in the few cycle laser pulses. We find that the CEP of laser pulses plays an important role in BTHG,leading to the enhancement and suppression of the BTHG.

High-order-harmonic generation (HHG) [1] of atoms and molecules in the intense laser fields, leading to the production of the coherent extreme-ultraviolet and attosecond pulses, has attracted much interest in the subject of ultrafast science and technology in the last decade.The essential features in HHG, such as the above-threshold harmonic plateau and cutoffs, can be well understood by the semiclassical three-step model [1,2].The strong field approximation (SFA) has been commonly adopted for studying the HHG above the ionization threshold. However, due to its complete neglect of the intermediate bound states and the Coulomb interaction in the final state, the SFA is not accurate to describe the below-threshold harmonic generation (BTHG).

In this work, we have presented the effects of CEP on the near-and below-threshold HHG in the few cycle laser fields. The HHG is obtained by solving the time-dependent Schrdinger equation (TDSE) of argon atom accurately and efficiently by means of the time-dependent generalized pseudospectral method for nonuniform spatial discretization of the Hamiltonian.

In Fig.1(a) and 1(b), we show the CEP dependence of the near-and below-threshold HHG of Ar atom driven by a few cycle laser pulses, respectively.In our calculation,the laser field has the following form:

$E(t) = E_0 f(t) = E_0 \cos^2\left(\frac{\pi t}{NT}\right)\cos(\omega t + CEP)$

where $f(t)$ is the cosine-squared pulse with 5 optical cycles (o.c.).E_0 and ω are the amplitude and frequency, respectively. We find that the near-and below-threshold HHG is sensitive to the CEP of the laser pulses.Namely,the yields of the near-and below-threshold HHG show a periodic change.To understand this process, we have performed the wavelet time-frequency transform and classical trajectories analysis.The results indicate that CEP of the laser pulses is responsible for the interference between different harmonic orders, leading to the coherent enhancement and suppression of the BTHG.

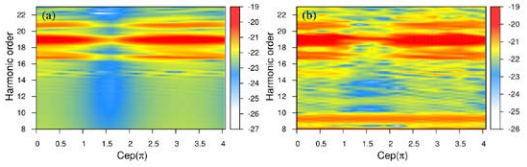

Figure 1. The near- and below-threshold HHG as a function of the CEP of the laser pulses with the intensity (a) 1.0×10^{13} W/cm^2(b) 3.0×10^{13} W/cm^2, respectively. The center wavelength used is 1800nm and the pulse duration is 5 optical cycles.

Acknowledgments

This work was supported by National Natural Science Foundation of China (11674268, 11764038, 12074239, 91850209); Natural Science Foundation of Guangdong Province (200110165892233, 2020A1515010927, 210206153460124); Department of Education of Guangdong Province (2018KCXTD011, 2019KTSCX038, 2020KCXTD012); Shantou University (NTF18030).

References

[1] F. Krausz *et al* 2009 *Rev. Mod. Phys* **81** 163-234
[2] P. Huang *et al* 2001 *Phys. Rev. A* **79** 043806

*E-mail: jiaozh@nwnu.edu.cn
†E-mail: lipch@stu.edu.cn

Photoelectron momentum distribution of Helium atom

Aldarmaa Ch[1*], Zorigt G[1] and Khenmedekh L[1]

[1]Department of Physics, School of Applied Sciences, Mongolian University of Science and Technology, Ulaanbaatar city, 14191, Mongolia

Synopsis Photoelectron momentum distribution (PMD) of the helium atom driven by linearly polarized strong laser field is studied, based on the numerical solution of the time-dependent Schrodinger equation (TDSE).

TDSE for hydrogen atom in the linearly polarized strong laser field is numerically solved using the Coulomb Wave Discrete Variable Representation (CWDVR) method [1].

We used the one active electron model with the variable nuclear charge Coulomb potential [2] for the atomic Hamiltonian. The final state wavefunction was taken at the moment t=3τ, where the τ is the laser pulse duration time. Interference pattern seen in the electron probability distribution remind the similar picture for the case of the Hydrogen atom. Further we calculated the PMD of the ejected electron. The ionization amplitude is obtained by projecting the final state wavefunction onto the stationary scattering wavefunction $\psi_k^-(r)$.

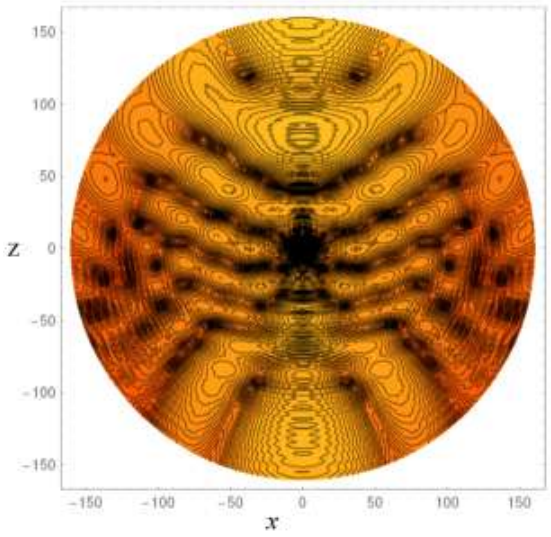

Figure 1. Electron probability density plot. The laser parameters are: frequency ω=0.4445, intensity I=1a.u., initial phase φ=-π/2, cycle number nc=2.

* E-mail: aldarmaa@must.edu.mn

Then PMD is equal to the square of the modulus of the amplitude. For the Helium atom, variable nuclear charge must be used in the stationary wavefunction $\psi_k^-(r)$ also.

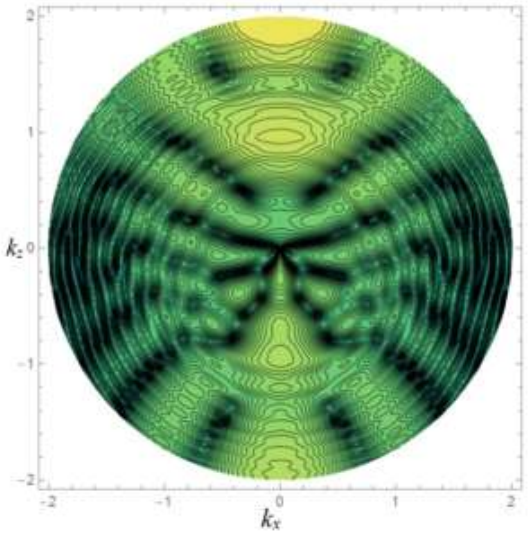

Figure 2. Photoelectron momentum distribution. The laser parameters are: frequency ω=0.4445, intensity I=1a.u., initial phase φ=-π/2, cycle number nc=2.

As it's seen from the figure (1), the interference pattern similar to the electron probability distribution turns out for the ejected electron momentum distribution. The laser pulse shape and parameters are taken as in the literature [2].

References

[1] G.Zorigt *et al* 2019 IJMA 10 , vol 5

[2] S.Borbely, A.Toth, D.G. Arbo, k.Tokesi and L.Nagy, Phys.Rev A99, 013416 (2019)

Glory interference spectroscopy of Sr atom

K Ferentinou[1], P Kalaitzis[1], S Danakas[1], F Lépine[2], C Bordas[2] and S Cohen[1] *

[1]Atomic and Molecular Physics Laboratory, Physics Department, University of Ioannina, 45110 Ioannina, Greece
[2]Institut Lumière Matière, Université Lyon 1, CNRS, UMR 5306, 10 rue Ada Byron 69622 Villeurbanne Cedex, France

Synopsis Near-threshold atomic photoionization under the presence of an external static electric field leads to slow (meV) photoelectron images that exhibit an intense peak at their center. This peak is due to the so-called glory scattering, whose pronounced magnitude oscillations as a function of photoelectron energy are connected to classical electron dynamics. This was recently demonstrated by employing two-photon threshold ionization of Mg atom. Here we extend our measurements to Sr atom, allowing comparison of the findings between different atoms as well as different photoionization schemes.

The term "glory scattering" denotes the divergence of the classical differential cross section when the deflection function goes through zero for a nonzero impact parameter. This critical effect also arises in near-threshold atomic photoionization under the presence of an external static electric field of strength F, whenever the linear polarization of the ionizing laser radiation is parallel to the static field direction. Then, glory scattering manifests itself as an intense peak at the center of the photoelectron momentum distribution recorded on a 2D position sensitive detector (see inset of Fig. 1(a)).

The gross magnitude variation of the glory peak as a function of energy comprises two local maxima (one at the classical saddle point energy E_{sp}=-2$\sqrt{F}$ au and one at ~0.775E_{sp}) and a steady decrease at higher energy [1]. In addition, the glory curve also displays oscillations of appreciable amplitude and intense beating effects, persisting even above the E=0 zero-field ionization limit (where they have no counterpart when F=0). More importantly, the "short time" Fourier transform of the E>0 glory spectrum allows the extraction of time of flight differences among various classical trajectories followed by the electron from the source to the center of the image.

The above quantum mechanical predictions on the hydrogenic glory signal were fully confirmed by an experimental study employing two-photon near-threshold ionization of ground state Mg atoms [2]. Nevertheless, for distinguishing between "universal" and atom-specific effects, these findings need to be re-examined by similar measurements and calculations on other non-hydrogenic atoms.

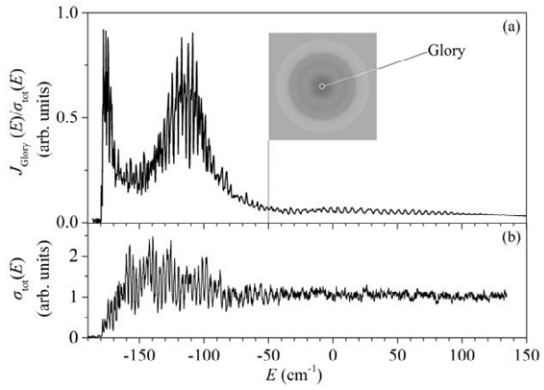

Figure 1. (a) Glory spectrum obtained by single photon ionization of ground state Sr atoms. Static electric field strength F≈850 V/cm. For avoiding systematic errors, the glory signal $J_{Glory}(E)$ at the image center (see the image at the inset) is scaled to the total electron signal. (b) The total ionization cross section $\sigma(E)$ (Sr^+ ions) which is proportional to the total electron signal.

To this purpose, we have recorded the glory signal corresponding to single photon ionization of ground state Sr atoms (Fig. 1(a)). It is evident that this glory spectrum exhibits all the aforementioned universal features, along with a number of atom-specific oscillating patterns attributed to E<0 Stark resonances (also present in the total ionization cross section of Fig. 1(b)). In fact, Sr target atom offers the possibility to trace atom-specific structures through the comparison between single- and two-photon ionization data recorded with otherwise identical conditions.

References

[1] Cohen S *et al* 2017 *J. Phys. B* **50** 065002
[2] Kalaitzis P *et al* 2020 *Phys. Rev A* **102** 033101

* E-mail: scohen@uoi.gr

Efficient two-dimensional localization of Rubidium atom using probe absorption in a microwave-driven five-level system

A Das[*], **M Hossain and J K Saha**[†]

Aliah University, Kolkata, 700160, India

Synopsis A microwave driven atom-laser five-level coupling scheme has been proposed to localize Rubidium atom in the 2D (X-Y) plane. Our investigation is based on the measurement of probe absorption technique which is easily realizable through experiments. The present work may be efficiently utilized in high-precision optical lithography.

Atom localization using quantum interference effects is one of the extensively discussed topics in the field of precision position measurement of atoms. Different atomic schemes have been put forward for high precision and high resolution two-dimensional (2D) [1] as well as three-dimensional (3D) [2] atom localization. In this context, we have proposed a five-level atom-laser coupling scheme in ^{87}Rb atom [Fig. 1(a)] for the spatial localization of atoms in 2D plane by applying orthogonal standing-wave laser fields.

In the proposed atomic configuration, a 780 nm optical probe laser (Pr) drives the transition between $5S_{\frac{1}{2}}$ ground state and $5P_{\frac{3}{2}}$ excited state. $5P_{\frac{3}{2}}$ state is connected to $33S_{\frac{1}{2}}$ and $33D_{\frac{5}{2}}$ Rydberg states by the pump laser (P1, P2) of wavelength 480 nm. The two Rydberg states are further coupled to another Rydberg state $34P_{\frac{3}{2}}$ by two microwave (MW) fields MW1 and MW2. Thus the four fields P1, P2, MW1, MW2 produce a close atom-field interaction loop that may be employed as an 'atomic Wheatstone bridge'. The mutually perpendicular standing-wave fields to localize the atom at a given (x, y) position are generated by P1 and P2.

The localization can be examined by plotting the normalized probe absorption as a function of position at different values of probe detuning (δ), initial phase difference (ϕ) between the MW fields and driving field strength. The peak maxima and position of the probe absorption in the position-dependent 2D-localization pattern [Fig. 1(b)] reflect the precise localization of the atom when it passes through the standing-wave fields. Moreover, the number of peaks in one period of the standing-wave fields give the conditional position probability. The related momentum distribution of the localized atom is an another aspect of our study to confirm the reasonable localization of atom within the uncertainty relation.

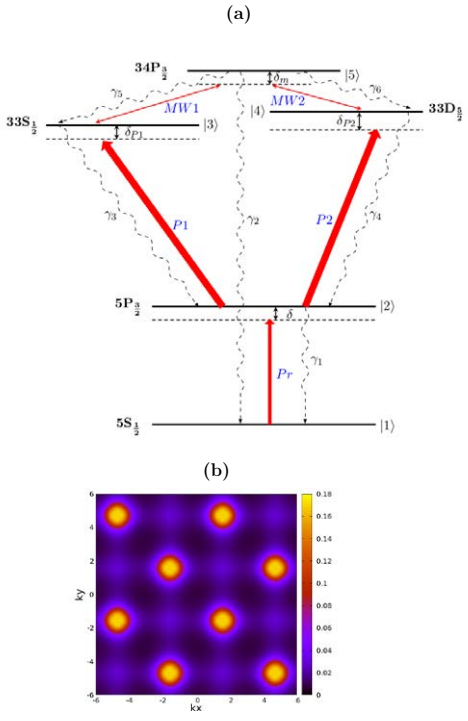

Figure 1. (a) Schematic diagram of microwave-driven five-level system in ^{87}Rb atom. (b) 2D atom localization pattern at $\phi = \pi$, δ=20 MHz.

References

[1] Chunling D *et al* 2011 *Phys. Rev. A* **84** 043840
[2] Zhiping W *et al* 2015 *J. Opt. Soc. Am. B* **32** 7

[*]E-mail: aparajita1223@gmail.com
[†]E-mail: jsaha84@gmail.com

Atom based vector magnetometry using coherent effects

B C Das[1], A Das[1], D Bhattacharyya[2] and S De[1]*

[1]Saha Institute of Nuclear Physics, HBNI, 1/AF Bidhannagar, Kolkata, 700064, India
[2]Department of Physics, Santipur College, Santipur, Nadia, West Bengal, 741404, India

Synopsis Vector magnetometry was studied using the electromagnetically induced transparency (EIT) with linear ⊥ linear polarization in ^{87}Rb D_2 transition. The dependence of the EIT on the directionality of the quantization axis and the relative orientation of the polarization of the applied electric field was studied experimentally. To understand the experimental observation, a theoretical study was done considering thirteen Zeeman levels numerically. Apart from the numerical solution, a toy model has also been developed to get an analytical response of the medium considering the velocity distribution of atoms. Further the magnetic field strength as well as the direction of the magnetic field were calculated using the analytical solution. The study can be helpful in order to make an atom based vector magnetometer.

The coherent interaction of the electric fields with the atomic medium which leads to the phenomena like electromagnetically induced transparency (EIT) and electromagnetically induced absorption (EIA) are highly sensitive to the external magnetic fields. Using this fact, magnetic field with good spatial resolution and high sensitivity can be measured. The narrow transmission peaks of the EIT can be used to develop an EIT based magnetometer.

We have studied the effects of longitudinal and transverse magnetic fields in a hyperfine Λ-type EIT system [1]. We have shown how the EIT resonance is highly sensitive to the magnetic field direction as well as the polarization direction of the applied electric fields. The selection rules of the EIT resonances can be controlled by controlling the polarization component of the laser fields with respect to the quantization axis. For the experiment we have chosen ^{87}Rb atoms in D_2 transition with linear ⊥ linear ($lin \perp lin$) polarization of the probe and the pump beams. With this geometry we can easily separate the probe beam from the pump beam and study the probe transmission only.

In addition to the experiment, Liouville's equation is solved numerically considering all the hyperfine Zeeman sub-levels in order to understand the underlying phenomena of the experimental observation. In addition to that, a toy model of nine level system has been developed to understand the interaction analytically by which we can study the explicit dependency on the angle of polarization ϕ and the direction of the magnetic field (θ).

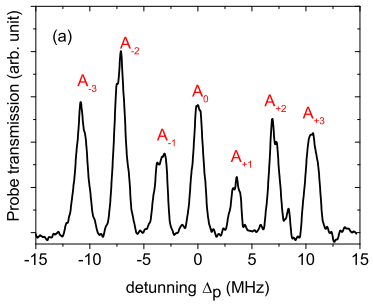

Figure 1. Experimentally observed spectrum for both (i) the magnetic field at 39^0 with respect to the propagation direction z-axis and (ii) the linear polarization axis of the probe beam kept fixed at 40^0 with respect to the x axis, assuming the probe and the pump makes an angle ϕ with the x and the y axis respectively.

We have calculated the magnetic field strength and the direction (θ) using a general formulation which considers the susceptibility of the medium for any value of θ and ϕ. This study can be helpful in the making and theoretical interpretation of a atomic vector magnetometer.

References

[1] Das B C *et al* 2021 *J Opt Soc Am B* **38** 584

*E-mail: sankar.de@saha.ac.in

Laser-assisted photoionization by a single attosecond circularly polarized XUV pulse

R Della Picca[1]*, M F Ciappina[2] and D G Arbó[3]

[1]CONICET and Centro Atómico Bariloche, CNEA, Bariloche, 8400, Argentina
[2]Physics Program, Guangdong Technion-Israel Institute of Technology, Shantou, Guangdong 515063, China
[3]Institute for Astronomy and Space Physics IAFE (UBA-Conicet), Buenos Aires, Argentina

Synopsis We consider the ionization of argon atoms induced by a attosecond extreme ultraviolet circularly polarized laser pulse assisted by an infrared field. We investigate the energy- and angle-resolved photoelectron spectrum in the streaking scenario.

The laser-assisted XUV photoelectric effect (LAPE) occurs when extreme ultraviolet (XUV) and infrared (IR) lasers overlap in space and time. In the streaking regime the XUV pulse is much shorter than the laser wavelength and the electron behaves like a classical particle getting linear momentum from the IR laser field at the instant of ionization. Provided that the fields of these two pulses are controlled with a subfemtosecond temporal resolution, the photoelectron spectra for different delays t_0 between the pulses, referred to as spectrograms, contain information about both the amplitude and the phase of both the XUV and the IR fields. Within this context, in a recent work it has been shown that the aymmetry in the photoelectron spectra allows to reconstruct the complete polarization state of the attosecond pulse, including its possible time dependence [1].

In the present work we study the energy- and angle-resolved photoelectron momentum distribution (PES) produced by an elliptically (in special circularly) polarized XUV pulse and assisted by a linearly polarized IR. We extend the recent theoretical approach based on the strong field approximation (SFA) [2] to the case of elliptical polarization. Within this approach the PES is determined by a leading contribution (kernel information) complemented by others derived from the periodicity and symmetry properties of the dipole transition matrix with respect to the infrared field. We investigate the PES and the asymmetry in the photoemission direction as a function of the delay, the relative intensities, and for different initial bound states.

In the figure we present the PES for argon $3s$ subject to a circularly polarized XUV attosecond pulse, where the typical streaking pattern following the shape of the square of the IR vector potential square (A_L^2) can be observed. From a classical viewpoint, the energy maxima in the perpendicular emission occur at

$$E(t_0) = [v_0^2 - A_L^2(t_0 + \tau_X/2)]/2, \qquad (1)$$

where $v_0 = \sqrt{2(\omega_X - I_p)}$ represents the initial classical velocity of the ejected electron [2].

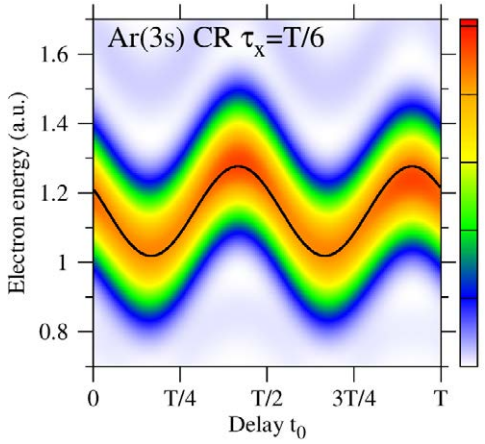

Figure 1. PES for a right circularly polarized XUV pulse with duration $\tau_X = T/6$ as a function of the delay t_0 for electronic emission perpendicular to the IR polarization vector. The black line corresponds to Eq. (1). The IR and XUV laser parameters are $\omega_L = 0.057$ with period $T = 2\pi\omega_L$, the electric amplitude of the IR (XUV) is 0.041 (0.01) and $\omega_X = 2.3$ (all in atomic units).

References

[1] Jiménez-Galán A *et al* 2018 *Nat. Comm.* **9** 850
[2] Della Picca R *et al* 2020 *Phys. Rev. A* **102** 041306

*E-mail: renata@cab.cnea.gov.ar

Photoionization of hydrogen confined in onion shells with Generalized Sturmians in the time-dependent frame.

A L Frapiccini[1] * and D M Mitnik[2]

[1] Instituto de Física del Sur, IFISUR, Departamento de Física, (UNS - CONICET), Bahía Blanca (B8000CPB), Argentina
[2] Instituto de Astronomía y Física del Espacio, IAFE, (UBA - CONICET), Buenos Aires (C1428EGA), Argentina

Synopsis In this work, we present a theoretical study of the photoionization for atomic hydrogen confined in onion fullerene compared with the bare H atom and the single fullerene case. We perform these calculations with a recently developed methodology using generalized Sturmian functions to numerically solve the time-dependent Schrödinger equation.

In recent years, the study of the response to an electromagnetic field of an atom encapsulated in a fullerene cage has been the subject of several theoretical works (see, for example, [1, 2]).

A special case of the fullerene is that of the so called fullerene onions or buckyonions, which consists of hollow carbon cages in which smaller buckyballs are encapsulated into larger ones [3–5]. Fullerene onions have been detected in the interstellar medium [6, 7] and were produced by synthesis by Ugarte in 1992 [8].

In a recent work [9], we proposed to use the generalized Sturmian functions (GSF) to numerically solve the time-dependent Schrödinger equation of a caged atom interacting with a laser pulse. We use and explicit integrating scheme known as Arnoldi, which is a Krylov subspace method.

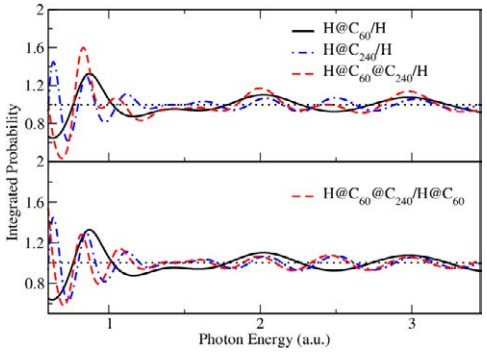

Figure 1. Integrated photoionization probability for the main peak (P peak) as a function of the photon energy

Here we use the GSF methodology to study the photoionization of atomic H encapsulated in fullerene onions, comparing the photoionization spectra for the $H@C_{60}$ and $H@C_{240}$ with the onion structure $H@C_{60}@C_{240}$, analyzing the confinement resonances for the main peak and the first ATI peak separately.

We present our calculations for the ionization of the bare H and caged atom interacting with an electromagnetic pulse having energies between 0.6 and 3.4 a.u.. The results for the photoionization differential probability integrated around the main peak as a function of the photon energy for the $H@C_{60}$ and $H@C_{60}@C_{240}$ are compared with the bare H atom probabilities. We got the expected confinement resonances, observing the increase in the number of oscillations in the onion fullerene with respect to the single-walled fullerene. The results for the main peak demonstrate that at high photon energies, the effect of the inner C_{60} and outer C_{240} cages for the onion fullerene are separable, which is not the case for lower photon energies.

References

[1] Dolmatov V K 2009 *Adv. Quantum Chem.* **58** 13
[2] Amusia M Y, Chernysheva L V 2020 *JETP Lett.* **112** 965
[3] Xu B S 2008 *Xinxing Tan Cailiao/New Carbon Materials* **23** 289–301
[4] Echegoyen L *et al* 2010 in *Chemistry of Nanocarbons* **Ch 19** 463
[5] Bartelmess J *et al* 1980 *J. Nanotechnol.* **5** 1980
[6] de Heer W A,Ugarte D 1993 *Chem. Phys. Lett.* **207** 480
[7] Iglesias-Groth S 2004 *Astrophys. J.* **608** L37
[8] Ugarte D 1992 *Nature* **359** 707
[9] Frapiccini A L, Mitnik D M 2021 *Eur. Phys. J. D* **75** 41

*E-mail: afrapic@uns.edu.ar

High order harmonic generation in semiconductors driven at near- and mid-IR wavelengths

D Freeman[1] *, S Yamada[2], K Yabana[2] and A Kheifets[1]

[1] Research School of Physics, Australian National University, Canberra, ACT, 2601, Australia
[2] Center for Computational Sciences, University of Tsukuba, Tsukuba 305-8577, Japan

Synopsis We study high order harmonics generation (HHG) in crystalline silicon and diamond subjected to near and mid-infrared laser pulses. We employ time-dependent density functional theory and solve the time-dependent Kohn-Sham equation in the single-cell geometry. We demonstrate that clear and clean harmonics spectra can be generated with careful selection of the pulse duration and the exchange-correlation functional. Furthermore, we implement dephasing effects through a mean displacement applied to a Si super-cell and compare our results with earlier calculation by Floss et al. [1] on diamond and by Tacogne-Dejean et al. [2] on Si.

High order harmonics generation (HHG) in solids has attracted efforts of many experimental and theoretical groups. Previous studies of HHG in condensed matter have been driven by improved harmonic intensities offered by the higher electron densities of solids compared to those offered by atomic gases. Experimental studies into HHG for thin films of bulk crystal targets [3] have shown such improvements. Studies have also recently expanded to consider structured metasurfaces and 2D layers like graphene.

In HHG of solids we consider an atomic lattice interacting with a strong oscillating electric field using femtosecond (10^{-15} s) laser pulses, by which a valence band electron is ejected to the conduction band, accelerated in the field and then recombined with its parent ion. This process results in the emission of a photon of energy proportional to the acceleration gained by the photoelectron. For solids, considerations must be made for the electron and hole dynamics in their respective bands.

Here we report on in-production work examing the HHG of diamond and silicon interacting with mid- and near-IR laser pulses of ~100 fs duration. Through the application of time dependent density functional theory, codified as SALMON-TDDFT [4], and motivated by recent literature investigating optimal thin film thickness for HHG signal strength [5], we demonstrate clear HHG spectra through careful parameter setting. Based on these results we review suggestions made in previous literature considering diamond [1] about the importance of solid-laser propagation effects and silicon [2] considering noisy and clean harmonics. Furthermore, we characterize the dephasing effect in HHG for diamond-like lattices through the application of molecular dynamics calculations, randomizing the atomic positions to simulate the lattice at temperature. Our results demonstrate improvement in the signal strength of HHG and suggest that cooling the lattice presents a great benefit for HHG processes.

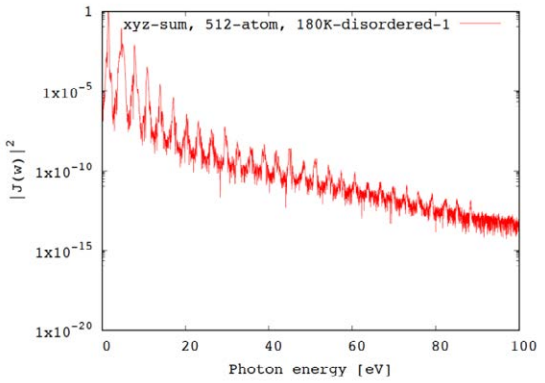

Figure 1. (Colour online) The HHG spectrum for a silicon super-cell of 512 atoms.

References

[1] Floss I *et al* 2018 *Phys. Rev. A* 97, 011401(R)
[2] Tancogne-Dejean et al. 2017 *Phys. Rev. Lett.* 118, 087403
[3] Ghimire S *et al* 2018 *Nat. Phys.* 7, 138
[4] Noda M *et al* 2019 *Comp. Phys. Commun.* 235, 356
[5] Yamada S *et al* 2021 *Phys. Rev. B* 103, 155426

* E-mail: u5562727@anu.edu.au

K-Shell Photoabsorption of the Silicon Isonuclear Sequence

M F Hasoglu,[1] T W Gorczyca,[2]* and S T Manson[3]

[1]Hasan Kalyoncu University, 27100 Sahinbey, Gaziantep, Turkey
[2]Department of Physics, Western Michigan University, Kalamazoo, MI 49008-5252, USA
[3] Department of Physics & Astronomy, Georgia State University, Atlanta, GA 30303-4106, USA

Synopsis We report the results of extensive R-matrix calculations for the K-shell photoabsorption of neutral silicon and all ions in the X-ray region.

Due to the latest high-resolution observations from X-ray telescopes, there is an increasing demand for accurate K-shell photoabsorption cross sections which plays an important role in modeling astrophysical plasmas, interpretation of observed spectra from distant cosmic emitters and determining elemental abundances in the interstellar medium (ISM). Previously, we computed K-shell photoabsorption for magnesium, oxygen, neon, and carbon, and these results were reliable for astrophysics modeling.

Photoabsorption cross sections for the isonuclear sequence neutral Si through Si^{11+}ions have been computed using an R-matrix method with the inclusion of important spectator Auger broadening effects of K-shell-excited autoionizing resonances. The spectroscopic orbitals are formed using Hartree-Fock methods and correlation orbitals are formed using multiconfiguration Hartree-Fock methods with the inclusion of single and double promotions to account for important orbital relaxation effects due to theK-shell vacancy.

Theoretical lowest and K-shell excited energies for the Si^+ target states in neutral Si cross section calculations are listed in Table 1.

Table 1. Some of the LS R-matrix for Si^+ and Si state energies in Ryd. compared to available NIST values.

Atomic State	R-mat	NIST
$1s^22s^22p^63s^23p[^3P]$	-0.6335	-0.5991
$1s^22s^22p^63s^23p[^2P^o]$	0.0000	0.0000
$1s2s^22p^63s^23p^2[^4P]$	135.2964	
$1s2s^22p^63s^23p^2[^2P]$	135.3416	
$1s2s^22p^63s^23p^2[^2D]$	135.4018	
$1s2s^22p^63s^23p^2[^2S]$	135.5095	

Fig. 1 shows our nuetral silicon K-shell photoabsorption cross sections with and without Auger broadening along with the earlier resonanceless independent-particle cross sections; above-threshold photoionization results [1]do not include resonance contributions, thus inadeqate for interpretation of high-resolution spectra.

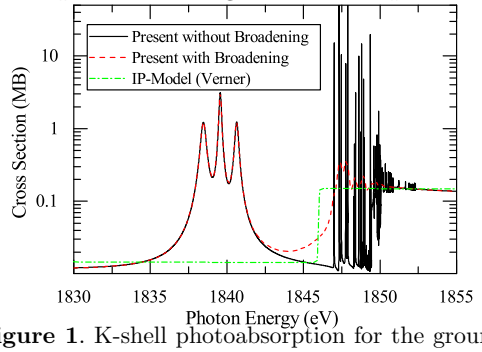

Figure 1. K-shell photoabsorption for the ground state of Si ($1s^22s^22p^63s^23p^2$ $[^3S]$) at the K-edge compared to independent-particle results [1].

The background cross section is in overall good agreement with earlier resonanceless results, implying that the outer L- and M-shell photoabsorption features are taken into account properly. Comparison with the earlier BPRM cross sections [2] for Si^+ - Si^{11+} ions shows good agreement in general for the resonance strengths and widths. Further, relativistic contributions in Si^{11+} are also calculated within the framework of a Breit-Pauli R-matrix method [3]. The computed cross sections have been used for the detailed analysis of the gaseous component of the atomic Si K edge by using high-resolution *Chandra* spectra of low-mass X-ray binaries [4].

References

[1] Verner D A *et al* 1993 *At. Data Nucl. Data Tables* **55** 233
[2] Witthoeft M C *et al* 2009 *Astrophys. J. Suppl. Ser.* **182** 127
[3] Hasoglu M F, Gorczyca T W, and Manson S T 2020 *Phys. Scr.* (Submitted)
[4] Gatuzz E *et al* 2020 *MNRAS* **498** L20

*E-mail: gorczyca@wmich.edu

Atomic ionization by twisted light in the region of autoionizing resonances

M D Kiselev[1,2,3] *, A N Grum-Grzhimailo[2,3] †, A Peshkov[4,5] and A Surzhykov[4,5]

[1]Faculty of Physics, Lomonosov Moscow State University, Moscow, 119991, Russia
[2]Skobeltsyn Institute of Nuclear Physics, Lomonosov Moscow State University, Moscow, 119991, Russia
[3]Department of Physics and Engineering, ITMO University, Saint Petersburg 197101, Russia
[4]Physikalisch-Technische Bundesanstalt, D-38116 Braunschweig, Germany
[5]Technische Universität Braunschweig, D-38106 Braunschweig, Germany

Synopsis Ionization of He atom in the region of 2snℓ and 2pnℓ autoionizing states (60-65 eV) by twisted photons is considered theoretically. The photoelectron angular distributions and cross sections are compared to the plane-wave results in the dipole and nondipole approximations.

In recent years, a considerable interest has been given to the application of twisted (or vortex) light beams in atomic physics. Owing to their helical phase fronts, ring-like intensity distributions and complex polarization patterns these beams may drastically affect the properties of fundamental light-matter interaction processes. During the recent years, for example, a number of experimental and theoretical studies have been performed to study excitation of atoms and ions by vortex photons [1]. It was shown, in particulatr, that twisted light modes can modify the selection rules of atomic transitions and efficiently induce higher-order multipole channels, which might be important for the development of a new generation of atomic clocks.

In contrast to bound-state transitions, less is currently known about photoionization of atomic targets by twisted light. To our knowlege, the vortex effects on ionization in the region of autoionizing states has not been studied so far. In this work we consider the photoionization of neutral helium atom in the energy range from 60 to 65 eV which corresponds to the formation of autoionizing states 2pnℓ and 2snℓ. The purpose of this study is to estimate the scale of the effects of ``twistedness'' on ionization in the region of overlapping Fano resonances of different angular momentum and parity.

The photoelectron angular distribution is given by expression

$$W^{tw}(\vartheta) = \frac{W_0^{tw}}{4\pi}\left[1 + \sum_{k=1,2\ldots} B_k^{tw} P_k(\cos\vartheta)\right],$$

where superscript 'tw' indicates twisted light, $P_k(x)$ is the Legendre polynomial, ϑ is the angle of emission with respect to the axis of the incoming photon beam. The anisotropy parameters B_k^{tw} depend on the ionization amplitudes of different multipoles as well as on spacial characteristics of the photon twisted beam and ensemble of the target atoms. Expressions for B_k^{tw} are derived within the spin density matrix and statistical tensor formalism [2,3]. To estimate the scale of the effect we took into account E1 and E2 multipole transitions. The partial photoionization amplitudes in the region of the helium autoionizing states were calculated by using B-spline R-matrix method [4]. We compare energy dependence of the cross sections and angular anisotropy parameters obtained for plane-wave and twisted photons over the sequence of the autoionizing states.

The results of this study will be presented at the conference.

This work is supported by the Russian Science Foundation (Project No. 21-42-04412) and by the Deutsche Forschungsgemeinschaft (Project No. 445408588).

References

[1] Schulz S *et al* 2020 *Phys. Rev. A* **102** 012812
[2] Surzhykov A *et al* 2015 *Phys. Rev. A* **91** 013403
[3] Balashov V V, Grum-Grzhimailo A N, Kabachnik N M *Polarization and Correlation Phenomena in Atomic Collisions* (Springer, Boston, 2000).
[4] Zatsarinny O 2006 *Comp. Phys. Commun.* **174** 273

* E-mail: md.kiselev94@gmail.ru
† E-mail: grum@sinp.msu.ru

Observation of photoion backward emission

S Grundmann[1]*, M Kircher[1], I Vela-Perez[1], G Nalin[1], D Trabert[1], N Anders[1], N Melzer[1], J Rist[1], A Pier[1], N Strenger[1], J Siebert[1], P V Demekhin[2], L Ph H Schmidt[1], F Trinter[1,3,4], M S Schöffler[1], T Jahnke[1], and R Dörner[1]†

[1]Institut für Kernphysik, Goethe-Universität, 60438 Frankfurt, Germany
[2]Institute of Physics and CINSaT, University of Kassel, 34132 Kassel, Germany
[3]Photon Science, Deutsches Elektronen-Synchrotron (DESY), 22607 Hamburg, Germany
[4]Molecular Physics, Fritz-Haber-Institut der Max-Planck-Gesellschaft, 14195 Berlin, Germany

Synopsis In photoionisation of single atoms and molecules, the emitted photoelectron might receive a larger momentum in light direction than the photon supplies. By means of momentum conservation, this entails that the atom or molecule (photoion) is attracted towards the light source. This counter-intuitive effect was predicted almost a century ago, but lacked experimental confirmation until recently.

Originally discovered by A. Einstein in 1905, the photoeffect has since become a powerful tool to explore structure and dynamics of matter and it is indespensable in modern technology. Surprisingly, even in its simplest manifestation—absorption of a single photon and subsequent emission of one electron from a single atom or molecule—the photoeffect itself is still the subject of ongoing research. In a recent work, we have comprehensively adressed the role of the photon momentum in photoionization of He and N_2. We have experimentally confirmed a 90-year-old prediction [1] of backward-directed ions created by interaction with light that exerts a forward-directed radiation pressure. Our fully-differential experimental data on He and N_2 one-photon ionization in an energy range of 300 eV–40 keV demonstrates how this surprising effect manifest: The photon momentum is imparted onto the photoion, which is essentially the system's center of mass. Moreover, the photon momentum brings in additional orbital angular momentum that leads to a forward tilt of the photoelectron angular distribution. The resulting forward-directed mean momentum of the photoelectron is balanced by a backward-directed momentum transfer to the ion which overcompensates the forward-directed photon momentum transfer. The measured mean momenta of photoelectrons and photoions in the light propagation direction are displayed in Fig. 1.

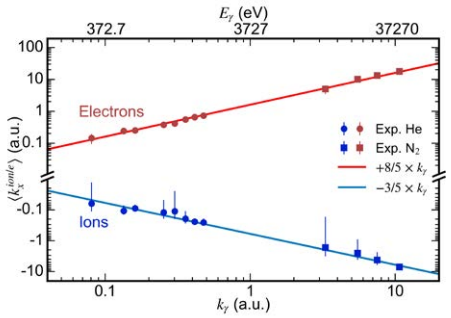

Figure 1. Mean value of electron (red) and ion (blue) momenta along the light propagation axis after photoionization as function of the photon momentum (bottom scale) and photon energy (top scale). The lines show theory predictions from Ref. [2]. The error bars are asymmetric because the y-axis is logarithmic.

References

[1] Sommerfeld A and Schur G 1927 *Ann. Phys.* **396** 409
[2] Chelkowski S, Bandrauk A D, and Corkum P B 2014 *Phys. Rev. Lett.* **113** 26005

*E-mail: grundmann@atom.uni-frankfurt.de
†E-mail: doerner@atom.uni-frankfurt.de

Sequential ionization of neutral Kr up to Kr^{3+} by intense femtosecond XUV pulses

E V Gryzlova[1]*, M D Kiselev[1,2], M M Popova[1,2], A A Zubekhin[2], G Sansone[3] and A N Grum-Grzhimailo[1]

[1]Skobeltsyn Institute of Nuclear Physics, Lomonosov Moscow State University, 119991 Moscow, Russia
[2]Physical Department, Lomonosov Moscow State University, 119991 Moscow, Russia
[3]Physikalisches Institut, Albert-Ludwigs-Universität Freiburg Hermann-Herder-Straße 3, 79104 Freiburg, Germany

Synopsis Sequential photoionization of krypton by intense extreme ultraviolet femtosecond pulses is studied theoretically for the photon energies below the 3d excitation threshold. The model is based on the solution of rate equations with photoionization cross sections of krypton obtained using R-matrix calculations. The ion yields and photoelectron spectra for various photon fluence are predicted.

Multiple ionization of atoms by intense pulses in the XUV has been observed since the first experiments at the free-electron laser FLASH [1]. Such studies are of great importance to benchmark theoretical models for the description of simple non-linear processes.

Our main purpose is to analyse theoretically and make predictions for sequential ionization of Kr at photon energies in the interval 50–80 eV. In this energy interval the 3*d*-hole is not produced and the Auger decay is excluded. To follow the dynamics of the state populations, we apply a method of solving rate equations extensively used in the description of sequential ionization of atoms by X-ray FEL pulses (see for example [2, 3]). Photoionization cross sections for variously charged Kr ions were calculated by the B-spline R-matrix approach [4], which fully takes into account non-orthogonality of the electron functions before and after the ionization.

As example we present the overall ionic yields at three fluences and two photon energies, presenting three typical regimes of ionization dynamics. Figures 1a,b,d show a typical situation for multiple ionization in a regime far from saturation, when the ions with higher charge have smaller yields, and the contribution of higher charge states is negligible. The opposite behavior is shown in Fig. 1e, in which nearly all ions are in highest allowed charged state, because a further ionization step is energetically forbidden for the photon energy of 50 eV. More uniform distribution in Figs. 1c,f show an intermediate regime, caused by an interplay between the cross sections, which decrease for increasing photon energies, and the laser fluence.

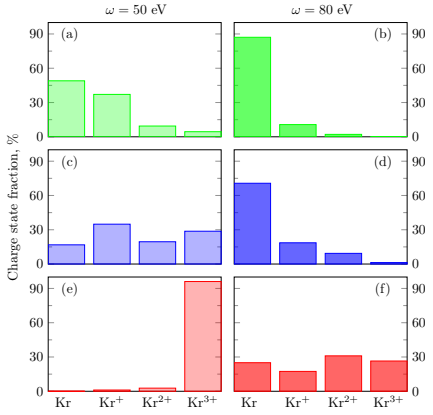

Figure 1. Charge-state yields for three fluences: $F = 40$ ph/Å^2 (**a,b**), $F = 100$ ph/Å^2 (**c,d**), and $F = 400$ ph/Å^2 (**e,f**) for the photon energies 50 eV (**a,c,e**) and 80 eV (**b,d,f**).

Detailed results including the photoelectron spectra will be presented at the conference.

This research was funded by the Russian Foundation for Basic Research, grant number 20-52-12023, and Deutsche Forschungsgemeinschaft, grant number 429805582.

References

[1] Sorokin *et al Phys. Rev. Lett.* 2007 **99** 213002
[2] Nakajima T, Nikolopoulos L 2002 *Phys. Rev. A* **66** 041402R
[3] Gryzlova E V *et al* 2020 *ATOMS* **8** 80
[4] Zatsarinny O 2006 *Comput. Phys. Commun.* **174** 273

*E-mail: gryzlova@gmail.com

Free-Electron Laser interacting with Atoms and Molecules

A Hadjipittas[1]*, H I B Banks, A Emmanouilidou[1]†

[1]University College London, WC1E 6BT, London, UK

Synopsis When atomic xenon interacts with an attosecond XUV pulse of photon energy 93 eV and 115 eV at an intensity of 10^{14} Wcm^{-2}, ions of Xe^{4+} and Xe^{5+} are formed. The Xe^{4+} ions are formed primarily via two sequential core electron photoionisations followed by two Auger decays while the Xe^{5+} ions are formed primarily via a single electron photoionisation followed by a shake-off ionisation, followed by a two-photon simultaneous absorption ionising one more electron and finally two consecutive Auger decay relaxations.

Free-electron lasers have a very high photon energy, allowing inner electron ionisation of atoms and molecules. Leaving a hole in an inner orbital makes the system unstable leading to its decay until it reaches a more stable configuration. The system can alter its electronic configuration and energy through the processes of Auger decay, shake-off or dissociation in the case of molecules. At the same time, other photo-ionisations can occur, leading to a variety of possible pathways the system can follow until it becomes stable

In our publication [1] we investigate the interaction between xenon atoms and attosecond XUV pulses of energies 93 eV and 115 eV at an intensity of 10^{14} Wcm^{-2}. Our goal is to identify the mechanisms responsible for the creation of Xe^{4+} and Xe^{5+} ions. We start by comparing our simulated ion yields with experimental data in table 1.

Table 1. Comparison of Ion yields with experiments. The intensity we used is 10^{14} Wcm^{-2}. The yields of all charged states add up to 1.

	This work	Ref. [2]	Ref. [3]
Xe^{+}	1.42	3.4	5.7
Xe^{2+}	74.8	77.6	68.6
Xe^{3+}	23.7	19.0	25.7
Xe^{4+}/Xe^{2+}	1.5×10^{-2}	4×10^{-3}	-

Next we identify the pathways leading to the formation of each ion yield. Since the ions of interest are the Xe^{4+} and Xe^{5+} we present the pathways leading to them in Fig. 1

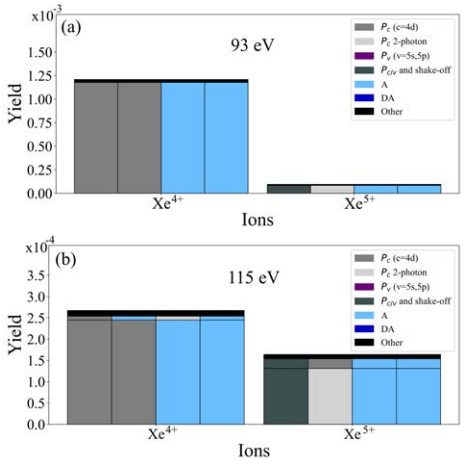

Figure 1. Pathways leading to Xe^{4+} and Xe^{5+} for an intensity of 10^{14} Wcm^{-2}. P_c (c = 4d) stands for a 4d ionisation via single-photon absorption; P_c 2-photon stands for 4d ionisation via two-photon absorption; P_v(v = 5s, 5p) stands for a 5s or 5p ionisation via single-photon absorption; $P_{c/v}$ and shake-off stands for ionisation via single-photon absorption followed by shake-off; A and DA stand for Auger decay and double Auger decay.

Xe^{4+} ions are mainly formed via two sequential core electron photoionisations followed by two Auger decays and Xe^{5+} ions are mainly formed via an electron photoionisation followed by a shake-off, followed by a two-photon core photoionisation and finally two Auger decays.

References

[1] Hadjipittas A. *et al* 2020 *Phys. Rev. A.* **102** 043108
[2] Bergues B. *et al* 2018 *Optica* **5** 237
[3] Holland D. M. P. *et al* 1979 *J. Phys. B.* **12** 2465

*E-mail: ucaphad@ucl.ac.uk
†E-mail: a.emmanouilidou@ucl.ac.uk

High-Harmonic Generation in the Water Window from mid-IR Laser Sources

K Finger[1], D Atri-Schuller[1], N Douguet[2], K Bartschat[1], and K R Hamilton[1]*

[1]Department of Physics and Astronomy, Drake University, Des Moines, IA 50311, USA
[2]Department of Physics, Kennesaw State University, Marietta, GA 30060, USA

Synopsis Using both a single-active electron (SAE) model and the multi-electron R-Matrix with Time-dependence (RMT) method, we investigate the response of neon atoms to near-IR laser fields, which results in the production of high-order harmonics within the water window.

Light sources with frequencies in the water window, which spans the K-edges of carbon and oxygen, can be used to image biological molecules in aqueous environments [1]. These soft X-rays can be produced, e.g., by synchrotron radiation, X-ray free-electron lasers, or high- harmonic generation (HHG) from mid-IR lasers, with the latter demonstrating the most promise for live-cell imaging with femtosecond time resolution [2].

However, describing harmonic generation in the mid-IR regime is a computationally difficult task, particularly if multi-electron effects are to be included in the calculation. We investigate the harmonic response of neon atoms to mid-IR laser fields (2000 – 3000 nm) using both a single-active electron (SAE) model [3] and the fully *ab initio* all-electron R-Matrix with Time-dependence (RMT) method [4]. The laser peak intensity and wavelength are varied to find optimal parameters for high-harmonic imaging in the water window. Comparison of the SAE and RMT results [5] shows excellent agreement between the resulting spectra, and parameters such as the cut-off frequency predicted by the classical three-step model [6].

Both the SAE and RMT methods can therefore be used to describe HHG in intense, near-IR laser pulses schemes. While more computationally demanding than the SAE model, RMT captures the multi-electron dynamics of the system, which have been shown to influence the appearance of the harmonic spectrum [7].

This work was supported by the United States National Science Foundation under PHY-1803844, PHY-2012078, OAC-1834740, and XSEDE PHY-090031, and the Frontera Pathways allocation PHY20028.

*E-mail: kathryn.hamilton@drake.edu

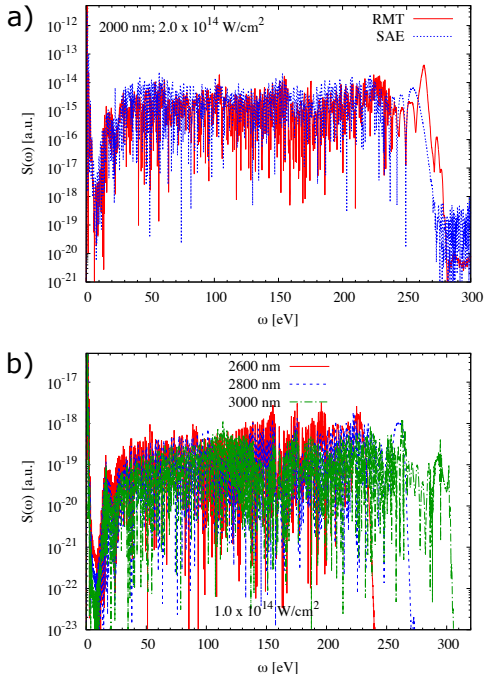

Figure 1. (a) Harmonic spectra for neon in a 2000 nm laser pulse with a peak intensity of 2×10^{14} W/cm^2. (b) Spectra determined by the RMT method in a 1×10^{14} W/cm^2 laser pulse with wavelengths ranging from 2600 nm to 3000 nm.

References

[1] Neutze R *et al* 2000 *Nature* **406** 752
[2] Fu Y *et al* 2020 *Commun. Phys* **3** 92
[3] Pauly T *et al* 2020 *Phys. Rev. A* **102** 013116
[4] Brown A C *et al* 2020 *Comp. Phys. Commun.* **250** 107062
[5] Finger K *et al* 2021 arXiv:2101.10547
[6] Corkum 1993 *Phys. Rev. Lett.* **71** 1994
[7] Mazza T *et al* 2015 *Nat. Commun.* **6** 6799

Photoionisation of Endohedral Alkali Atoms in Fullerene Cages

N M Hosea[1]*, J Jose[2], H R Varma[1]

[1]Indian Institute of Technology, Mandi, Himachal Pradesh, 175005, India
[2]Indian Institute of Technology, Patna, Bihar, 801106, India

Synopsis Photoionisation cross section and angular distribution parameter of Na atom trapped inside a fullerene molecule is studied. The effects due to charge transfer between the atom and the enclosing shell are also studied.

A multi-electron atom trapped inside a fullerene has gained a lot of attention in the recent years. Entrapment of an atom in a cage leads to the interesting features on the confined atomic spectra such as confinement resonances[1], Inter-Coulombic decay (ICD)[2], hybridisation[3] *etc.* The comparison of free and confined atomic spectra provides insights into the role of various interactions involved in the photoionisation dynamics at a fundamental level. This knowledge helps us develop applications especially in fields of nanoscience and technology[4]. Comparatively less work has been done in the study of photoionisation of confined open shell systems due to their complex spectra.

Here, we present a preliminary study on the photoionisation studies of sodium inside a fullerene cage. We have studied the photoionisation cross section and angular distribution parameter of this system using GRASP[5] and RATIP [6].

The cage is modelled by a spherical, short range, attractive shell potential[7]. As alkali metals have valence electrons, we considered different scenarios associated with the charge transfer from the atom to the fullerene cage and vice versa ($Na^-@C_{60}^+$ and $Na^+@C_{60}^-$). All these results are compared with the $Na@C_{60}$ to gain understanding of the role of various interactions present in the system.

In Figure 1 is shown the 3s cross section of $Na^-@C_{60}^+$ obtained along with the $Na@C_{60}$. This is done at a single configuration level of Na^- and Na. The confinement oscillations are present in both the systems. For the case of $Na^-@C_{60}^+$ very sharp resonances are present near the threshold.

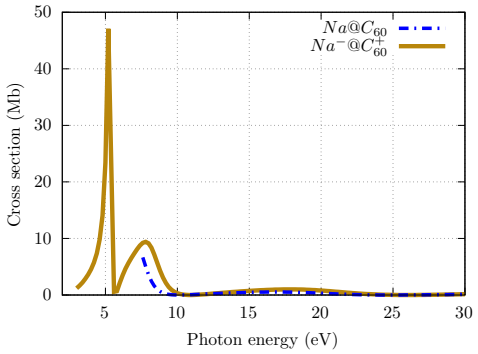

Figure 1. Photoionisation cross section of endohedral fullerene, $Na@C_{60}$ and $Na^-@C_{60}^+$.

Acknowledgement

Two of the authors, N M Hosea and Dr Hari Varma, extend our gratitude to Science and Engineering Research Board, Department of Science and Technology, Government of India for funding this work.

References

[1] V. K. Dolmatov 2016 *Academic Press, New York, Vol. 58, pp.13–68.*
[2] De R, Magrakvelidze M *et al* 2016 *J. Phys. B: At. Mol. Opt. Phys. 49 11LT01*
[3] Dakota Shields *et al* 2020 *J. Phys. B: At. Mol. Opt. Phys. 53 (2020) 125101 (8pp)*
[4] Simon. C. Benjamin *et al* 2006 *J. Phys.: Condens. Matter 18, S867–S883*
[5] F.A. Parpia *et al* 1996 *Computer physics communications, 94(2-3):249–271.*
[6] S. Fritzsche *et al* 2012 *Comput. Phys. Commun.*
[7] V. K. Dolmatov *et al* 2006 *Phys. Rev. A : 73, 013201*
[8] C. Y. Lin and Y. K. Ho, 2013 *Few-Body Systems : 54, 1*
[9] J.P Connerade *et al* 2000 *J. Phys. B : At. Mol. Opt. Phys. 33 2279*

*E-mail: nishita.hosea@gmail.com

Highly efficient XUV generation through high-order frequency mixing

M Khokhlova[1] * and V Strelkov[2]

[1]Max Born Institute for Nonlinear Optics and Short Pulse Spectroscopy, Berlin, 12489, Germany
[2]Prokhorov General Physics Institute of the Russian Academy of Sciences, Moscow, 119991, Russia

Synopsis We study the generation of coherent XUV using intense laser fields in a rapidly ionising gas. We show that the blue shift during propagation is a dominant limitation for the high-harmonic generation efficiency for visible or near-UV drivers. We introduce a new spatial scale, the blue-shift length, which sets the upper bound for its quadratic growth. Moreover, we show that this restriction can be overcome by adding a weak mid-IR field: the phase-matched high-order frequency-mixing process does not suffer from this blue shift, and the generated XUV intensity grows quadratically.

The generation of bright, coherent XUV light via frequency conversion of intense laser drivers is a problem of both fundamental and technological importance. Increasing the intensity of the generated high harmonics by raising the intensity of the driving field only works up to a point: at high intensities, rapid ionisation of the medium limits the conversion efficiency.

We identify the dominant limiting mechanism — the combined effect of phase matching and the blue shift of the driving field during its propagation in a rapidly ionising medium [1]. We introduce a new spatial scale, the blue-shift length, which sets the upper bound for the quadratic intensity growth of the harmonics.

Moreover, we show analytically and numerically (solving the propagation equation coupled with the TDSE) that this seemingly fundamental restriction can be overcome by using an additional generating weak mid-IR field. For specific combinations of frequencies of the generating fields, the corresponding high-order frequency-mixing (HFM) process does not suffer from the blue shift of the drivers and phase mismatch [Fig.1(a)], and thus its efficiency grows quadratically with propagation distance [Fig.1(b)].

Our results thus open a new route for highly efficient generation of XUV light, the first step of which has been taken already via an observation of high-order parametric generation [2].

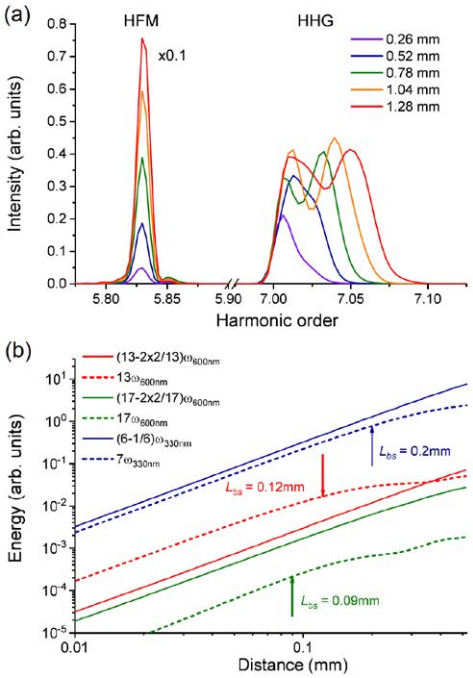

Figure 1. Numerical results. (a) Spectra of the XUV fields generated via HHG and HFM processes by fundamental (330 nm) and weak low-frequency (1980 nm) fields at several propagation distances. (b) Energies of harmonics (dashed) and HFM components (solid) as functions of the propagation distance. The initial wavelength of the fundamental field is 600 nm and of the low-frequency field is 5.1 μm (green lines) or 3.9 μm (red lines); blue lines correspond to the case in (a). The blue-shift length (arrows) sets the end of quadratic growth for the HHG emission.

References

[1] Khokhlova M and Strelkov V 2020 *New J. Phys.* **22** 093030
[2] Hort O *et al* 2021 *Opt. Express* **29** 5982

*E-mail: m.khokhlova@imperial.ac.uk

Generation of highly-elliptical resonant high-order harmonics

M Khokhlova[1]*, M Emelin[2], M Ryabikin[2], and V Strelkov[3]

[1]Max Born Institute for Nonlinear Optics and Short Pulse Spectroscopy, Berlin, 12489, Germany
[2]Institute of Applied Physics of the Russian Academy of Sciences, Nizhny Novgorod, 603950, Russia
[3]Prokhorov General Physics Institute of the Russian Academy of Sciences, Moscow, 119991, Russia

Synopsis We study resonant high-harmonic generation by tin ions in an elliptically-polarised laser field. We show that the yield of resonant harmonics does not drop with the fundamental ellipticity as rapidly as for nonresonant harmonics. Moreover, the ellipticity of resonant harmonics is significantly higher than for usual off-resonant ones. This introduces a prospective source of quasi-monochromatic coherent XUV with controllable ellipticity, potentially up to circular.

XUV sources are powerful tools for tracking and control of electron dynamics in atoms and molecules. An important handle of these tools is the polarisation of the emission: circularly-polarised (CP) XUV pulses recently have become extremely valuable due to their broad involvement in a growing number of experimental techniques for the study of structural, electronic, and magnetic properties of matter, such as chiral molecules and magnetic materials.

The naive approach to create CP harmonics via high-harmonic generation (HHG) by atoms in an elliptically-polarised (EP) field fails immediately: although the harmonic ellipticity grows with the driver's ellipticity [1], their yield drops exponentially with the fundamental ellipticity [2]. Thus, HHG in an atomic gaseous medium driven by an EP laser field does not appear as a reasonable candidate for EP XUV sources.

We suggest a new way to generate bright XUV with tunable polarisation via HHG more efficiently, avoiding overcomplicated experimental schemes. Our approach [3] is based on the process of resonant HHG [4, 5] in EP fields and follows the idea of the four-step model: the electron gets trapped in an autoionising state, which is much less localised than the ground state. This means that for fields with high ellipticities, the electron completely misses the ground state, but can still participate in the resonant mechanism.

To prove this idea, we study numerically the resonant HHG in an EP laser field by solving the 3D TDSE for a singly ionised tin atom in a strong laser field. We show that the resonant harmonic yield behaves anomalously as opposed to the rapid decrease of the nonresonant harmonic with the driver's ellipticity (Fig.1).

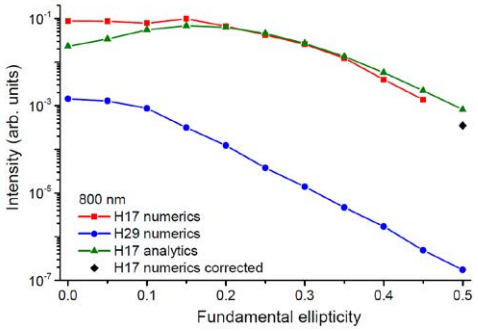

Figure 1. Harmonic intensity as a function of the driver's ellipticity. Resonant (red) and one of nonresonant (blue) harmonic intensities calculated within the SAE TDSE. Green shows analytical resonant contribution.

As a result, for the ellipticities above the threshold one, only the resonant harmonic is generated. Moreover, the ellipticity of resonant harmonics is higher than the usual nonresonant ones, without compromising the harmonic yield. This offers us an attractive new route for the generation of quasi-monochromatic XUV with high ellipticity.

References

[1] Antoine P *et al* 1997 *Phys. Rev. A* **55** 1314
[2] Budil K *et al* 1993 *Phys. Rev. A* **48** R3437
[3] Khokhlova M *et al Phys. Rev. A* in press arXiv
[4] Ganeev R *et al* 2006 *Opt. Lett.* **31** 1699
[5] Strelkov V *et al* 2014 *Phys. Rev. A* **89** 053833

*E-mail: m.khokhlova@imperial.ac.uk

Gas-phase helium double ionization induced by Compton scattering

M Kircher,[1]* G Kastirke,[1] M Weller,[1] L Ph H Schmidt,[1], I Vela-Pérez,[1] M Waitz,[1] T Mletzko,[1] S Grundmann,[1] D Kirchner,[1] A Khan,[2] F Trinter,[1] S Houamer,[3] O Chuluunbaatar,[4] I P Volobuev,[5] T Jahnke,[1] M S Schöffler,[1] Y V Popov,[5] and R Dörner[1]†

[1]Institut für Kernphysik, J. W. Goethe Universität, Max-von-Laue-Str. 1, D-60438 Frankfurt, Germany
[2]Institut für Ionenphysik und Angewandte Physik, Universität Innsbruck, Technikerstr. 25/3, A-6020, Austria
[3]LPQSD, Department of Physics, Faculty of Science, University Sétif-1, 19000, Setif, Algeria
[4]Joint Institute for Nuclear Research, Dubna, Moscow region 141980, Russia
[5]Skobeltsyn Institute of Nuclear Physics, Lomonosov Moscow State University, Moscow 119991, Russia

Synopsis We present a differential study on Compton scattering with $h\nu = 40\,\text{keV}$ on gas-phase helium. Comparing experimental and theoretical cross sections, we find a strong influence of electron-electron correlations in the final state, thus showing the invalidity of the independent-particle approximation in this energy regime.

Single-photon double ionization (DI) in helium can be induced by multiple processes. Usually, one can explain the process in two steps: the first electron is ionized (in our case the ionization is induced by Compton scattering). If the electron's energy is low, it can "knock-out" the second electron, a process referred to as Two-Step-1. For high electron energy, this process is suppressed. However, the removal of one electron from the initial system disturbs the electronic state of the singly-charged intermediate cation. The disturbed state has an overlap with the continuum, resulting in about 1% of all cases in a second low-energy electron being emitted. This process, referred to as shake-off (SO), does not require electron-electron correlations in the final state. Therefore, within the independent-particle approximation (IPA), SO is the sole underlying process of double ionization. Within the IPA, the first electron is removed instantaneously from the system, i.e., its final state is described by a plane wave (PW) and no *e*-*e* correlations in the final state exist. Hence, DI *only* happens due to initial state *e*-*e* correlations.

In the experiment, we induce helium DI by Compton scattering at a photon energy of 40 keV. We detect one of the two electrons in coincidence with the He^{++} ion using a COLTRIMS spectrometer [1]. To investigate the influence of final-state *e*-*e* correlations, we calculate the singly differential cross sections (SDCS) as seen in Fig. 1. Here, we compare two different final states of the system. First, we use a PW for the first electron and a Coulomb wave with charge $Z = 2$ for the second electron (solid, black line), i.e., we assume an IPA model. Second, we use the well-known Brauner-Briggs-Klar (BBK) wave function [2] (dashed, red line), taking into account the full *e*-*e* correlations in the final state.

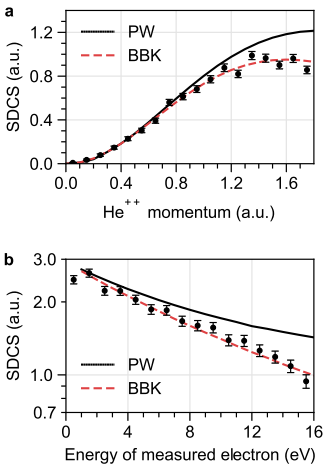

Figure 1. Singly differential cross sections for different final states. The experimental data is normalized to the red-dashed curve. Note the logarithmic scale of the y-axis in panel **b**.

References

[1] J Ullrich et al. *Rep. Prog. Phys.* **66**, 1463–1545 (2003)
[2] M Brauner et al. *J. Phys. B: At. Mol. Opt. Phys.*, **22**, 2265–2287 (1989)

*E-mail: kircher@atom.uni-frankfurt.de
†E-mail: doerner@atom.uni-frankfurt.de

Ultra-precise Rydberg atomic localization using spatially dependent fields

T Kirova[1 *], N Jia[2], S H Asadpour[3], H R Hamedi[4], J Qian[5], and G Juzeliūnas[4]

[1]Institute of Atomic Physics and Spectroscopy, University of Latvia, Riga, LV-1004, Latvia
[2]The Public Experimental Center, University of Shanghai for Science and Technology, Shanghai 200093, China
[3]Department of Physics, Iran University of Science and Technology, Tehran, 13114-16846, Iran
[4]Institute of Theoretical Physics and Astronomy, Vilnius University, Vilnius, LT-10257, Lithuania
[5]Department of Physics, School of Physics and Electronic Science, East China Normal University, Shanghai 200062, China

Synopsis We propose theoretical schemes for strongly confined atomic localization using interacting Rydberg atoms in a coherent population trapping ladder configuration, where a standing wave or an optical vortex is applied in the second step of the ladder. Our numerical simulations show that both scenarios lead to ultra-precise Rydberg localization on the nanometer scale. Compared to the standing wave localization method, the vortex beam can provide an ultra-precise two-dimensional localization solely at the zero-intensity center.

Atom localization (the spatial confinement of atoms with high precision) has been of continuous interest in quantum mechanics, while modern quantum optics tools have made its experimental realization possible. Current investigations have been driven by practical applications in nanolithography [1], laser cooling and trapping [2], and other areas of atomic physics [3]. Many problems arise when it comes to feasible localization of Rydberg atoms, due to the difficulty in confining them in a small region with high density. The strong van der Waals (vdW) interactions enhance the nonlinear properties of Rydberg media via the dipole blockade [4], opening new opportunities for quantum optics and quantum information applications [5]. The latter makes the experimentally achievable precise localization of highly excited Rydberg atoms an important one.

We propose theoretical schemes for strongly confined atomic localization using interacting Rydberg atoms in a coherent population trapping ladder configuration.

In the first scenario a standing-wave is used as a coupling field in the second step of the ladder [6]. Depending on the degree of compensation of the Rydberg level energy shift (induced by the vdW interaction), by the coupling field detuning, we distinguish between a partial antiblockade (PA) and a full antiblockade regimes. While a periodic pattern of tightly localized regions can be achieved for both regimes, the PA allows much faster convergence of the spatial confinement, resulting in high-resolution (below 1 nm) Rydberg state-selective superlocalization for higher-lying Rydberg levels. For lower-lying Rydberg levels, the PA leads to an anomalous change of spectra linewidth, confirming the importance of using a stable uppermost state to achieve the superlocalization regime.

In the second scenario we propose a robust localization of the highly-excited Rydberg atoms by applying a doughtnut-shaped optical vortex in the second step of the ladder scheme [7]. Compared to the standing wave localization method, the vortex beam can provide an ultra-precise two-dimensional localization solely at the zero-intensity center, within a confined excitation region down to the nanometer scale.

Our results pave the way to developing new sub-wavelength localization techniques, by reducing the excitation volumes to the level of nanometers, representing feasible implementation for the future experimental applications.

* E-mail: teo@lu.lv

References

[1] Boto A N *et al* 2000 *Phys Rev Lett.* ***85*** *2733*
[2] Phillips W D 1998 *Rev Mod Phys.* ***70*** *721*
[3] Adams C S *et al* 1994 *Rev Rep.* ***240*** *143*
[4] Lukin M D 2001 *Phys Rev Lett.* ***87*** *037901*
[5] Saffman M *et al* 2010 *Rev Mod Phys* ***82*** *2313*
[6] Kirova T *et al* 2020 *Opt Lett.* ***45*** *5440*
[7] Jia N *et al* 2020 *Opt Express. 28 36936*

Probing ultrafast coherent dynamics in core-excited xenon by using attosecond XUV-NIR transient absorption spectroscopy

D Kolbasova[1,2]*, M Hartmann[3], R Jin[1], A Blättermann[3], C Ott[3], S-K Son[1], T Pfeifer[3], and R Santra[1,2]

[1]Center for Free-Electron Laser Science CFEL, Deutsches Elektronen-Synchrotron DESY, Notkestrasse 85, 22607 Hamburg, Germany
[2]Department of Physics, Universität Hamburg, Notkestrasse 9-11, 22607 Hamburg, Germany
[3]Max-Planck-Institut für Kernphysik, Saupfercheckweg 1, 69117 Heidelberg, Germany

Synopsis Here, we present our theoretical research on the capability of attosecond transient absorption spectroscopy to characterize the dynamics ultrafast coherent dynamics in core-excited atoms. In particular, we clarify which aspects of the dynamics can be revealed when the wave packets are probed using an NIR pulse and analyze why the inner-shell hole dynamics is more difficult to probe than the dynamics of the excited electron.

We investigate the capability of attosecond transient absorption spectroscopy (ATAS) to characterize the dynamics of inner-shell-excited systems. In the transient absorption spectroscopy setup considered, wave packets are prepared by an attosecond XUV pulse and probed by a femtosecond NIR pulse. By using this, we study coherent electron dynamics in core-excited xenon atoms. We perform a theoretical analysis of the transient absorption signal as a function of the time delay between the XUV pump and NIR probe pulses, treating the excitation pulse perturbatively and the probe pulse nonperturbatively [1]. We demonstrate that inner-shell hole dynamics is much more difficult to detect than Rydberg-electron dynamics, because the dynamics of the inner-shell hole is defined mostly by the degree of coherence of the wave packet initially created by the XUV pulse, whereas Rydberg electrons get strongly dressed by the NIR pulse, thereby producing strong quantum coherence effects that are reflected in the ATAS.

Our theoretical predictions are compared with experimental results (Figure 1). Our analysis suggests that, in order to detect inner-shell hole dynamics using an NIR probe field, it is necessary to minimize the effect of the laser field on the Rydberg levels, which can be done by decreasing the field exposure time and by using fields that are far off-resonance. We show that the presence of a dressing field or a slight modification of the spectrum of the probe pulse can dramatically change the simulated ATAS results. Thus, our work also suggests that a precise NIR pulse characterization in the target region behind the HHG gas cell is necessary for a qualitatively and quantitatively accurate interpretation of experimental ATAS data, due to the high sensitivity of Rydberg electrons to the NIR electric fields.

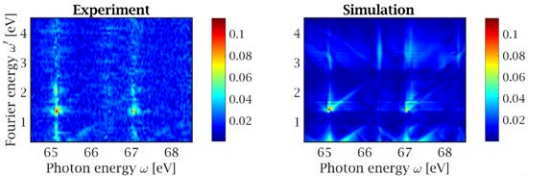

Figure 1. Comparison of an experimental and simulated transient absorption XUV spectra of Xe. In simulation, the nominal pulse shape from the experiment is used.

References

[1] Kolbasova D *et al* 2021 *Phys. Rev. A* **103** 043102

*E-mail: daria.kolbasova@desy.de

Self-induced splitting of Kα emission lines in zinc

Š Krušič[1]*, A Mihelič[1], K Bučar[1] and M Žitnik[1]

[1]Jožef Stefan Institute, Jamova cesta 39, SI-1000 Ljubljana, Slovenia

Synopsis We present a theoretical study of superfluorescence of $K\alpha$ emission in zinc after K-shell photoionization with intense attosecond x-ray laser pulses. The developed model, which accurately describes both spontaneous emission and the coupling of states in strong electromagnetic fields, predicts a splitting of the $K\alpha_1$ emission line due to a self-induced Autler-Townes effect, that could be observed with standard high resolution x-ray spectrometers. Subfemtosecond pulse duration is crucial for the manifestation of this phenomenon in zinc with a K-hole lifetime of only 394 as.

While superfluorescence has been extensively studied in the optical regime [1], its observation in the x-ray domain has only recently become possible with the development of free-electron lasers capable of producing the required high intensity radiation [2]. In the optical regime, superfluorescence is usually observed by detecting the characteristic temporal profile of the radiation emitted in the fluorescent decay of an excited state in a target with population inversion. This is not feasible in the x-ray domain because the duration of the emitted pulses is on the order of the excited state lifetime, which for core-hole states is well below one picosecond.

Another difficulty in studying x-ray superfluorescence stems from a lack of reliable theoretical modeling. Since superfluorescence develops from spontaneous emission, a successful model must describe both the quantum field fluctuations in the absence of external electric fields, as well as the interaction of strong electric fields with matter in the nonlinear regime [1]. The most widely used model of superfluorescence is based on the semiclassical Maxwell-Bloch equations with spontaneous emission described by a stochastic noise term [3]. Recently, a model based on quantum correlation functions has been demonstrated for a two-level system [4]. However, both models are inadequate when dealing with multilevel systems and competing decay channels.

We present a theoretical model of superfluorescence in extended multilevel targets based on a combination of propagation equations for the quantum correlation functions and Maxwell-Bloch equations [5]. Such a description overcomes the key deficiencies of the two constituent sets of equations, i.e., inaccurate treatment of spontaneous emission or modeling of multilevel systems. The theoretical model is employed to study the spectral properties of the $K\alpha_{1,2}$ emission in zinc at ~ 8630 eV, after photoionization by high intensity free-electron laser pulses with photon energy 9750 eV and duration of a few hundred attoseconds (Fig. 1). The calculations predict a clear splitting of the amplified $K\alpha_1$ emission line after reaching saturation, which could be observed with the present-day resolution of x-ray spectrometers. The short pump pulse duration with respect to the excited state lifetime is crucial for the manifestation of this effect. Realization of such an experiment in the x-ray domain has only recently become feasible with the demonstration of attosecond FEL pulses [6].

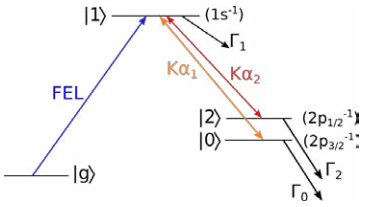

Figure 1. Schematic representation of the processes following 1*s* photoionization by a short FEL pulse, that are described in the model.

References

[1] Gross M and Haroche S 1982 *Phys. Rep.* **93** 301
[2] Emma P *et al* 2010 *Nat. Photon.* **4** 641
[3] Larroche O *at al* 2000 *Phys. Rev. A* **62** 043815
[4] Benediktovitch A *et al* 2019 *Phys. Rev. A* **99** 013839
[5] Krušič Š *et al* 2020 *Phys. Rev. A* **102** 013102
[6] Duris J *et al* 2019 *Nat. Photon.* **14** 30

*E-mail: spela.krusic@ijs.si

Continuous variable quantum state tomography of electron wavepackets

H Laurell[1,†*], D Finkelstein-Shapiro[2], C Guo[1], M Ammitzböll[1], R Weissenbilder[1], L Neoricic[1], M Gisselbrecht[1], C Arnold[1], T Pullerits[3], A L'Huillier[1] and D Busto[1]

[1]Department of Physics, Lund University, Box 118, SE-221 00 Lund, Sweden
[2]Instituto de Qumica, Universidad Nacional Autnoma de Mexico
[3]Chemical Physics and NanoLund, Lund University, Box 118, SE-221 00 Lund, Sweden

Synopsis We propose a continuous variable quantum state tomography protocol for photoelectron wavepackets ionized by absorption of attosecond pulses. The protocol has been verified with simulations on autoionizing wavepackets in helium and argon.

Quantum state tomography (QST) is the gold standard for quantum measurements. By performing a series of projective measurements on an unknown quantum state, QST aims at measuring the density matrix describing the system. The density matrix tells us everything we could possibly want to know about a state. It provides information on the population of the different quantum states in the system and the degree of coherence between them.

The development of attosecond light sources since the beginning of the century has opened the possibility to investigate electronic dynamics in real time. Due to the high photon energy of attosecond pulses, their interaction with matter results in the ejection of electron wave packets (EWP), which correspond to a superposition of continuum states. QST protocols have been proposed and demonstrated for the characterization of attosecond electron pulse trains [1, 2], whose spectrum is composed of discrete energies. However, these methods cannot be used for the characterization of EWPs with a continuous spectrum.

Here we propose a novel quantum state tomography protocol, Kvanttillstånd tomogRafi av AttoseKund ElektroNvågpaket (KRAKEN), for photoelectron wavepackets. We use a bichromatic infrared probe field consisting of two narrowband spectral peaks. By varying the probe delay relative to the XUV, an interferogram is measured from which a subdiagonal of the density matrix can be reconstructed. By then scanning the frequency difference of the two spectral components, a full density matrix can be reconstructed. This method enables the measurement of continuous variable density matrices of EWPs with very high spectral resolution. Additionally this method is robust to temporal and spectral jitter and ultimately sensitive to intrinsic quantum decoherence.

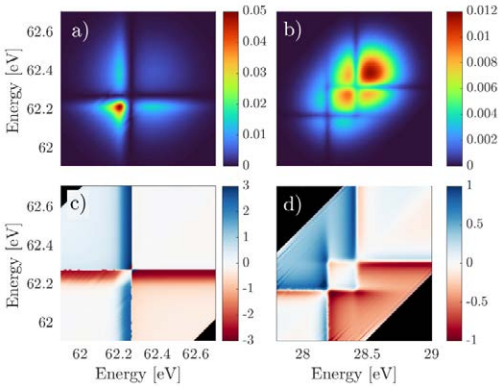

Figure 1. a) Amplitude and c) phase of the 2s2p density matrix. b) Amplitude and d) phase of the $3s^{-1}4p$ density matrix.

Figure 1 shows the density matrices for the 2s2p Fano resonance in helium and the $3s^{-1}4p$ Fano resonance in argon. The $3s^{-1}4p$ resonance is a mixed state due to the incoherent addition of the $j = 1/2$ and $j = 3/2$ continua. This is manifested as the damping of the coherences. The characterization of decoherence on the attosecond time scale is likely to uncover new aspects of ultrafast electron correlations.

References

[1] K. E. Priebe et. al., *Nature Photonics*, 11(12):793–797, 2017.
[2] C. Bourassin-Bouchet et. al., *Phys. Rev. X*, 10:031048, Aug 2020.

*E-mail: hugo.laurell@fysik.lth.se

Electron choreography at the attosecond time scale

J Vaughan, B Unzicker, S Burrows, B Tatum, D Arthur, T Olsson, S Jain, T Hart, P Stringer, and G M Laurent *

Department of Physics, Auburn University, 380 Duncan Drive, Auburn, AL 36849, United States of America

Synopsis In this work, we report on coherent control of electron dynamics in atoms via attosecond pulse-shaping. We show that the photoelectron emission from argon gas produced by absorption of an attosecond pulse train (APT) made of odd and even harmonics can be manipulated along the direction of polarization of the light by tuning the spectral components (amplitude and phase) of the pulse.

With the recent development of extreme ultraviolet (XUV) light sources with attosecond duration, new capabilities emerge for controlling quantum dynamics in matter with an unprecedented level of precision down to the natural timescale of electron motion. So far, attosecond control has been mostly achieved with pump/probe schemes where an attosecond-pump pulse triggers a given electronic process, and a phase-locked femtosecond-probe field is used to steer its dynamics [1]. The system under scrutiny is thus controlled by varying the time delay between the two pulses.

An alternative approach consists of shaping the spectral components of the attosecond pulse to control the dynamics. Within the widely accepted three-step model describing attosecond pulse generation via HHG, the spectral components are defined by the electron wavepacket trajectories (also referred to as quantum orbits) in the driving laser field. By tailoring the temporal waveform of the femtosecond driving field, the quantum orbits can then be tuned giving some control over the spectral components of the attosecond pulse train (APT). Two-color femtosecond waveforms, for example, have proved to be very efficient in manipulating quantum orbits in the HHG process. The literature is rich with experimental and theoretical studies reporting the dependence of both the spectrum and the polarization of the resulting APT on the temporal profile of such synthetized waveforms [2].

In this work, we show how the APT's spectral phases can be manipulated by varying the intensity ratio r and the relative phase ϕ between the two components of the driving field. As an application for such a spectral pulse shaping technique, we also report on a coherent control experiment where the photoelectron emission from atoms generated by tailored attosecond pulses in presence of relatively weak IR field is manipulated along the direction of polarization of the light by tuning the spectral phases of the APT [3]. Emission patterns where photolelectrons are emitted in the same direction or, conversely, are emitted in opposite directions depending on their energy can be obtained by tuning the spectral components of the pulse, as shown in Fig. 1.

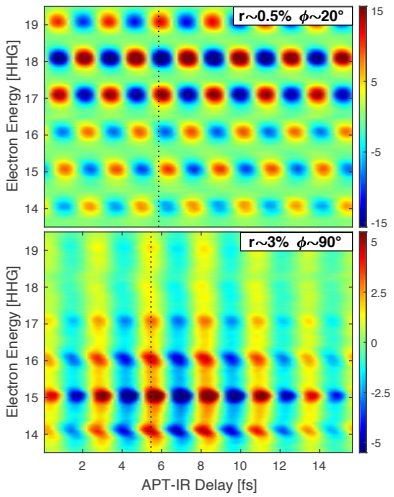

Figure 1. Density plots of the asymmetric components of the photoelectron emission as a function of the time delay between the APT and IR fields and the photoelectron energy.

References

[1] Mauritsson J *et al* 2008 *Physical Review Letters* **100** 073003
[2] Mauritsson J *et al* 2006 *Physical Review Letters* **97** 013001
[3] Unzicker B *et al* 2021 *New Journal of Physics* **23** 013019

*E-mail: glaurent@auburn.edu

Dynamics of enhancement and suppression of the frequency-comb emission via high-order harmonic generation in few-cycle pulse trains

C T Liang[1,2], P C Li[1,2]*, and S I Chu[3,4]

[1]Research Center for Advanced Optics and Photoelectronics, Department of Physics, College of Science, Shantou University, Shantou, Guangdong 515063, China
[2]Key Laboratory of Intelligent Manufacturing Technology of MOE, Shantou University, Shantou, Guangdong 515063, China
[3]Center for Quantum Science and Engineering, and Center for Advanced Study in Theoretical Sciences, Department of Physics, National Taiwan University, Taipei 10617, Taiwan
[4]Department of Chemistry, University of Kansas, Lawrence, Kansas 66045, USA

Synopsis We present an *ab initio* nonperturbative study of enhanced and suppressed high-order harmonic generation (HHG) of the He atom driven by the few-cycle pulse trains. The HHG is calculated by solving the three-dimensional time-dependent Schrödinger equation utilizing the time-dependent generalized pseudospectral method. We find that the frequency comb structures show immense enhancement and suppression in different regimes. The underlying physical mechanism of enhancing and suppressing HHG is illustrated by the interference effect of the HHG spectra originating from each short laser pulse.

The femtosecond frequency-comb techniques are promoting new frontiers in ultrafast science, such as providing a powerful new tool for observing the bound-state quantum electron dynamics (QED) [1]. Extending these methods into vacuum ultraviolet (VUV) and extreme ultraviolet (XUV) spectral region is highly desirable since this would, for instance, allow novel precision QED tests [2]. Recently, high-order harmonic generation (HHG) of atoms and molecules driven by intense laser pulse trains, as an alternative method for the coherent VUV and XUV radiation at ultrahigh repetition rates, has been increased considerably. It has been shown that the frequency-comb HHG of the He atom can provide a potential novel coherent XUV light source [3]. However, compared with the extensively studied feature of HHG [4], the dynamics of the frequency comb structures are still largely unexplored.

In Figure 1(a), we present the HHG power spectrum of the He atom by few-cycle pulse trains. Figs 1(b), (c), and (d) represent the detailed and enlarged graphs of the H43.04, H59, and H82.03 harmonics in the HHG spectrum. The most significant feature is the suppressed frequency comb structure and the giant enhanced sub-peak near the H43.04, and the giant enhanced higher peak near the H82.03, comparing with the plateau regular frequency-comb HHG structure in H59, which are observed for the three regions near-threshold, plateau, and near-cutoff. Our results indicate the few-cycle pulse trains provide the strong-field-driven atoms, molecules, and plasma to generate the VUV new light sources.

*E-mail: pchli@stu.edu.cn

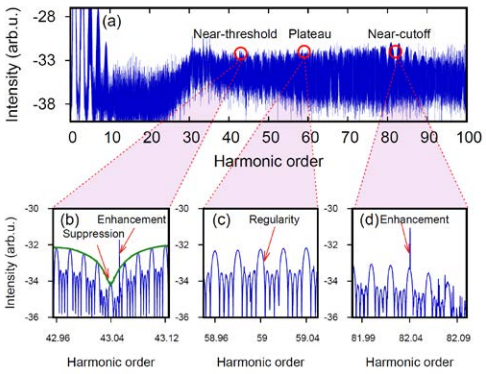

Figure 1. **(a)** HHG spectrum generated by laser field of a train of five pulses. **(b)**, **(c)**, and **(d)** are the enlarged graphs of the H43.04, H59.0, and H82.04 harmonics in the HHG spectrum, respectively, which illustrated the distinct frequency comb structures of the HHG in detail.

Acknowledgements

This work was supported by the NSFC (11764038, 12074239), Natural Science Foundation of Guangdong Province (200110165892233, 2020A1515010927, 210206153460124), Department of Education of Guangdong Province (2018KCXTD011, 2019KTSCX038), and Shantou University (NTF18030).

References

[1] Biesheuvel J *et al* 2016 *Nat. Commun.* **7** 10385
[2] Zhou C L *et al* 2020 *Nat. Photonics.* **10** 1038
[3] Carrera J J *et al* 2009 *Phys. Rev. A.* **79** 063410
[4] Li P C *et al* 2015 *Nat. Commun.* **6** 7178

Time-resolved ionization of atoms in plasmas by short laser pulses

C Y Lin *

Department of Physics, Soochow University, Taipei, 111, Taiwan (ROC)

Synopsis A hybrid computation scheme using the time-dependent approach is developed to explore the laser-driven ionization of atoms in plasmas. With the Yukawa and modified Debye-Hückel potentials used to model the plasma environments, the calculations of photoelectron energy spectrum and the time evolution of ionization probability for various Debye screening lengths are performed. The influence of shape resonances caused by plasma screening on the Wigner time delay of atomic ionization is illustrated.

In the present work, we develop a hybrid computation scheme using the time-dependent approach to explore the laser-driven ionization of atoms embedded in plasmas. For weakly coupled (classical) plasmas, electron densities range from $\sim 10^{6}$ to $\sim 10^{14}\mathrm{cm}^{-3}$ and temperatures range from $\sim 10^{-1}$ to $\sim 10^{4}$eV, the Yukawa (screened Coulomb potential) or so called Debye-Hückel potential has been extensively adopted to depict the potential of atoms embedded in plasmas. However, for the dense quantum plasmas with higher plasma density, the modified Debye-Hückel model (i.e., exponential-cosine-screened Coulomb potential) [1] is more appropriate to model the screening effect of plasms. The screening effects caused by the both models are characterized by the Debye screening length, which is a function of plasma density and temperature. The variation of the Debye length could lead to shape resonances [1] and Cooper minima [2] in atomic photoionization.

To solve the time-dependent Schrödinger equation, the finite-element discrete variable representation (FE-DVR) and the short iterative Lanczos (SIL) method [3] are employed for the spatial discretization and temporal propagation of atomic wavefunctions, respectively. Within the framework of FE-DVR, the matrix of the kinetic energy operator is sparse and structured, whereas the potential matrix elements are diagonal. With these features, the Hamiltonian matrix is amenable to efficient parallelization.

SIL method is implemented to perform the time propagation. The Lanczos algorithm constructs a set of orthonormal basis, which makes the Hamiltonian matrix tridiagonal. Through standard algorithms, the tridiagonal Hamiltonian can be quickly diagonalized leading to a time propagator expressed simply in terms of eigenvalues and eigenvectors of Hamiltonian in the Krylov space.

The screening effects due to the Yukawa and modified Debye-Hückel potentials on ionization processes driven by short laser pulses are investigated. We calculate the photoelectron energy spectrum and the time evolution of ionization probability for various Debye screening lengths to illustrate the shift of energy level caused by plasma effects. The shape resonances would emerge for a certain range of Debye screening lengths due to the quasi-bound states, which are converted from bound states and sustained by the potential barrier. The Wigner time delays [4] of atomic ionization in plasmas are explored focusing on specific regions, where shape resonances appear. The variations of Wigner time delays with Debye screening lengths are discussed, while the significant influence of shape resonances on the Wigner time delay is demonstrated.

References

[1] Lin CY and Ho YK 2010 *Eur. Phys. J. D* **57** 21
[2] Lin CY and Ho YK 2010 *Phys. Rev. A* **81** 033405
[3] Schneider B *et al* 2016 *Advances In Quantum Chemistry* **72** 95
[4] Wigner EP 1955 *Phys. Rev.* **98** 145

* E-mail: cylin@gm.scu.edu.tw

Probing sub-cycle oscillation dynamics of high-order harmonic generation of Na atom

H C Liu[1,2], P C Li[1,2,*], and S I Chu[3,4]

[1]Research Center for Advanced Optics and Photoelectronics, Department of Physics, College of Science, Shantou University, Shantou, Guangdong 515063, China
[2]Key Laboratory of Intelligent Manufacturing Technology of MOE, Shantou University, Shantou, Guangdong 515063, China
[3]Center for Quantum Science and Engineering, and Center for Advanced Study in Theoretical Sciences, Department of Physics, National Taiwan University, Taipei 10617, Taiwan
[4]Department of Chemistry, University of Kansas, Lawrence, Kansas 66045, USA

Synopsis We present an *ab initio* calculation by means of solving the time-dependent Schrödinger equation of Na atom in mid-infrared and ultraviolet (UV) laser fields. By changing the time delay between the two laser fields, we find that the excited states and dressed states play an important role in the sub-cycle oscillations. Our results provide a potential approach for the production of vacuum UV light source.

The study of atomic and molecular processes has been a subject of much interest in modern ultrafast science and technology in the past two decades [1, 2]. Recently, some experimental studies have been carried out on AC Stark shifts of He atom on attosecond scale [3]. However, little research has been done on the interaction between lasers and alkali metal atoms. Our results provide a physical insight into the sub-cycle dynamics of Na atom.

In this work, we focus on an *ab initio* study of Na atom by means of mid-infrared (IR) and ultraviolet (UV) laser fields. The time-dependent Schrödinger equation (TDSE) can be solved by means of the time-dependent generalized pseudospectral (TDGPS) method [4]:

$$i\frac{\partial\psi(\mathbf{r},t)}{\partial t} = H\psi(\mathbf{r},t) = [H_0+V(\mathbf{r},t)\psi(\mathbf{r},t)]. \quad (1)$$

Here, H_0 and $V(\mathbf{r},t)$ represent the unperturbed atom Hamiltonian and the time-dependent atom-field respectively. In Figure 1, we present the photon emission spectrum as a function of the time delay between the IR pulse and the UV pulse for the excited states and the virtual states. In the left pattern, the UV (IR) first indicates that the UV laser field arrives on the target before the IR (UV) pulse, and these black dotted lines represent the 3rd, 5th and 7th harmonic respectively, which originated form virtual oscillation structure. In the right pattern, it is clearly seen that the photon emission spectrum related to the excited states is very norrow and sharp.

*E-mail: pchli@stu.edu.cn

In summary, we have performed an *ab initio* of investigate sub-cycle photon emission dynamics behavior of Na atom at different time delay. We find that sub-cycle oscillation is produced by the virtual structures and the excited states. Our results provide a potential method for obtaining a vacuum UV light source.

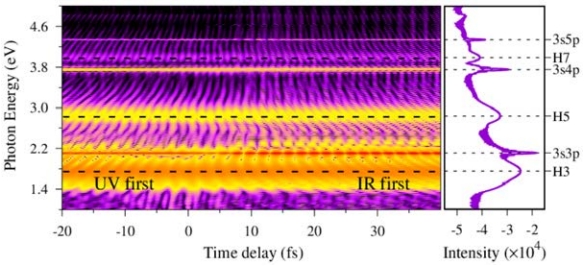

Figure 1. Photon emission energy spectrum as a function of the time delay between the IR pulse and the UV pulse.

Acknowledgments

This work was supported by the NSFC (11764038, 12074239), NSF of Guangdong Province (200110165892233, 2020A1515010927, 210206153460124), Department of Education of Guangdong Province (2018KCXTD011, 2019KTSCX038), and STU (NTF18030).

References

[1] Hentschel M H *et al* 2001 *Nature* **414** 509
[2] Heslar J *et al* 2014 *Phys. Rev. A* **89** 052517
[3] Michael C *et al* 2012 *Phys. Rev. Lett.* **109** 073601
[4] Tong X M *et al* 1997 *Chem. Phys.* **217** 119

Near-threshold dynamics in strong laser field

J. Liu[1] *, Y. Huang[1,2], J. Zhao[1], X. Wang[1] and Z. Zhao[1]

[1]Department of Physics, National University of Defense Technology, Changsha, 410073, People's Repulic of China
[2]National Innovation Institute of Defense Technology, AMS, Beijing 100071, People's Republic of China

Synopsis Physical processes near threshold in strong-field ionization are complex owing to the important role of manyintermediate states. Two typical near-threshold processes in few-cycle laser pulses, the generations of Rydberg electrons and terahertz waves, are investigated using classical trajectory Monte Carlo simulations. We find that the optimal phases for terahertz wave generation and creation of the Rydberg state in few-cycle laser pulses are opposite. This finding can be applied to further experiments on attosecond electron dynamics.

It is difficult to describe the behaviors of physical systems near threshold due to the lack of accurate physical models. For an atom or a molecule exposed to a high-intensity laser pulse, many highly nonlinear strong-field phenomena appear above the ionization threshold such as high harmonic generation, high-above-threshold ionization, and nonsequential double ionization. The involved dynamics can be well understood with a three-step model where the strong-fieldapproximation serves as an analytical tool to describethe rescattering process. Recently, investigations of dynamics near the ionization threshold are drawing more attention, like low-energy structure, frustrated tunneling ionization, below-threshold high-order-harmonic generation, and terahertz (THz) wave generation. The importance of interplay between the Coulomb potential and the laser field in the dynamics of the electron wave packet is proved in these near-threshold phenomena.

The pulse duration of THz wave is of (or near) the same order as the orbital time of a highly excited Rydberg electron and the classical trajectory method considering the Coulomb potential is well applicable in both Rydberg states and THz wave generation in a strong field. Although both escaping electrons and rescattering electrons can contribute to Rydberg state and photocurrent generation, the proportion of different kinds of trajectories varies dramatically. For photoelectron yields and the corresponding asymmetry change with the kind of trajectory; electrons which have soft collisions with the atomic core make the main contribution to THz wave generation[1]. Electrons released in a narrow time window before the extrema of the oscillating laser field, which experience no rescattering, mainly contribute to Rydberg state generation[2].

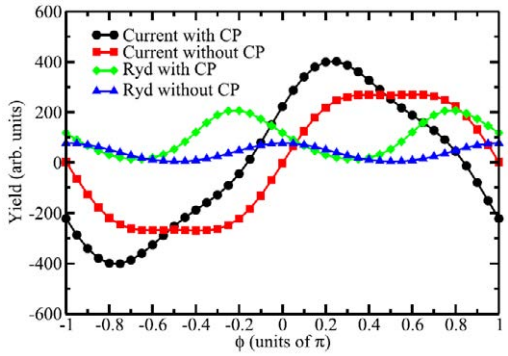

Figure 1. **Comparison of Rydberg states and photocurrent yields as a function of the CEP φ**

In this work, a complete physical picture of strong-field ionization is developed including the generations of THz waves and Rydberg states. For the two near-threshold processes, the correlated modulations and similar time scales are analyzed to decode the Coulomb focusing effect on the electronic dynamics. The connection between Rydberg states and THz waves makes it possible to measure their yields simultaneously. As shown in Fig. 1, modulations of photocurrents and Rydberg states have almost-opposite optimal phases whether with the Coulomb potential[3].

References

[1] Zhang D. *et al* 2012 *Phys. Rev. Lett* **109** 243002
[2] Eilzer S. *et al* 2014 *J. Phys. B* **47** 204014
[3] Liu J. *et al* 2020 *Phys. Rev. A* **102** 023109

* E-mail: liujinlei@nudt.edu.cn

Relativistic effects in the Cooper minima and angular distributions of photoelectrons in heavy elements

S Baral[1], S Saha[1], J Jose[1], P C Deshmukh[2,3], A K Razavi[4] and S T Manson[4*]

[1]Department of Physics, Indian Institute of Technology Patna, Bihta, Bihar 801103, India
[2]Department of Physics and CAMOST, Indian Institute of Technology Tirupati,Renigunta Road, Tirupati 517506, India
[3]Department of Physics, Dayananda Sagar University, Kudlu Gate, Hosur Road,Bengaluru 560114, India
[4]Department of Physics and Astronomy, Georgia State University, Atlanta, GA 30303, USA

Synopsis A systematic evolution of the Cooper minimum and the dipole angular distribution asymmetry parameter, β, as function of Z is investigated, with a special focus on the impact of relativistic effects in the photoionization of high-Z atoms..

Among various attributes of atomic photoionization, Cooper minimum (CM) in the cross-section and the photoelectron angular distribution have attracted much attention owing to their sensitivity to relativistic and correlation effects [1, 2]. The present work investigates the impact of relativistic effects on the photoelectron angular distribution asymmetry parameter β and the CM in a few high-Z atoms (Hg (Z=80), Rn (Z=86), Ra (Z=88), No (Z=102), Cn (Z=112), and Og (Z=118)) employing the Dirac-Fock (DF) and the Relativistic Random-Phase Approximation (RRPA) [3].

For an *ns* subshell, the CM in $ns \rightarrow \varepsilon p_{3/2}$ and $ns \rightarrow \varepsilon p_{1/2}$ transitions often occur at different energies, and the energy difference increases with increasing Z. The energy location of the CM displays interesting features as a function of Z. The minimum in $ns \rightarrow \varepsilon p_{1/2}$ channels moves down to discrete energies below the threshold and that in the $ns \rightarrow \varepsilon p_{3/2}$ shifts up in energy [4]. We extend the study on the locus of the CM to a series of subshells in high-Z atoms to examine if there is any new phenomenology at high-Z. We find that there are further curious behaviours resulting from competition between Coulomb attraction and spin-orbit interactions which lead to the location of the $ns \rightarrow \varepsilon p_{3/2}$ CM to continue to increase in photoelectron energy, with increasing Z, with the $6s \rightarrow \varepsilon p_{3/2}$ reaching almost 1 keV for Og. In addition, the $ns \rightarrow \varepsilon p_{3/2}$ CM for 4s and 5s, which move below therishold at lower Z, move into the continuum at high-Z owing to the spin-orbit repulsive force in the $ns \rightarrow \varepsilon p_{3/2}$ channels.

Although it is well known that β_{ns} deviates from 2.0 due to the relativistic effects, what about in the energy region away from the CM? To examine the asymptotic values of β_{ns}, which depend on the dipole phase shift difference $\delta p_{3/2}$-$\delta p_{1/2}$, plotted in Fig. 1, and shows that the phase shift difference increases as a function of Z. This leads to a deviation of β_{ns} from 2.0 asymptotically, even if the radial matrix elements of the two relativistic channels are equal, and the deviation is seen to increase with Z.

STM thanks DOE, Office of Science under Grant DE-FG02-03ER15428, JJ thanks SERB through the project no. ECR/2016/001564, SB and SS thank MHRD, India.

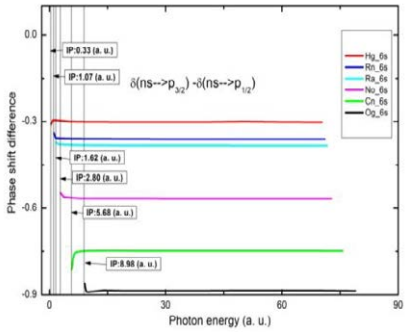

Figure 1. Phase shift difference (in radians) as a functions of photon energy (in a.u.).

References

[1] J. W. Cooper 1962 *Phys. Rev.* **128,** 681
[2] T.E.H. Walker and J.T. Waber 1973 *Phys. Rev. Lett.* **30,** 8
[3] W. R. Johnson and K. T. Cheng 1979 *Phys. Rev. A.* **20,** 978
[4] R.Y. Yin and R.H. Pratt 1987 *Phys. Rev. A* **35** 1149

* E-mail: smanson@gsu.edu

Photoionization branching ratios of spin-orbit doublets in heavy elements at high energy: Relativistic and interchannel coupling effects in Hg

C. R. Munasinghe[1], S T Manson[1*] and P C Deshmukh[2]

[1]Department of Physics and Astronomy, Georgia State University, Atlanta, GA 30303, USA
[2]Department of Physics, Indian Institute of Technology Tirupati, Tirupati, Andhra Pradesh 517506, India

Synopsis Photionization branching ratios of spin-orbit doublets in Hg are calculated over a broad range of energies up to several keV using the relativistic-random-phase approximation (RRPA). The results demonstrate both strong relativistic and interchannel coupling effects in the regions of inner-shell thresholds.

Photoionization studies of spin-orbit doublets in atoms are of interest in that they spotlight relativistic interactions. Absent relativity, the branching ratio for an n*l* doublet far above threshold (where the difference in binding energy is irrelevant) would just be the statistical ratio, $(l+1)/l$. It was predicted many years ago that relativistic interaction would cause the ratio to be below the statistical value [1,2] and this prediction was recently born out experimentally for Ar and Xe [3]. In addition it has been found that correlation in the form of interchannel coupling has a profound effect on the branching ratios for outer-shell doublets in the vicinity of inner-shell thresholds [3,4].

To further understand this phenomenology, we have studied the photoionization of Hg from threshold to about 3.6 keV using the relativistic random-phase approximation (RRPA) [5]. All relativistic channels from the valence 6s down to the 3s subshell are included in the calculation. In addition, truncated calculations have been performed omitting certain correlations to focus on how each coupling affects the results.

As an example, the 5p branching ratio in the vicinity of the 3d thresholds are shown in Fig. 1. Looking at the fully coupled (red) curve, it is evident that the coupling with the 3d channels induces not only an overall shift in the branching ratio, but also strongly energy-dependent structures above each of the thresholds. The green and yellow curves show how the results are affected when the coupling with the channels from one or the other 3d subshells is omitted. And the upper (blue) curve shows the result when the coupling with the 3d channels is completely omitted, thereby proving that the shift and the structure of this branching ratio is indeed the result of interchannel coupling with the photoionization channels from the 3d subshells.

This work was supported by DOE, Office of Science under Grant DE-FG02-03ER15428.

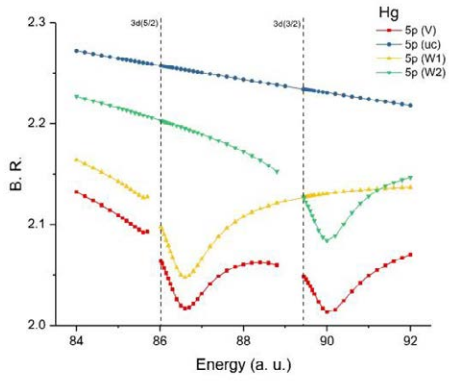

Figure 1. Branching ratio (B. R.) of the Hg 5p doublet in the vicinity of the 3d thresholds at various levels of truncation of the RRPA as a function of photon energy (in a.u.); red (complete coupling), blue (no 3d coupling), green (no $3d_{5/2}$ coupling), yellow ($3p_{3/2}$ coupling). Vertical lines show the 3d subshell thresholds.

References

[1] T.E.H. Walker and J.T. Waber 1973 *Phys. Rev. Lett.* **31,** 8
[2] Y. S Kim, R. H. Pratt and A. Ron 1981 *Phys. Rev.* **24,** 1889
[3] R. Püttner, *et al* 2021 *J. Phys B* In press
[4] W. Drube *et al* 2013 *J. Phys. B* **46** 245006
[5] W. R. Johnson and K. T. Cheng 1979 *Phys. Rev. A.* **20,** 978

* E-mail: smanson@gsu.edu

Disentangling photoelectron vortices in strong field ionization

A S Maxwell[1,2]*, Y Kang[2], X Barcons Planas[1], E Pisanty[1†], M Ciappina[1†], A F Ordonez[1], G S J Armostrong[3], A C Brown[3], C F d M Faria[2], and M Lewenstein[1†]

[1]ICFO - Institut de Ciencies Fotoniques, Av. Carl Friedrich Gauss 3, 08860 Castelldefels (Barcelona), Spain
[2]Department of Physics & Astronomy, University College London, Gower Street, London WC1E 6BT, UK
[3]CTAMOP, School of Mathematics and Physics, Queen's University Belfast, BT7 1NN, Northern Ireland, UK

Synopsis We present in-depth overview of recently published and ongoing research into the orbital angular momentum of photoelectrons in strong field processes. Developing a modified strong field approximation enables an understanding of the basic dynamic of the photoelectron OAM. This theoretical framework is then used to explore the strong-field photoelectron OAM for a range of issues. Firstly, we discuss their role in forming interference vortices, and then investigate the ability to probe chiral states using the OAM. Finally, we demonstrate how the OAM of two photoelectrons can be shown to be entangled in non-sequential double ionization.

The orbital angular momentum (OAM) of a free particle is a quantized observable, which leads to a rotating vortex in light or matter waves [1]. *Twisted* light and electrons have huge potential in imaging and control of matter. The study of OAM in attosecond physics is of great interest and is a rapidly advancing field. Almost all the attention has been devoted to the study of the OAM of incident and emitted light. In high-harmonic generation (HHG) a twsited driving field can be used to produce twisted UV light [2] and this has been manipulated in a myriad of ways [3]. However, little attention has been paid to the OAM of the photoelectrons.

We investigate the OAM of a photoelectron freed in strong-field ionization by developing an adapted version of the well-known strong-field approximation (SFA) [4]. This allows the derivation of conservation laws for the OAM twisted electrons. We find that the condition for the circular fields can be related to the famous ATI peaks. Employing this new framework we provide an alternative interpretation on existing experimental work of vortex interferences caused by strong field ionization mediated by two counter-rotating circularly polarized pulses separated by a delay [5]. We find very good agreement between photoelectron momentum distributions computed with the SFA, as well as with the methods Qprop and R-Matrix, see Fig. 1. These results are used to discuss interferometric and other methods for detecting OAM of the photoelectrons in strong field experiments.

Exploiting a construction of chiral states from hydrogenic orbitals allows analytical and numerical results that demonstrated how chirality is encoded in the photoelectron OAM. Finally, we investigate entanglement in the correlated two-electron strong field process non-sequential double ionization. The conditions required to generate pairs of photoelectrons with entangled OAM are explored, along with considerations about how this could be measured in experiment and whether this could be a useful resource.

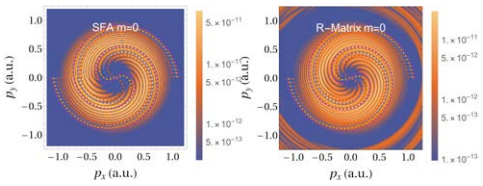

Figure 1. Interference vortices formed by two counter rotating circularly polarized pulses model by the SFA and R-Matrix with time-dependence.

References

[1] K. Y. Bliokh et al. *Phys. Rep.* **690** no. 2017, pp. 1–70 (2017).
[2] M. Zürch et al. . *Nat. Phys.* **8** no. 10, pp. 743–746 (2012). C. Hernández-García et al. *Phys. Rev. Lett.* **111**, p. 083602 (2013).
[3] L. Rego, K. M. Dorney, N. J. Brooks et al. *Science* **364** no. 6447, p. 1253 (2019). E. Pisanty et al. *Nat. Photonics* **13** no. August, pp. 569–574 (2019).
[4] Y. Kang, E. Pisanty et al. and A. S. Maxwell EPJ D (in press) (2021). arXiv:2102.07453
[5] A. S. Maxwell, G. S. J. Armstrong, M. F. Ciappina et al. *Faraday Discuss.* arXiv:2010.08355

*E-mail: andrew.maxwell@icfo.eu
†see [4, 5] for full address list

Control of Parent-Ion Coherence in Helium Ion Ensemble

S Mehmood[1]*, E Lindroth[2] and L Argenti[1,3]†

[1] Dept. of Phys., University of Central Florida, Orlando, 32826, USA
[2] Dept. of Phys., Stockholm University, Stockholm, Sweden
[3] CREOL, University of Central Florida, Orlando, 32826, USA

Synopsis We show that the pump-probe delay in an attosecond ionization setup can be used as a control knob to tune the coherence between shake-up ionic states of helium. From the picosecond dipole beating caused by relativistic interactions it is possible to reconstruct the polarization of the ion at the time of its inception.

Attosecond pulses can ionize atoms in a coherent process. Since the emerging fragments are entangled, however, each preserves only a fraction of the initial coherence [1], thus limiting the chance of guiding the ion subsequent evolution. In this work, we use *ab initio* simulations of pump-probe ionization of helium above the $2s/2p$ threshold to demonstrate how this loss of coherence can be controlled [2]. A broadband XUV pump pulse in association with an IR probe pulse with controllable delay activate several multi-photon paths to the shake-up ionization of the helium atom, some of which proceed through intermediate $2\ell n\ell'$ autoionizing states [3]. The Interference between direct and multi-photon ionization paths gives rise to a partial coherence between the $2s$ and $2p$ states of the ion, controllable via the pump-probe delay τ. The coherence between the ionic $2s$ and $2p$ states, which are degenerate in the non-relativistic limit, results in a stationary, delay-dependent electric dipole. From the picosecond real-time beating of the dipole, caused by the fine-structure splitting of the $n = 2$ manifold, it is possible to reconstruct all the original coherences between the ionic states. The coherence between antiparallel-spin states, in particular, is a sensitive probe of relativistic effects in attosecond photoemission.

We simulate this process by solving the time-dependent Schrödinger equation for the atomic system in the presence of the external pulses [3, 4]. The density matrix of the system is computed at the end of the pulse from the partial photoionization amplitudes [3, 5], as a parametric function of the pump-probe delay. The relativistic terms in the ionic Hamiltonian are taken into account for the subsequent evolution of the isolated ion. The slow fine-structure evolution, therefore, maps the attosecond modulation of the ionic density to a temporal domain three orders of magnitude larger.

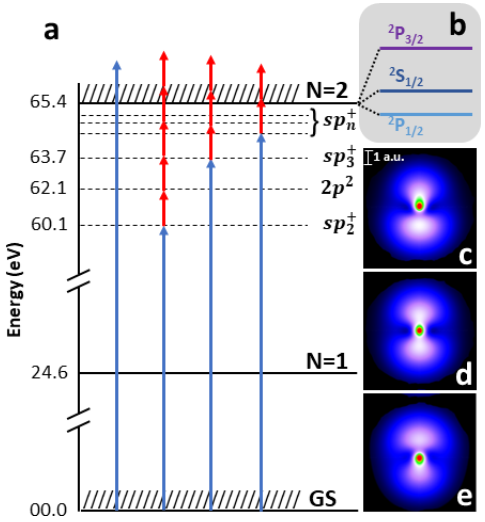

Figure 1. a) Several multi-photon paths interact to give rise to $2s - 2p$ coherence. c-e) Ion electron density at $\tau = 0$, 1, and 2 fs exhibits asymmetry due to ionization in the presence of polarized IR field. b) Due to the fine-structure splitting of the $n = 2$ He^+ level, the ionic dipole fluctuates, thus mapping the attosecond dependence of initial ionic coherence to the picosecond timescale.

References

[1] S Pabst *et al.* 2011 *Phys. Rev. Lett.* **106** 053003
[2] S Mehmood *et al.* arXiv:2012.11040 [physics.atom-ph]
[3] L Argenti and E Lindroth 2010 *Phys. Rev. Lett.* **105** 053002
[4] C Ott *et al.* 2014 *Nature* **516** 7531
[5] L Argenti *et al.* 2013 *Phys. Rev. A* **87** 053405

*E-mail: saadiphy@knights.ucf.edu
†E-mail: luca.argenti@ucf.edu

Photoelectron spectroscopy of laser-dressed atomic helium

S Meister[1]*, A Bondy[2,3], K Schnorr[4], S Augustin[4], H Lindenblatt[1], F Trost[1], X Xie[4], M Braune[5], R Treusch[5], B Manschwetus[5], N Schirmel[5], H Redlin[5], N Douguet[6], T Pfeifer[1], K Bartschat[2], and R Moshammer[1]

[1]Max-Planck-Institute for Nuclear Physics, 69117 Heidelberg, Germany
[2]Department of Physics and Astronomy, Drake University, Des Moines, IA 50311, USA
[3]Department of Physics, University of Windsor, Windsor, Ontario N9B 3P4, Canada
[4]Paul Scherrer Institute, 5232 Villigen, Germany
[5]Deutsches Elektronen-Synchrotron, 22607 Hamburg, Germany
[6]Department of Physics, Kennesaw State University, Marietta, GA 30060, USA

Synopsis Photoelectron emission from excited states of laser-dressed atomic helium is analyzed with respect to laser intensity-dependent excitation energy shifts and angular distributions. In the two-color extreme ultraviolet (XUV)-infrared (IR) measurement, the XUV photon energy is scanned between 20.4 eV and the ionization threshold at 24.6 eV, revealing electric dipole-forbidden transitions for a temporally overlapping IR pulse ($\approx 10^{12}$ W cm^{-2}). The interpretation of the experimental results is supported by numerically solving the time-dependent Schrödinger equation in a single-active-electron approximation.

This investigation employs XUV radiation from the FLASH (free-electron laser in Hamburg) in combination with a synchronized IR laser (800 nm). The temporal delay between pulses of both sources can be adjusted freely and the XUV photon energy is scanned in the region of excited states in helium. Emitted photoelectrons are measured by means of a reaction microscope which allows to infer angular distributions in 4π solid angle and kinetic energies.

In the trivial case of subsequent IR pulses, the XUV first excites the atom to nP states. In the second step the excited atom gets ionized by absorbing few IR photons of the subsequent pulse.

For overlapping pulses several additional pathways open up. As both radiation fields are simultaneously present, the XUV-photon absorption can be accompanied by IR-photon absorption or emission of the laser-dressed atom. For example, in the combined absorption of one XUV and absorption/emission of one IR photon, the helium atom can be excited from the $1s^2\,{}^1S$ ground state to $1sns\,{}^1S$ and $1snd\,{}^1D$ states, respectively [1]. Finally the excited atom can be ionized by absorbing additional IR photons. In general, these states are denoted as *dark states*. In similar transient absorption measurements, they were dubbed as *light-induced states* (LIS) [2].

*E-mail: severin.meister@mpi-hd.mpg.de

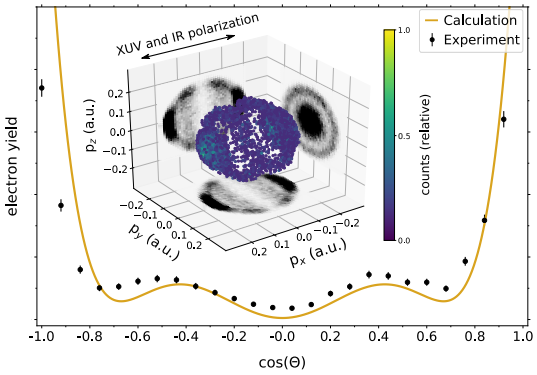

Figure 1. 3D PAD for emission from $1s3d\,{}^1D$ state.

Besides the assignment of these states, we analyze their excitation energies and photoelectron angular distributions as a function of laser intensity [3]. The experimental results are reproduced and verified by numerically solving the time-dependent Schrödinger equation (cf. Figure 1). Furthermore, the two-color scheme allows to vary the relative polarization of both radiation sources. This additional degree of freedom is employed to change the magnetic quantum number m and to deliberately switch on and off ionization via certain states.

References

[1] S. Meister *et al* *Phys. Rev. A*, 102:062809, 2020..
[2] S. Chen *et al* *Phys. Rev. A*, 86:063408, 2012.
[3] S. Meister *et al* *in press*, 2021

The work was supported by the US NSF (KB,AB,ND).

First complete test of polarization transfer in elastic scattering of hard x-rays

W Middents[1,2 *], G Weber[1,3], M Vockert[1,2], U Spillmann[3], A Gumberidze[3], P Pfäfflein[1,2,3], A Volotka[1], A Surzhykhov[4] and Th Stöhlker[1,2,3]

[1]*Helmholtz-Institut Jena, D-07743 Jena, Germany*
[2]*Friedrich-Schiller-Universität-Jena, Institut für Optik und Quantenelektronik, D-07743 Jena, Germany*
[3]*GSI Helmholtzzentrum für Schwerionenforschung GmbH, D-04291 Darmstadt, Germany*
[4]*Technische Universität Braunschweig, D-38106 Braunschweig, Germany*

Synopsis We present an experiment on the polarization transfer in Rayleigh scattering of highly linearly polarized hard x-rays on an atomic target. The experiment was recently performed at the synchrotron PETRA III at DESY and for the first time allowed to analyze the polarization properties of the scattered beams when leaving the polarization plane of the initial highly polarized beam.

Elastic scattering of hard x-rays on atomic targets describes a fundamental interaction process in the relativistic photon-matter interaction regime where both the energy of the initial and the scattered photon are the same. For photon energies up to several hundred keV this process is dominated by the 2nd order QED process of Rayleigh-scattering, the scattering of photons from bound electrons [1]. Elastic scattering is highly polarization-sensitive making the analysis of polarization transfer a suitable tool for a stringent test of the underlying theory [2].
For a long time experiments addressing the polarization-dependant features of elastic scattering were restricted to scenarios where either the differential scattering cross section for a linearly polarized incident beam or the polarization of the scattered radiation resulting from an unpolarized incident beam was measured [3]. For the first time both the polarization of the incoming radiation as well as the scattered radiation were measured simultaniously was realized by our group in 2015 [4] using the highly linearly polarized synchrotron beam of PETRAIII at DESY and a new prototype detector being a 2D sensitive strip detector serving as a highly sensitive Compton polarimeter [5]. This study where scattering within the polarization plane of the initial beam was analyzed showed, well in accordance with theory, a strong dependence of the degree of polarization of the scattered beam on the scattering angle ϑ and the degree of polarization of the initial beam.
Recently we performed an additional study on the polarization transfer in elastic scattering were for the first time ever we left the polarization plane of the initial beam. For the experiment we again used the beamline P07 of PETRAIII at DESY. The photon beam with a beam energy of 175 keV was scattered on a thin gold foil (Z=79) and then detected by a prototype Compton polarimeter under several angles inside and outside of the polarization plane of the initial beam. Preliminary results already show that the orientation of the polarization vector is strongly affected by the chosen detection geometry outside of the polarization plane of the initial photon beam.

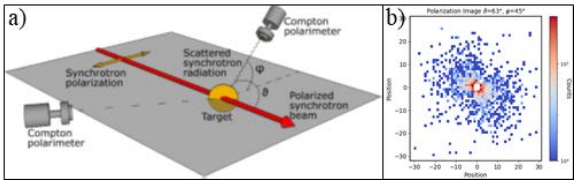

Figure 1. a) Sketch of the experimental setup. The incident synchrotron beam is scattered on a gold target and detected by a Compton polarimeter. b) Exemplary measurement image of the Compton polarimeter. The image shows the angular distribution of photons being Compton scattered on the detector crystal.

This research has been conducted in the framework of the SPARC collaboration. Financial support by ErUM-FSP APPA (BMBF n° 05P19SJFAA) is acknowledged.

References

[1] P.P. Kane et al., Phys. Rep. **140**, 75 (1986)
[2] Strnat et al. Phys. Rev. A **103**, 012801 (2021)
[3] S. C. Roy et al., Phys. Rev. A **34**, 1178 (1986)
[4] K.-H. Blumenhagen et al., New J. Phys. **18**, 103034 (2016)
[5] G. Weber et al., J. Phys.: Conf. Ser. **583**, 012041 (2015)

* E-mail: wilko.middents@uni-jena.de

Calculation of multiphoton ionization amplitudes and cross sections of few-electron atoms

A Mihelič[1,2*], **M Horvat**[2†]

[1]Jožef Stefan Institute, Ljubljana, Slovenia
[2]Faculty of Mathematics and Physics, University of Ljubljana, Slovenia

Synopsis We present a theoretical method for the calculation of multiphoton ionization amplitudes and cross sections of few-electron systems. The method is based on an extraction of partial wave amplitudes from a scattering wave function, which is calculated by solving a system of driven, time-independent Schrödinger equations. We use the new approach to calculate multiphoton ionization cross sections of hydrogen and helium atoms and the asymmetry parameters of photoelectron angular distributions for multiphoton ionization of the helium atom.

Sources of short, intense, coherent radiation operating in the ultraviolet and x-ray spectral regions, such as free-electron lasers (FELs) and high-order harmonic generation (HHG) sources, make it possible to study processes in atoms and molecules which unfold on the femto- and subfemtosecond time scales. These sources can be used to both probe and control the evolution of the system under investigation. When the incident intensity is high enough, more than one photon can be absorbed before atomic ionization or molecular fragmentation takes place.

Theoretical description of multiphoton ionization is particularly demanding when the number of photons absorbed exceeds the number of photons required to ionize the target (above threshold ionization, ATI) or when the continua are resonant (structured). While a direct solution of the time-dependent Schrödinger equation is usually the preferred way of studying photoexcitation or photoionization, this may not, generally, be feasible, for example, when the pulse duration exceeds a few tens of femtoseconds. In this case, the calculation of ionization probabilities, cross sections, or amplitudes, either by using the lowest-order perturbation theory or the non-perturbative Floquet approach, may be undertaken.

We present a novel method for the calculation of multiphoton ionization amplitudes and cross sections of few-electron atoms and molecules [1]. The method, which is an extension of the past work [2, 3, 4, 5] and is based on exterior complex scaling [6], allows the calculations to be performed using simulation volumes of modest sizes. Partial ionization amplitudes are extracted from a solution of a system of driven, time-independent Schrödinger equations. More specifically, the method relies on a description of the outgoing-wave part of the scattering state in terms of a small number of Coulomb waves with fixed wave numbers inside the nonscaled spatial region.

We demonstrate the applicability of the method by calculating two-, three-, and four-photon ionization amplitudes and cross sections of hydrogen and helium atoms over a wide range of photon energies. Furthermore, we calculate the asymmetry parameters used to characterize photoelectron angular distributions from two-, three-, and four-photon ionization of helium.

References

[1] Mihelič A, Horvat M 2021 *arXiv* **2103.16422**
[2] McCurdy C W, Rescigno T N 2000 **62** 032712
[3] Horner D A *et al* 2007 **76** 030701(R)
[4] Horner D A *et al* 2008 **77** 030703(R)
[5] Mihelič A 2018 *Phys. Rev. A* **98** 023409
[6] McCurdy C W, Martín F 2004 *J. Phys. B* **37** 917

*E-mail: andrej.mihelic@ijs.si
†E-mail: martin.horvat@fmf.uni-lj.si

Observation of the quantum shift of a backward rescattering caustic by carrier-envelope phase mapping

T Mizuno[1]*, N Ishii[1], T Kanai[1], P Rosenberger[2], D Zietlow[2], M F Kling[2,3], O I Tolstikhin[4], T Morishita[5] and J Itatani[1]

[1]The Institute for Solid State Physics, The University of Tokyo, Kashiwa, Chiba 277-8581, Japan
[2]Physics Department, Ludwig-Maximilians-Universität München, D-85748, Garching, Germany
[3]Max Planck Institute of Quantum Optics, D-85748, Garching, Germany
[4]Moscow Institute of Physics and Technology, Dolgoprudny 141700, Russia
[5]Institute for Advanced Science, The University of Electro-communications, Chofu-shi, Tokyo 182-8585, Japan

Synopsis We measure rescattering photoelectron momentum distribution (PEMD) generated in strong-field ionization of Xe atoms by using a carrier-envelope phase (CEP)-stable few-cycle field. A cutoff structure of PEMD is analyzed by the adiabatic theory of rescattering. This theory predicts that the cutoff, wherein the PEMD begins to exponentially decay, is located at a quantum caustic that is shifted towards higher energies with respect to the corresponding classical caustic at which long and short backward rescattering trajectories coalesce. The observed position of the cutoff in the PEMDs agrees well with the adiabatic theory, confirming the quantum shift of the caustic.

Photoionization of an atom and molecule in intense field is the most fundamental process in strong field Physics [1, 2]. Recent theoretical work predicts that the quantum caustic, where the photoelectron momentum distribution (PEMD) begins to exponentially decay, is shifted to higher energy than the corresponding classical caustic, at which long and short backward rescattering trajectories coalesce [1].

In this work, we experimentally and theoretically investigate photoelectron momentum distributions (PEMDs) for Xe atoms near the rescattering caustic by a carrier-envelope phase (CEP)-stable few-cycle field [3]. We use linearly-polarized intense IR fields at 1600 nm with a pulse duration of about 13.8 fs from an OPCPA system. The PEMD of Xe atom in the parallel direction to the polarization is measured by a time-of-flight photoelectron spectrometer as a function of the CEP.

Figure 1 shows measured and calculated PEMDs near the cutoff. In the top figure, an associated half cycle of the electric field with a calculated PEMD is shown. Thin and thick arrows indicate the classical and quantum caustics, respectively. One can clearly see two half-cycle cutoffs, which are assigned to corresponding half cycles of HCO(0) and HCO(1), which are depicted in the figure. By comparing measured PEMDs to calculated ones by the adiabatic theory, we verify the quantum shift of the caustic.

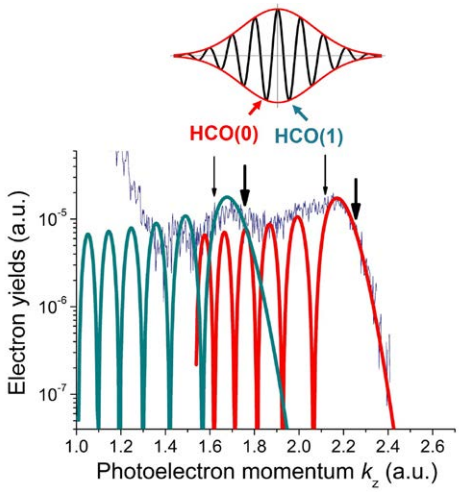

Figure 1. Measured PEMDs (black curve) at the CEP of 0 at an intensity of 2.6×10^{13} W/cm^2, and a pulse duration of 13.8 fs. The red and green curves show calculated PEMDs for HCO(0) and HCO(1).

References

[1] Morishita T and Tolstikhin O I, 2017 *Phys. Rev. A* **96**, 053416
[2] Geiseler H *et al*, 2016 *Phys. Rev. A* **94**, 033417
[3] Mizuno T *et al*, submitted to *Phys. Rev. A*

*E-mail: mizuno.tomoya@issp.u-tokyo.ac.jp

Attosecond electron dynamics near the ionization threshold in Ne

M Moioli[1,*], K R Hamilton[2], H Ahmadi[1], D Ertel[1], M Schmoll[1], M M Popova[3], E V Gryzlova[3], A N Grum-Grzhimailo[3], M D Kiselev[3], D Atri-Schuller[2], G P Menning[2], K Bartschat[2], C D Schröter[4], R Moshammer[4], T Pfeifer[4], and G Sansone[1].

[1]Physikalisches Institut, Universität Freiburg, 79106 Freiburg, Germany;
[2]Department of Physics and Astronomy, Drake University, Des Moines, Iowa 50311, USA;
[3]Skobeltsyn Institute of Nuclear Physics, Lomonosov Moscow State University, 119991 Moscow, Russia;
[4]Physical Department, Lomonosov Moscow State University, 119991 Moscow, Russia

Synopsis Attosecond pulses are suitable tools to unveil the ultrafast behaviour of electrons. We report results for photoionization of neon focusing the attention on the dynamics near the ionization threshold.

In recent years, attosecond spectroscopy has played a central role in exploring the electronic dynamics in atoms and molecules [1].

Electronic processes can be investigated using a two-color photoionization scheme from which it is possible to obtain information on the photoionization time delay (PTD) acquired by the electron undergoing the photoionization process [2].

A technique known as RABBITT (Reconstruction of Attosecond Beating By Interference of Two-photon Transitions) is commonly used to access the PTDs [3]. Photoionization occurs using synchronized XUV (extreme ultraviolet) and IR (infrared) pulses, which are delayed with respect to each other [4].

Usually, the XUV pulses are composed of a frequency comb of odd harmonics with photon energies above the ionization potential (IP) of the target medium. In the present case, one harmonic has a photon energy below the IP of neon, thus leading to excitation of an intermediate bound state before being ionized by absorbing an additional IR photon. The phase of the sideband oscillation generated through this XUV-excitation and IR-ionization process will be compared with the ones associated with the mechanism commonly considered, where both of the harmonics involved bring the electrons immediately to the continuum through direct ionization.

The time delays can be decomposed into a term inherent to the group delay of the different harmonics (τ_{GD}) and an atomic time delay (τ_a). It will be shown that the delay τ_a determined from one harmonic below and one above the ionization threshold largely deviates from the value expected for sidebands generated only above the threshold. The variation is attributed to excited states of neon that can be effectively populated by the harmonic of the XUV pulse train below the photoionization threshold.

Our experimental findings are supported by three different theoretical approaches: all-electron R-Matrix with Time Dependence (RMT), the single-active electron (SAE) approximation, and perturbation theory (PT).

Figure 1 depicts the experimental and theoretical sideband oscillations (SB) for SB14 (the harmonic 13 is below the ionization threshold of neon) and SB16 (both harmonics 15 and 17 are above the ionization threshold of neon), which are almost out of phase.

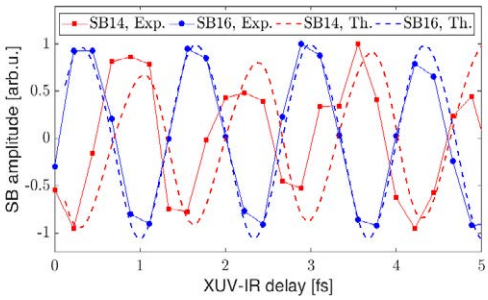

Figure 1. Comparison of experimental and theoretical sideband oscillations for the SB14 and SB16 case in neon. Laser pulses centered at 800 nm with duration of 30 fs are used in both cases.

References

[1] Krausz F and Ivanov M 2009 *Rev. Mod. Phys.* **81** 163
[2] Dahlström J M, L'Huillier A, and Maquet A 2012 *J. Phys. B* **45** 183001
[3] Paul P M *et al* 2001 *Science* **292**1689
[4] Ahmadi H *et al* 2020 *J. Phys. Photonics* **2** 02406

* E-mail: matteo.moioli@physik.uni-freiburg.de

Phase and amplitude characterization of partial waves in an attosecond continuum electron wavepacket

H Niikura[1] *, S Patchkovskii[2], P Peng[3], M J J Vrakking[2], and D M Villeneuve[3]

[1]Department of Applied Physics, Waseda University, Tokyo, 169-8555, Japan
[2]Max-Born-Institut, Berlin, D-12489, Germany
[3]Joint Attosecond Science Laboratory, National Research Council of Canada, Ottawa, K1A0R6, Canada

Synopsis We completely characterize the phase and amplitude of partial waves in a continuum electron wavepacket that is produced by an attosecond XUV and IR laser pulses .

A wavefunction is characterized by the phase and amplitude distributions in a real or momentum space. Recent attosecond technology has provided the way of measuring photoionization phases or delays using two-color ionization processes with attosecond XUV and IR laser pulses. In an atomic case, the electron wavepacket produced in photoionization is a result of coherent and incoherent superposition of several quantum states with magnetic numbers, m, and the orbital angular quantum numbers,ℓ. Besides, the phase of photoelectrons is influenced by the spectral phase of attosecond pulses. Hence, direct comparison between measurements and theory is more complicated.

We show that phase and amplitude of partial waves in a continuum electron wavepacket can be completely characterized from experiments. We use neon as a precursor atom. Two-color ionization by XUV and IR pulses produces a continuum electron wave packet which consists of the p- ($\ell = 1$) and f-($\ell = 3$) waves with m = 0 and m = ±1 through the intermediate s-($\ell = 0$) and d-($\ell = 2$) states from the 2p ground state.

First, we experimentally and theoretically demonstrate that tuning the photon energy of the XUV and the IR intensity, the photoelectron with m = 0 is isolated from m = ±1 [1-2]. Using TDSE and model calculations [2], we reveal that when the photon energy of the IR laser pulse is nearly resonant with the AC-stark shifted energy separation between the Rydberg states, the energy levels of m = 0 are separated from m = ±1 states. Figure 1 shows the measured velocity map images (VMI) that contain mainly the (a) m = 0 and (b) m = ±1 of the f-waves. Second, using three-path interference in the XUV-IR photoionization process, we decompose the continuum electron wavepacket into the partial waves [1,3]. We measured the VMI images of photoelectrons ionized by the IR pulse and the attosecond XUV pulse trains which contains both even and odd harmonics as a function of the XUV-IR delay. The XUV pulse with odd and even harmonics was produced by focusing both the IR (ω) and its second harmonic (2ω) into Ar gas. By fitting the photoelectron angular distribution as a function of the delay with the simulated distribution, we obtain the amplitude and phase of each partial wave produced by H13+IR, H14 and H15-IR.

We further disentangle the phases of partial waves into the phases caused by atto-chirp of the XUV pulse from the atomic phase [3]. We obtained the spectral phase of the XUV pulse by measuring the spectra as a function of the ω-2ω delay. With this information, we isolate the atomic phase of each partial wave. From these phases and amplitudes, we re-construct the continuum electron wavepackets produced by individual ionization pathways.

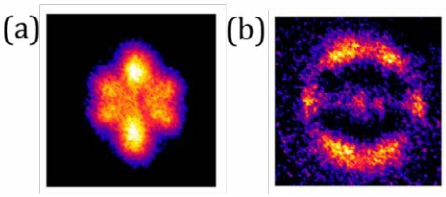

Figure 1. The measured velocity map images for mainly (a) m=0 and (b) m=±1of the f-wave.

References

[1] Villeneuve *et al* 2017 *Science* **356**, 1150.
[2] Patchokovskii S et al 2020 *J. Phys. B:At Mol. Opt. Phys.* **53** 134002.
[3] Peng P et al *in preparation*.

* E-mail: niikura@waseda.jp

Frustrated tunneling dynamics in ultrashort laser pulses

E Olofsson[1], S Carlström[1] and J M Dahlström[1]*

[1]Department of Physics, Lund University, Box 118, SE-221 00 Lund, Sweden

Synopsis We have studied frustrated tunneling ionization in ultrashort pulses using two methods. The first is a model based on the strong field approximation, and the second is numerically solving the time-dependent Schrödinger equation. As the carrier–envelope phase of the pulse is varied, we observe modulations in the distribution of population in the principal quantum number, and we find that the two methods we have used agree qualitatively for $n \geq 4$. We have also explored the role of continuum states in the context of the Schrödinger equation, in order to investigate the recapture mechanism of frustrated tunneling.

In addition to the process of tunneling ionization, one also finds a nonzero Rydberg state population, when an atom is subjected to an intense, low frequency laser pulse. This process is known as frustrated tunneling ionization, and has been explained with a classical model where the electron tunnels close to the peaks of the electric field, and is later captured by the atomic potential [1]. We have studied frustrated tunneling in Hydrogen with ultrashort pulses using a theory based on the strong field approximation (SFA) [2], and compared it to results obtained by solving the time-dependent Schrödinger equation (TDSE). We used pulses of 800 nm wavelength, a 2 fs pulse duration and intensities on the order of 10^{14} W/cm^2.

The SFA model that was used relies on a saddle point approximation that is supplemented with additional constraints to ensure that the trajectory associated to a solution of the saddle point equation will have have an energy and angular momentum that corresponds to a particular Rydberg state. Since we are dealing with short laser pulses, the carrier–envelope phase (CEP) becomes important. The solutions to the modified SFA equations show an intricate dependence on CEP and angular momentum l. As the CEP is varied in our TDSE simulations, we see a modulation in the total population of states with different principal quantum numbers n, see Fig. 1, that the SFA theory can qualitatively reproduce for $n \geq 4$. However, for $n = 2, 3$ we do not see agreement between the TDSE and SFA results. Additionally, when we resolve the CEP variations in l, we do not find agreement between TDSE and SFA for any n.

In conclusion, we have showed that population transfer to Rydberg states in ultrashort, intense pulses can be interpreted by frustrated tunneling. To support this conclusion, we have also performed TDSE simulations where the continuum states are either removed entirely from the state space, or damped during propagation, and find that the continuum states must be included in order to get the correct Rydberg state population.

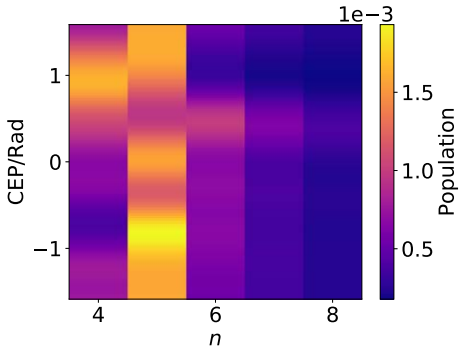

Figure 1. CEP dependence of the Rydberg population with principal quantum number n, calculated with the TDSE.

References

[1] Nubbermeyer T *et al* 2008 *Phys. Rev. Lett.* **101** 233001

[2] Popruzhenko S V 2017 *J. Phys. B: At. Mol. Opt. Phys.* **51** 014002

*E-mail: marcus.dahlstrom@matfys.lth.se

Doubly excited states driven by intense XUV FEL pulses

C Ott[1*], L Aufleger[1], A Magunia[1], and T Pfeifer[1]

[1]Max-Planck-Institut für Kernphysik, Heidelberg, 69117, Germany

Synopsis Using intense extreme ultraviolet (XUV) ultrashort free-electron laser (FEL) pulses it is possible to resonantly tune to specific transitions in atoms and molecules giving direct access to short-lived multi-electron excited states. Here we present results on the near-resonant driving of a two-electron autoionizing dipole transition in helium through intense XUV pulses and find regimes for achieving a short-lived population inversion as well as spectral redistribution for near-resonant gain of the XUV transmission.

Within nonlinear XUV-FEL light-matter interaction, a key scientific question is how exactly do resonant multi-electron transitions respond to and in turn influence the interaction with these pulses. Being embedded in the ionization continuum at XUV and x-ray photon energies, these transitions are naturally short lived, hence new effects can be expected when using shorter and shorter FEL pulses, nowadays approaching the attosecond regime.

Previously we have experimentally observed a significant modification of the absorbance line shape of the $1s^2$ – 2s2p autoionizing two-electron transition in helium when driven by intense XUV FEL pulses [1]. Supported by an analytical model these findings have been associated to transient light-induced energy shifts. Considering also the stochastic nature of the FEL pulses, the influence of the pulse duration on the spectral absorbance has been identified [2]. Furthermore, detuning effects of this strongly coupled autoionizing transition have been discussed [3].

Here we present new findings on the near-resonant driving of the $1s^2$ – 2s2p two-electron transition in helium (see Fig. 1). More specifically, Fig. 1c reveals a regime of negative absorbance, i.e., gain, (shown in light blue) when driven with blue-detuned FEL pulses. Most interestingly this regime does not directly coincide with the observation of a near-resonantly driven transient population inversion within the 17 fs autoionization lifetime, shown in Fig. 1d (yellow/orange colors). These results demonstrate how different FEL pulse parameters can be utilized to reach exotic states of matter at ultrafast timescales.

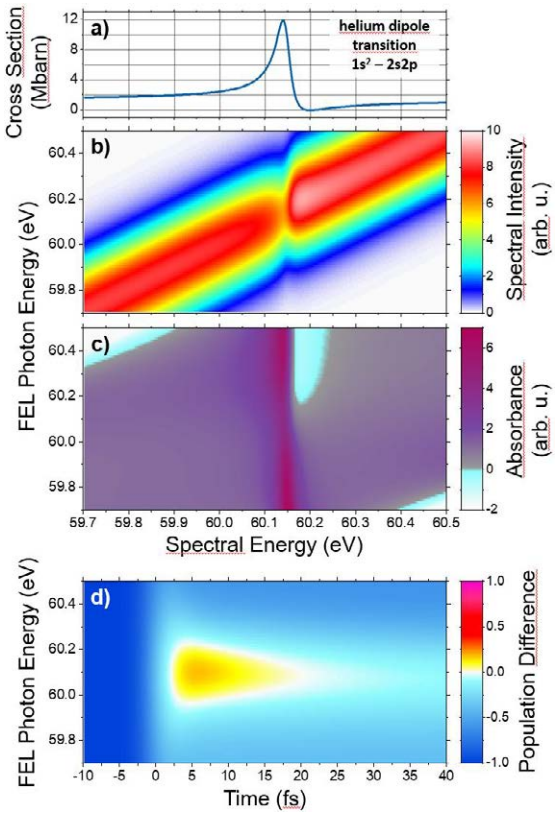

Figure 1. XUV optical response of helium driven by intense FEL pulses (5 fs FWHM, 10^{15} W/cm^2). a) weak-field photoabsorption cross section. b,c) transmitted spectral intensity (b) and absorbance (c) of intense XUV pulses transmitted through a cloud of helium atoms. d) transient population difference $N_{2s2p} - N_{1s2}$.

References

[1] Ott C *et al* 2019 *Phys. Rev. Lett.* **123** 163201
[2] Aufleger L *et al* 2020 *J. Phys. B* **53** 234002
[3] Magunia A *et al* 2020 *Appl. Sci.* **10** 6153

* E-mail: christian.ott@mpi-hd.mpg.de

Time-dependent optimized coupled-cluster method for laser-driven multielectron dynamics

H Pathak[1], T Sato[1,2,3]* and K L Ishikawa[1,2,3]†

[1]Department of Nuclear Engineering and Management, School of Engineering, The University of Tokyo, 7-3-1 Hongo, Bunkyo-ku, Tokyo 113-8656, Japan
[2]Photon Science Center, School of Engineering, The University of Tokyo, 7-3-1 Hongo, Bunkyo-ku, Tokyo 113-8656, Japan
[3]Research Institute for Photon Science and Laser Technology, The University of Tokyo, 7-3-1 Hongo, Bunkyo-ku, Tokyo 113-0033, Japan

Synopsis We report the development of an explicitly time-dependent coupled-cluster method considering optimized orthonormal orbitals within the flexibly chosen active space, called the time-dependent optimized coupled-cluster (TD-OCC) method, including double and triple excitation amplitudes (TD-OCCDT), and the most popular approximation to this method, TD-OCCD(T) for studying laser-driven dynamics. These methods are size extensive and gauge invariant, with a polynomial cost scaling. We employ these methods to Kr exposed to an intense laser field.

In recent years there has been sharp progress in strong-field physics and ultrafast science [1]. Accurate and affordable theoretical methods are needed for understanding and predicting strong-field and ultrafast phenomena. The multi-configuration time-dependent Hartree-Fock [2, 3] based on the full-configuration interaction within the time-dependent orbitals, and the time-dependent complete-active-space self-consistent-field (TD-CASSCF) [4] which introduces the flexible orbital subspacing, are the most reliable methods for systematically solving time-dependent Schrödinger equation. The computational cost of these methods scale factorially with the number of electrons.

Alternatively, the size-extensive and polymomial cost-scaling coupled-cluster method [5], which relies on the exponential wavefunction, is an appealing choice to address strong-field phenomena. We have developed an explicitly time-dependent coupled-cluster method considering optimized orthonormal orbitals within the flexibly chosen active space, called the time-dependent optimized coupled-cluster (TD-OCC) method, including double excitations (TD-OCCD) and double and triple excitations (TD-OCCDT) [6]. Recently, we also formulated the method called TD-OCCD(T), which approximately includes the effect of triple excitations as a time-dependent, orbital-optimized extension of the popular CCSD(T) in quantum chemistry. The computational cost of TD-OCCD(T) scales as $O(N^7)$ with N being the number of active orbitals, an order of magnitude lower than for the parent TD-OCCDT. As the first application of this method, we study electron dynamics in Kr subject to an intense near-infrared laser fields (Fig. 1).

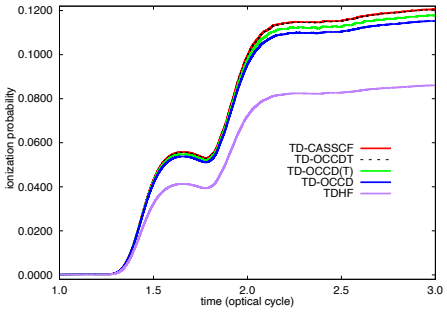

Figure 1. Time evolution of single ionization probability of Kr irradiated by a laser pulse with a wavelength of 800 nm and a peak intensity of 2×10^{14} W/cm^2 calculated with time-dependent Hartree-Fock (TDHF), TD-OCCD, TD-OCCD(T), TD-OCCDT and TD-CASSCF methods.

References

[1] Mauro N *et al* 2017 *Chem. Rev.* **117** 10760
[2] Kato T *et al* 2004 *Chem. Phys. Lett* **392** 533
[3] Caillat J *et al* 2005 *Phys. Rev. A* **71** 012712
[4] Sato T *et al* 2013 *Phys. Rev. A* **88** 023402
[5] Bartlett R J 1981 *Ann. Rev. Phys. Chem* **32** 359
[6] Sato T *et al* 2018 *J. Chem. Phys* **148** 051101

*E-mail: sato@atto.t.u-tokyo.ac.jp
†E-mail: ishiken@n.t.u-tokyo.ac.jp

Complete characterization of one-photon electron wave packets

J Peschel[1]*, D Busto[1], M Plach[1], M Bertolino[1], M Hoflund[1], S Maclot[1,2], H Wikmark[1], F Zapata[1], M Gisselbrecht[1], J M Dahlström[1], A L'Huillier[1], and P Eng-Johnsson[1]

[1]Department of Physics, Lund University, P.O. Box 118, 22100 Lund, Sweden,
[2]Physics Department, University of Gothenburg, Sweden

Synopsis Using angular-resolved attosecond interferometry, we show that we are able to characterize both amplitude and phase of different angular momenta partial waves resulting from the photoionization of the outer shell of neon atoms.

Ionization of atoms and molecules by absorption of broadband extreme ultraviolet radiation results in continuum electron wave packets. These wave packets are mathematically described by a complex wave function with an amplitude and phase. The determination of such wave functions has been a great challenge over the years, since direct measurements generally only give access to the modulus square of the amplitude. Any temporal dynamics involved in the process of photoionization, which requires the determination of the spectral amplitude and phase, remain hidden.

Recent developments in attosecond interferometry have opened up the possibility to reveal phase information via two-photon transitions. The second photon is essential to creating an interference between different pathways in order to probe the phase. It however adds complexity, which makes it difficult to disentangle the different angular momentum channels resulting from the ionization of electrons with non-zero angular momentum. We present a method that enables us to determine the one-photon scattering phases from the ionization of the $2p^6$-ground state of neon to s- and d-continuum states using angular-resolved reconstruction of attosecond beating by interference of two-photon transitions (RABBIT) [1]. Whereas a conventional RABBIT experiment measures the phase differences between photoelectrons ejected with different energies as an average of the angular momentum channels involved, we obtain the difference in phase between the angular momentum partial waves resulting from single photon ionization, as a function of the kinetic energy.

The method is based on a fitting algorithm applied to the photoelectron angular distribution, which makes use of the angular anisotropy involved in a multi-channel ionization process. Our approach extends the methods presented in previous work by Fuchs *et al.* in helium [2] as well as Joseph *et al.* in neon and argon [3]. We make use of Fano's propensity rule for continuum-continuum transitions [4], in order to reduce the number of unknown parameters in the fitting procedure. In combination with the scattering phases, we are able to retrieve the channel-resolved one-photon amplitudes from data taken without an infrared field present. Combining the amplitude and phase completely reconstructs the one-photon wave packet. The experimentally retrieved values are in good agreement with the prediction by angular-channel-resolved many-body perturbation theory simulations. While we present data acquired in neon, our approach is easily applicable to argon and in a modified version to larger atoms like xenon and krypton.

References

[1] Paul P M *et al.* 2001 *Science* **292** 1689
[2] Fuchs J *et al.* 2020 *Optica* **7** 154
[3] Joseph J *et al.* 2001 *J. Phys. B: At. Mol. Opt. Phys* **53** 184007
[4] Busto D *et al.* 2019 *Phys. Rev. Lett.* **123** 133201

*E-mail: jasper.peschel@fysik.lth.se

Optical excitation function of 4^1P_1 Zn state

M Piwiński[1] *and Ł Kłosowski[1]

[1]Institute of Physics, Faculty of Physics, Astronomy and Informatics, Nicolaus Copernicus University in Toruń, Grudziądzka 5, 87-100 Toruń, Poland

Synopsis The optical excitation function of 4^1P_1 zinc state excited by electron impact in the energy range 10 – 50 eV is presented. The experimental data are in very good agreement with previous theoretical convergent close-coupling (CC29) and B-spline R-matrix (BSR23) results.

The emission cross-section (ECS) for the 4^1P_1 state of zinc atoms has been measured. The experiment was conducted in a vacuum chamber with typical pressure of $3x10^{-7}$ mbar. The zinc atomic beam was produced by a resistively heated oven and collimated with a two-stage aperture system. The temperature of the oven reservoir was kept at 343^OC and the nozzle at 353^OC. Such conditions provided a number density of zinc atoms of the order of $10^{10}/cm^3$ in the interaction region.

The monochromatic electron beam was produced by an electron gun and monitored using a custom-made Faraday cup and precise multimeter. The sources of atomic and electron beams were used before in our coincidence experiments [1].

The zinc atoms were collided with electrons and excited from the ground to the 4^1P_1 state. The fluorescence photons (214 nm) were selected by a broadband filter and detected with a photomultiplier tube in the direction perpendicular to both electron and atomic beam. The experimental set-up was similar to the apparatus used in our previous optical excitation studies of calcium [2] and cadmium [3].

The obtained data are presented together with existing theoretical and experimental results (see Fig. 1). Present data are in very good agreement with theoretical convergent close-coupling (CC29) and B-spline R-matrix (BSR23) results. However, the explanation of significant discrepancies with other theoretical and experimental results require further research in a wider range of collision energies.

The present work is a continuation of our systematic studies on inelastic electron scattering on atoms with closed outer ns^2 shell (He [4], Ca [5], Cd [6, 7] and Zn [8, 9, 10]).

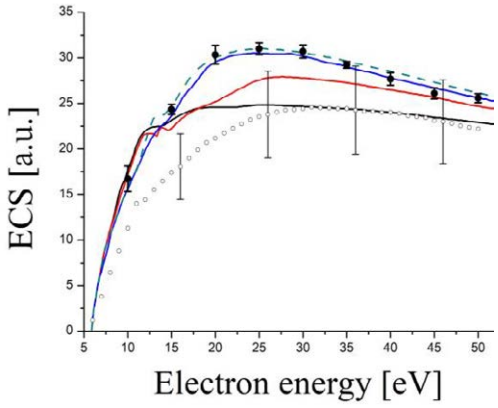

Figure 1. An optical excitation function (ECS) of 4^1P_1 Zn state. Experimental data: ● – present, ○ – Napier *et al*. Theoretical models: -- CC29, - BSR23, - BSR49, - CCC206, see explanation in Napier *et al* [11].

References

[1] Piwiński M. *et al.* 2013 *Eur. Phys. J. Special Topics* **222**, no. 9, 2273
[2] Dziczek. D. *et al.* 1998 *Acta Phys. Pol A* **93**, no. 5-6, 717
[3] Dziczek. D. *et al.* 2003 *Acta Phys. Pol A* **103**, no. 1, 3
[4] Kłosowski Ł. *et al.* 2009 *Phys. Rev. A* **80**, no. 6, 062709
[5] Dyl D. *et al.* 1999 *J. Phys. B: At. Mol. Opt. Phys.* **32**, no. 3, 837
[6] Piwiński M. *et al.* 2002 *J. Phys. B: At. Mol. Opt. Phys.* **35**, no. 18, 3821
[7] Piwiński M. *et al.* 2006 *J. Phys. B: At. Mol. Opt. Phys.* **39**, no. 8, 1945
[8] Piwiński M. *et al.* 2012 *Phys. Rev. A* **86**, no. 5, 052706
[9] Piwiński M. *et al.* 2015 *Phys. Rev. A* **91**, no. 6, 062704
[10] Piwiński M. *et al.* 2018 *J. Phys. B: At. Mol. Opt. Phys.* **51**, no. 8, 085002
[11] Napier S. A. *et al* 2009 *Phys. Rev. A* **79**, 042702

* E-mail: Mariusz.Piwinski@fizyka.umk.pl

Time, frequency, and angle-resolved quantum beats in the autoionizing nf' states of Argon

A Plunkett[1], M A Alarcón[2], J K Wood[3], C H Greene[2], and A Sandhu[1,3]*

[1]Department of Physics, University of Arizona, Tucson, AZ, 85721, USA
[2]Department of Physics, Purdue University, West Lafayette, IN, 47907, USA
[3]College of Optical Sciences, University of Arizona, Tucson, AZ, 85721, USA

Synopsis An electron wavepacket comprised of neutral autoionizing states between the two ionization thresholds of Argon is prepared using a femtosecond two-color excitation. A time-delayed infrared pulse ionizes the wavepacket leading to interferences in the continuum. In contrast to the conventional photoionization studies, we monitor this interference by resolving modulation of the autoionization process. This approach yields high resolution in both time and frequency, enabling us to extract the relative phases between the constituent states.

We prepare and study an electronic wavepacket comprised of autoionizing Rydberg states in Argon, situated between the spin-orbit split ground states of the Argon ion. The wavepacket is created using a two-color extreme ultraviolet (XUV) + near infrared (NIR) pulses that excite Argon atoms from their ground state to the $(^2P_{1/2})nf'$ manifold. The prime indicates that the Rydberg electrons are attached to an ion core in the spin-orbit excited $^2P_{1/2}$ state.

The nf' wavepacket evolves in time and decays via autoionization, leading to a free electron and an ion core in its ground state, $^2P_{3/2}$. We interrupt the natural autoionization process with a time-delayed infrared (IR) 1200nm, 60fs laser pulse, photoionizing the metastable nf' states. Both the autoionized and the photoionized electrons are collected in a Velocity Map Imaging spectrometer allowing their kinetic energy and angular distribution to be measured. The bandwidth of the IR pulse allows the continuum states to interfere, leading to quantum beats in the photoelectron spectrum as a function of time delay. This time-resolved photoionization approach limits the energy resolution to the bandwidth of the ionizing pulse[1, 2]. Instead, here we monitor the delay-dependence of the autoionization yield to obtain high resolution in both time and energy, allowing us to extract quantify the intricate details of wavepacket dynamics.

The IR pulse, in addition to photoionizing the wavepacket to continuum, also couples the autoionizing wavepacket back to itself through two-photon absorption-emission transitions. This interaction redistributes the amplitudes based on the quantum phases of the constituent states. Thus, we can selectively enhance or diminish the amplitudes of individual states in the wavepacket, controlling the autoionization yields of individual states. We obtain the time-dependent relative phase information with high energy resolution, limited only by the linewidth of autoionization. The experimental results agree extremely well with simulations that employ multi-channel quantum defect theory and perturbative analysis of the quantum interferences as function of time, energy, and angle.

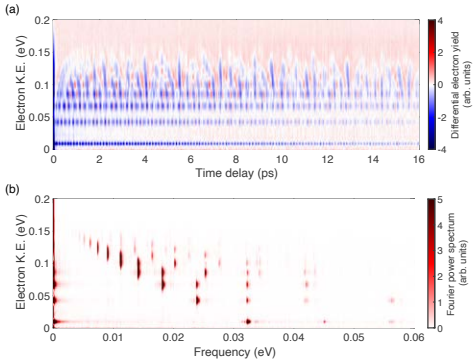

Figure 1. (a) Experimental differential electron spectrogram showing the modulation of autoionization yield due to the presence of a time-delayed IR pulse. (b) Fourier spectrogram of (a) showing beats that correspond to pairs of states with $\Delta n = 1, 2, 3...$

References

[1] Forbes R *et al* 2018 *Phys. Rev. A* **97** 063417
[2] Zamith S *et al* 2000 *Eur. Phys. J. D* **12** 255

*E-mail: asandhu@email.arizona.edu

Compton decay of positronium

Yu. V. Popov[1,2], **I.S. Stepantsov**[3], **I.P. Volobuev**[1]

[1] SINP, Lomonosov Moscow State University, Moscow, Russia
[2] BLTP, Joint Institute for Nuclear Research, Dubna, Russia
[3] Physics Faculty, Lomonosov Moscow State University, Moscow, Russia

Synopsis We study the Compton single ionization of positronium in comparison with the same of hydrogen [1]. The initial photon energy of a few keV allows one to apply the non-relativistic approach. Interesting differences in the behavior of various differential cross sections of the process are observed. In particular, the conditions were found, under which the electron and positron move parallel to each other with equal velocities. This suggests that the probability of annihilation is suppressed in this continuum state, and it is likely to be a long-lived one.

The recent experiments on Compton scattering using a new experimental technique [2] gave rise to a new wave of interest to this old effect discovered 100 yeas ago. To describe the process of Compton decay of positronium we use the so-called A^2 approximation with the vector potential

$$\frac{1}{c}\vec{A}(\vec{r},t) = \sqrt{\frac{2\pi}{\omega}}\,\vec{e}\,e^{i(\vec{k}\vec{r}-\omega t)} + \sqrt{\frac{2\pi}{\omega_1}}\,\vec{e}_1\,e^{-i(\vec{k}_1\vec{r}-\omega_1 t)} \tag{1}$$

Here $\vec{e}(\vec{e}_1)$ are linear polarizations of the initial (final) photons, $\vec{k}(\vec{k}_1)$ are their momenta, $(\vec{k}\cdot\vec{e}) = 0$, and the energy of the photon is $\omega = kc$, . After some simplifications due to the large value of ω, the full differential cross section (FDCS) of the process reads

$$FDCS = \frac{\alpha^4}{(2\pi)^3} p_1 \sum_{e,e_1} |M|^2, \tag{2}$$

where

$$\sum_{e,e_1}|M|^2 = 2^7\pi Z^5(1+\cos^2\theta)\left(\frac{2\pi\zeta}{\exp(2\pi\zeta)-1}\right)\times$$
$$\left|\frac{Q}{2}\left[(Q^2/4-(|\vec{p}_1-\vec{Q}/2|+iZ)^2\right]^{-1+i\zeta}\times\right.$$
$$\left[\frac{[Q/2-(|\vec{p}_1-\vec{Q}/2|+iZ)\cos\gamma]}{[(\vec{p}_1-\vec{Q})^2+Z^2]^{2+i\zeta}} + \right.$$
$$\left.\left.\frac{[Q/2+(|\vec{p}_1-\vec{Q}/2|+iZ)\cos\gamma]}{[p_1^2+Z^2]^{2+i\zeta}}\right]\right|^2, \tag{3}$$

with

$$\cos\gamma = \frac{(\vec{p}_1\cdot\vec{Q})-Q^2/2}{Q\sqrt{p_1^2-(\vec{p}_1\cdot\vec{Q})+Q^2/4}}.$$

Here $\vec{Q} = \vec{k}-\vec{k}_1$, $\quad Q \approx 2k\sin(\theta/2)$ is the momentum transfer, $\vec{p}_1$ is the electron momentum, θ is the photon scattering angle. In Eq. (3) $\zeta = -1/|2\vec{p}_1-\vec{Q}|$ is the positronium Coulomb number, $Z = 0.5$ is the effective charge.

Some results of the calculations are presented in Fig. 1. One clearly sees the resonances along the line $E_e = (\omega^2/2c^2)\sin^2(\theta/2)$. This condition appears, if $|\zeta| \to \infty$, which means that the electron and positron move parallel to each other with equal velocities. In this case there is a pole in FDCS (2). In such a continuum state the pair does not annihilate, and it can live until one particle radiates a low energy photon, after which the particles fall in a bound state and annihilate immediately. It is analogous to the transition of an atomic electron to an excited state, but it does not live long in this state. It is also interesting to investigate the possibility of stabilizing such a state.

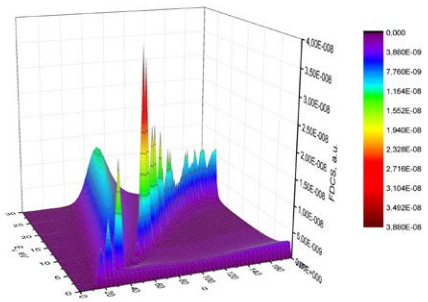

Figure 1. FDCS (atomic units) of Compton positronium decay versus the energy E_e(eV) of the emitted electron and the photon scattering angle θ. The photon energy is $\omega = 5$ keV

References

[1] S. Houamer*et al.* 2020 *EPJD* **74**, 81

[2] M.Kircher *et al.* 2020 *Nature Physics* **16(4)**, 756

[1]E-mail: popov@srd.sinp.msu.ru

Iterative Faddeev-like approach for the calculation of atomic bound state populations in laser-atom interactions

Yu. V. Popov[1,2], A. Galstyan[3], F. Mota-Furtado[4], P. F. O'Mahony[4], and B.Piraux [3]

[1] SINP, Lomonosov Moscow State University, Moscow, Russia
[2] BLTP, Joint Institute for Nuclear Research, Dubna, Russia
[3] Université catholique de Louvain, Institute of Condensed Matter and Nanosciences, Louvain-la-Neuve, Belgium
[4] Department of Mathematics, Royal Holloway, University of London, United Kingdom

Synopsis Earlier we considered iterative expansion of the ionization probability amplitude based on Faddeev 's decomposition [1]. This iterative series involves successively both the Coulomb, and the Volkov propagators. Here we calculate excitation probabilities of atomic hydrogen exposed to a laser pulse. The convergence of such a series strongly depends on the electric field frequency.

In Faddeev–like approach [1] , we write the full wave packet as $|\Psi(t)\rangle = |\Psi_1(t)\rangle + |\Psi_2(t)\rangle$ where $|\Psi_1(t)\rangle$ and $|\Psi_2(t)\rangle$ obey

$$(i\frac{\partial}{\partial t} - H_0 - V_c)|\Psi_1(t)\rangle = V_c|\Psi_2(t)\rangle,$$
$$(i\frac{\partial}{\partial t} - H_0 - V_d(t))|\Psi_2(t)\rangle = V_d(t)|\Psi_1(t)\rangle,$$

with the initial conditions $|\Psi_1(0)\rangle = |1s\rangle$, $|\Psi_2(0)\rangle = 0$. During the numerical calculations of these coupled equations we sum up previous n terms and normalise this total wave function to 1: $\langle\Psi^{(n)}|\Psi^{(n)}\rangle = 1$.

In these equations the dipole potential is

$$V_d = ib'(t)(\vec{e}\cdot\vec{\nabla}_r) + \zeta'(t),$$

with

$$b'(t) = \frac{1}{\omega}\sqrt{\frac{I}{I_0}}\sin^2(\pi\frac{t}{T})\sin(\omega t),$$

and

$$\zeta(t) = \frac{1}{2}\int_0^t d\xi\,\left[b'(\xi)\right]^2.$$

I is the pulse peak intensity, I_0 is the atomic unit of intensity and ω is the photon energy. The pulse vanishes for $t \le 0$ and $t \ge T$ where $T = 2\pi N/\omega$ is the total pulse duration, N being the total number of optical cycles within the pulse. V_c is the Coulomb potential.

Results of numerical calculations are presented in Fig.1 for $\omega = 0.1$ a.u. (≈ 460 nm) for ns states with $n = 2,...,6$. The convergence takes place after about 30 iterations, below we see quite chaotic behaviour. An analogous picture follows for np states. The higher frequency, the less number of iterations is needed. Unfortunately, we could not reach the convergence for the frequency $\omega = 0.057$ a.u. (≈ 800 nm). After about 35 iterations, the accumulation of round-off errors severely limits the accuracy of the calculations. But it is already clear even from Fig.1, that keeping only 2 or 3 terms is far from being enough to draw serious physical conclusions .

This approach can be readily extended to multi-electron atoms and in the first place, to helium. As for atomic hydrogen, system of coupled equations stay valid with the Coulomb potential replaced by the full binding potential of the atom. In this context, it is more convenient to use the hyperspherical coordinates since the stationary Schrödinger equation for the atom has the same structure as the corresponding equation for atomic hydrogen except that the nuclear charge in the expression of the Coulomb potential is replaced by an angle dependent effective charge.

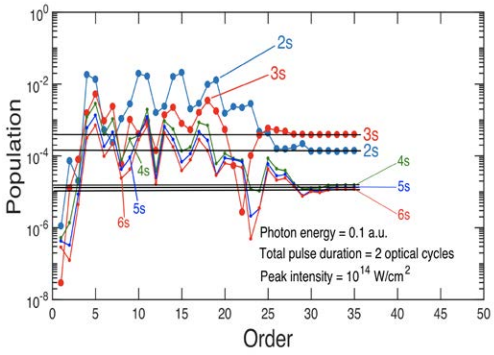

Figure 1. Population of ns states of atomic hydrogen versus orders of the Faddeev–like series. Photon energy is 0.1 a.u., $N = 2$, $I = 10^{14}$ W/cm^2. Straight lines are the exact (numerical) solutions of the corresponding Schrödinger equation.

References

[1] A. Galstyan *et al.* 2017 *EPJD* **71(4)**, 93

[1]E-mail: popov@srd.sinp.msu.ru

Compton ionization of atoms as a new method of dynamical spectroscopy

Yu. V. Popov[1,2], O. Chuluunbaatar[2], S. Houamer[3], I.P. Volobuev[1]

[1] SINP, Lomonosov Moscow State University, Moscow, Russia
[2] BLTP, Joint Institute for Nuclear Research, Dubna, Russia
[3] Faculty of Science, University Setif-1, Setif, Algeria

Synopsis We study the Compton single ionization of atoms as a method of dynamical spectroscopy in comparison with the famous (e,2e) electron momentum spectroscopy.

In a recent paper [1], a possibility to measure the full differential cross section (FDCS) of the reaction of single Compton ionization of a helium atom without detecting the scattered photon has been demonstrated. A comparison of the experimental data with the theory based on the nonrelativistic A^2 model has shown a good applicability of this model to the case of low (of the order of several keV) photon energies. Here we discuss the possibility of using such reactions for studying the momentum profile of the active electron in the target atoms.

We use a very simple vector potential

$$\frac{1}{c}\vec{A}(\vec{r},t) = \sqrt{\frac{2\pi}{\omega_1}}\,\vec{e}_1\, e^{i(\vec{k}_1\vec{r}-\omega t)} + \sqrt{\frac{2\pi}{\omega_2}}\,\vec{e}_2\, e^{-i(\vec{k}_2\vec{r}-\omega_1 t)} + (c.c.) \qquad (1)$$

Here $\vec{e}_1(\vec{e}_2)$ are linear polarizations of the initial (final) photons, $\vec{k}_1(\vec{k}_2)$ are their momenta, $(\vec{k}_j\cdot\vec{e}_j)=0$, and the energy of a photon is $\omega = kc$.

The full differential cross section (FDCS) of the process reads

$$\frac{d^3\sigma}{dE_e d\Omega_e d\Omega_1} = \frac{\alpha^4}{(2\pi)^3}\, p\, \left(1-\frac{E_e+I_p}{\omega_1}\right) \times (1+\cos^2\theta)|T_1+T_2-2T_3|^2, \qquad (2)$$

where

$$T_1(\vec{p},\vec{Q}) = \langle\tilde{\Phi}^-(\vec{p})|e^{i\vec{Q}\cdot\vec{r}_1}|\Phi_0\rangle;$$

$$T_2(\vec{p},\vec{Q}) = \langle\tilde{\Phi}^-(\vec{p})|e^{i\vec{Q}\cdot\vec{r}_2}|\Phi_0\rangle;$$

$$T_3(\vec{p},\vec{Q}) = \langle\Phi_0|e^{i\vec{Q}\cdot\vec{r}}|\Phi_0\rangle\langle\tilde{\Phi}^-(\vec{p})|\Phi_0\rangle. \qquad (3)$$

Here $\vec{Q}=\vec{k}-\vec{k}_1$, $\quad Q\approx 2k\sin(\theta/2)$ is the momentum transfer, $\vec{p}$ is the electron momentum, θ is the photon scattering angle.

Only the amplitude T_1 carries the information about the momentum profile like in the process (e,2e). Both other terms distort this information. We can reduce the influence of these terms collecting the experimental results not for all photon scattering angles, but only for the angles larger than an angle θ_0.

[1]E-mail: popov@srd.sinp.msu.ru

Such calculations for the single differential cross section $SDCS = d\sigma/dE_e$ are presented in Fig.1 for various angles θ_0. For the estimates, we use the simplest Hilleraas model of the wave function of helium atom

$$\Phi_0(\mathbf{r_1},\mathbf{r_2}) = \phi(r_1)\phi(r_2), \quad \phi(r) = \sqrt{\frac{Z^3}{\pi}}e^{-Zr}$$

with $Z = 27/16$. The final state is the Coulomb wave with $Z = 1$.

Thus, the large angles (backscattering) allow one to get a reliable momentum profile of the active electron even for relatively small electron energies.

The advantages of the Compton ionization as a method of dynamical spectroscopy over (e,2e) electron momentum spectroscopy (EMS) are also discussed in the report.

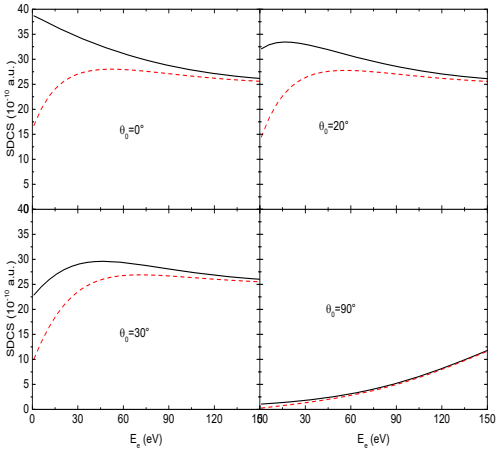

Figure 1. SDCS (atomic units) as a function of the emitted electron energy E_e. The photon energy is $\omega = 10$ keV. The cutoff angles θ_0 are shown in the figures. The solid curve is the result of the calculation with only T_1, the dashed curve is the sum of all terms in Eq. (2)

References

[1] M.Kircher *et al.* 2020 *Nature Physics* **16(4)**, 756

Theoretical and experimental studies of the Te atom

L Radžiūtė[1]*, G Gaigalas[1] and J Kwela[2]

[1]Institute of Theoretical Physics and Astronomy, Vilnius University, Vilnius, 10257, Lithuania
[2]Institute of Experimental Physics, University of Gdansk, Gdansk, 80-952, Poland

Synopsis Multiconfiguration Dirac-Hartree-Fock (MCDHF) and relativistic configuration-interaction methods (RCI) were used in the present work to calculate atomic properties like: energy levels, transition rates and hyperfine structure constants of Te atom. Methods are implemented in the general-purpose relativistic atomic structure package GRASP2018. Theoretical and experimental results were compared with the NIST database.

Atomic state functions and atomic properties of Te I ground state $[\mathrm{Kr}]4d^{10}5s^25p^4$ in search M1-E2 interference in the Zeeman effect were computed using active space method. Active space was increased by four layers of virtual orbitals in our computation scheme. Orbital symmetry was restricted up to h. Active space was generated by single and double substitutions from $5s$ and $5p$ orbitals (RCI^a). Single and restricted double substitutions were done from $4s$, $4p$, and $4d$ core shells in to the virtual orbitals (RCI^b), to include core-core and core-valence electron correlations. The Breit interaction and quantum electrodynamics corrections (QED) were included at RCI computations in both schemes. Obtained energy values of states of the ground configuration of Te I are compared with NIST [1] data in Table 1.

Table 1. Energy values (in cm $^{-1}$) of Te I compared with NIST database.

^ML_J	RCI^a	RCI^b	NIST [1]
$^3P_2$	0	0	0
$^3P_1$	4521	4837	4750.712
$^3P_0$	4678	5004	4706.495
$^1D_2$	10724	11221	10557.877
$^1S_0$	23402	24641	23198.392

The M1 and E2 type rates are compared with semi-empirical data [2]. Semi-empirical calculations done in intermediate coupling with HFR basis functions in the framework of the Slater-Condon theory. Expansion for configuration was: $5s^25p^4 + 5s5p^45d + 5s^25p^2\{5d^2, 5f^2\} + 5p^45d^2 + 5s^25p^3\{4f, 5f\} + 5p^5\{4f, 5f\} + 5p^6$. Forbidden transition probabilities are compared with our computed in Figure 1. Only those lines for which interference is possible were selected for comparison. Our computed E2 type transitions rates are given in Coulomb gauge. Fig. 1 shows good agreement between our results and semi-empirical data from [2].

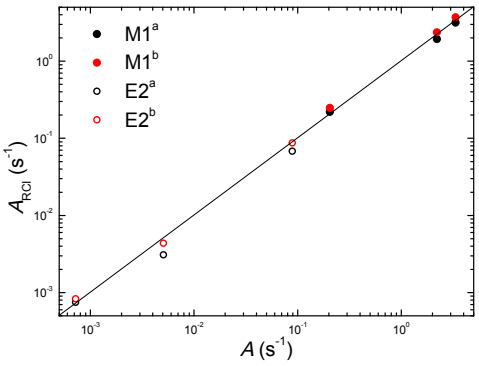

Figure 1. M1 and E2 type transition rates compared with semi-empirical data [2].

Experimental data ant other atomic properties will be provided during the conference.

Acknowledgment: This project has received funding from European Social Fund (project No 09.3.3-LMT-K-712-19-0080) under grant agreement with the Research Council of Lithuania (LMTLT).

References

[1] Kramida A E *et al* NIST Atomic Spectra Database (ver. 5.8), [Online]. Available: [2021, March 9]. National Institute of Standards and Technology, Gaithersburg, MD.
[2] Biémont E *et al* 1995 *Astronomy and Astrophysics Supplement series* **111** 333-346

*E-mail: laima.radziute@tfai.vu.lt

Multi-color pump-probe experiments at the European XFEL

D. E. Rivas[1 *], S. Serkez[1], T. M. Baumann[1], R. Boll[1], W. Decking[2], S. Dold[1], A. de Fanis[1], L. Fröhlich[2], N. Gerasimova[1], J. Grünert[1], M. Guetg[2], P. Grychtol[1], M. Huttula[4], M. Ilchen[1], F. Jastrow[2], S. Karabekyan[2], A. Koch[1], V. Kocharyan[2], Y. Kot[2], E. Kukk[5], J. Laksman[1], T. Maltezopoulos[1], T. Mazza[1], M. Planas[1], E. Saldin[2], P. Schmidt[1], E. Schneidmiller[2], M. Scholz[2], S. Tomin[2], S. Usenko[1], M. Vannoni[1], M. Veremchuk[3], M. Yurkov[2], I. Zagorodnov[2], G. Geloni[1], and M. Meyer[1]

[1]European XFEL, Schenefeld, 22869, Germany
[2]Deutsches Elektronen-Synchrotron, Hamburg, 22607, Germany
[3]Kyiv National University, Kyiv, 01033, Ukraine
[4]University of Oulu, Oulu, 90014, Finland
[5]University of Turku, Turku, 20500, Finland

Synopsis We present first results on multi-color pump-probe experiments at the European XFEL. We deliver ultrashort X-ray pulses at two wavelengths with controllable relative delays and combine them with a synchronized, intense optical laser. As a proof-of-principle demonstration we perform laser-dressed photoelectron spectroscopy in atoms and molecules, and show characterization and control of the spectral and temporal properties of the FEL pulses under different modes of operation.

Pump-probe spectroscopy with two-color soft X-ray FEL pulses allows the investigation of site-selective charge transfer dynamics [1] or performing nonlinear spectroscopy involving inner-shells [2]. Using an additional optical laser enables additional control of valence electronic states during the inner-shell soft X-ray nonlinear interaction or novel phase-sensitive applications through state-mixing [3]. Here we will present first results on the new multi-color pump-probe capabilities at the soft X-ray branch of the European XFEL.

The SASE3 soft X-ray undulator currently generates broadly tunable, mJ-level FEL pulses in the 500-3000 eV spectral region. Recently, it was upgraded with a magnetic chicane at the center of the undulator which provides up to picosecond delays for the electron bunch and can deliver two mJ-level pulses of different wavelengths and controllable relative delay [4].

As a first demonstration we deliver these pulses to the SQS instrument and combine them with an intense optical laser. Figure 1 shows a resulting neon photoelectron spectrum as a function of optical laser delay, demonstrating the possibility of a combined time-resolved measurement involving inner- and valence-states through the use of two-color, monochromatic FEL pulses and an optical laser.

First results of multi-color experiments in Ne, N_2 and CH_3F will be presented. The results highlight the new capability of manipulating the spectro-temporal properties of the fields, and enable novel possibilities for investigating dynamics in gas-phase atoms and molecules.

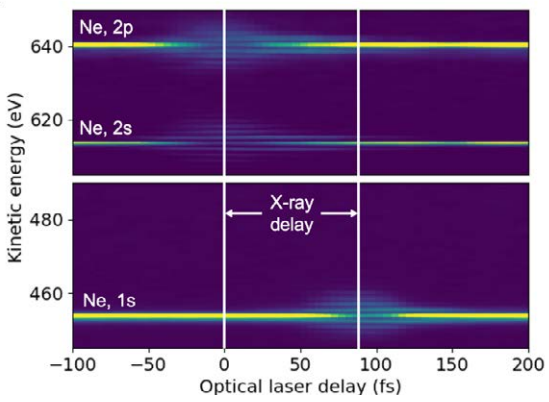

Figure 1. Laser-dressed, neon photoelectron spectrum of a two-color x-ray pulse as a function of optical laser delay. The "sidebands" dressing effects show that the ultrashort, monochromatic FEL pulses of 660 and 1320 eV, addressing the Ne 2s,2p and 1s states, respectively, are delayed by 90 fs.

References

[1] Picón A *et al* 2018 *Phys. Rev. A* **98** 043433
[2] Eichman U *et al* 2020 *Science* **369** 6511
[3] Maroju P K *et al* 2020 *Nature* **578** 386
[4] Serkez S *et al* 2020 *Appl. Sci.* **10** 2728

* E-mail: daniel.rivas@xfel.eu

RABBITT spectrograms using the semi-relativistic R-matrix with time-dependence approach

L. Roantree*, J. Wragg, C. P. Ballance, A. C. Brown†, and H. W. van der Hart.

School of Mathematics and Physics, Queen's University of Belfast, Belfast, Northern Ireland

Synopsis We demonstrate the modelling of the "Reconstruction of Attosecond Beating By Interference of Two-photon Transitions" (RABBITT) technique within R-Matrix with Time-dependence (RMT) theory. As a demonstration, we extract phase information induced by the [Ne]$3s3p^6 4p\ ^1P$ resonance.

Attosecond spectroscopy has enabled experiments to investigate how Fano resonance profiles build up over time. Experimental techniques, underpinned by theory, have recently been developed in order to characterise phase relations within these profiles, for example the RABBITT approach [1, 2]. Through these, the phases of the associated ionization processes are shown to be of critical importance in the final resonance profile of an atomic state.

To obtain accurate ionisation phases in multielectron systems, a good description of the atomic physics is essential. The R-Matrix with Time-dependence (RMT) code suite has been designed specifically to describe the influence of atomic structure on ultrafast-atomic dynamics. Recently, the code has been extended to enable the inclusion of spin-orbit interactions using the Breit-Pauli approximation [3].

In this contribution, we investigate the potential of the RMT codes for the numerical study of rainbow RABBITT, in which phase changes induced by an atomic resonance are traced as a function of energy across a RABBITT sideband [4, 5, 6]. Ar atoms are irradiated by an attosecond extreme ultra-violet (XUV) pulse train with a central frequency given by the 17th harmonic of a fundamental IR field with wavelength around 780 nm, combined with the weak, fundamental IR pulse. This XUV pulse train is scanned across the $3s3p^6 4p$ resonance.

For our initial numerical results, we focus on the lower sideband 'SB16', corresponding to either absorption of a 15ω photon and an ω photon, or absorption of a 17ω, photon and emission of an ω photon, where ω is the energy of the fundamental IR field.

Figure 1 shows the RABBITT spectrogram focused around SB16. The spectrogram shows the change in the photoelectron energy distribution across this sideband as a function of time delay between the XUV pulse train and IR field [2]. The figure shows an imprint of the resonance through a notable asymmetry within sideband SB16.

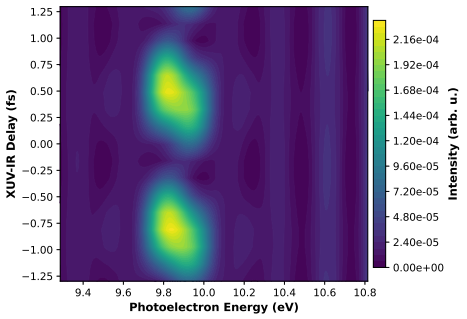

Figure 1. A RABBITT spectrogram showing variation in photoelectron yield of the sideband below the $3s3p^6 4p$ resonance in argon as a function of time delay between an on-resonance attosecond pulse train and an IR field.

References

[1] Véniard V, Taïeb R, and Maquet A, *Phys. Rev. A* **54** 721
[2] Muller H 2002 *Appl. Phys. B* **74** s17–s21
[3] Brown A C *et al* 2020 *Comput. Phys. Commun.* **250** 107062
[4] Kotur M *et al* 2016, *Nat. Commun.* **7** 10566
[5] Gruson V *et al* 2015, *Science 354* 734
[6] Turconi M *et al* 2020 *J. Phys. B: At. Mol. Opt. Phys.* **53** 184003

*E-mail: lroantree01@qub.ac.uk
†E-mail: andrew.brown@qub.ac.uk

Non-linear multiphoton ionisation dynamics of xenon upon irradiation by highly intense soft X-ray free-electron laser pulses

A Rörig[1,2]*, T M Baumann[1], B Erk[3], M Ilchen[1], J Laksman[1], T Mazza[1], M Meyer[1], V Musić[1], S Pathak[4], D E Rivas[1], D Rolles[4], R Santra[2,5,6], J M Schäfer[5], S Serkez[1], P Schmidt[1], S Usenko[1], S-K Son[5,6] and R Boll[1]†

[1]European XFEL, Holzkoppel 4, 22869 Schenefeld,
[2]Department of Physics, Universität Hamburg, 22761 Hamburg, Germany
[3]Deutsches Elektronen-Synchrotron (DESY), Notkestraße 85, 22607 Hamburg, Germany
[4]J. R. Macdonald Laboratory, Department of Physics, Kansas State University, Manhattan, KS 66506, USA
[5]Center for Free-Electron Laser Science (CFEL), Notkestraße 85, 22607 Hamburg, Germany
[6]The Hamburg Centre for Ultrafast Imaging, Luruper Chaussee 149, 22761 Hamburg, Germany

Synopsis Results on photon-energy-dependent multiphoton ionisation of xenon using intense soft X-ray FEL pulses at the SQS instrument at the European XFEL will be presented. Ion yields for charge states up to Xe^{41+} were recorded over a wide photon-energy range (700-1800 eV) in small steps while maintaining high pulse energy (several mJ). Thereby, we observed distinct ion-yield variations in the charge-state distributions as a function of the photon energy due to inner-atomic resonances.

The development of X-ray free-electron lasers in the last decade has enabled the detailed investigation of multiphoton processes in atoms and molecules in the hard and soft X-ray regime. Very high charge states are mainly produced via a sequence of single-photon absorptions and subsequent decay processes. The underlying dynamics critically depends on the pulse energy, photon energy [1][2][3][4] and other pulse parameters. Additionally, in multiply charged heavy atoms, resonant excitation of inner-shell electrons into unoccupied valence orbitals or densely spaced Rydberg states can enhance the photoionisation yield in the soft X-ray regime, called REXMI (resonance-enabled X-ray multiple ionisation) pathways [5].

At the SQS instrument, ion time-of-flight spectrometry was utilised to determine the charge-state distributions as a function of photon energy. The variable-gap undulators of SASE3 at the European XFEL facilitate scanning the photon energy. To provide a constant number of photons on the target, a gas attenuator was used to compensate for the increased pulse energy with decreasing photon energy.

Fig. 1 shows the variation of the charge-state distribution of atomic xenon as a function of photon energy. Besides a general trend to increase the highest charge state produced with increasing photon energy, structured distributions are clearly visible that can be related to transient resonances, such as 3d → 4f or 3p → 4d. The experimental results are in good qualitative agreement with quantitative calculations using the XATOM toolkit [6].

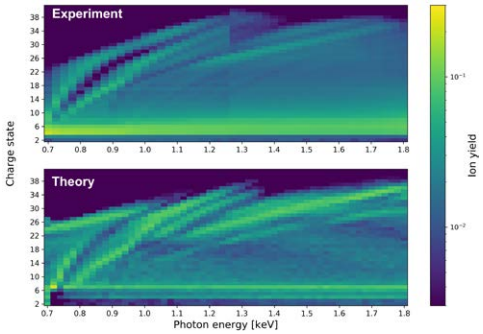

Figure 1. Experimental data and calculations using XATOM: charge-state distribution as a function of photon energy.

References

[1] Young L *et al* 2010 *Nature* **466** 56-61
[2] Rudek B *et al* 2012 *Nat. Photon.* **6** 858-865
[3] Fukuzawa H *et al* 2013 *Phys. Rev. Lett.* **110** 173005
[4] Son S-K *et al* 2020 *Phys. Rev. Research* **2** 023053
[5] Rudek B *et al* 2018 *Nat. Commun.* **9** 4200
[6] Jurek Z *et al* 2016 *J. Appl. Cryst.* **49** 1048-1056

*E-mail: aljoscha.roerig@xfel.eu
†E-mail: rebecca.boll@xfel.eu

Atomic Few-Photon Ionization out of an Optical Dipole Trap

K. Romans[1] *, B. Acharya[1], A. Dorn[2], and D. Fischer[1] †

[1]Missouri University of Science and Technology, Rolla, MO 65401, USA
[2]Max-Planck Institute for Nuclear Physics, 69117 Heidelberg, Germany

Synopsis We observe the effect of introducing an optical dipole trap laser to the ionization of a ground state atomic target initially exposed to a femtosecond laser pulse. New pathways to the continuum are seen in electron and recoil ion momentum spectra and can be "controlled" by adjusting the relative intensity of the two fields and central wavelength of the fs-pulse. Different central wavelengths that utilize resonance enhancement are used to study the degree of control over the ionization channels.

In the last decade, several types of laser atom traps have been used to provide a target for the study of atomic collisions and fragmentation dynamics. These traps stand out over conventional gas targets because they enable a tremendous level of control of the target state. Amongst other things, it can provide a very high level of spatial control of the target atoms [1], it is possible to excite and polarize the electronic state of the target [2], the gas cloud can be cooled down to ultra-low temperatures even reaching quantum degeneracy [3], and molecular targets can be formed, for instance by means of photo-association [4].

In the present study, we explore how an infrared optical dipole trap (ODT) laser affects the ionization dynamics of atoms subjected to a femtosecond laser pulse. We begin with a lithium-6 target held in an all-optical trap (AOT) [2]. A switching scheme is implemented that allows the lithium atoms to drop into the 2s ground. The atoms are then ionized by the absorption of a few photons in the field of a femtosecond laser pulse with a central wavelength of 735 nm. Electron and recoil ion momentum vectors are then measured using the COLTRIMS (cold target recoil ion momentum spectroscopy) technique. These measurements are then repeated with a 1070 nm continuous wave ODT laser superposed over the fs field and target.

Measured electron momentum spectra are shown in Figure 1. The fs laser field is polarized linearly along the y-axis and propogates along the z-axis (which is also the target's quantization axis). The ODT field is linearly polarized in the xy-plane at roughly 45 degrees with respect to the y-axis and propagates in the same plane an additional 90 degrees.

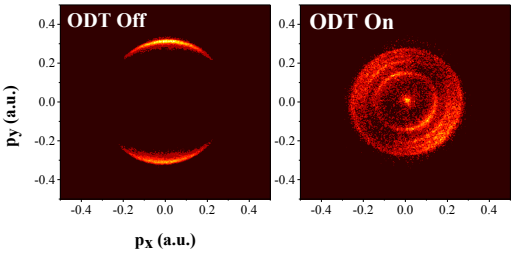

Figure 1. Electron momentum in the xy-plane for the fs-pulse with the ODT laser off (left) and on (right).

At low fs laser intensities, a large fraction of the observed ionization events are caused by the interaction with the ODT field. The additional photons, along with the reduced fs field, create new pathways to the continuum and significantly increase the rate. Controlling these pathways is the subject of current inquiry as the relative intensity of the two fields and central wavelength of the fs field produces fascinating spectra that will be discussed in this contribution in detail.

This work was supported by the NSF under grant PHY-1554776

References

[1] Santra B and Ott H 2015 *J. Phys. B: At. Mol. Opt. Phys.* **48** 122001
[2] de Silva AHN *et al.* 2021 *Phys. Rev. Lett.* **126** 023201
[3] Wessels P *et al.* 2018 *Comm. Phys.* **1** 32
[4] Niels Kurz 2021 Dissertation, University of Heidelberg

* E-mail: klrnyc@mst.edu
† E-mail: fischerda@mst.edu

Angular anisotropy parameters for photoionization delays

S Saha*, J Vinbladh, J Sörngård, A Ljungdahl and E Lindroth†

Department of Physics, Stockholm University, AlbaNova University Center, SE-106 91 Stockholm, Sweden

Synopsis Anisotropy parameters describing the angular dependence of the photoionization delay are defined. The parametrization has a form very similar to that traditionally used for cross sections, but the new β-parameters are complex. Results for the measurable *atomic delay* will be presented.

The photoelectron angular distribution is conveniently described with angular anisotropy parameters [1]. For linearly polarized light and within the dipole approximation:

$$\frac{d\sigma}{d\Omega} = \frac{\sigma_{int}}{4\pi}\left(1 + \sum_{n=1}^{N} \beta_{2n} P_{2n}\left(\cos\theta\right)\right) \qquad (1)$$

where P are Legendre polynomials and θ is the detection angle relative to the polarization axis. N is the number of exchanged photons and σ_{int} is the cross section integrated over all angles.

Attosecond techniques such the *Reconstruction of Attosecond Beating by Interference of Two-photon Transitions* are based on interference of electron wavepackets that are released by an XUV pulse train and then modified by absorption or emission of an IR photon. This creates spectral *sidebands* that oscillate with the delay between the light fields, and which carry information on the phase of the electron wave packet. The spectral derivative of this phase can be interpreted as a delay. Rather recently angle-resolved experiments [2, 3] have highlighted that not only cross sections (amplitudes), but also delays (phases) depend on angle.

Here we define anisotropy parameters, describing the angular dependence of the measurable two-photon *atomic delay*, τ_A. The parametrization is similar to that in Eq. (1):

$$\tau_A\left(\theta\right) = \tau_A^{int} + \frac{1}{2\omega}\arg\left(1 + \sum_{n=1}^{2} \tilde{\beta}_{2n} P_{2n}\left(\cos\theta\right)\right)$$

where τ_A^{int} is the angular integrated atomic delay and ω is the laser frequency. The new $\tilde{\beta}$-parameters, are closely related to the ordinary parameters in Eq. (1), but they are complex. Also the the underlying one-photon *Wigner delay*, τ_W, can be similarly parametrized.

Angular dependent delays for ionization from the outermost s-shell in rare gases will be presented. The s-shell Wigner delay is isotropic in a non-relativistic framework, but the presence of two channels, $s \rightarrow p_{1/2}, p_{3/2}$, relativistically allow for an angular dependence. The atomic delay, being due to a two-photon process will, on the other hand, always allow for an angular dependence. Results for xenon are shown in Fig. 1.

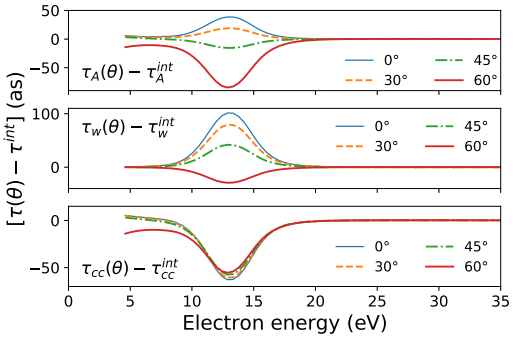

Figure 1. Ionization from Xe($5s$). The top panel shows $\tau\left(\theta\right) - \tau^{int}$ for the measurable *atomic delay*. The middle panel displays it for the underlying *Wigner delay*. Here the angular dependence is of purely relativistic origin, and significant only around the so-called Cooper minimum. The bottom figure shows the *difference* between the *atomic delay* and the *Wigner delay* (labelled *cc-delay*). It is clear that for low electron energies the angular dependence is mainly a two-photon effect, while the Cooper minimum region is dominated by the one-photon contribution.

References

[1] Cooper J & Zare RN 1968, *J.Chem.Phys.* **48** 942
[2] Heuser S *et al* 2016 *Phys. Rev. A* **94** 063409
[3] Cirelli C *et al* 2018 *Nat. Commun.* **9** 955

*E-mail: soumyajit.saha@fysik.su.se
†E-mail: Eva.Lindroth@fysik.su.se

Hundred years ago: Alfred Landé's half-integer quantum numbers and g-factor 2

H. Schmidt-Böcking[1]*, G. Gruber[1], W. Trageser[1] and H. J. Lüdde[2]

[1] Institut für Kernphysik, Universität Frankfurt, Max-von-Laue-Str. 1, 60438 Frankfurt, Germany
[2] Theoretische Physik, Universität Frankfurt, Max-von-Laue-Str. 1, 60438 Frankfurt, Germany

Synopsis A description of the historic path of the discoveries by Alfred Landé.

Alfred Landé is one of the great pioneers of modern quantum physics. His name can be found in every textbook on the fundamentals of quantum physics. In 1921 at the Frankfurt University, with his work [1, 2] on the normal and anomalous Zeeman effect (NZE and AZE)) he empirically discovered fundamentally important properties of the coupling of the inner-atomic magnetic moments and thus on the angular momentum in atoms. Hundred years ago the multiplet structure of the AZE was the greatest mystery of atomic physics and all attempts of physicists such as Bohr, Sommerfeld, Einstein, Planck and others were in vain. Asym Barut and Alwyn van der Mere honored Alfred Landé in [3] as the discoverer of the so-called g-factor. Landé was able to predict the multiplet structure in the photon emission of atoms both for the NZE and for the AZE.

From the analysis of the series of the different multiplet structures Landé empirically derived a working hypothesis of the existence of half-integer quantum numbers. From the energy shifts of the spectral lines Landé then deduced also that the classical Larmor precision with g-factor one was unable to explain the AZE and he introduced a g-factor > 1, accounting for expected deviations from classical physics. For an angular momentum of $k = 1/2$ Landé found that the g-factor was 2. We will describe in our contribution the historic path of Landé's discovery.

Based on this findings Landé was the first to explain in 1923 the results of the Stern Gerlach experimental in the correct quantum mechanical scheme [4].

References

[1] Landé A 1921 *Z.Phys.* **5** 231–241
[2] Landé A 1921 *Z.Phys.* **5** 398–405
[3] Barut A O and van der Mere A 1988 *D. Reidel Publishing Company, ISBN 90-277- 2594-2* 557
[4] Landé A 1923 *Z.Phys.* **24** 441–444

*E-mail: schmidtb@atom.uni-frankfurt.de

Attosecond-resolved multi-photon multiple ionization dynamics

M Kretschmar[1] J Tümmler[1] I Will[1] T Nagy[1] M J J Vrakking[1] and B Schütte[1]*

[1]Max-Born-Institut, 10247 Berlin, Germany

Synopsis We demonstrate attosecond control over the multi-photon multiple ionization dynamics of argon using an intense attosecond source based on high-harmonic generation. We find that the Ar^{2+} ion yield is only weakly modulated in an XUV-XUV autocorrelation measurement, which is attributed to the sequential absorption of two photons required to generate Ar^{2+}. In contrast, the Ar^{3+} autocorrelation trace shows strong oscillations, which is a signature of the direct absorption of at least two XUV photons.

XUV pulses have until recently either not been short enough or sufficiently intense to study multi-photon multi-electron dynamics with attosecond time resolution. This is currently changing, both due to the generation of attosecond pulses at free-electron lasers [1] and because XUV intensity scaling of high-harmonic generation (HHG) sources has enabled highly nonlinear ionization of atoms, leading to the observation of charge states up to Ar^{5+} [2]. This was the result of the absorption of at least 10 XUV photons induced by a very short attosecond pulse train [3].

Here we demonstrate attosecond control over the multi-photon multiple ionization of Ar atoms, studying both Ar^{2+} and Ar^{3+} ions. Our previous results indicated that two photons are required for the generation of Ar^{2+} [2], which may be absorbed either sequentially or via direct two-photon double ionization (TPDI). In this process, two photons simultaneously interact with two electrons, and electron-electron correlation plays an important role. The generation of Ar^{3+} was found to be a four-photon absorption process [2], potentially involving many different pathways and making any prediction very difficult. A split-and-delay unit was used to generate two replicas of an intense attosecond pulse train covering a photon energy range from 16 to 32 eV, with an intensity of 10^{14} W/cm^2 each. The corresponding autocorrelation measurement for Ar^{2+} is depicted in Fig. 1(a) and shows weak modulations, whereas the autocorrelation measurement for Ar^{3+} shown in Fig. 1(b) exhibits strong oscillations with a period of about 1.3 fs (corresponding to half the oscillation period of the fundamental laser). The weak modulation in the Ar^{2+} scan shows that, while direct two-photon absorption plays a role, the more dominant pathway is sequential ionization. In contrast, the strong modulation in the Ar^{3+} trace demonstrates that direct absorption of at least two XUV photons is important, since only this can explain the dependence of the Ar^{3+} ion yield on the XUV peak intensity that changes as a function of the XUV-XUV time delay.

*E-mail: Bernd.Schuette@mbi-berlin.de

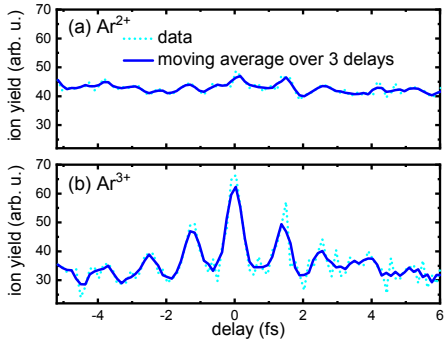

Figure 1. Attosecond-resolved XUV autocorrelation measurement in Ar. (a) While the Ar^{2+} ion yield is weakly modulated as a function of the XUV-XUV time delay, (b) the Ar^{3+} exhibits strong oscillations with a period of 1.3 fs.

Our results provide novel opportunities for the investigation of multi-electron dynamics and electron-electron correlation on attosecond timescales. An important advantage of these experiments is the negligible influence of strong-field effects, which are often present in state-of-the-art attosecond experiments that use a combination of one XUV and one near-infrared pulse.

References

[1] Duris J *et al* 2020 *Nat Photon* **14** 30
[2] Senfftleben B *et al* 2020 *J Phys Photonics* **2** 034001
[3] Major B *et al* 2020 *J Phys Photonics* **2** 034002

Above threshold ionization of Argon with ultrashort orbital angular momentum beams

A Sen[1] *, A Sinha[2] , R Gopal[3] and V Sharma[2]

[1]Indian Institute of Science Education and Research, Pune
[2]Indian Institute of Technology, Hyderabad
[3]Tata Institute of Fundamental Research, Hyderabad

Synopsis The photoionization of Argon in the multiphoton to above-threshold ionization regime with moderately intense ultrashort laser pulses endowed with orbital angular momentum has been studied. The spectra are compared with those obtained from Gaussian laser beams.

In a moderately intense (10^{12}-10^{15} W/cm^2) ultrashort (~25 fs) laser field an atom can be ionized with the absorption of multiple photons beyond the ionization threshold, it is known as Above Threshold Ionization (ATI)[1]. ATI occurs through several resonant and non-resonant multiphoton ionization channels. These ATI structures can be observed in the photoelectron spectrum. The photoelectron spectrum shows several sub-structures within each ATI order due to transient resonance of the AC-Stark-shifted Rydberg states. The complete momentum information of the ejected electrons can reveal the participating Rydberg states of the atom.

Finite light beams with an azimuthal dependence of the phase over the beam are said to possess an orbital angular momentum (OAM), which can be generated through holograms, spiral plates, or ring resonators, etc. Light-matter interaction with these beams raises a fundamental question on the nature of the transfer of this property of light to matter [2].

In experiments so far, only with macroscopic systems, has the OAM of the light beam manifested. In this talk, I will describe our experiments on the photoionization with linearly polarized, ultrashort (~25 fs) intense (10^{12}-10^{13} W/cm^2) laser pulses endowed with a definite OAM (l =1) using "Reaction Microscope"[3]. Photoionization with these laser pulses is through non-resonant multi-photon processes or tunnel ionization through the suppression of the Coulomb barrier of the atom. The talk will highlight the differences in the photoelectron spectrum as observed under similar conditions with non-structured Gaussian laser pulses.

References

[1] Freeman *et al.*, *Physical Review Letters* **59**, 10, 1092-1095 (1987)
[2] A. Picon *et al.*, New Journal of Physics **12**, 083053 (2010)
[3] J. Ullrich *et al.*, Rep. Prog. Phys Journal Abbreviation **66**, 1463-1545 (2003)

* E-mail: arnab.sen@students.iiserpune.ac.in

A Fully Relativistic Approach to Photoionization of Alkali Atoms

A Singor[1]*, D V Fursa[1] and I Bray[1]

[1]Department of Physics and Astronomy, Curtin University, Perth, WA 6102, Australia

Synopsis A fully relativistic method for calculating photon-atom scattering cross sections has been developed for scattering on quasi one-electron systems. This method has been applied to the calculation of photoionization cross sections from the ground and excited states of the alkali atoms: lithium, sodium, potassium, rubidium and cesium. The importance of accounting for relativistic effects and core polarisation is demonstrated.

The Kramers-Heisenberg-Waller (KHW) matrix elements [1, 2] provide a fully quantum mechanical description of photon-atom scattering to second order in perturbation theory. Since the development of the KHW matrix elements in the mid 1920's photon-atom scattering cross sections have proved to be essential for applications such as modelling radiative transport, opacities, Raman spectroscopy, and quantum illumination and radar.

We have extended a method recently used to calculated Rayleigh and Raman cross section for hydrogen [3] and the alkali atoms [4] to allow for a fully relativistic atomic structure model. Alkali atom bound state wave functions are calculated by diagonalising the Dirac Hamiltonian in a basis of Dirac L-spinors that are commonly used in the RCCC method [5, 6]. We use a central local potential produced by frozen core electrons which includes an equivalent local exchange term and polarisation potential. Pole terms that arise from integration over the continuum are handled using a well-known Gaussian quadrature method to implement principal value integration, which requires the evaluation of exact continuum eigenfunctions. For the alkali atoms, Rayleigh and Raman cross sections are dominated by contributions from the resonant transition between the ground state and first excited p state, thus photoionization cross sections provide a far more sensitive test of the accuracy of both the method and atomic structure model.

Photoionization cross sections from the s states of the alkali atoms: sodium, potassium, rubidium and cesium have a minimum in the cross section occurring just above the ionization threshold. This minimum occurs due to the dipole matrix element vanishing. In non-relativistic quantum theory this leads to the minimum being zero. In relativistic quantum theory there is a phase difference between the $p_{1/2}$ and $p_{3/2}$ continuum waves, which leads to the dipole matrix elements vanishing at different energies. This produces the distinctive non-zero minimum in the cross section called the Cooper-Seaton minimum. Obtaining a Cooper-Seaton minimum in the correct location and with the correct depth requires core polarisation and relativistic effects to be accurately accounted for. We perform calculations using a modified form of the electric dipole operator which accounts for core polarisation.

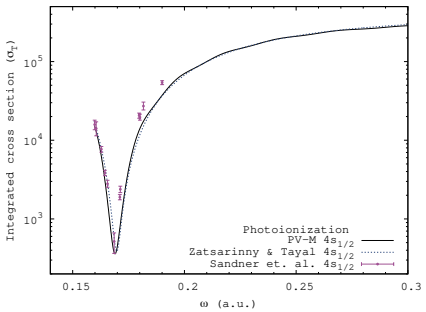

Figure 1. Photoionization from the ground state of potassium with comparison to the calculations of Zatsarinny and Tayal [7] and the experimental data of Sandner *et al.* [8]

References

[1] H. A. Kramers and W. Heisenberg 1925 *Z. Phys.* **31** 681.
[2] I. Waller 1929 *Z. Phys.* **58** 75.
[3] K. McNamara, D. V. Fursa, and I. Bray 2018 *Phys. Rev. A* **98** 043435.
[4] A. Singor *et al* 2020 *Atoms* **8** 57.
[5] D. V. Fursa and I. Bray 2008 *Phys. Rev. Lett.* **100** 113201.
[6] D. V. Fursa, C. J. Bostock and I. Bray 2009 *Phys. Rev. A* **80** 022717.
[7] O. Zatsarinny, and S. S. Tayal 2010 *Phys. Rev. A* **81** 043423.
[8] W. Sandner *et al* 1981 *Phys. Rev. A* **23** 2732.

*E-mail: adam.singor@postgrad.curtin.edu.au

Investigating photo-double-resonances in neon beyond the 1s threshhold

L Sommerlad[1]*, S Grundmann[1], A Pier[1], O D McGinnis[1], T Jahnke[1,2], R Dörner[1] and F Trinter[1,3,4]†

[1]Institut für Kernphysik, Goethe-Universität, 60438 Frankfurt, Germany
[2]European XFEL, 22869 Schenefeld, Germany
[3]Photon Science, Deutsches Elektronen-Synchroron (DESY), 22607 Hamburg, Germany
[4]Molecular Physics, Fritz-Haber-Institut der Max-Planck-Gesellschaft, 14195 Berlin, Germany

Synopsis Due to electronic correlation, a single photon can excite two electrons at once. We have measured and verified the position of such photo-double-resonances above the 1s threshold in neon over a broad photon energy range.

Electrons in atoms are not independent from each other and electronic correlations is an intriguing quantum mechanical phenomenon which has not yet been fully understood. Photo-double-resonance and photo-double-ionization (PDI) are exemplary processes for electronic correlations in which one single photon excites or detaches two electrons in an atom or molecule.

Using a COLTRIMS reaction microscope and synchrotron radiation of the P04 beamline at PETRA III (DESY), we have experimentally confirmed previous measurements of 1s2p and 1s2s resonance peaks in Neon. Furthermore, we were able to create charge state and energy resolved differential cross-sections in the region of the resonances. The electron energy was calibrated by the known 1snp Rydberg states below the 1s threshold [1]. The main peaks of the double resonances were identified and their photon energy positions were compared with the ones listed in Refs. [1] and [2]. As depicted in Fig. 1 there are 3 main peaks: The first peak at 902.4 eV belongs to the [1s2p]$3p^2$ state and the second at 905.3 eV to the [1s2p]3p4p state, both resulting from an excitement of one 1s and one 1p electron. The third peak at 924.7 eV belongs to the [1s2s]3s3p state.

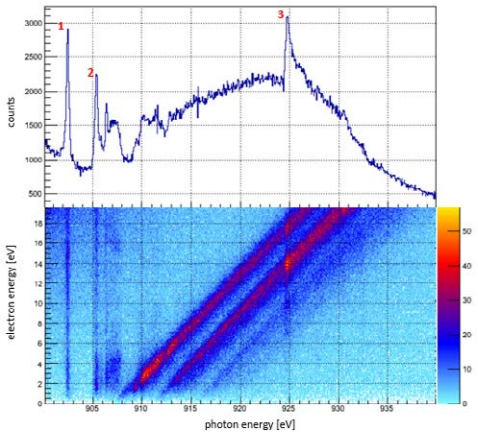

Figure 1. Energy and charge state resolved differential cross-section of the 1s2p and 1s2s double resonances in neon resulting in doubly charged neon ions.

The diagonal lines starting at roughly 907 eV observable in Fig.1 suggest additional photoelectrons. The nature of these electrons requires further investigation.

References

[1] K. C. Prince *et al* 2005 *Journal of Electron Spectroscopy* **144-147** 43-46
[2] Kato et al *et al* 2006 *J. Phys. B.* **39** 2059

*E-mail: sommerlad@atom.uni-frankfurt.de
†E-mail: trinter@atom.uni-frankfurt.de

Resonance-enhanced multiphoton ionization in the x-ray regime

S-K Son[1,2*], A C LaForge[3†], D Mishra[3], M Ilchen[4,5], S Duncanson[3], E Eronen[6], E Kukk[6], S Wirok-Stoletow[1,7], D Kolbasova[1,7], P Walter[8], R Boll[4], A De Fanis[4], M Meyer[4], Y Ovcharenko[4], D E Rivas[4], P Schmidt[4], S Usenko[4], R Santra[1,2,7], and N Berrah[3]

[1]Center for Free-Electron Laser Science CFEL, DESY, 22607 Hamburg, Germany
[2]The Hamburg Centre for Ultrafast Imaging, 22761 Hamburg, Germany
[3]Department of Physics, University of Connecticut, Storrs, Connecticut 06269, USA
[4]European XFEL GmbH, 22869 Schenefeld, Germany
[5]Institut für Physik und CINSaT, Universität Kassel, 34132 Kassel, Germany
[6]Department of Physics and Astronomy, University of Turku, 20014 Turku, Finland
[7]Department of Physics, Universität Hamburg, 22607 Hamburg, Germany
[8]Linac Coherent Light Source, SLAC National Accelerator Laboratory, Menlo Park, California 94025, USA

Synopsis Here, we report on resonance-enhanced multiphoton ionization (REMPI) of argon atoms in the short wavelength regime using ultraintense x rays from the European XFEL. We will demonstrate the differences of x-ray REMPI from conventional REMPI and discuss why.

Multiphoton ionization is one of the fundamental nonlinear processes when matter interacts with intense laser fields. In particular, REMPI [1] has been a widely-used spectroscopic technique due to high sensitivity and selectivity. X-ray free-electron lasers have offered new avenues for studying x-ray multiphoton ionization [2]. Extending REMPI to the x-ray regime, however, requires entirely different physical processes and interpretation. Conventional REMPI at long wavelengths relies on the resonant excitation of a valence electron where the only relaxation pathway is radiative decay. On the other hand, a core-excited state after x-ray resonant excitation is subject to Auger decay, which is orders of magnitude faster than radiative decay. Thus, the complex interplay between Auger processes and REMPI renders this process challenging to fully resolve in the x-ray regime.

We present a first observation of REMPI in the x-ray regime [3]. We observe nonlinear ionization to create Ar^{17+}, where photon energies are insufficient to directly ionize a $1s$ electron. With the aid of state-of-the-art theoretical modeling, we attribute the ionization to a two-color REMPI-like process where the second harmonic creates a $1s \rightarrow 2p$ transition and the fundamental pulse subsequently ionizes the system. The measured resonance profile of x-ray REMPI shows a broad, asymmetric, red-shifted distribution, as shown in Figure 1, which is a clear distinction from the conventional REMPI case. Moreover, theoretical results demonstrate a strong pulse-length dependence of the resonance profile. Our analysis shows that the REMPI process occurs not only for Ar^{16+} but also for lower charge states, where multiple ionization competes with Auger lifetimes. We find the observed broadband nature and pulse-length dependence of the resonance profile to be due to overlapping resonances with lower Ar charge states.

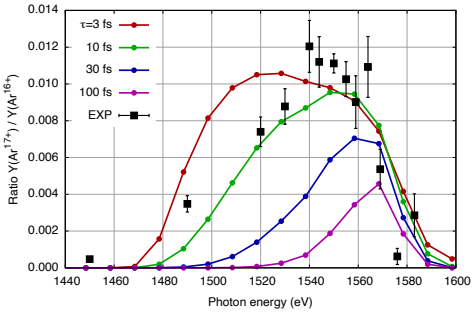

Figure 1. Experimental resonance spectral profile of the x-ray REMPI process, compared to theoretical results for different pulse lengths.

References

[1] Lambropoulos P 1976 *Adv. At. Mol. Phys.* **12** 87
[2] Young L *et al* 2010 *Nature* **466** 56; Hoener M *et al* 2010 *Phys. Rev. Lett.* **104** 253002; Rudek B *et al* 2012 *Nat. Photon.* **6** 858; Fukuzawa H *et al* 2013 *Phys. Rev. Lett.* **110** 173005
[3] LaForge A C *et al* 2021 submitted

*E-mail: sangkil.son@cfel.de
†E-mail: aaron.laforge@uconn.edu

XUV pump – XUV probe measurements for femtosecond ionization processes

K Takahashi*, K Nishimiya and A Suda

Department of Physics, Tokyo University of Science, Chiba, 278-8510, Japan

Synopsis To investigate the relaxation processes such as autoionization, femtosecond pump-probe experiments using high-order harmonics in the region of 10-30 eV was started up. The XUV pump-XUV probe system and time-of-flight analyzed system for photoion/photoelectron were installed. Using xenon high-order harmonics, the time-of-flight photoelectron and photoion spectra of argon were obtained under the zero delay time condition.

It is known that the lifetimes of ultrafast relaxation processes such as autoionization associated with inner-shell excitation and ionization of atoms and molecules are on the order of femtosecond (10^{-15} s). To directly observe such processes, it is necessary to use a probe pulse with a time resolution of attosecond (10^{-18} s) – femtosecond. Recently, high-order harmonics (HHs) generated by using a high-intensity femtosecond pulse laser and X-ray free electron laser with a pulsewidth from atto-to-femto second have been performed.

To investigate the relaxation processes related to the multi-electrons dynamics such as autoionization, we have started up pump-probe measurements using HHs in the region of extreme ultraviolet (XUV). In this study, an XUV pump- XUV probe system has been developed and a photoion/ photoelectron analysis system has been installed.

The XUV beam line was driven by a Ti: sapphire laser chirped pulse amplification (CPA) system (800 nm, 10 mJ/pulse, 35 fs, 10 Hz). The beam was focused by a convex lens (f = 4 m) into a gas cell (10 cm long) statically filled with xenon (Xe) (0.8 kPa). The IR and XUV radiation were co-propagating toward a silicon coated split-delay mirror placed at the Brewster's angle for the IR. The XUV beam was reflected at the mirror and focused by a gold-coated toroidal mirror into a target gas.

XUV pump-XUV probe system was performed by the split-delay mirror consisted of a fixed mirror that moved manually and a mirror that moved by piezo actuator (they are 70 mm height x 10 mm width x 10 mm depth).

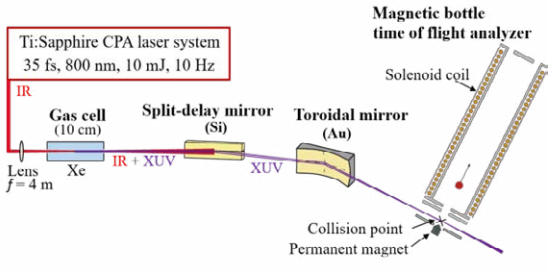

Figure 1. Schematic of the experimental setup.

The photoion time-of-flight (TOF) mass spectrometer was a Wiley-McLaren type. A permanent magnet was placed very close to the reflection electrode in the first acceleration region. In addition, a solenoid coil was introduced on the outside of the drift tube. The mass analysis of photoions was performed under the condition of accelerated electric field, while photoelectron energy was analyzed under the condition of non-electric field and magnetic field created by the permanent magnet and the solenoid coil. The photoelectron energy was analyzed by its flight time. Photoions or photoelectrons were detected by a microchannel plate.

As a first step, we succeeded to obtain the photoion TOF spectrum and the photoelectron spectrum of argon under the condition of zero delay time. In the photoelectron spectrum, the energy resolution $\Delta E/E$ was about 0.1-0.2 in the range of photoelectron energy of about 1-10 eV. In the future, we will investigate the delay time dependence of photoions and photoelectrons.

Reference

[1] Wiley W C and McLaren I H 1955 *Rev. Sci. Instrum.* **26** 1150

* E-mail: karin_takahashi@rs.tus.ac.jp

Theoretical study of the holographic structures induced by strong ultrashort pulses

A Taoutioui[1] * **and K Tőkési**[1] †

[1]Institute for Nuclear Research, Debrecen, 4026, Hungary

Synopsis We present a theoretical investigation of the holographic interference patterns in the two-dimensional photoelectron momentum distribution (PMD) by varying the number of optical cycles of the driving laser pulse. The PMDs are evaluated by solving the time-dependent Schrödinger equation (TDSE). We found that the PMD patterns are very sensitive to the number of optical cycles. Our calculations show the formation and coexistence of the spider-like and fishbone-like structures in the same PMD pattern. Furthermore, the formation of the fan-like structure is also discussed.

In strong field physics, the electron dynamics after ionization is responsible of many strong field phenomena such as High Harmonic Generation (HHG) [1] and High above threshold Ionization (HATI) [2] which are understood by means of scattering processes of the released electron wave packets by their parent ion in the presence of the driving laser field.

The scattering process of the ejected electrons with their parent ion plays a crucial role and leaves a footprint on the PMD patterns as well. The direct ionized wave packet can interfere with the forward or back-scattered scattered wave packets which leads to the intra-cycle holographic patterns such as spider-like structure [3], fishbone-like structure and the low-energy fan-like structure [4]. These patterns are very sensitive to the carrier-envelope phase in case of few-cycle pulses. We can see both, fishbone like and spider-like structures in the forward or in the backward directions of the momentum distribution by varying the carrier-envelope phase of the laser pulse. So far, the formation of the holographic patterns are still not well understood and need further detailed investigations.

In this work, we present TDSE results of atomic hydrogen interacting with sine square pulses applying various number of optical cycles N_c, from $N_c = 1$ to $N_c = 8$. The used linearly polarized electric field is $\mathbf{E(t)} = E_0 sin(\frac{\omega t}{2N_c})^2 sin(\omega t)\mathbf{e_z}$ where $E_0 = 0.0533$ a.u. and $\omega = 0.057$ a.u.. Fig. 1 shows the energy spectra of photoelectrons and the corresponding PMDs for atomic hydrogen. According to Fig. 1, the fishbone-like structure is formed in the backward direction in the case of two-cycle pulse but in three-cycle pulse case (not shown here) shows a coexistence of the fishbone like, spider-like and fan-like structures in the same pattern.

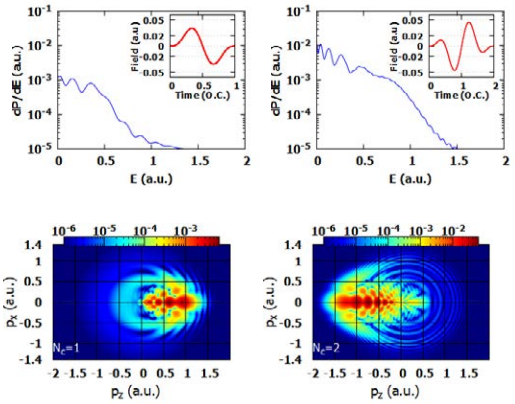

Figure 1. The photoelectron energy spectra (first row) and two-dimensional momentum distribution (second row) of atomic hydrogen induced by one-cycle (first column) and two-cycle (second column) pulses.

The work was support by the Bilateral relationships between Morocco and Hungary in science and technology (S&T) under the project number 2018-2.1.10-TÉT-MC-2018-00008.

References

[1] Krause J L *et al* 1992 *Phys. Rev. Lett.* **68** 3535
[2] Paulus G G *et al* 1994 *Phys. Rev. Lett.* **72** 2851
[3] Huismans Y *et al* 2011 *Science* **331** 6013
[4] Figueira de Morisson Faria C *et al* 2020 *Rep. Prog. Phys.* **83** 034401

*E-mail: Abdelmalek.taoutioui@atomki.hu
†E-mail: tokesi.karoly@atomki.hu

Photoelectron - residual ion entanglement in streaked and multi-sideband interferometric photoemission: an *ab initio* approach

H Shi and U Thumm

Department of Physics, Kansas State University, Manhattan, Kansas 66506, USA

Synopsis We calculated *ab initio* IR-streaked and multi-sideband (SB) interferometric (RABBITT) XUV photoemission (PE) spectra to investigate electronic correlation effects during the ionization of helium atom.

We extended our finite-element discrete-variable-representation (FE-DVR) code for the *ab initio* calculation of single- and double photoionization of gaseous helium atoms [1] to explore the effects of electronic correlation on attosecond time- and emission-angle-resolved PE spectra.

Our calculated IR-streaked XUV PE spectra and relative PE time delays between direct ionization (n=1) and shake-up ionization to the He^+ ($n = 2$) channel (i) agree with experimental and theoretical data in [2] and (ii) allow us to scrutinize the relevance of the residual excited He^+ ($n = 2, 3$) ion's transient induced dipole on the photoemission dynamics (Fig.1).

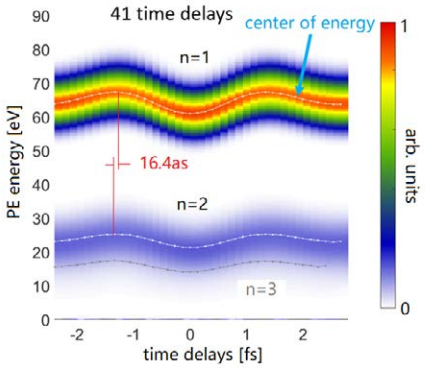

Figure 1. Single-90-eV-photon XUV photoemission spectrum of He, streaked by an 800 nm laser pulse, for direct (n=1) and shake-up ionization to the He^+ ($n = 2, 3$) channels. The relative streaking time delay between the $n = 1$ and $n = 2$ channels is 16.4 as. The $n = 3$ shakeup trace is weak and spectrally overlaps $n = 2$ trace.

To further investigate photoelectron interactions with the residual ion via laser-driven continuum-continuum transitions, we calculated *ab initio* multi-sideband interferometric spectra [3] of gaseous helium (Fig. 2). These enable us to address the imprint of laser-dressed electronic interactions (i) in relative sidebands phase shifts and (ii) by comparing *ab initio* calculated multi-sideband spectra (Fig. 2c) and with spectra modeled in single active electron (SAE) approximation (Fig. 2b).

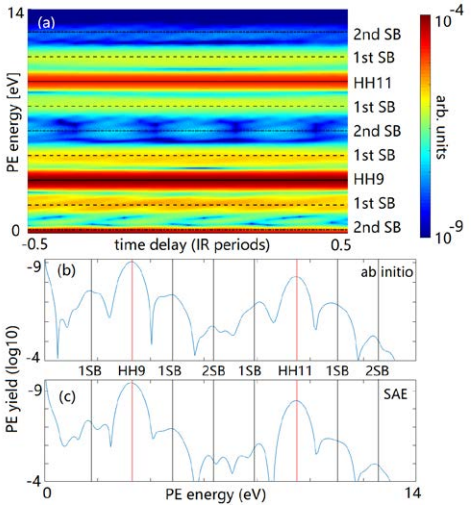

Figure 2. **(a)** Multi-sideband RABBITT spectrum of He for an attosecond pulse train (APT) composed of the 5th - 11th odd harmonics of a 400 nm fundamental laser and assisted by a delayed 800 nm laser pulse. **(b)** Lineout of (a) at zero delay. **(c)** Spectrum for temporally overlapping APT and assisting IR laser (zero delay)in SAE approximation.

This work is supported by the US DoE and NSF.

References

[1] Liu A and Thumm U 2015, *Phys. Rev A* **91**, 043416
[2] Ossiander M *et al.* 2017, *Nat. Phys.* **13**, 280
[3] Bharti D *et al.* 2021, *Phys. Rev A* **103**, 022834

Effect of SOIAIC on the angle-resolved time delay in the photoionization of Ar inside fullerene anion

A Thuppilakkadan[1]*, S Banerjee[2], H R Varma[1]

[1]School of Basic Sciences, Indian Institute of Technology Mandi, Kamand, H.P. 175005, India
[2]Department of Physics, Indian Institute of Technology Madras, Chennai 600036, India

Synopsis The effect of spin-orbit activated interchannel coupling (SOIAIC) has been studied on the time delay profile of $2p_{\frac{3}{2}}$ photoionization in $Ar@C_{60}^{-1}$. The time delay profile is found to have strong angular anisotropy in the region where SOIAIC features are present.

A number of studies, in the past, have revealed the role of spin-orbit activated interchannel coupling (SOIAIC) on the photoionization dynamics. As a result of the SOIAIC effect, the photoionization parameter corresponding to $j = l + \frac{1}{2}$ gets modified in the vicinity of the $j = l - \frac{1}{2}$ ionization threshold [1, 2]. In a recent work, it is shown that the SOIAIC effect profoundly alters the cross-section in the photoionization of high-Z atoms due to strong spin-orbit interaction [3].

Photoionization studies of an atom trapped inside a fullerene ($A@C_{60}$) provides a great platform to study the role of external environment on the dynamics of the atom inside. Such studies have important applications in the various fields of science and engineering. The distinctive feature of such systems is the existence of confinement oscillations in the photoionization spectra. Earlier Govil et al [4] have shown that confinement resonances can induce the SOIAIC effect. Recently, Keating et al [5] have studied the SOIAIC effect in the Wigner time delay of Hg, Rn, and Ra which are trapped inside a fullerene.

Here we report the SOIAIC effect in the angle-resolved Wigner time delay of a comparatively low-Z atom such as Ar trapped inside fullerene anion $\left(Ar@C_{60}^{-1}\right)$. In this case, the role of shape resonance is replaced by the Coulomb confinement resonances (CCRs) present in such anionic confinement system. We have studied the SOIAIC effect in the $2p_{\frac{3}{2}}$ time delay in the vicinity of $2p_{\frac{1}{2}}$ ionization energy.

Figure 1 shows the time delay profile of $2p_{\frac{3}{2}}$ in the region of $2p_{\frac{1}{2}}$ CCR. With the inclusion of channels from $2p_{\frac{1}{2}}$ (16 channel), the time delay profile shows significant variation as compared to 14 channel (channels from $2p_{\frac{1}{2}}$ not included). Before 9.56 a.u photon energy, the time delay is found to show strong angular anisotropy. After 9.56 a.u. the angular anisotropy is vanished. Detailed analysis of confinement enhanced SOIAIC features on the angular time delay will be carried out and will be presented at the conference.

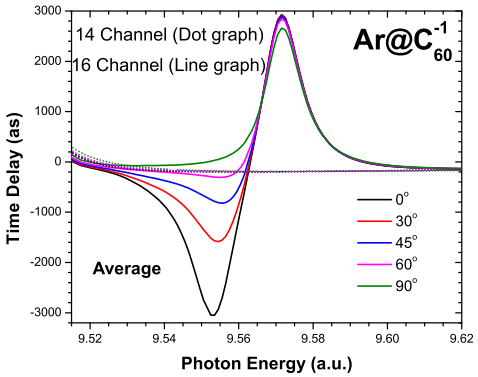

Figure 1. Wigner time delay of the $2p_{\frac{3}{2}}$ subshell of $Ar@C_{60}^{-1}$

This work is partially supported by DST-SERB (India) grant EMR/2016/002695 (HRV).

References

[1] Amusia M Y *et al* 2002 *Phys. Rev. Lett.* **88** 093002
[2] Banerjee S *et al* 2020 *Phys. Rev. A* **101** 043411
[3] Jose J *et al* 2020 *Phys. Rev. A* **102** 022813
[4] Govil K *et al* 2009 *J. Phys. B: At. Mol. Opt. Phys.* **42** 065004
[5] Keating D A *et al* 2017 *J. Phys. B: At. Mol. Opt. Phys.* **50** 175001

*E-mail: afsal_t@students.iitmandi.ac.in

Towards the coherent control of Penning collisions between metastable helium atoms

A Tsoukala[1] *, L Bienkowski[1], T Sixt[1], N Vanhaecke, F Stienkemeier[1] and K Dulitz[1]

[1]Institute of Physics, University of Freiburg, Hermann-Herder-Str. 3, 79104 Freiburg, Germany

Synopsis Our research focuses on understanding the mechanistic details of reactive collisions in order to enable control of their outcome. We are currently setting up an experimental apparatus which will allow for control of such reactions in the phase domain.

The coherent control of reactive collisions, which relies on the interference between two or more reaction paths, has been long sought for [1]. We are in the process of realizing an experiment, in which we coherently control the Penning collisions between metastable helium atoms in the 2^3S_1 and 2^1S_0 states.

Our control scheme is based on the preparation of a coherent superposition of the M_J=-1 and M_J=+1 quantum states in the He(2^3S_1) via an off-resonant two-photon Rabi excitation scheme. The two states are coupled by light of counter-rotating circular polarization, which also imprints its phase onto each state. By varying the phase difference between the two circularly polarized light components, the relative phase between the involved reaction pathways follows the same trend. This control scheme will for a precise tuning of the overall reaction cross section. Our detection scheme is based on monitoring of ions, produced in the collision process, on a time-of-flight detector.

In this contribution, I will describe our experimental apparatus and its characterization.

* E-mail: alexandra.tsoukala@physik.uni-freiburg.de

References

[1] Moshe Shapiro and Paul Brumer 2012 *Quantum Control of Molecular Processes* (WILEY-VCH)

Near-threshold two-photon double ionization of Kr in the VUV

L. Varvarezos[1*], S. Düsterer[2], M. D. Kiselev[3,4,5], R. Boll[2,6], C. Bomme[2,7], A. De Fanis[6], B. Erk[2], C. Passow[2], S. M. Burkov[5], G. Hartmann[2,8,9], M. Ilchen[9,6], P. Johnsson[10], T. J. Kelly[11], B. Manschwetus[2], T. Mazza[6], M. Meyer[6], D. Rompotis[6,2], O. Zatsarinny[12], E. V. Gryzlova[3], A. N. Grum-Grzhimailo[3] and J. T. Costello[1]

[1]School of Physical Sciences, Dublin City University, Dublin 9, Ireland
[2]Deutsches Elektronen-Synchrotron (DESY), Notkestrasse 85, D-22607 Hamburg, Germany
[3]Skobeltsyn Institute of Nuclear Physics, Lomonosov Moscow State University, Moscow 119991, Russia
[4]Lomonosov Moscow State University, Faculty of Physics, 119991 Moscow Russia
[5]Pacific National University, Tihookeanskaya Str., 139, Khabarovsk 680035, Russia
[6]European XFEL, Holzkoppel 4, 22869 Schenefeld, Germany
[7]Institut rayonnement-matiere de Saclay (Iramis), CEA Saclay Bat 524, Gif-sur-Yvette cedex, F-91191, France
[8]Helmholtz-Zentrum Berlin für Materialien und Energie GmbH, Albert-Einstein-Straße 15, D-12489 Berlin, Germany
[9]Institut für Physik und CINSaT, Universität Kassel, Heinrich-Plett-Str. 40, 34132 Kassel, Germany
[10]Department of Physics, Lund University, PO Box 118, SE-221 00 Lund, Sweden
[11]Department of Computer Science and Applied Physics, Galway-Mayo Institute of Technology, Galway Campus, T91 T8NW Galway, Ireland
[12]Department of Physics and Astronomy, Drake University, Des Moines, Iowa 50311, USA.

Synopsis This work focuses on two-photon double ionization of Kr, upon interaction with free electron pulses in the vacuum ultraviolet (VUV). Angle-averaged and angle-resolved photoelectron measurements are reported in order to investigate the effect of the autoionizing resonances on the photoelectron angular ditrsibutions. The experimental findings are complemented by theoretical calculations.

We report angle-integrated and angle-resolved photoelectron measurements in near-threshold two-photon double ionization (TPDI) of Kr irradiated by free-electron laser (FEL) pulses in the vacuum-UV [1] photon energy region.

As shown in Figure 1, the angle-integrated measurements allow for the observation of the $^2P_{3/2}$ and $^2P_{1/2}$ components in the first ionization step, at approximately 11.20 eV and 10.50 eV, respectively. Three more photoelectron peaks, attributed to the second-ionization step, are also discernible.

Regarding the angle-resolved measurements, the photoelectron angular distributions (PADs) are compared with the results of semirelativistic R-matrix calculations [2]. As reported by Augustin et al. [3] it is found that the presence of autoionizing resonances within the bandwidth of the exciting FEL pulse strongly influences the PADs. The large spin-orbit interaction, inherent in 4p-subshell hole states of Kr, permits us to resolve and study PADs associated with some of the fine-structure components of the singly and doubly charged Kr ions.

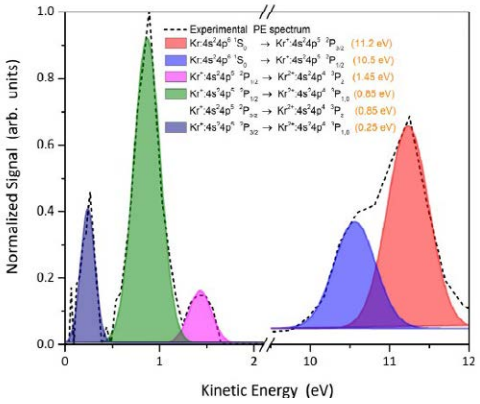

Figure 1. A representative experimental angle-averaged photoelectron spectrum for an FEL intensity of approximately 2.5×10^{13} W/cm^2.

References

[1] L. Varvarezos *et al* 2021 *Phys. Rev. A.* **103** 022832
[2] O. Zatsarinny 2006 *Comput. Phys. Commun.* **174** 273
[3] S. Augustin *et al* 2018 *Phys. Rev. A.* **98** 033408

* E-mail: lazaros.varvarezos2@mail.dcu.ie

The TMO Instrument: Opportunities and Plans for Time-resolved Atomic, Molecular and Optical Science at LCLS-II

P. Walter [1]*, J. Cryan [1,2], X. Cheng [1], R. Coffee [1,2], D. Fritz [1], J. James [1], A. Kamalov [1], M-F. Lin [1], X. Li [1], R. Obaid [1], T. Wolf [1,2], and J.C. Castagna[1]

[1]SLAC National Accelerator Laboratory, 2575 Sand Hill Road, Menlo Park, CA 94025, USA. [2]Stanford PULSE Institute, SLAC National AcceleratorLaboratory, 2575 Sand Hill Road, Menlo Park, CA 94025, USA.

Synopsis The new designed Time-resolved Atomic, Molecular and Optical Science end station, will be configured to take full advantage of both the high per pulse energy from the copper accelerator (120 Hz) as well as high average intensity and high repetition rate (1 MHz) from the superconducting accelerator. TMO will support many experimental techniques not currently available at LCLS and will have two X-ray beam focus spots. Thereby, TMO will support AMO science, strong-field and nonlinear science and a new dynamic reaction microscope.

The unique capabilities of LCLS, the world's first hard X-ray FEL, have had significant impact on advancing our understanding across a broad range of scientific fields, from fundamental atomic and molecular physics, to condensed matter, to catalysis and structural biology. A major upgrade of the LCLS facility, the LCLS-II project, is now underway. LCLS-II is being developed as a high-repetition rate X-ray laser with two simultaneously operating, independently tunable FELs. It features a 4 GeV continuous wave superconducting linac that is capable of producing uniformly spaced (or programmable) ultrafast X-ray laser pulses at a repetition rate up to 1 MHz spanning the energy range from 0.25 to 5 keV. Furthermore, the XLEAP sub-femtosecond soft X-ray pulse generation program is scalable to LCLS-II repetition rate [1].

The Time-resolved atomic, Molecular and Optical Science (TMO) instrument, one of the three new LCLS-II instruments with a energy range from 0.25 to 2 keV, will support AMO science, strong-field and nonlinear science, and a new dynamic reaction microscope. TMO will support many experimental techniques not currently available at LCLS and will have two X-ray focus spots.

At the first focus spot of the TMO instrument we will offer the possibility to install standardized modular stations (roll in and out) which can be set up, aligned and commissioned outside the hutch and then get installed for operations. These highly standardized stations will be optimized for performing high energy, high resolution, time- but also angular-resolved photoelectron spectroscopic measurements by using high resolution iTOF and eTOF, double-sided-VMI [2] or coaxial-VMI [3], and the future MR-COFFEE endstation [4].

At the second focus spot a new reaction microscope endstation will house a COLTRIMS type spectrometer to accommodate extreme vacuum, sub-micron focus spot size, and target purity requirements as dictated by coincidence experiments. The accumulation of data will be performed on an event-by-event basis using the 1 MHz full repetition rate of LCLS-II.

We would like to present some of the important science opportunities, new capabilities and instrumentation being planned for NEH 1.1 (TMO) at LCSL-II.

*E-mail: pwalter@slac.stanford.edu

References

[1] Marinelli, A., et al., Tunable Isolated Attosecond X-ray Pulses with Gigawatt Peak Power from a Free-Electron Laser. Nature Photonics, (2019). https://doi.org/10.1038/s41566-019-0549-5

[2] Osipov, et. l., (2018). The LAMP instrument at the Linac Coherent Light Source free-electron laser. Review of Scientific Instruments, 89(3), 035112. https://doi.org/10.1063/1.5017727

[3] Cryan, J., et. al., (2018). A co-axial velocity map imaging spectrometer for electrons. AIP Advances, 8(11), 115308. https://doi.org/10.1063/1.5046192

[4] **M**ulti **R**esolution **C**ookiebox **O**ptimized for **F**uture **F**ree **E**lectron laser **E**xperiments. https://arxiv.org/abs/2103.07603

Mechanism of below-threshold high-order harmonic generation of Na in the intense elliptically polarized laser field

Z-B Wang[1], Z-H Jiao[1]*, S-F Zhao[1]P-C Li[2,3]

[1]College of Physics and Electronic Engineering, Northwest Normal University, Lanzhou 730070, China
[2]Research Center for Advanced Optics and Photoelectronics, Department of Physics, College of Science, Shantou University, Shantou, Guangdong 515063, China
[3]Key Laboratory of Intelligent Manufacturing Technology of MOE, Shantou University, Shantou, Guangdong 515063, China

Synopsis We explore the mechanism of below-threshold harmonic generation (BTHG) of Na atom in the intense elliptically polarized laser fields by solving the time-dependent Schrödinger equation accurately in space and time. An intuitive physical picture is demonstrated by the analysis of the quantum channels of electron in BTHG.

High-order-harmonic generation (HHG) of atoms and molecules in intense laser fields, leading to the production of the coherent extreme-ultraviolet (XUV) and attosecond pulses, has attracted much interest in the subject of ultrafast science and technology in the last decade. In addition, most theoretical studies have focused on the HHG generated by linearly polarized laser fields[1]. Recently, the polarized HHG driven by bichromatic counterrotating circularly polarized laser fields has attracted much interest[2]. It allows one to generate XUV radiation and attosecond pulse trains with controlled polarization properties and carries the potential to generate isolated circularly polarized attosecond pulses.

We explore the mechanism of below-threshold harmonic generation (BTHG) of Na atom subjected to intense elliptically polarized intense mid-infrared laser fields. The Na atom is described by an accurate model potential which reproduces both the bound- and exited- states energies. In Figure 1(a) and 1(b), we present the comparison of the BTHG of Na atom in the z and x direction, respectively. The laser pulse has a sine-square pulse shape and the duration is 20 optical cycles. The results show that the yields of the BTHG generated by the elliptically polarized laser fields are high when the ellipticity is decreased. Namely, the yields of the BTHG are sensitive to the ellipticity of the laser fields. This results provide a potential method to control the enhancement of the BTHG by the polarized laser field. Combining with a synchrosqueezing transform of the quantum time-frequency spectrum and an extended semiclassical analysis, the role of quantum channels on the BTHG processes are clarified.

*E-mail: jiaozh@nwnu.edu.cn

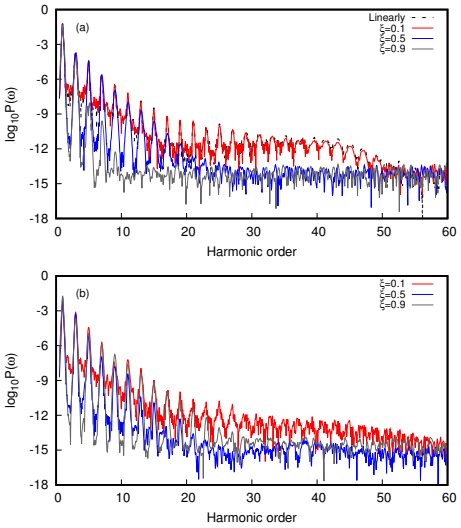

Figure 1. Comparison of the HHG power spectrum of Na atom driven by elliptically polarized laser fields in the z (a) and x (b) direction, respectively.

Acknowledgements

This work was supported by the National Natural Science Foundation of China (11674268, 11764038, 12074239), Natural Science Foundation of Guangdong Province (200110165892233, 2020A1515010927, 210206153460124), Department of Education of Guangdong Province (2018KCXTD011, 2019KTSCX038, 2020KCXTD012), and Shantou University (NTF18030).

References

[1] Li P C *et al* 2015 *Nat. Commun.* **6** 7178
[2] Kfir O *et al* 2015 *Nat. Photon.* **9** 99

Is carrier envelope phases of multi-color laser pulses necessarily optimized to generate shorter isolated attosecond pulses?

K Yang[1], G L Wang[1]* and X X Zhou[1]†

[1]College of Physics and Electronic Engineering, Northwest Normal University, Lanzhou, 730070, China

Synopsis Isolated attosecond pulses (IAP) can be generated from high-order harmonic generation driven by multicolor laser pulse. Our optimizations with genetic algorithm show that carrier envelope phases for each spectral components are not necessarily to be precisely controlled to generate shorter IAP, which could facilitate the operation of the experiment.

The attosecond (as) pulse is an important tool to detect the ultrafast dynamic behavior of electrons in atoms, molecules and nanomaterials [1]. Isolated attosecond pulse (IAP) with pulse width ∼50 as [2, 3] are now available in some laboratories from high-order harmonic generation (HHG). It is still necessary to obtain shorter attosecond pulses for strong field physics and attosecond science.

Besides some commonly used "optical gating" techniques, such as amplitude gating, ionization gating, polarization gating, double optical gating, a multi-color driving field is also a potential scheme to generate strong short IAP. This configuration has the advantage of capability to gate the harmonic emission driven by longer pulses with respect to other schemes, enhancing the harmonic yield and increasing the cutoff energy relatively easily. In this case, the driving laser field can be written as

$$E(t) = \sum_{j=1}^{n} E_j f(t-\tau_j) \cos\left[\omega_j(t-\tau_j) + \varphi_j\right], \quad (1)$$

where E_j is the electric field amplitude, $f(t)$ is the Gaussian pulse envelope $f(t) = e^{-2\ln 2t^2/\tau^2}$, τ is the pulse duration (FWHM), ω_j is laser angular frequency, φ_j is carrier envelope phase (CEP), τ_j is time delay. With the accurate parameters $\{E_j, \omega_j, \tau_j, \varphi_j\}$ an ideal arbitrary optical waveform can be achieved. Here, the most demanding is how to precisely control the CEPs, especially for experiment, which can be avoided in the generation of shorter IAP?

We simulate HHG and corresponding IAP with strong field approximation, the laser parameters are optimized via genetic algorithm (GA). Figure 1 shows our main results for 2-color case, where τ =6 fs, λ_1 is fixed as 800 nm, total laser peak intensity is 1.0×10^{15}W/cm^2, $\tau_1 = 0$ and $\varphi_1 = 0$. We compare the results in two cases, one is the fully optimization, the other with the constrain of $\varphi_j = 0$ in the optimization. It is found that the CEP has little influence on the optimized electric field waveforms, generated harmonic spectra and IAP, showing that CEP for each spectral components are not necessarily to be precisely controlled.

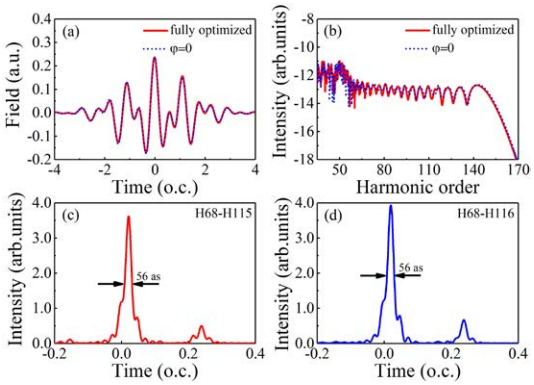

Figure 1. Comparison of results with the constrain of $\varphi_j = 0$ and fully optimized . (a) The electric field waveforms. (b) High-order harmonic spectra of Ne. (c)(d) Corresponding shortest IAPs.

This work was supported by the National Natural Science Foundation of China (Grant Nos. 11864037, 91850209).

References

[1] Föhlisch A *et al* 2005 *Nature.* **436** 373
[2] Li J *et al* 2017 *Nat. commun.* **8** 186
[3] Gaumnitz T *et al* 2017 *Opt. Express* **25** 27506

*E-mail: wanggl@nwnu.edu.cn
†E-mail: zhouxx@nwnu.edu.cn

Implementation and validation of the relativistic attosecond transient absorption theory within the dipole approximation

F Zapata[1*], J Vinbladh[1,2], E Lindroth[2] and J M Dahlström[1,2]

[1]Department of Physics, Lund University, 22100 Lund, Sweden
[2]Department of Physics, Stockholm University, 10691 Stockholm, Sweden

Synopsis In the present work, the relativistic attosecond transient absorption equations are derived from the time-dependent Dirac equation. Simulations on the Hydrogen atom validate our relativist theory and, thanks to the development of the novel relativistic TD-CIS method, different ATAS scenarios are explored in heavy atoms.

Attosecond transient absorption spectroscopy (ATAS) is used to study electron coherence and motion in atoms and molecules [1]. Typically, an intense laser field is used to prepare an electron wave packet in the target system and a XUV pulse is used to probe the dynamics.

All studies so far are based on *non-relativistic* ATAS theory [2], although the importance of spin-orbit coupling was demonstrated already by the first ATAS experiment which targeted Krypton [3]. Numerical calculations including spin-orbit effects have been done by few authors (i.e. Pabst *et al.* [4] and Baggesen *et al.* [5]) but without a fully relativistic approach.

In the present work [6], a *relativistic* ATAS theory is derived, implemented and validated within the dipole approximation based on the time-dependent Dirac equation.

In the non-relativistic limit, it is found that the absorption agrees with the well established non-relativistic theory based on the time-dependent Schrödinger equation. Time-dependent simulations have been performed using the Dirac equation and the Schrödinger equation for the Hydrogen atom in two different attosecond transient absorption scenarios. These simulations validate our relativistic theory.

The present work can be seen as a first step in the development of a more general relativistic attosecond transient absorption spectroscopy method for studying heavy atoms, but it also suggests the possibility of studying relativistic effects, such as Zitterbewegung [7], in the time domain.

References

[1] Beck A R *et al* 2015 *Chem. Phys. Lett.* **624** 119

[2] Wu M *et al* 2016 *J. Phys. B: At. Mol. Opt. Phys.* **49** 062003

[3] Goulielmakis *et al* 2010 *Nature* **466** 062003

[4] Pabst S *et al* 2012 *Phys. Rev. A* **86** 063411

[5] Baggesen J C *et al* 2012 *Phys. Rev. A* **85** 013415

[6] Zapata F *et al* 2021 *Electron. Struct.* **3** 014002

[7] Maquet A and Grobe R 2002 *J. Mod. Opt.* **49** 02001

* E-mail: felipe.zapata@matfys.lth.se

New source for tuning the effective Rabi frequency in multiphoton ionization

W Li[1,2], Y Lei[1,2], X Li[1,2], T Yang[1,2], M Du[1,2], Y Jiang[1,2], J Li[1,2], A Liu[1,2], L He[1,2], P Ma[1,2], S Luo[1,2], D Zhang[1,2]* and D Ding[1,2]†

[1]Institute of Atomic and Molecular Physics, Jilin University, Changchun, 130012, China
[2]Jilin Provincial Key Laboratory of Applied Atomic and Molecular Spectroscopy, Jilin University, Changchun, 130012, China

Synopsis The Autler-Townes effect due to near resonance transition between 4s-4p states are mapped out in the photo-electron-momentum distribution and manifests it as a splitting in the photo-electron kinetic energy spectra. The energy splitting fits well with the calculated Rabi frequency at low laser intensities and shows clear deviation at laser intensities above 1.5×10^{11} W/cm^2. An effective Rabi frequency formulae including the ionization process explains the observed results. Our results demonstrate the possibility to tune the effective coupling strength with the cost of the number of particles.

We have observed the tuning of the effective Rabi frequency in the resonance multiphoton ionization of potassium atoms [1]. The coupling strength between two resonantly coupled state are directly mapped out in the kinetic energy distribution of the photoelectrons. The coupling strength deviates significantly from the simple Rabi frequency as the laser intensity increases due to the non-negligible contribution of ionization rate as shown in Fig. 1. Our results shows the possibility to control the interaction between optical field and the atomic system with the cost of the losing populations. This finding might offer new tuning nobs to the fields of manipulating atom with intense laser fields. For example, a second control laser can be used to drive the populations into some dark states where the effective Rabi frequency can be tuned. With our findings, we would like to point out that identifying ionization channel based on the kinetic energy spectrum of the emitted electrons in strong field ionization process when the system has complex energy levels should receive extra cares. Not only resonances might be involved in the ionization and make the kinetic energy shift or split significantly, but also the detection procedure itself can induce considerable deviations from intuitive expectation.

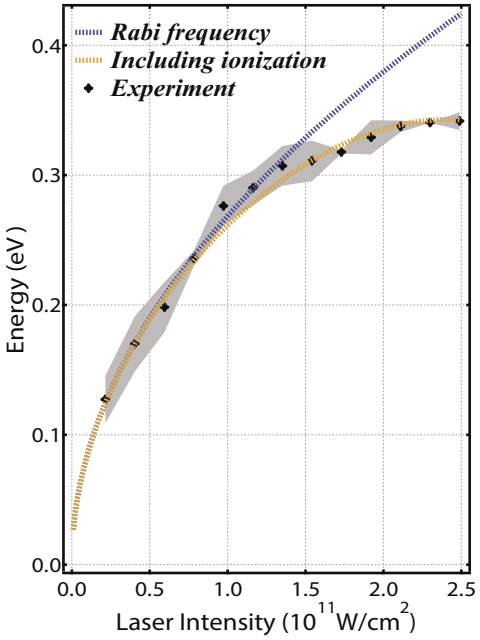

Figure 1. The Aulter-Townes splitting as a function of laser intensities. The black dot represents the experimentally measurements. The grey shadow is the standard deviation with ten individual measurements. The blue dot line is the Rabi frequency. The orange dot line is the effective Rabi frequency.

References

[1] Li W *et al* 2021 *Chin. Phys. Lett.* **38** 053202

*E-mail: dongdongzhang@jlu.edu.cn
†E-mail: dajund@jlu.edu.cn

Coherent control of He $2s^2$ population by XUV light

M Žitnik[1]*, A Mihelič[1], K Bučar[1], Š Krušič[1], R Squibb[2], R Feifel[2], I Ismail[3], P Lablanquie[3], J Palaudoux[3], O Plekan[4], M Di Fraia[4], M Coreno[4], M Manfredda[4], A Simoncig[4], P Rebernik Ribič[4], F Sottocorona[4], E Allaria[4,5], K C Prince[4], C. Callegari[4] and F Penent[3]

[1] Jožef Stefan Institute, Jamova cesta 39, SI-1000 Ljubljana, Slovenia
[2] University of Gothenburg, Department of Physics, SE-412 96 Gothenburg, Sweden
[3] Laboratoire de Chimie Physique-Matière et Rayonnement (UMR 7614), Sorbonne Université, CNRS, 4 Place Jussieu, 75252 Paris Cedex 05, France
[4] Elettra-Sincrotrone Trieste, Strada Statale 14 - km 163.5, I-34149 Basovizza, Trieste, Italy
[5] Now at Deutsches Elektronen-Synchrotron DESY, Notkestrasse 85, 22607 Hamburg, Germany

Synopsis The relative phase of overlapping ω and 3ω light pulses was tuned to control the population of $2s^2$ state in He by interference of $\omega+\omega$ and $3\omega-\omega$ two-photon excitation paths. The population was monitored by observing the total electron yield due to $2s^2$ autoionization decay. The maximum yield occurs when the relative phase of the two colors is equal to the phase difference of atomic amplitudes governing the two excitation paths. A displacement of the position of the maximum autoionization yield in the phase reference frame signals the presence of an additional phase-shifting effect in the ω and/or 3ω light paths between the source and the target and provides a measure of the corresponding phase shift.

Quantum mechanics offers a unique possibility to control transition probability by setting up relative amplitudes of two or more paths leading from one initial to one final state. A combination of coherent light beams is usually employed to drive the target to the desired reaction channel. The basic two-color scheme was pioneered by Shapiro and others [1] and uses a fundamental and its third harmonic, where the transition occurs due to the combined effect of the three-photon ($\omega+\omega+\omega$) and single-photon absorption (3ω).

The last decade has seen rapid development of intense free-electron laser (FEL) sources [2] and the question arises whether the coherent control can be executed entirely by using the extreme ultraviolet (XUV) light. We report here the results of an experiment at the free electron laser facility FERMI where the novel $\omega+\omega$ and $3\omega-\omega$ two-photon interference scheme (Fig. 1),

$$\begin{array}{ccccc} & \nearrow^{\omega+\omega}\searrow & & & \\ \mathrm{He}(1s^2) & & \mathrm{He}(2s^2) & \rightarrow & \mathrm{He}^+(1s)+e^-(E_2), \\ & \searrow_{3\omega-\omega}\nearrow & & & \end{array}$$

is employed to manipulate the population of $2s^2$ doubly excited state in He. While 2ω and $\omega+\omega$ absorption paths were recently combined to measure angle-resolved phases in atomic photoemission [3], coherent control of the state population by XUV light has not been previously demonstrated.

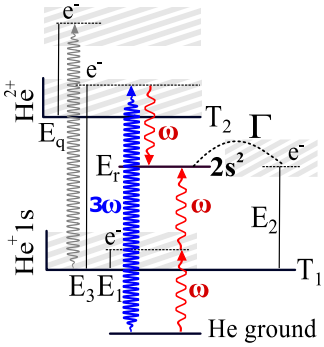

Figure 1. Shematic energy level diagram for emitted electrons when double of light frequency ω is tuned to He $2s^2$ state with excitation energy E_r and lifetime Γ^{-1}. Ionization thresholds of He and He^+ are denoted by T_1 and T_2 respectively. Electron kinetic energies are denoted by E_i, $i=1-3$.

References

[1] Chan C K, Brumer P and Shapiro M 1991 *J. Chem. Phys.* **94** 2688
[2] Seddon E A *et al* 2017 *Rep. Prog. Phys.* **80** 115901
[3] You D *et al* 2020 *Phys. Rev. X* **10** 031070

*E-mail: matjaz.zitnik@ijs.si

Relativistic R-matrix study on the photoionization process of highly charged tungsten ions

Y H An[1], Z W Wu[1]* and C Z Dong[1]†

[1]Key laboratory of Atomic and Molecular Physics & Functional Materials of Gansu Province, College of Physics and Electronic Engineering, Northwest Normal University, Lanzhou, 730070, P. R. China

Synopsis The single-photon photoionization process of highly charged W^{59+}-W^{61+} and W^{63+} ions from their respective ground states have been studied by using the DARC package based on the relativistic R-matrix theory. For the ground-state photoionization of W^{63+} ions, the direct and resonant ionization limits are obtained and the identified resonance peaks are found.

The photoionization process is one of the most basic processes, in which light interacts with atoms or ions. The photoionization cross section of atoms or ions is an important parameter for simulating the opacity of laboratory and astrophysical plasmas. The central temperature of fusion plasmas in the International Thermonuclear Experimental Reactor (ITER) under construction will exceed 30keV [1], which would make the wall material tungsten become more or less tungsten ion (greater than W^{64+}) impurities into the plasmas.

In this work, the direct and resonant single-photon photoionization of W^{63+} ions from their ground state $1s^22s^22p^63s\ ^2S_{1/2}$ and four lowly excited states $1s^22s^22p^63p\ ^2P_{1/2,3/2}$ and $1s^22s^22p^63d\ ^2D_{3/2,5/2}$ has been studied within the framework of the relativistic R-matrix method and the multiconfigurational Dirac-Fock method [2]. The direct ionization limit and the convergence limit of the Rydberg series ions are ideatified in detail, and the resonance energies are given. The photoionization of the ground states of W^{59+}-W^{61+} ions is systematically studied. The corresponding energy levels and resonance energies are gained by analyzing the direct ionization limit and the convergence limit of the Rydberg series. Moreover, the ground-state photoionization cross sections of W^{63+}-W^{59+} ions are compared with each other, and the change of photoionization cross sections with the number of valence electrons is analyzed, as shown in Figure 1. We expect that the present work could fill the existing vacancy of essential studies on the photoionization of tungsten ions and be helpful to the diagnosis and simulation of fusion plasmas together with available photoionization data for tungsten ions with other charge states.

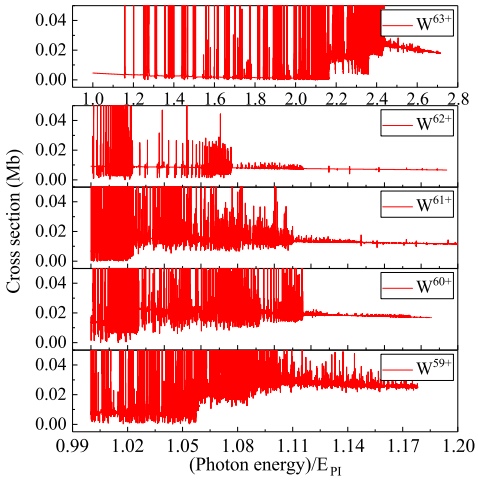

Figure 1. (Color online) The ground-state photoionization cross sections of W^{63+}-W^{59+} ions are compared with each other. E_{PI} is the direct ionization limit of tungsten ions.

This work is funded by the National Key Research and Development Program of China (2017YFA0402300) and the National Natural Science Foundation of China under Grant Nos. 11874051, 11804280, and 11864036.

References

[1] T Pütterich *et al* 2008 *Plasma Phys. Control. Fusion* **50** 085016
[2] Y H An *et al* 2021 *J. Phys. B: At. Mol. Opt. Phys.* **54** 065001

*E-mail: zhongwen.wu@nwnu.edu.cn
†E-mail: dongcz@nwnu.edu.cn

Dissociative ionization pathways of guanine tautomers

A Rebelo[1,2], D Bou-Debes[1*], J. Bockova[1], K L Nixon[3], J-C Poully[4] and S Eden[1]

[1] School of Physical Sciences, The Open University, Walton Hall, Milton Keynes, MK7 6AA, UK
[2] CEFITEC, Department of Physics, FCT - Universidade NOVA de Lisboa, P-2829-516 Caparica, Portugal
[3] School of Life, Health, and Chemical Sciences, The Open University, Walton Hall, Milton Keynes, MK7 6AA, UK
[4] CIMAP, Normandie Univ, ENSICAEN, UNICAEN, CEA, CNRS, Boulevard Henri Becquerel, BP, France

Synopsis 10 different direct dissociations (as opposed to sequential dissociations) have been observed from excited isolated guanine$^+$. This number is far higher than reported for other ionized nucleobases and provides the first experimental evidence supporting tautomer-dependence in the dissociative ionization of a DNA/RNA base.

Gas-phase guanine targets contain significant populations of multiple tautomers [1], whereas the other four DNA/RNA bases exist in just one or two dominant forms in the gas-phase. This mixed target composition complicates efforts to assign experimentally-observed fragment ions to calculated dissociation pathways. Furthermore, guanine is the most thermally-labile DNA/RNA base, making it difficult to achieve adequate target densities from conventional oven sources without thermal decomposition. These challenges can explain why dissociative ionization experiments on guanine are scarce despite longstanding interest in the radiation response of nucleic acid components.

Metastable dissociation experiments are invaluable for identifying fragmentation pathways as they allow fragment ions to be traced to direct dissociations of excited guanine$^+$ or to sequential dissociation processes. We applied the mapping method described by Bockova *et al* [2] to identify the dissociations that took place in a reflectron time-of-flight mass spectrometer several microseconds after multi-photon ionization. The guanine target was produced using a laser-based thermal desorption method [3] and thermal decomposition was avoided by applying the lowest desorption temperature (404±5 K) reported for an experiment on guanine to date.

The present results (Figure 1) reveal 9 new metastable dissociation pathways, as well as confirming 7 previously-reported ones [2]. Taking together the present and previous experiments, 10 different direct dissociation pathways of guanine$^+$ have now been identified experimentally, compared with just one each from previous experiments on adenine, uracil, and thymine [4,5]. The remarkably large number of different direct dissociations of guanine$^+$ is likely to be at least partly due to the variety of different tautomers in the neutral targets. This interpretation is consistent with theoretical predictions of tautomer-dependence in the dissociation pathways of guanine$^+$ [6].

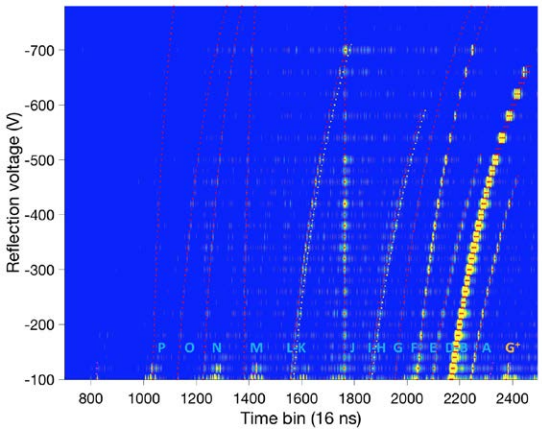

Figure 1. Reflectron TOF mass spectra of multi-photon ionized (225 nm, 7×10^6 Wcm^{-2}) guanine mapped against reflection voltage. The curved bands A-P identify dissociations that took place several microseconds after ionization. Experimental signals shown in yellow are compared with simulated bands in red.

References

[1] Zhou J *et al* 2009 *J. Phys. Chem. A* **113**(17) 4829–4832
[2] Bockova J *et al* 2019 *Int. J. Mass. Spectrom.* **442** 95-101
[3] De Camillis S *et al* 2015 *Phys. Chem. Chem. Phys.* **17** 23643–23650.
[4] Rice J M and Dudek G O 1967 *J. Am. Chem. Soc.* **89**(11), 2719–2725
[5] Rice J M and Dudek G O 1965 *J. Am. Chem. Soc.* **87**(20), 4569-4576
[6] Cheng *et al* 2010 *Phys. Chem. Chem. Phys.* **12** 4667–4677

* Presenting author daniel.bou-debes@open.ac.uk

Diagnosis for electron temperature and density of laser-produced Al-Sn alloy plasma based on optical emission spectrometry

Y Du, M G Su*, S Q He, J Z Liu, Q Min, S Q Cao, D X Sun, Y B Fu†, C Z Dong

Key laboratory of Atomic and Molecular Physics & Functional Materials of Gansu Province, College of Physics and Electronic Engineering, Northwest Normal University, Lanzhou, 730070, China

Synopsis The visible spectra of laser-produced Al-Sn alloy plasma were measured using a spatio-temporally resolved spectroscopy technique. Based on the simple structure and isolated spectral lines feature of the Al species, the corresponding electron temperature and density are diagnosed utilizing both, the Saha-Boltzmann plot method and modified semi-empirical Stark broadening formula, respectively. The evolution with time at 1.0 mm distance from the target surface is given.

The research on the transient diagnosis of laser-produced plasma (LPP) is helpful to understand the radiation characteristics and dynamic processes of atoms and ions in plasma, and its spectral diagnosis can provide information about electron temperature and density. Optical emission spectrometry is an effective and simple way to obtain the plasma parameters.

In this work, the temporally-resolved emission spectra generated by a 1064 nm wavelength with a power density of 4.5×10^{9} W/cm^{-2} is used to produce plasma from the Al-Sn alloy (Al : Sn = 1 : 1) in vacuum at 1.0 mm distance from the target. Based on the spectral lines of Al species, the corresponding electron temperature was obtained using the Saha-Boltzmann plot [1] and the electron density was determined using modified semi-empirical Stark broadening formula [2].

Fig. 1(a) and (b) give the evolution of electron temperature and density of LPP with delay time, respectively. Clearly, the electron temperature and density gradually decrease due to the expansion of plasma, and tend to be stable as the time increases. The insert figures in show the Saha-Boltzmann plot at 100 ns, and the determined temperature is 10187 K (Fig. 1(a)) and the full width at half maximum (FWHM) of Al III 355.09 nm line at 100 ns obtained by Lorentz fitting, and the determined electron density is 4.55×10^{16} cm^{-3} (Fig. 1(b)).

Based on the above analysis, we realized the diagnosis for LPP of medium- and high-Z element, that is, doping low-Z element in the target of medium- and high-Z element, and diagnosing the LPP through the isolated spectral lines from the low-Z element.

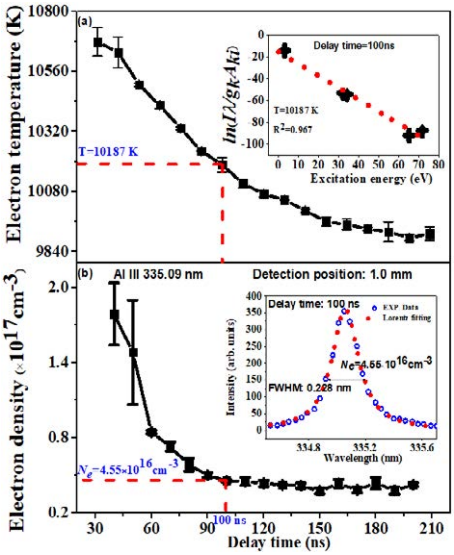

Figure 1. The evolution of electron temperature and density of laser Al plasma with delay time.

This work was supported by the National Key Research and Development Program of China (Grant no. 2017YFA0402300), the National Natural Science Foundation of China (NSFC) (Grant nos. 12064040, 11874051, 11904293, and 61965015); the Special Fund Project for Guiding Scientific and Technological Innovation of Gansu Province (2019zx-10), and the Funds for Innovative Fundamental Research Group Project of Gansu Province (20JR5RA541).

References

[1] Aguilera J A *et al* 2004 *J. Spectrochimica Acta Part B Atomic Spectroscopy* **59** 1861-1876.
[2] Heading D J *et al* 1997 *J. Phys. Rev. E* **56** 936.

* E-mail: nwnu_sumg@163.com; † E-mail: fuyb@nwnu.edu.cn

Photodetachment studies of CH^- using a cryogenic storage ring

G Eklund[1]*, M K Kristiansson[1], K C Chartkunchand[2], E K Anderson[3], M Simpson[4], H T Schmidt[1], H Zettergren[1], H Cederquist[1], and W D Geppert[1]

[1]Department of Physics, Stockholm University, Stockholm, 10691, Sweden
[2]Atomic, Molecular and Optical Physics Laboratory, RIKEN, Saitama 351-0198, Japan
[3]Department of Physics and Astronomy, Aarhus University, 8000 Aarhus C, Denmark
[4] Institut für Ionenphysik und Angewandte Physik, Universität Innsbruck, Technikerstraße 25, 6020 Innsbruck, Austria

Synopsis We perform time-dependent photodetachment spectroscopy on CH^- stored in a cryogenically cooled storage ring. Three thresholds are observed, corresponding to detachment from the first three excited rotational states. From these measurements we extract the rotational constant and electron affinity of the system. We further determine the lifetime of an excited metastable $^1\Delta$ electronic state.

We have used the electrostatic cryogenic storage ring facility DESIREE [1, 2] to study the relaxation of a beam of CH^-. The ion beam is probed using time-dependent near-threshold photodetachment spectroscopy, where the additional electron of the negative ion is removed. The resulting neutral CH are no longer confined in the storage ring, and are detected as they leave the ring (see e.g. [3]). By varying the photon energy in the vicinity of the previously observed electron affinity of CH [4], the integrated photodetachment signal as a function of photon energy is measured as shown in Figure 1, for two storage time intervals.

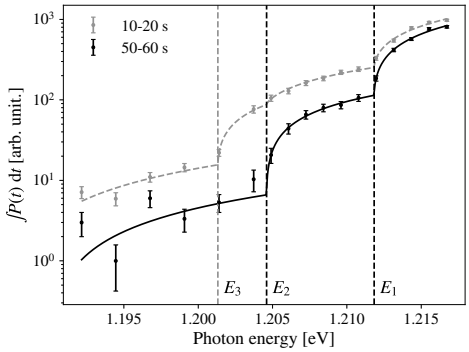

Figure 1. Integrated photodetachment signal as a function of photon energy, for two different time intervals. Three thresholds are observed, corresponding to detachment form the first three excited rotational states of CH^-.

At the 50-60 s time interval, the ions have had time to relax as they are stored in the cryogenic environment. Two distinct transitions are observed, which are assigned to detachment from the first two excited rotational states of CH^-. From the observed thresholds we are able to extract the rotational constant of the electronic ground state of CH^-, $B = 1.81 \pm 0.06$ meV, in agreement with available calculations [5]. We also determine the electron affinity of CH, $E_{EA} = 1.2155 \pm 0.0001$ eV, which is lower than previously observed [4].

CH^- has an excited electronic state of $^1\Delta$ symmetry. This state is long lived, since no electric-dipole transition to the $^3\Sigma$ ground state is possible. We perform state selective photodetachment of this state, for storage times up to 100 s, and extract a lifetime of 14.7 ± 0.3 s, which is about a factor of 2.5 longer than previously calculated [5] and measured [6].

References

[1] R D Thomas *et al* 2011 *Rev. Sci. Instrum.* **82** 065112
[2] H T Schmidt *et al* 2013 *Rev. Sci. Instrum.* **84** 055115
[3] H T Schmidt *et al* 2013 *Phys. Rev. Lett.* **119** 073001
[4] A Kasdan *et al* 1975 *Chem. Phys. Lett.* **31** 78
[5] S Srivastava and N Sathyamurthy 2012 *J. Chem. Phys.* **137** 214314
[6] M Okumura *et al* 1986 *J. Chem. Phys.* **85** 1971

*E-mail: gustav.eklund@fysik.su.se

Photoionization and MFPADS in polyatomic molecules with XCHEM

P Fernández-Milán[1] *, V J Borràs[1] †, J González-Vázquez[1] ‡ and F Martín[1,2,3] §

[1]Universidad Autónoma de Madrid, Madrid, 28049, España
[2]Instituto Madrileño de Estudios Avanzados en Nanociencia (IMDEA-Nanociencia), Madrid, 28049, España
[3]Instituto de Física de la Materia Condensada (IFIMAC), Madrid, 28049, España

Synopsis In recent years, the XCHEM methodology has been successfully applied to describe photoionization of many-electron atoms and diatomic molecules. In this communication we present the application of XCHEM to describe the photoionization of polyatomic molecules along with its MFPADS, the newest extension to the XCHEM package.

The recent XCHEM [1] code allows the study of photoionization considering the effect of electron correlation in the configuration interaction picture and taking into account the coupling between several continua.

It is especially appropriate for the study of low energy ionization, when the electron still feels the ionic core and electron correlation still plays a role; as recently shown in a study of the Hopfield resonant series in the nitrogen molecule [2].

At the core of the XCHEM method lies the hybrid Gaussian-B-spline basis [3] (GABS). It consists of a set of monocentric gaussians (MC) centered at the center of mass (CoM) of the molecule and a box of B-splines that ranges from a distance to the CoM R_0 to a sufficiently far distance R_∞. XCHEM couples this basis with the polycentric gaussian (PC) basis that results from a standard quantum chemistry calculation (QCP). The R_0 distance is chosen so that the overlap between PC gaussians and B-splines is negligible. The MC gaussians serve as a bridge communicating B-splines and PC gaussians.

The XCHEM model wavefunction is constructed by augmenting with a single electron in the GABS basis as well as in the PC guassians of the active space of the parent ions.

$$\Psi = \sum_i c_i \Xi_i + \sum_{\alpha j} c_{\alpha j} \Phi_{\alpha j} \qquad (1)$$

where Ξ represent short-range states, that come from optimizing the CI vector while maintaining the same set of orbitals. The second term represents an augmentation in each of the considered α parent ions by using all the available orbitals j, be it PC gaussians, MC gaussians or B-splines.

This model has been applied mainly to small systems: atoms like hydrogen, helium and neon [4] and diatomics as hydrogen and nitrogen. In this communication we present results for the photoionization of medium-sized molecules.

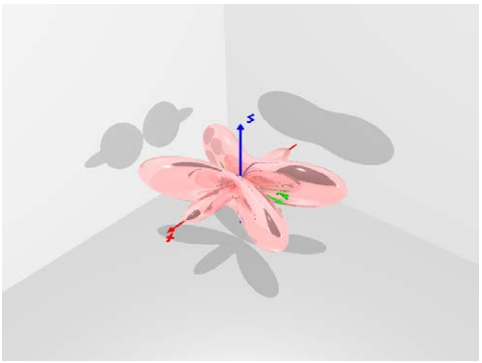

Figure 1. MFPAD for the ionization of pyrazine to the ^2A_g cation at 10.20 eV, computed with the XCHEM package.

References

[1] Marante C *et al* 2017 *J. Chem. Theory Comput.* **13** 499–514
[2] Klinker M *et al* 2018 *J. Phys. Chem. Lett.* **9** 756-762
[3] Marante C *et al* 2014 *Phys. Rev. A* **90** 012506
[4] Marante C *et al* 2017 *Phys. Rev. A* **96** 022507

*E-mail: pedro.fernandezm@uam.es
†E-mail: josep.borras@uam.es
‡E-mail: jesus.gonzalezv@uam.es
§E-mail: fernando.martin@uam.es

Time evolution of copper-aluminum alloy laser-produced plasmas in vacuum

C L Gao, Q Min*, J Z Liu, S S Hu, Y Du, Y H Wu, S Q Cao, D X Sun, C Z Dong and M G Su†

Key Laboratory of Atomic and Molecular Physics & Functional Material of Gansu Province, College of Physics and Electronic Engineering, Northwest Normal University, Lanzhou, 730070, China

Synopsis The temporal and spatial distribution characteristics for Cu and Al ions in the plasma are clarified. These results will be helpful for understanding the dynamics of the different ions during expansion of multi-element laser-produced plasma and its applications.

Only few theoretical simulations of multi-element laser-produced plasmas have been reported [1], and most of them focus on simple systems related to low Z elements. Such systems are far from meeting the requirements of analysis of practical applications. Using a program developed for multi-element laser-produced plasma simulation based on the radiation hydrodynamics model combined with experimental spectrum, ion/electron densities and plasma temperature as well as their time evolutions were obtained. The temporal and spatial distribution characteristics for Cu and Al ions in the plasma are clarified. These results will be helpful for the understanding the dynamics of the different ions during expansion of multi-element laser-produced plasma and its applications.

The spatio-temporally evolution of plasma parameters is the most effective way to accurately understand the evolution characteristics of plasma dynamics. For clarity, Fig. 6(a) and (b) shows spatial distributions of the Al and Cu particle density at time delays of 40 ns and 80 ns, respectively. From the distribution for Al ions, the number density of Al particles in the center reaches 6.79×10^{17} cm^{-3} at 40 ns, whereas the number density of Cu particles is 3.39×10^{17} cm^{-3}, the particle number density of Cu is half of that of Al. This is consistent with the initial condition given by us. Al III and II ions dominate at 40 ns, whereas Al atoms, Cu atoms, and Cu I ions are distributed relatively close to the edge of the plasma. With increasing the time delay, the plasma further expands and cools. From Fig. 6(b), the size of the plasma plume at 80 ns is nearly twice as large as that at 40 ns. Similarly, the number density of Al ions in the center falls to 4.7×10^{17} cm^{-3}, whereas that of Cu particles falls to 2.35×10^{17} cm^{-3}. Similarly, higher ionizations degrees are more distributed in the core of the plasma. While lower degrees of ionizations are distributed farther away from the target surface and closer to the edge of the plasma.

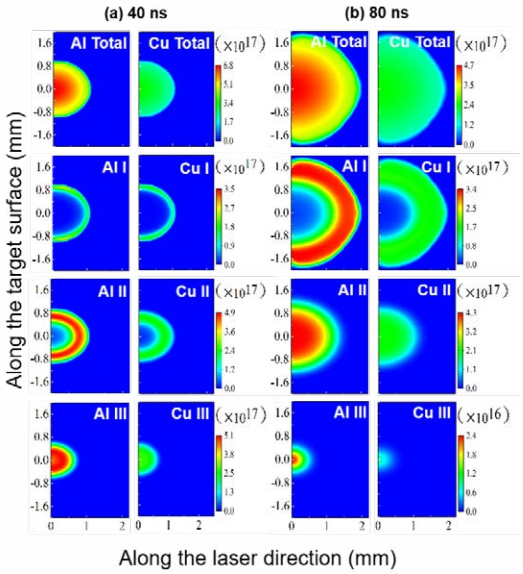

Figure 1. Spatial distributions of Al and Cu particle densities at delay times of (a) 40 ns and (b) 80 ns.

This work was supported by the National Key Research and Development Program of China (Grant no. 2017YFA0402300), the National Natural Science Foundation of China (NSFC) (Grant nos. 12064040, 11874051, 11904293, and 61965015).

References

[1] Min Q *et al* 2018 *Opt. Express* **26** 7176.

†E-mail: sumg@nwnu.edu.cn
*E-mail: mq_lpps@nwnu.edu.cn

Investigation of linear and circular photon polarizations in two-photon $2s \to 1s$ transitions in one-electron ions

V. A. Knyazeva[1]*, K. N. Lyashchenko[2] and O. Yu. Andreev[1,3]

[1]St. Petersburg State University, 7/9 Universitetskaya nab., St. Petersburg, 199034, Russia
[2]Institute of Modern Physics, Chinese Academy of Sciences, Lanzhou 730000, China
[3]Petersburg Nuclear Physics Institute named by B.P. Konstantinov of National Research Centre "Kurchatov Institute", Gatchina, Leningrad District 188300, Russia

Synopsis We have investigated the differential transition probability for two-photon $2s \to 1s$ decay in one-electron ions with respect to the polarization of the emitted photons. On the basis of the accurate relativistic calculation, we introduced a two-parameter approximation, which makes it possible to describe the two-photon angular-differential transition probability for the polarized emitted photons with high accuracy. Using this approximation we investigated the emission of photons with linear and circular polarizations. We also investigated the transition probabilities for the polarized initial and final electron states. The investigation was performed for ions with atomic numbers $1 \leq Z \leq 120$.

We investigated two-photon decay of $2s$ state of one-electron ions with atomic numbers $1 \leq Z \leq 120$. The angular distribution of the emitted photons is determined by the dominant E1E1 transitions, which gives $1 + \cos^2\theta$ distribution, where θ is the angle between the momenta of the emitted photons. The deviation from this distribution in the nonrelativistic limit was investigated in [1]. The deviation leads to an asymmetry of the angle-differential transition probability. The reason for this deviation is the interference between E1E1 and the higher multipoles (mainly E2E2 and M1M1). This asymmetry for unpolarized emitted photons investigated in [2].

Based on our relativistic calculations and works [1, 3], we introduced a two-parameter approximation, which makes it possible to describe the two-photon angular-differential transition probability for the polarized emitted photons with high accuracy. The accuracy of this approximation is 10^{-3}% for light ions, remaining within 1% even for the superheavy ions (for the photons with equal energies). Within the two-parameter approximation, the asymmetry factor determines the asymmetry of the angle-differential transition probability. The asymmetry factor calculated by the nonrelativistic formula [1] shows a significant deviation from the relativistic calculation for heavy ions. In particular, for superheavy elements, the deflection reaches 3 times. The main contribution to the asymmetry factor is made by the negative continuum of the Dirac spectrum.

*E-mail: viknyazeva16@gmail.com

For precision experiments, it can be important that a nonzero asymmetry factor, even for light ions, could be a source of nonresonant corrections [4].

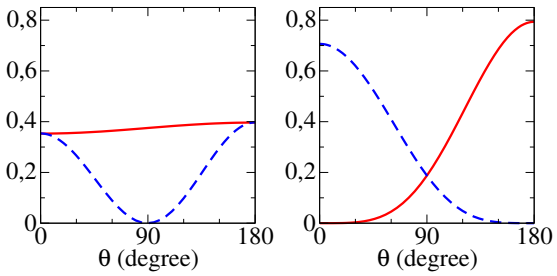

Figure 1. The normalized differential transition probabilities as a function of the angle between the momenta of the emitted photons (θ) for the photons with equal energies. In the left graph, the red solid line represents the equal linear polarizations of the photons, the blue dashed line represents the different linear polarizations of the photons. In the right graph, the red solid line represents the equal circular polarizations of the photons, the blue dashed line represents the different circular polarizations of the photons. The data are presented for uranium.

References

[1] C. K. Au, 1976 *Phys. Rev. A* **14** 531
[2] A. Surzhykov, J. P. Santos, P. Amaro, and P. Indelicato 2005 *Phys. Rev. A* **71** 022509
[3] N. L. Manakov *et al.* 2000 *Journal of Physics B* **33** 4425
[4] O. Y. Andreev, L. N. Labzowsky, G. Plunien, and D. A. Solovyev 2008 *Physics Reports* **455** 135

Experimental and theoretical studies of excited states in Ir-

M K Kristiansson[1]*, S Schiffmann[2,3], J Grumer[4], J Karls[5], N de Ruette[1], G Eklund[1], V Ideböhn[5], N D Gibson[6], T Brage[2], H Zettergren[1], D Hanstorp[5] and H T Schmidt[1]

[1]Department of Physics, Stockholm University, AlbaNova, SE-106 91 Stockholm, Sweden [2]Division of Mathematical Physics, Department of Physics, Lund University, Box 118, SE-221 00 Lund, Sweden [3]Spectroscopy, Quantum Chemistry and Atmospheric Remote Sensing (SQUARES), CP160/09, Université libre de Bruxelles (ULB), B 1050 Bruxelles, Belgium [4]Theoretical Astrophysics, Department of Physics and Astronomy, Uppsala University, Box 516, SE-751 20 Uppsala, Sweden [5]Department of Physics, University of Gothenburg, SE-412 96 Gothenburg, Sweden [6]Department of Physics and Astronomy, Denison University, Granville, Ohio 43023, USA

Synopsis Combined experimental and theoretical investigations into the binding energies and lifetimes of the excited states of Ir^- are presented.

We have used laser photodetachment to investigate anions of iridium produced in a cesium sputter ion source and stored in the cryogenic storage ring, DESIREE [1]. Due to the excellent DESIREE vacuum conditions, the ions can be stored for many hundreds of seconds, and relaxation of long lived metastable levels can thereby be studied. The iridium anion has been studied experimentally, before and the electron affinity is known to a high level of accuracy [2]. The lowest lying excited state was recently observed, and its binding energy was measured using photoelectron spectroscopy [3]. Another previous study measured the binding energy of a second excited state using two-photon spectroscopy [4].

We investigate the existence of further excited states, and study the two previously observed states and measure their lifetimes. By carefully selecting the photon energy, we can photodetach different excited states and measure their lifetimes. We locate the threshold for detachment from the lowest lying excited level and find that the binding energy agrees with a previous measurement. We find the lifetime of this excited state to be longer than the storage time of the beam of 1230 ± 100 seconds. We measure the lifetime of the second excited state investigated in [4] to be 133 ± 10 ms (see Figure 1). Finally we observe a third excited state that has previously not been predicted to be bound. We determine the lifetime of that state to be 172 ± 35 ms.

*E-mail: moa.kristiansson@fysik.su.se

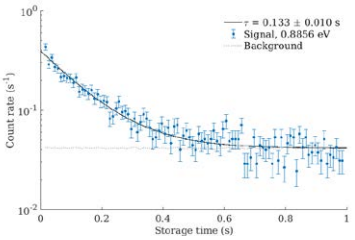

Figure 1: Photodetachment signal for the second excited state where an exponential fit gives a lifetime of 0.133 ± 0.010 s.

Complementary to our experiments, we perform fully relativistic Multi configuration Dirac-Hartree-Fock calculations in order to extract binding energies and lifetimes of the excited states. The calculations agree well with our experimental results in most cases. There are, however, some complications when more advanced correlation models are used, which motivate further developments of atomic structure computational strategies and programs for the open d- and f-shells atomic anion systems.

References

[1] Schmidt, H T, et al. Review of Scientific Instruments. 2013: 055115

[2] Bilodeau RC, et al. Physical Review A. 1999: 012505

[3] Y. Lu, et al. The Journalof Chemical Physics. 2020: 034302

[4] Thogersen J, et al. Physical Review Letters. 1996: 2870-3

Numerical simulation of the interaction between nanosecond laser and silicon target

Xingbang Liu, Qi Min*, Qiang Liu, Siqi He, Haidong Lu, Maogen Su , Chenzhong Dong

Key Laboratory of Atomic and Molecular Physics and Functional Material of Gansu Province, College of Physics and Electronic Engineering, Northwest Normal University, Lanzhou 730070, China.

Synopsis Developed a two-dimensional axisymmetric model for ns-laser ablation considering the Knudsen layer and plasma shielding effect. In particular, the evolution of target surface during laser ablation is studied.

A ns-laser ablation has been extensively applied to the micromachining [1], pulsed laser deposition, laser-induced breakdown spectroscopy (LIBS) [2], and material surface treatment [3] in recent years. The development of each application is closely related to the physical mechanism of the interaction between laser pulse, target and plasma.

A two-dimensional axisymmetric model for ns-laser ablate the silicon target is established based on the time-dependent heat transfer equation and fluid equations. Such equations are coupled by the Knudsen layer condition. The equations of state of the plasma are described by a real gas approximation, which divides the internal energy into the kinetic (thermal) energy of atoms, ions and electrons, ionization energy and the excitation energy of atoms and ions. This model is suitable for the case that the temperature of the target surface is lower than the critical temperature.

To intuitively show the temperature distribution of plasma during laser ablation, two-dimensional contour of the Si plasma temperature in *r-z* plane at 15, 20, 25 and 30 ns are shown in Fig. 1. It is clearly seen that the plasma has been formed at 15 ns and the maximum temperature has reached 1.4 eV. Therefore, the subsequent laser pulse will be absorbed by the plasma, which makes the plasma temperature continue to rise and the laser energy reaching the target surface will be reduced. At 20 ns, due to the continuous input of laser energy, the maximum temperature of the plasma reaches 3.9 eV.

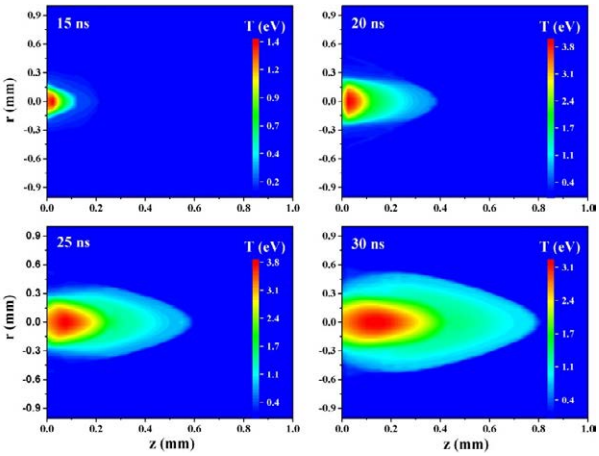

Figure 1. The temperature distributions of the Si plasma in *r-z* plane for the delay times of 15, 20, 25, and 30 ns, respectively.

This work is supported by the National Key Research and Development Program of China under Grant No.2017YFA0402300, the Natural Science Foundation of China under Grant Nos.11904293, 12064040 and 11874051.

References

[1] Dubey A K and Yadava V 2008 *Int. J. Mach. Tools Manuf.* 48 609
[2] Hahn D W and Omenetto N 2010 Appl. Spectrosc. 64 335A
[3] Musztyfaga-Staszuk M M 2017 *Int. J. Thermophys.* 38 130

* E-mail: mq_lpps@163.com

Asymmetry in emission of photons with left- and right-hand circular polarizations in two photon decay

K N Lyashchenko [1]*, V A Knyazeva [2], O Yu Andreev [2,3] and D Yu [1,4]

[1]Institute of Modern Physics, Chinese Academy of Sciences, Lanzhou 730000, China
[2]St. Petersburg State University, 7/9 Universitetskaya nab., St. Petersburg, 199034, Russia
[3]Petersburg Nuclear Physics Institute named by B.P. Konstantinov of National Research Centre Kurchatov Institute, Gatchina, Leningrad District 188300, Russia
[4]University of Chinese Academy of Sciences, Beijing 100049, China

Synopsis Two-photon decay of $2s$ state in H-like ions is investigated. We report that asymmetry in the emission of photons with left- and right-hand circular polarizations can be observed in this transition if the initial state has the certain polarization. This asymmetry can be used to measure the polarization of ion beams. In the reverse process (two-photon excitation), the asymmetry can be applied to produce polarized ion beams.

We investigated the two-photon decay of $2s$ state in H-like ions

$$2s \quad \rightarrow \quad 1s + \gamma_1 + \gamma_2 \,.$$

We show that in this process the asymmetry in the emission of the left- and right-hand photons takes place if the initial state has the certain polarization. We introduce the asymmetry parameter Ξ as

$$\Xi \quad = \quad \frac{\left| M^{--}_{m_i}(\alpha) - M^{++}_{m_i}(\alpha) \right|}{\frac{1}{2}\left(M^{++}_{m_i}(\alpha) + M^{--}_{m_i}(\alpha) \right)} \,,$$

where $M^{\lambda_1\lambda_2}_{m_i}(\alpha)$ denote the differential trantision probabilities of the two-photon decay with certain projection of the total angulat momentum of the initial $2s$ state m_i and certain circular polarizations of the emitted photons λ_1 and λ_2. The axis of quantization is defined by angle α: angle between the quantization axis and the normal to the plane formed by the photon momenta. We assume that the polarization of the final $1s$ state is not observed.

It was found that Ξ strongly depends on the energies and directions of the emitted photons as well as on the angle α. In Fig. 1 we present the asymmetry parameter Ξ for uranium ion as a function of the angle between momenta of the photons θ for $x = \frac{\omega_1}{\omega_1+\omega_2} = 0.25$, where ω_j is the energy of the photon $(j = 1, 2)$.

The left- and right-hand photons are emitted differently by ions with different polarizations what can be used in the measurement of the ion-beam polarizations. The detection of circularly polarized high-energy photons is connected with technical difficulties. It can be circumvented utilizing the following features of the two-photon decay. First, the asymmetry effect takes place even if we sum over the polarization of one of the photons. Second, the photon emission spectrum is continuous. Thus, we propose to measure the ion-beam polarization by measuring the polarization of only the low-energy photon, leaving the polarization of the high-energy photon unresolved.

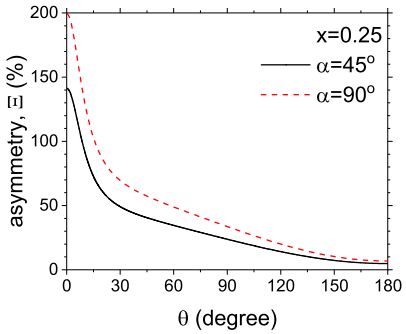

Figure 1. The asymmetry parameter Ξ as a function of the angle between momenta of the emitted photons.

Another implementation of the asymmetry effect can be found in the reverse process. The final $2s$ state can obtain polarization if the H-like ion initially being in the ground state is excited by two photons with certain circular polarizations. It can be used for the production of polarized ion beams.

*E-mail: k.n.lyashenko@impcas.ac.cn

Laser-induced ionization of ions from high brightness ion sources

F. Machalett,[1, 2, 3,*] B. Ying,[1, 2, 3] P. Wustelt,[1, 2, 3] V. Huth,[1] M. Kübel,[1, 2, 3] L. Bischoff, [4] N. Klingner,[4] W. Pilz,[4] Th. Stöhlker, [1, 2, 3] and G. G. Paulus[1, 2, 3]

[1]Institute of Optics and Quantum Electronics, Friedrich Schiller University Jena, 07743 Jena, Germany
[2]Helmholtz Institute Jena, Fröbelstieg 3, 07743 Jena, Germany
[3]GSI Helmholtz-Zentrum für Schwerionenforschung, 64291 Darmstadt, Germany
[4]Helmholtz-Zentrum Dresden-Rossendorf, 01328 Dresden, Germany

Synopsis Au and Si ions from high brightness liquid metal ion sources (LMIS) are used as ionic targets for strong-field laser interaction with femtosecond laser beams. Field ionization processes in the field emission source at electrostatic fields of some 10 V/nm allow the generation of various metallic and metalloid ion beams with charge states such as Au^{2+} and Si^{2+}. Studying the ionization in strong femtosecond laser fields with intensities of up to 10^{16} W/cm^2, we observed for these elements charge states of up to of Au^{11+} and Si^{4+}.

Using ionic laser targets enables to investigate interesting fundamental systems of light-matter interaction, such as He^+, H_2^+[1] and molecules that only arise in the ion source, e.g. HeH^+ [2]. In this work we generated ion beam targets for the investigation of strong-field laser interactions with metal and metalloid ions. To increase the density of these targets we adapted a high-brightness liquid metal ion source (LMIS), oiginally applied in focused ion beam systems [3,4], to an ion bam system for 3D coincidence momentum spectroscopy. The ions are emitted from a liquid Au-Si eutectic alloy and are generated by electrostatic field evaporation and field ionization. Using an E x B-Filter in the beamline, several different ion species could be detected: Si^{2+}, Si^+, Au^{2+}, Au^+, Au_2^+, Au_3^+ and Au_3^{2+}. The monoatomic and noble metal molecular ions are now available to carry out studies on ultrafast laser-induced fragmentation and ionization.

We investigated the ultrafast laser-induced ionization resulting in higher charge states after the multiple ionization of Au^+ and Si^{2+} ions. Laser intensities of up to 10^{16} W/cm^2 allow the observation of up to 10-times ionization of the Au^+-ions and three-times ionization of Si^{2+}-ions. By utilizing two-color sculpted laser fields to control the double ionization process on the attosecond time scale, we confirmed the resolution of the recoil ion momenta for the detection of heavy atoms.

Our results demonstrate that the manifold of emerged experimental techniques of attosecond physics can be extended to the until now rarely explored range of various metal and metalloid targets.

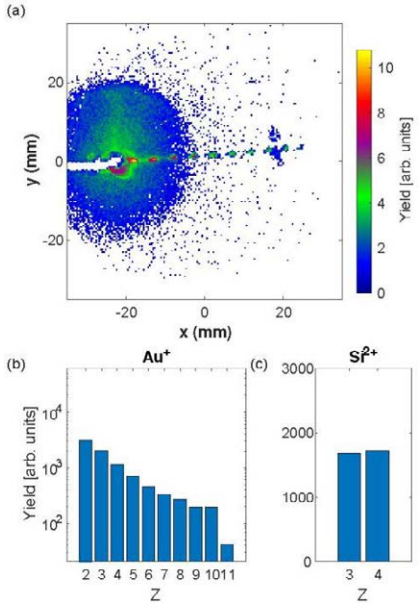

Figure 1. Multiple ionization of singly charged gold and doubly charged dsilicon ions: (a) Position-resolved detection of the laser-induced higher charge states after multiple ionization of Au^+ at an intensity of $3 \cdot 10^{16}$ W/cm^2. Different charge states are separated by horizontal and vertical electric fields after the laser interaction. The Au^+-beam is blocked by a Faraday cup before the detector. The structure around the Faraday cup is produced by fragments from gold molecules. (b) and (c) relative yields of different charge states for Au and Si respectively.

References

[1] T. Rathje, et al., *Phys. Rev. Lett.* **111**, 093002 (2013).
[2] P. Wustelt, et al., *Phys. Rev. Lett.* **121**, 073203 (2018).
[3] F. Machalett, P. Seidel, Focused Ion Beams and Some Selected Applications, EAP, Wiley 2019.
[4] L. Bischoff, et al., *Appl. Phys. Rev.* **3**, 021101 (2016).

* E-mail: info@nanovativ.de

Photodetachment studies of the metastable states of Si^- ions at the Cryogenic Storage Ring

D Müll[1]*, F Grussie[1], K Blaum[1], S George[1], J Göck[1], M Grieser[1], R von Hahn[1], Z Harman[1], Á Kálosi[2,1], C H Keitel[1], C Krantz[1], C Lyu[1], O Novotný[1], F Nuesslein[1], D Paul[1], V C Schmidt[1], S Singh[1], S Sunil Kumar[1,3], X Urbain[4], A Wolf[1], and H Kreckel[1]

[1]Max-Planck-Institut für Kernphysik, 69117 Heidelberg, Germany
[2]Columbia Astrophysics Laboratory, Columbia University, New York, 10027 USA
[3]Department of Physics and Center for Atomic, Molecular, and Optical Sciences and Technologies, Indian Institute of Science Education and Research (IISER) Tirupati, 517507, India
[4]Institute of Condensed Matter and Nanosciences, Université Catholique de Louvain, Louvain-la-Neuve B-1348, Belgium

Synopsis We used the Cryogenic Storage Ring (CSR) at the Max Planck Institute for Nuclear Physics to carry out detailed studies of the lifetimes of metastable states of silicon anions. We make use of the long storage times and reduced blackbody radiation field inside the CSR to monitor the decay of the long-lived ^2D-states as well as the weakly-bound ^2P-states, for which we find a lifetime of ∼22 s. Furthermore, we employ the Multi-Configuration Dirac–Hartree–Fock (MCDHF) formalism for updated calculations of the radiative lifetimes, which show very good agreement with the present measurements.

We have used the Cryogenic Storage Ring (CSR) [1] to study the metastable states of the silicon anion. The Si^- ions were produced in a sputter ion source, accelerated to 58 keV kinetic energy, and stored in the ultra-high cryogenic vacuum of the CSR, using only electrostatic deflection elements. We used several continuous-wave laser systems at various wavelengths and a tunable pulsed Optical Parametric Oscillator (OPO) laser to obtain information about the decay of the metastable anionic states by selective photodetachment. Our data shows evidence for the existence of very long-lived metastable ions with lifetimes of several hours, which we attribute to the ^2D metastable states. Coincidence counting with the pulses of the OPO laser at 2450 nm reveals very weakly-bound and sparsely-populated metastable states with a lifetime of ∼ 22 s that we assign to the ^2P-levels, as their predicted binding energy is very close to the neutral ground state. Moreover, we compare our experimental results to state-of-the-art calculations using the MCDHF approach to derive the radiative lifetimes of all metastable states of Si^-. While previous theoretical work [2, 3] shows considerable deviations from our experimental results, our updated independent calculations agree very well with the experimentally observed decay of the metastable signals.

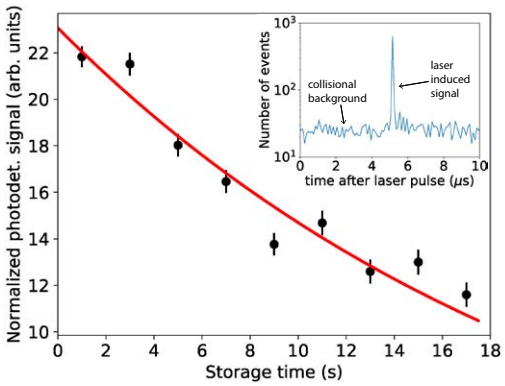

Figure 1. Background-subtracted normalized photodetachment signal obtained using the pulsed OPO laser. The laser was operated at 2450 nm to photodetach exclusively the weakly-bound ^2P states. The red line shows a single exponential fit, yielding a lifetime $\tau = (22.2 \pm 2.5)$ s. Inset: Neutral counts as a function of time after the laser pulse.

References

[1] von Hahn R *et al* 2016 *Rev. Sci. Instr.* **83** 023201
[2] O'Malley S M, Beck D R *J. Phys. B: At. Mol. Phys.* **35** 4301
[3] Andersson P *et al* 2006 *Phys. Rev. A* **73** 032705

*E-mail: damian.muell@mpi-hd.mpg.de

Cooling dynamics of C_{60}^- in new time domains

J.E. Navarro Navarrete[1]*, M. Kristiansson[1], M. Gatchell[1], H. Cederquist[1], H.T. Schmidt[1], and H. Zettergren[1]

[1]Department of Physics, Stockholm University, SE-114 21, Stockholm, Sweden

Synopsis A study of spontaneous and laser induced decays of C_{60}^- has been performed in DESIREE with the aim to follow the cooling dynamics in new time domains.

Astronomical observations and gas phase spectroscopic studies have proven that fullerenes exists throughout the interstellar media (ISM) [1]. How they are formed and survive are outstanding and unsolved follow-up questions. To address the latter, the knowledge of the cooling rates of these clusters is of outmost importance in order to benchmark statistical models describing their survival probabilities in the ISM [2].

We have performed studies of C_{60}^- at the cryogenic electrostatic ion storage ring facility DESIREE. By taking advantage of the excellent vacuum conditions, the spontaneous and laser induced decays can be followed on longer time scales compared to room temperature devices [3].

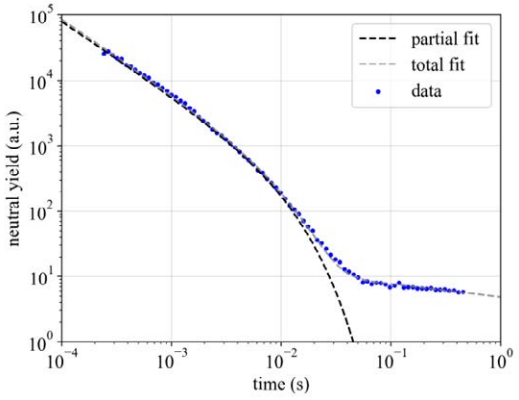

Figure 1. A typical spontaneous decay curve fitted with a quenched power law ($\propto t^{p1}e^{-t/\tau}$) up to 10 ms (black dotted line). The fitted parameters are p_1 = -1.138(3) and τ = 10.5(1) ms.

A typical spontaneous decay curve is shown in Figure 1. On short timescales, ranging up to a few ms, a power law decay (close to 1/t) is observed, as expected for a broad internal energy distribution for which electron emission is the dominating decay process. After approximately 5 ms and consistent with [3], the decay is quenched. This is attributed to a radiative cooling process with a characteristic time of 10 ms.

Furthermore, we have performed pilot studies of laser induced decays in DESIREE on timescales ranging up to 10 s using a similar technique as in the room temperature measurements reported by Sundén *et. al.* [3,4]. In this approach a single photon is absorbed by the cluster in order to shift up its energy distribution by the same amount of energy as the absorbed photon. This leads to an enhanced delayed signal that provides an absolute energy scale over time from which energy loss rates can be determined. By performing these types of experiments in DESIREE we aim to provide information about the absolute electron emission rates in new time domains.

References

[1] E.K. Campbell *et.al.* Nature **523,** 322-323 (2015)
[2] O. Berné *et.al.* A&A **550**, 4 (2013)
[3] A. E. K. Sundén *et al.* Phys. Rev.Lett. **103**, 143001 (2009)
[4] K. Hansen Phys. Rev. A **102**, 052823 (2020)

* E-mail: jose.navarrete@fysik.su.se

Multiple Photodetachment of Silicon Anions at the Si K-Edge

A Perry-Sassmannshausen[1]*, T Buhr[1], M Martins[2], S Reinwardt[2], F Trinter[3,4], A Müller[5], S Fritzsche[6,7] and S Schippers[1]†

[1]I. Physikalisches Institut, Justus-Liebig-Universität Gießen, 35392 Gießen, Germany
[2]Institut für Experimentalphysik, Universität Hamburg, 22761 Hamburg, Germany
[3]Institut für Kernphysik, Goethe-Universität Frankfurt am Main, 60438 Frankfurt am Main, Germany
[4] Molecular Physics, Fritz-Haber-Institut der Max-Planck-Gesellschaft, 14195 Berlin, Germany
[5]Institut für Atom- und Molekülphysik, Justus-Liebig-Universität Gießen, 35392 Gießen, Germany
[6]Helmholtz-Institut Jena, 07743 Jena, Germany
[7]Theoretisch-Physikalisches Institut, Friedrich-Schiller-Universität Jena, 07743 Jena, Germany

Synopsis We report on new measurements of m-fold photodetachment ($m = 3, \ldots, 6$) of silicon anions via K-shell excitation and ionization. The experiments were carried out using the photon-ion merged-beams setup PIPE at the PETRA III synchrotron light source. Previous studies were confined to L-shell detachment. Our new experimental data extend to photon energies of up to 1900 eV. They exhibit two resonances, with one of them only visible in the detachment channels with $m \geq 4$. We also carried out theoretical calculations which account for all fine-structure excitations and show quite good agreement with the experiment.

Negative atomic ions are of great fundamental interest because the extra electron is bound by a short-range attractive force due to the polarization of the atomic core, i.e., solely by correlation effects. The inner-shell photoionization dynamics in these ions is particularly rich since the valence electron is subject to strong relaxation effects upon creation of the core hole. Following up on previous experiments with O^- [1], F^- [2], and C^- [3] ions, we report here on multiple photodetachment of Si^- ions via K-shell excitation and ionization. Previous studies on photodetachment of silicon anions were restricted to L-shell detachment [4].

In the present study, which is the first addressing K-shell detachment of an anion with M-shell valence electrons, we investigated multiple ($m = 3, \ldots, 6$) photodetachment of silicon anions with photon energies between 1830 and 1900 eV. The data for triple-detachment exhibit one rather broad maximum at ∼1839 eV as shown in Fig. 1. In the other detachment channels, which are not shown in the figure, one additional maximum at about 1842 eV is visible. Our accompanying theoretical calculations suggest that the observed resonance features consist of several fine-structure components.Good agreement between experiment and theory has been achieved for the absorption cross section. To predict the final charge-state distributions, cascade calculations were performed in addition, which still leave room for some improvement. We thank the beamline team, K. Bagschik, F. Scholz, J. Seltmann, and M. Hoesch, for assistance in using beamline P04. This research was funded by BMBF (Grant Nos. 05K19GU3 and 05K19RG3) and from DFG (Project No. Schi 378/12)

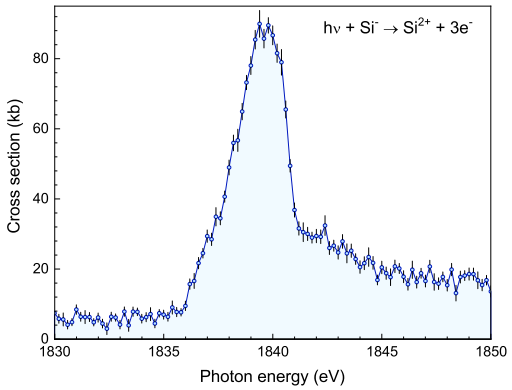

Figure 1. Measured cross section for triple-photodetachment of $Si^-(1s^2\,2s^2\,2p^6\,3s^2\,2p^3)$ ions.

References

[1] Schippers S *et al* 2016 *Phys. Rev. A* **94** 041401(R)
[2] Müller A *et al* 2018 *Phys. Rev. Lett.* **120** 133202
[3] Perry-Sassmannshausen A *et al* 2020 *Phys. Rev. Lett.* **124** 083203
[4] Schrange-Kashenock G 2016 *J. Phys. B: At. Mol. Opt. Phys.* **49** 115201

*E-mail: alexander.perry-sassmannshausen@physik.uni-giessen.de
†E-mail: stefan.schippers@physik.uni-giessen.de

Nonlinear resonances in the motion of ions in the linear Paul trap

K Pleskacz*, Ł Kłosowski and M Piwiński

Institute of Physics, Faculty of Physics, Astronomy and Informatics, Nicolaus Copernicus University in Toruń, Grudziądzka 5, 87-100 Toruń, Poland

Synopsis Nonlinear resonances were observed as the ions' escape from the trapping region which is caused by rapid increase of their kinetic energy gained from the electric field of the trap. Numerical simulation for different trapping conditions were carried out to compare trajectories of ions in the trap. Fourier transform was applied to determine and compare the characteristic frequencies of ion motion. Numerical simulations data will be presented and discussed with the experimental results.

Paul traps use alternating electric field with radio frequency Ω, which in combination with quadrupole trap geometry, provide trapping potential with eigenfrequency ω. In a system with perfect layout, quadrupole potential would be created. In the real trap, imperfections in the geometry lead to multipoles of higher orders in the quadrupole potential. These limitations cause formation of nonlinear resonances in the motion of ions in the potential of the trap. Such phenomena can be observed as the ions' escape from the trapping region at certain conditions, expressed with two dimensionless stability parameters a and q, which can be used to plot a stability diagram. The resonances occur at q and a values, where Mathieu equation solutions are stable. In the stability diagram they form characteristic lines which were observed experimentally and discussed in our previous work [2].

The numerical simulations for different trapping conditions were carried out to obtain trajectories of ion (Fig 1a, 1b and 1c). Fourier analysis of motion spectra was performed. The differences between spectra in frequency domain allowed the identification of conditions corresponding to the nonlinear resonances. The discrepancies between adiabatic approximation and numerical simulation data are observed (Fig 1d) and will be discussed in the poster.

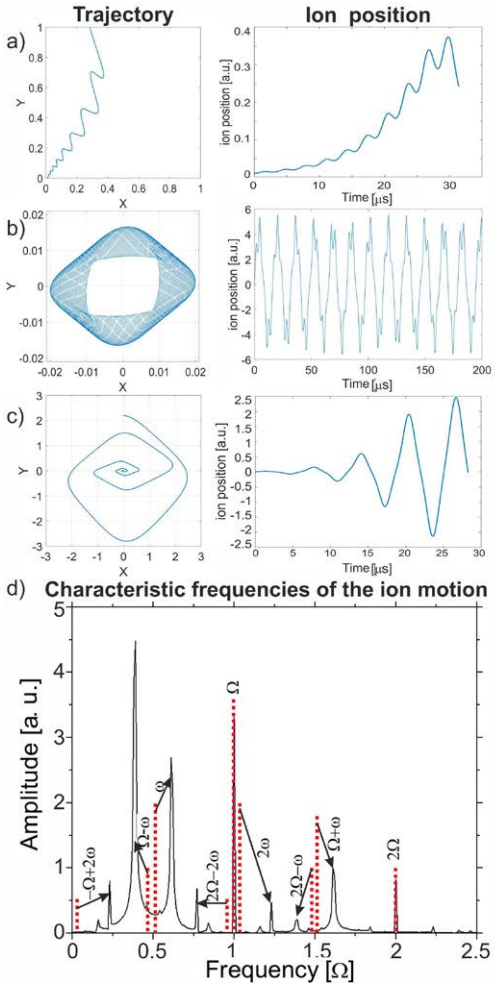

Figure 1. The numerical simulation for different trapping conditions. Ion trajectory and position of ion in one direction in the trapping potential: a) below stability region (low q value), b) stable conditions, c) above stability region (high q value). Item d) presents spectra in frequency domain of ion motion in the trap. Frequencies associated with radio (Ω) and eigenfrequency (ω) are presented: ——— simulation data, ····· adiabatic approximation.

* E-mail: pleskacz@doktorant.umk.pl

References

[1] Major F *et al.* 2005 *Springer* Charged Particle traps

[2] Kłosowski Ł *et al.* 2018 *J. Mass Spectrom.* **53,** 541-547

HILITE - stored ions for non-linear laser-ion experiments

S. Ringleb[1] *, N. Stallkamp[1,2] †, M. Kiffer[1], B. Arndt[3], S. Kumar[4], G. G. Paulus[1,5], W. Quint[2,6], Th. Stöhlker[1,2,5], M. Vogel[2]

[1]Friedrich-Schiller-Universität, 07743 Jena, Germany
[2]GSI Helmholtzzentrum für Schwerionenforschung GmbH, 64291 Darmstadt, Germany
[3]Goethe Universität Frankfurt, 60323 Frankfurt, Germany
[4]Inter-University Accelerator Centre, 110067 New Delhi, India
[5]Helmholtz-Institut Jena, 07743 Jena, Germany
[6]Ruprecht Karls-Universität Heidelberg, 69120 Heidelberg, Germany

Synopsis We present a Penning trap setup which is designed to prepare a well-defined and pure ion target for experiments with high-intensity and high photon-energy lasers. The setup is equipped with an external ion source which is capable of producing bunches of a highly charged ions. In experiments at the FLASH laser facility we observed interactions of trapped ions with high-energy photons.

The development of free-electron lasers with photon energies in the XUV to X-ray regime opens up new possibilities to investigate non-linear laser-matter interaction. Particularly, the K-shell electrons of certain ions are accessible by multi-photon ionisation. Here, ionic systems with only one active electron are of particular interest - especially hydrogen-like systems. In these systems, ionisation cross sections can be predicted by theoretical models with little computational effort and can be hence compared with the experimental values. It is also possible to measure the laser intensity in case the ionisation cross sections are known.

To this end, we have built, commissioned and operated the HILITE (**H**igh-**I**ntensity **L**aser **I**on-**T**rap **E**xperiment) Penning trap. The trap of the so-called *open-endcap* design allows both laser and ion access from outside (figure 1a). The ions are produced externally by an Electron-Beam Ion Trap (EBIT), selected by a Wien filter, and captured dynamically in the trap centre [1].

For example, C^{2+} and C^{5+} ions have been captured, detected inside the ion trap and stored for roughly a quarter of an hour. In addition, we have characterised the ion trap content destructively after ion ejection using time-of-flight spectroscopy. For ion-cloud formation, a cycle time of less than one minute is aspired, for which the current storage time is sufficient. Last year we have moved the HILITE Penning trap to a photon user facility for the first time, in the present case FLASH at DESY in Hamburg. We have connected both systems and brought the trap back in operation successfully. We have had to deal with unexpected bad vacuum conditions which has allowed us only the storage of C^{2+} - ions for a short time. We have used the 10 Hz master clock of the FLASH FEL to synchronise the ion capture, ejection and detection procedure with the laser pulses. During laser-ion interaction, the ions have been located about 20 mm around the trap centre in axial direction where the laser waist diameter has been nearly constant. This allowed for a good overlap of the stored ions with a laser focus of a well-known shape. The interaction of the laser with the stored ions has lead to loss of the initially stored C^{2+} ions which can be assigned to laser ionisation (figure 1b).

We will present the setup, the commissioning results and results from our first beamtime. We will also present envisaged upgrades of the setup.

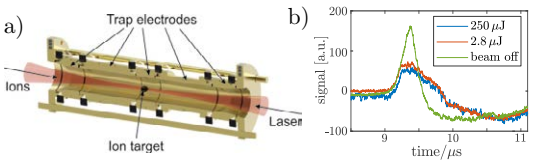

Figure 1. a) Experiment principle. Ions are stored in the trap and irradiated by an intense laser. b) Comparision of the time-of-flight signals of the ejected ions with and without laser interaction.

References

[1] Stallkamp N *et al* 2020 *X-Ray Spectrom* **49**(2020) 188-191

*E-mail: stefan.ringleb@uni-jena.de
†E-mail: n.stallkamp@hi-jena.gsi.de

Photodetachment cross sections and radiative lifetimes of the metastable states of Si^- ions

S Singh[1*], C Lyu[1†], Z Harman[1], and C H Keitel[1]

[1]Max Planck Institute for Nuclear Physics, 69117 Heidelberg, Germany

Synopsis The objective of the present work is to calculate the photodetachment cross sections, electron affinities, transition energies, and radiative lifetimes of all the metastable states of Si^- ions by using the Multiconfiguration Dirac-Hartree-Fock (MCDHF) approach. The present results are compared with recent experiments and other theoretical works.

Negative atomic ions attract growing attention from experimentalists as well as theorists, as they prove to be a benchmark system to study electronic structures. Since the outermost electron is weakly bound to the neutral atom, correlation effects dominantly determine the structure of the anions. This poses a challenge in computing structural and dynamical properties. Thus, so far there have been very few theoretical studies of photodetachment of negative ions beyond the first row of the periodic table.

In this work we have calculated photodetachment cross sections, electron affinities, fine-structure splittings, transition energies and radiative lifetimes of all the metastable states of the Si^- ion. All atomic state functions for the description of the neutral atoms as well as the negatively charged Si^- ions have been generated by means of the Multiconfiguration Dirac-Hartee-Fock (MCHDF) method [1]. Here, we have used the grasp2K [2] and RATIP codes [3] to carry out dedicated calculations of the photodetachment cross section of all anionic states of Si^- at two specific photon energies, namely, at 0.89 eV and 1.95 eV. The choice of the photon energies is motivated by very recent low-background measurements with the Cryogenic Storage Ring (CSR) of the Max Planck Institute for Nuclear Physics in Heidelberg, Germany. To independently predict the electron affinities, fine-structure splittings, transition energies and radiative lifetimes we have used the MCDHF method in combination with the relativistic configuration interaction approach. These calculations were performed using the GRASP2018 code [1], performing a systematic expansion of the atomic states in terms of a large number of configuration state functions to obtain accurate predictions.

The calculations are compared with the recent experiments [4] and other theoretical works. Detailed results will be presented during the conference.

* E-mail: suvamsingh18sep@gmail.com
† E-mail: lyu@mpi-hd.mpg.de

References

[1] Fischer C F *et al* 2019 *Comput. Phys. Commun.* **237** 184
[2] Jönsson P *et al* 2007 *Comput. Phys. Commun.* **177** 597
[3] Fritzsche S 2012 *Comput. Phys. Commun.* **183** 1525
[4] Müll D *et al* 2020 submitted

Measurement and analysis of the emission spectrum of laser-produced Zn plasma in the range of 7-14 nm

S Q He, M G Su*, Y Du, H Y Li, H D Lu, S Q Cao, Q Min, D X Sun and C Z Dong†

Key laboratory of Atomic and Molecular Physics & Functional Materials of Gansu Province, College of Physics and Electronic Engineering, Northwest Normal University, Lanzhou, 730070, China

Synopsis We measured and analyzed the emission spectrum of laser-produced Zn plasmas in the range of 7-14 nm. The dominant transition arrays were identified as $3p^63d^n$-$3p^63d^{n-1}f$ from Zn^{6+} to Zn^{9+} ions with aid of the Hartree-Fock calculations with configuration interaction effects. The plasma parameters have been obtained by comparison of experimental and simulated spectrum based on a steady-state collisional-radiative (CR) model.

Highly charged ions of the middle- and high-Z elements exist widely in astrophysical, fusion plasmas and laboratory plasmas. Spectral structure analysis of highly-charged ions ablated by high power laser pulse can reveal abundant information on plasmas, such as electron temperature, electron/ion density, particle and energy transport, and the evolution of these parameters.

In the present work, we observed the EUV spectrum of laser produced Zn plasma in the 7-14 nm wavelength range. The 3d-4f resonance transition arrays from Zn^{6+} to Zn^{9+} ions dominate the spectrum, which has been identified with the aid of the Hartree-Fock method with configuration interaction (HFCI) using Cowan's codes [1]. Table 1 shows the wavelength range together with the number of transition lines. Our calculation predicted that the contribution of $3p^63d^n$-$3p^63d^{n-1}$ mf (m=5-7) transitions from Zn^{6+} to Zn^{9+} is very small in this region. Whowever, lines that arose from the $3p^63d^n$-$3p^63d^{n+1}$ transitions of Zn^{6+} to Zn^{9+} are overlapping and concentrated in 12-16 nm.

Table 1. The wavelength range and number of lines of 3d-4f from Zn^{5+} to Zn^{9+} ions.

Ions	Wavelength range(nm)	Number of lines
Zn^{5+}	12.89-17.62	2380
Zn^{6+}	11.25-15.63	4492
Zn^{7+}	9.66-12.70	4376
Zn^{8+}	8.55-10.76	2369
Zn^{9+}	7.63-9.12	676

The plasma parameters were estimated by comparing experimental and simulated spectra, based on the assumption of a normalized Boltzmann distribution among excited states and a steady-state collisional-radiative model [2]. The experimental spectrum, simulated spectra and ion fractions are shown in **Figure** 1. The results provide further understanding of radiation properties of highly charged ions of the middle- and high-Z elements.

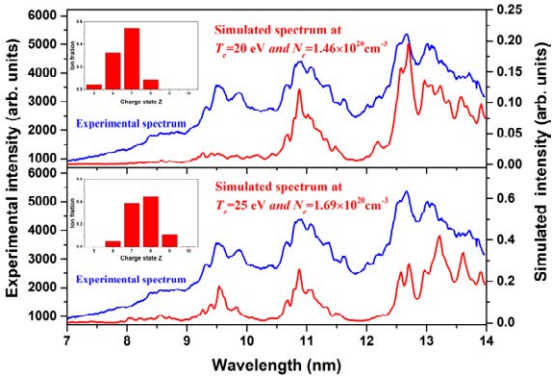

Figure 1. Comparisons between the experimental spectrum and simulated spectra.

This work is supported by the National Key Research and Development Program of China (Grant no. 2017YFA0402300), the Natural Science Foundation of China (NSFC) (Grant nos. 11874051, 11564037, 61741513). the Special Fund Project for Guiding Scientific and Technological Innovation of Gansu Province (2019zx-10), and the Funds for Innovative Fun-damental Research Group Project of Gansu Prov-ince (20JR5RA541).

References

[1] Cowan R D 1991 *The Theory of Atomic Structure and Spectra*(Berkeley, CA: University of California Press).

[2] Colombant D *et al* 1973 *J. Appl. Phys.* **44** 3524.

* E-mail: nwnu_sumg @163.com
† E-mail: dongcz@nwnu.edu.cn

Redefined vacuum approach and gauge-invariant subsets in two-photon-exchange diagrams

R. N. Soguel[1,2,3]*, A. V. Volotka[4], E. V. Tryapitsyna[5], D. A. Glazov[5], V. P. Kosheleva[1,2,3], and S. Fritzsche[1,2,3]

[1]Theoretisch-Physikalisches Institut, Friedrich-Schiller-Universität Jena, Jena, 07743, Germany
[2]Helmholtz-Institut Jena, Jena, 07743, Germany
[3]GSI Helmholtzzentrum für Schwerionenforschung GmbH, Darmstadt, 64291 Germany
[4]Department of Physics and Engineering, ITMO University, St. Petersburg, 197101, Russia
[5]Department of Physics, St. Petersburg State University, St. Petersburg, 199034, Russia

Synopsis The two-photon-exchange diagrams for atoms with single valence electron are investigated. Calculation formulas are derived for an arbitrary state within the rigorous bound-state QED framework utilizing the redefined vacuum formalism. The redefined vacuum approach enables the identification of eight gauge-invariant subsets and, thus, efficiently check the consistency of the obtained results. The gauge invariance of found subsets is demonstrated both analytically (for an arbitrary state) as well as numerically for $2s$, $2p_{1/2}$, and $2p_{3/2}$ valence electron in Li-like ions.

The treatment of the interelectronic interaction remains a cornerstone for accurate theoretical predictions of the energy levels in many-electron atoms or ions. Within the bound-state QED, the interelectronic interaction is usually treated perturbatively as an expansion over the number of exchanged photons. Recent review by Indelicato [1] suggests the necessity to extend the two-photon-exchange computations to systems with more complicated electronic structures. Derivations performed so far used zeroth-order many-electron wave-function constructed as a Slater determinant (or sum of Slater determinants) with all electrons involved [2, 3, 4]. Such a derivation becomes increasingly difficult for many-electron systems. The vacuum redefinition in QED, which is extensively used in MBPT to describe the states with many electrons involved, could be a path towards an extension of two-photon-exchange calculations to other ions and atoms.

The employment of the redefined vacuum approach allowed us to identify the gauge-invariant subsets at two- and three-electron diagrams and separate between the direct and exchange contributions at two-electron graphs. The possibility of checking the gauge invariance allows us to control the correctness of the derived expressions and verify the numerical calculations by comparing the results for each identified subset in different gauges. Moreover, the identification of gauge-invariant contributions within this approach paves the way for calculating the higher-order corrections, which can be split into gauge-invariant subsets and tackled one after the other.

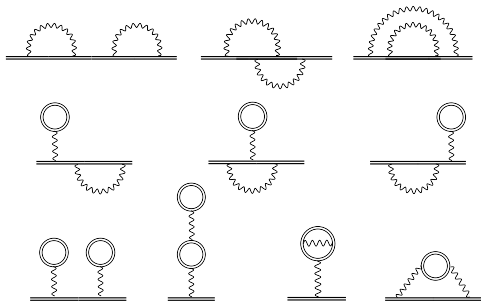

Figure 1. One-electron two-loop Feynman diagrams. Double lines indicate electron propagators in the external potential V. Wavy line corresponds to the photon propagator.

References

[1] P. Indelicato 2019 *J. Phys. B.* **52** 232001
[2] S. A. Blundell *et al* 1993 *Phys. Rev. A* **48** 2615
[3] V. M. Shabaev *et al* 1994 *Phys. Rev. A* **49** 4489
[4] J. Sapirstein *et al* 2015 *Phys. Rev. A* **91** 062508

*E-mail: romain.soguel@uni-jena.de

Coulomb corrections to Delbrück scattering

J Sommerfeldt[1,2]*, R A Müller[1,2], V A Zaytsev[3], A V Volotka[4], and A. Surzhykov[1,2]

[1]PhysikalischTechnische Bundesanstalt, D38116 Braunschweig, Germany
[2]Technische Universität Braunschweig, D38106 Braunschweig, Germany
[3]Department of Physics, St. Petersburg State University, 199034 St. Petersburg, Russia
[4]Helmholtz Institute Jena, D07743 Jena, Germany

Synopsis We present an efficient theoretical approach to calculate amplitudes for Delbrück scattering which accounts for the interaction with the nucleus to all orders including the Coulomb correction.

Delbrück scattering is the process in which a photon is elastically scattered by the Coulomb field of a nucleus or ion via the production of virtual electron-positron pairs.

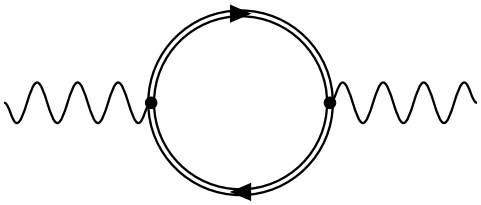

Figure 1. Leading order Feynman Diagram for Delbrück scattering.

It is one of the few non-linear quantum electrodynamical processes that can be observed experimentally [1]. However, despite the strong motivation for the theoretical analysis of Delbrück scattering, most of the previous studies have been limited to approximations regarding the coupling between the virtual electron positron pairs and the nucleus. For example, many authors have used the first order Born approximation which neglects terms of the order $(\alpha Z)^4$ and higher in the amplitude [2, 3]. The accuracy of this approximation wanes for higher nuclear charges which are of particular experimental interest. Other methods, like the high-energy large- and small-angle approximation, also have strong limitations on the parameter regimes in which they are applicable [4].

In this contribution, therefore, we present an efficient approach to calculate amplitudes for Delbrück scattering. Our formalism is based on the exact analytical Dirac-Coulomb Green's function and, hence, accounts for the interaction with nucleus to all orders including the Coulomb corrections. The numerical convergence is accelerated by solving the radial integrals analytically to all orders in the asymptotic case. Numerical results for the angle differential cross section of Delbrück scattering are presented which, by comparing them with the first order calculations, suggest that our method can produce accurate results for arbitrary scattering angles within a reasonable computation time.

Acknowledgments

This work is supported by the GSI Helmholtz Centre for Heavy Ion Research under the project BSSURZ1922 and by the DFG under the project SU658/4-1.

References

[1] Jarlskog G *et al* 1973 Phys. Rev. D **8**, 3813-3823
[2] Papatzacos P and Mork K 1975 Phys. Rev. D **12**, 206218
[3] Bar-Noy T and Kahane S 1977 Nuclear Physics A 288, 132140
[4] Falkenberg *et al* 1992 Atomic Data and Nuclear Data Tables 50, 127

*E-mail: jonas.sommerfeldt@ptb.de

Measurements of the 2*s*-2*p* transitions in stored and cooled relativistic $^{12}C^{3+}$ ions by means of laser spectroscopy

D Winters[1*], M Bussmann[2], A Bußß[3], C Egelkamp[3], L Eidam[4], V Hannen[3], ZQ Huang[5], D Kiefer[4], S Klammes[1,4], Th Kühl[1,6,7], M Loeser[2], X Ma[5], W Nörtershäuser[4,8], H-W Ortjohann[3], R Sanchez[1], M Siebold[2], Th Stöhlker[1,6,9], J Ullmann[4,6,8], J Vollbrecht[3], Th Walther[4,8], HB Wang[5], Ch Weinheimer[3], D Winzen[3]

[1]GSI Helmholtzzentrum für Schwerionenforschung GmbH, 64291 Darmstadt, Germany
[2]Helmholtzzentrum Dresden-Rossendorf, 01328 Dresden, Germany
[3]Westfälische Wilhelms-Universität, 48149 Münster, Germany
[4]Technische Universität Darmstadt, 64289 Darmstadt,Germany
[5]Institute of Modern Physics Chinese Academy of Sciences, 730000 Lanzhou, China
[6]Helmholtz Institut Jena, 07743 Jena, Germany
[7]Johannes Gutenberg-Universität, 55099 Mainz, Germany
[8]Helmholtz Forschungsakademie Hessen für FAIR (HFHF), Campus Darmstadt, Germany
[9]Friedrich-Schiller-Universität, 07737 Jena, Germany

Synopsis The 2*s*-2*p* transitions in stored and cooled Li-like carbon ions were measured by means of laser spectroscopy at the Experimental Storage Ring of the GSI Helmholtzzentrum für Schwerionenforschung in Darmstadt, Germany, for a relativistic velocity of β=0.47 (γ=1.13). Using a new cw UV laser system (257 nm) and a novel XUV photon detection system, the 2*s*-2*p* transition wavelengths were determined with a relative precision of $\Delta\lambda/\lambda$=8.4x10^{-6} and compared with earlier experimental data and with theoretical calculations.

As part of the preparations for future laser experiments at FAIR, a commissioning beam-time with Li-like carbon ions at the Experimental Storage Ring (ESR) at GSI Helmholtzzentrum für Schwerionenforschung GmbH in Darmstadt was carried out. This allowed for tests of two new UV (257 nm) laser systems [1,2] and one novel XUV photon detection system [3]. Such laser and detection systems will also be used for laser cooling of bunched relativistic ion beams at the heavy-ion synchrotron SIS100. During the test beam-time, the $^2S_{1/2}$ – $^2P_{1/2}$ and $^2S_{1/2}$ – $^2P_{3/2}$ transition wavelengths in $^{12}C^{3+}$-ions were measured by means of precision laser spectroscopy. These transitions are of interest for atomic structure calculations and for the astrophysical community. Special emphasis was placed on a careful calibration of all experimental components and a thorough analysis of the systematic uncertainties. Firstly, a pure beam of $^{12}C^{3+}$ ions was injected into the ESR and cooled by means of electron cooling to obtain a relative momentum spread of $\Delta p/p \approx 10^{-5}$. Then, the carbon ions, which were initially in the $^2S_{1/2}$ state, were excited using the cw laser sytem to the $^2P_{1/2}$ or $^2P_{3/2}$ state, depending on the velocity of the ions. After only a few ns, the excited states decayed and the forwardly emitted fluorescence was detected using the *in vacuo* moveable XUV photon detection system. By varying the high-voltage of the electron cooler, the velocity of the ions was changed. For a fixed laser wavelength, the fluorescence of the ions was then recorded versus the electron cooler voltage. The 2*s*-2*p* transition wavelengths were obtained with a relative precision of $\Delta\lambda/\lambda$=8.4x10^{-6}. Good agreement between the ESR experiment and theory has now been obtained.

This research has been conducted in the framework of the SPARC collaboration, FAIR Phase-0 supported by GSI. This work was supported by the German Federal Ministry of Education and Research (BMBF, ErUM-FSP APPA) under grant numbers: 05P15PMFAA, 05P18RDFAA, 05P09RDFA3, 05P12RDRB2, 05P15RDFA1 and 05P16ODFA1. D Winzen. and J Ullmann acknowledge support from HGS-HIRe.

References

[1] Beck T *et al.* 2016 Optics Letters **41**, 4186-4189
[2] Siebold M *et al.* 2016 Laser Photonics Rev. **10**, 673-680
[3] Egelkamp C *et al.* 2015 GSI Scientific Report, APPA-MML-AP-13

*E-mail: d.winters@gsi.de

Few-atoms scattering mechanisms in XUV photoemission from WSe_2

M J Ambrosio[1], E Plesiat [2], P Decleva [3], P M Echenique[1], R Díez Muiño [1,4] * and F Martín [2,5] †

[1] Donostia International Physics Center, 20018 San Sebastián (Spain)
[2] Instituto Madrileño de Estudios Avanzados de Nanociencia, Campus de Cantoblanco, 28049 Madrid (Spain)
[3] Dipartamento di Scienze Chimiche e Farmaceutiche, Universitá di Trieste, 34127 Trieste (Italy)
[4] Centro de Física de Materiales (CSIC/UPV-EHU), 20018 San Sebastián (Spain)
[5] Departamento de Química, Universidad Autónoma de Madrid, 28049 Madrid (Spain)

Synopsis We analyze the scattering and interference processes involved from WSe_2 XUV photoemission via a molecular cluster model.

Inspired by the time resolved photoelectron spectra from dichalcogenide WSe_2 measured by Siek *et al.* [1], we perform cluster-based single photon calculations to elucidate the complex scattering processes that the photoelectron experiences inside the solid.

Our cluster approach is based on a partial wave expansion complemented by smaller off-center partial wave expansion to enhance convergence near each atomic core, where the available kinetic energy introduces a strongly oscillatory behavior to wave functions, and thus, the one-center expansion [2, 3]. The main expansion contains a top angular momentum in the order of 20, whereas the off-center ones are kept to one unit more than the highest-angular-momentum value for their atom's bound states. The electron interactions with the other electrons is incorporated with an LB94 density functional model [4].

The molecular clusters that model the interaction of the photoelectron with the neighboring atoms in the solid belong to either C3v or D3h groups.

In this contribution we present results for the smallest clusters we considered, namely WSe_3, WSe_6, W_3Se, Se_2 and W_3Se_2, on top of the corresponding isolated atoms. Figure 1 contains the comparison of photoemission cross sections (left) and Wigner time delays (right) in terms of the polar emission angle θ and the kinetic- and photon energy, for a fixed azimuthal angle $\phi = 0°$ for WSe_3 (top) and WSe_6 (bottom). The W atom is placed at the origin, with the Se layers lying above and below. The yellow lines denote the θ angle at which the Se atoms lie.

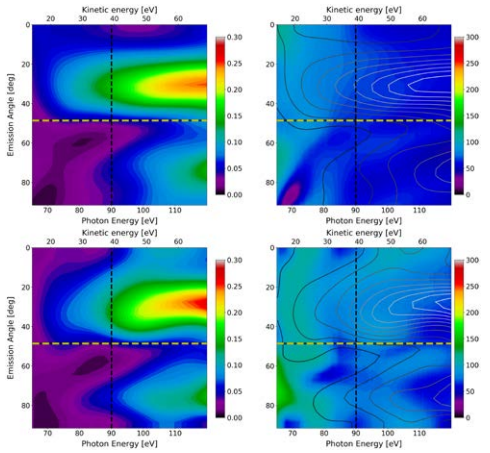

A clear effect that stems from the comparison is that for normal emission there is a rebound effect on the bottom layer of Se atoms. This leads to increases in the upwards emitted photocurrent and also affects the Wigner time delay for WSe_6, which are not present for WSe_3. However, the large structure present for at $\theta \approx 30°$ only requires the top layer of Se atoms to originate, meaning it is the result of constructive interference between the direct emission from the central W atom and the photocurrent deflected by the top level Se atoms.

References

[1] F. Siek *et al.* 2017 *Science*, **357** 1274-1277.
[2] D. Toffoli *et al.* 2002 *Chem. Phys.*, **276** 25-43.
[3] D. Toffoli *et al.* 2016 *J. Chem. Theory Comput.*, **12** 4996–5008.
[4] R. van Leeuwen *et al.* 1994 *Phys. Rev. A*, **49** 2421.

*E-mail: rdm@ehu.eus
†E-mail: fernando.martin@uam.es

Tracing back the scattering mechanisms in XUV photoemission from WSe_2 cluster models

M J Ambrosio[1], P M Echenique[1], R Díez Muiño [1,2] * and F Martín [3,4] †

[1] Donostia International Physics Center, 20018 San Sebastián (Spain)
[2] Centro de Física de Materiales (CSIC/UPV-EHU), 20018 San Sebastián (Spain)
[3] Instituto Madrileño de Estudios Avanzados de Nanociencia, Campus de Cantoblanco, 28049 Madrid (Spain)
[4] Departamento de Química, Universidad Autónoma de Madrid, 28049 Madrid (Spain)

Synopsis We analyze the scattering contribution from every atom in XUV photoemission from WSe_2.

In order to study the photoelectron dynamics from WSe_2 we introduce a cluster scattering model able to include the emitting atom and, selectively, its neighbors, and infer where the different scattering contributions originate. The method considers an approximation for a first order scattering process, where the zeroth order is approximated by an outgoing spherical wave weighted by the single-atom photoemission transition amplitude –can be supplied by any method [1, 2]– which acts as the incident wave at each scatterer J. DFT potentials [3] for W and Se localize strongly, and the resulting First Born scattering amplitude by atom J coming from source I is calculated analytically as follows:

$$f^{B1}_{I,J}(\mathbf{k}_f) = \frac{1}{4\pi}\langle\Phi(\mathbf{k}_f)|U_J|\Phi(\mathbf{k}_{JI})\rangle. \qquad (1)$$

From the above transition amplitude we obtain the physically measurable magnitudes: the fully differential cross section (FDCS) and Wigner time delay.

In Fig. 1 our focus is to dissect the FDCS and Wigner time delay for W4f photoemission from a WSe_6 cluster by looking at the emission from smaller fragments: WSe_2 (top), WSe_4 (middle) and the complete WSe_6 cluster (bottom). We display both magnitudes in terms of the polar emission angle θ and the kinetic and photon energies for azimuthal orientation $\phi = 0°$ as indicated in the leftmost depictions. As an example, consider the emission along $\phi = 0°$: there are FDCS peaks above the θ at which the Se atoms lie (yellow lines). The contributions come both from the atom closest to the emission path, but also due to constructive interference from the two Se atoms in the opposite direction. The time delay comparison in between the attests to the longer pathway required by part of the photocurrent rebounding off the Se atoms on the left towards the right.

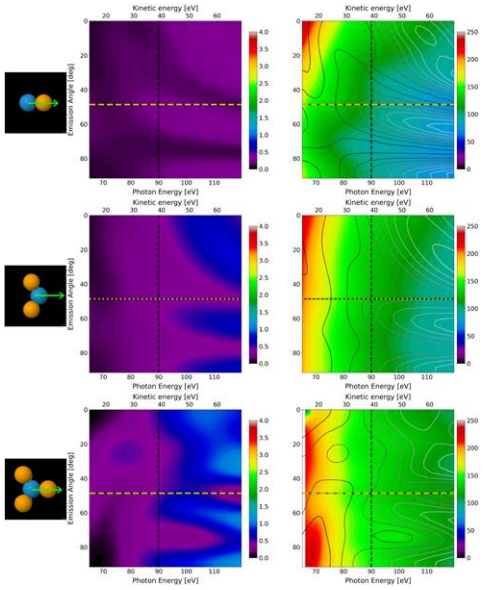

The method applies to larger cluster systems, where tracing back the origin of FDCS structures becomes increasingly complex.

References

[1] D. Toffoli *et al.* 2002 *Chem. Phys.*, **276** 25-43.
[2] D. Toffoli *et al.* 2016 *J. Chem. Theory Comput.*, **12** 4996–5008.
[3] G.te Velde *et al.* 2001 *J. Comp. Chem*, **9** 931–967.

*E-mail: rdm@ehu.eus
†E-mail: fernando.martin@uam.es

Unrevaling of inter- and intra-molecular interactions in homogeneous and hydrated uracil clusters

J Chiarinelli[1] *, L Avaldi[1], P Bolognesi[1], M C Castrovilli[1], A Domaracka[3], S Indrajith[3], S Maclot[4,5], G Mattioli[1], A Milosavljevic[2], C Nicolafrancesco[2,3], C Nicolas[2], P Rousseau[3]

[1] *CNR-Istituto di Struttura della Materia, Area della ricerca di Roma1, Monterotondo, Italy*
[2] *Synchrotron SOLEIL, L'Orme de Merisiers, 91192, Saint Aubin, BP48, 1192, Gif-sur-Yvette Cedex, France*
[3] *Normandie Université, ENSICAEN, UNICAEN, CEA, CNRS, CIMAP, 14000 Caen*
[4] *Departmentof Physics, University of Gothenburg, Origovagen 6B, 41296, Gothenburg, Sweden*
[5] *Department of Physics, Lund University, P.O. Box 118, 22100 Lund, Sweden*

Synopsis The electronic structure of homogenoeus and hydrated uracil clusters in the gas phase are investigated by X-ray photoemission spectroscopy and DFT calculations. This combined approach allowed to sheld light on inter- and intra-molecular interactions in clusters.

X-ray photoemission spectroscopy, XPS, is a suitable tool to probe the chemical environment of a specific atom in a system. In this work XPS has been used to study the different molecular interactions (H-bond, π-stacking, dispersion interactions) at work in homogeneous and hydrated uracil (U) clusters in the gas phase. The measurements have been performed at the Pleiades beam line [1] using a gas aggregation source, developed at CNRS-CIMAP [2] and coupled to an end station equipped with a Scienta R4000 photoelectron spectrometer. The measured C, N and O 1s XPS spectra of the clusters display a shift with respect to isolated uracil molecules [3] due to the variation of the molecular connections in the clusters (Fig.1). DFT-based simulations [4] to calculate the binding energy of each atom in the cluster and molecular dynamics simulations to determine the cluster structure have been performed. Our strategy is based on a bottom-up approach that selects aggregates with increasing numbers of uracil (2-50) and water (0-60) molecules to disentangle the effects of the different interactions in the cluster. The results of the homogeneous clusters show that the approach, which relies on computational simulations starting from the crystallographic structure of uracil, produces an excellent agreement with the experiments, while in the mixed clusters an interesting evolution of the cluster structure with different levels of hydration is observed.

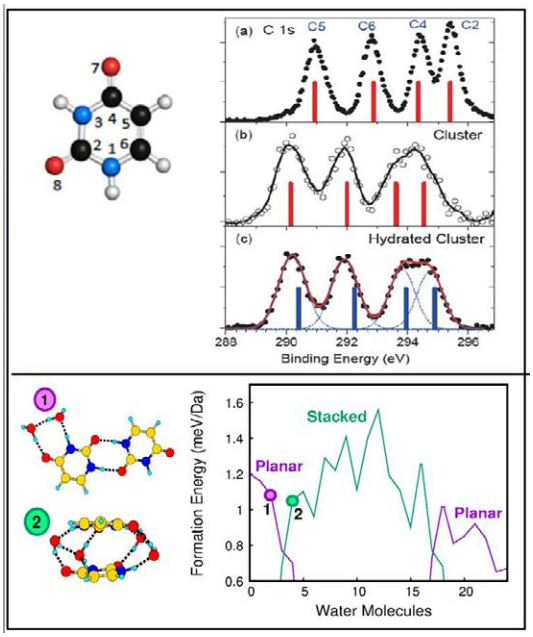

Figure 1. Top: C1s XPS spectra of Uracil molecules [3], homogeneous and hydrated clusters (a,b,c respectively). **Bottom**: formation energy per mass unit versus number of water molecules in a hydrated Uracil dimer.

References

[1] *A. Lindblad et al 2013 Rev. Sci. Instr. 84, 113105*
[2] *C. Nicolafrancesco et al 2021 Eur J Phys D 75, 117*
[3] *V. Feyer et al 2009 J. Phys. Chem. A 113, 5736*
[4] *P Giannozzi et al 2009 J. Phys. Condens. Matter, 21, 395502*

* E-mail: Jacopo.Chiarinelli@ism.cnr.it

An experimental and theoretical investigation of the valence photoemission spectra of uracil clusters

L Avaldi[1] *, P Bolognesi[1], J D Bozek[2], A Casavola[1], M C Castrovilli[1], J Chiarinelli[1], A.Domaracka[3], S Indrajith[3], S Maclot[4], G Mattioli[1], A R.Milosavljevic[2], F Morini[5], C Nicolafrancesco[2,3] and P Rousseau[3]

[1] CNR - Istituto di Struttura Della Materia (CNR - ISM), Area della Ricerca di Roma 1, Monterotondo Scalo, Italy
[2] Synchrotron SOLEIL, L'Orme de Merisiers, 91192, Saint Aubin, BP48, 1192, Gif-sur-Yvette Cedex, France.
[3] Normandie Univ., ENSICAEN, UNICAEN, CEA, CNRS, CIMAP, 14000 Caen, France.
[4] Physics Department, University of Gothenburg, Origovägen 6B, 41296 Göteborg, Sweden.
[5] Hasselt University, X-LAB, Agoralaan, 3590 Diepenbeek, Belgium

Synopsis The valence electronic structure of uracil clusters in the gas phase has been investigated by photoemission spectroscopy and DFT calculations.

Molecular clusters are weakly bonded systems with properties different from those of a single molecule or a bulk material. The study of the weak interactions in gas-phase clusters of increasing size can provide information on structures and mechanisms at work in both the liquid and condensed phases. To this aim, the valence shell spectrum of uracil clusters has been investigated.

The measurements have been performed at the Pleiades beam line [1] of SOLEIL synchrotron using a gas aggregation source, developed at CIMAP [2] and coupled to an end station equipped with a Scienta R4000 photoelectron spectrometer.

The DFT theoretical approach adopted can provide quite accurate results for outer-valence electronic states. The ground state geometrical parameters of the dimer, tetramer and hexamer of uracil are taken from Mattioli et al. [3]. The clusters have been cut out from the uracil crystal structure, and equilibrium geometries have been found by fully relaxing all the molecules accommodated in large cubic supercells using a plane-wave/pseudopotential/supercell approach, as implemented in the Quantum-ESPRESSO package.

The outer valence vertical ionization energies were calculated using the Outer Valence Green's Function (OVGF) methods [4,5] testing split valence double and triple zeta basis sets of different size. The calculations were performed using Gaussian 09 [6].

In fig.1 a comparison between OVGF predictions of the photoemission spectra of dimer, tetramer and hexamer and the experimental spectrum of the uracil cluster is shown.

Starting from uracil dimer, we analyze greater aggregates such as tetramer and hexamer. From our theoretical results, we observe a shift towards lower binding energy of the HOMO and outer orbitals and, as can be expected, a strong packaging of the states as the number of molecules in the cluster increases.

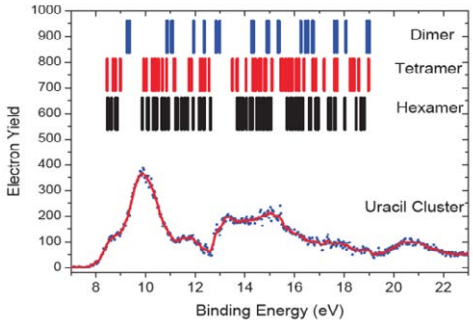

Figure 1. Comparison between OVGF predictions of the photoemission spectrum of dimer, tetramer and hexamer and the experimental spectrum of the uracil cluster.

References

[1] *A. Lindblad et al. 2013 Rev. Sci. Instr. 84, 113105*
[2] *C. Nicolafrancesco et al 2021 Eur J Phys D 75, 117*
[3] *G. Mattioli et al. 2020 Sci. Rep. 10, 13081*
[4] *L. S. Cederbaum et al. 1977 Adv. Chem. Phys. 36, 205*
[5] *W. von Niessen et al. 1984 Comput. Phys. Rep. 1, 57*
[6] *M. J. Frisch et al. GAUSSIAN 09, Revision B.01, Gaussian, Inc., Wallingford, CT, 2009*

* E-mail: lorenzo.avaldi@ism.cnr.it

Angle-resolved Photoelectron Spectroscopy of large Water Clusters ionized by an XUV Comb

L Colaizzi[1,2,*], L Ban[3], A Trabattoni[1], V Wanie[1,4], K Saraswathula[1], E P Månsson[1], P Rupp[5,6], Q Liu[5,6], L Seiffert[7], E A Herzig[7], A Cartella[1,8], B L Yoder[3], F Légaré[4], M F Kling[5,6], T Fennel[7], R Signorell[3], F Calegari[1,2,8,9†]

[1]Center for Free-Electron Laser Science, DESY, 22607 Hamburg, Germany
[2]Physics Department, Universität Hamburg, 22761 Hamburg, Germany
[3]Laboratory of Physical Chemistry, ETH Zürich, 8093 Zürich, Switzerland
[4]Institut National de la Recherche Scientifique, J3X 1S2, Varennes (Qc), Canada
[5]Max Planck Institute of Quantum Optics, , 85748 Garching, Germany
[6]Department of Physics, Ludwig-Maximilians-Universität München, 85748 Garching, Germany
[7]Institute of Physics, University of Rostock, 18059 Rostock, Germany
[8]The Hamburg Centre for Ultrafast Imaging, Universität Hamburg, 22761 Hamburg, Germany
[9]Institute for Photonics and Nanotechnologies CNR-IFN, 20133 Milano, Italy

Synopsis We performed angle-resolved photoelectron spectroscopy of water clusters ionized by an extreme-ultraviolet attosecond pulse train. A clean signature of the clusters was isolated from the water monomer contribution, to be used for time-resolved attosecond spectroscopy.

Detailed knowledge about photo-induced electron dynamics in water is key to the understanding of several biological and chemical mechanisms, in particular for those resulting from ionizing radiation [1]. While several studies reporting on detailed low-energy electron scattering cross sections in amorphous ice, liquid water and large water clusters [2] and a time-resolved approach to investigate electron scattering in water has been reported [3], such investigations in gas-phase water clusters have shown to be a promising bridge in between the gas and liquid phase, allowing for many technological limitations to be overcome and setting a clear route to perform attosecond-resolved spectroscopy of hydrated molecules. Indeed, extreme ultraviolet (XUV) attosecond pulses may be used to photoionize a water sample and to investigate the electron dynamics and transport properties with extremely high temporal resolution [4].

We report a method to obtain photoelectron spectra from neutral water clusters following ionization by an extreme-ultraviolet (XUV) harmonic comb. Typically, a large background signal in the experiment arises from water monomers and carrier gas used in the cluster source (Fig. 1). We describe a protocol to quantify this background in order to eliminate it from the experimental spectra. We disentangle the accumulated XUV photoionization into contributions from the species under study and the photoelectron spectra from the clusters. This study demonstrates feasibility of background free photoelectron spectra of large water clusters illuminated with XUV combs and paves the way for the detailed time-resolved analysis of the underlying dynamics.

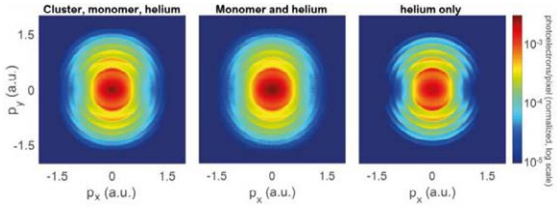

Figure 1. Angle-resolved photoelectron momentum distributions obtain after XUV comb photoionization in three different target conditions: (a) water clusters were present in the interaction region as a mixture with water monomers and He; (b) mixture of water monomers and He; (c) pure He. The photoelectron spectra (a,b,c) were fully symmetrized along x and y axes and plotted in log scale.

References

[1] Sanche, L. 2009 Nature 461, 358–359
[2] S. Hartweg, et al. 2017 Phys. Rev. Lett. 118(10), 103402
[3] Jordan, I et al. 2020 *Science* 369.6506 , 974-979
[4] L. Seiffert et al. 2017 Nature Phys 13, 766–770

* E-mail: lorenzo.colaizzi@desy.de
† E-mail: francesca.calegari@desy.de

Enhancement in the yield of O_2^+ ions from photo-ionized CO_2 clusters

S Ganguly[1*], D Barreiro-Lage[2], N Walsh[3], B Oostenrijk[1], S Sörensen[1], S Diaz-Tendero[2] and M Gisselbrecht[1]

[1]Department of Physics, Lund University, Lund, SE-221 00, Sweden
[2] Departamento de Quimica - Módulo 13, Universidad Autonoma de Madrid, Madrid, 28049, Spain
[3]MAXIV laboratory, Lund University, Lund, SE-221 00, Sweden

Synopsis The understanding of photochemical processes in molecular clusters induced by ionizing radiation is still at its infancy. Unlike molecular CO_2, C 1s-ionized CO_2 clusters dissociate by efficiently producing O_2^+, which can be of relevance to planets with CO_2-rich atmospheres. Combining the 3-D momentum ion imaging technique with *ab initio* molecular dynamics simulations, we investigate the dissociation dynamics. We find that O_2^+ production is enhanced when a structural transition takes place after photoionization.

Clusters studies improve our fundamental understanding of evolution of matter from a single molecule to an infinite solid. Recent quantum chemical calculations predict that pure CO_2 clusters exist at high altitudes in the CO_2-rich Martian atmosphere as cloud precursors [1]. Interaction of light with atmospheric particles is ubiquitous. At these high altitudes (60-100 km), ionizing radiation is abundant and can induce dissociation reactions in CO_2 clusters. Previous studies have reported that ionized CO_2 clusters can dissociated into O_2^+ ions [2, 3], but the details of the process are unexplored.

We investigate the production of O_2^+ from core-ionized CO_2 clusters, using 3-D momentum coincidence imaging technique. CO_2 clusters were ionized using soft X-Rays (320 eV) from the MAX-lab synchrotron in Sweden. The measured O_2^+ yield from the ionized CO_2 clusters is substantially higher than molecular studies [4] as shown in Figure 1. The dramatic increase in yield is due to the presence of intermolecular interactions in clusters, that opens specific reaction pathways.

The ion-momentum analysis shows that O_2^+ ions can be produced via two different sequential dissociation processes in the clusters; and these are dependent upon the cluster size. Quantum chemical calculations allow us to propose different reaction pathways. The simulations show that the most efficient quantum yield of the photoreaction leading to O_2^+ is when the mother cluster ion has an icosahedral structure. We believe that these reactions are relevant to the chemistry of CO_2-rich Martian atmosphere and may contribute to the O_2^+ concentration in the ionosphere [5].

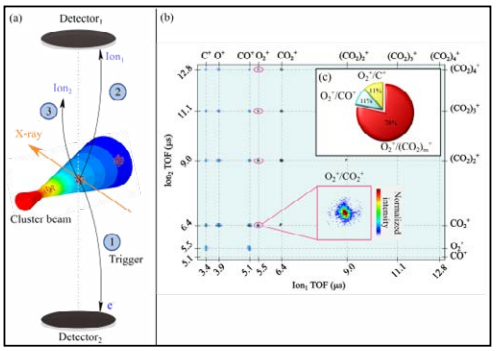

Figure 1. (a) A schematic of the experiment showing a typical double coincidence measurement. Detector$_1$ measures 3-D momentum of the ions. (b) 2-D coincidence map of time-of-flights (TOFs) of ions produced by CO_2 clusters made up to about 20 molecules ionized by X-ray photons (320 eV). All the cluster dissociation channels producing O_2^+ ions are highlighted in red. (c) Contribution of the different dissociation channels to the overall O_2^+ production from clusters.

References

[1] Ortega IK *et al* 2011 *Comput. Theor. Chem.* **965.2-3**: 353-358
[2] Romanowski G *et al* 1989 *Int. J. Mass Spectrom. Ion Processes* **95.2**: 223-239
[3] Heinbuch S *et al* 2016 *J. Chem. Phys.* **125.15**: 154316
[4] Laksman J *et al* 2012 *J. Chem. Phys.* **131**: 104303
[5] Haider SA *et al* 2011 *Rev. Geophys.* **49.4**: RG4001

* E-mail: smita.ganguly@sljus.lu.se

Exploring photoelectron angular distributions emitted from molecular dimers by two delayed intense laser pulses

V Hanus[1,2 *], S Kangaparambil[1], S Larimian[1] , M Dorner-Kirchner[1], X Xie[1, 3], A Baltuška[1] and M Kitzler-Zeiler[1]

[1]Photonics Institute, Technische Universitat Wien, Vienna, 1040, Austria, EU
[2]Wigner Research Centre for Physics, Institute for Solid State Physics and Optics, Budapest, 1121, Hungary, EU
[3]SwissFEL, Paul Scherrer Institute, Villigen PSI, 5232, Switzerland

Synopsis Two delayed laser pulses with different polarization allowed us to extract distributions of second emitted electron from double ionization of molecular dimers. Simulation shows that deformation of photoelectron distribution in dimers stems from scattering on neighboring molecule. Based on this result we demonstrate that the electron momentum space in the dimer case can be separated, allowing to extract information about the ionization pathway from the photoelectron angular distributions.

Tracing molecular dynamics induced by a pump pulse to observe the angular distributions of photoelectrons combined with coincidence imaging of the photoion momenta can provide unique insight into the intra-molecular dynamics with femtosecond resolution. In specific case, the rotating electric field vector of the probe pulse can be exploited for mapping laser-sub-cycle time to electron momentum, a concept known as angular streaking. Our aim is to extend existing methods from isolated molecules, to study dynamics in more complicated systems such as molecules in a compound. This effort is motived by the fact that most molecular processes in nature take place by interaction with more than one molecule [1].

In this work [2] we describe experiments and simulations investigating to what extent photoelectron angular distributions (PAD) measured with a strong, elliptically polarized laser field can be used to extract structural and dynamical information from molecules bound in a hetero-dimer complex. We studied with a reaction microscope the PADs from sequential double ionization N_2N_2 and N_2O_2 dimers during two delayed intense laser pulses. Using different polarization state for pump (linear) and probe (elliptical) pulse we isolated electrons that were emitted by action of the probe. Comparing PAD of second electron, see Fig. 1(a) with the case of an isolated molecule we observe change of its shape. Using simulations, we attribute this shape change to the scattering of the electron on the neighboring ion, see Fig. 1(b-e) just created by preceding laser pulse. Aligning the molecule, we showed that electrons originating from different sides of the molecule contribute to different parts of PAD.

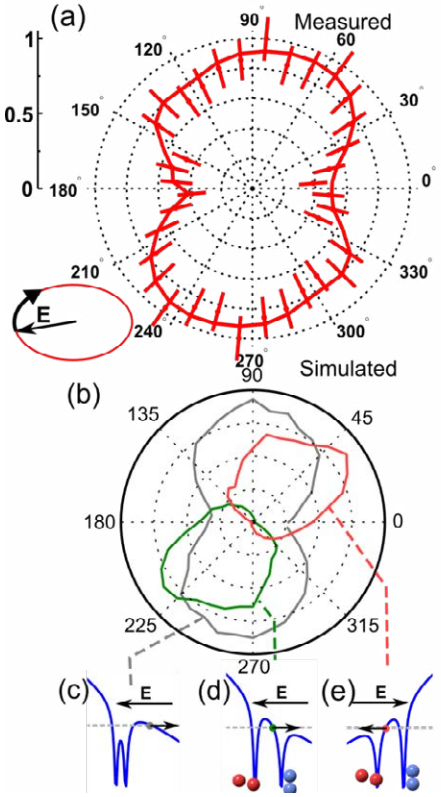

Figure 1. (a) Measured PAD of 2nd emitted electron upon ionization of N_2O_2 dimer. Using simuation (b), the shape of the distribution can be explained by several emission scenarios (c, d, e) that contribute to distribution.

References

[1] Weinberg DR *et al. 2012 Ch Rev.* **112**, 4016
[2] Hanus V et al. 2020 *Phys Rev A*, **102**, 053115

*E-mail: hanus.vaclav@wigner.hu

Attosecond spectroscopy of size-resolved water clusters

X. Gong[1,2,*], S. Heck[1,*], D. Jelovina[1], C. Perry[1], K. Zinchenko[1], H. J. Wörner[1,†]

Laboratorium für Physikalische Chemie, ETH Zürich, 8093 Zürich, Switzerland State Key Laboratory of Precision Spectroscopy, East China Normal University, Shanghai, China
∗ These authors contributed equally to this work.
† e-mail: hwoerner@ethz.ch

Synopsis We report photoionization time-delay measurements of size-resolved water clusters and find a continuous increase towards cluster sizes with 4-5 molecules and little change for larger clusters. We show that these delays directly reflect the spatial extension of the created electron hole, which first increases with cluster size and then partially localizes through the onset of structural disorder that is characteristic of large clusters and bulk liquid water.

Electron dynamics in water are of fundamental importance for a broad range of phenomena[1-3], but their real-time study has so far remained limited to the femtosecond time scale[4-5]. Here, we introduce attosecond size-resolved cluster spectroscopy and build up a molecular-level understanding of the attosecond electron dynamics in water. We measure the effect that the addition of single water molecules has on the photoionization time delays of water clusters. We find a continuous increase of the delay for clusters containing up to 4-5 molecules and little change towards larger clusters. The experimental data is supported by quantum-scattering calculations, which agrees very well as displayed in Figure 1. We show that these delays directly reflect the spatial extension of the created electron hole, which first increases with cluster size and then partially localizes through the onset of structural disorder that is characteristic of large clusters and bulk liquid water. These results establish a previously unknown sensitivity of photoionization delays to electron-hole delocalization and reveal a direct link from electronic structure to attosecond photoemission dynamics. Our results also bridge the technological, theoretical and conceptual gaps between gas-phase and liquid-phase attosecond spectroscopies.

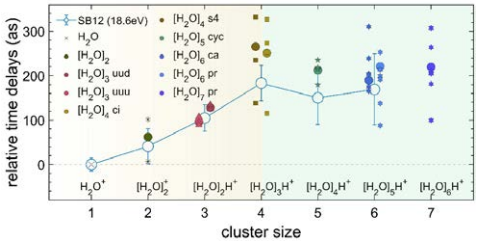

Figure 1. Time delays for photoionization out of the $1b_1$ band of water clusters, relative to H_2O, measured in SB12 (empty circles). The calculated delays were obtained for a kinetic energy of 6.0 eV. They are provided for each individual orbital of the $1b_1$ band (small symbols) and as a cross-section-weighted average over the band (filled symbols).

References

[1] Sanche, L, 2009 *Nature* **461** 358-359
[2] Boudaiffa, B, 2000 *Science* **287** 1658–1660
[3] Garrett, B. C., 2005 *Chemical Reviews* **105** 355–389
[4] Svoboda, V., 2005 *Science Advances* **6** eaaz038
[5] Loh, Z. H., 2020 *Science* **367** 179–182

From momenta to structure: Coulomb explosion imaging of small helium clusters

J Kruse[1]*, **M Kunitski**[1]†, **R Dörner**[1]

[1]Institut für Kernphysik, Goethe Universität, Frankfurt am Main, 60483, Germany

Synopsis Small helium clusters (He_2, He_3 and He_4) are unique quantum systems that have extremely fragile bound states of huge spatial extent. One of these states is the famous Efimov state in He_3. We study structures and field-induced dynamics of these states by Coulomb explosion imaging: trimers are ionized by a femtosecond laser pulse and the ion momenta gained in the subsequent Coulomb explosion are measured by a COLTRIMS reaction microscope. Here we present two approaches for the reconstruction of the cluster structure from the measured ion momenta.

The van der Waals interaction between helium atoms is extremely weak, such that the He-He potential supports only one bound state in the helium dimer ($^4He_2$), which has a binding energy of only 150 neV [1]. Due to this near-resonant character of the He-He interaction, the ^{4}He trimer has an excited state, which is of Efimov nature [2].

The spatial structure of small helium clusters can be investigated via Coulomb explosion imaging. A cluster is ionized by an intense femtosecond laser pulse. The momenta, which the helium ions gain during the subsequent Coulomb explosion, encode information about the structure of a cluster, such that $\mathrm{KER} = \sum_i 1/R_i$, where KER is kinetic energy release and R_i are interatomic distances in a cluster. This relation can be directly used for obtaining the interatomic distance in the dimer. In case of larger clusters the structural reconstruction is not that straightforward, and requires advanced reconstruction algorithms.

The first reconstruction approach that we have developed for the helium trimer is based on a two-dimensional lookup table [2]. The geometry of three vectors with the property $\mathbf{p}_1 + \mathbf{p}_2 + \mathbf{p}_3 = \mathbf{0}$ can be encoded using two-dimensional Dalitz coordinates, which represent the internal normalized coordinates of a trimer. These vectors can be momentum vectors in the center of mass system or position vectors in the center of coordinate system. Using this representation we map the spatial Dalitz space with the momentum Dalitz space by solving numerically Newton's EOM. The relation is saved into a lookup table, and used later for reconstruction.

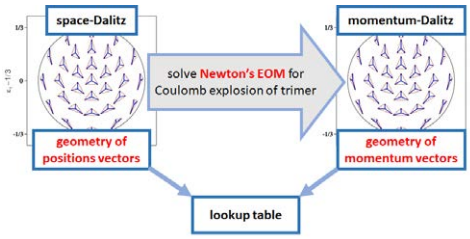

Figure 1. Structure reconstruction for trimers using the lookup table approach in two-dimensional Dalitz coordinates.

The second reconstruction algorithm is more general one and thus can be applied not only for trimers but for larger clusters as well. In this approach an initial guess structure is optimized using a global optimization technique until the simulated momenta corresponding to this structure will match the measured ones.

The advantages and drawbacks of two reconstruction approaches will be discussed. Both algorithms are going to be used for investigation of the field-induced dynamics in small helium clusters [3].

References

[1] Zeller S *et al* 2016 *PNAS* **113** 14651
[2] Kunitski M *et al* 2015 *Science* **348** 551
[3] Kunitski M *et al* 2020 *Nat. Phys.* **17** 174

*E-mail: kruse@atom.uni-frankfurt.de
†E-mail: kunitski@atom.uni-frankfurt.de

Investigation of the increase in ICD efficiency with the number of nearest neighbors – first experimental results on Kr clusters

C Küstner-Wetekam[1*], L Marder[1], A Ehresmann[1], A Hans[1]

[1]Institute of Physics and CINSaT, University of Kassel, 34132 Kassel, Germany

Synopsis Non-local decay mechanisms play an important role in the relaxation of electronic vacancies in dense media such as biological samples. Rare gas clusters can be used as a prototype system for experiments to explore these mechanisms in a less complex environment. Here, we show proof for the increase in efficiency of core-level interatomic Coulombic decay (ICD) with the number of neighbors when compared to the local Auger decay.

To understand fundamental processes of radiation chemistry in realistic samples it is necessary to study prototypical systems, where a molecule or atom is surrounded by neighbors. Weakly bound van-der-Waals clusters are one possible system in which novel relaxation pathways occur. One such relaxation pathway is the Interatomic Coulombic Decay (ICD), a non-local electronic decay mechanism which was theoretically predicted in 1997 and experimentally confirmed in 2004 [1,2]. Ever since, this field of research is rapidly growing.

To estimate the impact of these non-local processes on real-life scenarios, it is important to know the efficiency compared to local relaxation pathways. Theoretical studies show a growing ICD efficiency with the number of nearest neighbors, but there has been no experimental proof so far [3].

Here, we use the decay of the 3*d* vacancy in Kr clusters to study the ICD efficiency in comparison to the well-known Auger decay. In an isolated Kr atom 3*d* photoionization leads to relaxation via Auger decay into different final states; we consider the $Kr^{2+}(4p^{-2})$ ionic ground state [4]. In a cluster, however, this 3*d* vacancy can also decay non-locally via core-level ICD [5]. Here, the vacancy is filled by a 4*p* electron of the ionized atom itself, but the excess energy is then transferred to a neighboring atom leading to two-site delocalized dicationic states $Kr^{+}(4p^{-1})Kr^{+}(4p^{-1})Kr_{n-2}$. Since the two decay channels are competing, it is possible to estimate the core-level ICD efficiency.

To investigate the dependence on the number of nearest neighbors, we exploit the icosahedral structure of rare gas clusters where an atom has a different number of neighboring atoms depending on its site in the cluster. While a bulk atom has 12 surrounding atoms, an atom on the surface has 6 (corner), 8 (edge), or 9 (face) neighbors.

Figure 1 shows a comparison of the site-selective electron spectra after 3*d* photoionization. When both spectra are normalized to their respective Auger signal, it is possible to see an increase in core-level ICD signal for bulk states.

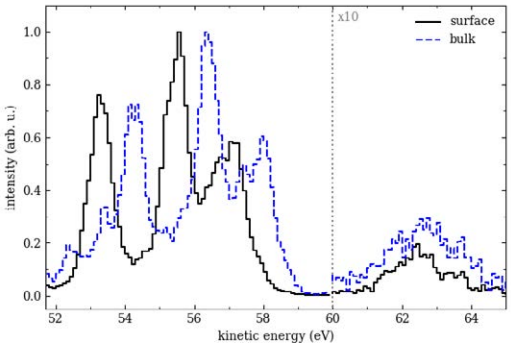

Figure 1 Electron spectra after 3*d* ionization of Kr clusters filtered for surface states (black solid) and bulk states (blue dashed).

A thorough more site-selective investigation of the broad cluster signal strongly indicates the expected increase of ICD efficiency with the number of neighbors.

References

[1] Cederbaum L *et al* 1997 *Phys. Rev. Lett* **79**, 4778-4781
[2] Jahnke T *et al* 2004 *Phys. Rev. Lett.* **93**, 163401
[3] Santra R *et al* 2001 *Phys. Rev. B* **64**, 245104
[4] Palaudoux J *et al* 2010 *Phys. Rev. A* **82**, 043419
[5] Hans A *et al* 2020 *Phys. Rev. Research* **2**, 012022(R)

* E-mail: c.kuestner-wetekam@uni-kassel.de

Structure of acetylene clusters in helium nanodroplets probed by Penning ionization electron spectroscopy

S Mandal[1]*, R. Gopal[2], M. Shcherbinin[3], A. D'Elia[4], H. Srinivas[5], R. Richter[6], M. Coreno[7,8], B. Bapat[1], M. Mudrich[3,9], S. R. Krishnan[9], and V. Sharma[10]

[1]Indian Institute of Science Education and Research, Pune 411008, India
[2]Tata Institute of Fundamental Research, Hyderabad 500107, India
[3]Department of Physics and Astronomy, Aarhus University, 8000 Aarhus C, Denmark
[4]IOM-CNR, Laboratorio TASC, Basovizza SS-14, km 163.5, 34149 Trieste, Italy
[5]Max-Planck-Institut für Kernphysik, 69117 Heidelberg, Germany
[6]Elettra-Sincrotrone Trieste, 34149 Basovizza, Italy
[7]Istituto di Struttura della Materia - Consiglio Nazionale delle Ricerche (ISM-CNR), 34149 Trieste, Italy
[8]INFN-LNF, via Enrico Fermi 54, 00044 Frascati, Italy
[9]Department of Physics and QuCenDiEm-Group, Indian Institute of Technology Madras, Chennai 600036, India
[10]Indian Institute of Technology Hyderabad, Kandi 502285, India

Synopsis We demonstrate Penning ionization electron spectroscopy as a useful technique to get insights into the structure and ionization dynamics of embedded acetylene (C_2H_2) clusters in helium (He) nanodroplets. Upon photoexcitation to $n = 2$ band, C_2H_2 cluster undergoes Penning ionization through He^* ($1s2s\ ^{3,1}S$), where the ion-mass correlated Penning electron spectra reveal the van der Waals character of the embedded cluster. We also report a new Penning ionization pathway stemming from $n = 4$ band, which competes with the dominant charge-transfer ionization channel from autoionized He in the droplets.

The spectroscopy of atomic and molecular clusters embedded in He nanodroplets is an active area of research as the nanodroplets act as ideal cryogenic hosts to the dopant clusters. Infrared spectroscopic technique is conventionally employed to probe the ro-vibronic structure of these clusters, wherein the embedded clusters are directly perturbed by the incident photons which are transparent to the host droplets [1]. However, when extreme-ultraviolet photons are used for such studies, due to the large photoexcitation cross-sections, efficient excitation occurs in the host rather than in the embedded cluster, and a rich class of intermolecular decay processes, such as Penning ionization, ensue in the dopant cluster upon relaxation of an excited host. In principle, coincident detection of energy-resolved Penning electrons and ions can give valuable information about the structure and ionization dynamics of the dopant cluster. However, the applicability of Penning electron ionization spectroscopy (PIES) to probe the molecular structure of the dopants in earlier study with organic acene molecules remained questionable due to the large inelastic scattering of Penning electrons with the host environment[2].

*E-mail: suddhasattwa.mandal@students.iiserpune.ac.in

This work establishes PIES as an important tool to probe the structure and ionization dynamics of C_2H_2 dopant clusters in He nanodroplets [3]. Upon $n = 2$ photoexcitation, C_2H_2 cluster is Penning ionized from He^* ($1s2s\ ^{3,1}S$), and the PIES in coincidence with C_2H_2 oligomer ions reveal the loosely-bound van der Waals nature of the cluster. Taking advantage of the tunability of synchrotron radiation, when photoexcited to $n = 4$ droplet band, a new Penning ionization channel, competing with the prominent charge-transfer ionization channel resulting from the autoionized droplet, is observed. Thus, our work will encourage further investigations of molecular complexes and nanostructures by utilizing PIES technique in the future, in particular using modern ultrafast spectroscopy such as femtosecond pump-probe in the XUV spectral range.

References

[1] Briant, M. *et al* 2018 *Phys. Chem. Chem. Phys.* **20**, 2597-2605
[2] Shcherbinin, M. *et al* 2018 *J. Phys. Chem. A* **122**, 7, 1855-1860
[3] Mandal, S. *et al* 2020 *Phys. Chem. Chem. Phys.* **22**, 10149-10157

Photoelectron spectroscopic characterization of non-supported $CaCl_2/MgCl_2$ and $MgBr_2/NaBr$ nanoparticles

M Patanen[1]*, E Pelimanni[1]†, C-M Saak[2], G Michailoudi[1], N Prisle[1,3] and M Huttula[1]

[1]Nano and Molecular Systems Research Unit, University of Oulu, P. O. Box 3000, 90014 Oulu, Finland
[2]Molecular and Condensed Matter Physics, Uppsala University, Ångströmlaboratoriet, 75237 Uppsala, Sweden
[3]Center for Atmospheric Research, University of Oulu, P. O. Box 4500, 90014 Oulu, Finland

Synopsis Synchrotron radiation excited X-ray photoelectron spectroscopy was used to study chemical composition of mixed inorganic nanoparticles grown from droplets using a spray drying method. Surface enrichment properties were found to strongly depend on the salt mixture and solvent used: no enrichment was observed in $MgCl_2/CaCl_2$ particles while extreme surface enrichment of Mg occurs in $NaBr/MgBr_2$ particles produced from aqueous solution. Mg enrichment was also observed for ethanol-dried particles, but with different behaviour as a function of relative solute concentration than for the aqueous case.

Spray drying is a common particle production method in e.g. ceramics, food, and pharmaceutical industries, but it also mimics naturally occurring phenomena such as creation of aerosol particles from breaking waves. Despite the importance of spray dried particles in technological applications and in nature, there is lack of knowledge of their formation processes and surface chemical composition. By using an extremely surface sensitive chemical analysis, synchrotron radiation excited X-ray photoelectron spectroscopy, we have carried out quantitative analysis of the surface segregation properties of Mg, Ca, and Na in *in situ* generated submicron particles. Experiments were carried out at SOLEIL synchrotron (Saint-Aubin, France) at PLEIADES beamline using an aerodynamic lens setup coupled with a VG-Scienta R4000 electron energy analyser [1]. Aerosol was produced with a constant output atomiser operated with N_2 and guided through two silica dryers or a cold trap and then fed to the aerodynamic lens system which focuses the nanoparticle beam to the interaction region with X-rays, ensuring constantly renewing substrate free sample. Relative ion concentrations and water content of the outermost few nm thick surface layer was determined based on XPS signals from particles generated from aqueous binary salt mixtures, $MgCl_2/CaCl_2$ and $NaBr/MgBr_2$. The role of the solvent was investigated by dissolving the Br-salts in an organic solvent, ethanol. Surface enrichment was monitored by varying salt mixing ratios and comparing the observed relative particle salt concentrations to those in the atomized solution. $CaCl_2/MgCl_2$ particles did not show any surface enrichment, as the data presented in Fig. 1 settle close to a curve assuming uniform distribution of components. Data on $MgBr_2/NaBr$ particles seem to fit better with assumed behaviour of core-shell like structures based on simple geometrical considerations. The difference between behaviour of ethanol and aqueous droplets can originate from hydrate formation.

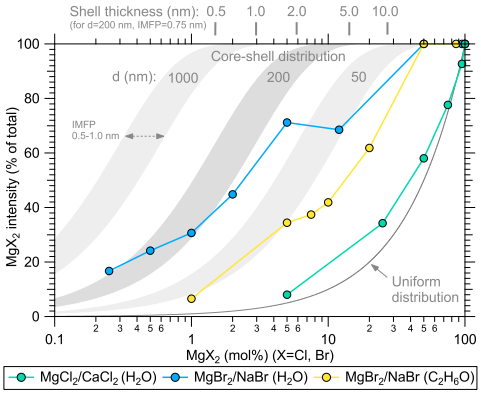

Figure 1. Experimental surface proportion of MgX_2 (X=Cl,Br) as a function of the molar mixing ratio in the atomized solution. Expected results from core-shell and uniform particles are presented with grey shaded areas and a line, respectively.

References

[1] Lindblad A, Söderström J, Nicolas C, Robert E, Miron C 2013 *Rev. Sci. Instrum.* **84**, 113105.

*E-mail: minna.patanen@oulu.fi
†E-mail: eetu.pelimanni@oulu.fi

Photoionization coherence of an alkali metal cluster confined in a giant fullerene ($Na_{40}@C_{540}$)

R Shaik[1], H R Varma[1]* and H S Chakraborty[2]†

[1]School of Basic Sciences, IIT Mandi, Himachal Pradesh, 175075, India
[2]Department of Natural Sciences, D. L. Hubbard Center for Innovation, Northwest Missouri State University, Maryville, Missouri 64468, USA

Synopsis We study the photoionization dynamics of Na_{40} confined in a giant fullerene C_{540} using a linear response density functional theory. The ionization spectra reveal the plasmonic contamination and the presence of inter-cluster Coloumbic decay (ICD) resonances.

Recent production of large fullerenes encapsulating clusters and nanocrystals [1] has paved the way to study interesting properties like dynamical coherent response between a metal cluster and a large fullerene. In the present work, we report photoionization calculations of Na_{40} inside the giant fullerene C_{540}.

The ground state of such an endohedral system, $Na_{40}@C_{540}$, is constructed using a jellium-based density functional theory (DFT) method. A gradient corrected approximation by van Leeuwen and Baerends (LB94) [2] for the exchange-correlation functional is employed. The photoionization (PI) dynamics of this system is then studied using a linear response framework of DFT, called time-dependent local density approximation (TDLDA). The ionization cross section is calculated as

$$\sigma_{PI}(\omega) = \sum_{nl} 2(2l+1)\left|\left\langle kl'\left|\delta V(\vec{r},\omega)\right|nl\right\rangle\right|^2,$$

where $\delta V = z + dV$ is the complex self-consistent field potential that includes both the dipole interaction (z) and the important electron correlation terms (dV). Here, nl denotes the occupied ionizing state and kl' are dipole-selected continuum states.

Fig.1(A) shows the cross section of the composite system $Na_{40}@C_{540}$ which is plotted in logarithmic scale to enhance the weaker features. Two broad plasmon-type peaks and a host of narrow resonances, comprising of various inner hole decays, are observed. Fig1(B) (inset) compares the cross section of Na_{40} ($Na_{40}@$) with its uncorrelated (dV=0) response which reveals significant contamination from C_{540} plasmons and the appearance of numerous inter-cluster Coulombic decays (ICD) resonances from the decay of C_{540} holes.

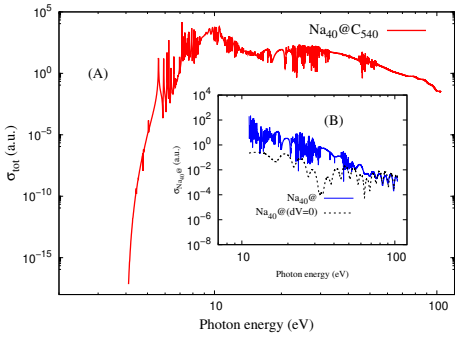

Figure 1. (A) Total photoionization cross-section of $Na_{40}@C_{540}$ and (B) total cross-section of Na_{40} inside C_{540} labeled as $Na_{40}@$.

Detailed comparisons between the results of $Na_{40}@C_{540}$ with that of isolated Na_{40} and C_{540} facilitate significant understanding of the plasmonic transfer and ICD resonances in the system.

Supported by the NSF-USA grant PHY-1806206 (HSC) and SERB-INDIA grant No. EMR/2016/002695 (HRV).

References

[1] Ugarte D 1993 *Chem. Phys. Lett.* **209** 99
[2] Van Leeuwen R *et al* 1994 *Phys. Rev. A* **49** 2421

*E-mail: hari@iitmandi.ac.in
†E-mail: himadri@nwmissouri.edu

Exchange-correlation functional with self-interaction corrections for many-atom systems

X M Tong*

Center for computational Sciences, University of Tsukuba, Tsukuba, Ibaraki 305-8573, Japan

Synopsis We propose a new exchange-correlation functional with self-interaction corrections for many-atom systems. The functional is constructed from atomic potentials with the self-interaction-correction. The test examples of CO, N_2 and H_2O show that the orbital energies have been improved significantly over the ones with conventional exchange-correlation functionals. Even better, the proposed functional can be separated from the self-consistent iteration so it does not increase the numerical efforts in density functional theory simulation.

Density functional theory (DFT) and time-dependent DFT are the most popularly used methods to study many-electron systems. The key ingredient in the theory depends on a universal exchange-correlation functional. Unfortunately, the universal functional is unknown, and there are hundreds, if not a thousand, proposed functionals, from simple local-density approximations (LDA), generalized gradient approximations (GGA) to more complicated meta-GGA forms with tuning parameters as documented in a library of exchange-correlation functionals [**?**].

On the other hand, the self-interaction-correction (SIC) exchange-correlation shows a great success for atoms [**?**] both for structures and dynamic processes. Direct extended the method to many-atom systems is impossible due to: (1) the functional is not well defined for degenerate states; (2) the numerical convergence is very slow. There are several works on how to remove the self-interactions for a specified system, but none works for broad many-atom systems. Given a physical observation that any proper SIC should go to the right asymptotic form for separate atomic limit for many-atom systems, we propose the following SIC form for many-atom systems as

$$v_{sic}(\mathbf{r}) = \sum_j \frac{e^{-2\kappa_j|\mathbf{r}-\mathbf{R}_j|}}{\omega(r)} v^j_{sic}(\mathbf{r}-\mathbf{R}_j),$$

with $\mathbf{R}_j, I_j, v^j_{sic}$ the position, ionization potential and atomic SIC potential of the $j-$th atom and $\omega(\mathbf{r}) = \sum_j e^{-2\kappa_j|\mathbf{r}-\mathbf{R}_j|}$, $\kappa_j = \sqrt{2I_j}$. The proposed functional returns to atomic SIC form when the atoms are far away from each other in the separated atomic limit. The details will be present in the conference.

The proposed SIC form only depends on the atomic information and it does not involve in the self-consistent iteration so it simplifies the simulation greatly. Table 1 shows the simulation results with the proposed SIC (LDA-SIC) compared with Hartree-Fock, conventional LDA results for H2O. Clearly we see the orbital energies have been improved significantly over the LDA and HF methods.

Table 1. Orbital energies of the ground state of H_2O. All energies are in eV.

Orbital	LDA	LDA-SIC	Expt.	HF[**?**]
$2a_1$	23.87	31.01	32.4	34.22
$1b_2$	11.97	18.93	18.7	16.16
$3a_1$	8.11	15.11	14.8	12.51
$1b_1$	6.15	13.01	12.6	10.68

We will also present the results for N_2, a homo-nuclear diatom molecule, *CO*, a hetero-nuclear diatom molecule, which show consistent improvements over the LDA and HF results. The possible application of the proposed functional for many-atom systems in a strong field by time-dependent density functional theory will be also discussed in the conference.

References

[1] M. A. L. Marques, M. J. T. Oliveira, and T. Burnus, 2012 *Comput. Phys. Commun.*, **183**, 10
[2] X M Tong and S I Chu, 1997 *Phys. Rev. A* **55**, 3406
[3] NIST Computational Chemistry Comparison and Benchmark Database, 2018, NIST Standard Reference Database Number 101 Release 19, Editor: Russell D. Johnson III.

*E-mail: tong.xiaomin.ga@u.tsukuba.ac.jp

Effect of incident pulse duration on generation of attosecond pulses during relativistic laser-cluster interaction

P Venkat[1]*, A R Holkundkar[2]† and T Otobe[1]‡

[1]Kansai Photon Science Institute, National Institutes for Quantum and Radiological Science and Technology(QST), Kyoto 619-0215, Japan
[2]Department of Physics, Birla Institute of Technology and Science, Pilani 333031, India

Synopsis Relativistic interaction of intense, ultrashort laser pulses with Deuterium clusters is simulated using molecular dynamics technique. Thomson scattered spectra are emitted during the interaction, consisting of higher order harmonics. These higher order harmonics are also a source of attosecond bursts of energy. The effect of varying pulse duration on the direction of power radiation and the duration of attosecond pulses is studied. It is found to be a significant parameter in the production of attosecond pulses and also has diagnostic potential with respect to the incident laser pulse.

Interaction of intense, ultrashort laser pulses with atomic clusters has been gaining a lot of traction in the past two decades, primarily because of the wide range of its applications in the field of high energy ion emission, soft X-ray sources, higher order harmonics and attosecond pulse generation, to name a few. The interaction of lasers with clusters approaches the relativistic regime when pulse intensity is of the order of 10^{18}W/cm^2 or higher i.e, the laser strength parameter $a_0 \geq 1$. During such an interaction, the magnetic field of the laser is significant enough to cause the $\vec{v} \times \vec{B}$ drift, due to which the oscillating electrons emit Thomson scattered radiation along a direction between the polarization and propagation axes of the pulse [1]. During this interaction, the higher order harmonics that are emitted show a certain phase relationship, which can be utilized for the production of attosecond pulses [1]. The higher harmonics spectra detected during the interaction and the attosecond pulses generated, depend significantly on the intensity of the incident laser pulse

Apart from the intensity dependence, incident laser pulse duration is an important parameter which influences the direction of the radiation emission and the duration of attosecond pulses. As the interacting pulses become extremely short i.e., of the order of few cycles, the dynamics and emitted radiation show significant changes. This is because intense, shorter pulses ionize the cluster nearly instantaneously, producing high energy ions and electrons[2]. However, unlike longer pulse interaction, the electrons don't experience prolonged oscillation in the laser field, which affects the Thomson scattered spectra and the associated attosecond bursts of energy. The $\vec{v} \times \vec{B}$ effect on the electrons is not pronounced enough in this case, thereby altering the direction in which maximum power is radiated. Reduced drift time also ends up lowering the duration of the attosecond pulses produced during the interaction. Thus, pulse duration is an important parameter which can help fine-tune the attosecond pulses produced and can also be potentially used for incident laser diagnostics.

In this work, we study the variation of incident pulse duration and its effect on the harmonics spectra and attosecond pulses generated during the interaction of intense laser pulses with Deuterium cluster. the radiation emission is studied using the model described in [1], based on the radiation effects described in [3].

References

[1] Prachi Venkat *et al* 2019 *Phys. Rev. Accel. Beams* **22** 084401
[2] Prachi Venkat *et al* 2016 *Phys. Plasmas* **23** 123106
[3] John David Jackson. *Classical Electrodynamics*. Wiley, New York, NY, 1975.

*E-mail: venkat.prachi@qst.go.jp
†E-mail: amol.holkundkar@pilani.bits-pilani.ac.in
‡E-mail: otobe.tomohito@qst.go.jp

Molecular photoionization studied with a complex Gaussian representation of the continuum states

A Ammar*, A Leclerc and L U Ancarani†

Université de Lorraine, CNRS, LPCT, Metz, 57000, France

Synopsis We study molecular photoionization by describing the photoelectron continuum state with a set of optimized complex Gaussian functions, within a monocentric and one-active-electron approach. Using a Slater-type expansion of the target orbital, all the necessary matrix elements become analytical, in both length and velocity gauges. This greatly facilitates the numerical evaluation of photoionization observables, *i.e.*, the cross section and the asymmetry parameter.

Real Gaussian-type orbitals (`rGTOs`) are widely used in molecular bound state calculations since their mathematical properties allow for closed form multicenter integrals. However, since nodeless `rGTOs` always go to zero, they are not suited to represent oscillating and non-decreasing continuum wavefunctions. Alternatively, complex Gaussian-type orbitals (`cGTOs`) –*i.e.* Gaussians with a complex exponent– intrinsically oscillate and should be more adapted to describe continuum states, such as those involved in collision processes.

In a recent study [1], we have developed an efficient optimization method to provide sets of `cGTOs` able to reproduce accurately –within a large radial box– continuum-type functions. These sets were used with success to evaluate analytically all matrix elements involved in the benchmark case of atomic hydrogen ionization, under photon or electron impact. In the present work, we pursue this approach by employing `cGTOs` to study molecular photoionization within a one-active-electron model; the initial and final wavefunctions are taken to be monocentric. Using Slater-type expansions for the initial molecular target, the necessary transition integrals are expressed in closed form, in both length and velocity gauges. The accuracy of our analytical `cGTOs` approach is checked by comparison with fully numerical results (see the example given in figure 1).

Work is ongoing to extend our proposal to a more realistic model by considering a multicentric initial state. In such a case, one can envisage studying the photoionization of large molecular systems since multicenter integrals involving `cGTOs` can be obtained analytically [2] and evaluated at a significantly reduced cost.

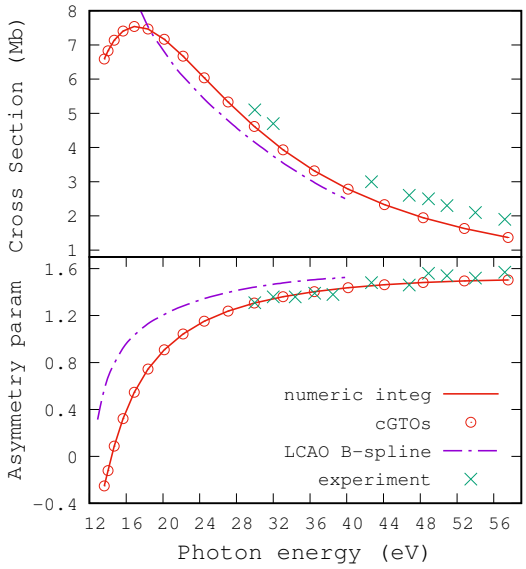

Figure 1. Photoionization cross section (top) and asymmetry parameter β (bottom) for orbital $1b_1$ of H_2O. The present closed form results (in velocity gauge) using `cGTOs` –optimized to reproduce a distorted radial continuum solution of a model potential– are confirmed by evaluating the integrals numerically, and are compared also with recent theoretical results [3] and experimental data [4].

References

[1] Ammar A *et al* 2020 *J. Comput. Chem.* **41** 2365
[2] Ammar A *et al* 2021 *Adv. Quantum Chem.* accepted.
[3] Moitra T *et al* 2020 *J. Phys. Chem. Lett.* **11** 5330
[4] Banna M S *et al* 1986 *J. Chem. Phys.* **84** 4739

*E-mail: aammar@irsamc.ups-tlse.fr
†E-mail: ugo.ancarani@univ-lorraine.fr

Attosecond Intramolecular-Scattering Delay

B Ghomashi[1], N Douguet[2] and L Argenti[3]*

[1]Physics Department, University of Colorado at Boulder, Boulder, CO 80309, USA
[2]Physics Department, Kennesaw University, Kennesaw, GA 30144, USA
[3]Physics Department and CREOL, University of Central Florida, Orlando, FL 32816, USA

Synopsis The photoionization of the CO molecule from the C−1*s* orbital deviates from the Franck-Condon approximation, due to the nuclear recoil associated to the photoelectron emission and intra-molecular scattering. We use an analytical model that reproduces the nuclear and electronic motion for this process to decompose the vibrationally-resolved photoemission delay in its localization and confinement components. Short pulses generate coherent vibrational ionic states with controllable vibrational delay compared to the sudden-photoemission limit.

Attosecond technology has opened the way to the study of electron dynamics at its natural time scale [1]. Photoionization chronoscopy, initially focused on atoms [2], should now explore the concerted ultrafast motion of electrons and nuclei, extending the perimeter of attosecond science to the real-time control of chemical reactions [3]. Understanding the interplay between the electronic motion initiated by an attosecond photoionization event and the subsequent nuclear motion is an essential component of this program.

When a molecule is ionized from a localized core orbital by an x-ray photon, the emerging photoelectron can either be directly ejected or collide with nearby nuclei. The interference between these ionization component gives rise to the well-known EXAFS interference pattern, and holographically encodes the molecular geometry [4]. Conversely, the intramolecular scattering process is resonantly enhanced, and so is the kinetic energy of the recoiling nuclei. The vibrationally-resolved spectrum bears an exquisitely sensitive signature of this energy transfer [5]. New pulsed x-ray sources, such as XFELS [6], make it now possible to study this phenomenon resolved in time. In this work, we simulate the real-time dynamics of the CO molecule following the C-1s ionization induced by a coherent soft-x-ray pulse using a simplified theoretical model. The vibrationally-resolved photoemission delay results from the interplay of two different phenomena, the localization of the photoelectron at its birth and its resonant confinement between the two nuclei. For short pulses, the ion is created in a partially coherent vibrational state: either in compression or in expansion, depending on the pulse central energy. The deviation of the nuclear Wigner distribution from the sudden-photoemission approximation can be interpreted as a vibrational delay due to intramolecular scattering.

*E-mail: luca.argenti@ucf.edu

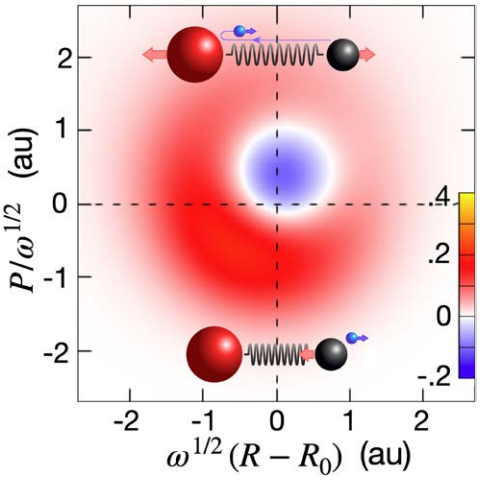

Figure 1. Wigner distribution of the vibrational state resulting from the C-1*s* core ionization events of the CO molecule by an attosecond x-ray pulse, when the photoelectron leaves on the C side. The interference between direct photoemission (compression) and intramolecular scattering (expansion) amplitudes results in a non-classical distribution.

References

[1] Ferrari F *et al* 2010 *Nature Phot.* **4** 875
[2] Pazourek R *et al* 2015 *Rev. Mod. Phys.* **87** 765
[3] Nisoli M *et al* 2017 *Chem. Rev.* **117** 10760
[4] Bressler C *et al* 2005 *Chem. Rev.* **104** 1781
[5] Plesiat E *et al* 2012 *Phys. Rev. A* **85** 023409
[6] Lindroth E *et al* 2019 *Nature Phys. Rev.* **1** 107

Femtosecond soft–X–Ray absorption spectroscopy of liquids with a water-window high-harmonic source

T. Balciunas[1*], Y. Chang[1], Z. Yin[2], C. Schmidt[1], K. Zinchenko[2], F. B. Nunes[2], V. Svoboda[2], A. Smith[2], E. Rossi[2], J-P. Wolf[1] and H-J. Wörner[2]

[1] GAP-Biophotonics, Université de Genéve, 1205 Geneva, Switzerland
[2] Laboratory for Physical Chemistry, ETH Zürich, 8093 Zürich, Switzerland

Synopsis We present time resolved X-ray spectroscopy of aqueous solutions and nano-solids samples utilizing a state-of-the-art high–harmonic table–top source covering the entire water-window range (284 - 538 eV). Our measurements represent the first extension of table-top XAS to the oxygen edge of a chemical sample in the liquid phase. In the time domain, our measurements resolve the gradual appearance of absorption features below the carbon K-edge of methanol during strong–field ionization, which trace the valence-shell ionization dynamics of the liquid alcohols with a temporal resolution of ~30 fs.

Table-top soft X-ray (SXR) sources driven by intense femtosecond lasers enabled time–resolved X–ray absorption spectroscopy (TRXAS) that has evolved into a powerful tool to investigate the structural and electronic dynamics of matter with element, site and orbital specificity. Pioneering transient–absorption experiments via high-order harmonic generation (HHG) were performed using near–infrared (NIR) laser–based sources with a cut–off limited to the extreme ultraviolet (XUV) photon energy range. Employing long-wavelength driving pulses allowed extending the HHG cut-off and XAS measurements into water-window [2]. The water-window spectral range spanning between the carbon and oxygen K absorption edges (284 and 538 eV respectively) opens the possibility to perform TRXAS measurements in liquid samples and solutions and covers absorption edges of biologically-relevant elements of carbon, nitrogen and oxygen.

The measurements presented in this contribution are enabled by merging the water-window soft X-ray transient absorption beamline driven by the 1.8 μm post-compressed pulses and the liquid flat-jet sample delivery system that provides sub-μm thickness samples of organic liquids, solutions and nanoparticles in the solution form [1]. As a proof-of-concept measurements we demonstrate time-resolved measurement of multi-photon induced dynamics in liquid alcohols at C K-edge, in molecular aqueous solutions at nitrogen K-edge and charge dynamics in TiO2 colloidal suspension probed at Ti L2,3-edge.

Our recent measurements in aromatic heretocyclic hydrocarbons and solutions reveal dynamics induced via multi-photon excitation. Comparing the measurements in liquid and gas phase, we are able to pinpoint differences in photoinduced dissociation dynamics in the condensed phase.

Furthermore, we demonstrate the proof-of-concept measurement of UV pulse (266 nm) induced charge dynamics in TiO_2 anatase nanoparticles in a colloidal solution. This allows studying charge-injection and the environment effects on the excitation and relaxation dynamics with element, site and orbital specificity.

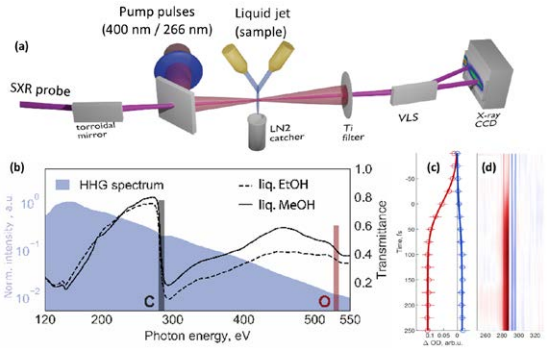

Figure 1. (a) experimental scheme; (b) measured transmission spectra of liquid ethanol and methanol at C-K and O-K absorption edges; (c, d) time evolution of transient absorption spectra of methanol pumped by 400 nm pulses. The lineouts (red and blue lines in (c)) correspond to the spectral bands shown in (d) that represent the formation of the cation (red) and the depletion of the ground state (blue).

References

[1] Smith A *et al J. Phys. Chem. Lett., 2020, 11, 1981–1988*
[2] Pertot Y *et al Science 2017, 10.1126/science.aah6114*

Formation of small hydrocarbons from polycyclic aromatic hydrocarbons via dissociative ionization in the interstellar medium

S Barik[1], R Chacko[1]*, and G Aravind[1]†

[1]Indian Institute of Technology Madras, Chennai, 600036, India

Synopsis Dissociative ionization processes of polycyclic aromatic hydrocarbon (PAH) molecules upon coupling with intense UV-field in the interstellar medium (ISM) is experimentally studied. The possible presence of CH_n^+ (n=4-6) in the UV-rich photo-dissociation regions of ISM is asserted. An interplay of H-migration and "roaming mechanism" in the formation of these ions from PAHs in ISM is proposed.

Polycyclic aromatic hydrocarbons (PAHs) are believed to be present everywhere in the interstellar medium (ISM). The formation of small hydrocarbons (C_mH_n) from large PAH molecules via UV-destruction plays a crucial role in the top-down physico-chemical processes in ISM. In the photon dominated regions (PDRs) of ISM, the PAHs can undergo photoionisation and dissociation, which could lead to formation of smaller hydrocarbons. In this work, the formation of small hydrocarbons via dissociative ionization of PAHs of astrophysical interests in the presence of intense UV-field were explored by performing multiphoton ionization and dissociation (MPI/ MPD) experiments on PAHs of different size and shape. An experimental setup was designed and built to do the MPI/ MPD experiments. The set-up consists of a pulsed valve for letting in the carrier gas seeded with the PAH molecules and a Wiley-Mclaren type double electric field linear time-of-flight mass spectrometer coupled with a pulsed nanosecond laser (Nd:YAG) with crystals for the generation of up to 4^{th} harmonics. The 4^{th} harmonic of the Nd:YAG laser which correspond to the 266 nm is focussed to the interaction region to generate intense UV-field. The laser intensity at the focal point is measured to be of the order of 10^{13} W/cm^2.

The molecules chosen for the study are anthracene, phenanthrene and pentacene, among which the first two are isomers. Anthracene and pentacene are linear PAH molecules, whereas phenanthrene possesses a bent structure. The molecules had undergone multiphoton ionization and dissociation under intense UV-field and revealed results of much astrophysical insights, especially about the top-down chemistry of the photon-dominated regions (PDRs) in the space. The laser power dependence of the yield of ionic fragments from anthracene, phenanthrene and pentacene are studied by recording the spectra at different laser intensities. We have observed the formation of smaller masses like H^+,C^+, CH_n^+ (n=4-6), C_2^+, $C_2H_n^+$ and $C_3H_n^+$. Formation of CH_n^+ (n = 4-6) from a larger precursor upon photodissociation has been probed for the first time. Fragments with H/C ratio higher than one cannot form by direct photodissociation of PAH molecules. We propose the potential role of roaming mechanism in PAHs in the ISM for the formation of smaller hydrocarbons with H/C ratio higher than one, especially for the fluxional ions CH_5^+ and CH_6^+. Roaming is a recently discovered reaction pathway different from the conventional reaction dynamics. The astrophysical significances of this work are discussed in the recent publication [1].

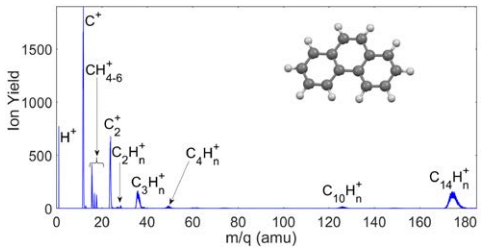

Figure 1. Multiphoton ionization and dissociation spectrum of phenanthrene.

References

[1] Chacko, R *et al* 2020 *ApJ* **896**(2) 130

*E-mail: robychako@gmail.com
†E-mail: garavind@iitm.ac.in

Photoionization and fragmentation of diketopiperazines. Computational and experimental efforts on the search of the 'seeds of life'

D Barreiro-Lage[1,*], P Bolognesi[2], J Charinelli[2], R Richter[3], H Zettergren[4], M H Stockett[4], L Carlini[2], S Díaz-Tendero[1,5,6] and L Avaldi[2]

[1]Departamento de Química, Módulo 13, Universidad Autónoma de Madrid, 28049 Madrid, Spain.
[2]Institute of Structure of Matter-CNR (ISM-CNR), 00015, Monterotondo, Italy.
[3]Elettra Sincrotrone Trieste, Basovizza (Trieste), Italy.
[4]Department of Physics, Stockholm University, Se-10691 Stockholm, Sweden.
[5]Condensed Matter Physics Center (IFIMAC), Universidad Autónoma de Madrid, 28049 Madrid, Spain.
[6]Institute for Advanced Research in Chemical Science (IAdChem), Universidad Autónoma de Madrid, 28049 Madrid, Spain

Synopsis In a combined experimental/theoretical study, we show how the interaction of VUV radiation with 2,5-Diketopiperazines can lead to the production of reactive oxazolidinone intermediates. The interaction of these intermediates with other neutral and charged fragments released in the molecular decomposition, leads either to reconstruction of the cyclic dipeptide or to the formation of longer linear peptide chains. Shedding light on the mechanisms of production of prebiotic building blocks is of paramount importance to understand the abiotic synthesis of relevant biologically active compounds.

The question of the origin of life has been discussed since before the birth of philosophy and hence, of science. Thales the Milesian considered water as the material entity that provided life, Heraclitus, on the other hand thought it was fire. Funny enough, we also agree that chemistry has the biggest role on it. In the search of pathways to the evolution of life on the early Earth, dynamic chemical processes involving peptide bond formation and cleavage mechanisms are thought to be of central importance [1].

Coupling of the condensation of α-amino acids into peptides with the peptide degradation 'returning' individual aminoacids might have provided an effective mechanism for reshuffling and building up the complexity of aminoacid sequences preceding the emergence of life. Considering this emergence of life as a process of evolution in a dynamic chemical network, α-amino acids and random oligopeptides shall have played an important role from the very beginning, acting as prebiotic 'seeds' that could lead to the formation of more complex systems. These processes of condensation and degradation rely on peptide bond formation and cleavage mechanisms. In this context, it has been proposed that the cyclic dipeptides (also known as 2,5-diketopiperazines, DKPs) [2], the simplest peptide derivatives found in nature, may have been precursors in the formation of longer peptide chains.

Photoelectron-photoion coincidence (PEPICO) measurements have allowed us to identify potential prebiotic activating agents and to investigate the energetics of their fragmentation channels. On the other hand, we have perfomed Quantum Chemistry calculations to unravel mechanisms that could lead to reorganization or peptide elongation [3], and thus, supporting the possible role of these DKP's as 'seeds' for biological life.

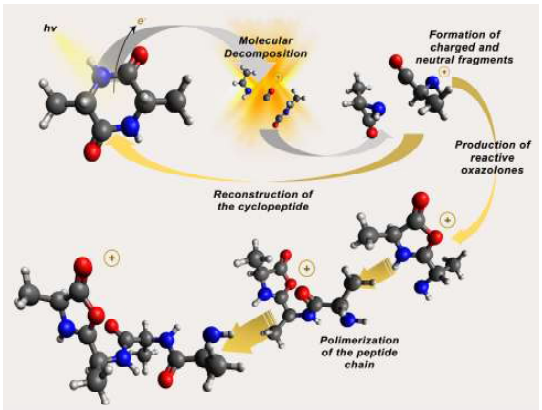

Figure 1. Interaction of VUV radiation with cyclo-(Alanine-Alanine) leading to molecular decomposition and to the production of reactive oxazolones.

References

[1] A Pross *et al.* 2011 *J. Sys. Chem.*, **2**, 1
[2] G Danger *et al.* 2012 *Chem. Soc. Rev.*, **41**, 5416–5429
[3] D Barreiro-Lage *et al.* 2021 *Submitted*.

*E-mail:dario.barreiro@uam.es

Asymmetric electron backscattering in strong-field ionization of chiral molecules

S Beauvarlet[1]*, D Rajak[1], O Kneller[2], S Rozen[2], A Comby[1], D Descamps[1], S Petit[1], V Blanchet[1], N Dudovich[2] and Y Mairesse[1]†

[1]CELIA-Universite de Bordeaux-CNRS-CEA, Talence, 33405, France
[2]Weizmann Institute of Science, Rehovot, 76100, Israel

Synopsis We photoionize chiral molecules by an intense elliptically polarized laser field. The angular distribution of the high energy photoelectrons shows a strong forward-backward asymmetry, resulting from their backscattering on the chiral ionic potential. The interference between direct and backscattered electrons opens the way to chiral photoelectron holography.

Strong laser fields offer unique properties to image the structure and dynamics of molecules in the gas phase. Tunnel ionization selectively releases electrons from the highest occupied orbitals and accelerates them along different possible pathways, depending on the ionization time. The electrons can directly escape the molecular potential, or be driven back to their parent ion and recollide. The photoelectron angular distribution (PAD) results from the coherent superposition of the different pathways, encoding information on the molecular potential through holography or laser-induced electron diffraction. As the complexity of the targets increases, retrieving structural information from the PAD becomes increasingly challenging because of orientational averaging over the randomly aligned molecules. Molecular alignment or coincidence electron-ion imaging both offer interesting solutions to this issue. Here we propose a different approach based on an orientational property which survives random alignment: molecular chirality.

When they are ionized by circularly polarized light, chiral molecules preferentially emit photoelectrons forward or backward relative to the laser propagation axis, depending on their handedness. This very sensitive chiroptical process named PhotoElectron Circular Dichroism (PECD) results from the scattering of the outgoing electrons in the chiral potential. In the strong-field regime, the influence of the potential is expected to vanish, leading to a weak PECD. Laser-driven electron backscattering could increase the sensitivity to the molecular potential, but this process is suppressed in circular polarization. To observe dichroism from chiral backscattering, we photoionize chiral molecules with an elliptically polarized strong laser field. The 3D PAD is measured in a velocity map imaging spectrometer using a tomographic method. In circular polarization, the PAD shows a doughnut structure (Fig 1a), with clear forward-backward (FB) asymmetry. With decreasing laser ellipticity, electrons appear in the 2-10 U_p kinetic energy range (Fig 1b), U_p being the ponderomotive energy. These electrons originate from backscattering and show strong FB asymmetries. In the region of overlap between direct and backscattered electrons, clear structures appear in the FB asymmetry and are found to be highly dependent on the molecular structure.
The observation of chiral-sensitive backscattering in strong-field ionization thus opens the way to chiral holographic imaging.

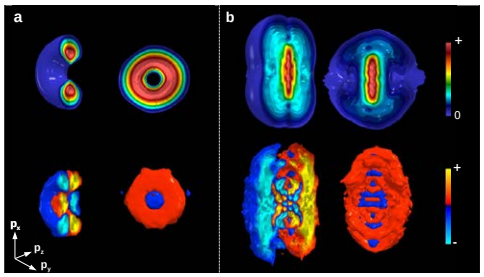

Figure 1. Cuts of the 3D photoelectron angular distribution (*up*) and its forward/backward asymmetric component (*down*) obtained by ionizing fenchone molecules with a circularly polarized (a) and low ellipticity (b) strong laser field.

*E-mail: sandra.beauvarlet@u-bordeaux.fr
†E-mail: yann.mairesse@u-bordeaux.fr

Step-by-step, state-selective tracking of sequential fragmentation dynamics of water dications by coincidence momentum imaging

T Severt[1*] Z L Streeter[2,3*], W Iskandar[2*], D Reedy[4], K A Larsen[2,5], D Call[4], E G Champenois[2,5], A Gatton[2,6], B Griffin[2], B Jochim[1], R Strom[2,6], M M Brister[2], A L Landers[6], D S Slaughter[2], J B Williams[4], R R Lucchese[2], T Weber[2], C W McCurdy[2,3] and I Ben-Itzhak[1†]

[1]J. R. Macdonald Laboratory, Physics Department, Kansas State University, Manhattan, Kansas 66506, USA
[2]Chemical Sciences Division, Lawrence Berkeley National Laboratory, Berkeley, California 94720, USA
[3]Department of Chemistry, University of California, Davis, California 95616, USA
[4]Department of Physics, University of Nevada Reno, Reno, Nevada 89557, USA
[5]Graduate Group in Applied Science and Technology, University of California, Berkeley, California 94720, USA
[6]Department of Physics, Auburn University, Alabama 36849, USA

Synopsis We demonstrate a method that enables step-by-step, state-selective tracking of sequential fragmentation of water following its double ionization by a single photon and measured with COLTRIMS.

During the fragmentation of polyatomic molecules, two or more bonds may break in a concerted manner (simultaneously) or sequentially (stepwise). Separating them and following their time evolution is key to better understanding of fragmentation dynamics. In this project [1], we focus on double ionization of heavy water by a single 61-eV photon, followed by sequential breakup via a $D^+ + OD^+$ intermediate into $D^+ + D^+ + O(^3P)$. Employing the native frames method [1,2], we identify, separate, and follow step-by-step, two state-specific sequential pathways of the intermediate OD^+. The signature of this sequential breakup is a uniform $N(\theta_{OD,D})$ distribution and $KER_{OD} < 2.25$ eV[‡], i.e. the expected KER for predissociation of OD^+ via the metastable $a\,^1\Delta$ and $b\,^1\Sigma^+$ states [3]. Some of the OD^+ ions undergo predissociation to the $D^+ + O(^3P)$ limit. Furthermore, we identify two pathways and the associated electronic states in the energy-correlation map shown in Fig. 1(a,b). Specifically, we separate the fragmentation of the $1\,^1B_1$ and $2\,^1A_1$ states of D_2O^{2+} into the $a\,^1\Delta$ and $b\,^1\Sigma^+$ states of OD^+ molecule, respectively.

Our classical trajectory calculations on the relevant *ab initio* potential energy surfaces verify the sequential fragmentation pathways, and enable the determination of the internal-energy and angular-momentum distributions of the OD^+ molecule. Moreover, the calculated and measured KER distribution in each of these pathways match very well, as shown in Fig. 1(c), where the inset shows the suppression at low KER due to the centrifugal barrier predicted by our theory.

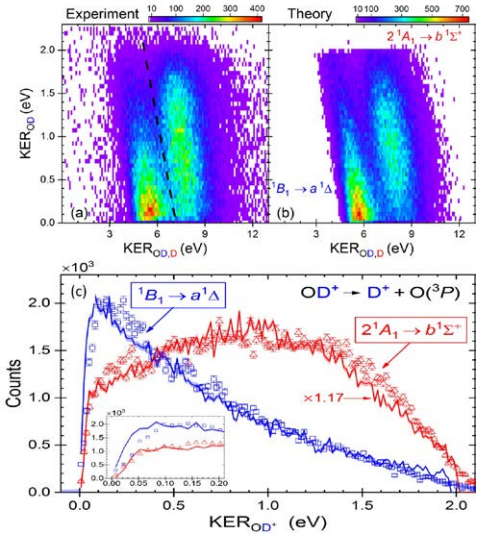

Figure 1. The (a) measured and (b) calculated KER correlation map of the first and second fragmentation step of D_2O, and (c) second step KER.

References

[1] Severt T, Streeter Z L *et al* – in preparation
[2] Rajput J *et al* 2018 Phys. Rev. Lett. **120** 103001
[3] de Vivie R *et al* 1987 Chem. Phys. **112**, 349

*T Severt, Z L Streeter, and W Iskandar, contributed equally by leading the data analysis, theoretical, and experimental aspects of the ALS campaign, respectively.
†E-mail: ibi@phys.ksu.edu
‡where $\theta_{OD,D}$ is the angle between the relative momenta associated with each step, and KER_{OD} is the second step KER.

Multi-photon and strong-field ionization of molecules in stationary and time-dependent R-matrix approaches

J Benda[1]*, Z Mašín[1], J D Gorfinkiel[2], G S J Armstrong[3], A C Brown[3], D D A Clarke[3], H W van der Hart[3], and J Wragg[3]

[1]Institute of Theoretical Physics, Faculty of Mathematics and Physics, Charles University, Prague, Czechia
[2]School of Physical Sciences, Faculty of STEM, The Open University, Milton Keynes, UK
[3]CTAMOP, School of Mathematics and Physics, Queen's University Belfast, Belfast, UK

Synopsis We use the R-matrix methodology to provide new insight into strong- and multi-photon ionization of molecules. In particular we perform a time-dependent simulation of the strong-field ionization of H_2O, where we observe correlation-driven redistribution of ionization yield. We also present a novel time-independent method for accurate calculation of below- and above-threshold multi-photon ionization amplitudes based on the molecular R-matrix approach and apply it to study resonant and non-resonant structures in two-photon cross sections for He, H_2 and CO_2.

We present selected theoretical results of our recently developed *ab initio* molecular method for description of interaction of multi-electron molecules with ultrafast strong or perturbative light fields. Our method is based on the well-known R-matrix theory, which divides the physical space into a region close to the target and its complement. In the "near" space, the multi-electron problem is solved using quantum-chemical methods, while in the "far" space we use single-particle channel expansion of the wave function. [1]

The method comes in two flavours: a time-independent one for calculation of the leading-order perturbation theory (LOPT) multi-photon cross sections for arbitrary number of absorbed photons (below or above the one-photon threshold), and a time-dependent one for direct solution of the Schrödinger equation for simulation of many-electron systems in electric fields of arbitrary strength, polarization and time dependence (RMT approach) [2]. In all cases the method allows for a flexible and sophisticated description of the multi-electron effects.

In this contribution we show the application of the time-independent method to calculation of the two-photon below- and above-threshold ionization of He, H_2 and CO_2 (see Fig. 1 for the latter) [3]. We also discuss application of the stationary approach to the analysis of a related two-photon process: the reconstruction of attosecond beating by two-photon transitions (RABITT).

Last but not least, we apply the time-dependent approach to strong-field ionization of H_2O in the coupled-channel model. We reveal the crucial role of multi-electron effects which manifest as correlation-driven redistribution of the total observable ionization yield and discuss the preferential ionization into various residual ion states and its dependence on the field intensity. [4]

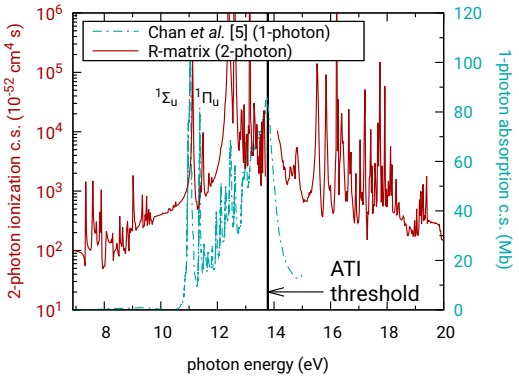

Figure 1. Two-photon ionization cross section of CO_2 summed over the final states X, A, B, C of the residual ion compared to one-photon absorption cross section measurement [5].

References

[1] Mašín Z *et al* 2020 *CPC* **249** 107092
[2] Brown A C *et al* 2020 *CPC* **250** 107062
[3] Benda J, Mašín Z 2021 *submitted*
[4] Benda J *et al* 2020 *Phys. Rev. A* **102** 052826
[5] Chan W F *et al* 1993 *Chem. Phys.* **178** 401

*E-mail: jakub.benda@utf.mff.cuni.cz

Strong-field-induced dissociation dynamics of tribromomethane ($CHBr_3$) studied using coincident ion momentum imaging

S. Bhattacharyya, K. Borne, F. Ziaee, S. Pathak, E. Wang, N. Marshall, A. Venkatachalam, A. Rudenko, D. Rolles*

J.R. Macdonald Laboratory, Department of Physics, Kansas State University, Manhattan, 66506, KS, USA

Synopsis Direct C-Br bond dissociation and H-migrated product formation of tribromomethane ($CHBr_3$) induced by intense near-infrared femtosecond laser pulses were investigated using the pump-probe technique in combination with ion-ion coincident Coulomb explosion imaging. The plausible mechanistic aspects of the dynamics are discussed.

Coulomb explosion imaging of molecules induced by an intense near-infrared (NIR) laser pulse is a powerful tool to understand the dynamics involved not only in bond-breaking but also in the formation of new chemical bonds that lead to transient molecular structures. Investigating the photo-induced isomerization and fragmentation dynamics of tribromomethane ($CHBr_3$) has been flourishing in recent years due to its photochemical features [1]. In the present work, the strong-field-induced dissociation dynamics of $CHBr_3$ were investigated as a function time delay between a pair of 28-femtosecond (fs) near-infrared laser pulses at a peak intensity of 6 x 10^{14} Wcm^{-2}. Pump-probe delay dependence signal is observed in the $Br^+ + CHBr_2^+$ and $HBr^+ + CBr_2^+$ two-body dissociation channels. The former is a direct dissociation while the latter requires hydrogen migration for H-Br bond formation.

Figure 1(a) shows the pump-probe delay dependence of the ionic kinetic energy release (KER) for the $HBr^+ + CBr_2^+$ channel. Two characteristic features are identified: A strong delay-independent bands between 3-5 eV, and a delay-dependent structure, marked by a superimposed blue dashed line, which evolves from 3 eV to 0.7 eV with increasing pump-probe delay. Similar features are observed for the $Br^+ + CHBr_2^+$ dissociation channel (not shown here). The total coincident ion counts for $Br^+ + CHBr_2^+$ and $HBr^+ + CBr_2^+$ channels is shown in Fig. 1(b). The observed delay dependence is modeled as the convolution of a Gaussian function with the product of a Heaviside function and a single exponential rise with time constant τ. The onsets of the dissociation are observed at 113 and 193 femtoseconds (fs) respectively. The likely scenario is that the vertically ionized parent ($CHBr_3^+$) holds the excitation energy in internal degrees of freedom before undergoing direct dissociation after a short period of time of 113 fs. It is likely that the H-migrated isomer is trapped in an additional potential energy well after the bond rearrangement causing 80 fs longer time for the dissociation onset. The experimental results are compared to Coulomb explosion simulations.

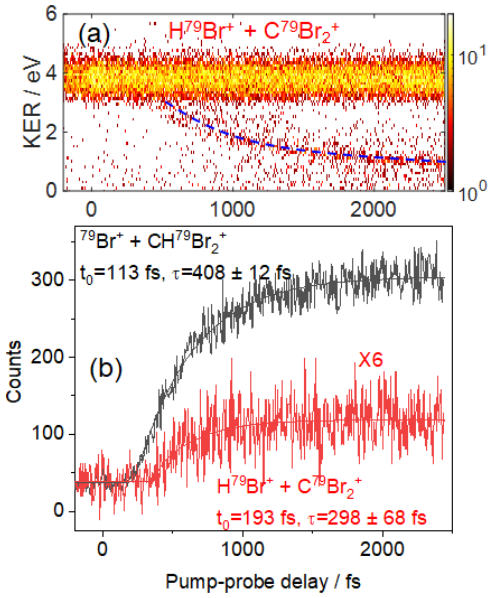

Figure 1. (a) Delay-dependence of the KER distribution for the $HBr^+ + CBr_2^+$ channel. (b) Delay dependence of the coincident ion counts for $Br^+ + CHBr_2^+$ and $HBr^+ + CBr_2^+$ channels.

References

[1] Toulson B W *et al* 2019 *Struct. Dyn.* **6** 054304

* E-mail: rolles@phys.ksu.edu

Probing influence of molecular environment and dynamic polarization in photoemission delays

Shubhadeep Biswas [1] *

[1] Physics Department, Ludwig-Maximilians-Universität Munich, D-85748 Garching, Germany
[2] Max Planck Institute of Quantum Optics, D-85748 Garching, Germany

Synopsis Measurement of molecular photoemission delays by attosecond streaking spectroscopy reveals the effect of molecular environment and dynamic polarizability in large molecules.

The advancement of attosecond chronoscopy has made it possible to reveal ultrashort time dynamics of photoionization [1]. Ionization delay measurements in atomic targets provide a wealth of information about the timing of the photoelectric effect [2], resonances, electron correlations and transport. The extension of this approach to molecules, however, presents great challenges. In addition to the difficulty of identifying correct ionization channels, it is hard to disentangle the role of the anisotropic molecular landscape from the delays inherent to the excitation process itself. Other than that the feature of dynamic polarizability in case of molecules, especially the larger ones, makes the problem even harder, however presents a rich play ground to see collective electron dynamics. Here, we first present the measurements of ionization delays from ethyl iodide around the 4d giant dipole resonance of iodine, which could disentangle the contribution of electron propagation effect within the molecular (ethyl group in this case) environment exclusively to the ionization delay [3]. In the second case to illustrate the effect of molecular dynamic polarization effect on ionization delay, we used ionization of C_{60} molecule around its well know giant dipole resonance at 20 eV. In both the cases, we employed attosecond streaking spectroscopy where an attosecond extreme ultraviolet (XUV) pulse ionizes the molecule around the energy of the respective giant resonances and the released electron is exposed to the ponderomotive force of a synchronized near-infrared (NIR) field, which yields a streaking spectrogram. Comparative phase analysis of the spectrograms corresponding to iodine 4d or C_{60} valance electrons with neon 2p emission permits extracting overall photoemission delays in both cases. In the ethyl iodide case the experimental results are compared to semi-classical and quantum scattering calculations. Here the outgoing electron, produced via inner shell ionization of the iodine atom in ethyl iodide, and thereby hardly influenced by the molecular potential during the birth process, acquires the necessary information about the influence of the functional ethyl group during its propagation. We find significant delay contributions that can distinguish between different functional groups, providing a sensitive probe of the local molecular environment [3]. This would stimulate to perform further angle resolved measurements in molecules to probe the potential landscape in three dimension. In case of C_{60}, the measurements are compared with simulations involving classical and quantum mechanical descriptions of fullerene under the effect of near infrared short laser pulses and subsequent propagation effect. This indicates a signatures of dynamic polarizability of the target and contribution from Eisenbud-Wigner-Smith type of delay, which encode the effect of collective excitation in time domain [4].

References

[1] Krausz F and Ivanov M 2009 *Rev. Mod. Phys.* **81** 163-234
[2] Schultze M *et al.* 2010 *Science* **328** 1658-1662
[3] Biswas S *et al.* 2020 *Nat. Phys.* **16** 778–783
[4] Biswas S *et al.* 2021 (in preparation)

* E-mail: shubhadeep.biswas@mpq.mpg.de

The XCHEM code: photoelectron angular distributions of the CO molecule

V J Borràs [1]*, L Argenti[2,3], J González-Vázquez[1] and F Martín[1,4,5]

[1]Departamento de Química, Módulo 13, Universidad Autónoma de Madrid, 28049 Madrid, Spain
[2]Department of Physics, University of Central Florida, Orlando, Florida 32186, USA
[3]CREOL, University of Central Florida, Orlando, Florida 32186, USA
[4]Instituto Madrileño de Estudios Avanzados en Nanociencia (IMDEA-Nano), Campus de Cantoblanco, 28049 Madrid, Spain
[5]Condensed Matter Physics Center (IFIMAC), Universidad Autónoma de Madrid, 28049 Madrid, Spain

Synopsis Study of the photoelectron angular distributions of the CO molecule in the presence of Feshbach resonances with the new implementation of the XCHEM code.

Due to the high photon energy of attosecond light sources, the theoretical description of attosecond experiments requires a proper representation of the ionization continuum. For polyelectronic molecules, the description of the ionization process requires the use of electronically correlated wave functions for the molecular bound states as well as the system's ionization continuum. Despite the huge success of state-of-the-art Quantum Chemistry Packages (QCP) for describing molecular bound sates, the combination with their ionization continuum at the same level of theory is still challenging.

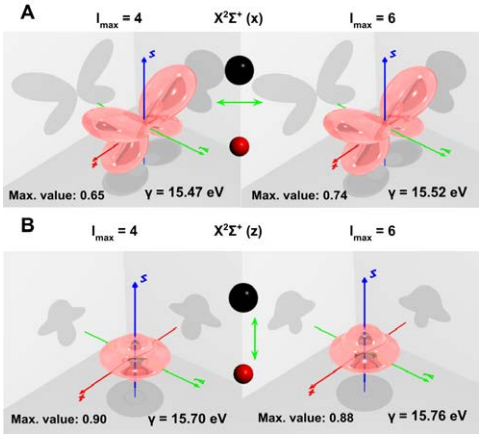

Figure 1: Convergence of the l_{max}=4 and l_{max}=6 XCHEM calculations for the MFPADs of the CO molecule at the top of two Feshbach resonances.

The XCHEM code, recently developed in our group, overcomes these difficulties by using a hybrid Gaussian-B-Spline (GABS) basis interfaced with existing QCPs via close-coupling scattering methods [1, 2]. The XCHEM approach has produced excellent results in different atomic and molecular systems [2, 3, 4, 5, 6, 7], encouraging us to go one step further.

The inherent anisotropy of molecules makes photoelectron angular distributions (PADs) an interesting observable to study, especially in the presence of Feshbach resonances where PADs are expected to change abruptly with the energy. The PADs, both in laboratory frame (beta asymmetry parameter) and in molecular frame (molecular-frame photoelectron angular distribution) have been just incorporated to the XCHEM code, allowing us to study them in more complicated systems such as CO and pyrazine.

In this presentation, we will focus on the results produced for the CO molecule that perfectly agree with previous results [8]. Our results also show that in the in the presence of Feshbach resonances abrupt changes in the PADs are observed.

References

[1] C. Marante et al., Phys. Rev. A 90, 012506 (2014).
[2] C. Marante et al., Chem. Theory Comp. 13, 499 (2017).
[3] L. Barreau, C. L. M. Petersson, M. Klinker, *et al.* Phys. Rev. Lett. 122, 253203 (2019).
[4] M. Klinkeret al., Phys. Rev. A,98, 033413 (2018).
[5] S. Poullain et al., Phys. Chem. Chem. Phys.,21, 16497 (2019).
[6] M. Klinker et al., J. Phys. Chem. Lett. 9, 756 (2018).
[7] C. Marante et al., Phys. Rev. A 96, 022507 (2017).
[8] A. Rouzée et al., J. Phys. B-At. Mol. Opt., 45, 074016 (2012)

*E-mail: josep.borras@uam.es

Non-ergodic fragmentation of protonated reserpine induced by fs-laser interaction

R Brédy[1]*, M Hervé[1], A Boyer[1], J M Brown[2], I Compagnon[1] and F Lépine[1]

[1]Univ Lyon, Université Claude Bernard Lyon 1, CNRS, Institut Lumière Matière, F-69622, Villeurbanne, France

[2]Waters Corporation, Stamford Avenue, Altrincham Road, Wilmslow, SK9 4AX, United Kingdom

Synopsis Fragmentation of gas phase protonated reserpine has been investigated using "on-the-fly" femtosecond laser activation/MS experiments. Non-statistical fragmentation triggered by multiphoton ionization is observed with activation at 800 nm. The mechanisms involve Coulomb repulsion between the proton site and the extra charge created by ionization. These results illustrate the use of ultrafast processes to unveil specific fragmentation patterns with the goal of studying the mechanisms behind fs-laser activation and the dynamics of the involved excited states.

Extracted from the root of Rauwolfia species, reserpine is used as drug treatment for hypertension or depression. In analytical sciences, reserpine is routinely employed as a chemical standard to calibrate and evaluate performances of mass spectrometers based on collision induced dissociation activation methods [1]. Despite these extensive uses the molecular physics properties of this model molecule are scarce.

Femtosecond-laser induced dissociation experiments conducted on amino-acids and peptides have demonstrated the interest of this activation method to generate non-statistical fragments [2] and/or fragments not accessible by conventional techniques. This is explained by the excitation and ionization mechanisms at play during the fs-laser interaction, multiphoton absorption or tunnel ionization depending on the laser peak intensity. In addition, the dissociation dynamics in such interactions can be investigated in pump-probe experiments thanks to the fs time resolution [3].

To explore fragmentation processes of protonated reserpine we have performed on-the-fly fs-laser interaction experiment by coupling a femtosecond laser with a triple quadrupole instrument, i.e., without trapping device [4]. This configuration ensures that one molecule interact with one single laser pulse. In mass spectra of protonated reserpine activated by 25 fs laser pulse at 800 nm (0 to 3.8×10^{14}W/cm^2), the observation of doubly charge reserpine and specific fragment m/z 414 show evidence of non-ergodic fragmentation, in contrast to fragmentation observed at 267 nm or CID [5].

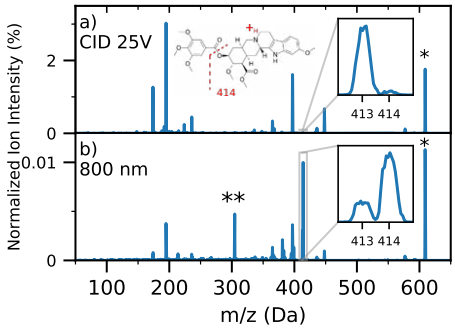

Figure 1. a) CID and b) 800 nm ($3.8\ 10^{14}$W/cm^2) fs-laser mass spectra of protonated reserpine. Parent ion at m/z 609 is marked by *, divided by a factor 10^3 in b). Doubly charge reserpine not observed in a) is marked by ** in b).

This specific fragmentation is attributed to Coulomb repulsion between the proton site and the extra charge created by ionization in the multiphoton and tunnel regimes.

References

[1] Kumar S *et al* 2016 *J. Pharm. Biomed. Anal.* **118** 183
[2] Kalcic C L *et al* 2012 *J. Phy. Chem. A* **116** 2764
[3] Reitsma G *et al* 2014 *Int. J. Mass. Spectrom.* **365-366** 365
[4] Hervé M *et al* 2019 *J. Phy. Chem. Lett.* **10** 2300
[5] Brédy R *et al* submitted

*E-mail: richard.bredy@univ-lyon1.fr

Molecular Frame Photoelectron Angular Distributions for Dissociation of 1,1-Dichloroethene ($C_2H_2Cl_2$) at the Chlorine L-edge

D Call[1]*, M Weller[4], G Kastirke[4], G Panelli[1], R A Strom[3], S Burrows[3], K Larsen[2], N Melzer[4], W Iskander[2], T Severt[5], I Ben-Itzhak[5], O Kostko[2], Th Weber[2], D Slaughter[2], V Davis[1], M Schöffler[4], R Dörner[4], T Jahnke[4], A L Landers[3], and J B Williams[1]†

[1]University of Nevada, Reno, NV, 89557, United States
[2]Lawrence Berkeley National Laboratory, Berkeley, CA, 94720, United States
[3]Auburn University, Auburn, AL, 36849, United States
[4]Goethe University Frankfurt, Frankfurt, 60323, Germany
[5]J.R. Macdonald Laboratory, Kansas State University, Manhattan, KS, 66506, United States

Synopsis L-edge photoionization of Cl followed by dissociation was performed on $C_2H_2Cl_2$. Results in the H^++H^++X dissociation channel show an unexpected number of electrons below 2 eV. Analysis found these low-energy electrons to have distinct Molecular Frame Photoelectron Angular Distributions (MFPADs) when compared to the two main photoelectron peaks.

Photoionization and dissociation of 1,1-Dichloroethene at the Chlorine L-edge measurements were performed with soft X-rays photons ($\gamma = 211.9$ eV) from the Advanced Light Source (ALS) on Beamline 9.0.1. Data was collected to examine the correlated momenta of the molecular fragments and the photoelectrons in coincidence, using the COld Target Recoil Ion Momentum Spectroscopy (COLTRIMS) method.

Chlorine has two 2p ionization thresholds separated by approximately 2 eV. Additionally, dissociation channels in the target molecule involving two separate H^+ ions contain an unexpected feature in the photoelectron energy spectrum located around 0 eV. Molecular Frame Photoelectron Angular Distributions (MFPADs) for different energy ranges show significant differences, as seen in Fig. 1. The molecular frame is defined from the two measured H^+ fragments' 3D momentum. This results in the two measured protons being located in this molecular frame at roughly $\phi \simeq 0$ & ± 180 and $cos(\theta) \simeq 0.6$. Assuming equilibrium molecular geometry, the two chlorine atoms are located at roughly $\phi \simeq 0$ & ± 180 and $cos(\theta) \simeq -0.6$. While the expected photoelectrons peaks show a preference for photoelectron emission off-angle between the C-Cl bond, the low-energy electrons show a clear preference to be emitted along the C-H bond with the strongest preference being seen in the lowest-energy electrons.

*E-mail: demitri.call@nevada.unr.edu
†E-mail: jbwilliams@unr.edu

Three possible explanations for the presence of low-energy electrons have been explored: shake-off events, knock-off events, and Post-Collisional Interaction (PCI) streaking effects[1]. PCI would correlate the measured low-energy electrons with Auger decay times in the low hundreds of attoseconds. Potential explanations for these low-energy electrons will be presented.

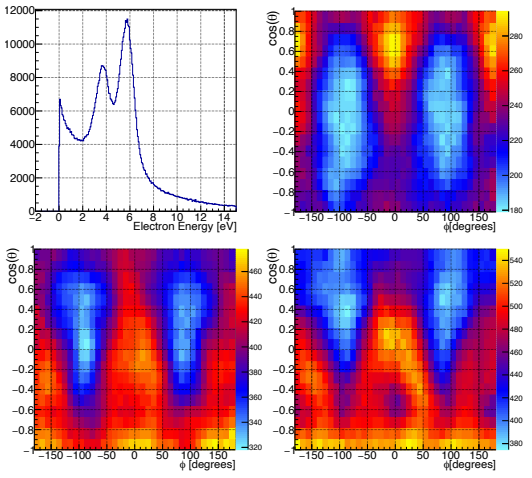

Figure 1. Above is a plot of electron energy (top left) and several MFPADs for different electron energies ranging from 0-2 eV (top right), 2-4.7 eV (bottom left), and 4.7-8.0 eV (bottom right).

References

[1] Trinter, F. *et al* 2013 *Phys. Rev. Lett.* **111** 093401

Metastable dications formation from chloronenzene probed by mass-selected Auger electron spectroscopy

LH Coutinho[1]*, C Nicolas[2], FA Ribeiro[3], A Milosavljevic[2], B Tenório[4], ACF dos Santos[1], J Bozec[2] and W Wolff[1]†

[1]Physics Institute, Federal University of Rio de Janeiro, Rio de Janeiro, 21941-972, Brazil
[2]Synchrotron SOLEIL, Gif-sur-Yvette, 91192, France
[3]Federal Institute of Rio de Janeiro, Rio de Janeiro, 26530-060, Brazil
[4]Technical University of Denmark, Department of Chemistry, Kongens Lyngby, 2800, Denmark

Synopsis We report the study of chlorobenzene photoionization by using synchrotron radiation at the Cl 2p and C 1s edges as part of a project aimed at elucidating metastable dicationic formation of aromatic compounds [1].

Important chemical compounds are derived from benzene by replacing one or more of its hydrogen or carbon atoms with another functional group, as in chlorobenzene, where the chlorine atom substitutes one hydrogen (C_6H_5Cl). It is found in several environmental matrices such as superficial and underground water, soil, air, biota, sediments, fertilizers, sewage sludge and recently in Mars craters [2].

Double charge transfer spectra, when OH^+ projectiles undergo electron-capture with chlorobenzene, observed the population of various excited states of $C_6H_5Cl^{++}$ [3]. Also, under 150 keV protons a significant yield of doubly and triple charged parent ions were observed [4].

In the present work, chlorobenzene photoionization was studied in the Cl 2p and C 1s edges, aiming at the investigation of these metastable dications under high dissociative conditions. For this purpose, Energy-Selected Auger Electron Photoion COincidende (ES-AEPICO) spectra were obtained by measuring the cationic molecular fragments in coincidence with electrons with kinetic energies in the Cl 2p and C 1s regions. Figure 1 presents mass selected Auger electrons spectra for the molecular dication $C_6H_5Cl^{++}$, the analogue molecular benzene dication $C_6H_4^{++}$ and the largest observed singly ionized fragment $C_5H_nCl^+$. A pronounced binding energy selectivity in the dications production was observed and is discussed in contrast with the behaviour of the singly ionized fragments, which are very similar to the total electrons distribution.

The experiment was conducted at the synchrotron facility SOLEIL, using photons from the undulator beamline PLÉIADES.

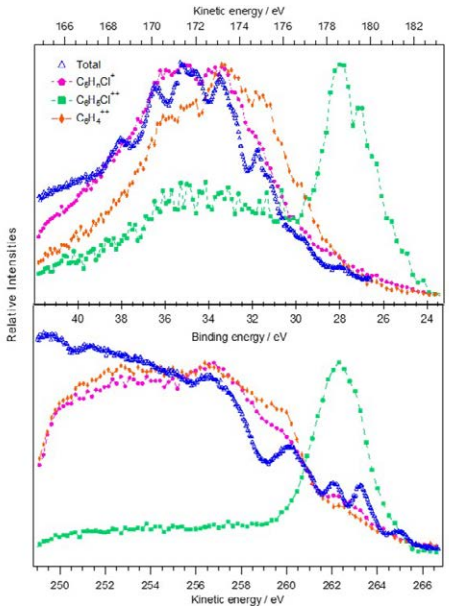

Figure 1. Total and mass selected Auger electron curves with kinetic energies in the Cl 2p (top) and C 1s (bottom) regions.

References

[1] Wolff W *et al.* 2020 *Journal Physical Chemistry. A* **124 9261–9271**.
[2] Freissinet C *et al.* 2015 *Journal of Geophysics Research: Planets* **120 495-514**.
[3] Harris F M *et al.* 1992 *Organic Mass Spectrometry* **27 261-269**.
[4] Fantuzzi F *et al.* 2018 *J. Am. Chem. Soc.* **140 4288–4292**.

*E-mail: lucia@if.ufrj.br
†E-mail: wania@if.ufrj.br

Observable Auger and inter-Coulombic decay hybrid resonances in the photoionization of endofullerenes

Ruma De[1] *, Esam Ali[1], Steven T Manson[2] and Himadri Chakraborty[1] †

[1] Department of Natural Sciences, D L Hubbard Center for Innovation, Northwest Missouri State University, Maryville, Missouri 64468, USA
[2] Department of Physics and Astronomy, Georgia State University, Atlanta, Georgia 30303, USA

Synopsis We compute the Auger-ICD hybrid resonances in the photoionization of Cl@C_{60} that reconfirms the effect's original prediction for Ar@C_{60}. The strength and width of some of these resonances suggest that they can be observed experimentally.

In loosely bound matter, the relaxation of an innershell vacancy resulting in the emission of an outershell electron at the same site of the system is the Auger process. This vacancy can also decay by transferring excess energy to a neighboring site to drive the emission. The latter is called the inter-Coulombic decay (ICD). Probing ICD processes in simpler vapor-phase materials is of considerable interest [1]. A class of such systems are endofullerene complexes, in which an atom placed in a fullerene makes them heterogeneous, nested dimers of weak bonding. For experiments, the synthesis techniques of endofullerenes are quickly developing [2].

The coherence between the Auger and ICD amplitudes to produce a novel class of resonances, the hybrid Auger-ICD (A-ICD) resonances, in the photoionization of atom-C_{60} hybridized levels was first predicted for Ar@C_{60} [3]. The new results presented here for Cl@C_{60} reconfirm the prediction of A-ICD resonances even for Cl which has a vacancy in the ground state compared to the closed shell Ar.

The calculation is carried out in the linear-response density functional theory (DFT) with the dipole response of the system to the incoming radiation [3]. The Kohn-Sham equations of the delocalized valence electrons are solved to obtain the ground state structures while the cage of 60 C^{4+} ions is jelliumized [4].

Figure 1 presents resonant hybrid A-ICD (RHA-ICD) features (A, B, C) for the decay of Cl 3*s* holes (identified) in the cross section of Cl@C_{60} symmetric and anti-symmetric hybrid level emissions. These window-type resonances of the symmetric level are seen to be sufficiently strong and wide favoring their experimental amenability. This trend was also found earlier for Ar@C_{60}, but for both hybrid level emissions. The other resonances seen in both curves are due to various C_{60} vacancy decays. This latter class of A-ICD features are harder to access due to their narrow widths because of the characteristic delocalized nature of C_{60} holes.

The current results may further motivate experiments to probe some of these resonances.

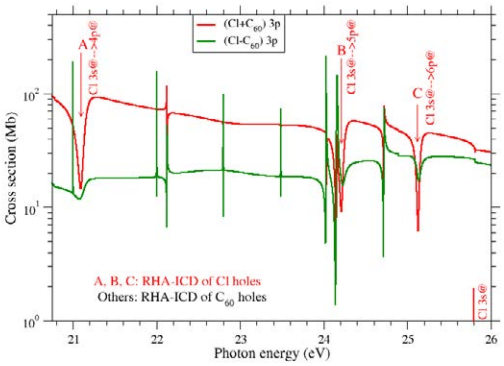

Figure 1. Symmetric (red) and anti-symmetric (green) hybrid level cross sections showing A-ICD resonances.

Supported by the National Science Foundation grant PHY-1806206 (HSC) and the US DoE, Office of Science, Basic Energy Sciences Grant DE-FG02-03ER15428 (STM).

References

[1] Jahnke T *et al* 2020 *Chem. Rev.* **120** 11295
[2] Popov A 2017 *Nanostruc. Sc. Tech. Ser. (Springer)*
[3] Javani M *et al* 2014 *Phys. Rev. A* **89** 063420
[4] Choi J *et al* 2017 *Phys. Rev. A,* **95** 023404

* E-mail: ruma@nwmissouri.edu
† E-mail: himadri@nwmissouri.edu

Attosecond Spectroscopy of Small Organic Molecules: XUV pump-XUV probe Scheme in Glycine

J. Delgado [1]*, M. Lara-Astiaso [2], J. González-Vázquez[2], P. Decleva[3], A. Palacios[2,4]†, F. Martín[1,2,5]

[1]Instituto Madrileño de Estudios Avanzados en Nanociencia, 28049 Madrid, Spain
[2]Departamento de Química, Módulo 13, Universidad Autónoma de Madrid, 28049 Madrid, Spain
[3]Dipartamento di Scienze Chimiche e Farmaceutiche, Universitá di Trieste, 34127 Trieste, Italy
[4]Institute for Advanced Research in Chemical Sciences (IAdChem), Universidad Autónoma de Madrid, 28049 Madrid, Spain.
[5] Condensed Matter Physics Center (IFIMAC), Universidad Autónoma de Madrid, 28049 Madrid, Spain

Synopsis We theoretically investigate the electron-nuclear dynamics arising in an attosecond two-color XUV-pump/XUV-probe experiment in glycine. A multi-reference static-exchange scattering method is combined with a trajectory surface hopping approach, thus explicitly accounting for the evaluation of the electronic continuum function, the nuclear wave packet distribution and the non-adiabatic couplings in the coupled electron-nuclear dynamics pumped upon ionization. We show that by engineering the initial electronic wave packet with the pump pulse, one can drive the cation dynamics into a specific fragmentation pathway.

The availability of coherent light sources with attosecond resolution (1 as=10^{-18} s) has opened the door to resolve electron dynamics in excited and ionized complex molecules. The early electron dynamics triggered in a biomolecule is at the heart of biological processes which are essential to life. Therefore, understanding the ultrafast charge dynamics that steer these processes has become a hot topic in the field of attosecond science. Attosecond time-resolve experiments allow us to retrieve images of this charge dynamics in molecules. The first experiment retrieving a sub-femtosecond ultrafast dynamics in a biomolecule was performed by using an as UV-pump/ fs IR-probe scheme in phenylananine [1]. The sub-fs charge fluctuations where associated with electronic coherences initiated by the as pump pulse. Theorical calculations to describe this experiment were initially performed considering that the nuclei of the molecule remained fixed in space [1],[2]. How long these electronic coherences can survive when nuclear motion comes into play is a question that has yet to be solved.

In the present study, we pursue to shed some light on this matter by theoretically describing the outcome of an attosecond two-color XUV-pump/XUV- probe scheme in glycine. The broadband pump pulse ionizes the molecule, creating a coherent superposition of cationic states, which evolve in time coupled to the nuclear motion until it is probed by the second XUV pulse. An explicit evaluation of the full-electron wave function in the continuum and the inclusion of non-adiabatic effects are carried out [3]. Both aspects have been addressed in this work by combining a multi-reference static-exchange method and a surface hopping approach, respectively. We have found that, in the absence of the probe pulse, ionization can lead to fragmentation of the glycine cation through the C-C or the C-N bonds. The lower electronic states of the cation are more likely to induce elongation of the C-C bond, while the higher excited states favor elongation of the C-N bond, both of which can ultimately break. We have found that by simply varying the central frequency of the pump pulse by a few eVs, one can alter the cation dynamics favouring specific fragmentation pathways. We have also investigated the role of the probe pulse in capturing the above dynamics, first by looking at the photoelectron spectra and then at the fragmentation yields, both as a function of the pump-probe delay.

*E-mail: jorge.delgado@imdea.org
†E-mail: alicia.palacios@uam.es

References

[1] Calegari *et al* 2014 *Science* **346** 336-339
[2] Kuleff, Cederbaum 2014 *J. Phys. B: At., Mol. Opt. Phys* **47** 124002
[3] Delgado *et al* 2021 *Faraday Discuss.* **Advance Article**

Photoelectron distributions from ionization via a synthetically chiral pulse

Z Dube[1] *, G Katsoulis[2], Y Mi[1], T Wang[1], G Ernotte[1], K Johnston[1], A Yu Naumov[1], D M Villeneuve[1], P B Corkum[1], A Emmanouilidou[2] and A Staudte[1]†

[1]National Research Council Canada, Ottawa, 100 Sussex Drive, Ottawa, Canada
[2]University College London, London, WC1E 6BT, UK

Synopsis Using a four-pulse, synthetically chiral pulse scheme, we study the photoelectron distributions of simple to complex targets in Cold Target Recoil Ion Momentum Spectroscopy: argon atoms, D_2 molecules, and propylene oxide, a chiral molecule.

Chiral enantiomers are notoriously difficult to differentiate as they have the same chemical and physical properties, yet they often have dramatically different biochemical functionality. Circularly polarized light has been shown to be able to distinguish between them, but the sensitivity is low, on the order of a few percent signal difference [1]. The reason for the weak optical response is that the wavelength is large compared to the molecule, and therefore the field appears 2-dimensional.

In 2019, Ayuso et al proposed a multi-pulse scheme to create an optical field with a locally chiral, i.e., a 3-dimensional electric field component. This scheme was predicted to yield a 100% signal difference between enantiomers in the high harmonic signal [2]. The predicted giant effect in the high harmonic spectrum so far remains untested by experiment. On the other hand, it is also unclear how sensitive the photoelectron response will be to the above scheme.

In this work, a Cold Target Recoil Ion Moment Spectroscopy (COLTRIMS) system is used to study the photoelectron distributions produced by Ayuso et al's multi-pulse scheme. A linearly polarized 800 nm pulse is split in two, and each subsequent pulse is used to generate a 400 nm second harmonic beam. Thereby we create two separate, independently controlled othorgonally polarized two colour (OTC) pulses for use in the experiment. The beams propagate in parallel, but not colinearly. When they are focused by a normal-incidence parabolic mirror in the COLTRIMS apparatus, both beams collapse with a 10° angle onto a supersonic gas jet. The combination of the non-collinear focusing with the 2-dimensional field of the OTC pulses creates an optical field in the focus, which has an electric field component that rotates through all three directions in every point in space, allowing for a locally chiral field. By changing the relative phases between the composite pulses, the degree of chirality of the effective field can be controlled. We are exploring the effect of this field on the photoelectron momentum distribution from single ionization.

In order to study levels of increasing complexity in photoelectron distributions, three different types of gas target are used: Argon atoms, D_2 molecules, and propylene oxide, a chiral molecule. The prelimary results of this experiment will be shown and discussed, and compared with theoretical computations using a semi-classical approach.

References

[1] R. Cireasa *et al*, Nat Phys, **11**, 654-658 (2015)
[2] D. Ayuso *et al*, Nat Phot, **13**, 866-871 (2019)

* E-mail: zack.dube@gmail.com
† E-mail: andre.staudte@nrc.ca

Fourfold differential Photoelectron Circular Dichroism

K. Fehre[1*], F. Trinter[2,3], N. M. Novikovskiy[4], G. Nalin[1],N. Anders[1], S. Eckart[1], D. Trabert[1], S. Grundmann[1], M. Kircher[1], A. Khan[1], R. Tomar[1], M. Hofmann[1], M. Waitz[1], I. Vela-Perez[1], H. Fukuzawa[5], K. Ueda[5],J. Williams[6], D. Kargin[7], M. Maurer[7], C. Küstner-Wetekam[4], L. Marder[4], J. Viehmann[4], A. Knie[4], R. Pietschnig[7], T. Jahnke[1], R Dörner[1*], Ph. V. Demekhin[4*] and M. S. Schöffler[1*]

[1]Institut für Kernphysik, Goethe-Universität, Max-von-Laue-Strasse 1, 60438 Frankfurt am Main, Germany
[2]Deutsches Elektronen-Synchrotron (DESY), Notkestrasse 85, 22607 Hamburg, Germany
[3]Molecular Physics, Fritz-Haber-Institut der Max-Planck-Gesellschaft, Faradayweg 4-6, 14195 Berlin, Germany
[4]Institut für Physik und CINSaT, Universität Kassel, Heinrich-Plett-Strasse 40, 34132 Kassel, Germany
[5]Institute of Multidisciplinary Research for Advanced Materials, Tohoku University, Sendai 980-8577, Japan
[6]Department of Physics, University of Nevada, Reno, Nevada 89557, United States
[7]Institut für Chemie und CINSaT, Universität Kassel, Heinrich-Plett-Strasse 40, 34132 Kassel, Germany

Synopsis We show the fourfold differential photoelectron circular dichroism for inner-shell photoionization to be equivalent to the influence of the helicity of the light onto the molecular frame angular distribution of a fixed in space asymmetric molecule.

The diffraction pattern of a photoelectron illuminating the molecule from within [1] provides detailed insights into, for example, the structure of the molecule [2]. The diffraction pattern of chiral molecules is sensitive to the helicity of the circularly polarized ionizing light and the orientation of the molecule relative to the light propagation axis. Even without access to the full 3d-orientation of the molecule (integration over all orientations), a forward/backward asymmetry with respect to the direction of light propagation survives even in the context of the electrical dipole approximation. Termed Photoelectron Circular Dichroism (PECD), the observation of this asymmetry has become a prime tool in the last two decades to investigate asymmetric molecules[3-5]. However, the integration over different molecular orientations inevitably leads to a loss of information. In a further development of the work by Tia et al. [6] we show that the signal strength and thus the sensitivity of the PECD for the fixed in space molecule is maximal and in this limiting case identical to the influence of the light helicity on the molecular frame photoelectron angular distribution (MFPAD) for certain molecular orientations. Employing the example of trifluoromethyloxirane ($C_3H_3F_3O$) upon O 1s photoionization, we discuss the symmetry properties of MFPADs resolved for the orientation of the molecule and connect it to the enhancement of the PECD going beyond 55 % signal strength.

References

[1] Landers A. *et al.* 2001 *Phys. Rev. Lett.* **87**, 13002
[2] arXiv:2101.03375
[3] Comby A. *et al* 2018 Nat. Commun. **9** 5212
[4] Ferré A. *et al* 2015 Nat. Photonics **9** 93
[5] Nahon L. *et al* 2015 JESRA **204** 322
[6] Tia M. *et al* 2017*J. Phys. Chem. Lett.*, **8**, 13, 2780–2786

* E-mail: fehre@atom.uni-frankfurt.de
* E-mail: schoeffler@atom.uni-frankfurt.de
* E-mail: doerner@atom.uni-frankfurt.de
* E-mail: demekhin@physik.uni-kassel.de

Strong Differential Photoion Circular Dichroism in Strong-Field Ionization of Chiral Molecules

K. Fehre[*1], S. Eckart[*], M. Kunitski[*], C. Janke[*], D. Trabert[*], M. Hofmann[*], J. Rist[*], M. Weller[*], A. Hartung[*], L. Ph. H. Schmidt[*], T. Jahnke[*], H. Braun[†], T. Baumert[†], J. Stohner[ł], Ph. V. Demekhin[†], M. S. Schöffler[*2] and R. Dörner[*3]

[*]Institut für Kernphysik Goethe-Universität Frankfurt Max-von-Laue-Str. 1, 60438 Frankfurt am Main, Germany
[†]Institut für Physik und CINSaT, Universität Kassel, Heinrich-Plett-Straße 40, 34132 Kassel, Germany
[ł]ZHAW Zurich University for Applied Sciences, Departement N, Campus Reidbach, Research Group Physical Chemistry Einsiedlerstrasse 31, 8820 Wädenswil, Switzerland

Synopsis In the strong field regime, the differential ionization probability is up to two orders of magnitude more sensitive to the helicity of the ionizing light than the total ionization yield.

Circular dichroism (CD) effects depict the difference in the absorption strength between left and right handed circularly polarized light occurring for the two enantiomers of a chiral substance. CD effects have received great attention in recent years with a variety of possible applications in, for example, the fields of absorption spectroscopy [1] or fluorescence spectroscopy [2]. Since the probability of absorption is directly linked to the probability of photoionization [3-5], an occurring CD can lead to observable differences in the absolute ion yield [6,7].

One promising route to enhance the visibility of CD effects is to examine vectorial observables such as electron emission angles rather than rates or yields. One prime example showing the strength of such an approach is the photoelectron circular dichroism (PECD), which is the normalized difference of photoelectron angular emission distributions from chiral molecules upon inversion of the light helicity.

In this contribution, we investigate the differential ionization probability of chiral molecules in the strong field regime as a function of the helicity of the incident light. To this end, we analyze the fourfold ionization of bromochlorofluoromethane (CHBrClF) with subsequent fragmentation into four charged fragments and different dissociation channels of the singly ionized methyloxirane (C_3H_6O). A variation of the differential ionization probability of several percent was observed.

References

[1] Kelly S. M. *et al* 2005 *Biochimica et biophysica acta* **1751**, 119
[2] Richardson F. S. *et al* 1977 *Chem. Rev.* **77**, 773
[3] Power E. A. et al 1974 *The Journal of chemical physics* **60**, 3695
[4] Boesl von Grafenstein U. *et al* 2006 *ChemPhysChem* **7**, 2085
[5] Lehmann C. S. 2020 *PCCP* **22**, 13707
[6] Breunig H. G. *et al* 2009 *ChemPhysChem* **10**, 1199
[7] Horsch P.*et al* 2012 *Chirality* **24**, 684

[1] E-mail: fehre@atom.uni-frankfurt.de
[2] E-mail: schoeffler@atom.uni-frankfurt.de
[3] E-mail: doerner@atom.uni-frankfurt.de

Enantiosensitive Structure Determination by Photoelectron Scattering on Single Molecules

K. Fehre[1*], G. Nalin[1], N. M. Novikovskiy[2,3], S. Grundmann[1], G. Kastirke[1], S. Eckart[1], F. Trinter[1,4], J. Rist[1], A. Hartung[1], D. Trabert[1], Ch. Janke[1], M. Pitzer[1], S. Zeller[1], F. Wiegandt[1], M. Weller[1], M. Kircher[1], M. Hofmann[1], L. Ph. H. Schmidt[1], A. Knie[2], A. Hans[2], L. Ben Ltaief[2], A. Ehresmann[2], R. Berger[5], H. Fukuzawa[6], K. Ueda[6], H. Schmidt-Böcking[1], J. B. Williams[7], T. Jahnke[8], R. Dörner[1], Ph. V. Demekhin[2*], and M. S. Schöffler[1*]

[1]Institut für Kernphysik, Goethe-Universität Frankfurt, Max-von-Laue-Straße 1, 60438 Frankfurt am Main, Germany
[2]Institut für Physik und CINSaT, Universität Kassel, Heinrich-Plett-Straße 40, 34132 Kassel, Germany
[3]Institute of Physics, Southern Federal University, 344090 Rostov-on-Don, Russia
[4] Molecular Physics, Fritz-Haber-Institut der Max-Planck-Gesellschaft, Faradayweg 4-6, 14195 Berlin, Germany
[5]Department of Chemistry, Philipps-Universität Marburg, Hans-Meerwein-Straße 4, 35032 Marburg, Germany
[6]Institute of Multidisciplinary Research for Advanced Materials, Tohoku University, Sendai 980-8577, Japan
[7]Department of Physics, University of Nevada, Reno, Nevada 89557, United States
[8]European XFEL GmbH, Holzkoppel 4, 22869 Schenefeld, Germany

Synopsis Combining Coulomb explosion imaging with photoelectron diffraction, we measure the 3D-structure of isolated chiral molecules in the gas-phase.

X-ray as well as electron diffraction are powerful tools for structure determination of molecules [1-3]. Electron diffraction methods yield Ångstrom-resolution even when applied to large systems [4] or systems involving weak scatterers such as hydrogen atoms [5]. For cases in which molecular crystals cannot be obtained or the interaction-free molecular structure is to be addressed, corresponding electron scattering approaches on gas-phase molecules exist [6,7]. Such studies on randomly oriented molecules, however, can only provide information on internuclear distances, which is challenging to analyze in case of overlapping distance parameters. Furthermore they do not reveal the handedness of chiral systems [8]. Here, we present a novel scheme to obtain information on the structure, handedness and even detailed geometrical features of the molecules in the gas phase. Using a loop-like analysis scheme employing input from ab initio calculations on the photoelectron scattering process, we were able to deduce the three dimensional molecular structure with great sensitivity regarding the position of individual atoms, as e.g. protons. To achieve this, we measure the molecular frame diffraction pattern of core-shell photoelectrons in combination with only two ionic fragments from a molecular Coulomb explosion. Our approach is expected to be suitable for larger molecules, as well, since typical size limitations regarding the structure determination by pure Coulomb explosion imaging are overcome by measuring in addition the photoelectron in coincidence with the ions.

References

[1] Zou, X. D., *et al* 2008 *Acta Cryst. A*. **64**, 149–160
[2] Woodruff, D. P. 2008 *Appl. Phys. A*. **92**, 439–445
[3] Kunde, T. et al 2019 *Angew. Chem. Int. Ed.* **58**, 666–668
[4] Zuo, J. M. *et al* 2003 *Science* **300**, 1419–1421
[5] Palatinus, L. *et al.* 2017 *Science* **355**, 166–169
[6] Hedberg, K. *et al.* 1991 *Science* **254**, 410-412
[7] Fokin, A. A., *et al* 2017 *J. Am. Chem. Soc.* **139**, 16696-16707
[8] Centurion, M. 2016 *J. Phys. B: At. Mol. Opt. Phys.* **49**, 062002

* E-mail: fehre@atom.uni-frankfurt.de
* E-mail: schoeffler@atom.uni-frankfurt.de
* E-mail: demekhin@physik.uni-kassel.de

Spectral Signature of Molecular Charge Migration

R. Fernández Carbón[1] * **and L. Argenti**[2] †

[1]Burnett School of Biomedical Sciences, University of Central Florida, FL 32816
[2]Dept. of Physics and CREOL, University of Central Florida, FL 32816

Synopsis We present an *ab initio* method to simulate the evolution of the correlated electronic state of a molecule under the action of arbitrarily polarized non-ionizing light pulses in the presence of decoherence, using the time-dependent Lindblad master equation. We apply the method to identify the spectral signature of charge migration in organic molecules of biological relevance.

Mounting experimental evidence suggests that the high efficiency of energy conversion in living beings, refined by natural selection over billions of years, relies on the quantum nature of charge transfer [1]. The recent development of attosecond laser technology allows us to study these ultrafast processes at the molecular level and natural time scale. To interpret the ultrafast electron dynamics of biomolecules, it is necessary to account for: i) correlation in excited electronic states, ii) the loss of electronic coherence caused by the progressive entanglement with the nuclear degrees of freedom and with electronic excited states in other molecules in the matrix, and iii) the non-perturbative character of the light matter interaction. Here we present a study on small organic molecules of biological relevance employing a new *ab initio* method to simulate the evolution of the correlated electronic state of a molecule under the action of arbitrarily polarized non-ionizing light pulses in the presence of decoherence. The electronic states are obtained from MCSCF calculations [2]. The effects of the driving pulses and decoherence are taken into account by numerically solving the time-dependent Lindblad equation [3] for the density matrix of the system. We reconstruct the susceptibility from the dipolar response of the light-dressed molecule, which is an experimental observable, and we use Becke's charge-partitioning algorithm [4] to theoretically predict the migration of charge associated to each spectroscopic signal. We demonstrate the potential of this method by mapping the profile of individual charge-migration modes in the molecule, and show how these modes are reproduced in the four-wave-mixing spectrum of the target.

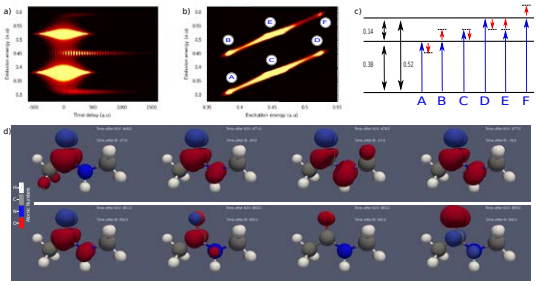

Figure 1. Simulation of the transient absorption spectrum and charge migration in N-Methylacetamide. a) Spectrum of the Y dipole component, as a function of the pump-probe delay (a.u.). b) 2D spectrum obtained by taking the Fourier transform of a) with respect to the time delay of the IR probe (Emission $[\omega]$ vs Excitation frequency $[\omega + \omega_\tau]$, in a.u.). c) Energy diagram of the relevant states in the molecule and of the main multi-photon paths responsible for the signals observed in a-b. d) Change of electronic density in N-Methylacetamide, with respect to the ground state, after a Y-polarized pump-probe pulse sequence; red and blue representing excess and depletion of electronic charge, respectively.

References

[1] Y Kim *et al* 2021 *Quantum Rep.* **3** 80
[2] I Fdez. Galván *et al* 2019 *J. Chem. Th. Comput.* **15** 5925
[3] F. Nathan and M. Rudner *et al* 2020 *Phys. Rev. B* **102** 115109
[4] H. Gharibnejad *et al* 2021 *Comput. Phys. Commun.* **263** 107889

*E-mail: rfernandez06@knights.ucf.edu
†E-mail: Luca.Argenti@ucf.edu

Interaction of ultra-short laser pulses with OCS molecules and determination of orientation of the (2,2,2) channel

A Ashrafi-Belgabad[1,2*], R Karimi[1,2], P Parvin[1], M Monfared[3], K Tian[2], E Irani[4], B Wales[2], É Bisson[5], S Beaulieu[5], M Giguère[5], J C Kieffer[5], F Légaré[5], J H Sanderson[2†]

[1]Amirkabir University of Technology (Tehran Polytechnic), 15875-4413, Tehran, Iran
[2]University of Waterloo, 200 University Avenue West, Waterloo, Ontario, Canada N2L 3G1
[3]Vienna University of Technology, Wiedner Hauptstraße 8-10, 1040, Vienna, Austria
[4]Tarbiat Modares University, P.O. Box 14115-175, Tehran, Iran
[5]Institut National de la Recherche Scientifique, Centre Énergie Matériaux Télécommunications,Varennes, QC J3X 1S2, Canada

Synopsis The kinetic energy released distribution and breakup orientation of OCS molecules probed by ultra-short laser pulses is investigated. The results show the breakup of OCS in which the molecule axis is parallel to the laser polarization is more probable than the case it is perpendicular.

In 1979, Kanter et.al. introduced a new technique in order to determine the structure of molecules called Coulomb explosion imaging (CEI) [1]. In this technique, the molecule under investigation ionizes very quickly on a femtosecond time scale and then breaks up, due to the Coulomb repulsion between the positively charged fragment ions. In contemporary femtosecond laser-based systems, this process occurs in a Time of Flight Mass Spectroscopy (TOFMS) apparatus which consists of a linear electric field that gives us an opportunity to capture ionic fragments in coincidence over 4π. The TOF apparatus ends in a Position Sensitive Detector (PSD) to record the position as well as time information [2]. From this information, we can obtain the momentum of the ionic fragments which contains within it an imprint of the initial position of the constituent atoms and thus allows us to obtain an image of the parent molecule structure.

Here we study the interaction of Carbonyl sulfide (OCS) molecules with ultra-short femtosecond pulses (sub 7fs) with the intensity of 3.2×10^{15} W/cm^2 by employing Coulomb explosion imaging using a TOFMS at the Advanced Laser Light Source (ALLS). In previous work, [3] Wales et al. studied the OCS^{3+} and OCS^{4+} dissociation and the kinetic energy released (KER) for different pulse durations from 7 – 500 fs. Here for the first time, we examine the KER of OCS^{6+} dissociation in the (2,2,2) channel, paying attention to the information which can be retrieved from the fragment and total KER, in terms of structure and alignment of the molecule.

Figure 1 shows the KER of all fragments and the total KER of the molecule, obtained over all orientations parallel to the laser polarization. We will present the results of KER and deduced geometry as a function of molecular alignment.

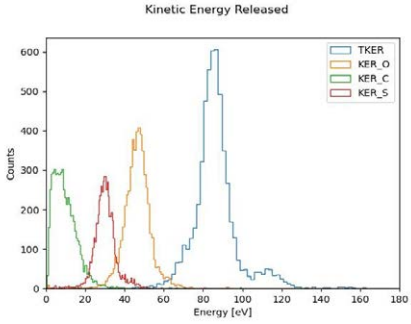

Figure 1. The KER of OCS^{6+} fragments in (2,2,2) channel

Furthermore, the laser-molecule interaction has been simulated for various initial alignments, using time-dependent density functional theory (TDDFT).

References

[1] Kanter, E. P., et al (1979). Physical Review A, 20(3), 834.
[2] Ibrahim, H., et al (2014). Nature communications, 5(1), 1-8.
[3] Wales, B., et al 2014 Journal of Electron Spectroscopy and Related Phenomena, 195, 332-336.

* E-mail: a32ashra@uwaterloo.ca
† E-mail: j3sanderson@uwaterloo.ca

Time-Resolved Images of Intramolecular Charge Transfer in Organic Molecules

F Fernández[1,2]*, J González[1]† A Palacios[1] and F Martin[1,2]

[1]Departamento de Química, Universidad Autónoma de Madrid, Madrid, 28049, Spain
[2]Instituto Madrileño de Estudios Avanzados en Nanociencia (IMDEA-Nano), Madrid, 28049, Spain

Synopsis In this work we simulate a pump-probe experiment to study the evolution of the charge transfer process in molecules of photovoltaic interest.

Ever since the first models of organic solar cells were proposed more than 40 years ago, the search for new materials with the ability to produce a charge separation, necessary for photovoltaic applications, has kept drawing the scientific community's attention.

Organic photovoltaic devices usually achieve charge photogeneration by using charge transfer complexes, which act as an intermediate step between exciton dissociation and charge extraction.

In order to capture the real time evolution of such electronic process, which takes place in the time range between tens of attoseconds to a few femtoseconds, a sub-femtosecond time-resolution is required. Therefore, in this work we propose the use of a pump-probe scheme employing ultrafast laser sources to track the charge transfer process using as target a typical donnor-acceptor molecule in the gas phase. In particular, we investigate the ultrafast dynamics following the excitation of para-nitroaniline (PNA), which has been extensively studied in a solvent, both theoretically [1, 6, 2] and experimentally [1, 5, 3, 4], while scarcer works have been performed in gas phase to date.

We thus propose the use of a pump-probe scheme, using a few-fs UV pulse to excite the target. The ensuying electron-nuclear dynamics will be later probed by a time-delayed attosecond XUV pulse which will ionize the molecule. The time-varying ionization yields are expected to capture the complex dynamics triggered in the excited molecule.

In a first approach, using the fixed nuclei approximation, we retrieve the time evolution of the excited wave packet by analyzing the electron density variation, computed through a transition density matrix formalism. The imprint of these dynamics is later retrieved into the cation with the time-delayed absorption of the probe pulse.

We later explored how these electron dynamics evolved when coupled with the nuclear degrees of freedom, when non-adiabatic couplings come into play. The coupled electron-nuclear motion is described by means of a surface-hopping method, i.e. within a semi-classical picture. In short, the time-dependent wave function is retrieved at each time step, computing the electronic structure on-the-fly by means of a quantum mechanical description, while the nuclear dynamics follows the classical equations of motion.

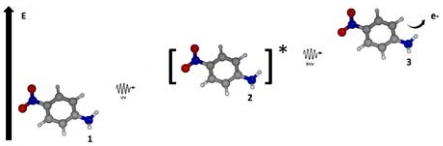

Figure 1. Diagram of the pump probe scheme.

References

[1] Kovalenko S *et al* 2000 *Chem. Phys. L.: Vol. Num. Pag.* **323** 3-4 312-322
[2] Bigelow R *et al* 1983 *Theoret. Chim. Acta: Vol. Num. Pag.* **63** 3 177-194
[3] Schuddeboom W *et al* 1996 *J. Phys. Chem: Vol. Num. Pag.* **100** 30 12369-12373
[4] Millefiori S *et al* 1977 *Spect. Chim. Acta: Vol. Num. Pag.* **33** 1 21-27
[5] Sinha H *et al* 1991 *J. Am. Chem. Soc.: Vol. Num. Pag.* **113** 16 6062–6067
[6] Kosenkov D *et al* 2011 *J. Phys. Chem. A: Vol. Num. Pag.* **115** 4 392–401

*E-mail: francisco.fernandez@imdea.org
†E-mail: jesus.gonzalezv@uam.es

Generalized Sturmians functions in prolate spheroidal coordinates for bound and continuum states of diatomic systems

A L Frapiccini[1]*, D M Mitnik[2], F A López[2] and L U Ancarani[3]

[1] Instituto de Física del Sur, IFISUR, Departamento de Física, (UNS - CONICET), Bahía Blanca (B8000CPB), Argentina
[2] Instituto de Astronomía y Física del Espacio, IAFE, (UBA - CONICET), Buenos Aires (C1428EGA), Argentina
[3] Université de Lorraine, CNRS, LPCT, 57000 Metz, France

Synopsis We propose and implement a spectral approach to describe bound and continuum states of diatomic systems. The method is based on Generalized Sturmian Functions in prolate spheroidal coordinates. We demonstrate the numerical efficiency by calculating photoionization cross sections.

The molecular ion H_2^+, and other one electron diatomics, are the simplest molecular quantum three-body problem with Coulomb interactions. In the fixed nuclei approximation, it is well known that prolate spheroidal coordinates possess the natural symmetry and make the Schrödinger equation separable [1].

With the aim of describing bound and continuum states for diatomic molecules, we develop and implement a spectral method that uses Generalized Sturmian Functions (GSF) in prolate spheroidal coordinates [2, 3]. For atomic systems, the GSF approach in spherical or hyperspherical coordinates has been applied with success [4, 5]. The main advantage is that an appropriate asymptotic behavior can be set upon all basis elements: an exponential decay for negative energy bound-like elements and oscillatory behavior for positive energy continuum-type elements. Inserting the correct physics into the basis makes the expansions converge rapidly which is particularly valuable when dealing with computationally expensive scattering problems.

For diatomic systems, we propose two different methods that use GSF in prolate spheroidal coordinates. The first one is an iterative 1d procedure in which one solves alternately the angular and the radial equations. The second method consists in representing the full Hamiltonian matrix in a two-dimensional GSF basis set, and its further diagonalization. In [2] we have shown that both methods provide accurate ground and excited states with very small basis. In [3] we deal with the continuum part of the spectrum. Figure 1 shows, for example, the oscillatory sinus-like behavior of the radial functions. The quality of our continuum states has been tested through time independent calculations of photoionization cross sections. Our results (in either length or velocity gauge) are in perfect agreement with benchmark calculations on the whole energy range (e.g. [6]), while using a much smaller basis set.

*E-mail: afrapic@uns.edu.ar

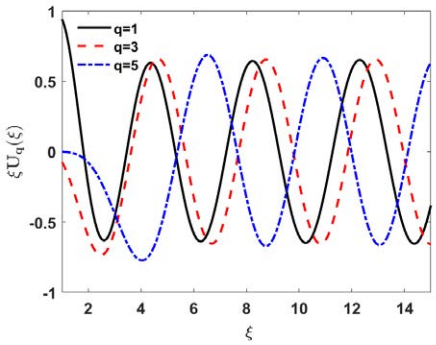

Figure 1. The continuum radial function $\xi U_q(\xi)$ for $m = 0$ and $q = 1, 3, 5$ zeros of the angular part, for energy $E = 1$ a.u. with 10 GSF.

References

[1] Bransden B H and Joachain C J 1983 *The Physics of Atoms and Molecules (Longamn Scientic and Technical: Harlow, UK).*
[2] Mitnik D M, López F A and Ancarani L U 2021 *Mol. Phys.* **e1881179**
[3] Mitnik D M *et al* submitted to *Adv. Quantum Chem.* March 2021
[4] Mitnik D M *et al* 2011 *Comp. Phys. Comm.* **182** 1145
[5] Gasaneo G *et al* 2013 *Adv. Quantum Chem.* **67** 153
[6] Bian X B 2014 *Phys. Rev. A* **90** 033403

Ab Initio Investigation on Bicircular High-Harmonic Spectroscopy of Molecular Chirality

Y Fukui[1], Y Orimo[1], T Teramura[1] , T Sato[1,2,3*] and K L Ishikawa[1,2,3†]

[1]Department of Nuclear Engineering and Management, School of Engineering, The University of Tokyo, 7-3-1 Hongo, Bunkyo-ku, Tokyo 113-8656, Japan
[2]Photon Science Center, School of Engineering, The University of Tokyo, 7-3-1 Hongo, Bunkyo-ku, Tokyo 113-8656, Japan
[2]Research Institute for Photon Science and Laser Technology, The University of Tokyo, 7-3-1 Hongo, Bunkyo-ku, Tokyo 113-0033, Japan

Synopsis We present numerical investigations, using *ab initio* wavefunction-based methods, on bicircular high harmonic spectroscopy (BHHS) of molecular chirality. The chiral selectivity of BHHS is quantitatively analysed for a range of chiral molecules both within and beyond the electric dipole approximation.

Left- and right-handed enantiomers (mirror reflections of each other which cannot be superimposed) of a chiral molecule have the same physical properties unless they interact with other chiral objects, such as another chiral molecule and circularly polarized light. Efficient identification and separation of enantiomers are highly demanded in many biological and industrial applications.

Bicircular high-harmonic spectroscopy (BHHS) is attracting attention as one of the new, promising chiral discrimination methods. It uses a two-color laser field consisting of a circularly polarized fundamental field of frequency ω and its counterrotating second harmonic 2ω. (See e.g, [1] and references therein.) In this study, we numerically analyse the chiral selectivity of BHHS for chiral molecules ranging from a simple one-electron model to L- and D-isomers of alanine, both within and beyond the electric dipole approximation.

For such numerical studies, one needs to (i) accurately describe multielectron dynamics in a molecule and (ii) take average of numerical results over the relative orientation between the molecule and the laser polarization to simulate experiments performed for randomly oriented molecules. Time-dependent multiconfiguration self-consistent-field (TD-MCSCF) methods [2] are ideally suited for addressing (i), and for the requirement (ii), we utilize a new implementation of TD-MCSCF on general curvilinear coordinate enabling accurate descritizations of molecular orbitals for aribitrary laser polarization, upon which an efficient method for the orientation averaging is implemented (Fig. 1).

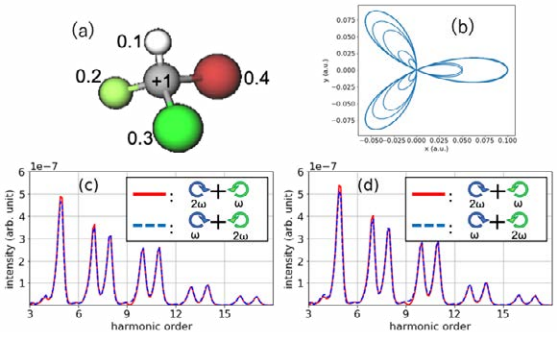

Figure 1. (a) A right-handed (R) isomer of a model one-electron chiral molecule with five potential centers having positive charges as depicted in the figure. (b) Counterrotating $\omega/2\omega$ bicircular laser field with ω corresponding to a wavelength of 911 nm, the peak intensity of 8.8×10^{13} W/cm^2, and the pulse duration (full-width at half maximum) of 13.7 fs. (c) HHG spectrum from the R-isomer of the chiral molecule shown in (a) irradiated by the bicircular field of (b) obtained for counterclockwise ω/clockwise 2ω field (solid line) and clockwise ω/counterclockwise 2ω field (dashed line), computed within the electric dipole approximation. The orientation average is taken by rotating the polarization plane about the molecule fixed in the laboratory frame. (d) Same as panel (c) but with the orientation averaging performed by rotating the molecule in the laboratory frame with a fixed laser polarization. A good agreement between the red and blue lines both in panels (c) and (d) (as expected in case of missing magnetic interaction) demonstrates a reliability of the present simulations.

References

[1] D. Ayuso *et al*, *Nat. Photonics*, **13**, 866 (2019).
[2] T. Sato and K. L. Ishikawa, *Phys. Rev. A*, **91**, 023417 (20

* E-mail: sato@atto.t.u-tokyo.ac.jp
† E-mail: ishiken@n.t.u-tokyo.ac.jp

Strong Field Ionization of H_2 in Circularly Polarized Two-Color Laser Fields

A Geyer[1] *, S Eckart[1], M Kunitski[1], D Trabert[1], N Anders[1], L Ph H Schmidt[1], M Schöffler[1], T Jahnke[1] and R Dörner[1]

[1]Institut für Kernphysik, Goethe-Universität, Frankfurt am Main, 60438, Germany

Synopsis We report on the strong field ionization of molecular hydrogen using circularly polarized two-color fields. The three-dimensional momentum distributions of the charged fragments are measured in coincidence using cold target recoil ion momentum spectroscopy (COLTRIMS). For the dissociation we observe low energy electrons in coincidence with high kinetic energy releases of the ions. We speculate that the low energy electrons are a fingerprint of inelastically recolliding electrons.

The strong field ionization of molecular hydrogen is experimentally investigated using counter-rotating circularly polarized two-color (CRTC) fields and co-rotating circularly polarized two-color (CoRTC) fields. The two-color fields (central wavelengths of 390 nm and 780 nm) are generated in an interferometric two-color setup [1] and the single color intensities are $I_{390} = 6.2 \cdot 10^{13}$ W/cm^2 and $I_{780} = 3.8 \cdot 10^{13}$ W/cm^2. The three-dimensional momentum distributions of the charged fragments are measured in coincidence using cold target recoil ion momentum spectroscopy (COLTRIMS) [2].

For the dissociation in a CoRTC field we observe low energy electrons in coincidence with high kinetic energy releases (KER) of the ions. Fig. 1a) shows the KER distribution for the dissociation of H_2 by a CoRTC field. b) and c) show the corresponding electron momentum distributions in the polarization plane for the blue and red shaded regions in a). For low KER (see Fig. 1b) the electron momentum distribution shows a typical CoRTC structure. For high KER (see Fig. 1c) this CoRTC structure vanishes and the electron momentum distribution shows a maximum at low electron energies.

A possible explanation is that the low energy electrons are due to recolliding electrons, which excite the molecule and lead to the high KER. We have simulated inelastically recolliding electrons with a semi-classical two-step (SCTS) simulation [3]. However, we were not able to confirm that the low-energy electrons arise from recollisions. If an explanation of the observed correlation of low energy electron and high KER is found, this might reveal recollision dynamics that are not covered by current semi-classical models.

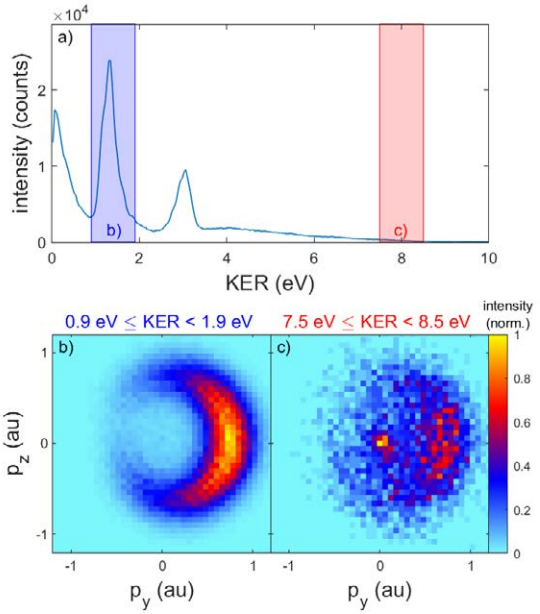

Figure 1. a) shows the kinetic energy release distribution for the dissociation of H_2 by a CoRTC field. b) [c)] shows the corresponding electron momentum distribution in the polarization plane for the blue [red] shaded region in a).

References

[1] Eckart S *et al* 2016 *Phys. Rev. Lett.* **117** 133202
[2] Jagutzki O *et al* 2002 *IEEE Transactions on Nuclear Science* **49** 2477
[3] Shvetsov-Shilovski N I *et al* 2016 *Phys. Rev. A* **94** 013415

* E-mail: geyer@atom.uni-frankfurt.de

A Multi-Center Quadrature Scheme for the Molecular Continuum

H Gharibnejad[1], N Douguet[2], B I Schneider[3]*, J Olsen[4] and L Argenti[5]†

[1]Computational Physics Inc., Springfield, VA 22151, USA; [2]Department of Physics, Kennesaw State University, Marietta, GA, 30060, USA; [2]Applied and Computational Mathematics Division, NIST, Gaithersburg, MD 20899, USA; [2]Department of Chemistry, Aarhus University, Aarhus C, DK; [2]Department of Physics and CREOL University of Central Florida, Orlando, FL 32816, USA

Synopsis We present a modification of the Becke partitioning scheme to compute polyatomic multi-center integrals involving both bound and continuum functions [1].

A common way to evaluate polycentric electronic integrals is to use Becke's grid partitioning scheme [2]. The Becke's scheme was designed for integrands that fall off rapidly at large distances, such as those approximating bound electronic states. When applied to states in the electronic continuum, however, this approach exhibits slow convergence and behaves improperly at large distances. Here, we present a modified version of Becke's scheme that is applicable to functions in the electronic continuum, such as those involved in molecular photoionization and electron-molecule scattering. The new approach ensures convergence, is efficient and achieves the desired accuracy for both bound and continuum functions.

In Figure 1, the weighting functions are shown for two possible schemes, one based on an atomic and one based on a molecular partitioning. Since both have been found to be equally accurate, and the atomic sphere approach is more straightforward to implement, it is the preferable method in practice. The accuracy of the method is demonstrated by evaluating integrals involving integrands containing Gaussian-Type Orbitals and Yukawa potentials on the atomic sites, as well as spherical Bessel functions centered on the master grid. These functions are representative of those encountered in realistic electron-scattering and photoionization calculations in polyatomic molecules. Some representative results which illustrate the differences in accuracy for the Becke's and modified Becke's approaches are shown in Table 1.

*E-mail: bis@nist.gov
†E-mail: luca.argenti@ucf.edu

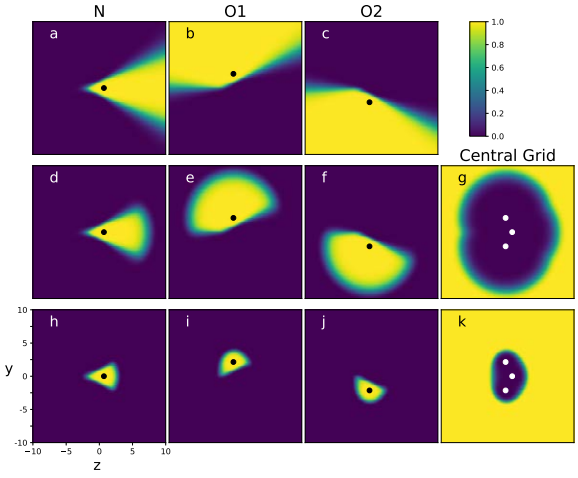

Figure 1. Atomic weights for the original (a-c) and for two flavors of the modified Becke's approach (d-g and h-k) for the NO_2 molecule. Atomic grid sizes are $R = 10$ a.u.

Table 1. Relative error between numerical and analytic results for the integration of spherical Bessel integrals for the Becke's and modified Becke's schemes.

Function	Method	Total Points	% error
j_0	Becke	974000	4.11[-2]
	Mod. Becke	876600	3.52[-12]
$r \cdot j_1$	Becke	1948000	1.16[-2]
	Mod. Becke	1753200	1.92[-11]

References

[1] Gharibnejad H *et. al.* 2021 *Comput. Phys. Commun.* **263** 107889
[2] Becke A D 1988 *J. Chem. Phys.* **89** 2993

Charge migration in aminophenol following sub-fs X-Ray pulses: Influence of nuclear effects and the XFEL shot-to-shot variation

G Grell[1,2]*, Z Guo,[3,4] A Marinelli[3,4], J P Cryan[3,5], A Palacios[2,6], and F Martín[1,2,7]†

[1]Instituto Madrileño de Estudios Avanzados en Nanociencia (IMDEA), Madrid, 28049, Spain
[2]Departamento de Química, Módulo 13, Universidad Autónoma de Madrid, Madrid, 28049, Spain
[3]SLAC National Accelerator Laboratory, Menlo Park, 94025, CA, USA
[4]Stanford University, Stanford, 94305, CA, USA
[5]Stanford PULSE Institute, SLAC National Accelerator Laboratory, Menlo Park, 94025, CA, USA
[6]Institute for Advanced Research in Chemical Sciences (IAdChem), Universidad Autónoma de Madrid, Madrid, 28049, Spain
[7]Condensed Matter Physics Center (IFIMAC), Universidad Autónoma de Madrid, Madrid, 28049, Spain

Synopsis Theoretical study regarding the attosecond charge migration in 4-aminophenol following sub-fs soft X-Ray ionization at 260 eV. The relative importance of the shot-to-shot variation of the XFEL pulses as well as the inclusion of ground state nuclear effects has been assessed based on ionization calculations carried out with the static-exchange B-spline DFT method.

Recently, X-Ray free electron laser (XFEL) facilities have been demonstrated to be capable of producing sub-fs soft X-Ray pulses, using the method of X-Ray laser-enhanced attosecond pulse generation (XLEAP) at the LCLS facility [1]. This makes it now possible to use tunable soft X-Ray pulses, carrying a much higher intensity than their respective high harmonic generation counterparts, enabling nonlinear spectroscopies to investigate attosecond electron dynamics in molecules.

We here present theoretical results describing the ultrafast charge dynamics induced in the 4-aminophenol molecule (C_6H_4-OH-NH_2) ionized with a sub-fs 260 eV pulse, i.e. below the carbon K-edge. The ionization calculations have been carried out using the static exchange B-spline DFT method that has been successfully applied in related previous studies at lower photon energies [2, 3]. In particular we scrutinize the influence of the shot-to-shot variation in terms of envelope, phase, and intensity by considering a set of 100 different X-Ray pulses generated from start-to-end simulations of the XFEL. Moreover, we examine the ground state nuclear effects in the resulting charge fluctuations. To this end we take into account an ensemble of molecular geometries sampled from the equilibrium Wigner distribution.

References

[1] Duris J *et al. Nat. Phot.* **14**, 30 (2020)
[2] Calegari F *et al. Science* **346**, 336 (2014)
[3] Lara-Astiaso M *et al. J. Phys. Chem. Lett.* **9**, 4570 (2018)

*E-mail: gilbert.grell@imdea.org
†E-mail: fernando.martin@imdea.org

Competition between suppression and enhancement of fragmentation of X-ray ionized organic molecules due to intermolecular decay of core vacancies

A Hans[1] *, D Bloß[1], L S Cederbaum[2], A Ehresmann[1], N V Kryzhevoi[2] and A Knie[1]

[1]Institute of Physics and CINSaT, University of Kassel, Kassel, 34132, Germany
[2]Institute of Physical Chemistry, University of Heidelberg, Heidelberg, 69120, Germany

Synopsis In Isolated molecules, Auger decay is the dominant decay path of electronic inner-shell vacancies, e.g., created by X-ray photoionization. We demonstrate that in an environment, direct intermolecular decay may outrun Auger decay, which has significant impacts on the resulting fragmentation of the ionized molecule.

X-ray induced radiation damage to small molecules is mainly governed by the Coulomb explosion of multiply charged states. Such states are usually populated by Auger decay as a consequence of inner-shell photoionization. Unless the molecule is very large to host two or more charges, it will thus be inevitably and irreversibly structurally damaged. Although it seems to be obvious, that this situation may change in an environment, due to the complexity of interactions and phenomana, a detailed picture of what happens if the molecule is, e.g., solvated, remains elusive. An understanding of the mechanisms underlying radiation damage of solvated molecules is, however, all the more important if theses shall be included into models of realistic scenarios in radiation biology [1].

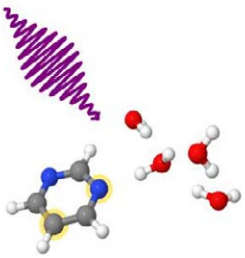

Figure 1. Schematic of the experimental principle. Microsolvated pyrimidine molecules are irradiated by X-rays. Depending on the site of ionization, the damage to the organic molecule may be suppressed or enhanced.

We mimic the response of biologically relevant matter to X-ray irradiation by exposing prototypical pyrimidine molecules solvated by few water molecules to soft X-ray synchrotron radiation (see Fig. 1). We explore the resulting fragmentation dynamics by applying photoelectron-photoion-photoion coincidence (PEPIPICO) spectroscopy. For isolated pyrimidine molecules, C 1s inner-shell ionization is followed solely by Auger decay and fragmentation into two (or more) ionic fragments [2,3]. For microsolvated pyrimidine, however, we observe intact parent ions in coincidence with water cluster ions.

We interpret our results by combining it with theoretical simulations, which reveal that direct intermolecular Coulombic decay (ICD) of the core vacancy is strongly competitive to Auger decay. In ICD, the core vacancy is filled by a valence electron of pyrimidine, but the ejected electron originates from a neighboring water molecule. For microsolvation by only four water molecules, intermolecular decay may already outrun Auger decay.

Our results strongly depend on the ionizing X-ray energy and the site of ionization. While for photon energies below the O 1s edge, only C and N of the pyrimidine may be ionized and the abovementioned damage suppression comes into play. For energies above the O 1s threshold, the effect may reverse. That means, after ionization of a water molecule an organic molecule in its vicinity may become ionized and potentially damaged by direct intermolecular decay.

References

[1] García Gómez-Tejedor G and Fuss M C 2012 *Radiation Damage in Biomolecular Systems* (Springer Netherlands)
[2] Itälä E *et al* 2011 *J. Electron Spectrosc. Relat. Phenom.* **184** 119
[3] Lin Y S *et al* 2015 *Chem. Phys. Lett.* **636** 146

* E-mail: hans@physik.uni-kassel.de

Directional fragmentation of methane in phase-locked ω-2ω intense laser fields

H Hasegawa[1], A Matsuda[1] and A Hishikawa[1,2] *

[1]Graduate School of Science, Nagoya University, Nagoya, 464-8602, Japan
[2]Research Center for Materials Science, Nagoya University, Nagoya, 464-8602, Japan

Synopsis Dissociative ionization and Coulomb explosion of CH_4 in ω-2ω intense laser fields are investigated by three-dimensional momentum imaging. Directional fragmentations along the laser polarization are observed. We discuss the asymmetry of fragmentation in terms of the molecular orientation to the laser polarization.

Shaped intense laser pulses provide unique methods to control chemical reactions. Two-color intense laser fields, consisting of fundamental (ω) and second harmonic (2ω) laser fields, have asymmetric electric field amplitudes. This characteristic feature has been used in selective breaking of equivalent chemical bonds as demonstrated with linear (CO_2 [1], C_2H_2 [2]) and bent (H_2O [3]) molecules. In the present work, the selective breaking of a tetrahedral molecule, CH_4, having four equivalent C-H bonds, is studied.

The output from a Ti: sapphire laser system (800 nm, 1 kHz, 50 fs) was introduced into an inline ω-2ω laser pulse generator [1]. The electric field can be expressed as $E_{\omega+2\omega} = E_\omega\cos(\omega t) + E_{2\omega}\cos(2\omega t + \phi)$, where the amplitude ratio of the 800 nm and 400 nm electric fields $E_{2\omega}/E_\omega$ was fixed to ~ 0.4. The relative phase ϕ between the two-color laser pulses was controlled using two fused silica wedge plates, and phase-locked by a feedback loop. The ω-2ω pulses, polarized parallel, were focused by a concave mirror (f = 75 mm) onto the CH_4 gas beam in an ultrahigh vacuum chamber. The momenta $\boldsymbol{p} = (p_x, p_y, p_z)$ of the fragment ions were obtained by using three-dimensional momentum imaging technique [1].

Four fragmentation processes, dissociative ionization (DI), $CH_4^+ \rightarrow H^+ + CH_3$ (1) and $CH_4^+ \rightarrow H + CH_3^+$ (2), and Coulomb explosion (CE) $CH_4^{2+} \rightarrow CH_3^+ + H^+$ (3) and $CH_4^{2+} \rightarrow CH_2^+ + H_2^+$ (4) are observed. The momentum image for H^+ fragments (Fig. 1(a)) exhibited two components. The smaller ($|\boldsymbol{p}| < 16$ a.u.) and larger ($|\boldsymbol{p}| \sim 25$ a.u.) components are assigned to DI (1) and CE (3), respectively. Anisotropic distributions along the laser polarization direction are observed.

To evaluate the asymmetry of directional fragmentation, an asymmetry parameter $A(\phi) = \frac{Y_+(\phi)-Y_-(\phi)}{Y_+(\phi)+Y_-(\phi)}$ is introduced. Here, Y_+ and Y_- are H^+ yields which have positive and negative momenta along the laser polarization direction. The asymmetry parameter of H^+ generated in DI (1) shows a clear relative phase dependence (Fig.1(b)). Asymmetry parameter maximizes at around $\phi \sim 0$, where H^+ ions from DI are preferentially emitted to the direction of the larger amplitude of the laser electric fields.

It is found that each fragmentation pathway shows a characteristic phase dependence, reflecting the ionization dynamics and the molecular dynamics in intense laser fields.

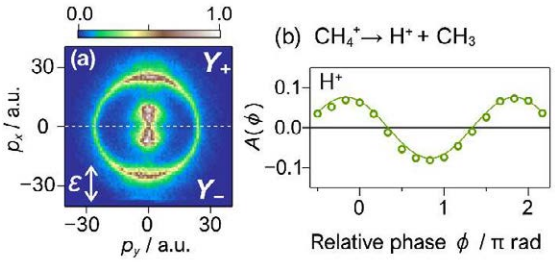

Figure 1. (a) Phase-averaged momentum image of the H^+ fragments ($|p_z| < 3$ a.u.). The laser polarization direction is denoted with ε. (b) Relative phase dependence of asymmetry parameter of H^+ generated in DI process ($|\boldsymbol{p}| < 16$ a.u.).

References

[1] T. Endo *et al.*, 2017 Phys. Chem. Chem. Phys. **19** 3550
[2] Q. Song *et al.*, 2015 J. Phys. B, **48** 094007
[3] E. Kechaoglou *et al.*, 2019 Phys, Chem. Chem, Phys. **21** 11259

* E-mail: hishi@chem.nagoya-u.ac.jp

What causes the angular dependence of photoionization time delays in a molecular shape resonance?

F Holzmeier[1,2] *, J Joseph[1], J C Houver[1], D Dowek[1] and R R Lucchese[3]†

[1]Université Paris-Saclay, CNRS, Institut des Sciences Moléculaires d'Orsay, Orsay, 91405, France
[2]Université Paris-Saclay, Synchrotron SOLEIL, Saint Aubin, 91190, France
[3]Lawrence Berkeley National Laboratory, Berkeley, California, 94720, USA

Synopsis The variation of single-photon ionization time delays in the NO molecule across a shape resonance angle-resolved in the molecular frame is found to originate from the interference of the angle-independent resonant and angle-dependent non-resonant contributions to the photoionization dipole amplitude.

The interaction of molecules with a single XUV photon induces ultrafast photoionization dynamics, which in turn influences their reactivity. Here, many-body interactions are crucial, and resonances, i.e., meta-stable states in the ionization continuum, often have a significant impact on the dynamics due to enhanced cross sections or temporary trapping of the outgoing electron. Photoionization time delays provide deep insights into these ultrafast dynamics on the attosecond time scale. For molecules, they depend dramatically on the emission direction in the molecular frame (MF) for each orientation of the molecule in the field frame [1], but have only been captured partially in an experiment so far [2]. Besides, in the XUV-IR RABBITT scheme used, the one-photon ionization dynamics is not elucidated for molecules due to their non-spherical symmetry [3].

Here, we completely resolve the experimental and computational MF angular dependence of time delays for one-photon ionization of the NO molecule into the $NO^+(c^3\Pi)$ state across the $4\sigma \rightarrow k\sigma^*$ shape resonance [4]. Large variations with energy (E) and emission angle (θ) are observed for the parallel transition and a multichannel Fano formalism reveals that the time delay profiles $\tau(E,\theta)$ result from the coherent superposition of the separated θ-independent resonant and θ-dependent non-resonant parts of the photoionization dipole amplitudes (PDA).

Experimental time delays are obtained from single-photon ionization measurements of molecular frame photoelectron angular distributions using synchrotron radiation at a series of photon energies. At each energy the complex valued partial-wave dipole matrix elements D_{lm} are extracted [5], and summed up coherently to the PDA, after being referenced to the phase of the (l=2, m=1) partial wave, which is not affected by the resonance. One-photon ionization time delays are then obtained as the energy derivatives of the PDA phases $\eta(E,\theta)$. They are found in good qualitative agreement with multichannel Schwinger configuration interaction calculations as shown in Figure 1.

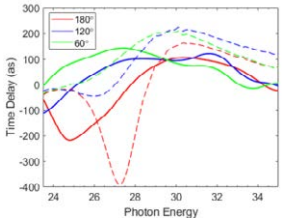

Figure 1. Experimental (full lines) and computed (dashed lines) time delays for NO ionization into the $NO^+(c^3\Pi)$ state for three different major emission angles in the MF for the parallel transition.

Comparing the resonant part of the PDA obtained in the Fano analysis and that computed for the same resonance in e-NO^+ scattering highlights the connection of photoionization time delays with Wigner scattering time delays.

References

[1] Hockett M *et al* 2016 *J. Phys. B: At. Mol. Opt. Phys.* **49** 95602.
[2] Vos J *et al* 2018 *Science* **360** 1326.
[3] Baykusheva D *et al* 2017 *J. Chem. Phys.* **146** 124306.
[4] Veyrinas K *et al* 2019 *J. Chem. Phys.* **151** 174305 and ref . therein
[5] Cherepkov N A *et al* 2000 *J. Phys. B : At. Mol. Opt. Phys.* **33** 4213-4236.

* E-mail: fabian.holzmeier@imec.be
† E-mail: rlucchese@lbl.gov

The Electronic Changes of Gas-Phase PAH cations Induced by Atomic Hydrogenation Attachment

Y.Huo[1*], M.Goulart[1], R.Hoekstra[1], V.Zamudio-Bayer[2], M.Kubin[2], T.Lau[2], M.Cangahuala[1], S. Faraji[1], T.Schlathölter[1]

[1]Zernike Institute for Advanced Materials, University of Groningen, Groningen, 9747AG, Nethrlands
[2]Institut für Methoden und Instrumentierung der Forschung mit Synchrotronstrahlung, Helmholtz-Zentrum Berlin Materialien und Energie, Berlin, 12489, Germany

Hydrogen attachment to gas-phase polycyclic aromatic hydrocarbon (PAH) cations has strong influences on molecular geometry and electronic structure. For instance, the planar aromatic PAH structure gradually transforms towards a puckered aliphatic structure upon sequential hydrogenation [1]. At the same time, the HOMO-LUMO gap is reduced by atomic hydrogen attachment [2]. We have studied the hydrogenation of PAH radical cations by means of soft X-ray spectroscopy. By combining synchrotron radiation and mass spectrometry, partial ion yields (PIY) for various photoionization channels were recorded as a function of photon energy and as a function of hydrogenation state. The recorded spectra were compared to spectra determined by time-dependent density functional theory (TDDFT), using Short Range Corrected (SRC) exchange-correlation functionals for core excitations. Hydrogenation for instance systematically shifts the 1s-π* resonance at 285eV to lower energies.

As PIY spectra allow to study the dependence of particular fragmentation channels on the final state of the core-excitation, we have investigated hydrogen loss from the molecular dication, both for $C_{24}H_{12}^{+}$ and for $C_{24}H_{13}^{+}$. Multiple hydrogen loss is facilitated by 1s-σ* transitions centered at 293eV. In singly hydrogenated PAHs, the 1s-σ* resonance even dominates of the 1s-π* resonances for loss of 6 hydrogen atoms or more (see Fig.1).

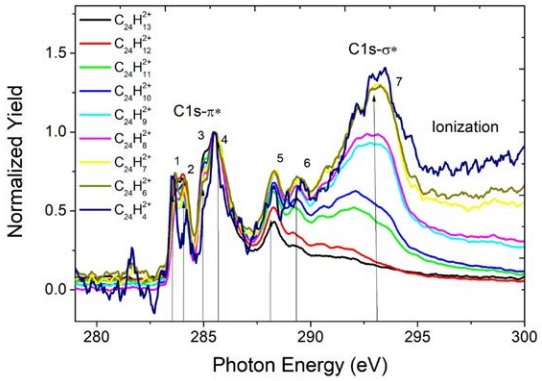

Figure 1. PIY for photoionization of singly hydrogenated coronene cations. Black: non-dissociative single ionization. Color: single ionization accompanied by hydrogen loss.

References

[1] Cazaux S *et al* 2019 *ApJ.*875:27
[2] Hammonds M *et al* 2009 *Phys.Chem.Chem. Phys* 11.4458

* E-mail: yining.huo@rug.nl

Radiative cooling dynamics of tetracene cations stored in DESIREE

S Indrajith[1]*, M C Ji[1], N Kono[1], A Al-Mogeeth[2], J Bernard[2], S Martin[2], C Joblin[3], H Cederquist[1], H T Schmidt[1], M H Stockett[1], and H Zettergren[1]

[1]Department of Physics, Stockholm University, Stockholm, 114 21, Sweden
[2]Institut Lumière Matière, UMR 5306 Université Lyon 1-CNRS, Université de Lyon, Villeurbanne cedex, 69622, France
[3]Institut de Recherche en Astrophysique et Planétologie, Université de Toulouse (UPS), CNRS, CNES, Toulouse, F-31028, France.

Synopsis We have studied the radiative cooling dynamics of a catacondensed PAH molecule, tetracene ($C_{18}H_{12}$) cation, in the cryogenic electrostatic storage ring DESIREE.

Polycyclic Aromatic Hydrocarbon molecules (PAHs) were proposed as possible carriers of the unidentified infrared bands in the 1980s and are since then believed to be distributed ubiquitously in the interstellar medium (ISM). Numerous experimental and theoretical studies on PAHs have been carried out in the past decades, with the aim to unravel how they are formed and may survive in such environments [1]. The cooling dynamics of the PAHs is a key to their survival and evolution in the ISM [2].

We study the radiative cooling dynamics of internally hot tetracene cations at the cryogenic electrostatic ion storage ring facility, DESIREE. The ions are produced by an electron cyclotron resonance (ECR) ion source, accelerated to 20 keV, mass selected and stored for 100 ms. The clean environment provided by DESIREE, essentially free from background collisions and blackbody radiation, is ideal to study slow relaxation processes of astrophysical interest. Our main goal here is to quantify experimentally both recurrent fluorescence and the IR cooling of the tetracene cations and see how they compare with studies of smaller catacondensed PAHs, like anthracene [3] and naphtalene [4].

In our experiment, we set laser pulses of different wavelengths to irradiate the stored ions at well-controlled storage times and the yield of neutral particles due to dissociation is monitored as a function of time. In Fig. 1, we show an example from a measurement where the tetracene cations have been exposed to 410 nm photons. The laser-induced decays reflect the time evolution of the internal energy distribution and how it is affected by radiative cooling. Thus by comparing the decay curves for different photon wavelengths and laser firing times, the radiative cooling dynamics may be followed in time [5]. This analysis is in progress and the results will be presented at the meeting.

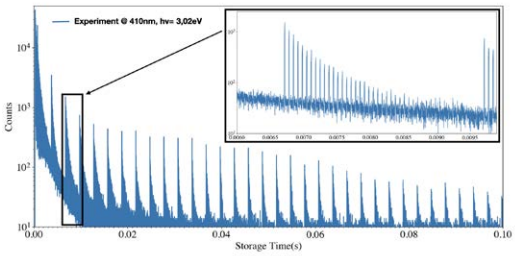

Figure 1. Yield of neutral particles as a function of storage time. The peaks separated by 3 milliseconds correspond to the laser induced signal from individual OPO laser pulses (photon wavelength: 410 nm). The zoom-in box shows series of peaks due to the laser-activated ions circulating around the ring.

References

[1] Joblin C and Tielens A G G M 2011 *EDP Sciences* **PAHs and the Universe**
[2] Montillaud J *et al.* 2013 *A& A* **552** A15
[3] Martin S *et al.* 2013 *Phys. Rev. Lett.* **110** 063003
[4] Saito M *et al.* 2020 *Phys. Rev. A* **102** 012820
[5] Martin S *et al.* 2015 *Phys. Rev. A* **92** 053425

*E-mail: suvasthika.indrajith@fysik.su.se

Investigation of relaxation pathways in D_2O^{2+} leading to D^++O^++D fragmentation channel

W Iskandar[1], K A Larsen[1,2], B Griffin[1,3], J B Williams[3], T Severt[4], B Jochim[4], I Ben-Itzhak[4], D Slaughter[2], and Th Weber[2]

[1] Chemical Sciences Division, Lawrence Berkeley National Laboratory, Berkeley, CA-94720, USA
[2] Graduate Group in Applied Science and Technology, University of California, Berkeley, USA
[3] Department of Physics, University of Nevada, Reno, NV-89557, USA
[4] J. R. Macdonald Laboratory, Department of Physics, Kansas State University, Manhattan, KS-66506, USA

Synopsis We present the investigation of relaxation dynamics on heavy water molecules after single photo double ionization. Among the multiple fragmentation channels arising from the dissociation of the D_2O dication, a very weak channel D^++O^++D is present. For this channel, we were able to identify and separate the autoionization process from the direct double ionization. For the direct process, the results show at least two distinct electronic states contributing to the fragmentation channel. Both dication states undergo sequential dissociaiton into D^++O^++D enabled by spin-orbit coupling.

The direct double ionization of water molecules followed by Coulomb explosion of the dication can lead to many fragmentation channels depending on the molecular state populated as well as on the rotational and vibrational mode of the molecule. Furthermore, water molecules can be excited to molecular states whose internal energies exceed their ionization potentials. These super-excited states are highly unstable and decay through various processes such as autoionizations, acting as doorway to sequential many body fragmentation. A detailed investigation of all possible fragmentation channels and their relaxation processes is necessary in order to achieve a complete understanding of the dissociation of water dication upon photo absorption. Recent combined experimental and theoretical work investigated the dissociation dynamics of H_2O following photoionization at 57 eV [1, 2] leading to OH^++H^+ and H^++H^++O fragmentation channels. The present work is devoted to the study of the rare D^++O^++D. The focus of this research is on the identification of the dissociation processes, molecular states, and their fragmentation scenarios leading to this breakup channel.

The experiments were performed at beamline 10.0.1.3 at the Advanced Light Source in Berkeley using 61.0 eV linearly polarized photons to investigate the fragmentation dynamics of D_2O molecular targets. COLd Target Recoil Ion Momentum Spectroscopy was employed to measure the 3D momenta of the emitted ions and electrons in coincidence. Two distinct processes, i.e. autoionization and direct ionization, were identified and isolated as visible in Fig.1. In the case of direct ionization, the results show at least two distinct states contributing to the breakup. From the balance of the excess enegy and the kinetic energy release we conclude that these states undergo multiple dissociation steps in order to produce D^++O^++D. For the autoionization process, the data indicates the participation of an excited cationic state located above the double ionization threshold of D_2O yielding an autoionizing electron with a fixed energy of about 0.5 eV, which is a signature of atomic oxygen autoionization.

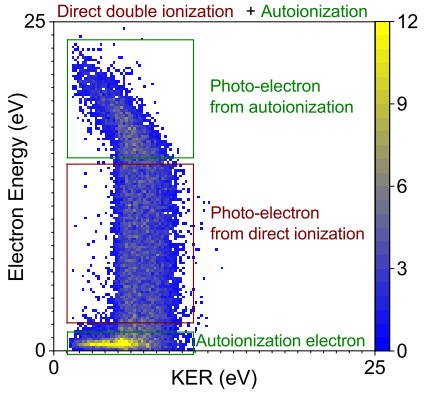

Figure 1. PDI yield of the D^++O^++D breakup as a function of the kinetic energy release (KER) and the kinetic energy of either emitted electron.

References

[1] Reedy D *et al.* 2018 *Phys. Rev. A* **98** 053430
[2] Streeter Z L *et al.* 2018 *Phys. Rev. A* **98** 053429

Non-dipole effects in the double ionization of atoms and molecules

G. P. Katsoulis[1]*, M. B. Peters[1], A. Staudte[2,3], R. Bhardwaj[3], T. Meltzer[1], P. B. Corkum[2], and A. Emmanouilidou[1]†

[1]Department of Physics and Astronomy, University College London, Gower Street, London WC1E 6BT, United Kingdom
[2]Joint Attosecond Laboratory, National Research Council and University of Ottawa, Ottawa, Ontario K1A 0R6, Canada
[3]Department of Physics, University of Ottawa, Ottawa, ON K1N 6N5, Canada

Synopsis Using a three-dimensional semiclassical model, we study the magnetic field effects in the double ionization of atoms and molecules. We identify striking signatures of those effects that can be experimentally observed.

We study the ionization of two-electron atoms and molecules, using a three-dimensional semiclassical model that accounts for non-dipole effects and the Coulomb singularities. We identify a prominent signature of magnetic field effects in the non-sequential double ionization of He [1, 2] and H_2 [3] where recollisions prevail. For both the atomic and the molecular case, we find that the recolliding electron has an asymmetry in the initial momentum along the propagation direction of light. For H_2 the recolliding electron back-scatters along the direction of light propagation, escaping opposite to the direction of change in momentum due to the magnetic field. This is in striking contrast to strongly-driven atoms where the recolliding electron forward scatters along the direction of light propagation. We attribute these distinct signatures to the different gate that the magnetic field creates jointly with a soft recollision in molecules compared to a hard recollision in atoms.

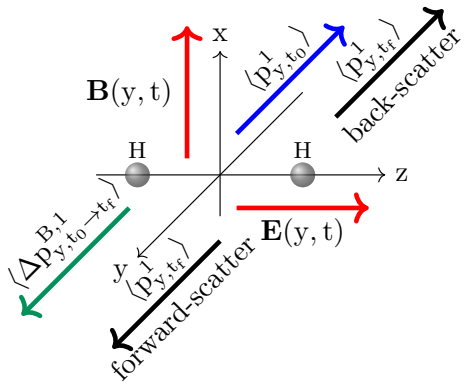

Figure 1. Schematic illustration of the electric and magnetic field of the laser pulse as well as of the average initial and final momentum of the recolliding electron along the direction of light propagation.

References

[1] A. Emmanouilidou and T. Meltzer 2017 *Phys. Rev. A* **95** 033405
[2] A. Emmanouilidou, T. Meltzer, and P. B. Corkum 2017 *J. Phys. B* **50** 225602
[3] G. P. Katsoulis, M. B. Peters, A. Staudte, R. Bhardwaj, and A. Emmanouilidou 2021 *Phys. Rev. A* **103** 033115

*E-mail: g.katsoulis@ucl.ac.uk
†E-mail: a.emmanouilidou@ucl.ac.uk

X-ray-induced anion production at the O K edge of simple alcohol molecules

A Kivimäki[1,2,*], J Koponen[1], E Pelimanni[1], C Stråhlman[3], K Chernenko[2], A R Abid[1] and M Patanen[1]

[1]Nano and Molecular Systems Research Unit, University of Oulu, 90014 Oulu, Finland
[2]MAX IV Laboratory, Lund University, 22100 Lund, Sweden
[3]Department of Materials Science and Applied Mathematics, Malmö University, 20506 Malmö, Sweden

Synopsis We have studied anion formation in simple alcohol molecules after the excitation and ionization of O 1s electrons. The measurements were performed by detecting coincidences between negative and positive ions.

Small molecules typically break into ionic and neutral fragments after the absorption of a soft X-ray photon, in particular if the process involves the transfer of an inner-shell electron to an empty molecular or Rydberg orbital or to the ionization continuum. Resulting core-hole states decay predominantly via resonant and normal Auger transitions (i.e., electron emission), whose final states are often dissociative. Dissociation studies at inner-shell edges have concentrated on the detection of ubiquitous positively charged fragments. However, partial ion yield studies at the K edges of small molecules such as water [1] have revealed that negative ions are also produced in dissocation processes following inner-shell photoexcitation and photoionization.

Stråhlman et al [2] have recently developed negative-ion/positive-ion coincidence (NIPICO) spectroscopy to study molecular dissociation channels involving anions. The technique is based on two ion time-of-flight (TOF) spectrometers, which are mounted opposite one another, and on the suppression of electrons by an external magnetic field. Due to the conservation of charge, two (three) positive ions are expected to be created together with a negative ion after resonant (normal) Auger decay. Such dissociation channels have indeed been observed [3].

The negative-ion TOF spectrometer of Ref. [2] has been transferred from Elettra (Trieste, Italy) to the MAX IV Laboratory (Lund, Sweden), where it has been coupled with the ion TOF spectrometer of the gas-phase end station [4] at the FinEstBeAMS beamline. The latter spectrometer is equipped with a Hex-anode delay-line detector, enabling the detection of multi-hit events. The new set-up has therefore an improved detection probability for identical positive ions (e.g., protons) originating from the same molecule. The first NIPICO experiments at FinEstBeAMS were performed for the four simplest alcohols: methanol, ethanol, 1-propanol, and 2-propanol. As an example, Figure 1 shows a part of the negative-ion/positive-ion/positive-ion coincidence map of ethanol measured at the photon energy of 537.1 eV, i.e. just below the O 1s ionization potential. The results of the experiments will be discussed.

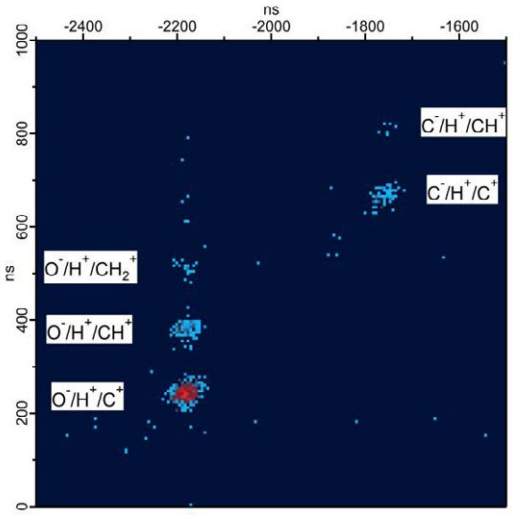

Figure 1. Some of the three-ion coincidences observed in ethanol at hν=537.1 eV.

References

[1] Stolte W C *et al* 2003 *Phys. Rev. A* **68** 022701
[2] Stråhlman C *et al* 2016 *Rev. Sci. Instrum.* **87** 013109
[3] Stråhlman C *et al* 2017 *Phys. Rev. A* **96** 023409
[4] Kooser K *et al* 2020 *J. Synchrotron Rad.* **27** 1080

* E-mail: antti.kivimaki@maxiv.lu.se

Multiphoton light-induced potential energy surfaces in H_2^+

Matthias Kübel[1,2,*], Michael Spanner[1], Zack Dube[1], Andrei Naumov[1], Marc J. J. Vrakking[3], Paul B. Corkum[1], David M. Villeneuve[1], and André Staudte[1]

[1] Joint Attosecond Laboratory, National Research Council and University of Ottawa, Ottawa, Ontario, Canada
2 Institute of Optics and Quantum Electronics, Friedrich Schiller University of Jena, D-07743 Jena, Germany
[3]Max-Born-Institut, Max-Born-Straße 2A, D-12489 Berlin, Germany

Synopsis *Using H_2^+ as an example, we demonstrate experimentally and theoretically that intense laser fields can produce unexpectedly structured angular distributions of photofragments. Floquet analysis indicates that the dynamics can be understood in the picture of light-induced potential energy surfaces. Here, both single and multiphoton couplings result in distinct features resembling conicial and non-conical intersection, respectively. Rovibronic dynamics in these complex potential energy landscapes underly our experimental results.*

In the focus of an intense laser pulse, the external forces acting on the constituents of a molecule are comparable to the internal forces. Hence, tailoring the temporal evolution of the intense laser field holds the promise to efficiently manipulate molecular dynamics. For example, the laser-dressing of electronic states in H_2^+ induces avoided crossings and light-induced conical intersections (LICI) that govern single-photon dissociation [1,2].

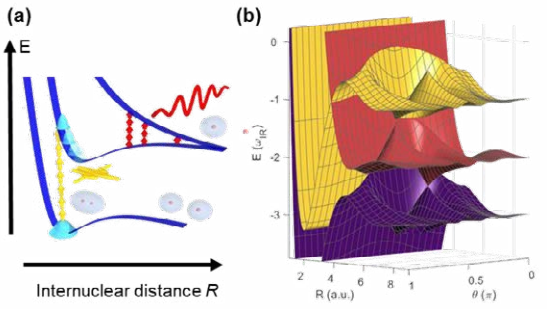

Figure 1. (a) Experimental scheme to probe light-induced non-conical intersections. Neutral H_2 is ionized by an intense few-cycle visible (760 nm) laser pulse. The molecular ion is subsequently dissociated in the presence of a mid-IR field (2300 nm) of moderate intensity. (b) Light-induced potential energy surfaces in the Floquet picture arising from the laser dressing of the two lowest-lying states of H_2^+ by a mid-IR laser field at 30 TW/cm².

Here, we explore the effect of the multiphoton analogue to LICIs, so-called non-conical intersections, on the photodissociation dynamics of H_2^+ [3]. In our experiment, we employ the two-pulse scheme depicted in Figure 1 (a). It allows us to prepare a coherent wave packet on the electronic ground state of H_2^+ and control the subsequent dissociation by tailoring amplitude and phase of the mid-IR laser field that dresses the angle-dependent molecular potential energy surfaces. An example of such surfaces is displayed in Figure 1(b).

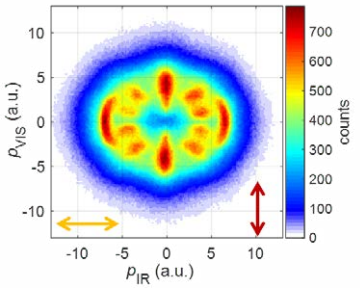

Figure 2. Experimental results showing the proton momentum distribution in the polarization plane. The arrows indicate the polarization directions of the visible and infrared laser pulses, respectively.

Figure 2 displays experimental results that exhibit a striking angular pattern which strongly contrasts with previously reported results, such as Ref. [2]. We discuss the role of multiphoton couplings and rotational dynamics in shaping the resulting angular distribution. Our results highlight to what remarkable extend molecular dynamics can be manipulated using tailored laser fields.

References

[1] Numico R, *et al*, 1999 *Phys. Rev. A* **60** 406
[2] Natan A, *et al* 2016 *PRL* **116** 143004
[3] Kübel M, *et al* 2020 *Nat. Commun.* **11** 2596

* E-mail: matthias.kuebel@uni-jena.de

The formative period in the X-ray-induced photodissociation of organic molecules

E. Kukk[1]*, H. Fukuzawa[2,3], J. Niskanen[1], K. Nagaya[4,3], K. Kooser[1,5], D. You[2], J. Peschel[6], S. Maclot[6], A. Niozu[4], S. Saito[2], Y. Luo[2], E. Pelimanni[7], E. Itälä[1], J.D. Bozek[8], T. Takanashi[2], M. Berholts[1,5], P. Johnsson[6] and K. Ueda[2,3]

[1]Department of Physics and Astronomy, University of Turku, FI-20014 Turku, Finland
[2]Institute of Multidisciplinary Research for Advanced Materials, Tohoku University, Sendai 980-8577, Japan
[3]RIKEN SPring-8 Center, Kouto 1-1-1, Sayo, Hyogo 679-5148, Japan
[4]Department of Physics, Kyoto University, Kyoto 606-8502, Japan
[5]Institute of Physics, University of Tartu, W. Ostwaldi 1, EE-50411 Tartu, Estonia
[6]Department of Physics, Lund University, 22100 Lund, Sweden
[7]Nano and Molecular Systems Research Unit, Faculty of Science, 90014 University of Oulu, Finland
[8]Synchrotron SOLEIL, L'Orme des Merisiers, Saint-Aubin, BP 48, FR-91192 Gif-sur-Yvette Cedex, France

Synopsis We investigated the dissociation dynamics and landscape of thiophene dications by femtosecond X-ray pulses from SACLA free electron laser. Near infrared light was found to be a sensitive probe of the excited electronic states populated by the Auger decay. It revealed an initial survival time of the parent molecule prior to forming an opened-ring geometry and dissociating, and underscored the importance of nonadiabatic couplings during this period.

We investigated the dissociation landscape of thiophene by femtosecond X-ray pulses from the SACLA free electron laser [1]. The S 2p core holes were filled by the Auger process creating dicationic states within a broad range of internal energy. The evolution of the ionized molecules was then monitored by a pump-probe experiment using a near-infrared (800 nm) laser pulse.

Ion-ion coincidence and ion momentum analysis reveals enhanced yields of ionic fragments from multi-body break-up of the ring, attributed to additional ionization of a highly excited fraction of the dicationic parent molecular states. The transient nature of the enhancement and its decay with about a 160 fs time constant, determined from this study, indicate the statistical survival time of the parent species before the dissociation events and the formation of an opened-ring parent geometry.

The near-infrared laser probe would not be a sensitive for the Auger final states but for the recently discovered (single-photon) laser-enabled Auger decay (LEAD) effect [2]. We demonstrate how the LEAD-activated NIR-probe technique works owing to the to the creation of highly excited electronic states by the Auger decay of the core-ionized molecules.

The prominence of electronic relaxation and geometry changes in the early photodynamics underscores the importance of nonadiabatic couplings during this period. We showed the feasibility of this experimental approach on the example of a medium-sized organic molecule. This technique would likely be beneficial also, for example, in time-tracing the early evolution of X-ray radiation damage in the molecular building blocks of much larger biomolecules.

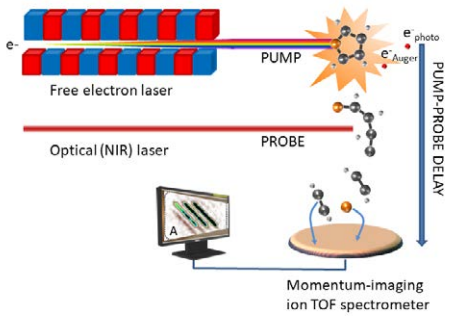

Figure 1. Schematic of the X-ray pump, near-infrared probe study of the early dissociation dynamics of thiophene.

References

[1] Kukk E *et al.* 2021 *Phys. Rev. Research* **3** 013221
[2] You D *et al.* 2019 *New J. of Physics* **21** 113036

*E-mail: edwin.kukk@utu.fi

Multi-photon ionization of photo-associated $X^1\Sigma_g^+(^6Li_2)$ dimers

N Kurz[1]*, T Pfeifer[1] and A Dorn[1]

[1]Max-Planck-Institut für Kernphysik, Heidelberg, 69117, Germany

Synopsis We report on kinematically complete multi-photon ionization experiments on $^6Li_2$ molecules trapped within a far-off resonant, optical dipole trap inside a reaction microscope. Weakly-bound $^6Li_2$ dimers are produced by single-color photo-association (PA) into the electronically excited $A^1\Sigma_u^+$ or $1^3\Sigma_g^+$ state from where fluorescence decay populates the $X^1\Sigma_g^+(^6Li_2)$ or $a^3\Sigma_u^+(^6Li_2)$ state, respectively, in highly excited vibrational states. We detect the $X^1\Sigma_g^+(^6Li_2)$ ground state molecules via 3-photon ionisation with ultrafast femtosecond laser pulses ($\tau = 30$ fs) at a central wavelength of 780 nm and measure directly the momenta of photoelectrons in coincidence with Li_2^+ recoil ions. The electron energies are found to be dominantly below 200 meV and the emission pattern is isotropic. Furthermore, we found ionization pathways which involve the IR dipole trap laser. Future experiments will include direct 1-photon ionization of the molecules using monochromatic UV radiation at 266 nm. This will enhance energy resolution and remove possible contributions from resonance-enhanced ionization.

Our experimental apparatus, a MOT reaction microscope [1] combined with an optical dipole force trap, makes it possible to investigate the photo-ionization dynamics of vibrationally highly-excited $^6Li_2$ molecules, so-called weakly-bound or halo dimers. Here we report on the production of $X^1\Sigma_g^+(\nu = 36)$ halo dimers via cw single-color PA [2] in the optical dipole-force trap. The halo dimers are ionized and the molecular ion and photoelectrons are detected in coincidence in a high-resolution charged particle momentum spectrometer. Due to dipole-selection rules, we were only able to detect molecules in the singlet system via 3-photon ionization. The detected photoelectrons had mostly energies below 200 meV (see Fig 1), which is in qualitative agreement with the calculated Franck-Condon factors in the accessible energy range (green curve in Fig 1). When the measurement will be performed with higher resolution by initiating a 1-photon transition using UV light, we will obtain more quantitative data on the dipole matrix elements and the Franck-Condon factors for the accessible vibrational states. The electron emission is isotropic. Additional ionization pathways were found. In one, the IR light of the optical dipole trap contributes to the molecular ion yield by ionizing an intermediate excited molecular state reached by absorption of two fs photons. In another one, the excited molecules formed during the PA process are directly ionized by absorption of two IR photons via an intermediate molecular state. This produces a continuous yield of molecular ground state ions $1^2\Sigma_g^+$ in the two lowest vibrational states. In order to exclude the participation of the IR field in the ionization process, the IR trapping field was pulsed.

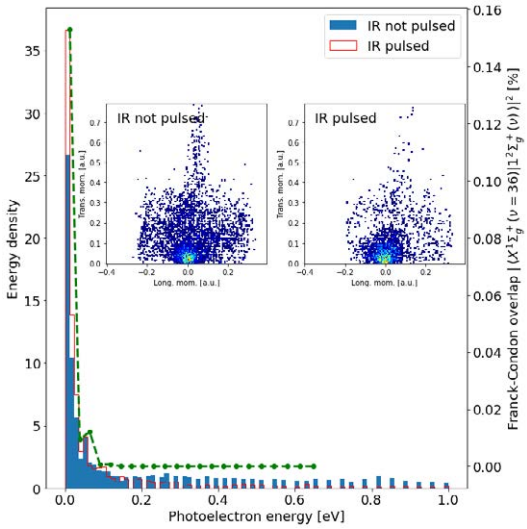

Figure 1. Photoelectron energies for photoelectrons from molecular ions.

Future studies might also focus on dissociative ionization of $^6Li_2$ dimers in order to obtain molecular frame photo-electron angular distributions or removal of all trapped atoms in order to do Coulomb explosion imaging of weakly-bound dimers.

References

[1] Schuricke, J *et al* 2011 *Phys. Rev. A* **83** 023413 **87** 123202
[2] Cote, R *et al* 1999 *Journal of Mol. Spect.* **195** 236-245

*E-mail: kurzn@mpi-hd.mpg.de

CHARGE REVERSING MULTIPLE ELECTRON DETACHMENT AUGER DECAY OF INNER-SHELL VACANCIES IN GAS-PHASE DEPROTONATED DNA

W Li[1]*, O Kavatsyuk[1,2], W Douma[1], X Wang[1], R Hoekstra[1], M Robinson[3], M Gühr[3], M Lalande[4], M Abdelmouleh[4], V Vizcaino[4], M Ryszka[4], J C Poully[4], T Schlathölter[1]†

[1] University of Groningen, Zernike Institute for Advanced Materials, Groningen, 9747AG, Netherlands.
[2] University College Groningen, Groningen, 9718 BG, Netherlands.
[3] Universität Potsdam, Institut für Physik und Astronomie, Potsdam, 14476, Germany.
[4] CIMAP UMR 6252 (CEA/CNRS/ENSICAEN/Université de Caen Normandie), Caen, 14070, France.

Synopsis The production of inner-shell vacancies in bio-molecular systems, in particular DNA, is one of the first steps in many types of biological radiation action. The accompanying Auger decay is considered responsible for a large part of the biological radiation damage. From the perspective of molecular damage, it makes a difference if one high-energy secondary electron is emitted or whether the Auger process is accompanied by many-electron detachment. In the latter case the molecular damage and break-up is expected to be more localized and prominent. Here we address the outstanding question how (un-)likely it is that inner-shell Auger decay in a single, large biomolecule is accompanied by many-electron detachment.

For the efficient production of inner-shell vacancies in light atoms, which make up biological tissue, we use soft X-rays. The energies of soft X rays are tuned on and over the respective K-shell absorption edges[1]. And in order to investigate the direct molecular response of DNA to inner-shell excitation and ionization without effects of the environment, we have studied soft X-ray photoabsorption on the doubly deprotonated oligonucleotide [dTGGGGT-2H]$^{2-}$ in gas-phase.

Fig.1 present direct evidence for the X-ray induced generation of positive fragment ions from deprotonated DNA. The dominating decay mechanism of the X-ray induced inner shell vacancy was found to be Auger decay with detachment of at least three electrons, leading to charge reversal of the anionic precursor and the formation of positively charged photofragment ions. The same process is observed in heavy ion (12 MeV C^{4+}) collisions with [dTGGGGT-2H]$^{2-}$ where inner shell vacancies are generated as well, but with smaller probability. K-vacancy Auger in DNA involving detachment of three or more low energy electrons instead of a single high energy electron has profound implications for DNA damage and damage modelling as secondary electron induced damage will be much more localized. The fragmentation channels, triggered by triple electron detachment Auger decay are predominantly related to protonated guanine base loss and even loss of protonated guanine dimers is tentatively observed. The fragmentation is not a consequence of the initial K-shell vacancy but purely due to multiple detachment of valence electrons, as a very similar positive ion fragmentation pattern is observed in fs-LID experiments.

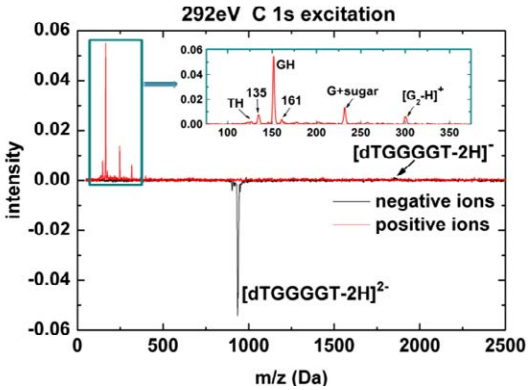

Figure 1. X-ray photoabsorption mass spectra of oligonucleotide dTGGGGT anions for 292 eV.

References

[1] Sadia B *et al* 2019 *Phys. Chem. Chem. Phys.* *21 30*
[2] Wen L *et al* 2019 *Chem. Eur. J.* *25 70*
[3] Dmitri E *et al* 2016 *Phys. Chem. Chem. Phys.* *18 37*

* E-mail: Wen.li@rug.nl
† E-mail: t.a.schlatholter@rug.nl

Implementation of multiconfiguration time-dependent Hartree-Fock method for diatomic molecules on prolate spheroidal coordinates

Y Li[1]*, T Sato[1,2,3] and K L Ishikawa[1,2,3]

[1]Department of Nuclear Engineering and Management, Graduate School of Engineering, The University of Tokyo, Tokyo 113-8656, Japan
[2]Photon Science Center, Graduate School of Engineering, The University of Tokyo, Tokyo 113-8656, Japan
[3]Research Institute for Photon Science and Laser Technology, The University of Tokyo, Tokyo 113-0033, Japan

Synopsis We report a numerical implementation of the multiconfiguration time-dependent Hartree-Fock (MCTDHF) method for diatomic molecules in intense laser fields. This method systematically incorporates electron-electron correlation for the system under consideration. As an example, we apply this method to the ionization of H_2 molecule. Our results for ionization probability as a function of internuclear distance show clear evidence of enhanced ionization.

Multielectron dynamics plays an important role when atoms and molecules are subject to ultrashort intense laser pulses. Numerical investigations of multielectron dynamics and correlation effects require highly nonperturbative treatments, which are very challenging. To tackle this challenge, the time-dependent multiconfiguration self-consistent-field (TD-MCSCF) methods have been developed [1, 2]. As one example of TD-MCSCF methods, we have developed and numerically implemented the time-dependent complete-active-space self-consistent-field (TD-CASSCF) method for atoms [3], with which stable and highly accurate simulations of strong-field phenomena are achieved within reasonable computational cost.

In this contribution, as one important kind of TD-MCSCF methods, we report 3-dimensional real-space implementation of the multiconfiguration time-dependent Hartree-Fock (MCTDHF) method for diatomic molecules. Our implementation adopts prolate spheroidal coordinates with spatial grids discretized by a finite-element discrete variable representation (FEDVR). Figure 1(a) shows the ground-state energy of H_2 as a function of internuclear distance. Excellent agreement with the exact energy is achieved. Figure 1(b) displays the ionization probability with respect to the internulcear distance. It is seen that enhanced ionization occurs at internuclear separation of 4.5 a.u., which is also in good agreement with that from the solution of the two-electron time-dependent Schrödinger equation (TDSE).

*E-mail: yangli@atto.t.u-tokyo.ac.jp

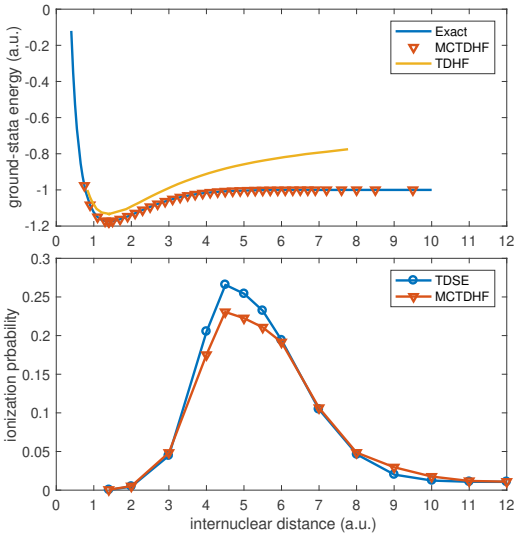

Figure 1. (a) Ground-state energy of H_2. The exact result was taken from [4]. (b) Ionization probability of H_2 in a 4-cycle 800-nm laser pulse with intensity of 1×10^{14}W/cm^2. The TDSE result was take from [5].

References

[1] Sato T *et al* 2013 *Phys. Rev. A* **88** 023402
[2] Ishikawa K L *et al* 2015 *IEEE J. Sel. Top. Quantum Electron* **21** 8700916
[3] Sato T *et al* 2016 *Phys. Rev. A* **94** 023405
[4] Sharp T E 1971 *Phys. Rev. A* **94** 023405
[5] Dehghanian E *et al* 2010 *Phys. Rev. A* **81** 061403(R)

Revealing molecular strong field autoionization dynamics

S Luo[1], J Liu[2], X Li[1], D Zhang[1], X Yu[1], D Ren[1], M Li[1], Y Yang[1], Z Wang[1], P Ma[1], C Wang[1], J Zhao[2], Z Zhao[2*] and D Ding[1†]

[1]Institute of Atomic and Molecular Physics, Jilin University, Changchun, 130012, China
[2]Department of Physics, National University of Defense Technology, Changsha, 410073, China

Synopsis We report a novel phenomenon of strong-field autoionization (SFAI) dynamics of CO^{+*} that is identified and investigated by channel-resolved angular streaking measurement combining with a laser-assisted autoionization calculation. Our results reveal that subcycle ac-Stark effect modulates the lifetime of the autoionizing state and controls the emission of SFAI electrons in molecular frame, which gives rise to the observed energy-dependent photoelectron angular distributions.

A quantum system in an excited state with energy higher than ionic states can couple with the ionic states by autoionization [1]. It is demonstrated that the coupling between autoionizing state with continuum can be tuned and tracked by adding a laser field, as shown in many ultrafast measurements [2]. Study on survival of autoionizing state in strong laser fields presents potential in enhancing the resonant high-harmonic generation and even composing an intense attosecond XUV pulse [3].

Here we perform a two-electron and two ion (2*e*-2*i*) coincident measurement of Coulomb explosion (CE) of CO in strong positively chirped laser fields (800 nm, 1.1×10^{15} W/cm^2, ~45 fs) using a reaction microscope setup. With a near-circularly polarized field (ε ~ 0.95), angular streaking method is employed to resolve the pathways of two electrons' detachment and to identify the autoionization channels.

A characteristic CE channel with low KER of 2.8-4.2 eV from CO^{+*} is observed. Two successively released electrons related to this channel are seperated according to their energy. One of the electrons shows a energy spectrum peaking around ~1 eV and extending to ~30 eV. And its angular distribution evolves gradually from a single peak to double peaks as energy increases, as shown in Fig. 1(a) and 1(b).

To interpret the observations, we model the SFAI theoretically as a strong field dynamical process with autoionizing state injection and decay. Calculated results agree well with that in experiment (see Fig. 1(c) and 1(d)). The simulation shows that, due to the subcycle ac-Stark effects in quantum systems with interacting bound and continuum configurations, the instantaneous response of molecules to the laser field strongly modifies the decay dynamics of autoionizing states, which induces the energy-dependent photoelectron angular distributions.

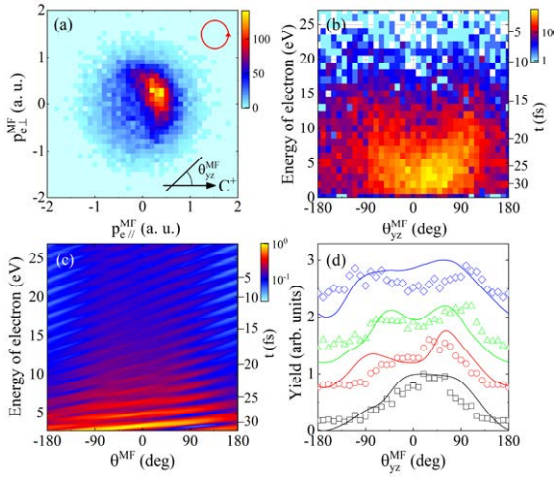

Figure 1. (a) Measured molecular-frame momentum distribution of electron from SFAI. (b) Measured and (c) calculated energy-dependent angular distributions of SFAI electron and (d) their evolution with energies at 0-3 eV, 3-6 eV, 6-12 eV and > 12 eV (dots for experiment and curves for calculation).

References

[1] Fano U 1961 *Phys. Rev.* **124** 1866
[2] Wang H *et al* 2010 *Phys. Rev. Lett.* **105** 143002
[3] Strelkov V *et al* 2010 *Phys. Rev. Lett.* **104** 123901

* E-mail: zhao.zengxiu@gmail.com
† E-mail: dajund@jlu.edu.cn

Retrieving molecular structure using machine learning of laser-induced electron diffraction

X Liu[1], K Amini[1], A Sanchez[1], B Belsa[1], T Steinle[1] and J Biegert[1,2,†]

[1]ICFO - Institut de Ciencies Fotoniques, The Barcelona Institute of Science and Technology, 08860 Castelldefels (Barcelona), Spain.
[2]ICREA, Pg. Lluís Companys 23, 08010 Barcelona, Spain.

Synopsis We implement a machine learning (ML) algorithm with a convolutional neural network (CNN) to laser-induced electron diffraction (LIED) technique to predict the three-dimensional molecular structure. We confirm our ML results by the strong correlation between experimental and simulated patterns and shown that the predicted molecular structure is accurate and reliable. Moreover, it also agrees well with the results from the previous publication. The combination of LIED with ML provides a new opportunity for retrieving large complex molecules.

Imaging ultrafast molecular dynamics addresses fundamental science, which helps us to understand the basics of chemical reactions. Laser-induced electron diffraction (LIED) [1, 2, 3], a strong-field variant of electron diffraction, is a state-of-the-art technique that directly retrieves the molecular structure with combined sub-atomic picometre and femtosecond spatio-temporal resolution. However, current retrieval algorithms are limited to few-atom molecular systems, becoming more challenging to identify extremum in a multi-dimensional solution space as the structural complexity increases.

Here, we first time implementing machine learning (ML) in LIED data that can accurately predict the three-dimensional (3D) molecular structure, which could be a potential candidate for retrieving large complex molecules. We train a convolutional neural network (CNN) to find the relationship between simulated molecular structures and their molecular interference signal through two-dimensional differential cross sections (2D-DCSs) from the simulated input database. The database split into training, validation and test set to validate the ML model. The different filters convolute across every source pixel of the input 2D-DCS map to provide a collection of feature maps (Fig. 1a). Subsequently, feature maps pass through the fully connected neural network by multiplying the weights of each neuron to predict the atomic position in the molecule (Fig. 1b). The predicted value is compared to the real value through the mean absolute error (MAE) (Fig. 1c). The whole process iterates from Fig. 1a to Fig. 1c to minimize the MAE and simultaneously optimize all of the parameters in the ML model. Once the ML model is validated, the experimental 2D-DCS map is used as an input to generate the molecular structure that most likely contributes to the measured interference signal shown in Fig. 1d. We take experimental data from two molecules, acetylene (C_2H_2) and carbon disulfide (CS_2). The predicted structures agree well with previous publications [1, 2].

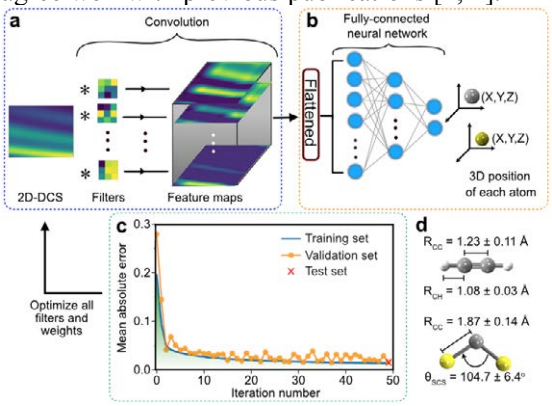

Figure 1. (a) A 2D-DCS convolute with different filters to generate feature maps. (b) The feature maps flatten to a 1D array and pass through the fully-connected neural network to predict the atomic position in the molecule. (c) At each iteration, all machine learning model parameters are simultaneously optimized to minimize the mean absolute error (MAE), which indicated the difference between predicted and real value. (d) Predicted structural parameters from machine learning.

References

[1]Pullen M G *et al* 2015 *Nat. Commun.* **6** 7262
[2]Amini K *et al* 2019 *PNAS* **116** 8173–8177
[3] Liu X *et al* 2019 *J. Chem. Phys.* **151** 024306

† E-mail: jens.biegert@icfo.eu

HHG-2ω attosecond stereo-photoionization unravel the shape resonance of N_2

V Loriot[1]*, A Marciniak[1], S Nandi[1], G Karras[1], M Hervé[1], E Constant[1], E Plésiat[2], A Palacios[2], F Martín[2,3,4], and F Lépine[1]

[1]Univ Lyon, Univ Claude Bernard Lyon 1, CNRS, Institut Lumière Matière, F-69622, VILLEURBANNE, France
[2]Departamento de Química, Módulo 13, Universidad Autónoma de Madrid, 28049 Madrid, Spain, EU
[3]Instituto Madrileño de Estudios Avanzados en Nanociencia (IMDEA-Nanociencia), Cantoblanco, 28049 Madrid, Spain, EU
[4]Condensed Matter Physics Center (IFIMAC), Universidad Autónoma de Madrid, 28049 Madrid, Spain, EU

Synopsis Photoionization time delay can be seen as a sensitive self-probe of the atomic or molecular potential. Nowadays, using attosecond interferometry, it is possible to perform such measurements using the RABBIT protocol. In this work, the ionization delay due to the shape resonance in the X-state N_2 has been observed, using the A-state as a reference signal. Compared to the standard RABBIT protocol, the dressing at 2ω has the advantage to separate the contributions in the measurement. Photoionization time delay can be retrieved using a specific analysis.

Attosecond science has recently brought the possibility to measure delays in photoionization of atomic and/or molecular targets. The RABBIT protocol (Reconstruction of Attosecond Beating By Interference of Two-photon transitions) offers this possibility with a temporal and spectral resolution [1]. This method is of high interest for molecular targets due to the richness of the processes that can take place in molecules. However, due to the rapid increase of the degree of complexity of molecular valence bands, spectral congestion of the RABBIT signal can take place and the information can be lost.

Recently, we developed an alternative method to the RABBIT protocol. The use of the second harmonic instead of the fundamental pulse as a dressing field reduces the spectral congestion. This method requires the measurement of the photoelectron spectrum on only one side of the laser polarization axis, that can be done using a velocity map imaging spectrometer (VMIS). We have shown that High Harmonic Generation (HHG)-2ω attosecond stereo-photoionization method allows to retrieve a similar information as the RABBIT method, using an appropriate analysis. For instance the attosecond pulse train (APT) can be reconstructed [2].

In this work, we take advantage of our method to measure photoionization time delays associated with the shape resonance of N_2. Since the two upper-most orbitals of N_2 are separated by ~1.5 eV, in contrast to the standard RABBIT method no overlap between the two contributions occurs when using the second harmonic of the Ti:Sa femtosecond laser.

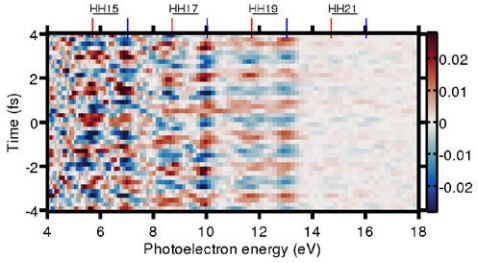

Figure 1. HHG-2ω attosecond stereo-photoionization measurement. Variation of the photoelectron spectrum ejected on one side of the polarization axis as a function of the APT-2ω delay.

Delays up to several tens of attosecond have been observed in the photoionization of the X-state [3]. This variation of the delay is a signature of the trapping of the electron wavefunction by the centrifugal potential barrier creating the resonance.

References

[1] Isinger M *et al* 2017 *Science* **358** 893
[2] Loriot V *et al* 2017 *J. Opt.* **19** 114003
[3] Loriot V *et al* 2020 *J. Phys. Photonics.* **2** 024003

*E-mail: vincent.loriot@univ-lyon1.fr

Electron-electron coincidence measurements of solvated molecules with a liquid micro-jet device.

B Lutet-Toti[1], L Huart[2], C Nicolas[2], A Kumar[2], D Céolin[2], J-P Renault[3], M-A Hervé du Penhoat[4], D Cubaynes[5], J.-M. Guigner[2], C Chevallard[3], J Bozek[2], P Lablanquie[1], I Ismail[1], F Penent[1], L Journel[1], and J Palaudoux[1]

[1]LCPMR, Sorbonne Université - UPMC, UMR CNRS 7614, Paris, France
[2]Synchrotron SOLEIL, Saint Aubin, France
[3]CEA, Université Paris-Saclay CNRS, NIMBE, 91191, Gif-sur-Yvette, France
[4]IMPMC, Sorbonne Université, UMR CNRS 7590, MNHN, Paris, France
[5] ISMO, Univ. Paris-Sud, Université Paris-Saclay, CNRS, Orsay, France

Synopsis Thanks to a magnetic bottle time-of-flight multi-electron spectrometer, we have filtered out the O 1s Auger spectra of the liquid phase and the gas phase in a liquid micro-jet environment. Interesting results are also shown in the C 1s case for a few benchmark molecules.

X-ray Photoelectron Spectroscopy (XPS) has proven to be a powerful asset for surface studies **[1]**. It is also emerging as the adequate choice to study biological samples **[2]**, especially with the increasing use of liquid micro-jet on synchrotron beamline. These new set-ups can help us to understand the energy transfer processes between organic molecules and the solvent, just after inner-shell ionization.

In this study, we used a new electron time-of-flight magnetic bottle spectrometer **[3] [4]**. It is composed of two parts: a permanent magnet (B~0.7T) which is placed just beneath the liquid micro-jet and a 1.2 m long flight tube, with a solenoid wrapped around (B~1mT), with a reduce entrance (Φ=5mm) to allow differential pumping (the vapor pressure around the liquid jet is in the 10^{-4} hPa range). When the Synchrotron light ionizes the molecules in the liquid jet, the electrons are driven by the magnetic field towards the flight tube and detected at the end by a micro-channelplate detector. Their energies are derived from the electrons' time-of-flight.

We studied a 1 molar sodium benzoate solution on the PLEIADES beamline (SOLEIL, France) in the liquid micro-jet. As a first example, we studied the O 1s photoelectron to probe the liquid-gas interface. We have recorded the coincidences between the O1s photoelectrons, and the subsequent Auger and we plot the corresponding two-dimensional map (**fig1**).

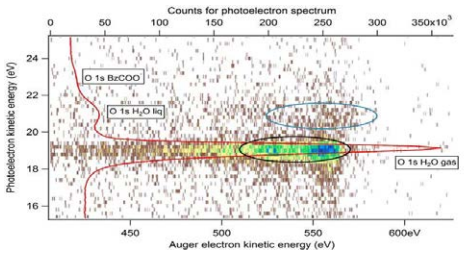

Fig 1: Overlap of two-dimensional electrons coincidence map and XPS spectrum.

Coincidence "islands" allow us to correlate the energies of these two electron types. By projecting the data on the y axis, we obtain the photoelectron spectrum (red curve). In this spectrum we observe three peaks corresponding to contributions from O1s of the gaseous water, the "liquid" water, and the solvated molecule. This first result can be followed by data filtering. In our events, we can separate in the Auger spectra the contribution from gas and liquid phases. We also applied the same coincidence method to other solvated molecules just above the C1s ionization threshold. For a given carbon site, we recorded the corresponding filtered Auger spectra. These spectra are different but, without any strong theoretical support, it is difficult to identify the final states of the solvated dications produced after Auger decay. Such experimental results will provide a severe test for theories.

[1] Siegbahn K 1970, *Phil. Trans. Roy. Soc. Lond. A.* **268**, 33-57
[2] Brown M A *et al* 2013, *Nano. Lett.*, **13**, 5403−5407
[3] Penent F *et al* 2005, *Phys. Rev. Lett.*, **95**, 083002
[4] Pohl M N *et al* 2017, *J. Phys. Chem. B*, **121**, 32, 7709–7714

Photoionization of the $(Mg@C_{60})^+$ cation: A hybrid model

M Magrakvelidze[1,3 *], S T Manson[2], and H S Chakraborty[3†]

[1]Science Department, Cabrini University, Radnor, Pennsylvania 19087, USA
[2]Department of Physics and Astronomy, Georgia State University, Atlanta, Georgia 30303, USA
[3]Department of Natural Sciences, D L Hubbard Center for Innovation, Northwest Missouri State University, Maryville, Missouri 64468, USA

Synopsis We investigate the photoionization of the singly positively charged ion of $Mg@C_{60}$ by implementing a DFT-based model that hybridizes photoamplitude signals from $Mg^+@C_{60}$ and $Mg@C_{60}^+$ configurations. The results predict interesting dynamical interferences.

The ground state electron hybridization between levels of atoms and fullerenes may occur from the near degeneracy of level energies. The observable consequences of this was earlier studied in various endofullerene molecules, for instance, in the context of resonant inter-Coulombic decay (ICD) photoionization processes for atoms like Ar, Kr confined in C_{60} [1,2]. However, a fundamentally different class of hybridization may arise from the near degeneracy of the total molecular energies that we focus in the current study.

The closeness of Mg 3*s* and C_{60} HOMO level-energies in $Mg@C_{60}$ suggests that the total ground state energies of its cation with configurations $Mg^+@C_{60}$ and $Mg@C_{60}^+$ are comparable. This near-degeneracy ensures hybridization between these configurations in the photoionization of a singly-charged $(Mg@C_{60})^+$ cation. We investigate the effect of this hybridization by comparing the photoionization properties of pristine $Mg^+@C_{60}$ and $Mg@C_{60}^+$ configurations with that of their hybrid in equal proportion of mixing at the level of photoamplitudes.

The calculation is performed in the framework of linear-response density functional theory (DFT) with the dipole response of the system to the incoming radiation [3]. The Kohn-Sham equations of the delocalized valence electrons are solved to obtain the ground state structures while the cage of 60 C^{4+} ions is jelliumized [4]. The photoionization cross sections, emission phases and Wigner time delays are calculated.

Figure 1 shows total photoionization cross sections of $Mg^+@C_{60}$ (in black), $Mg@C_{60}^+$ (in blue) and their hybrid configuration (in red). As noted, the cross section for the hybrid system is systematically lower than the two pristine system cross sections, which are themselves close, at the energies shown. This likely indicates that effect of the interference in the coherent mixing of the two configurations is destructive.

A detailed look at different energy ranges, for individual subshell emissions and phase (Wigner time delay) properties show a diverse range of interference effects.

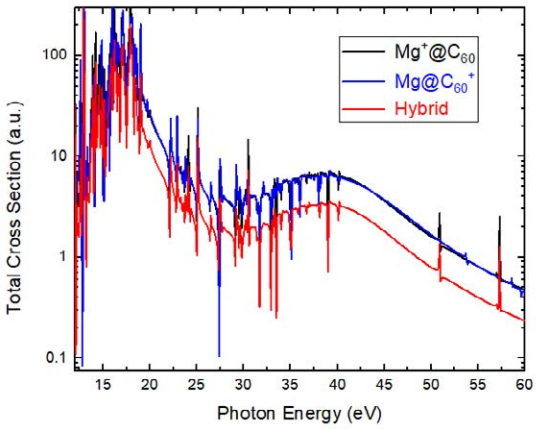

Figure 1. Total photoionization cross section of the configurations $Mg^+@C_{60}$ (black) $Mg@C_{60}^+$ (blue) and their hybrid $(Mg@C_{60})^+$ (red).

Supported by the National Science Foundation grant PHY-1806206 (HSC) and the US DoE, Office of Science, Basic Energy Sciences Grant DE-FG02-03ER15428 (STM).

References

[1] Magrakvelidze M *et al* 2016 *Eur. Phys. J. D* **70**:96
[2] De R *et al* 2016 *J. Phys. B* **49** 11LT01
[3] Shields D *et al* 2020 *J. Phys. B* **53**, 125101
[4] Choi J *et al* 2017 *Phys. Rev. A,* **95** 023404

* E-mail: mm12133@cabrini.edu
† E-mail: himadri@nwmissouri.edu

Revealing the influence of molecular chirality on tunnel-ionization dynamics

S Beaulieu[1], S Beauvarlet[1], V Blanchet[1], E Bloch[1], A Comby[1], D Descamps[1], N Dudovich[2], B Fabre[1], S Larroque[1], Y Mairesse[1]*, S Petit[1], B Pons[1], S Rozen[2], R Taïeb[3], A J. Uzan[2]

[1] Université de Bordeaux - CNRS - CEA, CELIA, UMR5107, F33405 Talence, France
[2] Weizmann Institute of Science, Rehovot, 76100, Israel
[3]Sorbonne Universités, UPMC Univ. Paris 6, CNRS-UMR 7614, LCPMR, 75252 Paris, France

Synopsis We theoretically and experimentally investigate the photoionization of chiral molecules using two-color laser fields in two complementary polarization configurations, bicircular and orthogonal, respectively acting as a chiral attoclock and a sub-cycle gated chiral interferometer. Comparing the angular distribution of electrons ejected forward or backward the laser propagation direction enables us to reveal the influence of the chiral potential in tunnel ionization dynamics.

In the past few years, new spectroscopic techniques based on strong laser fields have emerged, such as high-order harmonic spectroscopy, laser-induced electron diffraction and holography. They give access to structural and dynamical information on atomic and molecular systems, with unprecedented spatial and temporal resolutions. Strong-field processes all rely on the same initial step, in which electrons tunnel through the target potential barrier lowered by the laser field. Tunnel ionization thus plays a key role in strong-field physics and attoscience. However the tunneling dynamics and the properties of the electron wavepacket at the tunnel exit often remain hidden beneath the influence of the subsequent electron scattering onto the long range part of the potential, which adds up coherently to the primary ionization process.

We present a joint experimental/theoretical endeavor to characterize the amplitude and the phase of the wavepackets launched at the exit of the tunnel. We use chiral molecules, whose photoionization by circularly polarized light produces forward/backward asymmetric electron distributions. This asymmetry provides a background-free signature of the influence of the chiral potential in the ionization process. We first implement the attoclock technique, using corotating bicircular two-color fields. The forward/backward asymmetry of the angular streaking of the electron momentum distribution reveals the influence of chirality on electron scattering, subsequent to tunnel ionization. In addition, a large forward/backward asymmetry in electron yield is observed. Calculations trace back the root of this asymmetry to tunnel ionization, whose amplitude is thus strongly sensitive to the chiral potential.

In order to access the phase of the chiral ionizing wavepackets, we introduce sub-cycle gated chiral interferometry. We employ an orthogonally polarized two-color laser field whose optical chirality is manipulated on a sub-laser cycle timescale. Numerical simulations show that the interference between direct and indirect electrons is very sensitive to the instantaneous chirality of the field (Fig. 1). This scheme thus enables us to disentangle the contribution of tunneling and scattering in the process. The results show that the combined action of the chiral potential and rotating laser field not only imprints asymmetric ionization amplitudes during the tunneling process, but also induces a forward/backward phase shift. The ionic potential thus influences the whole coherent properties of tunneling wavepackets.

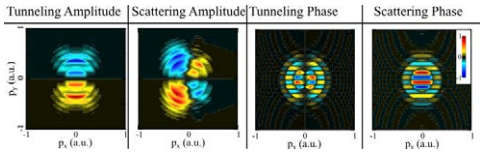

Figure 1. Simulated forward-backward asymmetric components of the electron distribution from different sources of chiral modulation.

*E-mail: yann.mairesse@u-bordeaux.fr

Time-resolved ultrafast fragmentation dynamics of 1-butanethiol

S Kumar[1,2] *, N Ekanayake[1], D Tikhonov [1,6], J Lee,[1,7], S Bari[1], R Boll[5], P Chopra[1,6], B Erk[1], D Garg[1,2], H Gleissner[2], S Gruet[1], J Lahl[3], S Maclot[3,4], J Peschel[3], D Rompotis[5], E Savelyev[1], N Schirmel[1], A Steber[1,6], P. Eng-Johnsson[3], M Schnell[1,6] and B Manschwetus[1] †

[1] Deutsches Elektronen Synchrotron (DESY), Notkestraβe 85, 22607 Hamburg, Germany
[2] Department of Physics, University of Hamburg, Germany
[3]Atomic Physics, Department of Physics, Lund University, Sweden
[4] Physics Department, University of Gothenburg, Sweden
[5] European XFEL, Schenefeld, Germany
[6] Institute of Physical Chemistry, Christians-Albrecht-Universität zu Kiel, Kiel, Germany
[7] The Chemistry Research Laboratory, University of Oxford, United Kingdom

The sulfur containing compounds in the atmosphere are produce from both the natural and anthropogenic combustion process. In recent years, Alkyl-thiols have excited great interest, mainly because of the experimental evidence of their presence in various environmental systems[1]. Here we present a study on the time-resolved UV photochemistry of 1-butanethiol molecule. Photoionization and fragmentation dynamics of 1-butanethiol molecule are investigated using a pump-probe technique. We used XUV beam from FLAH at 6.86 nm wavelength (181 eV) and UV pulses 266 nm wavelength from the third harmonic of a femtosecond NIR laser to perform the time-resolved pump-probe experiment at CFEL-AG Multi-Purpose (CAMP) endstation[2] at beamline 1 (BL1). After excitation with the UV pulses, the molecule undergoes fragmentation mainly into three reaction channels[3], for example most probable reaction channel produces SH and C_4H_9 (Fig.1. (a)). We can follow the fragmentation using the XUV pulses, which photo-ionize the 2p level of the sulfur atom in the molecule. Afterwards the sulfur atom undergoes rapid Auger decay that leads to the creation of double charge state on the sulfur. These charges will distribute over the molecule, if it has not yet dissociated. Therefore, based on the measured S^{2+} yield (Fig. 1. (b)) we can estimate the dissociation time. This work is under progress and we look forward to study the disscociation dynamics of the molecules using the photoelectron spectrum.

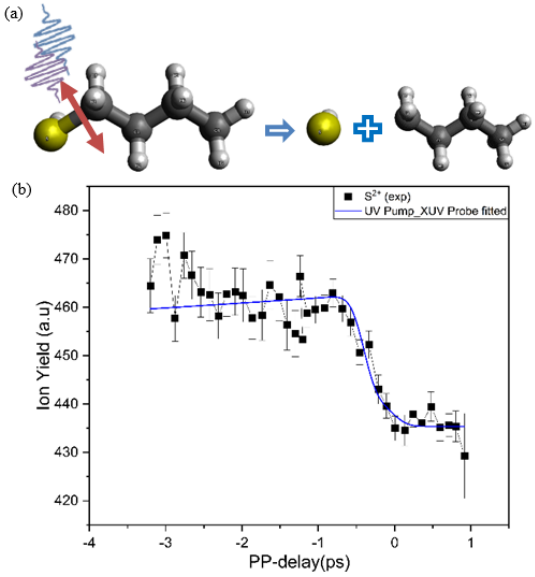

Figure 1. (a) The molecular dissociation of 1-butanethiol (b) Time dependent ion yield of S^{2+} ion.

References

[1] Levy A. *et al.* 1970 *Env. Sci. & Tech.* **4** 653
[2] Erk B. *et al.* 2018 *J. Sync. Rad.* **25** 1529
[3] Ross P.L. *et al.* 1993 *J. Phys. Chem.* **97** 1072

* E-mail: sonu.kumar@desy.de
† E-mail: bastian.manschwetus@desy.de

Photoionization of endohedral molecules: $N_2@C_{60}$

P. Decleva[1] and S. T. Manson[2*]

[1]Istituto Officina dei Materiali IOM-CNR and Dipartimento di Scienze Chimiche e Farmaceutiche, Universita' di Trieste, Via Giorgieri 1, I-34127 Trieste, Italy

[2]Department of Physics and Astronomy, Georgia State University, Atlanta, GA 30303, USA

Synopsis Calculations of the photoionization of the $1\sigma_g$, $1\sigma_u$, and $2\sigma_g$, states of the $N_2@C_{60}$ molecule are performed at the density functional theory (DFT) level taking full account of the molecular geometry of both N_2 and the C_{60}. The results show unexpected differences between the σ_g and σ_u levels.

The capability of the C_{60} cage to encapsulate atoms [1] and, more recently. small molecules [2] gives rise to a new class of systems with fascinating characteristics, still largely unexplored. The present work investigates the photoionization of the the $1\sigma_g$, $1\sigma_u$, and $2\sigma_g$ levels of the confined N_2 molecule at the density funcrtional theory (DFT) level with full account of the molecular geometry using methods described earlier [3].

The results for the the $1\sigma_g$ and $1\sigma_u$ states are shown in Fig. 1 for both the free N_2 molecule and $N_2@C_{60}$. For the free molecule, the $1\sigma_g$ state, the cross section shows the well-known shape resonance at about 420 eV, while the $1\sigma_u$ is essentially monotone decreasing. The confinement introduces confimement resonances [4] into the cross sections of both states, albeit with important differences. First of all, in the $1\sigma_u$ channel the confinement resonances show up simply as modulations of the free cross section as is generally the case for atoms [1]. For the $1\sigma_g$ channel, the form is rather different. The combination of these confinement resonances with the native shape resonance in the confined $1\sigma_g$ channel gives rise to a more complex feature in that energy range with a kind of splitting into a double peak structure, and some minor peaks in the low energy region. This seems to indicate that the native $1\sigma_g$ shape resonance and the confinement resonances interact coherently, and in a complicated manner, despite former being molecular in origin and the latter being essentially geometrical. To our knowledge, this type of interaction beteen a shape resonances and confinement resonances had not been seen for confined atoms,

A most interesting feature is the regular interleaving of the resonances, seen clearly in Fig. 1, between the $1\sigma_g$ and $1\sigma_u$ photoionization channels This interleaving is evidently a signature of the different parity of the initial states and that of the corresponding continuum waves. This effect too has not been seen in atoms.

This work was supported by DOE, Office of Science under Grant DE-FG02-03ER15428.

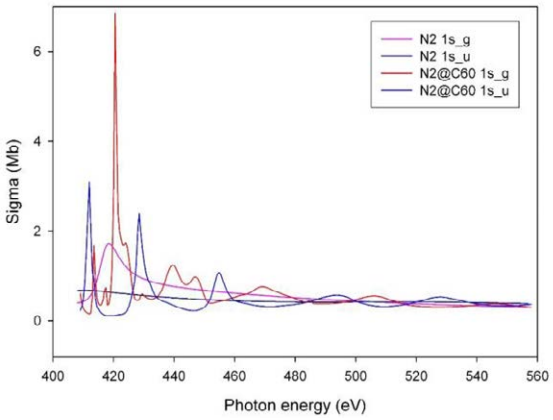

Figure 1. Photoionization cross section of the the $1\sigma_g$ and $1\sigma_u$ states of $N_2@C_{60}$ and free N_2.

References

[1] V. K. Dolmatov et al 2004 *Radiation Phys. Chem.* **70,** 417
[2] V.Kuznetsov 2020 *Molecules* **25,** 2437
[3] A. Ponzi, P.Decleva and S. T Manson 2015 *Phys. Rev. A.* **92,** 063422
[4] J. P. Connerade, V. K. Dolmsatov and S. T. Manson 2000 *J. Phys. B* **33** 2279

* E-mail: smanson@gsu.edu

Impact of aliphatic bonds on the stability of VUV photoprocessed PAHs under relevant astrophysical conditions

A. Marciniak[1] * A. Bonnamy[1], V. Rao Mundlapati[1], G. Mulas[1,2], M. Vilas-Varela[3], D. Peña[3] and C. Joblin[1] †

[1]IRAP, Université de Toulouse (UPS), CNRS, CNES, 31400 Toulouse, France
[2] INAF – Osservatorio Astronomico di Cagliari, Via della Scienza 5, I-09047 Selargius (CA), Italy
[3]CiQUS, Universidade de Santiago de Compostela, 15782 Santiago de Compostela, Spain

Synopsis We measured the VUV photoprocessing kinetics of bare, alkylated and superhydrogenated PAH cations isolated in astrophysical conditions. We obtained new insights into the competition between fragmentation, isomerization and radiative cooling. We emphasize the role of pentagonal rings in the molecular stability.

The interaction of polycyclic aromatic hydrocarbons (PAHs) with VUV light plays a crucial role in the physical and chemical evolution of photodissociation regions (PDRs). In addition of emission in the well-known aromatic infrared bands (AIBs) [1], fragmentation [2] can be involved, leading to selection effects favoring specific sizes and structures. In this context, despite their lower stability, PAHs containing aliphatic C-H bonds are considered as good candidates for the 3.4 μm AIB [3, 4].

We have combined a 10.5 eV photon source with the cryogenic ion trap PIRENEA [5] to study the impact of aliphatic bonds on the photostability of PAH cations in conditions relevant to PDRs [6]. The pyrene and coronene cations and their alkylated (methyl and ethyl sidegroups) and superhydrogenated derivatives have been irradiated over long timescales (∼1000 s). The measured photofragmentation cascades are analyzed with a simple kinetics model which enabled to derive fragmentation pathways, rates and branching ratios. Results show that PAHs with aliphatic bonds have a higher fragmentation rate and carbon losses compared to bare PAHs. Their fragmentation cascade can lead to species carrying a peripheral pentagonal cycle, which are as stable as or even more stable than the bare PAHs. From a detailed analysis of the kinetics curves and comparison of the fragmentation and photoabsorption rates (Figure 1), we are able to identify species for which there exists a competition between fragmentation, isomerization and radiative cooling.

This work provides further evidence for the role of isomerization processes, including the H-migration process [7], in the dissociation of PAHs. The formation of aliphatic C-H bonds resulting from this process could lead to an additional contribution to the 3.4 μm AIB. Our study also suggests that PAHs with peripheral pentagonal rings are abundant in PDRs.

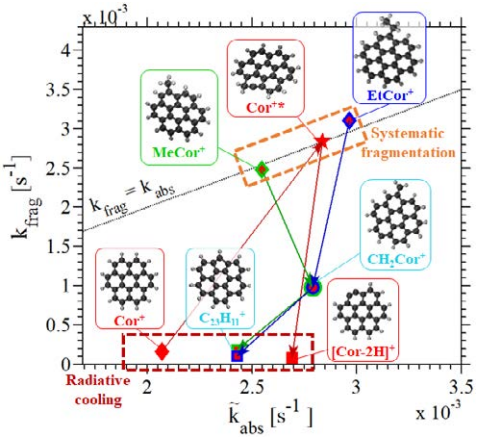

Figure 1. Fragmentation rates of coronene, methyl- and ethyl-coronene and their VUV photoinduced fragments as a function of their photoabsorption rates.

References

[1] A. Leger *et al.* 1989 *A&A*, **216**, 148-164
[2] J. Montillaud *et al.* 2013 *A&A*, **552**, A15
[3] C. Joblin *et al.* 1996 *ApJ*, **448**, 610-620
[4] M. P. Bernstein *et al.* 1996 *ApJ*, **472**, L127-L130
[5] C. Joblin *et al.* 2002 *EAS Pub. Series*, **4**, 73-77
[6] A. Marciniak *et al.* 2021 *arXiv*, **2103.03890**
[7] G. Trinquier *et al.* 2017 *Mol. Astrophys.*, **7**, 27-36

*E-mail: alexandre.marciniak@irap.omp.eu
†E-mail: christine.joblin@irap.omp.eu

Polarization control in two-color water molecule ionization

L Martini[1]*, D I R Boll[1,2], A Palacios[2,3] and O A Fojón[1,4]

[1]Laboratorio de Colisiones Atómicas, Instituto de Física Rosario (CONICET-UNR), 2000 Rosario, Argentina
[2]Depto. de Química, Módulo 13, Facultad de Ciencias, UAM, 28049 Madrid, España
[3]Institute of Advance Research in Chemical Science (IAdChem), UAM, 28049 Madrid, España
[4] Escuela de Ciencias Exactas y Naturales, FCEIA, UNR, 2000 Rosario, Argentina

Synopsis We investigate a polarization control scheme in two-color two-photon water molecule ionization by means of second-order time dependent perturbation theory. Recent experiments have shown dependencies with the light polarization in above threshold laser assisted ionization of water molecules. At the photoelectron energies these experiments were performed, the soft-photon approximation exhibits discrepancies with the measurements. We unveil that these discrepancies might be associated to the coulombic nature of the scattering process for continuum-continuum transitions.

The basic reactions that involve the water molecule are essential to understand the interaction between radiation and biological tissue, as it is composed mainly of water. Among the reactions of interest, the ionization of molecules in the gas phase has been investigated in numerous studies. The current availability of a great variety of experimental configurations of two-color ultra-short pulses allows new perspectives on the electronic dynamics induced in the water molecule. In this work, we investigate by means of second-order time-dependent perturbation theory (SOTDPT) [1], the dependencies with polarization in a pump-probe scheme for water molecules. In these reactions, an extreme ultraviolet (XUV) ultra-short pulse ionizes the water molecule leading to a smooth photoelectron energy distribution. Then, the photoelectron can exchange additional photons with an infrared (IR) laser producing secondary peaks in the energy spectrum known as sidebands. The intensity of these sidebands presents an oscillatory behaviour as the relative polarization angle between the XUV and IR pulses varies. It has a maximum for collinear polarization of the fields and a minimum for fields with perpendicular polarization.

In previous experiments the same behaviour was measured for laser assisted photoionization of water molecules [3]. These experiments were carried out at photoelectron energies for which predictions obtained with the soft-photon approximation (SPA) show discrepancies with the measurements. In the figure, we show our results for the sideband intensity for water molecules, for two basis sets (BS) [2], as a function of the relative polarization angle together with SPA calculations and experiments.

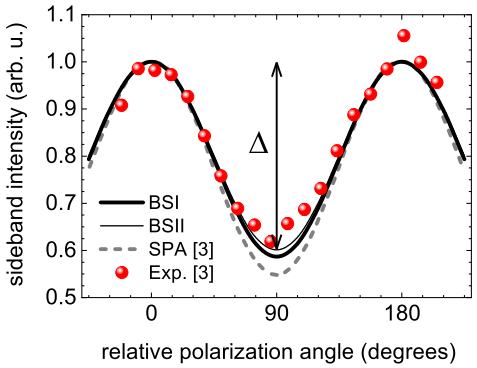

Figure 1. Sideband intensity as a function of the relative polarization angle for water molecules. Black curve and thin black curve, SOTDPT calculations using the basis set I and II respectively. Gray dashed curve, SPA calculations from Leitner *et al* [3]. Red circles, experimental values obtained by Leitner *et al* [3].

With our model, we improve the description of the experimental data and show that the discrepancies presented by the SPA can be attributed to the coulombic nature of the scattering process for continuum-continuum transitions.

References

[1] Boll D I R *et al* 2020 *Phys. Rev. A* **101** 013428
[2] Martini L *et al* 2019 *J. Phys. B: At. Mol. Opt. Phys.* **52** 105204
[3] Leitner T *et al* 2015 *Phys. Rev. A* **91** 063411

*E-mail: martini@ifir-conicet.gov.ar

Weak-field asymptotic theory of tunneling ionization of the hydrogen molecule including core polarization, spectator nucleus, and internuclear motion effects

H Matsui[1] , O I Tolstikhin[2] and T Morishita[1]

[1]The University of Electro-Communications, Chofu-shi, 182-8585, Japan
[2]Moscow Institute of Physics and Technology, Dolgoprudny, 141700, Russia

Synopsis We theoretically study the tunneling ionization of the hydrogen molecule in a static electric field. We calculate the tunneling ionization rate based on the leading-order many-electron weak-field asymptotic theory, and successively incorporates core polarization, spectator nucleus, and internuclear motion effects. Our calculation results with including these physical effects well describe ab initio calculations with the fixed nuclei approximation as well as the experimental results on the anisotropy of strong-field ionization of H_2 and D_2. These results indicate that all the effects have essential roles in the tunneling ionization process of the hydrogen molecule.

When the atoms and molecules are exposed to an intense low-frequency (~10^{14}W/cm^2, ~800nm) laser field, the tunneling ionization process occurs. This is one of the most fundamental processes in strong-field physics. In this process, the electron tunnels through the field-distorted nuclear Coulomb potential barrier. As the laser field can be regarded as a static electric field, this process can be characterized by the ionization rate Γ.

Especially for molecules, the rate Γ strongly depends on the molecular alignment angle with respect to the direction of the external field F. For the hydrogen molecule, the rate Γ has a maximum value $\Gamma_\parallel$ (a minimum value $\Gamma_\perp$) when its molecular axis is parallel (perpendicular) to the field. Therefore, the ratio of these two rates $\Gamma_\parallel/\Gamma_\perp$ characterizes the anisotropy of the molecular tunneling ionization process. The anisotropy ratios $\Gamma_\parallel/\Gamma_\perp$ were measured for H_2 [1] and D_2 [2]. However, as far as we know, these results have not been reproduced satisfactorily.

In our study, we calculated the rate Γ based on the leading-order many-electron weak-field asymptotic theory (ME-WFAT), and successively incorporates the physical effects described below. The results of the ratio $\Gamma_\parallel/\Gamma_\perp$ are shown in Figure 1 [3]. Brown densely dotted line shows the result of the Hartree-Fock method with the single active electron approximation as a reference. Red solid line shows the ME-WFAT result. Green dashed line shows the result including the core polarization effect, and blue dotted line further including the spectator nucleus effect. Black and magenta dash-dotted lines show the results with the internuclear motion for H_2 and D_2, respectively. We also plot the corresponding solid lines for the ratios of yields for H_2 and D_2, where the shape of the laser pulse is considered. All the effects change the results dramatically, and the final results well describe the experimental results [1, 2]. These results indicate that all the effects have essential roles in the tunneling ionization process of the hydrogen molecule.

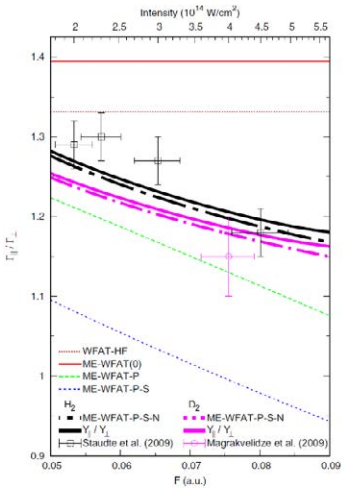

Figure 1. Ratio of the ionization rates in the parallel and perpendicular geometries $\Gamma_\parallel/\Gamma_\perp$ as a function of the field strength F [3]. The top axis shows the intensity of circular polarized laser field.

References

[1] A Staudte *et al* 2009 *Phys. Rev. Lett.* **102** 033004
[2] M Magrakvelidze *et al* 2009 *Phys. Rev. A* **79** 033408
[3] H Matsui *et al* 2021 *Phys. Rev. A* **103** 033102

Imaging SF_6 using Molecular Frame Photoelectron Angular Distributions

O D McGinnis[1]*, S Grundmann[1], A Pier[1], L Sommerlad[1], D Tsitsonis[1], M S Schöffler[1], T Jahnke[1,2], R Dörner[1] and F Trinter[1,3,4]†

[1]Institut für Kernphysik, Goethe-Universität, 60438 Frankfurt, Germany
[2]European XFEL, 22869 Schenefeld, Germany
[3]Photon Science, Deutsches Elektronen-Synchroron (DESY), 22607 Hamburg, Germany
[4]Molecular Physics, Fritz-Haber-Institut der Max-Planck-Gesellschaft, 14195 Berlin, Germany

Synopsis Photoelectron angular distributions can be used to image the structure of fixed-in-space molecules. Here, we apply this technique to display the six-fold symmetry of SF_6. We find that the structure determination works better if photoionization targets the sulfur instead of the fluorine.

The geometrical structure of molecules can be determined by means of angle-resolved photoelectron spectroscopy through a COLTRIMS reaction microscope (see, e.g., Ref.[1]). In the present work, we apply this method to a heavy molecule (SF_6) that exhibits high symmetry. In particular, we investigate the sensitivity of the approach on the spatial origin of the photoelectron wave (S 1s or F 1s).

Utilizing the wide spectrum of photon energies available at the P04 beamline at PETRA III (DESY), we were able to target either the inner or outer atoms of our target molecule (sulfur hexafluoride, SF_6). To target the inner atom (sulfur) we chose an energy of 2515 eV, for the outer atoms (fluorine) we chose 725 eV. In both cases, the photoelectron originated from the 1s shell of the respective atom with 28 eV kinetic energy. For our analysis, we used data points that contained either two or three detected ions. To fix the molecular frame of reference eventually, we selected detection events that contained at least two F+ with momentum vectors that enclosed a mutual angle of roughly 90°.

With the molecule fixed we can generate the MFPADs, shown in Fig. 1. One observes that for the ionization of Sulfur 1s, the Structure of SF_6 is clearly represented in the MFPAD. For the ionization of Fluor 1s however, the MFPAD is dominated by an isentropic distribution, with only a slight preference of photoelectron emission in the direction of one of the Fluor. As the molecular potential shapes the MFPADs [2], we speculate that due to the different spatial origins, the photoelectron wave experiences different molecular potentials, resulting in the observed variations between the two MFPADs.

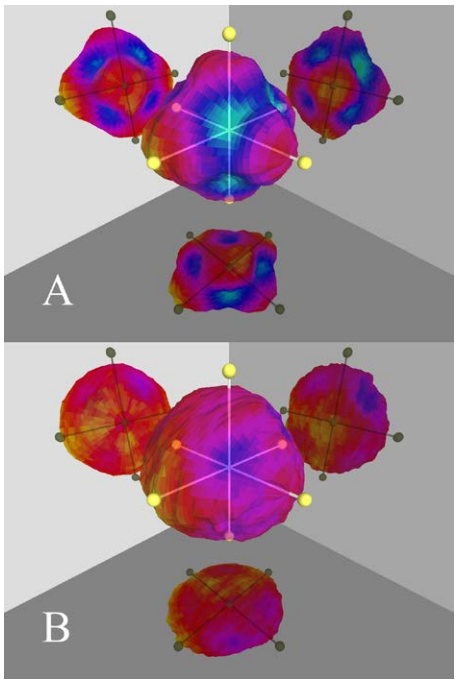

Figure 1. 3D electron angular distribution in fixed molecular frame for decays that resulted in two or three Ions with at least two F^+ Ions.
A) 2515 eV Photons B) 725 eV Photons

References

[1] Williams J B *et al* 2012 *Phys. Rev. Lett.*, **108** 233002
[2] Landers A *et al* 2001 *Phys. Rev. Lett.*, **87** 013002

*E-mail: mcginnis@atom.uni-frankfurt.de
†E-mail: trinter@atom.uni-frankfurt.de

Accurate R-matrix photoionization models for intermediate-sized molecules

T Meltzer[1]* **and Z Mašín**[1]

[1]Institute of Theoretical Physics, Faculty of Mathematics and Physics, Charles University, V Holešovičkách 2, 180 00 Prague 8, Czech Republic

Synopsis We introduce a novel variational R-matrix model, polarization-consistent coupled Hartree-Fock, which is applied to formic acid. We compare this with traditional methods, such as, static exchange plus polarization (SEP) and close-coupling (CC). We find that our new model provides significantly improved results compared to standard SEP calculations, and furthermore, the results are in close agreement with more expensive CC calculations. This paves the way towards accurate photoionization calculations for even larger molecules.

Photoionization of molecules is an important process that occurs across the Universe e.g., in natural or man-made plasmas, interstellar medium and planetary atmospheres. We are interested in the application of the R-matrix method, as implemented in the UKRMol+ code [1], to calculate accurate state-resolved photoionization cross sections and asymmetry parameters.

To date, photoionization calculations using the UKRMol+ codes have largely been restricted to either di- or tri-atomics e.g., H_2 and H_2O [2], CO_2 [3] etc. However, in this work we extend the applicability of the UKRMol+ code to study a 5 atom system – formic acid (HCOOH). Formic acid is of interest because it is a likely precursor to biological life on Earth and its dimer is one of the simplest prototypes for a dihydrogen bonded system. For the monomer we present brand new results for state-resolved, single-photon ionization cross sections and angular distributions.

To compute accurate cross sections we introduce a novel photoionization model called, Polarization-Consistent Coupled Hartree-Fock (PC-CHF) which we compare against traditional models; Static Exchange plus Polarization (SEP) and Close-Coupling (CC) [1]. The PC-CHF model is designed to sit somewhere between SEP and CC. It removes fully the deficiencies of the SEP model associated with unphysical pseudo-resonances, an issue we have identified as an important limiting factor in photoionization calculations. It does so by coupling all polarization configurations to the corresponding HF-like ionic states. Secondly, unlike CC we explicitly include all the couplings to the ionic states implied by the set of polarization configurations. The same behaviour can be obtained with the CC approach but in practice it will typically require including more ionic states than is computationally feasible. In summary, the PC-CHF model provides greatly improved results compared to the standard SEP approach, whilst maintaining close agreement with more expensive CC calculations.

*E-mail: thomas.meltzer@utf.mff.cuni.cz

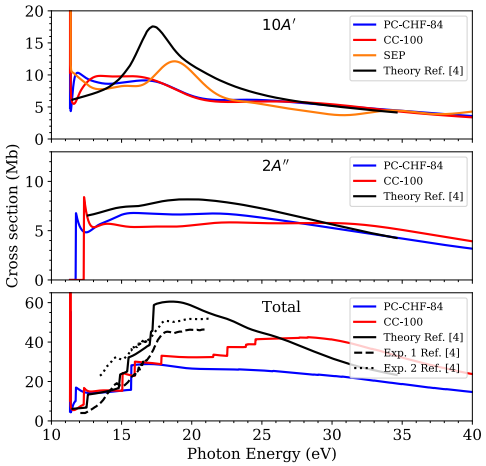

Figure 1. Photoionization cross sections for HCOOH for the two lowest-lying ionic states, 10 A′ (top) and 2 A″ (middle) and the total cross section (bottom). The R-matrix results PC-CHF (blue), CC (red) and SEP (orange) are compared with theory and experiments of Fujimoto *et al.* [4].

References

[1] Mašín Z *et al* 2020 *CPC* **249** 107092
[2] Benda J *et al* 2020 *Phys. Rev. A* **102** 052826
[3] Harvey A *et al* 2014 *J. Phys. B* **47** 215005
[4] Fujimoto M. M. *et al* 2020 *JPCA* **124** 6478

A comprehensive study of the dissociation processes of water after core ionisation

N Melzer[1]*, J Rist[1], L Kaiser[1], K Klyssek[1], C Schwarz[1], N Anders[1], J Siebert[1], D Tsitsonis[1], I Vela Perez[1], D Trabert[1], M Kircher[1], S Grundmann[1], L Ph H Schmidt[1], V Davis[3], F Trinter[1,2], J B Williams[3] and T Jahnke[4]†

[1]Institut für Kernphysik, Goethe University Frankfurt, 60438 Frankfurt, Germany
[2]Molecular Physics, Fritz-Haber-Institut der Max-Planck-Gesellschaft, 14195 Berlin, Germany
[3]University of Nevada, Reno, 89557, United States
[4]European XFEL, Holzkoppel 4, Schenefeld, 22869, Germany

Synopsis O 1*s* photoionization and dissociation of H_2O was investigated by performing a photoenergy-scan in a range of 20 eV above the K-threshold using a COLTRIMS reaction microscope and synchrotron radiation. Our comprehensive study shows, for example, that the H^++H^++O^+ breakup channel depicts a dependence of the dissociation geometry on the Kinetic Energy Release (KER) of the ions. β, which is defined as the angle between the two protons, increases for a lower KER, resulting in an almost linear breakup of the molecule.

We have performed a comprehensive study on the photoionization and dissociation of H_2O by removal of an Oxygen K-electron. For our study, the photon energy was scanned in a range between 539 and 561 eV (the O 1*s* threshold is located at 539.7 eV [1]) at the BESSY synchrotron on Beamline U49-2. COLd Target Recoil Ion Momentum Spectroscopy (COLTRIMS) was used to measure the correlated momenta of the ionic fragments and the photoelectrons in coincidence.

From the measured momenta, we obtained the dissociation angles of the molecule, which show a strong dependence on the Kinetic Energy Release (KER) in case of a three-particle breakup of the molecule into H^++H^++O^+ (see Fig. 1, top right). The distribution of the relative emission angle between the two protons β [2] depicts preferentially larger values with decreasing KER. For lower KERs, β extends to almost 180°, which corresponds to a linear breakup of the molecule.

In addition, $\alpha_{1,2}$, which are the angles between the emission directions of the oxygen ion and the two protons, show a similarly interesting behavior. Figure 1 (bottom row) depicts the correlation of α_1 and α_2 for different KER ranges of 10−18 eV and 25−50 eV. These KER ranges correspond to two significant peaks occurring in the KER distribution (Fig. 1, top left). The angular distribution is broader for smaller KER values.

Further results including molecular-frame photoelectron angular emission distributions will be presented.

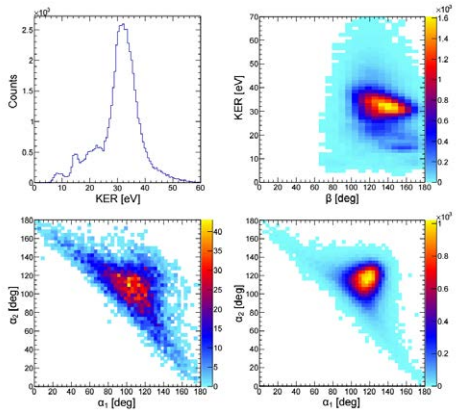

Figure 1. KER distribution for a breakup of H_2O into H^++H^++O^+ after O-K-shell ionization (top left). Dependence of β (see text) on the KER (top right). Bottom row: Correlation maps of α_1 and α_2 (see text) for two different KER regions. The KER ranges from 10−18 eV (bottom left) and from 25 − 50 eV (bottom right).

References

[1] I Ishii *et al* 1987 *J. Chem. Phys.* **87** 4344
[2] D Reedy *et al* 2018 *Phys. Rev. A* **98** 053430

*E-mail: melzer@atom.uni-frankfurt.de
†E-mail: till.jahnke@xfel.eu

Clocking enhanced ionization of H_2 with rotational wavepackets

Y Mi[1,2] *, P Peng[1], N Camus[2], X Sun[2], P Fross[2], D Martinez[2], Z Dube[1], P B Corkum[1], D M Villeneuve[1], A Staudte[1], R Moshammer[2] and T Pfeifer[2]

[1]Joint Attosecond Science Laboratory, National Research Council and University of Ottawa, Ottawa, K1A 0R6, Canada
[2]Max-Planck Institute for Nuclear Physics, Heidelberg, 69117, Germany

Synopsis The laser-induced rotational wavepacket of hydrogen molecules has been experimentally observed in real time by using two sequential 25-fs laser pulses and a reaction microscope. By measuring the time-dependent yields of the above-threshold dissociation and the enhanced ionization of the molecule, we observed a few-femtosecond time delay between the two dissociation pathways.

We demonstrate that rotational wavepackets of hydrogen molecules can serve as an ultrafast clock for probing time delays of the molecular dissociation dynamics on the few-femtosecond timescale within a single multi-cycle pulse [1].

In an experiment, 25-fs, 800-nm laser pulses are focused into the reaction microscope where they intersect a supersonic H_2 gas jet. An orthogonally polarized pump-probe scheme is applied, which ensures that the dissociation events induced by the pump pulses can be separated from those induced by the probe.

Figure 1(a) shows the kinetic-energy release (KER) distribution as a function of the time delay between the pump and the probe pulses. The peaks of the KER centered at 1.1 and 5.4 eV correspond to the above-threshold dissociation (ATD) and the enhanced ionization (EI) processes, respectively. Distinct delay-dependent oscillation structures in both channels are observed. The time-resolved yields of ATD (blue circles) and EI (red squares) have been extracted and plotted in Fig. 1(b). A Fourier transform was performed on their time-dependent traces, shown for ATD (blue) and EI (red) in Fig. 1 (c). Two main frequencies, 10.6 and 17.6 THz, were observed for both channels, which agree well with the rotational transitions of H_2, J: 0→2 and J: 1→3, respectively. This confirms that the rotational wavepackets are created in the H_2 molecule by the pump pulse. As both ATD and EI are sensitive to the molecular alignment, their time-resolved yields reflect the rotational wave packet of H_2.

Although ATD and EI show identical oscillation structures, which were mapped by the rotational wave packets in the hydrogen molecules, a clear time delay in their traces was observed, as is visible in Fig. 1(b). In order to extract this time delay, we fit their yields by the superposition of n cosine functions. The fit results of ATD and EI for H_2 are plotted in Fig. 1(b). Figure 1(d) shows the same curves as in Fig. 1(c) for a shorter time window between 250 and 350 fs. The delay from the fit is $\delta t = 5.5 \pm 0.7$ fs.

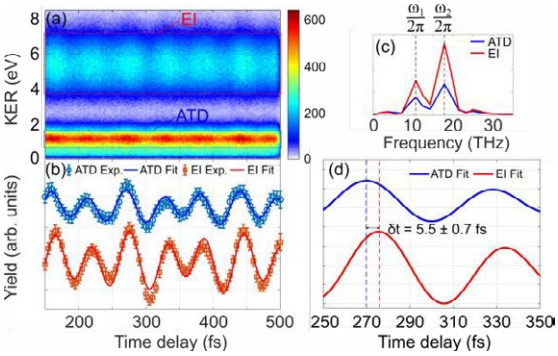

Figure 1. (a) Kinetic-energy release distribution of H+ as a function of the pump-probe delay. (b) Time-resolved yields of ATD and EI. (c) Fourier transform of the time-resolved yields of ATD and EI. (d) Enlargement of the fitted curves of ATD and EI for delays of 250 - 350 fs.

This method provides the general concept of a molecular rotational clock, which can be extended to other molecules for extracting temporal information of multiple sequential dissociation processes.

References

[1] Yonghao Mi *et al* 2001. *Phys. Rev. Lett.* **125** 173201

* E-mail: ymi@uottawa.ca

Ultrafast Isomerization Dynamics in Small Molecules

D Mishra[1]*, J Reino-González[2], A C LaForge[1], M McDonnell[1], R Obaid[1], S Díaz-Tendero[2], F Martín[2] and N Berrah[1]†

[1]Department of Physics, University of Connecticut, Storrs, Connecticut, 06269, USA
[2]Departamento de Quimica, Modulo 13, Universidad Autonoma de Madrid, Madrid, 28049, Spain

Synopsis We present a comparative study of laser-induced single and double hydrogen migration as well as fragmentation dynamics for a few small organic molecules, namely acetonitrile, 1- and 2- propanol, using pump-probe spectroscopy in combination with Coulomb explosion imaging. While direct C-C bond fragmentation is more likely than hydrogen migration in the case of the propanol isomers, interestingly, the opposite is true for acetonitrile, where isomerization through single and double hydrogen migration leads to more stable isomers as compared to the original linear structure.

Laser-induced ionization of molecules leads to changes in their molecular structures and by extension, their chemical properties via different types of characteristic processes such as single and double hydrogen migration and fragmentation. In particular, double hydrogen migration is a more complex isomerization process involving the motion of two hydrogen atoms within a molecule and was recently studied in ethanol [1]. The timescale for such fast hydrogen migration dynamics varies from a few femtoseconds in acetylene [2] to hundreds of femtoseconds in ethanol.

Here, we present the time-resolved measurements of isomerization and fragmentation dynamics observed in acetonitrile [3] and 1- and 2-propanol. Fig. 1 shows the primary channels of fragmentation, single and double hydrogen migration (SHM, DHM) and hydrogen loss channels in acetonitrile. We observe that SHM and DHM are the primary isomerization channels, showing higher yields than direct fragmentation of the C-C bond which has no hydrogen migration (NHM). In contrast, for both 1- and 2-propanol, the direct breakup is the only pathway observed in double coincidences and a SHM channel with low yield in triple coincidences. No DHM is observed in the ionization of 1- and 2-propanol.

The molecular dynamics presented in this work were investigated with IR pump-IR probe pulses combined with a coincident imaging spectrometer, which gives the full three-dimensional momentum information for each detected fragment. The experimental results are interpreted by state-of-the-art ab initio molecular dynamics calculations.

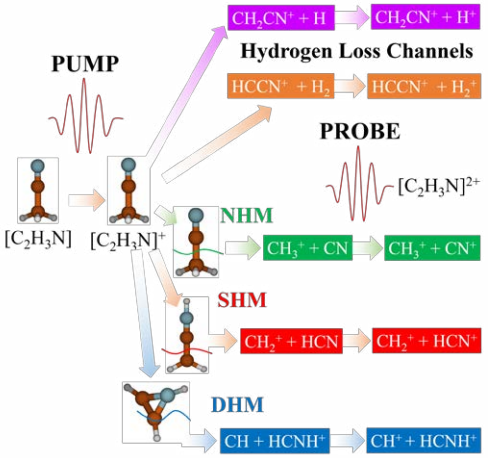

Figure 1. Primary channels of H^+ (pink) and H_2^+ (orange) loss, NHM (green), SHM (red) and DHM (blue) observed in the acetonitrile cation.

The experiment was funded by NSF award No. 1700551. The theory was funded by the MICINN - Spanish Ministry of Science and Innovation for projects PID2019-105458RB-I00.

References

[1] Kling N. G *et al.* 2019 *Nat. Commun.* **10** 2813
[2] Hishikawa A. *et al.* 2007 *Phys. Rev. Lett.* **99** 258302
[3] McDonnell M. *et al.* 2020 *J. Phys. Chem. Lett.* **11** 6724

*E-mail: debadarshini.mishra@uconn.edu
†E-mail: nora.berrah@uconn.edu

Probing molecular shape resonances in attosecond time-scale

S Nandi[1,2 *], E Plésiat[3], S Zhong[1], A Palacios[3], D Busto[1], M Isinger[1], L Neoričić[1], C L Arnold[1], R J Squibb[4], R Feifel[4], P Decleva[5], A L'Huillier[1], F Martín[3] and M Gisselbrecht[1]

[1]Department of Physics, Lund University, 22100 Lund, Sweden
[2]Univ Lyon, Univ Claude Bernard Lyon 1, CNRS, Institut Lumière Matière, F-69622 Villeurbanne, France
[3]Departamento de Química, Módulo 13, Universidad Autónoma de Madrid, 28049 Madrid, Spain
[4]Department of Physics, University of Gothenburg, 41296 Göteborg, Sweden
[5]Dipartimento di Scienze Chimiche e Farmaceutiche, Universitá di Trieste and IOM-CNR, 34127 Trieste, Italy

Synopsis Following molecular photoionization, an outgoing electron can be trapped by a potential barrier before escaping to the continuum. As the nuclei in the molecule vibrate, the shape of this barrier is modified and hence, the corresponding trapping time is changed. Here, we show that in valence-ionized N_2 molecule a mere change of 2% in the bond-length, amounting to a tiny change in the barrier, can lead to the photoelectron emission being delayed by almost 200 attoseconds. Our result poses a limit on the applicability of Franck-Condon principle in photo-excited molecules.

Shape resonances emerge from spatial confinement of a particle by a potential barrier. In photon-molecule interaction, such a barrier may prevent a photoelectron from reaching the ionization continuum instantaneously. In the meantime, the nuclei in the photoionized molecule may move, modifying the 'shape' of the barrier. This can, in turn, affect significantly the photoionization process [1].

Here, we studied the well-known $3\sigma_g^{-1}$ shape resonance in N_2 molecule [2] using the attosecond interferometric protocol: RABBIT (reconstruction of attosecond beating by interference of two-photon transitions) [3]. By detecting the photoelectrons with high spectral resolution that allowed us to resolve vibrational levels in the *X* and *A* electronic states of N_2^+, we could measure how the changes in the centrifugal barrier, induced by nuclear motion, can affect the associated molecular photoionization time delays.

We found that the time delay difference between the vibrational levels v′=1 and v′=0 for the *X*-state in N_2^+ ion varies by almost 200 attoseconds across the shape resonance region [see, Fig. 1(a)], whereas it remains more or less unchanged for the *A*-state [see, Fig. 1(b)]. Using theoretical calculations that explicitly describe the photoionization process and take into account the vibration of the molecular ion [4], we attribute this variation in photoionization time delay to a change in bond-length of ~0.02 Å only. The strong photon-energy dependence of the relative time delay between the two vibrational levels in the *X*-state disappears completely if one neglects the nuclear motion of the molecule [5]. Our results with attosecond time resolution illustrate that near a shape resonance the molecular photoionization process can no longer be described by the well-known Franck-Condon principle, which decouples the movement of the nuclei from the electronic relaxation, assumed to be instantaneous.

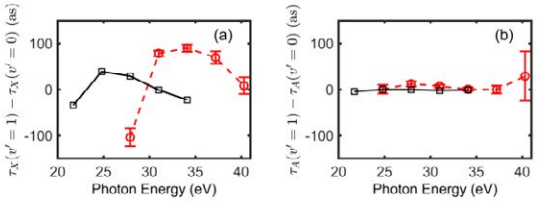

Figure 1. Photoionization time delay (τ) difference between the vibrational levels v′= 1 and 0 for the (a) *X*-state and the (b) *A*-state in N_2^+. Red circles, experiment; black squares, theory. Excellent agreement in magnitude between theory and experiment can clearly be noticed.

References

[1] Piancastelli, M N 1999 J. Elec. Spec. Relat. Phenom. **100** 167
[2] Dehmer J L *et al* 1979 Phys. Rev. Lett. **43** 1005
[3] Paul P M *et al* 2001 Science **292** 1689
[4] Plésiat E *et al* 2018 Chem. A Eur. J. **24** 12061
[5] Nandi S *et al* 2020 Sci. Adv. **6** eaba7762

* E-mail: saikat.nandi@univ-lyon1.fr

Photodissociation of homo- and heteronuclear rare gas molecular ions

A A Narits[1]*, K S Kislov[1]† and V S Lebedev[1]

[1]P.N.Lebedev Physical Institute of Russian Academy of Sciences, Moscow, 119991, Russian Federation

Synopsis We present the results of a theoretical study of the photodissociation of molecular cations in low-temperature plasmas of rare gas mixtures. Particular attention is paid to the qualitative differences in the spectra obtained for homonuclear and heteronuclear ions.

Low-temperature plasmas of noble gas mixtures are commonly used as active media for high-power gas lasers and sources of VUV radiation [1]. In addition to atomic ions such plasmas normally contain homonuclear, Rg_2^+, and heteronuclear, $RgRg2^+$ (Rg, Rg2 = Xe, Kr, Ar, Ne, He) ions. It is well-known that even minimal concentrations of the molecular ions may have a critical impact on the properties of the plasmas owing to the presence of efficient recombination and relaxation mechanisms realized via non-adiabatic energy exchange between the free electrons of the plasma and the electronic subsystem of the molecular ion. The co-existence of multiple atomic and molecular species allows for a variety of different collisional and radiative relaxation processes in the plasmas of rare gas mixtures. This makes such plasmas a challenging research subject for both theory and experiment.

We carry out a theoretical study of photodissociation of noble gas molecular ions at room and elevated gas temperatures. The bound-free transitions are described using original semi-quantal approach taking into account the contributions from the entire rovibrational manifold [2, 3] and *ab initio* calculations of electronic terms and electronic oscillator strengths. In addition to photodissociation of homonuclear cations which can be reasonable described using approach [3], we performed calculations for heteronuclear species containing heavy rare gas elements (Xe, Kr, Ar). Such ions are characterized by low dissociation energies and strong spin-orbit coupling. To provide an accurate description of the oscillator strengths we carried out CASSCF calculations and then improved the results using N-electron valence state perturbation theory. The relativistic effects are considered in the framework of the second-order Douglas-Kroll-Hess (DKH) approach.

The cross sections of photodissociation and bound-free photoabsorption coefficients were obtained for heavy ions containing Xe, Kr, Ar, Ne, He in the spectral range of 100 – 900 nm. We show that the results for homo- and heteronuclear ions exhibit qualitative differences. The specifics of the spectra of $RgRg2^+$ ions are attributed to the spin-orbit coupling spectra and to the multi-reference character of the wave functions of the excited electronic states. Our results agree well with the experimental data available.

The dependences of the photodissociation cross sections on the magnitude of the gas temperature is studied in the range of T = 300 – 6000 K. We demonstrate that the cross sections as functions of T and $\hbar\omega$ vary greatly with the decrease of the binding energy of the molecular ions. The integral photoabsorption coefficients are calculated for several ratios of the concentrations of the ions. The relative roles of the bound-free transitions in different molecular ions are determined for plasma conditions typical of the discharge afterglows.

This work is supported by Russian Science Foundation (grant No. 19-79-30086).

References

[1] Lomaev M I, Sosnin E A, Tarasenko V F 2015 *Chem. Eng. Technol.* **39** 39
[2] Lebedev V S, Presnyakov L P 2002 *J. Phys. B: At. Mol. Opt. Phys.* **35** 4347
[3] Kislov K S, Narits A A, Lebedev V S 2020 *Bull. Lebedev Phys. Inst.* **47** 308

*E-mail: narits@sci.lebedev.ru
†E-mail: kislov@lebedev.ru

Electronic structure of the ground states and low-lying excited states of CoB and NiB

J J Neville[1]* **and E C Anderson**[1]

[1]Department of Chemistry, University of New Brunswick, Fredericton, NB E3B 5A3, Canada

Synopsis The electronic structures and molecular constants of CoB and NiB in their ground states and lowest energy excited states have been determined using CAS-SCF and MCQDPT methods.

Electronic structure and bonding studies of many transition metal–boride compounds have been reported over the past decade, including recent high resolution laser spectroscopy studies of NiB[1] and CoB[2]. The recent studies confirmed the assignment of the ground states of the two diatomic molecules as $X^2\Sigma^+$ and $X^3\Delta_3$, respectively. Fitting and analysis of the experimental spectra have allowed determination of molecular constants for the ground states and observed excited states; insight into the electronic configurations and bonding in the excited states has been obtained, although some uncertainty remains regarding the precise nature of the observed excited states. Theoretical study of these molecules has focussed on the ground states[3], with only limited information available as to the nature of the excited states. The current study seeks to provide more detailed descriptions of both the ground and excited states of these molecules.

We have calculated the electronic structure of the cobalt and nickel monoborides in their ground electronic states and several low-energy excited states. A multiconfiguration approach is necessary to describe the electronic structure of these open shell diatomic molecules. We have used a complete active space self-consistent field (CAS-SCF) with a 10 orbital active space consisting of all valence shell orbitals and electrons (metal 4s, 3d, boron 2s, 2p). State energies and potential energy curves have been obtained for the ground states of the two molecules and the five lowest energy excited states of the same multiplicity (triplet for CoB and doublet for NiB). In addition, MCQDPT perturbation theory calculations have been performed for the ground states and selected excited states at the equilibrium geometries of the ground states and bound excited states. Bonding in the two molecules is analyzed and spectroscopic parameters are extracted from the computational results. The current results are compared with the previous calculated results for the NiB and CoB ground states[3] and experimentally-determined spectroscopic constants from high resolution laser-induced fluorescence spectrosopy[1, 2].

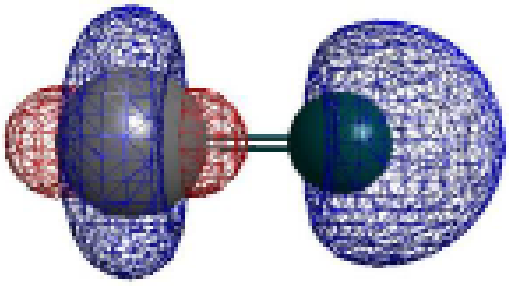

Figure 1. Valence 2σ molecular orbital of CoB.

References

[1] Goudreau ES, Adam AG, Tokaryk DW, Linton C. High resolution laser spectroscopy of the [20.6]0.5-$X^2\Sigma^+$ transition of nickel monoboride, NiB. 2015 *J. Mol. Spectrosc.* **314** 13–18

[2] Dore JM, Adam AG, Tokaryk DW, Linton C. Hyperfine analysis of the (2, 0) [18.3]3-$X^3\Delta_3$ transition of cobalt monoboride. 2019 *J. Mol. Spectrosc.* **360** 44–48

[3] Tzeli D, Mavridis A. Electronic structure and bonding of the 3d transition metal borides, MB, M=Sc, Ti, V, Cr, Mn, Fe, Co, Ni, and Cu through all electron *ab initio* calculations. 2008 *J. Chem. Phys.* **128** 034309

*E-mail: john.neville@unb.ca

Multi-fragment momentum imaging of polyatomic molecules using an electro-optic light modulator and an imaging polarimeter

T Okino[1]*, and K Midorikawa[1]

[1]Attosecond Science Research Team, RIKEN Center for Advanced Photonics, 2-1 Hirosawa, Wako-shi, Saitama, 351-0198, Japan

Synopsis In the velocity map imaging method, one specific ion species should be selected to record the momentum images due to the lack of the time resolution of image sensor. We developed multi-fragment momentum imaging method by recovering the temporal information of fragment ions with time-polarization tagging method in which the fluorescence from the MCP/phosphor is temporally modulated by an electro-optic light modulator to have one-to-one correspondence between the time-of-flight of fragment ions and the angle of polarization, and the angle of polarization is recorded by an imaging polarimeter.

Velocity map imagigng (VMI)[1] method is one of the starndard experimental approaches for investigating the ultrafast dynamics of atoms and molecules. In the standard VMI, the temporal resolution of detection system is not sufficient enough to assign the fragment ion speices. Recently, the advanced hybrid detectors such as PImMS[2] and Tpx3Cam[3] are available for recording the momentum images of all kinds of fragment ions simultaneously, but the number of pixels is not sufficient to record the high-resolution momentum images.

In this work, we developed multi-fragment momentum imaging (MFMI) using a phosphor screen with a-few-ns fluorescence lifetime, an electro-optic light modulator (EO-LM), and an imaging polarimeter[4]. With the time-polarization tagging, the time-of-flight (TOF) of fragment ions can be retrieved with the temporal resolution better than 100 ns which is sufficient for assigning the mass of fragment ion species.

The schematic diagram of MFMI is shown in Fig.1(a). The fluorescence from MCP/phosphor assembly is converted into linear polarization using a linear polarizer. After passing the linear polarizer, the PLZT EO-LM temporally modulates the angle of linear polarization (AoLP) as a function of the TOF of fragment ions monotonically. The AoLP, expressed as $\mathrm{AoLP} = 0.5\tan^{-1}(S_2/S_1)$ using Stokes parameters (S_1, S_2), is recorded with the imaging polarimeter composed of four-directional wiregrid polarizer arrays on the CMOS image sensor.

*E-mail: tomoya.okino@riken.jp

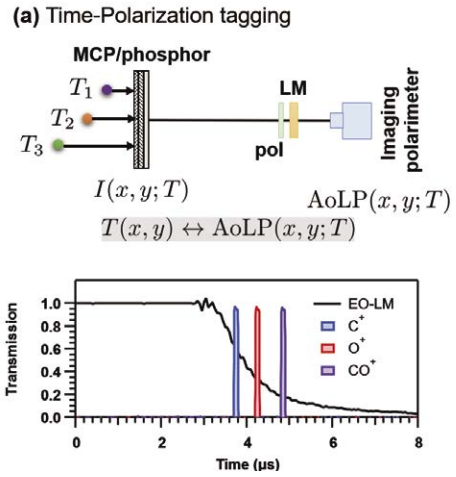

Figure 1. (a) Scheme of MFMI. (b) Temporal response of PLZT EO-LM and TOF of fragment ions from CO_2.

In Fig.1(b), the temporal response of the PLZT EO-LM is shown with the TOF of fragment ion species generated from carbon dioxide molecule (CO_2) exhibiting one-to-one correspondence between the EO-LM transmission and the TOF of fragment ions. Because the number of pixels is larger than 1MP, the high-resolution momentum images of all kinds of fragment ion species can be captured simultaneously.

References

[1] Eppink A T J B and Parker D H 1997 *Rev. Sci. Instrum.* **68**, 3477
[2] Clark A T *et al* 2012 *J. Phys. Chem. A* **116**, 10897
[3] Fisher-Levine M and Nomerotski A 2016 *J. Instrum.* **11**, C03016
[4] Maruyama Y *et al* 2018 *IEEE Trans. Electron Devices* **64**, 2544

XUV photoionization dynamics of N_2O molecule

Juan J. Omiste[1]*, Vicent Borràs[1], Jesús González-Vázquez[1], Fernando Martín[1,2]

[1]Departamento de Química, Universidad Autónoma de Madrid, Madrid 28049, Spain
[2]Instituto Madrileño de Estudios Avanzados en Nanociencia (IMDEA-Nanociencia), Cantoblanco, Madrid 28049, Spain

Synopsis We theoretically investigate the photoionization dynamics of the N_2O molecules using the XCHEM approach.

We present a theoretical study of the photoionization dynamics of the N_2O molecule induced by an XUV attosecond laser pulse. To do so, we use the XCHEM method [1, 2], which works in the close-coupling framework to account for the molecular electronic correlation in the bound region and the electronic continuum, at the level of accuracy of multireference configuration interaction methods. Thus, the XCHEM method is a perfect tool to investigate the N_2O molecule, since the electronic correlation plays a key role in its structure and photoionization dynamics, manifested in the high density of resonances and satellite states [3, 4].

We specially focus in the role of the resonances on the total and partial photoionization cross sections as well as in the Wigner-time delays.

These results constitute a relevant theoretical support to experiments aiming to measure the RABBIT spectrum in molecules as well as to record the dissociation following single-photon photoionization in the attosecond scale.

References

[1] Marante C *et al* 2017 *Phys. Rev. A* **96** 022507
[2] Marggi Poullain S *et al* 2019 *Phys. Chem. Chem. Phys.* **21** 16497-16504
[3] Gelius U. 1974 *J. Electron Spectros. Relat. Phenomena* **5** 985-1057
[4] Domcke W. *et al* 1979 *Chem. Phys.* **40** 171-183

*E-mail: juan.omiste@uam.es

Asymmetric electron angular distributions in stimulated Compton scattering from H_2 irradiated with soft-x ray laser pulses

A Sopena[1,2], A Palacios[1,3] *, F Catoire[2], H Bachau[2†] and F Martín[1,4,5]

[1]Departamento de Química, Módulo 13, Universidad Autónoma de Madrid, 28049 Madrid
[2]Centre des Lasers Intenses et Applications, Université Bordeaux-CNRS-CEA, 33405 Talence Cedex, France
[3]Institute for Advanced Research in Chemical Sciences, Universidad Autóma de Madrid, 28049 Madrid, Spain
[4]Instituto Madrileño de Estudios Advanzados (IMDEA) en Nanociencia, Cantoblanco, 28049 Madrid, Spain
[5]Condensed Matter Physics Center (IFIMAC), Universidad Autónoma de Madrid, 28049 Madrid, Spain

Synopsis We investigate photoionization of the hydrogen molecule exposed to intense ultrashort soft X-ray pulses, with frequencies ranging from 0.5 to 1.6 keV. The photoelectron spectra reveal the clear signature of stimulated Compton scattering. The interference between dipole and non-dipole quantum paths induces an asymmetry in the photoelectron angular distributions, which varies strongly with the light polarization and propagation directions with respect to the molecular orientation.

The last two decades have seen the rise of X-ray free electron lasers (XFELs) throughout the world, providing ultra-short pulses with unprecedented intensities (10^{20} W/cm^2), over a large range of photon energies going from VUV to hard X-ray domain. Besides the achievements in terms of brilliance, tremendous activity has been also devoted to the generation and control of XFEL pulses with sub-fs and even attosecond durations [1]. Extending X-ray in the attosecond domain is of crucial interest in a wide range of fundamental problems such as, for instance, to resolve in time the dynamics of electronic rearrangement in atoms after core excitation or ionization [2]. New avenues are also opened to explore nonlinear response in X-ray regime, like direct two-photon ionization of atoms [3] or nonlinear Raman and Compton scattering processes [4].

In the present paper, we present a novel scheme of stimulated Compton scattering (SCS) on the hydrogen molecule using a highly intense ultrashort X-ray pulse with frequencies ranging from 0.5 to 1.6 keV. We solve the time-dependent Schrödinger equation including the explicit evaluation of dipole and non-dipole terms. The short wave length of the X-ray pulse breaks down the commonly employed dipole approximation and it is found that the coherent contributions of dipole and nondipole effects lead to a symmetry breaking in the photoelectron emission, which strongly depends on the X-ray wave length and the molecular orientation (see Fig. 1). This is a pure nonlinear effect captured in the low-energy lying electrons emitted after absorption and subsequent stimulated emission of photons within the energy bandwidth of the pulse.

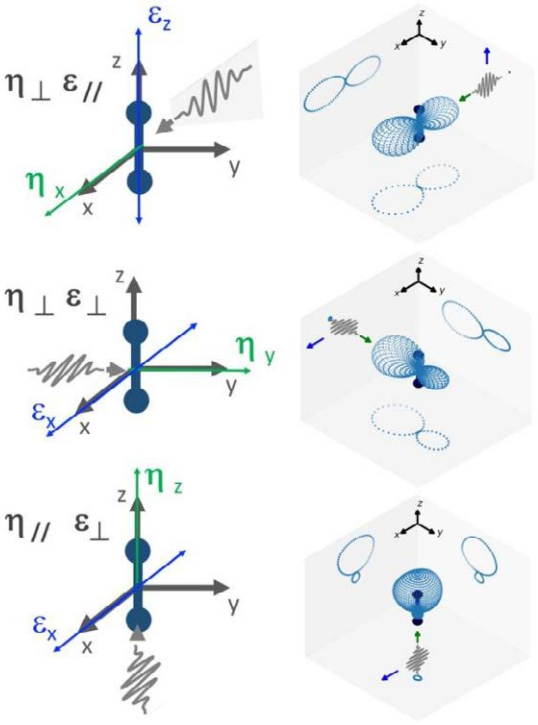

Figure 1. MFPADs integrated over a range of electron energies [0-2.5 au] for 1.1 keV pulse with a duration of 68 as and an intensity of 10^{18} W/cm^2.

References

[1] Hemsing E *et al* 2014 *Rev Mod Phys* **86** 897
[2] Huang S *et al* 2017 *PRL* **119** 154801
[3] Doumy G *et al* 2011 *PRL* **106** 083002
[4] Kircher M *et al* 2020 *Nat. Phys.* **16** 756

* E-mail: alicia.palacios@uam.es
† E-mail: henri.bachau@u-bordeaux.fr

Chiral photoelectron angular distributions from ionization of achiral atomic and molecular species

A Pier[1,*], K Fehre[1], S Grundmann[1,†], I Vela-Perez[1], N Strenger[1], M Kircher[1], D Tsitsonis[1], J B Williams[2], A Senftleben[3], T Baumert[3], M S Schöffler[1], P V Demekhin[3], F Trinter[4,5], T Jahnke[1] and R Dörner[1]

[1]Institut für Kernphysik, Goethe-Universität, 60438 Frankfurt, Germany
[2]Department of Physics, University of Nevada, Reno, Nevada 89557, USA
[3]Institut für Physik und CINSaT, Universität Kassel, 34132 Kassel, Germany
[4]Photon Science, Deutsches Elektronen-Synchrotron (DESY), 22607 Hamburg, Germany
[5]Molecular Physics, Fritz-Haber-Institut der Max-Planck-Gesellschaft, Faradayweg 4-6, 14195 Berlin, Germany

Synopsis We show that the combination of two achiral components—an atomic or molecular target plus a circularly polarized photon—can yield chirally structured photoelectron angular distributions.

Chiral molecules display a chirally structured photoelectron angular distribution upon photoionization. However, the concept of chirality can be applied to any three-dimensional object. We investigated if achiral atomic or molecular species can also display a chiral photoelectron angular distribution (PAD) under certain geometric configurations

We used the P04 beamline at PETRA III (DESY) and applied a reaction microscope to investigate carbon K-shell photoionization of CO followed by Auger decay at 310 eV photon energy and the one-photon double ionization of He at 255 eV and 800 eV.

We found that for photoionization of CO, the angular distribution of carbon K-shell photoelectrons is chiral when the molecular axis is neither perpendicular nor (anti)parallel to the light propagation axis [see Fig. 1 d) and e)]. In photo-double-ionization of He, the distribution of one electron is chiral if the other electron is oriented like the molecular axis in the former case and if the electrons are distinguishable by their energy. In both scenarios, the circularly polarized photon defines a plane with a sense of rotation and an additional axis is defined by the CO molecule or one electron.

We showed that in order to produce such a chirally structured electron angular distribution, an unambiguous coordinate frame of well-defined handedness is necessary but not sufficient and that additional electron-electron interaction or scattering processes are needed to create the chiral angular distribution.

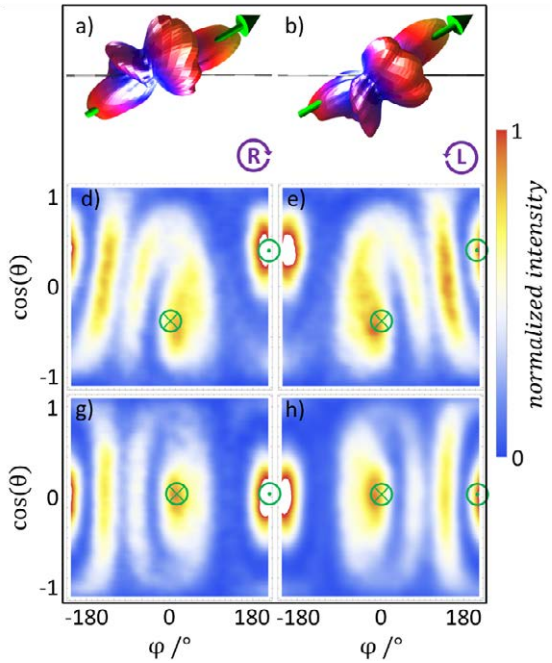

Figure 1. Measured photoelectron angular distributions of the carbon K-shell electron emission of CO, obtained from circularly polarized light at 310 eV. The panels on the left [right] correspond to right-handed [left-handed] circularly polarized light.

References

[1] Pier A *et al* 2020 *Phys. Rev. Research.* **2** 033209

* E-mail: pier@atom.uni-frankfurt.de
† E-mail: grundmann@atom.uni-frankfurt.de

Theoretical Attosecond Pump-Probe Photoelectron Spectroscopy of CF_4 and N_2

E. Plésiat[1*], A. Palacios[2], P. Decleva[3], and F. Martín[1,2,4]

[1] Instituto Madrileño de Estudios Avanzados en Nanociencia (IMDEA Nano), Campus de Cantoblanco, 28049 Madrid
[2] Departamento de Química,Universidad Autónoma de Madrid, 28049 Madrid (Spain)
[3]Dipartimento di Scienze Chimiche e Farmaceutiche, Universitá di Trieste, 34127 Trieste (Italy)
[4]Condensed Matter Physics Center (IFIMAC), Universidad Autónoma de Madrid, 28049 Madrid (Spain)

Synopsis Attosecond spectroscopy offers the possibility to track and control electron dynamics in molecules. We are reporting here a theoretical description of two different attosecond pump-probe techniques, applied to CF_4 and N_2, respectively. The photoelectron spectra of CF_4 subject to a single attosecond pulse in the presence of a VIS field capture the complex dynamics due to ultrafast charge fluctuations. In N_2, the vibrationally resolved RABBIT spectra reveal the variations of the centrifugal barrier as a function of the nuclear degrees of freedom.

Since the first experimental demonstration of attosecond (as) pulses in 2001 [1], many progresses have been achieved in attosecond technology. In particular, it is now possible to control electron dynamics in atoms [2], diatomic [3] and polyatomic molecules [4]. A widely used approach to perform such time-resolved studies is the attosecond pump-probe spectroscopy. We present here the results of attosecond pump-probe simulations on CF_4 and N_2.

For CF_4, a single attosecond XUV pump and a VIS probe pulse are used (see [5] for details). Depending on the time delay between the two pulses, a VIS photon can be absorbed by the photoelectron, being further promoted in the continuum, or can lead to excitations in the remaining ion. These quantum paths will interfere leading to visible fluctuations in the PES as a function of the time delay.

For N_2, we are using the RABBIT (reconstruction of attosecond beating by interference of two-photon transitions) interferometric method. The resulting vibrationally resolved PES (see Figure 1) exhibits sidebands which oscillate as a function of the time delay between the pump (train of attosecond XUV pulses) and the probe (dressing NIR) pulse. The fitting of these sidebands [1] gives access to the molecular two-photon ionization time. By comparing the photoionization time delays extracted for two vibrational levels (v'=0 and v'=1) of the $3\sigma_g^{-1}$ channel, we are able to capture the changes associated with nuclear motion on the centrifugal barrier that sustains the shape resonance [6].

* E-mail: etienne.plesiat@imdea.org

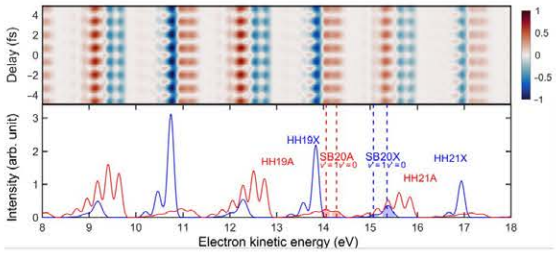

Figure 1. Vibrationally resolved RABBIT spectra of N_2. Upper panel: Difference between PES obtained with XUV+NIR and XUV only, as a function of delay. Lower panel: XUV+NIR PES averaged over all delays for the $3\sigma_g^{-1}$ (blue) and $1\pi_u^{-1}$ (red) photoionization channels.

The theoretical methodology consists in solving the time-dependent Schrödinger equation in a basis of Kohn-Sham orbitals and using the exclusive probability formalism to include interchannel couplings [5]. The basis is obtained in the dipole and static-exchange approximations by solving the Kohn-Sham Hamiltonian using a B-spline multicenter approach and the LB94 functional [7]. The CF_4 calculations are performed in the fixed nuclei approximation while the N_2 calculations include the nuclear motion in the Born-Oppenheimer approximation.

References

[1] Paul P. M. et al. 2001 *Science* 292, 1689
[2] Kiesewetter D. et al. 2018 *Nature Phys.* 14, 68
[3] Sansone G. et al. 2010 *Nature* 465, 763
[4] Calegari F. et al. 2014 *Science* 346, 336
[5] Plésiat E. et al. 2018 *Chem. Eur. J.* 24, 12061
[6] Saikat N. et al. 2020 Sci. Adv. 6, eaba7762
[7] Toffoli D. et al. 2002 *Chem. Phys.* 276, 25

ASTRA, a new close-coupling approach for molecular ionization

J M Randazzo[1,2], J Olsen[3], H Gharibnejad[4], B I Schneider[4], L Argenti[1,5]*

[1]Department of Physics, University of Central Florida, Orlando, FL, USA. [2]now at Consejo Nacional de Investigaciones Científicas y Técnicas, Argentina. [3]Department of Chemistry, Aarhus University, Denmark, EU. [4]National Institute of Standards and Technology, Gaithersburg, MD, USA. [5]CREOL, the College of Optics, University of Central Florida, Orlando, FL, USA.

Synopsis We present preliminary results of a new close-coupling package of codes for the calculation of single and, prospectively, double time-resolved molecular photoionization. ASTRA takes full advantage of compact state-of-the-art quantum-chemistry methods of molecular electronic structure, based on high-order transition density matrices and large-scale configuration interaction. This paves the way to accurate and efficient calculations employing highly correlated ionic targets.

Correlated electronic motion is at the core of light-induced chemical transformations. Until recently, the study of time-resolved attosecond electron-dynamics has focused on processes in which only a single extreme-ultraviolet (XUV) photon is absorbed and a single electron is liberated. New x-ray sources together with XUV-pump XUV/soft-x-ray-probe schemes promise dramatically increased time resolution. Soft-x-ray probes can excite localized core electrons, giving rise to new phenomena such as intramolecular photoelectron scattering and multiple photoionization. The theoretical description of the time evolution of these processes will be key to track the motion of correlated electron pairs.

Here we present a new approach towards the time-dependent close-coupling scheme for single and double multi-channel molecular photoionization and an implementation of the single ionization in the new ASTRA (AttoSecond TRAnsitions) code. ASTRA implements new formulas and associated algorithms to compute close-coupling matrix elements, which make use of high-order transition density matrices (TDM) between arbitrary-spin excited ionic states of the target molecule. The TDMs needed by the program are obtained from correlated ionic states employing a general-active-space formalism [1]. The TDMs used in ASTRA, are obtained from the LUCIA CI code developed by J. Olsen [2]. The ASTRA code also requires hybrid gaussian-numerical basis sets and integrals, which are currently obtained from the public GBTOlib library, developed by Zdenek Masin [3], and longer term will be based on polycentric expansions using a new numerical integration scheme [4]. Molecular orbitals are currently obtained from MCSCF calculations in DALTON [5], which will eventually be superseded by orbitals from LUCIA, which allows for averages over states of different symmetry and multiplicity.

We will present preliminary calculations of stationary electronic states of the N_2 molecule computed with ASTRA and compare them with the results of a in-house CI-singles benchmark code, for which the TDMs are exactly known.

References

[1] Helgaker T, Jorgensen P, Olsen J 2000 *Molecular Electronic-Structure Theory* Ed. Wiley
[2] Helgaker T *et al.* 2012 *Chem. Rev.* **112** 543.
[3] Masin Z *et al.* 2020 *Comp. Phys. Commun.* **249** 107092.
[4] Gharibnejad H *et al* 2021 *Comput. Phys. Commun.* **263** 107889
[5] Aidas K *et al.* 2014 *Comp. Mol. Sci.* **4** 269.

*E-mail: Luca.Argenti@ucf.edu

Photodouble ionization of water under different excess energy and energy sharing regimes

J M Randazzo[1]*, G Turri[2], P Bolognesi[3], L Avaldi[3] and L U Ancarani[4]

[1]Consejo Nacional de Investigaciones Científicas y Técnicas, Argentina.
[2]Embry-Riddle Aeronautical University, Physical Sciences Department, Daytona Beach, FL, USA
[3]CNR-Istituto di Struttura della Materia, Area della Ricerca di Roma 1,00015 Monterotondo Scalo, Italy
[4]Université de Lorraine, CNRS, LPCT, 57000 Metz, France

Synopsis Photodouble ionization of water molecules has been investigated at two excess energies and different energy sharing regimes. Experimentally, differential cross sections were measured via the angular resolved coincidence detection of the emitted electrons. Theoretically, within a first order treatment of the interaction, we consider the target as a two active electrons system, and therefrom we evaluate the scattering wavefunction of the two photoelectrons. This approach provides a satisfactory global agreement with the observed rich angular distributions.

The understanding of photodouble ionization (PDI) is of great interest because the process is dominated by electronic correlation. The most detailed information on PDI can be achieved via the measurement of the triple differential cross section (TDCS), i.e. a cross section differential in the excess energy and the direction of the two photoelectrons. For two-electron atomic systems [1], advanced understanding of PDI mechanisms has been achieved through experimental and theoretical studies of electron-electron coincidence angular distribution; for diatomic and polyatomic molecules, such investigations are scarse. In this combined experimental and theoretical work, we study the PDI of water.

In the measurements [2], performed at the Gas Phase beamline of Elettra at a fixed photon energy, coincidence angular distributions have been measured for three directions ($\theta_1 = 0^o$, 30^o or 60^o) of one electron with respect to the photon polarization direction. Two sets of TDCS are reported: at 20 eV above threshold under an equal energy sharing regime [3], and at 32 eV above threshold and unequal energy sharing [4].

The measured data are compared with a theoretical calculation in which the ten-electron molecule is first reduced to a two-electron system; then, using a model two-electron potential, a partial wave set of driven equations is solved accurately by means of the Generalized Sturmian Method. The average over all possible molecular orientations is taken into account and performed analytically. Both the measured and calculated TDCS present rich multilobe angular distributions which reflect the complex dynamics of the electron pair. According to the spectroscopy of the water dication H_2O^{2+} and the experimental energy resolution, several molecular states may contribute. In spite of this extra uncertainty and considering the theoretical approximations, we found an overall satisfactory experiment-theory agreement (see, for example, figure 1).

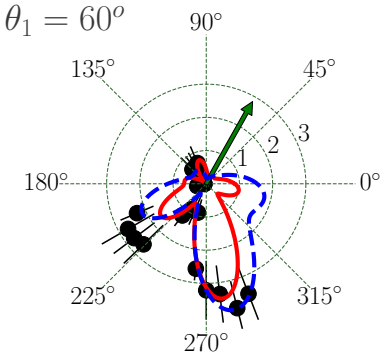

Figure 1. TDCS of water measured at 74 eV photon energy in the condition of unequal energy sharing (E_1 = 25 eV and E_2 = 7 eV) for a fixed direction θ_1 (green arrow) of one photoelectron compared with the theoretical predictions in length (solid red) and velocity (dashed blue) gauges.

References

[1] Avaldi L and Huetz A 2005 *J. Phys. B* **38** S861
[2] Turri G *et al* 2019 *J. Phys. B.* **52** 07LT01
[3] Randazzo J M *et al* 2020 *Phys. Rev. A* **101** 033407
[4] Bolognesi P *et al* 2021 *J. Phys. B.* **54** 034002

*E-mail: randazzo@cab.cnea.gov.ar

Physics informed statistical analysis reveals key processes in simulated X-ray induced Coulomb explosion

B Richard[1,2,4]*, **J Schäfer**[1,3], **Z Jurek**[1], **L Inhester**[1] **and R Santra**[1,2,3,4]

[1]Center for Free-Electron Laser Science, DESY, 22607 Hamburg, Germany
[2]Department of Physics, Universität Hamburg, 20355 Hamburg, Germany
[3]Department of Chemistry, Universität Hamburg, 20146 Hamburg, Germany
[4]The Hamburg Centre for Ultrafast Imaging, 22761 Hamburg, Germany

Synopsis We decompose data from molecular dynamics simulations describing Coulomb explosion of a iodopyridine molecule induced by exposition to an X-ray free-electron laser (XFEL) using various flavors of principal component analysis (PCA). We find that the work along major PCA components highlights key processes of the fragmentation dynamics. Moreover, we demonstrate that particular processes leave fingerprints in the final coincident momentum data.

Recent advances in measurement technology together with novel high-repetion XFELs make it possible to gather data from X-ray-induced Coulomb explosion containing coincidence information from all atoms composing the system [1]. We aim to explore the potential uses of these new data by investigating how key mechanisms of the charge redistribution and fragmentation dynamics leave fingerprints in the final momentum data. Our general strategy is to decompose the motion of atoms via principal component analysis (PCA) and to examine the resulting components to obtain physical insights into the Coulomb explosion.

Analysis of the position of atoms via PCA is an established method in the context of equilibrium MD simulations. However, it turns out to be unsuitable for the far from equilibrium situation of a Coulomb explosion. We thus propose to apply PCA on the forces during the Coulomb explosion. We also develop a more specific analysis and diagnostic method based on decomposing the released energy into work along each PCA component.

To test this procedure we apply it to a simulated data set of the Coulomb explosion of a iodopyridine molecule that has been computed in the context of one of the first experiments at the Small Quantum Systems instrument (SQS) at the European XFEL [1, 2]. Strong competition between the first and second components of the force PCA is identified which underlines the major role of the collision between the iodine atom and the closest carbon atom during the fragmentation of the molecule. Moreover, our analysis reveals that the ionization dynamics and collisions between ions leave distinct patterns in the coincident final momentum data.

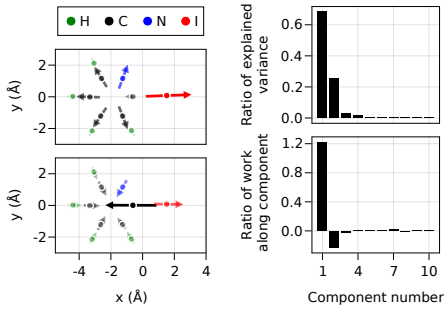

Figure 1. Left panel: the two first components of the force-PCA superimposed on the iodopyridine equilibrium structure. Top right panel: ratio of explained variance for the first PCA components. Bottom right panel: work along each of the first PCA components normalized by the total kinetic energy. Negative work corresponds to a component working against the final energy release.

This way, we demonstrate how coincidently detected ion momenta give us major insights into the charge redistribution and fragmentation dynamics of molecules exposed to intense X-ray radiation.

References

[1] R Boll *et al* 2020 *Submitted*
[2] Z Jurek *et al* 2016 *Journal of Applied Crystallography* **49** 1048

*E-mail: benoit.richard@cfel.de

Measuring the Photoelectron Emission Delay in the Molecular Frame

J Rist[1]*, K Klyssek[1], N M Novikovskiy[2,3], M Kircher[1], I Vela-Pérez[1], D Trabert[1], S Grundmann[1], D Tsitsonis[1], J Siebert[1], A Geyer[1], N Melzer[1], C Schwarz[1], N Anders[1], L Kaiser[1], K Fehre[1], A Hartung[1], S Eckart[1], L Ph H Schmidt[1], M S Schöffler[1], V T Davis[4], J B Williams[4], F Trinter[5,6], R Dörner[1], P V Demekhin[2], and T Jahnke[7†]

[1]Institut für Kernphysik, Goethe-Universität Frankfurt, Frankfurt, 60438, Germany
[2]Institut für Physik und CINSaT, Universität Kassel, Kassel, 34132, Germany
[3]Institute of Physics, Southern Federal University, Rostov-on-Don, 344090, Russia
[4]Department of Physics, University of Nevada, Reno, NV 89557, USA
[5]FS-PETRA-S, Deutsches Elektronen-Synchrotron DESY, Hamburg, 22607, Germany
[6]Molecular Physics, Fritz-Haber-Institut der Max-Planck-Gesellschaft, Berlin, 14195, Germany
[7]European X-Ray Free-Electron Laser Facility GmbH, Schenefeld, 22869, Germany

Synopsis Using the COLTRIMS technique and semi-continuous synchrotron radiation, the photoelectron emission delay of CO core electrons is measured with attosecond precision. This is achieved without the need of attosecond pulses, but is instead realized via the method of the so-called *complete experiment*, where the emission delay is extracted from the molecular frame photoelectron angular distribution. The measured delay map shows a high dependency on both the emission angle in the molecular frame as well as on the electron energy. Our findings are in excellent agreement with theoretical predictions.

For our study, we used a COLd Target Recoil Ion Momentum Spectroscopy (COLTRIMS) setup and performed a photon-energy scan between 0 eV and 20 eV above the carbon K-shell of CO, covering the Σ-shape resonance. The light was provided by the BESSY II synchrotron at the beamline U49-2_PGM-1.

That setup allowed us to measure the energy-dependent molecular frame photoelectron angular distribution (MFPAD) of the outgoing electron which is shown in Fig. 1(b) for the case of molecules oriented along the polarization axis of the light. We used a simple model consisting of the spherical harmonics up to $l \leq 4$ with $m = 0$ to fit the outgoing-electron wave function.

Following the predictions of Eisenbud and Wigner, Bederson, and Cherepkov [1-4] about the complete experiment, the derivative of the wave function's complex phase with respect to the energy yields the so-called Wigner phase which can be interpreted as an emission time (or Wigner time) delay t_w:

$$t_w(E,\theta) = \hbar \frac{d}{dE} \arg[\psi_{elec}(E,\theta)]$$

The Wigner time delay extracted from the fit results of our measured data is depicted in Fig. 1(a).

More details, a comparison of the twodimensional Wigner map with theoretical predictions, and the case of other molecular orientations will be presented as well.

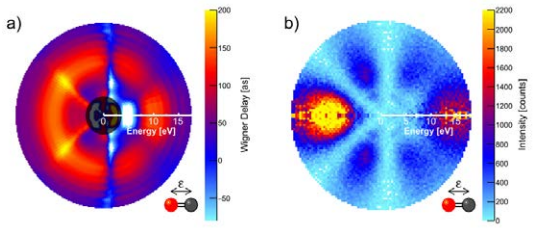

Figure 1. (a) Angle-dependent Wigner delay map in the molecular frame, where the molecule is oriented along the light's polarization axis. The electron energy is shown as the distance from the center, while the Wigner delay is encoded in the color scheme. **(b)** The corresponding MFPAD in the same representation as in panel (a). It is noticeable that prominent features in the Wigner delay map occur at the same angles as the minima in the MFPAD.

References

[1] Eisenbud L 1948 *PhD thesis, Princeton Univ.*
[2] Wigner E P 1955 *Phys. Rev.* **98**, 145-147
[3] Bederson B 1969 *Comm. At. Mol. Phys.* **1**, 41-45
[4] Cherepkov N A 1983 *Adv. At. Mol. Phys.* **19**, 395-447

* E-mail: rist@atom.uni-frankfurt.de
† E-mail: till.jahnke@xfel.eu

Probing ultrafast light-induced interconversion reactions in cyclic molecules

D Rolles[1 *], K Borne[1], M Bonanomi[2,3], J P Figueira Nunes[4], J Cooper[5], A Venkatachalam[1], O Plekan[2], C Callegari[2], A Rudenko[1], A Kirrander[5], P M Weber[6], M Centurion[4] and the QD/NB Collaboration[7]

[1]J.R. Macdonald Laboratory, Department of Physics, Kansas State University, Manhattan KS, 66506, USA
[2]Elettra-Sincrotrone Trieste S.C.p.A., 34149 Basovizza, Trieste, Italy
[3]CNR-IFN, 20133 Milano, Italy
[4]Department of Physics and Astronomy, University of Nebraska–Lincoln, Lincoln, Nebraska 68588, USA
[5]School of Chemistry and Centre for Science at Extreme Conditions, University of Edinburgh, Edinburgh EH9 3FJ, UK
[6]Department of Chemistry, Brown University, Providence, Rhode Island 02912, USA
[7]See bit.ly/3sWHJp4 for a full list of collaborators

Synopsis We have studied the UV-induced interconversion between two multicyclic hydrocarbons, quadricyclane (QD) and norbornadiene (NB), using a combination of time-resolved photoelectron spectroscopy, ultrafast electron diffraction, and ab-initio quantum chemistry calculations. The reaction is triggered by the absorption of a 200-nm photon that excites the molecules to a Rydberg manifold and proceeds via competing electronic relaxation pathways that return the molecule to the (hot) ground state resembling either the QD or NB geometry.

Quadricyclane (QD) and norbornadiene (NB) are isomers with the chemical formula C_7H_8 that can interconvert upon absorption of an ultraviolet (UV) photon. The reaction involves an ultrafast conversion from a highly strained three membered ring in QD to less strained five and six membered rings in NB, and vice versa. The NB-QD pair is considered as a candidate for a molecular solar energy storage since the conversion from NB to QD stores energy that can be released in the back-conversion from QD to NB. Since both QD and NB are stable compounds, this system also provides an opportunity to study passage through a conical intersection "from both directions", which is not possible in many other systems.

We have studied both directions of the interconversion reaction using time-resolved XUV photoelectron spectroscopy (TRPES) at the FERMI free-electron laser as well as using ultrafast electron diffraction (UED) at the SLAC MeV-UED facility. The XUV TRPES experiment yields somewhat different time constants and reveals additional de-excitation pathways when exciting at 200 nm compared to a previous UV-TRPES study conducted at 208 nm [1].

Figure 1 shows the XUV photoelectron spectra for pump-probe delays up to 1 ps, zoomed in to binding energies below 9 eV. We observe a prominent depletion in the signal from cold QD (~8 eV) on a time scale consistent with our instrument response function of ~80fs (FWHM), followed by a recovery attributed to the formation of "hot" (i.e., vibrationally excited) ground-state molecules in either QD or NB geometry on a timescale consistent with the findings of the UED experiment. We also observe an ultrafast increase in photoelectron yield in a broad range of binding energies corresponding to electronically excited molecules, followed by a rapid decay and shift of the spectral intensity towards higher binding energies.

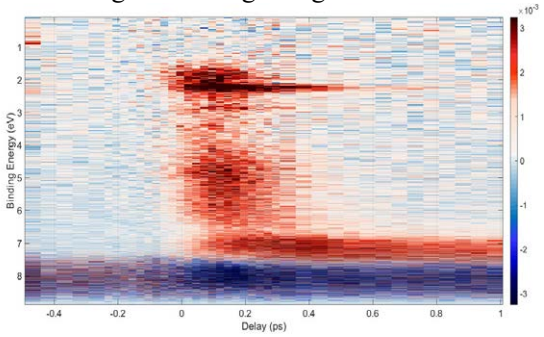

Figure 1. Time-dependent difference photoelectron spectrum ("pump on" minus "pump off") in the binding energy (BE) region corresponding to the lowest BE-peak of "cold" ground-state QD (~8 eV), hot ground-state products (~7 eV), and electronically excited molecules in the QD Rydberg states (~2 eV).

Supported by the CSGB Division, BES, U.S. Department of Energy, award DE-SC0020276.

References

[1] Rudakov F and Weber P M 2012 *J. Chem. Phys.* **136** 134303

* E-mail: rolles@phys.ksu.edu

Molecular retrieval from two-dimensional LIED photoelectron spectra upon strong-field ionization

A. Sanchez[1,*], K. Amini[1,*], S.-J. Wang[2], T. Steinle[1], B. Belsa[1], J. Danek[2], A.T. Le[2,3], X. Liu[1], R. Moshammer[4], T. Pfeifer[4], M. Richter[5], J. Ullrich[4,5], S. Gräfe[6], C.D. Lin[2], J. Biegert[1,7,†]

[1]*ICFO - Institut de Ciencies Fotoniques, The Barcelona Institute of Science and Technology, 08860 Castelldefels (Barcelona), Spain.*
[2]*Department of Physics, J. R. Macdonald Laboratory, Kansas State University, 66506-2604 Manhattan, KS, USA.*
[3]*Department of Physics, Missouri University of Science and Technology, Rolla, MO 65409.*
[4]*Max-Planck-Institut für Kernphysik, Saupfercheckweg 1, 69117, Heidelberg, Germany.*
[5]*Physikalisch-Technische Bundesanstalt, Bundesallee 100, 38116 Braunschweig, Germany.*
[6]*Institute of Physical Chemistry and Abbe Center of Photonics, Friedrich-Schiller-Universität Jena, Helmholtzweg 4, 07743 Jena, Germany.*
[7]*ICREA, Pg. Lluís Companys 23, 08010 Barcelona, Spain.*

Synopsis Laser-Induced Electron Diffraction (LIED) is a strong-field technique capable of extracting the precise atomic configuration of an isolated gas-phase molecule with picometre spatial and attosecond temporal precision. In contrast to existing methods that extract molecular structure in the laser frame, we introduce a method ZCPs (zero-crossing points) that directly retrieves the molecular structure in the laboratory frame avoiding the tedious conversion laser to the laboratory frame. Here, we apply the ZCP-LIED method to the asymmetric top molecule carbonyl sulfide OCS. We benchmark our model with a Fourier-based retrieval method and our quantum-classical calculations. All indicate the same asymmetrically stretched and bent field-dressed configuration.

Common to most scattering methods, imaging larger molecules or dynamics systems with little a priori knowledge can be exacerbated. For example, some targets require precision in the bond angle rather than in the bond distance. To circumvent the problem, we introduce a simple molecular retrieval method based on the identification of critical points in the oscillating molecular interference scattering signal from the full two-dimensional (energy and angle) electron scattering spectra as shown in Fig.1a and Fig.1b.

The distribution of experimental ZCP positions for different scattering angles is displayed in Fig. 1c. The molecular interference term is evaluated by averaging over a bandwidth of $\Delta p = 0.1$ a.u., corresponding to the detected momentum error. Fig.1d shows the number of angles where the ZCPs fall below or above the magenta dashed line within 0.1 a.u. We can thus estimate the error of each ZCP, and, in turn, calculate the error of the retrieved bond lengths. We find a stretch of the C-S bond-length $R_{CS} = 1.70 \pm 0.02$ Å ($R_{CO} = 1.18 \pm 0.02$ Å, $R_{OS} = 2.74 \pm 0.03$ Å) resulting in an O–C–S bond angle of $\Phi_{OCS} = 144 \pm 5°$.

Finally, we explain the retrieved bent molecular structure with mixed quantum-classical calculations. The field-dressed OCS molecules result in a significantly bent geometry due to the Renner–Teller effect and 8-10 cycles (fwhm) Mid-Ir laser pulse duration [1,2].

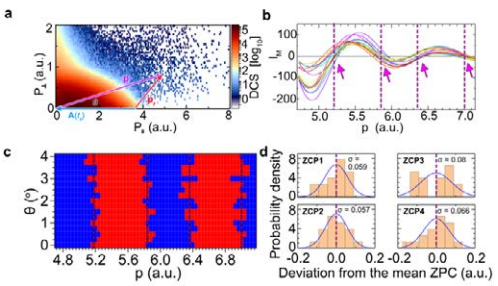

Figure 1. **a** Two-dimensional map of transverse ($P\perp$) and longitudinal ($P_{\parallel}$) electron momentum distribution. **b** Molecular interference signal, I_M, in the laboratory frame as a function of scattering momentum, p, for 17 laboratory scattering angles. **c** Two-dimensional map of the negative (blue squares) and positive (red squares) parts of the molecular interference signal as a function of scattering angle and momentum. The magenta dashed vertical lines and arrows in panels (**b**) and (**c**) indicate the mean positions of the zero-crossing points (ZCPs) over all scattering angles. **d** Frequency of occurrences of finite-width distributions of each averaged experimental ZCP obtained from panel (**c**).

References

[1] Amini K *et al* 2019 PNAS **116**, 8173-8177
[2] Sanchez A et *al* 2021 Nature Communications **12**, 1520

† E-mail: jens.biegert@icfo.eu

High Resolution Mass Spectrometry and Velocity Map Imaging for Ultrafast Electron Dynamics in Biomolecules

K Saraswathula[1 *], E P Månsson[1 †], V Wanie[1,3], L Colaizzi[1,4], S Ryabchuk[1,5], F Légaré[3], A Trabattoni[1], F Calegari[1,2,4,5]

[1] Center for Free-Electron Laser Science, Deutsches Electronen-Synchrotron, Notkestr. 85, Hamburg, 22607, Germany
[2]Institute for Photonics and Nanotechnologies, National Research Council, Piazza Leonardo da Vinci 32, Milano, 20133, Italy
[3] Institut National de la Recherce Scientifique, 1650 Blvd, Lionel Boulet, Varennes (Qc), J3X1S2, Canada
[4] Physics Department, University of Hamburg, Luruper Chaussee 149, Hamburg, 22761, Germany
[5]The Hamburg Centre for Ultrafast Imaging, Universität Hamburg, 149 Luruper Chaussee, Hamburg, 22761, Germany

Synopsis We present a new design and characterization of a velocity-map-imaging electron spectrometer combined with a reflectron mass spectrometer. Combined with attosecond and femtosecond pump-probe methods, it will enable studies of non-adiabatic ultrafast dynamics in complex molecules.

Pump-probe experiments with few-fs and sub-fs temporal resolution are excellent tools to investigate ultrafast dynamics in large molecules such as amino acids [1] and DNA bases, or nanosized systems such as C_{60} and dielectric nanoparticles. We recently studied single nucleosides in a XUV-pump NIR-pump experiment by resolving dissociated ionic fragments according to their masses [2]. For studying larger molecules, a high mass resolution is required for distinguishing between different isotopes or protonated species. With our double-sided spectrometer, electron-ion covariance measurements are now possible.

The spread in the ion's starting position and initial velocity causes difficulty in resolving adjacent masses. The spread in position can be cancelled out by employing Wiley-Mclaren focusing with drift tubes typically shorter or containing accelerating electric fields. Kinetic energy spread can be reduced by applying higher extraction voltage or a longer drift tube, although the latter is difficult to combine with Wiley-Mclaren focusing. A VMI electron spectrometer on the opposite side imposes further constraints for the applied voltages. These restrictions are lifted by inserting a reflectron [3] where ions are decelerated and reflected. Its tunable electric field can reduce the position spread error even at high extraction voltages and long drift tube lengths.

Simulations show that masses of up to 1500 u can be resolved at room temperature and 150 u for 2-eV dissociation fragments with simultaneous VMI of electrons up to 30 eV.

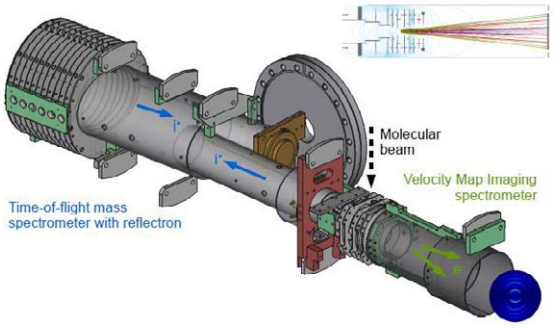

Figure 1. A schematic diagram of the double-sided spectrometer.

In this work we will also be presenting preliminary experimental results of photoelectron and mass spectroscopy experiments where we performed electron-ion covariance measurements of Acetone excited by a UV-pump and probed by NIR pulses.

References

[1] Calegari F *et al* 2014 *Science : 346, 336-339*
[2] Månsson E P *et al* 2017 *Phys. Chem. Chem. Phys:* 19, 19815
[3] Scherer S *et al 2006 International Journal of Mass spectrometry: 251, 73*

* E-mail: krishna.saraswathula@desy.de
† E-mail: erik.maansson@desy.de

Studying vibrational cooling and Renner-Teller interaction of the C_4O^- anion through resonant photo-dissociation at CSR

V C Schmidt[1]*, M Ončák[2], S George[3], K Blaum[1], M Grieser[1], P Fischer[3], R von Hahn[1], Á Kálosi[4,1], H Kreckel[1], P M Mishra[1], D Müll[1], O Novotný[1], F Nuesslein[1], L Schweikhard[3] and A Wolf[1]

[1]Max-Planck-Institut für Kernphysik, 69117 Heidelberg, Germany
[2]Innsbruck Physics Research Center, Universität Innsbruck, 6020 Innsbruck, Austria
[3]Institut für Physik, Universität Greifswald, 17487 Greifswald, Germany
[4]Columbia Astrophysics Laboratory, Columbia University, New York, 10027 New York, USA

Synopsis Photo-induced electron detachment and fragmentation of the astrophysically relevant C_4O^- anion were studied. To this end, a tunable, pulsed OPO laser was used to induce resonant dissociation into CO and C_3^- fragments. The fragmentation process in dependence of photon energy as well as its evolution with storage time were investigated in the Cryogenic Storage Ring (CSR) in Heidelberg. Preliminary results provide insights into the anion's geometry and decay channels of different vibronic excitations.

The study of cooling dynamics and ground-state properties of molecular ions is one of many research goals at the Cryogenic Storage Ring (CSR) at the Max-Planck-Institut für Kernphysik in Heidelberg. The CSR is a fully electrostatic storage ring, which can be cooled down to a few kelvin and reaches residual gas densities down to 100 cm^{-3} [1]. Thus, the ring provides a unique research environment enabling the study of gas-phase ion species in a very low radiation field and almost free of collisional background.

Here we present investigations of the carbon-based molecule C_4O^-, which is predicted to be observable in interstellar clouds [2]. Its detection requires a detailed knowledge of the anion's vibronic structure. Past studies of this molecule have left open questions about its geometry as well as its electron affinity. A previous measurement of photon absorption properties of C_4O^- in a neon matrix revealed multiple absorption resonances attributed to vibronic transitions [3].

For our measurement internally hot C_4O^- ions were produced in a sputter source and injected into the CSR. They were probed with different photon energies, using a pulsed OPO laser at various storage times to monitor their internal excitations. Neutral and charged fragments were measured in coincidence by two detectors.

The results include resonant fragmentation ($C_4O^- + h\nu \rightarrow C_3^- + CO$) in the photon energy region of about 21 300 cm^{-1} to 29 000 cm^{-1}. The resonance curves exhibit changes in shape and height attributed to cooling dynamics of the anions inside the CSR. One feature is attributed to the radiative cooling of a vibrational hot band. Furthermore, the possible onset of the electron detachment channel is visible around 29 000 cm^{-1}. We will present our experimental results together with a detailed theoretical investigation of the observed features. In particular, the molecule's geometry and vibronic structure were calculated, revealing that both initial and final electronic state of the observed transitions suffer from a Renner-Teller interaction.

*E-mail: viviane.schmidt@mpi-hd.mpg.de

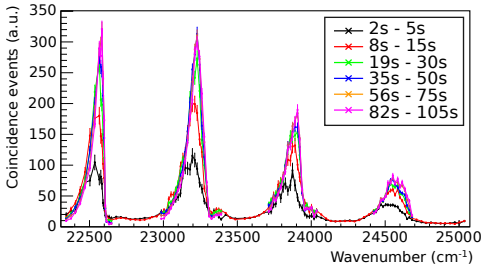

Figure 1. Coincidence events for the process: $C_4O^- + h\nu \rightarrow C_3^- + CO$ as a function of photon energy for different storage times in the energy photon region 22 400 cm^{-1} to 25 000 cm^{-1}.

References

[1] von Hahn R *et al.* 2016 *Rev. Sci. Instrum.* **87** 063115
[2] Adams N G *et al.* 1989 *Astron. Astrophys.* **220** 269-271
[3] Riaplov E *et al.* 2001 *J. Phys. Chem. A* **105** 4894-4897

The two-electron cusp in the ground states of He and H_2 investigated via quasifree double photoionization

S Grundmann[1], V V Serov[2], F Trinter[3,4], K Fehre[1], N Strenger[1], A Pier[1], M Kircher[1], D Trabert[1], M Weller[1], J Rist[1], L Kaiser[1], A W Bray[5], L Ph H Schmidt[1], J B Williams[6], T Jahnke[1], R Dörner[1], M S Schöffler[1,†] and A S Kheifets[5]

[1]Institut für Kernphysik, Goethe-Universität, Max-von-Laue-Strasse 1, D-60438 Frankfurt, Germany
[2]Department of Theoretical Physics, Saratov State University, Saratov 410012, Russia
[3]Photon Science, Deutsches Elektronen-Synchrotron (DESY), Notkestrasse 85, D-22607 Hamburg, Germany
[4]Molecular Physics, Fritz-Haber-Institut der Max-Planck-Gesellschaft, Faradayweg 4-6, D-14195 Berlin, Germany
[5]Research School of Physics, Australian National University, Canberra ACT 2601, Australia
[6]Department of Physics, University of Nevada, Reno, Nevada 89557, USA

Synopsis Kinematically complete double ionization measurements of He (H_2) induced by 800 eV circularly polarized photons are presented, accompanied by ab initio nonperturbative calculations. These confirm that the quasifree mechanism becomes the dominating double ionization mechanism in H_2 and originates from the electron-electron cusp region.

The interaction of photons with atoms and molecules is dominated by electronic dipole transition. Consequently the photon can only couple with a single electron and double ionization only occurs due to initial or final state interaction. These are commonly referred to as shake-off (SO) and electron knock-off (two-step-one, TS1). However at higher energies, when higher order terms of the light-matter-interaction come into play, the so-called quasifree mechanism (QFM) arises. While this process was predicted more than four decades ago [1], the experimental proof was made rather recently [2]. Each of the double ionization mechanisms exhibit an unique kinematically fingerprint, which makes it easy to identify. For SO the electron energy sharing is rather asymmetric with the SO-electron being very low energetic. Also the angle between slow and fast electron is nearly isotropic. For the TS1 the electron energy sharing can be of any value, dominating at asymmetric values as well and a classically 90 ° angle between both electrons. Both processes also transfer a rather big momentum to the nucleus.

For the QFM in contrast the photon couples directly to an electron-pair, leaving the nucleus at rest and both electrons being emitted back-to-back. In this CUSP-region the two electrons are spatially close together. In [3] it was also shown that an electron, emitted via QFM, exhibits not a dipolar shape, but rather a quadrupole shape [3]. In this presentation we will discuss what happens if instead of Helium, hydrogen molecules (H_2) are investigated [4]. Can QFM occur at all? And if yes, is it similar strong as in the highly correlated atomic system helium? Upon the removal of the electrons, the molecule will explode in two protons, giving an additional handle on the internuclear separation of the nuclei at the instant of ionization. Is there any dependency of QFM as function of the internuclear separation to be expected and observed? This mostly experimental study, which was performed using a COLTRIMS momentum imaging setup, is accompanied by calculations.

References

[1] M. Y. Amusia et al. J. Phys. B, **8**, 1248 (1975)
[2] M. S. Schöffler et al. Phys. Rev. Lett., **111**, 013003, (2013)
[3] S. Grundmann et al., Phys. Rev. Lett., **121**, 173003, (2018)
[4] Grundmann et al., Phys. Rev. Res. **2**, 033080, (2020)

† E-mail: schoeffler@atom.uni-frankfurt.de

Unravelling the electronic structure of isolated metalloporphyrins by metal L-edge spectroscopy

K Schubert[1 *], M Guo[2], K Atak[1], S Dörner[1], C Bülow[3], B v Issendorff[4], S Klumpp[1], J T Lau[3,4], P S Miedema[1], T Schlathölter[5], S Techert[1,6], M Timm[3], X Wang[5], V Zamudio-Bayer[3], L Schwob[1] and S Bari[1 †]

[1]Deutsches Elektronen-Synchrotron DESY, Hamburg, 22607, Germany
[2]Division of Chemical Physics, Chemical Center, Lund University, Lund, SE-22100, Sweden
[3]Helmholtz-Zentrum Berlin für Materialien und Energie, Berlin, 14109, Germany
[4]Physikalisches Institut, Albert-Ludwigs-Universität Freiburg, Freiburg, 79104, Germany
[5]Zernike Institute for Advanced Materials, University of Groningen, Groningen, 9747AG, The Netherlands
[6]Institut für Röntgenphysik, Georg-August-Universität Göttingen, Göttingen, 37077, Germany

Synopsis The electronic structure and orbital-specific deexcitation pathways of the cobalt(III) protoporphyrin IX cation have been investigated by a combination of tandem mass spectrometry and X-ray absorption spectroscopy at the cobalt L-edge. The analysis of the experimental data has been supported by quantum-mechanical restricted active space calculations.

Metalloporphyrins (MPs) are organometallic molecules widely found in nature and composed of a porphyrin ring coordinating a metal ion in the ring cavity center. Their particular electronic structure makes MPs ideally suited for a number of applications, from biological functions to the usage in electronic devices.

The electronic structure and functional activity of metalloporphyrins are determined by the type of the metal, its oxidation and spin state as well as axial ligands around the metal center. To understand their properties it is hence of great importance to probe the local electronic structure of the metal center. The electrospray ionisation technique allows the study of the intrinsic properties of MPs to be achieved by performing studies in the gas phase, i.e. in an environment-free and controlled chemical state.

Here, we applied near-edge X-ray absorption mass spectrometry (NEXAMS) and quantum-mechanical restricted active space calculations to investigate the electronic structure of the metal-active site of the cryogenically cooled isolated cobalt(III) protoporphyrin IX cation ($CoPPIX^+$) and its deexcitation pathways upon resonant absorption at the cobalt L-edge [1]. The comparison between experiment and theory shows that $CoPPIX^+$ is in a $^3A_{2g}$ triplet ground state and that competing excitations to metal-centered non-bonding and antibonding σ* molecular orbitals lead to distinct deexcitation pathways (see figure 1). The experiments were carried out at the UE52_PGM Ion Trap beamline of the BESSY II synchrotron (HZB, Berlin).

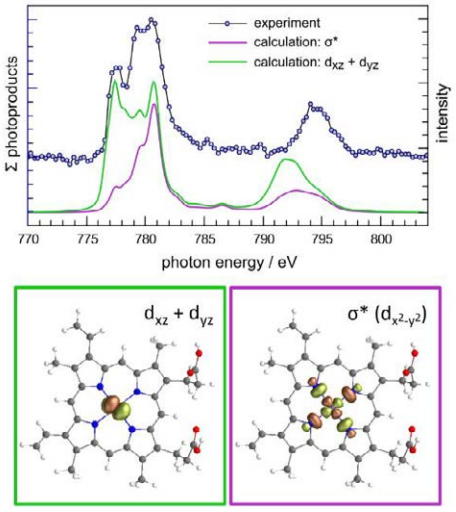

Figure 1. Experimental total ion yield and calculated contributions of the non-bonding d_{xy}, d_{yz} and antibonding σ^* orbitals to the X-ray absorption spectrum of $CoPPIX^+$ at the cobalt L-edge.

References

[1] Schubert K, Guo M *et al* 2021 *Chem. Sci.* 12 3966-3976

* E-mail: kaja.schubert@desy.de
† E-mail: sadia.bari@desy.de

Near edge X-ray absorption mass spectrometry applied to peptides: structure and site-selective dissociation.

S Dörner[1], L Schwob[1*], K Atak[1], R Boll[2], C Bülow[3], B v Issendorff[4], J T Lau[3,4], T Schlathölter[5], K Schubert[1], S Techert[1,6], M Timm[3], V Zamudio-Bayer[3], and S Bari[1]

[1]Deutsches Elektronen-Synchrotron DESY, Hamburg, 22607, Germany
[2] European XFEL, Schenefeld, 22869, Germany.
[3]Helmholtz-Zentrum Berlin für Materialien und Energie, Berlin, 14109, Germany
[4]Physikalisches Institut, Albert-Ludwigs-Universität Freiburg, Freiburg, 79104, Germany
[5]Zernike Institute for Advanced Materials, University of Groningen, Groningen, 9747AG, The Netherlands
[6]Institut für Röntgenphysik, Georg-August-Universität Göttingen, Göttingen, 37077, Germany

Synopsis We examined the capabilities of near edge X-ray absorption mass spectrometry to investigate the interplay between electronic and geometric structures as well as site-selective dissociation pathways. The experiments have been performed on two models pentapeptides at all relevant atomic edges.

Over the past decades, peptides and proteins have been investigated in the gas phase using state-of-art electrospray ionization sources, ion guiding in radiofrequency electric fields and mass spectrometric techniques. In order to obtain new insights into the electronic and structural properties of such biomolecules, VUV and soft X-ray photo-absorption experiments have been carried out at synchrotron facilities, which offer a broad photon energy range and a high photon flux. In particular, near-edge X-ray absorption mass spectrometry (NEXAMS), which is an action-spectroscopy technique based on the resonant photoexcitation of core electrons, has been of growing interest in the past few years for investigating the spatial and electronic structure of biomolecules. It has been used successfully to unravel different aspects of the photodissociation of peptides and to probe conformational features of proteins.

It is a current question to which extent the resonant photoabsorptions are sensitive toward effects of conformational isomerism, tautomerism, and intramolecular interactions in gas-phase peptides. Additionally, in the soft X-ray regime, the high degree of localization of the deposited energy allows getting a deeper understanding on the dissociation processes. However, identifying products of site-selective dissociation in large biomolecules is challenging at the carbon, nitrogen, and oxygen edges because of the high number of these atoms and related chemical groups. Probing the inner shells of a single sulfur atom within a biomolecule as the one and only excitation site is a promising way to overcome this obstacle.

We present here recent results from NEXAMS studies of cryogenically cooled gas-phase leucine enkephalin $[LeuEnk+H]^+$ and methionine enkephalin $[MetEnk+H]^+$ at the carbon, nitrogen, and oxygen K-edges[1] as well as sulfur L-edge[2]. The experiments were carried out at the UE52_PGM Ion trap beamline of the BESSY II synchrotron (HZB, Berlin).

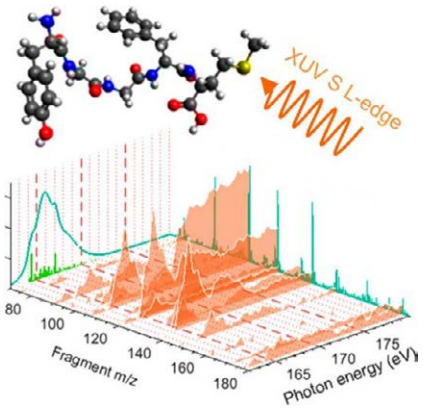

Figure 1. NEXAMS spectra obtained at the sulfur L-edge for $[MetEnk+H]^+$.

References

[1] Dörner S *et al* 2021 *J. Am. Soc. Mass Spectrom.* 32, 3, 670-684
[2] Schwob L *et al* 2020 *J. Phys. Chem. Lett.* 11, 4, 1215-1221

* E-mail: lucas.schwob@desy.de

Unraveling the most significant collective coordinate influencing time-resolved x-ray absorption spectra in ionized urea and its dimer

Y Shakya[1,2] *, L Inhester[1] †, C Arnold[1,2,3], R Welsch[1,3] and R Santra[1,2,3]

[1] Center for Free-Electron Laser Science, DESY, Notkestrasse 85, 22607 Hamburg, Germany
[2] Department of Physics, Universität Hamburg, Jungiusstrasse 9, 20355 Hamburg, Germany
[3] Hamburg Centre for Ultrafast Imaging, Luruper Chaussee 149, 22761 Hamburg, Germany

Synopsis We theoretically study the dynamics of urea and its dimer upon valence ionization and show how these dynamics can be probed via time-resolved x-ray absorption spectroscopy. By employing statistical analysis techniques on the simulated *ab initio* trajectories following ionization, it is demonstrated that time-dependent intensity variations in the spectra of urea can be linked to vibrations along specific collective coordinates. For the urea dimer, we find that ionization induces proton transfer, which can be traced through specific features in its spectra.

Probing the early dynamics of chemical systems following ionization is essential for our understanding of radiation damage. Time-resolved x-ray absorption spectroscopy (TRXAS) on a femtosecond timescale, in combination with appropriate simulations, can provide crucial insights into the ultrafast processes that occur upon ionization due to its element-specific probing nature. However, it can be very challenging to get a clear interpretation of the spectral features. Even when theoretical simulations are available, a direct interpretation of time-dependent changes in the spectra is often complicated due to the high dimensionality of the data.

In this theoretical study, we investigate the response of urea and its dimer to ionizing radiation and how it can be probed via TRXAS [1]. We show how statistical analysis techniques, in particular partial least square regression, can help to unravel specific structural dynamics in a molecule that induce time-dependent changes in the x-ray absorption spectra. By applying this technique, collective coordinates that most influence TRXAS are obtained from simulated *ab initio* nonadiabatic trajectories of valence-ionized urea and its dimer. These trajectories are obtained using a similar methodology presented in Ref. [2, 3] employing Tully's fewest switches surface hopping approach using Koopmans' theorem to describe the ionized system. The ability of TRXAS to reveal rich insights into the ionization-induced dynamics of urea and its dimer at carbon, nitrogen, and oxygen K-edges is hence shown.

For urea, we elucidate the possibility to trace the effects of specific molecular vibrations in its TRXAS. For its dimer, where ionization triggers a proton transfer reaction, we show how the spectra can reveal specific details on the progress of a proton transfer reaction. Furthermore, deeper valence ionization, which triggers dynamics in excited states of the ionized system, results in electronic relaxation dynamics through nonadiabatic transitions that are reflected via blueshifts in the TRXAS.

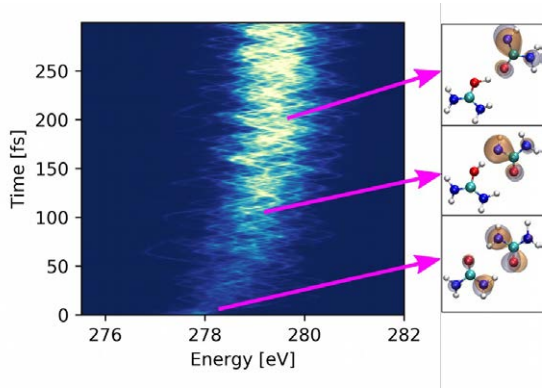

Figure 1. Calculated time-resolved x-ray absorption spectra of urea dimer at the C K-edge following HOMO ionization. Proton transfer coordinate along with the hole orbital is shown on the right at different times along the spectra.

References

[1] Shakya Y *et al* Submitted
[2] Loh Z-H *et al* 2020 Science **367** 179–182
[3] Khalili K *et al* 2019 Struct. Dyn. **6** 044102

* E-mail: yashoj.shakya@desy.de
† E-mail: ludger.inhester@cfel.de

Sub-femtosecond control of entangled two-electron states

F Shobeiry*, P Fross, H Srinivas, D Bharti, T Pfeifer, A Harth and R Moshammer

Max Planck Institute for Nuclear Physics, Heidelberg, 69117, Germany

Synopsis We present kinematically complete experiments on photodissociation of H_2 using a combination of XUV and IR pulses and demonstrate how the interplay of entangled two-electron states leads to symmetry breaking in the emission direction of the photoelectron with respect to the ejected proton. We show that the symmetry breaking can be controlled with the delay between two pulses on a sub-femtosecond time scale. Our experimental results are supported by a semiclassical simulation based on the WKB approximation.

The emission direction of the photoelectron with consecutive dissociation of the molecule is symmetric with respect to the ejected proton as long as the parity of the electron wave function is well-defined. This symmetry can, however, be broken by mixing states with opposite parities with the help of an external field. So far, this asymmetric emission was introduced using a single photon [1,2], where a time-resolved control is not possible, or in the multi-photon regime for the proton in the lab frame, where a strong asymmetric IR field is responsible for the asymmetric charge localization on one of the nuclei [3-5]. We experimentally present a novel method to introduce and control the molecular-frame symmetry breaking between the emission direction of the electron and the H^+ photoion during dissociative photoionization. This is achieved by manipulating the entangled two-electron states using a few controlled XUV and IR photons and their delay on a sub-fs time scale.

We perform XUV-IR pump-probe measurements using a 50-kHz laser amplifier (1030 nm). The main part of the beam is used to produce XUV light using high-harmonic generation, and a small portion is delayed in time using a translation stage. Both beams are focused into a reaction microscope (COLTRIMS) to interact with a gas target of H_2 where we retrieve vector momenta of the ejected electron and H^+, detected in coincidence. The molecular-frame asymmetry is defined as $A = \frac{N_{\alpha<90} - N_{\alpha>90}}{N_{\alpha<90} + N_{\alpha>90}}$, where $N_{\alpha<90}$ and $N_{\alpha>90}$ are the number of events where the electron and proton are emitted in the same and the opposite hemisphere, respectively. Fig. 1 shows a clear time-dependent asymmetry parameter in a region where ground-state dissociation (pathway 1) and bond-softening (pathway 2) overlap resulting in a coherent superposition

$$|\psi\rangle = \alpha \overbrace{|A_u\rangle\,|B_g\rangle}^{\text{pathway 1}} + \beta \overbrace{|A_g\rangle\,|B_u\rangle}^{\text{pathway 2}}, \qquad (1)$$

where $|A\rangle$ and $|B\rangle$ denote the wave function of the free and bound electrons with gerade (g) and ungerade (u) symmetries, respectively.

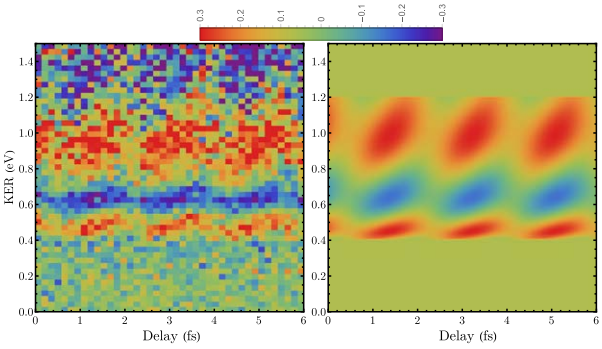

Figure 1. Asymmetry parameter A as a function of the delay between XUV and IR pulses for the experiment (left) and semi-classical simulation (right).

We show that we can manipulate the coherent superposition of an entangled two-electron system (in an analogy to a phase gate on a two-qubit system) on a sub-fs time scale. This ultrafast few-photon conceptual approach can have promising consequences in quantum computing.

References

[1] Martín F *et al* 2007 *Science* **315** 5812
[2] Fischer A *et al* 2013 *Phys. Rev. Lett.* **110** 213002
[3] Kling M *et al* 2006 *Science* **312** 5771
[4] Sansone S *et al* 2010 *Science* **465** 763766
[5] Kremer M *et al* 2009 *Phys. Rev. Lett.* **103** 213003

*E-mail: shobeiry@mpi-hd.mpg.de

Two-dimensional electron momentum distributions in ionization of water molecule by a strong laser field

N I Shvetsov-Shilovski[1] *, A Taoutioui[2] † and K Tőkési[2,3]

[1]Institut für Theoretische Physik, Leibniz Universität Hannover, Hannover, 30167
[2]Institute for Nuclear Research, Hungarian Academy of Sciences, Debrecen, 4001, Hungary

Synopsis We investigate the ionization of the water molecule by strong linearly polarized few-cycle laser pulse by solving the time-dependent Schrödinger equation and applying the semiclassical two-step model. We present two-dimensional electron momentum distributions, energy spectra, and angular distributions. The deviations from the case of the hydrogen molecule are revealed and analyzed.

The ionization of molecules by strong laser pulses has attracted considerable interest in both experiment and theory, see, e.g., Ref. [1]. It is clear that the strong-field ionization of a molecule is much more complicated that the same process in an atom. This is due to the extra degrees of freedom associated with the nuclear motion, the corresponding time scales, and the complicated shape of the electronic orbitals. As the result, the solution of the time-dependent Schrödinger equation (TDSE) in three spatial dimensions for a molecule interacting with an intense laser pulse is possible only for the simplest molecules selecting the most relevant degrees of freedom. Therefore, development and testing of simplified theoretical approaches to ionization of molecules by strong laser fields are very important.

For simplicity we used the single active electron and frozen core hydrogenic approximation of water. In this approximation the water molecule is treated as two bodies and the electrons from the highest occupied molecular orbital ($1b_1$) are considered. The photoelectron momentum distribution of electrons generated in ionization of H_2O molecule are calculated by solving the three-dimensional TDSE and using the semiclassical two-step (SCTS) model [2], see Fig. 1. We analyze the discrepancies between the TDSE and the SCTS and propose modification of the semiclassical approach aimed at better agreement with the fully quantum results.

We reveal and discuss differences in electron momentum distributions, energy spectra, and angular distributions compared to the case of the hydrogen molecule [3]. Special attention is paid to the fanlike interference structure in the low-energy part of the momentum distributions that is particularly sensitive to the molecular potential. The obtained results will be used as a benchmark for further studies of strong-field ionization of water molecule.

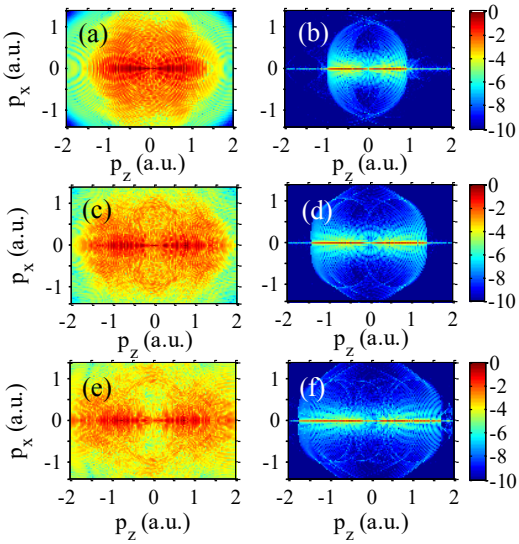

Figure 1. The two-dimensional photoelectron momentum distributions for the H_2O molecule ionized by a laser pulse with duration of 8 cycles and wavelength of 800 nm calculated from the numerical solution of the TDSE [(a), (c), and (e)] and the SCTS model [(b), (d), and (f)]. Panels [(a), (b)], [(c), (d)], and [(e), (f)] correspond to the intensities of 1.0×10^{14} W/cm^2, 2.0×10^{14} W/cm^2, and 3.0×10^{14} W/cm^2, respectively. A logarithmic color scale in arbitrary units is used. The distributions are normalized to the maxima. The laser field is linearly polarized along the z axis.

References

[1] Wiese J, *et al* 2021 *Phys. Rev. Res.* **3** 013089
[2] Shvetsov-Shilovski N I, *et al* 2016 *Phys. Rev. A* **94** 013415
[3] Shvetsov-Shilovski N I, *et al* 2019 Eur. Phys. J. D **73** 37

* E-mail: nikolay.shvetsov@itp.uni-hannover.de
† E-mail: abdelmalek.taoutioui@atomki.hu and tokesi@atomki.hu

Tracing the dynamics in photoexcited hydrocarbons: cyclical vs conjugated

S Sorensen[1*], S Oghbaie[1], N Walsh[1,2], B Oostenrijk[1], J Laksman[1,3], E P Månsson[1,4] and M Gisselbrecht[1]

[1]Department of Physics, Lund University, Box 118, Lund, 221 00, Sweden
[2]MAXIV laboratory, Lund University, Box 118, Lund, 221 00, Sweden
[3]EU-XFEL, DESY, Hamburg, Germany.
[4]Center for Free-electron Laser Science, DESY, Hamburg, Germany

Synopsis We present two examples of experimental studies that are combined with theoretical calculations of the potential energy surfaces of the investigated molecules with the aim to understand the evolution of the molecule after excitation of the C 1s electron. The experiments illuminate fragmentation processes of doubly-charged states in cyclopropane and butadiene populated via direct double ionization and via excitation of C1s electrons.

Photoinduced nuclear dynamics via bond lengthening or symmetry break can lead to preferential fragmentation or isomerization. Cyclical molecules are interesting as a model for probing whether ring distortion via the Jahn-Teller effect, for example, will open up different dissociation pathways upon splitting of degenerate states. Cyclopropane has a three-member carbon 'triangular ring' with the ground state geometry in D_{3h} symmetry. Due to the large strain of this ring, ionization of an electron from degenerate orbitals readily destabilizes the molecule. Calculations show that the minimum energy path from these states indeed leads to very different fragmentation channels [1] as shown in Fig. 1. Resonant excitation to valence states of different symmetries can initiate nuclear dynamics, and populate these inner-valence states.

Butadiene is the simplest conjugated hydrocarbon but exhibits several conformational changes in the dication. We present a comprehensive study of fragmentation of dication states, and study how these states are populated after core electron excitation. The inner-valence states have been studied using direct double ionization and calculations of the dication states are correlated to fragmentation channels in the measured spectra [2].

Experiments were carried out at MAX-Lab using the 3D multicoincidence ion imaging spectrometer developed in our research group [3], and at the MAX IV FLEXPES beam line.

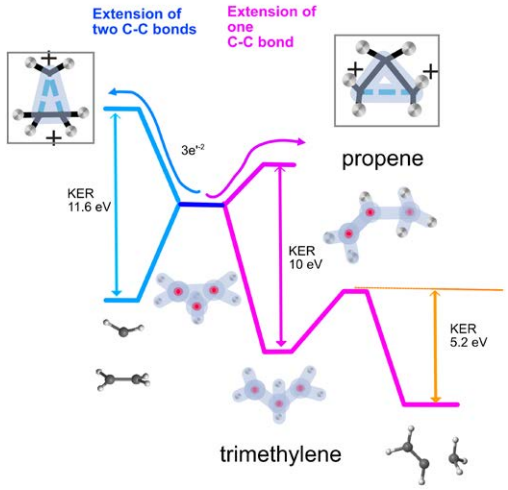

Figure 1. Schematic diagram showing that the Jahn-Teller effect in the $3e'^2$ dication states splits electronic states, leading to geometry changes for extension of one or two C-C bonds in cyclopropane. The relevant fragment channels are sketched. Adapted from ref [1].

References

[1] Oghbaie S *et al* 2017 *Phys Chem Chem Phys* **19** 19631
[2] Oghbaie S et al 2015 *J Chem. Phys* **143** 114309
[3] Laksman J et al 2013 *Rev Sci Instrum* **84** 123113

* E-mail: stacey.sorensen@sljus.lu.se

Competitive Dehydrogenation and Backbone Fragmentation of Super-Hydrogenated PAHs

M H Stockett[1,†*], L Avaldi[2], P Bolognesi[2], J N Bull[3], L Carlini[2], E Carrascosa[4], J Chiarinelli[2], R Richter[5], and H Zettergren[1]

[1]Fysikum, Stockholms Universitet, Stockholm, Sweden
[2]CNR-Istituto di Struttura della Materia, Area della Ricerca di Roma 1, Rome, Italy
[3]School of Chemistry, University of East Anglia, Norwich, United Kingdom
[4]Laboratoire de Chimie Physique Moléculaire, École Polytechnique Fédérale de Lausanne, Lausanne, Switzerland
[5]Elettra Sincrotrone Trieste, Trieste, Italy

Synopsis The photo-stability of super-hydrogenated PAHs is assessed using the Photo-Electron Photo-Ion Coincidence technique.

Super-hydrogenated Polycyclic Aromatic Hydrocarbons (PAHs) have been suggested to catalyze the formation of H_2 in certain regions of space, but it remains unclear under which circumstances this mechanism is viable given the reduced carbon backbone stability of super-hydrogenated PAHs. We report a laboratory study on the stability of the smallest pericondensed PAH, pyrene ($C_{16}H_{10+N}$, with $N = 4$, 6, and 16 additional H atoms, see Figure 1), against photodestruction by single vacuum ultraviolet photons using the Photo-Electron Photo-Ion Coincidence (PEPICO) technique [1]. For 4H-Pyr ($N = 4$), we observe a protective effect of hydrogenation against the loss of native hydrogens, in the form of an increase in the appearance energies of the $C_{16}H_9^+$ and $C_{16}H_8^+$ daughter ions compared to those reported for pristine pyrene ($C_{16}H_{10}$). No such effect is seen for 6H- or 16H-Pyr, where the weakening effect of replacing aromatic bonds with aliphatic ones outweighs the buffering effect of the additional hydrogen atoms. The onset of fragmentation occurs at similar internal energies for 4H- and 6H-Pyr, but is significantly lower for 16H-Pyr. In all three cases, H-loss and C_mH_n-loss ($m \geq 1$, carbon backbone fragmentation) channels open at approximately the same energy. The branching fractions of the primary channels favor H-loss for 4H-Pyr, C_mH_n-loss for 16H-Pyr, and are roughly equal for the intermediate 6H-Pyr. Figure 1 shows the branching fractions of the first few fragment groups from the PEPICO measurement at a common electron binding energy of 13.6 eV, corresponding to the highest photon energy expected to impinge on PAHs in photodissociation regions. We conclude that super-hydrogenated pyrene is probably too small to support catalytic H_2-formation, while trends in the current and previously reported data suggest that larger PAHs may serve as catalysts up to a certain level of hydrogenation [1].

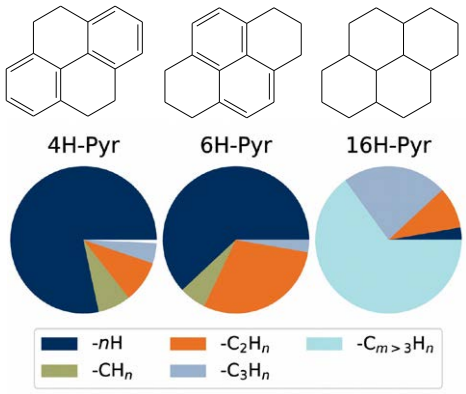

Figure 1. Structures of tetrahydropyrene (4H-Pyr, $C_{16}H_{14}$), hexahydropyrene (6H-Pyr, $C_{16}H_{16}$), and hexadecahydropyrene (16H-Pyr, $C_{16}H_{26}$). Comparison of the branching fractions of the first few fragment groups at a binding energy of 13.6 eV.

References

[1] Stockett M H *et al* 2021 *Astrophys. J.* **Accepted**

*E-mail: Mark.Stockett@fysik.su.se

Adiabatic theory of strong-field ionization of molecules with nuclear motion

J Svensmark[1] * O I Tolstikhin[2] and T Morishita[1]

[1]Institute for Advanced Science, The University of Electro-Communications, Tokyo, 182-8585, Japan
[2]Moscow Institute of Physics and Technology, Dolgoprudny, 141700, Russia

Synopsis The adiabatic theory for molecules is developed. This theory excels at describing laser-molecule interaction for long-wavelength laser pulses in the infrared and terahertz regimes. Using the theory quantitatively accurate observables such as the photo-electron momentum distribution can be calculated from first principles.

In recent years there has been an increased interest in laser pulses in the mid-infrared and terahertz regimes in the strong field community. With such pulses it could become possible to measure molecular dynamics in detail. However, most theoretical methods are unable to describe what happens in these regimes, due to the large ranges of the dynamic variables involved. Unlike such methods, the adiabatic theory of ionization for atoms [1, 2] works well in this regime, since it exploits the slow variations of the laser field compared to motion inside the atom.

Here we present the recently developed extensions of the adiabatic theory to molecules (AAnf) [3]. It treats nuclear motion in addition to all interactions among nuclei, electrons and the laser field. We will demonstrate the accuracy of the theory by comparing with exact solutions of the time-dependent Schrödinger equation (TDSE), as shown in Figure 1. We will also show an application of the theory to explain why the energy width of the vibrational state distribution in the molecular ion shrinks when isotopes with heavier nuclear masses are used.

Recently we have also been working on including the effect of rescattering into the theory. Building upon the work in Ref. [4], this makes it possible to recreate the nuclear wave packet in the molecular ion from measurements of the photo-electron distributions over nuclear vibrational states.

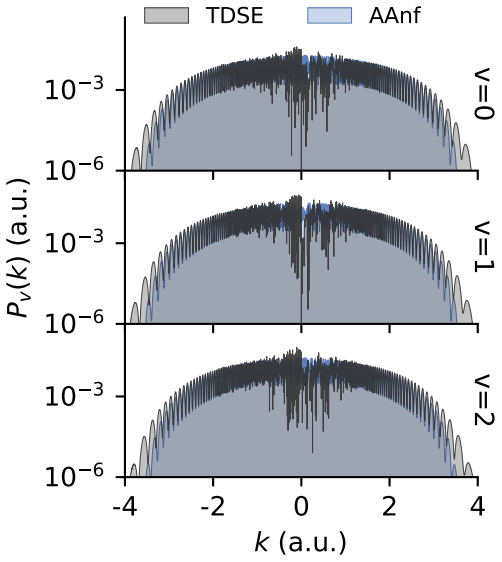

Figure 1. Photo-electron momentum distribution resolved in vibrational channels of the molecular ion v. Agreement is seen across a large range of photo-electron momenta k.

References

[1] Tolstikhin O I, Morishita T, Watanabe S. 2010 *Phys Rev A* **81, 033415**
[2] Tolstikhin O I, Morishita T. 2012 *Phys Rev A* **86, 043417**
[3] Svensmark J, Tolstikhin O I, Morishita T. 2020 *Phys Rev A* **101, 053422**
[4] Morishita T, Tolstikhin O I. 2017 *Phys Rev A* **96 053416**

*E-mail: jenssss@uec.ac.jp

Gauge-invariant time-dependent configuration interaction singles method for molecules: extracting photoelectron momentum distribution

T Teramura[1] *, T Sato[1,2,3] and K L Ishikawa[1,2,3]

[1]Department of Nuclear Engineering and Management, Graduate School of Engineering, The University of Tokyo, 7-3-1 Hongo, Bunkyo-ku, Tokyo 113-8656, Japan
[2]Photon Science Center, Graduate School of Engineering, University of Tokyo, 7-3-1 Hongo, Bunkyo-ku, Tokyo 113-8656, Japan
[2]Research Institute for Photon Science and Laser Technology, University of Tokyo, 7-3-1 Hongo, Bunkyo-ku, Tokyo 113-0033, Japan

Synopsis We present an extraction of photoelectron momentum distribution of general three-dimensional molecules within the gauge-invariatn time-dependent configuration interaction singles method. The extraction is carried out by the time-dependent surface flux method.

Phototoelectron energy has been a fundamental observable since the dawn of quantum mechanics. In recent attosecond science, photoelectron momentum distribution (PMD) from molecules is a key experimental probe and theoretical evaluation of the PMD is demanded.

For accurate description of time evolution of multielectron systems, we have developed the gauge-invariant time-dependent configuration interaction singles method (TDCIS) method [1, 2] and successfully implemented to general three-dimensional molecules. Our gauge-invariant formulation enables one to enjoy computational efficiency thanks to velocity gauge treatment of the laser-electron interaction Hamiltonian.

Extracting PMD from the computed wavefunction is not a tribial task, since the ejected photoelectron is highly delocalized in real spece. If one naively tried to extract photoelectron by projecting onto plane waves, one would be forced to keep delocalized electronic wave packet entirely in the simulation box. This would result in unacceptable number of grid points especially for the case of molecules.

For cost-effective evaluation of the PMD from multielectronic wavefunction, Orimo *et al* applied the time-dependent surface flux (tSURFF) method to the time-dependent multiconfiguration self consistent field method [3]. In the tSURFF method, instead of storing electronic wave packet inside the simulation box, electron flux going through a surface is used to evaluate the PMD. The electron outside the surface is regarded as a photoelectron which can be absorbed by exterior complex scaling (ECS). The combination of the tSURFF method and the ECS sifnificantly reduces the size of the simulation box.

We have successfully applied the tSURFF method to the gauge-invariant TDCIS method. In figure 1, we show the PMD from H_2 molecule irradiated by a laser pulse with a photon energy of 30 eV and an intensity of 10^{13} W/cm^2. The laser pulse is polarized parallel to the molecular axis ($\theta = 0$). The photoelectron with $|p| = 1$ is consistent with the calculated ionization energy of 16.3 eV.

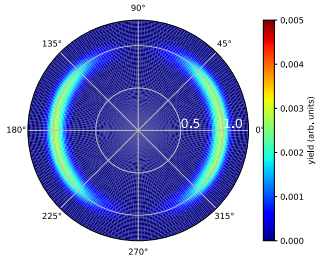

Figure 1. Photoelectron momentum distribution from H_2 molecule with parallely polarized laser pulse with a photon energy of 30 eV and an intensity of 10^{13} W/cm^2.

References

[1] Sato T *et al* 2018 *Appl. Sci.* 8 322
[2] Teramura T *et al* 2019 *Phys. Rev. A* 100 043402
[3] Orimo Y *et al* 2019 *Phys. Rev. A* 100 013419

* E-mail: teramura@atto.t.u-tokyo.ac.jp

Mapping of light-induced potentials in the strong-field dissociation of O_2^+

P M Abanador and U Thumm

Department of Physics, Kansas State University, Manhattan, Kansas 66506, USA

Synopsis We examine the imprints of light-induced potentials (LIPs) on the dissociation dynamics of O_2^+ molecular ions, as observed in angle-resolved fragment kinetic-energy-release (KER) spectra. By numerically solving the time-dependent Schrödinger equation (TDSE) within the Born-Oppenheimer approximation, we follow the vibrational and rotational motion of O_2^+ molecular ions exposed to 800-nm, 40-fs laser pulses. For peak intensities between 10^{13} and 10^{14} W/cm^2, we calculate angle-resolved KER spectra, which reveal characteristic energy- and angle-dependent fringe structures associated with the LIPs.

Floquet theory elucidates underlying mechanisms behind fundamental molecular strong-field processes. Within this Floquet description, LIPs result from the dipole-coupling between molecular Born-Oppenheimer (BO) states in the presence of a laser field [1, 2]. Notably, the *bond hardening* mechanism refers to transient population trapping in light-induced vibrational potential wells [3]. We have recently theoretically demonstrated the role of bond hardening in a pulse-duration-dependent molecular stabilization effect during the dissociation of O_2^+ molecular ions [4].

We further explored how the bond hardening mechanism and associated LIPs might be revealed in experiments. By numerically solving the TDSE, we analyzed the rovibrational dynamics of O_2^+ molecular ions interacting with infrared (IR) laser pulses and calculated observable, angle-resolved fragment kinetic-energy-release (KER) spectra.

Figure 1 compares our numerical results for the lowest IR-pulse peak intensity considered in [5] from calculations that include rotational excitations (2D) with simplified calculations in which the rotational motion is frozen (1D). For the given peak intensity, the angle-resolved KER spectra from 1D and 2D calculations are almost indistinguishable. This indicates that the rotational motion is of marginal relevance. The TDSE results reveal striking fringe structures that shift downward in energy for increasing alignment angles $0 \leq \theta \leq \pi/2$. To explain this downward trend, we compared our TDSE results with a Floquet model, based on the vibrational energies in the light-induced potential well [5].

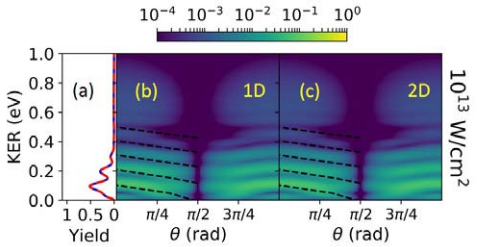

Figure 1. (a) Total, angle-integrated KER spectra for an 800-nm, 40-fs pulse with a peak intensity of 10^{13} W/cm^2. TDSE calculations without (1D) and including rotational excitations (2D) are represented by red dashed and blue solid curves, respectively. Corresponding angle-resolved KER spectra are shown for (b) 1D and (c) 2D TDSE calculations. Superimposed black dashed lines show the lowest five vibrational levels in the light-induced Floquet bond-hardening well (see Eq. (4) in Ref. [5]).

This work was supported by the Chemical Sciences, Geosciences, and Biosciences Division, Office of Basic Energy Sciences, Office of Science, U.S. DoE Award DEFG02-86ER13491 and, in part, NSF grant PHY 1802085.

References

[1] Aubanel E E *et al* 1993 *Phys. Rev. A* **48** R4011
[2] Chu S-I and Telnov D A 2004 *Phys. Rep.* **390** 1
[3] Ibrahim H *et al* 2018 *J. Phys. B* **51** 042002
[4] Abanador P M *et al* 2020 *Phys. Rev. A* **101** 043410
[5] Abanador P M and Thumm U 2020 *Phys. Rev. A* **102** 053114

Angular dependence of the Wigner time delay upon tunnel ionization of H_2

D Trabert[1]*, K Fehre[1], N Anders[1], A Geyer[1], S Grundmann[1], M S Schöffler[1], L Ph H Schmidt[1], T Jahnke[1], R Dörner[1], M Kunitski[1], and S Eckart[1]†

[1]Institut für Kernphysik, Goethe Universität, Frankfurt am Main, 60438, Germany

Synopsis We show experimental data on the Wigner time delay for tunnel ionization of H_2 molecules and demonstrate its dependence on the emission direction of the electron with respect to the molecular axis. To understand the microscopic origins of the changes of the Wigner time delay, we present a simple model which shows very good agreement with our experimental findings.

When a very strong light field is applied to a molecule an electron can be ejected by tunneling [1]. In order to quantify the time-resolved dynamics of this ionization process, the concept of the Wigner time delay can be used [2]. We find that the Wigner time delay depends on the tunneling direction of the electron relative to the molecular axis.

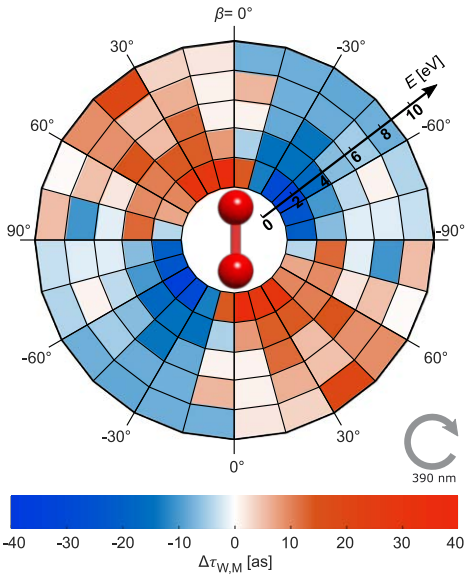

Figure 1. Experimentally retrieved changes of the Wigner time delay, $\Delta\tau_{W,M}$ as a function of the electron energy E and β (relative angle between electron momentum vector and the molecular axis of H_2 in the polarization plane).

Our experimental findings are based on our results [3] from studying single ionization of molecular hydrogen in the strong field regime. We use a corotating circular two-color (CoRTC) laser field (780 nm 390 nm) that is dominated by the second harmonic [4, 5]. The three dimensional momenta of the fragments are recorded using Cold Target Recoil Ion Momentum Spectroscopy (COLTRIMS) as experimental technique [6]. We investigate sub-cycle interferences in the measured electron momentum spectra as a function of the molecular orientation by using the technique of holographic angular streaking of electrons (HASE) [7]. We find, that the observed changes in the Wigner time delay can be quantitatively explained by elongated/shortened travel paths of the emitted electrons, which occur due to spatial shifts of the electrons' birth positions after tunneling. Our work provides an intuitive perspective towards the Wigner time delay in strong-field ionization.

References

[1] Keldysh L W 1965 *Sov. Phys. JETP* **20** 1307
[2] Wigner E P 1955 *Phys. Rev.* **98** 145
[3] Trabert D *et al* 2021 *Nat. Commun.* **12** 1697
[4] Han M *et al* 2018 *Phys. Rev. Lett.* **120** 073202
[5] Eckart S *et al* 2020 *Phys. Rev. A* **102** 043115
[6] Jagutzki O *et al* 2002 *IEEE Trans. Nucl. Sci.* **49** 2477
[7] Eckart S 2020 *Phys. Rev. Research* **2** 033248

*E-mail: trabert@atom.uni-frankfurt.de
†E-mail: eckart@atom.uni-frankfurt.de

Angular emission distribution of O 1s photoelectrons of uniaxially oriented methanol

L Kaiser[1], K Fehre[1], N M Novikovskiy[2,3], J Stindl[1], D Tsitsonis[1], G. Gopakumar[4], I Unger[4,5], J Söderström[4], O Björneholm[4], M Schöffler[1], T Jahnke[1], R Dörner[1], F. Trinter[1,5,6 *] and Ph V Demekhin[2]

[1]Institut für Kernphysik, Goethe-Universität, Max-von-Laue-Str. 1, 60438 Frankfurt am Main, Germany
[2]Institut für Physik und CINSaT, Universität Kassel, Heinrich-Plett-Str. 40, 34142 Kassel, Germany
[3]Institute of Physics, Southern Federal University, 344090 Rostov-on-Don, Russia
[4]Department of Physics and Astronomy, Uppsala University, Box 516, 75120 Uppsala, Sweden
[5]Deutsches Elektronen-Synchrotron DESY, Notkestr. 85, 22607 Hamburg, Germany
[6]Molecular Physics, Fritz-Haber-Institut der Max-Planck-Gesellschaft, Faradayweg 4-6, 14195 Berlin, Germany

Synopsis We present the angular emission distribution of O 1s photoelectrons of uniaxially oriented methanol and show the corresponding experimental and theoretical three-dimensional molecular-frame photoelectron angular distributions.

The angular distribution of O 1s photoelectrons emitted from uniaxially oriented methanol is studied experimentally and theoretically [1]. We employed circularly polarized photons of an energy of $h\nu$ = 550 eV for our investigations. We measured the three-dimensional photoelectron angular distributions of methanol, with the CH_3—OH axis oriented in the polarization plane, by means of cold target recoil ion momentum spectroscopy [2]. The experimental results are interpreted by single active electron calculations performed with the single center method [3]. A comparative theoretical study of the respective molecular-frame angular distributions of O 1s photoelectrons of CO, performed for the same photoelectron kinetic energy and for a set of different internuclear distances, allows for disentangling the role of internuclear distance and the hydrogen atoms of methanol as compared to carbon monoxide.

We will present the predicted emission distributions of O 1s photoelectrons of CO, computed for circularly polarized light with negative helicity and a photoelectron kinetic energy of 8.5 eV at different internuclear distances, the comparison of the molecular-frame photoelectron angular distributions (MFPADs) of O 1s photoelectrons of CO and CH_3OH, at the equilibrium internuclear distance $R_{C-O} = R_{CH3-OH}$ = 2.696 a.u. of CH_3OH, the comparison of the measured and computed two-dimensional MFPADS of O 1s photoelectrons of methanol, as well as the comparison of the measured and computed three-dimensional MFPADs of O 1s photoelectrons of methanol (see Fig. 1).

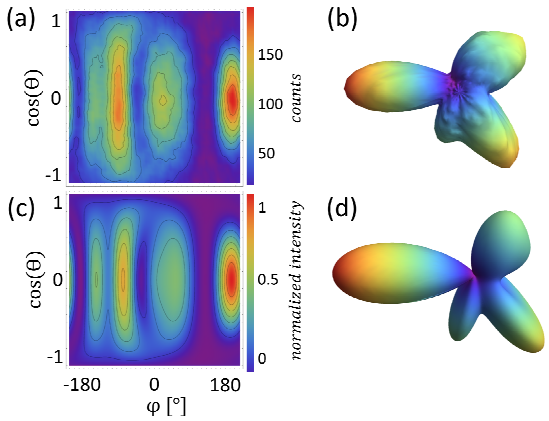

Figure 1. Comparison of the measured [(a) and (b)] and computed [(c) and (d)] three-dimensional MFPADs of O 1s photoelectrons of methanol, obtained for circularly polarized light with negative helicity and photoelectron kinetic energy of 8.5 eV. In panels (b) and (d), the light propagates out of the page plane (the polarization plane), and the molecule is oriented horizontally with the OH^+ ion pointing to the right. Panels (a) and (c) show the same three-dimensional MFPADs in a color-map representation as functions of the polar and azimuthal angles.

References

[1] Kaiser L *et al* 2020 *J. Phys. B: At. Mol. Opt. Phys.* **53** 194002
[2] Dörner R *et al* 2000 *Phys. Rep.* **330** 95
[3] Demekhin Ph V *et al* 2011 *J. Chem. Phys.* **134** 024113

* E-mail: trinter@atom.uni-frankfurt.de

Atomic-resolution of momentum spectrum from tunnel ionization for the study of ionization-induced hole localization

I. S. Wahyutama[1] *, K. Lopata[2,3], M. B. Gaarde[1], and K. J. Schafer[1]

[1]Department of Physics and Astronomy, Louisiana State University, Baton Rouge, Louisiana 70803, US
[2]Department of Chemistry, Louisiana State University, Baton Rouge, Louisiana 70803, USA
[3]Center for Computation and Technology, Louisiana State University, Baton Rouge, Louisiana 70803, USA

Synopsis We use weak-field adabatc theory (WFAT) to disentangle the atomic contributions to the momentum spectrum of molecular tunnel ionization in C_6HBr. We find that when the molecular axis forms an angle of 22° with a DC force that points from H to Br, ionization happens exclusively from the Br atom. When the molecule is flipped, the ionization decreases and most electrons come from H and the two neighboring C atoms. This result can be helpful in studies that require reliable information on which atoms are most likely to contribute to tunnel ionization, such as in charge migration studies.

Tunnel ionization plays an important role in strong field processes such as ionization and high harmonic generation. Owing to its exponential sensitivity to electron binding energies, tunnel ionization can potentially be utilized as a tool to create a localized hole in molecules.

In this work, we demonstrate how we can choose which site in a molecule we want almost all ionizations to occur by involving halogen and choosing certain field-molecule orientation. In Fig. 1, using integral representation of WFAT [1] we show the transverse momentum distribution (TMD) [2] of ionized electrons from C_6HBr molecule oriented at 22° (upper half) and 156° (lower half) relative to a DC field of magnitude 0.02 a.u. pointing in the positive z direction. In the upper half, when the force points from H to Br ends, we can see that effectively all electrons are ionized from around Br atom. When the force points from Br to H end (lower half), most electrons come from C atom indicated by the number 7 with some visible contributions from the neighboring C and H atoms.

This observation demonstrates that it is possible to concentrate ionization only around a particular atom in a molecule if we place a halogen at the desired site and orient the molecule such that the halogen is at the side where it is intuitively the easiest to pull an electron from. This behavior may be employed in, e.g. charge migration studies where researchers desire a way to reliably create an initial localized hole. When the hole has started to propagate, it can also be useful in the study of the hole dynamic using ionization probe to see how the dynamic affects the atomic contribution.

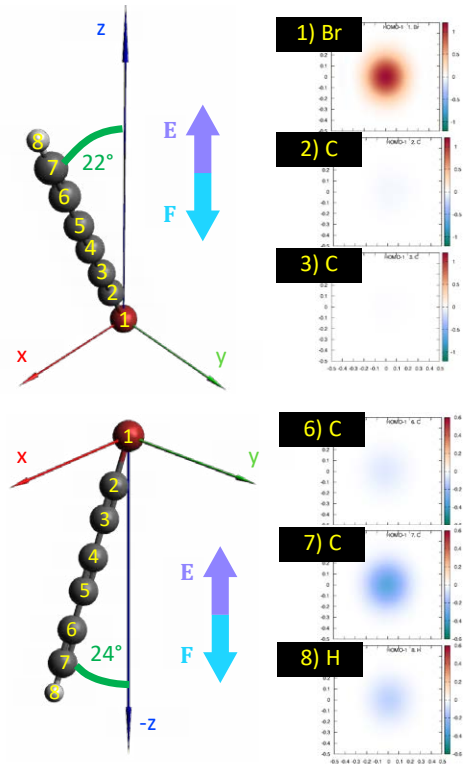

Figure 1. Atom-resolved TMD for orientations where the force points from H end to Br end (upper half) and where it points from Br to H (lower half). The contributions from other atoms not shown are vanishing.

References

[1] A. I. Dnestryan and O. I. Tolstikhin 2016 *Phys. Rev. A* **93**, 033412.
[2] V. N. T. Pham *et al* 2014, *Phys. Rev. A* **89** 033426.

* E-mail: wahyutama1@lsu.edu

Intramolecular hydrogen transfer in gas-phase DNA induced by site-selected resonant core excitations

X Wang[1, *], S Rathnachalam[1], K Bijlsma[1], W Li[1], V Zamudio-Bayer[2,3], M Kubin[2], M Timm[2], B von Issendorff[3], J. Tobias Lau[2], R Hoekstra[1], S Faraji[1], T Schlathölter[1, †]

[1] ZIAM, University of Groningen, Nijenborgh 4, 9747AG Groningen, The Netherlands
[2] Helmholtz Zentrum Berlin für Materialien und Energie, 12489 Berlin Germany.
[3] Physikalisches Institut, Universität Freiburg, 79104 Freiburg, Germany

Synopsis We present experimental evidence for intramolecular hydrogen transfer in d(^{F}UAG) tri-oligonucleotides in the gas phase. Soft X-ray partial ion yield spectroscopy reveals hydrogen migrations towards the nucleobases from the sugar-phosphate backbone in the process of resonant core de-excitations. We identify the most plausible intramolecular hydrogen bonds in the system by DFT calculations of ground state geometry structures and non-covalent interactions. It is likely that these bonds play a key role in the hydrogen transfe processr.

Hydrogen bonding, as one of the most important weak chemical interaction, widely exist in all kinds of biomolecules, such as proteins and DNA, which play an important role in many biological process [1]. Hydrogen migrations can happen along intermolecular or intramolecular hydrogen bonds, as an efficient way of energy relaxation in DNA [2].

In this work, we employ partial ion yield spectroscopy to investigate [d(^{F}UAG)+H]$^{+}$ photofragmentation at the P L-edge and an the C, N, O and F K-edges. We focus on hydrogen transfer as stimulated by resonant soft X-ray absorption. The experimental quantity of interest is the relative intensity of nucleobase fragments B^{+} and BH^{+}, formed by glycosidic bond cleavage accompanied bysingle and double hydrogen transfer, respectively.

A^{+}, AH^{+}, G^{+} and GH^{+} are the main photon induced products and their spectra exchibit very similar resonances partial ion yield spectra at the C, N, O, F and P inner shell edges. TD-DFT core excitation calculations are in good agreement with this experimental data [3].

The ratio between B^{+} and BH^{+} yields reflects the DNA excited-state dynamics as it is a measure for the relative strength of the second H transfer channel. Resonances in the B^{+}/BH^{+} spectrum are a clear indication for resonant X-ray induced hydrogen migrations. As a consequence, hydrogen bonds appear to play a critical role in soft X-ray induced dynamics of DNA where they act as a bridge for molecular exited-state decay.

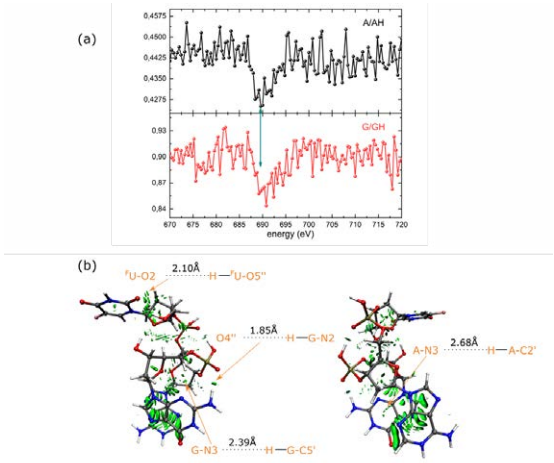

Figure 1. (a) Fragment ion yield ratios of [d(^{F}UAG)+H]$^{+}$, induced by fluorine K-edge X-ray photons (A=adenine, G=guanine). The green arrow shows more hydrogen transfer to the nucleobases by resonant X-ray absorptions (b) non-covalent interaction surfaces of [d(^{F}UAG)+H]$^{+}$, four nucleobase-related hydrogen bonds are indicated.

References

[1] Šponer, J et al 2001 Biopolymers: Original Research on Biomolecules, 61(1), 3-31.
[2] Schultz, T et al 2004 Science, 306(5702), 1765-1768.
[3] Wang, X et al 2021 PCCP (submitted)

* E-mail: xin.wang@rug.nl
† E-mail: t.a.schlatholter@rug.nl

Light-induced dissociation dynamics of Br_2

T Wang[1*], Z Dube[1], Y Mi[1], X Ding[1,2], G Ernotte[1], B Bergues[1,3,4], A S Johnson[5], C Vozzi[6], A Yu Naumov[1], D M Villeneuve[1], P B Corkum[1], and A Staudte[1 †]

[1]Joint Attosecond Science Laboratory, NRC & University of Ottawa, 100 Sussex Drive, Ottawa, Canada
[2]University of Michigan, Ann Arbor, Michigan 48109, USA
[3]Physics Department, Ludwig-Maximilians-Universität Munich, Am Coulombwall 1, 85748 Garching, Germany
[4]Max Planck Institute of Quantum Optics, Hans-Kopfermann-Straße 1, 85748 Garching, Germany
[5]ICFO, Barcelona Institute of Science and Technology, 08860, Castelldefels, Barcelona, Spain
[6]Istituto di Fotonica e Nanotecnologie, CNR, Italy

Synopsis By using Cold Target Recoil Ion Momentum Spectroscopy and a pump-probe experiment, we follow the breaking of a molecular bond and simultaneously the separation of atoms in dissociating Br_2 by observing single and double ionization processes. In the same experiment we can also follow the vibrational wave packet dynamics in the Br_2^+ molecular ion.

When a chemical bond breaks, the valence electrons in the bond re-arrange and, consequently, also the atoms in a molecule re-arrange and separate. Coulomb explosion imaging (CEI) is widely regarded as a very sensitive probe to study molecular geometry, because the observable ion kinetic energy from a Coulombic repulsion is very sensitive to the internuclear distance [1]. However, imaging changes in the molecular geometry does not necessarily reveal insight into the underlying electronic re-arrangement.

Here, using Cold Target Recoil Ion Momentum Spectroscopy (COLTRIMS) and a pump-probe experiment on the Br_2 molecule we show that the actual bond breaking occurs on a time scale that is not differentiated with CEI.

For the experiment we use a weak, linearly polarized, 400nm, 40fs pump pulse and a strong, linearly polarized, 800nm, 25fs probe pulse. A single photon absorption at 400nm couples the X with the C state of Br_2. The excited Br_2 then dissociates and is probed with photo ionization [2]. Fig.1(a) shows the Br^+ energy spectrum vs pump probe delay. Region A results from single ionization and reflects the chemical bond breaking [2], while region B is caused by double ionization and measures the separation distance of neutral dissociating bromine molecule.

For negative delays we monitor the vibrational wave packet on the manifold of bound states of the molecular ion, shown in Fig.1(b), There is a clear oscillation structure with about 100fs oscillating period in the negative delay time range, which means several bound state Br_2^+ wave packets are created [3] by the strong 800nm pulse and then are probed by the weak 400nm pulse.

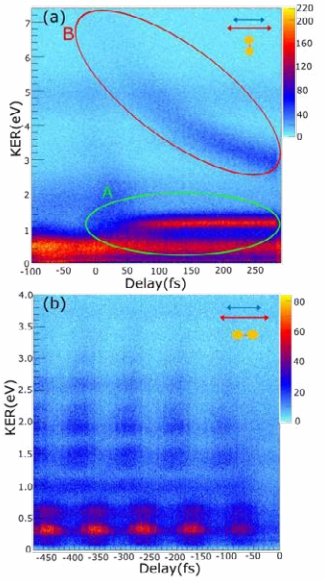

Figure 1 Br^+ yield as a function of pump-probe delay and kinetic energy of the detected Br^+. a) Region A: Br^+ from single ionization of dissociating Br_2. Region B: Br^+ from doubly ionized Br_2. b) Br^+ from Br_2^+.

References

[1] M. Pitzer *et al*, Science **341**, 1096 (2013).
[2] W. Li *et al,* PNAS **107**, 20219 (2010).
[3] Y. Kobayashi *et al,* Phys. Rev. A **102**, 051102 (2020).

* E-mail:twang110@uottawa.ca
† E-mail: andre.staudte@nrc.ca

Soft X-ray induced excitation, ionization, and fragmentation of isoxazole at the K-edges

T. J. Wasowicz[1*], A. Kivimäki[2,3], and R. Richter[4]

[1]Division of Complex Systems Spectroscopy, Gdansk University of Technology, 80-233 Gdańsk, Poland
[2]Nano and Molecular Systems Research Unit, University of Oulu, P.O. Box 3000, 90014 Oulu, Finland
[3]MAX IV Laboratory, Lund University, P.O. Box 118, 22100 Lund, Lund Sweden
[4]Elettra – Sincrotrone Trieste, Area Science Park Basovizza, 34149 Trieste, Italy

Synopsis Excitation, ionization, and fragmentation of isoxazole (C_3H_3NO) have been investigated experimentally using the near edge X-ray absorption fine structure (NEXAFS), ion time-of-flight (TOF) spectrometry combined with pulsed-field ionization, and the photoelectron-photoion coincidence (PEPICO) technique.

Various molecules that play a significant role in many different fields of chemistry, medicine, and biology contain heterocyclic rings with oxygen and nitrogen heteroatoms. One of such bioactive compounds is isoxazole. It is a prototypical molecule due to its distinctive ring structure consisting of one oxygen atom and one nitrogen atom at adjacent positions. For that reason, isoxazole has specific electronic properties and chemical reactivity that cause, for example, unique photodissociation mechanisms [1]. Despite the importance of this molecule in the synthesis of new pharmaceuticals and agrochemicals, the literature concerning its electronic structure and decomposition mechanisms is scarce.

Therefore, the present work explores the ionization and fragmentation of inner-shell excited isoxazole molecules at the photon energies encompassing the C, N, and O *K*-edges. The experiments were performed at the Gas Phase beamline of the Elettra synchrotron radiation laboratory (Trieste, Italy) utilizing a TOF mass spectrometer modified for pulsed-field ionization measurements [2], [3].

The total ion yields (TIY) were first measured at each inner-shell edge without field ionization. Secondly, the total yields of high-Rydberg (HR) fragments and energetic photons were recorded exploiting field ionization in the spectrometer, while suppressing cations produced in the interaction region. As an example, Figure 1a) shows such yields recorded at the C1s edge of isoxazole. The HR yield (blue curve) resembles the TIY (black curve) only in the region of the C 1s resonances. Above the C 1s ionization potential (IP), prominent bands occur that are attributed to the production of neutral fragments in HR states. To identify the HR fragments and fragmentation processes, PEPICO spectra (Fig. 1b) have been measured, and for comparison, the TOF spectra were also measured at the selected energies using pulsed field ionization (see Fig. 1c).

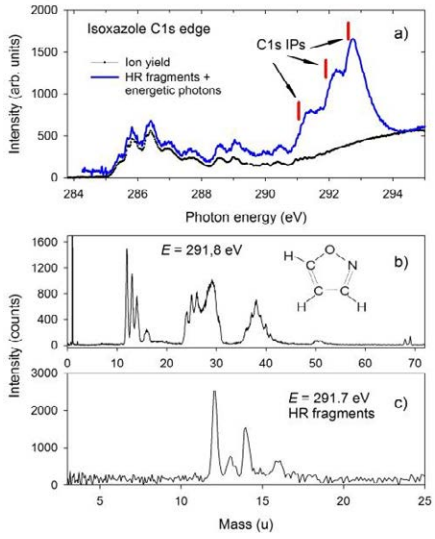

Figure 1. a) The total ion yield (TIY) of isoxazole measured near the C1s edge without field ionization and the total yield of HR fragments obtained after applying field ionization. b) A typical mass spectrum measured just above the first C1s IP. c) Field ionization mass spectrum of neutral HR fragments.

References

[1] Zubek M *et al* 2014 *J. Chem. Phys.* **141** 064301
[2] Kivimäki A *et al* 2015 *J. Chem. Phys.* **143** 114305
[3] Kivimäki A *et al* 2021 *J. Phys. Chem. A* **125** 713

* E-mail: tomasz.wasowicz1@pg.edu.pl

Dissociative photo-double-ionization of tetrahydropyran and 3,4-dihydropyran

T. J. Wasowicz[1*], A. Kivimäki[2,3], and R. Richter[4]

[1]Division of Complex Systems Spectroscopy, Gdansk University of Technology, 80-233 Gdańsk, Poland
[2]Nano and Molecular Systems Research Unit, University of Oulu, P.O. Box 3000, 90014 Oulu, Finland
[3]MAX IV Laboratory, Lund University, P.O. Box 118, 22100 Lund, Lund Sweden
[4]Elettra – Sincrotrone Trieste, Area Science Park Basovizza, 34149 Trieste, Italy

Synopsis Dissociative photo-double-ionization of tetrahydropyran ($C_5H_{10}O$) and 3,4-dihydropyran (C_5H_8O) molecules, whose structures differ in one C=C double bond, has been studied in the 23-35 eV energy range using vacuum ultraviolet (VUV) synchrotron radiation excitation combined with ion time-of-flight (TOF) spectrometry and photoelectron-photoion coincidence (PEPICO) technique.

Small changes in the structure of molecules can invoke substantial modifications in their physico-chemical properties. For instance, during hydrogenation of furan, a five-membered aromatic compound consisting of four carbon atoms and one oxygen atom, four hydrogen atoms are attached and two double C=C bonds are lost, whereby the molecule becomes tetrahydrofuran. This bond rearrangement modifies the aromaticity of the new molecule and, in general, gives decreased stability compared to furan.

In the present communication, we will discuss whether an even smaller change in the bond rearrangement will modify the stability of a new molecule compared to a previous arrangement with a similar set of atoms. In particular, we provide results on the dissociative photo-double-ionization of the six-membered heterocyclic molecules containing oxygen, namely tetrahydropyran (THP, $C_5H_{10}O$) and 3,4-dihydropyran (DHP, C_5H_8O). DHP has a non-aromatic ring with five carbon atoms and one oxygen atom. It contains one double bond. By removing the double bond by two more hydrogen atoms, we get a saturated six-membered ring of tetrahydropyran. The experiments were carried out at the Gas Phase Photoemission beamline at the Elettra-Sincrotrone radiation facility exploiting VUV excitation and ion time-of-flight spectrometer [1] utilizing the PEPICO technique.

Double ionization produces a doubly charged parent ion and two correlated electrons. These doubly charged ions are usually very reactive, short-living species that easily dissociate into ionic fragments through many-body fragmentation. Several well-resolved dissociation channels have been identified in the coincidence maps of both molecules (Figures 1a and b), and their coincidence yield curves have been obtained in the photon energy range from their appearance energies up to 35 eV (see Figures 1c and d). The present experimental study aims at elucidating the mechanisms of these dissociation channels in DHP and THP. In particular, we will show how the character of the bond arrangement in DHP and THP influences the generation of two- and three-body charge separation reactions occurring at the lowest energies.

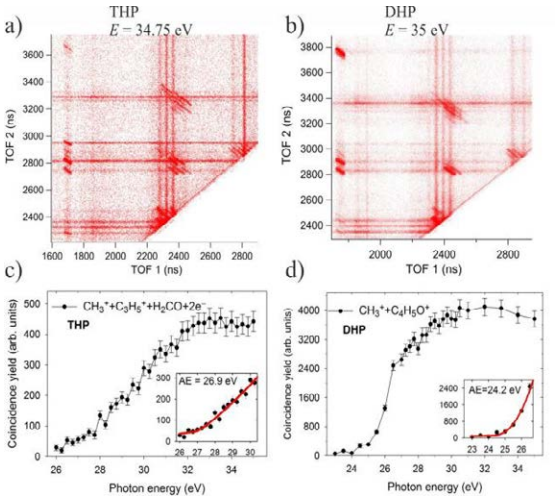

Figure 1. A typical coincidence map of a) THP measured at 34.75 eV and b) DHP measured at 35 eV. Panels c) and d) show the coincidence yields and appearance energies of the lowest energy fragmentation channels triggered by double ionization in each molecule.

References

[1] Kivimäki A *et al* 2015 *J. Chem. Phys.* **143** 114305

* E-mail: tomasz.wasowicz1@pg.edu.pl

Angularly Resolved Photoelectron Spectra from Photoionized Benzene

N L Wong[1] *, J Howard[1], E Sokell[1] †, P Bolognesi[2] and L Avaldi[2]

[1]School of Physics, Science Centre North, University College Dublin, Belfield Dublin 4, Ireland
[2]CNR-Istituto di Struttura della Materia, Area della Ricerca di Roma 1, 00015 Monterotondo Scalo, Italy

Synopsis A set of hemispherical electron energy analyzers provided angle resolved single photoelectron spectra (PES) of benzene (C_6H_6). Analysis of the spectra is planned to examine the spectra's relation to electron emission angle. Designs for a new spectrometer to further investigate the photoionization of benzene and other carbon containing molecules are presented.

Aromatic hydrocarbons are characterized by a planar structure with overlapping π molecular orbitals and delocalized electrons, and a standard example is benzene. Aromatic hydrocarbons have exhibited interesting properties, such as superconductivity at high temperatures [1] and excellent thermal properties; and the molecules are important to biological and astronomical processes, as well as combustion.

The work presented was accomplished at the GasPhase Beamline at Elettra. Outside the vacuum chamber, a test tube held the liquid benzene, which was freeze-pump-thawed to remove gases. After heating, the benzene flowed through a gas line into the interaction region, where the spot diameter of the linearly polarized photon beam was ~200 μm.

Within the experimental chamber, 10 hemispherical electron energy analyzers are mounted 30 degrees apart in groups of 3 and 7 on two independent frames. The two frames were positioned in the perpendicular plane, and [2] describes the apparatus and triple differential cross section acquisition method in more detail.

Figure 1. displays the PES of benzene recorded at a photon energy of 80eV, by 6 of the 7 analyzers mounted on the same frame. The curves in Figure 1 have not been internormalized nor has the transmission efficiency of the analyzers been accounted for yet. It has been suggested that the PES could inform the electron angle of emission [3], so the data processing will also investigate the connection. Previous studies have not looked at the angular distribution of the photoelectron emission in this way.

A new spectrometer design is planned to further investigate the photoionization of benzene

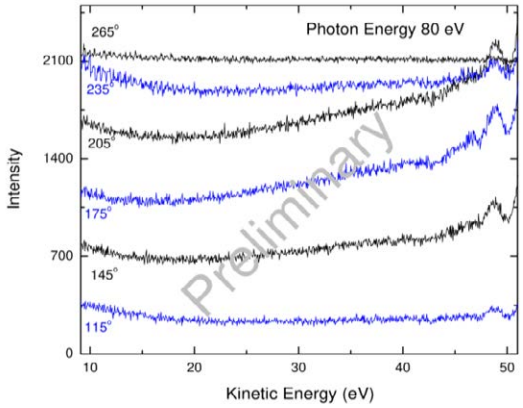

Figure 1. Preliminary PES from 80 eV photoionized benzene for 6 analyzers in kinectic energy vs intensity in counts. The angle of each analyzer is with respect to the polariziton axis of the light.

in conjunction with the development of a lab-based soft x-ray (SXR) source. Coincidence velocity-map imaging (VMI) is the primary candidate for the spectrometer, because the method can measure the TOF and velocity distribution of photoproducts [4,5]. Several configurations of coincidence VMI with photoionizing SXRs exist and inform the design of the new spectrometer [4,5,6].

References

[1] Rosseinsky M J and Prassides K 2010 *Nature* **464** 39
[2] Bolognesi P *et al* 2004 *J. Of Electron Spectrosc. Relat. Phenom.* **141** 105
[3] Wehlitz R *et al* 2012 *Phys. Rev. Lett.* **109** 193001
[4] Rading L *et al* 2018 *Appl. Sci.* **8** 998
[5] Sztáray B *et al* 2017 *J. Chem. Phys.* **147** 013944
[6] Zhao A *et al* 2017 *Rev. Sci. Instrum.* **88** 113104

* E-mail: nicholas.wong1@ucdconnect.ie
† E-mail: emma.sokell@ucd.ie

Near-infrared strong field induced fragmentation and ionization of toluene captured by ultrafast electron diffraction

Y Xiong[1], K Borne[2], A M Carrascosa[3], S K Saha[1], K J Wilkin[1], M Yang[4] ,S Bhattacharyya[2] , K Chen[2], W Du[3], L Ma[3] , N Marshall[2] , J P F Nunes[1], S Pathak[2], Z Phelps[2], X Xu[3], H Yong[3], K Lopata[4], P M Weber[3], A Rudenko[2], D Rolles[2], M Centurion[1]

[1]University of Nebraska-Lincoln, Lincoln, Nebraska, 68588, USA
[2]Kansas State University, Manhattan, Kansas, 66506, USA
[3]Brown University, Providence, Rhode Island, 02912, USA
[4]Louisiana State University, Baton Rouge, Louisiana, 70803, USA

Synopsis The fragmentation products of strong-field ionized toluene are determined using ultrafast electron diffraction and momentum-resolved time of flight ion mass spectrometry.

Gas phase ultrafast electron diffraction (UED) has been successfully applied to capture structural dynamics in neutral molecules photo-excited by femtosecond laser pulses, but so far UED has not been applied to study dynamics in ionized molecules. Here we present an investigation of ionization, fragmentation and isomerization of toluene by a near-infrared intense femtosecond laser pulse. We use momentum-resolved coincidence time-of-flight ion mass spectrometry (TOF-MS) to determine the main reaction products and relative yields of toluene cations, and a 90 kilo-electron-volt gas phase UED setup to distinguish structural isomers, and to determine the structure and relative yields of the ionized molecules generated from toluene. With the help of *ab initio* electron scattering calculation, the UED measurement can determine the absolute yield of the main reaction channels, including isomers. The UED retrieved yields are in in a good agreement with the TOF-MS measurement. The electron diffraction signal is in good agreement with *ab initio* scattering calculation, while scattering computations based on independent atom model are not able to provide a good approximation for scattering from ions. These results demonstrate an avenue for combining UED and TOF-MS measurements, and opens the door to studying structural dynamics triggered by ionization.

E-mail: ywxiong@huskers.unl.edu

The investigations of excitation dynamics of the inner-shell excitation of the nitrogen

Yuan-Chen Xu[1], Xiao-Jiao Du[1], Li-Han Wang[1] and Lin-Fan Zhu[1]*

[1]Hefei National Laboratory for Physical Sciences at Microscale and Department of Modern Physics, University of Science and Technology of China, Hefei, Anhui 230026, People's Republic of China

Synopsis The energy levels and dynamic parameters of atoms and molecules are the fundamental physical properties and the basic issues for atomic and molecular physics. The excitation dynamics of the inner-shell excitation of the nitrogen has been investigated by electron scattering and inelastic X-ray scattering method.

As the primary atmosphere constituent of Earth and some satellites such as Titan and Triton, the dynamic parameters of nitrogen molecule plays an important role in understanding the nature of the atmosphere [1, 2]. The dynamic parameters for the inner-shell excitations of nitrogen are of great significance to the obtaining the structure information of nitrogen molecule. Furthermore, nitrogen molecule is one of the homonuclear diatomic molecules, and thus photon-impact and electron-impact studies are of interest from the viewpoint of atomic and molecular spectroscopy. Electron impact and X-ray scattering are useful tools for the study of inner-shell core excited states of molecules and can provide much information about spectroscopic energies, structural parameters, vibrational states and resonant structures.

In this work, the generalized oscillator strengths (GOSs) of the inner-shell excitations of nitrogen have been determined by X-ray scattering method in Shanghai Synchrotron Radiation Facility. Besides, the optical oscillator strength (OOS) has been obtained by extrapolating the GOSs to the limit of the squared momentum transfer $K^2 \rightarrow 0$. The GOS of the $1s \rightarrow 1\pi_g$excitation of nitrogen are shown in the Fig.1.

In addition, although valence electrons are clearly delocalized in molecular bonding frameworks, researchers have long debated whether the core vacancy created in a homonuclear diatomic molecule by absorption of a single x-ray photon is localized on one atom or delocalized over both [3, 4, 5]. In this work, the electron energy loss spectra of the inner shell excitations $1\sigma_{g/u} \rightarrow 1\pi_g$ of nitrogen have been measured at different scattering angle with an incident electron energy of 1500 eV. With the aid of peakfit software, the splitting value of inner shell excitations $1\sigma_{g/u} \rightarrow 1\pi_g$ is obtained to be about 90 meV which supports the hypothesis that the electrons in the inner shell of nitrogen molecules are delocalized.

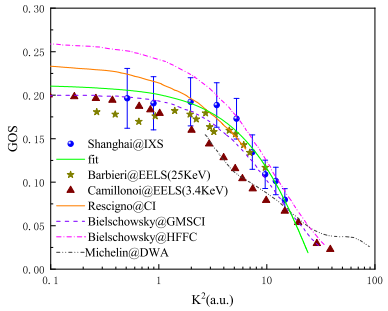

Figure 1. The GOSs of the inner shell excitation of nitrogen.

References

[1] D. J. Strickland *et al* 1999 *J. Quant. Spectrosc. Radiat. Transfer* **62** 689
[2] D. B. Jones *et al* 2006 *Planet. Space Sci.* **54** 45
[3] M. S. Schöffler *et al* 2008 *nature* **320** 920
[4] J. Adachi *et al* 2007 *J. Phys. B* **40** F285
[5] M. Ehara *et al* 2006 *J. Chem. Phys.* **124** 124311

*E-mail: lfzhu@ustc.edu.cn

Femtosecond Dynamics of Solvated Biomolecules Studied by Flat-jet X-ray Absorption Spectroscopy

Z Yin[1 *], Y P Chang[2], T Balciunas[2], Y Shakya[3,4], G Fazio[1], L Inhester[3], R Santra[3,4,5], J P Wolf[2], and H J Wörner[1†]

[1]Laboratorium für Physikalische Chemie, ETH Zürich, 8093 Zürich, Switzerland
[2]GAP-Biophotonics, Université de Géneve, 1205 Geneva, Switzerland
[3]Center for Free-Electron Laser Science, DESY, Notkestrasse 85, 22607 Hamburg, Germany
[4]Department of Physics, Universität Hamburg, Jungiusstrasse 9, 20355 Hamburg, Germany
[5]Hamburg Centre for Ultrafast Imaging, Luruper Chaussee 149, 22761 Hamburg, Germany

Synopsis Photoinduced excitation and ionization of matter are essential for a wide range of bio-chemical phenomena. In many cases, multiphoton ionization can lead to ultrafast structural dynamics, which constitutes an experimental challenge to follow in real-time, due to to the lack of sufficient time resolution. Here, we present experimental evidence of coupled electron-nuclear dynamics in a solvated biomolecule utilizing a water window high-harmonic-generation source coupled with a sub-µm thin flat jet. Theoretical simulations support the observation of valence-hole-induced structural dynamics.

Light-induced dynamics are essential for various bio-chemical processes, like e.g. vision [1]. However, it is experimentally challenging to follow associated ultrafast reaction processes in real-time.

In this work, we present femtosecond time-resolved X-ray absorption spectroscopy (trXAS) of aqueous urea (CH_4N_2O) solution utilizing a high-harmonic-generation (HHG) source covering the essential carbon and nitrogen edges as depicted in Figure 1. The inherently broadband HHG pulse allows to probe both edges simultaneously and is therefore ideal for XAS [2]. XAS is an element and site-specific method and very popular in investigating the electronic properties of matter including intermolecular dynamics in a liquid environment [3]. Furthermore, we utilized a sub-µm thin flat jet to record artefact-free XAS in transmission mode [4]. The time-resolved results on the C and N K-edge contain complementary information about the ionization-induced chemical dynamics. A distinct feature is a blue shift of a band at the carbon K-edge. The shift occurs within the first 700 fs before it stabilizes, which we attribute to chemical dynamics like proton dynamics originating from biomolecular interactions with its environment. Theoretical simulations and XAS calculations of several urea dimers and urea-water geometries can reproduce the main spectral features and support the experimental findings. The theoretical results indicate that charge dynamics drive the structural rearrangement and leave geometric specific spectral fingerprints on the electronic properties.

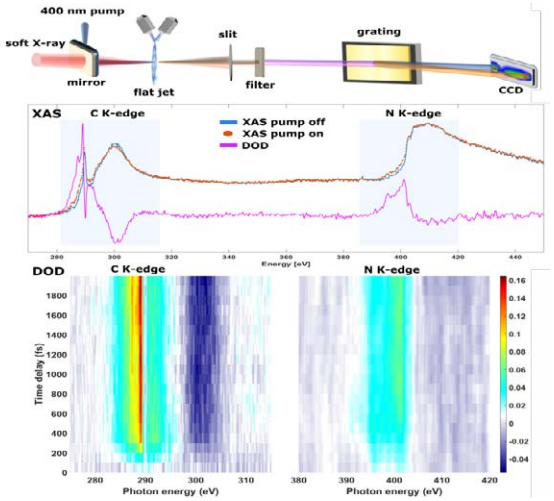

Figure 1. Top: Illustration of the experimental scheme. An intense 400 nm pump creates a valence hole on the sample and then probed by a delayed soft X-ray pulse. **Middle:** The X-ray absorption spectrum of 10 M urea solution at the carbon and nitrogen K-edges with (orange), without pump (blue) and the integrated difference (pink). **Bottom:** Time resolved DOD signal on the carbon and nitrogen K-edge indicating spectral features arising from coupled electronic-nuclear dynamics.

References

[1] Kumpulainen T *et. al.* 2017 *Chem. Rev.* **117** 10826–108939
[2] Smith A D, et. al. 2020 J. Phys. Chem. Lett. **11** 1981–1988
[3] Smith J W, et. al. 2017 Chem. Rev. **117**, 13909-13934
[4] Yin Z et al, 2020 J. Phys. Photonics **2**, 044007

* E-mail: yinz@ethz.ch, † E-mail: hansjakob.woerner@phys.chem.ethz.ch

The Laser-driven Anharmonic Oscillator: Ground-state dissociation of the Helium hydride molecular ion by mid-infrared pulses

B. Ying,[1,2] P. Wustelt[1,2] , M. Kübel,[1,2] F. Oppermann,[3] S. Mhatre[4], L. Yue,[4] A. Max Sayler,[1,2] M. Lein,[3] S. Gräfe,[4] and G. G. Paulus[1,2*]

[1]Institute of Optics and Quantum Electronics, Friedrich Schiller University Jena, Germany
[2]Helmholtz Institute Jena, Germany
[3]Institut für Theoretische Physik, Leibniz Universität Hannover, Germany,
[4]Institute of Physical Chemistry, Friedrich Schiller University Jena, Germany

Synopsis Utilizing a diatomic prototype molecular system, HeH^+, we show that mid-infrared laser pulses can drive the nuclear motion in the anharmonic potential of the electronic ground state, increasing its energy above the potential barrier and facilitating dissociation of a diatomic molecule by purely vibrational excitation.

The vibrational motion of molecules is a fundamental example of an anharmonic oscillator. If light couples directly to the vibrational degrees of freedom of the molecule, absorption of photons can transfer population from lower to higher vibrational bound, or even continuum states, while remaining on the same electronic state [1]. The ground electronic surface is of enormous general importance for chemical syntheses which are predominantly carried out on the ground state.

We present a direct measurement of molecular photodissociation of the HeH^+ molecule induced by purely vibrational excitation [2]. Efficient dissociation requires the match of the periodicity of the driving force to the eigenfrequency of the system, which for HeH^+ is 11.5fs. Experimentally, this is realized by combining a molecular ion beam target, coincidence 3D momentum spectroscopy and mid-infrared laser pulses produced by an optical parametric amplifier. The dissociation yield for different periodicities of the driving laser is displayed in Fig.1.

The measured laser-driven dynamics can be adequately described by the intuitive model of a driven anharmonic oscillator. The uneven spacing of vibrational states in the anharmonic potential results in characteristic wavelength dependence of the dissociation probability [3].

We compared the wavelength-dependent response of the helium hydride molecular cation to both classical and quantum mechanical calculations. The very good agreement of the experimental results with both classical and quantum simulations shows that the results can be interpreted applying the anharmonic oscillator analogies and removes any uncertainties through electronic excitation.

Additionally, we examined the measured momenta of the fragments after dissociation. This allows us to identify the different dissociation pathways starting from different vibrational states.

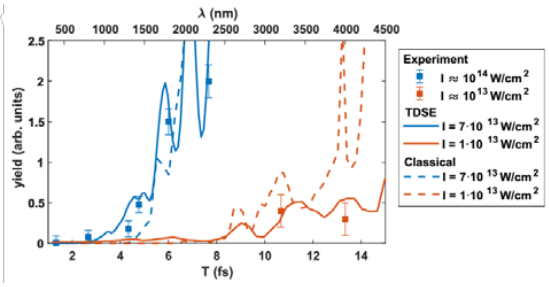

Figure 1. Frequency-dependent response of HeH^+: Yield for the dissociation as function of the periodicity of the driving field and laser wavelength (upper abscissa). Measured results are displayed together with one-dimensional TDSE- and classical simulations.

In conclusion, we have studied experimentally and computationally multiphoton dissociation of HeH^+ on the electronic ground state. Our study provides insight to the rich dynamics of anharmonic quantum oscillator systems and laser-controlled ground-state chemistry.

References

[1] Chelkowski, S. *et al,* 1990. *Phys. Rev. Lett.* **65**, 2355
[2] Wustelt P, *et al.*, 2018 *Phys. Rev. Lett.* **121**, 073203
[3] Ursrey, D. *et al.* 2012, *Phys. Rev. A* **85**, 023429

* E-mail: gerhard.paulus@uni-jena.de

A composite velocity map imaging spectrometer for ions and 1 keV electrons

B Ding[1,2], W Xu[1] , R Wu[1], Y Feng[1], L Tian[1] , and X Liu[1*]

[1]School Physical Science and Technology, ShanghaiTech University, Shanghai 201210, China
[2]University of Chinese Academy of Sciences, Beijing 100049,China

Synopsis Velocity map imaging spectrometer (VMI) is widely used to measure the momentum distribution of the charged particles with the kinetic energy of a few tens of electronVolts. Here, we report on our recently built composite VMI spectrometer that can simultaneously measure both electrons image and ions image. In the SIMION simulation, we extended the electron kinetic energy up to 1 keV at high resolution about 2%, at the same time measure the ions with the kinetic energy of 10 eV. In the tests using monochromatic soft x-ray from Shanghai Synchrotron Radiation Facility and femtosecond laser, we measured the image of electrons with kinetic energies up to 510 eV with a resolution of 1.5%, and the ions image with the kinetic energy of 5.6 eV when the electron arm's maximum detectable energy is 100 eV.

Since the pioneering work of Eppink and Parker[1], velocity map imaging was widely used in atomic and molecular physics. Recently, with the development of the femtosecond laser and the free-electron lasers, scientists find it's more and more necessary to build a VMI spectrometer that is capable of imaging electrons with kinetic energies up to keV or even higher.

To increase the kinetic energy boundary of the VMI spectrometer, several modifications of the standard Eppink-Parker setup have been conducted[2,3]. Here, we report on a composite velocity map imaging spectrometer, which is capable of mapping the electrons with kinetic energies up to 1 keV and low energies ions simultaneously, and experimentally demonstrate imaging of electrons with energies up to 510 eV with a resolution about 1.5%.

To test the performance of the electron arm, we shipped the spectrometer to the bending-magnet beamline BL02B02 at the Shanghai Synchrotron Radiation Facility. The test is done by measuring the photoelectrons image of Ar 2p photoionization with the photon energy tuned from 350 eV to 760 eV. Figure 1(a) show the invert photoelectron image for photoionization of Ar atoms at a photon energy of 760 eV. The corresponding photoelectrons spectrum was shown in Figure 1(b) at different photon energy from 350 to 760 eV. The relative energy resolution is about 1.5% at the energy of 510 eV.

We tested the capabilities of the ion arm with the femtosecond laser. Figure 1(c) shows the inverted momentum image of O^+ ions when the the electron arm's maximum detectable energy is 100 eV. The corresponding kinetic energy spectrum obtained via angular integration of the momentum spectrum within a range of 30° in the direction perpendicular to the laser polarization is shown in Figure 1(d). It needs to be emphasized that, the corresponding resolution of ion arm gets worse when the electron arm's maximum detectable energy increases.

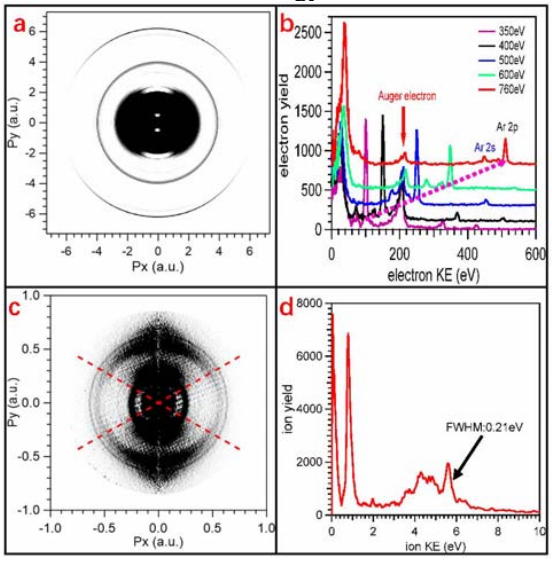

Figure 1. The experiment tests results of composite velocity map imaging. The relative energy resolution is 1.5% at the energy of 510 eV of electron arm, and 3.8% at the energy of 5.6eV of ion arm when the the electron arm maximum detectable energy is 100 eV.

References

[1] Eppink *et al* 1997 *Rev.Sci.Instrum.*68,3477
[2] Kling *et al* 2014 *J.Instrum.*9(05),P05005
[3] Schomas *et al* 2017 *J.Chen.Phys.*147,013942

* E-mail: liuxj@shanghaitech.edu.cn

Efficient extreme-ultrabiolet multi-band high-order wave mixing in silica

F Campi[1 *], S Roscam Abbing[1], A-Y Zhang[1], M van der Geest[1], and P M Kraus[1,2]

[1]Advanced Research Center for Nanolithography, Science Park 106, 1098 XG Amsterdam, The Netherlands
[2]Department of Physics and Astronomy, and LaserLaB, Vrije Universiteit, De Boelelaan 1105, 1081 HV Amsterdam, The Netherlands

Synopsis High-harmonic generation in dielectrics is a recently demonstrated technique that results in extreme-ultraviolet emission, albeit at comparatively lower yield than in gaseous media. In this work, we greatly enhance emission from silica and we relate the observation to multi-band dynamics via a multilevel model.

The recently discovered emission of high-order harmonics from solids [1] under intense laser-pulse irradiation is testing our understanding of strong-field solid-light interactions, while simultaneously opening avenues towards new all-solid coherent short-wavelength table-top sources.

High-harmonic generation from solids holds a strong appeal as a coherent, short-wavelength light source: extreme-ultraviolet pulses generated in solids impose less stringent requirements on the vacuum apparatus, provide a prospective of shrinking down the physical size of setups, and the possibility of high-harmonic generation at higher repetition rates, while exhibiting similar spectral and temporal characteristics as high harmonics generated in gases.

To date, broadband spectra from solids have been generated well into the extreme ultraviolet [2], but the comparatively low conversion efficiencies still lag behind those of gas high-harmonic sources, and have hindered wider-spread applications.

In this contribution, we overcome the low conversion efficiency of all-solid high-harmonic sources through efficient extreme-ultraviolet wave mixing by crossing an intense fundamental 800-nm pulse with its second harmonic under a small angle in a fused silica substrate. We develop a few-level model, which fully reproduces the experimentally observed far-field patterns (Figure 1) as well as the scaling of all extreme-ultraviolet wave mixing orders as a function of driving intensity. Moreover, our model reveals that the laser-driven population transfer between the valence band and the two lowest conduction bands causes the large conversion-efficiency increase. This laser-driven population transfer physically resembles an injection current. Thus our contribution supports the only recently proposed mechanism of injection-current-driven high-harmonic generation [3] as the underlying cause of extreme-ultraviolet emission in solids.

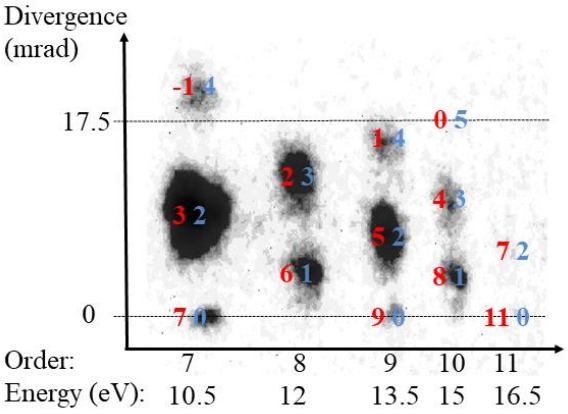

Figure 1. Typical far-field resolved extreme-ultraviolet emission. Numbers on the wave mixing orders indicate the photon combinations of 800-nm (red) and 400-nm (blue) photons that lead to that emission channel.

References

[1] S. Ghimire, et al., *Nature Physics,* **2011**, 7, 138.
[2] T. T. Luu, et al., *Nature*, **2015**, 521, 498.
[3] P. Juergens, et al., *Nature Physics*, **2020**, https://doi.org/10.1038/s41567-020-0943-4.

* E-mail: f.campi@arcnl.nl

Unified real and momentum space collision picture of high-order harmonic generation in solids

R Zuo[1], S Yang[1], X Song[1], W Yang[1], T Meier[2] and M Ciappina[3,4]*

[1]Department of Physics, Shantou University, Shantou, Guangdong 515063, China [2]Department of Physics and Center for Optoelectronics and Photonics Paderborn (CeOPP), University of Paderborn, Warburger Str. 100, D-33098 Paderborn, Germany [3]Physics Program, Guangdong Technion - Israel Institute of Technology, Shantou, Guangdong 515063, China [4]Technion - Israel Institute of Technology, Haifa, 32000, Israel

Synopsis We reveal that, in the electron-hole re-collision model of solid-state high-order harmonic generation (HHG), the electron and its associated hole can elastically scatter by other neighboring atoms when their wavelength approaches the atomic size. We demonstrate that this process can dramatically influence the occurrence of the electron-hole pair recombination, which is the underlying mechanism of the experimentally observed anisotropy in the interband bulk crystal HHG. We link the electron/hole backward (forward) scattering with the Van Hove singularities (critical lines) of the solid band structure.

In the theoretical study of high-order harmonic generation (HHG) from solids, the electron-hole recombination, also known as recollision, has been considered as the main mechanism of interband solid-HHG [1, 2]. Different from atomic HHG, in solid-HHG the electron and the left-behind hole move in periodic potentials, making collisions with other neighboring atoms in the lattice highly probable. Up to date, it's still unclear the underlying mechanisms behind the electron/hole dynamics, i.e. if the electron/hole recombine with the neighboring atoms or if they are scattered away. How all these phenomena possibly affect the high-harmonic emission are open questions.

Here we propose and establish a transparent collision and recombination picture for interband HHG in semiconductors by providing a direct mapping between the band structure and the collision dynamics [3]. Our results support the fact that the electron does not directly recombine with but is scattered by the neighboring atoms. When driven by a linear polarized laser field, the backward scattering of the electron/hole by the neighboring atoms would be facilitated, whereas the forward scattering would be suppressed. Therefore, the recombination of the electron with its associated hole. This mechanism represents the principal reason of the solid-like anisotropic HHG. Moreover, we clarify that delocalization of HHG in solids can be attributed to the fact that the electron and its left-behind hole experience different times of backward scattering. In this way, they recombine at a different atomic sites from the one they were born. Most importantly, our research link the electron/hole backward scattering with Van Hove singularities, and forward scattering with some critical lines in the band structure, thus building a clear mapping between the solid band structure and its harmonic spectrum. Our research gives an unified and whole new explanation of many aspects of previous experimental observations and theoretical findings [2, 4–6].

References

[1] Zaks B *et al* 2012 *Nature* **483** 580
[2] Vampa G *et al* 2015 *Nature* **522** 462
[3] Zuo R *et al* 2021 *submitted*
[4] Osika E *et al* 2017 *Phys. Rev. X* **7** 021017
[5] Reis Y *et al* 2017 *Nat. Phys.* **13** 345
[6] Uzan A *et al* 2020 *Nat. Photon.* **14** 183

*E-mail: marcelo.ciappina@gtiit.edu.cn

Attosecond x-ray transient absorption spectroscopy in graphene

G Cistaro[1] †, L Plaja[2], F Martín[1,3,4] and A Picón[1]

[1]Departamento de Química, Universidad Autónoma de Madrid, 28049 Madrid, Spain
[2]Grupo de Investigación en Aplicaciones del Láser y Fotónica, Departamento de Física Aplicada, University of Salamanca, E-37008, Salamanca, Spain
[3]Instituto Madrileño de Estudios Avanzados en Nanociencia (IMDEA-Nanociencia), Cantoblanco, 28049 Madrid, Spain
[4]Condensed Matter Physics Center (IFIMAC), Universidad Autónoma de Madrid, 28049 Madrid, Spain

Synopsis Real-time observations of the coherent electron dynamics induced by ultrashort light pulses is becoming possible in the last years, thanks to new devices and new experimental techniques. We show a theoretical work that predicts the information that might be extracted from an ATA spectrum in a monolayer of graphene.

Exciting core electrons in condensed matter systems is a promising technique to extract information about the electron dynamics and the geometry of the system, as it has already been explored in atoms and molecules; since core bands are flat in k-space, electrons coming from those are expected to efficiently probe the dynamics of the other electrons that are located close to the Fermi level energy.

Pump-probe techniques are well used nowadays to track the photoinduced dynamics. It consists in the analysis of the response of a system by comparing two different situations: when two laser pulses act and when one of them is switched off.

We performed calculations by evolving the density matrix of graphene by computing the Bloch equations, which also include the core bands, in order to simulate a pump-probe experiment. Here we consider as a probe an attosecond X-ray pulse, which is nowadays possible by the recent advances of HHG laser-based sources. Those pulses excite electrons from core bands, but also they are very short, in the attosecond time scale, which is the "real-time" scale of electron motion; so, this laser pulse takes a "snapshot" of the electron cloud. The other pulse is in the mid-IR regime. On one hand, it excites electrons from valence to conduction around and through the Dirac cone. On the other hand, it drives the electrons coming from the core orbitals within the conduction band.

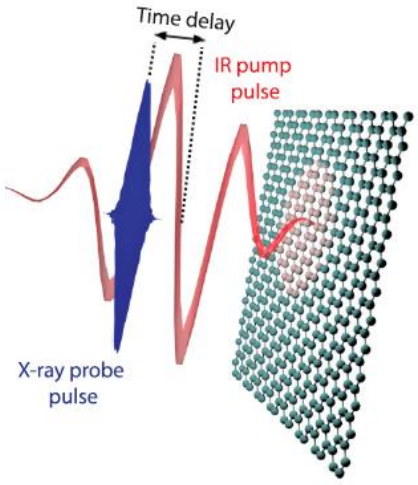

Figure 1. Schematic representation of the pump-probe technique used in this work. An ultra-fast X-ray pulse is sent to the system together with a mid-IR pulse, at different time delays between them.

With the two lasers acting, we can therefore observe the real-time motion of electrons close to the Dirac cone and at the same time probe the coherent motion of electrons in the whole conduction band, in particular at the Van Hove singularities.

References

[1] Cistaro G *et al* 2021 *Physical Review Research* **3.1** 013144

† E-mail: giovanni.cistaro@uam.es

Multi-octave Parametric Amplification for Ultrashort Laser Pulses

JAC Dilrukshi[1], J Stephen[1] and TJ Hammond[1*]

[1]Attosecond Condensed Matter Experiments Lab, University of Windsor, Windsor ON N9B 3P4 Canada

Synopsis We develop and characterize a parametric amplifier based on Kerr instability, a $\chi^{(3)}$ process. Through modelling and experiments, we demonstrate gain factors exceeding 50/mm. Temporal measurements find the amplified pulse duration a factor of 5X shorter than the seed.

Optical parametric amplifiers (OPAs) deliver intense ultrashort pulses with broadly tuneable frequencies, useful for strong field physics, high harmonic generation, and attosecond experiments. Currently, this nonlinear amplification scheme relies on the second order nonlinearity, $\chi^{(2)}$,which is made possible only by crystals without centro-symmetry. More recently, investigations into a non-collinear setup show an increase in the phase matching bandwidth, leading to the creation even shorter pulses [1]. In this paper, we discuss our research involving amplification of ultrashort pulses using wide bandgap materials with centrosymmetry, previously reported as Kerr instability amplification (KIA) [2].

We find that by using these crystals that exploit the next order nonlinearity, $\chi^{(3)}$,we can choose our amplifying medium from a more general class of crystals and still can generate gain factors of g = 50 /mm, or amplification factors of > 10^{12} [3]. Without the constraint of centrosymmetry, we have a greater crystal selection by varying the bandgap, thermal properties, and linear and nonlinear indices of refraction.

We developed pulse propagation models to optimize the critical parameters for amplification, and we find that the amplified pulse duration is much shorter than the pump and can be independent of the seed. We test several high bandgap dielectrics to optimize our scheme, such as YAG, YVO_4, and MgO.

In **Fig. 1**, we show three different that this experiment can be separated into three regimes: **A** non-degenrate cascaded four-wave mixing (ND4WM) converts the seed beam (in blue circle) across multiple octaves, separated beams phase matched from the near IR to the UV; **B** with the pump pulse first, a hole forms in the seed beam caused by multi-photon absorption; **C** optimized for amplification, the initial spectrum is amplified and significantly broadened. We experimentally demonstrate near-octave spanning amplification and that KIA is closely linked to ND4WM . We also spectrally and temporally characterize the amplified pulses to show agreement with theory.

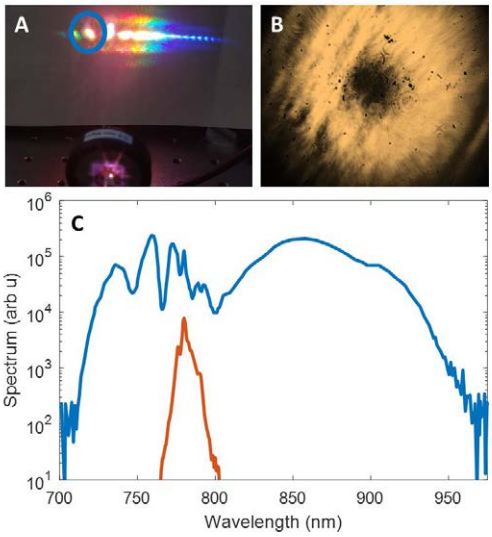

Figure 1. A 4WM output with converted beams, blue circle amplified seed; **B** Hole in seed beam showing multi-photon absorption; **C** Amplified spectrum (blue) from initial spectrum (orange).

References

[1] H Fattahi *et al* 2014 *Optica* **1** 45-63
[2] G Vampa *et al* 2018 *Science* **359** 673-675
[3] M Nesrallah *et al* 2018 *Optica* **5** 271-278

* E-mail: thammond@uwindsor.ca

Limits to the observation of low kinetic energy electrons from liquid water compared to water clusters

S Malerz[1], F Trinter[1,2], U Hergenhahn[1]*, A Ghrist[1,3], H Ali[1], C Nicolas[4], C-M Saak[5], C Richter[1], S Hartweg[4], L Nahon[4], C Lee[1,6], C Goy[7], M Förstel[8], D M Neumark[6], G Meijer[1], I Wilkinson[9], B Winter[1] and S Thürmer[10]

[1]Dept. MP, Fritz-Haber-Institut, 14195 Berlin, Germany
[2]Inst. for Nuclear Physics, University Frankfurt, 60348 Frankfurt, Germany
[3]Dept. of Chemistry, USC, CA 90089, USA; [4]Synchrotron SOLEIL, 91192 Gif sur Yvette, France
[5]Dept. of Physics and Astronomy, Uppsala Univ., SE-75120 Uppsala, Sweden
[6]Dept. of Chemistry, UC Berkeley, CA 94720, USA; [7]CMWS, DESY, 22607 Hamburg, Germany
[8]Dept. of Physics, TU Berlin, 10623 Berlin, Germany; [9]Dept. PS-ALTS, HZB, 14109 Berlin, Germany
[10]Dept. of Chemistry, Kyoto University, Kyoto 606-8502, Japan

Synopsis We present data on the photoemission of low kinetic energy electrons from liquid water. We show that severely distorted line shapes are observed at kinetic energies below a limit of approximately 10-14 eV. This behaviour is not dependent on the orbital producing the electrons. No such behaviour is observed in spectra from a free jet of water clusters ($\langle N \rangle = 135$).

Transport of energetic electrons through gases and dense media is invariably determined by electron scattering. In photoemission experiments, by choosing a sufficiently dilute target, the influence of that can be avoided in gas-phase experiments, but inelastic scattering inevitably becomes noticeable as soon as atomic or molecular clusters are considered. In solids and liquids, inelastic scattering is known to produce pronounced, structureless backgrounds in the kinetic energy distribution, which hardly have been explored in detail for the latter.

Here, we present experimental data on the photoemission of electrons with low kinetic energy ($< 30\,\mathrm{eV}$) from $\langle N \rangle = 135$ water clusters and from liquid water, probed in the form of a liquid microjet in vacuum. For water clusters, data for the valence band ranging down to the ionization threshold will be shown; equivalent spectra have been recorded for liquid water. Moreover, XPS data for the Cl 2*p*-core level of an aqueous solute (NaCl) near the respective ionization threshold will be shown (see Fig. 1).

We show that cluster valence-band features can well be observed at kinetic energies as low as one eV (see also [1]), while in liquid water both valence and core-level features are blended into a structureless continuum of inelastically scattered electrons as soon as kinetic energies decrease below a limit of approximately 10 eV. This is attributed to an interplay of the change in inelastic mean free path with various channels for inelastic energy loss at kinetic energies, for which the electron impact ionization channels known from gas-phase work are closed [2].

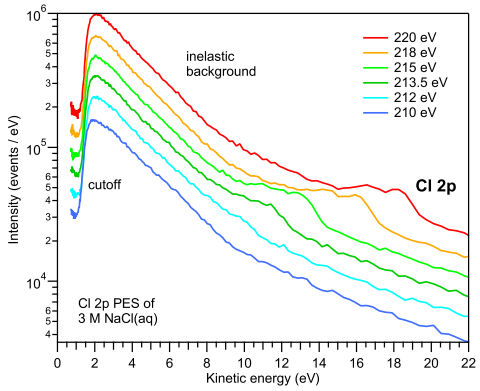

Figure 1. XPS spectrum of a 3-molar aqueous solution of NaCl in the vicinity of the Cl 2p ionization edge. The Cl 2p photoelectron peak cannot be distinguished from the inelastic background at kinetic energies smaller than approx. 10 eV.

References

[1] Hartweg S *et al* 2017 *Phys. Rev. Lett.* **118** 103402
[2] Malerz S *et al* 2021 *Phys. Chem. Chem. Phys.* **23** 8246–8260

*E-mail: uhe@fhi.mpg.de

Edge-state contributions to high-order harmonic generation in topological insulators

C Jürß[1] * and D Bauer[1] †

[1]Institute of Physics, University of Rostock, 18051 Rostock, Germany

Synopsis The high-order harmonic generation of a topological insulator (Haldanite) is calculated. The systems are finite. One specific peak in the spectrum shifts towards smaller frequencies as the flakes become larger. The frequency of the peaks follows the same law as expected for an electronic movement along the edge with the group velocity given by the band structure of the edge-state.

Topological insulators are a special kind of solid state material. They are insulating in their interior, called bulk, and conducting on their edges. This gives rise to edge currents, currents that move without dissipation along the edges of a topological insulator without scattering into its bulk. These currents are topologically protected against perturbations to the system.

In our work, we study the so called Haldane model [1]: a two-dimensional topological insulator with a honeycomb structure described in tight-binding approximation. In order to make the system topological, the sublattice symmetry and the time-reversal symmetry has to be broken. The sublattice symmetry is broken by assigning an alternating on-site potential, the time-reversal symmetry by including a complex hopping between the next-nearest neighbors. This system is called "Haldanite".

In this work, the influence of the edge states and edge currents to the high-order harmonic spectrum is investigated. Therefore, finite flakes illuminated by an intense, ultrashort laser pulse are simulated. Usually, photons with energies that are multiples of the incidents photon energy are emitted. In a recent paper we show that the presence of edge states can have an influence on the harmonic spectrum of Haldanite [2]. In this presentation, however, we focus on finite size effects.

The harmonic spectra of finite flakes show a strong peak with a comparable yield to the fundamental harmonic. The energy of this peak shifts towards smaller energies as the system size becomes larger. The peak is indicated by a red dot in the spectra, see Figure 1.

As the flakes become larger (larger N), the length of the edge of the flakes increases as well. By assuming that the group velocity of the edge state (given by the derivative of the band structure of the edge states) is independent from the size of the flake, the time that the edge current needs to move around the edge of the flake should increase for larger systems. Hence, the frequency of the edge current decreases.

We show that the frequency-shift of the peaks follow the same law as expected for the frequency of the edge current with a constant group velocity. Furthermore, the velocity obtained from the frequencies of the peaks is similar to the group velocity of the edge state derived from the band structure.

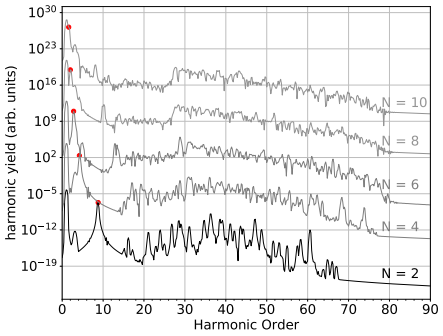

Figure 1. Harmonic yield for different sizes of the Haldanite-flakes (large N means large flakes). The yield is multiplied by a factor of $10^{7(N/2-1)}$.

References

[1] F. D. M. Haldane 1988 *Phys. Rev. Lett.* **61** 2015
[2] C. Jürß and D. Bauer 2021 arXiv:2103.14671 [cond-mat.mes-hall]

*E-mail: christoph.juerss@uni-rostock.de
†E-mail: dieter.bauer@uni-rostock.de

High-harmonic generation in Fibonacci quasicrystals

F Navarrete* **and D Bauer†**

Institute of Physics, University of Rostock, 18051 Rostock, Germany

Synopsis

In this contribution we analyze the characteristics of the high-harmonic generation (HHG) spectra of quasicrystals (QCs), compared to that of crystals of the same composition. In particular, we investigate the spectrum of a one-dimensional (1D) type of QC, a Fibonacci chain, which is a paradigmatic case. We found an extension of the secondary plateau as well as a substantial decrease of the intraband region of the spectra. This study shows the potential of HHG spectroscopy to scrutinize the band structure of this exotic state of matter, as well as to assess the influence of long-range order effects in the optical properties of solids.

The mechanism of HHG in solids has been theoretically studied over the last two decades, and experimentally determined only a decade ago [1]. While many conclusions have been drawn for this process in crystals, it has also been predicted a strong dependence of the HHG spectrum on the topology of the sample [2]. The latter motivated us to explore the strong-field response of QCs [3], which might provide interesting technological applications and also insight on fundamental questions of its electron dynamics. Even though in our study we focus on a simplified model for QCs, the Fibonacci chain, these conclusions might also be extrapolated to both synthesized [3] and natural QCs [4]

We solved the time-dependent Schrödinger equation in real space for a model potential which is formed by the sequential tiling of two potentials $L(x)$ and $R(x)$. Each of the tile potentials is the mirror image of the other, and consists of two potential wells of different depth as is shown in Fig. 1(a) and 1(b). Each chain is formed by the sequence: $V_0 = L$, $V_1 = LR$, $V_2 = LLR$, $V_3 = LRLLR$, ..., $V_n = V_{n-2}V_{n-1}$, where V_i is a Fibonacci chain of order i.

We performed the time propagation for lattices ranging from V_0 to V_3, establishing periodic boundary conditions (to focus on bulk effects), incorporating crystal-momentum contributions along the full Brillouin zone, and including bands up to an energy corresponding to a filled valence band in the pristine case V_0, to ensure convergence [5]. This systematic study allowed us to analyze the progressive emergence of long-range order effects on the HHG spectra of Fibonacci chains of increasing complexity.

In Fig. 1(c) we show the HHG spectra for V_0 and V_3 for a 10-cycle driving field of 2500nm wavelength and 0.23 V/Å field-strength. It is possible to infer that while the intraband region of the spectrum (corresponding to harmonics up to the 11th) decreases, the secondary plateau (harmonics from 23th to 43th) is extended by approximately 20 harmonic orders.

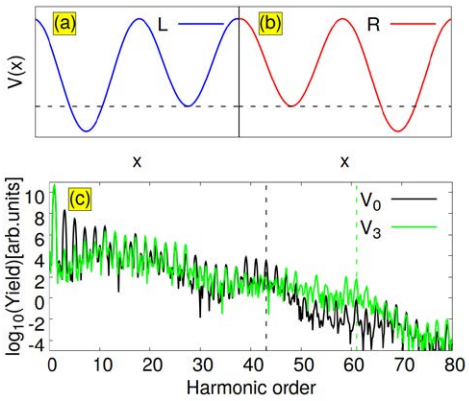

Figure 1. (a) Tile potential $L(x)$. (b) Tile potential $R(x)$. (c) HHG Yield for V_0 and V_3 for a 10-cycle driving field of 2500nm wavelength and 0.23 V/Å field-strength.

References

[1] Ghimire S *et. al.* 2011 *Nat. Phys.* **7** 138
[2] Bauer D and Hansen K K 2018 *Phys. Rev. Lett.* **120** 177401
[3] Shechtman D *et. al.* 1984 *Phys. Rev. A* **53** 1951
[4] Bindi L *et. al.* 2009 *Science* **324** 1306
[5] Navarrete F *et. al.* 2019 *Phys. Rev. A* **100** 033405

*E-mail: francisco.navarrete@uni-rostock.de
†E-mail: dieter.bauer@uni-rostock.de

Coherent diffractive extreme-ultraviolet generation from nanostructured silica

S D C Roscam Abbing,[1*], Z Zhang,[1], R Kolkowski[2], F Campi,[1], A F Koenderink[2], P M Kraus[1*]

[1]Advanced Research Center for Nanolithography (ARCNL), Science Park 106, 1098 XG Amsterdam, The Netherlands

[2]Center for Nanophotonics, AMOLF, Science Park 104, 1098XG Amsterdam, The Netherlands

Synopsis We demonstrate high-harmonic generation inside structured silica, enabling the generation of structured XUV beams, useful for spectroscopy, metrology and imaging.

High-Harmonic Generation (HHG) is driving the research field of attosecond science through the generation of coherent extreme-ultraviolet (XUV) pulses, and enables lensless imaging and metrology with high resolution. HHG from a solid medium was only demonstrated more recently [1], and specifically silica is shown to generate harmonics extending into the XUV regime [2]. Generation from a solid has the advantage that the medium can be structured [3]. Here, we demonstrate HHG from various structured silica samples, and generate spatially structured XUV beam profiles, see Fig. 1. First experiments are performed in periodic structures with micron-sized features. The structures imprint phase and amplitude on either the generated harmonics or on the fundamental wavefront, leading to diffraction of the XUV pulses. Using classical diffraction theory we model the experimental results quantitatively. Also, we use the experimental data to determine the height of the structures and the field distribution inside the micron-sized structures. In addition we generate harmonics inside nanometer-sized structures, fabricated using e-beam lithography. Generation from these sub-fundamental-wavelength structures demonstrates the sensitivity of HHG to the near-field properties of the involved wavelengths. Specifically, we investigate how the relative polarization of the incoming driving field, with respect to the structures, influence the amplitude and polarization of the structured HHG emission. Again, we confirm our understanding with simulations, based on a finite-element method. The simulations predict that generation inside our periodic nanometer-sized structures leads to elliptically and circularly polarized harmonics. Finally, we also generate from complex aperiodic structures, and can replicate the obtained diffraction pattern very well with simulations, see Fig. 1. In addition, the iterative reconstruction of the recorded diffraction patterns, demonstrates the use of solid-state HHG from structured materials for imaging and metrology purposes. In conclusion, we have demonstrated the generation of structured XUV pulses. Our results pave the way towards extreme-ultraviolet super resolution imaging, and direct manipulation of extreme-ultraviolet beams through nano engineered samples.

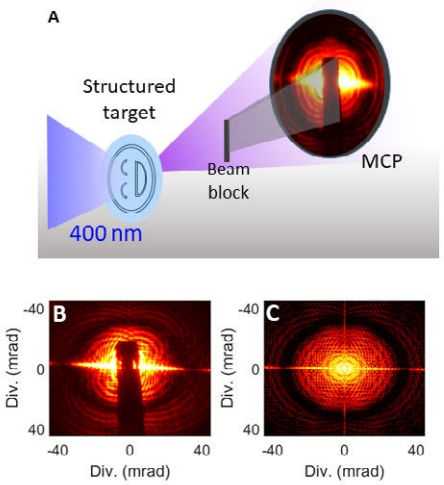

Figure 1. A) Schematic of experimental setup. B) Measured diffraction of target in A. C) Simulated diffraction pattern of target in A.

References

[1] Ghimire S *et al* 2011 *Nature physics* 7(2) 138-141
[2] Luu TT *et al* 2015 *Nature* 521(7553) 498-502
[3] Sivis M *et al* 2017 *Science* 357(6348) 303-306

On the precision limits in a single-event quantum measurement of electron momentum and position

H. Schmidt-Böcking[1]*, S. Eckart[1], H. J. Lüdde[2] G. Gruber[1], and T. Jahnke[3]

[1] Institut für Kernphysik, Universität Frankfurt, Max-von-Laue-Str. 1, 60438 Frankfurt, Germany
[2] Theoretische Physik, Universität Frankfurt, Max-von-Laue-Str. 1, 60438 Frankfurt, Germany
[3] European XFEL, Holzkoppel 4, 22869 Schenefeld, Germany

Synopsis A modern state-of-the-art measurement of momentum and position of a single electron at a given time and the precision limits for their experimental determination are discussed from an experimentalists point of view.

A modern state-of-the-art quantum measurement† of momentum and position of a single electron at a given time‡ and the precision limits for their experimental determination are discussed from an experimentalists point of view. We show - by giving examples of actually performed or experiments - that in a single reaction between quantum particles at a given time only their momenta but not their positions in the reaction process can be measured with high sub-atomic resolution. This momentum resolution in a single event measurement depends only the properties of the classical detection system. The resolution is de-facto "unlimited". This fundamental disparity between the conjugate variables of momentum and position is due to the fact that during a single-event measurement only the total momentum but not position is conserved as function of time. We highlight, that (other than prevalently perceived) Heisenberg's "Uncertainty Relation" UR does not limit the achievable resolution of momentum in a single-event measurement. Thus, Heisenberg's statement that in a single-event measurement only either the position or the momentum (velocity) of a quantum particle can be measured with high precision contradicts a real experiment. The UR states only a correlation between the mean statistical fluctuations of a large number of repeated single-event measurements of two conjugate variables. A detailed discussion of the real measurement process and its precision with respect to momentum and position is presented.

A single-event measurement can only provide information on the particle's properties back in the past but never allow a prediction of future properties, since the impact of a particle on the detector changes its momentum and location in an uncontrollable way.

*E-mail: schmidtb@atom.uni-frankfurt.de
†The wording "Quantum measurement" as used here represents a short form for the measurement of parameter values of atomic particles involved in a single scattering process.
‡"at a given time" corresponds to the extremely short time duration of the quantum particle reaction process.

High-Resolution Momentum Imaging: From Stern's Molecular Beam Method to the COLTRIMS Reaction Microscope

T. Jahnke[1], V. Mergel[3], O. Jagutzki[2+4], A. Czasch[2+4], K.Ullmann[2+4], R. Ali[5], V. Frohne[6], T. Weber[7], L. P. Schmidt[2], S. Eckart[2], M. Schöffler[2], S. Schössler[2+4], S. Voss[2+4], A. Landers[8], D. Fischer[9], M. Schulz[9], A. Dorn[10], L. Spielberger[11], R. Moshammer[10], R. Olson[9], M. Prior[7], R. Dörner[2], J. Ullrich[12], C. L. Cocke[13], and H. Schmidt-Böcking[2+4]*,

[1] European XFEL, Holzkoppel 4, 22869 Schenefeld, Germany
[2] Institut für Kernphysik, Universität Frankfurt, Max-von-Laue-Str. 1, 60438 Frankfurt, Germany
[3] Patentconsult, 65052 Wiesbaden, Germany
[4] Roentdek GmbH, 65779 Kelkheim, Germany
[5] Department of Physics, The University of Jordan, Amman 11942, Jordan
[6] Department of Physics, Holy Cross College, Notre Dame, 46556 IN, USA
[7] Chemical Sciences, LBNL, Berkeley, CA 94720, USA
[8] Department of Physics, Auburn University, Auburn, AL 36849, USA
[9] Department of Physics, Missouri S&T, Rolla, MO 65409, USA
[10] MPI für Kernphysik, 69117 Heidelberg, Germany
[11] GTZ, 65760 Eschborn, Germany
[12] PTB, 38116 Braunschweig, Germany
[13] Department of Physics, Kansas State University, Manhattan, Kansas 66506, USA

Synopsis A review on the historic developments from Otto Stern's molecular beam method to modern COLTRIMS reaction microscopes.

Multi-particle momentum imaging experiments are now capable of providing detailed information on the properties and the dynamics of quantum systems in Atomic, Molecular and Photon (AMO) physics. Historically, Otto Stern can be considered the pioneer of high-resolution momentum measurements of particles moving in a vacuum and he was the first to obtain sub-atomic unit (a.u.) momentum resolution. A major contribution to modern experimental atomic and molecular physics was his so-called molecular beam method, which he developed and employed in his experiments. With this method he discovered several fundamental properties of atoms, molecules and nuclei. As corresponding particle detection techniques were lacking during his time, he was only able to observe the averaged footprints of large particle ensembles.

Today it is routinely possible to measure the momenta of single particles, because of the tremendous progress in single particle detection and data acquisition electronics. A "state-of-the-art" COLTRIMS reaction microscope can measure, for example, the momenta of several particles ejected in the same quantum process in coincidence with sub-a.u. momentum resolution. Such setups can be used to visualize the dynamics of quantum reactions and image the entangled motion of electrons inside atoms and molecules. This review will briefly summarize Stern's work and then present in longer detail the historic steps of the development of the COLTRIMS reaction microscope. Furthermore, some benchmark results are shown which initially paved the way for a broad acceptance of the COLTRIMS approach. Finally, a small selection of milestone work is presented which has been performed during the last two decades.

*E-mail: schmidtb@atom.uni-frankfurt.de

An application of a Si/CdTe Compton camera for the polarization measurement of hard x-rays

Y Tsuzuki[1,2]*, S Watanabe[3,2], S Oishi[4], N Nakamura[4], N Numadate[4,5], H Odaka[1,2], Y Uchida[6], H Yoneda[7], T Takahashi[2,1]

[1]Department of Physics, The University of Tokyo, 7-3-1, Hongo, Bunkyo, Tokyo 113-0033, Japan
[2]Kavli Institute for the Physics and Mathematics of the Universe (WPI), Institutes for Advanced Study (UTIAS), The University of Tokyo, 5-1-5 Kashiwa-no-Ha, Kashiwa, Chiba, 277-8583, Japan
[3]Institute of Space and Astronautical Science, Japan Aerospace Exploration Agency, 3-1-1 Yoshinodai, Chuo Sagamihara, Kanagawa, 252-5210, Japan
[4]Institute for Laser Science, The University of Electro-Communications, Chofu, Tokyo 182-8585, Japan
[5]Komaba Institute for Science, The University of Tokyo, 3-8-1 Komaba, Meguro, Tokyo 153-8902, Japan
[6]Department of Physics, Hiroshima University, 1-3-1 Kagamiyama, Higashi-Hiroshima, Hiroshima 739-8526, Japan
[7]RIKEN Nishina Center, 2-1 Hirosawa, Wako, Saitama 351-0198, Japan

Synopsis We applied a Compton camera, which consists of pixelated multi-layer silicon (Si) and cadmium telluride (CdTe) semiconductor detectors, to hard x-ray observations. We measured the degree of polarization of radiative recombination x-rays from highly charged krypton (Kr) ions. The uncertainty of the result is sufficiently small to probe relativistic and QED effects in future experiments.

Polarization of hard x-rays emitted through interactions between highly charged heavy ions and electrons is of significant importance for diagnostics of relativistic quantum effects. For example, dielectronic recombination (DR) x-rays emitted from highly charged high-Z ($Z > 70$) ions are estimated to be polarized and affected by relativistic and quantum electrodynamics (QED) interactions [1]. A new polarimetric method for high-Z ions with sufficient sensitivity and accuracy is required.

We have developed a new Compton camera, named the EBIT-CC, equipped with pixelated multi-layer silicon (Si) and cadmium telluride (CdTe) semiconductor detectors. It is capable of determining three-dimensional positions of interactions between incident photons and detector materials. One can derive the azimuthal angular distribution of photons scattering in the detectors, thereby the degree of polarization of incoming x-rays. Its design is detailed in [2].

We performed an experiment using the EBIT-CC, a germanium (Ge) spectrometer, and the Tokyo Electron Beam Ion Trap (Tokyo-EBIT) [3] in the University of Electro-Communications. Radiative recombination x-rays were emitted from the highly charged krypton (Kr) ions toward the detectors.

As a result, we evaluate the degree of polarization to be 0.962 ± 0.023 from data (see Fig. 1). The uncertainty of our result is sufficiently small to probe the relativistic and QED effects on the polarization of DR x-rays from high-Z ions in future experiments [4].

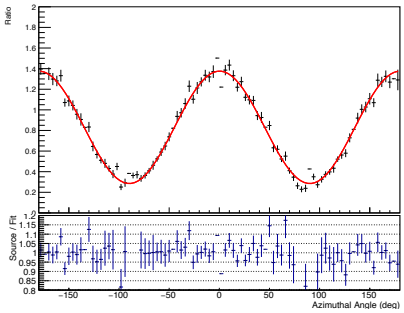

Figure 1. Modulation curve for the Kr radiative recombination (black dots) and the best-fit model (red line). Cited from [5]

References

[1] Nakamura N 2016 *J. Phys. B: At. Mol. Opt. Phys.* **49** 212001
[2] Watanabe S *et al* 2014 *Nucl. Inst. and Meth. A* **765** pp. 192-201
[3] Nakamura N *et al* 1997 *Phys. Scr.* **1997** 362
[4] Tong XM *et al* 2015 *J. Phys. B: At. Mol. Opt. Phys.* **48** 144002
[5] Tsuzuki Y *et al* 2021 submitted for publication.

*E-mail: yutaka.tsuzuki@ipmu.jp

From molecules to liquid jets - synchrotron research on isolated species and condensed samples

N Walsh[1]*, V Ekholm[1], T Gallo [1,2], S Ganguly[1,2], A Kivimäki[1], E Kokkonen[1], C Preger [1,3], N Punnakayathil[1], M Scardamaglia[1], K Sigfridsson Clauss[1] and G Öhrwall[1]

[1]MAX IV Laboratory, Lund University, Lund 22484, Sweden
[2]Division of Synchrotron Radiation Research, Lund University, Lund 22362, Sweden
[3]Ergonomics and Aerosol Technology, LTH, Lund University, Lund 22362, Sweden

Synopsis MAX IV is a Swedish national large-scale research laboratory that hosts the world's first 4th generation light source. The facility delivers soft x-ray and hard x-ray radiation for research in chemistry, physics, the life sciences, cultural heritage and materials science. Here, we highlight the facilities that are available for AMO/LDM (Atomic, Molecular, Optical / Low Density Matter) research at MAX IV. We present both current experimental capabilities and new capabilities that are under development for gas-phase and liquid-phase research at MAX IV.

Research investigating the interaction of light with molecules, clusters and liquids/aqueous solutions enables a fundamental understanding of the properties of these samples, as well as an understanding of various processes that occur in nature, or that are relevant to industrial and technological development. Traditionally, AMO/LDM science at MAX-lab has utilized techniques such as photoelectron spectroscopy, molecular jet/cluster beam generation and liquid microjet generation. MAX IV has a number of LDM-relevant beamlines that together cover a broad photon energy range (4-2400 eV). FinEstBeAMS, FlexPES, HIPPIE and SPECIES enable research in areas such as high-resolution photoelectron spectroscopy and angle-resolved electron spectroscopy on molecules, clusters and liquid jets, Ambient Pressure XPS on liquid jet/laboratory generated nanoparticles, Time-Of-Flight Mass Spectrometry, electron energy resolved multi-coincident PEPIPICO and negative ion - positive ion coincidence spectroscopy. Further beamlines that intend to offer possibilities for AMO/LDM research include FemtoMAX in the short pulse facility and Veritas which aims to offer gas-phase and liquid jet RIXS. On the 3 GeV ring, absorption spectroscopy on liquid samples is already a possibility at Balder and the beamline is looking towards the development of a new liquid jet sample delivery system for hard X-ray research.

In addition to the above, we are also actively expanding our LDM equipment portfolio – developing new experimental capabilities to complement the established techniques. The ICE (Ions in Coincidence with Electrons) endstation is a new addition to MAX IV. The ICE spectrometer is a reaction microscope spectrometer that enables the measurement of the 3-D momentum distribution of particles produced in photoreactions. ICE is currently available for expert commissioning and will soon be available to the broader user community. Two new sample delivery systems are also under development in collaboration with the MAX IV user community - an aerodynamic lens and a flat liquid jet setup. Veritas and it's collaborators are also developing a sample delivery system for gas-phase RIXS.

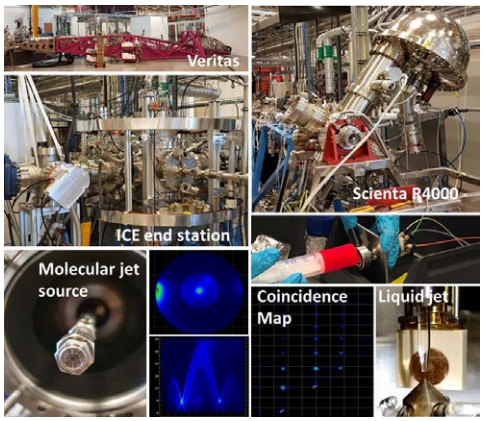

Figure 1. LDM-relevant facilities at MAX IV

*E-mail: noelle.walsh@maxiv.lu.se

Intermolecular Coulombic decay in liquid H_2O and D_2O: the role of proton transfer

Pengju Zhang[1] *, **Tran Trung Luu**[1,2] and **Hans Jakob Wörner**[1] †

[1]Laboratory for Physical Chemistry, ETH Zürich, Vladimir-Prelog-Weg 2, 8093 Zürich, Switzerland
[2]Department of Physics, The University of Hong Kong, Pokfulam Road, Hong Kong, People's Republic of China

Synopsis Electron-electron coincidence measurements were performed on both liquid H_2O and D_2O by combining a monochromatized table-top high-harmonic generation (HHG) source with a liquid micro-jet. We find that the efficiency of intermolecular Coulombic Decay (ICD) (γ) is below unity in both liquids and determine a relative efficiency of $\gamma(H_2O)/\gamma(D_2O)=0.87 \pm 0.03$.

As a ubiquitous, electron-correlation-driven relaxation process, interatomic or intermolecular Coulombic decay (ICD) [1] plays an essential role in understanding the dynamics of energy transfer in weakly-bound complexes and liquids following inner-valence or core-level ionization. ICD is particularly relevant in the context of radiation damage because it is an efficient source of slow (0-10 eV) electrons, which are the main vectors of radiation damage to living tissues surrounded by an aqueous environment [2].

We have recently obtained the first evidence of ICD following inner-valence ionization of liquid H_2O [3]. In the present work, we address the role of nuclear motion in the ICD process. For this purpose, we directly compare the ICD-electron yields from liquid H_2O and D_2O. The efficiencies of ICD process in both samples is determined both less than 1, and the ratio of ICD efficiencies between liquid H_2O and D_2O is determined to be 87% ±3%.

Our results indicate the existence of competing processes which evolve on a timescale comparable to that of ICD. The most likely candidate is proton transfer, as in the case of water clusters[4]. In contrast to preliminary predictions regarding liquid water [4], our results suggest that proton transfer is likely to close the ICD channel, which would explain both the ICD efficiencies being lower than unity and the lower ICD efficiency of D_2O. Supporting theoretical results will be presented at the conference.

Our present experimental methodology moreover opens a direct pathway to the measurement of the ICD lifetime in liquid water via attosecond interferometry [5].

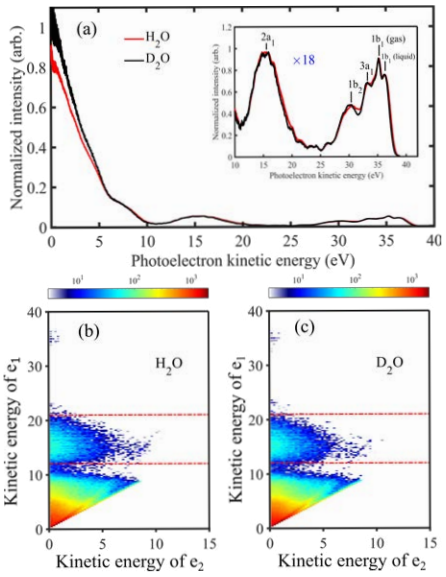

Figure 1. (a) Photoelectron spectrum of liquid water recorded with XUV pulses centered at 48 eV (normalized to the liquid $1b_1$ peak). (b) and (c) Coincidence maps of electron pairs created by ionization of liquid H_2O and D_2O, respectively. The area between the two red lines is dominated by $2a_1$-photoelectron–ICD electron pairs.

References

[1] L. S. Cederbaum *et al* 1997 *Phys. Rev. Lett.* **79** 4778-4781
[2] E. Alizadeh *et al* 2015 *Annu. Rev. Phys. Chem.* **66** 379-398
[3] P. Zhang *et al* 2021 *submitted.* arXiv:2103.15014
[4] C. Richter *et al* 2018 *Nat.Commun.* **9** 4988
[5] I. Jordan *et al* 2020 *Science* **369** 974

*E-mail: pengju.zhang@phys.chem.ethz.ch
†E-mail: hwoerner@ethz.ch

Ultrafast relaxation of photoexcited electrons in fullerenes and endofullerenes

E Ali[1]*, M E Madjet[1,2] , O Vendrell[3] , M Carignano[4], and H S Chakraborty[1†]

[1] Department of Natural Sciences, D L Hubbard Center for Innovation, Northwest Missouri State University, Maryville, Missouri 64468, USA
[2] Max-Planck-Institut für Physik Komplexer Systeme, Nöthnitzer Straße 38, 01187 Dresden, Germany
[3] Theoretical Chemistry, Institute of Physical Chemistry & Centre forAdvanced Materials, Heidelberg University, Im Neuenheimer Feld 229& 225, 69120 Heidelberg, Germany
[4] Department of Biomedical Engineering, Northwestern University,Evanston, IL 60208, USA

Synopsis We study the relaxation of photoexcited electrons in C_{60} and $Mg@C_{60}$ molecules by using *ab initio* non-adiabatic molecular dynamics based on DFT. The simulated population dynamics driven by the electron-phonon couplings evolves in ultrafast time scales and opens excellent opportunities to measure these processes by two-photon transient absorption spectroscopy as well as photoelectron spectroscopy.

Understanding of the dynamics of photoinduced "hot" electron relaxation in fullerenes and endofullerenes is invaluable in organic photovoltaics that use these materials [1]. With the possibility of easy production of gas-phase C_{60} and with remarkable advances in synthesis methods of endohedral C_{60} in gas phase, in solution or as thin films [2], these systems render eminent natural laboratories to probe the relaxation proces. First, they can support surgical level-to-level excitations. Second, they can showcase the pristine decay and charge transfer or even charge oscillation dynamics between atom and C_{60}. Third, the details of the transient intermediate state populations can potentially map out excited state structures. Therefore, these molecules can be of particular appeal for both ultrafast transient absorption spectroscopy and time-resolved photoelectron spectroscopy.

The computational methodology adopted has a two-prong approach [3]. (i) An independent particle method based on a DFT frame that uses B3LYP exchange-correlation functional. (ii) A configuration-interaction singles (CIS) description of the many-body effects. These descriptions of the electronic structure combine with the fewest-switch surface hopping approach.

Figure 1 depicts a cartoon of Mg $3s \rightarrow 3p$ photoexcitation in $Mg@C_{60}$. It also presents simulated energy-time map of the decay of the initial excited state and the subsequent population dynamics during the relaxation including the charge transfer and transient captures [3]. In general, the decay and transfer times are found to be in ten's of femtoseconds (fs) while that for transient events to be longer that 100 fs. This contour map is comparable to standard experimental spectrograms of energy versus laser pump-probe time-delay.

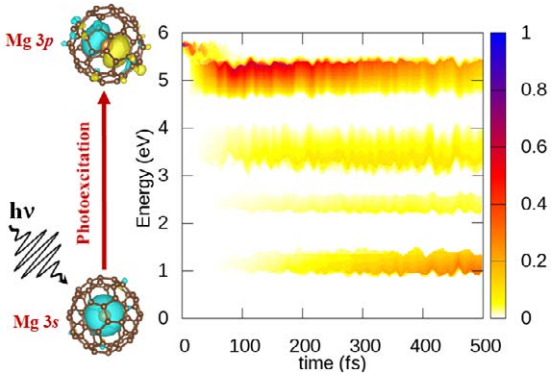

Figure 1. Energy-time map of $Mg@C_{60}$ transient excited electronic state population from DFT/B3LYP level.

Similar results (not shown) for pristine C_{60}, which is far more readily amenable for experiments, show attractive details of dynamics following selective photoexcitations to further allure experimental initiatives.

Supported by National Science Foundation grant PHY-1806206 and Bartik High-Performance Cluster under National Science Foundation Grant CNS-1624416, NWMSU

References

[1] Collovini S *et al* 2018 *Sust. En. Fuels* **2** 2480
[2] Popov A 2017 *Nanostruc. Sc. Tech. Ser. (Springer)*
[3] M. Madjet *et al* 2021 *Phys. Rev. Lett.* **(accepted)**

* E-mail: eali@nwmissouri.edu
† E-mail: himadri@nwmissouri.edu

Translationally-invariant Generalized-Volkov approach for time-resolved WSe_2 photoemission

M J Ambrosio[1], P M Echenique[1], R Díez Muiño[1,2]* and F Martín[3,4]†

[1] Donostia International Physics Center, 20018 San Sebastián (Spain)
[2] Centro de Física de Materiales (CSIC/UPV-EHU), 20018 San Sebastián (Spain)
[3] Instituto Madrileño de Estudios Avanzados de Nanociencia, Campus de Cantoblanco, 28049 Madrid (Spain)
[4] Departamento de Química, Universidad Autónoma de Madrid, 28049 Madrid (Spain)

Synopsis We examine features WSe_2 time-resolved photoemission with a translationally-invariant model.

We calculate time-resolved photoemission processes from core states of WSe_2, a transition metal dichalcogenide studied by Siek *et al.* [1]. A diagram of the process is depicted in Fig. 1 (top). Our formulation consists of a translationally invariant generalized-Volkov final-state model with initial states described as combinations of localized orbitals. The localized orbitals, coming from the built-in models from GPAW [2], are averaged in the x, y plane, as all the spatial dependence for the initial- and final state is assumed to take place along the normal direction z. The XUV and IR fields, on the other hand, do include their three spatial components and can match the experimental orientations.

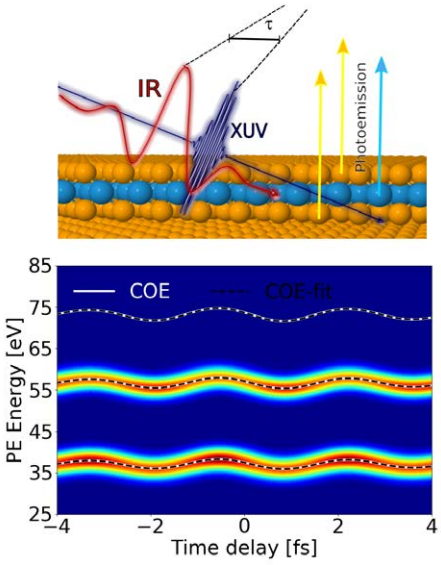

As WSe_2 is not a pure material, the energy-dependent mean free path and dielectric function are not widely available and we used the values calculated in the supplemental material of Ref. [1] and from a GPAW [2] calculation respectively.

Figure 1 (bottom) shows the energy- and delay-dependent spectrum, with emission from Se3d, W4f and Se4s from bottom to top. A simple integration of the streaking traces produces the centers of energy in terms of the XUV-IR time delay, which are then fitted to extract the photoemission delays. We use the Se4s state as the zero-delay reference.

We explore the use of different model potentials for the Generalized-Volkov final states. The former are extracted from 3D calculations with GPAW [2] for the WSe_2 periodic system reduced to 1D by averaging or by choosing the pathway to go over either the W or Se atoms. The use of averaged potentials yielded the photoemission delays in better agreement with the experimental times.

Our study also reveals that considering the core states as completely single core as opposed to Bloch-type combinations leads to an insignificant time-delay change, with a mean free path of 10 au.

References

[1] F. Siek *et al.* 2017 *Science*, **357** 1274-1277.

[2] J. Enkovaara *et al.* 2010 *J. Phys.: Condens. Matter*, **22** 253202.

*E-mail: rdm@ehu.eus
†E-mail: fernando.martin@uam.es

Optical response and valley pseudospin of WSe_2 monolayer: 2D Maxwell scheme

A Hashmi[1†], S Yamada[2], A Yamada[2], K Yabana[2] and T Otobe[1*]

[1]Kansai Photon Science Institute, National Institutes for Quantum and Radiological Science and Technology (QST), Kyoto 619-0215, Japan
[2]Center for Computational Sciences, University of Tsukuba, Tsukuba 305-8577, Japan

Synopsis: We present an effective method based on the Maxwell-TDDFT scheme, the combined classical Maxwell plus time-dependent Kohn-Sham (TDKS) equations to describes the propagation of electromagnetic fields in the weak field limit. The present scheme has a great advantage to analyze electron dynamics as well as electromagnetic field analysis with ultrashort pulse without extra computational cost. Our theoretical description named 2D Maxwell is appropriate for extremely thin layers. Results of electron dynamics obtained by 2D Maxwell agree well with the results of TDKS which validates our description.

Time-dependent density functional theory (TDDFT) combined with linear response theory has successfully been proved to describe electronic excitations in molecules and solids[1]. The effectiveness of electron dynamics calculations based on TDDFT is further enhanced by combining it with Maxwell equations[2]. The combined scheme known as Maxwell-TDDFT formalism has been successfully applied to crystalline solids[3].

Maxwell-TDDFT scheme is quite comprehensive but a high computational cost limits its applicability. Thus to overcome this problem, we present an approach by assuming zero-thickness for extremely thin two-dimensional layers and use the linear-response treatment to calculate the transmission and reflection by 2D conductivity in the weak field limit[3].

WSe_2 monolayer is used to validate our method. A comparison of 2D Maxwell and TDKS method with and without spin-orbit coupling (SOC) is made for electron dynamics calculations. 2D Maxwell calculation of excitation energy and electric current coincides accurately with the TDKS method validates the reliability of our method.

Electromagnetic field analysis is done by calculating the transmission and reflection. In Figure. 1(a, b), the electric field after the interaction with WSe_2 monolayer is shown. The incident pulse is split into transmitted and reflected waves. The transmission is dominated, while reflection is very weak. Due to the difference in bandgap (w/o SOC 1.5 eV, with SOC 1.24 eV) because of SOC, reflection is strongly affected.

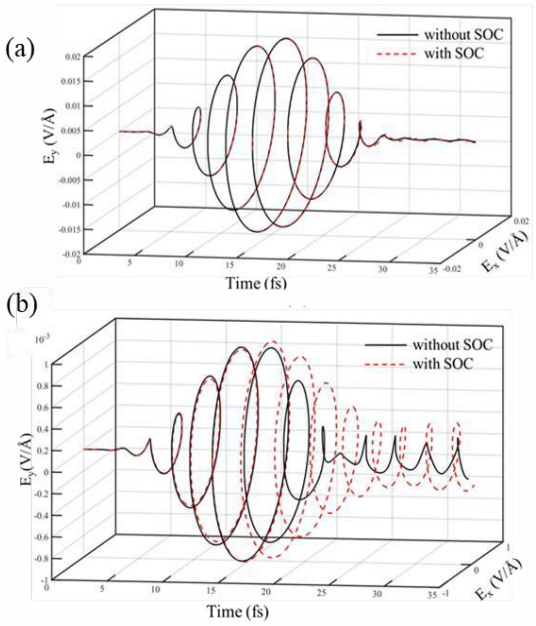

Figure 1. Time evolution of the electromagnetic field for (a) transmitted waves (b) reflected waves.

To get an understanding of valley pseudospin, we calculate the k-resolved electron populations. We observed that the valley degeneracy is lifted and only K or K′ electron is excited by changing the helicity of the laser.

References

[1] Laurent A D *et al* 2013 *International Journal of Quantum Chemistry* **113** 2019
[2] Yabana K *et al* 2012 *Phys. Rev. B* **85** 045134
[3] Yamada S *et al* 2018 *Phys. Rev. B* **98** 245147

* E-mail: otobe.tomohito@qst.go.jp
† E-mail: hashmi.arqum@qst.go.jp

Mechaninism of multi-plateau high-order harmonic generation in solid

L Lin[1,2], P C Li[1,2,*], and S I Chu[3,4]

[1]Research Center for Advanced Optics and Photoelectronics, Department of Physics, College of Science, Shantou University, Shantou, Guangdong 515063, China
[2]Key Laboratory of Intelligent Manufacturing Technology of MOE, Shantou University, Shantou, Guangdong 515063, China
[3]Center for Quantum Science and Engineering, and Center for Advanced Study in Theoretical Sciences, Department of Physics, National Taiwan University, Taipei 10617, Taiwan
[4]Department of Chemistry, University of Kansas, Lawrence, Kansas 66045, USA

Synopsis We schematically study the high-order harmonic generation (HHG) in solid driven by intense laser pulses using a one-dimensional model periodic crystal. The HHG is obtained by numerically solving the time-dependent Schrödinger equation in the velocity gauge. We show that the intensity-dependent multiple plateaus in HHG of the solid. By performing the semiclassical analysis, we find that the Bloch scattering plays a significant role in multi-plateau high-order harmonic generation in solid.

High-order harmonic generation (HHG) is typical nonlinear optical phenomena in the process of laser-matter interaction. It has enabled the generation of coherent extreme ultraviolet source in the attosecond time scale [1]. However, the previous works have found that HHG in solid has different physical mechanism compared with HHG from gas target. HHG in solid is obtained by numerically solving the time-dependent Schrödinger equation in the velocity gauge:

$$i\hbar\frac{\partial}{\partial t}\psi_{nk}(t) = H(t)\psi_{nk}(t), \tag{1}$$

$$H(t) = \left[\frac{p^2}{2m} + V(x)\right] + \frac{e}{m}A(t)p. \tag{2}$$

We discretize the wave function by expanding it with the Bloch basis [2]:

$$H_0\phi_{nk} = \varepsilon_{nk}\phi_{nk}. \tag{3}$$

Where ε_{nk} is the dispersion relation in band n with a crystal momentum k, and the $A(t)$ is the vector potential. For the model periodic potential, we employ the Mathieu-type lattice potential [3]:

$$V(x) = -V_0\left[1 + \cos(2\pi x/a)\right]. \tag{4}$$

In Fig.1(a), we have prensented the HHG spectrum with the laser amplitude of $E_0 = 1.644V/nm$. It's clear seeing that result shows multiple plateaus. In our calculation, the result of multi-plateau feature is optained by the k-space semi-classical trajectory model [4]. Fig.1(b) shows the harmonic spectrum as a function of the laser amplitude E_0. We find that the transition from single- to multi-plateau structure takes place suddenly when the vector potential amplitude is increasing.

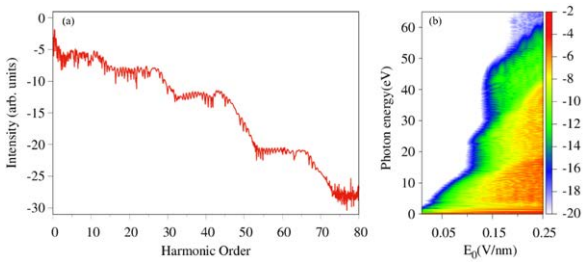

Figure 1. **(a)** HHG spectrum with the laser amplitude of $E_0 = 1.644V/nm$. **(b)** Harmonic spectrum as a function of the laser amplitude E_0.

*E-mail: pchli@stu.edu.cn

Acknowledgments

This work was supported by the NSFC (11764038, 12074239), NSF of Guangdong Province (200110165892233, 2020A1515010927, 210206153460124), Department of Education of Guangdong Province (2018KCXTD011, 2019KTSCX038), and STU(NTF18030).

References

[1] Salieres P *et al* 1999 *Advanced in Atomic, Molecular,and Opt. Phys.* **41** 83
[2] Korbman M *et al* 2012 *New J. Phys.* **15** 013006
[3] Wu M X *et al* 2015 *Phys. Rev. A* **91** 013405
[4] Ikemachi T *et al* 2017 *Phys. Rev. A* **95** 043416

Effects upon the grazing interaction of microfocus bremsstrahlung with surfaces of different lengths

V A Smolyanskiy*, M M Rychkov and V V Kaplin

R&D Laboratory for Betatron Tomography of Large Objects, Tomsk Polytechnic University; Tomsk; 7, Savinyh street 634028 Tomsk; Russian Federation

Synopsis The experimental results of studying the grazing interaction of microfocus bremsstrahlung radiation with the edge surfaces of plastic and steel plates. High-quality images of the objects are shown to be realized due to the small horizontal size of the radiation source when the edge surfaces of the plates are oriented at grazing angles to the axis of the radiation cone. The possible involvement of edge-phase contrast in image formation, which is determined by radiation refraction on the lateral faces of the plates, is discussed.

Results on the generation of microfocus hard bremsstrahlung radiation for the case of the grazing incidence of electrons of an 18-MeV betatron beam on the surface of a tantalum foil with a thickness of 13 μm and a length of 2.5 mm along the electron beam were presented in [1]. A significant dependence of the angular distributions of the hard bremsstrahlung radiation on the thin-target orientation, which is not observed for the normal incidence of electrons on its surface, was shown.

In this paper, we present experimental results on the study of the grazing interaction of microfocus hard bremsstrahlung generated by electrons with an energy of 18 MeV in a betatron Ta target with the edge surfaces of plastic plates 10 and 4 mm in thickness, steel plates 10, 5, and 0.9 mm in thickness, and lead foils 25 μm in thickness. These results (when the soft part of the emission spectrum is suppressed by absorption in the heavy material of the Ta target) are shown in comparison with those obtained using the microfocus radiation generated in a Si target when the radiation of the soft part of the spectrum was not absorbed in the lighter material of the target and (mostly) formed an object image [2].

The radiation from the Ta target is much harder than the radiation from the Si target due to the absorption of the soft part of the spectrum by heavy tantalum. The image of the edge of an object for the case of a Si target is formed by radiation with a photon energy of several tens of keV due to the maximal sensitivity of the film in this photon-energy range. In this case, the photons of the hard part of the spectrum do not have time to contribute to the formation of the image during exposure. For a Ta target, the image is formed by much harder radiation when the soft part of the spectrum is suppressed.

Nevertheless, in the images of the plates, sufficiently sharp edge images are observed, which is determined by the microfocus (13 μm) of the radiation. The overall unsharpness of the edge image depends on the transmission geometry, radiation scattering in the near-edge region of the plate, film characteristics, and interaction of radiation with the film (secondary processes and the range of secondary electrons in the film). The effect of geometric blurring of the absorption image of the plate edge due to the size of the radiation source in our case is 19.5 μm, which is comparable to the distance between possible refractive intensity stripes. The effect of additional geometric blurring of the absorption image of the plate edge due to inclination of the edge surface depends on the value of its inclination angle relative to the radiation direction and can be very significant for thick plates. The intrinsic unsharpness of the X-ray film, which can be sufficiently large (tens of microns) with hard radiation, is also important [3].

References

[1] M.M. Rychkov, V.V. Kaplin, S.I. Kuznetsov et al. J. of Surface Investigation. 13/4 (2019)
[2] M.M. Rychkov, V.V. Kaplin, E.L. Malikov et al. J. of Nondestr. Evaluation. 37/1 (2018) 13
[3] M.M. Rychkov, V.V. Kaplin, and V.A. Smolyanskiy J. of Surface Investigation. 15/2 (2021)

* E-mail: vsmol@tpu.ru

High Harmonic Generation from MgO crystals by two-color pulses

F Navarrete[1,2] and U Thumm[1]

[1]Department of Physics, Kansas State University, Manhattan, KS 66506, USA

[2]Institute of Physics, University of Rostock, 18051 Rostock, Germany

Synopsis We simulated high-harmonics generation (HHG) in model crystals by few-cycle pulses composed as the phase-coherent superposition of a mid-infrared fundamental pulse and its second harmonic. We adjusted the model-crystal parameters to reproduce the lowest band gap of MgO. By varying the ratio between the two spectral components and their delay (relative phase) at fixed pulse energy, we controlled the driving-pulse temporal profile. For specific amplitude ratios and delays, we find an up to five-fold enhancement of the HHG yield and can modify the cutoff frequency.

HHG from gaseous atoms is relatively well understood, but is still debated [1] and has been scrutinized experimentally only recently [2] for solid targtes [1]. While HHG is usually driven by single intense mid-IR laser pulses, recent studies analyzed the effects of coherently adding a second delayed pulse of higher frequency on the frequency response of the solid sample and HHG yield [1,3].

We investigated intra- and interband contributions to HHG in MgO model semiconductors, driven by the phase-coherent superpositions of 3200 and 1600 nm laser pulses with adjustable delay and intensity ratio. We solved the time-dependent Schrödinger equation in single-active-electron approximation by expanding the active electron's wave function in a basis of adiabatically field-dressed Bloch (Houston) states, including crystal momenta in the entire Brillouin zone

We performed systematic numerical calculations over a large parameter range of amplitude ratios and time delays of the two pulses to characterize the enhancement of the HHG yield and the variation of the cutoff frequencies. We explained both effects analytically within a semiclassical saddle-point approximation. The resulting spectrum is composed of both even and odd harmonics. For specific pulse shapes we find an up to fivefold increase of the integrated HHG yield relative to a single-frequency driving laser pulse of equal pulse energy (Fig. 1).

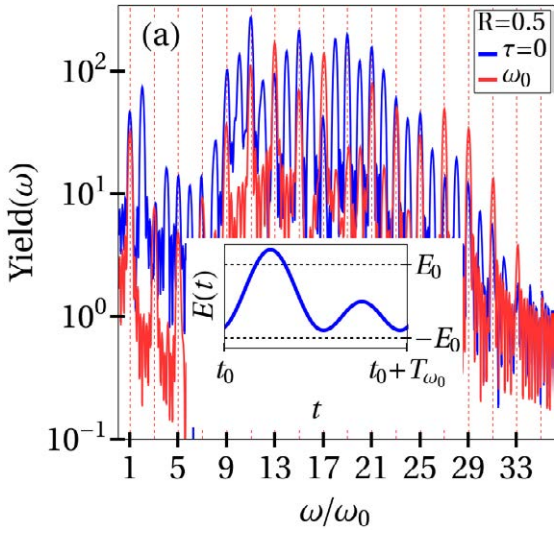

Figure 1. HHG spectrum of a bichromatic pulse (black line) in comparison with the spectrum generated by the monochromatic 3200 nm primary pulse (red line). The electric-field amplitude of the monochromatic pulse is 0.15 V/Å. The bichromatic pulse shape is shown in the inset and maximizes the peak bichromatic electric-field strength. For these parameters we find a twofold increase of the integrated HHG yield

Supported by the US DOE and DoD.

[1] Navarrete F *et al* 2019 *Phys. Rev. A* **100,** 033405
[2] Ghimire S *et al* 2011 *Nat. Phys.* **7** 138
[3] Luu T T and Wörner H J 2018 *Phys. Rev.A* **98**, 041802(R)
[4] Navarrete F and Thumm U 2020 *Phys. Rev. A* **102**, 063123

* E-mail: thumm@phys.ksu.edu

Enhanced high-harmonic generation yield in doped semiconductors

V E Nefedova[1], S Fröhlich[1], F Navarrete[2,3], N Tancogne-Dejean[4], D Franz[1], A Hamdou[1], S Kaassamani[1], D Gauthier[1], R Nicolas[1,5], G Jargot[6,7], M Hanna[6], P Georges[6], M F Ciappina[8,9,10], U Thumm[2,*], W Boutu, and H. Merdji[1]

[1]Ultrafast Nanophotonics group, LIDYL, CEA-CNRS-Université Paris-Saclay, France
[2]Department of Physics, Kansas State University, Manhattan, USA
[3]Institute of Physics, University of Rostock, Germany
[4]Max Planck Institute for the Structure and Dynamics of Matter and CFEL, Hamburg, Germany
[5]Department of Natural Sciences, Lebanese American University, Beirut, Lebanon
[6]Université Paris-Saclay, Institut d'Optique, CNRS, Laboratoire Charles Fabry, Palaiseau, France
[7]Fastlite, Antibes, Sophia Antipolis, France
[8]ICFO-Institut de Ciences Fotoniques, The Barcelona Institute of Science and Technology, Spain
[9]Physics Program, Guangdong Technion – Israel Institute of Technology, Shantou, Guangdong, China
[10]Technion – Israel Institute of Technology, Haifa, Israel

Synopsis High-order harmonic generation (HHG) from semiconductors is a promising candidate for promoting compact coherent extreme ultraviolet (XUV) light sources. Tailoring the band gap of MgO crystals with very low Cr dopant concentrations, we measured the HHG yield in the XUV domain. Our observations are supported by a numerical model that emphasizes the importance of defect states in the MgO crystal.

When an intense electric field interacts with a semiconductor or a dielectric, electron-hole pairs are formed. These are then accelerated by the field and emit coherent radiation up to high multiples of the fundamental frequency via inter- and intra-band electronic transitions in the solid. HHG from doped crystals is a new source of coherent extreme ultraviolet (XUV) attosecond radiation and candidate for assembling efficient XUV sources.

We present a method for increasing the HHG yield from solids by modifying and controlling the electronic configuration of the active medium. The Cr dopants in magnesium oxide (MgO:Cr) introduce impurity and vacancy states that change the minimum band gap. Since the interband HHG yield is proportional to the solid's minimum band-gap energy [3], its reduction is expected to increase the HHG yield [4].

Figure 1 show our first experimental determination of the measured increased HHG efficiency, supported by our numerical calculations based on the solution of the semiconductor Bloch equations [5].

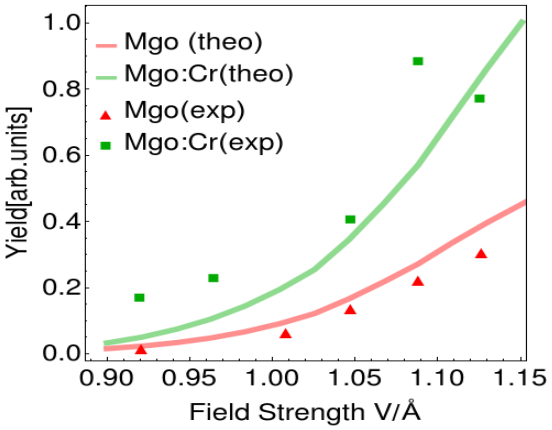

Figure 1. HHG yield for MgO and MgO:Cr as a function of the driving-laser peak-electric-field strength.

Supported by the US DoE and DoD.

[1] Vampa G, *et al.,* 2015 IEEE *J. Sel. Top. Quantum Electron.* **21**, 8700110
[3] Navarrete F, et al., 2019 *Phys. Rev. A* **100**, 033405
[4] Huang T, *et al.,* 2020 *Phys.Rev. A* **96**, 043425
[5] Nefedova V, *et al.* 2020 arXiv:2001.00839, App. Phys. Lett., accepted for publication

* E-mail: thumm@phys.ksu.edu

Investigation of the mode symmetries in Sapphire phoXonic cavities

H. Bentarki[1,†], A. Makhoute[1,2], K Tökési[3,*]

[1] Physics of Radiation and Laser-Matter Interactions, Faculty of Sciences. Moulay Ismail University. B.P. 11201, Zitoune, Meknes, Morocco
[2] Affiliation with laboratory and/or University name, city, zip code, country
[3] Institute for Nuclear Research (ATOMKI), Debrecen, 4026, Hungary

Synopsis In this work we present theoretical studies of the acousto-optic interaction in 2D Sapphire phoXonic crystal drilled with holes. Our study focuses on the acousto-optic couplings inside a phoXonic cavity by taking into account two coupling mechanisms, the photoelastic effect and effect of movement of the interfaces. We found that the elastic and the electromagnetic energy can be confined simultaneously inside a cavity created by modifing one hole in the perfect structure.

Recently several studies have looked at the possibility of finding periodic structures that behave both as photonic and phononic crystal [1] with the concept of phoXonic crystal. The interest of such an artificial crystal is to provide the possibility of confining the optical and acoustic energy in an extremely small volume in order to exalt the interactions between these two types of waves. These properties make these artificial crystals interesting for many applications in integrated optics for the realization of new components such as micro guides with low losses, micro sources laser.

The interest of studying these artificial crystals is to improve the performance of optical devices by controlling the propagation of electromagnetic waves in the presence of elastic waves.[2]

In this work, we investigated the opening of simultaneous photonic and phononic band gaps in a simple square periodic array of holes drilled in Sapphire substrate.

The goal is to study the acousto-optic coupling, based on both photo-elastic and opto-mechanical mechanisms, in periodic structures with simultaneous photonic and phononic band gaps. The acousto-optic interaction generates a phonon thanks to the excitation of the cavity by the confinement of the optical wave. The aim in this field being to seek a maximum coupling of this interaction, and this also due to a strong confinement of the waves in the micro cavities.

The photoelastic effect (PE) and the effect of the movement of the interfaces (MI) are two mechanisms that contribute to the acousto-optical interaction.

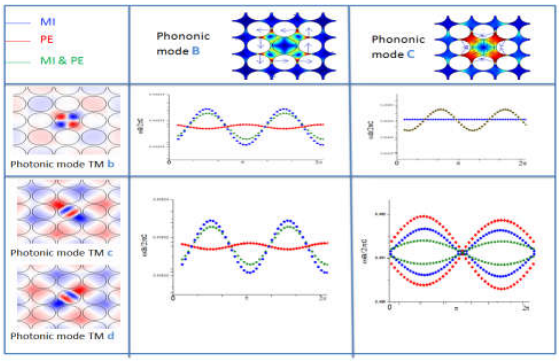

Figure 1. (Color online) Modulation of the TM modes (b), (c) and (d) during a period T = 2π/Ω of acoustic oscillations for the phononic modes (B) and (C) in the Sapphire matrix. The colors blue, red and green show respectively the effects of movement of the interfaces (MI), photoelastic (PE) and both at once (MI + PE).

The work was support by the by the Bilateral relationships between Morocco and Hungary in science and technology (S&T) under the project number 2018-2.1.10- TÉT-MC-2018-00008.

References

[1] Martin Maldovan et Edwin L. Thomas, "Simultaneous localization of photons and phonons in two dimensional periodic structures". Applied Physics Letters, 88(25): 251907, 2006.
[2] H. Bentarki, A. Makhoute, K. Tökési and A. El karkri " Signatures of the mode symmetries in Sapphire phoXonic cavities" (To be published).

* E-mail: tokesi@atomki.hu
† E-mail: bentarki.houda@gmail.com

Inorganic-organic lead trihalide perovskites as potential extreme ultraviolet scintillators

M. van der Geest*[,1], L. McGovern[2], G. Grimaldi[2], S. van Vliet[1], H.Y. Zwaan[1], N. Sadegh[1], B. Ehrler[2], P.M. Kraus[1,3]

[1]Advanced Research Center for Nanolithography, Science Park 106, 1098 XG, Amsterdam, The Netherlands.
[2]AMOLF, Science Park 102, 1098 XG, Amsterdam, The Netherlands.
[3] Department of Physics and Astronomy, and LaserLaB, Vrije Universiteit, De Boelelaan 1105, 1081 HV Amsterdam, The Netherlands

Synopsis We present extreme ultraviolet radiation sensitive scintillator candidates in the form of thin film methylammonium lead halide perovskites and discuss their macroscopic response and dynamics as observed through various surface and bulk sensitive experimental techniques.

Inorganic-organic lead trihalide perovskites are a class of versatile materials with properties, such as damage resistance, facile synthesis, high quantum efficiency and short absorption lengths for relevant wavelengths, that make them interesting in applications such as solar cells, lasers and LED's. The same properties that make these perovskites interesting for the aforementioned applications, also make them interesting for applications as high energy radiation scintillators, something which has not been extensively investigated in the case of extreme ultraviolet (XUV) radiation.[1,2] With the advent of extreme UV based nanolithography as well as concerns related to XUV radiation damage in space-based solar cells, being able to detect and potentially even utilize this radiation is of great interest.

We present the applicability of two methylammonium lead trihalide perovskites as XUV scintillators. The perovskites were exposed to a pulsed XUV source based on high harmonic generation (HHG), during and after which the luminescence, surface chemistry and morphology were characterized and contrasted to fresh unexposed samples. We will discuss the rather complicated photobleaching and luminescence recovery dynamics that can be observed during continuous exposure and compare them to established XUV scintillators such as sodium salicylate (Figure 1). We relate these observations to morphological and chemical changes that become apparent through, among others, atomic force microscopy (AFM) and X-ray photoelectron spectroscopy (XPS). We will also discuss the time-resolved emission of these perovskites and how it compares to established time-resolved emission experiments excited by visible and deep UV excitation.[3] Lastly, we discuss how these dynamics, combined with the surface chemistry and luminescence recovery results make the perovskites suitable as novel XUV scintillators and which challenges remain.

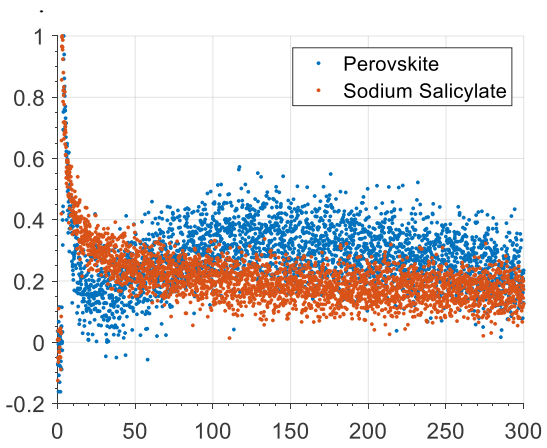

Figure 1. Bleaching dynamics of a methylammonium lead halide perovskite compared to established XUV scintillator sodium salicylate.

References

[1] Wei, H et al, 2016, Nat Phot, vol. 10, 5, pp. 333-339
[2] Chen, Q et al, 2018, Nature, vol. 561, pp 88-93
[2] Richter, J et al, 2016, Nat Comm, vol. 7, pp. 1-8

* E-mail: M.vdGeest@arcnl.nl

Three mathematical models of photons

I Bersons[1], R Veilande[1 *] and O Balcers[2]

[1]Institute of Atomic Physics and Spectroscopy, University of Latvia, Riga, LV-1004, Latvia
[2]Engineering Faculty, Vidzeme University of Applied Sciences, Valmiera, LV-4201, Latvia

Synopsis: New ideas that mathematically describe a free propagated photon are proposed. To validate them, they should be tested experimentally.

There is growing interest on the interaction of matter and light, as well as the single quantum technologies where the main element is a photon. But there is not a complete understanding of what a photon is exactly. We compare 3 different mathematical models of a photon [1]:

1. The theory of photons is based on the quantization of Maxwell equations which was reduced to the quantization of an infinite number of linear harmonic oscillators. The quantization procedure provides the correct energy and momentum of the photon and perfectly describes the creation and annihilation of photons. The quantization of the field is the cornerstone of the quantum field theory and, especially, quantum electrodynamics. Despite the great success of the quantization of light, the physics of this procedure is not so clear: what is there that oscillates and where are photons located in time and space? The definition of a photon as a first excited state of a single mode of the quantized electromagnetic field is rather abstract.

2. If we look at the photon as a stable object that is localized in space, the same definition is valid for a soliton. The several nonlinear equations (that could be reduced to the nonlinear Schrödinger equations) with the three dimensional electromagnetic soliton type solution were proposed [2-3]. In these models the nonlinearity in the Maxwell equations is introduced by small, finite components of polarization and magnetization in a vacuum along the direction of propagation of light. The one- and two-soliton solutions are found in a vacuum and in dielectrics (see Figure 1a).

3. Combining the mathematics of the first and second models, the new photon model is proposed [1] (see Figure 1b). The free propagating photons are described by the vector potential, the function, which is a product of harmonic oscillator eigenfunction with the coordinate ωt-$\boldsymbol{kr}$ and the Gaussian functions of the transverse coordinates. The interaction potential between the photons and the charged particle differs from the potential derived by the traditional quantization method only with the definition of the harmonic oscillator coordinates.

The reflection and refraction of photons on the boundary between two dielectrics is considered [4]. The amplitudes of the reflected and transmitted photons are determined by the Fresnel formulas, such as for the plane waves, but the transverse size of the transmitted photons in the plane of incidence changes with the angle of incidence changing.

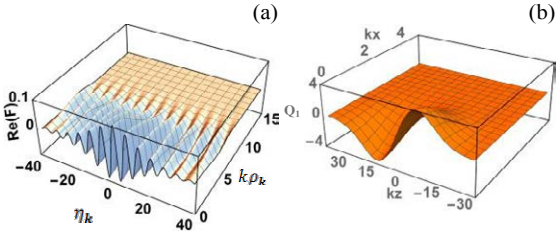

Figure 1. The cross section of the real part of the dimensionless vector potential: (a) the photon-soliton model; with dependence on the polar radius $k\rho_k$ and $\eta_k=\omega t$-$\boldsymbol{kr}$; (b) the new model for the one photon state; with dependence on the coordinates x and z ($y=0$), $\boldsymbol{k}$ is the wave vector.

RV gratefully acknowledges support by ERDF project No. 1.1.1.1/18/A/155.

References

[1] I.Bersons, R.Veilande, and O.Balcers *"Mathematical models of photons"*, submitted to the *Journal of Mathematical Physics*
[2] I.Bersons, R.Veilande and O.Balcers, *Phys.Scr.* **91**, 065201 (2016)
[3] I.Bersons, R.Veilande and O.Balcers, *Phys.Scr.* **95**, 025203 (2020)
[4] I.Bersons, R.Veilande, and O.Balcers *"Reflection and refraction of photons"* in preparation.

* E-mail: rita.veilande@lu.lv

Dependence of low-frequency THz radiation on electron population distributions from graphene

Z Guan[1], G L Wang[1]* and X X Zhou[1]†

[1]College of Physics and Electronic Engineering, Northwest Normal University, Lanzhou, 730070, China

Synopsis We study on characteristics of terahertz (THz) radiation from mono-layer graphene driven by normal incident two-color laser pulses. It is found that THz spectra in low frequency region depend sensitively on phase difference of driving laser pulses. Our simulations further show that the dependence of low-frequency THz radiation on phase difference of two-color laser pulses is affected by the asymmetry parameters which is determined by electron population distributions.

Recently, interaction between light and graphene materials has attracted considerable interest due to special physical and chemical properties of graphene. THz radiation is one of the important nonlinear optical phenomena in the interaction of laser pulses and graphene materials [1]. Due to weak radiation strength, THz ouput has hardly been observed in the experiment at normal incidence of the pump beam so far [2]. In one of our recent work, we propose a scheme to enhance THz field by using few-cycles laser pulses [3]. Here, we investigate properties of terahertz (THz) radiation from mono-layer graphene in two-color laser pulses. Our results show that THz spectra in low frequency region depend sensitively on phase difference of two-color laser pulses. We define an asymmetry parameter of electron population difference between conduction band and valence band to interpret depence of low-frequency THz emission on phase difference.

In Fig.1(a), we present the dependence of low-frquency radiation on phase difference of two-color laser pulses (λ_1=800 nm and λ_2=400 nm), the pulses duration is 63.96 fs, total peak intensity is 3.159×10^{11}W/cm^2, intensity ratio I_1/I_2=2, carrier envelope phase (CEP) of fundamental frequency laser pulses ϕ_1=0. It is found that the THz yield ($\int_{0.1\mathrm{THz}}^{10\mathrm{THz}} |\mathbf{E}_{\mathrm{THz}}(\omega)|^2 d\omega$) displays a periodic variation in π period with changing of ϕ_2. When ϕ_2=0, the THz radiation is very weak, then it quickly reaches its maximum at $\phi_2=\pi/2$. Figure 1(b) shows the dependence of the asymmetry parameters on ϕ_2, the asymmetry parameters is related to electron population difference between conduction band and valence band at end of laser pulses. We define it as $\xi=\frac{P_+-P_-}{P_++P_-}$, where $P_+=\int_0^\infty dk_x \int_{-\infty}^{\infty}(\rho_{cc}(\mathrm{k},\mathrm{t_f})-\rho_{\mathrm{vv}}(\mathrm{k},\mathrm{t_f}))\mathrm{dk_y}$, $P_-=\int_{-\infty}^0 dk_x \int_{-\infty}^{\infty}(\rho_{cc}(\mathrm{k},\mathrm{t_f})-\rho_{\mathrm{vv}}(\mathrm{k},\mathrm{t_f}))\mathrm{dk_y}$, here, $\rho_{cc}(\mathrm{k},\mathrm{t_f})$ and $\rho_{cc}(\mathrm{k},\mathrm{t_f})$ are electron populations in conduction band at t_f=∞ and electron populations in valence band at t_f=∞, respectively. From Fig.1(b), it is found that asymmetry parameters ξ displays a periodic variation in 2π period with changing of ϕ_2 and ξ^2 displays a periodic variation in π period with changing of ϕ_2. The dependence of low-frquency radiation on ϕ_2 can be well described by change of ξ^2 with ϕ_2.

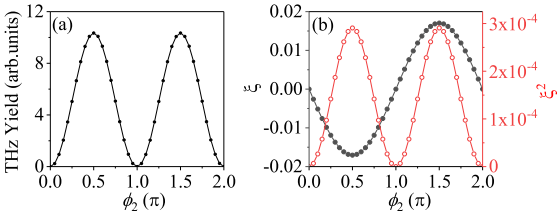

Figure 1. Dependence of (a) low-frequency THz yield (0.1-10 THz) and (b) asymmetry parameters on ϕ_2 (ϕ_1=0).

Acknowledgments This work was supported by the National Natural Science Foundation of China (Grant Nos.11764038, 11864037 and 91850209).

References

[1] Bahk Y M *et al* 2014 *ACS Nano.* **8** 9089
[2] Maysonnave J *et al* 2014 *Nano Lett.* **14** 5797
[3] Guan Z *et al* 2021 *Chin. Phys. Lett.* (Accepted)

*E-mail: wanggl@nwnu.edu.cn
†E-mail: zhouxx@nwnu.edu.cn

INDEX

Last Name	First Name	Proposal Title	Abstract Topic (Projectile)	Room Letter	Poster #	Page #
Arthur-Baidoo	Eugene	Selective fragmentation in the tirapazamine molecule by low-energy electrons	Lepton	Room G	G05	282
Ashrafi	Aydin	Orientation of OCS molecular fragments following irradiation by 7fs laser pulses	Photon	Room L	L40	483
Ayuso	David	Ultrafast, all-optical and highly enantio-sensitive imaging of molecular chirality	Speaker	Progress Report		28
Bachi	Nicolás	Classical description of the electron-impact ionization of Carbon	Lepton	Room E	E01	210
Bagdia	Chandan	Ionization and fragmentation of PAH molecules by swift projectile ions	Heavy	Room B	B06	136
Bakhiet	Mohammedelnazier	EUV spectral measurements and theoretical investigation of Mo^{4+}-Mo^{17+} ions in laser-produced plasmas	Photon	Room I	I09	339
Balciunas	Tadas	Femtosecond soft–X–Ray absorption spectroscopy of liquids with a waterwindow high-harmonic source	Photon	Room L	L18	464
Barik	Saroj Kumar	Formation of small hydrocarbons from polycyclic aromatic hydrocarbons via dissociative ionization in the interstellar medium	Photon	Room L	L19	465
Barrachina	Raul Oscar	On how classical uncertainties enfeeble quantum coherence	Speaker	SR (Room B)	B08	61
Barrachina	Raul Oscar	On how a target atom might hide in plain sight due to a loss of coherence of the projectiles beam	Heavy	Room B	B07	137
Barreiro-Lage	Darío	Photoionization and fragmentation of diketopiperazines. Computational and experimental efforts on the search of the 'seeds of life'	Photon	Room L	L20	466
Beauvarlet	Sandra	Asymmetric electron backscattering in strong-field ionization of chiral molecules	Photon	Room L	L21	467
Belsa	Blanca	Imaging the ultrafast umbrella (inversion) motion in ammonia	Speaker	SR (Room L)	L22	62
Benda	Jakub	Multi-photon and strong-field ionization of moleculesin stationary and time-dependent R-matrix approaches	Photon	Room L	L24	469
Benis	Emmanouil	State-resolved KLL cross sections of single electron capture in collisions of swift $C^{4+}(1s2s\ ^3S)$ ions with gas targets	Heavy	Room A	A05	95
Benis	Emmanouil	Pauli Shielding and Breakdown of Spin Statistics in Multielectron, Multi-Open-Shell Dynamical Atomic Systems	Heavy	Room A	A06	96
Ben-Itzhak	Itzik	Step-by-step, state-selective tracking of sequential fragmentation dynamics of water dications by coincidence momentum imaging	Photon	Room L	L23	468
Bernitt	Sonja	PolarX-EBIT: A versatile tool for high-resolution resonant photoexcitation spectroscopy with highly charged ions	Lepton	Room F	F04	245
Bertolino	Mattias	Multiphoton interaction phase shifts in attosecond science	Photon	Room I	I10	340
Bettega	Marcio	Electron scattering by molecules relevant to plasma processing	Lepton	Room H	H01	317
Bharti	Divya	Multi-Sideband RABBITT in Atomic Hydrogen and Argon: Theory and Experiment	Photon	Room I	I11	341
Bhattacharyya	Surjendu	Strong-field-induced dissociation dynamics of tribromomethane ($CHBr_3$) studied using coincident ion momentum imaging	Photon	Room L	L25	470
Bhogale	Abhijeet	Ionization of water under the impact of 250 keV proton beam	Heavy	Room B	B09	138
Biedma	Luis	Numerical methods for few body problems in atomic physics	Photon	Room I	I12	342
Biela-Nowaczyk	Weronika	Higher-order recombination processes in HCl's	Speaker	Progress Report		29
Bijlsma	Klaas	Energy transfer from keV and lower energy Sn ions to H_2 molecules	Heavy	Room B	B10	139

Last Name	First Name	Proposal Title	Abstract Topic (Projectile)	Room Letter	Poster #	Page #
Biswas	Shubhadeep	Probing influence of molecular environment and dynamic polarization in photoemission delays	Photon	Room L	L26	471
Blondel	Christophe	Direct absorption measurements of the two-photon excitation cross-section of the 6p'[3/2]$_2$ and 6p'[1/2]$_0$ levels of Xe I with a new analytical formula	Photon	Room I	I13	343
Bocan	Gisela	Very grazing incidence effects on fast He diffraction from KCl(001)	Heavy	Room D	D09	200
Boll	Diego	Two-photon single ionization of helium: from below-threshold to doubly-excited states	Speaker	Progress Report		30
Bondy	Aaron	Two-photon decay rates in heliumlike atoms: Finite-nuclear-mass effects	Photon	Room I	I14	344
Bordas	Christian	Photoionization microscopy in the time domain: classical atomic chronoscopy	Photon	Room I	I15	345
Borisova	Gergana D.	Strong-field ionization of FEL-prepared doubly excited states in helium	Photon	Room I	I16	346
Borovik	Alexander	Status of the Transverse Free-Electron Target for the Heavy-Ion Storage Ring CRYRING@ESR	Lepton	Room F	F05	246
Borovik	Oleksandr	Autoionization and direct ionization of Cs atoms by electron impact	Lepton	Room E	E02	211
Borràs	Vicent J.	The XCHEM code: photoelectron angular distributions of the CO molecule	Photon	Room L	L27	472
Bou-Debes	Daniel	Dissociative ionization pathways of guanine tautomers	Photon	Room K	K21	427
Bouwman	Dennis	Neutral dissociation of methane by electron impact and a complete and consistent cross section set	Lepton	Room G	G06	283
Boyer	Alexie	Ultrafast dynamics of correlation bands following XUV molecular photoionization	Speaker	SR (Room L)	L28	63
Boyle	Daniel	Electron-impact dissociation of H_2 and its isotopologues into neutral fragments	Lepton	Room G	G07	284
Bray	Abbie	Beyond Born-Type Methods in Investigating the Core Dynamics of Excited Helium	Photon	Room I	I17	347
Brédy	Richard	Non-ergodic fragmentation of protonated reserpine induced by fs-laser interaction	Photon	Room L	L29	473
Bromley	Steven	Time-Dependent Close-Coupling Calculations of nl-resolved cross sections for collisions of bare Ne and Mg incident on atomic hydrogen and helium between 1 - 5 keV/amu	Heavy	Room A	A07	97
Brown	Andrew	The R-matrix with time (RMT) project	Photon	Room I	I18	348
Brown	Graham	Optical Measurement of Photorecombination Time Delays	Photon	Room I	I19	349
Buhr	Ticia	Comprehensive investigation of nondipole effects in photoionization of the He 1s and Ne 2s shells	Photon	Room I	I20	350
Bulhakova	Alla	Processes of excitation of glutamine molecules by electron impact	Lepton	Room G	G08	285
Bulhakova	Alla	Ionization and fragmentation of glutamic acid and glutamine molecules in the gas phase by electron impact	Lepton	Room G	G09	286
Bulhakova	Alla	Single ionization of valine amino acid molecule	Lepton	Room G	G10	287
Busto	David	Probing electronic coherence in the vicinity of Fano resonances using high resolution photoelectron interferometry	Photon	Room I	I21	351
Call	Demitri	Molecular Frame Photoelectron Angular Distributions for Dissociation of 1,1-Dichloroethene ($C_2H_2Cl_2$) at the Chlorine L-edge	Photon	Room L	L30	474
Callegari	Carlo	Two-photon ionization using superradiant light from a Free-Electron Laser	Photon	Room I	I22	352

Last Name	First Name	Proposal Title	Abstract Topic (Projectile)	Room Letter	Poster #	Page #
Camper	Antoine	Production of antihydrogen pulses at AEgIS	Speaker	SR (Room H)	H18	64
Campi	Filippo	A high-harmonic generation source for ultrafast X-ray imaging and spectroscopic applications driven by a high-power mid-infrared optical parametric chirped-pulse amplifier	Photon	Room I	I23	353
Campi	Filippo	Efficient extreme-ultrabiolet multi-band high-order wave mixing in silica	Photon	Room O	O02	559
Cariker	Coleman	Stabilization of an autoionizing polariton in attosecond transient absorption	Photon	Room I	I24	354
Carlini	Laura	Photoemission and state-selected fragmentation in cyclic dipeptides containing an aromatic amino acid	Speaker	SR (Room L)	L31	65
Carlström	Stefanos	Core hole motion revealed through interference in above-threshold ionization	Photon	Room I	I25	355
Cassidy	Jack	Positron binding and annihilation with nitrogen- and oxygen-containing molecules	Lepton	Room E	E23	231
Chacko	Roby	Dissociation dynamics of C_nN^- (n = 1-3, 5-7) anions and formation of smaller anions in the interstellar and circumstellar mediums	Heavy	Room A	A08	98
Chakrabarti	Kalyan	Electron collision with CH: negative ion states and cross sections	Lepton	Room F	F33	271
Champenois	Caroline	The physics of radio-frequency traps in a collision physics perspective	Speaker	Tutorial		23
Champenois	Caroline	Using Coulomb collisions in a radio-frequency trap to detect a single heavy molecule	Heavy	Room C	C02	165
Chen	Dongyang	Ultraviolet photon detection system for precision laser spectroscopy of Lithium-like $^{16}O^{5+}$ ions at CSRe	Heavy	Room C	C03	166
Chen	Yang-Yang	Role of carrier-envelope phase on below-threshold high-order harmonic generation of Ar atom	Photon	Room I	I26	356
Cheng	Rui	Dynamic charge-changing processes in Ne^{7+} ions collision with Ar atoms near the Bohr velocity	Heavy	Room A	A09	99
Chiarinelli	Jacopo	Unrevaling of inter- and intra-molecular interactions in homogeneous and hydrated uracil clusters	Photon	Room L	L03	449
Chiarinelli	Jacopo	An experimental and theoretical investigation of the valence photoemission spectra of uracil clusters	Photon	Room L	L04	450
Chrétien	Renaud	Inversion of coherent backscattering with interacting Bose-Einstein condensates in two-dimensional disorder : a Truncated Wigner approach	Heavy	Room A	A10	100
Chuluunbaatar	Aldarmaa	Photoelectron momentum distribution of œlium atom	Photon	Room I	I27	357
Ciappina	Marcelo	Unified real and momentum space collision picture of high-order harmonic generation in solids	Photon	Room O	O03	560
Cistaro	Giovanni Consalvo	Attosecond x-ray transient absorption spectroscopy in graphene	Photon	Room O	O04	561
Čížek	Martin	On implementation of PO formalism into R-matrix calculations.	Lepton	Room G	G11	288
Cohen	Samuel	Glory interference spectroscopy of Sr atom	Photon	Room I	I28	358
Colaizzi	Lorenzo	Angle-resolved Photoelectron Spectroscopy of large Water Clusters ionized by an XUV Comb	Photon	Room L	L05	451
Cornetta	Lucas	Solvent effects in low energy electron scattering	Speaker	Progress Report		31
Corrêa De Freitas	Thiago	Low-energy electron collisions with cubane	Lepton	Room G	G12	289
Coutinho	Lucia	Metastable dications formation from chloronenzene probed by mass-selected Auger electron spectroscopy	Photon	Room L	L32	475

Last Name	First Name	Proposal Title	Abstract Topic (Projectile)	Room Letter	Poster #	Page #
Eckart	Sebastian	Holographic Angular Streaking of Electrons (HASE)	Speaker	SR (Room I)	I32	68
Eklund	Gustav	Photodetachment studies of CH^- using a cryogenic storage ring	Photon	Room K	K23	429
Esponda	Nicolás	Distorted wave models for electron emission by impact of dressed proyectiles	Heavy	Room A	A11	101
Fabrikant	Ilya	Semiclassical theory of laser-assisted dissociative recombination	Lepton	Room F	F07	248
Fabrikant	Ilya	Collisions of excited Ps with antiprotons: Ps break-up and antihydrogen formation	Lepton	Room F	F08	249
Fehre	Kilian	Fourfold differential Photoelectron Circular Dichroism	Photon	Room L	L36	479
Fehre	Kilian	Strong Differential Photoion Circular Dichroism in Strong-Field Ionization of Chiral Molecules	Photon	Room L	L37	480
Fehre	Kilian	Enantiosensitive Structure Determination by Photoelectron Scattering on Single Molecules	Photon	Room L	L38	481
Fernandez	Ruben	Spectral Signature of Molecular Charge Migration	Photon	Room L	L39	482
Fernández	Francisco	Time-Resolved Images of Intramolecular Charge Transfer in Organic Molecules	Photon	Room M	M01	484
Fernández Milán	Pedro	Photoionization and MFPADS in polyatomic molecules with XCHEM	Photon	Room K	K24	430
Figueira Nunes	Joao Pedro	Imaging the structural dynamics in the photo-induced proton transfer reaction of o-nitrophenol by Ultrafast Electron Diffraction	Speaker	SR (Room H)	H03	69
Franz	Jan	Cooling of C_2^- in ion traps with H_2 as a partner gas	Heavy	Room B	B13	141
Franz	Jan	Monte-Carlo simulations of electron emission from liquid water	Lepton	Room H	H14	327
Frapiccini	Ana	Photoionization of hydrogen confined in onion shells with Generalized Sturmians in the time-dependent frame.	Photon	Room I	I33	362
Frapiccini	Ana	Generalized Sturmians functions in prolate spheroidal coordinates for bound and continuum states of diatomic systems	Photon	Room M	M02	485
Freeman	David	High order harmonic generation in semiconductors driven at near- and mid-IR wavelengths	Photon	Room I	I34	363
Fuchs	Sebastian	High-Resolution Electron-Ion Collision Spectroscopy with Slow Cooled Pb^{78+} Ions in the CRYRING@ESR Storage Ring	Lepton	Room F	F09	250
Fukui	Yoshimitsu	Ab Initio Investigation on Bicircular High-Harmonic Spectroscopy of Molecular Chirality	Photon	Room M	M03	486
Gancewski	Maciej	Quantum calculations of O_2-N_2 scattering: Ab initio investigation of the N_2-perturbed fine structure lines in $O_2(X^3\Sigma_g^-)$	Heavy	Room B	B14	142
Ganguly	Smita	Enhancement in the yield of O_2^+ ions from photo-ionized CO_2 clusters	Photon	Room L	L06	452
Gao	Chunli	Time evolution of copper-aluminum alloy laser-produced plasmas in vacuum	Photon	Room K	K25	431
Garcia	Isaac	An investigation into low temperature dielectronic recombination rate coefficients	Lepton	Room E	E04	213
Geyer	Angelina	Strong Field Ionization of H_2 in Circularly Polarized Two-Color Laser Fields	Photon	Room M	M04	487
Gharbi	Chaima	Sodium isocyanide: helium potential energy surface and astrophysical applications	Heavy	Room D	D11	202
Gharibnejad	Heman	A Multi-Center Quadrature Scheme for the Molecular Continuum	Photon	Room M	M05	488
Ghosh	Soumen	Bound positron molecule annihilation resonances beyond fundamental modes	Lepton	Room E	E25	233
Goetz	Esteban	Quantum control of entangled photon pair emission in electron-ion collisions by laser-synthesized photoelectron wave packets	Lepton	Room F	F10	251

Last Name	First Name	Proposal Title	Abstract Topic (Projectile)	Room Letter	Poster #	Page #
Herczku	Peter	A new experimental apparatus for ion and electron impact studies on astrophys-ical ice analogues	Heavy	Room D	D01	192
Hergenhahn	Uwe	Limits to the observation of low kinetic energy electrons from liquid water compared to water clusters	Photon	Room O	O06	563
Hernández-García	Carlos	Light pulses structured at the attosecond timescale	Speaker	IUPAP PT		27
Hillenbrand	Pierre-Michel	K-shell vacancy production in slow Xe^{54+} - Xe collisions	Heavy	Room A	A15	105
Hofierka	Jaroslav	Many-body theory calculations of positron-atom binding energies using a Gaussian-orbital basis	Lepton	Room E	E07	216
Holzmeier	Fabian	What causes the angular dependence of photoionization time delays in a molecular shape resonance?	Photon	Room M	M11	492
Horton	Reese	Electron Energy Deposition in H_2	Lepton	Room G	G16	293
Hosea	Nishita Manohar	Photoionisation of Endohedral Alkali Atoms in Fullerene Cages	Photon	Room J	J01	370
Hu	Xiaoqing	Fragmentation dynamics of molecular ions in cluster environment	Speaker	Progress Report		38
Huo	Yining	The Electronic Changes of Gas-Phase PAH cations Induced by Atomic Hydrogenation Attachment	Photon	Room M	M12	493
Iacob	Felix	Reactive Electron Collision Dynamics And Rate Coefficients With Isotopologues of Beryllium Monohydride	Lepton	Room F	F12	252
Iacob	Felix	Electron-induced excitation and recombination of BeH^+ ions and isotopologues: reactional dynamics and rate coefficients	Lepton	Room F	F13	253
Ibrahim	Heide	A molecular road movie: capturing roaming molecular fragments in real time	Speaker	SR (Room M)	M13	72
Illescas	Clara	Excitation, electron capture and ionization in Be^{4+}+H(n = 1; 2) collisions: a comparative study	Heavy	Room C	C10	173
Indrajith	Suvasthika	Ion and electron induced molecular growth inside of linear hydrocarbons clusters	Heavy	Room B	B01	131
Indrajith	Suvasthika	Radiative cooling dynamics of tetracene cations stored in DESIREE	Photon	Room M	M14	494
Inhester	Ludger	Inner-shell-ionization-induced femtosecond structural dynamics of water molecules imaged in real time at an x-ray free-electron laser	Speaker	SR (Room M	M15	73
Iskandar	Wael	Investigation of relaxation pathways in D_2O^{2+} leading to $D^+ + O^+ +$ D fragmentation channel	Photon	Room M	M16	495
Jablonski	Lukasz	The role of internal dielectronic excitation in relaxation of Rydberg hollow atoms	Heavy	Room D	D13	204
Jiang	Jun	Theoretical study on the hyperpolarizability of Li atoms	Heavy	Room A	A16	106
Jorge	Alba	Classical trajectory time-dependent mean-field calculations for ion-molecule collisions	Speaker	Progress Report		39
Jozwiak	Hubert	Collisional effects in the self- and H_2-perturbed spectra of D_2	Heavy	Room B	B16	143
Jozwiak	Hubert	Ab initio investigation of the CO-N_2 quantum scattering: The collisional perturbation of the pure rotational R(0) line in CO	Heavy	Room B	B17	144
Juhász	Zoltán	Rotational excitation followed by collision-induced molecular dissociation in 10-keV $O^+ + H_2$ and O+ + D2 collisions	Heavy	Room B	B18	145
Jürß	Christoph	Edge-state contributions to high-order harmonic generation in topological insulators	Photon	Room O	O07	564
Kadokura	Rina	Accurate experimental cross sections for electron and positron scattering.	Speaker	Progress Report		40

Last Name	First Name	Proposal Title	Abstract Topic (Projectile)	Room Letter	Poster #	Page #
Kálosi	Ábel	Dissociative recombination of OH^+ at the Cryogenic Storage Ring	Speaker	SR (Room F)	F35	74
Kanda	Sohtaro	Search for metastable muonic atoms toward observation of atomic parity violation	Lepton	Room E	E08	217
Kanika	Kanika	Laser-Microwave Double-Resonance Spectroscopy: Toward Measurement of Magnetic Moments in Heavy, Highly Charged Ions.	Heavy	Room C	C11	174
Kariuki	Peter	Distorted Wave Born Approximation and Optical Potential Methods in Calculation of Cross Sections for Electron-Potassium Elastic Scattering	Lepton	Room E	E09	218
Karman	Tijs	Microwave control of ultracold molecular collisions	Speaker	Progress Report		41
Kartoshkin	Victor	Transfer of angular momentum at the interaction between spin polarized metastable helium atoms	Heavy	Room A	A17	107
Katsoulis	Georgios	Non-dipole effects in the double ionization of atoms and molecules	Photon	Room M	M17	496
Kazinski	Peter	Generation of twisted photons by charged particles in cholesteric liquid crystals with large pitch	Lepton	Room H	H10	323
Kheifets	Anatoli	Time resolved atomic ionization processes and tests of the fundamental threshold laws	Speaker	SR (Room J)	J02	75
Khokhlova	Margarita	Highly efficient XUV generation through high-order frequency mixing	Photon	Room J	J03	371
Khokhlova	Margarita	Generation of highly-elliptical resonant high-order harmonics	Photon	Room J	J04	372
Kiataki	Matheus	Bulk water effect upon Π^*_1 orbital of the 1-methyl-4-nitroimidazole	Lepton	Room H	H04	318
Kimura	Naoki	Laser spectroscopy of forbidden transitions between metastable excited states of I^{7+} in an electron beam ion trap	Speaker	SR (Room C)	C12	76
Kircher	Max	Gas-phase helium double ionization induced by Compton scattering	Photon	Room J	J05	373
Kirchner	Tom	Proton collisions with fluorine-containing biomolecules: an exploratory study based on an independent atom model including geometric overlap	Heavy	Room B	B19	146
Kirova	Teodora	Ultra-precise Rydberg atomic localization using spatially dependent fields	Photon	Room J	J06	374
Kislov	Konstantin	Resonant dissociative excitation of rare gas molecular ions by electron impact	Lepton	Room F	F36	273
Kivimäki	Antti	X-ray-induced anion production at the O K edge of simple alcohol molecules	Photon	Room M	M18	497
Knyazeva	Victoria	Investigation of linear and circular photon polarizations in two-photon 2s → 1s transitions in one-electron ions	Photon	Room K	K26	432
Kolbasova	Daria	Probing ultrafast coherent dynamics in core-excited xenon by using attosecond XUV-NIR transient absorption spectroscopy	Photon	Room J	J07	375
Koncevičiūtė	Jurgita	Electron-impact double ionization of B^+	Lepton	Room F	F14	254
Kono	Naoko	Spontaneous decay of highly excited C_2^-: electron emission versus fragmentation	Heavy	Room C	C13	175
Kossoski	Fábris	Applications and developments of the Schwinger multichannel method to electron-molecule collisions	Lepton	Room G	G17	294
Kristiansson	Moa	Experimental and theoretical studies of excited states in Ir-	Photon	Room K	K27	433
Kruse	Jan	From momenta to structure: Coulomb explosion imaging of small helium clusters	Photon	Room L	L09	455
Krusic	Spela	Self-induced splitting of Kωemission lines in zinc	Photon	Room J	J08	376

Last Name	First Name	Proposal Title	Abstract Topic (Projectile)	Room Letter	Poster #	Page #
Kübel	Matthias	Multiphoton light-induced potential energy surfaces in H_2^+	Photon	Room M	M19	498
Kukk	Edwin	The formative period in the X-ray-induced photodissociation of organic molecules	Photon	Room M	M20	499
Kumagai	Yoshiaki	Ultrafast electronic and nuclear dynamics in the nanoparticle induced by the hard-x-ray laser	Speaker	Progress Report		42
Kundu	Narayan	Effect of slicing in velocity map imaging for the study of dissociation dynamics in electron collision with isolated molecules	Lepton	Room G	G18	295
Kurz	Niels	Multi-photon ionization of photo-associated $X^1\omega_g^+(^6Li_2)$ dimers	Photon	Room M	M21	500
Küstner-Wetekam	Catmarna	Investigation of the increase in ICD efficiency with the number of nearest neighbors – first experimental results on Kr clusters	Photon	Room L	L10	456
La Mantia	David	RDEC for F^{9+} and F^{8+} Ions on Graphene: First Observation	Heavy	Room A	A18	108
La Mantia	David	Developing Compact Neomagnet Electron Beam Ion Trap and Penning Trap Beyond 0.7 T at NIST	Lepton	Room F	F15	255
LaForge	Aaron	Ultrafast resonant interatomic Coulombic decay induced by quantum fluid dynamics	Speaker	Progress Report		43
Lamour	Emly	Status of the FISIC platform for future ion-ion collisions	Heavy	Room D	D02	193
Lapicki	Gregory	Updated compilation, universal empirical and theoretical fits for K x-ray production cross sections by protons	Heavy	Room A	A19	109
Laurell	Hugo	Continuous variable quantum state tomography of electron wavepackets	Photon	Room J	J09	377
Laurent	Guillaume	Electron choreography at the attosecond time scale	Photon	Room J	J10	378
Li	Wen	CHARGE REVERSING MULTIPLE ELECTRON DETACHMENT AUGER DECAY OF INNER-SHELL VACANCIES IN GAS-PHASE DEPROTONATED DNA	Photon	Room M	M22	501
Li	Xiaokai	Revealing molecular strong field autoionization dynamics	Photon	Room M	M24	503
Li	Yang	Implementation of multiconfiguration time-dependent Hartree-Fock method for diatomic molecules on prolate spheroidal coordinates	Photon	Room M	M23	502
Liang	Chang-Tong	Dynamics of enhancement and suppression of the frequency-comb emission via high-order harmonic generation in few-cycle pulse trains	Photon	Room J	J11	379
Lin	Chih-Yuan	Time-resolved ionization of atoms in plasmas by short laser pulses	Photon	Room J	J12	380
Lin	Long	Mechanism of multi-plateau high-order harmonic generation in solid	Photon	Room O	O19	575
Liu	Hechuan	Probing sub-cycle oscillation dynamics of high-order harmonic generation of Na atom	Photon	Room J	J13	381
Liu	Jinlei	Near-threshold dynamics in strong laser field	Photon	Room J	J14	382
Liu	Xin	Precision Measurements of $^2P_{1/2}$-$^2P_{3/2}$ M1 Transitions in Boron-like S^{11+} and Cl^{12+} at EBIT	Lepton	Room F	F16	256
Liu	Xingbang	Numerical simulation of the interaction between nanosecond laser and silicon target	Photon	Room K	K28	434
Liu	Xinyao	Retrieving molecular structure using machine learning of laser-induced electron diffraction	Photon	Room M	M25	504
Loetzsch	Robert	High resolution measurement of the $2p_{3/2}$→$2s_{1/2}$ intra-shell transition in He-like uranium	Heavy	Room A	A20	110
Loriot	Vincent	HHG-2w attosecond stereo-photoionization unravel the shape resonance of N_2	Photon	Room M	M26	505

Last Name	First Name	Proposal Title	Abstract Topic (Projectile)	Room Letter	Poster #	Page #
Lozano	Ana I.	Methanol fragmentation probed in electron transfer experiments	Heavy	Room B	B20	147
Lu	Q	Visible lines from W^{8+} and W^{10+} in electron beam ion trap	Lepton	Room F	F17	257
Lutet-Toti	Bastien	Electron-electron coincidence measurements of solvated molecules with a liquid micro-jet device.	Photon	Room M	M27	506
Lyashchenko	Konstantin	Asymmetry in emission of photons with left- and right-hand circular polarizations in two photon decay	Photon	Room K	K29	435
Ma	Wanlu	A transverse electron target for electron-impact ionization of highly charged ions at the 320 kV platform	Lepton	Room F	F18	258
Ma	Xinwen	Atomic physics research at HIAF and future perspectives	Heavy	Room C	C14	176
Ma	Xinwen	APEX: A collaboration on Atomic Processes at EXtremes	Heavy	Room D	D03	194
Machalett	Frank	Laser-induced ionization of ions from high brightness ion sources	Photon	Room K	K30	436
Maclot	Sylvain	Cage-opening dynamics of adamantane	Speaker	Progress Report		44
Magrakvelidze	Maia	Photoionization of the $(Mg@C_{60})^+$ cation: A hybrid model	Photon	Room M	M28	507
Maiorova	Anna	Structured ion beams produced by radiative recombination of twisted electrons	Speaker	SR (Room C)	C15	77
Mairesse	Yann	Revealing the influence of molecular chirality on tunnel-ionization dynamics	Photon	Room M	M29	508
Majima	Takuya	Coincidence measurements between secondary ions and scattered projectiles in collisions of MeV-energy heavy ion with submicron droplets	Heavy	Room D	D14	205
Maltsev	Ilia	How to observe the vacuum decay in supercritical heavy-ion collisions	Heavy	Room C	C16	177
Mandal	Aditi	Ionization of atoms and molecules by twisted electron beams	Speaker	Progress Report		45
Mandal	Suddhasattwa	Structure of acetylene clusters in helium nanodroplets probed by Penning ionization electron spectroscopy	Photon	Room L	L11	457
Manschwetus	Bastian	Time-resolved ultrafast fragmentation dynamics of 1-butanethiol	Photon	Room M	M30	509
Manson	Steven	Relativistic effects in the Cooper minima and angular distributions of photoelectrons in heavy elements	Photon	Room J	J15	383
Manson	Steven	Photoionization branching ratios of spin-orbit doublets in heavy elements at high energy: Relativistic and interchannel coupling effects in Hg	Photon	Room J	J16	384
Manson	Steven	Photoionization of endohedral molecules: $N_2@C_{60}$	Photon	Room M	M31	510
Mansouri	Abdelaziz	Double ionization of argon by impact of fast electrons	Lepton	Room E	E10	219
Marciniak	Alexandre	Impact of aliphatic bonds on the stability of VUV photoprocessed PAHs under relevant astrophysical conditions	Photon	Room M	M32	511
Marjollet	Adrien	Initial state-selected molecular reactive scattering with non-equilibrium ring polymer molecular dynamics.	Heavy	Room B	B21	148
Martin	Fernando	Attosecond molecular science: a theoretical point of view	Speaker	Tutorial		24
Martini	Lara	Polarization control in two-color water molecule ionization	Photon	Room M	M33	512
Martini	Paul	Splashing of cold doped helium nanodroplets	Heavy	Room B	B02	132
Marucha	Alex	Relativistic Distorted Wave Approach to Electron Impact Excitation of Argon Gas Using a Complex Potential	Lepton	Room E	E11	220
Masin	Zdenek	Dissociative ω^* states in electron-molecule collisions and their interpretation	Lepton	Room G	G19	296

Last Name	First Name	Proposal Title	Abstract Topic (Projectile)	Room Letter	Poster #	Page #
Matsui	Hirokazu	Weak-field asymptotic theory of tunneling ionization of the hydrogen molecule including core polarization, spectator nucleus, and internuclear motion effects	Photon	Room M	M34	513
Maxwell	Andrew	Disentangling photoelectron vortices in strong field ionization	Photon	Room J	J17	385
Mccann	Michael	Theoretical and experimental determination of Au I-III lines withinCollisional-Radiative and LTE plasma regimes.	Lepton	Room E	E12	221
Mcginnis	Owen Dennis	Imaging SF_6 using Molecular Frame Photoelectron Angular Distributions	Photon	Room M	M35	514
Mehmood	Saad	Control of Parent-Ion Coherence in Helium Ion Ensemble	Photon	Room J	J18	386
Meister	Severin	Photoelectron spectroscopy of laser-dressed atomic helium	Photon	Room J	J19	387
Meltzer	Thomas	Accurate R-matrix photoionization models for intermediate-sized molecules	Photon	Room M	M36	515
Melzer	Niklas	A comprehensive study of the dissociation processes of water after core ionisation	Photon	Room M	M37	516
Mendes	Mónica	Low energy electron interactions with 5-aminoimidazole-4-carboxamide	Speaker	SR (Room G)	G20	78
Mendez	Alejandra	Universal scaling rule for the ionization of molecules by impact of ions	Heavy	Room B	B22	149
Méndez	Luis	Theoretical study of collisions of multicharged ions with water molecules	Heavy	Room B	B23	150
Menz	Esther	First Dielectronic-Recombination Experiments at CRYRING@ESR	Speaker	Progress Report		46
Menz	Esther Babette	Neutral Particle Imaging for Beam Analysis at CRYRING@ESR	Heavy	Room D	D04	195
Mezei	Janos Zsolt	New insights in the low energy electron-driven reactivity of molecular cations	Lepton	Room F	F37	274
Mi	Yonghao	Clocking enhanced ionization of H_2 with rotational wavepackets	Photon	Room M	M38	517
Middents	Wilko	First complete test of polarization transfer in elastic scattering of hard x-rays	Photon	Room J	J20	388
Mifsud	Duncan V.	High-Fluence S^+ Implantation in Simple Oxide Astrophysical Ice Analogues	Heavy	Room B	B24	151
Mihelic	Andrej	Calculation of multiphoton ionization amplitudes and cross sections of few-electron atoms	Photon	Room J	J21	389
Mishra	Debadarshini	Ultrafast Isomerization Dynamics in Small Molecules	Photon	Room M	M39	518
Mizuno	Tomoya	Observation of the quantum shift of a backward rescattering caustic by carrier-envelope phase mapping	Photon	Room J	J22	390
Moioli	Matteo	Attosecond electron dynamics near the ionization threshold in Ne	Photon	Room J	J23	391
Montanari	Claudia	Lanthanides, the importance of 4f electrons in the energy loss	Heavy	Room A	A21	
Mootheril Thomas	Deepthy Maria	Electron-Impact single ionization of lithium: Benchmark data	Lepton	Room E	E13	222
Moreira	Giseli	The electron-thiophene scattering dynamics under the influence of multichannel coupling effects	Speaker	SR (Room G)	G21	79
Moreira	Giseli	Calculated cross sections for elastic scattering of slow positrons by polar molecules	Lepton	Room E	E28	236
Mori	Nicolas	Calculation of the single differential cross section for electron-impact ionization of atoms and molecules	Lepton	Room G	G22	297
Morimoto	Yuya	Scattering of attosecond electron pulse trains by atomic targets	Speaker	Progress Report		47
Mozejko	Pawel	Cross sections measurements and calculations for low energy electron scattering from titanium tetrachloride	Lepton	Room G	G23	298

Last Name	First Name	Proposal Title	Abstract Topic (Projectile)	Room Letter	Poster #	Page #
Mozejko	Pawel	Total cross section calculations for electron-impact ionization of germanium tetrafluoride, GeF_4, and germanium tetrachloride, $GeCl_4$, molecules	Lepton	Room G	G24	299
Muckenhuber	Helmut	Irradiation of Au-nano-islands with highly charged ions and characterization with AFM and SEM	Heavy	Room B	B03	133
Müll	Damian	Photodetachment studies of the metastable states of Siωions at the Cryogenic Storage Ring	Photon	Room K	K31	437
Nandi	Saikat	Probing molecular shape resonances in attosecond time-scale	Photon	Room M	M40	519
Narits	Alexander	Photodissociation of homo- and heteronuclear rare gas molecular ions	Photon	Room N	N01	520
Navarrete	Francisco	High-harmonic generation in Fibonacci quasicrystals	Photon	Room O	O08	565
Navarro Navarrete	José Eduardo	Cooling dynamics of C_{60}- in new time domains	Photon	Room K	K32	438
Neville	John	Electronic structure of the ground states and low-lying excited states of CoB and NiB	Photon	Room N	N02	521
Ni	Hongcheng	Nonadiabatic Subcycle Linear Momentum Transfer in Tunneling Ionization	Speaker	Progress Report		48
Niggas	Anna	Interatomic Coulombic decay driving the de-excitation of highly charged ions inside of atomically thin materials	Heavy	Room C	C17	178
Niikura	Hiromichi	Phase and amplitude characterization of partial waves in an attosecond continuum electron wavepacket	Photon	Room J	J24	392
Niraula	Prashanta	Target used to study radiative-double electron capture in single-layer graphene	Heavy	Room A	A22	112
Nuesslein	Felix	New Lifetime Limit of the Ground State Vinylidene Anion H_2CC^-	Heavy	Room B	B25	152
Numadate	Naoki	Polarization of radiative recombination X-rays in highly charged Bi ions	Lepton	Room F	F19	259
Okada	Kunihiro	Rotational cooling effect on the reaction rate constant of rotationally cold $Ca^+ + CH_3F \rightarrow CaF^+ + CH_3$ reaction	Heavy	Room C	C18	179
Okino	Tomoya	Multi-fragment momentum imaging of polyatomic molecules using an electro-optic light modulator and an imaging polarimeter	Photon	Room N	N03	522
Okumura	Takuma	High resolution measurement of electronic K x rays from muonic atoms in metal	Lepton	Room H	H15	328
Okutsu	Kenichi	Design of a charged particle transport method using electrostatic field	Lepton	Room H	H05	319
Olofsson	Edvin	Frustrated tunneling dynamics in ultrashort laser pulses	Photon	Room J	J25	393
Omiste Romero	Juan José	XUV photoionization dynamics of N_2O molecule	Photon	Room N	N04	523
Onitsuka	Yuuki	An atomic momentum spectroscopy study for elucidating the range of the validity of the plane wave impulse approximation	Lepton	Room E	E29	237
Orbán	Andrea	Engineering intermolecular interactions with light to prevent destructive ultracold collisions	Heavy	Room B	B26	153
Orszagh	Juraj	Oxygen excitation induced by electron impact	Lepton	Room G	G25	300
Ott	Christian	Doubly excited states driven by intense XUV FEL pulses	Photon	Room J	J26	394
Oxley	Paul	Measurements of Charge Transfer Cross Sections for Hydrogen Ion Impact on Lithium at Low Energies	Heavy	Room A	A23	113
Palacios	Alicia	Asymmetric electron angular distributions in stimulated Compton scattering from H_2 irradiated with soft-x ray laser pulses	Photon	Room N	N05	524
Panelli	Guglielmo	Investigating resonant low-energy electron attachment to formamide	Lepton	Room G	G26	301

Last Name	First Name	Proposal Title	Abstract Topic (Projectile)	Room Letter	Poster #	Page #
Papp	Peter	Formation of negative ions from gas-phase and clusters of precursor molecules for FEBID and EBISA by low-energy electron impact	Lepton	Room G	G01	278
Passalidis	Stylianos	Charge exchange and excitation cross sections in Li^{2+}-H collisions in the intermediate impact energy domain	Heavy	Room A	A24	114
Patanen	Minna	Photoelectron spectroscopic characterization of non-supported $CaCl_2/MgCl_2$ and $MgBr_2$/NaBr nanoparticles	Photon	Room L	L12	458
Pathak	Himadri	Time-dependent optimized coupled-cluster method for laser-driven multielectron dynamics	Photon	Room J	J27	395
Paul	Anirban	Electron impact ion-pair dissociation dynamics of nitrous oxide	Lepton	Room G	G27	302
Paul	Raka	Neutralization of fullerene- and PAH-cations in collisions with atomic anions	Heavy	Room B	B27	154
Peng	Peng	Coherent control of ultrafast XUV transient absorption	Speaker	SR (Room N)	N06	80
Perry-Sassmannshausen	Alexander	Multiple Photodetachment of Silicon Anions at the Si K-Edge	Photon	Room K	K33	439
Peschel	Jasper	Complete characterization of one-photon electron wave packets	Photon	Room J	J28	396
Peters	Matthew	Frustrated ionization in strongly driven triatomic molecules	Lepton	Room G	G28	303
Pier	Andreas	Chiral photoelectron angular distributions from ionization of achiral atomic and molecular species	Photon	Room N	N07	525
Pindzola	Michael	Neutron Impact Ionization of the Fluorine Atom	Heavy	Room A	A25	115
Pindzola	Michael	Electron Impact Ionization of the Neon Atom	Lepton	Room E	E14	223
Pisanty	Emilio	The imaginary part of the high-order harmonic cutoff	Speaker	SR (Room J)	J29	81
Piwiński	Mariusz	Optical excitation function of 4^1P_1 Zn state	Photon	Room J	J30	397
Plésiat	Etienne	Theoretical Attosecond Pump-Probe Photoelectron Spectroscopy of CF_4 and N_2	Photon	Room M	N08	526
Pleskacz	Katarzyna	Nonlinear resonances in the motion of ions in the linear Paul trap	Photon	Room K	K34	440
Plowman	Corey	Differential studies of proton-hydrogen collisions	Heavy	Room A	A26	116
Plunkett	Alexander	Time, frequency, and angle-resolved quantum beats in the autoionizing nf' states of Argon	Photon	Room J	J31	398
Poline	Mathias	Study of charge transfer reactions between oxygen ions in a unique cryogenic double storage ring apparatus.	Heavy	Room C	C19	180
Pop	Nicolina	The low-energy scattering of electrons on $H_2^+$and HD^+: Dissociative recombination and ro-vibrational transitions	Lepton	Room F	F21	260
Popov	Yuri	Compton decay of positronium	Photon	Room J	J32	399
Popov	Yuri	Iterative Faddeev-like approach for the calculation of atomic bound state populations in laser-atom interactions	Photon	Room J	J33	400
Popov	Yuri	Compton ionization of atoms as a new method of dynamical spectroscopy	Photon	Room J	J34	401
Priti	Priti	Collisional-radiative modeling of the EUV spectrum of W^{6+}–W^{13+}ions observed in an electron beam ion trap	Heavy	Room C	C20	181
Purkait	Malay	Single-electron capture by He^+ from helium at intermediate energies	Heavy	Room A	A27	117
Quinto	Michele	Electron loss of neutral hydrogen atom impacting on water molecule	Heavy	Room A	A28	118
Quinto	Michele	Electron removal in neutral hydrogen – atom collisions	Heavy	Room A	A29	119

Last Name	First Name	Proposal Title	Abstract Topic (Projectile)	Room Letter	Poster #	Page #
Rabadán	Ismanuel	Single charge capture in collisions of protons with poliatomic molecules	Heavy	Room B	B28	155
Radžiūtė	Laima	Theoretical and experimental studies of the Te atom	Photon	Room J	J35	402
Rai	Subam	Charge exchange interactions of 9 – 51 keV Sn^{3+} with H2 molecules	Heavy	Room B	B29	156
Randazzo	Juan Martin	The confined Helium atom with a moving nucleus	Heavy	Room D	D05	196
Randazzo	Juan Martin	ASTRA, a new close-coupling approach for molecular ionization	Photon	Room M	N09	527
Randazzo	Juan Martin	Photodouble ionization of water under different excess energy and energy sharing regimes	Photon	Room N	N10	528
Rankovíc	Miloš	Vibrational autodetachment following excitation of electronic resonances	Speaker	Progress Report		49
Rawlins	Charlie	Many-body theory calculations of positron scattering and annihilation in H_2, N_2, CH_4 and CF_4	Speaker	SR (Room E)	E30	82
Rehill	Una	Rotational excitation of H_2 by electron impact with the molecular convergent close-coupling method	Lepton	Room G	G30	304
Richard	Benoît	Physics informed statistical analysis reveals key processes in simulated X-ray induced Coulomb explosion	Photon	Room N	N11	529
Ringleb	Stefan	HILITE - stored ions for non-linear laser-ion experiments	Photon	Room K	K35	441
Rist	Jonas	Measuring the Photoelectron Emission Delay in the Molecular Frame	Photon	Room N	N12	530
Rivas	Daniel E.	Multi-color pump-probe experiments at the European XFEL	Photon	Room J	J36	403
Roantree	Luke	RABBITT spectrograms using the semi-relativistic R-matrix with time-dependence approach	Photon	Room J	J37	404
Roerig	Aljoscha	Non-linear multiphoton ionisation dynamics of xenon upon irradiation by highly intense soft X-ray free-electron laser pulses	Photon	Room J	J38	405
Rolles	Daniel	Probing ultrafast light-induced interconversion reactions in cyclic molecules	Photon	Room N	N13	531
Roman	Viktoriya	Critical minima in the differential cross sections of electron elastic scattering by the atoms of 2nd and 3rd periods	Lepton	Room E	E15	224
Roman	Viktoriya	Electron-impact excitation cross section of the 190.8 nm ($6s6p\ ^3P^o_1$ -> $6s^2\ ^1S_0$) intercombination line of the Tl^+ ion	Lepton	Room F	F22	261
Roman	Viktoriya	Absolute cross-section of electron-impact excitation of the In^+ ion ω158.6 nm resonance line	Lepton	Room F	F23	262
Roman	Viktoriya	Emission cross-sections of the ω182.2 and ω143.4 nm Pb+ ion spectral lines	Lepton	Room F	F24	263
Roman	Viktoriya	Elastic electron scattering by the amino acid threonine molecule	Lepton	Room G	G31	305
Roman	Viktoriya	Resonances in the low-energy electron interaction with the D-ribose molecule	Lepton	Room G	G32	306
Romans	Kevin	Atomic Few-Photon Ionization out of an Optical Dipole Trap	Photon	Room J	J39	406
Roscam Abbing	Sylvianne	Coherent diffractive extreme-ultraviolet generation from nanostructured silica	Photon	Room O	O09	566
Roy Chowdhury	Madhusree	Radiosensitizing effect of halouracils in hadron therapy	Speaker	SR (Room B)	B30	83
Rui	Jinglin	Theoretical study of resonant electron recombination process of Si^{11+} ions	Lepton	Room F	F25	264
Rupp	Daniela	Time-resolved imaging of light-induced dynamics in isolated nanoparticles	Speaker	Progress Report		50
Saalmann	Ulf	Proper time delays from streaking measurements	Speaker	SR (Room J)	J40	84

Last Name	First Name	Proposal Title	Abstract Topic (Projectile)	Room Letter	Poster #	Page #
Saha	Jayanta	Atomic systems under plasma and cavity confinements	Speaker	Progress Report		51
Saha	Soumyajit	Angular anisotropy parameters for photoionization delays	Photon	Room K	K01	407
Sanchez	Aurelien	Molecular retrieval from two-dimensional LIED photoelectron spectra upon strong-field ionization	Photon	Room N	N14	532
Sanchez	Sergio	Elastic positron collision with acetone molecule: a study in the low-energy region	Lepton	Room E	E31	238
Sanchez	Sergio	METHYLATION EFFECT ON ELECTRON SCATTERING:GLYCOLIC ACID AND LACTIC ACID	Lepton	Room G	G33	307
Sarantseva	Tatiana	Retrieving of an attosecond pulse waveform based on the high harmonic generation	Speaker	Progress Report		52
Saraswathula	Krishna Chaitanya	High Resolution Mass Spectrometry and Velocity Map Imaging for Ultrafast Electron Dynamics in Biomolecules	Photon	Room N	N15	533
Šarmanová	Martina	Nonlocal multidimensional vibrational dynamics of anions: Testing of various Krylov subspace methods on model examples	Lepton	Room F	F38	275
Scarlett	Liam	Rovibrationally-resolved electron scattering on H2: Molecular convergent close-coupling calculations	Speaker	PR (Room G)	G34	53
Scheier	Paul	Cold physics and chemistry: collisions, ionization and reactions inside helium nanodroplets	Speaker	Tutorial		25
Schiller	Arne	Observing the submersion of rubidium clusters in helium nanodroplets	Heavy	Room B	B04	134
Schmidt	Viviane Charlotte	Studying vibrational cooling and Renner-Teller interaction of the C_4O^- anion through resonant photo-dissociation at CSR	Photon	Room N	N16	534
Schmidt-Böcking	Horst	Ultra-fast dynamics in quantum systems revealed by particle motion as clock	Heavy	Room B	B31	157
Schmidt-Böcking	Horst	Hundred years ago: Alfred Lande's half-integer quantum numbers and g-factor 2	Photon	Room K	K02	408
Schmidt-Böcking	Horst	On the precision limits in a single-event quantum measurement of electron momentum and position	Photon	Room O	O10	567
Schmidt-Böcking	Horst	High-Resolution Momentum Imaging: From Stern's Molecular Beam Method to the COLTRIMS Reaction Microscope	Photon	Room O	O11	568
Schmidt-May	Alice	Experimental branching fractions of the mutual neutralization of lithium cations and hydrogen anions at DESIREE	Heavy	Room C	C22	182
Schneider	Barry	A Science Gateway for Atomic and Molecular Physics: Democratizing Atomic and Molecular Physics Research and Education	Lepton	Room H	H06	320
Schöffler	Markus	On the quest for projectile coherence in C^{6+}/He collisions	Heavy	Room A	A30	120
Schöffler	Markus	The two-electron cusp in the ground states of He and H_2 investigated via quasifree double photoionization	Photon	Room N	N17	535
Schubert	Kaja	Unravelling the electronic structure of isolated metalloporphyrins by metal L-edge spectroscopy	Photon	Room N	N18	536
Schulz	Michael	Interference effects in fully differential cusp electron production cross sections for p + He collisions	Heavy	Room A	A31	121
Schury	Daniel	Planned Laboratory Studies of N_2 reacting with H_3^+ Isotopologues	Heavy	Room C	C23	193
Schütte	Bernd	Attosecond-resolved multi-photon multiple ionization dynamics	Photon	Room K	K03	409
Schwob	Lucas	Near edge X-ray absorption mass spectrometry applied to peptides: structure and site-selective dissociation.	Photon	Room N	N19	537
Segui	Silvina	Oscillator model: A new approach to study the interaction ofexternal charged particle with 2D materials. Application to graphene	Lepton	Room H	H16	329

Last Name	First Name	Proposal Title	Abstract Topic (Projectile)	Room Letter	Poster #	Page #
Sen	Arnab	Above threshold ionization of Argon with ultrashort orbital angular momentum beams	Photon	Room K	K04	410
Shahi	Abhishek	VMI photoelectron spectroscopy probing the rotational cooling dynamics of hot trapped OH^- ions	Speaker	SR (Room K)	K36	86
Shaik	Rasheed	Photoionization coherence of an alkali metal cluster confined in a giant fullerene ($Na_{40}@C_{540}$)	Photon	Room L	L13	459
Shakya	Yashoj	Unraveling the most significant collective coordinate influencing time-resolved x-ray absorption spectra in ionized urea and its dimer	Photon	Room N	N20	538
Shalenov	Erik	Ionization and recombination coefficients of the dense nonideal hydrogen plasma: effects of screening and quantum diffraction	Lepton	Room E	E16	225
Shalenov	Erik	Investigation of electron runaway process on the basis of effective potential taking into account dynamic screening	Lepton	Room F	F26	265
Sheil	John	Transitions between multiply-excited states and their contribution to opacity in laser-driven tin plasmas for EUV lithography	Lepton	Room F	F27	266
Shobeiry	Farshad	Sub-femtosecond control of entangled two-electron states	Photon	Room N	N21	539
Shvetsov-Shilovskiy	Nikolay	Two-dimensional electron momentum distributions in ionization of water molecule by a strong laser field	Photon	Room N	N22	540
Sigaud	Lucas	Neutral H_2 production from ethylene electron and photon ionization	Lepton	Room G	G35	308
Silva	Murilo	Elastic and electronically inelastic scattering of low-energy electrons by the 2H-pyran molecule.	Lepton	Room G	G36	309
Simonet	Juliette	Ultrafast electron cooling in an expanding ultracold plasma	Speaker	SR (Room D)	D19	87
Singh	Chandra Shekhar	Electron impact excitation of autoionizing states of lithium and potassium using distorted wave method with absorption potential	Lepton	Room E	E17	226
Singh	Suvam	Photodetachment cross sections and radiative lifetimes of the metastable states of Si^- ions	Photon	Room K	K37	442
Singor	Adam	A Fully Relativistic Approach to Photoionization of Alkali Atoms	Photon	Room K	K05	411
Siqi	He	Measurement and analysis of the emission spectrum of laser-produced Zn plas-ma in the range of 7-14 nm	Photon	Room K	K38	443
Sixt	Tobias	Quantum-state-controlled Penning collisions of ultracold lithium atoms with metastable atoms and molecules	Heavy	Room A	A32	122
Smolianskiy	Vladimir	Effects upon the grazing interaction of microfocus bremsstrahlung with surfaces of different lengths	Photon	Room O	O20	576
Soguel	Romain	Redefined vacuum approach and gauge-invariant subsets in two-photon-exchange diagrams	Photon	Room K	K39	444
Sommerfeldt	Jonas	Coulomb corrections to Delbrück scattering	Photon	Room K	K40	445
Sommerlad	Laura	Investigating photo-double-resonances in neon beyond the 1s threshhold	Photon	Room K	K06	412
Son	Sang-Kil	Resonance-enhanced multiphoton ionization in the x-ray regime	Photon	Room K	K07	413
Sorensen	Stacey	Tracing the dynamics in photoexcited hydrocarbons: cyclical vs conjugated	Photon	Room N	N23	541
Souza Barbosa	Alessandra	Electron and Positron scattering by lactic acid molecule	Lepton	Room E	E32	239
Souza Barbosa	Alessandra	Carboxylation effects in low-energy electron scattering by molecules	Lepton	Room G	G37	310
Spicer	Kate	Differential direct scattering and electron capture in proton-helium collisions at intermediate energies	Heavy	Room A	A33	123

Last Name	First Name	Proposal Title	Abstract Topic (Projectile)	Room Letter	Poster #	Page #
Srivastav	Sumit	Fragmentation dynamics of CO_2^{4+}: Contributions of different electronic states	Heavy	Room B	B32	158
Stankiewicz	Kamil	Accurate theoretical studies from first principles of HD-He collisional system in molecular spectra	Heavy	Room B	B33	159
Steydli	Sebastien	Measurement of ion-induced desorption yields for accelerator vacuum application	Heavy	Room C	C24	184
Stockett	Mark	Competitive Dehydrogenation and Backbone Fragmentation of Super-Hydrogenated PAHs	Photon	Room N	N24	542
Stolarczyk	Nikodem	The first comprehensive data set of beyond-Voigt line-shape parameters for the H_2-He system for the HITRAN database	Heavy	Room B	B34	160
Stolarczyk	Nikodem	CO-Ar collisions: sub-percent agreement between ab initio model and experimental spectra at pressures varying within four order of magnitude	Heavy	Room B	B35	161
Svensmark	Jens	Adiabatic theory of strong-field ionization of molecules with nuclear motion	Photon	Room N	N25	543
Swann	Andrew	Positron cooling in N_2 and CF_4 gases	Lepton	Room E	E33	240
Szabo	Paul	Sputtering of Planets and Moons by Ion Impact	Speaker	Progress Report		54
Szabo	Gabriel	Generation of picosecond ion pulses using a fast pulse electron beam ion source	Heavy	Room C	C25	185
Táborský	Jiří	Comparison of classical trajectory and quantum calculations of reactions of O^- with H_2 at low temperatures	Heavy	Room C	C26	186
Tachibana	Yuichi	Direct observation of atomic motion in molecules using atomic momentum spectroscopy	Speaker	Progress Report		55
Takahashi	Karin	XUV pump – XUV probe measurements for femtosecond ionization processes	Photon	Room K	K08	414
Takahashi	Naoto	p-wave elastic collisional properties of Fermi gases confined in quasi-2D	Heavy	Room A	A34	124
Tamuliene	Jelena	Fragmentation of tyrosine under low-energy electron impact	Heavy	Room B	B36	162
Tanis	John	Radiative double-electron capture for $F^{9,8+}$ ions in gas and thin-foil targets*	Heavy	Room A	A35	125
Taoutioui	Abdelmalek	Transfer ionization cross sections in collisions between bare light ions and Helium atom	Heavy	Room A	A36	126
Taoutioui	Abdelmalek	Theoretical study of the holographic structures induced by strong ultrashort pulses	Photon	Room K	K09	415
Tarek	Khatit	Theoretical study of the collision dynamics in electron-impact ionization of atomic and molecular targets	Lepton	Room G	G39	311
Tayal	Swaraj	Electron-impact excitation of Sc II	Lepton	Room F	F28	267
Teramura	Takuma	Gauge-invariant time-dependent configuration interaction singles method for molecules: extracting photoelectron momentum distribution	Photon	Room N	N26	544
Thiam	Guillaume	Electron-attachment energies predicted using TD-DFT methods	Lepton	Room G	G40	312
Thumm	Uwe	Strong-field photoelectron emission from metal nanoparticles	Speaker	SR (Room O)	O12	85
Thumm	Uwe	Photoelectron –- residual ion entanglement in streaked and multi-sideband interferometric photoemission: an ab initio approach	Photon	Room K	K10	416
Thumm	Uwe	Mapping of light-induced potentials in the strong-field dissociation of O_2^+	Photon	Room N	N27	545
Thumm	Uwe	High Harmonic Generation from MgO crystals by two-color pulses	Photon	Room O	O21	577

Last Name	First Name	Proposal Title	Abstract Topic (Projectile)	Room Letter	Poster #	Page #
Thumm	Uwe	Enhanced high-harmonic generation yield in doped semiconductors	Photon	Room O	O22	578
Thuppilakkadan	Afsal	Effect of SOIAIC on the angle-resolved time delay in the photoionization of Ar inside fullerene anion	Photon	Room K	K11	417
Tokesi	Karoly	Computer simulations of the spatial and temporal distribution of 1 MeV proton microbeam guided through a poly(tetrafluoroethylene) macrocapillary	Heavy	Room D	D15	206
Tokesi	Karoly	Interecations of electrons and positrons with two-dimensional proton lattice	Lepton	Room H	H17	330
Tokesi	Karoly	Investigation of the mode symmetries in Sapphire phoXonic cavities	Photon	Room O	O23	579
Tong	Xiaomin	Exchange-correlation functional with self-interaction corrections for many-atom systems	Photon	Room L	L14	460
Trabert	Daniel	Angular dependence of the Wigner time delay upon tunnel ionization of H_2	Photon	Room N	N28	546
Travnikova	Oksana	Photo-induced molecular catapult. Imaging molecular rotation during ultrafast dissociation.	Speaker	SR (Room N)	N29	88
Trinter	Florian	Multi-coincidence Studies of Molecules using Synchrotrons and XFELs	Speaker	Progress Report		56
Trinter	Florian	Angular emission distribution of O 1s photoelectrons of uniaxially oriented methanol	Photon	Room N	N30	547
Trnka	Jiří	Theoretical study of electron-impact vibrational excitation of isocyanic acid HNCO using two dimensional nonlocal model	Lepton	Room G	G41	313
Tsikritea	Andriana	Charge transfer reactions of polar molecules and rare gas ions	Speaker	SR (Room C)	C27	89
Tsoukala	Alexandra	Towards the coherent control of Penning collisions between metastable helium atoms	Photon	Room K	K12	418
Tsuzuki	Yutaka	An application of a Si/CdTe Compton camera for the polarization measurement of hard x-rays	Photon	Room O	O13	569
Tukhfatullin	Timur	Studies of DD reactions in Deuterated Crystals at HELIS in astrophysical energy region	Heavy	Room D	D06	197
Tukhfatullin	Timur	Half-Wavelength-Crystal channeling of relativistic heavy ions and its possible application	Heavy	Room D	D07	198
Tukhfatullin	Timur	HWC Channeling of Relativistic Isotopes	Heavy	Room D	D08	199
Utamuratov	Ravshan	Positron collisions with alkali atoms	Lepton	Room E	E18	227
Van Der Burgt	Peter	Fragmentation of anthracene molecules following double ionization by 70 eV electron impact	Lepton	Room G	G42	314
Van Der Geest	Maarten	Inorganic-organic lead trihalide perovskites as potential extreme ultraviolet scintillators	Photon	Room O	O24	580
Vanhaele	Guillaume	NOON states with ultracold bosonic atoms via resonance- and chaos-assisted tunneling	Heavy	Room A	A37	127
Varvarezos	Lazaros	Near-threshold two-photon double ionization of Kr in the VUV	Photon	Room K	K13	419
Vasileva	Daria	Polarization phenomena in electron resonant elastic scattering on one-electron ions	Speaker	SR (Room F)	F29	90
Veilande	Rita	Three mathematical models of photons	Photon	Room O	O25	581
Venkat	Prachi	Effect of incident pulse duration on generation of attosecond pulses during relativistic laser-cluster interaction	Photon	Room L	L15	461
Vincenti	Henri	Probing strong-field QED using high-power lasers Doppler-boosted by curved relativistic plasma mirrors	Speaker	Progress Report		57

Last Name	First Name	Proposal Title	Abstract Topic (Projectile)	Room Letter	Poster #	Page #
Visentin	Giorgio	Accurate binding energy of Yb dimer (Yb_2) from ab initio calculations and ultracold photoassociation spectroscopy	Heavy	Room A	A38	128
Wahyutama	Imam	Atom-resolution of momentum spectrum from a single tunnel ionization for the study of ionization-induced hole localization	Photon	Room N	N31	548
Walsh	Noelle	From molecules to liquid jets - synchrotron research on isolated species and condensed samples	Photon	Room O	O14	570
Walter	Peter	The TMO Instrument: Opportunities and Plans for Time-resolved Atomic, Molecular and Optical Science at LCLS-II	Photon	Room K	K14	420
Wang	Enliang	Fragmentation dynamics of hydrated tetrahydrofuran induced by electron impact ionization	Speaker	Progress Report		58
Wang	Enliang	The role of the environment in quenching the production of H_3^+ from the dicationic clusters of methanol	Lepton	Room F	F39	276
Wang	Guoli	Is carrier envelope phases of multi-color laser pulses necessarily optimized to generate shorter isolated attosecond pulses?	Photon	Room K	K16	422
Wang	Guoli	Dependence of low-frequency THz radiation on electron population distributions from graphene	Photon	Room O	O26	582
Wang	Hanbing	Simulation of bunched Schottky spectrum for laser-cooled O^{5+} ions at CSRe	Heavy	Room C	C28	187
Wang	Lihan	The study of the low-lying valence-shell excitations of carbon tetrachloride by fast electron impact	Lepton	Room G	G43	315
Wang	Shu-Xing	Precise determination of the transition energy with fluorine-like nickel utilizing a low-lying dielectronic resonance	Lepton	Room F	F30	268
Wang	Tian	Light-induced dissociation dynamics of Br_2	Photon	Room N	N33	550
Wang	Xia	Theoretical study on the tune-out wavelengths of the ground state of Ba atom	Heavy	Room A	A39	129
Wang	Xin	Intramolecular hydrogen transfer in gas-phase DNA induced by site-selected resonant core excitations	Photon	Room N	N32	549
Wang	Zhi-Bin	Mechanism of below-threshold high-order harmonic generation of Na in the intense elliptically polarized laser field	Photon	Room K	K15	421
Wasowicz	Tomasz	Marks of charge transfer and complexes formation processes revealed in cat-ion-induced fragmentation spectra of pyridyne	Heavy	Room B	B37	163
Wasowicz	Tomasz	Soft X-ray induced excitation, ionization, and fragmentation of isoxazole at the K-edges	Photon	Room N	N34	551
Wasowicz	Tomasz	Dissociative photo-double-ionization of tetrahydropyran and 3,4-dihydropyran	Photon	Room N	N35	552
Watanabe	Noboru	Measurement of the forward-backward asymmetry in electron impact ionization of CO	Lepton	Room G	G44	316
Wen	Wei-Qiang	Rate Coefficients for Dielectronic Recombination of C-Like $^{40}Ca^{14+}$	Lepton	Room F	F31	269
Werl	Matthias	Measuring charge exchange and energy loss of highly charged ions colliding with surfaces under grazing incidence	Heavy	Room D	D16	207
White	Andrew	Electron-impact ionization and excitation of Si^+ for applications in laboratory and astrophysical plasmas.	Lepton	Room F	F32	270
Wilde	Robyn	Positronium Scattering by O_2 and CO_2	Lepton	Room E	E34	241
William	Noah	Positron impact excitation of lowest autoionizing state of potassium atom using distorted wave method with absorption and polarization potentials	Lepton	Room E	E19	228
Winters	Danyal	Measurements of the 2s-2p transitions in stored & cooled relativistic $^{12}C^{3+}$ ions by means of laser spectroscopy	Photon	Room K	K41	446
Wolff	Wania	On the stability of the aromatic molecules benzonitrile and toluene under electron impact in Titan´s atmosphere	Lepton	Room H	H07	321

Last Name	First Name	Proposal Title	Abstract Topic (Projectile)	Room Letter	Poster #	Page #
Wong	Nicholas	Angularly Resolved Photoelectron Spectra from Photoionized Benzene	Photon	Room N	N36	553
Xing	Xiaodong	Non-radiative charge exchange in an ultracold Li-Ba^{+} hybrid trap	Heavy	Room C	C29	188
Xiong	Yanwei	Near-infrared strong field induced fragmentation and ionization of toluene captured by ultrafast electron diffraction	Photon	Room N	N37	554
Xu	Shenyue	Delayed fragmentation of propyne and allene in collisions with highly charged ions	Heavy	Room B	B38	164
Xu	Yuan-Chen	The investigations of excitation dynamics of the inner-shell excitation of the nitrogen	Photon	Room N	N38	555
Yamaguchi	Atsushi	Development of an RF-carpet gas cell to obtain an ion beam of thorium-229	Speaker	Progress Report		59
Yamashita	Takuma	Relativistic effects on loosely bound states of positronic alkali-metal atom	Speaker	PR (Room E)	E21	60
Yamashita	Takuma	Antihydrogen positive ion formation in antihydrogen-positronium collision	Lepton	Room E	E20	229
Yasuda	Kazuhiro	Four-body calculation of muonic molecular resonances in the electron cloud	Lepton	Room H	H11	324
Yin	Zhong	Femtosecond Dynamics of Solvated Biomolecules Studied by Flat-jet X-ray Absorption Spectroscopy	Photon	Room N	N39	556
Ying	Bo	The Laser-driven Anharmonic Oscillator: Ground-state dissociation of the Helium hydride molecular ion by mid-infrared pulses	Photon	Room N	N40	557
Yusuke	Naito	Spin-state dependence of the Charge-Exchange collision in a hybrid system of ultracold ^{6}Li atoms and $^{40}Ca^{+}$ ions	Heavy	Room C	C31	189
Zapata	Felipe	Implementation and validation of the relativistic attosecond transient absorption theory within the dipole approximation	Photon	Room K	K17	423
Zaytsev	Sergey	Single ionization of helium by high energy proton impact using the parabolic Sturmians representation	Heavy	Room A	A40	130
Zaytsev	Sergey	Laser-assisted elastic electron scattering by Xe in the quasi-Sturmian-Floquet approach	Lepton	Room E	E22	230
Zhang	Dongdong	New source for tuning the effective Rabi frequency in multiphoton ionization	Photon	Room K	K18	424
Zhang	Pengju	Intermolecular Coulombic decay in liquid H_2O and D_2O: the role of proton transfer	Photon	Room O	O15	571
Zhang	Yu	Hydrogen migration in the dissociation of hydrocarbon dications	Lepton	Room F	F40	277
Zhongkui	Huang	Absolute Rate Coefficients for Dielectronic Recombination of Na-like Kr^{25+}	Lepton	Room H	H12	325
Zhu	Binghui	Observation of X-ray spectroscopy from H-like Lead at CRYRING@ ESR	Heavy	Room C	C32	190
Žitnik	Matjaž	Coherent control of He $2s^2$ population by XUV light	Photon	Room K	K19	425
刘	一乐	Collisional-radiative model of the visible spectrum of W^{13+} ion	Heavy	Room C	C33	191
张	天成	Ionization potentials is one of the fundamental properties of the superheavy elements.	Heavy	Room D	D17	208

www.ICPeac2021.ca